COLLECTED WORKS OF
KS KRISHNAN

NATIONAL PHYSICAL LABORATORY
DR. K.S. KRISHNAN ROAD
NEW DELHI-110012

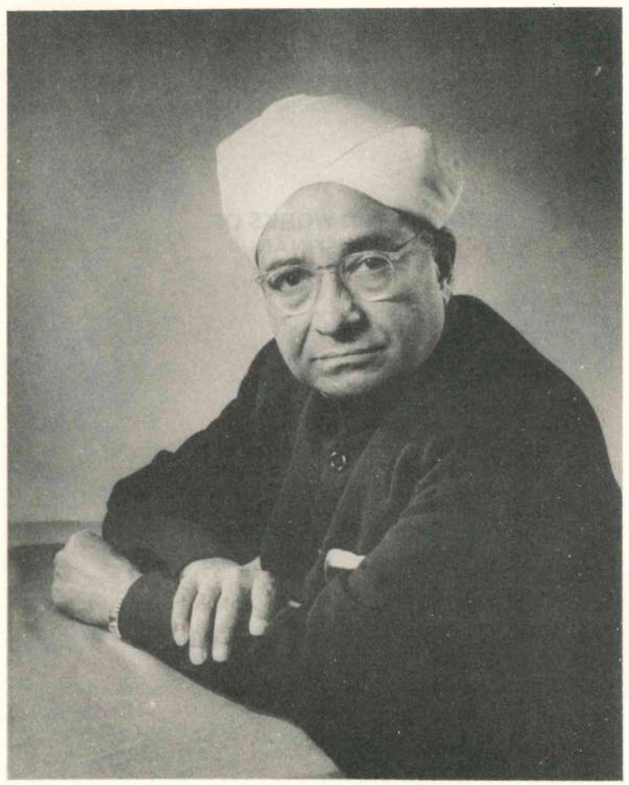

COLLECTED WORKS OF
K S KRISHNAN

NATIONAL PHYSICAL LABORATORY
DR. K.S. KRISHNAN ROAD
NEW DELHI-110012
1988

Cover Design:
PRADIP BANERJEE

Printed by INSDOC, Hillside Road, New Delhi-110012.

FOREWORD

It gives me great pleasure in writing the Foreword to the collected Research Contributions of Late Prof. K.S. Krishnan, F.R.S. Prof. K.S. Krishnan ranks as one of the most outstanding Indian Scientists whose contributions are respected all over the world. Efforts are being made to bring out the collected papers of all outstanding Indian Scientists. This volume gives in one place an account of the original researches of Prof. Krishnan in spectroscopy, magnetism, thermionic emission and other areas of his interest. I hope this volume will be useful to all the Scientists. Dr. Krishan Lal and some of his colleagues have made the necessary efforts in bringing out this volume.

A.P. Mitra

A.P. MITRA
DIRECTOR-GENERAL
COUNCIL OF SCIENTIFIC AND INDUSTRIAL RESEARCH
NEW DELHI

19.2.1988

REMARKS OF DIRECTOR, NPL

The National Physical Laboratory was fortunate to have Sir K.S. Krishnan as its founder Director who guided the destiny of this laboratory for nearly fourteen eventful years. All his acts were directed towards making NPL into a laboratory that works, committed to the cause of science and development. He was one of the outstanding scientists of the country, who was associated with many remarkable discoveries including his association with Sir C.V. Raman on studies of molecular scattering of light which ultimately led to the discovery of Raman effect. Sir Krishnan had a penetrating insight into the basic physics of a problem presented to him and one would be able to discern it in his publications which has been brought together in this volume of "Collected Works". One can also notice from this collection that in this overspecialized world today Krishnan's breadth of interest was remarkable. He worked on areas as diverse as scattering of light from liquids and gases, magnetism and structure of matter, thermionic emission and optical and transport properties of the condensed phase of matter. I am sure even today we shall be benefitted by browsing through his research papers brought together in this volume specially because of the physical principles emphasized and illuminated in these papers.

S.K. Joshi

S K JOSHI
DIRECTOR
NATIONAL PHYSICAL LABORATORY
NEW DELHI

19.2.1988

PREFACE

It has been a matter of great pleasure and privilege for me to be entrusted with the responsibility of bringing out a Volume containing all important research papers of Late Prof. K.S. Krishnan, F.R.S. This work was initiated at the suggestion of Dr. A.P. Mitra, Director-General, CSIR during his tenure as Director, National Physical Laboratory. Dr. S.K. Joshi has been showing keen interest in this project.

This Volume contains nearly 130 papers which cover all major scientific interests of Prof. Krishnan including spectroscopy, magnetism and thermionic emission. We have also included tributes paid to him by well-known Scientists like Prof. K.R. Ramanathan Prof. Sydney Chapman, Prof. Dame Kathleen Lonsdale and Dr. H.J. Bhabha. These contributions throw light on different aspects of Prof. Krishnan's personality.

A subject index and a list of collaborators of Prof. K.S. Krishnan have been included. A few photographs of Prof. Krishnan recorded during his tenure at the NPL have also been incorporated.

It was quite a time consuming task. All the original journals from which the material was to be reproduced were not available in any one library. Indeed even all the libraries in Delhi could not provide all the material. Some of the papers had to be obtained from abroad. A large number of persons helped us in this effort. The name of Prof. Krishnan aroused strong positive feelings in all the persons whom we contacted for this purpose.

It is a great pleasure to acknowledge the cooperation I received from all persons who were approached in connection with this Volume. Shri V. Ramachandran of INSDOC New Delhi and his colleagues have put in every effort to bring out a volume of good quality. Shri T N. Rajan, INSDOC, helped us in getting good copies of some of the important research papers. It is a pleasure to acknowledge the cooperation received from the NPL Library. A large number of journals were borrowed from the library of the Indian Agricultural Research Institute, New Delhi. I am indebted to the Librarian and other staff and Dr. Nam Prakash and Shri V.K. Sharma of NRL. Shri G Bhagavannarayana, Dr. S.K. Halder, Dr. R.V. Ananthamurthy and Dr. S.D. Sharma of NPL were of great help.

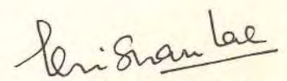

(KRISHAN LAL)
DEPUTY DIRECTOR
NATIONAL PHYSICAL LABORATORY
NEW DELHI

19.2.1988

CONTENTS

Professor K. S. Krishnan, F.R.S.*

PROFESSOR K. S. Krishnan, distinguished physicist, philosopher and *Acharya*, will be sixty years old on 3 December 1958. On that auspicious occasion, we wish to convey to him our cordial felicitations and good wishes for his continued good health, activity and service to science, philosophy and international goodwill for many, many years to come.

Creative thinkers like Krishnan with understanding, critical judgement and tolerance, men who have a mind of their own and carry out their inner *dharma* unperturbed by changing fashions, men who "explore the explorable and quietly venerate the inexplorable" are not to be found in large numbers in any country. When we do find such persons, we do well to honour them.

Kariamanikkam Srinivasa Krishnan was born in the village of Watrap near Srivilliputtur in the Tirunelveli (now Ramnad) district in Tamilnad. His father was a scholar of the old school deeply versed in Tamil and Sanskrit religious literature. He spent a good part of his time in pilgrimages to South Indian temples, particularly to Srirangam and Tirupathi. Krishnan had his early schooling in Watrap and Srivilliputtur and was brought up in a rural atmosphere. After matriculation, he had his collegiate education first in the American College, Madura, and later in the Christian College, Madras. After graduating in physics from the Christian College, he was for a few years a Demonstrator in Chemistry in the same college. He took his teaching seriously and was a very popular teacher. I have heard that he used to conduct informal lunch-hour discussion classes which were attended by large number of students from all the neighbouring colleges and in which any questions in mathematics, physics or chemistry could be raised and would be answered there and then, starting from first principles.

Being of an enquiring turn of mind and anxious to qualify himself for a life of scientific study and research, Krishnan went to Calcutta to study physics under Professor C. V. Raman. He joined the University College, Calcutta, for his M.Sc. Professor Raman's lectures which have a range, penetration and fascination, all their own, influenced Krishnan greatly and he absorbed from Raman a deep and abiding interest in optics and molecular physics. For some reason, Krishnan did not take the M.Sc. examination, but Professor Raman accepted him as a research student in the Indian Association for the Cultivation of Science, 210 Bowbazar Street. This was in 1923. Krishnan continued to work there as a research scholar till December 1928, when he left for Dacca as a Reader in Physics in the university there.

The period of Krishnan's stay in the Indian Association for the Cultivation of Science was a period of exceptional activity. The new subject of molecular scattering of light and of X-rays was being rapidly developed by Professor Raman and there were a number of bright young men from all over India working in the Association under his unique leadership in various aspects of the subject. Krishnan entered into his work with great enthusiasm. He made a characteristically thorough experimental study of the scattering of light in a large number of pure liquids, worked on many problems in the classical theory of the diffraction of light and started work on the magnetic anisotropy of gaseous molecules and of crystals (nitrates and carbonates). He collaborated with Professor Raman in making a detailed examination of the change in the nature of the light which was found to be associated with molecular scattering. As is well known, these studies led to the discovery of the Raman Effect.

In October 1928, Professor Arnold Sommerfeld of Germany was a Guest Professor of the Calcutta University and he delivered a course of seven lectures on modern developments of quantum theory. Krishnan took careful notes of the lectures. As Professor Sommerfeld says, "the first three and the last two lectures were worked out by

*This article is reproduced, with kind permission, from the Souvenir Volume published by Dr K. S. Krishnan's Sixtieth Birthday Celebrations Committee, New Delhi.

With Pt. Nehru, Bhatnagar, Swaran Singh and others

Sixtieth birthday celebration of Dr. K.S. Krishnan at NPL

Mr K. S. Krishnan in a very independent way". The lectures were later published by the Calcutta University.

Professor Krishnan was in the Dacca University from 1929 to 1933. With Dr S. N. Bose as Professor of Physics and his old friend Dr T. Vijayaraghavan, Reader in Mathematics, and with Mr Langley as Vice-Chancellor, Mr Krishnan found a congenial atmosphere in Dacca and threw himself heart and soul into his teaching and research activities. It was there that he developed his elegant and precise experimental methods to test out the idea that the magnetic anisotropy of a diamagnetic or paramagnetic crystal could be correlated with the anisotropy of the individual molecules and their relative orientations and that in favourable cases the precise orientation of molecules in the unit cell could be determined from magne-crystallic measurements. He worked out simple methods of measuring accurately feeble susceptibilities and anisotropies, making effective use of quartz fibre suspensions and liquid baths of varying susceptibilities for immersing the crystals. With his students, B. C. Guha, S. Banerjee and N. C. Chakravarty, he made measurements on a large number of crystals, both diamagnetic and paramagnetic.

The papers entitled "Investigations in magne-crystallic action", which were published in the next few years by Professor Krishnan and his students in the *Philosophical Transactions of the Royal Society* and in the *Physical Review*, are mines of information regarding the magnetic properties of diamagnetic and paramagnetic crystals. The work of Krishnan and his students and of Dr Kathleen Lonsdale established the fruitfulness of magnetic methods as a valuable supplement to the methods of X-ray analysis for determining the architecture of crystals.

When Professor Raman left Calcutta in 1933, Krishnan was invited to take up the post of Mahendralal Sircar Professor of Physics in the Indian Association for the Cultivation of Science. There were no regular teaching duties attached to the post and a return to the old familiar cosmopolitan surroundings of 210 Bowbazar was welcome to Krishnan. The magnetic and optical properties of crystals together with their structure analysis by X-rays, and the various ways in which the anisotropy of crystal units manifest themselves in the bulk properties of the crystals continued to occupy his attention. To the second Calcutta period belongs the work of Krishnan, Bose and Mookherjee on the magnetic properties of salts of the rare earth and iron groups including a detailed comparison of their extensive experimental measurements with the conclusions which follow from the theoretical work of Van Vleck and Penney and Schlapp on the crystalline electric fields of such crystals. In paper V in the series on magne-crystallic action published in the *Philosophical Transactions of the Royal Society*, there is detailed discussion of the susceptibilities and anisotropies of these crystals and of the conditions which determine to what extent the temperature variation of their susceptibilities will follow the Curie Law. To the same period also belongs a characteristically significant paper by Gangulee and Krishnan on "The magnetic and other properties of free electrons in graphite" (*Proc. roy. Soc.*, 1941). In this paper, the authors show that the diamagnetism of graphite is almost wholly along the hexagonal axis, that in a graphite crystal, one electron per carbon atom is free to move in the basal plane but not in a perpendicular direction, or in other words, the electrons in such a crystal form a two-dimensional electron gas, and that the theoretical properties of such an electron gas can be verified in detail from a study of the magnetic properties of graphite. From the measured values of the diamagnetism of graphite at different temperatures varying from $-90°$ to $1270°$K., they conclude that the energy distribution of electrons in graphite conforms to Fermi-Dirac distribution.

Professor Krishnan's contributions to physics were recognized by the invitations he received from Lord Rutherford in Cambridge and Sir William Bragg in London to give a course of lectures in the Cavendish Laboratory and in the Royal Institution (1937). He later visited a number of universities in Europe and was awarded the University Medal by the University of Liége for his scientific achievements. In 1939, he was invited to participate in an International Symposium on Magnetism at Strasbourg. Krishnan was elected to the Fellowship of the Royal Society in 1940.

In 1942, Krishnan was offered the post of Professor of Physics in the University of Allahabad which had been vacant for some years after the departure of Professor M. N. Saha to Calcutta. Krishnan always enjoyed

teaching and discussion. The Professorship in Allahabad gave him an opportunity to review, in a systematic and comprehensive way, before senior students the various problems of classical scattering of light, X-rays and electrons, of statistical thermodynamics, and quantum theory and wave mechanics. Despite the difficult conditions created by the war, Krishnan and his associates were able to do a good amount of investigational work on these subjects. In particular may be mentioned his work with Dr A. B. Bhatia giving a critical review of Einstein's theory of light scattering in homogeneous media as reflection from thermal elastic waves and a new and illuminating method of summing up the intensities of the elastic waves. They also treated on a unified basis the scattering of X-rays by fluids and of low velocity electrons by liquid metals and by alloys.

As an offshoot of the analysis of elastic waves in a homogeneous medium caused by fluctuations of density, Krishnan was led to the study of the mathematical problem of the summation of certain infinite series of a class of functions which are of special importance in physics. He showed that with functions whose Fourier transforms satisfy two simple conditions, the sum of the infinite series could be obtained just as well by rectangulation as by integration, and that this was not an approximate, but a rigorous result. Krishnan's paper " On the equivalence of certain infinite series and the corresponding integrals " in the *Journal of the Indian Mathematical Society* (Vol. 12, 1948) shows the range and power of the method.

Even before the gaining of independence, it was felt by many Indian scientists and statesmen that there was a great need for national laboratories in different branches of science and technology in India. With the achievement of independence, the Government of India decided to start such laboratories, and the laboratories for chemistry and physics were the first ones to be started. Professor Krishnan was offered the Directorship of the National Physical Laboratory. Although the acceptance of this meant getting away from teaching and research, at least temporarily, Krishnan accepted the offer and took over the duties in 1947.

A good deal of Krishnan's time during the next few years was taken up in administrative duties and committee work, but still he was able to keep up active interest in scientific research. Evidence for this is found in his work with Dr S. K. Roy on the frequencies and anharmonicities of alkali halide crystals and on a critical analysis of the difference between the characteristic frequencies which appear in the dispersion formulae of Drude and Lorentz. In the Drude formula, the frequencies are characteristic of the medium, and in the Lorentz formula, they are characteristic of the oscillators when unaffected by the polarization field. At about the same time, there began to appear a series of four brilliant papers on thermionics with Dr S. C. Jain. Thermionics began to interest Krishnan when he was in Allahabad. He had suggested in 1944 a new method of determining the saturation pressure of electrons by effusion through a small aperture in a uniformly heated chamber of graphite whose inside could be coated with different materials. Like cavity radiation for the study of black body radiation, this method has several advantages. With the assistance of Dr Jain, he started experimental work at the National Physical Laboratory and, in a few years, they were able to determine with great accuracy the thermionic constants of graphite, the metals of the iron group and of the monovalent metals, copper, silver and gold. In their final paper they discussed the energy barrier at the surface of a monovalent metal, on the thermodynamic potential of the electrons and on the work function in metals. They showed that the observed variation of the work function was as though the electrons in the metal and in the vapour formed the two phases of a single component thermodynamic system. They showed further that the thermal expansion of the lattice and the thermal agitation of the atoms in the lattice both affected the work function of the metal, but that the effects of the two practically cancelled each other.

Another problem which is of an applied physical nature and has engaged Krishnan's attention in the National Physical Laboratory is the distribution of temperature along a thin rod (or wire) electrically heated *in vacuo*. In modern electrical technology, electrically heated wires find extensive use in various devices, such as electric lamps, valves of various kinds, cathodes of X-ray tubes, etc. The functioning and efficiency of these devices depend largely on the manner in which the temperature, and depending on it, other properties, are distributed along the wire.

With the collaboration of Dr Jain, Krishnan attacked this problem both from a theoretical and an experimental point of view. On the theoretical side, the authors formulated the appropriate differential equation and solved it in a practically usable form both for long and short filaments. On the experimental side, they carried out measurements on thin rods of Acheson graphite and platinum filaments, and verified the theoretical results. Moreover, they compared these theoretical results with the empirical findings of many investigators who had studied the subject before and found very satisfactory agreement. They thus brought orderly thinking into a complex but very practical subject and made the way easier for further advances.

I have mentioned above only the major items of work in which Krishnan himself was personally engaged, for they bring out clearly his broad outlook, his carefulness in the choice of problems, the masterly combination of theoretical and experimental methods of approach, the depth, thoroughness and maturity of his treatment and the elegance of his presentation of results. I do not propose to discuss the various other studies and projects, both in the National Physical Laboratory and elsewhere, in which he has taken interest and guided or helped. Scientists in India know how freely he gives of his knowledge and time. I should not, however, fail to mention his intimate, active and uninterrupted association with the Department of Atomic Energy from its very beginning.

Believing as Krishnan does that science alone cannot solve all problems in life, he combines an earnest study of the classics of Indian religious literature with the study and practice of science, and endeavours to *live* a life of religious faith. The combination of *Vinaya* (humility) with *Vignyan* (critical understanding), which has become natural to him, makes it easy for people of all stations in life to feel at ease in his company.

It is not surprising that Krishnan is much sought after for giving addresses and discourses not only on scientific but also on literary and philosophical subjects. He has great respect for Indian scholars of Sanskrit and other Indian languages who have been brought up in the traditional Indian way. Being himself a writer of distinction on philosophic and scientific subjects in Tamil, Tamil and Sanskrit scholars all over India and in Ceylon find him congenial and stimulating company, and take delight in inviting and honouring him at their conferences and assemblies.

Krishnan has been the recipient of many honours both in India and abroad. He is a past President of the Indian Science Congress, of the National Academy of Sciences and of the National Institute of Sciences. He is a Founder-Member of the International Union of Crystallography. He has been Vice-President of the International Union of Pure and Applied Physics and of the International Council of Scientific Unions. Krishnan's quick grasp of essentials and the brevity and lucidity of his exposition make him a respected member in international scientific meetings and assemblies.

In 1955, the U.S. National Academy of Sciences invited Krishnan to be their chief guest at their annual meeting as the representative of Indian Science. This is an honour which had been previously given to the President of the Royal Society, London, the President of the Royal Netherlands Academy and the President of the Swedish Academy. At the ceremonial dinner of the Academy, Krishnan spoke on India's forward outlook on science and technology and also explained how that outlook was tempered by her own basic philosophy and sense of values. After the meeting, President Bronk wrote to Krishnan, " You did much to emphasize and strengthen the friendly bonds between scientists of your country and ours, and thus fostered the traditional international unity of science ".

Next year, in 1956, Krishnan was elected a Foreign Associate of the National Academy of Sciences. This is a high honour indeed as the total number of Foreign Associates today is only 60, of whom 9 are physicists. In the same year, at the request of the All India Radio, Krishnan gave in Delhi the second series of Sardar Vallabhbhai Patel Memorial Lectures, taking as his theme " The New Era in Science ".

The Government of India recently honoured Krishnan by appointing him a National Professor — an honour which he shares with Professor C. V. Raman and Professor S. N. Bose. The whole country wishes Krishnan many years of active happy life, searching, learning and teaching, in his own quiet and confident way.

K. R. RAMANATHAN

During the visit of Prince Philips

At an important CSIR meeting at NPL library

Sir K. S. Krishnan & the International Geophysical Year

PROFESSOR SYDNEY CHAPMAN

President, Special Committee for the International Geophysical Year, Brussels

IT is a pleasure to take part in the celebration of the sixtieth birthday of my distinguished friend and colleague Sir K. S. Krishnan, F.R.S., by contributing to this special volume. Such a volume on this occasion is a fitting tribute to the high distinction he has won as a scientist and administrator, and to the many services he has rendered to science and to his country and to the community of nations. His personal scientific researches have been recognized by the conferment upon him of many high honours. As a teacher he has fostered the scientific spirit and enthusiasm of his country's youth. As Director of a great scientific institution he has furthered the scientific and economic advance of India.

Here, however, I would specially write of his association with that remarkable world-wide scientific enterprise — the International Geophysical Year (IGY) 1957-58. Only his colleagues on the National IGY Committee for India can fully know the leadership and the support he has given, as President of that Committee, in developing India's IGY participation and programme. But the scope and excellence of that programme redounds to his credit, which he will be the first to wish to share with his many distinguished fellow officers and colleagues on the Committee, and with the still greater number of his countrymen and countrywomen who are taking a direct personal part in the programme.

Sir K. S. Krishnan has not only led and supported the plans for India's share in the IGY, he has also given it valuable support on the international level, in his capacity as Vice-President of the International Council of Scientific Unions (ICSU) for the past six years. This eminent position has given him a voice in the formation and progress of the Special Committee for the International Geophysical Year (CSAGI) — Comité Spécial de l'Année Géophysique Internationale — over which I have had the honour to preside. As a leading member of the Bureau of ICSU he has shared the executive responsibility resting on that Bureau for the multitudinous scientific affairs associated with ICSU; and not least as regards the IGY and the reports by CSAGI to ICSU, his scientific knowledge and experience have fitted him to give counsel solidly based.

To turn now to the IGY programme of India, it is good to record that India took part in every one of the fourteen divisions of the international programme. The Meteorological Department of India, as one of its many valuable contributions to the programme, received the notices of Alerts and Special World Intervals, and relayed them to All India Radio to be broadcast at specific times of the day. These broadcasts included a daily report on the sun's activity, received from the Kodaikanal Observatory. This observatory was an important member of the chain of solar stations that girdle the earth, whose regular programmes of observation were extended and intensified during the IGY — so that the sun was then observed with a degree of completeness and detail never before approached. The Nizamiah Observatory, Hyderabad, also contributed to this achievement, by its observations of solar flares.

The India Meteorological Department played an active role in its own most distinctive sphere, as a member of the World Meteorological Organization (WMO) in the execution of India's part in the meteorological IGY programme drawn up jointly by CSAGI and WMO. It gave valuable support also to the IGY auroral programme, by directing ten of its stations to watch regularly for the aurora at specific times. Its exploration of the atmosphere by balloons included, besides the usual meteorological elements, the measurement of the electrical potential gradient and electrical conductivity of the air.

In geomagnetism the same Department extended its normal observatory recording by the maintenance of additional stations at Trivandrum and Chidambaram, supplementing the permanent magnetic station at Kodaikanal, to study the equatorial electrojet. Projects related to the World Magnetic Survey that is to form a deferred part of the IGY were carried out by the Survey of India and the Hydrographic Department of the Indian Navy.

The IGY airglow programme of observation was advanced by observations at four stations, Mt Abu, Gulmarg, Dharwar and Poona. The cosmic ray neutron programme was executed at four stations, Ahmedabad, Kodaikanal, Gulmarg and Darjeeling, and there were cubical meson telescopes at five stations, and ionization chamber studies at Howrah. The Physical Research Laboratory at Ahmedabad (Director, Professor K. R. Ramanathan) took an active part in the airglow and cosmic ray programmes, and also in the WMO scheme of ozone studies — in which India employed no less than six Dobson spectrophotometers.

The many-sided IGY ionospheric programme was very actively undertaken in India, with eight observatories for vertical incidence recording. The pre-IGY measurements of ionospheric drift were extended by an additional station, making four in all. Absorption measurements were also made at four stations.

The Survey of India and the National Physical Laboratory co-operated in the programme of Latitudes and Longitudes, including the use of a Danjon impersonal astrolabe and a Markowitz moon camera.

Three glaciers, at Gangotri, Shigri and Machhoi were re-visited and studied after 57 years, by the Geological Survey of India.

The Survey of India extended its oceanographic activities, among other ways by increasing the number of its normal tide-gauge stations from fifteen to twenty-one. The India Meteorological Department made associated observations at each tide station.

India took part in the IGY satellite tracking programme by means of a Schmidt precision camera installed at the Uttar Pradesh State Observatory at Naini Tal; the camera was a gift from the Smithsonian Astrophysical Observatory at Harvard.

India co-operated also in the IGY programmes for seismology, earth tides, gravity measurement and nuclear radiation.

In this connection I would like to recall a fine passage of the Presidential Address of Sir K. S. Krishnan's friend and colleague, Professor K. R. Ramanathan, given at the opening Assembly of the International Union of Geodesy and Geophysics at Toronto, on 3 September 1957.

"The ICSU and the CSAGI have done a great job. The greatest single achievement of organized science in history was perhaps the building of the first atom bomb. It required the bringing together of many top-ranking scientists, technologists and organizers on an unprecedented scale. But they were top-ranking men, and of a few countries only. The IGY is in my view an undertaking of greater magnitude and difficulty, because it has involved the bringing together of workers of many nations with differing ideologies and in very varying stages of scientific development. A keen, diligent observer with modest education in any corner of the world has a respected place in the IGY scheme. The approach is human and earthy, and the potentialities for the unification of mankind are infinitely greater."

Among Dr Krishnan's many other achievements that will be recalled in this birthday celebration, the part he has played in this great enterprise of the IGY must not be forgotten.

KARIAMANIKKAM SRINIVASA KRISHNAN*

1898-1961

Foundation Fellow 1935

INDIA lost a distinguished physicist and philosopher in the death, after a third heart attack, of KARIAMANIKKAM SRINIVASA KRISHNAN. His contributions to science and his achievements especially in physics won international recognition for India.

Krishnan was born on 4 December 1898, in the village of Watrap, in the Tirunelveli (now Ramnad) District of Tamilnad (Madras State). His father was a Brahmin farmer-scholar of the old school, deeply versed in Tamil and Sanskrit religious literature, who spent a good part of his time in pilgrimages to South Indian temples, particularly to Srirangam and Tirupathi. From him Krishnan inherited an abiding love of religion and philosophy and a thorough knowledge of the Tamil language and literature, and of Sanskrit. His mother was very intelligent and an excellent organizer.

His early schooling was in the rural surroundings of his native village and at the Hindu High School at nearby Srivilliputtur. In a broadcast talk on All India Radio he once described the palm-leaf manuscript of which, in the first standard, two or three leaves were written every day until by the end of the year it had become a good-sized 'book' containing a vast amount of general information. It included, among other things, formulae for identifying the constellations in the night sky and mnemonics for determining time from the position of the constellation nearest to the zenith. This, he said, was not merely book knowledge but was accompanied by actual observations on the night sky. It was typical of Krishnan's encyclopaedic memory that late in life, when confronted with a question on astronomy, he was able to give a convincing answer from his recollection of the palm-leaf manuscript.

His subsequent education was partly in the American College, Madura, and then in the Christian College, Madras, where, after taking his degree in physics, he became a Demonstrator in Chemistry. He was meticulous in seeing that every fresh student knew exactly how to make observations and how to record the results of experiments. In later life he himself took much trouble to write both tersely and lucidly. At the request of some of the students he began an informal lunch-hour discussion to which they could bring any questions in physics, mathematics or chemistry. After a time so many students came from other Madras colleges that even the big gallery of the lecture room was full to overflowing. One of his students, who

*Reproduced from the *Biographical Memoirs of Fellows of the Royal Society*, Volume 13, 1967.

afterwards became Principal of Andhra University College, Waltair, has written: 'I learnt more physics in that half an hour in Krishnan's class than during the rest of the regular lectures, as his explanation of physical concepts was wonderfully lucid.' He was also much loved for his kindly and sympathetic manner.

In 1920 Krishnan went to Calcutta, attracted by the fame of the growing school of physics being developed by Professor C. V. Raman at the University College of Science. There he attended post-graduate classes, but showed such a keen interest in and aptitude for research in optics and molecular physics that Raman, realizing Krishnan's abilities, took him as a Research Associate in the Indian Association for the Cultivation of Science, 210 Bowbazar Street, where he at first lived with other young research workers in the dormitories. Here, it was said, he could hold his room-mates spell-bound with tales from the epics and of the ancient saints and philosophers. His day in the laboratory began at 6 a.m., often after an early walk and a cold bath. As he was a great football fan, many an evening would be spent with his colleagues watching a match in the Eden Gardens. He also used to take a very lively interest in political movements and personalities, and was a strong nationalist. At one time he thought it unbecoming to go abroad in search of Western learning and even took to writing his scientific papers in Tamil; but time mellowed him in this respect (although he always retained a spirit of sturdy independence of thought and action) and he grew to love Western literature. He was a voracious reader all his life and afterwards said (in the broadcast previously mentioned, published in the *Souvenir* in honour of his 60th birthday, 1958):

> 'Walter Scott, Dickens, Thackeray, Stevenson, Cervantes, Dumas and Victor Hugo and Conan Doyle linger in my memory as my favourite authors at this time, Plato and Aristotle in translations, Shakespeare, Milton and Shelley, Swift, Addison, Boswell, Newman, Mathew Arnold, Walter Pater and Charles Lamb at a later age and Tolstoy, Ibsen and Bernard Shaw still later. Some of them naturally stand out much more prominently than others in my memory. I should specially mention *Don Quixote*, *Pickwick Papers*, *Vanity Fair* and *Book of Snobs*, *Essays of Elia*, *Essay and Discourses* of Stuart Mill, some of the prose writings of Swift and Whitehead, *Alice in Wonderland* and *Through the Looking Glass*, most of which I have re-read later.
>
> 'Among the popular scientific books that made a great impression on me I should specially mention Tyndall's *Fragments*, *Microbe Hunters* by Paul de Kruif, *Men of Mathematics* by Eric Bell, *A Mathematician's Apology* by Hardy, and the biographies of Kelvin, Helmholtz, Lord Rayleigh, Maxwell and Tait.
>
> 'Among the serious scientific writings, the collected papers of Lord Rayleigh have been my constant companion for nearly 38 years and I can-

> not think of a better model for a research worker. One of the research papers of Einstein I have read off and on during the same period, and every time I read it I get something new out of it. Some of the papers of Niels Bohr had over me even more profound influence.'

All this he could take in his stride without the least interruption to the quality or quantity of his scientific work. Given the opportunity by Professor C. V. Raman, who was a source of great inspiration to all his students, Krishnan plunged deeply into an experimental study of the scattering of light in a large number of liquids, and its theoretical interpretation; he also began work on the magnetic anisotropy of gaseous molecules and of crystals (nitrates and carbonates). He collaborated with Raman in making a detailed examination of the changes in the frequency and polarization of light which was found to be associated with molecular scattering. These concentrated studies led to the discovery of the *Raman effect* in 1928.

In October 1928 Professor A. Sommerfeld visited Calcutta and gave a course of seven lectures on 'Modern developments in wave mechanics'. Krishnan took careful notes and undertook the task of preparing the lecture course for publication by Calcutta University as a book. In so doing he developed five of the lectures in an independent way and was commended by the visiting Professor for his originality and scholarship in supplying elegant mathematical proofs.

From 1929 to 1933 Krishnan served as a Reader in Physics at Dacca University where he found a very congenial atmosphere for teaching and research, with Professor S. N. Bose as Head of the Physics Department. Here he turned his attention to the subject of magnetic properties of crystals in relation to their structure, and developed elegant and precise experimental techniques to measure the magnetic anisotropy of dia- and paramagnetic crystals. He was able to correlate the anisotropy of crystals with the anisotropy and arrangement of the individual molecules or ionic groups. In suitable cases, from magne-crystallic measurements, the orientation of molecules in the unit cell could be determined. Krishnan and his students also developed methods for the accurate measurement of feeble susceptibilities and anisotropies. The papers he published during this period in collaboration with B. C. Guha, S. Banerjee and N. C. Chakravorty were the foundation stones of the modern fields of crystal magnetism and magneto-chemistry.

Krishnan was invited in 1933 to take up the post of Mahendralal Sircar Professor of Physics in the Indian Association for the Cultivation of Science, Calcutta. This infused in him a new enthusiasm and a fresh impetus. With Mookherji and Bose as co-workers, he continued vigorously the study of the magnetic properties of the salts of the rare earth and iron groups and integrated the results of measurements on the crystalline electric fields of crystals with the theoretical conclusions of Van Vleck, Penney and Schlapp. Many of his papers on magne-crystallic action were published in the *Philosophical*

Transactions of the Royal Society. At about the same time, Ganguli and Krishnan, in a classic paper in the *Proceedings of the Royal Society* (1941), established that the diamagnetism of graphite is very large indeed along the hexagonal axis and that certain of the electrons in such a crystal form a two-dimensional electron gas. Further, from the temperature-variation study, they concluded that the energy distribution of electrons in graphite obeyed Fermi-Dirac statistics.

The outstanding achievements of Krishnan could not remain unnoticed. He was invited by Lord Rutherford to the Cavendish Laboratory, Cambridge, and by Sir William Bragg to the Royal Institution, London, to give course of lectures in 1937. The Liège University Medal was awarded to Krishnan as a recognition of his scientific achievements.

Krishnan became the Professor of Physics in the University of Allahabad in 1942. Here he was concerned with teaching and research. In discussion with senior students, he reviewed in a systematic way various problems of the classical scattering of light, X-rays and electrons, of quantum theory, wave mechanics and statistical thermodynamics. Together with his students, he was able to carry out some important investigations in these subjects in spite of administrative duties and war-time difficulties.

Krishnan undertook a theoretical investigation in collaboration with A. B. Bhatia on the electrical conductivities of metals and alloys. He found that the scattering of electrons can be almost wholly attributed to local thermal fluctuations in density of the type studied by Smoluchowski and Einstein. This study could be easily extended to binary alloys also. In the case of alloys, the large increase in the resistivity due to alloying was shown to be due to fluctuations in the concentration of the alloying metal rather than to fluctuations in density. With this, a simple approach was found for discussing the electrical properties of metals and alloys as order-disorder phenomena.

Then came independence for India and its new leaders saw in Krishnan an outstanding senior scientist of international reputation. He was offered the Directorship of the National Physical Laboratory, New Delhi, which he accepted, though it meant sacrificing his natural desire for teaching. The post carried with it large administrative responsibilities. These did not deter Krishnan from continuing his activities in his chosen fields of research. With S. K. Roy, he analysed the differences between the characteristic frequencies which appear in dispersion formulae and published a series of papers in the *Proceedings of the Royal Society* and elsewhere which resolved certain doubts regarding the original formulae of Drude and Lorentz and gave many new and significant results.

At the National Physical Laboratory Krishnan also turned his attention to problems in the thermionics in collaboration with S. C. Jain. He suggested a new method of determining the saturation pressure of electrons by passing them through a small aperture in a wall of a uniformly-heated graphite chamber whose inside could be coated by any metal. This was a new

technique which avoided the need for degassing the surface of a metal and, at the same time, allowed the determination of the thermionic constants and their temperature coefficients. In particular, the data for the monovalent and transition metals present some interesting features inasmuch as the method is analogous to that of obtaining black-body radiation which is independent of the emissivity of the walls of the chamber.

He devoted both theoretical and experimental attention to the study of the distribution of temperature along a thin rod or wire which is electrically heated *in vacuo*. The temperature distribution was found to be parabolic near the centre, logarithmic a little farther away and approximately similar to that of an infinitely long filament near the ends. These studies have a practical application to modern industry in connexion with electrical technology.

The problem of temperature distribution along a heated tube was also solved by Krishnan and Sundaram. They calculated, in a straightforward way, the radiative transfer of energy in the hollow core of the tube. The expression they obtained bears a close similarity to that of the lattice conductivity of a dielectric cylinder at very low temperatures, in which the diffusion of the phonons is responsible for conduction and their free path is also determined, as in this case, by the diameter of the cylinder.

In the last few years of his life he gave much thought to obtaining an integrated picture of the problems of the solid state.

Krishnan loved mathematical reasoning and his skill as a mathematician would have gained him international recognition even without his great ability as an experimental physicist. He was deeply moved by a by-product of pure mathematical interest thrown up during the course of a physical investigation. At the same time, although a pure scientist himself, he strongly deprecated any division between pure and applied mathematics or science and when, in 1955, the U.S. National Academy of Sciences invited him to be the guest speaker at their Annual Dinner (a privilege that only the Presidents of the Royal Society, of the Royal Netherlands Academy and of the Swedish Academy had previously enjoyed) he seized the opportunity of extolling the purely cultural values of technological training and showed how India was trying to improve this aspect of her national life. Professor Van Vleck said afterwards of his speech: 'He quoted extensively from Whitehead and it was his speech that prompted me to read some of Whitehead's writings'.

Krishnan also believed firmly that international cooperation in science was one of the best ways of promoting understanding between nations and he was himself an ideal ambassador for India because his humility, simplicity and humour, combined with his scientific and cultural erudition and an all-too-rate fund of common sense won him friends all over the world. He never lacked an appropriate anecdote with which to drive home a moral or disarm a critic, or just to entertain. Nehru once remarked that he did not remember meeting Krishnan on any occasion when he had not told him

some new story. But Nehru also said of him on his sixtieth birthday: 'He is a great scientist, but something much more. He is a perfect citizen, a whole man with an integrated personality.'

Krishnan was the recipient of many honours both in India and abroad. He was elected a Fellow of the Royal Society, London, in 1940 and was knighted in 1946. He was associated with the work of many national and international scientific bodies: Chairman, Scientific Advisory Committee, UNESCO; Vice-President, International Council of Scientific Unions and of the International Union of Pure and Applied Physics; Chairman, Indian National Committee, URSI; Chairman, Indian National Committee for IGY and Chairman, Sub-Commission for Cooperation with UNESCO. He was, with P. P. Ewald, M. v. Laue and W. L. Bragg, a Founder-Member of the International Union of Crystallography, and afterwards a member of its Executive Committee. In 1956, Krishnan was elected a Foreign Associate of the U. S. National Academy of Sciences; in 1959 he was the guest speaker at the Geneva Convention of the International Telecommunications Union.

Dr. Krishnan had an active association with the work of many scientific organizations and establishments in India. He was President, Section of Physics, Indian Science Congress in 1940 and its General President in 1949. He was President also of the National Academy of Sciences and of the National Institute of Sciences. He was the Chairman, Board of Research in Nuclear Science; Member, Atomic Energy Commission, Board of Engineering Research, Standing Board of Astronomy and the University Grants Commission. He served the Council of Scientific and Industrial Research from its very inception in various capacities, as a member of the Governing Body and the Board of Scientific and Industrial Research, and on many of its Research Committees. As a member of the Editorial Board, he contributed significantly to the growth and progress of the *Journal of Scientific and Industrial Research*.

The title of Padma Bhushan was awarded to him by the President of India in 1954, and he was the first recipient of the Bhatnagar Memorial Award in March 1961. The Government of India honoured Krishnan by appointing him a National Professor—an honour which he shared with a very few great Indian scholars. But he did not live long to enjoy this honour. Just before he died he was planning to take the first long leave of a lifetime, to visit a son in England and a daughter in the U.S.A., whose little son he had never seen. He loved playing with his grandchildren at home.

He left behind him his wife, two sons and four daughters.

(The first draft of this notice was prepared by the late Dr. H. J. Bhabha, F.R.S., and was found amongst his papers late in 1966.)

KATHLEEN LONSDALE

H. J. BHABHA

BIBLIOGRAPHY

1925. On the molecular scattering of light in liquids. *Phil. Mag.*, **50**, 679-715.
1926. A discussion of the available data on light-scattering in fluids. *Proc. Indian Ass. Cultiv. Sci.*, **9**, 251-270.
1926. (With SIR C. V. RAMAN) On the diffraction of light by spherical obstacles. *Proc. phys. Soc. Lond.*, **38**, 350-353.
1926. Are gaseous molecules orientated in a magnetic field ? *Indian. J. Phys.*, **1**, 35-44.
1926. (With SIR C. V. RAMAN) The electrical polarity of molecules *Nature, Lond.*, **118**, 302.
1927. (With SIR C. V. RAMAN) Magnetic double-refraction in liquids I. Benzene and its derivatives. *Proc. R. Soc.*, A, **113**, 511-519.
1927. (With SIR C. V. RAMAN) Electric double-refraction in relation to the polarity and optical anisotropy of molecules I. Gases and vapours. *Phil. Mag.*, **3**, 713-723.
1927. (With SIR C. V. RAMAN) Electric double-refraction in relation to the polarity and optical anisotropy of molecules II. Liquids. *Phil. Mag.*, **3**, 724-735.
1927. (With SIR C. V. RAMAN) The diffraction of light by metallic screens. *Proc. R. Soc.*, A, **116**, 254-267.
1927. Magnetic double-refraction in paramagnetic gases. *Indian J. Phys.*, **1**, 245-254.
1927. (With SIR C. V. RAMAN) La constante de birefringence magnetique de benzene. *C. r. hebd. Séanc. Acad. Sci. colon.*, **184**, 449-451.
1927. (With SIR C. V. RAMAN) The magnetic anisotropy of crystalline nitrates and carbonates. *Proc. R. Soc.*, A, **115**, 549-554.
1927. (With SIR C. V. RAMAN) A theory of electric and magnetic birefringence in liquids. *Proc. R. Soc.*, A, **117**, 1-11.
1927. (With SIR C. V. RAMAN) The Maxwell effect in liquids. *Nature, Lond.*, **120**, 726-727.
1928. (With SIR C. V. RAMAN) A theory of light scattering in liquids. *Phil. Mag.*, **5**, 498-512.
1928. (With SIR C. V. RAMAN) A theory of the optical and electrical properties of liquids. *Proc. R. Soc.*, A, **117**, 589-599.
1928. (With SIR C. V. RAMAN) A theory of the birefringence induced by flow in liquids. *Phil. Mag.*, **5**, 769-783.
1928. (With SIR C. V. RAMAN) A new type of secondary radiation. *Nature, Lond.*, **121**, 501-502.
1928. (With SIR C. V. RAMAN) The optical analogue of the Compton effect. *Nature, Lond.*, **121**, 711.
1928. (With SIR C. V. RAMAN) A new class of spectra due to secondary radiation I. *Indian J. Phys.*, **2**, 399-419.
1928. (With SIR C. V. RAMAN) The negative absorption of radiation. *Nature, Lond.*, **122**, 12-13.
1928. (With SIR C. V. RAMAN) Polarization of scattered light-quanta. *Nature, Lond.*, **122**, 169.
1928. (With SIR C. V. RAMAN) Molecular spectra in the extreme infra-red. *Nature, Lond.*, **122**, 278.
1928. The Raman effect in crystals. *Nature, Lond.*, **122**, 477-478.
1928. Influence of temperature on the Raman effect. *Nature, Lond.*, 122, 650.
1928. (With SIR C. V. RAMAN) Rotation of molecules induced by light. *Nature, Lond.*, **122**, 882.
1928. The Raman effect in X-ray scattering. *Nature, Lond.*, **122**, 961-962.
1929. (With SIR C. V. RAMAN) The production of new radiations by light scattering I. *Proc. R. Soc.*, A, **122**, 23-35.
1929. (With S. RAMACHANDRA RAO) The anisotropy of the polarization field in liquids. *Indian J. Phys.*, **4**, 39-55.
1929. The Raman spectra of crystals. *Indian J. Phys.*, **4**, 131-138.
1929. The influence of molecular form and anisotropy on the refractivity and dielectric behaviour of liquids. *Proc. R. Soc.*, A, **126**, 155-164.
1930. Are black soap films birefringent ? *Indian J. Phys.*, **4**, 385-404.
1930. (With A. C. DASGUPTA) Pleochroism and crystal structure. *Nature, Lond.*, **126**, 12.
1931. Das magnetische verhalten von Ammoniummanganosulfat Hexahydrat bei niedrigen Temperaturen. *Z. Phys.*, **71**, 137-140.
1931. (With A. SARKAR) The dispersion of polarization of light scattering. *Indian J. Phys.*, **6**, 193-205.
1931. The magnetic anisotropy of ions of the type XO_3. *Phys. Rev.*, **38**, 833-834.
1932. Magnetic analysis of molecular orientations in crystals. *Nature, Lond.*, **130**, 313.
1932. Magnetic constants of benzene, naphthalene and anthracene molecules. *Nature, Lond.*, **130**, 698-699.
1933. (With B. C. GUHA & S. BANERJEE) Investigations on magne-crystallic action I. Diamagnetics. *Phil. Trans.*, A, **231**, 235-262.
1933. (With N. C. CHAKRAVORTY & S. BANERJEE) Investigations on magne-crystallic action II. Paramagnetics. *Phil. Trans.*, A, **232**, 99-115.
1933. (With S. M. MITRA) Negative polarization in fluorescence. *Nature, Lond.*, **131**, 204-205.
1933. (With S. BANERJEE) Feeble anisotropies in paramagnetic crystals. *Curr. Sci.*, **1**, 239-240.
1933. (With S. BANERJEE) Orientations of molecules in *p*-benzoquinone crystal. *Nature, Lond.*, **131**, 653-654.
1933. (With A. C. DASGUPTA) The pleochroism and the birefringence of the NO_3 ion in crystals. *Indian J. Phys.*, **8**, 49-66.
1933. (With B. MUKHOPADHYAY) Pleochroism and birefringence in crystals. *Nature, Lond.*, **132**, 411.

1933. (With S. Banerjee) Molecular orientations in *p*-diphenylbenzene crystal. *Nature, Lond.*, **132**, 968-969.
1933. The principal optical polarizabilities of the naphthalene molecule. *Indian J. Phys.*, **8**, 431-436.
1934. Magnetic anisotropy of graphite. *Nature, Lond.*, **133**, 174-175.
1934. Large artificial crystals of graphite. *Phys., Rev.*, **45**, 115.
1934. Crystal structure of 1, 3, 5-triphenylbenzene. *Nature, Lond.*, **133**, 497.
1934. (With A. C. Guha) Photo-dissociation of the NO_3 ion and its dependence on the polarization of the exciting light-quantum. *Curr. Sci.*, **2**, 476-477.
1934. (With P. K. Seshan) Absorption spectra in single crystals of Polynuclear hydrocarbons. *Curr. Sci.*, **3**, 26-27.
1934. (With A. C. Guha)- The absorption spectra of nitrates and nitrites in relation to their photo-dissociation. *Proc. Indian Acad. Sci.*, **1**, 242-249.
1934. (With P. K. Seshan.) Orientations of impurity molecules included in crystals. *Z. Kristallogr. Kristallgeom.*, **89**, 538-540.
1935. (With S. Banerjee) Investigations on magne-crystallic action III. Further studies on organic crystals. *Phil. Trans.*, A, **234**, 265-298.
1935. (With S. Banerjee) Stark splitting of the ^6S level of the manganous ion in crystalline fields. *Nature, Lond.*, **135**, 873.
1935. (With L. K. Narayanaswamy) The photo-dissociation of single crystals of potassium and sodium nitrates under polarized light. *Curr. Sci.*, **3**, 417.
1935. (With S. Banerjee) An othorhombic crystalline modification of 1.2; 5.6-dibenzanthracene. *Z. Kristallogr. Kristallgeom.*, A, **91**, 170-172.
1935. (With S. Banerjee) The magnetic anisotropy and crystal structure of 1.2; 5.6- dibenzanthracene. *Z. Kristallogr. Kristallgeom.* A, **91**, 173-180.
1935. (With S. Banerjee) The entropy of manganous ammonium sulphate hexahydrate at temperatures close to absolute zero in relation to magnetic anisotropy of the salt at room temperatures. *Proc. Indian Acad. Sci.*, A, **2**, 82-85.
1935. (With N. Ganguli) The influence of 'swelling' on the abnormal unidirectional diamagnetism of graphite crystals. *Curr. Sci.*, **3**, 472-473.
1935. (With S. Banerjee) A simple method for studying the magnetic susceptibilities of very small crystals. *Curr. Sci.*, **3**, 548.
1936. (With S. Banerjee) Investigations on magne-crystallic action IV. Magnetic behaviour of paramagnetic ions in the S-state in crystals. *Phil. Trans.*, A, **235**, 343-366.
1936. (With K. Lonsdale) Diamagnetic anisotropy of crystals in relation to their molecular structure. *Proc. R. Soc.*, A, **156**, 597-613.
1936. (With A. Mookherji) The magnetic anisotropy of copper sulphate pentahydrate, $CuSO_4.5H_2O$, in relation to its crystal structure. I. *Phys. Rev.*, **50**, 860-863.
1936. (With P. K. Seshan) On the fluorescence spectra of impurity molecules included in crystals. *Rapports sur la photoluminescence presentés a la réunion internationale de photoluminescence, Warsaw*, May, 289-299.
1937. (With N. Ganguli) Temperature variation of the abnormal unidirectional dia-magnetism of graphite crystals. *Nature, Lond.*, **139**, 155-156.
1937. (With A. Mookherji) The magnetic anisotropy of $Cs_3[CoCl_4]$. *Phys. Rev.*, **51**, 528.
1937. (With A. Mookherji) The magnetic anisotropy of four-coordinated Co^{++} ions in crystals. *Phys. Rev.*, **51**, 774.
1937. Magnetic and optical properties of crystals (Abstracts of three lectures given in the Cavendish Laboratory, Cambridge, April 1937). *Nature, Lond.*, **139**, 810.
1937. (With A. Mookherji) Magnetic anisotropy of rare earth sulphates and the asymmetry of their crystalline fields. *Nature, Lond.*, **140**, 549.
1937. (With A. Mookherji) Crystal structure and the magnetic anisotropy of $CuSO_4.5H_2O$. *Nature, Lond.*, **140**, 896-897.
1938. (With A. Bose) Coupling between the orbital and the spin angular momenta of paramagnetic ions from magnetic measurements. *Nature, Lond.*, **141**, 329.
1938. (With A. Mookherji) Investigations on magne-crystallic action V. Paramagnetic salts of the rare earth and the iron groups. *Phil. Trans.*, A, **237**, 135-159.
1938. (With D. C. Chakrabarty) The polarization of the absorption lines of single crystals of rare earth salts. *J. chem. Phys.*, **6**, 224-225.
1938. (With S. Banerjee) Magnetic studies on rhodochrosite, $MnCO_3$. *Z. Kristallogr. Kristallgeom.*, A, **99**, 499-508.
1938. (With A. Mookherji) The magnetic anisotropy of copper sulphate pentahydrate, $CuSO_4.5H_2O$, in relation to its crystal structure, II. *Phys. Rev.*, **54**, 533-539.
1938. (With A. Mookherji) The magnetic anisotropy of copper sulphate pentahydrate, $CuSO_4.5H_2O$, in relation to its crystal structure, III. *Phys. Rev.*, **54**, 841-845.
1938. (With S. Banerjee) Magnetic anisotropies and the valencies of paramagnetic atoms in crystals. *Nature, Lond.*, **142**, 717.
1938. (With P. K. Seshan) Directional variations in the absorption and the fluorescence of the chrysene molecule. *Proc. Indian Acad. Sci.*, A, **8** (Raman Number), 487-498.

1939. (With A. Mookherji & A. Bose) Investigations on magne-crystallic action VI. Further studies on paramagnetic crystals. *Phil. Trans.*, A, **238**, 125-148.
1939. (With S. Banerjee) The magnetic anisotropy of manganite crystal in relation to its structure. *Trans. Faraday Soc.*, **35**, 385-387.
1939. Jahn-Teller theorem and the arrangement of water molecules around paramagnetic ions in aqueous solutions. *Nature, Lond.*, **143**, 600.
1939. (With N. Ganguli) Temperature variation of the magnetic anisotropy of graphite. *Z. Kristallogr. Kristallogeom.*, A, **100**, 530-536.
1939. (With S. Banerjee) Magnetic studies on braunite, $3Mn_2O_3.MnSiO_3$. *Z. Kristallogr. Kristallogeom.*, A, **101**, 507-511.
1939 (With N. Ganguli) Large anisotropy of the electrical conductivity of graphite. *Nature, Lond.*, **144**, 667.
1939. The magneitc anisotropy of crystals I. Paramagnetic crystals II. Organic crystals. *Collection scientifique institut internationale de cooperation intellectuelle.* (Report of the meeting on 'Magnetism', arranged by the Institute of Strasbourg in May 1939.)
1940. The diamagnetism of the mobile electrons in aromatic molecules. Presidential Address to the physics section of the Indian Science Congress, Madras session.
1940. Landau diamagnetism and the Fermi-Dirac energy distribution of the metallic electrons in graphite. *Nature, Lond.*, **145**, 31-32.
1940. Electronic specific heat of graphite. *Nature, Lond.*, **145**, 388.
1940. (With S. L. Chorghade & T. S. Ananthapadmanabhan) Dimorphism of diphenyl octatetraene crystals. *Nature, Lond.*, **146**, 333.
1940. (With S. L. Chorghade & T. S. Ananthapadmanabhan) On an orthorhombic crystalline modification of diphenyl octatetraene. *Trans. Faraday Soc.*, **36**, 1153-1155.
1941. Magnetic and thermal properties of $CuSO_4.5H_2O$ at low temperatures. *Nature, Lond.*, **147**, 87-88.
1941. (With N. Ganguli) The magnetic and other properties of the free electrons in graphite. *Proc. R. Soc.*, A, **177**, 168-182.
1944. (With A. B. Bhatia) Investigations on the resistivities of binary alloys I. Order-disorder alloys of the CuZn type under equilibrium conditions. *Proc. natn. Acad. Sci. India*, A, **14**, 153-180.
1945. (With A. B. Bhatia) Electrical resistance of liquid metals. *Nature, Lond.*, **156**, 503
1948. (With A. B. Bhatia) Light scattering in homogeneous media regarded as reflection from appropriate thermal elastic waves. *Proc. R. Soc.*, A, **192**, 181-195.
1948. (With A. B. Bhatia) Diffuse scattering of the Fermi electrons in monovalent metals in relation to their electrical resistivities. *Proc. R. Soc.*, A, **194**, 185-205.
1948. A simple result in quadrature. *Nature, Lond.*, **162**, 215-216.
1948. On the equivalence of certain infinite series and the corresponding integrals. *J. Indian math. Soc.*, **12**, 79-88.
1950. Anharmonicity of the lattice oscillations in the alkali halide crystals, *Nature, Lond.*, **166**, 114, 571.
1951. (With Sanat Kumar Roy) The frequencies and the anharmonicities of the normal modes of oscillation of alkali halide crystals I. Lattice oscillations. *Proc. R. Soc.*, A, **207**, 447-460.
1951. (With Sanat Kumar Roy) Elastic constants of alkali halide crystals. *Nature, Lond.*, **168**, 869-870.
1951. (With Sanat Kumar Roy) The frequencies and the anharmonicities of the normal modes of oscillation of alkali halide crystals II. Low frequency acoustic modes. *Proc. R. Soc.*, A, **210**, 481-497.
1952. (With S. C. Jain) Thermionic constants of graphite. *Nature, Lond.*, **169**, 702-703.
1952. (With Sanat Kumar Roy) Polarization field and the acoustic modes of oscillation of alkali halide crystals. *Nature, Lond.*, **170**, 159.
1952. (With S. C. Jain) The thermionic constants of metals and semiconductors I. Graphite. *Proc. R. Soc.*, A, **213**, 143-157.
1952. (With Sanat Kumar Roy) Evjen's method of evaluating the Madelung constant. *Phys. Rev.*, **87**, 581-582.
1952. (With S. C. Jain) The thermionic constants of the iron group of metals. *Nature, Lond.*, **170**, 759.
1952. (With Sanat Kumar Roy) The dispersion formulae and the polarization fields. *Phil. Mag.*, **43**, 1000-1002.
1952. (With S. C. Jain) The thermionic constants of metals and semiconductors II. Metals of the first transition group. *Proc. R. Soc.*, A, **215**, 431-437.
1952. (With P. G. Klemens) The temperature variation of the thermo-dynamic potential of a degenerate electron gas. *Phil. Mag.*, **43**, 1224-1225.
1952. (With S. C. Jain) Thermionic constants of metals determined by a new method. Paper read at the URSI general assembly at Sydney.
1953. (With Sanat Kumar Roy) The polarization fields and the resonance frequencies of the alkali halide crystals. *Phil. Mag.*, **44**, 19-32.

1953. (With S. C. Jain) Thermionic constants of metals and semi-conductors III. Monovalent metals. *Proc. R. Soc.*, A, **217**, 451-461.
1954. (With S. C. Jain) Temperature distribution along a [illegible] electrically heated *in vacuo*. *Nature, Lond.*, **173**, 166.
1954. (With S. C. Jain) The distribution of temperature along a thin rod electrically heated *in vacuo* I. Theoretical. *Proc. R. Soc.*, A, **222**, 167-180.
1954. (With S. C. Jain) Temperature distribution in an electrically heated filament. *Nature, Lond.*, **173**, 820.
1954. (With S. C. Jain) The distribution of temperature along a thin rod electrically heated *in vacuo* II. Theoretical (continued). *Proc. R. Soc.*, A, **225**, 1-7.
1954. (With S. C. Jain) The distribution of temperature along a thin rod electrically heated *in vacuo* III. Experimental. *Proc. R. Soc.*, A, **225**, 7-18.
1954. (With S. C. Jain) The distribution of temperature along a thin rod electrically heated *in vacuo* IV. Many useful empirical formulae verified. *Proc. R. Soc.*, A, **225**, 19-32.
1954. (With S. C. Jain) Thermionic constants of metals and semi-conductors IV. Monovalent metals (continued). *Proc. R. Soc.*, A, **225**, 159-172.
1954. (With S. C. Jain) Determination of thermal conductivities at high temperatures. *Br. J. appl. Phy.*, **5**, 426-430.
1954. Thermionic properties of monovalent metals. Proc. of Commission VII, 11th General Assembly, URSI (The Hague), p. 136. (Titles of papers read).
1955. (With S. C. Jain) The distribution of temperature along a thin rod electrically heated *in vacuo*. V. Time lag. *Proc. R. Soc.*, A, **227**, 141-154.
1955 (With S. C. Jain) The distribution of tempeature along a thin rod electrically heated *in vacuo*. VI. End-losses. *Proc. R. Soc.*, A, **229**, 439-445.
1955. (With Sanat Kumar Roy) The polarization field in an ionic crystal and its influence on the reststrahlen frequency. Read at the Symposium on the Physics of the Solid State, held during the Silver Jubilee Session of the National Academy of Sciences at the University of Lucknow, 27 December. *Proc. natn. Acad. Sci. India*, A, **25**, 50-57.
1956. (With S. C. Jain) Thermionic constants of semiconductors. *Nature, Lond.*, **177**, 285.
1956. (With S. K. Roy) The Drude dispersion formula shown to be applicable to any medium irrespective of the polarization field. *Phil. Mag.*, **1**, 926-933.
1956. The new era of science. (Sardar Vallabbhai Patel lectures.) The Publication Division, Government of India.
1960. (With R. Sundaram) Radiative transfer of energy in the core of a heated tube. *Nature, Lond.*, **188**, 483-484.
1960. (With R. Sundaram) The distribution of temperature along electrically heated tubes and coils I. Theoretical. *Proc. R. Soc.*, A, **257**, 302-315.
1960. Effect of specular reflections on the radiation flux from a heated tube. *Nature, Lond.*, **187**, 135.
1960. Some aspects of the scientific background to telecommunications. (Address as guest speaker at the International Telecommunication Banquet, Geneva, November 1959). *Telecommun. J. Geneva*, No. 8.
1961. (With S. C. Jain) Qu[illegible]g of cation vacancies in doped crystals of sodium chloride. *Nature, Lond.*, **191**, 162-163.

LXXV. *On the Molecular Scattering of Light in Liquids.*

By K. S. Krishnan *.

1. *Introduction.*

THE theory of molecular scattering of light in liquid media has been worked out recently by Raman †, Ramanathan ‡, Gans §, and others. Their results in general indicate that in a medium consisting of anisotropic molecules, there is, in addition to the polarized scattering due to density fluctuations, a scattering due to the optical anisotropy of the molecules of the liquid. The total intensity of the light scattered in a direction perpendicular to the direction of the incident light is given by the formula

$$I = \left\{ \frac{\pi^2 RT\beta}{18N\lambda^4}(n^2-1)^2(n^2+2)^2 \right\} \times \frac{6(1+r)}{6-7r}, \quad . \quad (1)$$

where I is the fraction of the incident light scattered transversely, per unit volume, per unit solid angle,
n is the refractive index of the medium,
λ is the wave-length of the incident light,
T is the absolute temperature,
R and N are the gas const. and Avogadro number respectively per gm. molec.,
β is the isothermal compressibility, and
r is the observed depolarization of the transversely scattered light.

The expression inside the double brackets, which can easily be recognized as the Einstein-Smoluchowski formula, gives the density scattering, and $\frac{6(1+r)}{6-7r}$ is the multiplying factor to be applied to that expression in order to take into account the anisotropy of the molecules. The theory of Raman and Ramanathan connects r with the optical anisotropy of the molecules in the gaseous condition, while that of Gans connects it with the observed value of electric double refraction (Kerr constant) of the liquid

The experimental results so far available regarding the

* Communicated by Prof. C. V. Raman, F.R.S.
† Raman, 'Molecular Diffraction of Light,' Calcutta, 1922; Raman & Ramanathan, * Phil. Mag. xlv. p. 213 (1923); Raman & Rao, Phil. Mag. xlv. p. 625 (1923).
‡ Proc. Ind. Assn. Cultn. Sc. viii. pp. 1–22 & 181–198 (1923).
§ *Zeits. f. Phys.* xvii. p. 353 (1923).

intensity and depolarization of the light scattered by liquids are meagre, only about 15 liquids having been studied by Martin and Lehrman * and Raman and Rao †. It was therefore felt that a more comprehensive experimental work was desirable, especially in order to determine more clearly the influence of the molecular constitution of the liquid. This paper describes a series of such measurements on the intensity, and the depolarization for different regions of the spectrum, of light scattered by about 65 liquids, with a general discussion of the results.

2. *Experimental Details.*

In drawing up the list of liquids to be examined, care was taken that most of the important groups might be fairly represented. The liquids were all Kahlbaum's pure chemicals except ortho- and para-xylenes, which were Merck's extra-pure, and benzyl alcohol which was obtained from a local firm. The liquids were directly transferred from the freshly opened bottles to the cleaned and dried bulbs in which they were to be examined (which were essentially of the same pattern as those used by Martin and later investigators); the bulbs were then exhausted and sealed. But no special precautions were taken in order to dry the liquids, since extreme drying was not considered necessary ‡.

The liquids were then obtained dust-free in one of the bulbs by repeated slow distillations and washing back to the other bulb. The liquids were tested for absence of dust particles by placing the bulb, immersed in water, at the focus of a powerful lens concentrating the rays reflected from the sun and looking against the transmitted light at a slight angle, when any dust particles floating in the liquid were brilliantly illuminated and could easily be detected.

In general, 4 or 5 distillations were sufficient to get the liquid perfectly dust-free, but in the case of methyl acetate, acetaldehyde, and some of the chlorides and bromides a larger number of distillations was necessary. In this respect water showed such a strong tendency to carry over dust particles in the process of distillation that the following special arrangements had to be made. A double bulb of the same pattern as in the other liquids but of pyrex glass, with the transverse connecting tube specially long and narrow,

* Journ. Phys. Chemistry, xxvi. p. 75 (1922).
† Phil. Mag. xlv. p. 625 (1923).
‡ In the case of benzene it was found that extreme drying in contact with phosphorus pentoxide for several months had very little effect on either the polarization or the intensity of the scattered light.

contained the liquid, which had originally been distilled over alkaline permanganate. The liquid was also distilled extremely slowly by keeping the bulbs at the room temperature and temperature of ice respectively. In spite of these precautions, the distillation had to be repeated more than a dozen times in order to get the water dust-free. After distillation the bulb had been allowed to stand for more than three months, and when examined later it was surprising to find that it contained such a large number of particles that it had to be redistilled before the experiment.

The bulbs were put away in suitable light-tight shelves, specially made for the purpose, so as to avoid continual exposure to the action of light.

The measurements were carried on inside a dark room into which a horizontal beam of sunlight was reflected by means of a heliostat of the single mirror type, through a small opening in the door. For observations on the imperfection of polarization of the transversely scattered light, the beam was concentrated by a lens of 20 cm. focal length whose aperture was limited to a small square portion at the centre, the actual size of the aperture varying, within certain limits, according to the intensity of the light scattered by the liquid, the object being to work with the smallest intensity consistent with the requisite amount necessary for accurate comparison. The largest aperture used (and that was while working with feebly scattering liquids like water and the alcohols or with coloured filters) was 2 cm. sq., while in other cases it was less, the usual size being 1·4 cm. sq.

The bulb containing the distilled liquid was blackened completely, excepting for three small windows—one for the entrance of light, one for its exit, and the third for observation. It was immersed in a small rectangular tank of distilled water (whose outside was also blackened, leaving similar openings), so as to minimize reflexion from the sides of the bulb. The position of the bulb was adjusted so that the rays might pass axially through the bulb, with the focus at its centre. This was tested by noting the position of the transmitted beam on the wall at the farthest end of the room. Even in extreme cases the maximum deviation of the rays from the axis of the track, as judged by the size of the same projection, was not more than 2° or 3°.

Just at the focus the track in the liquid was found to be practically parallel, and a small length of the track at this portion, limited by a sharp, clean cut rectangular aperture in a thin metal plate attached to the observation side of the tank, was chosen for observation. The imperfection of

polarization of the transversely scattered light was measured by the usual method due to Cornu, with the help of a double-image prism and nicol mounted on a stand so as to be capable of independent rotation about the same axis. The two images of the track were brought in a line so as *just* to touch each other. The axis of the prism-nicol combination was now adjusted so as to be exactly perpendicular to the axis of the track in the bulb, the two images appearing in the centre of the field of view. Any slight inaccuracy in this adjustment would not of course, as Rayleigh has pointed out, appreciably affect the result. Particular care was taken to cover up the passage of the scattered light from the observation window to the prism-nicol combination with a black cloth, so as to avoid any extraneous illumination of the field of view. The background was quite satisfactory.

Any slight discontinuity in width at the line of contact of the two images, when they had been brought in a line, which might arise if the aperture limiting the length of the track were not exactly in front of the focus, was remedied by slightly moving either the condensing lens or the aperture. Otherwise serious error might creep in, since the eye would compare only the portions of either image immediately adjoining the line of separation. In order further to guard against this error, the observations were always repeated with the double-image prism turned over 180°, and thus with the position of the strong and weak images interchanged. But in general there was not any appreciable difference between the two sets of readings. For each position of the prism two sets of readings were taken, rotating the nicol in its mount between the two sets so as to get the readings on different parts of the scale. For each position of equality two readings were taken approaching from either side. In order to minimize the action of light, if any, on the liquid, the light was kept on only for just the time necessary for taking observations.

In connexion with the remarks above on the discontinuity in width of the two images at the line of contact, it might be supposed that it would be an advantage to use a narrow parallel beam for the incident light instead of the convergent beam. However, owing to the converging action of the spherical bulb of liquid the actual track inside the bulb would cease to be parallel. An incident divergent beam is also out of the question, since the actual divergence ought to be capable of continual variation in order that on entering the various liquids the tracks inside might be parallel. Of course, all this trouble can be avoided if we use the same

liquid for the tank as is contained inside the bulb, but this is also not quite practicable when working with a large number of liquids.

In the case of a number of liquids, the imperfection of polarization was measured also for different parts of the spectrum, using for the purpose coloured filters. Where any difference was detected between the values for different portions of the spectrum the liquid was tested for fluorescence, by the method used by Ramanathan *, by transferring the coloured filters from the path of the incident beam to that of the scattered beam and testing whether the value for the imperfection was altered.

For measurements of the relative intensities of the scattered light a telescope objective of about 140 cm. focal length was used to concentrate the rays. The objective was limited, as before, by an aperture 1·4 cm. sq.; the beam emerging out of the telescope was very nearly parallel, and the central portion of this concentrated beam was allowed to pass through another aperture 4 mm. sq. before passing through the bulb. The bulb was immersed as in depolarization measurements in a tank, the liquid used in general in the tank being distilled water. But for liquids having a high refractive index, *i. e.* above 1·5, in order to avoid errors arising from the magnification of the track in the bulb due to its sphericity, a mixture of benzene and carbon disulphide having nearly the same refractive index as the liquid inside the bulb was used.

A block of homogeneous, colourless Jena glass, 2 cm. thick, was chosen as a secondary standard, its scattering being of the same order of magnitude as in most of the liquids and forming a perfect colour match with the same. The glass block, which was completely blackened, excepting for the usual three windows, was placed in the bath in front of the bulb to be compared and closely touching it, the beam of light passing transversely through the place of contact. Two small similar portions of the tracks on either side were selected for comparison, by using two rectangular apertures in a line, with a short opaque portion between them, which served to cut out the light diffused at the surface of contact. The diffusion was unavoidable, so that the two portions of the track compared had to be separated by a few mm. (4 mm.); and due to this separation the comparison was by no means as accurate as in the case of polarization measurements. The comparison was made with the help of an

* *Loc. cit.*

Abney rotating sector photometer. The secondary standard was finally compared with a freshly prepared bulb of ethyl ether

3. *Results.*

In Table I. are given the results of the measurements on the imperfection of polarization of the scattered light with white light and also with coloured filters interposed in the path of the incident and scattered light. The ratio of the weaker component, having its vibrations parallel to the incident beam, to the stronger component having its vibrations perpendicular to the same, is expressed as a percentage. In general, only blue and orange filters were used and occasionally green. Even though red would have been preferable to orange, being at the end of the spectrum, the latter was used owing to the much larger intensity of the light transmitted.

TABLE I.

Depolarization of the Light transversely scattered by the Liquids at 30° C.

White incident light.

Substance.	Weak component / Strong component ×100	Substance.	Weak component / Strong component ×100.
PARAFFINS AND UNSATURATED FATTY HYDROCARBONS.		CHLORIDES.	
Pentane	7·8	Propyl chloride	16·3
Isopentane	5·6	Isopropyl chloride	16·2
Hexane	9·9	Isobutyl chloride	16·5
Heptane	10·0	Allyl chloride	36
Octane	12·9	Methylene chloride (Dichlormethane)	31
β-isoamylene (Trimethyl Ethylene)	25·8	Ethylene chloride	36
BROMIDES.		Chloroform (Trichlormethane)	24·2
Ethyl bromide	25·0	Carbon tetrachloride (Tetrachlormethane)	6·1
Propyl bromide	25·0	Silicon tetrachloride	5·8
Isobutyl bromide	26·4		
Allyl bromide	59		
Ethylene bromide	61		

TABLE I. (*continued*).

Substance.	Weak component / Strong component ×100. White light.	Orange filter in the path of: incident light.	Orange filter in the path of: scattered light.	Green filter in the path of: incident light.	Green filter in the path of: scattered light.	Blue filter in the path of: incident light.	Blue filter in the path of: scattered light.
SULPHUR COMPOUNDS.							
Carbon bisulphide	69	68·5	70	...	...	71	73
Methyl sulphide	12·9						
Ethyl sulphide	18·2						
FATTY ACIDS.							
Formic acid	5·,						
Acetic acid	47	47	47	..	...	48	48
Propionic acid	41	41	42	42	41·5	49	47
Butyric acid	40	36	39	41·5	44	68	55
OXIDES (ANHYDRIDES).							
Acetic anhydride	43						
Propionic anhydride	44						
Ethyl ether	9·1	8·0	9·3	8·3	8·9	10·9	8·8
BENZENE AND ITS DERIVATIVES.							
Benzene	47	47	47	48	48	50	51
Toluene (Methyl benzene)	52·5	52·5	52	55 (?)	51	57·5	59
Ethyl benzene	53	54	53	53	55	53	59
Ortho-xylene	40	40	38	...	...	42	41
Meta-xylene	57	56	60	...	...	64	61
Para-xylene	66	66	67	..	...	67	68
Benzyl chloride	58	56	61	...	...	73	54
Benzal chloride	55	52	55	...	...	71	53
Chlorobenzene	58	57·5	58	61 (?)	61 (?)	56	55
Bromobenzene	65						
Nitrobenzene	74						
Aniline	60						
Ortho-nitrotoluene	82						
Meta-nitrotoluene	83						

TABLE I. (*continued*).

$$\frac{\text{Weak component}}{\text{Strong component}} \times 100.$$

Substance.	White light.	Orange filter in the path of		Green filter in the path of		Blue filter in the path of	
		incident light.	scattered light.	incident light.	scattered light.	incident light.	scattered light.
ALCOHOLS.							
Methyl alcohol	8·2	6·0	8·0	...	...	12·6	7·4
Ethyl alcohol	6·8	5·3	7·1	...	...	10·5	6·8
Propyl alcohol	7·6	7·1	9·9	...	...	11·0	7·2
Isopropyl alcohol	7·2	5·0	6·7	...	...	10·7	7·2
Butyl alcohol	11·5	9·3	11·0	...	...	14·9	11·0
Isobutyl alcohol	11·2	7·3	11·8	...	...	16·3	9·0
Tertiary butyl alcohol (Trimethyl carbinol) ...	6·2	4·1	5·8	...	...	9·2	5·6
Amyl alcohol (inactive) .	11·9	9·8	12·5	...	..	27·9	10·8
Allyl alcohol	29·3	29·6	29·4	34	31	38	37
Benzyl alcohol	65	62	63	...	...	67	66
ESTERS.							
Methyl formate	28·1						
Ethyl formate	22·1	21·3	21·6	...	...	20·7	19·6
Propyl formate	21·0	21·0	21·1	18·1	20·4	18·6	17·7
Ethyl acetate	23·3						
Propyl acetate	21·7						
ACETALDEHYDE AND KETONES.							
Acetaldehyde	20·0	18·9	19·4	...	...	21·6	19·0
Dimethyl ketone	23·6						
Methyl ethyl ketone ...	17·4	16·6	18·1	...	...	25·5	18·2
Diethyl ketone	36	18·0	36	...	...	78	24·9
Methyl propyl ketone ...	19·6						
Water	9·6	8·5	11·8	7·9	9·5	14·5	9·9

The orange filter, as tested by a direct-vision spectroscope, transmitted the region of the spectrum from greenish yellow to red; the green filter transmitted, in addition to green, a little blue and a small region at the extreme red; the blue filter, while transmitting mostly blue and violet, allowed to a more or less extent almost the whole visible region to pass. Thus the light transmitted by the filters extended over large regions. However, since the observations were all visual and the purpose was to test in a general way the influence of the frequency of the incident vibrations on the depolarization, homogeneity was not considered necessary.

In Table II. the observed intensities with white incident light are given in terms of the light scattered by ethyl ether. Ether was chosen for comparison since its intensity is of the proper magnitude and the liquid is easily got pure and is not acted on by light. The figures in the table give the actual values obtained by experiment, no correction having been made either for absorption or for reflexion at the various surfaces. For the small distances involved, the absorption, even when not wholly accounted for by scattering, would be quite negligible. As for the reflexions, in the case of the track in the liquid, 2 water-glass and 2 glass-liquid surfaces had to be taken into account more than in the case of the track in glass, and since the incidences were normal, a little calculation shows that, even in extreme cases, the loss would not be appreciable.

In the case of nitro-benzene and nitro-toluene, which were coloured greenish yellow, a filter of about the same colour was used in the path of the incident light.

4. *Discussion of Results.*

(i.) *Feeble fluorescence and its influence on the polarization of the scattered light.*

In some of the liquids given above, the imperfection is affected by transferring the coloured filter from the path of the incident beam to that of the scattered beam. This may be considered as a very feeble kind of fluorescence. To see how this would influence the polarization, let us, for example, consider the case where the blue region of the spectrum excites a fluorescence which lies mainly in the green. With the blue filter in the path of the incident beam, the scattered light would be mixed up with the fluorescent light, and if we assume, as we may reasonably, that the fluorescent light is mostly unpolarized, the light observed would show an abnormal imperfection of polarization. On transferring the

TABLE II.—Intensity of the transversely scattered Light.

Substance.	r.	n_D.	$\beta \times 10^6$ per atm.	Intensity at 30° C. (Ether = 1). Calculated.	Observed.	Values obtained by other investigators.	Remarks.
Pentane	·078	1·353	235	1·12	1·14		
Isopentane	·056	1·352	238	1·06	1·06		
Hexane	·099	1·374	169	0·99	1·00	1·13 at 18°C. (M.L.)	
Heptane	·100	1·387	142	0·92	1·00		
Octane	·129	1·396	128	0·94	0·96		
β-isoamylene	·258	1·381	199	1·78	1·54		
Ethyl bromide	·250	1·423	144	1·71	1·58		
Allyl bromide	...	...	...	..	3·10		
Ethylene bromide	...	.	...	...	3·42		
n-Propyl chloride	...	. .	...	...	1·34	.. ...	Background not satisfactory owing to white deposit on the sides of the bulb.
Isopropyl chloride	...	...	...	...	1·38		
Allyl chloride	...	...	...	.	1·47		
Methylene chloride	...	...	...	...	1·24		
Ethylene chloride	·36	1·445	87	1·60	1·44		
Chloroform	·242	1·446	110	1·50	1·26		
Carbon tetrachloride	·061	1·462	114	1·14	1·02		
Silicon tetrachloride	...	...	...	...	1·13		
Carbon bisulphide	·685	1·642	101	21·3	13·0	18·6 (R.R.) 12·8 (M.L.)	
Methyl sulphide	...	...	..	...	1·22		
Ethyl sulphide	...	...	...	...	1·33		
Formic acid	...	...	...	...	1·22		
Acetic acid	·47	1·373	98·5	1·50	1·19		
Propionic acid	...	...	...	...	1·24		
Butyric acid	...	..	...	...	1·19		
Acetic anhydride	...	...	...	...	1·01	.....	Liquid left over after distillation distinctly coloured, indicating decomposition.
Propionic anhydride	...	...	...	...	1·41		

Ethyl ether	·080	1·352	212	1·00	1·00		
Benzene	·47	1·507	103	3·90	3·15	3·64 (R.R.) 2·82 (M.L.)	
Toluene	·525	1·501	97	4·28	3·53	3·45 (R.R.) 3·21 (M.L.)	
Ethyl benzene	·53	1·502	92	4·17	3·18		
Meta-xylene	·57	1·502	91	4·82	3·87		Calculated values not quite reliable since a small error in r makes a large difference. Aniline not quite free from dust particles. Ortho-nitrotoluene contains a number of dust particles and its intensity was calculated for 14° C. from the values of n and $\frac{\partial n}{\partial p}$.
Para-xylene	·66	1·501	94	7·61	4·61		
Benzyl chloride	† ...	...	...	...	3·50		
Benzal chloride	† ...	...	...	...	3·21		
Chlorobenzene	·58	1·531	80	5·27	4·10	4·11 (M.L.)	
Bromobenzene	·65	1·568	72	8·21	4·92		
Nitrobenzene	·74	$n_D = 1·548$	53	10·0	10·5		
Aniline	·60	1·599	48	5·18	3·42	.....	
Ortho-nitrotoluene	·82	..	...	·29	9·40		
Meta-nitrotoluene	...	...	...	...	9·80		
Methyl alcohol	·060	1·329	131	0·49	0·78	·58 (R.R.) ·54 (M.L.)	Liquid left over after distillation is coloured dark brown.
Ethyl alcohol	·053	1·363	121	0·59	0·58	·72 (R.R.) ·56 (M.L.)	† A yellow filter was used in the path of the incident light in working with Benzyl and Benzal chlorides.
n-Propyl alcohol	·071	1·385	105	0·63	0·62	0·73 (M.L.)	
Isopropyl alcohol	·050	1·380	112	0·62	0·60		
n-Butyl alcohol	·093	1·400	97	0·68	0·65		
Isobutyl alcohol	·073	1·397	105	0·69	0·74	0·79 (M.L.)	
Trimethyl carbinol	·041	1·388	120	0·69	0·69		
Amyl alcohol (inactive)	·098	1·408	110	0·82	0·74	0·84 (M.L.)	
Allyl alcohol	·296	1·419	100	1·29	1·22		
Benzyl alcohol	·62	1·547	60	5·20	2·93		
Methyl formate	...	...	...	...	1·09	.....	Not quite dust-free.
Ethyl formate	..	...	...	...	1·00		
Propyl formate	·210	1·379	120	0·94	0·94		
Ethyl acetate	·233	1·372	125	0·98	0·98		
Propyl acetate	...	...	...	...	0·95		
Acetaldehyde	...	...	...	...	0·89		
Dimethyl ketone	·236	1·358	130	0·92	0·81	.....	Show a tendency to decomposition.
Methyl ethyl ketone	..	...	...	...	0·80	.....	
Diethyl ketone	·18	1·392	110	0·88	1·06	.....	
Water	·085	1·336	45	0·19	0·21	0·19 (M.L.) 0·19 (R.R.)	

R.R.—Raman and Rao, *loc. cit.* M.L.—Martin and Lehrman, *loc. cit.*

blue filter to the path of the scattered beam, however, the imperfection would become normal. If, instead of a blue filter, we use a green filter, normal polarization would be observed when the filter is in the path of the incident beam, and an abnormally high polarization when in the path of the scattered beam.

Of the liquids investigated, water, ether. all the monohydric alcohols, benzyl and benzal chlorides, methyl ethyl ketone, diethyl ketone, and to a slight extent butyric acid and acetaldehyde, exhibit a feeble fluorescence. From a comparison of the values for the two positions of the filter it is evident that in all the cases mentioned above, the exciting region is at the blue end of the spectrum. the excited region coming much lower down, including to an appreciable extent the orange.

Now, since the orange is in the excited region far removed from the exciting region, on the longer wave-length side, we may safely assume that the value for the ratio of the components obtained with orange incident light is the normal value, there being no question of fluorescence here. Comparing with this value the value with the blue filter in the path of scattered light, we find the latter is generally the higher, leading to either of the following two conclusions:— (1) The exciting region extends higher up the spectrum than the blue, say to the v , so that a part of the fluorescent light due to the violet is in the blue, of course without prejudice to the exciting power of blue itself. (2) The normal value of the depolarization for blue light is itself greater than the value for orange. The latter seems to be more probable.

It must be pointed out here that the above liquids are not fluorescent to anything like the same extent as what are usually known as fluorescent substances. Except in the case of a few liquids, practically no difference of colour was noticeable between the two images of the track while using blue incident light, which shows that the amount of light fluoresced is only a small fraction of the scattered light; and when we remember that the scattered light per unit volume is of the order of 10^{-4} to 10^{-5} of the incident light, we can have an idea of the magnitude of the effect. In fact, it is theoretically possible to calculate the ratio of the intensity of the fluoresced light in a direction transverse to the incident beam to the light scattered in the same direction, *provided we assume that fluorescence is entirely independent of scattering and is a superposed phenomenon.* Thus, taking for example the case

of ether, the ratio $= \frac{2\theta}{108{\cdot}8}$, where $\frac{8{\cdot}8+\theta}{100+\theta} = \frac{10{\cdot}9}{100}$, *i. e.* 4 per cent. In the case of methyl alcohol it is about 10 per cent., while with amyl alcohol it is about 40 per cent., and with benzal chloride as high as 80 per cent.

It is significant that, among the liquids examined, those which show this type of fluorescence have a certain family relationship: thus the list includes water and all the monohydric alcohols which have the OH radicle in common, acetaldehyde and the two ketones which have the CO radicle in common, and the fatty acids having the COOH radicle, and benzyl and benzal chlorides. They are also, in general, liquids whose molecules are known to be polar.

(ii.) *Influence of wave-length.*

Coming next to the question of the effect of wave-length on the depolarization, we have already pointed out that among the fluorescent substances, the normal value for the blue might be greater than the normal value for the orange; and this seems to be particularly true of butyric and propionic acids. Among the non-fluorescent liquids, allyl alcohol, and to a less marked extent benzene, toluene, ethyl benzene, and benzyl alcohol seem to show a similar increase as we proceed from orange to blue.

(iii.) *Relation between depolarization and chemical constitution.*

We may take for consideration the values obtained with orange incident light in the case of liquids which have been examined with coloured filters, and with white light in other cases. Of course, for a proper discussion of the relation between the optical anisotropy of the molecule and its constitution, we must proceed on data for the gaseous state. However, there are certain prominent features which might well be pointed out here.

One principal point that strikes us at the outset is that optical anisotropy does not always go hand in hand with the asymmetry of shape of the molecule. For example, the long chain compounds of the paraffin series show much smaller imperfection of polarization than the ring compound benzene. But within the same series of compounds, increased symmetry causes more perfect polarization. This is well illustrated by the normal and iso-compounds of the paraffin series, by the three isomerides of butyl alcohol, and by the three chlorine substitution products of methane, CH_2Cl_2, $CHCl_3$, and CCl_4. The last case is of particular interest, as with the accepted

structure of the compound with tetrahedral symmetry, we might expect the scattered light to be completely polarized. The actual value obtained (6·1 per cent.), though much smaller than the earlier value of Raman and Rao, is still too large to be attributed to experimental error. In the case of $SiCl_4$ the ratio is of the same order, namely 5·8 per cent.*

In a strictly homologous series of paraffins and alcohols, the depolarization generally increases as we go up the series, while, in the fatty acids, anhydrides and esters, the value decreases. The effect of the unsaturation of carbon on the anisotropy of the molecule is quite marked, the value for the unsaturated compounds being much higher than that for the corresponding saturated compounds, as is clear from Table III. given below.

TABLE III.

Unsaturated.	r (per cent.).	Saturated.	r (per cent.).
β-iso amylene	25·8	Isopentane	5·6
Allyl bromide	59	Propyl bromide ...	25·0
Allyl chloride	36	Propyl chloride ..	16·3
Allyl alcohol	[illegible]	Propyl alcohol	7·1

When we come to the aromatic compounds, the most striking feature is the very large value for the depolarization characteristic of all of them, the value in certain cases approaching the limit ($\frac{6}{7}$=86 per cent.), showing that the "density scattering" in these cases is small in comparison with "orientation scattering." The values for the three isomeric xylenes may be pointed out here as illustrating the marked influence of the relative positions of the side chains on the anisotropy of the molecule.

(iv.) *Intensity of the scattered light.*

In column 5 of Table II. are given the intensities of the transversely scattered light calculated from the Einstein-Smoluchowski formula, with the correction factor for imperfect polarization already mentioned (equation (1)), and in

* A redetermination of the ratio for CCl_4 vapour has been recently made in this laboratory by Mr. A. S. Ganesan, who has obtained the value 1·8 per cent. A similar determination for SiCl vapour and for CH_4 would be of interest.

column 6 the observed intensities. Both are expressed as ratios referred to transverse scattering by ethyl ether as unit. Columns 2, 3, and 4 give the values of r, n, and β respectively used in the calculation. For reasons given at length by Ramanathan in an addendum to a recent paper *, the refractive indices (n) of the liquids for the F line have been adopted for calculation. They were taken from Landolt-Börnstein Tables (1923) and reduced to the temperature of the experiment, viz. 30° C., by using the Lorentz-Mosotti formula and the known constants of thermal expansion. In a few cases where direct experimental data for the refractive index were not available, the values have been calculated from the atomic refractivities.

The most reliable data we have regarding the isothermal compressibilities of liquids for *30° C. and 1 atm. press.* are those of Tyrer †. He has experimentally determined the adiabatic compressibilities at different temperatures, for the range 1–2 atm., and from thence calculated the isothermal compressibilities. However, the other investigators, excepting Gay ‡, have determined the isothermal compressibilities directly, and since, as has been pointed out by Tyrer, it is extremely difficult to eliminate the heat of compression while working with small ranges of pressure changes, the direct measurements by the majority of investigators at low pressures give values somewhere between the isothermal and adiabatic compressibilities. Naturally the values obtained by the different investigators do not agree among themselves.

The values of Tyrer have been adopted wherever available, in other cases the values of other investigators (taken from 'Piezochemie' by Cohen and Schut) have been used, the closeness of the agreement between their values and those of Tyrer, where they are both available, being used as a criterion for choosing from among them. In this respect the values obtained by Röntgen § (1–8 atms. and at 3° C.–6° C. and about 18° C.), when extrapolated to 30° C., agree best with Tyrer's. In some liquids which have been investigated only at high pressures the values for 1 atm. had to be extrapolated from the scanty data at higher pressures.

Before preceeding to compare the calculated and observed values of the intensity, there is one other point regarding the calculation, pointed out to the writer by Prof. Raman, which

* Phys. Rev. xxi. p. 564 (1923).
† Journ. Chem. Soc. London, cv. p. 2534 (1914).
‡ *Comptes Rendus*, clvi. p. 1979 (1913).
§ *Wied. Ann.* xliv. p. 1 (1891).

must be mentioned here. The original expression obtained by Einstein for the fraction of the incident light scattered transversely per unit volume per unit solid angle was

$$I_1 = \frac{2\pi^2 RT}{N\lambda^4} \cdot \frac{n^2\left(\frac{\partial n}{\partial p}\right)^2}{\beta} . \quad . \quad . \quad . \quad . \quad (2)$$

Now $\frac{\partial n}{\partial p}$ has been measured directly by experiment for some liquids by Röntgen and Zehnder * and recently by Himstedt and Wertheimer †, and Eisele ‡, and might be used in the calculation. But since the number of liquids for which such data are available is small, the value of $\frac{\partial n}{\partial p}$ given by the Lorentz-Mosotti relation has been used in all cases for the sake of uniformity, thus getting the Einstein formula in the usual form.

$$I_2 = \frac{\pi^2 RT\beta}{18N\lambda^4}(n^2-1)^2(n^2+2)^2. \quad . \quad . \quad . \quad (3)$$

However, we can get a general idea of the error involved in such a substitution by seeing how nearly $\frac{I_1}{I_2}$ for the F line and 30° C. is equal to unity. No direct data are available for calculating $\frac{\partial n}{\partial p}$ and thence $\frac{I_1}{I_2}$ *for the* F *line and 30° C.* But a calculation of the values of the ratio $\frac{I_1}{I_2}$ for different wave-lengths from the experimental values of $\frac{\partial n}{\partial p}$ obtained by Himstedt and Wertheimer and Eisele, and for different temperatures from the values obtained by Röntgen and Zehnder, shows that the variation of $\frac{I_1}{I_2}$, if any, with wave-length or temperature is very small. We may therefore take those values (given in column 3 of Table IV.) as applying equally well for the F line and 30° C. Column 4 of the same table gives those values relative to ether, and they are obviously the correction factors to be applied on this account to the calculated values of the intensity relative to ether in column 5 of Table II.

* *Wied. Ann.* xliv. p. 22 (1891).
† *Ann. der Phys.* lxvii. p. 395 (1922).
‡ *Ann. der Phys.* lxxvi. p. 396 (1925).

TABLE IV.

	Liquid.	I_1/I_2 for the liquid.	$\frac{I_1/I_2 \text{ for the liquid.}}{I_1/I_2 \text{ for ether.}}$
1.	Water	·79	·91
2.	Hexane	·97 (?)	1·12
3.	Chloroform	·90	1·04
4.	Carbon bisulphide	·80$_5$	·93
5.	Benzene	·80$_5$	·93
6.	Toluene.....	·80	·92
7.	Ethyl benzene	·73	·84
8.	Chlorobenzene	·82	·95
9.	Bromobenzene	·75	·87
10.	Nitrobenzene	·81	·94
11.	Methyl alcohol	·89	1·03
12.	Ethyl alcohol	·87	1·01
13.	Propyl alcohol.....	·87	1·01
14.	Isopropyl alcohol	·89	1·03
15.	Butyl alcohol	·89	1·03
16.	Isobutyl alcohol	·90	1·04
17.	Benzyl alcohol.....	·63	73
18.	Dimethyl ketone	·85	·98
19.	Ethyl ether	·86$_5$	1·00

Thus, even though the absolute values of the intensity calculated by the two methods, viz. eqns. (2) and (3), widely disagree, the correction factors for the values relative to ether except in the case of liquids with high ref. index, water and hexane are very nearly equal to unity.

Now, coming to the actual comparison of the observed and calculated values of the intensity of the transversely scattered light, we find that in a large number of liquids the agreement is all that could be desired, especially when we consider the experimental imperfections and the uncertainties in the values of β used in the calculation. In a few of the other liquids the discrepancy might probably be explained away. Thus in the case of β-isoamylene and ethyl bromide the difference might be neglected. And with acetic acid it might be due to the presence of water, since it shows a strong tendency to adsorb it and, as already mentioned, no special precautions were taken to dry the liquids. However, data for calculating the values for the other fatty acids and

anhydrides might help us in settling this point. Diethyl ketone is so strongly fluorescent that the track with white light shows a distinct greenish tinge. Hence the larger observed value might be due to the contribution from fluorescence, since white incident light was used for intensity measurements. Dimethyl ketone is probably fluorescent like the other two ketones examined, in which case, the white light value for r used in the calculation would certainly be too high, and that would explain the higher calculated value. Further, the ketones show a strong tendency to decomposition.

With ethylene chloride, chloroform, and carbon tetrachloride the observed values are definitely smaller than the calculated values, and they might be classed along with the liquids to be mentioned below. But the discrepancy in these cases is not sufficiently large to justify any conclusion based on them.

Thus even in the above liquids, we cannot say definitely that there is disagreement with theory.

However, we are still left with CS_2 and all the aromatic compounds (even nitrobenzene is probably no exception) where, as a rule, the observed values in terms of ether as a standard are much smaller than the calculated values, even taking into account the correction already mentioned for the value of $\frac{\partial n}{\partial p}$ used in the calculation. Here the theoretical expressions for the intensity seem definitely to break down.

5. *Summary.*

1. The paper describes measurements of the intensity and the imperfection of polarization for different regions of the spectrum, of the light scattered transversely by 65 different dust-free liquids, mostly carbon compounds.

2. It is found that some of the liquids are feebly fluorescent, the blue end of the spectrum, in general, exciting fluorescence, the fluorescent light being in the less refrangible region. An estimate is made of the magnitude of this effect.

3. In some of the liquids there seems to be a genuine dependence on wave-length of the depolarization; the imperfection of polarization increases as the wave-length diminishes.

4. Some prominent features of the relation between the depolarization and chemical constitution are pointed out.

5. The theoretical formula for the intensity is found to

fail in the case of high refractive index liquids (which are also, in general, liquids which show a high depolarization).

In conclusion, the writer has great pleasure in expressing his indebtedness to Prof. C. V. Raman for his kind interest in the work. The experiments were for the most part carried out in the spring and summer of 1924, in the Physical Laboratory of the Indian Association for the Cultivation of Science.

210 Bowbazaar Street,
Calcutta, India.
April 16, 1925.

LXXVI. *Note to "Refraction and Electron Constraint in Ions and Molecules"*.* *By* CHARLES P. SMYTH, *Department of Chemistry, Princeton University, Princeton, N.J., U.S.A.*†

A METHOD similar to that which I have employed for calculating the refractions of electron groups was proposed by K. Fajans and C. A. Knorr in a communication to the Bunsengesellschaft ‡, which had escaped my attention. Two months after the correction and dispatch of the proof, but before the actual publication of my paper, "Refraction and Electron Constraint in Ions and Molecules," I was enabled by Professor Fajans to examine the manuscript of an unpublished dissertation by Dr. Knorr, in which this method was applied and a large number of results obtained identical with those appearing in my paper. Although the work of Professor Fajans and Dr. Knorr, which will be published shortly, does not cover precisely the same ground as that covered by my paper and although differences in the details of interpretation are apparent, their work, done quite independently, may be regarded as agreeing substantially with mine.

Munich, Germany.
July 30, 1925.

* Phil. Mag. August 1925, p. 361.
† Communicated by the Author.
‡ *Chem. Zeit.* xlviii. p. 403 (1924).

4

A Discussion of the Available Data on Light-scattering in Fluids.

By

K. S. Krishnan, Research Scholar in the Indian Association for the Cultivation of Science.

I. Different Theories of Scattering

In a recent paper on light scattering, M. Y. Rocard [1] has made a comparison of the theories of Ramanathan, King and Gans. For a medium consisting of anisotropic molecules oriented at random, Ramanathan [2] gets for the ratio of the weak component to the strong in the transversely scattered light, when the incident light is unpolarised, the expression

$$r=\frac{6\delta}{\frac{5RT\beta n}{N}\left(\frac{\nu^2+2}{3}\right)^2+7\delta} \qquad \ldots (1)$$

where

$$\delta=\frac{A^2+B^2+C^2-AB-BC-CA}{(A+B+C)^2}$$

A, B, C being the optical moments induced in a molecule when placed in a field of unit intensity parallel respectively to its three principal anisotropic axes;

R and N are the gas constant and Avogadro number respectively per gram molecule,

[1] *Comptes Rendus*, Aug. 3rd, 1925.

[2] Proc. Ind. Assn. Cultn. Sc., viii, pp. 1-22 & 181-198 (1923).

T is the absolute temperature,

β in the isothermal compressibility,

n is the number of molecules per unit volume, and

ν is the refractive index of the medium.

For the total fraction of the incident unpolarised light, scattered transversely per unit volume, per unit solid angle, he gets

$$I=\frac{\pi^2RT\beta}{18N\lambda^4}(\nu^2-1)^2(\nu^2+2)^2\cdot\frac{6(1+r)}{6-7r} \qquad \ldots (2)$$

For isotropic molecules it obviously reduces to the Einstein-Smoluchowski expression.

King's theory,[1] which is also molecular, leads on the other hand to the values [2]

$$r=\frac{6\delta}{\frac{5RT\beta n}{N}+7\delta} \qquad \ldots (3)$$

and

$$I=\frac{\pi^2RT\beta}{2N\lambda^4}(\nu^2-1)^2\frac{6(1+r)}{6-7r} \qquad \ldots (4)$$

Gans,[3] on the other hand, from purely thermodynamical considerations, has obtained an expression for r in terms of the Kerr constant (Electric double refraction) of the medium:

$$r=\frac{48\pi\nu\lambda B}{\frac{1}{3}\beta(\nu^2-1)(\nu^2+2)(k-1)(k+2)+56\pi\nu\lambda B} \qquad \ldots (5)$$

[1] Nature, cxi, p. 667 (1923).

[2] King really uses the adiabatic compressibility. However, for the purpose of our present discussion, we shall use the isothermal.

[3] *Zeits. f. Physik*, xvii, p. 353 (1923).

where k is the dielectric constant and B is the Kerr constant, as usually defined

$$\left(i.e., = \frac{\nu_2 - \nu_1}{\lambda E^2} \right).$$

According to Langevin's theory of the Kerr effect, for non-polar molecules, which is the case contemplated by Gans's theory,

$$B^1 = \frac{(\nu^2-1)(\nu^2+2)}{4\nu\lambda}\left(\frac{k+2}{3}\right)^2 \frac{\Theta}{\frac{A+B+C}{3}} \qquad \ldots (6)$$

where

$$\Theta = \frac{1}{45}\frac{N}{RT}\left\{(A-B)(A'-B')+(B-C)(B'-C')+(C-A)(C'-A')\right\}.$$

A′, B′, C′ are the constants of electrical anisotropy corresponding to the optical constants A, B, C.

The above expression for the Kerr constant, assumes that the principal axes of electrical and optical anisotropy coincide. Now let us make some simplifying assumptions, analogous to those made by Gans in his discussion, regarding the relation between the constants of electrical and optical anisotropy. Thus, let us suppose that

$$\frac{A'}{A} = \frac{B'}{B} = \frac{C'}{C}.$$

Then the above ratio

$$= \frac{A'+B'+C'}{A+B+C}$$

$$= \frac{\frac{k-1}{k+2}}{\frac{\nu^2-1}{\nu^2+2}};$$

[1] Langevin's actual expression for B [*Le Radium*, vii, p. 249 (1910)] refers to the simple case when the anisotropic molecule has an axis of symmetry. The expression given here is a generalisation of Langevin's, taken from Debye, Marx's "*Handbuch der Radiologie*," Bd. VI, p. 768.

and the expression for the Kerr constant reduces to

$$B = \frac{(k-1)(k+2)(\nu^2-1)(\nu^2+2)N}{120\pi RTn\lambda\nu}\delta \qquad \ldots (7)$$

Substituting this value in (5) we have

$$r_{\text{Gans}} = \frac{6\delta}{\frac{5RT\beta n}{N}+7\delta}, \qquad \ldots (8)$$

which is identical with (3).

For I, Gans's theory leads to the same expression as Ramanathan's (Expn. 2).

Thus we find that for r, King and Gans get identical values which are, however, different from Ramanathan's, while for I, Ramanathan's expression is the same as Gans's, but different from that of King. It is needless to point out that, in the case of vapours and gases sufficiently rare that ν^2 is very nearly equal to unity, the different expressions agree.

Recently, measurements have been made in this laboratory, on the scattering constants of a number of vapours and liquids; and it is proposed in the present paper to ascertain how far the different theories fit in with the experimental facts—leaving alone, for the present, all considerations regarding the theoretical merits of the different hypotheses underlying the above theories.

II. Intensity of the Scattered Light

Table I gives the values of I for a number of liquids, *relative to ethyl ether*, calculated by the two formulæ [(2) and (4)], along with the observed values for comparison.

TABLE I

Liquid	r	Authority	r adopted	I CALCULATED ETHER=1		I OBSERVED. Ether=1	Authority
				Ramanathan-Gans	King		
Pentane	·072	M. L	·075	1·11	1·11	1·14	K
	·078	K					
Isopentane ...	·056	K	...	1·06	1·06	1·06	K
Hexane	·100	M. L	·100	0·99	0·96	1·13	M. L
	·099	K				1·00	K
Heptane	·127	M. L(2)	·114	0·95	0·90	1·00	K
	·100	K					
Octane	·129	K	...	0·94	0·89	0·96	K
β-isoamylene ...	·258	K	...	1·78	1·71	1·54	K
Ethyl bromide ...	·250	K	...	1·71	1·55	1·58	K
Ethylene chloride ...	·36	K	...	1·60	1·40	1·44	K
Chloroform [1] ...	·238	G	·240	1·49	1·31	1·26	K
	·242	K					
	·150	R R.	·150	1·21	1·06		
	·150	M(2)					
Carbon tetrachloride ...	·045	G	·053	1·12	0·96	1·02	K
	·061	K					
Carbon bisulphide ...	·64	G	...	16·4	10·9	12·8	M.L
	·685	K	...	21·3	14·1	13·0	K
Acetic acid ...	·439	G	·455	1·43	1·39	1·19	K
	·47	K					
Benzene ...	·47	K	...	3·90	3·13	2·82	M.L
						3·64	R. R
						3·2	R
						3·15	K

[1] It is surprising that the two sets of values for r for cloroform agreeing perfectly among themselves, should however differ so widely from each other.

TABLE I (*contd.*)

Liquid	r	Authority	r adopted	I CALCULATED ETHER=1		I OBSERVED. Ether=1	Authority
				Ramanathan-Gans	King		
Toluene	·490	M. L	·51	4·06	3·29	3·21	M. L
	·507	G				3·45	R. R
	·525	K				3·53	K
Ethyl benzene ...	·53	K	...	4·17	3·37	3·18	K
Meta Xylene ...	·57	K	...	4·82	3·90	3·87	K
Para Xylene ...	·583	G		5·22	4·23	4·61	K
Chlorobenzene ...	·58	K		5·27	4·09	4·11	M.L
						4·10	K
Bromobenzene ...	·618	G	·635	7·59	5·59	4·92	K
	·65	K					
Nitrobenzene ...	·74	K		10·0	7·6	10·5	K
Aniline	·60	K		5·10	3·59	3·42	K
O-nitro-toluene ...	·82	K		29	22	9·40	K
Methyl alcohol ...	·060	K		0·49	0·51	0·54	M.L.
						0·58	R.R.
Ethyl alcohol ...	·053	K		0·59	0·58	0·56	M,L.
						0·72	R.R.
						0·58	K
n-Propyl alcohol ...	·071	K		0·63	0·60	0·73	M.L
						0·62	K
Isopropyl alcohol ...	·050	K		0·62	0·59	0·60	K
n-Butyl alcohol ...	·093	K		0·68	0·64	0·65	K
Isobutyl alcohol ...	·073	K		0·69	0·65	0·79	M.L
						0·74	K
Trimethyl carbinol ...	·041	K		0·69	0·66	0·69	K
Amylic alcohol (inactive)	·098	K		0·82	0·76	0·84	M.L
						0·74	K

TABLE I (*contd.*)

Liquids	r	Authority	r adopted	I CALCULATED ETHER = 1		I OBSERVED. Ether = 1	Authority
				Ramanathan-Gans	King		
Allyl alcohol ...	·296	K		1·29	1·18	1·22	K
Benzyl alcohol ...	·62	K		5·20	3·95	2·93	K
Propyl formate ...	·210	K		0·94	0·91	0·94	K
Ethyl acetate ...	·228	M(1)	·230	0·97	0·95	0·98	K
	·233	K					
Dimethyl ketone ...	·170	G	·20	0·85	0·84	0·81	K
	·236	K					
Diethyl ketone ...	·18	K		0·88	0·84	1·06	K
Water	·085	K		0·19	0·19	0·19	M.L
						0·19	R.R
						0·21	K

Authorities —

M (1)—Martin, Journ. Phys. Chemistry, xxiv, p. 478 (1920).
M L—Martin and Lehrman, *ibid*, xxvi, p. 75 (1922).
R R—Raman and Rao, Phil. Mag., xlv, p. 625 (1923).
R—Ramanathan, Phys. Rev., xxi, p. 564 (1923).
M L (2)—Martin and Lehrman, Journ. Phys. Chemistry, xxvii, p. 558 (1923).
M (2)—Martin, *ibid*, xxviii, p. 1284 (1924)
G—R. Gans, *Zeits. f. Phys.* xxx, p. 231 (1924).
K—K. S. Krishnan, Phil. Mag. l, p. 697 (1925).

From the Table we can easily see that in the case of liquids with refractive indices of the same order of magnitude as in ether, the agreement of the values calculated by either formula with the observed values is quite satisfactory; and, as we should expect, there is not much to choose between the two. But in the case of highly refractive liquids (which have also, in general, a large value for r), while King's formula continues to be valid, the other formula gives values for I consistently higher than the observed values.

Of course for a fair comparison of the two expressions for I, one should take into consideration the absolute values. But here, owing to the extreme smallness of I (of the order of 10^{-6}) the uncertainties in the measurements are naturally much greater and the results obtained by different investigators support either theory indifferently. Thus Martin and Leherman,[1] using some intermediary standards, have compared the intensity of the light scattered by liquid ether with that of the incident light and they get for the mercury line 4358 A°. $I = 9{\cdot}2 \times 10^{-6}$ agreeing perfectly with the value $8{\cdot}85 \times 10^{-6}$, given by King's formula, as against $14{\cdot}6 \times 10^{-4}$, given the formula of Ramanathan and Gans.

On the other hand, Raman and Rao,[2] in determining the Avogadro constant from the absolute scattering by distilled water, get values for I which seem to support Ramanathan-Gans formula. Further, we have the measurements of Raman[3] on the intensity of water in terms of ether vapour, of Ramanathan[4] on saturated ether vapour at different temperatures and also of ether above the critical temperature, in terms of liquid ether, and those of Raman and Ramanathan[5] on carbon dioxide, both liquid and vapour at high pressures, in terms of carbon dioxide at N. T. P., which fit in with Ramanathan-Gans formula.[6]

In view of the above conflicting results, it would be extremely interesting to redetermine the absolute intensity for some liquid, say ether. In spite of the experimental difficulties it ought to be possible at least to decide between the

[1] *Loc. cit.*
[2] *Loc. cit.*
[3] Proc. Roy. Soc A, ci, p. 64 (1922).
[4] *Ibid*, cii, p. 151 (1922)
[5] Proc. Roy. Soc. A, civ, p. 357 (1923)
[6] We have no reason to doubt the validity of the theoretical expressions for vapours, especially after the recent measurements on atmospheric transparency, the experiments of Lord Rayleigh on the transparency of gases [Proc. Roy. Soc. A, xcv, p. 155 (1918)] and the work of Cabannes (*Journ. de Physique*, Series VI, Tome 1, p. 129 (1920) and Daure (*Comptes Rendus*, June 29th, 1925) on the determination of the Avogadro number from gaseous scattering. Hence all the intensity measurements relative to vapours, referred to in the paper, may be considered absolute.

two expressions, since one gives a value for ether about 1·6 times that given by the other. The author proposes to take up the work shortly.

III. Depolarisation of the Scattered Light

In Table II are given the values of δ (which may be taken as an expression for the anisotropy of the medium), calculated from r by (1) and (3), as also the values of δ calculated from the Kerr constant B by (7). Since most of the available data for B refer to the D line, all the calculations have been made for that wave-length. We confine ourselves to the case of non-polar molecules.

Table II

Liquid	r	$\delta \times 10^3$ calculated from r		$B \times 10^7$ * for D line at 20°C	Authority †	$\delta \times 10^3$ calculated from B.
		Ramanathan	King-Gans			
Pentane ...	·075	5·0	3·1	·050	L	3·1
Isopentane ...	·056	3·7	2·3	·050	Ka.	3·1
Hexane	·109	4·5	2·7	·045	S	2·7
				·056	L	3·4
Heptane	·114	4·0	2·3	·071	S	2·7
				·105	L	4·0
Octane	·129	3·8	2·2	·077	S	2·6
				·136	L	4·5

* Where the values given by the investigators are relative to CS_2, they have been converted to absolute values, using Chaumont's value for CS_2—$B = 3·226 \times 10^{-7}$ for the D line and 20°C.

† *Authorities:*—

S—Schmidt, *Ann. der Phys.*, vii, p. 142 (1902).
L—Leiser—quoted by Bergholm, *Ann. der Phys.*, liv, p. 511 (1917).
Mc—McComb, Phys. Rev., xxix, p. 525 (1909).
C—Chaumont, *Ann. de Physique*, IX series, iv, p. 61 (1915).
B—Becker, *Ann. der Phys.*, lxxvi, p. 849 (1925).
Ka—Taken from "*Beziehungen Zwischen physikalischen Eigenschaften und chemischer Konstitution*" by H. Kauffmann, Stuttgart.....1920, p. 387.

Table II (*contd.*)

Liquid	r	$\delta \times 10^3$ calculated from r		$B \times 10$ for D line at 20°C	Authority	$\delta \times 10^3$ calculated from B.
		Ramanathan	King-Gans			
Carbon tetrachloride ...	·053	2·4	1·2	·074	Ka	2·6
Carbon bisulphide ...	·685	255	106	3·226	C	84
	·64	189	79			
Benzene	·47	45	22	·593	Mc	18·5
Meta-xylene ...	·57	48	24	·858	B	17·5
Para-xylene ...	·583	52	26	·74	S	19
				·73	L	

When we remember the large variations in the Kerr constant data obtained by different investigators, and the sensitiveness of δ to small variations in r and B, the agreement, in general, between the Kerr constant values of δ and the scattering values of δ, should be considered satisfactory. Here again, in the case of highly refractive liquids, King-Gans expression seems to give better agreement than Ramanathan's.

IV. Anisotropy calculated from Liquid and Vapour States.

The agreement between the values of the anisotropy calculated from r and from B for liquids, raises the question how far these values represent the real anisotropy of the individual molecules, as contemplated by the molecular theories. Of course in the vapour state, where the molecules are sufficiently far apart to exert any mutual influence, we may reasonably suppose that the theoretical formula gives the real anisotropy of the molecules. The values of δ calculated from the liquid and vapour states are given in Table III for comparison.

TABLE III

Substance	ρ liquid	δ × 10³ calculated from ρ liquid: Rama-nathan	δ × 10³ calculated from ρ liquid: King-Gans	ρ vapour	Autho-rity	ρ vapour adopted	δ × 10³ calcula-ted from ρ vapour
	·075	5·0	3·1	·012	R	·012	10·1
				·012	C. G		
Pentane				·028	R. R	·027	23
				·025	V.		
Isopentane	·056	3·7	2·3	·012	C. G		10·1
Hexane	·100	4·5	2·7	·015	C. G		12·7
				·021	Rn		18
Heptane	·114	4·0	2·3	·031	Gn		27
Octane	·129	3·8	2·2	·027	Gn		23
β-isoamylene ...	·258	20	12·1	·061	Gn		55
Ethyl bromide ...	·250	22	12·4	·032	Rn		28
Chloroform ...	·240	15·7	8·4	·030	R		
	·150	8·6	4·6	·032	Gn	·031	27
Carbon tetrachloride ...	·053	2·4	1·2	·019	Gn		16
Carbon bisulphide ...	·685	255	106	·120	R		
	·64	189	79	·167	Gn	·143	143
				·143	Rn		
Ethyl ether	·080	5·3	3·2	·032	Gn	·031	27
				·030	Rn		
Benzene	·47	45	22	·068	R.R		
				·066	Gn	·067	61
				·067	Rn		
Toluene	·51	43	22	·064	Gn		58
m-Xylene	·57	48	24	·067	Gn		61
Chlorobenzene ...	·58	55	27	·078	Gn		72

TABLE III (*contd.*)

Substance	ρ liquid	δ × 10³ calculated from ρ liqnid: Rama-nathan	δ × 10³ calculated from ρ liqnid: King-Gans	ρ vapour	Autho-rity	ρ vapour adopted	δ × 10³ calcula-ted from ρ vapour
Bromobenzene ...	·635	69	31	·078	Gn		72
Nitrobenzene ...	·74	115	53	·056	Rn		50
Aniline	·60	46	20	·049	Rn		43
Methyl alcohol ...	·060	6·2	3·9	·027	Gn		23
Ethyl alcohol ...	·053	3·6	2·2	·017	Gn		14·5
n-Propyl alcohol ...	·071	3·5	2·1	·020	Gn		17
Iso-propyl alcohol ...	·050	2·5	1·5	·019	Gn		16
n-Butyl alcohol ...	·093	3·6	2·1	·020	Gn		17
Isobutyl alcohol ...	·073	3·0	1·7	·019	Gn		16
Allyl alcohol ...	·296	23	12·7	·052	Gn		46
Propyl formate ...	·210	9·7	5·7	·035	Gn		30
Ethyl acetate ...	·230	12·4	7·4	·034	Gn		29·5
Dimethyl Ketone ...	·200	14·1	8·6	·048	Gn		42

Authorities :—

R—Lord Rayleigh, Proc. Roy. Soc., A, xcv, p. 155 (1918).
V—R. Venkateswaran, Trans. Chem. Soc., cxxi, p. 2655 (1922).
R. R.—Raman and Rao, Phil. Mag., xlvi, p. 426 (1923).
Gn—A. S. Ganesan, Phil. Mag., xlix, p. 1216 (1925).
C.G.—Cabannes and Gauzit, *Journ. de Physique et le Radium*, Series VI, Tome vi, p. 182 (1925).
Rn—K. R. Ramanathan—unpublished.

One can easily see that, even though in the case of high depolarisation liquids like benzene, its derivatives, carbon bisulphide, etc., the anisotropies calculated from the liquid and vapour states are more or less the same, in other cases the "effective anisotropy" in the liquid state is much smaller

than the anisotropy in the vapour state. Probably it is due to *temporary* molecular groupings, of the kind suggested by Raman,[1] having a higher degree of optical symmetry than the individual molecules. This change in "effective anisotropy" in the liquid state can be explained in a general way. Taking for example a long molecule like pentane, when there is a close packing of the molecules, as in the liquid state, the influence on any atom in the molecule, of the atoms in the neighbouring molecules might compare favourably with the influence of the atoms in the same molecule; and this might conduce to a greater optical symmetry of the molecule. But in the case of a molecule like benzene, where the influence of the atoms in the same molecule is already large, the contributions from the atoms of the neighbouring molecules might be small in comparison, in which case, the influence of close packing on the anisotropy would also be small.

It would have been interesting to confirm from Kerr constant data this change in the "effective anisotropy" as we pass from the vapour to the liquid. But we have not sufficient data for B for vapours. However, we have seen how δ from ^{r} liquid agrees satisfactorily with δ from ^{B} liquid, and there is no reason why δ from ^{r} vapour should not agree with δ from ^{B} vapour.[2]

[1] Nature cxi, p. 428 (1923).

[2] For CO_2, $r = \cdot 107$ [mean of the values ·117 of Rayleigh, ·106 of Raman and Rao and ·098 of Cabannes and Granier] gives

$$\delta = \cdot 102;$$

while Szivessy's value [*Zeits. f. Physik*, xxvi, p. 323 (1924)] for the Kerr const., $B = \cdot 24 \times 10^{-10}$ per atm., for the D line and 17·5°C (which agrees closely with Hansen's $\cdot 23 \times 10^{-10}$) gives

$$\delta = \cdot 077.$$

In the case of N_2O, the value $r = \cdot 143$ of Raman and Rao gives $\delta = \cdot 143$; and the value of Cabannes and Granier $r = \cdot 122$ gives. $\delta = \cdot 118$. From Hansen's value for the Kerr const, $B = \cdot 48 \times 10^{-10}$ per atm. (Szivessy's report in *Jahrbuch der Radioaktivität*, 1919) δ comes out to be ·125.

The other vapours for which we have data both for B and for r, have polar molecules and they will be discussed in a later paper.

V. Variation of the Anisotropy in Liquids with Temperature

We have seen how the anisotropy calculated from the liquid state is in general, much smaller than that calculated from the vapour. Now in the case of some liquids, *viz.*, ether,[1] pentane,[2] heptane,[3] benzene,[3] and carbon bisulphide [4] the depolarisation of the scattered light has been studied for different temperatures up to the critical point; and with the help of these data, we can follow continually the change in the anisotropy as we pass gradually from the liquid to the gaseous state. But there is one difficulty in calculating δ at higher temperatures; we have no compressibility measurements for some of these liquids. For ether and pentane, β can be calculated from the pressure-volume curves of Ramsay and Young [5] and Rose—Innes and Young [6] respectively, and these values have been used in the calculations below. But for the other three liquids we have no such data. Also the equations of state cease to give even rough approximations for β as we approach the critical point. However, we have seen in Part II that the values of the intensity of the scattered light calculated by King's formula [Eqn. (4)] agree satisfactorily with the observed values. *Assuming the validity of that expression*, β has been calculated for heptane and benzene (relative to the known compressibilities at room temperature)

[1] K. R. Ramanathan, Proc. Roy. Soc., A, cii, p. 151 (1922).

[2] R. Venkateswaran, Trans. Chem. Soc., cxxi, p. 2655 (1922).

[3] Martin and Lehrman, Jour. Phy. Chem., xxvii, p. 558 (1923).

[4] K. R. Ramanathan, not published.

[5] Phil. Trans. Roy. Soc., A., clxxviii, p. 57 (1887).

[6] Phil. Mag., V series, xlvii, p. 355 (1899).

from the corresponding observed values of the intensity of the scattered light.

When we come to CS_2, Amagat's values [1] for the compressibility extend only up to 100° C ; and for higher temperatures, we have no data even for the intensity of the scattered light from which to calculate β as in the case of heptane and benzene. Thus, for want of other means of calculating the compressibility, it was assumed that the compressi ility of CS_2 at any required temperature is the same as the compressibility of liquid CO_2 at the same "reduced temperature" $(\frac{T}{T_c})$ For the latter substance, we have of course the pressure—volume measurements of Jenkin[2] at different temperatures.

The other data were taken from Landolt-Börnstein Tables (1923). The refractive indices at higher temperatures were calculated from the experimental values of the molecular refractivity at the room temperature and the known densities, using the Lorentz-Mos- : relation.

For CS_2, no direct measurements of the density are available for higher temperatures, and the values were therefore interpolated between the known densities at ordinary temperatures and at the critical point, using for the purpose the temperature (reduced) variation curve of the density of liquid CO_2.

The calculated values of δ are given in Tables IV to VIII. In the case of ether, pentane and CS_2, the authors' values were plotted and smoothened.

[1] Taken from "*Piezochemie*," by Cohen and Schut, Leipzig, 1919, pp. 112 and 100.

[2] Proc. Roy. Soc. A., xcviii, p. 170 (1920).

TABLE IV—*Ether.*

Temp. °C	r	$\delta \times 10^3$ Calculated.	
		Ramanathan.	King-Gans.
35	·080	5·8	3·6
60	·079	7·2	4·5
90	·074	9·2	6·0
100	·071$_5$	10·5	6·9
150	·024	16·0	11·3
175	·015	19·7	14·6
185	·014	40	31
190	·013	115	90
Critical temp. = 193·6°C		$\delta \times 10^3$ from r vapour = 27	

TABLE V—*n-Pentane.*

Temp. °C	r	$\delta \times 10^3$ Calculated.	
		Ramanathan.	King-Gans.
30	·072	5·2	3·2
120	·048	12·0	8·1
140	·023	7·1	4·9
150	·017$_5$	7·0	4·9
160	·015	7·8	5·6
170	·014	11·4	8·3
Critical temp = 197·2°C		$\delta \times 10^3$ from r vapour = 10·1	

TABLE VI—*n-Heptane.*

Temp. °C	r	$\delta \times 10^3$ Calculated.	
		Ramanathan.	King-Gans.
20	·127	4·6	2·7
100	·100	4·0	2·5
200	·038	4·8	3·3
225	·026	5·9	4·2
240	·020	7·2	5·3
250	·017	8·6	6·4
260	·0165	11·6	9·0
Critical temp. = 266·85°C.		$\delta \times 10^3$ from r vapour = 27	

TABLE VII—*Benzene.*

Temp. °C	r	$\delta \times 10^3$ Calculated.	
		Ramanathan.	King-Gans.
20	·485	49	24
100	·394	50	26
200	·154	40	24
250	·061	46	30
260	·045	63	42
270	·025	68	47
280	·015	142	102
Critical temp. = 288°C		$\delta \times 10^3$ from r vapour = 61	

TABLE VIII—*Carbon bisulphide.*

Temp. °C	r	$\delta \times 10^3$ Calculated.	
		Ramanathan.	King-Gans.
30	·67	248	101
100	·545	147	66
150	·42	100	49
180	·325	137	71
200	·26	153	82
210	·225	131	72
Critical temp. = 273°C.		$\delta \times 10^3$ from r vapour = 143.	

It is necessary here to draw attention to the serious experimental difficulties in the measurement of the depolarisation of the light scattered by liquids under very high pressures. The unavoidable strain produced in the glass walls or windows, as the case may be, through which observations are made, will introduce errors, which will be most conspicuous near the critical point, where the weak component is very small. When we remember also the difficulties of securing good back-ground in high pressure work, it is needless to point out that, in spite of the precautions taken by the investigators, the values for r near the critical temperature can only be taken as approximate.

However, without laying any stress on the actual calculated values of δ, we can see in a general way that in the case of ether, pentane and heptane, as the temperature is increased, the anisotropy, according to either formula, also increases, continually approximating to the value calculated from the vapour state, but not actually reaching it even near the critical point. For benzene, King-Gans formula leads to

the same conclusion; while for benzene according to Ramanathan's formula and for CS_2 according to either formula, the calculated values of δ at different temperatures are almost of the same order of magnitude as in the vapour, and the variations of individual values are more or less indifferent.

If, as we have supposed in Part IV, the smaller value of the anisotropy calculated from the liquid state, as compared with the value calculated from the vapour state, is due to the influence of the atoms of the neighbouring molecules, consequent upon the closer packing in the liquid state, it is not difficult to understand this continual approximation of δ liquid to δ vapour as we approach the critical temperature.

VI. Summary and Conclusion

1. The theories of light-scattering of Ramanathan, King and Gans lead to different expressions for the intensity and the depolarisation of the scattered light. Attempt is made to test how far they fit in with experimental facts.

2. Relative measurements of the intensity, agree much better with King's expression than with Ramanathan-Gans expression. However the evidence of absolute measurements is not unanimous.

3. The anisotropy calculated from scattering measurements agrees satisfactorily with that calculated from Kerr constant, King-Gans formula giving slightly better agreement.

4. The anisotropy calculated from the liquid state is, in general, smaller than the value calculated from the vapour. A general explanation is suggested.

5. The anisotropy calculated from the liquid is found to increase with rise of temperature, continually approximating to the anisotropy in the vapour state, but not actually reaching it even near the critical point.

The author's thanks are due to Prof. C. V. Raman for his kind suggestions.

210, Bow Bazar Street,
Calcutta,
26th December, 1925.

XXXIV.—ON THE DIFFRACTION OF LIGHT BY SPHERICAL OBSTACLES.

By Prof. C. V. Raman, *F.R.S.*, and Mr. K. S. Krishnan.

Abstract.

The diffraction of light inside the shadow, thrown by a small source of light, of a sphere and a circular disc of the same diameter, was studied, with special reference to the relative intensities of the central bright spots. With the source at about 2 metres from the obstacles, with a quarter-inch polished steel ball, the bright spot could be detected visually up to 3 cm. behind the obstacle, while with a steel disc of the same diameter, with the edges perfectly sharp, smooth and circular, the spot could be traced up to 2 cm.

The relative intensities of the two spots were studied at different distances behind the obstacles, qualitatively by photography and quantitatively by visual photometry. At small distances behind the obstacles, the spot inside the shadow of the sphere is much feebler than the disc-spot, however approximating to the latter as we reach farther back from the obstacles, but even at 100 cm. remaining appreciably feebler.

A general explanation is suggested.

I. Introduction.

IT has long been known* that at the centre of the shadow of a spherical obstacle thrown by a small source of light there is a bright spot similar to that found in the shadow of a circular disc; and, in fact, a spherical obstacle is often used instead of a disc to demonstrate the formation of the bright spot at the centre of the shadow of a circular boundary. It is usually assumed by experimenters† that at a point on the axis of the shadow a circular disc and a sphere of equal radius would give practically identical results. This, however, is not actually the case, and it is the purpose of this Paper to draw attention to the notable differences that exist between the effects observed in the two cases.

II. The Intensity of the Bright Spot.

To compare the effects obtained in the shadow of a spherical obstacle and a circular disc of equal size, it is convenient to mount them side by side on a glass plate, so that the bright spots at the centres of their shadow may be seen at the same time. In most of our observations we used a quarter-inch (diameter) steel ball and an accurately made steel disc of the same size, cut on the lathe so as to have a sharp circular edge of razor-like smoothness and sharpness. They were attached by specks of wax, with sufficient space between them, to a glass plate, and held at a distance of about two metres from the source.

The diffraction patterns within the shadow of disc and sphere were seen simultaneously through a lens of sufficiently wide field of view. When a bright source of light is used, it is convenient to use a plate with two holes cut in it, to correspond with the shadow of the sphere and the disc, and place it in the field of view so as to cut off all extraneous light except that diffracted into the region of shadow. The removal of the glare outside the region of shadow is very helpful, and with this

* Rayleigh, Sc. Papers, Vol. V, p. 112. *See* also A. O. Rankine, Proc. Phys. Soc., Vol. 37, p. 267 (1925).

† Hufford, Phys. Rev., Vol. 7, p. 545 (1916).

arrangement it is possible to trace the bright spots in the centre of the shadow up to within 3 cm. of the object in the case of the sphere, and to less than 2 cm. in the case of the disc, thus testifying to the accuracy of the edges. A series of photographs were taken of the diffraction patterns with the source of light 179 cm. in front of the obstacles, and with the object plane of the camera at different distances behind them. Some of these are reproduced here (Figs. 1, 2, 3, 4). In the photographs the diffraction pattern on the right corresponds to the sphere and that on the left to the disc. We can easily see that the central white spots in the case of the sphere are much less bright than in the case of the disc. Thus, in Fig. 1, which corres-

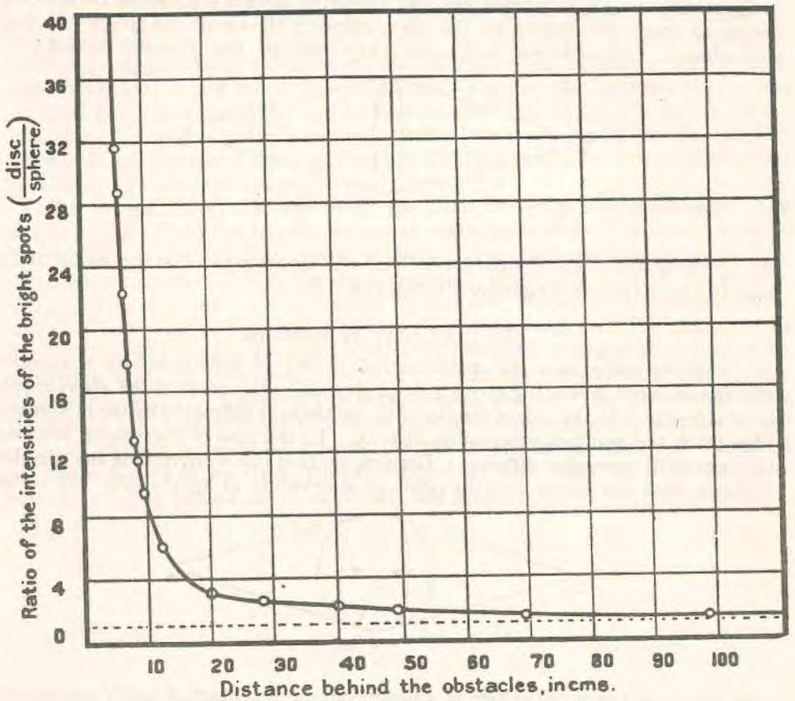

Fig. 5.

ponds to a distance of about 11 cm. behind the obstacles, the spot in the case of the sphere is invisible in the photograph. At 13 cm., as shown in Fig. 2, it is just visible. At 25 cm. (Fig. 3) it is still much feebler than for the disc, and at 40 cm. (Fig. 4) the difference in intensity of the two bright spots is still conspicuous. Further, we see in the photographs that the general illumination within the geometrical shadow is much greater for the disc than for the sphere. The spots in the shadow of the sphere were distinctly reddish in comparison with those for the disc, and the photographic intensity thus differed more than the visual intensity.

A quantitative study of the relative intensities of the central white spots of the two diffraction patterns was made with the help of an Abney rotating sector photometer placed just in front of the obstacles, and looking for the diffraction patterns through the eye-glass with the two apertures in its focal plane, mentioned already. The source of light was at a distance of 232 cm. in front of the obstacles. The results are shown in the graph on p. 351 (Fig. 5). Owing to the difference in colour, some uncertainty arises in the visual estimates of equality of intensity. Further, for short distances behind the obstacles the comparison was by no means easy, owing to the spots having a very small size, and appearing against a luminous background. Owing to these circumstances, the measurements shown in the graph are only approximate. Nevertheless, they sufficiently indicate the general character of

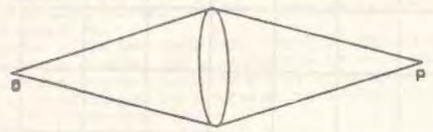

FIG. 6*a*.

the phenomenon. The dotted line in Fig. 5 is the asymptote to the curve, and is slightly above the line of equality of intensities.

III. DISCUSSION OF RESULTS.

Without going into the mathematical theory of diffraction by a spherical obstacle, it is not difficult to give a general physical explanation of the above experimental results. In the case of the disc (Fig. 6*a*) the rays diffracted by the illuminated edge reach the point of observation directly. In the case of the sphere, however, the position is somewhat different. Drawing tangent cones enveloping the spherical obstacle, with the source and the point of observation as apexes (Fig. 6*b*), we see

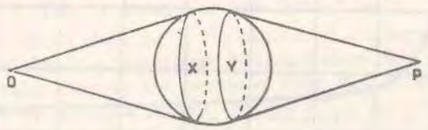

FIG. 6*b*.

that they now touch the sphere at different circles of contact, X and Y respectively. Thus, the circle of contact Y, from which diffracted rays originating at the surface can reach the point of observation, lies within the region of geometrical shadow, and not at its edge, as in the case of the disc. The disturbance incident on the surface of the sphere has to creep round it, as it were, over the arc XY before the rays diffracted out by the sphere can reach the point of observation, and must suffer a very considerable diminution in the process. Thus, we can see that the intensity of the central white spot in the diffraction pattern of a sphere will be less than in the case of the disc at the same distance behind by a quantity depending on the length of the arc XY between the circles of contact of the tangentially incident and diffracted rays. Now the length of this arc will be the greater the nearer the point of observation

approaches the sphere, so that the intensity of the sphere-spot, as compared with the disc-spot, ought to decrease as we approach the obstacles. Proceeding in the opposite direction, the intensity at large distances will approach that of the disc, but still will be smaller than the latter by an amount which will depend on the distance of the source from the obstacle.

That the foregoing way of viewing the matter is not fanciful, but is really a statement of the physical processes occurring in the case, is evident from the following observations. A microscope is focussed tangentially on the circle of contact X already mentioned, which appears as a luminous edge in the field of view. If now the microscope is shifted laterally into the region of the geometrical shadow, we find that it has also to be drawn back longitudinally towards Y in order to keep the diffracting edge of the sphere in focus, whereas in the case of the disc such longitudinal movement is not found to be required. Further, the luminous edge of the sphere is found to diminish in brightness much more rapidly than in the case of the disc when the observer's eye is moved laterally into the region of shadow. Similar differences are also found when we compare the diffraction into the region of shadow by a sharp straight edge and by the edge of a cylinder.

We recognise that the explanation we have offered is only qualitative. The reality of the effects described is, however, unquestionable, and we have no doubt that a quantitative explanation will be forthcoming when the diffraction problem is considered on the basis of the electromagnetic theory for the case of the large sphere. This problem has been handled by Poincaré, Nicholson, Macdonald, Bromwich, G. N. Watson and others. The Paper by Macdonald, on "The Diffraction of Electric Waves Round a Perfectly Reflecting Obstacle,"* might in particular be referred to, as the analysis contained in it approaches most closely to the point of view from which we have explained our experimental results. The formulæ given by Macdonald are, however, not in a form capable of immediate application to the problem without considerable labour. As the experimental work was completed last summer, and as we are at present engaged on other work, we have thought it best not to defer publication of the results any longer.

* Phil. Trans. R.S., A.210, 113 (1910). For other references *see* Bateman, "Electrical and Optical Wave Motion."

Are Gaseous Molecules Orientated in a Magnetic Field?

BY

K. S. KRISHNAN

Research Scholar in the Indian Association for the Cultivation of Science.

Introduction.

Glaser,[1] working on the diamagnetic susceptibilities of hydrogen, nitrogen and carbon dioxide at low pressures, has obtained some very interesting results. As the pressure is gradually lowered, the susceptibilities decrease proportionately only up to a certain pressure which depends on the nature of the gas and, to some extent, on the value of the magnetic field. Below this point the susceptibilities are greater than, and approach at low pressure three times, the value one would expect if the original rate of decrease with pressure had been maintained throughout. With slightly improved apparatus he has later[2] extended these observations to the case of carbon monoxide, which is also diamagnetic.

Glaser explains these "anomalies" by assuming that there is a tendency for the molecules to set themselves in a definite direction under a magnetic field and that this setting would require some time owing to the moment of inertia of the molecules. The effect of collisions would be

[1] Ann. der Physik 76, 459, 1924. See also Physik. Zeits. 26, 212, 1925.
[2] Ann. der Physik 78, 641, 1926.

to hamper this setting up. Hence so long as the time between two collisions is small in comparison with the time required for the molecules to set themselves, there will be no orientation of the molecules; and this will be the case at the higher pressures. But when the pressure is lowered, the time between two collisions begins to be comparable with the time of setting of the molecules and orientation will appear and consequently an increase in susceptibility. The orientation will, however, be complete only when the time between two collisions becomes large; this will correspond to the low pressures where the susceptibilities are again proportional to the pressure.

Thus the orientation theory explains in a simple way the observed facts. But probably the strongest argument in its favour is the natural explanation it offers for the three-fold values of the apparent molecular susceptibilities at low pressures; this is actually the ratio of the value of the susceptibility when the molecules have all set themselves in any particular direction, to the value when they are orientated at random.[3]

Also Glaser finds that the actual pressures at which the anomalous values begin to appear for the different diamagnetic gases investigated, can be expressed as an empirical function of the moment of inertia of the respective molecules; which seems further to support the orientation theory.

However, there are some real difficulties in accepting the theory. For instance, it is reasonable to suppose that all the molecules above—H_2, N_2, CO and CO_2—possess an axis of symmetry, *viz.*, the line joining the atomic nuclei. "Owing to the relatively large mass of the nuclei, it is only about the line joining them that the molecule will acquire an appreciable magnetic moment under the influence of the field.[4]"

[3] Stoner, Nature 115, 302, 1925.
[4] Stoner, *loc. cit.*

If Glaser's factor 3 is to be explained, these nuclear axes, which previously were orientated at random, should all point in the same direction on the introduction of the magnetic field. This cannot be reconciled with the existence of rotation of the molecules about axes perpendicular to their axes of symmetry, required by the theory of specific heats, etc.

Hence it would be extremely instructive to verify by independent methods whether there is real orientation of the molecules under the conditions of Glaser's experiments. Such methods are not difficult to devise.

Double Refraction.

For instance, if there is actual orientation of the molecules in a magnetic field, then owing to their optical anisotropy, the medium will become doubly refracting. We can calculate the magnitude of this effect.

Let us take for example the case of carbon dioxide at 50 mm. pressure; at this pressure it is evident from Glaser's curves that the orientation, if any, of the molecules should be complete. When there is orientation, the line joining the C- and the two O-nuclei, which we might call the axis of the molecule, will set itself parallel to the field.

Now let μ be the normal refractive index of carbon dioxide *i.e.*, the refractive index when the molecules are orientated at random; and let $\mu_\parallel$ and $\mu_\perp$ be the refractive indices, when the CO_2-molecules are all orientated with their axes along the magnetic field, for vibrations parallel and perpendicular respectively to the magnetic field.

Also let A, B be the optical moments induced in a molecule of CO_2 per unit light vector incident along and perpendicular to its axis respectively.

Then according to the usual theory of dielectric polarisation, remembering that, for the small pressures we are

considering, the μ's are very nearly equal to unity, we have

$$\left.\begin{aligned} \mu_\parallel - 1 &= 2\pi\nu.\mathrm{A} \\ \mu_\perp - 1 &= 2\pi\nu.\mathrm{B} \\ \text{and}\quad \mu - 1 &= 2\pi\nu.\frac{\mathrm{A}+2\mathrm{B}}{3} \end{aligned}\right\} \quad \ldots \quad \ldots \quad \ldots \quad (1)$$

where ν is the number of molecules per unit volume.

Now $\frac{\mathrm{A}}{\mathrm{B}}$ can be calculated from measurements on light-scattering. According to Rayleigh's theory[5] of scattering by anisotropic molecules, the ratio of the components of the transversely scattered light is given by

$$r = \frac{2(\mathrm{A}^2+\mathrm{B}^2-2\mathrm{AB})}{4\mathrm{A}^2+9\mathrm{B}^2+2\mathrm{AB}} \quad \ldots \quad \ldots \quad \ldots \quad \ldots \quad (2)$$

For carbon dioxide, taking $r = \cdot 107$ (mean of the values $\cdot 117$ of Rayleigh,[6] $\cdot 106$ of Raman and Rao[7] and $\cdot 098$ of Cabannes and Granier[8]) we get from (2)

$$\frac{\mathrm{A}}{\mathrm{B}} = 2 \cdot 41.$$

This agrees well with the value $2 \cdot 42$ calculated by Ramanathan[9] from the structure of the CO_2-molecule and does not differ much from the value $2 \cdot 15$ calculated from the Kerr constant measurements of Hansen[10] and Szivessy.[11]

[5] Phil. Mag., 35, 373, 1918. Collected papers, Vol. VI, p. 540.
[6] Proc. Roy. Soc., A, 97, 435, 1920.
[7] Phil. Mag., 46, 426, 1923.
[8] Journ. de Physique, VI, Series, Tome IV, p. 429, 1923.
[9] Proc. Roy. Soc. A, 107, 684, 1925.
[10] Quoted by Szivessy, Jahrbuch der Radioaktivität, 1920.
[11] Zeits. f. Phys. 26, 342, 1924.

For the room temperature, *viz.* 25°C, and 50mm. pressure, we have from the tables, for the sodium light,

$$\mu - 1 = 2{\cdot}71 \times 10^{-4} :$$

so that, using (1) and (2) we get

$$\mu_{\parallel} - 1 = 4{\cdot}44 \times 10^{-4}$$

$$\mu_{\perp} - 1 = 1{\cdot}84 \times 10^{-4}\ ^{10}$$

Thus supposing a beam of plane polarised light traverses carbon dioxide perpendicular to the magnetic field, if the vibrations are parallel to the field, there will be a path retardation of $1{\cdot}73 \times 10^{-5}$ cms. *i.e.*, about 0·3 of a wavelength of sodium light for each centimetre length of path across the magnetic field; while vibrations perpendicular to the magnetic field will be accelerated by about 0·15 of a wavelength per centimetre of path.

The author used an interference arrangement in which one of the interfering beams traversed a tube of carbon dioxide lying between the flat pole-pieces of an electromagnet, perpendicular to the magnetic field, while the other traversed a similar tube of carbon dioxide, in communication with the first, placed outside the field. The second tube served merely as a compensator. White light was incident and the

[10] Similar calculation gives the following values for the other gases (at 25°C and 50 mm. pressure):—

	$\mu - 1$	$\mu_{\parallel} - 1$	$\mu_{\perp} - 1$
Hydrogen	$0{\cdot}838 \times 10^{-5}$	$1{\cdot}14 \times 10^{-5}$	$0{\cdot}687 \times 10^{-5}$
Nitrogen	$1{\cdot}80 \times 10^{-5}$	$2{\cdot}48 \times 10^{-5}$	$1{\cdot}46 \times 10^{-5}$
Carbon monoxide	$2{\cdot}02 \times 10^{-5}$	$2{\cdot}71 \times 10^{-5}$	$1{\cdot}67 \times 10^{-5}$

The values refer to the sodium line.

interference fringes were observed through a micrometer eye-piece and a nicol.

The field between the pole pieces was estimated at about 10,000 gausses, and it was fairly uniform over a diameter of about 8 cms.

With this arrangement and with the nicol rotated for transmitting vibrations parallel to the magnetic field, if there is complete orientation of the molecules on putting on the field there should be a shift, at 50 mm. pressure, of the interference system, by more than two fringe-widths. For perpendicular vibrations, the shift should be in the opposite direction by more than one fringe-width.

However in the actual experiment there was no shift for either of the components, even though a shift of a tenth of a fringe-width could easily have been detected. A preliminary experiment was performed with carbon dioxide from a commercial cylinder at various pressures from 1 atmosphere down to about 10 mm. of mercury and the experiment was repeated afterwards with pure dry carbon dioxide with entirely negative results in both cases.

There is another familiar form in which the double refraction, if any, could be detected, *viz.*, to allow light polarised at an angle of 45° to the magnetic field to traverse the tube of carbon dioxide lying between the pole-pieces of the magnet and to extinguish the transmitted light with a crossed nicol. For unit length of track across the field, in carbon dioxide at 25°C. and 50 mm. pressure, the vibrations perpendicular to the magnetic field will gain in phase about $0{\cdot}9\pi$, over the vibrations parallel to it, so that when the field is put on, there should be a restoration of light, the actual illumination of the field of view varying as the pressure is gradually altered.

The experiment was tried with carbon dioxide at different pressures down to about 10 mm. of mercury, with a tri-field

Lippich polariser and a nicol; and there was no restoration of light when the magnetic field was put on.

It need hardly be pointed out that the partial orientation of the molecules in the field, due to the differences in their magnetisability along and perpendicular to their axes, which will be determined by Boltzmann's theorem, will be very small; and the double refraction arising therefrom (the Cotton-Mouton effect) will be entirely negligible.

Light-scattering.

We have another very interesting method of studying the orientation of molecules, which, however, is not so delicate as the above methods. Suppose a beam of light is traversing any medium perpendicular to a magnetic field, and the light scattered perpendicular both to the track and to the magnetic field is examined.

Taking carbon dioxide again, in the absence of the magnetic field, when the molecules are orientated at random, owing to the optical anisotropy of the CO_2-molecules, the scattered light is imperfectly polarised, the ratio of the components being, as already mentioned, equal to ·107. But suppose the magnetic field is put on and all the CO_2-molecules set themselves with their axes along the field. Then from the theory of scattering by anisotropic molecules it is obvious that none of the molecules in the field can give rise to vibrations along the incident light. Also the vibration in the scattered light, parallel to the magnetic field, will be entirely due to that component of the incident unpolarised light which is vibrating in the same direction, *i.e.*, vibrating along the axes of the CO_2-molecules. Thus, when the field is put on, the transversely scattered light will become *perfectly polarised* with its vibrations parallel to the field. But the total intensity will not be appreciably altered because, according to the Einstein-Smoluchowski expression the ratio of the

intensities before and after the introduction of the field will be equal to

$$\frac{(\mu-1)^2 \cdot \frac{6(1+r)}{6-7r}}{\frac{1}{3}(\mu_1-1)^2}$$

which, on evaluation is found to be very nearly equal to 1[15].

The scattering by carbon dioxide was studied in the usual way; the gas was contained in a glass cross of about 1·8 cms. diameter, and the transversely scattered light was examined through a double-image prism adjusted to transmit vibrations parallel and perpendicular to the incident track. At a fourth of an atmosphere there was no change in the depolarisation in a field of about 4,000 gausses. When however the pressure was further reduced, though the stronger component was distinctly visible even at a tenth of an atmosphere, the weaker component could not be recognised clearly, as the imperfections in the background, particularly the light diffused from the edges of the apertures used inside the cross, became conspicuous. Hence it was not possible to test whether the weaker image disappears at still lower pressures, when the field is put on. The author hopes to repeat the experiment with a bigger glass cross and under better conditions.

Paramagnetic Gas.

In the later work mentioned, Glaser has also investigated the paramagnetic gas oxygen and he finds that over the whole range investigated, *viz.*, from 16 atmospheres down to about 20 mm. the susceptibility is always proportional to the pressure. He explains the absence of anomalies similar to those observed for diamagnetic gases by remarking that, with the magnitude of the paramagnetic moment one

[15] In the cases of hydrogen, nitrogen and carbon monoxide the total intensity is slightly diminished (is about 0·8 to 0·9 times).

should expect the anomalous region only at very high pressures; which means that a paramagnetic gas at ordinary pressures corresponds to the last stage in a diamagnetic gas where the molecules are completely orientated along a particular direction.

But actual experiments with oxygen at different pressures down to less than 10 mm. of mercury, by the interference method, failed to detect any double refraction in a field of about 10,000 gausses.[14] Again light transversely scattered by the gas at atmospheric pressure failed to show any change in its depolarisation in a field of about 4,000 gausses.

On the other hand, some recent experiments by Debye and Huber.[15] on nitric oxide and other substances seem to throw doubt even on the existence of the partial orientation of para-magnetic molecules in a magnetic field required by Langevin's classical theory, not to talk of any complete orientation.

Summary and Conclusion.

Glaser has observed some "anomalies" in the diamagnetic susceptibilities of gases at low pressures; which he explains by assuming that the molecules, under these conditions, set themselves in a particular direction in a magnetic

[14] For oxygen at atmospheric pressure and 25°C.

$$\mu - 1 = 2{\cdot}48 \times 10^{-4}$$

$$\mu_{\parallel} - 1 = 3{\cdot}91 \times 10^{-4}$$

and $$\mu_{\perp} - 1 = 1{\cdot}77 \times 10^{-4}$$

for sodium light. For 8 cms. of path across the field, as was the case in the actual experiment, if there had been complete orientation, there should have occurred a shift of the interference system by

$$\frac{8 \cdot (3{\cdot}91 - 2{\cdot}48) \cdot 10^{-4}}{5{\cdot}89 \times 10^{-5}}$$

or 20 fringe-widths for vibrations parallel to the magnetic field and by 10 fringe-widths, in the opposite direction, for vibrations perpendicular to the magnetic field.

[15] See Debye, Zeits. f. Phys. 36, 300, 1926.

field. The present paper describes some experiments which failed to show any such setting up of the molecules. Thus an interference method failed to detect any change in refractive index when a magnetic field was put on; with the gas between two crossed nicols there was no restoration of light in the field; and the depolarisation of the transversely scattered light did not show any change in the field.

The actual magnitudes of the effects to be expected, according to the orientation theory, in the above experiments, are calculated and are found to be far too large to escape detection in case they existed.

Our uniformly null experiments lead therefore to the conclusion that the molecules are not orientated in a magnetic field under the conditions of Glaser's experiments and that we have to look for an explanation of the "anomalies" observed in the diamagnetic susceptibilities of gases at low pressures elsewhere.

The author wishes to thank Professor C. V. Raman who suggested the work and took great interest in its progress.

The Electrical Polarity of Molecules.

ON attempting to correlate the electrical double-refraction (Kerr effect) of gases and vapours which has been measured by Leiser, Hansen and Szivessy, with the optical anisotropy of the molecules determined from observations on light-scattering, it is found that electrically polar molecules generally exhibit a Kerr effect which is very large in relation to their optical anisotropy. This indicates that the orientative action of the field on the molecule in such cases is chiefly due to the permanent electric doublet present in it, and is much larger than would be the case if the molecules were non-polar. In the case of molecules having an axis of optical symmetry to which the electric doublet is parallel, or is inclined at some known angle, it is possible to calculate the permanent electric moment from the value of the Kerr constant and the constant of depolarisation of the scattered light. Conversely, if the moment is known, the inclination of the electric doublet to the optic axis can be found. For example, in the case of the simple dipole molecule HCl, we may assume the optic axis to be parallel to the doublet.

The constant of depolarisation as recently measured by Ramanathan is 0·010, and the Kerr constant from the measurements of Hansen = $0{\cdot}90 \times 10^{-10}$. From this, considering the orientative action of the field to be due only to the permanent doublet, we find its moment to be $1{\cdot}06 \times 10^{-18}$ electrostatic units, while if the orientative couple on the induced doublet is also taken into account as in the case of non-polar molecules, the value of the permanent moment comes out to be $1{\cdot}04 \times 10^{-18}$. The recent determination by Zahn from dielectric constant measurements gives $1{\cdot}03 \times 10^{-18}$, thus showing good agreement.

When the optical ellipsoid of the molecule has three unequal axes, measurements of the factor of depolarisation and of the Kerr constant are by themselves insufficient for an accurate determination of the electric moment. But if the moment is known from measurements of the dielectric constant, the data mentioned are of much assistance in fixing the position of the axis of the doublet. For example, if the Kerr constant of a substance is negative, we can assert definitely that the axis of the permanent doublet does not coincide with the longest axis of the optical ellipsoid. It is interesting to note in this connexion that, so far as is known, all substances having a negative Kerr constant are polar.

C. V. RAMAN.
K. S. KRISHNAN.

210 Bowbazaar Street,
Calcutta, India.

Magnetic Double-Refraction in Liquids. Part I.—Benzene and its Derivatives.

By Prof. C. V. RAMAN, F.R.S., and K. S. KRISHNAN.

(Received September 6, 1926.)

1. *Introduction.*

Many organic liquids exhibit a feeble double-refraction when they are placed in a strong magnetic field and a beam of light traverses the substances in a direction transverse to the lines of force. The magnitude of this effect, which was discovered in 1907 by Cotton and Mouton, depends very largely on the chemical structure of the molecule. Hydrocarbons belonging to the aliphatic series and the aromatic series are strikingly different in their behaviour; hexane, for instance, showing no detectable effect, while benzene is an example of a liquid showing a measurable double-refraction. We propose in the series of papers of which this is the first, to discuss this phenomenon in its relation to the structure of molecules and their magnetic properties. For this purpose we shall use the theory of Langevin, which explains magnetic double-refraction as an effect arising from the orientative action of the field on the molecules (assumed to be magnetically and optically anisotropic) and connects the absolute value of the Cotton-Mouton constant with the values of the optical refractivity and of the magnetic susceptibility of the molecule along three mutually perpendicular axes. To enable the formula of Langevin to be used

for the purpose of calculating the absolute value of the Cotton-Mouton constant, it is necessary to have data concerning, firstly, the magnetic character of the molecule, and, secondly, its optical anisotropy. In regard to the latter, we propose to utilise the data obtained from observations on light-scattering in the liquids concerned. In regard to the magnetic anisotropy of the molecules, we shall endeavour to connect the indications furnished by the data on magnetic double-refraction with considerations of atomic and molecular structure and the well-known theory of diamagnetism, also due to Langevin.

2. *Theory of Magnetic Double-Refraction.*

We shall here merely quote the formula due to Langevin, the derivation of which is very conveniently set out in a recent article by Debye.* The Cotton-Mouton constant C_m of double-refraction is given by the relation

$$C_m = \frac{n_p - n_s}{\lambda H^2} = \frac{3(n_0^2-1)^2}{80\pi n_0 \lambda k T \nu} \cdot \frac{[(A-B)(A'-B')+(B-C)(B'-C')+(C-A)(C'-A')}{(A+B+C)^2}, \quad (1)$$

where A, B, C are the moments induced along the three mutually perpendicular axes of the optical ellipsoid of the molecule by unit electric force in the incident light-waves, acting respectively along the three axes, and A′, B′, C′ are the magnetic moments induced in the molecule by unit magnetic force acting in the same three directions. H is the acting magnetic field, λ is the wave-length of the light, k is the Boltzmann constant, T the absolute temperature, ν the number of molecules per unit volume, n_0 the refractive index of the liquid outside the field, and n_p and n_s are the principal refractive indices in the field. The quantities A, B, C are connected with the refractive index n_0 of the liquid by the relation

$$\frac{A+B+C}{3} = \frac{3}{4\pi\nu} \cdot \frac{n_0^2-1}{n_0^2+2}. \quad (2)$$

The quantities A′, B′, C′ are connected with the magnetic susceptibility of the medium by the relation

$$\frac{A'+B'+C'}{3} = \frac{\chi}{\nu}, \quad (3)$$

where χ is the susceptibility per unit volume.

It will be noticed that the Cotton-Mouton constant depends essentially on the differences of the magnetic susceptibilities of the molecules along the three directions which form the axes of the optical ellipsoid of the molecule.

* P. Debye, 'Marx's Handbuch der Radiologie,' vol. 6, pp. 754–76.

3. *The Optical Anisotropy of the Molecule.*

Observations on the state of polarisation of the light scattered by a gas or vapour enables us to evaluate directly an expression which depends on the differences (A − B), (B − C), and (C − A) between the optical properties of the molecule along its principal optical axes. The light scattered by an ideal spherically symmetrical molecule in a direction transverse to the incident unpolarised beam would be completely polarised. In all actual cases, however, the light so scattered is imperfectly polarised, indicating that the molecule is not optically isotropic. The state of polarisation is usually indicated by the ratio of the intensities of the two components of vibration in the scattered light. The ratio r of the intensity of the feeble component to the stronger component is connected with the values of A, B, C, by the relation

$$r = \frac{6[(A-B)^2+(B-C)^2+(C-A)^2]}{10(A+B+C)^2+7[(A-B)^2+(B-C)^2+(C-A)^2]}. \quad (4)$$

In the case of dense fluids, the problem of determining the relation between the optical anisotropy of the molecule and the state of polarisation of the transversely scattered light is not quite simple, as we have to take into account the influence of neighbouring molecules on each other and the effect of local fluctuations of density and molecular orientation on the optical field at any point in the medium. Various theories differing mainly in detail have been proposed, and the question how far they are in agreement with the available observations on light-scattering has been discussed in a recent paper by one of us.* Two formulæ of nearly identical form have been proposed, connecting the effective anisotropy of the molecule in the liquid state with the state of polarisation of the scattered light. The first formula is

$$r = \frac{6[(A-B)^2+(B-C)^2+(C-A)^2]}{10kT\beta\nu\left(\frac{n_0^2+2}{3}\right)^2(A+B+C)^2+7[(A-B)^2+(B-C)^2+(C-A)^2]}, \quad (5)$$

where β is the compressibility of the medium.

A second formula which has been proposed is

$$r = \frac{6[(A-B)^2+(B-C)^2+(C-A)^2]}{10kT\beta\nu(A+B+C)^2+7[(A-B)^2+(B-C)^2+(C-A)^2]}. \quad (6)$$

The quantity δ given by the expression

$$\delta = \frac{[(A-B)^2+(B-C)^2+(C-A)^2]}{(A+B+C)^2} \quad (7)$$

* K. S. Krishnan, 'Proc. Ind. Assn. Cultn. Sc.,' vol. 9, p. 251 (1926).

defines the optical anistropy of the molecule and should be the same for the vapour and the liquid state. For many substances, however, the value of δ calculated by either formula from the scattering by the liquid is rather less than that calculated from the vapour, indicating that the effective optical anisotropy of the molecules may be diminished by reason of their close packing or actual association in the liquid. For this reason it seems appropriate, in any discussion bearing on the liquid state, to consider the values of the molecular anisotropy determined from observations on light-scattering in liquids. An extensive and careful study of the scattering in no fewer than 65 different liquids has been recently carried out in the authors' laboratory.* We propose to utilise the data thus gathered in our discussion of magnetic double-refraction.

The data available are not sufficient to decide absolutely whether formula (5) or formula (6) is to be preferred. Instead of rejecting one or the other, it seems preferable to retain and use both formulæ and to compare the results thus obtained.

4. *The Cases of Hexane and Benzene.*

Observations on light-scattering both in vapours and in liquids indicate that the hydrocarbons of the paraffin series exhibit a smaller degree of optical anisotropy than those of the aromatic series. The depolarisation factor r for the vapours of hexane and cyclohexane are 1·68 per cent. and 0·86 per cent. respectively. The corresponding values of r for liquid hexane and liquid cyclohexane are 9·9 per cent. and 8 per cent. The values of r for benzene vapour and liquid are respectively 4·4 per cent. and 47 per cent., being thus considerably larger than for either hexane or cyclohexane. From the value of r the value of δ may be easily calculated for the substances mentioned.

Table I.

	Benzene.	Hexane.	Cyclohexane.
$\delta \times 10^{36}$ from vapour	77	28·6	14·5
$\delta \times 10^{36}$ from liquid { 1st formula, equation (5)	90	$8{\cdot}9_6$	6·5
$\delta \times 10^{36}$ from liquid { 2nd formula, equation (6)	45	5·3	3·6
Refractive index	1·505	1·378	1·429
C_m	$5{\cdot}90 \times 10^{-12}$	Not detectable	Not detectable

* K. S. Krishnan, 'Phil. Mag.,' vol. 50, p. 697 (1925).

It will be noticed that in the case of hexane and cyclohexane, δ for the liquid is strikingly less than δ for the vapour. The difference is not so conspicuous in the case of benzene vapour and liquid, and, indeed, is of the opposite sign when formula (5) is used to calculate δ.

In the numerator of the expression for δ the expression

$$[(A - B)^2 + (B - C)^2 + (C - A)^2]$$

appears, while in that for the Cotton-Mouton constant the expression

$$[(A - B)(A' - B') + (B - C)(B' - C') + (C - A)(C' - A')]$$

occurs. It will be seen that the differences in the value of the Cotton-Mouton constant for the three substances are of a larger order of magnitude than those in the value of δ. The molecular refractivities and magnetic susceptibilities of the three substances are not very different. Hence, in order to explain the great differences in the value of the Cotton-Mouton constant, it is necessary to assume that the differences in the magnetic anisotropy of benzene and hexane are not less pronounced than the differences in their optical anisotropy. In fact, the data compel us to assume that hexane is practically isotropic magnetically, and that benzene, on the other hand, exhibits a remarkable degree of magnetic anisotropy.

An interesting sidelight on the relation between chemical structure and magnetic anisotropy of carbon compounds is furnished by the observations of Owen* and Honda and Také Sonê† on the diamagnetic properties of the element carbon in the two forms of diamond and graphite. These authors have found that diamond, as might be expected from the fact that it belongs to the cubic system, shows no diamagnetic anisotropy. Graphite, on the other hand, shows a very large magnetic anisotropy, its susceptibility parallel to the hexagonal axis being about seven times as large as in perpendicular directions.

5. *Calculation of the Cotton-Mouton Constant.*

In order to evaluate absolutely the value of the Cotton-Mouton constant, we shall now assume that the benzene molecule has an axis of optical symmetry. This seems justifiable, particularly in view of the fact that chemical evidence shows that the six carbon atoms and the six hydrogen atoms in the ring are all equivalent. If the ring were a plane structure, then the axis of symmetry would obviously be the six-fold axis perpendicular to the plane of the ring. On

* M. Owen, 'Ann. der Physik,' vol. 37, p. 657 (1912).

† Kôtarô Honda and Také Sonê, 'Sc. Rep. Tôhoku Imperial Univ.,' series I, vol 2, p. 25 (1913).

the other hand, even if the configuration of the molecule were a puckered ring in which alternate carbon atoms lie above and below a certain plane, the normal to this plane would still be an axis of optical symmetry. Ramanathan* has discussed the explanation of the optical anisotropy of the benzene molecule and given very good reasons for the belief that there is an optical axis of symmetry, and that the optical moment induced by the field of a light-wave in a direction parallel to this axis is considerably smaller than in directions perpendicular to it. If we combine this with the idea suggested by the case of graphite, that the diamagnetic susceptibility is numerically greater along this line than in perpendicular directions, we get a positive value for the Cotton-Mouton constant, as actually observed. The existence of an axis of optical symmetry makes A = B. The expressions for C_m and δ then reduce to

$$C_m = -\frac{(n_0^2-1)(n_0^2+2)}{60n_0\lambda kT}\cdot\frac{A-C}{2A+C}[3C' - (A'+B'+C')] \qquad (8)$$

and

$$\delta = 2\left(\frac{A-C}{2A+C}\right)^2. \qquad (9)$$

Now $A'+B'+C'$ is a constant proportional to the total susceptibility $= \theta$, say. Then C_m can be written in the form

$$C_m = -\frac{(n_0^2-1)(n_0^2+2)}{60n_0\lambda kT}\cdot(3C'-\theta)\sqrt{\frac{\delta}{2}}. \qquad (10)$$

We can easily compute the values of the Cotton-Mouton constant corresponding to different values for the ratio C'/θ. If $C' = \theta$, then the entire magnetic susceptibility of benzene is concentrated in one direction only; in other words, it is magnetisable only along the axis of optical symmetry. The ratio C'/θ thus represents the fraction of the total magnetic susceptibility concentrated along this axis. In row 2 of Table II the theoretical value of the Cotton-Mouton constant for different values of the ratio C'/θ is shown, the value of δ being derived from formula (5). In row 3 of Table II the theoretical values of the Cotton-Mouton constant are shown similarly, δ being derived from formula (6). The observed value of the Cotton-Mouton constant $= 5{\cdot}90 \times 10^{-13}$. A comparison of this value with those shown in the table indicates that according to either method of calculation we have to assume that a considerable proportion of the magnetic susceptibility of benzene is concentrated in one direction, in order that the observed and calculated values of the Cotton-Mouton constant might agree. According to row 2 we should find the ratio of

* K. R. Ramanathan, 'Roy. Soc. Proc.,' A, vol. 110, p. 123 (1926).

the susceptibility along the principal axis to that in perpendicular directions to be 17 : 10, while according to row 3 the ratio is 21 : 10.

Table II.—Observed Value of the Cotton-Mouton Constant $= 5{\cdot}90 \times 10^{-13}$.

		0·60	0·55	0·50	0·45	0·40	0·333
Cotton-Mouton constant calculated from—	formula (5) $\times 10^{13}$	12·6	10·2	7·85	5·49	3·14	0
	formula (6) $\times 10^{13}$	8·88	7·21	5·55	3·89	2·22	0

6. *Interpretation of the Observed Results.*

The remarkable magnetic anisotropy of the benzene ring indicated by the foregoing investigation demands an explanation. In the entire structure of the molecule we have 42 electrons in all outside the atomic nuclei. Of these, 12 electrons belong to the K rings of carbon, and the size of their orbits is so small that they cannot contribute appreciably to the diamagnetic susceptibility of the molecule. We are thus left with 30 electrons which contribute to magnetic susceptibility and can or may take part in the chemical binding of the atoms. Pauling* has recently suggested a plane structure for the benzene ring in which 12 electrons are held in pairs in orbits binding the carbon and hydrogen atoms, 12 electrons in pairs connect the neighbouring carbon atoms, and the 6 remaining electrons form three pairs which connect each carbon atom with the one opposite to it directly across the ring. This structure would make the molecule diamagnetic. If we make the further assumption that at least 12 of the electron orbits are in the plane of the ring, we would have an explanation of the observed magnetic anisotropy of the molecule. If, on the other hand, the molecule is not a plane structure but is a puckered ring, an even larger proportion of the orbits may be orientated in planes approximately parallel to the ring consistently with its observed magnetic anisotropy.

7. *Some Benzene Derivatives.*

When one or more of the hydrogen atoms in benzene is replaced by other atoms or groups, we shall no longer be justified in taking the optical ellipsoid of the molecule to be a spheroid of revolution. If, however, the replacing atoms or groups are not themselves strongly anisotropic optically, we may, as a rough approximation, assume the derivative to have an optical axis of symmetry and

* L. Pauling, 'Jour. Am. Chem. Soc.,' vol. 48, p. 1139 (1926).

calculate the magnetic anisotropy of the molecule in the same way as was done in the case of benzene. Instead of following the latter procedure, however, it would perhaps be of greater interest to attempt to calculate the Cotton-Mouton constant for these derivatives, assuming that the atoms or groups which replace the hydrogen to be magnetically isotropic, and leave the magnetic anisotropy of the rest of the benzene ring unaffected. Let us take, for example, ethyl benzene ($C_6H_5 . C_2H_5$). It has already been mentioned that the aliphatic hydrocarbons exhibit a much smaller magnetic anisotropy, if any, than the aromatics. Hence to a first approximation we may assume that the contribution from the ethyl radical to the magnetic susceptibility of the molecule would be the same along the three optic axes. If, also, the contribution from the benzene ring to the susceptibilities along these axes be supposed to be unaffected, it will easily be seen that the factor $(3C' - \theta)$ in expression (10) will remain unaltered, since the increase in C' will be a third of the increase in θ. Thus the expression for the Cotton-Mouton constant reduces to

$$C_m = \text{constant} \times \frac{(n_0^2 - 1)(n_0^2 + 2)}{n_0} \sqrt{\delta}. \qquad (11)$$

The constant can be evaluated from the observed value of C_m for benzene, and will be different according as we use formula (5) or (6) for calculating δ. The values of the Cotton-Mouton constant so calculated are given in Table III. The

Table III.

Liquid.	Depolarisation factor × 100.	Refractive index for 0·578μ	Susceptibility per gram molecule × − 10^6	$\delta \times 10^2$		Cotton-Mouton constant × 10^{10}.		
						Calculated		
				from formula (5)	from formula (6)	using δ from formula (5)	using δ from formula (6)	Observed.
Benzene	47	1·505	5·74	90	45	5·9	5·9	5·90
Toluene	51	1·499	6·99	86	43	5·7	5·7	6·20
Ethyl benzene	53	1·498	8·20	78	39	5·4	5·4	5·44
m-Xylene	57	1·501	8·21	95	48	6·0	6·0	6·33
p-Xylene	58	1·498	8·21	103	52	6·2	6·2	6·83
Chlorobenzene	58	1·528	7·52	111	53	6·9	6·8	7·29
Bromobenzene	63·5	1·563	8·62	137	63	8·3	8·0	6·50
Aniline	60	1·589	6·51	92	40	7·2	6·7	4·03
Benzyl chloride	56	1·542	8·76	78	37	6·0	5·8	6·12
Benzal chloride	52	1·568	10·55	57	26	5·4	5·2	6·02

air agreement between the calculated and observed values shows that in all these cases, except perhaps those of aniline and bromobenzene, our assumptions are not far from the truth.

8. *Summary.*

The paper contains a discussion of the magnetic double-refraction exhibited by liquid benzene and some of its derivatives on the basis of the Langevin theory, utilising the data for optical anisotropy of the molecules derived from observations on light-scattering. The following is a summary of the results obtained :—

(1) A comparison of magnetic double-refraction and light-scattering by hexane, cyclohexane and benzene shows that the differences between the aromatic and the aliphatic hydrocarbons in respect of magnetic anisotropy must be even more pronounced than their differences in respect of their optical anisotropy.

(2) Making the justifiable assumption that the optical ellipsoid of the benzene molecule is an oblate spheroid of revolution, it is shown that the observed value of the Cotton-Mouton constant can only be explained on the assumption that the molecule exhibits a very pronounced magnetic anisotropy, the susceptibility in the direction of the axis being about twice as large as in perpendicular directions.

(3) As an explanation of this result, it is suggested that at least 12 of the electron orbits binding the atoms in the molecules must be orientated in a plane parallel to the ring.

(4) The absolute value of the Cotton-Mouton constant has been calculated for some of the simpler benzene derivatives in which it can be assumed without serious error that the optical ellipsoid is still a spheroid of revolution, and that the group which replaces the hydrogen atom is magnetically isotropic. The calculated and observed values are in fair agreement.

LXXI. *Electric Double-Refraction in Relation to the Polarity and Optical Anisotropy of Molecules.*—Part I. *Gases and Vapours.* *By* Prof. C. V. Raman, *F.R.S.*, *and* K. S. Krishnan *.

1. *Introduction.*

As is well known, Kerr discovered that fluids when placed in an electrostatic field exhibit a feeble birefringence. The accepted explanation of the effect is that the electrostatic field exercises an orientative influence on the molecules, that the latter possess an intrinsic optical anisotropy, and that, in consequence of the molecular orientation, the fluid as a whole becomes optically anisotropic. In

* Communicated by the Authors.

the original form of the theory, due to Langevin, it is assumed that the molecules are both electrostatically and optically anisotropic, and that the orientative action of the field is due to the couple exerted by it on the induced doublets in the molecules. In the later form of the theory, due to Born *, the orientative effect exerted by the field on the permanent electric doublet, if any, present in the molecule is also taken into account. We propose in the series of papers of which this is the first, to discuss the available data regarding electric double-refraction in the light of these theories, and to corrrelate them with what is known regarding the optical anisotropy of molecules from observations on light-scattering, and regarding the permanent electric moment from the observed variation of the dielectric constant with temperature.

2. *The Kerr Constant Data for Gases and Vapours.*

The simplest case to consider is naturally that of gases and vapours, as here the mutual influence of the molecules is negligible. The available data regarding the Kerr constant in the gaseous state are, however, very scanty, and the corresponding data regarding light-scattering have also not been obtained for all the substances. The variation of dielectric constant with temperature is also not known for many vapours. Such figures as are available are, however, very interesting, and are collected together in Table I. The second column gives the Kerr constant for the sodium line for one atmosphere pressure at 20° C., compiled from the measurements of Leiser †, Hansen ‡, and Szivessy §. Column 3 gives the ratio, r, of the components of polarization in the light transversely scattered by the vapours, when the incident light is unpolarized, from the measurements by Rayleigh ‖, Cabannes ¶ and others. The last column gives the permanent electric moments of the molecules as calculated by Zahn ** and others.

* For a good account of the subject, see P. Debye, Marx's 'Handbuch der Radiologie,' Bd. vi. pp. 754–776.

† R. Leiser, *Ver. d. Deutsch. Phys. Gesell.* xiii. p. 908 (1911).

‡ D. E Hansen, quoted by G. Szivessy, *Jahrbuch der Radioaktivität*, xvi. p. 414 (1920).

§ G. Szivessy, *Zeits. f. Phys.* xxvi. p. 328 (1924).

‖ Lord Rayleigh, Proc. Roy. Soc. A, xcv. p. 155 (1918).

¶ J. Cabannes and J. Granier, *Comptes Rendus*, clxxxii. p. 885 (1926); *Journ. d. Physique* [VI], p. 429 (1923). See also K. R. Ramanathan and N. G. Srinivasan, Phil. Mag. i. p. 491 (1926), and W. H. Martin and A. F. W. Cole, Chem. Abs. xx. p. 1752 (1926).

** C. T. Zahn, Phys. Rev. xxvii. p. 455 (1926); and also C. P. Smyth, Journ. Amer. Chem. Soc. xlvi. p. 2151 (1924).

TABLE I.

Gas or Vapour.	Kerr const. for the D line for 1 atm. press. at 20° C., K×10¹⁰.	Depolarisation factor, r×100.	Approximate value of the permanent moment, ×10¹⁸.
Ethyl chloride	8·7	1·64	2·3 (?)
Methyl bromide.....	8·2	.....	Polar.
Acetaldehyde	10·0	.....	1·69 (from liquid at 10° C.).
Methyl chloride.....	5·45	1·52	Polar.
Ethyl nitrate	15·0	.....	1·57 (from liquid at 20° C.)
Phosgene.....	1·4	.....	.....
Carbon dioxide	0·24 (at 17°·5 C.).	9·8	Non-polar.
Cyanogen	0·68	12·0 (?)	0·62 (from liquefied gas at 23° C.).
Hydrogen cyanide.....	14·7	.....	1·22 (from liquid at 21° C.).
Acetylene	0·29	4·6	Non-polar.
Ammonia	0·59 (at 17°·9 C.).	1·0	1·44
Nitrous oxide	0·48	12·2	Non-polar.
Chlorine	0·35	4·1	Non-polar.
Hydrogen chloride ...	0·90	1·0	1·03
Hydrogen sulphide ...	0·26	1·0	1·02
Sulphur dioxide.....	−1·67 (at 17°·3 C.).	4·9 (?)	1·61
Nitrogen	No appreciable double refraction at 2 atm. press.	3·75	Non-polar.
Oxygen		6·45	Non-polar.
Nitric oxide		2·6	Slightly polar.
Carbon monoxide		3·4	Almost non-polar ($\mu = 0{\cdot}13 \times 10^{-18}$).

It is very significant that all the substances which possess a large Kerr constant have molecules which are electrically polar. Amongst the non-polar molecules, the gases CO_2 and N_2O are distinguished by the possession of a large optical anisotropy, as will be evident from the values of the depolarization factor in column 3 of the table, and yet, as will be seen from the data, they exhibit only a relatively feeble Kerr effect; oxygen, which is strongly anisotropic

optically but is also non-polar, shows hardly any observable Kerr effect. This suggests immediately that, in the case of molecules which are electrically polar, the orientative influence of an electrostatic field is chiefly due to the couple exerted on the permanent electric doublet present in the molecule. The expression for the Kerr constant of a vapour sufficiently rare to obey Boyle's law is

$$K = \frac{n_p - n_s}{\lambda E^2} = \frac{3\pi\nu}{\lambda}(\theta_1 + \theta_2), \quad \ldots\ldots (1)$$

where ν is the number of molecules per unit volume, λ is the wave-length of the incident light, E the acting electrostatic field, and n_p and n_s are the refractive indices for light-vibrations along and perpendicular to the field.

$$\theta_1 = \frac{1}{45kT}[(A-B)(A'-B') + (B-C)(B'-C') + (C-A)(C'-A')], \quad (2)$$

and $$\theta_2 = \frac{1}{45k^2T^2}[(A-B)(\mu_1^2-\mu_2^2) + (B-C)(\mu_2^2-\mu_3^2) + (C-A)(\mu_3^2-\mu_1^2)], \quad (3)$$

where k is the Boltzmann constant per molecule; T is the absolute temperature; A, B, C are the moments induced in a molecule along its three principal axes of optical anisotropy by unit electric force in the incident light-waves acting respectively along these directions; A′, B′, C′ are similar moments induced along the same three directions by unit *electrostatic* field; and μ_1, μ_2, μ_3 are the components along these directions of the permanent electric moment of the molecule.

3. *Electrically Non-Polar Molecules.*

For a non-polar molecule such as CO_2, $\theta_2 = 0$ and we are only concerned with θ_1. It is not unreasonable in such cases to assume, as has been done by Gans*, that

$$\frac{A'}{A} = \frac{B'}{B} = \frac{C'}{C}.$$

Then this ratio $= \frac{\delta - 1}{n_0^2 - 1}$, where δ is the dielectric constant of the vapour and n_0 is the refractive index of the vapour

* R. Gans, *Ann. der Physik*, lxv. p. 97 (1921).

outside the field. The expression (2) for θ_1 therefore reduces to

$$\theta_1 = \frac{1}{45kT}\frac{\delta-1}{n_0^2-1}[(A-B)^2+(B-C)^2+(C-A)^2]. \quad (4)$$

Now, from the theory of light-scattering by optically anisotropic molecules the factor of depolarization, r, of the transversely-scattered light is given by

$$r = \frac{6[(A-B)^2+(B-C)^2+(C-A)^2]}{10\left[\frac{3(n_0-1)}{2\pi\nu}\right]^2+7[(A-B)^2+(B-C)^2+(C-A)^2]}. \quad (5)$$

From (1), (4), and (5) we may readily obtain as the relation between the Kerr constant and the factor of depolarization

$$K = \frac{3(n_0-1)(\delta-1)}{4\pi\nu\lambda kT}\cdot\frac{r}{6-7r}. \quad . \quad . \quad . \quad (6)$$

Table II. gives the values of the Kerr constant calculated from r according to this expression, for a few non-polar molecules for which data are available. The close agreement between the calculated and observed values shows the validity of the assumptions made.

TABLE II.

Gas or Vapour.	Depolarization factor, $r\times100$.	$(n_0-1)\times10^4$ for D line per atm. at 20° C.	$(\delta-1)\times10^4$ per atm. at 20° C.	Kerr constant per atm. at 20° C. $K\times10^{10}$.	
				Calculated.	Observed.
Carbon dioxide ...	9·8	4·18	8·93	0·28	0·24 (at 17°·5 C.).
Nitrous oxide	12·2	4·73	10·6	0·48	0·48
Acetylene	4·6	5·62	12·43	0·23	0·29
Chlorine	4·1	7·28	.....	0·30	0·35
Nitrogen	3·75	2·79	5·40	0·04	Not appreciable.
Oxygen	6·45	2·52	5·06	0·06	
Carbon monoxide.	3·4	3·12	6·38	0·05	

4. *Polar Molecules: Determination of Electric Moment.*

For polar molecules θ_1 is usually small in comparison with θ_2; and since it appears as a small correction term in the expression for the Kerr constant, we may, to a sufficient

approximation, determine θ_1 in the same way as for non-polar molecules. There is one difference, however, between the two cases: for non-polar molecules the ratio $\frac{A'}{A} = \ldots = \frac{\delta-1}{n_0^2-1}$, where δ is the *observed* dielectric constant; for polar molecules, on the other hand, this ratio $= \frac{\epsilon-1}{n_0^2-1}$, where ϵ is the contribution to the dielectric constant δ from the *induced* electric moments alone of the molecules, the contributions from the permanent moments being entirely omitted. ϵ can be evaluated from the temperature variation of the dielectric constant at a constant density by means of the well-known formula of Debye,

$$\delta = \epsilon + \frac{a}{T}, \quad . \quad . \quad . \quad . \quad . \quad . \quad . \quad (7)$$

where a is a constant for the molecule independent of the temperature. Theoretically, ϵ should be equal to the square of the refractive index extrapolated for infinite wave-length, provided, of course, the values of refractive index used for extrapolation refer to a region of the spectrum far removed from absorption bands.

θ_2, however, cannot be evaluated completely unless we know the position of the permanent electric moment and the form of the optical ellipsoid of the molecule. In the simple cases, however, when the optical ellipsoid is a spheroid of revolution, say B = C, and the permanent moment is either parallel to the axis of the spheroid (*i. e.* the A-axis) or is inclined to it at some known angle α, θ_2 can be connected numerically with the optical anisotropy of the molecule as determined from observations on light-scattering. Thus, in expression (3) for θ_2, putting B = C and $\mu_1^2 = \mu^2\cos^2\alpha$ and $\mu_2^2+\mu_3^2 = \mu^2\sin^2\alpha$, and using eqn. (5), we have

$$\theta_2 = \pm\frac{(n_0-1)\mu^2}{30\pi\nu k^2T^2}(2\cos^2\alpha-\sin^2\alpha)\sqrt{\frac{5r}{6-7r}}, \quad (8)$$

the + or − sign being taken according as the optical ellipsoid is prolate or oblate, *i. e.* according as $A \gtrless B\,(=C)$.

Thus we get a simple relation connecting the Kerr constant with the factor of depolarization and the permanent moment of the molecules. Instead of calculating the Kerr constant, however, it would be of greater interest to calculate the permanent moments from the known values of K and r; and we give here as examples the calculations for a few simple cases.

(1) *HCl.*—From direct considerations of symmetry the optical ellipsoid will be one of revolution about the line joining the H- and Cl-nuclei, and this direction will also be the axis of the electric doublet of the molecule. Now let us assume with Bragg * that the optical anisotropy of a molecule is due, at least in a large measure, to the mutual influence of the electric doublets induced in the different atoms of the molecule by the field of the light-waves. In the case of HCl it directly follows that the optical polarizability of the molecule along the line of the nuclei will be greater than for perpendicular directions; *i. e.*, $A > B = C$ and $\alpha = 0$.

From Table I. $K = 0{\cdot}90 \times 10^{-10}$ per atm., from which we get, using eqn (1),

$$\theta_1 + \theta_2 = 2{\cdot}23 \times 10^{-25};$$

while from the value $r = 0{\cdot}010$ for the depolarization factor,

$$\theta_1 = 0{\cdot}07 \times 10^{-25},$$

so that

$$\theta_2 = 2{\cdot}16 \times 10^{-25};$$

and hence we obtain

$$\mu = 1{\cdot}04 \times 10^{-18} \text{ E.S.U.},$$

agreeing perfectly with the value

$$\mu = 1{\cdot}03 \times 10^{-18} \text{ E.S.U.}$$

obtained recently by Zahn from dielectric constant measurements.

(2) *CH_3Cl.*—Here the three H-atoms may reasonably be assumed to lie at the corners of an equilateral triangle, the C- and Cl-atoms lying on a line drawn through the centroid of the triangle perpendicular to its plane. Considerations of symmetry require the axis of the permanent doublet to be along the latter line and the optical ellipsoid to be one of revolution about this line, which, on actual calculation of the optical anisotropy by Bragg's method, is found to be the major axis. Thus we have, as before,

$$A > B = C \quad \text{and} \quad \alpha = 0.$$

The value $K = 5{\cdot}45 \times 10^{-10}$ per atm. gives

$$\theta_1 + \theta_2 = 1{\cdot}35 \times 10^{-24}.$$

* W. L. Bragg, Proc. Roy. Soc. A, cv. p. 370 (1924); cvi. p. 346 (1924). See also K. R. Ramanathan, same Proc. cvii. p. 684 (1925).

From $r = 0{\cdot}0152$

$$\theta_1 = 0{\cdot}03 \times 10^{-24};$$

$$\therefore \quad \theta_2 = 1{\cdot}32 \times 10^{-24},$$

whence

$$\mu = 1{\cdot}66 \times 10^{-18} \text{ E.S.U.}$$

(3) *C_2H_5Cl.*—Here there is some uncertainty regarding the form of the optical ellipsoid. However, we shall assume for simplicity

$$A > B = C \quad \text{and} \quad \alpha = 0.$$

From the values in Table I. we get, as before,

$$\theta_1 + \theta_2 = 2{\cdot}16 \times 10^{-24},$$

$$\theta_1 = 0{\cdot}07 \times 10^{-24};$$

$$\theta_2 = 2{\cdot}09 \times 10^{-24},$$

which corresponds to

$$\mu = 1{\cdot}76 \times 10^{-18} \text{ E.S.U.}$$

It has already been mentioned that θ_2 is usually large in comparison with θ_1. The above calculation shows that actually, in the cases of HCl and C_2H_5Cl, θ_2 is 30 times larger than θ_1, and for CH_3Cl it is about 40 times larger.

Regarding CH_3Cl and C_2H_5Cl, we have no reliable data for the dielectric constant from which to calculate the permanent moment independently and compare with the values obtained here. However, we have no reason to doubt that they are the proper values (especially for CH_3Cl). In fact, in certain special cases where we can be certain about the form of the optical ellipsoid and the position of the axis of the electric doublet, this method of calculating the electric moment of the molecule promises to be at least as sensitive as the dielectric constant method. Thus, for instance, in the case of CH_3Cl Hansen gives the value of the Kerr constant relative to carbon bisulphide liquid to three significant digits. Assuming therefore that the value is correct to 3 per cent. (which would admit of an error as high as 6 per cent. in the measurement of r), the calculated value of the permanent moment will be correct to less than 2 per cent.

5. *Polar Molecules*: *Determination of Electric Axis.*

In the case of molecules having an axis of optical symmetry, to which the permanent doublet is inclined at a known angle, we have seen that it is possible to calculate the

permanent moment from the value of the Kerr constant and the constant of depolarization of the scattered light. *Vice versa*, if the moment is known from measurements of the dielectric constant, the inclination of the electric doublet to the optic axis can be found. The latter procedure promises to be of interest in certain cases, *e. g.* some of the simple derivatives of benzene. Regarding the benzene molecule, we have strong reasons to believe that the optical ellipsoid is an oblate spheroid of revolution with its axis perpendicular to the plane of the ring*. If one or more of the H-atoms be replaced by other atoms or groups which are not themselves strongly anisotropic optically, we can still, to a first approximation, consider the derivative to have an axis of optical symmetry; and thus, if we know the values of the Kerr constant, of the factor of depolarization, and of the permanent moment, we can locate the direction of the moment with respect to the axis. In the case of simple derivatives like chlorobenzene or bromobenzene, for example, it would be particularly interesting to ascertain whether the moment lies in the plane of the ring, since it might probably throw light on the vexed question whether the ring is plane or puckered. But, unfortunately, we have no data for the Kerr constant of any of the benzene derivatives in the vapour state, even though a fair number of them have been studied with respect to their light-scattering. However, we shall have something more to say on this point when we discuss the case of the liquids.

6. *Explanation of Negative Kerr Constants.*

Probably the strongest argument in favour of Born's theory of electric double-refraction is the natural explanation it offers for the negative value of the Kerr constant obtained in some cases. If the permanent electric moment of the molecule lies along directions of smaller optical polarizability of the molecule, then, owing to the couple exerted by the external field on the doublet, the molecule tends to orientate with the direction of smaller optical polarizability along the field. Hence the refractive index for light-vibrations parallel to the field is less than for vibrations perpendicular to it; i. e., $n_2 < n_0$ and the medium exhibits a negative double-refraction. It is significant in this connexion to note that in all cases in which the Kerr constant is negative the molecule is known to be electrically polar.

As an instructive illustration of the dependence of the sign of the Kerr effect on the constitution of the molecule,

* K. R. Ramanathan, Proc. Roy. Soc. A, cx. p. 123 (1926).

let us consider here the chloromethanes. Monochloromethane has a positive value for the Kerr constant, and this, we have seen, agrees with that expected from theoretical considerations. On the other hand, di- and tri-chloromethanes are known to exhibit a negative Kerr effect in the liquid state. We shall presently see that this is also in agreement with what we should expect on theoretical grounds.

(1) $CHCl_2$.—First let us take $CHCl_3$. Analogous to the structure of CH_3Cl, already mentioned, the three Cl-atoms may be assumed to lie at the vertices of an equilateral triangle with the C- and H-atoms on a line perpendicular to its plane. From direct considerations of symmetry it is obvious, as for CH_3Cl, that the optical ellipsoid of the molecule will be a spheroid of revolution with its axis along the line of the C- and H-atoms, which will also be the axis of the permanent doublet. Now, by far the greatest contribution to the refractivity of the molecule comes from the three chlorine atoms; and since they are in a plane, owing to the mutual influence of the doublets induced in them, the optical polarizability of the $CHCl_3$ molecule perpendicular to this plane will be smaller than for directions in the plane: *i. e.*, the optical polarizability of the molecule along the axis of its permanent doublet is less than for perpendicular directions. Hence its double-refraction in an electric field will be negative.

In our previous notation

$$A < B = C \quad \text{and} \quad \alpha = 0,$$

and it is obvious from eqn. (8) that θ_2 will be negative.

(2) CH_2Cl_2.—Here we may reasonably assume the two Cl-atoms to lie at the ends of a straight line and the two H-atoms at the ends of another, the two lines being perpendicular to each other and to the line joining their middle points. The C-atom will lie on the last line, which will also, from considerations of symmetry, be the axis of the electric doublet of the molecule. Regarding the optical ellipsoid of the molecule, we are obviously not justified, consistently with the above structure, in assuming an axis of symmetry. But since the contribution to the refractivity of the molecule from the C- and the two H-atoms is much smaller than the contribution from the two Cl-atoms, we may, without being altogether wide of the mark, consider the optical ellipsoid to be a prolate spheroid with its axis along the line joining the two Cl-atoms; *i. e.*, perpendicular to the axis of the electric

doublet. Hence we have

$$A > B = C \quad \text{and} \quad \alpha = \frac{\pi}{2};$$

so that here again, according to (8), θ_2 will be negative.

(3) *CH_3Cl.*—Here, as we have seen in para. (4) above,

$$A > B = C \quad \text{and} \quad \alpha = 0,$$

and hence θ_2 is positive.

More extensive data regarding the Kerr constant and light-scattering in gases and vapours with electrically polar molecules are obviously desirable, and we have initiated experimental work with this object.

7. *Summary.*

1. An attempt is made in this paper to correlate, on the basis of Born's theory of electric double-refraction (Kerr effect), the available data on the Kerr effect of gases and vapours, with the optical anisotropy of molecules as determined from observations on light-scattering, and with the polarity of the molecules as determined from dielectric constant measurements.

2. In the case of molecules which are electrically polar, it is found that the orientative action of an electrostatic field on the molecule is due chiefly to the couple exerted on the permanent electric doublet present, and is much larger than would be the case if the molecules were non-polar.

3. For non-polar molecules, with the simplifying assumptions of Gans regarding the relation between the constants of electric and optical anisotropy, we can calculate the values of the Kerr constant from the factor of depolarization of the scattered light in good agreement with the observed values.

4. In the case of polar molecules having an axis of optical symmetry, to which the permanent moment is parallel or is inclined at a known angle, it is possible to calculate the value of the moment from the Kerr constant and the factor of depolarization. Calculations are given for a few cases.

5. On the other hand, if the moment of the doublet is known, its direction can be determined from the same data. The applicability of the method to simple benzene derivatives is pointed out.

6. The significance of the negative value of the Kerr constant is discussed in the light of Born's theory, with special reference to its dependence on molecular structure, as evidenced in the chloromethanes.

210 Bowbazaar Street, Calcutta.
15th September, 1926.

LXXII. *Electric Double-Refraction in Relation to the Polarity and Optical Anisotropy of Molecules.*—Part II. *Liquids.* *By* Prof. C. V. Raman, *F.R.S.*, *and* K. S. Krishnan *.

1. *Introduction.*

In Part I.† the electric double-refraction (Kerr effect) in gases and vapours was discussed in relation to the optical anisotropy of molecules as determined from observations on light-scattering. It was found that in the case of electrically non-polar molecules their electrostatic anisotropy is sufficient to account for the orientative couple exerted by the field on them, and thus for the observed double-refraction. On the other hand, in the case of molecules known to be electrically polar, the orientative couple is in a large measure due to the permanent doublets present in them, and the actual magnitudes involved were shown in certain simple cases to be in quantitative agreement with what one should expect from Born's theory of the Kerr effect. In this part we propose to extend the discussion to the case of liquids. Here, of course, owing to our imperfect knowledge of the liquid state, the problem is more complicated. There are, however, certain prominent features of the phenomenon which are of interest, and admit of at least an approximate comparison between observation and theory.

2. *Kerr Constant Data in Liquids.*

The electric double-refraction in liquids has been studied extensively by Schmidt ‡, Leiser §, McComb ‖, and others, while data for the scattering of light in some 65 liquids (chiefly organic) are available from measurements made by K. S. Krishnan ¶. In the following Table (I.) are given the data for some typical cases. Column 2 gives the relative values of the Kerr constant, carbon bisulphide, as usual, being taken as 100; column 3 gives the factor of depolarization of the scattered light; and column 4 the values of the dielectric constant.

* Communicated by the Authors.

† *Suprà*, p. 718.

‡ W. Schmidt, *Ann. der Physik*, vii. p. 142 (1902).

§ For collected data, see H. Kauffmann, 'Beziehungen zwischen physikalischen Eigenschaften und chemischer Konstitution,' Enke, Stuttgart, 1920, pp. 385–389.

‖ H. E. McComb, Phys. Rev. xxix. p. 525 (1909).

¶ K. S. Krishnan, Phil. Mag. l. p. 697 (1925).

TABLE I.

Liquid.	Kerr constant, $CS_2=100$.	Depolarization factor, $r \times 100$.	Dielectric constant δ at 20° C.
Hexane	1·73	9·9	1·729
Cyclohexane	2·30	8	2·05
Heptane	3·26	11·4	.. ...
Octane	4·21	12·9	1·945
β-iso amylene	7·9	25·8	2·191
Propyl chloride	234	16·3	7·70
Methylene chloride	−36	31	8·3
Ethylene chloride	146	36	9·96
Chloroform	−103	24·0	4·853
Carbon tetrachloride	2·3	5·3	2·190
Carbon bisulphide	100	68·5	2·593
Acetic acid	130	45·5	6·02
Propionic acid	43	41	3·12 (at 18° C.)
Ethyl ether	−19·2	8·0	4·351
Benzene	18·4	47	2·284
Toluene	23·3	51	2·368
Ethyl benzene	23·4	53	2·417
m-Xylene	26·6	56	2·392
p-Xylene	22·6	58·3	2·15
Chlorobenzene	280	57·5	5·65
Bromobenzene	280	63·5	5·2
Nitrobenzene	7900	74	36·95
Aniline	−38	60	6·936
o-Nitrotoluene	5400	82	26·2
m-Nitrotoluene	5520	83	23·6
Benzyl alcohol	−477	62	13·0
Water	123	8·5	80·5
Methyl alcohol	30	6·0	31·2
Ethyl alcohol	23·8	5·3	25·8
Propyl alcohol	−78	7·1	22·2
Butyl alcohol	−113	9·3	19·2
Isobutyl alcohol	−111	7·3	20·0
Trimethyl carbinol	154	4·1	11·4
Ethyl formate	138	21·3	8·27
Ethyl acetate	52	23·0	6·11
Acetone	505	20·0	22·58

It will be seen that, just as in the case of vapours, all the liquids which have a large Kerr constant are characterized by the possession of strongly polar molecules, as will be evident from the dielectric constant data in column 4. In fact, the variations in the values of the Kerr constant are even more pronounced than in the case of vapours. This is really what we should expect from theoretical considerations. The influence of the electrical polarity of the molecules on the Kerr effect is here twofold. One is its direct contribution to the orientative couple exerted on the molecule by the external field, just as in the gaseous state. The other arises in the following way: owing to the influence of neighbouring molecules, the actual field tending to orientate any particular molecule is $\frac{\delta+2}{3}$ times the external imposed field, where δ is the dielectric constant. Since, in the case of polar molecules, the value of the dielectric constant is large, and since the double refraction varies as the square of the acting field, the enormous influence of the polarity of the molecules on the magnitude of the Kerr effect is readily understood.

The theoretical expression for the Kerr constant of a liquid is

$$K = \frac{\pi\nu(n_0^2+2)^2}{3n_0\lambda}\left(\frac{\delta+2}{3}\right)^2(\theta_1+\theta_2), \quad . \quad . \quad . \quad (1)$$

where the different letters have the same significance as in Part I., θ_1 and θ_2 being given, as before, by the relations

$$\theta_1 = \frac{1}{45kT}[(A-B)(A'-B') + (B-C)(B'-C') + (C-A)(C'-A')], \quad . \quad (2)$$

$$\theta_2 = \frac{1}{45k^2T^2}[(A-B)(\mu_1^2-\mu_2^2) + (B-C)(\mu_2^2-\mu_3^2) + (C-A)(\mu_3^2-\mu_1^2)]. \quad . \quad (3)$$

For convenience we shall denote the term on the right-hand side of equation (1), which is proportional to θ_1, by K_1, and the term proportional to θ_2 by K_2, so that

$$K = K_1 + K_2.$$

3. *Non-Polar Molecules.*

In the case of non-polar molecules $\theta_2=0$, and with the assumptions of Gans regarding the relation between the

constants of electrostatic and optical anisotropy, viz., $\frac{A'}{A}=\frac{B'}{B}=\frac{C'}{C}$, this ratio $=\frac{\delta-1}{\delta+2}\Big/\frac{n_0^2-1}{n_0^2+2}$, and hence the expression for θ_1 reduces to

$$\theta_1=\frac{1}{45kT}\frac{\delta-1}{\delta+2}\cdot\frac{n_0^2+2}{n_0^2-1}[(A-B)^2+(B-C)^2+(C-A)^2]. \quad (4)$$

It remains to evaluate the constants of optical anisotropy in the above expression from scattering measurements. It might be imagined that the anisotropic constants would be characteristic of the molecule, and could thus be easily evaluated from the vapour state, as in Part I.; but, as a matter of fact, owing probably to temporary molecular groupings, the optical anisotropy calculated from the liquid state is, in general, found to be less than that calculated from the vapour; and in any discussion concerning the liquids it is only appropriate that we should use the former value for the optical anisotropy. Two slightly different expressions have been proposed connecting the depolarization factor r with the constants of optical anisotropy—

$$r=\frac{6[(A-B)^2+(B-C)^2+(C-A)^2]}{10kT\beta\nu\left(\frac{n_0^2+2}{3}\right)^2(A+B+C)^2+7[(A-B)^2+(B-C)^2+(C-A)^2]} \quad (5a)$$

and

$$r=\frac{6[(A-B)^2+(B-C)^2+(C-A)^2]}{10kT\beta\nu(A+B+C)^2+7[(A-B)^2+(B-C)^2+(C-A)^2]}, \quad (5b)$$

where β is the isothermal compressibility and $(A+B+C)$ is given by the relation

$$\frac{n_0^2-1}{n_0^2+2}=\frac{4\pi}{3}\nu\frac{A+B+C}{3}. \quad (6)$$

Since the experimental data available at present are not sufficient to decide definitely between the two expressions *, we shall use both of them here. From (4) and (5) we thus have

$$\theta_1=\frac{9\beta(\delta-1)(n_0^2-1)}{8\pi^2\nu(\delta+2)(n_0^2+2)}\cdot\left(\frac{n_0^2+2}{3}\right)^2\cdot\frac{r}{6-7r} \quad (7a)$$

or

$$\theta_1=\frac{9\beta(\delta-1)(n_0^2-1)}{8\pi^2\nu(\delta+2)(n_0^2+2)}\cdot\frac{r}{6-7r}, \quad (7b)$$

* See K. S. Krishnan, Proc. Ind. Assn. Sc. ix. p. 251 (1926).

and hence

$$K=\frac{\beta(n_0^2-1)(n_0^2+2)(\delta-1)(\delta+2)}{24\pi n_0\lambda}\left(\frac{n_0^2+2}{3}\right)^2\cdot\frac{r}{6-7r} \quad (8a)$$

or

$$K=\frac{\beta(n_0^2-1)(n_0^2+2)(\delta-1)(\delta+2)}{24\pi n_0\lambda}\cdot\frac{r}{6-7r}. \quad (8b)$$

Table II. shows the values of the Kerr constant calculated according to these expressions for all the non-polar liquids for which we have the necessary data.

TABLE II.

Liquid.	r $\times 100$.	n_0.	δ.	Kerr constant $\times 10^7$. Calculated according to (8a)	Calculated according to (8b)	Observed.
Pentane	7·5	1·356	...	0·082	0·050	0·050
Isopentane	5·6	1·353	...	0·059	0·036	0·050
Hexane	9·9	1·375	1·729	0·074	0·044	0·045 0·056
Cyclohexane	8	1·427	2·05	0·080	0·044	0·074
Heptane	11·4	1·386	...	0·102	0·060	0·071 0·105
Octane.....	12·9	1·397	1·945	0·116	0·067	0·077 0·136
Carbon tetrachloride.	5·3	1·461	2·190	0·068	0·036	0·074
Carbon bisulphide ...	68·5 64·0	1·627	2·593	9·79 7·24	4·08 3·02	3·226
Benzene	47	1·501	2·284	1·45	0·72	0·593
m-Xylene	56	1·497	2·392	2·20	1·10	0·858
p-Xylene	58·3	1·496	2·15	1·96	0·98	0·74 0·73

All the constants refer to the D line and 20° C.

Considering the uncertainties in the evaluation of the anisotropic constants from r, the agreement between the calculated and observed values in Table II. should be considered satisfactory. Equation (8*b*), which corresponds to the relation (5*b*) for the optical anisotropy, gives better agreement in the case of highly refractive liquids. In the

following discussion we shall use the same expression for the anisotropy consistently; the main conclusions, however, will not be seriously affected when the relation (5 *a*) is used.

Polar Molecules.

Here also θ_1 can be evaluated in the same way as for non-polar molecules, the ratio $\frac{A'}{A} = \ldots$ being now equal to $\frac{\epsilon-1}{\epsilon+2}\Big/\frac{n_0^2-1}{n_0^2+2}$, where ϵ is given by Debye's relation

$$\frac{\delta-1}{\delta+2} = \frac{\epsilon-1}{\epsilon+2} + \frac{4\pi}{3}\nu\frac{\mu^2}{3kT}. \quad . \quad . \quad . \quad . \quad (9)$$

μ is the "effective value" of the permanent electric moment of the molecule, which is different in general from the real moment of the individual molecules, owing to the well-known phenomenon of association of polar molecules; its actual magnitude varies naturally with temperature. Hence ϵ can not be evaluated easily from the temperature dependence of the dielectric constant, as in the vapour state; but it is possible to calculate it on the basis of Debye's dipole-theory from dielectric constant measurements at different temperatures of very dilute solutions of the liquid in a non-polar solvent like benzene, carbon bisulphide, or carbon tetrachloride*. However, for the purpose of our present discussion we can take ϵ to a first approximation to be equal to the square of the refractive index extrapolated for zero frequency.

Thus we obtain the relation

$$K_1 = \frac{\beta(n_0^2-1)(n_0^2+2)(\epsilon-1)(\delta+2)^2}{24\pi n_0\lambda(\epsilon+2)}\frac{r}{6-7r}. \quad (10)$$

The problem of determining θ_2, however, is very complicated. It is possible to evaluate θ_2 only when we know the form of the optical ellipsoid and the position of the permanent electric moment. Even in the gaseous state, where these quantities refer to the *individual molecules*, our information regarding them extends only to very simple cases. When, on the other hand, we have to deal, as in the liquid state, with certain "effective values" of these quantities which, we have *prima facie* reasons to believe, can no longer be identified with the values for the individual molecules, the problem is naturally very complicated. We

* See P. Debye, *Handbuch der Radiologie*, Bd. vi. p. 633.

have therefore to limit ourselves to a more or less general discussion.

Let us first consider a somewhat simple case, say chloroform. It has already been shown in Part I. that the optical ellipsoid of the $CHCl_3$ molecule is an oblate spheroid of revolution, with the permanent doublet along its axis.

The value of the permanent moment calculated according to equation (9) from the dielectric constant for the liquid at 20° C., taking ϵ to be equal to the square of the refractive index extrapolated for infinite wave-length, comes out to be equal to $1{\cdot}07\times10^{-18}$ e.s.u., which is slightly less than the value $1{\cdot}25\times10^{-18}$ calculated by Smyth* from the vapour.

Also the optical anisotropy, defined by, say,

$$\frac{(A-B)^2+(B-C)^2+(C-A)^2}{(A+B+C)^2},$$

calculated from the liquid state = ·017, as against ·028 from the vapour.

For reasons already indicated we shall take the former value and assume that the axis of the electric moment has the same position in the molecule as in the state of vapour. On calculation we get

$$K_1 = 0{\cdot}47\times10^{-7} \quad \text{and} \quad K_2 = -5{\cdot}9\times10^{-7},$$

$$\text{and therefore} \quad K = -5{\cdot}4\times10^{-7},$$

as compared with the observed value $-3{\cdot}32\times10^{-7}$. The assumption made in the calculation that the permanent doublet is along the direction of minimum optical polarizability would give to the calculated Kerr constant the maximum possible negative value. If, however, owing to molecular association in the liquid state, the position of the effective moment is altered, the calculated value of the Kerr constant would be diminished, and would then agree better with the observed value. Even as it stands, the results of the calculation furnish strong support to Born's expression for the Kerr constant in preference to that due to Langevin. The latter gives for chloroform the value $+1{\cdot}02\times10^{-7}$, which has the wrong sign, and is also numerically much smaller than the observed value.

A negative value for the Kerr constant cannot be explained on the basis of Langevin's theory unless we make the improbable assumption that the maximum electrostatic polarizability of the molecule is along directions of smaller

* C. P. Smyth, Journ. Am. Chem. Soc. xlvi. p. 2151 (1924).

optical polarizability—an assumption which cannot be reconciled with the ideas of Bragg regarding the cause of electrostatic and optical anisotropy, viz., as being due to atomic interaction.

5. *The General Case.*

In general there is considerable uncertainty both as regards the form of the optical ellipsoid and the position of the permanent moment, even for the individual molecules. For the present we shall, for the purpose of tentative calculations, assume that the effective optical ellipsoid is a spheroid of revolution whose axis coincides with the axis of the permanent doublet, the spheroid being taken as prolate or oblate according as the Kerr constant is positive or negative. This would obviously be far from the truth in most cases, and it is not surprising that we find in several cases large differences between the calculated and observed values as shown in Table III. It is significant, however, that the calculated values are always numerically higher than the observed, which is what we should expect, as the assumptions made are such as make the calculated value of the Kerr constant numerically a maximum.

TABLE III.

Liquid.	$K_1\times10^7$.	$K_2\times10^7$.	Kerr constant $\times10^7$.	
			Calculated $=K_1+K_2$.	Observed.
Propyl chloride	0·72	16·3	17·0	7·55
Methylene chloride ...	1·26	−9·6	−8·3	−1·16
Ethylene chloride	2·12	35·5	37·6	4·71
Acetic acid	1·18	12·2	13·4	4·19
Propionic acid	0·38	2·3	2·7	1·39
Ethyl ether.....	0·22	−1·49	−1·27	−0·618
Ethyl formate	0·74	18·2	18·9	4·45
Ethyl acetate	0·49	10·4	10·9	1·68
Acetone	3·6	120	124	16·3

6. *Monohydric Alcohols.*

Since the value of the Kerr constant depends on the angle between the axis of the electric moment of the molecule and its optic axis, which in its turn depends on the chemical structure of the molecule, we should expect certain

similarities in the behaviour of molecules of the same type. That is actually what we find, for instance, in the case of the monohydric alcohols. Table IV. shows in column 2 the observed values of K; column 3 gives the values of K_1 calculated according to equation (10); column 4 gives $K-K_1=K_2$; and the last column gives the values of K_2 directly evaluated on the assumption that the optical ellipsoid is a prolate spheroid of revolution with the permanent moment perpendicular to the axis of the spheroid.

TABLE IV.

Liquid.	$K\times10^7$ observed.	$K_1\times10^7$.	$K-K_1=K_2\times10^7$.	$K_2\times10^7$ calculated directly.
Methyl alcohol	0·97	1·41	−0·44	−40
Ethyl alcohol.....	0·768	0·96	−0·19	−32
Propyl alcohol	−2·52	0·99	−3·51	−31
Butyl alcohol.....	−3·65	1·01	−4·66	−29
Isobutyl alcohol	−3·58	0·90	−4·48	−29

It will be seen that the values of K_2 in column 4 are far smaller numerically than the values calculated according to the above assumptions. Theoretically the contribution from the permanent moment to the Kerr constant will be nothing when it makes an angle of 54° 44′ with the axis of the optical spheroid (corresponding to the condition $2\cos^2\alpha-\sin^2\alpha=0$). The small values of K_2 in column 4 therefore suggest that in the case of the alcohols the permanent moments, instead of being perpendicular to the optical axis, are inclined to it at an angle not much greater than 55°. Indeed, there is reason to believe that in the monohydric alcohols the OH group, which is chiefly responsible for the polarity, is inclined to the hydrocarbon chain at an angle which may vary slightly with the length of the chain.

7. *Some Benzene Derivatives.*

Let us take another example—simple derivatives of benzene. As in Part I., the optical ellipsoids of these molecules can be roughly considered to be oblate spheroids of revolution. Table V. gives the calculations for some of

these molecules, assuming that the permanent moment is in the plane of the ring. In the case of aniline and benzyl alcohol, for which the Kerr constant is negative, the moment is taken to be perpendicular to the plane, a supposition which, however, is *a priori* much less probable than that of a moderate inclination to the plane of the ring.

TABLE V.

Liquid.	$K_1 \times 10^7$.	$K_2 \times 10^7$.	Kerr constant $\times 10^7$. Calculated $= K_1 + K_2$.	Kerr constant $\times 10^7$. Observed.
Toluene	0·80	0·31	1·11	0·753
Ethyl benzene	0·84	0·42	1·26	0·754
Chlorobenzene	3·15	10·3	13·5	9·1
Bromobenzene	3·99	10·0	14·0	9·1
Nitrobenzene	184	770	950	256
Aniline	3·74	−29	−25	−1·23
Benzyl alcohol	12·0	−130	−118	−15·4

For toluene and ethyl benzene the contribution from the electrical polarity of the molecule is very small. In other cases the calculated values of the Kerr constant are numerically larger than the observed values, thus pointing to an inclination of the permanent moments to the plane of the ring. Whether this inclination arises from a distortion, due to the heavy substituents, of the benzene ring, which is otherwise plane, or whether it is due to the fact that ths ring is puckered, and consequently the substituent atoms like Cl or Br are attached to the ring at an angle, cannot be decided without further data, especially for the vapour.

8. *Temperature Dependence of the Kerr Constant.*

We now come to the question of the variation of the Kerr constant of liquids with temperature. We have seen that the value of the optical anisotropy and of the permanent moment calculated from the liquid state is less than that calculated from the vapour. As the temperature is raised, the values continually approach the value for the vapour.

Therefore any discussion of the temperature dependence of the Kerr constant of liquids must naturally take this variation into account. However, since the scattering measurements are not available at different temperatures, we shall, to a first approximation, assume the anisotropic constants to be independent of temperature, and shall only take into consideration the change in the effective value of the permanent moment μ, as given by eqn. (9). We shall also suppose that when the effective value of μ changes, its position with respect to the optic axes is not altered. With these assumptions the expression for the Kerr constant can be written in the form

$$K \propto \frac{(n_0^2-1)(n_0^2+2)(\delta+2)^2}{n_0 T}\left(1+\phi\frac{\mu^2}{T}\right), \quad . \quad (11)$$

where ϕ is a constant independent of temperature. ϕ can be evaluated from the known values of the quantities involved, at 20° C.

Table VI. includes all the liquids whose Kerr constant has been investigated over a long range of temperature. Column 3 gives the ratio of the values of K at the extreme limits of the range of temperature over which they have been studied, calculated according to (11). The observed values of the ratio are given in column 4 for comparison.

TABLE VI.

Liquid.	Limits of the range of temperature over which investigated. t_1 (0° C.).	t_2 (0° C.).	Kerr const. at t_2° C. / Kerr const. at t_1° C. Calculated.	Observed.	Observer *.
Toluene	−78·5	18	0·56	0·58	L. W.
	−20	100	0·51	0·59	B.
Chlorobenzene	−20	100	0·30	0·39	B.
Bromobenzene	−20	100	0·33	0·41	B.
Nitrobenzene	5·5	25	0·76	0·74	S.
Ethyl ether	−78·5	18	0·17	0·26	L. W.
Chloroform	−20	55	0·40	0·42	B.

* L. W.—N. Lyon and F. Wolfram, *Ann. der Phys.* lxiii. p. 739 (1920).
B.—C. Bergholm, *Ann. der Phys.* lxv. p. 128 (1921).
S.—G. Szivessy, *Zeit. f. Phys.* ii. p. 30 (1920).

Considering the nature of the assumptions made, the agreement between the calculated and the observed values is quite satisfactory, so that measurements on the temperature dependence of the Kerr constant of liquids, far from disproving Born's expression, actually support it.

9. *Summary.*

1. In this part the discussion of the available data on electric double-refraction in relation to the polarity and optical anisotropy of the molecules is extended to the liquid state.

2. It is found that, just as in the case of vapours, all the compounds which exhibit a large Kerr effect are characterized by the possession of electrically polar molecules, the influence of the polarity on the Kerr constant being here even more pronounced than in the case of vapours.

3. In the case of non-polar molecules the moments induced in the molecules when placed in an electrostatic field are sufficient to account quantitatively for the observed double-refraction.

4. In simple cases of polar liquids like chloroform, where we have definite information regarding the form of the optical ellipsoid and the position of the electric moment, the observed Kerr constant is in numerical agreement with that calculated on the basis of Born's theory, which takes into account also the orientative couples exerted by the external field on the permanent doublets present in the molecules.

5. Even in the general case there is nothing to throw doubt on the validity of Born's theory. In the case of alcohols, for instance, the contribution from the permanent moments to the Kerr constant is found to be very small, and this is explained on the assumption of suitable positions for the permanent moment, which are not improbable from our knowledge of their structure. In the cases of benzene derivatives, also, the moments are apparently inclined to the plane of the ring.

6. Measurements on the dependence on temperature of the electric double-refraction of liquids support the validity of Born's expression for the Kerr constant.

210 Bowbazaar Street, Calcutta.
30th September, 1926.

The Diffraction of Light by Metallic Screens.

By Prof. C. V. Raman, F.R.S., and K. S. Krishnan.

(Received June 13, 1927.)

1. *Introduction.*

Gouy* discovered that when a metallic screen with a sharp and highly-polished edge is held in the path of a pencil of light, its boundary appears as a luminous line diffracting light through large angles, both into the region of shadow (interior diffraction) and into the region of light (exterior diffraction). He noticed further that this diffracted light is strongly polarised, but in perpendicular planes in the two regions mentioned; the colour of the diffracted light and its state of polarisation depend in a remarkable manner on the material of the screen and on the extent to which its edge is rounded off in the process of polishing. When the edge is viewed through a double-image-prism from within the shadow, only that image appears coloured which is more intense and is polarised with the magnetic vector parallel to the edge. The second image which is fainter and is polarised with the electric vector parallel to the edge, appears perfectly white. When the incident light is polarised in any arbitrary azimuth, the diffracted light is found to exhibit elliptic polarisation. These and other results have been confirmed by later observers.†

Gouy's experimental results were discussed by Poincaré on the basis of the electromagnetic theory of light in two memoirs published in the "Acta Mathematica."‡ The special case of an ideal screen (plane or wedge-shaped), supposed perfectly-reflecting and having a sharp edge, is amenable to complete theoretical treatment, and was dealt with by Poincaré himself, and later in a rigorous manner by Sommerfeld,§ and following him by numerous other mathematicians. The behaviour of actual metallic screens, however, differs considerably from that found theoretically for this ideal case. Though attempts have been made by Poincaré himself in the memoirs quoted, and later also by Epstein,‖ to take the nature of the screen and the rounding of its edge into account, it cannot be said that Gouy's observations have so far received a complete or satisfactory explanation. We propose in this paper to discuss more particularly the

* 'Ann. Chim. et Physique,' vol. 8, p. 145 (1886).
† W. Wien, 'Wied. Ann.,' vol. 28, p. 117 (1886).
‡ 'Acta Mathematica,' vol. 16, p. 297 (1892), and vol. 20, p. 313 (1896).
§ 'Math. Annalen,' vol. 47, p. 317 (1896).
‖ 'Diss. Munich'; also 'Encyklop. d. math. Wissensch.,' vol. V (3), p. 491.

influence of the material of the screen on the diffraction by a sharp edge, and to show how it may be explained in a very simple manner. The case of rounded edges is reserved for discussion in a separate paper.

In the fifth section of his first memoir, Poincaré discussed the electromagnetic boundary conditions at the surface of an imperfectly conducting screen, and made the important remark that the extreme smallness of the depth to which an optical disturbance penetrates into any actual metal, should considerably simplify the theory. In his actual attempt, however, to discuss the problem of diffraction by an imperfectly conducting screen, he made no use of the elegant mathematical methods and results contained in the earlier parts of his memoir, and contented himself with a qualitative discussion on the basis of the Kirchhoff formulation of Huygens' Principle. The treatment given does not, as was indeed remarked by Poincaré himself, appear capable of leading to quantitative results. In the course of our paper, we shall sh how it is possible to apply the Fresnel-Huygens' Principle with success to the problem of diffraction by imperfectly-conducting screens. It is more convenient, however, to base our treatment in the first instance on a modification of the known exact solutions for the case of perfectly-reflecting screens or wedges.

2. *Theory.*

Sommerfeld's solution of the wave-equation in cylindrical co-ordinates for the case of a semi-infinite screen which is a perfect reflector and lies in the xz-plane, with its edge along the z-axis, is

$$u = \mathrm{F}(\rho, \phi, \phi_0) \mp \mathrm{F}(\rho, \phi, -\phi_0). \qquad (1)$$

The upper (minus) sign refers to the case in which the plane of polarisation and the plane of incidence are parallel to each other; (we shall refer to this as the $\|^r$ case), and u then denotes the electric force parallel to the edge. The lower (plus) sign refers to the case in which the plane of polarisation of the incident light is perpendicular to the plane of incidence (we shall refer to this as the $\perp^r$ case), u then denoting the magnetic force parallel to the edge.

$$\mathrm{F}(\rho, \phi, \phi_0) = \left(\frac{i}{\pi}\right)^{\frac{1}{2}} e^{i\frac{2\pi t}{T}} e^{ik\rho\cos(\phi-\phi_0)} \int_{-\infty}^{\tau} e^{-i\lambda^2} d\lambda, \qquad (2)$$

where

$$\tau = \sqrt{2k\rho} \,.\, \cos\tfrac{1}{2}(\phi - \phi_0).$$

The expression (2) has the property that when τ is positive and sufficiently large, which is the case when $\pi + \phi_0 > \phi > 0$, the function tends to the limiting value $e^{i\frac{2\pi t}{T}} e^{ik\rho\cos(\phi-\phi_0)}$, which represents a train of plane waves incident on

the screen in a direction making an angle ϕ_0 with its plane; when τ is negative and sufficiently large, which is the case when $\pi + \phi_0 < \phi < 2\pi$, the function tends to the limit zero. $\mathrm{F}(\rho, \phi, -\phi_0)$ is obtained by writing $-\phi_0$ for ϕ_0. When $\pi - \phi_0 > \phi > 0$ it tends to the limit $e^{i\frac{2\pi t}{T}} e^{ik\rho\cos(\phi+\phi_0)}$, which represents a plane train of waves reflected from the screen. When $\pi - \phi_0 < \phi < 2\pi$, $\mathrm{F}(\rho, \phi, -\phi_0)$ tends to the limit zero.

Now the solutions (1) satisfy the conditions $u = 0$ and $\frac{\partial u}{\partial \phi} = 0$ respectively, on both faces of the screen, supposed to be infinitely thin and perfectly reflecting, that is, when $\phi = 0$ and also when $\phi = 2\pi$. Now any actual screen to be opaque must be of finite thickness, hence a solution of the form (1) or any simple modification of it cannot be expected to represent the behaviour of such screens *completely*. Nevertheless, as already mentioned above, a metallic screen of a thickness which is only a small fraction of a wave-length, is practically opaque, and this makes it possible to represent its behaviour with a high degree of accuracy by a comparatively simple modification of (1). Consider expressions of the form

$$u = \mathrm{F}(\rho, \phi, \phi_0) - (\mathrm{C}_s + i\mathrm{D}_s) \,.\, \mathrm{F}(\rho, \phi, -\phi_0) \qquad (3)$$

and

$$u = \mathrm{F}(\rho, \phi, \phi_0) + (\mathrm{C}_p + i\mathrm{D}_p) \,.\, \mathrm{F}(\rho, \phi, -\phi_0) \qquad (4)$$

in which the (numerical) factors $\mathrm{C}_s + i\mathrm{D}_s$ and $\mathrm{C}_p + i\mathrm{D}_p$ are so chosen that they represent the amplitude of the wave reflected at the illuminated face of the particular screen used, for the particular angle of incidence under consideration. Equation (3) refers to the $\|^r$ case, and (4) to the $\perp^r$ case. Since $\mathrm{C}_s + i\mathrm{D}_s$ and $\mathrm{C}_p + i\mathrm{D}_p$ are functions only of the angle of incidence ϕ_0, (3) and (4) continue to satisfy the wave-equation and represent distributions of light and shadow of the same general character as those indicated by (1), with this difference, however, that the disturbance on the illuminated face of the screen expressed by (3) and (4) will have the actual values corresponding to the screen used, while (1) corresponds to a screen with properties which cannot be physically realised. We are therefore justified in expecting that (3) and (4) would represent the disturbance throughout the whole field in the actual problem much more accurately than the Sommerfeld formulæ.

To understand the physical significance of the formulæ, it is best to use the asymptotic expressions for the functions for large values of ρ. We have, when $\cos\frac{1}{2}(\phi - \phi_0)$ is positive,

$$\mathrm{F}(\rho, \phi, \phi_0) \sim e^{i\frac{2\pi t}{T}} e^{ik\rho\cos(\phi-\phi_0)} + \frac{i^{3/2} e^{i\frac{2\pi t}{T}} e^{-ik\rho}}{2\sqrt{2\pi k\rho} \,.\, \cos\frac{1}{2}(\phi - \phi_0)}, \qquad (5)$$

while when $\cos \frac{1}{2}(\phi - \phi_0)$ is negative, there is a similar expression in which the first term is missing. Similarly when $\cos \frac{1}{2}(\phi + \phi_0)$ is positive, we have

$$F(\rho, \phi, -\phi_0) \backsim e^{i\frac{2\pi t}{T}} e^{ik\rho\cos(\phi+\phi_0)} + \frac{i^{3/2} e^{i\frac{2\pi t}{T}} e^{-ik\rho}}{2\sqrt{2\pi k\rho}\,.\cos\frac{1}{2}(\phi+\phi_0)}, \qquad (6)$$

and a similar expression in which the first term is missing, if $\cos \frac{1}{2}(\phi + \phi_0)$ is negative. The general expression for the light diffracted by the edge is either

$$E_z = \frac{i^{3/2} e^{i\frac{2\pi t}{T}} e^{-ik\rho}}{2\sqrt{2\pi k\rho}} \left[\frac{1}{\cos\frac{1}{2}(\phi-\phi_0)} - \frac{C_s + iD_s}{\cos\frac{1}{2}(\phi+\phi_0)}\right] \qquad (7)$$

or

$$H_z = \frac{i^{3/2} e^{i\frac{2\pi t}{T}} e^{-ik\rho}}{2\sqrt{2\pi k\rho}} \left[\frac{1}{\cos\frac{1}{2}(\phi-\phi_0)} + \frac{C_p + iD_p}{\cos\frac{1}{2}(\phi+\phi_0)}\right]. \qquad (8)$$

3. *An Alternative Treatment.*

The formulæ (7) and (8) may also be derived in the following manner based on the Fresnel-Huygens' Principle. It is readily shown that the wave-equation in cylindrical co-ordinates,

$$\frac{\partial^2 u}{\partial\rho^2} + \frac{1}{\rho}\frac{\partial u}{\partial\rho} + \frac{1}{\rho^2}\frac{\partial^2 u}{\partial\phi^2} + \frac{\partial^2 u}{\partial z^2} - \frac{1}{c^2}\frac{\partial^2 u}{\partial t^2} = 0, \qquad (9)$$

is exactly satisfied by putting

$$u = e^{i\frac{2\pi t}{T}} \frac{e^{-ik\rho}}{2\sqrt{2\pi k\rho}} \cos\tfrac{1}{2}(\phi + \varepsilon), \qquad (10)$$

which represents a cylindrical wave of Poisson's type diverging from the z-axis. A plane wave incident on the xz-plane in the direction ϕ_0 is transmitted through the part of the plane to the left of the edge and is reflected from the part on the right. To find the disturbance diverging from the edge of the screen, at any point very distant from it, we divide the area of the xz-plane adjacent to the edge into half-period strips parallel to it on either side, and show in the usual way that the effect of the transmitted wave reduces to one-half of the first half-period strip on one side of the edge, and that the effect of the reflected wave reduces to that of a similar strip on the other side. Assuming that each of these strips is the origin of a cylindrical wave of the type appearing in (10), we may write the total disturbance at (ρ, ϕ) diverging from the origin, in the form

$$u = e^{i\frac{2\pi t}{T}} \frac{e^{-ik\rho}}{2\sqrt{2\pi k\rho}} [A_0 \cos\tfrac{1}{2}(\phi + \alpha) + B_0 \cos\tfrac{1}{2}(\phi + \beta)], \qquad (11)$$

where A_0, B_0, α and β have to be so chosen as to give the amplitudes and phases of the divergent waves correctly. Now the width of either half-period strip is easily shown to be

$$\frac{\lambda}{4\cos\frac{1}{2}(\phi-\phi_0)\cos\frac{1}{2}(\phi+\phi_0)},$$

and we may assume, as is usual in the elementary diffraction theory, that the amplitudes A_0 and B_0 are proportional to this width. It is necessary that the term in (11) proportional to A_0, contributed by the transmitted wave, remains finite when $\phi = \pi - \phi_0$, and that proportional to B_0, contributed by the reflected wave, remains finite when $\phi = \pi + \phi_0$, as these directions do not coincide with the respective directions of travel of these waves. We are thus obliged to assume that $\alpha = \phi_0$ and that $\beta = -\phi_0$. The equation (11) then reduces to

$$u = e^{i\frac{2\pi t}{T}} \frac{e^{-ik\rho}}{2\sqrt{2\pi k\rho}} \left[\frac{A}{\cos\frac{1}{2}(\phi-\phi_0)} + \frac{B}{\cos\frac{1}{2}(\phi+\phi_0)}\right], \qquad (12)$$

where A and B are suitably chosen constants. As in the elementary diffraction theory we write

$$A = e^{-i\frac{\pi}{4}} = i^{3/2},$$

which expresses the difference of path of $\lambda/8$ between a parent plane wave and the divergent cylindrical wave from a laminar strip cut out of it. The value of B relatively to A evidently depends on the change of amplitude and phase occurring in reflection at the surface of the screen. We write therefore

$$B/A = -(C_s + iD_s) \quad \text{or} \quad +(C_p + iD_p),$$

according to the state of polarisation of the incident beam. The formulæ (7) and (8) are then reproduced.

4. *Explanation of Ellipticity of the Diffracted Light.*

From expressions (7) and (8) the ellipticity of the light diffracted through large angles, when the incident light is polarised in any arbitrary azimuth, follows as an immediate consequence. We shall consider first the case of normal incidence on a plane screen. We have then

$$C_s + iD_s = C_p + iD_p = \frac{n(1 - i\kappa) - 1}{n(1 - i\kappa) + 1}.$$

Taking for the case of a steel edge and for $\lambda = 5{\cdot}80 \times 10^{-5}$ cm., $n\kappa = 3{\cdot}24$ and $n = 2{\cdot}46$, we have $C_s + iD_s = C_p + iD_p = 0{\cdot}69 - i \times 0{\cdot}29$. With these numerical values and writing the expressions in the square brackets on the right-

hand side of (7) and (8) in the form $F_s + iG_s$ and $F_p + iG_p$ respectively, the values of $F_s^2 + G_s^2$ and of $F_p^2 + G_p^2$ for various angles of observation, and the phase differences between these two components are shown in Table I.

Gouy noticed that with a sharp steel edge, the light diffracted into the region of shadow shows no sensible ellipticity when the deviation is less than 45°. For larger deviations, it becomes sensible, the $\parallel^r$ component being in advance of the $\perp^r$ component, the difference of path being, however, always numerically less than $\lambda/4$. It will be seen that this is in general agreement with the figures for the difference of path shown in the fifth column of Table I. The table also indicates the interesting result that in the region of exterior diffraction, the path difference changes sign and increases in a continuous manner up to the boundary of reflection, when it becomes half a wave-length, while according to the Sommerfeld formulæ there is a sudden reversal of phase when the diffracted ray lies in the continuation of the plane of the screen.

Table I.—Diffraction by Steel Edge : Normal Incidence.

$\parallel^r$ and $\perp^r$ indicate plane of polarisation parallel and perpendicular respectively to the plane of incidence.

$$\lambda = 5{\cdot}80 \times 10^{-5} \text{ cm.}$$

Region of observation.	Direction of diffracted ray ϕ.	Intensity of $\parallel^r$ component $F_s^2+G_s^2$.	Intensity of $\perp^r$ component $F_p^2+G_p^2$.	Difference of path between the components $\frac{\delta_p-\delta_s}{\lambda}$.	Difference of path according to Sommerfeld formulæ.
	°				
Boundary of reflection....	90	—	—	0·50	0·50
Exterior diffraction (region of illumination)	120	15·0	3·9	0·45	0·50
	150	6·7	0·38	0·35	0·50
	180	5·9	0·36	0·15	—
	210	8·0	1·55	0·06	0
	240	21·1	10·0	0·03	0
Boundary of shadow.....	270	—	—	0	0
Interior diffraction (region of shadow)	285	49	70	−0·01	0
	300	10·0	21·1	−0·03	0
	315	3·6	11·4	−0·04	0
	330	1·55	8·0	−0·06	0
	345	0·72	6·4	−0·09	0
	360	0·36	5·9	−0·15	—

5. *Effect of Oblique Incidence.*

When the light is incident on the screen obliquely at an angle θ (measured as usual from the normal) we have

$$C_s + iD_s = -\frac{\cos\theta - \sqrt{n^2(1-i\kappa)^2 - \sin^2\theta}}{\cos\theta + \sqrt{n^2(1-i\kappa)^2 - \sin^2\theta}}, \tag{13}$$

and

$$C_p + iD_p = \frac{n^2(1-i\kappa)^2\cos\theta - \sqrt{n^2(1-i\kappa)^2 - \sin^2\theta}}{n^2(1-i\kappa)^2\cos\theta + \sqrt{n^2(1-i\kappa)^2 - \sin^2\theta}}, \tag{14}$$

At normal incidence (13) and (14) are equal, and at grazing incidence they are again equal but opposite in sign. At the principal incidence (which lies between 70° and 80° for most metals) the difference of path between the $\parallel$ and $\perp^r$ components of the reflected wave amounts to $\lambda/4$ and then rapidly diminishes to 0 as grazing incidence is approached. With the help of the formulæ (7), (8), (13) and (14) the intensity of the two components of the diffracted light and their phase-difference can be calculated for any angle of incidence and of observation. Let us first consider moderately oblique incidence. Two cases have naturally to be distinguished, viz., when the incidence is from the screen-side of the normal, and when it is from the farther side. Tables II and III give the values for a steel screen when $\phi_0 = 135°$ and 45°, respectively, for yellow light. It can be seen that the effects observed in interior and exterior diffraction are no longer similar to each other.

Table II.—Diffraction by a Steel Edge. $\phi_0 = 135°$.

Region of observation.	Direction of diffracted ray ϕ.	Intensity of $\parallel^r$ component $F_s^2+G_s^2$.	Intensity of $\perp^r$ component $F_p^2+G_p^2$.	Difference of path between the components $\frac{\delta_p-\delta_s}{\lambda}$.
	°			
Exterior diffraction	135	4·6	0·30	0·23
	180	3·8	0·35	0·14
	225	4·9	0·8	0·09
	270	12	4·0	0·04
	285	24	11	0·03
	300	75	48	0·02
Boundary of shadow.....	315	—	—	0
Region of shadow	330	41	75	−0·02
	345	6·0	27	−0·05
	360	0·7	18	−0·17

In the case considered in Table II, the region of shadow is of much smaller angular width, and the degree of polarisation and also the ellipticity increase rapidly as we approach the plane of the screen ($\phi = 360°$). On the other hand, in Table III the region of shadow is much wider, and the polarisation and ellipticity of the diffracted light increase less rapidly with increasing deviation of the diffracted ray. In exterior diffraction these effects are reversed.

Table III.—Diffraction by a Steel Edge. $\phi_0 = 45°$.

Region of observation.	Direction of diffracted ray ϕ.	Intensity of $\parallel^r$ component $F_s^2+G_s^2$.	Intensity of $\perp^r$ component $F_p^2+G_p^2$.	Difference of path between the components $\frac{\delta_p-\delta_s}{\lambda}$.
	°			
Exterior diffraction	135	—	—	0·45
	165	28	2·3	0·32
	195	31	8·4	0·06
Boundary of shadow	225	—	—	0
Region of shadow	255	9·6	22	−0·03
	285	1·5	7·0	−0·06
	315	0·5	4·2	−0·09
	345	0·2	3·3	−0·14
	360	0·1	3·1	−0·17

6. *Diminished Intensity of Diffracted Light.*

If we compare the figures shown in Tables II and III with those calculated from Sommerfeld's formulæ for a perfectly reflecting screen, we find that the effect of imperfect conductivity of the screen is not only to introduce elliptic polarisation, but also to diminish the total intensity of the diffracted light and the ratio of the components of vibration for specified angles of incidence and diffraction. In fact, these effects are all closely related to one another, and become the more striking when the incidence is very oblique.

In Table IV the case of oblique incidence on a steel edge has been worked out and shown. It is assumed that $\phi_0 = 170°$, that is, only 10° short of grazing incidence. The figures for the steel edge and for a perfectly reflecting screen are shown side by side for comparison, and it will be seen that the intensity of the $\perp^r$ component is diminished to one-fifth of its value, on the surface of the screen, by reason of the imperfect conductivity, while that of the $\parallel^r$ component is very slightly increased. Nevertheless, the ratio of the $\perp^r$ and $\parallel^r$ components remains large, showing that even at such incidences the polarisation remains large. We have to approach grazing incidence still more closely before the

Table IV.—Diffraction by a Steel Edge. $\phi_0 = 170°$.

Region of Shadow.

Direction of diffracted ray ϕ.	Intensity of $\parallel^r$ component for a *perfect conductor*.	Intensity of $\parallel^r$ component for *steel* $F_s^2+G_s^2$.	Intensity of $\perp^r$ component for *steel* $F_p^2+G_p^2$.	Intensity of $\perp^r$ component for a *perfect conductor*.	Difference of path between the components for *steel* $\frac{\delta_p-\delta_s}{\lambda}$.
°					
350	—	—	—	—	0
352	2590	2600	3100	4060	−0·01
354	460	480	750	1280	−0·02
356	119	128	313	746	−0·04
358	23	28	170	571	−0·07
360	0	0·9	109	527	−0·23

diminution of the $\perp^r$ component is such as to produce a striking diminution of the completeness of polarisation. From formulæ (7), (8), (13) and (14) it follows that, at grazing incidence, the diffracted light should be unpolarised at all angles.

The foregoing considerations help to explain, at least in part, the interesting observation of Gouy that for given directions of the incident and diffracted rays, the intensity of the diffracted light is a *maximum* when the plane of the screen bisects the angle between these two directions. According to Sommerfeld's formulæ the intensity should be a *minimum* for this position of the screen. Owing, however, to the imperfect conductivity of actual screens, as we have seen, the intensity falls off in approaching the extreme cases in which the light is incident grazingly on the screen from either direction. As we shall see later, other circumstances, as, for instance, the finite angle formed by the faces of the screen at the edge, or the actual rounding off of the latter, would also operate in the direction of diminishing the intensity of the diffracted light in the two extreme positions of the screen. Hence the intermediate position for the screen actually gives the maximum instead of the minimum intensity for the diffracted rays in the particular direction.

7. *Explanation of Diffraction Colours.*

The wave-length enters in the expression for the intensity of the diffracted light in two distinct ways. Referring to (7) and (8) it will be seen that the intensity is inversely proportional to k, that is, proportional to the wave-length. The longer wave-lengths would thus tend to be more prominent in

the light diffracted by the edge than in the incident light. This effect would operate both on the parallel and perpendicular components of vibration in the diffracted light. The colour of the diffracted light is also influenced, and in an entirely different way, by the factors $C_s + iD_s$ and $C_p + iD_p$ appearing in (7) and (8), which are, in general, functions of the wave-length of the incident light. If we confine ourselves to the case of normal incidence, $C_s + iD_s$ and $C_p + iD_p$ are identical in magnitude. But the former appears with a negative sign in (7) and the latter with a positive sign in (8). Hence, if a particular wave-length appears with a strengthened amplitude in (8) it will appear with a weakened amplitude in (7), and *vice versa*. This, taken together with the proportionality to λ already mentioned, furnishes an explanation of the difference in the colour of the parallel and perpendicular components of the light diffracted into the region of shadow, which was discovered by Gouy for metals such as copper and gold. It can easily be seen that in the region of shadow the longer wave-lengths which are strongly reflected by the metal would be much enhanced in the perpendicular component, while the corresponding weakening in the parallel component would be almost insensible. In the region of exterior diffraction, these features are interchanged.

Table V.—Gold Screen. $\phi_0 = 90°$ (Normal Incidence).

Direction of diffracted ray ϕ.	$(F_s^2+G_s^2)\ \lambda \times 10^5$, for $\lambda \times 10^5 =$			$(F_p^2+G_p^2)\ \lambda \times 10^5$, for $\lambda \times 10^5 =$		
	4·20.	5·80.	7·00.	4·20.	5·80.	7·00.
°						
270	—	—	—	—	—	—
285	217	282	326	279	408	508
300	48·3	59·0	64·4	80·4	125	159
315	19·1	22·1	22·1	41·8	68·3	88·7
330	9·56	10·7	9·50	28·1	48·5	63·9
345	5·44	6·36	4·87	22·1	40·2	53·6
360	3·41	4·86	3·48	19·5	37·6	50·7

In Table V the intensity of the diffracted light has been calculated for the case of a gold screen using the following data :—

$\lambda = 7{\cdot}00 \times 10^{-5}$ cm. ; $n = 0{\cdot}280$, $n\kappa = 3{\cdot}800$;
$\lambda = 5{\cdot}80 \times 10^{-5}$ cm. ; $n = 0{\cdot}415$, $n\kappa = 2{\cdot}750$;
$\lambda = 4{\cdot}20 \times 10^{-5}$ cm. ; $n = 1{\cdot}570$, $n\kappa = 1{\cdot}800$.

From the table it will be seen that in the region of shadow $(F_s^2 + G_s^2)\lambda$ has practically the same value for different wave-lengths, while $(F_p^2 + G_p^2)\lambda$

increases in value as we proceed towards the red end of the spectrum. The increase with wave-length is much more marked for large angles of diffraction than for small angles. Further, $F_p^2 + G_p^2$ is always greater than $F_s^2 + G_s^2$, the ratio between the two increasing with the angle of diffraction. From these facts, it follows that when the region of shadow is examined, the $\|^r$ component of the diffracted light will be perfectly white, while the $\perp^r$ component, which is in fact much stronger than the other, will exhibit an orange-yellow tint, the colouration being the more marked, the further we go into the region of shadow. The same colour effects will be noticeable also in the region of exterior diffraction, the $\|^r$ and $\perp^r$ components now, however, exchanging places.

8. *Intensified Colours at Oblique Incidences.*

While the variation with wave-length of the intensity of the $\perp^r$ component shown in Table V is marked enough, it is not exceptionally large, being in fact of the same order of magnitude as the variation of the reflecting power of the metal with wave-length. This is in agreement with observation, for Gouy found that the sharpest metallic edges do not show particularly vivid colours by diffraction. When, however, the incidence on the screen is made oblique, the colours of the $\perp^r$ component should become more lively. To understand why this should be the case, we have only to refer to section 6 above, in which it was shown that the imperfect reflectivity of the metal results in a diminution of the intensity of the diffracted light in comparison with the theoretical value for a perfectly reflecting screen, and that this diminution becomes the more marked as the incidence of the light on the screen becomes more oblique. Those wave-lengths, however, for which the reflecting power of the metal approaches unity, persist in nearly full strength in the $\perp^r$ component of the diffracted light, and hence determine its colour in increasing measure as the obliquity of the screen is increased. It is to be noted also that the colour should appear at smaller deviations of the ray in interior diffraction, and at larger deviations in exterior diffraction, or *vice versa*, according to the position of the screen.

In Table VI the case of a gold screen, for a position of the screen 10° short of grazing incidence, has been worked out and the intensities of the $\|^r$ and $\perp^r$ components are shown for six different wave-lengths, the direction of observation considered being along the surface of the screen in the region of shadow. The normal reflecting power of the metal for the same wave-lengths is also shown for comparison.

Table VI.—Gold Edge. $\phi_0 = 170°$, $\phi = 360°$.

$\lambda \times 10^5$ (cm.).	Intensity of $\parallel^r$ component $(F_s^2+G_s^2)\ \lambda \times 10^5$.	Intensity of $\perp^r$ component $(F_p^2+G_p^2)\ \lambda \times 10^5$.	The reflection coefficient.
4·00	9·9	200	0·360
4·60	12·5	210	0·358
5·20	17·5	240	0·608
5·80	10·5	470	0·827
6·20	8·8	650	0·889
7·00	7·1	1000	0·930

It will be noticed that the intensity of the $\parallel^r$ component varies but little with wave-length, while the $\perp^r$ component shows large intensities in the orange and red regions in the spectrum. The effect in the latter case is of a highly selective character, becoming pronounced only for the wave-lengths for which the reflecting power of the metal approaches unity.

When the figures shown in Table VI are computed after the manner employed by the late Lord Rayleigh* for discussion of the colours of thin plates, and plotted in Maxwell's colour-triangle, it is found that the $\parallel^r$ component is perfectly white, while the $\perp^r$ component is of a rich orange-yellow colour.

The case of other metals may be worked out in a similar manner. In Table VII are given the reflection-coefficients and the colour of the diffracted light as observed by Gouy and Wien, for a number of metals. The general relationship between them is fairly clear from the figures. In the case of the whiter metals, of course, the colour is largely determined by the factor λ appearing in the expression for the intensity of the diffracted light.

Table VII.—Reflection Coefficients and Diffraction Colours.

For $\lambda \times 10^5$ =	4·20	4·50	5·00	5·50	6·00	6·50	7·00	Colour of $\perp^r$ component of diffracted light.
Silver	0·866	0·905	0·913	0·927	0·926	0·935	0·946	Pale yellow.
Copper	0·33	0·37	0·44	0·48	0·72	0·80	0·83	Red.
Steel	0·52	0·54	0·55	0·55	0·55	0·56	0·58	Reddish white.
Platinum	0·518	0·547	0·584	0·611	0·642	0·663	0·69	Yellow.
Zinc	0·803	0·806	0·805	0·789	0·774	0·771	0·770	Colour insensible.
Tin	—	0·605	0·670	0·686	0·706	0·713	0·716	Greenish yellow.

* Lord Rayleigh, 'Scientific Papers,' vol. 2, p. 498.

9. *Diffraction by Metallic Wedges.*

Poincaré considered the case of a perfectly reflecting wedge in his first memoir, and showed that if the surfaces of the wedge are given by the angles $\phi = 0$ and $\phi = \chi$, the rays diffracted from its edge have an amplitude proportional to

$$\left[\frac{1}{\cos\frac{\pi^2}{\chi} - \cos\frac{\pi}{\chi}(\phi-\phi_0)} \mp \frac{1}{\cos\frac{\pi^2}{\chi} - \cos\frac{\pi}{\chi}(\phi+\phi_0)}\right]. \qquad (15)$$

As the result of a more elaborate analysis, Wiegrefe* found for the cylindrical wave diverging from a wedge-shaped edge the identical expression given by (15) with the multiplying factor

$$-i^{3/2}e^{i\frac{2\pi l}{\lambda}}e^{-ik\rho}\sqrt{\frac{\lambda}{\rho}}\cdot\frac{\sin\frac{\pi^2}{\chi}}{2\chi}. \qquad (16)$$

On putting $\chi = 2\pi$, the formulæ (15) and (16) reduce to those for the case of a perfectly reflecting plane screen. In the case of an imperfectly conducting wedge, we modify expression (15) and write it in the form.

$$\left[\frac{1}{\cos\frac{\pi^2}{\chi} - \cos\frac{\pi}{\chi}(\phi-\phi_0)} - \frac{C_s+iD_s}{\cos\frac{\pi^2}{\chi} - \cos\frac{\pi}{\chi}(\phi+\phi_0)}\right], \qquad (17)$$

or

$$\left[\frac{1}{\cos\frac{\pi^2}{\chi} - \cos\frac{\pi}{\chi}(\phi-\phi_0)} + \frac{C_p+iD_p}{\cos\frac{\pi^2}{\chi} - \cos\frac{\pi}{\chi}(\phi+\phi_0)}\right], \qquad (18)$$

where C_s, D_s, C_p, D_p have the same significance as previously, and are functions of the angle of incidence of the light on the illuminated side of the wedge.

From formula (15) it appears that along the two surfaces of the wedge $\phi = 0$ and $\phi = \chi$, the diffracted light should be completely polarised with the intensity of the $\parallel^r$ component zero, and that of the $\perp^r$ component finite. As the rear surface of the wedge limits the region of shadow, it follows as a consequence that the polarisation-effects should usually appear at smaller deviations of the diffracted ray in the case of a wedge than for a plane screen. When the imperfect reflecting power of the metal is taken into account, as in formulæ (17) and

* A. Wiegrefe, 'Ann. d. Physik,' vol. 39, p. 449 (1912).

(18), it would also follow, for the reasons stated, that the colours of the diffracted light should also be observable at smaller deviations and be generally more striking than for a plane screen.

10. *Summary.*

1. The paper contains a discussion of the observations of Gouy on the intensity, colour and polarisation of the light diffracted through large angles by metallic screens and wedges with polished edges. The well-known expressions due to Poincaré and Sommerfeld referring to diffraction by perfectly-reflecting screens and wedges, are modified so as to take into account the changes of phase and amplitude which occur when light is reflected at the surface of a metal. The modified formulæ are then discussed.

2. The formulæ show that when the incident light is plane-polarised in any arbitrary azimuth, the light diffracted through large angles is elliptically polarised, the sign of the ellipticity being different in interior and exterior diffraction.

3. In interior diffraction, the component polarised in the plane of incidence is white, while the perpendicular component is coloured, the colour depending on the nature of the metal. In exterior diffraction, these effects are reversed.

4. The effect of imperfect conductivity is to make the intensity of the diffracted light less and less as the incidence becomes more and more oblique. This diminution is least for the wave-length for which the reflection-coefficient is largest. The colour-effects arise in this way and therefore become more prominent at oblique incidences.

12. Magnetic Double-Refraction in Paramagnetic Gases.

By

K. S. Krishnan.

1. *Introduction.*

The theory of spatial quantization of electron-orbits in a magnetic field was put forward independently by Sommerfeld and Debye in 1916 as a necessary basis for the quantum treatment of the Zeeman-effect. In contradistinction to the classical theory of paramagnetism, in which all orientations of the electron-orbits responsible for the permanent magnetic moments of atoms or molecules are equally probable in an external magnetic field, in the limit when the field is vanishingly small, the theory of spatial quantization assumes that only certain discrete orientations are possible. The theory may now be taken to be fairly well established directly in the case of *atomic* magnetic carriers by the recent experiments of Stern and Gerlach on the deviation of a stream of atoms in a non-homogeneous magnetic field; and indirectly in the case of *molecular* magnetic carriers by the work of Pauli, Sommerfeld and others on the calculation of the magnitude of the elementary magnetic moments from measurements of paramagnetic susceptibility.

Recently attempts have been made to get some evidence of such orientations by independent optical methods. For instance Schütz,[1] Fraser [2] and others have looked for double-refraction in a strong magnetic field, in the vapours of

[1] W. Schütz, quoted by W. Gerlach, Phys. Zeits. 26, 820, 1925.
[2] R. Fraser, Phil. Mag. 1, 885, 1926.

sodium and potassium and in oxygen, which are all paramagnetic. Schütz used fields up to 15,000 gauss, and even though his optical arrangement was capable of detecting a difference between the two principal refractive indices equal to 6×10^{-6} in the case of sodium and potassium vapours, and a difference equal to 3×10^{-10} in the case of oxygen, there was no evidence of any double refraction. The vapours of sodium and potassium have one Bohr magneton per atom,[3] and according to the rules of spatial quantization, will set themselves with their magnetic moments either along or against the direction of the incident field, the probability of their taking up the one or the other position being determined by Boltzmann's theorem. If we assume along with Langevin and others that the elementary magnetic moments are rigidly fixed to the carriers, knowing the optical anisotropy of the atoms, we can easily calculate the magnitude of the magnetic double-refraction to be expected. But we have no data for determining the optical anisotropy of either sodium or potassium. In the case of oxygen we have the necessary data for calculating the double refraction, but nitric oxide with one Bohr magneton per molecule (oxygen has two), being much simpler, we shall give the calculations for this case.

2. *Double-Refraction of Nitric Oxide in a Magnetic Field.*

If we accept Bragg's[4] ideas regarding the optical anisotropy of molecules as arising from the mutual interaction of the electric doublets induced in the different atoms by the electric field of the incident light-waves, NO-molecule being diatomic, should be optically symmetrical with respect to the line joining the N- and O-nuclei, the refractivity of the

[3] J. B. Taylor, Phys. Rev. 28, 576, 1926.

[4] W. L. Bragg, Proc. Roy. Soc. A., 105, 370, 1924; see also K. R. Ramanathan, same Proceedings, 107, 684, 1925.

molecule for light-vibrations along the optic axis being greater than for vibrations in perpendicular directions.

Let A, B (A>B) be the moments induced in a molecule of NO per unit electric force in the incident light-wave, acting respectively along and perpendicular to its optic axis. Also let α be the angle which the permanent magnetic moment of the molecule makes with the same axis. Then in a magnetic field, if we neglect the diamagnetic polarisation of the molecule, the refractivity of the medium for light-vibrations parallel and perpendicular to the magnetic field are given by the relations

$$\left.\begin{aligned} n_{\parallel}-1&=2\pi\nu[A\cos^2\alpha+B\sin^2\alpha]\\ n_{\perp}-1&=2\pi\nu\left[A\frac{\sin^2\alpha}{2}+B\left(1-\frac{\sin^2\alpha}{2}\right)\right]\end{aligned}\right\}\quad\ldots\ (1)$$

where ν is the number of molecules per c. c. of the medium in the magnetic field, which may be taken to be the same as the number outside the field since the change of volume due to magnetostriction is quite negligible. (For NO, in a field of 15,000 gauss, $\frac{\delta\nu}{\nu}$ is about 7×10^{-6} at room temperature.)

The refractivity of the medium outside the field is given by

$$n-1=2\pi\nu\frac{A+2B}{3}.\quad\ldots\ (2)$$

Now from the theory of light-scattering by anisotropic molecules the ratio $\frac{A}{B}$ can be evaluated with the help of the formula

$$\frac{A-B}{A+2B}=\sqrt{\frac{5r}{6-7r}},\quad\ldots\ (3)$$

where r is the ratio of the intensity of the components of the imperfectly polarised light scattered transversely by the medium, when the incident light is unpolarised.

For NO, from the measurements of Cabannes and Granier,[5] $r=0{\cdot}026$, which gives

$$\frac{A}{B}=1{\cdot}53.$$

Taking the refractivity at 25°C. and 1 atm. pressure

$$n-1=2{\cdot}69\times10^{-4},$$

we get

$$2\pi\nu A=3{\cdot}50\times10^{-4}$$

and

$$2\pi\nu B=2{\cdot}29\times10^{-4}.$$

Substituting in (1) we obtain

$$\left.\begin{aligned} n_{\parallel}-1&=3{\cdot}50\times10^{-4}\cos^2\alpha+2{\cdot}29\times10^{-4}\sin^2\alpha\\ n_{\perp}-1&=2{\cdot}29\times10^{-4}+0{\cdot}60\times10^{-4}\sin^2\alpha\end{aligned}\right\} \quad \ldots\ (4)$$

Case I. $\alpha=0$, *i.e.*, the permanent magnetic moment is along the line joining the N- and O- nuclei.

$$n_{\parallel}-1=3{\cdot}50\times10^{-4}$$

$$n_{\perp}-1=2{\cdot}29\times10^{-4}.$$

Hence when a magnetic field is put on, light vibrations parallel to the field are retarded by about $1{\cdot}4\lambda$ for each cm. lengh of track across the magnetic field, while the perpendicular vibrations are accelerated by about $0{\cdot}7\lambda$ per cm.

Case II. $\alpha=\frac{\pi}{2}$ *i.e.*, the magnetic moment is perpendicular to the optic axis.

In this case

$$n_{\parallel}-1=2{\cdot}29\times10^{-4}$$

$$n_{\perp}-1=2{\cdot}90\times10^{-4}.$$

[5] J. Cabannes and J. Granier, Journ. de Physique Series VI, 4, 429, 1923.

so that parallel vibrations are accelerated by $0{\cdot}7\lambda$ per cm. of path, while the perpendicular vibrations are retarded by about $0{\cdot}4\lambda$ per cm.

Thus for either of the positions assumed above for the direction of the magnetic moment of the molecule, which seem to be the only probable ones, the change of refractive index due to the magnetic field is sufficiently large to be detected by ordinary interference methods.

But an actual interference arrangement in which one of the interfering beams traversed a length of over 8 cms. of nitric oxide across a magnetic field of about 10,000 gauss, gave entirely negative results, in conformity with the observations on the paramagnetic substances already mentioned. Various pressures from 1 atm. down to a few mm. of mercury were tried.

In connection with this negative result it must be pointed out that for the value of α satisfying the condition

$$\cos^2\alpha=\tfrac{1}{3}\ (i.e.,\ \alpha=54°44'),\ n_{\parallel}=n_{\perp}=n;$$

i.e., the difference between the principal refractive indices in a magnetic field and the mean refractive index outside the field vanishes, the difference being numerically small for values of α not far different from this value. For these directions of the permanent moment, we should therefore expect no detectable change in refractive index in a magnetic field. These directions, however, seem to be highly improbable.

3. *Magnetic Double-Refraction of Oxygen according to the Classical Theory.*

The negative result is not peculiar to the quantum theory. Even if we assume, as in the classical theory of paramagnetism of Langevin, that all orientations of the elementary magnetic moments are equally probable in a magnetic field, of course in the limit when the field vanishes, we still get a value for the double-refraction of oxygen, for

instance, which could not have escaped detection in Schütz's experiments in case it exists.

As in the case of NO it is reasonable to assume that O_2-molecule has an axis of optical symmetry, *viz.*, the line joining the two O-nuclei. If as before, α denotes the angle which the permanent magnetic moment μ of the molecule makes with the optic axis, we have according to the classical theory [6],

$$n_{\parallel} - n_{\perp} = \frac{(n^2-1)(n^2+2)}{4n} \cdot \frac{\theta_1+\theta_2}{\gamma} \cdot H^2, \quad \ldots (5)$$

where

$$\theta_1 = \frac{1}{45k^2T^2} \cdot (A-B)(2A'-B'-C')$$

and

$$\theta_2 = \frac{\mu^2}{45k^2T^2} (A-B)(2\cos^2\alpha - \sin^2\alpha)$$

$$\gamma = \frac{A+2B}{3},$$

A, B have the same significance as before. A', B', C' are the diamagnetic moments induced in a molecule of oxygen per unit magnetic field incident along, and in two mutually perpendicular directions at right angles to its optic axis. H is the incident magnetic field, and k is Boltzmann's constant.

A little calculation shows that for oxygen, θ_1 which depends on the diamagnetic anisotropy of the molecule, is entirely negligible in comparison with θ_2. If we take the diamagnetic values for oxygen calculated by Pascal from its compounds, even assuming that the molecule (O_2) is polarisable diamagnetically only along its optic axis, θ_1 is only about $\frac{1}{400}$ of θ_2 (numerically) when $\alpha=0$, and about $\frac{1}{200}$

[6] See P. Debye, Handbuch der Radiology Band VI, p. 769.

of θ_2 when $\alpha=\frac{\pi}{2}$, which as in the case of NO, seem to be the only probable values for α.

Since n is very nearly equal to 1,

$$n_{\parallel} - n_{\perp} = \frac{n-1}{10k^2T^2} \cdot \mu^2 \cdot H^2 \frac{A-B}{A+2B}(2\cos^2\alpha - \sin^2\alpha)$$

$$= \frac{n-1}{10k^2T^2} \cdot \mu^2 \cdot H^2 \sqrt{\frac{5r}{6-7r}} \cdot (2\cos^2\alpha - \sin^2\alpha) \quad \ldots (6)$$

From the susceptibility measurements of Bauer and Piccard [7]

$$\left(\chi = \frac{0{\cdot}03158}{T}\right)$$

μ on calculation, still according to the classical theory, comes out to be equal to $2{\cdot}62\times10^{-20}$.

At 1 atm. pressure and 20°C., which may be taken as the temperature of Schütz's experiment,

$$n-1 = 2{\cdot}53\times10^{-4}.$$

Also $r = 0{\cdot}0645$ (Cabannes and Granier).

$$\therefore \quad n_{\parallel} - n_{\perp} = 2{\cdot}60\times10^{-18}H^2(2\cos^2\alpha - \sin^2\alpha).$$

For

$$H = 15{,}000 \text{ gauss}$$

$$n_{\parallel} - n_{\perp} = 6\times10^{-10}(2\cos^2\alpha - \sin^2\alpha). \quad \ldots (7)$$

When $\alpha=0$,

$$n_{\parallel} - n_{\perp} = 12\times10^{-10}$$

and is hence four times the amount which Schütz could have detected, and when $\alpha=\pi/2$,

$$n_{\parallel} - n_{\perp} = -6\times10^{-10}$$

which is about twice the amount.

[7] E. Bauer and Piccard, Journ. de Physique Series VI, 1, 97, 1920.

Thus even calculating according to the classical theory, there is no evidence of orientation of paramagnetic molecules in a magnetic field.

The same conclusions have been drawn by Debye and Huber[8] from the negative results of some experiments on nitric oxide and other substances. The molecules of NO, in addition to possessing a permanent magnetic moment, also have a small electric moment. When placed in a magnetic field, if the molecules orientate, owing to their electrical polarity they will induce a difference of potential between two parallel plates placed transversely to the magnetic field. But in their actual experiment there was no such potential difference. It might however be pointed out here that if the electric moment of the molecule is perpendicular to the magnetic moment, which is not improbable, even if there is orientation of the molecules when the field is put on, they will not induce any difference of potential.

4. *Discussion of the Results.*

A natural explanation which would suggest itself for the negative results mentioned in the previous sections, is that if paramagnetic molecules do not orientate as a whole in a magnetic field, the electron-orbits responsible for the moments of the molecules might be free to rotate without disturbing the rest of the molecule. In the case of sodium and potassium, where according to the generally accepted ideas, the single electron in the outermost orbit accounts for the paramagnetism, there is not much difficulty in considering it to be free to rotate independently of the rest of the atom. But the explanation is not without difficulties in the case of NO, for instance. The idea is not new and has been put forward to explain the observed validity of Curie's law in the case of paramagnetic crystals.

[8] P. Debye, Zeits. f. Phys. 36, 300, 1926; A. Huber, Phys. Zeits. 27, 619, 1926.

However the above assumption is not by itself sufficient to account for the absence of any double-refraction in a magnetic field. We will have further to assume that the contributions from these paramagnetic electron-orbits to the optical anisotropy of the molecule is quite negligible. Thus, for instance, in the case of sodium and potassium we will have to assume that the difference in the deformability of the outer electron-orbit due to the electric field of the incident light-waves, when the field is acting in the plane of the orbit and when it is acting perpendicular to the plane, is very small. But when we remember that even the inert gases like argon, krypton and xenon, with closed and symmetrical configurations exhibit an appreciable optical anisotropy, as evidenced by the imperfect nature of the polarisation of the light transversely scattered by them[9], it is rather difficult to understand how the outermost electron-orbit in sodium or potassium can be so perfectly isotropic.

5. *Summary.*

According to the theory of spatial quantization, which may be taken to be fairly well established, the molecular magnetic moments in nitric oxide, equal to one Bohr-magneton each, should all orientate in a magnetic field with their axes either along or against the field. If the moments are rigidly fixed to the molecules, the latter being optically anisotropic, the medium should exhibit a double refraction as a consequence of the orientation.

The magnitude of the double refraction to be expected is calculated. But actually no such double-refraction could be detected.

The negative result is then shown to be not peculiar to the quantum theory. In the case of oxygen, for instance, Schütz could not discover any double-refraction in a strong

[9] See J. Cabannes and A. Lepape, Comptes Rendus 179, 825, 1924.

magnetic field, while calculation accordng to the classical theory shows that the effect could not have escaped detection in Schütz's experiment in case it exists.

It is therefore evident that paramagnetic molecules do not orientate, at least as a whole, in a magnetic field.

Some difficulties in the different explanations that might be suggested for these negative results, are pointed out.

In conclusion the author wishes to express his best thanks to Prof. C. V. Raman for his kind interest in the work.

210, Bowbazar Street, Calcutta,
The 6th December, 1926.

OPTIQUE. — *La constante de biréfringence magnétique du benzène.* Note de MM. **C.-V. Raman** et **K.-S. Krishnan**, présentée par M. Brillouin.

Dans un récent Mémoire (1), nous avons discuté les valeurs de la constante de Cotton-Mouton de biréfringence du benzène et de quelques dérivés à l'état liquide. Comme on sait, la théorie de Langevin explique l'effet Cotton-Mouton comme dû aux molécules qui sont magnétiquement et optiquement anisotropes, leur orientation dans le champ étant la cause pour laquelle le liquide devient biréfringent. Dans ledit Mémoire les résultats pour l'anisotropie optique, dérivés des observations sur la diffu-

(1) C. V. Raman and K. S. Krishnan, *Proc. Roy. Soc. Lond.*, A, 113, 1927, p. 511.

sion de la lumière sont combinés avec les valeurs connues de la constante de Cotton-Mouton afin de déterminer le degré d'anisotropie magnétique des molécules.

Dans cette Communication nous nous proposons de montrer comment, par des suppositions simples sur la structure de la molécule de benzène et sur l'anisotropie optique connue de la même molécule, nous pouvons évaluer directement la constante de Cotton-Mouton, pour la comparer avec la valeur observée.

Pauling (1) a suggéré une structure hexagonale, pour la molécule du benzène, dans laquelle 12 électrons relient ensemble les atomes de charbon et d'hydrogene; 12 électrons relient les atomes de charbon voisins; les six autres forment les trois paires reliant chacune deux atomes de charbon en position para. Nous adoptons cette structure et présupposons que quelques-unes des orbites d'électrons, de ceux qui relient les atomes de charbon et d'hydrogène, restent dans le plan de l'hexagone, tandis que les autres restent dans les plans perpendiculaires à l'hexagone. Les calculs de biréfringence sont faits de la manière suivante. La constante de Cotton-Mouton est donnée par la relation (voir le Mémoire cité)

$$C_m = -\frac{(n_0^2-1)(n_0^2+2)}{60\, n_0 \lambda k T}(3C'-\theta)\sqrt{\frac{\delta}{2}},$$

dans laquelle n_0 est l'indice de réfraction en dehors du champ, $\frac{\theta}{3}$ est la susceptibilité diamagnetique de chaque molécule, en moyenne pour toutes les orientations, C' est sa susceptibilite mesuree perpendiculairement au plan de l'hexagone; δ est une constante exprimant l'anisotropie optique de la molécule. Les autres lettres ont leur signification habituelle. On trouve par le degré de dépolarisation (47 pour 100) de la lumiere diffuse, que δ est 0,090 si la formule de Ramanathan (2) est employée ou 0,045 si l'on emploie la formule de Gans (3). La susceptibilité connue du benzène montre que θ est $-27{,}4\times10^{-29}$ pour chaque molécule. D'après la supposition faite plus haut, la valeur de C' est déterminée entièrement par les orbites de six paires d'électrons reliant les atomes de charbon et d'hydrogène, supposés être dans le plan de l'hexagone; les autres orbites ne contribuent pas à la susceptibilité en direction perpendiculaire a ce plan. La contribution à la

(1) L. Pauling, *Journal Am. Chem. Soc.*, 48, 1926, p. 1139.
(2) K. R. Ramanathan, *Proc. Ind. Ass. Sc.*, 8, 1923, p. 181.
(3) R. Gans, *Zeit. für Phys.*, 17, 1923, p. 353.

susceptibilité pour chaque liaison entre le charbon et l'hydrogène peut être considérée être la même, quand on prend la moyenne de toutes les orientations, comme on trouve dans les séries des hydrocarbones aliphatiques, et peut être calculée par les susceptibilités connues de ces derniers composés. On trouve de cette manière

$$C' = 6\times(-2{,}2)\times10^{-29} = -13{,}2\times10^{-29}.$$

D'ou

$$C_m = 6{,}7\times10^{-12} \quad \text{si} \quad \delta = 0{,}090$$

et

$$C_m = 4{,}8\times10^{-12} \quad \text{si} \quad \delta = 0{,}045.$$

Si, d'un autre côté, nous prenons les suppositions que tous les orbites charbon-charbon sont dans le plan de l'hexagone et que les orbites charbon-hydrogène sont dans les plans perpendiculaires à cet hexagone,

$$C' = -27{,}4\times10^{-29} + 13{,}2\times10^{-29} = -14{,}2\times10^{-29}.$$

D'où les valeurs calculées

$$C_m = 8{,}4\times10^{-12} \quad \text{ou} \quad 5{,}9\times10^{-12},$$

qui correspondent aux deux valeurs de δ ci-dessus (Ramanathan, Gans).

La valeur observée est

$$C_m = 5{,}90\times10^{-12}.$$

OPTIQUE. — *Sur le vent d'éther.* Note (1) de MM. **A. Piccard** et **E. Stahel**, transmise par M. Pierre Weiss.

La Note de M. E. Brylinski (2) suggère quelques remarques :

1° Toutes nos mesures ayant relevé des vents d'éther inférieurs à l'erreur probable de nos mesures, on ne peut rien en conclure en faveur des résultats de Miller, comme le fait M. Brylinski.

2° Nous avons fait nos mesures à Bruxelles après avoir pris connaissance des dernieres publications de Miller (3) dans lesquelles il déclare formellement qu'il ne trouve pas de différence notable entre le vent d'éther de la plaine et celui du Mont Wilson et nous avons mentionné ce dernier fait

(1) Séance du 14 février 1927.
(2) *Comptes rendus*, 184, 1927, p. 192.
(3) *Science*, 63, 1926, p. 433.

The Magnetic Anisotropy of Crystalline Nitrates and Carbonates.

By K. S. Krishnan and Prof. C. V. Raman, F.R.S.

(Received March 27, 1927.)

1. *Introduction.*

Recent work in the field of magnetism emphasises the relation between the crystal structure and magnetic properties of solids. Such relations exist in all crystals whether ferromagnetic, paramagnetic or diamagnetic. We propose in this paper to discuss the explanation of the anisotropy of diamagnetic crystals, particularly some nitrates and carbonates with regard to which we have data from the measurements of Voigt and Kinoshita* and very recently of Rabi.† These substances are especially simple because, as is well-known from the work of Kossel, Bragg and others, they consist of charged ions held together by electrostatic forces, so that we can attribute the magnetic anisotropy of the crystal to that of the individual ions. Thus, for instance, in the case of sodium and potassium nitrates we may reasonably look for the explanation of observed magnetic anisotropy of the crystal in the structure of the nitrate ion, since presumably the metallic ions are more or less isotropic. It is significant in this connection that nitric acid solution has been found by Cotton and Mouton‡ to exhibit a measurable magnetic birefringence, thus indicating that the NO_3^- ion has a pronounced magnetic anisotropy even in the liquid state. It is possible to estimate this anisotropy in a purely optical way by combining the data for magnetic double-refraction with the measurements of the depolarisation of the light scattered in nitric acid. It is found that the magnetic anisotropy of the NO_3 group thus found, practically agrees with that necessary, as remarked above, to explain the magnetic properties of the crystalline nitrates.

2. *Relation between Structure and Magnetic Properties.*

The crystal structures of sodium nitrate and calcite have been investigated by X-ray methods and the two crystals are found to be homœomorphous. They have an axis of trigonal symmetry. The NO_3 or CO_3 groups are built up of three oxygen atoms at the corners of an equilateral triangle with the nitrogen or carbon atom at the centre, the plane of the triangle being perpendicular to

* 'Ann. d. Physik,' vol. 24, p. 492 (1907).
† 'Phys. Rev.,' vol. 29, p. 174 (Jan., 1927).
‡ 'Ann. Chim. et Phys.,' vol. 28, p. 209 (1913).

the trigonal axis. Potassium nitrate and aragonite, on the other hand, belong to the rhombic system; but here also the three oxygen atoms are arranged symmetrically round the nitrogen or carbon atoms in a plane perpendicular to the "c" axis.

In the following table are given the principal diamagnetic susceptibilities for these crystals :—

Compound.	Crystal system.	Axis along which susceptibility is measured.	Susceptibility per gm. molec. $\times -10^6$.	Average susceptibility per gm. molec. $\times -10^6$.
$NaNO_3$	trigonal	∥ trig. axis	29·5	25·9
		⊥ trig. axis	24·1	
$CaCO_3$ (calcite)	trigonal	∥ trig. axis	40·0	37·8
		⊥ trig. axis	36·4	
KNO_3	rhombic	∥ "c" axis	35·6	31·7
		∥ "b" axis	29·7	
		∥ "a" axis	29·9	
$CaCO_3$ (aragonite)	rhombic	∥ "c" axis	44·4	40·8
		∥ "b" axis	38·7	
		∥ "a" axis	39·2	

Sodium nitrate and calcite are magnetically uniaxial owing to the possession of an axis of trigonal symmetry. For potassium nitrate and aragonite, however, the susceptibilities along the "b" and "a" axes are different. But the difference is very small, so that for all practical purposes we may treat them also as magnetically uniaxial crystals. In all the cases quoted in the table, the susceptibility along the axis, which we shall denote by $\chi_\parallel$, is numerically greater than the susceptibility, $\chi_\perp$, perpendicular to the axis. It is also significant that $\chi_\parallel - \chi_\perp$ is very nearly the same for the two nitrates, and not very different for the two forms of calcium carbonate. It suggests immediately that the nitrate and carbonate ions are, at least in a very large measure, responsible for the magnetic anisotropy of the respective crystals.

3. *Relation to Magnetic Birefringence.*

Before proceeding to connect the magnetic anisotropy of the NO_3^- ion in the crystals with its anisotropy as deduced from observations on magnetic double-refraction of nitric acid (liquid), we may point out that we would not be justified in assuming that the NO_3^- ion is necessarily identical in the two cases. For instance, it is well-known from the investigations of Oxley* that many dia-

* 'Phil. Trans.,' A, vol. 214, p. 109 (1914).

magnetic substances show an appreciable change of susceptibility on crystallisation, suggesting a re-adjustment of the electron-orbits as we pass from the liquid to the crystalline state. We cannot therefore expect any exact numerical agreement between the values of the anisotropy of the NO_3^- ion calculated from the two states.

The constant of magnetic birefringence (Cotton–Mouton constant) of nitric acid has been measured by Cotton and Mouton and $= 6{\cdot}3 \times 10^{-14}$ at about 16° C. for light of wave-length $\lambda = 5{\cdot}78 \times 10^{-5}$ cm. They, however, used acid of density 1·49, which corresponds to a concentration of about 90 per cent. Since the magnetic birefringence of water is negligibly small, we will not be far out if we estimate the value of the constant for 100 per cent. acid at

$$6{\cdot}3 \times 10^{-14} \times \frac{10}{9} = 7{\cdot}0 \times 10^{-14}.$$

In order to evaluate the magnetic anisotropy of the molecule from the Cotton-Mouton constant, we require to know the optical constants of the molecule. From the recent work of Bragg* on the birefringence of crystalline nitrates, we have very strong reasons to believe that HNO_3 molecule possesses an axis of optical symmetry, which is perpendicular to the plane of the NO_3^- ion; the moment induced in the molecule by unit field of the incident light-waves, acting along this axis, equal to C, say, being less than when it is acting perpendicular to it (= A). On actual calculation from Bragg's data, the ratio of these moments C/A comes out equal to 0·60. However, since the Cotton-Mouton constant refers to the liquid state it is only proper that we should use the value of the optical anisotropy calculated from measurements under the same conditions. Recently careful measurements have been made in the authors' laboratory by Mr. S. Venkateswaran† on the depolarisation of the light scattered by nitric acid of different concentrations. The value of the depolarisation factor extrapolated for 100 per cent. acid = 0·64. Calculating from this value we get

$$C/A = 0{\cdot}38 \text{ or } = 0{\cdot}50,$$

according to the two hypotheses that have been proposed for light-scattering. Even though the experimental data at present available are not sufficient to decide definitely which of the two hypotheses is correct, the data are more in accord with the hypothesis which gives the latter value of C/A, viz., 0·50.‡

* 'Roy. Soc. Proc.,' A, vol. 106, p. 346 (1924).
† 'Indian Journal of Physics,' vol. 1, p. 235 (1927).
‡ See K. S. Krishnan, 'Proc. Indian Ass. Sci.,' vol. 9, p. 251 (1926).

Now the magnetic anisotropy of HNO_3 molecule can be calculated from the Cotton-Mouton constant, C_m of liquid nitric acid, with the help of the relation

$$C_m = -\frac{(n_0^2-1)(n_0^2+2)}{30 n_0 \lambda k T} \cdot \frac{A-C}{2A+C} \cdot (C'-A'),$$

where n_0 is the refractive index of the liquid outside the field, k is Boltzmann's constant, C′ and A′ are the susceptibilities of the molecule along and perpendicular to the axis respectively. A being greater than C, it is evident from the above expression that in order to get a positive value for magnetic birefringence, as is actually observed, C′ should be numerically greater than A′, *i.e.*, the diamagnetic susceptibility of the NO_3^- ion along its axis should be numerically greater than for perpendicular directions—in conformity with the observations on crystals.

Actually substituting values for C_m and C/A in the expression, we obtain

$$C' - A' = -6{\cdot}7 \times 10^{-30}$$
$$\text{or } -8{\cdot}8 \times 10^{-30}$$

corresponding to the two values of C/A.

Now according to the assumptions we have made

$$\chi_\parallel = N C'$$
and $$\chi_\perp = N A'$$

where N is the Avogadro number per gram molecule.

Therefore $$\chi_\parallel - \chi_\perp = -4{\cdot}1 \times 10^{-6}$$
or $$-5{\cdot}3 \times 10^{-6},$$

which may be compared with the observed values

$$-5{\cdot}4 \times 10^{-6} \text{ for } NaNO_3$$
and $$-5{\cdot}8 \times 10^{-6} \text{ for } KNO_3.$$

It may also be mentioned incidentally that the absolute value of the susceptibility of NO_3^- ion is the same in the crystals and in nitric acid. If from the average susceptibilities of $NaNO_3$ and KNO_3 we deduct the contributions from the Na^+ and K^+ ions as given by Joos,* we get for the average susceptibility of NO_3^- ion respectively the values—

$$\chi = -(25{\cdot}9 - 6{\cdot}5) \times 10^{-6} = -19{\cdot}4 \times 10^{-6}$$
and $$\chi = -(31{\cdot}7 - 14{\cdot}5) \times 10^{-6} = -17{\cdot}2 \times 10^{-6}$$

per gram molecule.

* G. Joos, 'Z. f. Physik,' vol. 32, p. 835 (1925).

The value calculated from Quincke's results for nitric acid of about 63 per cent. concentration

$$= -17 \times 10^{-6} \text{ per gm. molecule.}^*$$

4. *Relation to the Structure of Ions.*

We have to look for the explanation of the observed magnetic anisotropy of the NO_3^- ion in its peculiar electronic structure. The three O-atoms are distributed symmetrically round the N-atom as centre, all of them lying in the same plane. Pauling† has recently suggested a dynamical model from entirely independent considerations, where he assumes six of the electrons to move in pairs in orbits connecting the central N-atom in turn with the three O-atoms, the other eighteen electrons being distributed about the three O-atoms. (Of course we exclude the K-electrons as contributing negligibly to the susceptibility.) If we now assume that the electron-orbits connecting the N- and O-atoms are in the plane of the atoms, and the other orbits are orientated more or less isotropically, the diamagnetic susceptibility perpendicular to the plane of NO_3^- ion will be numerically greater than for directions in the plane by an amount equal to the contribution from the six binuclear orbits. Taking the other electron-orbits to be all of equal size, it is found on calculation, from the assumption made above, that the susceptibility of a binuclear orbit should be much less than that of one of the other orbits. Too little is known at present regarding multinuclear electron-orbits to enable us to verify how far this conclusion is in accord with the general theory of diamagnetism. The results seem to suggest that these binuclear orbits, if elliptical, should have a large eccentricity.

However, the main conclusion that the anisotropy arises from the six binuclear orbits, seems to gain a further support from the fact that the CO_3^- ion, which has an essentially similar structure, exhibits a magnetic anisotropy (defined by $\chi_{\parallel} - \chi_{\perp}$) almost the same as for the NO_3^- ion. In this connection it need hardly be emphasised that further data on the magnetic susceptibilities of a number of crystals of this type, *e.g.*, nitrates, silicates, carbonates and borates, would be highly desirable and we have initiated experimental work in this direction.

* The susceptibility of nitric acid is assumed, consistently with our assumptions, to be entirely due to the NO_3 ion, the hydrogen atom, having lost its electron, contributing nothing to it.

† L. Pauling, 'J. Am. Chem. Soc.,' vol. 48, p. 1139 (1926).

5. *Summary.*

Crystals of sodium and potassium nitrates exhibit a marked diamagnetic anisotropy, the susceptibility perpendicular to the plane of the NO_3^- ion being greater than for directions in the plane; the difference of susceptibility in the two directions is the same for the two crystals.

Attributing this anisotropy to that of the NO_3^- ion, it is found that its magnitude is exactly what we should expect from the known value of the magnetic birefringence (Cotton-Mouton effect) of nitric acid liquid.

An explanation is suggested on the basis of its electronic structure; CO_3^- ion which has essentially the same structure, gives almost the same anisotropy.

PROCEEDINGS OF
THE ROYAL SOCIETY.

Section A.—Mathematical and Physical Sciences.

A Theory of Electric and Magnetic Birefringence in Liquids.

By Prof. C. V. Raman, F.R.S., and K. S. Krishnan.

(Received July 25, 1927.)

1. *Introduction.*

The double refraction exhibited by liquids when placed in an electrostatic field is ascribed in the theory of Langevin* to an orientation of the molecules produced by the field, the orientative couple arising from assumed electrical anisotropy of the molecule. If an optical anisotropy of the molecule is postulated in addition, the birefringence of the liquid follows as a necessary consequence. Born† modified the Langevin theory by including also the orientative effect of the field on the molecule due to the permanent electric moment, if any, possessed by it. The optical anisotropy and electrical polarity of the molecule postulated in these theories can be independently determined from observations of light-scattering and dielectric constant in the vapours of the substances. In two recent papers‡ we have attempted to discuss how far the available data for the Kerr effect can be reconciled with the theories of Langevin and Born. The main result emerging is that these theories fail to give the magnitude of the Kerr constant in *liquids* correctly in terms of the constants of the molecule as determined in the gaseous condition. This failure is illustrated in Table I for a number of liquids having non-polar molecules for which the optical anisotropy is known from observations on light-scattering in the vapour.

It appears hardly likely that the failure of the Langevin theory indicated by the figures in Table I can be ascribed to a real change in the optical anisotropy of the molecule when it passes from the condition of vapour to that of liquid. It seems rather that the explanation must lie in the inadequacy of the theory itself. We accordingly propose in this paper to put forward a theory of electric and magnetic double refraction, in which the fundamental premises of Langevin and Born are revised.

* 'Le Radium,' vol. 9, p. 249 (1910).
† 'Ann. der Physik,' vol. 55, p. 177 (1918).
‡ 'Phil. Mag.,' vol. 3, pp. 713 and 724 (1927).

Table I.

Liquid.	Depolarisation of the light scattered by the corresponding vapour.	Kerr constant × 10^6.	
		Calculated according to Langevin's theory.	Observed.
	Per cent.		
Pentane	1·28	17·9	5·0
Isopentane	1·2	16·2	5·0
Hexane	1·41	19·7	4·5 5·6
Heptane	1·40	30	7·1 10·5
Octane	1·66	43	7·7 13·6
Carbon tetrachloride	0·6	14·4	7·4
Carbon bisulphide	10·7	390	322·6
Benzene	4·40	122	59·3
Cyclohexane	1·26	26	7·4

2. *The Polarisation Field in Liquids.*

Both Langevin and Born assume that, while the molecule individually is anisotropic, the polarisable matter present round it is so distributed that the local polarisation field acting on the molecule is independent of its orientation in the field. There is reason to believe that this assumption cannot be correct in a dense fluid, and that, in addition to considering the anisotropy of the molecule itself, we have also to postulate an anisotropic distribution of polarisable matter in its immediate neighbourhood. For the purpose of a purely formal mathematical theory it is unnecessary to discuss in detail how such anisotropic distribution of matter arises. We assume only that the orientation of the molecule determines the distribution of matter around it, and therefore also the local polarisation field acting on it. That the polarisation field acting on a molecule may vary with its orientation in the liquid has been previously suggested by other writers, notably Havelock* and Lundblad.† But while these writers have put forward the hypothesis as an independent theory of electric double refraction, we, on the other hand, consider it only as modifying the premises of the Langevin-Born theory, and find that its effect, in general, is actually to diminish the magnitude of the Kerr effect to be expected. Independent evidence in support of the hypothesis is furnished by studies of X-ray diffraction, by the deviations from the Lorentz refraction formula, and by observations of light-scattering, in liquids. In order, however, not unduly to lengthen this paper, we refrain from presenting this evidence here, and will merely assume the existence of the "anisotropic" polarisation field.

* 'Roy. Soc. Proc.,' A, vol. 84, p. 492 (1911).
† 'Optik der dispergierenden Medien,' p. 57 (Upsala, 1920).

The average value of m_z taken over all the molecules is given by

$$\overline{m_z} = \frac{\int e^{-\frac{u}{kT}} m_z \sin\theta \, d\theta \, d\phi \, d\psi}{\int e^{-\frac{u}{kT}} \sin\theta \, d\theta \, d\phi \, d\psi}, \tag{9}$$

which, after a long calculation, reduces to

$$\overline{m_z} = \frac{B_{1z} + B_{2z} + B_{3z}}{3} + 2(\Theta_{1z} + \Theta_{2z})\frac{E^2}{2}, \tag{10}$$

where

$$\Theta_{1z} = \frac{1}{45kT}[(A_1 - A_2)(B_{1z} - B_{2z}) + (A_2 - A_3)(B_{2z} - B_{3z}) + (A_3 - A_1)(B_{3z} - B_{1z})] \tag{11}$$

$$\Theta_{2z} = \frac{1}{45k^2T^2}[(M_1^2 - M_2^2)(B_{1z} - B_{2z}) + (M_2^2 - M_3^2)(B_{2z} - B_{3z}) + (M_3^2 - M_1^2)(B_{3z} - B_{1z})] \tag{12}$$

Also

$$\chi_{0z} = \nu\overline{m_z}. \tag{13}$$

Case II.—The light-vector is perpendicular to the electrostatic field, say, along the x-axis.

We can show, just as in Case I, that the average contribution from a molecule to the optical moment along the x-axis is given by

$$\overline{m_x} = \frac{B_{1x} + B_{2x} + B_{3x}}{3} - (\Theta_{1x} + \Theta_{2x})\frac{E^2}{2}, \tag{14}$$

where

$$\left.\begin{aligned} B_{1x} &= b_1(1 + q_1\chi_{0x}) \\ B_{2x} &= b_2(1 + q_2\chi_{0x}) \\ B_{3x} &= b_3(1 + q_3\chi_{0x}) \end{aligned}\right\}, \tag{15}$$

χ_{0x} being the optical susceptibility of the medium along the x-axis.

$$\chi_{0x} = \nu\overline{m_x}. \tag{16}$$

$$\Theta_{1x} = \frac{1}{45kT}[(A_1 - A_2)(B_{1x} - B_{2x}) + (A_2 - A_3)(B_{2x} - B_{3x}) + (A_3 - A_1)(B_{3x} - B_{1x})]. \tag{17}$$

$$\Theta_{2x} = \frac{1}{45k^2T^2}[(M_1^2 - M_2^2)(B_{1x} - B_{2x}) + (M_2^2 - M_3^2)(B_{2x} - B_{3x}) + (M_3^2 - M_1^2)(B_{3x} - B_{1x})]. \tag{18}$$

From equations (10) and (14)

$$\overline{m_z} - \overline{m_x} = \tfrac{1}{3}(b_1q_1 + b_2q_2 + b_3q_3)(\chi_{0z} - \chi_{0x}) + [2(\Theta_{1z} + \Theta_{2z}) + (\Theta_{1x} + \Theta_{2x})]\frac{E^2}{2}. \tag{19}$$

If n_p and n_s are the refractive indices of the medium for vibrations along and perpendicular to the field,

$$\overline{m_z} = \frac{n_p^2 - 1}{4\pi\nu}; \quad \overline{m_x} = \frac{n_s^2 - 1}{4\pi\nu},$$

$$\overline{m_z} - \overline{m_x} = \frac{n_p^2 - n_s^2}{4\pi\nu} = \frac{n_0(n_p - n_s)}{2\pi\nu}, \tag{20}$$

n_0 being the mean refractive index of the medium.

Also

$$\chi_{0z} - \chi_{0x} = \nu(\overline{m_z} - \overline{m_x}). \tag{21}$$

From (20), (21) and (19) we have

$$n_p - n_s = \frac{2\pi\nu}{n_0} \cdot \frac{2(\Theta_{1z} + \Theta_{2z}) + (\Theta_{1x} + \Theta_{2x})}{1 - \frac{\nu}{3}(b_1q_1 + b_2q_2 + b_3q_3)} \cdot \frac{E^2}{2}. \tag{22}$$

Since the values of the optical susceptibility of the medium along and perpendicular to the field are nearly equal, we may write in equation (22)

$$\Theta_{1z} = \Theta_{1x} = \Theta_1$$

and

$$\Theta_{2z} = \Theta_{2x} = \Theta_2,$$

where

$$\Theta_1 = \frac{1}{45kT}[(A_1 - A_2)(B_1 - B_2) + (A_2 - A_3)(B_2 - B_3) + (A_3 - A_1)(B_3 - B_1)], \tag{23}$$

$$\Theta_2 = \frac{1}{45k^2T^2}[(M_1^2 - M_2^2)(B_1 - B_2) + (M_2^2 - M_3^2)(B_2 - B_3) + (M_3^2 - M_1^2)(B_3 - B_1)], \tag{24}$$

$$\left.\begin{aligned} B_1 &= b_1(1 + q_1\chi_0) \\ B_2 &= b_2(1 + q_2\chi_0) \\ B_3 &= b_3(1 + q_3\chi_0) \end{aligned}\right\}, \tag{25}$$

χ_0 being the mean value of the optical susceptibility of the medium.

Also

$$\chi_0 = \nu \frac{b_1(1+q_1\chi_0) + b_2(1+q_2\chi_0) + b_3(1+q_3\chi_0)}{3},$$

$$= \frac{\nu\gamma_0}{1 - \frac{\nu}{3}(b_1q_1 + b_2q_2 + b_3q_3)}, \tag{26}$$

where

$$\gamma_0 = \frac{b_1 + b_2 + b_3}{3}.$$

Substituting in (22), we finally obtain for the Kerr constant

$$K = \frac{n_p - n_s}{\lambda E^2} = \frac{n_0^2 - 1}{4n_0\lambda} \cdot \frac{3(\Theta_1 + \Theta_2)}{\gamma_0}. \tag{27}$$

When the polarisation field acting on the molecules is isotropic,

$$p_1 = p_2 = p_3 = \frac{4\pi}{3},$$

and also

$$q_1 = q_2 = q_3 = \frac{4\pi}{3};$$

$$\Theta_1 = \frac{1}{45kT}[(a_1 - a_2)(b_1 - b_2) + (a_2 - a_3)(b_2 - b_3) + (a_3 - a_1)(b_3 - b_1)]\left(\frac{\delta+2}{3}\right)^2 \cdot \frac{n_0^2+2}{3} \tag{28}$$

and

$$\Theta_2 = \frac{1}{45k^2T^2}[(\mu_1^2 - \mu_2^2)(b_1 - b_2) + (\mu_2^2 - \mu_3^2)(b_2 - b_3) + (\mu_3^2 - \mu_1^2)(b_3 - b_1)]\left(\frac{\delta+2}{3}\right)^2 \cdot \frac{n^2+2}{3}, \tag{29}$$

where δ is the dielectric constant of the medium ; and expression (27) naturally reduces to that given by the Langevin-Born theory.*

In the above discussion we have entirely neglected the effect of electrostriction, since it will not affect the value of the *difference* in refractive indices for vibrations along and perpendicular to the incident field.

5. *Comparison of Theory and Observation.*

In order to apply the foregoing modified formula to any actual liquid, we have to make some assumptions regarding the origin of the anisotropy of the polarisation field. The anisotropy might arise in the following way. We replace for simplicity the molecules in the medium by the equivalent doublets

* See Debye, Marx's ' Handbuch der Radiologie,' vol. 6, p. 768.

placed at their respective centres. The finite size of the molecules imposes naturally a limit to the closeness of approach of the doublets towards each other. Round any particular molecule as centre we can describe a closed surface, entry into which by other molecules is excluded by reason of their finite size. The form of the surface will naturally be determined by the shape of the molecule and will therefore, in general, be non-spherical, *i.e.*, the distribution of polarisable matter around the molecule under consideration will have no spherical symmetry with respect to it, and hence arises an anisotropy in the polarisation field.

We may provisionally represent this surface by an ellipsoid having the molecule at its centre, and consider, as an approximation, the distribution as well as the orientation of the molecules outside to be entirely fortuitous. Then the polarisation field at the centre of the ellipsoid will be equivalent to that due to a surface charge $-\chi E\cos\theta$ per unit area at any point of the surface of the ellipsoid the normal to which makes an angle θ with the direction of E.

Let us consider two simple cases.

Case I.—The ellipsoid is a prolate spheroid of revolution ;

$$b = c = \sqrt{1-e^2}\,.\,a,$$

say, where a, b, c are the semi-axes of the ellipsoid. The polarisation constants along the axes are*

$$p_1 = 4\pi\left(\frac{1}{e^2} - 1\right)\left(\frac{1}{2e}\log\frac{1+e}{1-e} - 1\right) \tag{30}$$

$$p_2 = p_3 = 2\pi\left(\frac{1}{e^2} - \frac{1-e^2}{2e^3}\log\frac{1+e}{1-e}\right). \tag{31}$$

As an example we may take pentane, which is a fairly elongated molecule. From X-ray measurements the cross-sectional diameter of the molecule is equal to 4·90 Å.U. and its length is about 8·7 Å.U. Hence, as an approximation, we may take for the semi-axes of the ellipsoid

$$a = \left(\frac{8\cdot7}{2} + \frac{4\cdot9}{2}\right)\text{Å.U.} = 6\cdot8\text{ Å.U.},$$

$$b = c = 4\cdot9\text{ Å.U.}$$

On calculation from these dimensions

$$p_1 = q_1 = 3\cdot15,$$

$$p_2 = p_3 = q_2 = q_3 = 4\cdot71.$$

* See Maxwell, ' Treatise on Electricity and Magnetism,' 3rd edn., vol. 2, p. 69.

We may also reasonably take the optical ellipsoid of the molecule to be a prolate spheroid of revolution about the geometrical axis of the molecule. Using for the depolarisation factor of the light scattered by the vapour the value $r = 0{\cdot}0128$ and for the refractivity at 0°C., $n - 1 = 1{\cdot}711 \times 10^{-3}$ per atm.,

$$b_1 = 12{\cdot}15 \times 10^{-24},$$
$$b_2 = b_3 = 9{\cdot}01 \times 10^{-24}.$$

Hence

$$A_1 = 17{\cdot}88 \times 10^{-24},$$
$$A_2 = A_3 = 15{\cdot}66 \times 10^{-24}.$$

Also

$$B_1 = 14{\cdot}74 \times 10^{-24},$$
$$B_2 = B_3 = 11{\cdot}88 \times 10^{-24}.$$

Therefore

$$K = 5{\cdot}5 \times 10^{-9},$$

as against $17{\cdot}9 \times 10^{-9}$ calculated according to the Langevin theory.

The observed value $= 5{\cdot}0 \times 10^{-9}$.

Case II.—The ellipsoid surrounding the molecule is an oblate spheroid of revolution:

$$a = b = \frac{c}{\sqrt{1-e^2}}.$$

Then

$$p_1 = p_2 = 2\pi\left(\frac{\sqrt{1-e^2}}{e^3}\sin^{-1}e - \frac{1-e^2}{e^2}\right), \tag{32}$$

$$p_3 = 4\pi\left(\frac{1}{e^2} - \frac{\sqrt{1-e^2}}{e^3}\sin^{-1}e\right). \tag{33}$$

As an example for this case we may take benzene. The X-ray diffraction pattern of the liquid has been critically studied by Prof. Sogani* and shows two rings corresponding to mean molecular distances of 4·90 Å.U. and about 3·42 Å.U. respectively. Solid benzene also gives very intense lines, corresponding to a spacing approximately equal to the above distances.† We may reasonably take these distances for the semi-axes of the ellipsoid

$$a = b = 4{\cdot}90 \text{ Å.U.},$$
$$c = 3{\cdot}42 \text{ Å.U.}$$

We then obtain

$$p_1 = p_2 = q_1 = q_2 = 3{\cdot}56;$$
$$p_3 = q_3 = 5{\cdot}44.$$

* 'Indian Journal of Physics,' vol. 1, p. 357 (1927).

† Broomé, 'Phys. Z.,' vol. 24, p. 124 (1923).

From $r = 0{\cdot}0440$ for the vapour and from the refractivity, assuming the optical ellipsoid of the molecule to be an oblate spheroid of revolution about the geometric axis, we get

$$b_1 = b_2 = 12{\cdot}33 \times 10^{-24},$$
$$b_3 = 6{\cdot}26 \times 10^{-24},$$
$$A_1 = A_2 = 22{\cdot}36 \times 10^{-24},$$
$$A_3 = 14{\cdot}63 \times 10^{-24}.$$

Also

$$B_1 = B_2 = 16{\cdot}61 \times 10^{-24},$$
$$B_3 = 9{\cdot}57 \times 10^{-24}.$$

Hence

$$K = 6{\cdot}2 \times 10^{-8},$$

as against the value $12{\cdot}2 \times 10^{-8}$ calculated according to Langevin's theory.

The observed value $= 5{\cdot}93 \times 10^{-8}$.

It is necessary to remark that, considering the nature of the assumptions made, the numerical agreement in these cases should not be unduly emphasised. It should be considered only as indicating that the effect of the anisotropy of the polarisation field is of the order of magnitude necessary to explain the deviation of Langevin's theory from observation.

An examination of Table I shows that in all cases the influence of the anisotropy of the polarisation field is to diminish the magnitude of the Kerr effect to be expected. On the above assumption of an ellipsoidal cavity this result finds a ready explanation in the fact that the longer geometrical dimension of the molecule—and therefore also of the ellipsoid—almost always goes hand-in-hand with the direction of greater electrical or optical polarisability of the molecule.

6. *Summary.*

In this paper a new theory of electric and magnetic double refraction in liquids is put forward, which can in essence be regarded as a modification of the Langevin-Born theory. It is assumed in the latter theory that, while the molecules themselves are anisotropic, their distribution round any particular molecule in the medium can be considered as being spherically symmetrical with respect to it. This assumption can hardly be correct in any actual liquid, so that the local polarisation field acting on any molecule must depend on its orientation. The Langevin-Born theory is accordingly modified so as to take this "anisotropy" of the polarisation field also into account.

Density of Vapour in Mercury Arc.

The modified expression for birefringence is in better accord with facts than the Langevin-Born expression. As a rule the effect of the "anisotropy" of the polarisation field is to diminish the magnitude of the birefringence to be expected. This is explicable as due to the fact that, in general, the longer linear dimension of a molecule tends to be also the direction of maximum electrical and optical susceptibility. The distribution of the molecules in a dense fluid therefore tends to be such that their mutual influence is equivalent to an apparent diminution in the anisotropy of the molecules.

The Maxwell Effect in Liquids.

CLERK MAXWELL many years ago surmised that viscous liquids in a state of flow should exhibit birefringence, and devised methods of observing the phenomenon. Vorländer and Walter (*Zeits. Phys. Chem.*, **118**, 1; 1925) have recently investigated no fewer than 172 liquids of known chemical composition by Maxwell's method, and their work has demonstrated conclusively that a great many pure liquids which cannot by any stretch of language be classed as colloids, exhibit birefringence when subjected to viscous flow. The Maxwell effect, as it may be called, is thus a characteristic property of pure liquids just as much as the power of exhibiting birefringence in strong electrostatic or magnetic fields. We wish briefly in this note to indicate a molecular theory of the Maxwell effect we have worked out which has proved itself very successful in explaining the observed phenomena.

It is easily seen that the stresses in flowing liquid can be considered as equivalent to a set of tensions and a set of pressures acting perpendicularly to each other, and at angles of 45° to the plane of sliding. When the liquid consists of molecules which are highly asymmetric in shape, there would be a tendency for the molecules to orientate under the influence of this system of stresses in such manner that the longest dimension of a molecule tends to lie along the axis of tensions and the shortest one along that of pressures; because such orientation would evidently result in the fluid, regarded as a densely packed assemblage of molecules, expanding along the direction of tensions and contracting along the direction of pressures, thus allowing the system of stresses to do work. By considering the work done during such deformation by the acting stresses as equivalent to the change of energy of the molecules resulting from orientation under a system of couples acting upon them, we can determine the latter in terms of the viscous forces and the asymmetry of shape of the molecules; it being remembered that the orientation is opposed by the thermal agitation of the fluid and that the resulting equilibrium is to be determined statistically in accordance with the Boltzmann principle.

The birefringence of the fluid resulting from the orientation of the molecules under the viscous stresses and their known optical anisotropy, is then readily worked out on lines analogous to those used by Langevin in his theory of electric and magnetic double refraction. The final expression obtained in this way for the difference between the refractive indices n_t and n_p for the vibrations along the axes of tensions and pressures respectively, is:

$$n_t - n_p = \frac{(n^2-1)(n^2+2)}{5nvkT} \cdot \frac{(a_1-a_2)(b_1-b_2)+(a_2-a_3)(b_2-b_3)+(a_3-a_1)(b_3-b_1)}{(a_1+a_2+a_3)(b_1+b_2+b_3)} \cdot \eta \frac{v}{c},$$

where n is the mean refractive index of the fluid, ν is the number of molecules per unit volume, k is the Boltzmann constant, T is the absolute temperature, a_1, a_2, a_3 are the linear dimensions of the molecule along the three principal axes, b_1, b_2, b_3 are the optical moments induced in the molecule along these axes by unit field acting on it successively along the same three directions, η is the coefficient of viscosity and v/c is the velocity gradient.

The birefringence calculated from our formula, utilising the optical anisotropy ascertained from observations on light scattering and the geometrical dimensions derived from X-ray data, comes out in excellent agreement with the determinations of Vorländer and Walter.

The extension of the theory to the case of colloidal solutions and gels is at present engaging our attention.

C. V. RAMAN.
K. S. KRISHNAN.

210 Bowbazar Street,
Calcutta, India, Sept. 17.

LI. *A Theory of Light-Scattering in Liquids.*

By Prof. C. V. Raman, *F.R.S., and* K. S. Krishnan *.

1. *Introduction.*

THE theory of light-scattering in gases with optically anisotropic molecules was discussed by the late Lord Rayleigh † and by Born ‡, whose investigations showed that the anisotropy results in the transversely scattered light becoming imperfectly polarized and also in making its intensity greater than for a gas of equal refractivity with isotropic molecules. In a monograph § by one of us, published in February 1922, and in further papers communicated shortly afterwards to the Philosophical Magazine ||, the case of dense fluids was dealt with, and it was shown that by considering the scattering due to the thermal fluctuations of density in the fluid and also the additional scattering due to the anisotropy and varying orientations of the molecules, the observed phenomena could be satisfactorily explained. A general theory of light-scattering in fluids from the molecular standpoint was worked out shortly afterwards in two papers by Dr. K. R. Ramanathan ¶. His treatment is very wide in its scope and is applicable equally to the case of polar and non-polar molecules. Dr. Ramanathan has returned again to the subject, and in a recent paper ** has examined critically the relation of his general theory to the special treatment worked out by R. Gans ††
for the restricted class of liquids with non-polar molecules.

An examination of the data for depolarization of the light scattered by fluids with the aid of Ramanathan's formulæ indicates an apparent change (usually a large diminution) in the optical anisotropy of the molecules of a given substance as it passes from the condition of vapour to that of liquid ‡‡. A similar discrepancy becomes apparent when the optical anisotropy of the molecule is determined from the

* Communicated by the Authors.
† Lord Rayleigh, Phil. Mag. vol. xxxv. p. 373 (1918).
‡ M. Born, *Deutsch. Phys. Gesell. Ver.* vol. xix. p. 243 (1917).
§ C. V. Raman, 'Molecular Diffraction of Light,' Calcutta Univ. Press (1922).
|| C. V. Raman and K. R. Ramanathan, Phil. Mag. vol. xlv. p. 113 (1923); C. V. Raman and K. S. Rao, vol. xlv. p. 625 (1922).
¶ K. R. Ramanathan, Proc. Ind. Assoc. Cult. Sc. vol. viii. pp. 1 & 181 (1923).
** K. R. Ramanathan, Indian Journal of Physics, i. p. 413 (1927).
†† R. Gans, *Zeits. für Physik*, xvii. p. 353 (1923).
‡‡ K. S. Krishnan, Proc. Ind. Assoc. Cult. Sc. ix. p. 251 (1926).

electric double refraction in the liquid *, using the well-known formula due to Langevin, and is compared with the value derived from observations on light-scattering in the vapour. As an explanation of this phenomenon it may of course be suggested that some kind of temporary grouping or association of neighbouring molecules occurs in the liquid in such a manner as to diminish their effective optical anisotropy. Such an assumption however, besides being artificial and qualitative, would appear difficult to sustain, particularly when it is noticed that the apparent diminution of optical anisotropy is quite as marked in liquids usually considered as "non-associated," *e. g.* the paraffins, as in others which are typically "associated" like the alcohols. The facts stated above necessitate a revision of the theory of light-scattering in liquids. It is proposed in this paper to put forward a theory which does not involve any artificial hypotheses and which offers a natural explanation of the observed facts.

2. *The Fundamental Postulates.*

Any satisfactory theory of our subject must consider the optical properties of the molecules composing the fluid, their distribution and orientations in space, and the field actually acting on them. We assume that the molecules are polarizable differently along three mutually perpendicular directions fixed to them, which might be called the principal optic axes of the molecules. As to their distribution and orientations in space, we have not at present full knowledge. The molecular aggregation in liquids is presumably intermediate in character between the two extreme cases of an ideal crystalline solid and a perfect gas. If we follow an individual molecule in a liquid over a sufficiently long time, it can take up all possible positions and orientations, and thus the conditions approximate to those of a gas. If, however, we consider a molecule in relation to its immediate neighbours, the analogy between the solid and liquid states is closer. We are not justified in treating the space-distribution as random, because the molecules have a finite size, and in the dense assemblage forming a liquid they would naturally restrain each other's freedom of movement to a considerable extent. On the other hand, we shall not be seriously in error if we assume the freedom of orientation of the molecules to be comparatively unrestricted in most liquids. It is true that in many actual cases the molecules

* C. V. Raman and K. S. Krishnan, Phil. Mag. iii. p. 727 (1927).

are highly unsymmetrical in shape, and hence in finding the probability of any particular configuration of neighbouring molecules, both spacing and orientation have to be considered together. Nevertheless, we may regard the effect of molecular collisions as equivalent approximately to a restriction of the possible arrangements of the molecules in space, while their freedom of orientation is retained.

To make our ideas more precise, we may fix our attention on a volume element in the liquid whose linear dimensions are large in comparison with the size of a molecule, and consider the spontaneous fluctuations in the number and orientations of the molecules contained in it. We shall make the following assumptions :—

(1) That the fluctuations in density of the fluid present in an element of volume δv are given by the usual Smoluchowski-Einstein expression

$$\overline{\delta n^2} = \frac{RT\beta n_0^2}{N\delta v}, \quad \ldots \ldots \quad (1)$$

where $\overline{\delta n^2}$ is the mean square of the deviation of the number of molecules per unit volume from its mean value n_0, R and N are the gas constant and Avogadro number respectively per gram molecule, β is the isothermal compressibility, and T is the absolute temperature.

(2) That the number of molecules in the volume element having at any instant any given orientation, will be the same as though all the molecules in the volume element were oriented entirely at random, and that fluctuations in orientations are entirely uncorrelated with the fluctuations in density.

3. *The Polarization Field in Liquids.*

We have next to consider the question of the field actually acting on any molecule in the liquid. In a gas this will evidently be the same as the field of the incident light-wave. In a liquid, however, we have also to take into account the field due to the doublets induced in the surrounding molecules. This "polarization field" is usually taken to be $\frac{4\pi}{3}\chi E$, where χ is the susceptibility of the medium per unit volume and E is the incident field, it being thus tacitly assumed that the polarization field acting on any given molecule is independent of its orientation in the field. This assumption would be valid, only if the molecules surrounding

it were distributed in such a manner as to be equivalent to a spherically symmetrical arrangement of polarizable matter. While this assumption may be justified for molecules at a sufficient distance from the one under consideration, it is not necessarily true in respect of its immediate neighbours. If the shape of a molecule departs greatly from spherical symmetry, it would be incorrect to regard the distribution of polarizable matter immediately surrounding it as completely symmetrical. The polarization field acting on a molecule must thus, in general, vary with its orientation in the external field. To express this "anisotropy" of the polarization field in mathematical language, we choose three mutually perpendicular axes fixed in the molecule such that when the incident field lies along any one of them, the polarization field is also in the same direction, and is given by $p_1\chi E$, $p_2\chi E$, or $p_3\chi E$, where p_1, p_2, p_3 are constants characteristic of the molecule for the given density and temperature of the liquid. It is quite possible to discuss the general case where these axes of the molecule are different from its optic axes. However, for simplicity we may assume that the two sets of axes are coincident in direction.

An important question which arises here is whether the local field acting on a molecule is influenced appreciably by the fluctuations of density and molecular orientation in its immediate neighbourhood. This question has been discussed by Ramanathan in his recent paper, and he has given reasons for assuming that the local field should be regarded as constant. His argument may be modified and expressed in the following way :—The local field arises in part from the external field, and in part from the polarization of the entire medium surrounding the molecule under consideration. If the distribution at any instant, of polarizable matter surrounding the molecule, can be regarded as spherically symmetrical, it can be shown by dividing up the medium into concentric spherical shells that the polarization field acting on the molecule at the centre is unaffected by either a diminution or an increase of density in its immediate neighbourhood. This conclusion remains valid even if there be fluctuations from spherical symmetry in the distribution of polarizable matter round the molecule, for it may be shown that this would give rise to a fluctuation of the polarization field which would be uncorrelated in sign with the local variation of density and may therefore be left out of account. The argument of Ramanathan appears to be correct, and, as we shall show later in the course of the paper, its validity remains substantially unaffected even when, as

in our present treatment, the polarization field acting on a molecule is assumed to vary with its orientation in the external field. We now proceed to modify the treatment of light-scattering given by Ramanathan so as to take the "anisotropy" of the polarization field into account.

4. *Radiation from a given Molecule.*

Let a beam of plane-polarized light be incident in the medium along the x-axis of a system of coordinates xyz fixed in space, the electric vector of the light-wave, equal to E, say, lying along the z-axis. Let us consider a molecule at O radiating under the influence of the light-wave. We choose the optic axes of the molecule as the axes of another coordinate system $\xi\eta\zeta$, of course rigidly fixed to the molecule, their orientation in space being defined with reference to the xyz axes by the usual Eulerian angles θ, ϕ, ψ. Then the cosines of the angles between the different axes are given by the following table

TABLE I.

	x.	y.	z.
ξ ...	$\alpha_{11}=\cos\theta\cos\phi\cos\psi - \sin\phi\sin\psi$.	$\alpha_{12}=\cos\theta\sin\phi\cos\psi + \cos\phi\sin\psi$.	$\alpha_{13}=-\sin\theta\cos\psi$.
η ...	$\alpha_{21}=-\cos\theta\cos\phi\sin\psi - \sin\phi\cos\psi$	$\alpha_{22}=-\cos\theta\sin\phi\sin\psi + \cos\phi\cos\psi$.	$\alpha_{23}=\sin\theta\sin\psi$.
ζ ...	$\alpha_{31}=\sin\theta\cos\phi$.	$\alpha_{32}=\sin\theta\sin\phi$.	$\alpha_{33}=\cos\theta$.

Now, if A, B, C be the moments induced in a molecule per unit field acting respectively along its three axes, then the actual moments induced in the molecule at O along its axes by the electric vector of the light-wave are

$$\left.\begin{aligned} &AE(1+p_1\chi)\alpha_{13},\\ &BE(1+p_2\chi)\alpha_{23},\\ \text{and}\quad &CE(1+p_3\chi)\alpha_{33}\end{aligned}\right\} \quad . \quad . \quad . \quad . \quad . \quad . \quad (2)$$

respectively. We may denote these expressions shortly by $A'E\alpha_{13}$, $A'E\alpha_{23}$, and $C'E\alpha_{33}$, where

$$\left.\begin{aligned} A'&=A(1+p_1\chi),\\ B'&=B(1+p_2\chi),\\ C'&=C(1+p_3\chi).\end{aligned}\right\} \quad . \quad . \quad . \quad . \quad . \quad . \quad (3)$$

When these moments are resolved along the x-axis, their sum is equal to

$$M_x=E(A'\alpha_{13}\alpha_{11}+B'\alpha_{23}\alpha_{21}+C'\alpha_{33}\alpha_{31}). \quad . \quad . \quad (4)$$

At a large distance d from the molecule measured along the y-axis, *i. e.* transversely to both the direction of vibration and the direction of propagation of the incident light, the amplitude of the x-component in the radiation from the given molecule is obviously equal to

$$\frac{k^2}{d}M_x, \quad . \quad . \quad . \quad . \quad . \quad . \quad . \quad (5)$$

where $$k=\frac{2\pi}{\lambda}.$$

Similarly, the amplitude of the z-component of the radiation from the given molecule will be equal to

$$\frac{k^2}{d}M_z, \quad . \quad . \quad . \quad . \quad . \quad . \quad . \quad (6)$$

where M_z is the sum of the resolved components along the z-axis, of the moments induced in the molecule, and is given by

$$M_z=E(A'\alpha_{13}^2+B'\alpha_{23}^2+C'\alpha_{33}^2). \quad . \quad . \quad . \quad (7)$$

5. *Orientation Scattering.*

We now imagine the space occupied by the fluid to be divided into a large number of equal volume elements forming the cells of a regular cubic space-lattice. The linear dimensions of the volume element are assumed to be small in comparison with a wave-length, and at the same time large enough to include a great many molecules. The fluctuations in the number and orientations of the molecules in any one element may, in the circumstances, be considered to be independent of the fluctuations in the adjoining ones. At any given instant the radiations from the different molecules in a volume element may be taken to be in the same phase; and in order to get their instantaneous aggregate effect at the point of observation, we have merely to add up the amplitudes due to the individual molecules. Thus, for instance, the amplitude, at any given instant, of the x-component of the radiation from a volume element δv will be given by

$$X=\frac{k^2}{d}\Sigma M_x, \quad . \quad . \quad . \quad . \quad . \quad . \quad . \quad (8)$$

where Σ denotes summation over all the molecules in δv.

We have next to compound the effects due to the different

volume elements. Since each of these contains a large number of molecules, which, as mentioned in section 2, are oriented at random, the average value of ΣM_x (given by (4)) taken over the different volume elements will be nothing. However, for any single element, ΣM_x will, in general, be finite, being as often positive as negative, its actual value being determined by the chance orientations at the given instant of the molecules present in it. The values of ΣM_x for different volume elements will thus be entirely uncorrelated, and the resultant effect is accordingly obtained by addition of the intensities (represented by the squares of the amplitudes), and not by addition of the amplitudes. Thus the problem reduces to one of finding the average value of the intensity taken over all the volume elements, and will evidently be the same as finding what is called in the theory of probabilities the "expectation" of intensity from a single volume element; *i. e.*, the mean value of the intensity to be expected after a very large number of trials in each of which the number and the orientations of the molecules present in it are rearranged arbitrarily according to the principles of statistical mechanics.

Since, as is evident from (1), the fluctuation of density is very small in comparison with the mean density, we may reasonably assume in the calculation that in the different trials the total number of molecules in the element of volume does not vary, only their orientations varying arbitrarily. The expectation of X^2 from δv will then be given by

$$\overline{X^2} = \frac{k^4}{d^2} \times \text{expectation of } (\Sigma M_x)^2 \text{ from } \delta v,$$

which can easily be shown to be equal to

$$\frac{k^4}{d^2} n_0 \delta v \, \overline{M_x^2}, \quad \ldots\ldots (9)$$

where $\overline{M_x^2}$ denotes the average value of M_x^2 taken over all the molecules in the element, *i. e.* over all orientations, and is therefore given by

$$\overline{M_x^2} = \frac{\int_{\theta=0}^{\theta=\pi}\int_{\phi=0}^{\phi=2\pi}\int_{\psi=0}^{\psi=2\pi} E^2(A'\alpha_{13}\alpha_{11} + B'\alpha_{23}\alpha_{21} + C'\alpha_{33}\alpha_{31})^2 \sin\theta \, d\theta \, d\phi \, d\psi}{\int_{\theta=0}^{\theta=\pi}\int_{\phi=0}^{\phi=2\pi}\int_{\psi=0}^{\psi=2\pi} \sin\theta \, d\theta \, d\phi \, d\psi} \quad \ldots\ldots (10)$$

$$= E^2 F, \quad \ldots\ldots (11)$$

where

$$F = \tfrac{1}{30}[(A'-B')^2 + (B'-C')^2 + (C'-A')^2]. \quad \ldots (12)$$

Then from (9) we get for the intensity of the x-component of the scattering per unit volume

$$I_x = \frac{k^4}{d^2} E^2 n_0 F. \quad \ldots\ldots (13)$$

Coming now to the z-component, we may write expression (7) for M_z shortly as

$$M_z = EL, \quad \ldots\ldots (14)$$

where

$$L = A'\alpha_{13}^2 + B'\alpha_{23}^2 + C'\alpha_{33}^2. \quad \ldots (15)$$

As before, by summing up the amplitudes of the radiations from the individual molecules in δr at any instant, we get for the resultant amplitude

$$Z = \frac{k^2}{d} E \Sigma L, \quad \ldots\ldots (16)$$

Σ, as before, denoting summation over all the molecules in δv. For convenience in discussion we can rewrite the expression in the form

$$Z = \frac{k^2}{d} E\left[\Sigma\frac{A'+B'+C'}{3} + \Sigma\left(L - \frac{A'+B'+C'}{3}\right)\right]. \quad (17)$$

$$= \frac{k^2}{d} E \frac{A'+B'+C'}{3} n\delta v + \frac{k^2}{d} E\Sigma\left(L - \frac{A'+B'+C'}{3}\right). \quad (18)$$

The two terms in (18) may be denoted by Z_1 and Z_2 respectively. We shall in the first place consider the second term Z_2, reserving a discussion of the other term to the next section.

At any instant the average value of $\Sigma\left(L - \frac{A'+B'+C'}{3}\right)$ for the different volume elements can easily be shown to be zero. But as in the previous case its actual value for any single element will be finite, in general, and will be determined wholly by the chance orientations of the molecules in it. Hence, so far as the second term of (18), viz. Z_2, is concerned, we have as before to add up the intensities due to the different volume elements in order to get the total intensity.

Following the same reasoning as in the case of the x-component, we get for the expectation of intensity on account of the second term of expression (18) from a volume element δv

$$\overline{Z_2^2} = \frac{k^4}{d^2} E^2 n_0 \delta v \overline{\left(L - \frac{A'+B'+C'}{3}\right)^2}, \quad \ldots (19)$$

where the bar over the last factor denotes averaging over

all orientations,

$$= \frac{k^4}{d^2} E^2 n_0 \delta v \times \tfrac{2}{45}[(A'-B')^2+(B'-C')^2+(C'-A')^2]. \quad (20)$$

$$= \frac{k^4}{d^2} E^2 n_0 \delta v \times \tfrac{4}{5} F. \quad . \quad . \quad . \quad . \quad . \quad . \quad . \quad . \quad . \quad . \quad (21)$$

Thus we get for the intensity of this part of the x-component, scattered per unit volume

$$I_{x2} = \frac{4}{3} \frac{k^4}{d^2} E^2 n_0 F. \quad . \quad . \quad . \quad . \quad . \quad . \quad (22)$$

The expression

$$I_x + I_{x2} = \frac{7}{3} \frac{k^4}{d^2} E^2 n_0 F \quad . \quad . \quad . \quad . \quad . \quad (23)$$

gives the "orientation" scattering per unit volume In the special case when $A'=B'=C'$, *i. e.* when the moments induced in a molecule are isotropic, $F=0$ and the orientation scattering naturally disappears.

6. *Density Scattering.*

We have still to consider the first term in (18), viz.

$$Z_1 = \frac{k^2}{d} E \frac{A'+B'+C'}{3} n \delta v. \quad . \quad . \quad . \quad (24)$$

$\frac{A'+B'+C'}{3}$ is the average moment induced in a molecule per unit external field, the average being taken over all directions of incidence of the field with respect to the molecule. The actual field on the molecule which produces this moment can be divided into three parts :—

(*a*) The external field.
(*b*) The field arising from the doublets outside a spherical volume element containing the molecule at its centre.
(*c*) The field arising from the molecules within the volume element.

For the reasons given in section 3, the fields (*a*) and (*b*) will be unaffected by the fluctuations of density in the volume element, and hence the corresponding contribution from these fields to the mean moment of the molecule, viz.

$$\frac{A+B+C}{3}\left(1+\frac{4\pi}{3}\chi\right),$$

can be regarded as constant.

The rest of the contribution to the mean moment, viz.

$$\tfrac{1}{3}(A\sigma_1+B\sigma_2+C\sigma_3)\chi, \quad . \quad . \quad . \quad . \quad (25)$$

$$\left.\begin{aligned} \sigma_1 &= p_1 - \frac{4\pi}{3}, \\ \sigma_2 &= p_2 - \frac{4\pi}{3}, \\ \sigma_3 &= p_3 - \frac{4\pi}{3}, \end{aligned}\right\} \quad . \quad . \quad . \quad . \quad . \quad . \quad . \quad (26)$$

comes from field (*c*) due to the immediate neighbours, and hence will vary directly with the fluctuation of n in the volume element. However, in any actual case $A\sigma_1+B\sigma_2+C\sigma_3$ is negligible in comparison with $A+B+C$ (generally 1 or 2 per cent.), and hence we may reasonably assume that the whole of the mean moment, *i. e.* $\frac{A'+B'+C'}{3}$, is independent of the fluctuations of n.

Expression (24) can then be written in the form

$$Z_1 = \frac{k^2}{d} E \frac{A'+B'+C'}{3} n_0 \delta v + \frac{k^2}{d} E \frac{A'+B'+C'}{3} \delta n \delta v. \quad (27)$$

The first term represents that part of the amplitude which will be constant for the different volume elements, and on compounding will cancel each other out by mutual interference, owing to the regularity in the arrangement of the volume elements in the medium. The amplitude represented by the second term, however, being determined by the chance fluctuation δn, will be uncorrelated for the different volume elements, and we shall have to add their squares to get the resultant intensity. Thus

$$\overline{Z_1^2} = \frac{k^4}{d^2} E^2 \left(\frac{A'+B'+C'}{3}\right)^2 \overline{\delta n^2} \delta v^2, \quad . \quad . \quad (28)$$

which, using (1) and the relation

$$n_0 \frac{A'+B'+C'}{3} = \frac{\mu^2-1}{4\pi}, \quad . \quad . \quad . \quad . \quad (29)$$

where μ is the refractive index of the medium, reduces to

$$\overline{Z_1^2} = \frac{k^4}{d^2} E^2 \frac{RT\beta}{N} \left(\frac{\mu^2-1}{4\pi}\right)^2 \delta v. \quad . \quad . \quad . \quad (30)$$

Thus we have for the "density scattering" per unit volume

$$I_{x1} = \frac{k^4}{d^2} E^2 \frac{RT\beta}{N} \left(\frac{\mu^2-1}{4\pi}\right)^2 . \quad . \quad . \quad . \quad . \quad (31)$$

The total intensity of the z-component

$$I_z = I_{z1} + I_{z2}, \quad \ldots \ldots \quad (32)$$

where I_{z1} and I_{z2} are given by (31) and (22) respectively.

7. *Depolarization and Intensity of the Scattered Light.*

If the incident light travelling along Ox is unpolarized, we shall have to take into consideration also the y-component of the primary vibrations, which, being along the direction of observation, will contribute equally to the intensities of the x- and z-components of the transversely scattered light, an amount given by (13).

Thus in this case the intensity of the x-component will be equal to $2I_x$ and that of the z-component to $I_z + I_x$, and the ratio of the components is given by

$$r = \frac{2I_x}{I_z + I_x} = \frac{2n_0F}{\frac{RT\beta}{N}\left(\frac{\mu^2-1}{4\pi}\right)^2 + \frac{7}{3}n_0F} \quad \ldots \ldots \quad (33)$$

Also the total intensity of the transversely scattered light expressed in terms of the incident intensity $I_0 = 2E^2$, becomes

$$I = I_0 \frac{\pi^2}{2d^2} \frac{RT\beta}{N\lambda^4} (\mu^2-1)^2 \frac{6+6r}{6-7r} \quad \ldots \ldots \quad (34)$$

In the special case when the polarization field is isotropic,

$$p_1 = p_2 = p_3 = \frac{4\pi}{3}$$

and

$$F = \tfrac{1}{3}I_0[(A-B)^2+(B-C)^2+(C-A)^2]\left(1+\frac{4\pi}{3}\chi\right)^2$$

$$= \tfrac{1}{3}I_0[(A-B)^2+(B-C)^2+(C-A)^2]\left(\frac{\mu^2+2}{3}\right)^2, \quad (35)$$

and the expressions r and I reduce naturally to those obtained recently by Ramanathan.

8. *Comparison with Experiment:* (a) *Intensity.*

We now proceed to consider how far the above expressions are in conformity with actual experimental results. First we take up the intensity of the transversely-scattered light. From a critical examination of the available data, it has

been shown by one of us* that relative measurements of intensity in a large number of organic liquids entirely support expression (34). We reproduce here the calculations for some typical cases for which we have accurate values for the compressibility from the measurements of Tyrer †.

TABLE II.

Liquid.	r (observed).	I (relative to ether=1) at 30° C.	
		Calculated according to (34).	Observed.
Water	0·085	0·10	0·13
Methyl alcohol	0·060	0·51	0·56
Ethyl alcohol	0·053	0·58	0·57
Ethyl acetate	0·230	0·95	0·98
Carbon tetrachloride	0·053	0·96	1·02
Chloroform	0·240	1·31	1·26
Acetic acid	0·455	1·39	1·42
Ethylene chloride	0·36	1·40	1·44
Ethyl bromide	0·250	1·55	1·58
Benzene	0·47	3·13	3·2
Toluene	0·51	3·29	3·4
Aniline	0·60	3·59	3·42
Meta xylene	0·57	3·90	3·87
Chlorobenzene	0·58	4·09	4·10
Nitrobenzene	0·74	7·6	10·5
Carbon bisulphide	0·64 0·685	10·9 14·1	12·9

Thus over the whole range of intensities from 0·2 to 13, relative to ether, the agreement between the observed and calculated values is very satisfactory. Nitrobenzene is the only exception, the discrepancy being too large to be attributable to error of measurement. However, since it shows a very high depolarization (the highest in the list), any impurity present in the liquid is likely to lower the observed value of r and consequently the calculated value of I considerably; whereas the actual intensity will be

* K. S. Krishnan, Proc. Ind. Assoc. Cult. Sc. ix. p. 251 (1926).
† D. Tyrer, Journ. Chem. Soc. cv. p. 2534 (1914).

increased. Further it is a coloured liquid. It would be of interest to repeat the measurement with a specially purified specimen.

Recently in the authors' laboratory, Mr. Ramachandra Rao * has studied the scattering by six typical organic liquids over a wide range of temperature up to the critical point. The relative values of the intensity at different temperatures again confirm the validity of the above expression for I.

Absolute measurements of intensity available also support expression (34), as will be evident from Table III. $\frac{I}{I_0}d^2$ gives, according to our notation, the fraction of the incident unpolarized light scattered transversely per unit volume of the liquid, per unit solid angle.

TABLE III.

Liquid.	λ in A.U.	Temperature ° C.	r.	$\frac{I}{I_0}d^2\times10^6$. Calculated according to (34).	$\frac{I}{I_0}d^2\times10^6$. Observed.	Observer.
Ethyl ether..	4358	20	0·080	8·85	9·2	Martin & Lehrman †.
Benzene	5440	15	0·41	8·85	10·7±0·55	Cabannes & Daure ‡.
			0·47	10·7		

9. *Comparison with Experiment:* (b) *Depolarization.*

Expression (33) enables us to determine the depolarization of the light scattered by a fluid in terms of A, B, C, the optical constants of the molecule and p_1, p_2, p_3, the constants of anisotropy of the polarization field. In the case of a rarefied fluid, the polarization field is very small and may be neglected. For a dense fluid, if we disregard the "anisotropy" of the field and assume that

$$p_1=p_2=p_3=\frac{4\pi}{3},$$

* S. Ramachandra Rao, Indian Journal of Physics, ii. p. 7 (1927).

† W. H. Martin and S. Lehrman, Journ. Phys. Chem. xxiv. p. 478 (1920).

‡ J. Cabannes and P. Daure, *Comptes Rendus*, clxxxiv. p. 520 (1927).

then the depolarizations in the liquid and gaseous states are connected by the simple relation

$$\frac{RT\beta}{N}n_0\cdot\frac{r_{liq.}}{6-7r_{liq.}}=\frac{r_{gas}}{6-7r_{gas}}. \quad . \quad . \quad . \quad (36)$$

The value of $r_{liq.}$ calculated from expression (36) usually, however, differs widely from the observed value. In the case of the carbon compounds, the differences are very marked in the case of the paraffins and the monohydric alcohols, the observed depolarization being much smaller than the calculated value; the differences are less conspicuous in the aromatic series of compounds.

A natural explanation of these facts is furnished by taking into account the anisotropy of the polarization field. It is sufficient as an illustration to consider the cases of the paraffin series of hydrocarbons. As is well-known from chemical considerations and from X-ray data, the molecules of these compounds form elongated chains of carbon atoms, to which the hydrogens are linked. The length of the chain is much greater than its cross-section. X-ray study of the liquid shows, as might be expected *a priori*, that the molecules lie much more frequently touching one another side to side and much less frequently end to end. In these circumstances it would obviously be incorrect to assume the polarization field acting on a molecule to be independent of its orientation in the field. A much closer approximation to the truth is to consider the molecule as equivalent to a doublet placed at the centre of a prolate ellipsoidal cavity scooped out of a continuous isotropic medium, the dimensions of the cavity being determined by those of the molecule. The values of p_1, p_2, p_3 are readily calculated from the expressions

$$p_1=4\pi\left(\frac{1}{e^2}-1\right)\left(\frac{1}{2e}\log\frac{1+e}{1-e}-1\right), \quad . \quad . \quad (37)$$

$$p_2=p_3=2\pi\left(\frac{1}{e^2}-\frac{1-e^2}{2e^3}\log\frac{1+e}{1-e}\right), \quad . \quad . \quad (38)$$

where e is given by

$$b=c=\sqrt{1-e^2}\,.\,a, \quad . \quad . \quad . \quad . \quad . \quad (39)$$

a, b, c being the axes of the cavity.

In Table IV. are given the values of the depolarization factor computed in this way, and those observed are tabulated for comparison. A satisfactory agreement is indicated.

TABLE IV.

All the quantities refer to 30° C.

Substance.	Dimensions of the molecule in A.U.		$\gamma_{gas.}$	$\gamma_{liq.}$ calculated from		γ_{liq} observed.
	$a.$	$b=c.$		(36). (Isotropic polarization field).	(33). (Anisotropic polarization field).	
Pentane ...	8·7	4·9	0·0136	0·21	0·074	0·075
Hexane ...	10·0	,,	0·015	0·31	0·087	0·100
Heptane...	11·3	,,	0·0158	0·38	0·083	0·127 0·100
Octane ...	12·6	,,	0·0186	0·46	0·105	0·129

10. *Summary.*

An examination of the data for the depolarization of the light scattered by fluids, with the aid of the molecular theory due to Ramanathan, indicates an apparent change, usually a large diminution, in the optical anisotropy of the molecules of a given substance, as it passes from the condition of vapour to that of liquid. In the present paper a new theory is put forward which offers a natural explanation of the foregoing fact without any artificial hypotheses. In the treatment of the optical properties of liquids usually given, the polarization field acting on a molecule is assumed to be independent of its orientation in the field. This assumption is not justifiable when the shape of the molecule departs greatly from spherical symmetry, and consequently the distribution of polarizable matter surrounding it ceases to be symmetrical. The strength of the polarization field will in these circumstances be dependent on the orientation of the molecule in the field, and may be expressed in terms of three constants characteristic of the molecule for the given density and temperature of the fluid. The theory of light-scattering is developed on this basis, and gives an expression for the intensity of scattering which is in close accord with facts. It also enables the depolarization of the scattered light in the liquid to be successfully calculated from that of the corresponding vapour, at least in those cases where the constants of anisotropy of the polarization field can be determined from the shape of the molecule.

210 Bowbazar Street,
Calcutta, India.
18th August, 1927.

A Theory of the Optical and Electrical Properties of Liquids.

By Prof. C. V. RAMAN, F.R.S., and K. S. KRISHNAN.

(Received September 19, 1927.)

1. *Introduction.*

Theories of the optical behaviour of liquids generally base themselves on the postulate that the well-known Lorentz formula $(n^2 - 1)/(n^2 + 2)\rho = \text{constant}$ correctly expresses the relation between the refractive index and density of a liquid. It has long been known, however, that this formula is at best only an approximation. The quantity $(n^2 - 1)/(n^2 + 2)\ \rho$ is found experimentally to be not invariable, its deviation from constancy becoming more and more marked as the density is increased. The change in the value of $(n^2 - 1)/(n^2 + 2)\rho$ in passing from the state of vapour to that of a liquid under ordinary conditions, is usually quite appreciable, as might be instanced by the case of benzene, for which Wasastjerna* found for the D-line a molecular refraction of 27·20 in the vapour state, while the corresponding value for the liquid is 26·18, that is, 3·8 per cent. lower. The deviations from the Lorentz formula appear most striking when we use it to compute the change in the refractive index of a liquid produced by alterations of temperature or pressure. Here, again, we might instance the case of benzene, for which the observed value of $dn/dt = -6{\cdot}4 \times 10^{-4}$ per degree Centigrade for the D-line at 20° C., and that of $dn/dp = 5{\cdot}06 \times 10^{-5}$ per atmosphere, while the calculated values are $dn/dt = -7{\cdot}15 \times 10^{-4}$ and $dn/dp = 5{\cdot}66 \times 10^{-5}$. The observed values are thus numerically about 10 per cent. smaller in either case, indicating that $(n^2 - 1)/(n^2 + 2)\ c$ diminishes more and more quickly as the density is increased. An expression of the form $(n^2 - 1)/(n^2 + 2)\ \rho = a - b\rho^2$, where a and b are positive constants, has been found to represent the refraction of carbon dioxide over a wide range of density more closely than the original Lorentz formula.† It has been deduced theoretically on certain suppositions regarding the magnitude of the polarisation field in liquids, which are, however, somewhat arbitrary in nature.

Considering next the electrical behaviour of liquids, we find that the formula proposed by Debye $(\varepsilon - 1)/(\varepsilon + 2)\ \rho = A + B/T$ is not adequate to explain

* 'Soc. Sci. Fenn., Phys.-Math.,' vol. 2, No. 13 (1924).

† Phillips, 'Roy. Soc. Proc.,' A, vol. 97, p. 225 (1920).

the dielectric properties of many known liquids. To illustrate this, we may again consider the case of benzene, whose dielectric constant has been determined over a wide range of temperatures* and pressures.† Since A and B in the formula are essentially positive constants, it follows that $(\varepsilon - 1)/(\varepsilon + 2)\ \rho$ should remain invariable when the liquid is compressed isothermally, and that it should *diminish* with rising temperature. Actually it is found with benzene that the quantity in question falls steadily with increasing pressure and *increases* with rising temperature. A similar apparently anomalous behaviour is shown by many other liquids whose molecules have a negligible electrical polarity. Liquids of marked electrical polarity show a diminution of $(\varepsilon - 1)/(\varepsilon + 2)\ \rho$ with rising temperature as demanded by the formula, but they deviate from it by showing a diminution of the same quantity when isothermally compressed, the latter effect being usually even more marked than for non-polar compounds.‡

It will be clear from the foregoing review that the existing theories of the optical and electrical behaviour of liquids are far from being satisfactory. It is proposed in this paper to put forward a new theory which appears to us competent to offer at least an insight into the whole range of facts referred to. We believe that it is capable of doing more, that is, of actually giving a quantitative explanation of the behaviour of actual liquids for which the necessary data for evaluating the constants appearing in our formulæ are available. In order, however, not to lengthen the paper unduly, we shall confine ourselves to a general discussion, leaving the details for fuller treatment in separate papers.

2. *The Refractivity of Liquids.*

We shall first consider the optical problem, which is relatively simple. In any satisfactory treatment of it we have necessarily to take into account the fact which has been clearly established by recent investigations, namely, that a liquid can be regarded as an optically isotropic medium only when we do not push the analysis of its structure into regions of molecular dimensions. In the first place, it is established by investigations on light-scattering that all known molecules are optically anisotropic, in other words, that they are polarisable to different extents in different directions. From this circumstance it follows that the refractivity of a liquid is really an average effect determined by the contributions of molecules variously orientated relatively to one another

* Isnardi, 'Z. f. Physik,' vol. 9, p. 153 (1922).
† Francke, 'Ann. d. Physik,' vol. 77, p. 159 (1925).
‡ Grenacher, 'Ann. d. Physik,' vol. 77, p. 138 (1925).

and to the field of the incident radiation. Further, it is known from X-ray studies that many actual molecules are highly asymmetric in their geometric form. In view of this fact we would not be justified in treating the distribution of polarisable matter surrounding any given molecule in a dense fluid as completely symmetrical. It follows, therefore, that the local field acting on any molecule due to the polarisation of its immediate neighbours, cannot be regarded as independent of the orientation of the molecule in the field. The study of light-scattering in liquids furnishes striking evidence in support of this idea and indeed enables us in simple cases to actually determine how the polarisation field acting on a molecule varies with its orientation with respect to the incident beam of light. We shall in what follows proceed to develop the theory of refraction in liquids on the assumption that the molecules are optically anisotropic and that the polarisation field acting on the molecule is a function of its orientation.

Let us choose the optic axes of any given molecule as the axes of a co-ordinate system ξ, η, ζ fixed to it, whose orientations with respect to another system of axes x, y, z fixed in space are given by the Eulerian angles θ, ϕ, ψ. Let b_1, b_2, b_3 be the moments induced in the molecule per unit field (due to a light-wave) *actually* acting on it respectively along its three axes ξ, η, ζ. When the external field is incident along any one of these axes, say along the ξ-axis, the polarisation field acting on the molecule will, in general, have components also along the η- and ζ-axes. Let p_{11}, p_{12}, p_{13} be the numerical factors which determine the polarisation fields acting along the ξ-, η-, ζ-axes when the external field is incident along the ξ-axis; and let p_{21}, p_{22}, p_{23} and p_{31}, p_{32}, p_{33} be similar factors when the external field lies along the η- and ζ-axes; $p_{ik} = p_{ki}$.

Suppose now the field of the incident light-wave, equal to E, say, lies along the z-axis. Then the moments induced in the molecule under consideration along its three axes are obviously

$$\left.\begin{aligned} & b_1\,[\alpha_1 + \chi\,(p_{11}\alpha_1 + p_{21}\alpha_2 + p_{31}\alpha_3)]\,\mathrm{E} \\ & b_2\,[\alpha_2 + \chi\,(p_{12}\alpha_1 + p_{22}\alpha_2 + p_{32}\alpha_3)]\,\mathrm{E} \\ & b_3\,[\alpha_3 + \chi\,(p_{13}\alpha_1 + p_{23}\alpha_2 + p_{33}\alpha_3)]\,\mathrm{E} \end{aligned}\right\} \quad (1)$$

and

respectively, where χ is the mean moment induced in unit volume of the fluid by unit field of the incident light-wave; $\alpha_1, \alpha_2, \alpha_3$ are the cosines of the angles which the ξ-, η-, ζ-axes make with the direction of the field E, and are given by

$$\alpha_1 = -\sin\theta\cos\psi; \quad \alpha_2 = \sin\theta\sin\psi; \quad \alpha_3 = \cos\theta. \quad (2)$$

These moments when resolved along the direction of the incident field are together equal to

$$[b_1(1+p_{11}\chi)\alpha_1^2 + b_2(1+p_{22}\chi)\alpha_2^2 + b_3(1+p_{33}\chi)\alpha_3^2 + \chi\{p_{12}(b_1+b_2)\alpha_1\alpha_2 + p_{23}(b_2+b_3)\alpha_2\alpha_3 + p_{31}(b_3+b_1)\alpha_3\alpha_1\}] \times \mathrm{E}. \quad (3)$$

Now the average values of α_1^2, α_2^2 and α_3^2 taken over all orientations of the molecules with respect to the incident field are equal to $\frac{1}{3}$, while the average values of $\alpha_1\alpha_2$, $\alpha_2\alpha_3$ and $\alpha_3\alpha_1$ vanish. Hence it readily follows that the average moment induced in a molecule in the medium by unit incident field is given by

$$m = \tfrac{1}{3}(b_1' + b_2' + b_3'), \quad (4)$$

where b_1', b_2', b_3' denote the coefficients of α_1^2, α_2^2, α_3^2 respectively in (3) above.

Further

$$\chi = \nu m = (n^2-1)/4\pi, \quad (5)$$

ν being the number of molecules per unit volume and n the refractive index.

Putting

$$p_{11} = \tfrac{4}{3}\pi + \sigma_1, \quad p_{22} = \tfrac{4}{3}\pi + \sigma_2, \quad p_{33} = \tfrac{4}{3}\pi + \sigma_3,$$

and using relation (5), we obtain from (4)

$$\frac{n^2-1}{n^2+2} = \frac{4\pi}{3}\nu\frac{b_1+b_2+b_3}{3} + \frac{n^2-1}{n^2+2}\nu\frac{b_1\sigma_1 + b_2\sigma_2 + b_3\sigma_3}{3}, \quad (6)$$

which may be written in the form

$$\frac{n^2-1}{n^2+2} = \nu C + \frac{n^2-1}{n^2+2}\nu\Phi, \quad (7)$$

where

$$\Phi = \tfrac{1}{3}(b_1\sigma_1 + b_2\sigma_2 + b_3\sigma_3) \quad (8)$$

and C is a constant characteristic of the molecule. We shall now consider three special cases.

Case (a):

$$\sigma_1 = \sigma_2 = \sigma_3 = 0,$$

and therefore

$$p_{11} = p_{22} = p_{33} = \tfrac{4}{3}\pi. \quad (9)$$

We find in this case that equation (7) reduces absolutely to the Lorentz formula.

The assumption (9) is equivalent to the supposition that the local field acting on the molecule is equal to that at the centre of a spherical cavity excavated around it.

Case (b):

$$\sigma_1 + \sigma_2 + \sigma_3 = 0,$$

and therefore

$$p_{11} + p_{22} + p_{33} = 4\pi. \quad (10)$$

If, in addition, $b_1 = b_2 = b_3$, *i.e.*, if the molecule is optically isotropic, equation (7) again reduces to the Lorentz formula. Equation (10) amounts to assuming that the local field acting on the molecule is equal to that at the centre of an ellipsoidal cavity with three unequal axes,* scooped around the molecule. It may also be interpreted in the sense that the *mean* polarisation field acting on the molecule averaged over all orientations is the same as at the centre of a spherical cavity.

Case (c):

$$\sigma_1 + \sigma_2 + \sigma_3 \neq 0.$$

This is equivalent to the assumption that the mean polarisation field differs from that obtainable at the centre of a spherical cavity around the molecule.

In Case (*a*) we obtain no deviation from the Lorentz formula at all. In Case (*b*) we obtain a deviation provided the molecule is optically anisotropic, and in Case (*c*) we may obtain a deviation from the Lorentz formula even for optically isotropic molecules.

3. *The Dielectric Constant of Liquids.*

For the corresponding electrical problem we choose the principal axes of electrostatic polarisability of the molecule as its ξ-, η-, ζ-axes. When an electrostatic field E is incident in the medium along the z-axis, the actual fields acting on the molecule along its axes are given by

$$\left.\begin{aligned} \mathrm{E}_1 &= [\alpha_1 + \chi_e(q_{11}\alpha_1 + q_{21}\alpha_2 + q_{31}\alpha_3)]\,\mathrm{E} \\ \mathrm{E}_2 &= [\alpha_2 + \chi_e(q_{12}\alpha_1 + q_{22}\alpha_2 + q_{32}\alpha_3)]\,\mathrm{E} \\ \mathrm{E}_3 &= [\alpha_3 + \chi_e(q_{13}\alpha_1 + q_{23}\alpha_2 + q_{33}\alpha_3)]\,\mathrm{E} \end{aligned}\right\}, \quad (11)$$

and

where χ_e is the mean electrostatic moment produced in unit volume of the medium per unit incident field; and the q's denote the constants of the static polarisation fields acting on the molecule, analogous to the p's in the optical problem. If μ_1, μ_2, μ_3 be the components of the permanent electric moment μ of the molecule resolved along the ξ-, η-, ζ-axes and a_1, a_2, a_3 the moments induced in it by unit field acting along these axes, the contribution from the

* See Routh, 'Analytical Statics,' vol. 2, p. 100.

molecule under consideration to the moment along the direction of the incident field is given by

$$\begin{aligned}\mathrm{L} = [&a_1(1+q_{11}\chi_e)\alpha_1^2 + a_2(1+q_{22}\chi_e)\alpha_2^2 + a_3(1+q_{33}\chi_e)\alpha_3^2 \\ &+ \{q_{12}(a_1+a_2)\alpha_1\alpha_2 + q_{23}(a_2+a_3)\alpha_2\alpha_3 + q_{31}(a_3+a_1)\alpha_3\alpha_1\}\chi_e] \times \mathrm{E} \\ &+ \mu_1\alpha_1 + \mu_2\alpha_2 + \mu_3\alpha_3. \qquad (12)\end{aligned}$$

The potential energy of the molecule in the field due to the existence of the permanent moment in it, is given by

$$\begin{aligned}u &= -(\mu_1\mathrm{E}_1 + \mu_2\mathrm{E}_2 + \mu_3\mathrm{E}_3) \\ &= -(\mathrm{M}_1\alpha_1 + \mathrm{M}_2\alpha_2 + \mathrm{M}_3\alpha_3)\,\mathrm{E}, \qquad (13)\end{aligned}$$

where

$$\left.\begin{aligned}\mathrm{M}_1 &= \mu_1 + \chi_e(q_{11}\mu_1 + q_{21}\mu_2 + q_{31}\mu_3) \\ \mathrm{M}_2 &= \mu_2 + \chi_e(q_{12}\mu_1 + q_{22}\mu_2 + q_{32}\mu_3) \\ \mathrm{M}_3 &= \mu_3 + \chi_e(q_{13}\mu_1 + q_{23}\mu_2 + q_{33}\mu_3)\end{aligned}\right\} \qquad (14)$$

By Boltzmann's theorem the number of molecules per unit volume whose orientations in the field correspond to the range $\sin\theta\, d\theta\, d\phi\, d\psi$ is equal to

$$c\, e^{-u/kT} \sin\theta\, d\theta\, d\phi\, d\psi, \qquad (15)$$

where c is a constant which can be evaluated from the obvious relation

$$c\int_{\theta=0}^{\theta=\pi}\int_{\phi=0}^{\phi=2\pi}\int_{\psi=0}^{\psi=2\pi} e^{-u/kT}\sin\theta\, d\theta\, d\phi\, d\psi = \nu, \qquad (16)$$

the total number of molecules per unit volume.

The average contribution from a molecule in the medium to the moment along the field

$$= \frac{\iiint e^{-u/kT}\,\mathrm{L}\sin\theta\, d\theta\, d\phi\, d\psi}{\iiint e^{-u/kT}\sin\theta\, d\theta\, d\phi\, d\psi} = m_e\mathrm{E}\ (\text{say}), \qquad (17)$$

the limits of integration being the same as in (16), and neglecting terms involving E^2 and higher powers of E. On actual evaluation of the integrals in (17) we obtain

$$\begin{aligned}m_e = &\frac{a_1(1+q_{11}\chi_e) + a_2(1+q_{22}\chi_e) + a_3(1+q_{33}\chi_e)}{3} \\ &+ \frac{1}{3kT}(\mathrm{M}_1\mu_1 + \mathrm{M}_2\mu_2 + \mathrm{M}_3\mu_3). \qquad (18)\end{aligned}$$

Further,

$$\chi_e = \nu m_e = \frac{\epsilon-1}{4\pi}, \qquad (19)$$

where ϵ is the dielectric constant.

Using this relation and putting

$$q_{11} = \tfrac{4}{3}\pi + s_1, \quad q_{22} = \tfrac{4}{3}\pi + s_2, \quad q_{33} = \tfrac{4}{3}\pi + s_3,$$

we obtain from (18)

$$\begin{aligned}\frac{\epsilon-1}{\epsilon+2} &= \frac{4\pi}{3}\nu\left(\frac{a_1+a_2+a_3}{3} + \frac{\mu^2}{3kT}\right) + \frac{\epsilon-1}{\epsilon+2}\nu\left\{\frac{a_1s_1+a_2s_2+a_3s_3}{3}\right. \\ &\qquad \left. + \frac{1}{3kT}(\Sigma\mu_i^2 s_i + 2\Sigma\mu_i\mu_k q_{ik})\right\} \\ &= \frac{4\pi}{3}\nu\left(\frac{a_1+a_2+a_3}{3} + \frac{\mu^2}{3kT}\right) + \frac{\epsilon-1}{\epsilon+2}\nu\left(\Psi + \frac{1}{3kT}\Theta\right), \qquad (20)\end{aligned}$$

where

$$\Psi = \tfrac{1}{3}(a_1s_1 + a_2s_2 + a_3s_3) \qquad (21)$$

and

$$\Theta = \mu_1^2s_1 + \mu_2^2s_2 + \mu_3^2s_3 + 2(\mu_1\mu_2q_{12} + \mu_2\mu_3q_{23} + \mu_3\mu_1q_{31}). \qquad (22)$$

The second term in (20) containing Ψ and Θ appears as an addition to the first term which is identical with Debye's expression. We may rewrite (20) in the form

$$\frac{\epsilon-1}{\epsilon+2} = \nu\left(\frac{4\pi}{3}\frac{a_1+a_2+a_3}{3} + \frac{\epsilon-1}{\epsilon+2}\Psi\right) + \frac{\nu}{3kT}\left(\frac{4\pi}{3}\mu^2 + \frac{\epsilon-1}{\epsilon+2}\Theta\right). \qquad (23)$$

The first term on the right-hand side of (23) has a form similar to the expression for refractivity obtained in the preceding section and does not explicitly involve the temperature. The second term, on the other hand, is inversely proportional to the absolute temperature.

4. *Discussion of the Theory.*

Our formulæ offer a natural explanation why with increase of density the Lorentz refraction-constant usually diminishes. Equation (7) runs

$$\frac{n^2-1}{n^2+2} = \nu\mathrm{C} + \nu\frac{n^2-1}{n^2+2}\Phi,$$

where

$$\Phi = \tfrac{1}{3}(b_1\sigma_1 + b_2\sigma_2 + b_3\sigma_3).$$

The expression for the dielectric constant of non-polar liquids is very similar,

see equation (23) above, and the following remarks may be regarded as applying equally well in respect of the same.

The constants b_1, b_2, b_3 represent the polarisabilities of the molecule along its optic axes and are therefore essentially positive. We shall, for the present at any rate, be justified in making the simplifying assumption, see equation (10) above, that $p_{11} + p_{22} + p_{33} = 4\pi$, in other words, that the polarisation field acting on the molecule *when averaged over all its orientations* is the same as at the centre of a spherical cavity. We have, then, $\sigma_1 + \sigma_2 + \sigma_3 = 0$, and it follows that σ_1, σ_2, σ_3 cannot all have the same sign.

If

$$\left.\begin{aligned} b_1 > b_2 > b_3 \\ \sigma_1 < \sigma_2 < \sigma_3 \end{aligned}\right\}, \quad (24)$$

and

it is easily shown that the value of Φ, that is, of $\frac{1}{3}(b_1\sigma_1 + b_2\sigma_2 + b_3\sigma_3)$ is necessarily negative. In other words, provided the condition stated in (24) is satisfied, the value of $(n^2 - 1)/(n^2 + 2)$ would necessarily have a smaller value than that given by the Lorentz formula.

The condition stated in (24) has a physical significance, namely, that the direction in the molecule corresponding to maximum polarisability is that along which the field due to its neighbours has a minimum value, and vice versa. That this condition would be satisfied in most cases seems highly probable. If we can regard the chemical molecule as roughly equivalent to an ellipsoidal particle of polarisable matter, its longest axis would be the one of maximum polarisability and its shortest axis that of minimum polarisability. If we consider a liquid composed of such molecules, it is obvious that the centre of a second molecule could approach that of the first most closely in the direction of the shortest axis, and least closely in the direction of its longest axis. The polarisation field due to its neighbours would be the sum of the fields due to the individual molecules occupying various positions with respect to it. If we consider a particular molecule in such position that the line joining the centres of the two molecules is parallel to the external field, its influence would appear as an addition to the field; while if the joining line is perpendicular to the field, its influence would be equivalent to a diminution of the external field. These effects would conspire to diminish the aggregate polarisation field acting on the molecule when the external field is along its longest dimension, and to increase it when the field is along its shortest dimension, in comparison with the case of spherical molecules. This is precisely the result which is required to satisfy the condition stated in (24) above.

It must, however, be remembered that the preceding argument is based on the assumption that the optical anisotropy of the molecule is determined by its geometric shape. The origin of the optical anisotropy of molecules as evidenced in observations on light-scattering has been the subject of discussion in recent papers.* It is found that pronounced asymmetry of geometric form does not necessarily mean pronounced optical anisotropy, the latter being determined by the chemical nature and arrangement of the atoms in the molecule. Nevertheless, the order of the geometric dimensions of a molecule in different directions is usually also the order of its optical polarisabilities along those directions. It must not be forgotten, however, that there may be exceptions to this rule.†

Returning now to formula (7), we may, since the second term on the right is much smaller than the first, write it in the form

$$\frac{n^2 - 1}{n^2 + 2} = \nu C (1 + \nu\Phi), \quad (25)$$

from which it is seen that apart from any possible variation of Φ with density or temperature, the correction to the Lorentz formula increases in importance with increasing density. There is *prima facie* reason to believe that Φ must itself increase numerically with increasing density of the fluid. To realise this, we recall the argument set out above regarding the relation between the geometric form of the molecule and the polarisation field acting on it. In the gaseous condition, or even in a dense vapour, there would ordinarily be almost complete freedom of orientation for the molecules. Further, the fraction of the time during which a molecule is in actual collision with a neighbour is a small part of the whole, and hence, in determining the polarisation field, we would not be sensibly in error in ignoring the non-spherical shape of the molecule altogether. It is only when the density becomes comparable with that of a liquid that a molecule is almost continually in collision with one or other of its neighbours, and that in evaluating the polarisation field we cannot ignore the restrictions imposed by the geometric form of the molecules on their relative positions and orientations. These considerations indicate a progressive change in the *character* of the polarisation field acting on a molecule as the density increases. At low densities, the field acting on a molecule would be appreciably the same as

* See K. R. Ramanathan, 'Roy. Soc. Proc.,' A, vol. 107, p. 684 (1924); vol. 110, p. 123 (1926). Also T. H. Havelock, 'Phil. Mag.,' vol. 3, pp. 156, 433 (1927).

† From some observations by Mr. I. Ramakrishna Rao in the authors' laboratory, on light-scattering in formic and acetic acid vapours, it appears that these form such exceptions. The available data on refractivity appear also to indicate an *increase* of the Lorentz constant of refractivity with increasing density.

if it were placed at the centre of a spherical cavity excavated around it, and would be independent of its orientation. At higher densities, the non-spherical shape of the molecule would begin to influence the results. A detailed treatment of the problem on the basis of the kinetic theory would be complicated by the circumstance that the molecules are themselves optically anisotropic and that therefore the mutual influence of two molecules depends both on their relative position and their relative orientation. Ignoring this difficulty, however, we may make the simplifying assumption that the surrounding molecules can be regarded as equivalent to a distribution of polarisable matter which is of uniform density and symmetrical except in a small region surrounding the given molecule. With increasing density, this small region and its lack of symmetry become of greater importance, until finally, when a density as great as that of the amorphous solid is reached, we shall not be much in error in regarding the molecule as practically embedded in a cavity having its own shape, the dependence of the polarisation field on the orientation of the molecule relatively to the external field then reaching its maximum value. We thus arrive at the general conclusion that the value of Φ increases numerically with increasing density, beginning with zero at low densities and reaching a limiting value at densities as high as those of the amorphous solid. The correction $\nu\Phi$ appearing in our modified form of the Lorentz formula must therefore increase at a greater rate than in proportion to the density, during a greater part of its course.

A clearer view of the whole subject may be obtained in the following way: In section 2, we obtained the expression (equation (4))

$$m = \tfrac{1}{3}(b_1' + b_2' + b_3'),$$

where

$$b_1' = b_1[1 + \chi(\tfrac{4}{3}\pi + \sigma_1)],$$

etc., etc., for the average moment induced in a molecule per unit external field. In a rarefied medium we have

$$m = \tfrac{1}{3}(b_1 + b_2 + b_3).$$

The ratios $b_1 : b_2 : b_3$ are a measure of the optical anisotropy of the molecule in the state of vapour. In the dense fluid the ratios $b_1' : b_2' : b_3'$ similarly indicate the optical anisotropy of the molecule as effectively modified by the influence of its neighbours. The preceding discussion shows that the result of such influence is to diminish these ratios and make them approach more nearly to unity, in other words, to diminish the effective optical anisotropy of the molecule, and that a diminution in refractivity is a necessary consequence of the same effect.

Independent evidence that the effect of increasing density is to cause an apparent diminution in the optical and electrical anisotropies of the molecule, is furnished by studies of the electrical birefringence of liquids, and by the study of the depolarisation of the light scattered by liquids at different temperatures. The authors have developed a theory of electric birefringence in liquids, and a theory of light-scattering in liquids, based on ideas very similar to those underlying the present paper, and find strong support for these theories in the experimental evidence available. The theory of light-scattering in liquids indicates that it is possible in simple cases to evaluate the quantities appearing in the formulæ of the present paper and thus offer a quantitative test of the proposed theory of refraction and dielectric behaviour. Very encouraging results have already been obtained in this direction, but to enter into these details would be foreign to the scope of this paper.

5. *Summary.*

A review of the experimental evidence shows that the existing theories of the refractivity and dielectric behaviour of liquids are inadequate to explain all that is known concerning the changes of these properties with density and temperature. A new theory is accordingly developed in this paper, which is based on the idea that the molecules of the fluid are optically and electrically anisotropic, and that, in addition, the polarisation field, acting on a molecule in a dense fluid, varies with its orientation relatively to the external field. The theory offers an immediate explanation why in general an *increased* density causes a *diminished* molecular refractivity as calculated from the Lorentz formula. It is shown that these changes in refractivity and dielectric constant are closely related to a change in the effective optical or electrical anisotropy of the molecules produced by the influence of its immediate neighbours. Similar ideas have been adopted in theories of electric birefringence and of light-scattering in liquids developed by the authors, which have found strong experimental support, and with the aid of which the anisotropic constants appearing in the formulæ of the present paper can be evaluated.

LXXIX. *A Theory of the Birefringence induced by Flow in Liquids.* *By* Prof. C. V. Raman, *F.R.S., and* K. S. Krishnan *.

1. *Introduction.*

THAT a viscous liquid such as Canada balsam exhibits optical anisotropy when mechanically agitated appears to have been first observed by Clerk Maxwell. The subject was later pursued by other investigators, notably by Kundt and his pupils, whose work will be found well summarized in an article by G. de Metz †. An extensive series of observations on the subject has been made recently by Vorländer and Walter ‡ with the arrangement, originally suggested by Maxwell, of placing the liquid in the gap between two coaxial cylinders and rapidly rotating the inner cylinder. A beam of plane-polarized light traversed the column of liquid in a direction parallel to the axis of the cylinders, and with the help of a suitable analyser and an auxiliary spectroscope, measurements were made of the birefringence exhibited by it. Vorländer and Walter examined in this way no fewer than 172 liquids, and have greatly extended our knowledge of the subject. An important outcome of their work is to shew that mechanical birefringence is observable in numerous common liquids having a definite chemical composition, including several which do not possess an exceptionally high viscosity; they found also that careful purification and removal of suspended "colloidal" matter from the liquids studied, by vacuum distillation, leaves the birefringence unaffected. Their work obliges us to conclude that the power to exhibit birefringence under mechanical flow is just as much a characteristic of pure liquids as, for instance, the power of exhibiting birefringence when placed in an electrostatic field.

It is proposed in this paper to develop a molecular theory of mechanical birefringence in liquids based on ideas somewhat similar to those successfully employed by Langevin and Born to explain electric double-refraction in liquids. The birefringence is regarded as arising from the optical anisotropy of the molecules, taken together with a tendency for them to orientate under the mechanical stresses within

* Communicated by the Authors.

† G. de Metz, *Scientia*, Gauthier-Villars, no. 26, Jan. 1906; see also Winkelmann's 'Handbuch der Physik,' Optik, pp. 1230–1236 (1906).

‡ D. Vorländer and R. Walter, *Zeits. Phys. Chem.* vol. cxviii. p. 1 (1925).

the fluid. The effective cause of such orientation is taken to be the non-spherical shape of the molecules.

It will be seen in the sequel that the theory succeeds not only in explaining the general features of the observed phenomena, but also in giving a value for the "Maxwell constant" in good agreement with observation.

2. *Molecular Orientation in Flowing Liquid.*

Stokes, in his memoir * on the internal friction of fluids, discussed the character of the stresses arising from viscous flow, and showed that in the case of a simple sliding motion

Fig. 1.

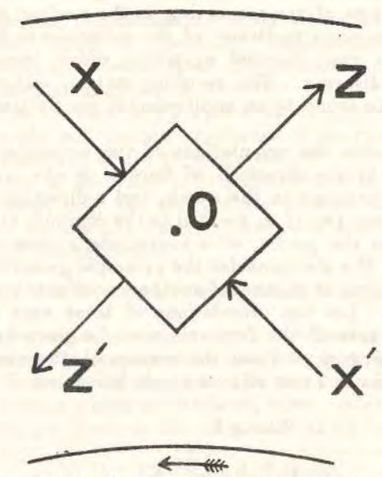

parallel to a plane the tangential stresses acting along the plane may be replaced by two sets of stresses, one set consisting of tensions and the other set of pressures acting along two directions which are mutually perpendicular and inclined at 45° to the line of flow. The direction of the tensions is parallel to the axis of extension and of the pressures to the axis of compression (see fig. 1, which represents a section of the fluid between the two cylinders, perpendicular to their common axis). The inner cylinder is assumed to rotate in the direction of the arrow, the outer one remaining fixed. The tensions and pressures shown in the figure are

* Sir George Stokes, Math. and Phys. Papers, Camb. Univ. Press, vol. i. p. 91.

each equal to $\eta\frac{v}{c}$ per unit area, where η is the coefficient of viscosity and $\frac{v}{c}$ is the radial velocity-gradient at O.

It is clear that if the molecules are highly asymmetrical in shape, the set of tensions and pressures pictured in fig. 1 would tend to cause them to orient in the fluid, in such manner that the longest dimension of a molecule lies along the axis of tensions and the shortest one along the axis of pressures. For such orientation would evidently result in the fluid (regarded as a densely-packed assemblage of molecules) expanding along the axis of z and contracting along the axis of x, the total volume remaining constant, thus allowing the system of stresses acting in the medium to do work. This orientative tendency of the molecules is, however, opposed by their thermal agitation, which tends to throw them into disarray. The resulting state of statistical equilibrium can be found by an application of the Boltzmann Principle.

In order to define the orientations of the molecules, we choose (see fig. 1) the direction of tension as the z-axis, the direction of pressure as the x-axis, and a direction perpendicular to these two (*i. e.* parallel to the common axis of the cylinders) as the y-axis, of a coordinate system $x\,y\,z$ fixed in space. We also consider the principal geometrical axes of each molecule as the axes of another coordinate system $\xi\,\eta\,\zeta$ fixed in it. Let the orientations of these axes with reference to the axes of the former system be given by the Eulerian angles θ, ϕ, ψ. Then the cosines of the various angles between the two sets of axes are as below :—

TABLE I.

	x.	y.	z.
ξ	$a_{11} = \cos\theta\cos\phi\cos\psi - \sin\phi\sin\psi$.	$a_{12} = \cos\theta\sin\phi\cos\psi + \cos\phi\sin\psi$.	$a_{13} = -\sin\theta\cos\psi$.
η	$a_{21} = -\cos\theta\cos\phi\sin\psi - \sin\phi\cos\psi$.	$a_{22} = -\cos\theta\sin\phi\sin\psi + \cos\phi\cos\psi$.	$a_{23} = \sin\theta\sin\psi$.
ζ	$a_{31} = \sin\theta\cos\phi$.	$a_{32} = \sin\theta\sin\phi$.	$a_{33} = \cos\theta$.

For allowing the Principle of Boltzmann to be applied to our present problem, we require an expression for the

potential energy of each molecule in the fluid in terms of its orientation with respect to the fixed coordinate axes $x\,y\,z$. A suitable form of expression is suggested by the following considerations. The stress acting in the medium is, as we have seen, $\eta\frac{v}{c}$, and if we divide this by the number of molecules ν per unit volume in the fluid, we obtain a quantity $\eta\frac{v}{c}\cdot\frac{1}{\nu}$, which has the physical dimensions of energy. It is therefore permissible to assume that the energy of each molecule, as determined by its orientation with respect to the axes of these stresses, is proportional to $\eta\frac{v}{c}\cdot\frac{1}{\nu}$, the coefficient of proportionality being a function of the angle-variables, which is physically dimensionless. Since by hypothesis the orientation of the molecules arises from their non-spherical shape, and since the positive and negative directions are necessarily equivalent, the potential energy of a molecule will remain unaffected if we rotate it through 180° round any of the ξ-, η-, ζ-axes.

In view of what has been said above, and considering for the present only the effect of the *tensions* along the z-axis, we may assume the potential energy of each molecule to be given by the expression

$$u = -(\omega_1 a_{13}^2 + \omega_2 a_{23}^2 + \omega_3 a_{33}^2)\cdot\eta\frac{v}{c}\cdot\frac{1}{\nu}, \qquad (1)$$

where ω_1, ω_2, ω_3 are constants determined by the geometric form of the molecule, which will later be evaluated. Then, from Boltzmann's theorem, the number of molecules per unit volume whose orientations, when under thermal equilibrium, are given by the range $\sin\theta\,d\theta\,d\phi\,d\psi$, is equal to

$$Ce^{-\frac{u}{kT}}\sin\theta\,d\theta\,d\phi\,d\psi, \qquad (2)$$

where C is the constant given by the relation

$$\nu = C\int_{\theta=0}^{\theta=\pi}\int_{\phi=0}^{\phi=2\pi}\int_{\psi=0}^{\psi=2\pi} e^{-\frac{u}{kT}}\sin\theta\,d\theta\,d\phi\,d\psi. \qquad (3)$$

In the orientated state the average potential energy per molecule in the medium is given by

$$\bar{u} = \frac{\iiint e^{-\frac{u}{kT}}u\sin\theta\,d\theta\,d\phi\,d\psi}{\iiint e^{-\frac{u}{kT}}\sin\theta\,d\theta\,d\phi\,d\psi}$$

the limits of integration being the same as in (3),

$$= -\frac{\omega_1+\omega_2+\omega_3}{3}\cdot\eta\frac{v}{c}\cdot\frac{1}{\nu} - \frac{2}{45k\bar{T}}\left[(\omega_1-\omega_2)^2+(\omega_2-\omega_3)^2 + (\omega_3-\omega_1)^2\right]\cdot\left(\eta\frac{v}{c}\cdot\frac{1}{\nu}\right)^2 . \quad (4)$$

If, on the other hand, the molecules are orientated entirely at random, then the average energy per molecule will be given by

$$\bar{u}_0 = \frac{\iiint u \sin\theta\, d\theta\, d\phi\, d\psi}{\iiint \sin\theta\, d\theta\, d\phi\, d\psi} = -\frac{\omega_1+\omega_2+\omega_3}{3}\cdot\eta\frac{v}{c}\cdot\frac{1}{\nu} . \quad (5)$$

The difference $\bar{u}_0-\bar{u}$ multiplied by ν gives the diminution of potential energy per unit volume in orientating the molecules contained in it, and is equal to

$$(\bar{u}_0-\bar{u})\nu = \frac{2}{45k\bar{T}}\left[(\omega_1-\omega_2)^2+(\omega_2-\omega_3)^2 + (\omega_3-\omega_1)^2\right]\cdot\left(\eta\frac{v}{c}\right)^2\cdot\frac{1}{\nu} . \quad (6)$$

3. *The Optical Effect of Molecular Orientation.*

We now proceed to find the double refraction which arises from this orientation of the molecules, here again confining our attention at first to the result of the tensions acting along the x-axis. Since the optic axes of the molecule will not, in general, coincide with its geometric axes $\xi\,\eta\,\zeta$, when a field (due to a light-wave) is incident along any one of these axes, say along the ξ-axis, the moment induced in the molecule will not be wholly along the ξ-axis, but will have components also along the η- and ζ-axes. Thus for unit field actually acting on the molecule along the ξ-axis, let b_{11}, b_{12}, b_{13} be the moments induced in it along its ξ-, η-, and ζ-axes respectively; and let b_{21}, b_{22}, b_{23}, and b_{31}, b_{32}, b_{33} be similar induced moments for unit field acting along the η- and ζ-axes respectively: $b_{ij}=b_{ji}$. We have two special cases to consider.

Case I.—The electric vector of the incident light-wave lies along the z-axis—*i. e.*, along the direction of the tension.

Let the optical field actually acting on each molecule in the same direction be denoted by E. Then the moments induced in the molecule under consideration along its axes,

when resolved along the direction of E, are together equal to

$$(b_{11}\alpha_{13}^2+b_{22}\alpha_{23}^2+b_{33}\alpha_{33}^2+2b_{12}\alpha_{13}\alpha_{23}+2b_{23}\alpha_{23}\alpha_{33}+2b_{31}\alpha_{33}\alpha_{13})\mathrm{E} \quad . \quad . \quad . \quad (7)$$

$$= m_z\mathrm{E}, \text{ say.} \quad . \quad . \quad . \quad . \quad . \quad . \quad . \quad (8)$$

Then the average value of m_z taken over all the molecules in the medium will be given by

$$\bar{m}_z = \frac{\iiint e^{-\frac{u}{kT}} m_z \sin\theta\, d\theta\, d\phi\, d\psi}{\iiint e^{-\frac{u}{kT}} \sin\theta\, d\theta\, d\phi\, d\psi} = \frac{b_{11}+b_{22}+b_{33}}{3} + 2\Theta\eta\frac{v}{c}\cdot\frac{1}{\nu} . \quad . \quad . \quad . \quad (9)$$

where

$$\Theta = \frac{1}{45k\bar{T}}[(\omega_1-\omega_2)(b_{11}-b_{22})+(\omega_2-\omega_3)(b_{22}-b_{33}) + (\omega_3-\omega_1)(b_{33}-b_{11})] . \quad . \quad (10)$$

Case II.—The light-vector lies along the x-axis.

Let us denote the actual field acting on each molecule along the x-axis by E. The moments induced in any molecule along its axes, when resolved along the x-axis, are together equal to

$$(b_{11}\alpha_{11}^2+b_{22}\alpha_{21}^2+b_{33}\alpha_{31}^2+2b_{12}\alpha_{11}\alpha_{21}+2b_{23}\alpha_{21}\alpha_{31}+2b_{31}\alpha_{31}\alpha_{11})\mathrm{E} \quad . \quad . \quad . \quad (11)$$

$$= m_x\mathrm{E}, \text{ say.} \quad . \quad . \quad . \quad . \quad . \quad . \quad . \quad (12)$$

The average value of m_x taken over all the molecules can be calculated as in the previous case, and comes out equal to

$$m_x = \frac{b_{11}+b_{22}+b_{33}}{3} - \Theta\eta\frac{v}{c}\cdot\frac{1}{\nu} . \quad . \quad . \quad . \quad (13)$$

From (9) and (13)

$$\bar{m}_z-\bar{m}_x = 3\Theta\eta\frac{v}{c}\cdot\frac{1}{\nu} . \quad . \quad . \quad . \quad (14)$$

Hitherto we have considered only the effect of the tensions $\eta\frac{v}{c}$ acting along the z-axis. The effect of the pressures of the same magnitude acting along the x-axis can be calculated in exactly the same way by considering them as tensions $=-\eta\frac{v}{c}$ along the x-axis, and thus we get

$$\bar{m}_x-\bar{m}_z = 3\Theta\times-\eta\frac{v}{c}\cdot\frac{1}{\nu} .$$

Thus, when the two effects are superposed, as in the actual liquid, we get for the difference in the values of the mean induced moments, for directions of vibration of the incident light along the z- and x-axes, the expression

$$\overline{m}_z - \overline{m}_x = 6\,\Theta\,\eta\,\frac{v}{c}\cdot\frac{1}{\nu}. \quad . \quad . \quad . \quad . \quad (15)$$

If we denote by n_z and n_x the refractive indices of the medium for light-vibrations along the z- and the x-axes respectively, by differentiating the well-known expression for refractivity

$$\frac{n^2-1}{n^2+2} = \frac{4\pi}{3}\nu\,.\,m, \quad . \quad . \quad . \quad . \quad . \quad (16)$$

we have

$$n_z - n_x = \frac{(n^2-1)(n^2+2)}{6n}\cdot\frac{\overline{m}_z-\overline{m}_x}{m}$$

$$= \frac{(n^2-1)(n^2+2)}{n}\cdot\frac{\Theta}{m}\cdot\eta\frac{v}{c}\cdot\frac{1}{\nu}, \quad . \quad (17)$$

where n is the refractive index and m is the mean moment induced in a molecule per unit field actually acting on it, in the randomly orientated state of the molecules. Obviously

$$m = \frac{b_{11}+b_{22}+b_{33}}{3}. \quad . \quad . \quad . \quad . \quad . \quad (18)$$

All the quantities in expression (17) for the birefringence of the medium are experimentally determinable, except Θ, which involves, as is evident from (10), the optical constants of the molecule and the constants $\omega_1, \omega_2, \omega_3$ appearing in expression (1) for the potential energy. We shall now proceed to consider how the quantities $\omega_1, \omega_2, \omega_3$ may be connected with the geometric form of the molecules.

4. *Molecular Shape and Molecular Orientation.*

Since, by hypothesis, the orientation of the molecules is the result of their non-spherical form, we may proceed to connect them in the following way. We idealize the molecules and consider them to have the form of ellipsoids with three unequal diameters, a_1, a_2, a_3. If we imagine the molecules to be arranged in contact with each other, their axes parallel, in the form of a rectangular parallelopiped having s molecules in each of its edges, the length of the latter would be sa_1, sa_2, sa_3 respectively. This is an extreme case, which illustrates the general principle that the effect of any general tendency of the molecules to orientate in

specific directions is to cause the density of molecules per unit length in different directions to become different. It is difficult to express this principle with complete precision in a mathematical form, particularly in the case of liquids, where the molecules are not always necessarily in contact with each other. Considering, however, the fact that the density of the type of liquid with which we are concerned here is usually not very different from that in the solidified state, the error in considering the molecules to be in contact with each other all the time would not be serious in any event; and since we are only concerned with ratios, the inaccuracy involved can practically be eliminated by considering the "effective" dimensions of a molecule in the liquid to be slightly different from what they are in the solidified state. Subject to these remarks, we may assume that a molecule arbitrarily orientated contributes to the linear dimension of the aggregate measured along the z-axis a length equal to

$$a_1\alpha_{13}^2 + a_2\alpha_{23}^2 + a_3\alpha_{33}^2. \quad . \quad . \quad . \quad . \quad (19)$$

If the molecules are arbitrarily orientated, the average effective length of the molecule along the z-axis is simply

$$\frac{\iiint (a_1\alpha_{13}^2 + a_2\alpha_{23}^2 + a_3\alpha_{33}^2)\sin\theta\,d\theta\,d\phi\,d\psi}{\iiint \sin\theta\,d\theta\,d\phi\,d\psi}$$

$$= \frac{a_1+a_2+a_3}{3}; \quad . \quad . \quad . \quad . \quad . \quad (20)$$

that is to say, the mean of the three diameters of the ellipsoid. Considering, however, the tendency of the molecules to orientate, due to the tensions along the z-axis in the fluid, we find the average length to be

$$\frac{\iiint e^{-\frac{u}{kT}}(a_1\alpha_{13}^2 + a_2\alpha_{23}^2 + a_3\alpha_{33}^2)\sin\theta\,d\theta\,d\phi\,d\psi}{\iiint e^{-\frac{u}{kT}}\sin\theta\,d\theta\,d\phi\,d\psi},$$

where u is given by expression (1),

$$= \frac{a_1+a_2+a_3}{3} + \frac{2}{45kT}[(\omega_1-\omega_2)(a_1-a_2)+(\omega_2-\omega_3)(a_2-a_3)$$

$$+(\omega_3-\omega_1)(a_3-a_1)]\,\eta\frac{v}{c}\cdot\frac{1}{\nu}. \quad (21)$$

The difference between (21) and (20) divided by (20) gives the effective expansion per unit length, along the z-axis, owing to the orientation of the molecules, as

$$\frac{2}{15kT}\cdot\frac{(\omega_1-\omega_2)(a_1-a_2)+(\omega_2-\omega_3)(a_2-a_3)+(\omega_3-\omega_1)(a_3-a_1)}{a_1+a_2+a_3}\times\eta\frac{v}{c}\cdot\frac{1}{\nu}. \quad . \quad . \quad . \quad . \quad (22)$$

Multiplying this by the tension $\eta\frac{v}{c}$ along the x-axis, we obtain the work done per unit volume resulting from the orientation of the molecules contained in it, an expression for which was obtained in an entirely different way in (6) above. Equating the two expressions, we have

$$(\omega_1-\omega_2)^2+(\omega_2-\omega_3)^2+(\omega_3-\omega_1)^2 = 3\frac{(\omega_1-\omega_2)(a_1-a_2)+(\omega_2-\omega_3)(a_2-a_3)+(\omega_3-\omega_1)(a_3-a_1)}{a_1+a_2+a_3} \quad . \quad . \quad . \quad (23)$$

The form of the equation immediately suggests as a solution

$$\frac{\omega_1-\omega_2}{a_1-a_2}=\frac{\omega_2-\omega_3}{a_2-a_3}=\frac{\omega_3-\omega_1}{a_3-a_1}=\frac{3}{a_1+a_2+a_3}, \quad . \quad (24)$$

which is readily seen to satisfy (23). For the special cases in which the molecule has the form of a prolate or oblate spheroid of revolution, the validity of (24) is rigorously demonstrable, and it seems justifiable to assume that it is generally true.

5. *Expression for the Maxwell Constant.*

Substituting (24) in (17) and (10) we obtain as the final expression for the birefringence

$$n_z-n_x=\frac{(n^2-1)(n^2+2)}{5n\nu kT}\times\frac{(a_1-a_2)(b_{11}-b_{22})+(a_2-a_3)(b_{22}-b_{33})+(a_3-a_1)(b_{33}-b_{11})}{(a_1+a_2+a_3)(b_{11}+b_{22}+b_{33})}\times\eta\frac{v}{c}. \quad . \quad . \quad . \quad . \quad . \quad . \quad . \quad (25)$$

$$=\nabla\cdot\eta\frac{v}{c}, \quad . \quad . \quad . \quad . \quad . \quad . \quad . \quad (26)$$

where ∇ is the constant of mechanical birefringence in the fluid, which may appropriately be called the Maxwel

constant, in honour of the discoverer of the effect. It will be seen from the equation that the value of the constant depends jointly upon the optical anisotropy of the molecule and upon the anisotropy of its geometric form.

We shall now proceed to consider how the theory set out above compares with the phenomena as observed in their general features.

Axes of Birefringence.—The theory indicates in agreement with observation that the two principal directions of vibration are mutually perpendicular, and inclined at 45° to the plane of sliding within the liquid.

Positive or Negative Birefringence?—The theory indicates that the sign of the birefringence depends on whether the expression

$$[(a_1-a_2)(b_{11}-b_{22})+(a_2-a_3)(b_{22}-b_{33})+(a_3-a_1)(b_{33}-b_{11})] \quad . \quad . \quad . \quad (27)$$

is positive or negative. It is easily seen that if $a_1>a_2>a_3$ and $b_{11}>b_{22}>b_{33}$, the expression in question is positive and the birefringence is therefore positive, while if $a_1>a_2>a_3$ and $b_{11}<b_{22}<b_{33}$, the birefringence will be negative. In other words, the sign of the double refraction depends on whether the optical constants of the molecule along its three axes follow the same sequence as the linear dimensions or follow the reverse order. If we can regard the chemical molecule as roughly equivalent to an ellipsoid of isotropic dielectric material, the former condition would be satisfied. It is thus readily understood why the great majority of the liquids examined by Vorländer and Walter exhibit positive birefringence. In fact, the only cases of negative birefringence contained in their table of results are the sodium and potassium salts of some of the higher fatty acids; the corresponding fatty acids themselves show positive birefringence.

Influence of Speed, Viscosity, and Temperature.—The theory indicates that the observed birefringence should be proportional to the speed of rotation. The experimental evidence appears to indicate that this is actually the case with most pure liquids. Where divergences appear, it seems not unlikely that they are due to disturbing causes, *e. g.*, departure from the assumed stream-line flow of the liquid, or a rise of the temperature of the liquid as a result of the rotation. The theory indicates a rapid fall of the birefringence with rising temperature, primarily because of the fall of the viscosity, the variation of the Maxwell constant itself with temperature being much less important. The experimental evidence fully supports this inference from theory.

Influence of Molecular Form.—The theory shows that, apart from the viscosity of the liquid, the birefringence should be specifically influenced by the form of the molecule, being greatest when the molecule is highly elongated and least when its form approaches spherical symmetry. The observations of Vorländer and Walter furnish ample evidence in support of this. They found that increasing the length of the chain in the fatty acid series increased the specific birefringence (or Maxwell constant as we call it), and introducing side-chains in the molecule diminishes it notably.

Influence of Optical Anisotropy.—The theory indicates that for molecules of given form the Maxwell constant should increase with increasing optical anisotropy and with increasing refractive index. Now it is known that organic liquids of the aromatic series exhibit in light-scattering a much higher degree of optical anisotropy than the aliphatic series, besides having usually a higher refractive index. On the other hand, the geometry of the benzene ring ensures a greater symmetry of form for simple benzene derivatives than for the aliphatic compounds. The two effects would thus set each other off to a considerable extent in the case of the simpler benzene derivatives. If, however, we consider long-chain compounds in which the benzene ring also appears, we may reasonably expect the increased optical anisotropy to manifest itself in an increased value for the Maxwell constant. Similarly it is known from observations on light-scattering that unsaturated carbon compounds show a high degree of optical anisotropy, and it follows that they should have a large Maxwell constant. Ample support for these inferences from theory is furnished by the observations of Vorländer and Walter.

Dispersion of Double-Refraction.—From our formula it will be seen that the wave-length does not appear explicitly in our formula. Since, however, the Maxwell constant is proportional to $(n^2-1)(n^2+2)/n$, where n is the refractive index, a not negligible degree of dispersion may be expected, as has indeed been observed in experiment.

6. *Absolute Value of Birefringence.*

To calculate the Maxwell constant for any liquid, we require to know the refractive index of the liquid, its molecular weight and density, the optical anisotropy of the molecules and their geometric form. The optical anisotropy of the molecules can be completely determined from measurements of the light-scattering in the liquid if the molecule has an axis of symmetry, and can at least be estimated in other cases from such measurements. The geometrical form

of the molecules is known, at least approximately, from chemical considerations and from X-ray studies. It is thus possible to calculate the value of the Maxwell constant absolutely for any liquid for which the data referred to above are available. Unfortunately, few of the liquids for which the mechanical birefringence is known have been investigated for light-scattering. We may, however, test the theory in the following way. The range of variation of the quantities appearing in the expression for the Maxwell constant is well known. The refractive index of most organic liquids ranges between 1·4 and 1·7. The ratio of molecular weight to density for the type of compounds under consideration ranges between 80 and 240. The ratio of the longest to the shortest dimension of the molecule may of course range theoretically from 1 to large values, but practically it may be taken as lying between 2 and 5 for most compounds which are liquids and show an appreciable birefringence under flow. The ratio of the maximum and minimum polarizabilities of the molecule along its different axes is known from the extensive investigations on light-scattering carried on at Calcutta for different types of organic compounds. It is usually about 1·1 for aliphatic hydrocarbons and saturated cyclo-compounds, 1·5 for aliphatic compounds containing strongly refractive groups, 1·9 for simple benzene derivatives, and about 2·3 for very highly anisotropic compounds such as chloronaphthalene, quinolene*, etc. We may group the data in such order as to have four representative classes, in which we have respectively very low, moderate, high, and very high values of the Maxwell constant as theoretically calculated. This has been done in Table II., in which, for simplicity of calculation, the molecule is assumed to have an axis of symmetry. The temperature assumed is 293° absolute.

For comparison with the values shown in Table II. we have analysed the data given by Vorländer and Walter in their paper. Of the 172 liquids studied, 37 were of very low viscosity and naturally did not yield any results. 15 other liquids having moderate or high viscosities also showed no indication of birefringence. This is not surprising in view of the fact that their optical arrangements did not permit a difference of path of less than 2 millimicrons to be detected. A liquid of moderately high viscosity, say 50 times that of water and having a Maxwell constant less than $0{\cdot}01 \times 10^{-9}$, would have shown no detectable birefringence in their experiments. The limit of detectability would

* These values give the *effective* anisotropies determined from observations of light-scattering in *the liquid state.*

be correspondingly larger for liquids of lower viscosity. It appears certain that an adequate explanation (viz., a low viscosity, or an insufficient optical or geometric anisotropy

TABLE II.—Calculated values of the Maxwell constant.

Class.	Refractive index.	Ratio of molecular weight to density.	Ratio of geometric axes $\frac{a_1}{a_2}=\frac{a_1}{a_3}$.	Ratio of optic axes $\frac{b_{11}}{b_{22}}=\frac{b_{11}}{b_{33}}$.	Maxwell constant $\times 10^9$.
I.....	1·4	80	2	1·1	0·03
II.....	1·5	120	3	1·5	0·4
III.....	1·6	180	4	1·9	1·5
IV.....	1·7	240	5	2·3	3·7

of the molecules) would be forthcoming in most cases in which they failed to detect any effect. It must also be remembered that in the expression

$$(a_1-a_2)(b_{11}-b_{22})+(a_2-a_3)(b_{22}-b_{33})+(a_3-a_1)(b_{33}-b_{11})$$

appearing in the Maxwell constant, b_{11}, b_{22}, b_{33} are the optical polarizabilities of the molecule, *not along its optic axes, but along its geometric axes.* Consequently, special cases may arise, if the optic and geometric axes are suitably inclined to each other, when the above expression will have very small values, even if the molecule possesses a large geometric and optical anisotropy.

Excluding the 52 liquids in which no effect was found, and the 12 compounds of potassium and sodium with the fatty acids which showed a negative birefringence, we have 108 liquids in which a normal effect was observed. From the dimensions of their apparatus (length of liquid column 4·68 cm., radii of the cylinders 1·15 cm. and 1·05 cm., and width of gap therefore =0·10 cm.), and the known viscosity of water at 20° C., relative to which the values for the different liquids are expressed, and the specific birefringence as tabulated by them, the values of the Maxwell constant in C.G.S. units can be ascertained. In Table III. the observed values of the Maxwell constant have been grouped into five classes and are shown for comparison with the figures in Table II.

It appears highly significant that the observed values for the great majority of the liquids cluster round that calculated on the reasonable assumptions that the refractive index is about 1·5, the molecular weight about 120, the density about 1, the ratio of length of the molecule to its thickness

TABLE III.—Observed values of the Maxwell constant ($\times 10^9$) for 108 liquids.

Observed values of $\nabla \times 10^9$.	Below 0·03.	Between 0·03 and 0·4.	Between 0·4 and 1·5.	Between 1·5 and 3·7.	Above 3·7.
Number of aliphatic and hydro-aromatic liquids.	12	44	12	—	—
Number of aromatic liquids.	—	22	15	2	1

about 3, and the ratio of its maximum and minimum optical polarizabilities about 1·5. It is equally significant that all the low values of the Maxwell constant belong to the aliphatic or hydro-aromatic compounds, and all the high values to the aromatic compounds, and that the average values for the two sets of compounds differ just in the way we should expect in view of the greater refractive index and optical anisotropy of benzene and its derivatives.

Finally, as an example of the degree of quantitative agreement to be expected, we shall take the case of *n*-octyl alcohol. We may approximately consider this as a prolate spheroid whose major axis is 12·6 Å.U. and whose minor axis is 4·9 A.U. Its refractive index is 1·430 and the molecular weight is 130·1.

The scattering of light in octyl alcohol has not been studied. We have, however, data for heptane and octane and also for ethyl, propyl, butyl, and amylic alcohols, and for all these compounds, assuming the optical ellipsoids of the molecules to be also prolate spheroids of revolution whose axes coincide with their respective geometric axes, the ratio $b_{11}:b_{22}$ is equal to 1·15. We may therefore with confidence assume the same value for *n*-octyl alcohol. From these data we find the Maxwell constant for *n*-octyl alcohol to be

Calculated value of $\nabla = 0{\cdot}125 \times 10^{-9}$.

From the measurements of Vörlander and Walter, taking the viscosity of octyl alcohol at 20° C. = 0·0895 (Landolt Tables),

Observed value of $\nabla = 0{\cdot}13 \times 10^{-9}$.

7. *Summary.*

In this paper a theory is developed for the effect discovered by Maxwell—viz., that a liquid in a state of viscous flow exhibits birefringence. The state of stress in the fluid consists of tensions and pressures in directions perpendicular to each other and inclined at 45° to the plane of sliding.

Frequency Variations of the Triode Oscillator.

When the molecules have an elongated form, these stresses tend to orientate them so that their direction of greatest length lies along the axis of tension, and that of shortest length along the axis of pressure. The tendency to orientation is, however, resisted by their thermal agitation, and the resulting state of statistical equilibrium may be found by the application of Boltzmann's Principle. The optical anisotropy of the molecules, taken together with the orientations referred to, causes the medium to become birefringent. The magnitude of the effect is proportional to the product of the viscosity and the velocity-gradient. The constant of proportionality, which is referred to as the Maxwell constant for the liquid, is evaluated in terms of the optical and geometrical anisotropies of the molecule, the refractive index, density, and molecular weight of the liquid, and Boltzmann's constant.

The data for 172 liquids recently obtained by Vorländer and Walter are critically discussed, and it is shown that the theory succeeds not only in giving an explanation of the general features of the phenomena observed, but also in giving quantitatively the observed values of the Maxwell constant.

210 Bowbazar Street,
Calcutta, India.
September 15, 1927.

A New Type of Secondary Radiation.

If we assume that the X-ray scattering of the 'unmodified' type observed by Prof. Compton corresponds to the normal or average state of the atoms and molecules, while the 'modified' scattering of altered wave-length corresponds to their fluctuations from that state, it would follow that we should expect also in the case of ordinary light two types of scattering, one determined by the normal optical properties of the atoms or molecules, and another representing the effect of their fluctuations from their normal state. It accordingly becomes necessary to test whether this is actually the case. The experiments we have made have confirmed this anticipation, and shown that in every case in which light is scattered by the molecules in dust-free liquids or gases, the diffuse radiation of the ordinary kind, having the same wave-length as the incident beam, is accompanied by a modified scattered radiation of degraded frequency.

The new type of light scattering discovered by us naturally requires very powerful illumination for its observation. In our experiments, a beam of sunlight was converged successively by a telescope objective of 18 cm. aperture and 230 cm. focal length, and by a second lens of 5 cm. focal length. At the focus of the second lens was placed the scattering material, which is either a liquid (carefully purified by repeated distillation *in vacuo*) or its dust-free vapour. To detect the presence of a modified scattered radiation, the method of complementary light-filters was used. A blue-violet filter, when coupled with a yellow-green filter and placed in the incident light, completely extinguished the track of the light through the liquid or vapour. The reappearance of the track when the yellow filter is transferred to a place between it and the observer's eye is proof of the existence of a modified scattered radiation. Spectroscopic confirmation is also available.

Some sixty different common liquids have been examined in this way, and every one of them showed the effect in greater or less degree. That the effect is a true scattering and not a fluorescence is indicated in the first place by its feebleness in comparison with the ordinary scattering, and secondly by its polarisation, which is in many cases quite strong and comparable with the polarisation of the ordinary scattering. The investigation is naturally much more difficult in the case of gases and vapours, owing to the excessive feebleness of the effect. Nevertheless, when the vapour is of sufficient density, for example with ether or amylene, the modified scattering is readily demonstrable.

C. V. Raman.
K. S. Krishnan.

210 Bowbazar Street,
Calcutta, India,
Feb. 16.

The Optical Analogue of the Compton Effect.

THE presence in the light scattered by fluids, of wave-lengths different from those present in the incident light, is shown very clearly by the accompanying photographs (Fig. 1). In the illustration (1)

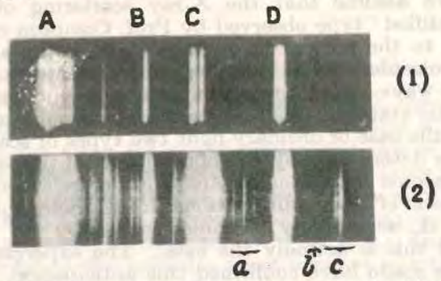

FIG. 1.—(1) Spectrum of incident light; (2) spectrum of scattered light.

represents the spectrum of the light from a quartz mercury vapour lamp, from which all wave-lengths greater than that of the indigo line have been filtered out. This line (4358 A.) is marked D in the spectrogram, and C is the group of lines 4047, 4078, and 4109 A. Spectrogram (2) shows the spectrum of the scattered light, the fluid used being toluene in this case. It will be seen that besides the lines present in the incident spectrum, there are several other lines present in the scattered spectrum. These are marked *a*, *b*, *c* in the figure, and in addition there is seen visually another group of lines which is of still greater wave-length and lies in a region outside that photographed. When a suitable filter was put in the incident light to cut off the 4358 line, this latter group also disappeared, showing that it derived its origin from the 4358 line in the incident radiation. Similarly, the group marked c in spectrogram (2) disappeared when the group of lines 4047, 4078 and 4109 was filtered out from the incident radiation by quinine solution, while the group due to 4358 A. continued to be seen. Thus the analogy with the Compton effect becomes clear, except that we are dealing with shifts of wave-length far larger than those met with in the X-ray region.

As a tentative explanation of the new spectral lines thus produced by light-scattering, it may be assumed that an incident quantum of radiation may be scattered by the molecules of a fluid either as a whole or in part, in the former case giving the original wave-length, and in the latter case an increased wave-length. This explanation is supported by the fact that the diminution in frequency is of the same order of magnitude as the frequency of the molecular infra-red absorption line. Further, it is found that the shift of wave-length is not quite the same for different molecules, and this supports the explanation suggested.

Careful measurements of wave-length now being made should settle this point definitely at an early date.

C. V. RAMAN.
K. S. KRISHNAN.

210 Bowbazar Street,
Calcutta, Mar. 22.

A New Class of Spectra due to Secondary Radiation. Part I.

BY

PROF. C. V. RAMAN, F.R.S., AND K. S. KRISHNAN.

(Plates XIII, XIV and XV.)

(Received for publication 7th May, 1928.)

1. *Introduction.*

The discovery of a new type of secondary radiation, distinct from either the classical scattering or ordinary fluorescence, has been recorded in an address delivered recently by one of us and published in the previous issue of this Journal.[1] Whenever light is diffused by the molecules of a transparent medium, the scattered radiations contain not only the wave-lengths present in the incident light but also radiations of modified frequency. The effect is most striking when the scattering medium is a dust-free liquid, and the incident radiations consist of sharply defined spectral lines, *e.g.*, the light of a quartz mercury lamp. It is then found that in the spectrum of the scattered light we have besides the incident lines also other new lines which are usually quite sharp A continuous spectrum may also be observed and is specially noticeable in certain liquids. The scattered radiation of

[1] "A New Radiation" by C. V. Raman, Ind. Jour. Phys., vol. 2, p. 387, 1928. See also C. V. Raman and K. S. Krishnan, Nature, vol. 121, p. 501, 31st March, 1928.

altered wave-lengths is partially polarised. Though the effects mentioned above are most readily studied with liquids, other media such as vapours, crystals and even amorphous solids exhibit the modified scattering, which is thus a universal phenomenon. The explanation was tentatively put forward that the new type of secondary radiation is produced when the incident quantum of radiation is partly absorbed by the molecule, shifting it to a higher level of energy, and is partly scattered. The difference between the frequencies of the incident and scattered radiations would thus correspond to a characteristic frequency of the molecule. Accepting this explanation it follows that corresponding to a given frequency of the incident radiation, we should expect a new line in the spectrum of the scattered radiation for each one of the characteristic frequencies of the molecule, that is to say, for each incident frequency we should expect as many lines of modified frequency as the molecule has characteristic electronic frequencies. Further, when the incident radiation contains several spectral lines, we should expect several sets of such modified lines in the scattered spectrum. The new type of secondary radiation should thus create for us a whole new class of spectra, and indeed as many new spectra as there are chemical substances suitable for study, multiplied by the number of spectral lines available in the light-source used.

The discovery of the new radiation thus opens up a wonderful avenue of research in spectroscopy. During the past few weeks we have succeeded in obtaining a number of spectrograms of the scattered radiation with the following liquids selected for their importance, namely, benzene, toluene, pentane, ether, methyl alcohol and water. The spectrograms obtained with benzene have been measured. It is proposed in this paper to detail the highly significant results which have emerged from the detailed study of the spectrograms for benzene, and from a qualitative study of the spectra obtained with the other liquids.

2. *Experimental Methods.*

As the source of illumination we used a commercial 3,000 C. P. mercury vapour lamp in quartz, made by the Hewittic Electric Company, which was found to be thoroughly reliable and efficient in its working. The light of the lamp was concentrated by an 8-inch glass condenser into a bulb containing the dust-free liquid under examination. The larger the bulb the more satisfactory are the conditions of observation and it is therefore desirable to use a bulb of clear non-fluorescent glass, having a diameter at least as large as the image of the quartz lamp formed by the condenser. On the other hand, a large bulb involves the use of a large quantity of the liquid and correspondingly greater expense. With liquids such as water or the common chemicals such as benzene, this is not a serious consideration. But in the case of the more costly chemicals it sets a limit to the size of the bulbs to be employed.

It is of importance that the liquid to be used for study should be chemically the purest available. For purpose of further purification, it is placed in a second large bulb connecting with the observation bulb, and transferred to the latter by distillation in *vacuum*. If the bulbs have been thoroughly cleansed before filling, a single distillation may suffice. It is usually advisable however to wash back the distilled liquid from the observation bulb to the distillation bulb several times. The distillation should be conducted at as low a temperature as possible. For this purpose the initial vacuum should be good, and the observation bulb is cooled with ice, so that the distillation occurs quickly when the second bulb is only moderately warmed. The final distillate is then obtained as a very clear liquid free from dust or other fluorescent impurity and is then used immediately for the optical observations.

The modified lines in the scattered spectrum can easily be seen with a pocket spectroscope. The most convenient direction of observation is that transverse to the path of the beam of light through the liquid, though of course any other direction of observation is theoretically permissible. The maximum intensity is obtained when the axis of the spectroscope is pointed along the direction of the image of the quartz lamp formed within the liquid, as the greatest depth of illuminated liquid is obtained in this way. For purpose of visual observation, it is helpful to exclude wave-lengths greater than 4358·3 A.U. from the incident light by placing in its path a violet glass, which completely cuts out the blue, green and yellow regions of the mercury spectrum. The spectrum of the modified scattering (lines and in some cases also bands and continuous spectrum) is then very conspicuous in the blue-green region of the spectrum. With a little practice the wave-lengths of the brightest modified lines can even be read off on the drum of a Hilger constant deviation spectrometer. Photographic study of the spectrum is, however, obviously the most convenient and accurate method for quantitative work, and indeed for the fainter lines the only method available.

The spectrograms reproduced with this paper (Plates XIII and XIV) were obtained with a Hilger E_2 quartz spectrograph, the reproductions being enlarged about twice from the original negatives. When sufficiently sensitive plates, *e.g.*, Ilford Iso-Zenith, are used, an exposure of a few hours is sufficient to obtain a fairly good spectrogram. In order, however, to obtain the fainter details, exposures of twelve or twenty four hours are desirable. As the quartz mercury lamp runs without attention, very long exposures can be given without any trouble or fatigue.

Usually the spectrograms are taken with the complete light from the mercury arc incident within the liquid. As the glass dome and condenser of the lamp cut out the extreme

ultraviolet, the incident radiation extends from about 3400 A. U. towards longer wave-lengths. Owing to the operation of the Rayleigh λ^{-4} law, the longer wave-lengths (except the most intense lines) are practically suppressed in the classical or unmodified scattering, and hence the numerous lines present in the visible region of the spectrum of the mercury arc do not trouble us much. Indeed such of the brighter incident lines as appear in the scattered spectrum serve as a convenient scale of wave-lengths.

If it is desired to use instead of the whole incident spectrum, only selected lines as the radiation to be scattered, this is done by placing suitable filters between the lamp and the observation bulb. A fresh strong solution of quinine sulphate followed by a blue glass serves to cut out everything except the 4358 A. U. line and its close companions, from the incident spectrum. A Corning ultra-violet glass filter (G 586) by itself passes a narrow region of the spectrum including the group of three lines near 3650 A. U.

A solution of potassium permanganate passes the strong lines 4047 A. U. and 4358 A. U. and their close companions. A strong solution of cobalt sulphocyanate in water is also useful. It transmits the group of lines near 4047 A. U. and suppresses the other bright lines in the ultra-violet and visible regions of the spectrum.

3. *Experimental Results.*

Fig. 1 in Plate XIII gives the direct spectrum of the mercury arc in quartz, up to and including the two yellow lines, the exposure being such as to give a satisfactory picture in which the brightest lines are not heavily overexposed. Figs. 2, 3 and 4 are the scattered spectra of benzene, toluene and pentane respectively. The two yellow lines do not appear in them while the lines in the violet and ultra-violet are somewhat overexposed. This is a natural consequence of

the Rayleigh λ^{-4} law for the classical scattering. On comparing Fig. 1 with Figs. 2, 3 and 4, it will be seen that the latter contain a great many new lines not present in the direct spectrum of the mercury arc. These lines will be referred to in what follows as modified lines. It will be noticed their intensity is comparable with that of some of the weaker unmodified lines.

Fig. 7 in Plate XIV is another direct spectrum of the mercury arc reproduced for comparison with Figs. 8, 9 and 10 in the same plate, which are the scattered spectra from pentane, ethyl ether and methyl alcohol respectively. Fig. 11 in Plate XIV represents the scattered spectrum from distilled water and Fig. 12 the spectrum of the incident light for comparison with it. (A violet filter had been used in the incident light which cut off the lines in the blue, green and yellow regions of the incident spectrum.)

Figs. 5 and 6 in Plate XIII are of special interest. Fig. 5 represents the spectrum of the mercury arc filtered through quinine sulphate solution and a blue glass, which transmit only the 4358·3 A. U. line and its close companions (the two feeble lines of shorter wave-length appearing to the left of it are due to stray light). Fig. 6 is the spectrum of the light thus filtered after being scattered by benzene liquid.

4. *Qualitative Study of the Spectra.*

A general scrutiny of the spectrograms reproduced in Plates XIII and XIV brings out several features of interest and importance.

In the first place it is clear from an inter-comparison of Figs. 2 and 6 both of which represent the scattering by liquid benzene, that when the quinine filter suppresses the bright lines in the incident spectrum, of shorter wave-length than 4358·3 A. U., it also suppresses from the scattered spectrum many of the modified lines with wave-lengths both greater and

smaller than 4358·3 A. U. With a potassium permanganate filter instead of quinine sulphate, we have the 4047 line in addition to the 4358 line in the incident spectrum, and several of the modified scattered lines suppressed previously re-appear.[2] On the other hand Corning glass (G. 586) ultra-violet filter, which transmits the 3650 lines and cuts out the 4047 and 4358 groups from the incident light, also cuts out all the modified scattered lines which appear when either quinine sulphate or potassium permanganate filters[3] are used. *It is thus clear that each line in the incident spectrum generates its own modified radiations in the scattered spectrum, independently of the other lines.*

All the modified scattered radiations seen in the spectrograms are generated by the intense lines lying in the region from 3650 to 4358 A. U. of the incident spectrum. That incident lines of longer wave-length are not equally effective is not surprising. For even the classical scattering of such wave-lengths becomes very weak in consequence of the Rayleigh λ^{-4} law, and the modified scattering, if any, due to such wave-lengths may also be expected to be feeble. Further, even if there were such lines they could hardly be expected to appear on the plates, owing to the relative insensitiveness of the photographic plate used, in the green and yellow regions. A careful visual examination may perhaps reveal them, but the attempts so far made have not been successful with the liquids studied in the present paper. The dependence of the intensity of the modified scattered lines on the wave-length of the incident lines, is a subject for further experimental research.

On Fig. 6 of Plate XIII, the modified lines due to the incident 4358·3 A. U. line, are all of longer wave-length, except

[2] See Plate XII. Figs. 3 and 4 reproduced in the address on "A New Radiation," Ind. Jour. Phys., vol. 2, part 3, facing p. 396.

[3] A spectrogram of the scattering by liquid benzene, with the Corning glass filter in the incident light, has been obtained, but is not reproduced in the present paper.

one, which appears feebly but quite clearly in the original negative, but is perhaps not visible in the reproductions. The existence of this line proves in a perfectly unmistakable way that *while a degradation of frequency is by far the most probable effect in light-scattering, an enhancement of frequency may also occur*. We shall have more to say about this line later on.

5. *Relation of Modified Scattering to Chemical Constitution.*

An inter-comparison of Figs. 2, 3, 4, 8, 9, 10 and 11 in the Plates shows in a striking way the manner in which the chemical constitution of the molecule influences the modified scattering. It is clear that each chemical substance has its own special type of modified scattering, no two of the spectra being exactly alike. Nevertheless, certain general similarities are noticeable in the scattered spectra due to compounds having similar chemical characters. For instance, in Plate XIV, the brightest groups of lines in the scattered spectra of the three aliphatic compounds pentane, ethyl ether, and methyl alcohol, are in approximately the same positions, one group of lines appearing in the region 4076 A. U. to 4100 A. U., a second group in the region 4500 A. U. to 4600 A. U., and a third group (visually very bright, but only very faintly visible in the photographs) in the region 4900 A. U. to 5000 A. U. Comparing the scattered spectra of the two aromatic compounds benzene and toluene, we see that toluene gives many more lines than benzene, but that the lines due to toluene are less intense, some of the brighter lines due to benzene and toluene are in nearly identical positions, and these differ distinctly from the positions of the brighter groups of lines obtained with the aliphatic compounds. On the other hand, a close comparison of the spectra due to toluene and ether shows certain similarities evidently connected with the presence in both the compounds of the methyl group CH_3.

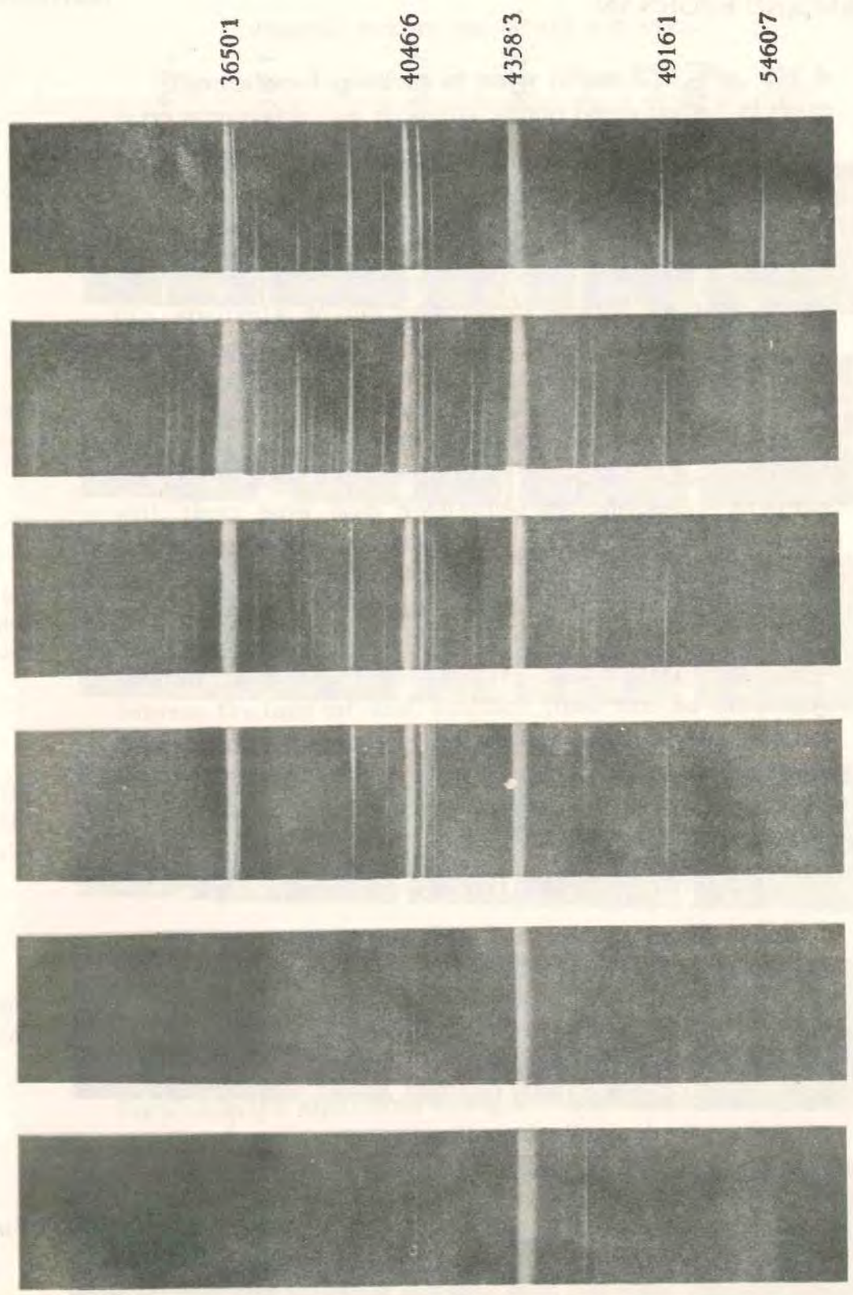

Fig 1

Fig 2
Benzene

Fig 3
Toluene

Fig 4
Pentane

Fig 5

Fig 6
Benzene

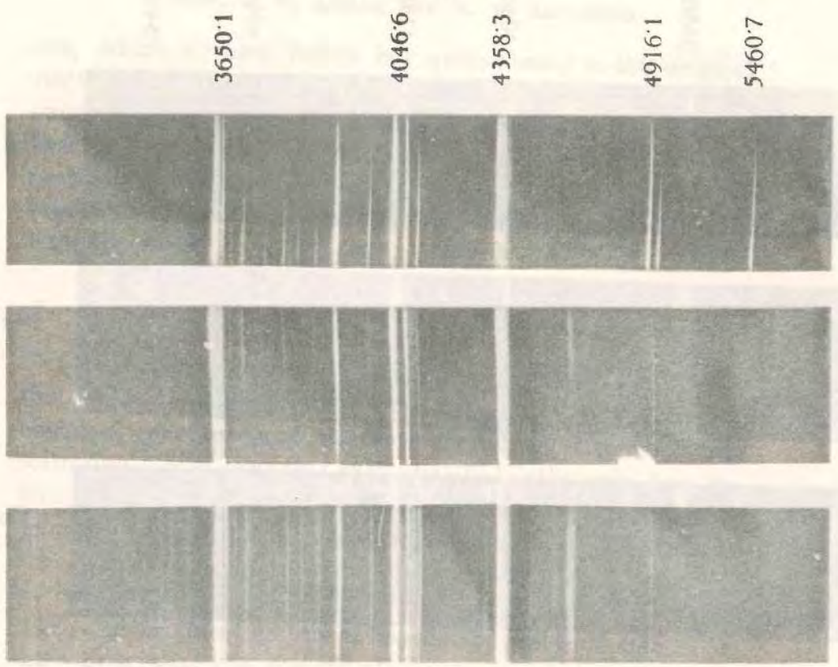

Fig 7

Fig 8
Pentane

Fig 9
Ethyl
Ether

Fig 10
Methyl
Alcohol

Fig 11
Water

Fig 12

The scattered spectrum of water (Plate XIV, Fig. 11) is very remarkable, as it shows bright bands instead of sharp lines. It is very interesting that methyl alcohol shows in addition to sharp lines, also diffuse bands, one of which is seen in Fig. 10, Plate XIV in the region 4100 A.D. to 4105 A.D., that is to say, in the same region as the first and brightest band obtained with water. We may presumably attribute this similarity to the presence in methyl alcohol, of the hydroxyl group OH.

Further discussion of the relationship between chemical constitution and the scattered spectra must evidently be postponed till a large number of compounds have been studied, and the positions and intensities of the modified lines observed with them have been determined and tabulated. Even the preliminary work described above, however, makes it clear that the scattered spectrum is practically a description in spectroscopic form, of the chemical constitution of the molecule. Since the lines are in many cases sharp and can therefore be very accurately measured, the frequency differences between the incident and modified lines can be accurately determined. The study of the scattered spectra thus promises to be of great importance for the future of chemistry as an exact science.

6. *Measurements of the Benzene Spectrum.*

The spectrum of the light scattered by liquid benzene, which is reproduced in Fig. 2 of Plate XIII, was measured with a Hilger travelling micrometer, and such of the lines appearing in it as were present in the direct spectrum of the mercury arc were located and identified by comparison with the photograph reproduced in Fig. I. From the known wave-lengths of the standard lines thus identified, the wave-lengths of the modified scattered lines appearing only in Fig. 2 and not in Fig. 1 were determined from the measurements, using

the Hartmann simplified interpolation formula. The wave-lengths of the modified scattered lines thus measured are probably accurate to 0·5 A. U. in the case of well-exposed lines, and to within 1·0 A. U. in the case of faint or diffuse lines. Greater accuracy should be possible if an iron arc be used as a comparison and the wave-lengths determined from the nearest standard lines by interpolation. The quartz spectrograph used provides in the blue region a dispersion of about 50 A. U. per mm. on the original negative. In view of the brightness and sharpness of the modified scattered lines, a dispersion much greater than this should prove useful and make a greater accuracy of measurement possible. The present work being of a preliminary nature, we have contented ourselves with determinations of wave-length to within 0·5 A. U. or 1·0 A. U. With the improvements mentioned above, a ten- or a hundred-fold increase of accuracy might well be hoped for.

TABLE I.

Spectrum of Benzene-Scattering.

Unmodified lines.			Modified lines.			Origin of the modified lines.	
Wave-length (in A.U.).	Wave number (in *vacuo* per cm.).	Intensity.	Wave-length (in A. U.).	Wave number (in *vacuo* per cm.).	Intensity.	Exciting lines (in A.U.).	Difference of wave numbers.
3341·5	29918	1					
3543·4	28213	3					
3561·7	28068	3					
3579·7	27927	0					
3598·0	27824	1 (Band)					
3615·8	27649	1					
3650·1	27389	100					
3654·8	27354	30					

TABLE I (*contd.*)

Spectrum of Benzene-Scattering.

Unmodified lines.			Modified lines.			Origin of the modified lines.	
Wave-length (in A. U.).	Wave number (in *vacuo* per cm.).	Intensity.	Wave-length (in A. U.).	Wave number (in *vacuo* per cm.).	Intensity.	Exciting lines (in A. U.).	Difference of wave numbers.
3663·3	27290	30					
3680·0	27166	3					
3704·3	26988	6					
			3732·8	26782	2	3650·1	607
			3737·7	26747	1	3654·8	607
			3746·6	26683	0	3663·3	607
3751·7	26647	5					
			3767·7	26534	0	3650·1	855
3771·0	26511	1					
			3787·1	26399	15	3650·1	990
3789·8	26379	10					
3801·7	26297	6					
			3813·4 imperfectly 3815·8	26216 resolved 26199	2 2	3650·1	1173
						3654·8	1155
3820·4	26168	5					
			3828·0	26116	0	3663·3	1174
3860·3	25897	5					
			3875·3	25797	1 (very broad)	3650·1	1592
			3891	25693	1	4046·6	−988
3895·3	25665	2					
3902·0	25621	6					
3906·5	25591	20					
3984·0	25098	8					
4046·6	24705	100					
4077·8	24516	30					
4108·9	24331	10					

TABLE I (*contd.*)

Spectrum of Benzene-Scattering.

Unmodified lines.			Modified lines.			Origin of the modified lines.	
Wave-length (in A. U.).	Wave number (in *vacuo* per cm.).	Intensity.	Wave-length (in A. U.).	Wave number (in *vacuo* per cm.).	Intensity.	Exciting lines (in A. U.).	Difference of wave numbers.
			4115·1	24294	3	3654·8	3060
			4125·1	24235	4	3663·3	3055
			4147·7	24103	1	4046·6	602
			4178·2	23927	0	4358·3	—989
			4190·6	23856	0	4046·6	849
			4215·5	23715	10	4046·6	990
			4248·8	23529	5	4077·8	987
						4046·6	1176
			4282·1	23346	0	4108·9	985
4339·2	23039	15					
4347·5	22995	30					
4358·3	22938	200					
			4476·4	22333	1	4358·3	605
			4525·8	22089	0	4358·3	849
			4543·3	22004	0	4347·5	991
			4554·9	21948	10	4358·3	990
			4593·6	21763	2	4358·3	1175
			4618·6	21646	10	4046·6	3059
			4658·9	21458	1	4077·8	3058
			4683·0	21348	1 (very broad)	4358·3	1590
4916·1	20336	5					
4960·4	20154	1					
			5029·6	19877	1	4358·3	3061
5460·7	18308	1					

TABLE II.

Spectrum of Benzene-Scattering.

(Only the 4358 A. U. group of lines were incident.)

Unmodified lines.			Modified lines.			Origin of the modified lines.	
Wave-length (in A. U.).	Wave number (in *vacuo* per cm.).	Intensity.	Wave-length (in A.U.).	Wave number (in *vacuo* per cm.).	Intensity.	Exciting line (in A. U.).	Difference of wave numbers.
			4178·5	23925	0	4358·3	—987
4339·2	23039	15					
4347·5	22995	30					
4358·3	22938	200					
			4476·4	22333	1	4358·3	605
			4524·3	22097	0	4358·3	841
			4534·5	22047	0	4339·2	992
			4543·4	22004	0	4347·5	991
			4555·1	21947	10	4358·3	991
			4593·9	21762	2	4358·3	1176
			4683·5	21346	1 (broad)	4358·3	1592
			5029·6	19877	1	4358·3	3061

TABLE III.

Analysis of the modified lines.

(The numbers within brackets give the relative intensities of the lines.)

	Shift of wave number of the modified lines.	Incident lines (in A. U.).	Shift of wave number of the modified lines.					
		3650·1 (100)	607 (2)	855 (0)	990 (15)	1173 (2)	1592 (1)	falls on an incident line 3060 (3)
		3654·8 (30)	607 (1)		falls on an incident line.	(?) 1155 (2)		
		3668·3 (30)	607 (0)		,,	1174 (0)		3055 (4)
	−988 (1)	4046·6 (100)	602 (1)	849 (0)	990 (10)	1176*		3059 (10)
		4077·8 (30)			987* (5)			3058 (1)
		4108·9 (10)			985 (0)			
		4339·2 (15)						
		4347·5 (30)			991 (0)			
	−989 (0)	4358·3 (200)	605 (1)	849 (0)	990 (10)	1175 (2)	1590 (1)	3061 (1)
		4339·2 (15)			99[illegible] (0)			
		4347·5 (30)			9[illegible] (0)			
	−987 (0)	4358·3 (200)	605 (1)	841 (0)	991 (10)	1175 (2)	1592 (1)	3061 (1)
Mean shift of wave number.	−988		606	849	990	1176	1591	3059
Wave-lengths corresponding to the frequency of the shifts.	10·13μ		16·50μ	11·78 μ	10·10μ	8·57μ	6·28μ	3·268μ

* The two modified lines marked with * coincide in position.

SPECTRA DUE TO SECONDARY RADIATION

In Table I, the wave-lengths of the lines in the scattered spectrum of benzene have been separated into two classes and shown under the headings "Unmodified lines" and "Modified lines" respectively, the former being the original lines present in the incident spectrum and the latter the additional lines present only in the scattered spectrum. Under the heading "Origin of the modified lines" are indicated the wave-length of the incident line which gives rise to each modified line, and the difference in wave number between the incident and the modified lines in question. The identification of the exciting line corresponding to each modified line is assisted and confirmed by observations and photographs with light-filters placed in the path of the incident light.

In Table II are shown the wave-lengths of the modified lines excited when only the 4358·3 A. U. line and its close companions are present in the incident spectrum.

In Table III is given an analysis of the data given in Tables I and II; against each of the strong lines present in the mercury arc spectrum, are shown the differences in wave-number between it and the modified lines to which it gives rise.

7. *Interpretation of Results.*

From the analysis of the measurements given in Table III several striking results emerge.

The first and most significant result is that the shift of the modified line with respect to the exciting line (measured in wave-numbers) is independent of the frequency of the exciting line. This is shown by the fact that the shift is the same for all exciting lines, within the limits of error in measurement.

The second most significant result is that very similar groups of lines are generated by each incident line in the spectrum. This is shown by the fact that for each incident

line, modified lines are to be found in known positions relative to it, or else, if they are absent, an adequate explanation is forthcoming, *e.g.*, insufficient intensity of the incident line, or of the modified line, or of both, or else the obscuration of a modified line by strong lines in the incident spectrum.

Thirdly, the order of the relative intensities within each group of modified lines appears to depend but little on the frequency of the line which excites the group. The shifts of +990 and of 3059 in wave-number give rise to the brightest modified lines in every case.

A fourth and most interesting result is that while most of the modified lines are *degraded* in frequency relatively to the exciting lines, an *enhancement* of frequency is also possible, though such modified line of enhanced frequency is usually of extremely low intensity. Further the *enhancement* of frequency of such line is equal to the *degradation* of frequency of another modified line. This is shown by the identity in magnitude (within the limits of accuracy of measurements) of the shifts of opposite signs shown in the first and fifth columns of Table III.

A fifth and rather curious result, which is probably not an accident, is that one of the shifts in wave-number (1591) is approximately the sum of two others (606+990=1596). It may be significant to note that the modified lines showing this shift appear distinctly more diffuse on the plate than other modified lines.

8. *Origin of the Modified Spectrum.*

The results set out above definitely prove the correctness of the explanation of the new type of secondary radiation advanced by one of us previously,* namely, that the incident quantum of radiation is partly absorbed and partly scattered

* Ind. Jour. Phys., vol. 2, part 3, p. 395, 1928.

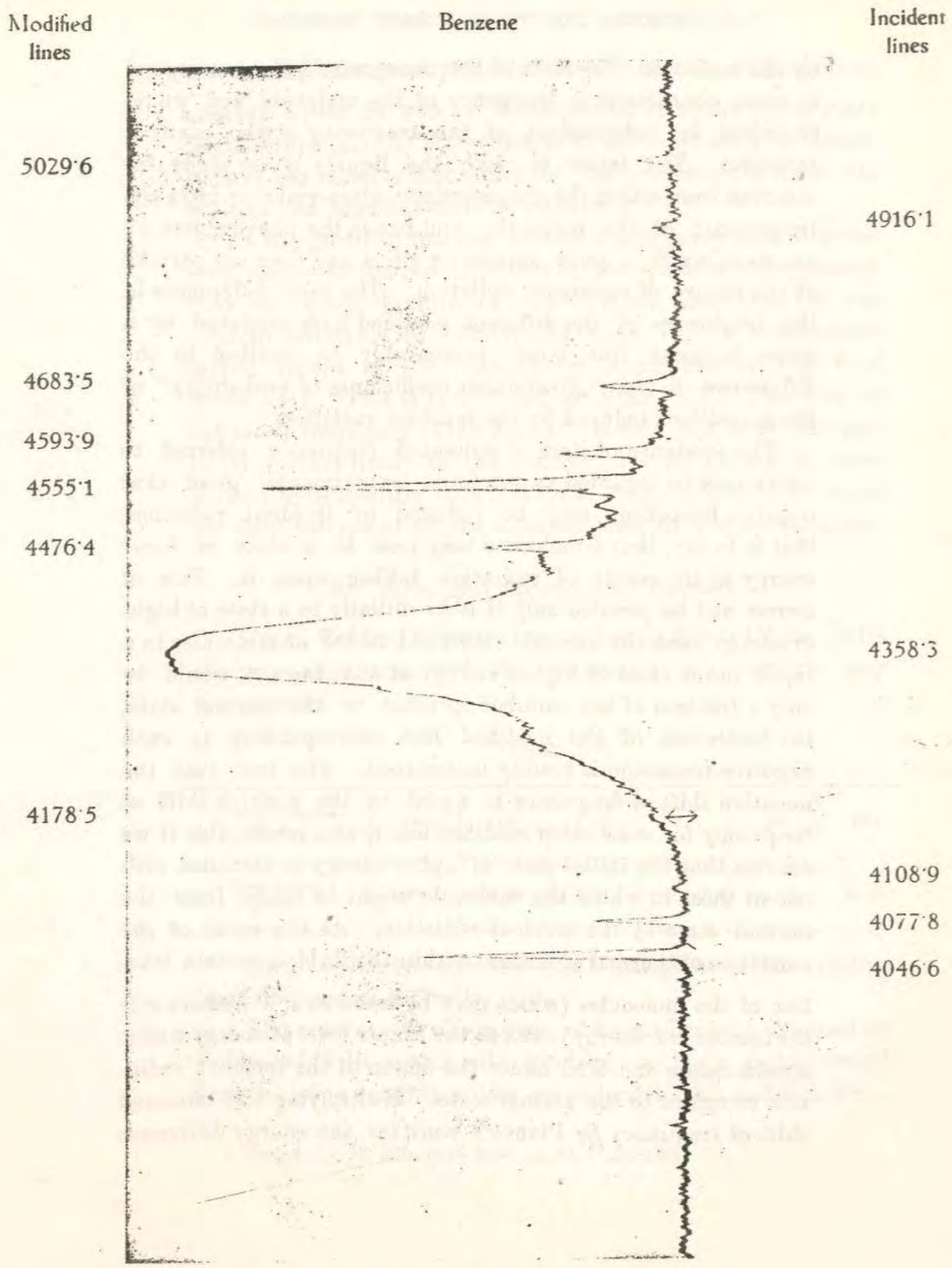

Microphotometered Spectrum of Scattering

by the molecule. The shift of frequency would then correspond to some characteristic frequency of the molecule and would therefore be independent of the frequency of the exciting radiation. The latter is, with the liquids under study, far removed from either the characteristic ultra-violet or infra-red frequencies of the molecule, and hence the phenomenon we are studying is a pure scattering effect and does not partake of the nature of resonance radiation. The great differences in the brightness of the different modified lines produced by a given incident line must presumably be ascribed to the differences in the "Einsteinian coefficients of probability" of the transitions induced by the incident radiation.

The existence of lines of enhanced frequency referred to above may be regarded as a definite experimental proof that *negative* transitions may be induced by incident radiation, that is to say, that a molecule may pass to a state of *lower* energy as the result of radiation falling upon it. This of course will be possible only if it be initially in a state of higher energy than the normal. As the number of molecules in a liquid in the state of higher energy at any instant would be only a fraction of the number present in the normal state, the feebleness of the modified line corresponding to such negative transition is readily understood. The fact that the negative shift of frequency is equal to the positive shift of frequency for some other modified line is also intelligible if we assume that the initial state of higher energy is identical with one of those to which the molecule might be raised from the normal state by the incident radiation. As the result of the existence of thermal agitation within the fluid, a certain fraction of the molecules (which may be taken as $e^{-\frac{w}{kT}}$, where w is the increase of energy) exist in the higher level of energy under consideration and tend under the action of the incident radiation to return to the normal state. Multiplying the observed shift of frequency by Planck's constant, the energy difference

w is readily calculated. Thus corresponding to a shift of wave number equal to 990, $e^{-\frac{w}{kT}}$ comes out as about $\frac{1}{120}$ at room temperature (*viz.* 30°*c.*), which is of the same order of magnitude as the relative intensities of the two modified lines with positive and negative shift of frequency.

As the modified lines of enhanced frequency do not appear very clearly in the reproductions of the spectrograms (though they are quite definite in the original negatives) it was thought advisable to exhibit the same with a microphotometric record of the spectrogram appearing as Fig. 6 of Plate XIII. This is reproduced as Plate XV. The line of enhanced frequency (4178·5 A. U.) is seen as a small but perfectly distinct hump in the record. Its feebleness in comparison with the line 4554·9 is quite evident, the latter being the most intense of all the modified lines in the spectrogram.

9. *Infra-Red Spectrum of Benzene.*

From Table III we extract below in Table IV the shifts of wave-numbers, and the wave-lengths to which they correspond.

TABLE IV.

Shift of wave-number.	3059	1591	1175	990	849	606
Wave-length (in μ).	3·268*	6·28	8·51	10·10*	11·78	16·50

Of these the two marked with a star give us the shifted lines of greatest intensity.

The curves of absorption of liquid benzene obtained by Coblentz[5] with a rock-salt spectroscope show rather broad troughs lying roughly at the wave-lengths 3·3 μ, 5·5 μ, 6·8 μ,

[5] Quoted by J. W. Ellis, Phys. Rev., vol. 27, p. 305, 1926.

8.7 μ, 9·9 μ and 11·9 μ, the most prominent of these being the one at 9·9 μ. Bell[6] gives an absorption curve for benzene obtained with his infra-red spectrometer in which a series of absorptions appear at 3·3 μ, 5.1 μ, 5·5 μ, 6·2 μ, 6·7 μ, 7·2 μ, 8·5 μ, 9·7 to 10·2 μ and 11·8 μ respectively. Of these the absorption at 3·3 μ is the sharpest and most prominent and may be certainly identified with the 3·268 μ shown in Table IV. The absorptions at 8·5 μ and 11·8 μ are also very prominent and have wave-lengths agreeing very closely with those shown in Table IV. The absorption between 9·7 μ and 10·2 μ, forms a very prominent feature. We may reasonably identify it with our wave-length 10·10 μ. In Bell's curve for benzene, the absorption at 6·2 μ is more shallow than that at 6·7 μ; but he points out that the absorption band at 6·2 μ is prominently shown by certain benzene derivatives such as aniline, and it is therefore not surprising to find the wave-length 6·28 μ, with which it may be identified, appearing in our Table IV, and not 6·7 μ. The absorptions at 5·1 μ, 5·5 μ and 7·2 μ also fail to appear in our Table IV. The reason for this is yet to be found.

From the foregoing comparison, it is clear that the wave-lengths appearing in Table IV correspond to certain fundamental frequencies of absorption of light by the benzene molecule. *Further it is evident that the shift of the modified lines in scattering by liquids, furnishes us with an extremely accurate method of determining these fundamental infra-red frequencies of the molecule*, and of the changes produced in it by varying the chemical constitution.

Attempts have been made by Ellis, Andrews and others to identify the infra-red frequencies of the molecule with the frequencies of relative oscillation of the chemically bonded atoms in the molecule. For instance, Bates and Andrews[7]

[6] F. K. Bell, Jour. Amer. Chem. Soc., vol. 57, p. 2814, 1925.

[7] J. R. Bates and D. H. Andrews, Proc. Nat. Acad. Sciences, Washington, vol. 14, p. 128, Feb. 1928.

identify the wave-lengths 3·3 μ and 9·9 μ respectively with the oscillations of the hydrogen-carbon bond, and the carbon-carbon bond, in benzene, and the latter[8] has even attempted to calculate the specific heat of liquids on the basis of certain assumed fundamental frequencies of vibration of the molecule. The relation between the modified scattering of light and the structure of the molecule, and specially its bearings on Franck's[9] recent work on photochemical decomposition will form the subject of a separate paper.

10. *Summary and Conclusion.*

(*a*) The paper concerns itself with a new class of spectra observed when light from a quartz mercury lamp is diffused within a liquid and the scattered light is spectroscopically analysed. A large number of new lines are observed in the scattered spectrum which are not present in the incident spectrum.

(*b*) The scattered spectra from benzene, toluene, pentane, ether, methyl alcohol and water have been photographed.

(*c*) Each liquid shows a distinctive scattered spectrum, but certain general similarities are exhibited by liquids having chemically similar groups in their composition.

(*d*) The scattered spectrum of benzene has been measured and analysed. From the measurements and also from special spectrograms obtained with single-line filters in the path of the incident light, it is shown that corresponding to each unmodified line in the spectrum there are seven modified lines observable, of which two are specially prominent. The frequency differences between the unmodified and modified lines are independent of the wave-length of the incident lines.

[8] D. H. Andrews, Proc. Roy. Acad., Amsterdam, vol. 29, p. 744, 1926.

[9] J. Franck, Trans. Farad. Soc., vol. 21, p. 536, 1925.

(*e*) Six out of the seven in the group of modified lines have frequencies lower than that of the exciting line while one has a higher frequency, the increase of wave number being numerically the same for it as the decrease of wave-number for one of the six lines of degraded frequency.

(*f*) The shift of frequency of the modified lines is found to agree with certain characteristic infra-red frequencies of the molecule and in fact the method is capable of yielding extremely accurate measurements of these frequencies.

(*g*) The observations are explicable on the supposition that the incident quantum of radiation may be absorbed in part and scattered in part by the molecule. If the molecule is initially in the normal state, the transition induced by the radiation must naturally be to a higher level of energy, and hence the scattered radiation will have a degraded frequency. But if the molecule is initially in a level of energy higher than the normal, the radiation will induce a return to the normal level, and in this case we get a modified scattered radiation of higher frequency than the incident. The possibility of such negative transitions induced by radiation is proved by the observations. The comparative feebleness of the modified line of higher frequency is readily explained on a thermodynamic basis.

We have much pleasure in acknowledging the valuable assistance received from Mr. S. Venkateswaran in the course of the experiments described in this paper.

The Negative Absorption of Radiation.

In Einstein's celebrated derivation of the Planck radiation formula, an equilibrium is considered to exist between three elementary processes: (1) a spontaneous emission from the atoms, (2) an absorption of energy by the atoms proportional to the energy density in the field, and (3) an induced emission of energy from the atoms, also proportional to the energy density. The third process can be described as a negative absorption of radiation, and is quite characteristic for Einstein's theory, as the omission of it from the equations leads to Wien's radiation formula instead of to Planck's. The negative absorption of radiation also figures prominently in the Kramers-Heisenberg theory of dispersion. The physical existence of such absorption has been up to now an article of faith rather than a proved experimental fact, and indeed some writers (Ornstein and Burger, S. N. Bose) have been tempted to question its reality.

A definite experimental proof is now forthcoming of the reality of negative absorption. We have discovered (Nature, April 21, 1928, p. 619) that when a liquid, for example, benzene, is irradiated by monochromatic light, the radiation scattered by the molecules contains several spectral lines of modified frequencies. Careful measurements have shown that the difference between the incident and scattered frequencies is exactly equal to an infra-red frequency of the molecule, so that the process of modified scattering involves the absorption of radiation by the molecule. As the molecule has several characteristic infra-red frequencies, we have an equal number of modified scattered lines. This is seen in the photograph reproduced in Fig. 1, which is from a spectrogram of the scattering by liquid benzene, of the light of the mercury arc from which practically everything except the 4358 A. group of lines had been filtered out. In the spectrogram, the wave-lengths in the incident radiation are marked in A., and the modified scattered lines are indicated by arrowheads. (It may be mentioned in passing that the benzene had not been completely purified, hence a marked continuous spectrum is also present in the modified scattering.) The brightest modified lines are of longer wave-length than 4358 A., and their frequencies are determined by the infra-red absorption lines at 16·55 μ, 11·78 μ, 10·10 μ, 8·51 μ, 6·27 μ, and 3·267 μ. (These wave-lengths can be determined more accurately in this way than with an infra-red spectrometer.)

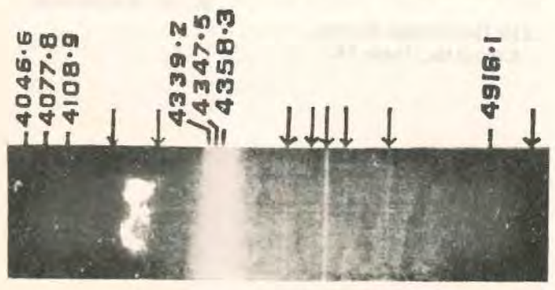

Fig. 1.

An inspection of the actual spectrogram, however, shows two modified lines of shorter wave-length than the exciting 4358·3 line, and the measurements show that their frequencies *exceed* that of the latter by the infra-red frequencies of the molecule, namely, those corresponding to 16·55 μ and 10·10 μ respectively. The presence of these lines proves simultaneously the existence in the liquid of molecules at levels of energy correspondingly higher than the normal, and the fact that the incident radiation induces a return to a lower state of energy; in other words, that there is a negative absorption of the radiation. The feebleness of the modified line of enhanced frequency, in relation to the modified line of degraded frequency, is consistent with the supposition that the transitions in either direction are equally probable, if we take into account the fact that the proportion of molecules in the liquid in a higher level of energy than the normal is small at the ordinary temperatures.

C. V. Raman.
K. S. Krishnan.

210 Bowbazar Street,
Calcutta,
May 15.

Polarisation of Scattered Light-quanta.

It is well known from the work of Barkla, Compton, and others that X-rays scattered through 90° by matter are completely polarised, irrespective of whether the electron remains bound or suffers ejection from the atom as the result of the impact of the quantum upon it. The recent discovery of a new type of light scattering with altered frequency (Nature, May 5, p. 711) makes it of importance to ascertain whether a light-quantum which is scattered with diminished energy is less perfectly polarised than in the ordinary case.

We have investigated this question with several liquids by analysing the scattered light with a spectrograph having a suitably orientated Nicol placed in front of its slit. The results obtained are extraordinarily interesting, as will be seen from Fig. 1. Fig. 1 (*b*) represents the spectrum of the incident light from the mercury arc. Fig. 1 (*a*) represents the spectrum of the scattered light from liquid benzene,

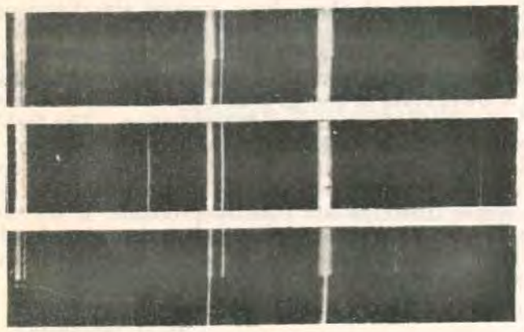

Fig. 1.

the upper and lower halves of the spectrogram corresponding respectively to the two principal directions of vibration. It is seen that some of the new lines which appear only in the scattered spectrum are actually polarised much more completely than the lines present in the incident spectrum. Further, the degree of polarisation varies greatly from line to line, some of the new lines being strongly polarised, others only very partially so. So large are the differences in polarisation that the relative intensity of the lines is quite different in the upper and lower halves of the spectrogram. In the case of amyl alcohol as well (Fig. 1 (*c*)) the new lines in the scattered spectrum are polarised to varying extents, and the continuous radiation appearing in it is also partially polarised.

The strong polarisation of the modified light scattering is intelligible in view of the analogy with the Compton effect. Since the different modified lines represent different electronic transitions induced in the molecule by the incident radiation, the varying extents of their polarisation may be interpreted as due to the optical anisotropy of the molecule being very different for different types of deformation. That some of the intense modified lines are polarised even more strongly than the unmodified lines need not occasion surprise, if we remember that the classical light scattering in a liquid is much less perfectly polarised than the scattering by the molecules of the corresponding vapour. If we assume that the modified scattering is an incoherent type of radiation, we should expect its intensity to be proportional to the density of the fluid, and its polarisation to be comparable with that of the classical scattering in the corresponding *vapour* (not liquid). These expectations appear to be not very far from the truth.

C. V. Raman.
K. S. Krishnan.

210 Bowbazar Street,
Calcutta, June 14.

Molecular Spectra in the Extreme Infra-Red.

The appearance in the spectrum of monochromatic light diffused by fluids, of new lines of modified frequency (*Ind. Jour. Phys.*, vol. 2, pp. 387 and 399; 1928), gives us a powerful, accurate, and convenient method of exploring molecular spectra, especially in the near and extreme infra-red regions. We have only to photograph the spectrum of the

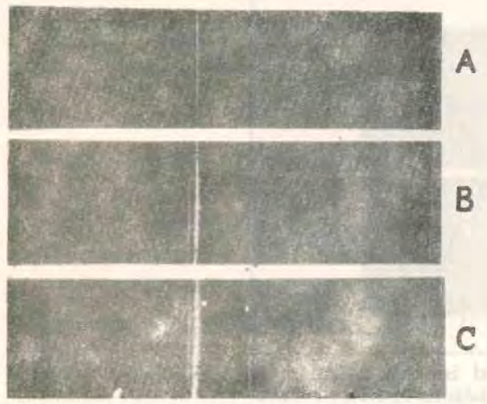

Fig. 1.

scattered light, and the frequency-differences between the incident light and the new radiations excited by it give us the molecular frequencies. As an illustration of what the method is capable of, we may mention the case of carbon tetrachloride, the spectrum of the mercury arc scattered by which is reproduced as Fig. 1 B, 1 A being the incident spectrum. The 4358 A. line, which is the principal exciter, is accompanied by three sharp lines close to it on the right, from which we deduce 45·4 μ, 31·8 μ, and 21·7 μ as wave-lengths of three hitherto unknown infra-red lines in the spectrum of the carbon tetrachloride molecule. In addition, we have a doublet 13·0 μ and 12·6 μ, the position of which as an unresolved line was approximately known from the work of Coblentz.

Fig. 1 C shows the nebulosity or continuous spectrum accompanying the 4358 line when it is scattered by benzene. The existence of a continuous radiation accompanying the lines and bands in the scattered spectrum from liquids has been pointed out by us earlier and is indeed visible in our published photographs. Its natural explanation would appear to be that it arises from a combination of the rotational frequencies of the molecule with the frequencies of the incident or scattered radiations, the impedance to the free rotation of the molecules in a dense fluid being the reason why such combination results in a continuous spectrum instead of discrete lines. The unmodified lines being the strongest, the nebulosity accompanying them appears very conspicuous. Incidentally, with reference to a recent interesting paper by Cabannes and Daure (*Comptes rendus*, June 4, 1928), we may direct attention to the distinctly imperfect symmetry of the nebulosity on the two sides of the 4358 line appearing in Fig. 1 C.

C. V. Raman.
K. S. Krishnan.

210 Bowbazar Street,
Calcutta, July 5.

The Raman Effect in Crystals.

THE thermal agitation of the atoms in solids results, as was shown by Raman (NATURE, Jan. 12, 1922, and Jan. 6, 1923), in a noticeable blue opalescence in the interior of such transparent crystals as quartz or ice when they are traversed by a strong beam of sunlight. In his address on the discovery of a new type of secondary radiation (*Indian Journal of Physics*, Mar. 31, 1928) Raman described observations showing that

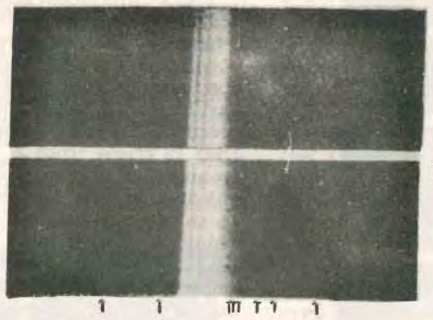

Fig. 1.

Fig. 2.

monochromatic light scattered in this manner by crystals is accompanied by radiations of altered wave-length in the same way as in the case of gases and liquids. The difference between the incident and scattered frequencies corresponds, of course, to a characteristic infra-red frequency of the crystal.

Some of the frequencies revealed in this way correspond to infra-red radiations of much greater wave-length than those known previously from the work of Rubens and others on the *rest-strahlen* from crystals. Fig. 1 represents the incident radiation (the 4358 A. group of the mercury arc), and Fig. 2 the spectrum of the light scattered in quartz, where the positions of the new lines are marked by arrow heads.

The wave-lengths of the longest radiations from quartz determined from these and other photographs are 118μ, 94μ, 78μ, 48·5μ, 37·4μ, and 21·5μ. Some of these have been overlooked by Landsberg and Mandelstam (*Comptes rendus*, July 9, 1928) and by I. R. Rao (*Ind. Jour. Phys.*, vol. 3, part I., August 1928), who have recently studied the Raman effect in quartz, apparently owing to the insufficient resolving power of their instruments.

K. S. KRISHNAN.

210 Bowbazar Street,
Calcutta, Aug. 16.

Influence of Temperature on the Raman Effect.

As has been emphasised by Prof. Pringsheim in his recent admirable report on the Raman effect (*Die Naturwissenschaften*, Aug. 3, 1928), there is a far-reaching and fundamental analogy between the be-

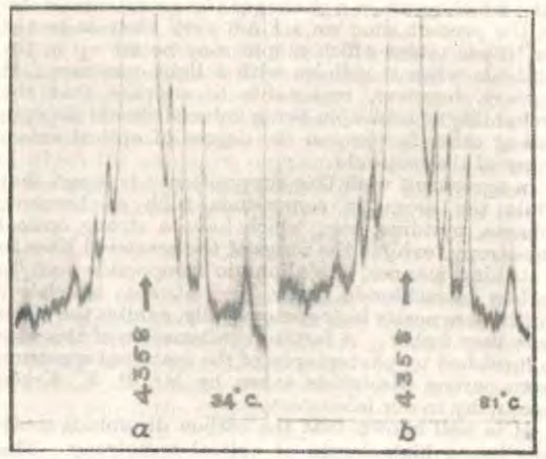

FIG. 1.

haviour of electrons and of light quanta during their collisions with material particles. The new lines appearing in the spectrum of the scattered light are the result of inelastic collisions or of super-elastic collisions of the light quanta with the molecules of the medium, according as the shift of frequency is towards longer or shorter wave-lengths. As has already been pointed out in an earlier communication (NATURE, July 7, 1928, p. 12), the lines with enhanced frequencies are usually of much smaller intensity than those degraded in frequency to an equal extent. The natural explanation of this is that comparatively few molecules are normally present in an excited state and therefore in a position to communicate energy to the light quantum. As the temperature rises, we should expect the number of such molecules to increase, and the proportion of super-elastic to inelastic collisions to rise *pari passu*.

The case of carbon tetrachloride is very suitable for an experimental test of this point, as there are numerous Raman lines with relatively small shifts of frequency in its scattered spectrum. I have made experiments which confirm this theoretical expectation. Figs. 1*a* and 1*b* are microphotometric records of the Raman spectrum of carbon tetrachloride excited by the 4358 group of the mercury arc, the former being taken at 34° C. and the latter at 81° C. It will be seen that the lines of higher frequency (towards the left) increase in intensity and those of lower frequency (towards the right) decrease in intensity when the temperature is raised.

K. S. KRISHNAN.

210 Bowbazar Street,
Calcutta, Sept. 6.

Rotation of Molecules induced by Light.

IN an earlier note to NATURE (Aug. 25, p. 278) we ventured to suggest that the nebulosity or wings which accompany the original lines of the mercury arc after scattering in benzene liquid, are the effect of those collisions of the incident light-quanta with the molecules which result in a change of their rotational state. At the present time we are not very clear as to the conditions under which a spin may be set up in the molecule when it collides with a light-quantum. It appears, however, reasonable to suppose that the probability of such spin being induced should depend, among other factors, on the degree of optical anisotropy of the molecule.

In agreement with this supposition it is found that while the aromatic compounds such as benzene, toluene, pyridine, etc., which have a strong optical anisotropy, exhibit the wings of the scattered lines in a striking manner, the aliphatic compounds such as carbon tetrachloride, ether, alcohol, etc., which are much more nearly isotropic optically, exhibit the effect only very feebly. A further confirmation of this idea is furnished by photographs of the scattered spectrum from carbon disulphide taken by Mr. P. V. Krishnamurthy in our laboratory.

It is well known that the carbon disulphide molecule has a high degree of optical anisotropy. The photographs show, as expected, besides some displaced lines, also strong wings accompanying the original lines of the mercury arc. Incidentally, we may mention that the wings appear to consist of unpolarised light.

C. V. RAMAN.
K. S. KRISHNAN.

210 Bowbazar Street,
Calcutta, Oct. 18.

The Raman Effect in X-ray Scattering.

THAT a quantum of radiation can be absorbed in part by an atomic system, and the remaining part scattered by it giving rise to a radiation of increased wave-length, has been demonstrated by recent work on the scattering of light in material media. In his address on "A New Radiation" (*Ind. Jour. Phys.*, vol. 2, p. 398, Mar. 31, 1928) Raman pointed out that precisely similar effects should also be observable in the case of X-ray scattering. In other words, in addition to the Compton type, we should also have other modified X-radiations scattered by the atom, in which the scattering electrons alter their positions in the atom, but remain bound to it. The frequencies of the radiations scattered by the atom would be

$$\nu' = \nu - \frac{E_l - E_k}{h},$$

where ν is the incident frequency, E_k is the energy of the initial level and E_l of the final level of the electron. When E_l is positive, it may have an arbitrary value, and, as has been shown by Wentzel and others, the scattered radiation is of the Compton type, in which the change of wave-length depends on the direction of observation. On the other hand, when E_l is negative, the electron remains bound to the atom, and we have a type of X-ray scattering completely analogous to that observed in the optical case. The frequency of the Raman type of X-ray scattering is independent of direction and is as sharply defined as that of the unmodified radiation.

Experiments to observe the new type of X-ray scattering here indicated have been in progress at Calcutta for some time. Meanwhile, results have been reported by Bergen Davis and Dana Mitchell (*Phys. Rev.*, vol. 32, p. 331 ; 1928) which may be regarded as a demonstration of its existence. Studying the scattered radiation from graphite excited by molybdenum Ka_1, they found three new lines the frequencies of which differed from that of the incident radiation by amounts corresponding to changes of energy level of the scattering electron by 279, 57, and 34 volts respectively. The first and the last may be identified with the transition of an electron from the K and L_1 levels respectively, to a level of very loose binding to the carbon atom. The radiation corresponding to a change of energy of 57 volts may be identified with the case in which both the L_1 electrons are shifted outwards. The latter supposition is not unreasonable in view of the well-known existence of double excitation in connexion with spark lines in the X-ray region of the spectrum.

K. S. KRISHNAN.

210 Bowbazar Street,
Calcutta, Oct. 25.

28.5.2025

Date:

MR. **or MS.** MANJU SHARMA

Adress: N.P.L. Library. PUSA.
64. Sangam Apartment. P. Vihar. N.D. 87

Email: Manju061@gmail.com.

REPRESENTATION

Subject: Re-fixation of pay under the 6th Central Pay Commission in terms of the CSIR O.M. No. 17/66/94-PP3 dated 23.05.2006 and final order dated 25.04.2017 of the Hon'ble High Court of Madras in *S. Stephenson & Ors.* v. *CECRI & Ors.* and *S.P. Kartikeyan* v. *Director, CECRI & Ors.*, being W.P. Nos. 34120-34121/2015 and having attained finality *vide* orders dated 04.07.2019, 19.11.2019, and 19.05.2022 of the Hon'ble Supreme Court of India in SLP (C) Diary No. 20493/2019, Review Petition (C) No. 35580/2019 and Curative Petition (C) No. 97/2021

Dear Ma'am/Sir,

1. By way of the present Representation, I request re-fixation of pay such that the benefits granted under the 6th Central Pay Commission *vide* the final order dated 25.04.2017 of the Hon'ble High Court of Madras in *S. Stephenson & Ors.* v. *CECRI & Ors.* and *S.P. Kartikeyan* v. *Director, CECRI & Ors.*, being W.P.Nos.34120-34121/2015 and having attained finality *vide* orders dated 04.07.2019, 19.11.2019, and 19.05.2022 of the Hon'ble Supreme Court of India in SLP (C) Diary No. 20493/2019, Review Petition (C) No. 35580/2019 and Curative Petition (C) No. 97/2021 to other similarly-placed employees of the CSIR are extended to me. In this regard, I draw your attention to certain orders of the Hon'ble Central Administrative Tribunal ("CAT"):

   a) Order dated 28.03.2023 in O.A. No. 3641/2022 before the Hon'ble CAT, Principal Bench titled *Harinder Pal Singh v. Dr. (Mrs.) N. Kalaiselvi*;
   b) Order dated 05.07.2023 in O.A. No. 3603/2022 before the Hon'ble CAT, Chandigarh Bench titled *Asha Rani v. Director, CSIO & Ors*;
   c) Order dated 07.08.2023 in O.A. No. 1844/2023 before the Hon'ble CAT, Principal Bench titled *Tapas Kumar Sahoo v. Union of India & Ors.*

28/05/25

O.A. Nos. 890-891/2011 before the Hon'ble CAT, Chennai Bench, *vide* the aforesaid final order of the Hon'ble High Court of Madras.

5. Accordingly, you are hereby called upon to:

- Re-fix my pay in order to extend the benefit of Grade Pay of ₹4600 in Pay Band-2 as per the recommendations of the 6th Central Pay Commission with effect from 01.01.2006 in terms of the final order of the Hon'ble High Court of Madras dated 25.04.2017 in W.P. Nos. 34120-34121/2015, such that my minimum basic pay as of 01.01.2006 is ₹17,140, and pay arrears accruing consequent upon such re-fixation; and
- Grant all consequential benefits and adjustments due on account of promotion and/or other related service events.

Sincerely,

Manju
28/5/25

Manju Sharma

The Production of New Radiations by Light Scattering.—Part I.

By Prof. C. V. Raman, F.R.S., and K. S. Krishnan.

(Received August 7, 1928.)

(Plates 1, 2.)

1. *Introduction.*

In two preliminary papers* we have recorded the discovery that when monochromatic light is scattered in a transparent medium (be it gas, vapour, liquid, amorphous solid or crystal), the diffused radiation ceases to be monochromatic, and several new lines or sometimes bands (associated in many cases with a continuous spectrum) appear in the spectrograms of the diffused radiation. Further, the new radiations are, in general, strongly polarised. That the phenomenon is entirely distinct from what is usually known as fluorescence is clear from the fact that the effect is observed when both the exciting radiation and the new radiations generated by it are far removed from the characteristic ultra-violet and infra-red frequencies of the medium. As an illustration we may mention the case of transparent crystalline quartz in which the effect is very well shown with the 4358 A.U. line of mercury as the exciting line, the new lines also appearing in the indigo-blue region of the spectrum. Our preliminary studies have proved conclusively that the effect arises in the following way: The incident quantum of radiation is either scattered as a whole, in which case we have the classical scattering, or else is absorbed in part by the molecules of the medium, the remaining part appearing as a scattered quantum. The part absorbed shifts the molecule to a level of energy

* Raman, 'Ind. J. Phys.,' vol. 2, p. 387 (1928); Raman and Krishnan, 'Ind. J. Phys.,' vol. 2, p. 399 (1928).

different from the initial state. The possibility of a process of this kind, in respect of the electronic state of an atom, was first contemplated by Smekal,* and figures prominently in the theory of dispersion due to Kramers and Heisenberg,† and in the papers of Schrödinger.‡ Our experiments furnish definite proof of the possibility of such processes, and show that they may occur also in such complicated systems as the molecules of a vapour or a liquid or even in a complete crystal. In the series of papers of which this is the first our further studies of the new radiations will be discussed.

2. *Experimental Methods.*

The experimental arrangements were exactly the same as those described in the previous papers. The liquids to be examined were rendered dust-free in the usual manner by repeated slow distillation *in vacuo*, and the final distillate was contained in a bulb of about 500 to 600 c.c. capacity. A 3000-c.p. mercury arc served as the source of monochromatic illumination and was concentrated with an 8-inch condenser, at the centre of the liquid bulb, which was kept immersed in a suitably blackened glass tank containing water. By interposing a strong solution of quinine sulphate and a plate of blue glass between the condenser and the liquid, practically all the lines of the incident mercury spectrum excepting the 4358·3 line and its close companions were cut out. In the case of carbon tetrachloride, where the modified lines were sufficiently close to the exciting line, no filters were used.

The spectrum of the scattered light was taken with a Hilger quartz spectrograph (E_3), using very rapid photographic plates (Ilford Iso-zenith, H. & D. 700). In the case of the single line pictures of benzene and toluene an exposure of about 40 hours was necessary, while for carbon tetrachloride, for which the complete mercury arc was incident, an exposure of only 25 hours was given.

3. *Experimental Results.*

In Plates 1 and 2 are reproduced the spectrograms of the scattering by benzene, toluene and carbon tetrachloride. The plates were measured with a Hilger travelling micrometer and the wave-lengths of the modified lines were calculated, using the mercury lines (feebly transmitted by the filters) as standards for reference. A simplified Hartmann formula was used for interpolation.

* 'Naturw.,' vol. 11, p. 873 (1923).
† 'Z. Physik,' vol. 31, p. 681 (1925).
‡ 'Abhandlungen zur Wellenmechanik, Leipzig. p. 112 (1927).

Table I.—Spectrum of Benzene Scattering.

Unmodified Lines.			Modified Lines.			Origin of the Modified Lines.	
Wave-length I.A.	Wave-number (*in vacuo* per cm.)	Intensity.	Wave-length I.A.	Wave-number (*in vacuo* per cm.)	Intensity.	Wave-length of the exciting line.	Difference of wave-numbers.
			4178·0	23928	0	4358·3	− 990
			4246·7	23541	0	4358·3	− 603
4339·2	23039	15					
4347·5	22995	30					
4358·3	22938	200					
			4476·4	22333	1	4358·3	605
			4525·8	22089	0	4358·3	849
			4534·5	22047	0	4339·2	992
			4543·4	22004	0	4347·5	991
			4555·1	21947	10	4358·3	991
			4593·9	21762	2	4358·3	1176
			4683·5	21346	1	4358·3	1592
			5029·6	19877	1	4358·3	3061
					Broad		

Table II.—Spectrum of Toluene Scattering.

Unmodified Lines.			Modified Lines.			Origin of the Modified Lines.	
Wave-length I.A.	Wave-number (*in vacuo* per cm.)	Intensity.	Wave-length I.A.	Wave-number (*in vacuo* per cm.)	Intensity.	Wave-length of the exciting line.	Difference of wave-numbers.
			4176·1	23939	0	4358·3	− 1001
			4213·7	23725	0	4358·3	− 787
			4262·3	23455	0	4358·3	− 517
			4315·6	23165	1	4358·3	− 227
4339·2	23039	15					
4347·5	22995	30					
4358·3	22938	200					
			4399·5	22723	2	4358·3	215
			4424·9	22593	1	4358·3	345
			4448·4	22474	0	4347·5	521
			4459·3	22419	2	4358·3	519
			4479·8	22316	1	4358·3	622
			4501·7	22208	0	4347·5	787
						4358·3	730
			4513·8	22153	4	4358·3	785
			4547·1	21986	0	4347·5	1009
			4558·0	21933	7	4358·3	1005
			4563·0	21909	1	4358·3	1029
			4591·0	21776	1	4358·3	1162
					Broad		
			4600·8	21729	2	4358·3	1209
			4638·0	21555	1	4358·3	1383
			4648·3	21507	0	4358·3	1431
			4664·0	21435	0	4358·3	1503
			4685·5	21336	2	4358·3	1602
			4994·3	20017	0	4358·3	2921
			5027·3	19886	1	4358·3	3052

Table III.—Spectrum of Carbon Tetrachloride Scattering.

Unmodified Lines.			Modified Lines.			Origin of the Modified Lines.	
Wave-length I.A.	Wave-number (*in vacuo* per cm.)	Intensity.	Wave-length I.A.	Wave-number (*in vacuo* per cm.)	Intensity.	Wave-length of the exciting line.	Difference of wave-numbers.
			4273·5	23393	1	4358·3	− 455
			4299·6	23251	2	4358·3	− 313
			4317·2	23157	2	4358·3	− 219
4339·2	23039	15					
4347·5	22995	30					
4358·3	22938	200					
			4400·3	22719	7	4358·3	219
			4418·5	22626	8	4358·3	312
			4447·3	22479	10	4358·3	459
			4509·3	22170	2	4358·3	768
			4514·0	22147	2	4358·3	791

4. *Infra-Red Spectra of the Molecules.*

As has been shown in our previous papers, the shift in frequency of the modified lines must correspond to a characteristic frequency of the molecule. In the following table are exhibited the shifts in wave-number of the different modified lines and the corresponding infra-red wave-lengths characteristic of the molecule. The infra-red absorption spectra of these liquids have been studied by Coblentz,* Bell† and others, and their values are also reproduced in the table for comparison.

Considering the uncertainties in the direct measurement of infra-red spectra, the agreement between the values of the characteristic wave-lengths calculated from light-scattering and those measured directly should be considered satisfactory; thus confirming the conclusions drawn in our previous papers regarding the origin of the modified lines.

* Quoted by J. W. Ellis, 'Phys. Rev.,' vol. 27, p. 305 (1926).
† 'J. Am. Chem. Soc.,' vol. 47, p. 2814 (1925).

Table IV.—Infra-Red Spectra of the Molecules.

Benzene.			Toluene.			Carbon Tetrachloride.		
Shift in wave-number.	Infra-red wave-length.		Shift in wave-number.	Infra-red wave-length.		Shift in wave-number.	Infra-red wave-length.	
	Calculated.	Observed (Bell).		Calculated.	Observed (Coblentz)		Calculated.	Observed (Coblentz)
Cm.$^{-1}$	μ	μ	Cm.$^{-1}$	μ	μ	Cm.$^{-1}$	μ	μ
3061	3·27	3·3						
			3052	3·28				
			2921	3·42	3·4			
			1602	6·24	6·2			
1592	6·28	6·2						
			1503	6·65				
			1431	6·99	6·9			
			1383	7·23				
			1209	8·27				
1176	8·57	8·5						
			1162	8·60	8·6			
			1029	9·71				
			1005	9·94	9·9			
991	10·09	9·7 to 10·2						
849	11·78	11·8				791	12·64	
			786	12·72	12·1			13
						768	13·02	
			730	13·69	13·9			
			622	16·07				
605	16·52							
			520	19·23				
						457	21·9	
			345	29·0				
						312	32·0	
						219	45·6	
			215	46·5				

5. *Light Scattering and Infra-Red Spectroscopy.*

Attention was drawn in our previous papers to the usefulness of light scattering as a convenient and accurate method in infra-red spectroscopy. In a single spectrogram taken in the visible region we get all the infra-red frequencies of the molecule simultaneously photographed, and they could be measured much more accurately than with an infra-red spectrometer. For example, in the case of sharp, bright lines, as some of those appearing in the spectrograms are, we can, with an instrument of larger dispersion and using suitable comparison standards, measure them correct to a hundredth of an Ångström unit, which corresponds in the near infra-red, say, 3 μ, to an accuracy of about 1 part in 60,000, and in the extreme infra-red, say, 20 μ, to 1 part

in 10,000. In fact, the accuracy is limited only by the width of the modified line.

The appearance in the scattered spectra of toluene and carbon tetrachloride of modified lines corresponding to several hitherto unknown frequencies of the molecules, in the extreme infra-red region as far as 46 μ,* emphasises the ready applicability of the method especially to regions not accessible to the ordinary infra-red spectrometer.

6. *Enhancement of Frequency in Light Scattering.*

While most of the modified lines are of smaller frequency than the exciting line there appear in all the three spectrograms (figs. 2, 3 and 5) some relatively feeble lines whose frequencies *exceed* the frequency of the exciting line by an infra-red frequency of the molecule. These lines are particularly conspicuous in the case of carbon tetrachloride, where corresponding to each of the three prominent lines on the longer wave-length side of the exciting line we have a weaker line on the shorter wave-length side. The appearance of these lines of enhanced frequency proves in the first place the existence in the liquid at ordinary temperatures of some molecules at a level of energy higher than the normal by that corresponding to an infra-red frequency of the molecule, and secondly, that the incident light induces a return of these molecules to the normal state. That is to say, while most of the molecules taking part in modified scattering are in the normal state and absorb a part of the incident light quantum, thus giving rise to a scattered radiation of smaller frequency, there is also a small number in the liquid, already in the higher level of energy, which under the influence of the incident radiation can be induced to part with their energy by a return to the normal state, thus giving rise to a scattered radiation of correspondingly higher frequency. In the existence of these lines of enhanced frequency we have for the first time a direct experimental proof of *induced emission* of radiation by molecules.

It may be of interest to recall in this place that the idea of an induced emission of radiation or what has sometimes been described as a "negative absorption of radiation," was first put forward by Einstein in his celebrated paper† on the derivation of Planck's radiation formula, and forms an essential feature of his theory. The idea also figures prominently in the theory of dispersion developed by Kramers and Heisenberg (*loc. cit.*).

* In fact in the case of toluene there is a line corresponding to even longer wave-lengths which could not, however, be measured in the particular negative.

† 'Phys. Z.,' vol. 18, p. 121 (1917).

The relative intensities of the positive and negative lines corresponding to a given molecular frequency ν can be easily calculated. The proportion of molecules in the higher level of energy is obviously given by the relation

$$f = e^{-\frac{h\nu}{kT}},$$

where h is the Planck constant, k is the Boltzmann constant per molecule, and T is the absolute temperature. If we assume, as we might reasonably, that the transitions of the molecule to and from the higher level are equally probable, then the above ratio, viz., $e^{-\frac{h\nu}{kT}}$ also represents the ratio of the intensities of the corresponding negative and positive lines.

Taking for example the case of carbon tetrachloride, corresponding to the shifts in wave number 219, 312 and 457 (cm.$^{-1}$) the calculated values for the ratio of intensities of the negative and positive lines are 1 : 2·8, 1 : 4·4 and 1 : 8·8 respectively, at the temperature of the experiment, viz., 30° C. Accurate measurements of the actual intensities of the lines have not been made. A rough estimate, however, of the intensities from the negative, using for comparison a series of graded exposures taken on the same negative and in the same region of the spectrum, gave the values 1 : 3, 1 : 5, and 1 : 10 respectively, in good agreement with the calculated values.

Conversely, we can take the observed intensity relationships between the different positive and the corresponding negative lines as an experimental verification of the assumption made in the earlier paragraph, that the forward and backward transitions of the molecule are equally probable. The probabilities of transitions of the molecule from the normal state to *different* energy levels are, of course, different, and the differences in the intensities of the different modified lines of degraded frequency are obviously due to this cause.

The rapid fall in the value of the ratio as ν increases offers a ready explanation why we do not get negative lines corresponding to large shifts of frequency. Also as the temperature is increased, since the proportion of molecules in a higher energy level also increases, we should expect the negative lines to brighten up relatively to the corresponding positive lines. Experiments are in progress to test this point.

7. *Continuous Spectrum accompanying the Scattered Lines.*

The molecular frequencies in the near and extreme infra-red, determining the shifts of the various modified lines discussed in the previous sections, are presumably vibrational frequencies. The question naturally arises whether

we should not expect also shifts corresponding to the pure rotational frequencies of the molecules. For example, in the case of benzene, taking the rotational frequency of the molecule to be of the order of 100 μ the corresponding shifts for the 4358 line will be slightly less than 20 A.U., and should be capable of being detected. A visual examination with a direct vision spectroscope, of benzene, toluene and some other liquids, showed a nebulosity or continuous spectrum accompanying the prominent lines in the scattered spectrum. The actual spectrograms reproduced here and in our earlier papers also show a general broadening of the lines. However, in view of the presence of a general photographic halation accompanying the bright lines—the plates used were not backed—we thought it desirable to take fresh pictures with a larger dispersion instrument, and they are reproduced here. Fig. 7 (Plate 2) shows the nebulosity accompanying the 4358 line scattered by liquid benzene, fig. 6 being the direct mercury spectrum diffused by a plate of ground glass, taken with the same instrument.* Fig. 8 shows the scattering by carbon tetrachloride where, however, the nebulosity is not so conspicuous as in benzene.

From the fact that in the case of benzene the extension of the nebulosity from the exciting line is of the same order of magnitude as the rotational frequency of the molecule, one is tempted, by analogy with the explanation of the origin of the modified lines, to attribute the nebulosity to a combination of the rotational frequencies of the molecule with the frequency of the incident radiation. Owing to the continual impedance to rotation which must be present in a dense medium, it is not difficult to understand why we get a continuous spectrum instead of discrete lines. In connection with this explanation it may be pointed out that the nebulosity extends unsymmetrically on the two sides of the exciting line, being more conspicuous on the longer wave-length side.

Whether the comparatively feeble continuous spectrum in carbon tetrachloride scattering is due to a smaller rotational frequency of the molecule or is in any way connected with its symmetrical nature, is more than we can venture to answer at present. Further observations, especially in the vapour state, or in the liquid at different temperatures, are obviously necessary before we can fully understand the origin of this nebulosity.

* In this connection see an interesting paper by Cabannes and Daure, 'Comptes Rendus, June 4, 1928.

8. *Polarisation of Scattered Radiations.*

In view of the imperfection in polarisation of the classical light-scattering at 90°, it becomes of importance to ascertain the nature of the polarisation of the modified radiations. For this purpose two spectrograms were taken with equal exposures and under identical conditions, side by side on the same plate, using a nicol in front of the slit of the spectrograph. During the first exposure the shorter axis of the nicol was perpendicular to the track in the liquid, and during the second, parallel to the track.

Fig. 9 gives the direct spectrum of the mercury arc, incident in the liquid, fig. 10 the scattered spectra of benzene, fig. 11 of carbon tetrachloride, and fig. 12 of amyl alcohol.

The following are some of the interesting results which emerge from a study of these spectrograms :—

(1) All the unmodified lines (*i.e.*, classical scattering) are polarised to practically the same extent.

(2) For a given shift of frequency, the modified lines excited by the different incident lines are polarised to the same degree, but differ in polarisation from the unmodified lines.

(3) The modified lines corresponding to different frequency shifts are polarised to different extents, the intensity of the weaker component varying from almost nothing to about 40 or 50 per cent. of that of the stronger line. For example, in the case of carbon tetrachloride, the most prominent modified line (which corresponds to a shift of 457 cm.$^{-1}$) is more or less completely polarised, while the other two prominent lines show a large imperfection in polarisation.

(4) The negative lines (*i.e.*, of enhanced frequency) are polarised to the same extent as the corresponding positive lines.

(5) The strong modified lines are usually more polarised than the feeble ones.

(6) The general continuous spectrum appearing in the scattering by amyl alcohol is also strikingly polarised.

A tentative explanation of these results regarding the polarisation of the modified lines may be suggested by analogy with the ideas put forward by the late Lord Rayleigh and by Born to explain the observed imperfection of polarisation of the classical scattering. In the classical theory the molecules of the medium behave under the influence of the incident light-vector, like oscillating doublets, which, as a consequence radiate out energy. If the moment induced in the molecule is in the same direction as the inducing force, the transverse

scattering would obviously be completely polarised. The imperfection in polarisation experimentally observed therefore suggests that there are three principal directions in the molecule mutually perpendicular to one another, only along which moments can be induced, and that to varying extents. If the incident force lies along any one of these directions the induced moment is along the same direction. In every other case we have to resolve the incident force along the principal axes of the molecule and then determine the corresponding moments induced in these directions. Incidentally, we may point out that on this basis, assuming the molecules to be independent scattering centres, as is very nearly the case in a gas, the ratio of the intensities of the two principal polarised components of the scattered light can never exceed 50 per cent., the latter limit being reached when the molecule is polarisable only along one axis.

Carrying now the analogy to the case of modified scattering let us tentatively assume that for a given energy transition of the molecule, there are three principal directions in the molecule, the Einstein coefficients of probability of transition under the influence of an external force incident respectively along these three directions being different. As regards the actual mechanism which leads to such an anisotropy we shall for the present leave it an open question. The imperfection in polarisation of the modified lines follows then as a necessary consequence. If, further, we take these principal axes, as well as the corresponding principal Einstein coefficients, to be different for different energy transitions of the molecule, the differences in the intensity and the degree of polarisation of the different modified lines are also readily explained. That for a given frequency shift the polarisation is independent of the inducing line is also obvious. The identity in the degree of polarisation of the positive and negative lines corresponding to a given frequency shift will then merely be a consequence of the equal probability of transitions in the positive and negative directions; that is to say, for the same reasons for which, as we pointed out in sec. 6, the intensities of the negative and positive lines are in the ratio of the number of molecules in a correspondingly higher level of energy, to the number in the normal state.

It is significant in connection with the above explanation that there is no modified line in the spectrograms for which the ratio of the intensities of the principal polarised components is greater than 50 per cent. Physically interpreted, this limiting value of the polarisation signifies that the vibration to which the frequency under consideration corresponds, can take place only along a definite axis in the molecule, which is *a priori* not improbable.

It remains now to discuss the relation between the polarisation of the unmodified radiations and that of the different modified ones. The modified radiations are presumably incoherent, i.e., the radiations at any given instant from neighbouring molecules have no definite phase relationship, so that the polarisation of the modified radiation would be characteristic of the molecule and independent of its state of aggregation. On the other hand, the unmodified radiations from neighbouring molecules are definitely correlated in phase, and their polarisation will be characteristic of the molecule only in the vapour state. Actual calculation shows the polarisation in the liquid state to be considerably smaller. Thus for a fair comparison we should take the polarisation of the modified lines as given by the spectrograms with that of ordinary classical scattering not in the liquid but in the vapour. The vapour values for the ratio of components of classical scattering are benzene 4·5 per cent., amyl alcohol, 1·2 per cent., and carbon tetrachloride 0·5 per cent.

On making the actual comparison we find that most of the modified lines are much less polarised than the unmodified ones. If we can take the degree of anisotropy of the transitions corresponding to the infra-red frequencies as evidenced by the imperfection of polarisation of the corresponding modified lines, as being typical of the anisotropy of all other kinds of energy transitions of the molecule which determine its refractivity, especially the electronic transitions of ultra-violet frequencies, then the smaller polarisation of the modified lines is easily understandable; because the anisotropy of the molecule as a whole, which determines the polarisation of classical scattering, is merely a resultant of the anisotropies of all the individual transitions (suitably weighted) of the molecule, and must, therefore, necessarily correspond to a greater spherical symmetry.

9. *Dependence on Wave-Length.*

It is well known that the classical scattering falls off rapidly with increasing wave-length, following Rayleigh's λ^{-4} law, and it will, therefore, be of interest to find how the intensity of the modified radiations depend on the wave-length of the exciting line. No quantitative measurements have yet been made which would enable us to decide this question. But we may draw attention here to the spectrogram of carbon tetrachloride scattering, which throws some light on the point. Comparing the intensities of the green λ 5460·7 line and the ultra-violet λ 3906·5 line of the mercury arc, as they appear in the spectrum of the scattered light the former line is much brighter, whereas comparing the modified lines excited by them, those excited by the green line are distinctly feebler than the ones excited by the ultra-violet line. It would

thus appear that the intensity of the modified line changes with wave-length even more rapidly than is indicated by Rayleigh's inverse fourth-power law.

This is further confirmed by visual observations on the spectrum of scattered light with a direct vision spectroscope. Though as seen through the spectroscope the scattered green mercury line is far more intense than the indigo or violet lines, the modified lines excited by the green line could not be detected, whereas those due to the violet and indigo lines are very conspicuous.

10. *Summary.*

In two preliminary papers the authors have shown that when any transparent medium, be it gas, vapour, liquid, amorphous solid or crystal, is irradiated by monochromatic light the radiations scattered by the molecules contain several spectral lines of modified frequencies, the difference between the incident and scattered frequencies corresponding to a characteristic infra-red frequency of the molecule. The present paper describes further studies on these radiations.

(*a*) Using the λ 4358 group of lines of the mercury arc as the exciting radiations, the scattered spectra of benzene, toluene and carbon tetrachloride have been photographed and measured.

(*b*) The characteristic infra-red frequencies of the molecules are calculated from the frequencies of the modified lines and are compared with the values obtained from direct measurements of infra-red absorption. The calculation gives several molecular frequencies hitherto unknown.

(*c*) The usefulness of light-scattering as a powerful, convenient and accurate method of exploring molecular spectra, is pointed out.

(*d*) While most of the modified lines are of smaller frequency than the exciting line, there are some relatively feeble lines whose frequencies exceed the frequency of the exciting line by an infra-red frequency of the molecule. In the appearance of these lines we have for the first time a direct experimental proof of *induced emission* (or negative absorption) of radiation by molecules.

(*e*) The scattered lines are sometimes accompanied by a nebulosity or continuous spectrum, extending unsymmetrically on the two sides. Its origin is discussed.

(*f*) The modified radiations scattered at 90° exhibit striking polarisation, the degree of polarisation being different for lines corresponding to different frequency shifts. A tentative explanation is suggested.

(*g*) Some preliminary remarks are made regarding the dependence of the intensities of the modified lines on the wave-length of the exciting line.

Production of New Radiations by Light Scattering.

DESCRIPTION OF PLATES.

PLATE 1.

FIG. 1 gives the spectrum of the mercury arc from which practically all the lines excepting the λ 4358 group have been cut out by interposing a solution of quinine sulphate and a blue glass plate.

FIG. 2 is the spectrogram of the radiations shown in fig. 1 when scattered by liquid benzene.

FIG. 3 is a similar spectrogram of the radiations scattered by toluene.

FIG. 4 is the direct spectrum of the mercury arc which was incident on carbon tetrachloride.

FIG. 5 being the corresponding scattered spectrum. Note the appearance of relatively feeble lines of enhanced frequency.

PLATE 2.

FIG. 6.—Spectrum of the λ 4358 group of lines diffused by a plate of ground glass.

FIG. 7.—Spectrum of the same as scattered by benzene. Note the nebulosity accompanying the scattered line, which is not present in fig. 6.

FIG. 8 shows the same line as scattered by carbon tetrachloride. The nebulosity is not so prominent as in benzene.

FIG. 9 gives the complete spectrum of the mercury arc used for polarisation measurements (for comparison with figs. 10 to 12).

FIG. 10.—Spectrum of the mercury arc scattered by benzene, taken with a nicol in front of the slit of the spectrograph. In (*a*) the shorter axis of the nicol was perpendicular to the track, while in (*b*) it was parallel to the track.

FIG. 11 shows similarly the polarisation of the scattered radiations from carbon tetrachloride.

FIG. 12 is a similar spectrogram of the radiations scattered by amyl alcohol. Note the continuous radiations are also partly polarised.

Fig. 1.—Incident Spectrum.

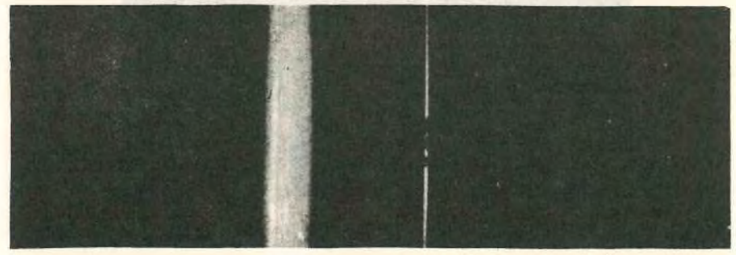

Fig. 2.—Benzene Scattering.

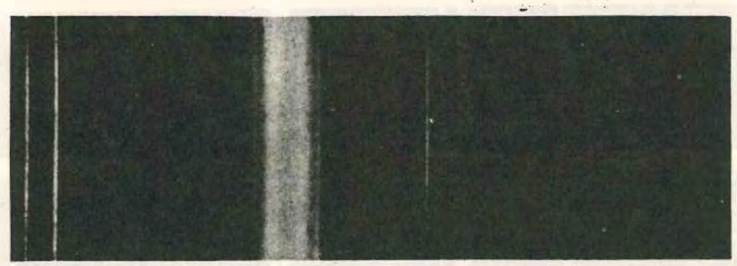

Fig. 3.—Toluene Scattering.

Fig. 4.—Incident Spectrum.

Fig. 5.—Carbon Tetrachloride Scattering.

Fig. 6.—Diffused by Ground Glass.

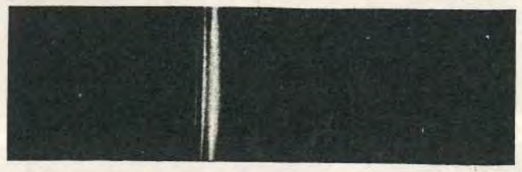

Fig. 7.—Scattered by Benzene.

Fig. 8.—Scattered by Carbon Tetrachloride.

Continuous Spectrum accompanying the Scattered Lines.

Fig. 9.—Incident Spectrum.

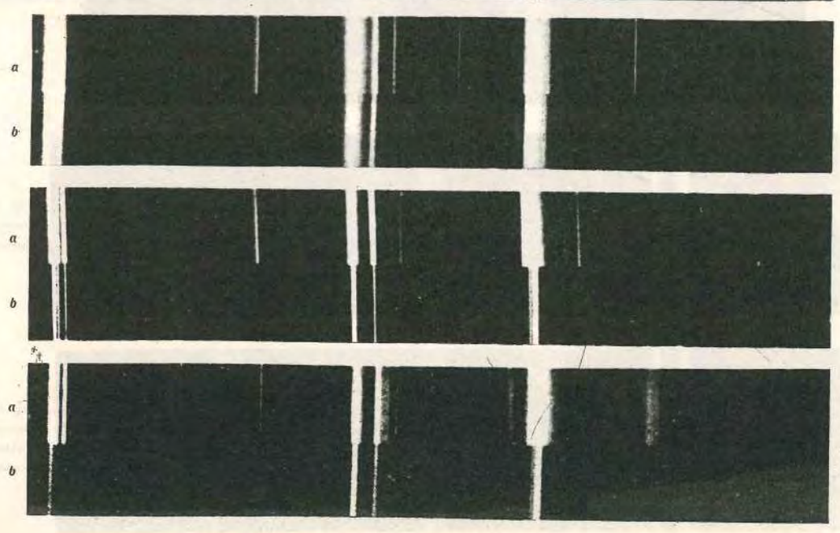

Fig. 10.—Benzene.

Fig. 11.—Carbon Tetrachloride.

Fig. 12.—Amyl Alcohol.

Polarisation of Scattered Radiations.

The Anisotropy of the Polarisation Field in Liquids.

By

K. S. Krishnan, *Reader in Physics, Dacca University*

and

S. Ramachandra Rao, *King's College, London.*

(*Received for publication, 20th April 1929.*)

Abstract.

The well-known expression of Lorentz for the polarisation field acting on any molecule in a refracting medium, due to the doublets induced in the surrounding ones, is applicable to actual liquid media consisting of optically anisotropic molecules only if the following conditions are satisfied. Firstly the distribution of the molecules surrounding the one under consideration should be spherically symmetrical and secondly their orientations with respect to it should be entirely fortuitous. The validity of these two conditions is discussed on the basis of recent evidence concerning the fine structure of liquids obtained by a study of their X-ray diffraction, and it is shown that in the case of molecules which are highly asymmetric in shape, e.g., the normal hydrocarbons of the paraffin series, though the latter assumption regarding the randomness of orientation, may be taken to be more or less justified, the spherical symmetry of distribution is far from being realised. The result is that the value of the polarisation field varies with the direction of the incident field with respect to the molecule; that is to say, it is anisotropic. The magnitude of this anisotropy is evaluated from X-ray data for some typical liquids, and also indirectly from measurements on light-scattering by them, and the two sets of values are in good agreement. The influence of the close packing or the density of the

molecules on the anisotropy of the polarisation field is then discussed on the basis of measurements on light-scattering at different temperatures. The anisotropy tends to approach asymptotically a certain maximum value, determined by the asymmetry of the molecule itself, at high densities, and again a minimum value of zero at very low densities, in conformity with our theoretical expectations.

1. *The Lorentz Theory of Refraction.*

In the well-known theory of refraction developed by Lorentz, each molecule in the refracting medium is supposed to behave under the influence of the incident light-wave as an isotropic electric doublet, and the main problem centres round the evaluation of the *actual* field acting on the molecule which induces this doublet. This field would obviously be different from the "field in the medium" since we have to take into account also the influence of the doublets induced in the surrounding molecules, *i.e.*, "the polarisation field." The latter is evaluated by Lorentz in the following manner. Round the given molecule as centre is described a sphere whose radius is small in comparison with the wave-length of the incident light, and at the same time large enough to contain a great many molecules. The contributions from the molecules inside and outside the sphere are then evaluated separately. As the sphere contains by supposition a great many molecules, the medium *outside* can for our present purpose be treated as continuous and uniformly polarised; and the field at the centre due to it will be equivalent to that of a surface charge on the sphere whose magnitude at any point the radius vector to which makes an angle θ with the direction of the field in the medium, is equal to $-P\cos\theta$ per unit area, where P is the mean polarisation of the medium (*i.e.*, the total moment induced in unit volume). On actual evaluation this part of the polarisation field arising from the molecules *outside* the sphere comes out equal to $4\pi P/3$.

The contribution from the molecules inside the sphere to the polarisation field acting on the given molecule at the centre is however more difficult to evaluate. Its value will obviously depend on the nature of their distribution. *In the special case where their distribution may be considered spherically symmetrical with respect to the given molecule* (a condition which according to Lorentz is approximately realised in fluid media) the contribution can be easily shown to be nothing. In this case the total polarisation field is equal to $4\pi P/3$ and we obtain directly the well-known Lorentz expression for refractivity for fluids.

In order that the above expression for the polarisation field may be applicable to a medium consisting of *optically anisotropic* molecules (as we have in general in actual fluids), *i.e.*, in order that the polarisation field acting on any specific molecule in the medium arising from the doublets induced in the surrounding ones may still be represented by $4\pi P/3$ the surrounding molecules *in addition to being distributed spherically symmetrically about the given molecule* have to satisfy the further condition that *their orientations with respect to it shall be entirely fortuitous.*

In view of the very general application that has been made of the above expression to actual liquids in all discussions concerning their optical and electrical properties, it would be of interest to enquire how far the above two conditions are satisfied in these cases.

2. *The Fine Structure of Liquids.*

Our knowledge of the internal constitution of liquids has been considerably extended during recent years by the study of their X-ray diffraction. Raman and Ramanathan[1] put forward in 1923 a theoretical explanation of the diffraction haloes

[1] C. V. Raman and K. R. Ramanathan, Proc. Ind. Assn. Sc., Vol. 8, p. 127 (1923).

observed when a thin layer of liquid is irradiated by a narrow pencil of monochromatic X-rays, according to which the X-ray halo gives us in effect an analysis of the fine structure into a "structural spectrum." Their paper contains a detailed discussion of how this structural spectrum is determined by the spacing and orientation of the molocules relatively to one another in the liquid. Extensive experimental investigations carried out since then by Sogani,[2] Stewart[3] and others have entirely confirmed and made more precise the ideas outlined in their paper and furnish us valuable information regarding the molecular structure of liquids.

Taking for example the normal saturated hydrocarbons of the paraffin series, Sogani finds that at room temperature, *viz.*, 30°C., pentane, hexane, heptane and octane give diffraction haloes which differ only in their degree of sharpness, the angular size of the haloes (18° with Kα copper radiation, corresponding to a spacing of 4·90 A.U.) being practically the same for the four liquids. That the size of the halo should remain constant in spite of the increase of the length of the chain of carbon atoms from five to eight, is remarkable enough, and its significance will become clearer when we remark that the quantity $n^{-1/3}$, where n is the number of molecules per unit volume, increases steadily as we go up the series, being 5·80 A.U. for pentane, 6·02 for hexane, 6·26 for heptane and 6·47 for octane (at the temperature of the experiment). The quantity $n^{-1/3}$ has the dimensions of a length, being in fact the edge of a unit cell in a cubic arrangement of n molecules per unit volume, and in the case of liquids with more or less symmetric (in geometric shape) molecules like cyclohexane, it is found to agree with the grating space deduced from the size of the X-ray halo. That there is no such agreement in the case of these long chain molecules indicates that their

[2] C. M. Sogani, Ind. Journ. Phys., Vol. 1, p. 357 (1927); Vol. 2, p. 97 (1928).

[3] G. W. Stewart and his collaborators, Phys. Rev., Vol. 30, p. 232, (1927) and several subsequent issues.

arrangement in space is of quite a different character. An explanation of the observed effects is obtained, as suggested by Sogani, if we imagine the molecules to be approximately equivalent to cylinders or ellipsoids of considerable length, loosely packed together in the liquid; the perpendicular distance between the axes of two neighbouring molecules would obviously tend to be more or less constant and independent of the length of the molecules, being in fact of the same order of magnitude as the diameter of any one of them. The X-ray facts are clearly in accord with such a supposition and suggest further that the grating space of 4·90 A.U. observed, represents the mean value of the perpendicular distance between the axes of neighbouring molecules in the liquids. A striking confirmation of these assumptions is furnished by the observation of Sogani that compounds such as lauric, palmitic, oleic, erucic and brassidic acids with molecules having the same cross-section but considerably greater lengths, continue to exhibit in the liquid state X-ray haloes of very nearly the same size as the earlier members of the paraffin series.

Thus if we consider any particular molecule in these liquids we may reasonably assume that the most probable distance of approach on its broadside of the neighbouring molecules, is 4·90 A. U. On the other hand the X-ray data give us no direct indication of the corresponding distance of approach of its neighbours along its length. It is *prima facie* obvious, however, that the latter distance should be the greater the greater the length of the molecule. Its actual magnitude can in fact be roughly estimated from the known density of the liquid. If we represent the most probable distance of approach to the given molecule from its end-on position by a and that for approach from its broadside by b (=4·90 A.U. in this case) the product ab^2 represents to a first approximation the *average* volume occupied by each molecule in the medium, and may therefore be put equal to $1/n$.

About the centre of the given molecule we may thus picture in a crude way an ellipsoid whose semi-axes—along and perpendicular respectively to the length of the molecule—are equal to a, b, b, which represents the *effective* closeness of approach from different directions, of its neighbours. That is to say, *in effect* it is as though the centres of the surrounding molecules can occupy all positions outside the ellipsoid, but are precluded from occupyiug any position inside it. The physical significance of such an ellipsoid which the molecule is supposed to carry with it in all its movements, is in fact obvious from direct considerations of geometry, when once we postulate a finite size and a highly elongated shape for the molecule.

Thus the first condition for the applicability of the Lorentz expression for the polarisation field, *viz.*, that regarding the spherical symmetry of distribution of the surrounding molecules, is far from being satisfied, at least in these liquids.

As to the second condition, *viz.*, that regarding the *random nature of the orientations* of the surrounding molecules with respect to it, the X-ray data give us much less definite evidence. All that the X-ray halo gives us is in effect a certain mean distance between any two molecules in the assemblage which is statistically the most probable; and in the case of the long chain paraffins this happens to be of the order of the lateral dimension of the molecule. But if we concentrate our attention on any particular molecule in the assemblage, whether in any reasonable time its immediate neighbours can take up all orientations with respect to it, is a question which cannot be answered from X-ray data alone. From the fact that in these long chain compounds the average linear dimension allotted to a molecule in the medium (*i.e.*, $n^{-\frac{1}{3}}$) is actually found to be much smaller than the length of the molecule, Sogani seems to suggest that the axes of two adjacent molecules must be *more or less parallel*

to each other; that is to say, the orientation of any molecule can *differ* from that of its neighbour only within certain small limits. It is true that the close packing of the molecules suggested by the above value of $n^{-\frac{1}{3}}$ might hamper their *freedom of orientation* with respect to their neighbours, but it need not necessarily conduce to a *parallel* alignment of the neighbouring molecules. Any such parallel allignment would endow the medium with properties not very different from those usually associated with "liquid crystals," which are quite distinct from the class of liquids we are considering here.

Measurements on light-scattering in these liquids furnish, on the other hand, definite evidence that no such parallelism in the orientation of neighbouring molecules actually exists; because it would mean an enormously greater "orientation scattering" (*i.e.*, that part of the scattering which arises from the optically anisotropic nature of the molecules and their varying orientations) than is experimentally observed. In fact measurements seem to suggest that neighbouring molecules are capable of taking up on an average all possible orientations relatively to one another, and we may therefore reasonably assume that this represents approximately the actual fact.[4]

[4] Dr. Sogani gives two reasons why we should consider the orientations of neighbouring molecules to be more or less identical: (1) The absolute available space for the molecule is not sufficient for random orientation. This point has been discussed above. (2) That the density does not change as the substance passes from the crystal state to that of a liquid. This is not true at least with the hydrocarbons under consideration. Though careful measurements are not available, it is well-known that ordinary paraffin—which is a mixture of a number of hydrocarbons—expands considerably on melting (see, *e.g.*, Thorpe, Diction . Appl. Chem.). Secondly the observed fact that when the liquid is gradually cooled below its melting point it becomes opaque, must be attributed to a large shrinkage in volume with the consequent—when taken together with its tendency not to form large crystals—formation of a large number of minute crevasses inside. Muller finds that these hydrocarbons when heated begin to be *translucent* (as contrasted with opaqueness at lower temperatures) a few degrees below the melting point, suggesting there is already an expansion before actual melting takes place, and he finds also that the X-ray diffraction spacing in the translucent state is different from that in the solid state.

3. *The Anisotropy of the Polarisation Field.*

We now proceed to discuss the influence of the fine structure of these liquids outlined in the previous section on the polarisation field. The general features of the influence are not difficult to understand without calculation. For example one can readily see that in the first place the field can no more be equal to $4\pi P/3$ and secondly that its actual value will depend on the *direction* of the incident electric vector with respect to the molecule. Let us consider the case when it is along the length of the molecule. The polarisation field is really an integrated effect of the contributions from all the surrounding molecules lying in various positions around it and supposed to to be orientated at random, those on the broadside of the molecule tending to diminish the field, while those along its length tend to increase it. In the particular case where their distribution is spherically symmetrical, we have seen that the resultant is equal to $4\pi P/3$. But as a matter of fact those on the broad side which tend to diminish it are able to approach very much closer to the molecule than those along its length, so that the resultant field must be considerably *less* than $4\pi P/3$ (say, $=p_1 P$ where $p_1<4\pi/3$). On the other hand if the incident field is perpendicular to the length of the molecule, it will be, for similar reasons, much *greater* than $4\pi P/3$ ($=p_2 P$, $p_2>4\pi/3$). Thus the polarisation field is no more isotropic and is a function of the direction of incidence with regard to the molecule.

The constants p_1 and p_2 can be evaluated in the following manner. We offer here a preliminary remark. We notice that the method adopted by Lorentz of dividing the surrounding medium into two parts by describing a sphere about the molecule *large enough to contain a great many molecules*, was

merely to ensure the separation of that part of the polarisation field which arises from the immediate neighbours and which requires for its evaluation a precise knowledge of the fine structure of the medium, from the part which is independent of any such fine structure. But when once we have decided on some reasonable assumptions regarding the structure, the above method of dividing the medium into two parts loses its significance, at least so far as the final results are concerned.

In fact in the present case it is very much simpler to consider the surrounding medium as a whole. In the last section we imagined an elongated ellipsoid to be described about each molecule (the long axis of the ellipsoid being along the length of the molecule) whose semi-axes are a, b, $b(a>b)$, which limits the effective closeness of approach of the surrounding ones; the latter are precluded from occupying any position inside the ellipsoid but can occupy all positions outside it equally well. Since they are also assumed to be oriented at random, we may treat the medium outside the ellipsoid as continuous and uniformly polarised. The calculation of the polarisation field then merely reduces to finding the field at the centre of an ellipsoidal cavity scooped out of an otherwise uniformly polarised medium, and the problem is exactly analogous to that of finding the constants of demagnetisation in ellipsoidal magnets, which has been discussed elaborately by Maxwell and others.[5] We thus immediately get for p_1 and $p_2(=p_3)$ the values

$$p_1=4\pi\left(\frac{1}{e^2}-1\right)\left(\frac{1}{2e}\log\frac{1+e}{1-e}-1\right) \quad \ldots (1)$$

$$p_2=p_3=2\pi\left(\frac{1}{e^2}-\frac{1-e^2}{2e^3}\log\frac{1+e}{1-e}\right) \quad \ldots (2)$$

[5] See Lord Rayleigh, Scientific Papers, Vol. IV, p. 307.

where e is the eccentricity of the ellipsoid defined by the usual relation

$$b=c=\sqrt{1-e^2}\ .a \qquad \ldots (3)$$

We can readily see that

$$p_1+2p_2=4\pi \ . \qquad \ldots (4)$$

In the case of the paraffins, taking for the semi-axes of the ellipsoid $b=c=4{\cdot}90$ A.U. and $a=\frac{1}{n\overline{b^2}}$, as explained in the previous section, the constants p_1 and p_2 can be calculated from (1) and (2) and their values are exhibited in Table I.

TABLE I.

Liquid.	Temperature.	Semi-axes of the ellipsoid.		p_1	$p_2=p_3$
		a in A.U.	$b=c$ in A.U.		
Pentane	30°C.	8·03	4·90	2·7	5·0
Hexane	,,	9·10	4·90	2·4	5·1
Heptane	,,	10·19	4·90	2·1	5·2
Octane	,,	11·29	4·90	1·9	5·4

4. *Evidence from Light-Scattering.*

The influence of the anisotropy of the polarisation field on the optical and electrical properties of liquids has been the subject of some recent papers,[6] where on the basis of some preliminary estimates of the anisotropy it is shown to offer a simple explanation of the observed discrepancies in the existing theories of electric and magnetic birefringence, of light-

[6] C. V. Raman and K. S. Krishnan, Proc. Roy. Soc. A, Vol. 117, pp. 1 and 589 (1927-8); Phil. Mag., Vol. 5, p. 498 (1928).

scattering and of refraction and dielectric polarisation, in liquids. For example in light-scattering, the apparent change in the optical anisotropy of a molecule as it passes from the state of vapour to that of a liquid can be attributed to a change in the constants of the polarisation field; and thus it is possible to calculate the latter constants purely from measurements on light-scattering, *i.e.*, by a method which is entirely independent of any specific assumptions regarding the origin of the anisotropy of the polarisation field. Since very reliable measurements on light-scattering are available for the paraffins both in the vapour and in the liquid states, it is proposed in this section to calculate the constants of the polarisation field from these data and see how far the values obtained in the previous section from direct considerations regarding the fine structure of these liquids, approximate to them.

We reproduce here only the final expression for the depolarisation factor of the light transversely scattered by a liquid, *viz.*,

$$r=\frac{2n\mathrm{F}}{kT\beta\left(\frac{\mu^2-1}{4\pi}\right)^2+\frac{7}{3}n\mathrm{F}} \qquad \ldots (5)$$

where r is the ratio of the intensities of the principal components (the incident light being unpolarised),

n is the number of molecules per c.c.,
k is the Boltzmann constant per molecule,
T is the absolute temperature,
β is the isothermal compressibility,
μ is the refractive index.

$$\mathrm{F}=\frac{1}{30}\left[\ (\mathrm{A}'-\mathrm{B}')^2+(\mathrm{B}'-\mathrm{C}')^2+(\mathrm{C}'-\mathrm{A}')^2\ \right] \qquad \ldots (6)$$

$$\left.\begin{aligned}\mathrm{A}'&=\mathrm{A}(1+p_1\chi)\\ \mathrm{B}'&=\mathrm{B}(1+p_2\chi)\\ \mathrm{C}'&=\mathrm{C}(1+p_3\chi)\end{aligned}\right\} \qquad \ldots (7)$$

where A, B, C are the moments induced along the three principal axes of the molecule, per unit field incident respectively along them, the p's are the corresponding constants of the polarisation field and χ is the susceptibility of the medium $\left(=\frac{\mu^2-1}{4\pi}\right)$.

In the case of the paraffins, if we take A to correspond to the long axis of the molecule, owing to its being an axis of symmetry,

$$B=C \text{ and } p_2=p_3 \quad \ldots \quad \ldots \quad (8)$$

The optical constants A, B, C can be readily calculated from the refractive index and the depolarisation factor for the vapour state, with the help of the relations,

$$\mu_{vap}-1=2\pi n_{vap}, \frac{A+B+C}{3} \quad \ldots \quad \ldots \quad \ldots (9)$$

and

$$\frac{(A-B)^2+(B-C)^2+(C-A)^2}{(A+B+C)^2}=\frac{10r_{vap}}{6-7r_{vap}}. \quad \ldots \quad \ldots (10)$$

All the quantities in expression (5) being thus known except p_1 and p_2 $(=p_3)$, the latter can be evaluated using the further relation [see (4)]

$$p_1+p_2+p_3=4\pi. \quad (11)$$

Table II gives the values of p_1 and p_2 calculated from (5). The corresponding values obtained in the previous section are reproduced from Table I for comparison. The agreement is surprisingly good.

TABLE II.

Substance.	Temp.	r		Constants of the polarisation field.			
				From scattering.		From liquid structure.	
		Vapour.	Liquid.	p_1	$p_2=p_3$	p_1	$p_2=p_3$
Pentane	30°C.	0·0132	0·072	2·5	5·0	2·7	5·0
Hexane	,,	0·0149	0·099	2·5	5·0	2·4	5·1
Heptane	,,	0·0158	0·126	2·1	5·2	2·1	5·2
Octane	,,	0·0186	0·129	1·8	5·4	1·9	5·4

5. *Benzene and Cyclohexane.*

Till now we have been considering the case of liquids consisting of highly elongated molecules. We now pass on to another equally simple case, *viz.*, that of flat disc-shaped molecules. Benzene and cyclohexane may be taken as typical of this class. Sogani gives for the spacing corresponding to the inner and outer limits of blackening in the photographs of the X-ray diffraction patterns of these liquids the values 6·2 and 3·2 A. U. respectively for benzene, and 6·4 and 4·6 A. U. respectively for cyclohexane. Consistently with the ideas developed in the earlier sections of this paper we may take these values to represent the effective closeness of approach to any given molecule in the medium, of its neighbouring ones, from its edge and its side respectively. The polarisation field acting on it will as before be the same as at the centre of a spheroidal cavity, which would however be oblate in this case. The constants will therefore be given by

$$p_1=p_2=2\pi\left(\frac{\sqrt{1-e^2}}{e^3}\sin^{-1}e-\frac{1-e^2}{e^2}\right) \quad \ldots \quad \ldots (12)$$

$$p_3=4\pi\left(\frac{1}{e^2}-\frac{\sqrt{1-e^2}}{e^3}\sin^{-1}e\right), \quad \ldots \quad \ldots (13)$$

where e is defined by

$$a=b=\frac{c}{\sqrt{1-e^2}} \quad \ldots \quad \ldots \quad (14)$$

Also as before $p_1+p_2+p_3=4\pi$.

The calculation of the same constants from light-scattering is also very similar to the case of elongated molecules. Only we have to put in equations (9) and (10) A = B > C (instead of A > B = C of the previous case) and in relations (7) $p_1=p_2$.

The values of the constants calculated by both the methods are given in Table III. Here again the two sets of values agree satisfactorily.

TABLE III.

Substance.	Temp.	$a=b$ A.U.	c A.U.	From liquid structure.		r		From scattering.	
				$p_1=p_2$	p_3	Vapour.	Liquid.	$p_1=p_2$	p_3
Benzene ...	30°C.	6·2	3·2	3·0	6·5	0·0445	0·405	3·0	6·6
Cyclohexane	,,	6·4	4·6	3·6	5·3	0·010	0·08	3·4	5·7

6. *Dependence on Temperature.*

From what has been discussed in an earlier section regarding the origin of the anisotropy of the polarisation field it would follow that it must essentially depend on the closeness of packing of the molecules, *i.e.*, on the density of the medium. The general features of the dependence can be made evident from direct considerations. As the density of the medium is diminished, say by raising its temperature, there is more free space available for the molecules to move about, and hence the ellipsoid which limits the effective

closeness of approach of the surrounding molecules tends to be more and more symmetrical until finally when the fraction of the whole time, during which the molecule is in actual collision with its neighbours becomes negligible, the ellipsoid approximates to a sphere. On the other hand if the temperature is continually diminished, we will soon reach a stage where the molecule is almost always in collision with its neighbours and the ellipsoid would have reached its maximum eccentricity, whose value is of course determined by that of the molecule itself. Taking the example of elongated molecules again, the ratio $\frac{p_2}{p_1}\left(=\frac{p_3}{p_1}\right)$ will thus approach asympotically a certain maximum value (determined by the asymmetry of the molecules) at sufficiently low temperatures, and again a minimum value of unity at sufficiently high temperatures. It can therefore be represented by a curve of the form shown in Fig. 1 which exhibits three distinct stages, the first and the third corresponding to a very slow variation of $\frac{p_2}{p_1}$ with temperature, and an intermediate stage where the variation is relatively very rapid.

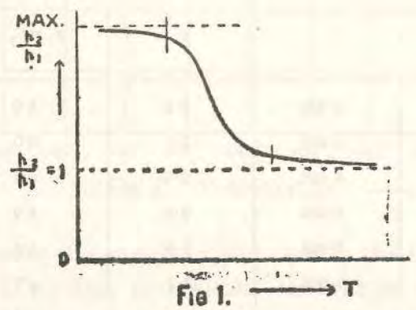

Fig 1.

Proceeding to the experimental evidence, we do not have sufficient data for the X-ray diffraction of liquids at different temperatures to enable us to calculate the polarisation constants

directly from the molecular structure. But measurements are available for light-scattering at different temperatures up to the critical point, from which we can calculate the constants indirectly as in section 4. The following Tables exhibit the values thus obtained, and they are plotted in Fig. 2.

TABLE IV. Pentane.

Temp. °C.	r	p_1	$p_2=p_3$	$\frac{p_2}{p_1}=\frac{p_3}{p_1}$
30	0·072	2·5	5·0	2·0
60	0·072	3·3	4·7	1·4
80	0·071	3·8	4·4	1·2
100	0·058	3·9	4·3	1·1
120	0·050	4·3	4·2	1·0
140	0·034	4·0	4·3	1·1
160	0·020	4·2	4·2	1·0

TABLE V.—Hexane.

Temp. °C.	r	p_1	$p_2=p_3$	$\frac{p_2}{p_1}=\frac{p_3}{p_1}$
30	0·099	2·5	5·0	2·0
50	0·098	2·7	5·0	1·9
70	0·095	2·8	4·9	1·8
80	0·089	2·8	4·9	1·7
100	0·082	2·9	4·8	1·6
120	0·062	3·1	4·7	1·5
140	0·050	3·3	4·6	1·4
160	0·039	3·4	4·6	1·3
180	0·025	3·4	4·6	1·3

TABLE VI.—Heptane.

Temp. °C.	r	p_1	$p_2=p_3$	$\frac{p_2}{p_1}=\frac{p_3}{p_1}$
20	0·127	2·2	5·2	2·4
100	0·100	2·1	5·2	2·4
200	0·038	2·4	5·1	2·2
225	0·026	2·8	4·9	1·8
240	2·020	3·2	4·7	1·4
250	0·017	3·8	4·4	1·2

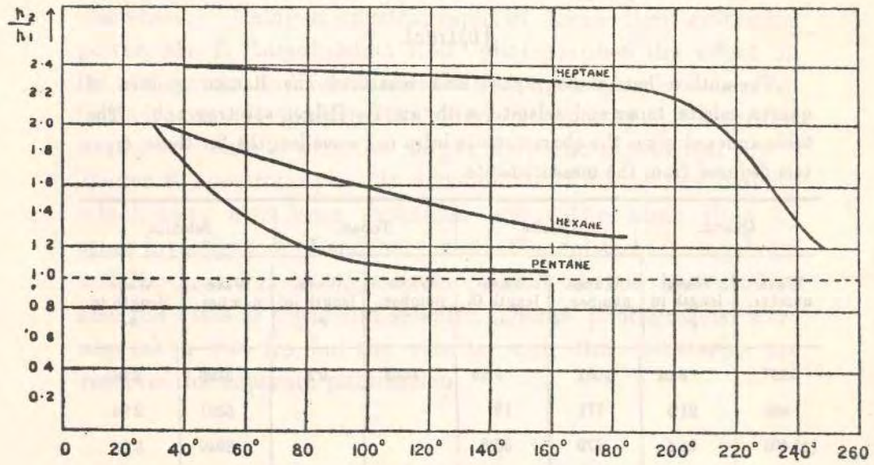

FIG 2.

On comparing the curves in Fig. 2 with the typical curve shown in Fig. 1, we find that within the range of temperatures investigated, pentane exhibits the second and the third stages, hexane only the second, while heptane (having the longest molecule of the three) shows also the first stage.

The Raman Spectra of Crystals*

BY

K. S. KRISHNAN

Reader in Physics, Dacca University.

(PLATE II)

(*Received for publication on the 25th January, 1929.*)

Abstract.

The author has photographed and measured the Raman spectra of quartz, calcite, topaz and selenite, with an E_2 Hilger spectrograph. The table annexed gives the characteristic infra red wave-lengths for these crystals deduced from the measurements.

Quartz.		Calcite.		Topaz.		Selenite.	
Wave-number.	Wave-length in μ.	Wave-number.	Wave-length in μ.	Wave-number.	Wave-length in μ.	Wave-number.	Wave-length in μ.
1157	8·64	1084	9·22	1053	9·5	3493	2·86
464	21·5	771	13			3397	2·94
(?) 408	24·5	279	35·8			3240	3·09
267	37·4	147	68			1134	8·81
206	48·5					1011	9·89
127	79						

* The photographs of the Raman spectra of these crystals were taken by the author at Calcutta during the two months 15th July to 15th September, 1928. The measurements of the plates and the writing up of the paper could not, however, be completed earlier owing to the author having been engaged in other very pressing duties and his subsequent transfer to the Dacca University.

Selenite which has water of crystallization shows three sharp lines in positions corresponding to those shown by ice, and two lines of somewhat longer wave-length than the prominent line shown by solutions of sulphates in water. The values for quartz and calcite are in satisfactory agreement with those reported by Pringsheim and Rosen and by R. W. Wood respectively.

1. *Introduction.*

Soon after the announcement of the discovery[1] of the Raman effect in a great variety of substances and in different physical states including that of a crystalline solid, detailed studies of the phenomenon were undertaken at Calcutta[2] and elsewhere. Using a spectrograph of large light-scattering power, Mr. I. Ramakrishna Rao[3] photographed the effect in ice and quartz, and found also that it could not be observed in rock-salt. It appeared that more satisfactory spectrograms would be obtained with the larger dispersion provided by a Hilger E_2 spectrograph. In addition to quartz[4] and calcite which have also been examined about the same time by other investigators (Landsberg and Mandelstam, Pringsheim and Rosen and R. W. Wood) the present author has studied also the cases of topaz and selenite. Some photographs were also taken with ice, but the results with this substance are reserved for separate publication.

2. *Experimental Methods and Results.*

The experimental arrangements were exactly the same as those described in earlier papers. The light from a 3000 c. p.

[1] C. V. Raman, Indian Journal of Physics, Vol. 2, p. 387 (1928).

[2] C. V. Raman and K. S. Krishnan, Indian Journal of Physics, Vol. 2, p. 399 (1928); Proc. Roy. Soc., A, Vol. 122, p. 23 (1929).

[3] I. Ramkrishna Rao, Ind. Jour. of Physics, Vol. 3, p. 123 (1928).

[4] A preliminary report on quartz was published in 'Nature' Vol. 122, p. 506 (1928).

mercury arc was concentrated on the crystal and the transversely scattered light was photographed with a Hilger E_2 spectrograph. The specimen of crystalline quartz used in the investigation was in the form of a large sphere and was kept immersed in a water bath. In the case of calcite and topaz (yellow Brazilian) which were in their natural form, a bath of liquid benzene was used to minimise reflection from the natural faces of the crystals. For selenite, however, which was available as a very large crystal no bath was considered necessary.

The actual spectrograms are reproduced in Plate II. The wave-lengths of the Raman lines appearing in the spectrum of the scattered light were calculated by simple interpolation from the known wave-lengths of the mercury lines also appearing in the spectrum. These values are exhibited in the following tables (I-IV) along with the wave-lengths of the incident mercury lines which respectively excite them. The difference in frequency between the exciting mercury line and any of the Raman lines produced by it is of course equal to a characteristic frequency of the medium, and the last columns in the tables give the characteristic frequencies so calculated. The values for the different crystals are collected together in Table V where their equivalent infra-red wavelengths are also given.

TABLE I.

Crystalline Quartz ($Si O_2$).

Exciting mercury lines.			Raman lines.			Difference in Wave-numbers.
Wave-length in A. U.	Wave-number per cm.	Intensity.	Wave-length in A. U.	Wave-number per cm.	Intensity.	
4046·6	24705	100	4012·9	24913	1 (Broad)	−208
			4025·9	24832	1	−127
			4067·4	24579	3	126
			4124·0	24241	5	464
4077·8	24516	30	4099·3	24388	1	128
			4156 3	24053	1	463
4339·2	23039	15	4427·8	22578	1	461
4347·5	22995	30	4437·3	22530		465
4358·3	22938	200	4272·0	23402	1	−464
			4319·8	23143	1	−205
			4332·6	22811	3	127
			4397·9	22732	4 (Broad)	206
			4409·6	22671	1	267
			4437·3*	22530		408
			4448·5	22473	8	465
			4589·9	21781	1	1157

TABLE II.

Calcite ($CaCO_3$).

Exciting mercury lines.			Raman-lines.			Difference in Wave-numbers.
Wave-length A. U.	Wave-number per cm.	Intensity.	Wave-length A. U.	Wave-number per cm.	Intensity.	
4046·6	24705	100	4092·8	24426	2	279
			4231·8	23624	3	1081
4358·3	22938	200	4386·5	22791	2 very broad	147
			4411·8	22660	2	278
			4510·0	22167	very feeble.	771
			4575·0	21852	2	1086

* The Raman line at λ 4437·3 corresponding to a shift of 465 wave-numbers from the mercury line λ 4347·5 which excites it, is broad whereas the Raman lines corresponding to the same shift excited by the other mercury lines are sharp Presumably the breadth indicates the presence of another line at this place excited by λ 4358·3.

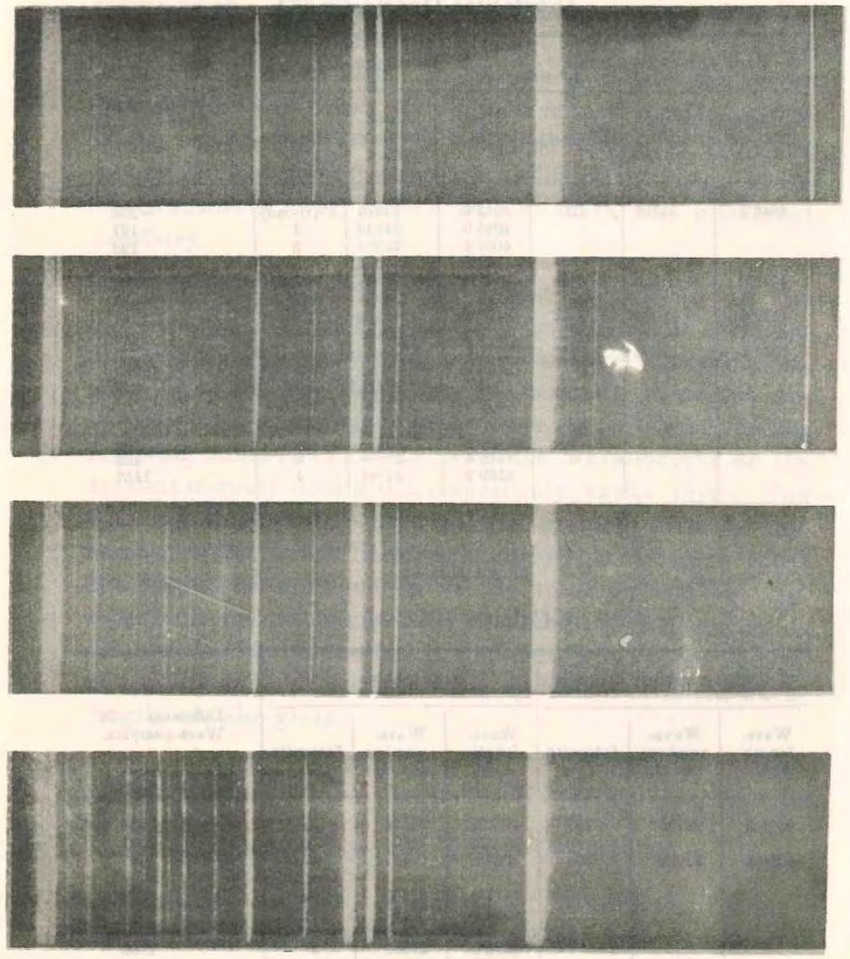

Raman Spectra of Crystals.
(a) Hg spectrum, *(b)* quartz, *(c)* calcite, *(d)* selenite.

TABLE III.

Topaz [$(Al.F)_2 SiO_4$]—yellow.

Exciting mercury lines.			Raman-lines.			Difference in Wave-numbers.
Wave-length A.U.	Wave-number per c.m.	Intensity.	Wave-length A.U.	Wave-number per c.m.	Intensity.	
4046·6	24705	100	4226·7	23652	Extremely feeble.	1053

TABLE IV.

Selenite (crystalline gypsum—$CaSO_4+2H_2O$).

Exciting mercury lines.			Raman-lines.			Difference in Wave-numbers.
Wave-length A.U.	Wave-number per cm.	Intensity.	Wave-length A.U.	Wave-number per cm.	Intensity.	
3650·1	27389	100	3789·8	26379	falls on an incident line.	1010
			3908·4	26250	1	1139
			4141·6	24138	1	3251
			4167·4	23989	5 diffuse.	3400
			4185·0	23888	1 diffuse.	3501
4046·6	24705	100	4219·7	23692	6	1013
			4241·5	23570	1	1135
			4655·3	21475	1	3230
			4691·3	21310	5 diffuse.	3395
			4711·5	21219	1 diffuse.	3486
4358·3	22938	200	4558·7	21930	4	1008
			4583·9	21809	1	1129

TABLE V.

Characteristic infra-red wave-lengths.

Quartz.		Calcite.		Topaz.		Selenite	
Wave-number.	Wave-length in μ.	Wave-number.	Wave-length in μ.	Wave-number.	Wave-length in μ.	Wave-uumber.	Wave-length μ.
1157	8·64	1084	9.22	1053	9·5	3493	2·86
464	21·5	771	13			3397	2·94
(?)408	24·5	279	35·8			3240	3·09
267	37·4	147	68			1134	8·81
206	48·5					1011	9·89
127	79						

3. *Discussion of Results.*

Among the spectrograms reproduced in this paper that of scattering by selenite is of special interest on account of the relatively large intensity of the Raman lines. These lines of selenite fall into two distinct groups. The first group consits of a strong line corresponding to the infra-red wave-length 9·89μ and a feeble line accompanying it corresponding to 8·81μ. These can be easily indentified as being due to the SO_4^{--} group in the crystal. Sulphuric acid and aqueous solutions of several sulphates have recently been investigated for their modified scattering by S. K. Mukherjee[5] and P. N. Sengupta and by S. Venkateswaran [6] and all of them are found to exhibit a Raman line corresponding to 10·2μ, which may therefore be taken as the characteristic frequency of the SO_4^{--}

[5] Proc. Indian Science Congress, Madras Session, 1929.
[6] In course of publication.

group. In selenite, as a result of the influence of the regularity of packing in the crystal the above line apparently splits into two (9·89μ and 8·81μ), besides being slightly shifted away from the exciting line.

The second group of Raman lines in selenite scattering is much further removed from the exciting line, and consists of a strong and fairly well-defined line corresponding to 2·94μ accompanied by two fainter lines one on either side of it corresponding respectively to 3·09μ and 2·86μ. The author has investigated the scattering by a large block of ice and the fact that it gives rise to Raman lines in very nearly the same positions as above, the relative intensities of these lines also being comparable, immediately suggests that this group in selenite must be attributed to its water of crystallization. Water also in the liquid state shows a broad Raman band in approximately the same position, the band itself though not resolved into lines, showing a distinct structure. This points to the influence of the crystal structure not only on the positions of the Raman lines but also on their sharpness.

That water retains its identity when it enters the crystal as water of crystallization is significant and is in conformity with the generally accepted ideas regarding its nature.

The influence of crystal structure on the characteristic molecular frequencies has been mentioned. The question naturally arises whether there may not be frequencies characteristic of the crystal as a whole and not of the individual molecules constituting it. The entire absence of any Raman lines in the scattered spectrum of *amorphous* quartz recently reported by Prof. Pringsheim throws some light on this point. Also the present author has studied the scattering by crystalline quartz at about 130°C. and finds that the Raman lines get very diffuse, thus showing that the thermal agitations of the atoms in the crystal tend to destroy the sharpness of the natural frequencies. It seems therefore probable that they are characteristic of the crystal as a whole.

However, very much longer exposures than those given by Prof. Pringsheim for amorphous quartz would be necessary in order to reveal modified radiations, if any, present in the form of very diffuse bands or as a general continuous spectrum, and experiments are in progress to test this point.

Whatever origin may be assigned to these characteristic frequencies of the medium, one would have expected that corresponding to each Raman line in the scattered spectrum there would be a peak in infra-red absorption and similarly a maximum in the metallic reflection in the same region, the relative values of the peaks at different characteristic frequencies showing at least a rough parallelism with the intensities of the corresponding Raman lines in the scattered spectrum. As has been shown in our previous papers, though there is in general a correspondence between the Raman lines and the infra-red absorption spectrum, it does not seem to hold always. The case of crystalline quartz affords a striking example of such a discrepancy, since the Raman line corresponding to the wave-length 8·5μ which is very prominent in infra-red reflection from the crystal, is so feeble that only in well exposed plates it is detectable at all. Further experiments on a large number of substances for which infra-red data are available, will be necessary in order to determine the exact nature of the relation between the intensities of the different Raman lines and those of the corresponding absorption maxima in the infra-red.

Department of Physics,
University of Dacca,
23rd January, 1929

The Influence of Molecular Form and Anisotropy on the Refractivity and Dielectric Behaviour of Liquids.

By K. S. Krishnan, Reader in Physics, University of Dacca, Dacca, India.

(Communicated by Sir Venkata Raman, F.R.S.—Received October 17, 1929.)

1. *Introduction.*

Recent investigations on the diffraction of X-rays by liquids throw considerable light on their molecular structure. One conspicuous result that emerges out of these investigations is that when the molecules are asymmetric in shape, as in general they are, their average distribution around any given molecule in the liquid is far from being spherically symmetrical with respect to it.* When the medium is under the influence of an electric field, the well-known Lorentz polarisation field acting on any given molecule, arising from the polarisation of the surrounding ones, will then naturally vary with the orientation of the exciting field with respect to the molecule. Independent evidence for such an "anisotropy" of the polarisation field is forthcoming when we correlate the measurements on electric double-refraction and on light-scattering in the liquid state with the corresponding values for the same substance in the state of vapour.† The general mathematical theory of refraction by dense media which takes into account this anisotropy of the polarisation field, has been developed in a recent paper.‡ It is proposed in the present communication to discuss the theory outlined in that paper in its relation to actual experimental results, confining ourselves mainly to one typical case, viz., benzene, for which accurate measurements are available for the various physical quantities appearing in the expressions.

2. *The Theory of Refraction.*

If we consider any given molecule in the medium, when the distribution of the surrounding molecules about it may be taken to be spherically symmetrical, the polarisation field acting on it is evidently equal to $\frac{4\pi}{3}\chi E$, where E is the

* See C. M. Sogani, 'Ind. Jour. Phys.,' vol. 2, p. 97 (1928).

† C. V. Raman and K. S. Krishnan, 'Roy. Soc. Proc.,' A, vol. 117, p. 1 (1927); 'Phil. Mag.,' vol. 5, p. 498 (1928).

‡ C. V. Raman and K. S. Krishnan, 'Roy. Soc. Proc.,' A, vol. 117, p. 589 (1928).

field in the medium and χ is the average optical susceptibility of the medium per unit volume, *i.e.*, the total moment induced per unit field per unit volume. ($\chi = (n^2 - 1)/4\pi$, n being the refractive index.) If, on the other hand, the average distribution is not spherically symmetrical, let $p_1\chi E$, $p_2\chi E$, $p_3\chi E$ be the values of the polarisation field when the incident field E is acting respectively along the three principal *optic* axes of the molecule;

$$p_1 + p_2 + p_3 = 4\pi. \tag{1}$$

In this case the final expression for the refractivity of the liquid—which it would be sufficient to quote here—comes out as

$$\frac{n^2-1}{n^2+2}\cdot\frac{1}{\nu} = \frac{C}{1-\nu\Phi}, \tag{2}$$

where

$$C = \tfrac{4}{3}\pi \cdot \tfrac{1}{3}(b_1 + b_2 + b_3), \tag{3}$$

and

$$\Phi = \tfrac{1}{3}(b_1\sigma_1 + b_2\sigma_2 + b_3\sigma_3), \tag{4}$$

b_1, b_2, b_3 being the moments induced in a molecule in the vapour state by unit field of the incident light-wave, acting respectively along its three optic axes, ν being the number of molecules per unit volume, and the σ's being given by the relations

$$p_1 = \frac{4\pi}{3} + \sigma_1, \quad p_2 = \frac{4\pi}{3} + \sigma_2, \quad p_3 = \frac{4\pi}{3} + \sigma_3. \tag{5}$$

Obviously from (1)

$$\sigma_1 + \sigma_2 + \sigma_3 = 0. \tag{6}$$

When the polarisation field is isotropic, the three σ's separately vanish and consequently also Φ, and relation (2) reduces, as it should, to the well-known Lorentz formula.

3. *Evaluation of the Constants.*

For the vapour state where the molecules are sufficiently rare, relation (2) reduces to

$$n - 1 = 2\pi\nu \cdot \tfrac{1}{3}(b_1 + b_2 + b_3), \tag{7}$$

which enables us to calculate $b_1 + b_2 + b_3$. The expression for the depolarisation of the light transversely scattered by the vapour, viz.,

$$r = \frac{6[(b_1-b_2)^2 + (b_2-b_3)^2 + (b_3-b_1)^2]}{10(b_1+b_2+b_3)^2 + 7[(b_1-b_2)^2 + (b_2-b_3)^2 + (b_3-b_1)^2]} \tag{8}$$

where r is the ratio of the intensities of the principal components, the incident light being supposed to be unpolarised, supplies a second relation connecting the optical constants of the molecule.

When the molecule may be assumed to possess an axis of symmetry, as in the case of benzene at least as an approximation, we get the necessary third relation, say,

$$b_1 = b_2, \tag{9}$$

and thus the b's are separately evaluated.

Regarding the constants of the polarisation field which appear in the expression for Φ, the different methods of calculating them are discussed in detail elsewhere,* and it will be sufficient here to mention that they yield fairly concordant results. For the purpose of our present paper, however, we use the values calculated from light-scattering data not only because they are the most reliable, but the calculation does not require any specific knowledge of the *origin* of the anisotropy of the polarisation field. We have for the liquid

$$r = 6\nu F/(3kT\beta\chi^2 + 7\nu F) \tag{10}$$

where

$$F = \tfrac{1}{30}[(b_1' - b_2')^2 + (b_2' - b_3')^2 + (b_3' - b_1')^2], \tag{11}$$

$$b_1' = b_1(1 + p_1\chi), \quad b_2' = b_2(1 + p_2\chi), \quad b_3' = b_3(1 + p_3\chi); \tag{12}$$

k is the Boltzmann Constant per molecule, T is the absolute temperature, and β is the isothermal compressibility. As before, $\chi = (n^2 - 1)/4\pi$.

Hence from the known values of the above constants and of the refractive index n (for which an approximate value will suffice here, calculated from the refractivity for the vapour, say, by using the Lorentz relation), the value of F may be calculated from (10) for any given temperature of the liquid.

For the benzene molecule when it is assumed as an approximation to possess an axis of symmetry, $p_1 = p_2$, and the expression for F simplifies to the form

$$\begin{aligned} F &= \tfrac{1}{15}(b_1' - b_3')^2 \\ &= \tfrac{1}{15}\left[(b_1 - b_3) + \frac{n^2-1}{4\pi}(b_1p_1 - b_3p_3)\right]^2 \end{aligned} \tag{13}$$

since b_1, b_3 and F are known, using again the approximate value for n, (13) becomes an equation connecting p_1 and p_3. With the help of relation (1), viz., $2p_1 + p_3 = 4\pi$, p_1 and p_3 may be evaluated.

4. *Refractivity in the Vapour and Liquid States.*

Very careful measurements on the refractivity of benzene have been made recently by Wasastjerna† with the specific object of determining accurately

* K. S. Krishnan and S. R. Rao, 'Ind. Jour. Phys.,' vol. 4, p. 39 (1929).

† 'Soc. Sci. Fenn., Phys.-Math.,' vol. 2, No. 13 (1924).

its change as the substance passes from the state of vapour to that of liquid, and they are therefore of particular interest for our present discussion. Using sodium light, he gets for the refractivity of the vapour $n - 1 = 0{\cdot}001821$ per atmosphere at 0° C. (This corresponds to a gram molecular refractivity of 27·20.) Using (7) we obtain from this value

$$2b_1 + b_3 = 32{\cdot}14 \times 10^{-24}. \qquad (14)$$

The polarisation of the light scattered by benzene vapour has been measured by Cabannes and Granier and by Rao, and they get identical values for r, viz., 0·0420; after correcting for the deviations from Boyle's law, Rao gives the value as 0·0445.*

The optical properties of the benzene molecule have been discussed by Ramanathan† in relation to its structure, and he has shown that the optical susceptibility of the molecule along its axis of symmetry is less than in perpendicular directions, *i.e.*, the optical ellipsoid of the molecule is an oblate spheroid of revolution; $b_1 = b_2 > b_3$.

Using relation (8) we get from the above value of r

$$b_1/b_3 = b_2/b_3 = 1{\cdot}98_3$$

and hence

$$b_1 = b_2 = 12{\cdot}83 \times 10^{-24}$$

$$b_3 = 6{\cdot}47 \times 10^{-24}$$

We now come to the calculation of the constants of the polarisation field. Light scattering by liquid benzene has also been investigated by Cabannes and Granier, and they get the following values‡:—

Table I.

Temperature ° C.	16.	50.	60.
r	0·420	0·390	0·375

In expression (2) neglecting $\nu\Phi$ in comparison with unity, we get as a first approximation for the refractive index of the liquid at 20° C., $n = 1{\cdot}525$, and using this approximate value in (10) and (13), and taking r at 20° C. as $0{\cdot}41_7$ from the above table, we obtain $p_1 = p_2 = 3{\cdot}06$, $p_3 = 6{\cdot}45$, and hence $\nu\Phi = -0{\cdot}031$. In view of (2) this signifies that the molecular refractivity

* See J. Cabannes, 'La diffusion moléculaire de la lumière,' Paris, 1929, p. 88.
† 'Roy. Soc. Proc.,' A, vol. 110, p. 123 (1926).
‡ See Cabannes, *loc. cit.*, p. 184.

for the liquid at 20° C. is less than the value for the vapour by 3·1 per cent., and would thus give for the refractive index of the liquid the value 1·506. Using this value of n as a *second* approximation in the calculation of p_1 and p_3, we obtain $p_1 = 2{\cdot}93$, $p_3 = 6{\cdot}71$, and hence

$$\nu\Phi = -0{\cdot}036.$$

This indicates a diminution of molecular refractivity of 3·6 per cent. as we pass from the vapour to the liquid at 20° C. This agrees almost exactly with the diminution of 3·8 per cent. experimentally obtained by Wasastjerna—his values for the gram-molecular refractivities for the vapour and liquid being respectively 27·20 and 26·18 (for sodium light).

Speaking in terms of refractive index, our calculated value comes out as 1·503 as against 1·525 calculated on the basis of the Lorentz formula, while the observed value is 1·501.

5. *Variation with Temperature.*

Any theory of refraction in order to be acceptable must predict successfully the dependence of the refractive index on temperature and pressure, since here the Lorentz formula is known to fail conspicuously. We therefore proceed to discuss these variations.

On differentiating (2) we obtain for the temperature coefficient of refractive index

$$\frac{dn}{dt} = -\frac{(n^2-1)(n^2+2)}{6n}\frac{\alpha - \nu\frac{d\Phi}{dt}}{1-\nu\Phi}, \qquad (14)$$

instead of the Lorentz expression

$$\frac{dn}{dt} = -\frac{(n^2-1)(n^2+2)}{6n}\alpha; \qquad (15)$$

where α is the coefficient of thermal expansion defined by $\alpha = -\frac{1}{\nu}\frac{d\nu}{dt}$. Also in (14)

$$\frac{d\Phi}{dt} = -\tfrac{1}{3}(b_1 - b_3)\frac{d\sigma_3}{dt} \qquad (16)$$

and thus dn/dt can be readily calculated when we know the variation of the constants of the polarisation field with temperature.

From the values of r at different temperatures exhibited in Table I we find on calculation that σ_3 decreases from 2·55 at 16° C. to 2·20 at 50° C.

Assuming the variation to be uniform over this range of temperature, we get roughly

$$\frac{d\sigma_2}{dt} = -0{\cdot}010,$$

and taking for α the value 0·001208, we obtain

$$\frac{dn}{dt} = -6{\cdot}14 \times 10^{-4} \text{ per degree Centigrade.}$$

The experimental values obtained by different investigators (taken from Landolt-Börnstein tables) vary from $-6{\cdot}13 \times 10^{-4}$ to $-6{\cdot}50 \times 10^{-4}$.

On the other hand, if we calculate on the basis of the Lorentz expression (15), taking for n the observed value of 1·501, we get

$$\frac{dn}{dt} = -7{\cdot}15 \times 10^{-4} \text{ per 1° C.}$$

But strictly speaking, we ought to use for n not the observed value but the value calculated by the Lorentz formula from the vapour state; if we do so, the failure of the Lorentz expression (15) becomes even more striking, because it then gives

$$\frac{dn}{dt} = -7{\cdot}56 \times 10^{-4} \text{ per 1° C.}$$

6. *Dependence on Pressure.*

Just as in the previous case, by differentiating (2) with respect to pressure we obtain

$$\frac{dn}{dp} = \frac{(n^2-1)(n^2+2)}{6n} \frac{\beta + \nu \frac{d\Phi}{dp}}{1 - \nu\Phi} \tag{17}$$

in place of the Lorentz expression

$$\frac{dn}{dp} = \frac{(n^2-1)(n^2+2)}{6n} \beta, \tag{18}$$

where β is the compressibility, given by $\beta = \frac{1}{\nu}\frac{d\nu}{dp}$.

We have no means of directly ascertaining the variation of Φ with pressure since light-scattering has not been investigated at different pressures. (In fact the accurate measurement of the dependence of r on pressure will involve very difficult experimental technique.) It is not, however, difficult to evaluate $d\Phi/dp$ in an indirect way. From what has been suggested in the introduction regarding the origin of the anisotropy of the polarisation field, viz., as arising

from the asymmetric shape and close packing of the molecules, one would naturally expect the constants of the polarisation field to depend only on the density of packing, the temperature as such having no influence. In that case we would have $\frac{d\Phi}{dt} \Big/ \frac{d\Phi}{dp} = -\frac{\alpha}{\beta}$, from which, in view of (14) and (17), we would obtain the relation

$$\frac{dn}{dt} \Big/ \frac{dn}{dp} = -\frac{\alpha}{\beta}, \tag{19}$$

That this is actually the case will be evident from Table II. It includes almost all the liquids for which we have accurate values for the compressibility, and for the temperature and pressure variations of refractive index.

Table II.*—For the D Line, at 20° C.

Liquid.	$-\frac{dn}{dt} \times 10^4$. calculated from Lorentz formula (15).	$-\frac{dn}{dt} \times 10^4$ observed.	$\frac{dn}{dp} \times \frac{\alpha}{\beta} \times 10^4$.
Acetone	5·66	5·46 (— ? —) 5·30 (0°–45°)	5·35
Carbon bisulphide	9·33	8·10 at 20° C.	8·34
Chloroform	6·30	5·88 (10°–20°)	5·92
Ethyl ether	6·16	5·86 (8°–21°)	5·69
Methyl alcohol	4·26	3·80 for C line 4·0 for F line	3·98
Ethyl alcohol	4·30	4·04 (8°–38°)	4·00
n-Propyl alcohol	4·01	3·86 (0°–45°)	3·73
Toluene	6·26	5·66 at 20° C.	5·63
Chlorobenzene	6·07	5·48 (9·6°–89·2°) 5·4 (— ? —)	5·40
Nitrobenzene	5·62	5·08 (25°–38°)	5·00

* The values used for the compressibility were mostly Tyrer's ('Journ. Chem. Soc.,' vol. 105, p. 2534 (1914)); those for dn/dp were taken from Röntgen and Zehnder, ('Wied. Ann.,' vol. 44, p. 22 (1891)), Himstedt and Wertheimer ('Ann. Physik,' vol. 67, p. 395 (1922)), and Eisele ('Ann. Physik,' vol. 76, p. 396 (1925)); and those for the other constants were taken from the standard tables. Both β and dn/dp refer to *isothermal* compression. The numbers within brackets in column 3 indicate the range of temperature used for determining dn/dt. In calculating on the basis of the Lorentz formula (column 2) the observed values of n have been used throughout.

The values given in columns 3 and 4 agree well among themselves,* though they differ considerably from those in column 2. This shows that in all cases the variation of Φ with temperature as such, if any, is negligible in com-

* That the small discrepancies should be due to experimental errors is suggested by the fact that the deviations are on both sides.

parison with its variation due to the change in density accompanying the temperature change.

Coming back to benzene, it naturally follows from the foregoing discussion that since the proposed expression gives the correct value for dn/dt it must necessarily also give the correct value for dn/dp; the actual calculated value is

$$\frac{dn}{dp} = 4{\cdot}87 \times 10^{-5} \text{ per atmosphere,}$$

while the experimental value obtained by Röntgen and Zehnder is $5{\cdot}06 \times 10^{-5}$. With these may be compared the values $5{\cdot}66 \times 10^{-5}$ and $5{\cdot}99 \times 10^{-5}$ calculated on the basis of the Lorentz formula, the former being obtained when the observed refractive index of the liquid is used in the calculation and the latter when the value corresponding to the molecular constants in the vapour state is used.

7. *Dielectric Constant of Benzene.*

All the foregoing discussions regarding refractive index are also applicable to the dielectric constant, provided the molecules do not possess any permanent electric moment, *e.g.*, benzene. We shall briefly state here the results of the calculation for this case.

In the vapour state we do not have any measurement of the dielectric constant of benzene which is sufficiently accurate for our present discussion. The latest measurement, as far as the writer is aware, seems to be that of Pohrt* (1913) who obtained for the vapour at 100° C.

$$\epsilon = 1{\cdot}00274$$

the last digit being correct to ± 1. We are not therefore justified in attaching to it the same weight as to Wasastjerna's measurements of refractivity in the vapour. Nevertheless even the approximate value is interesting as $\frac{\epsilon - 1}{\epsilon + 2} \cdot \frac{1}{\nu}$ calculated on this basis comes out about 5 per cent. higher than the value for the liquid, the difference being of the order of magnitude suggested by the theory.

Coming to the variation with temperature

$$\frac{d\epsilon}{dt} = -\frac{(\epsilon - 1)(\epsilon + 2)}{3} \frac{\alpha - \nu \frac{d\Phi}{dt}}{1 - \nu\Phi}, \qquad (20)$$

* 'Ann. Physik,' vol. 42, p. 583 (1913).

where Φ would have practically the same value as for the optical case, and we thus obtain on calculation

$$\frac{d\epsilon}{dt} = -18{\cdot}9 \times 10^{-4} \text{ per } 1° \text{ C.}$$

as against the experimental value of $-19{\cdot}8 \times 10^{-4}$ very recently obtained by Hartshorn and Oliver.* The Lorentz expression on the other hand, even using for ϵ in the calculation the observed value, gives

$$\frac{d\epsilon}{dt} = -22{\cdot}2 \times 10^{-4} \text{ per } 1° \text{ C.}$$

Similarly our proposed formula gives for $d\epsilon/dp$ the value $14{\cdot}9 \times 10^{-5}$ per atmosphere as against $17{\cdot}6 \times 10^{-5}$ given by the Lorentz expression, while the experimental value of Cagniard†, viz., $1{\cdot}39 \times 10^{-10}$ per dyne per square centimetre corresponds to $14{\cdot}1 \times 10^{-5}$ per atmosphere.

8. *Conclusion.*

We may collect here for convenience the various numerical results obtained.

Table III.—For Benzene at 20° C.

	According to Lorentz formula.	According to proposed formula.	Observed.
For sodium light—			
n	1·525	1·503	1·501
$\frac{dn}{dt} \times 10^4$	−7·15, −7·56	−6·14	−6·13 to −6·50
$\frac{dn}{dp} \times 10^5$	5·66, 5·99	4·87	5·06
$\frac{d\epsilon}{dt} \times 10^4$	−22·2	−18·9	−19·8
$\frac{d\epsilon}{dp} \times 10^5$	17·6	14·9	14·1

It is significant that the calculation of n, which involves a knowledge of the *absolute* value of r for the liquid which is known accurately, gives a value which leaves nothing to be desired. On the other hand, the calculations of the variations of n with temperature and pressure involve a knowledge of the *variation* of r with temperature, the experimental values for which are not so

* 'Roy. Soc. Proc.,' A, vol. 123, p. 664 (1929).
† 'Comptes Rendus,' vol. 183, p. 873 (1926).

reliable, and it is therefore not surprising that the agreement in these cases with the observed values is not as good as might be desired; we have very little doubt that, when sufficiently accurate measurements for the temperature coefficient of r are forthcoming, the agreement will be better. In any case the improvement over the Lorentz formula is quite evident; it may be pointed out in this connection that the modification of the Lorentz theory underlying the present paper has not been proposed *ad hoc*, but follows as a necessary consequence of the ideas suggested by entirely independent considerations, viz., investigations on X-ray diffraction, light-scattering and electric double-refraction in the liquid state.

Summary.

The theory of the optical and electrical properties of liquids outlined in a paper by Raman and Krishnan is here applied to the case of benzene for which the necessary data are available. The deviations from the Lorentz refraction formula are, according to the theory, the effect jointly of the non-spherical shape of the molecule which results in the local polarisation field being anisotropic, and of the optical anisotropy of the molecule itself. Data on light-scattering by benzene and its variation with temperature furnish the constants appearing in the formulæ. The change in the Lorentz refraction "constant" in passing from vapour to liquid, and the effect of temperature and pressure variations on the same "constant" are successfully evaluated numerically, in satisfactory agreement with experiment. The application of the theory to the dielectric behaviour of liquid benzene is equally successful.

Are Black Soap Films Birefringent?

By

K. S. Krishnan,

Reader in Physics, Dacca University.

(*Received for Publication, 2nd July, 1929.*)

(Plate X)

Abstract.

In view of the recent investigations of Perrin and others on the structure of stratified soap films, we should expect them to be optically birefringent, behaving as uniaxial crystals with their optic axes perpendicular to their surfaces. The present paper contains a discussion of some unpublished observations by Sir C. V. Raman on soap bubbles of various thicknesses placed between crossed Nicols in monochromatic light, which were undertaken in the hope of finding some evidence of such birefringence. It is found that the optical behaviour of black soap bubbles stands in marked contrast with that of thicker bubbles which display vivid colours. For example, while the edge of the black bubble as seen through crossed Nicols is intensely luminous, the portions inside being more or less dark, with thicker bubbles the edge is actually darker than the portions of the bubble further from the margin. Also, while in the case of the black bubble, a slight rotation of the analysing Nicol from exact crossing destroys the possibility of observing the dark cross except at the vicinity

of the luminous edges, with the thicker bubbles the dark cross persists in the form of the familiar hyperbolic isogyres even after a considerable rotation of the analyser. These and other differences in the optical behaviour of thin and thick bubbles are discussed and it is shown that these differences are just what we should expect from bubbles of *isotropic* material having their respective thicknesses; and they give us no information regarding the optical anisotropy or otherwise of black bubbles.

1. *Structure of Soap Films.*

It is well-known from the recent work of Perrin[1] that stratified soap films can exist which are built up of discrete layers of the same thickness. Starting with the thinnest film which reflects very little light and which consists of only one such layer, as we go on adding layer after layer, the reflected light exhibits in succession different stages of blackness, becoming lighter and lighter until it is more or less white, and then passes through straw-yellow, orange-red and dark-red of the first order, to violet and other colours of the second order. In one typical experiment with a film of potassium oleate solution, Perrin was able to count as many as forty layers having a total thickness of 2150 A.U., seventeen, of thickness 920 A.U., corresponding to the different blacks and greys, another seventeen of the same thickness corresponding to reflection of colours of the first order, and the remaining six, 310 A.U. thick, exhibiting second order colours. Perrin's observations thus give for the fundamental thickness of the unit layer the value 54-52 A.U. These results have been fully confirmed by Wells[2] whose more accurate measurements, however, give for

[1] J. Perrin, Ann. de Physique, Vol. 10, p. 160 (1918). For an excellent account of this films, see Sir William Bragg's discourse before the Royal Institution, Jan. 16, 1925, reprinted in "Nature."

[2] P. V. Wells, Ann. de Physique, Vol. 16, p. 69 (1921).

the thickness of the unit layer the slightly smaller value of 42 A.U.

The above lamellar structure has also been verified by an entirely different method by de Broglie and Friedel,[1] who have studied the diffraction of monochromatic X-rays by thin films of sodium, potassium and ammonium, oleate solutions. They obtain in each case three well-defined rings, whose radii and relative intensities suggest that they are the first, second and third order diffraction spectra, corresponding to a regular spacing of 43·5 A.U. between two adjacent layers. This value is in excellent agreement with that of Wells.

Perrin has also suggested that the material of the unit layer is not the oleate itself, but oleic acid formed by its hydrolysis. From the investigations of Langmuir, Hardy, Adam and others on the spreading of monomolecular oil films on water, it is well-known that in the case of the long chain fatty acids, the effective area of spreading is independent of the length of the chain, and is determined only by its cross section, leading to the conclusion that the acid molecules stand out perpendicular to the surface, presumably with their active carboxyl ends attached to the water molecules on the surface. With oleic acid, the thickness of the film has been estimated by this method at about 23 A.U. From the fact that this is just half the thickness of the unit soap film, it has been suggested that the latter consists of two such layers of oleic acid molecules, the molecules of each layer being packed side by side, with their lengths perpendicular to the surface, and being joined to the molecules of the other layer by their active carboxyl ends which meet at the centre; at the two outer surfaces of the double layer, the molecules present only their inactive methyl ends.

Such a structure in the first place fits well with the physical properties of soap films, *e.g.*, the stability, the abnor-

[1] M. de Broglie and F. Friedel, Comptes Rendus, Vol. 176, p. 708 (1923).

mal surface tension, the ease with which one layer can slide over another, etc. Secondly it is fully supported by the results of the X-ray investigation of the long chain fatty acids in the crystalline state, where also the molecules appear in double-layers of the type suggested above for the unit soap film. The stability of the double layer, as strikingly contrasted with the feeble binding between one double layer and its neighbour, is evidenced also in the crystals by their flakiness. Again the spacing between these double-layers has in the case of oleic acid, approximately the same value as in the soap film, *viz.*, 36 A.U.

In view of these and other considerations which we refrain from discussing here,[1] the molecular structure of the unit soap film described above may be taken to be well established.

2. *The Birefringence and its Investigation.*

The regular orientation of the molecules of the soap film postulated by the above structure will evidently render the film doubly refracting. Investigations on light-scattering by the earlier members of the fatty acids definitely point to an optical anisotropy of the molecules, their polarisability along their lengths being about 10 to 20% more than for perpendicular directions. That is to say, in the soap film where all the molecules are oriented with their axes perpendicular to the surface, if we neglect their mutual influence, the refractivity for vibrations normal to the plane of the film will be correspondingly greater than for vibrations in the plane. Their mutual influence would of course reduce to some extent the above value of the ratio of the refractivities in the two directions; still the ratio would differ appreciably from unity the film behaving as a positive uniaxial crystal with its optic

[1] For detailed discussion, see Bragg, *loc. cit.*

axis perpendicular to the surface. It would therefore be of interest to study the behaviour of soap-films of various thicknesses under polarised light.

The usual method of examining uniaxial crystalline plates cut perpendicular to the optic axis, "under convergent light" between crossed Nicols, is however not applicable to these films owing to their extreme thinness. A little calculation shows that even at very large angles of incidence, the path difference between the ordinary and extraordinary rays is only a very small fraction of a wave-length. It would, therefore, be more convenient to use parallel monochromatic light and study the restoration of light produced by introducing a soap film between two crossed Nicols at various large angles of incidence. But the method would enable us to study the transmission for only one angle at a particular setting, and from this point of view a fairly large spherical bubble would be much more advantageous, since the restoration of light by the different portions of the bubble would correspond to various angles of incidence, and the transmission pattern would give a complete picture of the dependence of the restoration on the angle of incidence.

In the following few pages are recorded some hitherto unpublished observations by Sir C. V. Raman with spherical soap bubbles and a discussion of them by the present writer undertaken at his instance.

3. *Thick Soap Bubbles in Polarised Light.*

A quartz mercury vapour lamp with a collimating lens and a green ray filter furnishes an intense beam of monochromatic light. Two large Nicols are employed, the first to polarise the beam, and the second as analyser. Between the two is placed a soap bubble, about 2 cms. in diameter blown from a solution of sodium oleate in water thickened by glycerine. The bubble rests on the top of the thin glass

tube from which it is blown, and drains slowly. When the Nicols are crossed, the bubble exhibits a dark cross whose arms are parallel to the planes of the polarisation of the two Nicols, and in addition a number of rings, the form and position of which depend on the thickness of the film and the degree of its uniformity. A thick and uniform soap bubble gives a large number of symmetrical rings. (See, for instance, Figs. 7, 8 and 9 in Plate X.) Non-uniform films show an unsymmetrical system of bands abutting on the edge of the bubble which then presents a curious appearance of being serrated instead of being spherical in shape. Thin uniform bubbles show relatively few rings (Figs. 5 and 6 in the plate), or even merely a dark cross on a bright field covering the whole bubble (Fig. 4). These phenomena simulate the effects due to a uniaxial crystal in convergent polarised light. They do not however indicate any birefringence of the film, but arise from the ordinary colours of thin films taken together with the rotation of the plane of polarisation of light which occurs in its passage through an obliquely held transparent plate. (A thin glass bubble shows the same phenomena.) This explanatian is readily shown to be correct by rotating the analysing Nicol a little one way or the other, when the dark cross transforms itself into two hyperbolic arcs lying in one or other of the opposite pairs of quadrants according to the position of the analysing Nicol, as shown in Diagram 1.

Diagram 1.

These arcs are the loci of points on the surface of the bubble in passing through which the plane of polarisation of the

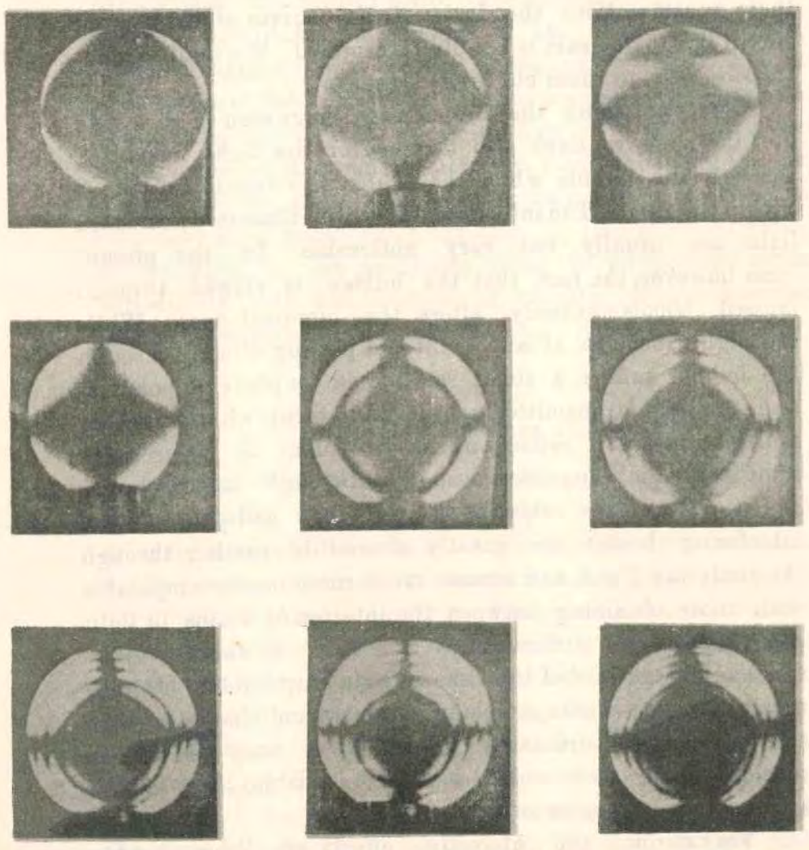

Figs. 1, 2, 3.

Figs. 4, 5, 6.

Figs. 7, 8, 9.

Soap Bubble between Crossed Nicols

transmitted light is rotated through equal angles. The rotation is zero for rays passing normally through the bubble and increases with increasing obliquity of incidence. It is zero for the planes of incidence which are either parallel or perpendicular to the plane of polarisation of the incident light, and maximum in a plane making 45° with either. From these considerations the form of the curves of darkness as shown in the diagram is readily interpreted. We shall, in what follows, refer to these curves as isogyres.

For explaining the interference rings seen in Figs. 5 to 9 of the plate, we have also to consider the light trasmitted through the bubble which has suffered internal reflections within the film. The interferences of thin films in transmitted light are usually not very noticeable. In the present case however, the fact that the bubble is viewed through crossed Nicols entirely alters the circumstances. While the light incident at any point and passing directly through the bubble suffers a small rotation in its plane of polarisation, the light transmitted at the same point after suffering multiple internal reflections has its plane of polarisation rotated in the *opposite* sense and through much larger angles. Hence the relations of amplitude and phase of the interfering beams are greatly altered in passing through the analysing Nicol, and become much more nearly comparable with those obtaining between the interfering beams in light *reflected* from the surfaces of a thin film. In fact the interferences in transmitted light shown by a soap bubble between crossed Nicols are comparable in vividness and character with the interferences ordinarily shown by a soap bubble in *reflected* light. The colour-sequence in white light indeed appears to be the same as in the latter case.

Very curious and interesting effects are observed when a moderately thick soap bubble is viewed in monochromatic light between crossed Nicols, and the plane of the analysing Nicol is swung through a small angle one way or the other.

The isogyres are then seen in approximately the same positions as in the case of a soap bubble which is too thin to show interference rings, but they are observed to become alternately less and more perfectly dark as they cross the successive bright and dark interference curves. If the latter are not very close together, as in moderately thin bubbles, the isogyres even appear distorted in form. These effects may be interpreted as due to the interference of the direct and multiply reflected beams of light causing a fluctuation in the state of polarisation of the transmitted light as we pass from point to point along the surface of the bubble. As the direct and multiply-reflected pencils emerging from the film are not polarised in the same way, and as they differ in phase, an ellipticity must result which involves an imperfect extinction of the light by the analysing Nicol to an extent varying periodically with the thickness of the film, thus accounting for the phenomena noticed above.

4. *Effects with Thin Bubbles.*

As the film drains a black spot forms at the top and gradually extends downwards so as to cover half or even more of the surface of the bubble until the latter finally bursts. The remarkable effect that is observed is the development of an intensely luminous crescent or a spherical boundary to the "black" portion of the bubble. This has its maximum brightness at angles making 45° with the planes of the polariser and analyser. The dark cross persists appearing as an interruption of the luminosity of the edge. Reproduced in Fig. 3 of the plate we have a photograph of these effects, the "black film" covering about one-fourth of the area of the bubble at the top. In Fig. 2 the "black film" has extended so as to cover half the bubble, and in Fig. 1 it includes quite three-fourths of the entire surface.

The luminosity of a "black bubble" as seen through crossed Nicols is most intense in a narrow region near the spherical edge where the light passes very obliquely through the film. Careful inspection shows, however, that the luminosity extends inwards, though feebly, to an appreciable extent, and that if the Nicols are exactly crossed, it is possible to make out the dark cross as an interruption in a faintly luminous background covering the entire area of the "black film." A very small rotation of the analysing Nicol one way or the other, however, destroys the possibility of observing the existence of the dark cross except in the vicinity of the luminous edges of the bubbles where it can be seen even if the two Nicols are not accurately set for extinction of the transmitted light.

Very interesting results are observed if a spherical bubble is initially blown so thin as not to show any interference-rings and the development of the "black spots" in it is watched with the Nicols not quite exactly crossed, so that instead of a dark cross we have two curved isogyres in the field. When a "black spot" moves over the surface of the bubble, it appears as a darker area on a brighter background, except when it passes over an isogyre, when its optical character reverses, and it appears as a *bright spot on a dark background*. This effect is so conspicuous that when the black spots are numerous and nearly cover a hyperbolic arc, the latter altogether loses its character as a dark curve on a bright background. When such is the case, the isogyres are visible (as a dark cross) only if the Nicols are *exactly crossed* but disappear more or less completely when the analysing Nicol is rotated through a small angle in either direction.

It should be emphasised that the appearance of a luminous crescent over the edge of the bubble as shown in Figs. 1 to 3 in the plate, is essentially a phenomenon characteristic of the "black bubble." With thicker bubbles of the kind illustrated in Figs. 4 and 5, the edge of the bubble instead of

being luminous, is actually darker than the portions of the bubble further from the margin. This cannot be made out from Figs. 4 and 5, as the dark edges naturally merge into the surrounding dark field. If the analysing Nicol be turned round very considerably so as to make the field surrounding the bubble quite luminous, then the dark edges of the bubble become easily visible. It stands in marked contrast with the behaviour of the edge of the "black bubble" which instead of being dark is intensely luminous and actually diffracts light through large angles.

5. *Transmission by an Isotropic Spherical Shell.*

From what has been described in the two previous sections it is evident that the "black" soap bubble exhibits under polarised light certain characteristic features which are not observed with thicker bubbles. The question naturally arises whether these characteristics are merely a consequence of their extreme thinness or whether they may be interpreted as indicating a birefringence of the black films as contrasted with the isotropic nature of thicker films. In order to be able to answer this question, it would be useful to calculate the transmission between crossed Nicols by a sherical bubble of *isotropic* material.

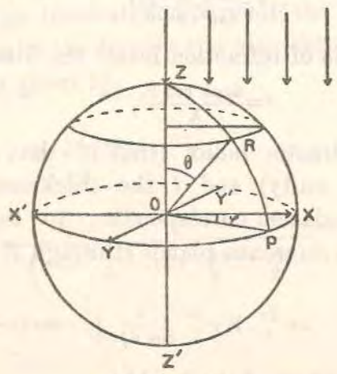

DIAGRAM 2.

Let ZO (see Diagram 2) be the direction of propagation of the parallel beam of polarised light incident on the spherical bubble having O for its centre, the direction of vibration being along the X-axis (positive along OX). Let us consider a small element of area on the surface of the bubble at a point R whose polar co-ordinates are θ, ϕ (OZ corresponding to the axis $\theta=0$, and ϕ being measured from the plane ZOX). If the incident vibration be represented by $a\,e^{i\omega t}$ at points on the tangential plane through Z, we can resolve it into two components :—

(1) $a\cos\phi\,e^{i\omega t}$ vibrating in the plane ZOP, *i.e.*, in the plane of incidence on the element of area at R;

(2) $a\sin\phi\,e^{i\omega t}$ vibrating perpendicular to the plane of incidence.

Considering first the vibration in the plane of incidence, it is easily shown that the ray through R, when it has reached the XY-plane after transmission through the front pair of surfaces of the bubble, can be represented by

$$a\cos\phi\,\frac{1-r_{\parallel}^{\,2}}{1-r_{\parallel}^{\,2}\,e^{-i\delta}}\cdot e^{i(\omega t-\epsilon)} \qquad \ldots\ (1)$$

where

$$r_{\parallel}=\frac{\tan(\theta-\theta_1)}{\tan(\theta+\theta_1)} \qquad \ldots\ (2)$$

θ_1 being the angle of refraction inside the film, and

$$\delta=\frac{4\pi\mu t\cos\theta_1}{\lambda} \qquad \ldots\ (3)$$

μ being the refractic index (that of the outside medium being taken as unity) and t the thickness of the film.—ϵ is the phase retardation corresponding to the path traversed between the two reference planes (through Z and O). In fact

$$\epsilon=\frac{2\pi}{\lambda}\cdot R+\frac{2\pi}{\lambda}\,\frac{t}{\cos\theta_1}\,\{\mu-\cos(\theta-\theta_1)\} \qquad \ldots\ (4)$$

where R is the radius of the bubble.

When the same ray has reached the tangential plane through Z', after passing through also the back pair of surfaces of the bubble, it can be represented by

$$a\cos\phi\,\left(\frac{1-r_{\parallel}^{\,2}}{1-r_{\parallel}^{\,2}\,e^{-i\delta}}\right)^2\cdot e^{i(\omega t-2\epsilon)} \qquad \ldots\ (5)$$

This expression can be rewritten in the form

$$a\cos\phi\cdot k_{\parallel}\,e^{i(\omega t-2\epsilon)}\,e^{-i.2\chi_{\parallel}} \qquad \ldots\ (6)$$

where

$$k_{\parallel}=\frac{(1-r_{\parallel}^{\,2})^2}{(1-r_{\parallel}^{\,2})^2+4r_{\parallel}^{\,2}\sin^2\frac{\delta}{2}} \qquad \ldots\ (7)$$

$$\text{and } \chi_{\parallel}=\tan^{-1}\left(\frac{r_{\parallel}^{\,2}\sin\delta}{1-r_{\parallel}^{\,2}\cos\delta}\right). \qquad \ldots\ (8)$$

After passing through the crossed analyser, which transmits vibrations only along the Y axis (taken positive along OY), the amplitude of the vibration will be given by

$$a\sin\phi\cos\phi\,k_{\parallel}\,e^{i(\omega t-2\epsilon)}\cdot e^{-i2\chi_{\parallel}}. \qquad \ldots\ (9)$$

Similarly starting with the second component of the incident light, vibrating *perpendicular* to the plane of incidence, its amplitude after transmission through the front and back pairs of surfaces of the bubble and also through the crossed analyser, will be given by

$$-a\sin\phi\cos\phi\cdot k_{\perp}\,e^{i(\omega t-2\epsilon)}\,e^{-i2\chi_{\perp}} \qquad \ldots\ (10)$$

where

$$k_{\perp}=\frac{1-r_{\perp}^{\,2}}{\left(1-r_{\perp}^{\,2}\right)^2+4r_{\perp}^{\,2}\sin^2\frac{\delta}{2}} \qquad \ldots\ (11)$$

$$r_{\perp}=\frac{\sin(\theta-\theta_1)}{\sin(\theta+\theta_1)} \qquad \ldots\ (12)$$

$$\text{and } \chi_{\perp} = \tan^{-1}\left(\frac{r_{\perp}^{2}\sin\delta}{1-r_{\perp}^{2}\cos\delta}\right). \qquad \ldots \quad (13)$$

Evidently ϵ has the same value as for the parallel component.

Combining vibrations (9) and (10) we obtain for the intensity of transmission through the crossed analyser, of the small bundle of rays under consideration (defined by the coordinates θ, ϕ),

$$I = a^{2}\sin^{2}\phi\cos^{2}\phi\left[k_{\parallel}^{2} + k_{\perp}^{2} - 2k_{\parallel}k_{\perp}\cos 2\left(\chi_{\perp} - \chi_{\parallel}\right)\right]. \quad \ldots \quad (14)$$

The point, R′ say, on the photographic plate to which this value of the intensity corresponds is easily determined. Let O′ be the centre and ρ the radius of the *image* of the bubble on the plate, and OX, OY the traces of the transmission axes of the polarising and analysing Nicols. Then $O'R' = \rho \sin\theta$; and the angle $R'O'X = \phi$. Thus (14) supplies a general expression for the illumination at various points on the transmission pattern.

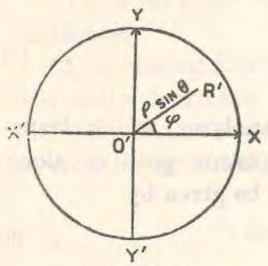

Diagram 8.

I being proportional to $\sin^2\phi\cos^2\phi$, the pattern is symmetrical with respect to the axes of the Nicols, these axes corresponding to zero illumination. For a given distance from the centre, the illumination is obviously a maximum for the diagonal positions ($\phi = 45°$, etc.).

The azimuthal variation of intensity does not, however, interest us here and we proceed to discuss directly the dependence on the distance from the centre, *i.e.*, the dependence on θ which arises from the factor inside the square brackets in (14). Taking $\theta = 1{\cdot}46$ (the refractive index of oleic acid liquid) the values of I/a^2 have been calculated for the diagonal positions ($\phi = 45°$) for various values of θ and also for different

thicknesses of the bubble. The calculated values are given in Table I. I/a^2 is obviously the ratio of the observed intensity of transmission to the intensity which would be observed if the bubble were removed and the analyser rotated through 90°, so as to have its axis parallel to that of the polariser; in the table it is expressed as a percentage.

TABLE I.

Radial distribution of intensity for the diagonal positions.

$\frac{I}{a^2} \times 100$

Thickness θ=	60°	70°	75°	80°	85°	88°	89°	90°
42 A. U. (=1 unit layer of soap film)	0·0	0·1	0·2	0·6	2·1	6·7	6·2	0
84 A. U. (=2 unit layers)	0·2	0·5	0·9	2·0	5·5	4·8	...	0
168 A. U. (=4 unit layers)	0·6	1·5	3·0	5·3	6·7	1·8	...	0
252 A. U. (=6 unit layers)	1·3	3·2	5·0	7·1	5·2	0·6	...	0
420 A. U. (=10 unit layers)	2·7	5·7	7·1	6·6	2·1	...	...	0
840 A. U. (=20 unit layers)	5·1	7·2	6·1	3·1	0·4	...	...	0
1260 A. U. (=30 unit layers)	5·6	7·0	5·0	2·0	0·2	...	...	0
1680 A. U. (=40 unit layers)	5·0	7·2	5·5	2·3	0·3	...	...	0

One significant result emerges from the values exhibited in the above table, *viz.*, that in the case of *black* bubbles the illumination is confined practically to the edge of the bubble. It is true that theoretically the illumination at the edge itself is zero. But this has no practical significance since the

smallest shift towards the centre gives a large restoration of light. For example for the thinnest film (of 42 A.U.) for a deviation of 1° from the edge the illumination is as high as 6%. When we remember that in the image of the bubble obtained on the photographic plate the distance from the centre is proportional to sin θ which changes very slowly when θ is in the neighbourhood of $\pi/2$, it is directly evident that for the black bubble the illumination must be confined mostly to the extreme edge, and it must fall off as we proceed towards the centre. On the other hand in the case of films sufficiently thick to exhibit vivid colours (consisting of say 20 to 40 unit layers) it is also clear that the region of maximum illumination shifts appreciably towards the centre, the portions adjoining the edge being more or less dark.

Thus the luminous crescent actually observed at the edge of black films, as contrasted with the dark edge of thicker films which exhibit colours, follows as a necessary consequence of their difference in thickness.

6. *Effect of Rotating the Analyser.*

We now proceed to discuss the influence of rotating the analysing Nicol on the restoration of light, again confining ourselves to the case of an isotropic spherical shell. For this purpose it is simpler to adopt the method indicated in Section 3 of considering *separately* the directly transmitted ray, and the ray which is transmitted at the same point after multiple internal reflections. Originally we have an incident polarised beam the components of whose amplitude parallel and perpendicular to the plane of incidence are respectively $a\cos\phi$ and $a\sin\phi$. After transmission through both the front and back pairs of surfaces of the bubble, it can conveniently be split up into the following components :—

(1) The ray transmitted *directly* by both the front and back films. Its principal components, parallel and

perpendicular respectively to the plane of incidence, are $a\cos\phi\,(1-r_{\parallel}{}^{2})^{2}$ and $a\sin\phi(1-r_{\perp}{}^{2})^{2}$. Its plane of polarisation is inclined at an angle $\phi_1-\phi$ to the plane of polarisation of the incident light, where

$$\tan\phi_1=\tan\phi\times\frac{(1-r_{\perp}^{2})^{2}}{(1-r_{\parallel}{}^{2})^{2}}.$$

Since $r_{\perp}>r_{\parallel}$, $\tan\phi_1$ is always less than $\tan\phi$; *i.e.*, the rotation of the directly transmitted light is towards the plane of incidence.

(2) The ray transmitted directly through one of the films (front or back) and after two internal reflections by the other. Its phase is behind that of (1) by δ. The principal components of its amplitude are $a\cos\phi\times r^{2}_{\parallel}(1-r^{2}_{\parallel})^{2}$ and $a\sin\phi\times r^{2}\perp(1-r^{2}\perp)^{2}$ respectively. Its plane of polarisation is therefore inclined at an angle $\phi_2-\phi$ to that of the incident light, where

$$\tan\phi_2=\tan\phi\,\frac{r^{2}_{\perp}(1-r^{2}_{\perp})^{2}}{r^{2}_{\parallel}(1-r^{2}_{\parallel})^{2}}$$

and the rotation will be in the same direction as the rotation of the directly transmitted ray [*viz.*, (1)] or in the opposite direction, according as $\frac{r^{2}_{\perp}(1-r^{2}_{\perp})^{2}}{r^{2}_{\parallel}(1-r^{2}_{\parallel})^{2}}$ is less than or greater than, unity.

(3) the ray transmitted after two internal reflections in either of the films, or directly through one of them and after 4 internal reflections inside the other, and so on.

Case A.—*Angle of incidence less than 60°.*

Let us first consider values of θ less than 60°. Both $r_{\perp}$ and $r_{\parallel}$ are small compared with unity and the amplitude of (2) is much smaller than that of (1). (Even for $\theta=60°$ it

is only about 9% ; for $\theta = 45°$ it is $5\frac{1}{2}$% ;) that of (3) is of course still smaller. It might therefore appear at first sight that the restoration of light when the bubble is viewed through the analyser would be given to a first approximation by that due to (1) alone, *i.e.*, to the directly transmitted beam alone. Thus one might suppose that when the analysing Nicol is swung over a small angle from its position for exact crossing, there will be more or less complete extinction at those points at which the rotation of the directly transmitted beam is the same as that of the analyser. But a moment's consideration will immediately convince us that this is not wholly true. As already indicated in Section 3, for the values of θ we are considering, the rotation of (2) is much larger (and in the opposite direction) than that of (1). In fact it almost approaches the limiting value of $\pi/4$ since the parallel component is practically extinguished even by two internal reflections. This larger rotation tends to compensate for its smaller amplitude, when viewed through the crossed analyser. That the contributions from (1) and (2) are actually comparable is evident from a simple calculation. Taking for example $\phi = 45°$ and $\theta = 60°$, the amplitude of (2) is only about 9% of that of (1) ; and since there are two such rays they give together an amplitude of about 18%. But their rotation is as large as 44° as compared with 10° of the directly transmitted beam in the opposite direction ; 18% of sin 44° is equal to 0·13 which is almost of the same magnitude as sin 10° (=0·17). Similarly when $\theta = 45°$, the combined amplitude of both the rays of type (2) is only 11% of that of (1), but the rotation of its plane of polarisation is $39\frac{1}{2}$° as compared with the $4\frac{1}{2}$° of (1). Thus the restoration between crossed Nicols depends as much on (2) as on (1), its actual value depending markedly on the phase difference δ between the two. Since their resolved amplitudes are thus comparable, the minimum value of the intensity of restoration may reach very small values as compared with the maximum.

(The minimum occurs when (1) and (2) are in the *same* phase, since their rotations with respect to the plane of polarisation of the incident light are in opposite directions.) This is exactly why under crossed Nicols we observe very vivid colours in white light transmission (Section 3) and also why the interference rings in monochromatic light are very distinct. Also in the latter case when the analyser is rotated slightly the illumination inside the isogyre fluctuates appreciably on crossing the interference rings. Again the same effect also explains the distorted appearance of the isogyre, when the interference rings are very sparse. In fact the contribution from (2) to the restored light stands out conspicuously in the case of very thin films, because for these films the restoration depends to a marked extent on the thickness. In the case of the blackest film for which δ is practically zero, when the analyser is crossed, (1) and (2) which are in the same phase, but rotated in opposite directions, would practically cancel each other out, and hence for the values of θ under considerations there would be no restoration of light, which is in agreement with the rigorous calculation of the previous section. In this case a slight rotation of the analyser towards quenching the contribution from the directly transmitted light, instead of diminishing the intensity in the field of view, would actually *increase* it. It would thus be impossible to observe the dark isogyres with such thin films, except when the Nicols are exactly crossed. This is also in agreement with observation.

On the other hand when we go to thicknesses of the order of say 30 layers (just too thin to exhibit vivid coloms) δ approaches π, and (1) and (2) together would compound into a plane polarised beam rotated with respect to the plane of polarisation of the incident light by about *twice* the angle over which (1) alone is rotated, and in the same direction. Of course the absolute value of the rotation will be very different for different points on the film. On rotating the

analyser we would naturally get the familiar dark isogyre, its position depending on the angle of rotation of the analyser.

This is doubtless the explanation of the apparently anomalous phenomenon described in Section 4 which is observed when we start with a soap bubble too thin to exhibit any interference rings, and watch the development of black spots in it with the analyser not exactly crossed. When a black spot appears on the isogyre it would naturally appear bright against a dark back-ground, because as we have seen, the small rotation of the analyser from the crossed position tends to increase the illumination of the "black film," whereas at the isogyre the thicker film itself is more or less completely dark.

Case B.—*Large angles of incidence.*

For very large angles of incidence, say about 80°, the rotation of component (2) is in the *same* direction as that of (1), and is also comparable with the latter in magnitude. But their amplitudes are also comparable, so that here again we are not justified in neglecting the component transmitted after multiple internal reflections.

Since in this case the planes of polarisation of (1) and (2) are rotated in the same direction, for the black film for which δ is very small, their amplitudes resolved along the axis of the analyser will reinforce each other and thus give strong restoration at the edge of the black bubble ; though as we have seen, for smaller values of θ for which (1) and (2) are rotated in opposite directions they cancel each other out by interference thus producing darkness. This is evidently in accordance with the results of the rigorous calculation for the black bubble given in the previous section and also agrees with actual observation.

Since for values of θ approaching $\pi/2$ (1) and (2) are rotated in the same direction, by a very slight rotation in this

direction, of the analyser from exact crossing we may be able to see the dark isogyre near the edges of the black bubble ; even though for smaller values of θ for which the rotations of (1) and (2) are in opposite directions, no trace of the isogyre could be detected. This again is in conformity with observation.

On the other hand for films sufficiently thick to exhibit colours (say 30 layers) the amplitudes of (1) and (2) are of opposite sign and are comparable in magnitude, and since near the edge their rotations are in the same direction and also comparable, the observed darkness at the edges of such bubbles is readily understood. Also it is evident that they would continue to be dark even after a considerable rotation of the analysing Nicol from its crossed position, while the portions of the bubble sufficiently removed from the edge will considerably brighten up, as well as the back ground surrounding the bubble ; and hence the darkness of the edges of such bubbles is rendered very conspicious by a rotation of the analysing Nicol from its crossed position. This is also in agreement with observation.

7. *Conclusion.*

From the foregoing discussion it follows that all the essential features observed with black soap bubbles under polarised light, which distinguish them from thicker bubbles, are merely direct consequences of their extreme thinness, and they do not give us information regarding the optical anisotropy or otherwise of black films.

Department of Physics.
University of Dacca, June 1929.

Pleochroism and Crystal Structure.

In a very important paper (*Phil. Mag.*, vol. 33, p. 521; 1917), Silberstein developed a theory of molecular refractivity based on the idea that the electric doublets induced by the field of the light wave in the atoms composing the molecule influence each other, the result of such atomic interaction largely depending on their relative distances and the geometric form of the molecule. One important consequence of Silberstein's theory, namely, that gaseous molecules should in general be optically anisotropic, is supported by observation, and has been worked out in detail by Ramanathan, Havelock, and others; it also forms the basis of W. L. Bragg's well-known and successful attempt to compute theoretically the birefringence of the solid carbonates and nitrates from their known crystal structure.

In the present note we desire to direct attention to another important consequence of Silberstein's theory, namely, that atomic interaction induces pleochroism in ions or molecules: such pleochroism would become accessible to observation when they are regularly oriented as in a crystal. In a recent paper (*Ind. Jour. Phys.*, vol. 4, p. 1; 1929), Sir C. V. Raman and S. Bhagavantam have indeed suggested that the colour and pleochroism of solid organic compounds arise in this way. We have made some observations on the absorption of *polarised ultra-violet light* in crystals of sodium and potassium nitrates which appear to be very significant in this connexion.

It is known from the X-ray evidence that the NO_3 ions form a plane structure normal to the trigonal axis in sodium nitrate and to the pseudo-hexagonal axis ('c' axis) in potassium nitrate. We have found that the selective absorption at about 3000 A. which appears in aqueous solutions of the nitrates manifests itself in the solid crystals only when the vibrations are in the plane of the NO_3 ions; vibrations of this frequency perpendicular to the plane of the NO_3 ions are freely transmitted by the crystals. Further, beyond about 2600 A. begins another region of strong absorption in the crystals which is also polarised in the same direction as the 3000 A. band. It is also found that while the refractive index of the ordinary ray shows a rapid increase even in the visible region with diminishing wave-length, the corresponding increase in that of the extraordinary ray is much slower. These observations taken together with W. L. Bragg's work on the birefringence of the nitrates appear to indicate that the basic ideas of Silberstein's theory are substantially valid.

K. S. Krishnan.
A. C. Dasgupta.

Physics Laboratory,
Dacca University,
Dacca, May 19.

Das magnetische Verhalten von Ammoniummanganosulfat-Hexahydrat bei niedrigen Temperaturen.

Von K. S. Krishnan in Dacca.

(Eingegangen am 2. Juni 1931.)

Die kürzlich von Jackson und de Haas ausgesprochene Vermutung, daß die magnetischen Momente des Mn^{++}-Ions im Ammoniummanganosulfatkristall sich mit der Richtung ändern, beruht auf Rechenfehlern. In Wirklichkeit verhält sich der genannte Kristall in wesentlich derselben Weise wie andere paramagnetische Kristalle.

Zahlreiche Messungen über die magnetische Suszeptibilität der Einzelkristalle des Siderits ($FeCO_3$) sind von Foëx[1]) ausgeführt worden. Das gleiche hat Jackson[2]) an einigen paramagnetischen Sulfaten und Doppelsulfaten untersucht. Diese Messungen zeigen, daß innerhalb einer weiten Temperaturspanne die drei hauptsächlichen spezifischen Suszeptibilitäten eines paramagnetischen Kristalls durch folgende Gleichungen von Weiss

$$\chi_i = \frac{C}{T - \Theta_i}, \quad i = 1, 2, 3,$$

dargestellt werden können. Diese Gleichungen legen die Auffassung nahe, daß Θ und daher auch das innere Weisssche Feld in dem Kristall für die drei magnetischen Achsen verschiedene Werte annimmt, während die Curiesche Konstante C bei Messungen in den verschiedenen Richtungen dieselbe bleibt. Beide Ergebnisse, die Konstanz von C und die Abhängigkeit des Θ von der Richtung, sind leicht verständlich und waren wohl zu erwarten.

Dagegen lassen die Ergebnisse einiger Messungen an Ammoniummanganosulfat [$MnSO_4 \cdot (NH_4)_2 SO_4 \cdot 6H_2O$] bei niedrigen Temperaturen, über die Jackson und de Haas kürzlich berichtet haben[3]), einen ganz anderen Ursprung der magnetischen Anisotropie dieses Kristalls vermuten. Nach ihnen soll die hauptsächliche spezifische Suszeptibilität in diesem Falle durch die Curiesche Relation

$$\chi_i = \frac{C_i}{T}, \quad i = 1, 2, 3,$$

[1]) G. Foëx, Ann. de phys. **16**, 174, 1921.
[2]) L. C. Jackson, Phil. Trans. Roy. Soc. (A) **224**, 1, 1923; **226**, 107, 1927.
[3]) L. C. Jackson u. W. J. de Haas, Proc. Amsterdam **31**, 846, 1928.

dargestellt werden. Das molekulare Feld scheint dabei für alle drei Achsen zu verschwinden, während die Curiesche Konstante eine deutliche Abhängigkeit von der Richtung zeigt. Tatsächlich entsprechen den drei magnetischen Achsen die folgenden Werte: 34,7, 29,4 und 22,2 Weisssche Magnetonen. Daß C mit der Richtung des wirksamen magnetischen Feldes in dem Kristall sich ändern sollte, ist sehr überraschend, vor allem wenn das molekulare Feld verschwindet. Es ist schwer verständlich, weshalb das Verhalten von Ammoniummanganosulfat so wesentlich verschieden sein sollte von dem der anderen Doppelsulfate, die, wie eingangs erwähnt, von Jackson untersucht worden sind. Auch wenn dasselbe Gesetz der Abhängigkeit von der Temperatur bis zur Zimmertemperatur aufrechtzuerhalten wäre, so würde es eine sehr beträchtliche Anisotropie für den Kristall erwarten lassen, da das Maximum der Suszeptibilität mehr als das Doppelte ihres Minimums beträgt, während tatsächlich bei gewöhnlichen Temperaturen der Unterschied zwischen Maximum und Minimum weniger als 1% ihrer absoluten Werte ausmacht[1]).

Im Hinblick auf die Schwierigkeiten, zu denen die Ergebnisse von Jackson und de Haas führen, schien eine neuerliche Berechnung der Hauptsuszeptibilitäten dieses Kristalls auf Grundlage ihrer tatsächlichen experimentellen Daten wünschenswert. Tatsächlich wichen die Ergebnisse einer solchen Nachrechnung stark von denen ab, die die Autoren selbst gegeben haben, obwohl unsere Gleichungen mit den ihrigen identisch waren, woraus man auf einen Fehler in ihrer Berechnung schließen kann. Bei der großen theoretischen Bedeutung der Ergebnisse mag es nicht unangebracht sein, hier die nachberechneten Werte zu geben.

Ammoniummanganosulfat kristallisiert im monoklinen System. In der Tabelle 1 bezeichnen χ_1 und χ_2 die hauptsächlichen spezifischen Suszeptibilitäten in der symmetrischen Ebene des Kristalls, d. h. der b (010)-

Tabelle 1[2]).

T	$\chi_1 \cdot 10^6$	$\chi_2 \cdot 10^6$	$\chi_3 \cdot 10^6$	ψ
$20{,}3_5^0$ K	627	451	548	— 63° 39′
19,0	678	474	589	— 63 1
17,0	747	539	662	— 63 0
15,0	841	617	748	— 63 27

[1]) I. I. Rabi, Phys. Rev. **29**, 174, 1927.

[2]) Es mag darauf hingewiesen werden, daß die Messungen von Jackson und de Haas einzig und allein die Lage der magnetischen Achsen und die Werte der Hauptsuszeptibilitäten bestimmen, und daß entgegen ihrer eigenen Annahme bei der Deutung ihrer Messungen keinerlei Zweifel obwalten kann.

Ebene, und χ_3 bezeichnet den Wert an der dritten magnetischen Achse, d. h. der b-Achse. Die letzte Spalte der Tabelle gibt den Winkel ψ an, welchen die χ_1-Achse mit der c-Achse bildet, positiv gerechnet im Sinne des *spitzen* Winkels β zwischen der c- und der a-Achse[1]).

Wie aus der letzten Spalte ersichtlich ist, ist der Wert von ψ praktisch bei allen Temperaturen derselbe, d. h. die Lage der magnetischen Achsen ist unabhängig von der Temperatur: ein Ergebnis, das mit den Beobachtungen Jacksons an anderen Doppelsulfaten übereinstimmt.

Was nun die Werte der Hauptsuszeptibilitäten anlangt, so zeigt eine kleine Rechnung, daß sie durch die Gleichungen

$$\chi_i = \frac{C}{T - \Theta_i}$$

dargestellt werden können, also auf dieselbe Weise wie bei den anderen Kristallen, wo C die gleiche Konstante für alle Achsen ist. In der Tat ergibt sich für diesen Kristall 0,0112 als Wert von C, was einem Wert von 29,4 Weisschen Magnetonen entsprechen würde. (Bei den Temperaturen der vorliegenden Messungen kann die Korrektur für den Diamagnetismus des Moleküls vernachlässigt werden.) Dieser Wert ist genau der gleiche wie jener, den Cabrera[2]) bei Messungen von Mangano-Nitrat-, -Sulfat-, -Chloridlösungen erhalten hat. Ferner ist es interessant, daß das Moment des Mn^{++}-Ions, wenn wir nur die Drehmomente der fünf Elektronen in den äußersten unvollständigen Schalen in Betracht ziehen, $4{,}97 \cdot 2 \cdot \sqrt{\frac{5}{2}\left(\frac{5}{2}+1\right)} = 29{,}4$ Weissche Magnetonen beträgt, was vollständig mit dem oben erwähnten Wert übereinstimmt.

Was Θ anlangt, so sind seine Werte aus Tabelle 2 ersichtlich.

Tabelle 2.

T	Θ_1	Θ_2	Θ_3
$20{,}3_5^0$ K	2,5	— 4,6	0
19,0	2,5	— 4,6	0
17,0	2,0	— 3,8	0
15,0	1,7	— 3,2	0

Man sieht, daß die Werte von Θ_1 und Θ_2 nur für die ersten beiden Temperaturen konstant sind, dann aber zahlenmäßig heruntergehen, wenn

[1]) Wir verwenden ψ in der gleichen Weise wie Jackson und de Haas; gewöhnlich berechnet man allerdings ψ positiv im Sinne des *stumpfen* Winkels β. (Siehe W. Finke, Ann. d. Phys. **31**, 149, 1910.)

[2]) B. Cabrera, Journ. de phys. (6) **3**, 443, 1922.

wir zu niederen Temperaturen fortschreiten. Auch hierin wieder ähnelt es anderen paramagnetischen Kristallen, die den gleichen Typ „Kryomagnetischer Anomalie" bei niederen Temperaturen zeigen.

Ammoniummanganosulfat verhält sich also durchaus in wesentlich derselben Weise wie andere paramagnetische Kristalle, und wir haben keinen experimentellen Beweis für die Annahme, daß die magnetischen Momente des Ions in dem Kristall sich mit der Richtung ändern, wie dies der Artikel von Jackson und de Haas nahezulegen scheint.

Dacca, Physikalisches Laboratorium der Universität, 11. Mai 1931.

The Dispersion of Polarisation of Light-Scattering

BY

K. S. KRISHNAN AND AMALENDU SARCAR.

(Plate VI)

1. *Introduction.*

As is well-known, the birefringence of crystals shows a remarkable dependence on wave-length, increasing in general rapidly as we proceed towards the ultra-violet. For example in the case of calcite the value of $n_o - n_e$ which is only 0·172 for the D-lines of sodium (589 mμ) rises to 0·207 at 300 mμ and to 0·327 at 200 mμ, the last value being almost double the first. We should expect a similar dependence on wave-length also for the optical anisotropy of individual molecules, because according to the theory of Silberstein,[1] developed by Bragg,[2] Ramanathan [3] and others, the optical anisotropy of molecules arises from essentially the same causes as are responsible for the birefringence of crystals, *viz.*, the mutual interaction of the optical doublets induced in the component atoms by the incident light-wave. Since the depolarisation of the light transversely scattered by the molecules in the fluid state is a measure of their optical anisotropy, the depolarisation should then exhibit a large dispersion.

[1] L. Silberstein, Phil. Mag., Vol. 33, p. 521 (1917).
[2] W. L. Bragg, Proc. Roy. Soc. A, Vol. 105, p. 320 (1924).
[3] K. R. Ramanathan, Proc. Roy. Soc. A, Vol. 107, p. 684 (1925).

2. *Discussion of Earlier Measurements.*

Some early investigations carried out by one of us on a large number of liquids, using sun-light filtered through suitable coloured glasses, did not show any large dependence on wave-length.[4] These measurements, however, so far as the dependence on wave-length is concerned, must necessarily be taken as only preliminary, since in the first place the incident light was not *monochromatic*, the filters used transmitting fairly large regions of the spectrum, and secondly, no attempt was made to isolate the classical scattering from the Raman radiations which, as we now know, always accompany them; however, the general result is not likely to be affected by either of these considerations. Taking the latter effect first, the Raman scattering is very much feebler than the classical scattering, being according to recent estimates[5] only a small fraction of the latter (about one or two per cent.). Since the Raman scattering is in general also polarised in the same direction as the classical scattering, the value of the depolarisation of the latter is not likely to be affected much by its admixture. When we consider the *variation* of this value with the wave-length, the influence of the Raman scattering will be even smaller, since it increases with practically the same rapidity as the classical scattering with the diminution of the exciting wave-length.[6]

The want of perfect monochromatism of the incident light used in these experiments does not also seriously affect the result when it is negative, as it happens to be; all that is necessary for establishing the independence on wave-length being that the spectral regions transmitted by the different filters should widely differ from one another—which was actually the case.

[4] K. S. Krishnan, Phil. Mag., Vol. 50, p. 697 (1925).

[5] S. C. Sirkar, Ind. Journ. Phys., Vol. 5, p. 159 (1930).

[6] See C. V. Raman and K. S. Krishnan, Proc. Roy. Soc. A, Vol. 122, p. 23 (1929); Ornstein and Rekveld, Zeits. für Physik,, Vol. 61, p. 593 (1930); S. C. Sirkar, *loc. cit.*

Mr. P. V. Krishnamurthy[7] has repeated the investigation by a method which in principle is an improvement on the previous method. He uses light from a mercury arc as source and investigates the polarisation of the different mercury lines scattered by the liquid with the help of a nicol and a quartz spectrograph. The method besides enabling the depolarisation to be determined for any particular wave-length, also automatically eliminates the effect, if any, of the Raman radiations. Mr. Krishnamurthy has studied by this method five or six liquids and gets in all cases a considerable change of the depolarisation with wave-length, in striking contrast with our results mentioned. As he proceeds from the yellow towards shorter wave-lengths, the depolarisation at first diminishes to a minimum and rises rapidly as we proceed further, the value for the 3,650 group of lines of mercury being about one and a half times (or even more in some cases) the value for the visible regions. What is more remarkable, the region of minimum value for the depolarisation factor is practically the same for all the liquids studied by him, *viz.*, in the violet. That the optical anisotropy of the molecules should depend on the wave-length is understandable or probably even to be expected as we have already mentioned in the introduction, but that it should reach a minimum value in the violet for all the molecules and again rise as we proceed towards the ultra-violet, is rather surprising. Also his absolute values for the depolarisation factor for the visible region differ considerably from those obtained by other investigators.

More recently Szivessy and Dierkesmann[8] have investigated the dispersion of the electric double-refraction (Kerr-effect) of some liquids. As is well-known, the magnitude of this effect depends on the optical as well as the electrical

[7] Quoted by A. S. Ganesan and S. Venkateswaran, Ind. Journ. Phys., Vol. 4, p. 339 (1929).

[8] G. Szivessy and A. Dierkesmann, Ann. der Physik, Vol. 3, p. 507 (1929).

anisotropy of the molecules, as also on the refractive index of the medium.[9] Szivessy's results in all cases show a slight increase of the effect as we go to the ultra-violet which is *wholly* explicable as being due to the increased refractive indices of the liquids without any change in the optical or electrical anisotropy of the molecules in the liquid, thus supporting the results of our measurements as against Mr. Krishnamurthy's.

In view of the conflicting nature of the results given above and the theoretical importance of an accurate determination of the dispersion, it was thought that a thorough investigation of one typical substance like benzene, over a wide range of wave-lengths would be desirable. The present paper describes the results of such an investigation.

3. *Use of Spectrograph in Polarisation Measurements.*

The general principle involved in the usual method of determination of the polarisation of the scattered light for different wave-lengths with the help of the spectroscope is as follows. A narrow parallel beam of light traverses the liquid, say, in a horizontal direction. The spectrograph is adjusted so as to have the axis of its collimator horizontal and normal to the track in the liquid; in this position the light that gets into the spectrograph would be the one transversely scattered by the liquid. As we know, this is partially polarised, the direction of vibration of the polarised part being vertical. If now a nicol is introduced in front of the slit of the spectrograph in the path of the scattered light, by having its transmission axis vertical and horizontal respectively, either of the two components in the scattered light can be separately transmitted into the spectrograph. By photographing the two polarised spectra in juxtaposition, as can be easily done by using a suitable Hartmann diaphragm for the slit of the

[9] See C. V. Raman and K. S. Krishnan, Phil. Mag., Vol. 3, pp. 713 and 724 (1927).

spectrograph, the two intensities can be compared. Indeed by using a steady source of illumination and by suitably adjusting their relative times of exposure so as to obtain equality of density on the photographic plate for any given wave-length, their relative intensities for this wave-length can be calculated.

Evidently any part of the spectrograph which is likely to affect the intensities of the two principal vibrations *differently* has to be carefully studied and if its behaviour is uniform the instrument has to be calibrated for the polarisation induced by these parts.

The present measurements were made with a Hilger quartz spectrograph (their new 'All-Metal' instrument). For the purpose of calibrating it for polarisation, a 'pointolite' lamp fed from a storage battery of constant voltage, with a ground glass plate in front of it, was used as the source of light. When the lamp has been burning for some time, its intensity may be taken to be practically constant. On viewing it through a Savart plate backed by a suitably oriented nicol, no fringes were visible, showing that the source of light was perfectly unpolarised. It was mounted on the line of axis of the collimator of the spectrograph and at a large distance from it so as to illuminate the slit quite uniformly. A square ended nicol of large aperture served to polarise the light falling on the slit. That the slit was uniformly illuminated and that the source of light was also quite steady were tested by taking two spectrograms in juxtaposition, using the Hartmann diaphragm, under the same exposure, the orientation of the nicol being the same in both cases. It was hardly possible to distinguish the two halves.

Next, two spectrograms were taken also in juxtaposition but one of them with the nicol so oriented as to transmit only vertical vibrations and the other with the nicol transmitting horizontal vibrations. They are reproduced in Fig. 1

(Plate VI) where the upper half of the picture corresponds to vertical vibrations and the lower half to the horizontal. The intensities of the two halves are no more equal, thus pointing to an appreciable difference in transmission by the spectrograph of the two vibrations. What is curious, their relative intensities show an alternating fluctuation as we move along the spectrum. For the region at about 5500 A.U. —the extreme right of the picture—the horizontal vibration is much stronger than the vertical, and it tends to approach the latter as we go towards the violet, the two becoming equal at about 4400 A.U. Further beyond, the horizontal component again increases, the whole region up to about 3900 A.U. showing distinctly a larger intensity for the horizontal. Beyond this wave-length the intensities are reversed, the vertical being now stronger. The two again approach at about 3300 A.U., and for shorter wave-lengths the vertical is always the stronger. Their relative values are roughly represented by the curve in Fig. 3.

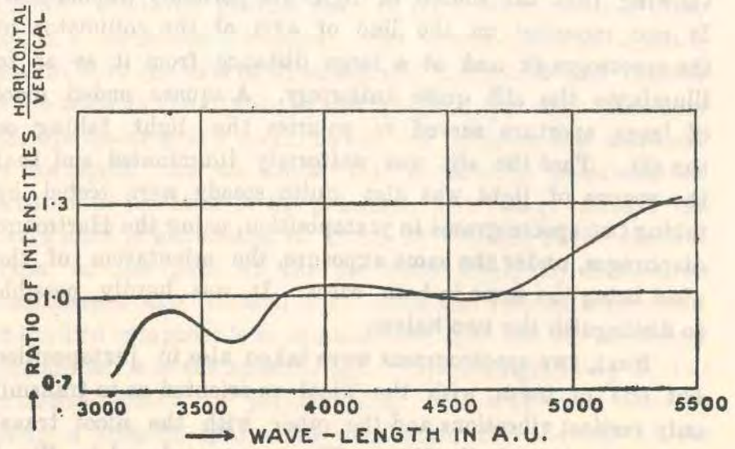

FIG. 3.

It would be of interest to locate the origin of the polarisation in the spectrograph. It is well-known that light on passage through narrow metallic slits are considerably polarised; but in the above experiment the slit was kept fairly wide, so that the polarisation due to the slit is eliminated. The only other obvious (at first sight) source of polarisation in the spectrograph would be the unequal reflection of the two components from the two faces of the prism. The vertical vibration would be more copiously reflected and would therefore be correspondingly feebler in transmission. But by itself this cannot account for the alternation in intensity actually observed, which suggests in addition some kind of rotation of the plane of polarisation of the light while traversing the spectrograph. That actually such a rotation takes place is shown by allowing plane polarised light to fall on the slit and analysing the light transmitted at the camera end. The latter is found to be elliptically polarised, its weaker principal component being however so much feebler than the stronger that it can be practically regarded as plane polarised. Its plane of polarisation is *widely* different for different wave-lengths.

It is not difficult to find the cause of this rotation since all the optical parts of the spectrograph are of crystalline quartz. First considering the prism, it is of the Cornu type consisting of two equal prisms of right- and left-handed quartz. For the ray for which the deviation by the prism is a minimum, the distance traversed in the two halves will be exactly the same and hence the rotations will compensate each other. Even for a wave-length for which the ray inside the prism deviates most from the previous track, calculation shows that the difference in thickness of right-handed and left-handed material traversed by it would, for prisms of the size used, be small even near the base; and the consequent rotation is only a few degrees. Thus the enormous rotations actually observed must be due to the lenses, and

are quite understandable since the rotation for quartz is about 21° per mm. for the D-line and very much more shorter wave-lengths. The rotation by the camera lens would not of course affect the relative intensities of the two components reaching the photographic plate, but that by the collimating lens would evidently determine the plane of polarisation at incidence on and emergence from the first and second prism faces respectively and hence the loss by reflection. The alternation in intensity observed on the photographic plate is a necessary consequence.

But this rotation would depend on what *part* of the collimating lens the ray is traversing ; experimentally the ratio of the two components transmitted does depend to some extent on the size of the aperture used in front of the camera lens and also on the position of the source of light in front of the spectrograph.

These limitations of the quartz spectrograph do not seem to have been recognised.

4. *Experimental Method adopted in the Present Measurements.*

From what has been said at the end of the last section it will be clear that the ratio of the intensities of the two vibrations, besides being different for different wave-lengths, also depends on the portion of the collimating lens of the spectrograph through which they traverse. This latter fact makes the calibration of the quartz instrument to some extent uncertain. Of course in a glass spectrograph or one of fused silica parts, the polarisation of the instrument for any given wave-length is exactly determinable. But the glass spectrograph can be used only over a limited range of the spectrum while fused quartz prisms and lenses are not usually available. For this reason it seemed desirable to use the ordinary quartz spectrograph and design a method of measurement which would be *independent of the polarisation of the instrument.*

The following experimental arrangement satisfies this condition. The principle of the method is essentially the same as in the well-known Cornu method of measuring partially polarised light which has been so frequently used in light scattering, with this difference, *viz.*, the scattered light after passage through the double image prism and nicol is analysed spectroscopically. A narrow horizontal beam of light from a mercury arc is sent through the liquid. The double image prism is placed in the path of the transversely scattered light and so oriented as to deviate in a vertical plane the rays passing through it. Immediately behind it is the nicol and further behind, a lens which focusses the two images of the track formed by passage through the double image prism, on the slit of the spectrograph. The two images will naturally fall one above the other crossing the length of the slit, and will correspond to vibrations in the scattered light which were initially vertical and horizontal respectively. On taking a spectrogram with the slit fairly open, a separate pair of tracks appears on the plate for each incident wave-length. By suitably rotating the nicol, the two tracks can be adjusted for equality of density on the photographic plate for any given mercury line and thus the depolarisation of the scattered light for the wave-length calculated. In Fig. 2, Plate VI, is reproduced one such picture (enlarged about $2\frac{1}{2}$ times) obtained with benzene liquid with an exposure of about 15 mins.

In this arrangement the window through which the scattered light passes from the liquid to the double image prism is of fused silica. All the other parts may be of *crystalline* quartz. Because in the first place the incident light being perfectly unpolarised, any lens or plate of crystalline material interposed normally in its path does not affect the nature of its polarisation. On the observation side also, *after leaving the nicol* the light corresponding to either of the two images of the track is plane polarised in the same direction determined by the orientation of the nicol, and hence any further passage

through either the crystalline lens used to focus them on the slit, or through the parts of the spectrograph will not affect their *relative* intensities. Thus the polarisation of the instrument is completely eliminated.

There are also other advantages in this arrangement. The source of light need not be steady, since any fluctuation in its intensity would not alter the relative intensities of the two images. Also the influence of stray light from the background, whose polarisation would in general be different from that of the liquid scattering, on the measurement of the latter, is eliminated ; since the images are here viewed against a background which is of the same intensity for both.[10]

5. *Results.*

Coming to the actual measurements on benzene it may be mentioned at the outset that the present measurements extend only to about 3100 A.U. on the ultra-violet side, since a double-image prism transparent to shorter wave-lengths was not available to us. When such a prism is available we hope to extend the measurements as far as the transparency of the liquid would allow.

The spectrogram reproduced in Fig. 2, Plate VI, shows tracks for the three prominent mercury wave-lengths-: λ3650, λ4047 and λ4358. The tracks for the green and yellow lines on one side, and for the 3341 and 3130 doublet on the other, are not shown in the picture, because when the tracks for these wave-lengths are of reproducible intensity, those for the other three are highly over-exposed. The actual values obtained for different wave-lengths are given in column 2 of the following table.

[10] See J. Cabannes, "La diffusion moleculaire de la lumiare," Paris, 1929, p. 102.

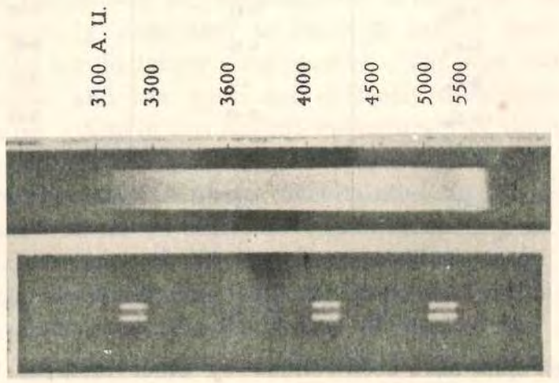

Fig. 1

Fig. 2

TABLE I.

Values for the depolarisation factor for liquid benzene at 25°-28°C.

λ in A.U.	Cornu method with quartz spectrograph.	Cornu method with incident monochromatic light.	With a glass spectrograph and only a nicol.
5790 } 5769 }	$0{\cdot}40_5$	...	0·43
5461	$0{\cdot}40_5$	0·41	0·42
4358	$0{\cdot}40_5$	0·41	0·41
4047	$0{\cdot}40_5$	...	0·41
3650	$0{\cdot}41_0$	0·42	0·41
3341	$0{\cdot}41_0$	...	...
3132 3126	$0{\cdot}41_0$	...	...

6. *Other Methods*

The values have been verified by other methods which are not however so accurate. For example instead of analysing the scattered light spectroscopically as has been done in the above measurements, the incident light was rendered monochromatic by interposing in its path suitable filters, and the scattered light after passing through the double prism and nicol, was photographed directly. The "Zeiss monochromator filters," B and C, served to transmit the 5461 line and the 4358 group respectively. For the 3650 group a Corning glass filter was used. The values obtained by this method are given in column 3 of Table I.

In this method the Raman radiations are not eliminated; their effect on the values, however, is not likely to be appreciable. (See section 2.)

Measurements have also been made, by the method discussed in Section 3, with a glass spectrograph specially constructed for the purpose, the scattering being analysed merely by a nicol placed in front of the slit of the spectrograph. The instrument was of course calibrated for its polarisation. A mercury lamp running at a constant voltage of 110 from a storage battery served as the source of illumination. The values obtained by this method are given in the last column of Table I.

In this method any residual stray light which could not be completely eliminated is likely to affect the values, especially for the longer wave-lengths. The high values for the yellow and the green are evidently to be attributed to this cause. Also in this method the accuracy of the measurements depends on the steadiness of the source.

Considering the above uncertainties in the latter two methods their results must be considered as fully confirming the values obtained by the Cornu method with spectral analysis, which are more reliable. They show unambiguously that over the range of wave-lengths investigated the *depolarisation factor for liquid benzene has practically the same value.*

7. *Scattering by Benzene Vapour.*

The constancy in the value of the depolarisation of liquid scattering for different wave-lengths and the consequent suggestion, at least at first sight, that the optical anisotropy of the benzene molecule is presumably also constant, makes an investigation of the scattering in the vapour state extremely desirable. Here the experimental difficulties are naturally very much greater. Some preliminary measurements have been made on the vapour at a pressure of one atmosphere at the temperature of boiling of the liquid. The values must be considered as very approximate. They seem to show that

when we pass from the green to about 3600 A.U. the depolarisation factor increases from 0·041 to about 0·047 in contrast with the behaviour of the liquid where the value *remains constant* over a much larger spectral range. We shall postpone discussion about the significance of these results till more accurate values for the vapour have been obtained.

Summary

The paper describes the results of measurements on the dispersion of polarisation of the light scattered by benzene both in the liquid state and in the state of vapour. It is found that while the depolarisation factor for the liquid remains constant over a wide range of the spectrum, the value for the vapour increases appreciably as we proceed towards the ultra-violet.

PHYSICS LABORATORY,
DACCA UNIVERSITY.

The Magnetic Anisotropy of Ions of the Type XO_3

In connection with the letters published recently in The Physical Review from W. H. Zachariasen and Maurice L. Huggins on the structure of ions of the type XO_3, the results of some magnetic measurements on these ions made by the present writer with Mr. B. C. Guha, may be of interest.

Among a large number of crystals measured by us for their magnetic anisotropy, are included some carbonates, viz., calcite, aragonite and strontionite, sodium and potassium nitrates and potassium chlorate, all of which are diamagnetic. Of these, calcite and sodium nitrate being trigonal crystals, have naturally an axis of both optical and magnetic symmetry. The other crystals are optically biaxial, but two of their principal refractive indices are so nearly equal that for practical purposes they may also be treated as uniaxial. Magnetically also it is found that they have an axis of similar pseudo-symmetry, the approximation to actual symmetry being even closer than in the optical case. The optical and magnetic symmetry axes are coincident. Table I gives for each crystal the difference between its principal susceptibilities, as also the difference between its principal refractivities—i.e., the magnetic and optical anisotropies of the crystal. $\chi_\parallel$ and $\chi_\perp$ in the table denote the values of the susceptibilities per gram molecule, along and perpendicular to the axis of symmetry respectively: R_e and R_0 denote similarly the gram molecular refractivities for the D-line, (defined as usual by $[(n^2-1)/(n^2+1)]M/\rho$), for vibrations along and perpendicular to the axis respectively.

Since the metallic ions in these crystals are presumably isotropic, and x-ray evidence suggests that the negative ions in them are oriented parallel to one another, the values given in the table for the magnetic and optical anisotropies of a crystal may be taken to represent respectively the magnetic and optical anisotropies of the negative ion present in it. It is significant that the values for the three carbonates are practically the same, as are also the values for the two nitrates.

TABLE I.

Crystal	$(\chi_\perp-\chi_\parallel)\cdot 10^6$	R_0-R_e
$CaCO_3$ (calcite)	4.1	2.94
$CaCO_3$ (aragonite)	4.1	2.41
$SrCO_3$	3.8	2.72
$NaNO_3$	4.7	4.83
KNO_3	4.8	4.32
$KClO_3$	−3.8	2.12

What is remarkable is whereas for the CO_3^{--} and NO_3^- ions the diamagnetic susceptibility along the axis of symmetry is numerically a *maximum*, in the case of the ClO_3^- ion it is numerically a *minimum* along its axis; although optically all the three ions behave similarly.

It may also be remarked that the values given in the table would suggest a positive magnetic double-refraction for the nitrate and carbonate ions in solution, and a negative value for the chlorate ion under the same conditions. Observations are available only for the nitrate ion and are in agreement with the above conclusion. (K. S. Kirshnan and C. V. Raman, Roy. Soc. Proc. **A115, 549, 1927.**) It would be interesting to confirm the negative magnetic double-refraction of the chlorate ion in solution.

K. S. KRISHNAN

Physics Laboratory,
Dacca University, India,
July 11, 1931.

Magnetic Analysis of Molecular Orientations in Crystals

By correlating the magnetic constants of a diamagnetic crystal with those of the individual molecules constituting it, calculated from measurements on the magnetic double refraction of the substance in the liquid state, or from other considerations, it is possible to obtain direct information regarding the orientations of the molecules in the crystal. In a paper which is in course of publication, the results of some magnetic measurements by Mr. S. Banerjee and me on a number of organic crystals are discussed from this point of view.

It is found that in favourable crystals it is possible by the above method to locate the precise molecular orientations. The cases of biphenyl and dibenzyl may be quoted here as examples. Both of them crystallise in the monoclinic prismatic class, in the space group C_{2h}^5. There are two molecules in their unit cells. Their orientations determined from the magnetic measurements are as follows. Let us for brevity define the directions of the lines joining the carbon atoms 4 and 1 in the molecule (in the usual notation), or the atoms 1′ and 4′, as the length of the molecule, and the plane of the benzene rings as the molecular plane. We then find that the lengths of both the molecules in the unit cell lie in the (010) plane in the obtuse angle β, their inclination to the c axis being 20·1° in biphenyl and 83·9° in dibenzyl. As regards the molecular planes, in either crystal, one half of the molecules have their planes inclined at +59° to the (010) plane and the other half at −59° to it.

In the case of dibenzyl, sufficient X-ray data are not available to enable us to test the above conclusions. Our results for biphenyl, however, are fully confirmed by the recent X-ray measurements of Dhar,[1] whose values for the above angular parameters are 20° and 58° respectively, which are almost the same as our values.

K. S. Krishnan.

Physics Laboratory,
University of Dacca, July 6.

[1] *Ind. J. Phys.*, 7, 43; 1932.

Magnetic Constants of Benzene, Naphthalene and Anthracene Molecules

In a recent communication[1], I have shown how, by a correlation of the principal susceptibilities of a diamagnetic crystal, with those of the constituent molecules, it is possible to determine the orientations of the molecules in the crystal. Conversely, where the orientations are already known from X-ray measurements, we can calculate the molecular magnetic constants from those of the crystal. The principal susceptibilities of naphthalene and anthracene molecules, calculated in this manner, are given in the following table. Two of the magnetic axes of the molecules lie in the plane of the benzene rings, one along the line joining the centres of the rings and the other perpendicular to this line. The third axis is normal to the plane of the rings. The susceptibilities along these axes, per gram molecule, are denoted by K_1, K_2 and K_3 respectively. The values for the benzene molecule, which are also included in the table, have been calculated (in the absence of magnetic data for the crystal) from measurements on magnetic double refraction and on light scattering in the liquid state; the calculation is possible since the molecule may be assumed to have an axis of symmetry.[2]

Molecule	$-K_1 \times 10^6$	$-K_2 \times 10^6$	$-K_3 \times 10^6$
Benzene	37·3	37·3	91·2
Naphthalene	39·4	43·0	187·2
Anthracene	45·9	52·7	272·5

It is remarkable that the numerical increase in susceptibility as we proceed from benzene to naphthalene and from naphthalene to anthracene is practically confined to one direction, namely, that which is normal to the plane of the molecules.

Also the normal to the plane is an axis of approximate magnetic symmetry; the ratio of the susceptibility along this axis to that in perpendicular directions increases from 2·4 in benzene to 4·5 in naphthalene and 5·5 in anthracene. It would be of interest to verify by measurements on molecules with continually increasing number of benzene rings in a plane, whether this ratio would reach a limiting value; and whether the limiting value would coincide with the observed value (about 10) of the ratio for carbon in graphite.

K. S. Krishnan.

Physics Laboratory,
University of Dacca,
Sept. 23.

[1] Nature, 130, 313, Aug. 27, 1932.
[2] C. V. Raman and K. S. Krishnan, *Proc. Roy. Soc.* A., 113, 511; 1927.

VII. *Investigations on Magne-Crystallic Action. Part I.—Diamagnetics.*

By K. S. KRISHNAN, *Reader in Physics, and* B. C. GUHA *and* S. BANERJEE, *Research Scholars, University of Dacca.*

(*Communicated by Sir* VENKATA RAMAN, *F.R.S.*)

(Received March 14—Revised July 25—Read November 10, 1932.)

CONTENTS.

INTRODUCTION.

It is well known, from the investigations of COTTON and MOUTON and others* on the magnetic double-refraction of liquids, that diamagnetic molecules in general are

* Various papers in 'C.R. Acad. Sci. Paris' and 'Ann. Chim. Phys.' (1908) to (1913); M. RAMANADHAM, 'Ind. J. Phys.,' vol. 4, p. 15 (1929). For calculation of the anisotropy, see RAMAN and KRISHNAN, 'Proc. Roy. Soc.,' A, vol. 113, p. 511 (1927).

magnetically anisotropic. When such molecules are arranged in a regular manner as they are in a crystal, the crystal, as a whole, will usually exhibit differences in susceptibility in different directions. The magnitude of these differences will evidently depend on the relative *orientations* of the molecules in the unit cell; their *positions* in the cell will have no direct effect, since the diamagnetic moments induced in the molecules are so feeble that their mutual influences are negligible.* Thus a correlation of the magnetic anisotropy of the crystal with that of the individual molecules constituting it, calculated from measurements on magnetic double-refraction in the liquid state, or from other considerations, is likely to give us useful information regarding the orientations of the molecules. This method of analysis of molecular orientations in crystals, which was first suggested by one of us,† promises, at any rate, in favourable circumstances, to be a useful supplement to X-ray methods of crystal analysis. Indeed, in certain crystals—as will be seen in the body of the present paper—the molecular orientations can thus be determined more easily and with greater accuracy than by X-ray methods.

Optical measurements in theory have the same value, but owing to strong mutual influences of the optical dipoles induced in the neighbouring molecules of the crystal, even in those cases where the molecules happen to be orientated in the same manner, the birefringence of the crystal, as a whole, does not *directly* give that of the individual molecules. In order to correlate the optical constants of the crystal with those of the molecules, the relative *positions* of the latter in the crystal have also to be considered; thus the problem is more complicated than in the corresponding magnetic case.

Measurements on paramagnetic single crystals are also of interest for very different reasons. The mutual interactions of the atomic magnetic moments are no longer negligible, so that the anisotropy of the crystal is not determined solely by that of the individual units of the crystal. Investigations over an extensive range of temperatures, by FOËX‡ on siderite and by JACKSON§ on some sulphates and double-sulphates, show that the principal magnetic susceptibilities of a paramagnetic crystal obey Weiss relations of the type

$$\chi_i = \frac{C}{T - \theta_i}, \quad i = 1, 2, 3,$$

where the Curie constant C is the same for all three axes, while θ's are different. This suggests that the anisotropy of the crystal arises from differences in the value of the

* See RAMAN and KRISHNAN, 'Proc. Roy. Soc.,' A, vol. 115, p. 549 (1927).

† KRISHNAN, 'Proc. Ind. Sci. Cong.,' Madras Session, January, 1929. Naphthalene was mentioned in this communication as a suitable crystal for the application of this method; the approximate molecular orientations in this crystal were first determined by this method. (BHAGAVANTAM, 'Proc. Roy. Soc.,' A, vol. 124, p. 545 (1929).) BHAGAVANTAM's results have been confirmed by more recent X-ray measurements (BANERJEE, 'Ind. J. Phys.,' vol. 4, p. 557 (1930)).

‡ 'Ann. Physique.,' vol. 16, p. 174 (1921).

§ 'Phil. Trans.,' A, vol. 224, p. 1 (1923) and vol. 226, p. 107 (1927).

inner Weiss field in different directions. Measurements on the magnetic anisotropy of paramagnetic crystals may, therefore, throw light on the dependence of the Weiss field on crystal structure, which, in our present state of knowledge regarding the nature of the Weiss field, would be very desirable.

In view of the above remarks regarding the importance of magne-crystallic investigations, extensive measurements on single crystals were undertaken by us about two years ago. This paper describes the results of these measurements. Part I of the paper deals with diamagnetic crystals; Section I refers to inorganic compounds; in Section II are given measurements on organic crystals, selected exclusively from the class of aromatic compounds on account of their remarkable magnetic anisotropy; in Section III some measurements on the change of susceptibility of crystals on melting are described; the results on organic crystals are discussed in Section IV, with special reference to molecular orientations in crystals. Extensive measurements have also been made on paramagnetic crystals, and they will form the subject-matter of Part II of the paper.

Section I.—Inorganic Crystals.

1. *Methods of Measuring Magnetic Anisotropy.*

One method of measuring the magnetic anisotropy of a crystal is to locate its principal magnetic axes, and to determine the actual susceptibilities along these directions. This has been done by Voigt and Kinoshita* and others. The method, however, is not sufficiently accurate to give the exact *differences* in susceptibility in different directions; this can be measured more precisely by a direct method.

When any diamagnetic crystal is suspended by a thin fibre, say, of quartz, in a magnetic field, besides the lateral force acting on the crystal which tends to move it to the weakest part of the field, there are also two different couples tending to rotate the crystal about the axis of suspension: (*a*) the couple due to the asymmetry of shape of the crystal and the non-homogeneity of the field, which tends to place its length perpendicular to the field, and (*b*) the couple due to the magnetic anisotropy of the crystal tending to set the axis of greater† susceptibility in the plane of oscillation, along the field. The former couple can be eliminated by using the material in the form of a sphere, and then the only couple that acts is that due to the anisotropy of the crystal. When the torsion of the fibre is known, this couple can be deduced either by observing the twist of the fibre, or preferably from the period of oscillation of the crystal sphere in the magnetic field. This method has been used by Stenger‡ and by König§ for measurements on quartz and calcite.

* 'Ann. Physik.,' vol. 24, p. 492 (1907).

† In the following pages the terms "greater" and "smaller" applied to susceptibility refer to its *algebraic* value.

‡ 'Wied. Ann.,' (Ann. Physik.), vol. 20, p. 304 (1883) and vol. 35, p. 331 (1888).

§ 'Wied. Ann.' (Ann. Physik.), vol. 31, p. 273 (1887).

It is not, however, necessary to use the crystal in the form of a sphere. The couple due to the asymmetry of shape can be eliminated almost as effectively by using a homogeneous magnetic field; such fields as are obtained in ordinary large magnets fitted with large-sized plane parallel pole-pieces, are found to be sufficiently homogeneous for the purpose. The crystal can then be used in whatever shape it is available, which is a great convenience, though the moment of inertia of the crystal about the axis of suspension is not easy to calculate; but it can be readily eliminated by making another observation on the period of oscillation outside the magnetic field. This method was, therefore, adopted in the following measurements.

Theory of Oscillations in a Magnetic Field.—Suppose that a crystal is suspended in a uniform magnetic field H. Let χ_1 and χ_2 be the maximum and the minimum values, respectively, of the gram molecular susceptibility of the crystal in the plane of oscillation. The χ_1 axis will naturally tend to place itself along the magnetic field. Let the torsion-head now be rotated, so that, when the crystal is in this position, the torsion of the fibre is zero. If the crystal be allowed to execute torsional oscillations about this position, and if T and T′ be the periods of oscillation when the field is on and when it is removed, it can easily be shown that

$$\chi_1 - \chi_2 = \frac{T'^2 - T^2}{T^2} \cdot \frac{c}{H^2} \cdot \frac{M}{m},$$

where c is the torsional constant of the fibre, m is the mass of the crystal, and M is its molecular weight. All the quantities on the right-hand side of the above equation being determinable, $\chi_1 - \chi_2$ is known.

Thus in order to determine the magnetic anisotropy of a crystal, it is sufficient to measure its periods of oscillation in a uniform magnetic field when suspended along different axes, and to compare them with the corresponding periods of oscillation outside the field.

2. *Experimental Arrangement.*

The Magnetic Field.—The magnet used in these measurements was of the usual type with replaceable pole-pieces. For the present purpose the plane parallel pieces were used. The current for the magnet was taken from a 110-volt storage supply of constant voltage, and was regulated by a water-cooled resistance. Before any measurements were made, the magnet was brought to a steady state by repeated reversals of the current, the final direction of the current in the coils always being kept the same. The field was measured in the usual manner with the help of an exploring coil and a ballistic galvanometer, with a standard mutual inductance for calibrating the latter.

In order to test the homogeneity of the field, a thin plate of Merck's "Extra Pure" sodium chloride (which crystallises in the cubic system and is therefore magnetically isotropic) was suspended centrally between the pole-pieces by a thin quartz fibre of known torsional constant. The dimensions of the plate in the horizontal plane were

13 mm. × 2 mm., one of them thus being more than six times the other. When a field of 5050 gauss was put on, there was a feeble rotation of the plate towards the equatorial position, evidently due to a small deviation from homogeneity in the field. The maximum value of the rotating couple—which obtains when the plate is nearly at 45° to the field—was measured. It was found to be equivalent to the couple which would act on the plate in an ideal homogeneous field if the susceptibility of the plate along its length were smaller than along its breadth by about 3 parts in 2,000.* Thus even for such extreme asymmetry of shape as in this plate, the effect of the non-homogeneity of field is very small, so that for the usual asymmetries involved, the effect will be negligible in comparison with that due to the magnetic anisotropy of the crystals.

The Mounting of the Crystals.—Fine quartz fibres were used for the oscillation measurements. The upper end of the quartz fibre was fixed to a graduated torsion-head. To the lower end was attached permanently a short length (about 7 or 8 mm.) of moderately thin glass fibre, to which the crystals could be attached readily.† The glass fibre being very short, and much stouter than the quartz fibre, the torsion of the whole suspension was that due to the latter alone. The torsional constant of the suspension was determined by oscillating from its end a circular disc of glass, about one of its diameters.

The attachment of the crystal to the fibre, so as to make any specific direction in the crystal vertical, was a matter of some difficulty, and had to be adjusted by repeated trials. A short focal length telescope fitted with a graduated eye-piece scale, which could be rotated through any known angle about the axis of the telescope tube, served for measurements in connection with the mounting of the crystal. In fact, with the help of the torsion-head for measuring rotations about a vertical axis, the graduated circle of the telescope for rotations about a horizontal axis, and the eye-piece scale for linear displacements, all the necessary adjustments and measurements on the crystal could easily be made.

3. *Results.*

Before proceeding to describe the experimental results, we explain the notation adopted in the paper.

In the case of magnetically uniaxial crystals, the gram molecular susceptibilities along and perpendicular to the axis are represented by $\chi_{\parallel}$ and $\chi_{\perp}$ respectively. In crystals that belong to the orthorhombic system, the three crystallographic axes are also the magnetic axes, and the values of the susceptibilities along them per gm. mol. are denoted by χ_a, χ_b and χ_c, respectively. For the monoclinic crystals (010) plane being a plane of symmetry must naturally contain two of the magnetic axes; we denote

* A similar measurement with a paramagnetic single crystal of ferric ammonium alum—which is also cubic—whose horizontal dimensions were 8 mm. × 1 mm. gave practically the same value, $\Delta\chi/\chi = 2\times10^{-3}$.

† Traces of shellac, which was tested and found to be feebly diamagnetic, were used as cement in all cases.

the gram molecular susceptibilities along them by χ_1 and χ_2, χ_1 *being greater than* χ_2. The angle which the χ_1-axis makes with the "*c*" axis of the crystal, *taken positive towards the obtuse angle* β between the "*c*" and the "*a*" axes, determines the positions of these two magnetic axes. (Since in most of the monoclinic crystals the (001) plane was well developed, the inclination of the χ_2-axis to this plane was directly measured. Calling this angle θ, measured positive from the "*a*" axis towards the obtuse angle β, it is connected with ψ by the simple relation $90° + \theta + \psi =$ obtuse β). The third axis is, of course, along the "*b*" axis, and the gm. mol. susceptibility along it is denoted by χ_3.

The results are shown in Table I. Column 3 of Table I gives the axis of suspension, column 4 the direction of setting of the crystal in the field, the fifth column the maximum difference in susceptibility $|\Delta\chi|$ in the plane of oscillation, and the sixth column the magnetic anisotropy of the crystal. In the case of orthorhombic and monoclinic crystals, though oscillations about two axes are sufficient to determine completely the anisotropy, measurements were made also with a third direction of suspension, so as to be able to check the results.

4. *Discussion of Results.*

The most striking result is the large value of the magnetic anistropy of the nitrates, carbonates and the chlorate, as contrasted with the more or less complete isotropy of the sulphates. We have seen that calcite and sodium nitrate have an axis of magnetic symmetry, while aragonite, strontianite, witherite, potassium nitrate and potassium chlorate may for practical purposes be considered to have the same in view of the close approximation in value of two of the principal susceptibilities. In Table II are collected together the differences in susceptibility of these crystals, along, and perpendicular to, their axes of symmetry. The last column in the table gives the differences between the principal gram molecular refractivities (defined as usual by $R = M(n^2-1)/(n^2+2)\rho$).

In striking contrast with these values are those for the sulphates which are given in Table III.

The strong anisotropy of the nitrates and carbonates receives a natural explanation in terms of the intrinsic anisotropy of the NO_3^- and CO_3^{--} ions and the parallel orientations of all the ions in the crystal. (The contribution to the susceptibility of the crystal from the metallic ions is presumably isotropic.) The fact that $\chi_{\perp} - \chi_{\parallel}$ has the same value for both the nitrates and nearly the same value for the four carbonates is then readily understood. Indeed, it is possible, as has been shown in a recent paper,* to calculate the actual magnetic anisotropy of the NO_3^- ion from the Cotton-Mouton constant of nitric acid (or of aqueous solutions of nitrates) and this value is found to be in satisfactory agreement with the observed value of $\chi_{\perp} - \chi_{\parallel}$ for the crystal.

Why the nitrate and the carbonate ions are so strongly anisotropic is difficult to understand. Presumably it is connected with their plane structure; graphite, benzene,

* C. V. Raman and K. S. Krishnan, 'Proc. Roy. Soc.,' A, vol. 115, p. 549 (1927).

TABLE I.

The unit adopted for the χ's is 10^{-6} of a c.g.s. electromagnetic unit.

Crystal.	Crystal system.	Mode of suspension.	Orientation in the field.	$\lvert\Delta\chi\rvert$.	Magnetic anisotropy.	Remarks.
1. Quartz (SiO_2) . .	Trigonal	Trigonal axis horizontal	Trigonal axis normal to field	0·12	$\chi_\perp - \chi_\parallel = 0{\cdot}12$	KÖNIG's value = 0·14. STENGER's value = 0·10 to 0·12.
2. Calcite ($CaCO_3$) . .	,,	,,	,, ,,	$4{\cdot}0_9$	$\chi_\perp - \chi_\parallel = 4{\cdot}0_9$	KÖNIG's value = 3·98 to 4·28.
3. Sodium nitrate ($NaNO_3$)	,,	,,	,, ,,	$4{\cdot}8_9$	$\chi_\perp - \chi_\parallel = 4{\cdot}8_9$	
4. Aragonite ($CaCO_3$) .	Orthorhombic	"a" axis vertical	"b" axis along field	$4{\cdot}2_9$		"c" axis is an axis of approximate magnetic symmetry.
		"b" ,,	"a" ,,	$4{\cdot}0_2$	$\chi_a - \chi_c = 4{\cdot}0_3$...	
		"c" ,,	"b" ,,	$0{\cdot}1_2$	$\chi_b - \chi_c = 4{\cdot}2_6$...	
5. Strontianite ($SrCO_3$)	,,	"b" ,,	"a" ,,	$4{\cdot}8_1$	$\chi_a - \chi_c = 4{\cdot}8_1$...	
		"c" ,,	"b" ,,	$0{\cdot}0_3$	$\chi_b - \chi_c = 4{\cdot}8_4$...	,, ,,
6. Witherite ($BaCO_3$) .	,,	(110) horizontal	"c" axis normal to field	$5{\cdot}0_3$		
		(110) vertical and "c" axis horizontal	,, ,,	$4{\cdot}9_7$	$\chi_a - \chi_c = 4{\cdot}9_3$...	,, ,,
					$\chi_b - \chi_c = 5{\cdot}0_7$...	
		"c" axis vertical	"b" axis along field	$0{\cdot}1_4$		
7. Potassium nitrate ($K NO_3$)	,,	"a" ,,	"b" ,,	$4{\cdot}8_7$		
		"b" ,,	"a" ,,	$4{\cdot}8_9$	$\chi_a - \chi_c = 4{\cdot}8_3$...	,, ,,
		"c" ,,	"b" ,,	$0{\cdot}0_8$	$\chi_b - \chi_c = 4{\cdot}8_7$...	
8. Barite ($BaSO_4$) . .	,,	"a" ,,	"b" ,,	$0{\cdot}7_2$		
		"b" ,,	"c" ,,	$0{\cdot}6_2$	$\chi_b - \chi_c = 0{\cdot}7_2$	
		"c" ,,	"b" ,,	$1{\cdot}3_4$	$\chi_c - \chi_a = 0{\cdot}6_2$	
9. Celestite ($SrSO_4$) . .	,,	"a" ,,	"b" ,,	$0{\cdot}7_4$		
		"b" ,,	"c" ,,	$0{\cdot}9_0$	$\chi_b - \chi_c = 0{\cdot}7_4$	
		"c" ,,	"b" ,,	$1{\cdot}6_8$	$\chi_c - \chi_a = 0{\cdot}9_0$	
10. Anhydrite ($CaSO_4$) .	,,	"a" ,,	"b" ,,	$0{\cdot}2_7$		Since the order of the magnetic axes is different from that in $BaSO_4$ and $SrSO_4$, the measurements were repeated with two other specimens with practically the same results.
		"b" ,,	"a" ,,	$0{\cdot}6_2$	$\chi_a - \chi_b = 0{\cdot}4_5$...	
		"c" ,,	"a" ,,	$0{\cdot}4_9$	$\chi_b - \chi_c = 0{\cdot}2_3$...	
11. Sulphur	,,	"a" ,,	"b" ,,	$0{\cdot}0_7$		
		"b" ,,	"c" ,,	$0{\cdot}2_3$	$\chi_b - \chi_c = 0{\cdot}0_7$	
		"c" ,,	"b" ,,	$0{\cdot}3_0$	$\chi_c - \chi_a = 0{\cdot}2_3$	
12. Selenite . . . . . ($CaSO_4{\cdot}2H_2O$)	Monoclinic	"b" ,,	"c" ,,	$1{\cdot}0_6$	$\psi = 0$	
		"c" ,,	"b" ,,	$0{\cdot}4_2$	$\chi_1 - \chi_2 = 1{\cdot}0_6$	
		(100) horizontal	"c" ,,	$0{\cdot}6_4$	$\chi_1 - \chi_3 = 0{\cdot}6_4$	
13. Potassium chlorate ($KClO_3$)	Monoclinic $\beta = 109°{\cdot}7$	"b" axis vertical	$\theta = -39°{\cdot}5$	$3{\cdot}7_1$	$\psi = +59°{\cdot}2$ ...	χ_1—axis is an axis of approximate magnetic symmetry.*
		"a" ,,	"b" axis normal to field	$2{\cdot}3_7$	$\chi_1 - \chi_2 = 3{\cdot}7_1$...	
		(001) horizontal	,, ,,	$1{\cdot}7_3$	$\chi_1 - \chi_3 = 3{\cdot}9_1$...	

* $KClO_3$ usually crystallises in the form of a pseudo-rhombohedron bounded by (001) and (110) planes. The above axis of approximate magnetic symmetry is found, on calculation, to be nearly along the trigonal axis of the rhombohedron, which is also known to be an axis of approximate optical symmetry.

TABLE II.

Crystal.	$\chi_\perp - \chi_\parallel$.	$R_\infty - R_r$ for sodium line.
$NaNO_3$	4·9	4·86
KNO_3	4·9	4·32
$CaCO_3$ (calcite)	4·1	2·99
$CaCO_3$ (aragonite)	4·1	2·41
$SrCO_3$ (strontianite)	4·8	2·77
$BaCO_3$ (witherite)	5·0	3·03
$KClO_3$	— 3·8	2·12

TABLE III.

Crystal.	$\chi_b - \chi_c$.	$\chi_c - \chi_a$.	$R_b - R_c$.	$R_c - R_a$.
$BaSO_4$	0·72	0·62	0·02	−0·28
$SrSO_4$	0·74	0·99	0·04	−0·20
$CaSO_4$	0·25	−0·65	0·12	−0·93

and naphthalene molecules may be cited as showing this connection. But, also, we know, independently, that a plane close-packing of atoms conduces to a large optical anisotropy, so that if the above relation is general we have an explanation of the relationship remarked by RAMAN and BHAGAVANTAM* that strong magnetic anisotropy is always associated with strong optical anisotropy.

On the other hand, in the case of the SO_4^{--} ions it appears from X-ray investigations† that the four oxygen atoms are disposed more or less symmetrically about the sulphur atom, being situated at the corners of a tetrahedron with the latter atom at the centre. In that case, the observed isotropic nature of the sulphates, both as regards their magnetic and optical properties, follows as a direct consequence. Here, too, may be mentioned the strong contrast in the depolarisation of the light transversely scattered by nitric and sulphuric acids, observed by VENKATESWARAN‡.

The magnetic behaviour of potassium chlorate is interesting and deserves special mention. The strong resemblance of this crystal to calcite and to sodium nitrate in several of its properties is well-known.§ Even though it belongs to the monoclinic system, it crystallizes in the form of rhombohedra like the latter crystals, and their planes of cleavage are also similar. Also the trigonal axis of the pseudo-rhombohedron,

* 'Ind. J. Phys.,' vol. 4, p. 57 (1929).

† EWALD and HERMANN, 'Strukturbericht,' p. 340 (1913–1926).

‡ 'Ind. J. Phys.,' vol. 1, p. 235 (1927).

§ See P. GROTH, "Chemische Kristallographie," Leipzig, vol. 2, p. 81 (1908).

as has already been remarked, is at once an axis of approximate optical and of magnetic symmetry. Optically, the crystal is negative just like the other two crystals; even the magnitude of the molecular birefringence is of the same order. But, magnetically, whereas for nitrates and carbonates $\chi_\perp - \chi_\parallel > 0$ for potassium chlorate $\chi_\perp - \chi_\parallel < 0$. This difference in sign is probably due to the fact that the ClO_3 ion is not plane as the NO_3^- and CO_3^{--} ions are, but pyramidal with Cl at the apex. Whatever may be the explanation, the above fact regarding the signs of $\chi_\perp - \chi_\parallel$ when taken together with the known negative birefringence of these crystals, would suggest a *negative* sign for the magnetic double-refraction of ClO_3^- ions in solution as contrasted with the positive sign for nitrate solutions. This is indeed so for the nitrate solutions; the magnetic double-refraction of chlorate solutions, however, does not seem to have been tested. *

Section II.—Organic Crystals.

1. *Measurements on Organic Crystals.*

In this section are described measurements on organic crystals. Investigations on magnetic double-refraction show that molecules of the aromatic class exhibit a pronounced magnetic anisotropy. In this respect, molecules having two or more benzene rings stand in a class by themselves; all the crystals studied in this paper are selected exclusively from this class of compounds. For reasons given in the introduction, our choice of crystals has been guided to a considerable extent by the list of substances for which preliminary X-ray measurements are available, we may then expect to supplement the information regarding the orientations of molecules in these crystals by that already obtained by the X-ray methods.

The differences in susceptibilities in different directions were measured in the same manner as described in the previous section by oscillating them about different axes. The organic crystals, however, were generally in the form of plates, and hence the influence of the residual non-homogeneity of the field on the setting of the crystal will naturally be greater than for the inorganic crystals. But the magnetic anisotropy of the organic crystals is also several times larger, so that the effect of the non-homogeneity of the field is also negligible in these crystals.

2. *Absolute Susceptibilities.*

Method of Measurement.—Since existing data for the magnetic susceptibilities of organic crystals are very meagre, the absolute susceptibilities have also been measured for these crystals. The method adopted is a null method of the type used recently by Rabi† for measurements on paramagnetic crystals. The principle of the method is as

* [*Note added November* 7, 1932.—In the 'Ind. J. Phys.' vol. 7, p. 317 (1932), Mr. Chinchalkar reports measurements on the magnetic double-refraction of aqueous solutions of sodium chlorate. The double-refraction is *negative* as predicted here: further, its numerical value is in agreement with that deduced from the magnetic and optical anisotropies of the ClO_3^- ion given in Table II. of the present paper.]

† 'Phys. Rev.,' vol. 29, p. 171 (1927).

follows. The crystal is suspended in a strong non-homogeneous field in a bath of liquid whose susceptibility can be varied at will. In general, there will be a lateral motion of the crystal when the field is put on, which will vanish when the volume susceptibility of the solution is the same as that of the crystal *in the direction of the field*. Thus the method of measurement of the susceptibility of the crystal along any specific direction consists in suspending the crystal so as to have this direction along the field and adjusting the susceptibility of the bath till there is no lateral motion when the non-homogeneous field is put on. If this direction does not correspond to the maximum susceptibility of the crystal in the horizontal plane, the crystal will tend to rotate from the above direction. Rabi prevents this rotation by using for the suspension a fibre of glass of sufficient thickness. The fibre must not be very thick since the lateral movements of the crystal will then be diminished considerably. Thus the fibre has to possess a large torsional couple and, at the same time, a small bending moment. These conditions being to some extent mutually unaccommodative, there is a limit to the sensitiveness of the above arrangement.

But in our investigations, since the differences in the principal susceptibilities are already known from the oscillational measurements, it is sufficient to determine the absolute susceptibility along *any one* direction in the crystal. We can conveniently choose the direction which actually sets itself along the field. In this case, we can replace the glass fibre of Rabi by a thin quartz fibre and thus the sensitiveness of the arrangement is considerably increased.

The Balancing Liquid Bath.—In all the crystals studied by us there was at least one principal magnetic axis along which the volume susceptibility was greater than that of water. Also the crystals were only sparingly soluble in water. Hence an aqueous solution of a paramagnetic salt was used as the liquid for the balancing bath. Manganese chloride was chosen as the solute in view of its large susceptibility. A standard solution of about one per cent concentration of Kahlbaum's pure manganese chloride was first prepared (the water used for the solution, as well as for later dilutions, was specially distilled for the purpose), and its exact strength was determined by chemical analysis by converting the chloride to the pyrophosphate. In the actual experiment, 50 c.c. of the solution at 29° C. gave on analysis 0·5717 gm. of $Mn_2P_2O_7$, which corresponds to 0·01014 gm. of $MnCl_2$ per c.c. of the solution. This standard solution was suitably diluted with known amounts of water and used in the bath, the precise dilution necessary for magnetically balancing the crystal being determined by repeated trials.

The Susceptibility of the Balancing Solution.—The volume susceptibility of the balancing bath has next to be calculated from its known concentration. Accurate measurements have been made by Cabrera and Duperier,* on the susceptibilities of solutions of $MnCl_2$ of different concentrations, and they find that the calculated susceptibility of $MnCl_2$ is very nearly the same for all concentrations. The smallest concentration measured by them was, however, about 3 per cent, which is much greater than the concentrations

* 'J. Phys. Rad.,' vol. 6, p. 121 (1925).

used here. Hence the value was carefully redetermined by comparing the susceptibility of the above solution with that of water by a modified Quincke method, which will be described in the next section in connection with the measurements on molten crystals. These measurements gave for the susceptibility of $MnCl_2$ at such low concentrations, the value $117{\cdot}9 \times 10^{-6}$ at 28·5° C., as against $115{\cdot}3 \times 10^{-6}$ calculated for the same temperature from the results of CABRERA and DUPERIER for higher concentrations. (The value for solid $MnCl_2$ is much lower, being equal to $105{\cdot}3 \times 10^{-6}$ per gm.)

The above value has been adopted in the following calculations. For small deviations of temperature from 28·5° C. the temperature coefficient of susceptibility of $MnCl_2$ in solution has been taken to be $-0{\cdot}43 \times 10^{-6}$ per 1° C.

3. *Densities of Organic Crystals.*

Since the volume susceptibility of the balancing solution gives at once that of the crystal along the field, it remains only to know the density of the crystal in order to calculate the corresponding gram molecular susceptibility. On a reference to the standard literature, one finds that the values for the densities of organic crystals given by different experimenters vary widely. This is not surprising; even in the case of substances which can be obtained in the form of large single crystals, TUTTON* remarks that measurements on several crystals are made and the *highest* value is adopted. The difficulties of measurement on organic substances, which are usually in the form of micro-crystals, are naturally greater, and hence the above discrepancies. In fact, it has been suggested by BRAGG† that the calculation of the density from the size of the unit cell determined by X-ray methods is likely to give a more accurate value than direct methods of measurement.

Thus it is clear that in our calculation of the gram molecular susceptibility of a crystal from its volume susceptibility we have to use the proper value of the density for the particular crystal used. This was determined by the "immersion" method, using a solution of zinc sulphate for the purpose.

The following observation made in the course of the measurements on densities appears to be worth mentioning. By taking a large crystal and continually subdividing it, the density of the heaviest piece is found to be considerably higher than that of the original crystal. The limiting value of the density so determined agrees in general with the value calculated from X-ray measurements.

Assuming that the deviation of the density of the actual crystal from the ideal density is due to inclusions of air, the gram molecular susceptibility χ of the crystal is connected with its volume susceptibility k (both χ and k being expressed in the usual unit, viz., 10^{-6} of a c.g.s. e.m.u.) by the relation,

$$\chi = \frac{kM}{\rho} - \left(\frac{1}{\rho} - \frac{1}{\rho_0}\right) M \cdot 0 \cdot 029,$$

* "Crystallography," p. 625.

† 'Proc. Phys. Soc.,' vol. 35, p. 167 (1923).

TABLE IV.

Crystal.	Crystal system.	Mode of suspension.	Orientation in the field.	$\lvert\Delta\chi\rvert$.	Magnetic anisotropy.	Remarks.
1. Naphthalene	Monoclinic $\beta = 122°{\cdot}8$	"b" axis vertical; "a" (001) vertical and the intersection of (001) and (110) horizontal	$\theta = +20°{\cdot}8$ "b" axis normal to field (001) at 68°·5 to field	122 13·9 92·5	$\chi_1 - \chi_3 = 122$ $\chi_1 - \chi_2 = 29{\cdot}3$ —	Calculated value of setting angle = 67°·3 and of $\Delta\chi = 92{\cdot}0$.
2. Anthracene	Monoclinic $\beta = 124°{\cdot}4$	"b" axis vertical	$\theta = +26°{\cdot}4$	Oscillation measurements were not made with this crystal. Absolute measurements were made along three directions. See Table V.		
3. Biphenyl	Monoclinic $\beta = 94°{\cdot}8$	"b" " "a" (001) horizontal	$\theta = -15°{\cdot}3$ "b" axis normal to field "a" "	83·1 29·7 40·1	$\chi_1 - \chi_3 = 83{\cdot}1$ $\chi_1 - \chi_2 = 35{\cdot}5$ —	Cal. $\Delta\chi = 41{\cdot}8$.
4. Dibenzyl	Monoclinic $\beta = 115°{\cdot}9$	"b" axis vertical (001) horizontal "a" axis vertical	$\theta = -58°{\cdot}0$ "a" axis along field "b" "	83·1 5·1 29·9	$\chi_1 - \chi_3 = 83{\cdot}1$ $\chi_1 - \chi_2 = 28{\cdot}4$ —	Cal. $\Delta\chi = 31{\cdot}4$.
5. Stilbene	Monoclinic $\beta = 114°{\cdot}1$	"b" " (001) horizontal "a" axis vertical	" "a" " "b" " "	56·6 0·8 58·0	$\chi_1 - \chi_3 = 56{\cdot}6$ $\chi_3 - \chi_1 = 0{\cdot}8$ —	Cal. $\Delta\chi = 57{\cdot}4$.
6. Benzophenone	Orthorhombic	"c" " "a" axis horizontal and (110) vertical (110) horizontal	" "a" " "c" axis normal to field " "c" "	0·6 61·0 61·3	$\chi_a - \chi_b = 0{\cdot}6$ $\chi_b - \chi_c = 60{\cdot}7$ —	Cal. $\Delta\chi = 61{\cdot}0$.

7. Benzil	Trigonal	Trigonal axis horizontal	45·6	$\chi_n - \chi_\perp = 45·6$		
		" a " "	42·7	$\chi_1 - \chi_3 = 42·7$		
		" b " "	4·4	$\chi_3 - \chi_1 = 4·4$		
		" b " "	46·3	—	Cal. $\Delta\chi = 47·1$.	
8. Azobenzene	Monoclinic $\beta = 114°·4$	" b " axis vertical (001) horizontal " a " axis vertical	48·5	$\chi_a - \chi_b = 15·0$		
		" c " "	15·0	$\chi_c - \chi_b = 48·5$		
		" a " "	33·9	—	Cal. $\Delta\chi = 33·5$.	
9. Hydrazobenzene	Orthorhombic	" c " "				
		" a " "				
		" b " "				
10. β-Naphthol	Monoclinic $\beta = 119°·8$	" b " "	86·0	$\chi_1 - \chi_3 = 86·0$		
		" a " "	7·6	$\chi_1 - \chi_3 = 18·1$		
		(001) horizontal	54·2	—	Cal. $\Delta\chi = 57·4$.	
11. Acenaphthene	Orthorhombic	" b " axis vertical	28·0	$\chi_a - \chi_c = 28·0$		
		" c " "	45·5	$\chi_b - \chi_c = 73·5$		
		" a " "	72·7	—	Cal. $\Delta\chi = 73·5$.	
12. Salol	Orthorhombic	" b " "	31·5	$\chi_a - \chi_c = 31·5$		
		" c " "	30·3	$\chi_b - \chi_c = 61·8$		
		" a " "	61·9	—	Cal. $\Delta\chi = 61·8$.	

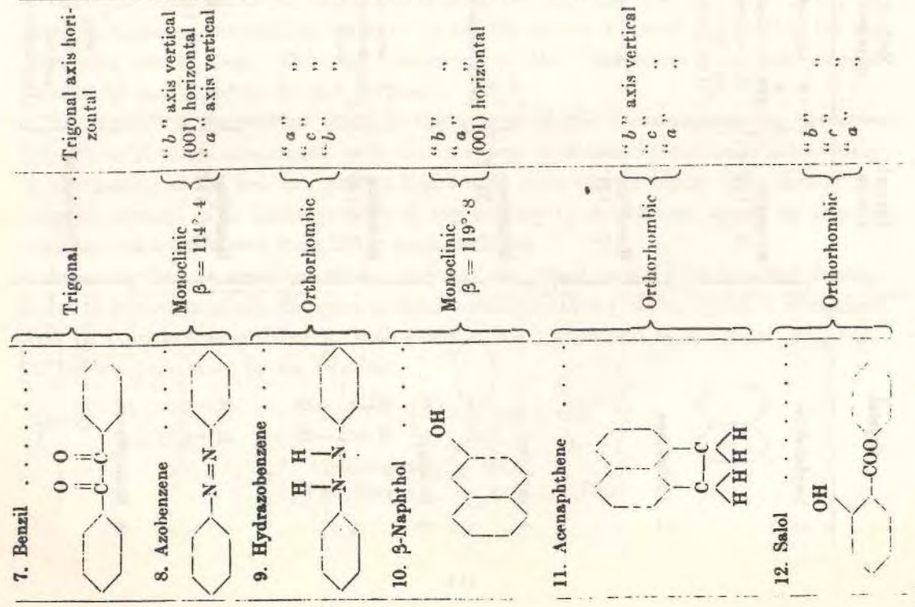

where ρ and ρ_0 are the densities for the actual crystal and for the ideal crystal respectively and M is its molecular weight. The second term is, in general, negligible.

4. *Results.*

The results of the oscillation measurements are given in Table IV. The different columns have the same significance as the corresponding columns in Table I and do not require any explanation. One extra oscillation measurement was also made with these crystals, as a check on the accuracy of the measurement, and the results are included in the Table. The calculated value of $|\Delta\chi|$ for this suspension is given in the final column for comparison with the observed value.

The results of the measurements on absolute susceptibilities are given in Table V. The second column gives the direction along which the susceptibilities were measured, and the next column the volume susceptibility of the bath and therefore of the crystal along the above direction, in the usual unit, viz., 10^{-6} of a c.g.s. e.m.u. The fourth column gives the density of the crystal. The principal gram molecular susceptibilities can thence be calculated with the help of the data given in Table IV. The principal magnetic constants for the crystal so calculated are given in column 5. The sixth column gives the arithmetic mean of the three principal susceptibilities of the crystal and the last column the value of the susceptibility of the substance calculated from the well-known additive law of PASCAL. The constants required in this calculation were all taken from the " International Critical Tables," vol. VI.

SECTION III.—CHANGE OF SUSCEPTIBILITY OF CRYSTALS ON MELTING.

1. *Some Remarks on Measurements in the Solid State.*

Before proceeding to discuss the results on organic crystals, described in the foregoing section, we may give here an account of some experiments on the change of susceptibilities of crystals on melting. In a well-known paper OXLEY* has given measurements of this change for a number of organic crystals. He finds that, in general, the susceptibility in the solid state is greater than that for the fused substance. The difference is usually of the order of 5 per cent; in exceptional cases, however, it is much higher, as, for example, in nitrobenzene, where it is 13 per cent. The value for the solid state in OXLEY'S experiment refers to the substance as obtained by solidifying the molten liquid in a glass bulb; the substance would naturally be in the form of micro-crystals. The question arises how far the orientations of such micro-crystals, when placed in a magnetic field can be assumed to be random. Especially in crystals like naphthalene, which are markedly anisotropic—the extreme values for this crystal are in the ratio of 4 : 1—there will be a strong orientative couple acting on the micro-crystals. Even a small rotation of the crystals under the influence of this couple will give a value for the susceptibility of the aggregate which will be appreciably higher than the mean value

* 'Phil. Trans.,' A, vol. 214, p. 109 (1914).

TABLE V.

Crystal.	Direction along which susceptibility was measured.	Vol. susceptibility.	ρ	Principal gm. mol. susceptibilities.	Mean susceptibility.	PASCAL'S additive value.
1. Naphthalene	⊥ to (001)	−0·461	1·081	$\chi_1 = -39{\cdot}4$ $\chi_2 = -161{\cdot}4$ $\chi_3 = -68{\cdot}7$ $\psi = +12{\cdot}0°$	−89·8	−89·5
2. Anthracene	Along χ_1 — axis ⊥ to (001) Along χ_2 — axis	−0·320 −0·578 −0·641	1·24	$\chi_1 = -45{\cdot}9$ $\chi_2 = -233{\cdot}2$ $\chi_3 = -91{\cdot}9$ $\psi = +8{\cdot}0°$	−123·7	−123·9
3. Biphenyl	Along χ_1 — axis	−0·466	1·132	$\chi_1 = -63{\cdot}4$ $\chi_2 = -146{\cdot}5$ $\chi_3 = -98{\cdot}9$ $\psi = +20{\cdot}1°$	−102·9	−104·3
4. Dibenzyl	,, ,,	−0·540	1·086	$\chi_1 = -90{\cdot}5$ $\chi_2 = -173{\cdot}6$ $\chi_3 = -118{\cdot}9$ $\psi = +83{\cdot}9°$	−127·7	−128·0
5. Stilbene	,, ,,	−0·626 −0·605	1·155 1·124	$\chi_1 = -97{\cdot}4$ $\chi_2 = -154{\cdot}0$ $\chi_3 = -96{\cdot}6$ $\psi = -65{\cdot}9°$	−116·0	−116·7
6. Benzophenone . . .	Along "*a*" axis	−0·583	1·206	$\chi_a = -88{\cdot}0$ $\chi_b = -88{\cdot}6$ $\chi_c = -149{\cdot}3$	−108·6	−108·6
7. Benzil	Along trig. axis	−0·474	1·244	$\chi_{\parallel} = -80{\cdot}0$ $\chi_{\perp} = -125{\cdot}6$	−110·4	−112·9
8. Azobenzene	Along χ_1 — axis	−0·576	1·198	$\chi_1 = -87{\cdot}5$ $\chi_2 = -130{\cdot}2$ $\chi_3 = -83{\cdot}1$ $\psi = -65{\cdot}6°$	−100·3	−113·6
9. Hydrazobenzene . .	Along "*c*" axis	−0·524	1·179	$\chi_a = -115{\cdot}4$ $\chi_b = -130{\cdot}4$ $\chi_c = -81{\cdot}9$	−109·2	−121·3
10. β-Naphthol	Along χ_1 — axis	−0·546	1·263	$\chi_1 = -62{\cdot}3$ $\chi_2 = -148{\cdot}3$ $\chi_3 = -80{\cdot}4$ $\psi = +9{\cdot}4°$	−97·0	−96·1
11. Acenaphthene . . .	Along "*b*" axis	−0·557	1·191	$\chi_a = -117{\cdot}6$ $\chi_b = -72{\cdot}1$ $\chi_c = -145{\cdot}6$	−111·8	−107·4
12. Salol	,, ,,	−0·551	1·299	$\chi_a = -121{\cdot}1$ $\chi_b = -90{\cdot}8$ $\chi_c = -152{\cdot}6$	−121·5	−122·9

The figures given in the last two columns of the Table agree in general. Azobenzene and hydrazobenzene are, however, striking exceptions.

for a single crystal. Hence, instead of comparing the susceptibility of the fused substance with that of the solidified micro-crystals, it was considered preferable to compare it with the mean of the three principal susceptibilities for a single crystal. Naphthalene and benzophenone were chosen for these measurements.

2. *Susceptibility of Fused Crystals.*

The susceptibility of the molten substance was compared with that of water by a modified Quincke method. Since a similar arrangement has been described in a recent paper by RANGANADHAM* we refer to this paper for the details of the arrangement. The principle of the method is as follows. The two liquids whose susceptibilities are to be compared are contained in two similar U-tubes. One limb of each tube is of small bore and lies in a uniform magnetic field, while the other, which lies outside the field, is of much larger diameter. The levels of the liquid menisci in the two narrow tubes are adjusted so as to be in the centre of the magnetic field. When the field is removed, the liquid menisci which were originally depressed will move up. The positions of the menisci both when the field is on and when it is removed, are photographed on the same plate with a camera having a large magnification—about 20 times. Since the images of the menisci are sharp lines, the changes of level of the two liquids which occur when the field is removed, can be compared accurately.

It can easily be shown that the above change of level, say, h, in the narrow tube when a field H is removed, is given by

$$h = \frac{H^2}{2g} \cdot \left(\frac{S}{S+\sigma}\right) \cdot \frac{k}{\rho} \ ,$$

where k is the volume susceptibility of the liquid, ρ is its density, g is the acceleration due to gravity, and σ and S are respectively the cross-sectional areas of the inner (*i.e.*, the narrow limb inside the magnetic field) and the outer limbs of the U-tube. Since the two U-tubes are of identical dimensions,† the ratio of the changes in level of the two liquids gives directly the ratio of their *specific* susceptibilities. As the temperature co-efficient of the specific susceptibility of a diamagnetic substance is very small (if not zero) any small uncertainty in the measurement of the temperatures of the two liquids will have no influence on the ratio.

3. *Results.*

Naphthalene (m.p. = 80·1° C.). The two U-tubes were wound separately with nichrome wires, so that each could be raised to any desired temperature. The tube containing molten naphthalene was kept exhausted, and was at 94° C. The other U-tube contained water at 32° C., and was kept exposed to air through a small side tap.

* 'Ind. J. Phys.,' vol. 6, p. 421 (1931).

† S being much greater than σ—actually about 60 times—any small difference in the diameters of the two U-tubes will not affect the results.

The ratio of the rise of molten naphthalene to that of water when the field was removed was 0·928, whence the susceptibility of the former comes out on calculation as $-0\cdot694 \times 10^{-6}$ per gm. In another series of measurements molten naphthalene at 100° C. was first compared with that of nitrobenzene at 90° C.; the latter was, in its turn, compared with nitrobenzene at 30° C., which was finally compared with water at the same temperature. All the tubes were kept exhausted. The experimental values for the ratios were 1·418, 0·976, and 0·707, respectively. Hence, the susceptibility of molten naphthalene at 100° C. $= -0\cdot704 \times 10^{-6}$, which agrees within the limits of experimental error with the previous value. Their mean corresponds to

$$\chi_{liq.} = -89\cdot5 \times 10^{-6} \text{ per gm. mol. at about } 100° \text{ C.}$$

This value may be compared with the mean value for the crystal $[= \frac{1}{3}(\chi_1 + \chi_2 + \chi_3)]$

$$\chi_{cryst.} = -89\cdot8 \times 10^{-6} \text{ per gm. mol. at about } 30° \text{ C.}$$

The difference is less than one-half of one per cent.

Benzophenone (m.p. = 48·5° C.). The specific susceptibility of the molten substance at 50° C. was 0·852 times that of water at 30° C., and is therefore equal to $-0\cdot612 \times 10^{-6}$ per gm. This corresponds to $-111\cdot5 \times 10^{-6}$ per gm. mol., whereas the mean gm. mol. susceptibility for the crystal $= -108\cdot6 \times 10^{-6}$ which is, numerically, about 2·5 per cent. less than for the liquid.

Oxley's value for this change is 6 per cent., which is much higher.

It is known that benzophenone possesses a large dipole moment, viz., $2\cdot5 \times 10^{-18}$ e.s.u., whereas naphthalene is non-polar. It would therefore be interesting to determine whether the difference in behaviour of benzophenone and naphthalene, as regards the change of susceptibility on melting, is typical of polar and non-polar molecules respectively. Experiments on other compounds which are in progress in the author's laboratory may be expected to throw light on this point.

Section IV.—Magnetic Analysis of Molecular Orientations in Crystals.

We now proceed to discuss the magnetic constants of organic crystals in relation to the orientations of the molecules in their unit cells. Among the crystals studied by us, naphthalene, anthracene, biphenyl and dibenzyl are of special interest from this point of view, since their unit cells contain only two molecules.

1. *Naphthalene.*

Naphthalene crystal belongs to the monoclinic prismatic class. Its structure has been studied by X-ray methods by Bragg* and Robertson,† and more recently by Banerjee (*loc. cit.*). The unit cell contains two molecules, for which Banerjee suggests

* "X-Rays and Crystal Structure," p. 233 (1924).

† 'Proc. Roy. Soc.,' A, vol. 125, p. 546 (1929).

a plane structure. As regards their orientations, he finds, in the the molecules in the unit cell have their lengths (*i.e.*, the lines j the constituent benzene rings) in the (010) plane making an angle axis in the obtuse angle β. Since from direct considerations of axis of the naphthalene molecule must be one of its magnetic axes (along its breadth in the plane of the benzene rings and along the of the rings, respectively) we should expect the above direction i one of the magnetic axes of the crystal. This is indeed so, because gave for the direction of the χ_1-axis $\psi = +12\cdot0°$, which is precisely by Banerjee from his X-ray measurements.*

Having fixed the directions of the *lengths* of the molecules, we orientations of their *planes*. Banerjee finds that they are inclined at respectively, to the (010) plane. In order to deduce the value of th magnetic measurements, a knowledge of the principal susceptibilities molecules, say, K_1, K_2 and K_3 along their lengths, their breadths an their planes, respectively, is necessary. A calculation of these con made by one of us from direct considerations of the structure of th method which has recently been used with success for the benzene susceptibility normal to the plane of the naphthalene molecule comes o lation to be about four times as much as for directions in the plane.‡ result with the known values for χ_1, χ_2 and χ_3 for the crystal the orie molecules can easily be calculated.

Magnetic Constants of the Naphthalene Molecule.—However, in view o information, already available from X-ray measurements, regarding orientations in the crystal, it will be more logical to use this to calcula values of the magnetic constants of the molecules, rather than to de orientations from their magnetic constants deduced from structural c which at best must be considered as only approximate. We directly pro The calculations are simple since we have the following relations :—

$$\chi_1 = K_1$$

$$\chi_2 = K_2 \cos^2 65° + K_3 \sin^2 65°$$

$$\chi_3 = K_2 \sin^2 65° + K_3 \cos^2 65°.$$

* It may be remarked here that the value of this angle given by the magnetic method is than the X-ray value, since the former is obtained by a direct measurement of the orien crystal when suitably suspended in a magnetic field. It is, however, a matter for satisfac values given by the two methods agree so closely.

† Raman and Krishnan, 'C. R. Acad. Sci. Paris,' vol. 184, p. 449 (1927).

‡ The calculations have not been published. The results are quoted by Bhagavantam, *loc*

Using the known values of the χ's for the crystal, we obtain for the principal susceptibilities of the *molecule**

$$K_1 = -39{\cdot}4$$
$$K_2 = -43{\cdot}0$$

and
$$K_3 = -187{\cdot}2.$$

Thus, the plane of the naphthalene molecule is almost a plane of magnetic symmetry. Also the susceptibility along the normal to the plane is about $4\frac{1}{2}$ times as much as for directions in the plane; this confirms the results of our calculations from its structure, referred to in an earlier paragraph.

Optical Constants of the Naphthalene Molecule.—Since any information regarding the physical constants of individual molecules is of great interest, we remark in passing that the above data for the magnetic constants of the naphthalene molecule enable us to calculate its optical constants also; other data necessary for the calculation are (1) refractivity, (2) depolarisation factor of light-scattering, and (3) Cotton-Mouton constant. The calculation† gives for the polarisabilities of the molecule along its length, its breadth and normal to its plane the values $26{\cdot}7 \times 10^{-24}$, $14{\cdot}2 \times 10^{-24}$ and $11{\cdot}5 \times 10^{-24}$ respectively, for the sodium line.

These values when taken together with the known orientations of the molecules in the crystal would suggest for the plane of its optic axes (010). This agrees with observation.

2. *Anthracene.*

We next consider anthracene. This crystal also belongs to the monoclinic prismatic class, and there are two molecules in the unit cell. On the basis of his X-ray measurements BANERJEE finds that the lengths of both the molecules (*i.e.*, the lines joining the centres of the three component benzene rings) lie in the (010) plane in the obtuse angle β at 9° to the "c" axis. The planes of the molecules, as in the case of naphthalene, are inclined at + 65° and − 65° to the (010) plane.

The above inclination of the long axes of the molecules to the "c" axis, viz., + 9°, is directly confirmed by our magnetic measurements, since $\psi = +8{\cdot}0°$. Concerning the orientations of the molecular planes, we will adopt, as we did for naphthalene, the results of the X-ray measurements and calculate the molecular magnetic constants. We thus obtain for the principal susceptibilities of the molecule along its length, along its breadth and along the normal to its plane respectively, the values

$$K_1 = -45{\cdot}9$$
$$K_2 = -52{\cdot}7$$
$$K_3 = -272{\cdot}5.$$

* The K's, just like the χ's, refer to one gm. mol. and are also expressed in the same unit, viz., 10^{-6} of a c.g.s. electromagnetic unit.

† The details of the calculation will be published elsewhere.

Here, also, the normal to the plane of the molecule is practically an axis of magnetic symmetry, in spite of the large geometric asymmetry in the plane.

3. *Benzene, Naphthalene and Anthracene.*

Knowing now the molecular magnetic constants of naphthalene and anthracene, it is desirable to calculate the constants for benzene in order to be able to compare the values for the three molecules. The necessary X-ray investigations, as well as magnetic measurements on crystalline benzene, are not available. The constants for benzene can, however, be calculated from its Cotton-Mouton constant and the depolarisation factor of its light-scattering, since we may without appreciable error assume the molecule to possess an axis of symmetry. Taking the Cotton-Mouton constant for liquid benzene at 18° C. as $5{\cdot}90 \times 10^{-13}$ and the depolarisation factor for transverse scattering of unpolarised incident light at the same temperature as 0·417, we get for the principal susceptibilities of the molecule, viz., K_1 and K_2 in the plane of the ring and K_3 normal to it, the values

$$K_1 = K_2 = -37{\cdot}3$$
$$K_3 = -91{\cdot}2.$$

The values for the three molecules are collected in Table VI.

TABLE VI.

Molecule	K_1	K_2	K_3	Mean K
Benzene	37·3	37·3	91·2	55·3
Naphthalene . . .	39·4	43·0	187·2	89·8
Anthracene	45·9	52·7	272·5	123·7

It is remarkable that as we proceed from benzene to naphthalene and from naphthalene to anthracene, the numerical increases in diamagnetic susceptibility are confined practically to one direction, viz., normal to the plane of the benzene rings.*

4. *Biphenyl and Dibenzyl.*

We next consider biphenyl and dibenzyl, which, in view of the fact that the X-ray measurements at present available are not sufficiently precise to determine the

* In the previous article, we have assumed the orientations of anthracene molecules given by X-ray measurements and calculated the K's. On the other hand, if complete X-ray analysis of the crystal had not been made, we could still have deduced the K's either from structural considerations, as for naphthalene, or preferably from the relation

$$K_i^{C_{14}H_{10}} - K_i^{C_{10}H_8} = K_i^{C_{14}H_{14}} - K_i^{C_6H_6}, \quad i = 1, 2, 3,$$

and thence determined solely from magnetic data the correct orientations of molecules in the unit cell.

'es in their unit cells, offer good scope for analysis by the

belongs to the monoclinic prismatic class. Its structure has
methods by HENGSTENBERG and MARK* and independently
'hey assign it to the space group C_{2h}^5. Its unit cell contains
er one takes the benzene rings in biphenyl to have a puckered
and MARK have done, or to have a plane structure by
xamethyl benzene, analysed by Mrs. LONSDALE,‡ and the
racene, according to BANERJEE, it is possible to satisfy the
e molecule in the crystal. In either case, the planes of
igs of any given molecule—their mean planes in the former
planes in the latter—have to be orientated in the same
e the orientations of these planes,§ without making any
he planes are puckered or not. *We will only assume that*
ve the same structure as in the benzene molecule.

alculate the magnetic constants of the biphenyl molecule
benzene. The mean gram molecular susceptibility of
numerically less than twice the susceptibility of the
s difference is clearly the contribution from the two
ı dropped out from the benzene rings in the formation
rst approximation, we assume that the above numerical
to dropping the H^- atoms, is the same along the three
le.‖ We then obtain for the principal susceptibilities
ı and K_2 along its length (*i.e.*, the line joining the
ıd breadth respectively in the plane of the benzene
the plane, the values

$$= K_2 = -\ 66{\cdot}9$$

$$K_3 = -\ 174{\cdot}7.$$

931).

929).

nzene ring is taken by HENGSTENBERG and MARK to be the
in the usual notation, the other two C-atoms, viz., 1 and 4,
ıe other hand, the "mean plane," referred to in this paper,
them, 1, 3, 5 lie on one side of this plane and the remaining
ame distance.

ı the truth; even if it is, since this contribution is small
nolecule (only about 7½ per cent), the particular manner
tions is a matter of little consequence.

On the other hand, the values for the crystal are

$$\left.\begin{aligned}\chi_1 &= -\ 63{\cdot}4\\ \chi_2 &= -\ 146{\cdot}5\\ \chi_3 &= -\ 98{\cdot}9\end{aligned}\right\};\quad \psi = +20{\cdot}1^\circ.$$

A correlation of the two sets of constants given above gives the following orientations for the two molecules in the unit cell of biphenyl. Let both the molecules have their planes parallel to (100) and their lengths along the "*c*" axis. In order to bring the molecules to their actual orientations, we have to give them the following rotations:

Firstly, a rotation about the "*c*" axis of one of the molecules through an angle λ and of the other through $-\lambda$;

Secondly, a rotation of both the molecules about the "*b*" axis through an angle of μ, the positive direction of the rotation being defined as being from the "*c*" axis to the "*a*" axis through the obtuse angle β; and

Thirdly, a rotation of the two molecules through angles $+\nu$ and $-\nu$ respectively, about the normal to the plane which contains the "*b*" axis and the direction of the lengths of the molecules obtaining after rotation (2) has been performed.

Evidently

$$\mu = \psi = +20{\cdot}1^\circ.$$

λ and ν can be evaluated from the following relations:*

$$\chi_1 = K_1 \cos^2\nu + (K_2\cos^2\lambda + K_3\sin^2\lambda)\sin^2\nu$$
$$\chi_2 = K_2\sin^2\lambda + K_3\cos^2\lambda$$
$$\chi_3 = K_1\sin^2\nu + (K_2\cos^2\lambda + K_3\sin^2\lambda)\cos^2\nu.$$

Solving them, we get

$$\lambda = 31^\circ$$
$$\nu = 0.$$

We thus find that the lengths of the molecules lie in the (010) plane in the obtuse angle β at 20·1° to the "*c*" axis, while the planes of the molecules are inclined at plus and minus 31° respectively to the "*b*" axis.

It would be interesting to confirm by further X-ray measurements on biphenyl the above assignment of orientations of the molecules in its unit cell.†

* Since we have already assumed that $\chi_1+\chi_2+\chi_3 = K_1+K_2+K_3$, only two of these relations are independent.

† [*Note added November* 7, 1932.—Further X-ray investigations on this crystal have recently been made by Mr. J. DHAR ('Ind. J. Phys.,' vol. 7, p. 43 (1932)), and they confirm the results of our magnetic analysis. In the first place Mr. DHAR finds that the lengths of the molecules lie in the (010) plane, in the obtuse angle β, at 20° to the "*c*" axis; our value for the angle is 20·1°. As regards the planes of the molecules, he finds that they are inclined at plus and minus 32° to the "*b*" axis; this is in close agreement with the values plus and minus 31° for this angle calculated by us from the magnetic data.]

Dibenzyl.—Dibenzyl also crystallizes in the monoclinic prismatic class, and has been assigned by HENGSTENBERG and MARK to the space group C_{2h}^5. The molecule is found to have a centre of symmetry, the unit cell containing two molecules.

The magnetic constants for the molecule can be calculated in the same manner as for biphenyl. In the same notation,

$$K_1 = K_2 = -91{\cdot}7$$
$$K_3 = -199{\cdot}5.$$

Correlating these with the values for the crystal, we obtain for the angular parameters λ, μ and ν that define the orientations of the molecules in the unit cell, again using the same notation as for biphenyl, the values

$$\lambda = 30^\circ$$
$$\mu = +83{\cdot}9^\circ$$
$$\nu = 0.$$

On comparing these values with those for biphenyl, we find that in both the crystals the molecular planes are inclined at about 30° to the "*b*" axis; also the lengths of the molecules lie in both cases in the (010) plane in the obtuse angle β. There is this essential difference, however, between the two crystals. Whereas in biphenyl the molecular lengths are inclined at 20·1° to the "*c*" axis, in dibenzyl they are almost normal to the "*c*" axis (actually at 83·9°). This difference is reflected in the dimensions of the unit cell, as we should expect; whereas the "*c*" axis is the longest axis for biphenyl ($a = 8{\cdot}22$ A, $b = 5{\cdot}69$ A, $c = 9{\cdot}50$ A), for dibenzyl the longest axis is the "*a*" axis, since $a = 12{\cdot}82$ A, $b = 6{\cdot}18$ A and $c = 7{\cdot}74$ A.

The optical observations on this crystal, viz., that the optic axes lie in (010) and that the bisectrix lies in the acute angle β, making a small angle with the "*c*" axis, are in agreement with the molecular orientations suggested here.

Before concluding this article, it may not be out of place to remark that the centro-symmetric structure of the molecules of biphenyl and dibenzyl points to a zero dipole moment for these molecules. This is in conformity with observation.*

5. *Azobenzene and Stilbene.*

We will first consider azobenzene. This crystal has recently been analysed by X-ray methods by PRASAD.† It is assigned to the space group C_{2h}^5 in the monoclinic prismatic class, with four molecules in the unit cell, whose dimensions are

$$a = 12{\cdot}65 \text{ A}, b = 6{\cdot}06 \text{ A}, c = 15{\cdot}60 \text{ A}; \quad \beta = 114{\cdot}4^\circ.$$

* W. LAUTSCH. 'Z. Phys. Chem.,' B, vol. 1, p. 115 (1928).
† 'Phil. Mag.,' vol. 10, p. 306 (1930).

"A remarkable feature of this crystal" according to PRASAD "is the nearly complete symmetry about the (20 $\bar{1}$) plane both in respect to the geometrical relations and to the intensities of reflection by corresponding planes." Using the above dimensions for the unit cell for calculation, we find that the (20 $\bar{1}$) plane is nearly normal to the "*a*" axis. We should therefore expect the normal to the (001) plane to be an axis of magnetic symmetry. This is actually so, because, in the first place, one of the principal magnetic axes, viz., the χ_3-axis, lies along that direction and, secondly, χ_1 has nearly the same value as χ_3; the values are

$$\chi_3 = -130{\cdot}2$$
$$\chi_1 = -87{\cdot}5$$
$$\chi_3 = -83{\cdot}1.$$

Since the number of molecules in the unit cell is 4, which is the maximum number necessary to complete the symmetry of the class, it is presumable that the molecule itself has no element of symmetry. This result appears surprising in view of the centro-symmetry of the biphenyl and dibenzyl molecules, but is supported by the magnetic observations. Suppose we assume that azobenzene has a structure similar to that of biphenyl or dibenzyl with a centre of symmetry. The molecular magnetic constants would then be

$$K_1 = K_2 = -64$$
$$K_3 = -172.$$

Correlating these values with those for the crystal, we get for the angular parameters λ, μ, ν in our usual notation

$$\lambda = 39^\circ$$
$$\mu = -65{\cdot}6^\circ$$
$$\nu = 48^\circ.$$

These values place the lengths of the molecules in the (001) plane, at an angle of 48° to the "*a*" axis and therefore at 42° to the "*b*" axis; *i.e.*, the long axes of the molecules lie nearer to the "*b*" axis than to the "*a*" axis. The dimensions of the unit cell, however, show that this conclusion cannot be correct. Thus, we find that the lengths of the two component benzene rings of the molecule—by the length of the ring we mean the line joining the C-atoms 4 and 1, or 1′ and 4′—cannot lie along the same line.

Also the *planes* of the two component benzene rings cannot be parallel to each other since in that case the value of χ_1 ought to be equal to −64, whereas it is actually equal to −87·5.

Thus solely from the magnetic data and the known axial ratio $a : b$, we can conclude, regarding the benzene rings of the azobenzene molecule, that they cannot have either their

lengths parallel to each other, or their planes parallel to each other. Hence the molecule has no element of symmetry—a conclusion in conformity with the X-ray evidence.

If we assume, not unreasonably, that the two halves of the azobenzene molecule are identical and that the greatest length of the molecule lies along the "a" axis, the magnetic constants suggest that the planes of the two benzene rings of the molecule are inclined at $+ 39°$ and $- 39°$, respectively, to the (001) plane, and that the lengths of the rings, as defined above, lie in the (001) plane at about $+ 48°$ and $- 48°$ to the "a" axis. Thus we get an estimate of the "twist" and the "folding up" of the two benzene rings of the azobenzene molecule in the crystal.

The weak birefringence of the azobenzene crystal observed by BHAGAVANTAM* is not difficult to understand on the basis of the above structure.

Coming to stilbene, which is also monoclinic and belongs to the C_{2h}^5 prismatic class, it is very similar in its crystal structure and in its magnetic properties to azobenzene. The existence of a pseudo-rhombic symmetry (just as in azobenzene) has been remarked by HENGSTENBERG and MARK)†; magnetically, the normal to the (001) plane (which is along the χ_2 axis) is an axis of symmetry.

This molecule also has no element of symmetry. The orientations of the two component benzene rings of the molecule with respect to each other, as also with respect to the crystallographic axes, can be estimated in the same manner as for azobenzene.

6. β-*Naphthol.*

Next we take β-naphthol. It belongs to the monoclinic prismatic class. The crystal has been analysed by BRAGG‡ and is found to contain 4 molecules in the unit cell.

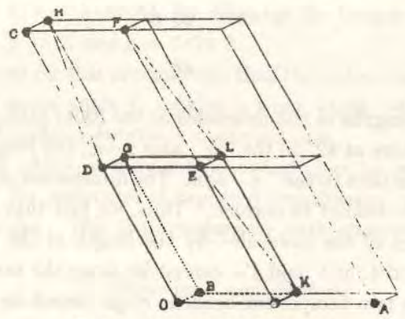

FIG. 1.—Unit cell of β-naphthol.

Taking the molecules at O, D, K and L, fig. 1, as belonging to the unit cell under consideration, their lengths are placed by BRAGG along the diagonals OG, DH, EK and

* 'Ind. J. Phys.,' vol. 4, p. 1 (1929).

† *Loc. cit.*, footnote on p. 294.

‡ 'Proc. Phys. Soc., Lond.,' vol. 34, p. 45 (1922).

FL respectively. As regards the magnetic evidence for their orientations, the constants for the crystal are

$$\left.\begin{aligned}\chi_1 &= - 62{\cdot}3\\ \chi_2 &= - 148{\cdot}3\\ \chi_3 &= - 80{\cdot}4\end{aligned}\right\};\quad \Psi = + 9{\cdot}4°.$$

Those for the molecule can be calculated from the known constants for naphthalene on the assumption that the small numerical increase in susceptibility of the molecule when we pass from naphthalene to β-naphthol, due to the replacing of a H-atom by the OH-group, takes place isotropically. Then the molecular susceptibilities along the length, breadth and the normal to the plane are, respectively,

$$K_1 = - 46{\cdot}6$$

$$K_2 = - 50{\cdot}2$$

$$K_3 = - 194{\cdot}4.$$

A correlation of the two sets of constants gives the following orientations for the molecules. Starting with all the molecules in the unit cell, having their planes parallel to (100) and their lengths along the "c" axis, we have, to give them the following rotations in order to bring them to their actual orientations in the crystal:—

(1) about the "c" axis: half the molecules through an angle λ and the other half through an angle $- \lambda$;

(2) about the "b" axis: all the molecules through an angle μ (the positive direction of μ being defined as before);

(3) about the normal to the plane containing the "b" axis and the directions of the lengths of the molecules obtaining after rotation (2) has been performed: half the molecules through an angle ν and the other half through $- \nu$.

The choice of the particular molecules for the positive and for the negative rotations in (1) and (3) is determined by the requirements of the symmetry of the crystal.

Calculation gives

$$\lambda = 34°$$

$$\mu = + 9{\cdot}4°$$

$$\nu = 34°.$$

7. *Acenaphthene.*

The crystal belongs to the orthorhombic class, having the fullest symmetry of that class. Its structure has been analysed by BRAGG.* There are 4 molecules in the unit cell. BRAGG provisionally places the planes of all the molecules in the (001) plane,

* 'Proc. Phys. Soc. Lond.,' vol. 34, p. 45 (1922).

their lengths making angles of about 30½° with the "*b*" axis on either side. (See fig. 2. The positions of the molecules in the unit cell are denoted in the figure by dots, and the directions of the lengths of the molecules by arrows.)

Magnetically, if we assume with BRAGG, that the lengths of the molecules lie in (001) plane, it is found on calculation that they make angles of plus and minus 24° with the "*b*" axis, while the molecular planes are inclined at about 41½° to the (001) plane.

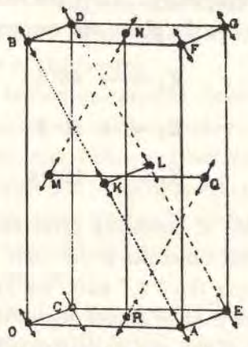

FIG. 2.—Unit cell of acenaphthene.

The known optical properties of the crystal are consistent with the orientations proposed here. Just as in the case of naphthalene, the optical polarisability of the acenaphthene molecule should be a maximum along its length and a minimum along the normal to its plane. From the molecular orientations, given in the previous paragraph, we should therefore expect the optical polarisability of the crystal to be a maximum along the "*b*" axis and a minimum along the "*c*" axis. This is actually the case, since the crystal shows a positive birefringence, the (100) plane being the axial plane and the "*b*" axis being the acute bisectrix.

8. *Conclusion.*

From what has been said in the previous pages it is clear that in favourable cases, *e.g.*, biphenyl and dibenzyl, it is possible from magne-crystallic measurements to determine the precise orientations of the molecules in the unit cell; in less favourable cases, *e.g.*, naphthalene and anthracene, some of the angular parameters defining the orientations can be so derived; even in complicated cases like stilbene and azobenzene, where it is not possible to obtain a unique solution, the magnetic data throw considerable light on the question, which would help us at least to decide between alternative orientations suggested by X-ray methods. In any case, it is obvious that no structure proposed by X-ray methods can be considered acceptable which cannot satisfactorily explain the observed magnetic properties of the crystal. Thus the magnetic method of analysis of molecular orientations in crystals promises to be a useful supplement to X-ray methods of analysis.

We have much pleasure in thanking the Government of Bengal and the University of Dacca for the grant of Research Scholarships to the two junior authors which made it possible for them to collaborate in this work.

Summary.

The paper describes a convenient method of determining the magnetic anisotropy of crystals by oscillating them about different axes in a uniform magnetic field. Amongst the inorganic crystals studied by this method were quartz, calcite, aragonite, strontianite, witherite, sodium and potassium nitrates, potassium chlorate, barite, celestite, anhydrite, gypsum and sulphur. It may be noted that while the nitrates and carbonates exhibit a large anisotropy, the sulphates are more or less completely isotropic.

The organic crystals investigated were naphthalene, anthracene, β-naphthol, acenaphthene, biphenyl, dibenzyl, benzophenone, benzil, azobenzene, hydrazobenzene and salol. In most of the above crystals the mean of the three observed principal susceptibilities agrees well with the value calculated for the substance from the well-known additive relations of Pascal. Azobenzene and hydrazobenzene are, however, exceptions in this respect, as the additive value is numerically much higher than the actual mean value for the crystal.

On comparing the mean susceptibilities of naphthalene and benzophenone crystals with the values obtained for these two substances in the fused state, it is found that while the susceptibility of naphthalene remains practically unchanged, benzophenone shows a diminution of 2½ per cent on melting. A possible connection between the dipole character of the molecule and such a change is indicated.

A correlation of the principal magnetic constants of the crystal with those of the individual molecules constituting it may be effected with the help of the data on magnetic birefringence and light-scattering. This offers a useful method of determining the orientations of the molecules in the crystal lattice, and is found to work very satisfactorily, leading to accurate results, two typical instances being biphenyl and dibenzyl.

IV. *Investigations on Magne-Crystallic Action. Part* II.—*Paramagnetics.*

By K. S. KRISHNAN, *Reader in Physics, and* N. C. CHAKRAVORTY *and* S. BANERJEE, *Research Students, Dacca University.*

(*Communicated by Sir* VENKATA RAMAN, *F.R.S.*)

(Received, December 1, 1932. Read, February 2, 1933.)

CONTENTS.

1. INTRODUCTION.

In Part I* we gave an account of some magnetic measurements on diamagnetic crystals. It is found that the diamagnetic anisotropy of a crystal can be satisfactorily explained in terms of the intrinsic anisotropy of the individual molecules (or ions) constituting it and their relative orientations. Thus by a study of the magnetic properties of diamagnetic crystals much useful information can be obtained regarding the anisotropies of molecules and their orientations in the crystal lattice.

The study of paramagnetic crystals is also of great interest, but for other reasons. Here the crystal-forces play an all-important part in determining their anisotropy, as opposed to diamagnetic crystals where the influence of crystal structure is indirect, and appears only so far as it determines the relative orientations of the molecules. The recent work of BETHE† on the Stark-splitting of the energy levels of a paramagnetic

* 'Phil. Trans,' A, vol. 231, p. 235 (1932).

† 'Ann. Physik,' vol. 3, p. 133 (1929); 'Z. Physik,' vol. 60, p. 218 (1930).

ion in a crystal, under the influence of the crystalline forces, and the discussions by VAN VLECK,* and by PENNEY and SCHLAPP† about the effect of this splitting on the magnetic behaviour of the ion, throw considerable light on the origin of the magnetic anisotropy in a paramagnetic crystal. From the point of view of these newer theories, especially in consideration of our present incomplete knowledge regarding atomic energy levels in crystals, extensive data on the anisotropies of paramagnetic crystals would be useful. The present paper describes the results of some direct measurements on anisotropy for a number of crystals.

Data are already available for several crystals from the susceptibility measurements that have been made by FINKE,‡ JACKSON,§ RABI‖ and others. Their results, however, do not show satisfactory agreement among themselves; even the directions of the magnetic axes in the crystal—which can easily be determined with accuracy—disagree considerably. Let us take, for example, the two cobalt salts that have been investigated by most of them, viz., $CoSO_4 . K_2SO_4 . 6H_2O$ and $CoSO_4 . (NH_4)_2SO_4 . 6\ H_2O$, both of which crystallize in the monoclinic system. The following table gives their magnetic constants. (The values of JACKSON refer to 17° C. and those of RABI to 27° C. FINKE does not mention the temperature.)

TABLE I.¶

Crystal.	ψ.	$\chi_1 - \chi_2$.	$\chi_1 - \chi_3$.	Mean χ.	Author.
$CoSO_4 . K_2SO_4 . 6H_2O$	° ′ −21 20 +20 2 −44	3360 2370 2550	−2090 1670 1760	12,750 11,080 9,830	FINKE. JACKSON. RABI.
$CoSO_4 . (NH_4)_2SO_4 . 6H_2O$ . .	−27 31 −31 18 −13	2570 1530 3200	2170 240 1490	10,050 9,690 10,050	FINKE. JACKSON. RABI.

For other crystals also, where comparison is possible, the discrepancies are of the same order of magnitude. In view of these discrepancies many crystals that have already been studied by them are also included in our present investigations.

* 'Phys. Rev.,' vol. 41, p. 208 (1932).

† *Ibid.*, vol. 41, p. 194 (1932).

‡ 'Ann. Physik,' vol. 31, p. 149 (1910).

§ 'Phil. Trans,' A, vol. 224, p. 1 (1924); vol. 226, p. 107 (1927); also JACKSON and DE HAAS, 'Proc. Amst. Acad. Sci.,' vol. 31, p. 346 (1928).

‖ 'Phys. Rev.,' vol. 29, p. 174 (1927).

¶ The notation adopted is the same as in Part I of this paper; χ_1 and χ_2 are the principal gram molecular susceptibilities in the b(010) plane, and χ_3 along the "b" axis; the χ_1 — axis ($\chi_1 > \chi_3$) makes an angle ψ with the "c" axis, and an angle $\beta - \psi$ with the "a" axis, β being obtuse. The unit for the χ's is 10^{-6} of a c.g.s. e.m.u.

2. *Discussion on Earlier Measurements.*

General method of measurement.—The method generally adopted in determining the magnetic anisotropy of a crystal is to measure the susceptibilities along different convenient directions in the crystal and thence to find the directions of the principal magnetic axes, and also the susceptibilities along them. For example, for a monoclinic crystal one such measurement along the "*b*" axis and three others along three other directions, suffice to determine all the four magnetic constants of the monoclinic crystal, viz., ψ and the three χ's. In place of one of these measurements a measurement on the crystal powder, which gives $\frac{1}{3}(\chi_1 + \chi_2 + \chi_3)$, is sometimes substituted.* Even though these measurements give the absolute values with fair accuracy,† they are not sufficiently precise to lead to reliable values either for the anisotropy of the crystal, that is, for the differences between the principal susceptibilities, or for ψ.‡ Thus in measuring the anisotropy a direct method will evidently be preferable to an indirect one.

JACKSON'S *method.*—JACKSON has developed and used one such method in his well-known investigations on the monoclinic crystal $CoSO_4 . (NH_4)_2SO_4 . 6H_2O$. Since, however, in his application of the method there are some serious errors, we discuss it here in some detail.

If a cylinder is cut out of the crystal and suspended with its axis vertical in a uniform horizontal magnetic field, there will be a couple tending to rotate it about the axis. Its magnitude will evidently be given by

$$C = \frac{1}{2}(\chi_I - \chi_{II}) \cdot \frac{m}{M} \cdot H^2 \cdot \sin 2\phi \quad . \quad . \quad . \quad . \quad . \quad . \quad . \quad . \quad (1)$$

where χ_I and χ_{II} are the maximum and the minimum values of the gram molecular susceptibility in the horizontal plane and ϕ is the angle which the direction of the field makes with the χ_I-axis. The sense of the couple will be such as to place the χ_I-axis (since $\chi_I > \chi_{II}$) along the field. By varying ϕ and measuring the maximum value of the couple (corresponding to $\phi = 45°$), $\chi_I - \chi_{II}$ is evaluated.

* For example, for the monoclinic crystal $MnSO_4 . (NH_4)_2 SO_4 . 6H_2O$, JACKSON and DE HAAS (*loc. cit.*) measure the susceptibility of the powder, and with single crystals the susceptibilities along the "*b*" axis and along two other directions. These measurements are sufficient to determine ψ and the three χ's uniquely; there is no ambiguity in the calculated value of ψ as JACKSON and DE HAAS remark. (See KRISHNAN, 'Z. Phys.,' vol. 71, p. 137 (1931).)

† With measurements on powdered crystals unless they are very closely packed, there will be a tendency for them to orientate in the field, especially when they are strongly anisotropic. Hence the assumption of random orientation is not always justifiable. We refer the reader to the discussions regarding measurements on solidified naphthalene in Part I. It should be remembered that with measurements on single crystals, individual crystals vary considerably in density, and the values given in the standard literature represent the *highest* values obtained from measurements on a large number of crystals (TUTTON, "Crystallography," p. 625).

‡ We must make an exception here to RABI's measurements. The "null method" which he adopts yields results of great accuracy.

JACKSON cuts three such cylinders of $CoSO_4 . (NH_4)_2SO_4 . 6H_2O$ with their axes perpendicular to the crystallographic planes (100), (010) and (001) respectively and thus determines *a*, *b* and *c*, where these denote $\chi_3 - \chi_c$, $\chi_1 - \chi_2$ and $\chi_3 - \chi_a$ respectively; here χ_a and χ_c are the gram molecular susceptibilities of the crystal along the "*a*" and the "*c*" axes respectively, and are therefore given by

$$\chi_a = \chi_1 \cos^2(\beta - \psi) + \chi_2 \sin^2(\beta - \psi) \quad . \quad . \quad . \quad . \quad . \quad . \quad . \quad . \quad (2)$$

$$\chi_c = \chi_1 \cos^2\psi + \chi_2 \sin^2\psi \, . \quad . \quad . \quad . \quad . \quad . \quad . \quad . \quad . \quad . \quad . \quad . \quad . \quad (3)$$

A fourth measurement is made by JACKSON on the crystal powder, which gives $\frac{1}{3}(\chi_1 + \chi_2 + \chi_3)$.

In the first place JACKSON seems to have measured only the *numerical* values of the couples acting on the crystal cylinders without taking any note of the *signs* of the couples. It happens that the positive signs which he assigns to $\chi_3 - \chi_a$ and $\chi_3 - \chi_c$ are incorrect in both the cases; actually both χ_a and χ_c are found to be greater than χ_3.*

Even when the proper signs are assigned to the above couples it is easy to see that the four measurements made by JACKSON are not sufficient to determine all the four magnetic constants of the monoclinic crystal uniquely. Solving for ψ, for example, we obtain

$$\sin(2\psi - \beta) = \frac{a - c}{b \sin\beta}, \quad . \quad . \quad . \quad . \quad . \quad . \quad . \quad . \quad . \quad . \quad . \quad . \quad (4)$$

which will, in general, give *two* different values for ψ† (with the corresponding ambiguity in the values for the χ's). This ambiguity in the value of ψ can be eliminated if in the course of the measurement of *b*—with the "*b*" axis of the crystal vertical—a further observation is made of the orientation of the crystal in the field, under zero torsion of the suspension fibre. However, JACKSON gives both the solutions for ψ, and chooses one of them for the reason that it happens to agree nearly with a previous determination by FINKE; whereas on calculation, with the proper signs for *a* and *c*, we find that neither of the solutions for ψ is near FINKE's value; the two solutions are $+ 58° 59'$ and $\overline{-} 42° 3'$ at 17° C., while FINKE's value is $- 27° 31'$.

3. *Method Adopted.*

Most of the crystals studied by us belong to the monoclinic system and our descriptions therefore, refer specifically to this crystal type. The present measurements may conveniently be divided into two parts.

(1) The determination of the principal magnetic axes and of the anisotropy of the crystal, *i.e.*, of ψ and of $\chi_1 - \chi_2$ and $\chi_1 - \chi_3$: ψ is measured *directly* by suspending the

* By definition $\chi_1 - \chi_3$ is always positive.

† Values of ψ differing from one another by multiples of π are, of course, taken to be identical.

crystal in a uniform magnetic field with its "b" axis vertical, and noting its orientation in the field. The influence of the asymmetry of shape of the crystal—which is discussed in detail in the next section—is usually negligible. When, however, the magnetic anisotropy is very small, as with manganese salts, the effect of the asymmetry cannot be neglected. With such salts it was eliminated by surrounding the crystal by a liquid bath having the same volume susceptibility as the crystal. This method of eliminating the effect of the asymmetry of shape was found to be more convenient than the usual method of using the crystal in the form of a cylinder; it is a great advantage to be able to use the crystal in its natural form, for then direct observations can be made on the dispositions of the different faces of the crystal in the field.

The magnetic anisotropy of the crystal was determined by suspending it about different suitable axes in the uniform field and finding the value of the couple tending to rotate it. Where the crystal was immersed in the liquid bath, the couple was measured statically from the rotation of the torsion head that was necessary to counterbalance it; for other crystals the couple was calculated from the periods of oscillation of the crystal in the field and outside it, and the method of measurement was the same as that adopted by us for diamagnetic crystals, and described in Part I.

(2) Measurement of the absolute susceptibility along any one direction. For this purpose RABI's "null method" was adopted, but, instead of the stout glass-suspension used by RABI—which was necessary in his measurements in order to prevent the rotation of the crystal in the field—a fine quartz-suspension was used. For our purpose a measurement of the susceptibility along *any* one direction in the crystal was sufficient, and hence we could choose that direction which naturally tends to lie along the field. The quartz suspension considerably improved the sensitiveness of the arrangement.

4. *Influence of the Asymmetry of Shape of the Crystal.*

Since in our measurements on magnetic anisotropy, the crystal was used in its natural form, it is necessary to have a correct estimate of the effect of the asymmetry of shape of the crystal on the measurements. For convenience in discussion, we may consider a magnetically isotropic body of highly asymmetric shape; when such a body is suspended in a "uniform" magnetic field, the effect of the asymmetry of shape will be two-fold. Firstly, even if the field is ideally homogenous (before the body is brought in), the body will tend to place its greatest length along the field, since the "demagnetising force" is then a minimum. This rotating couple will, however, be very small. For extreme asymmetry where the body is in the form of a very thin plate with its plane vertical, the rotating couple will be equivalent to that caused by a magnetic anisotropy in the body whose magnitude is given by

$$\frac{\Delta k}{k} = 4\pi k, \quad \ldots\ldots\ldots\ldots\ldots \quad (5)$$

where k is the volume susceptibility of the plate. Even for strongly paramagnetic bodies ($k = 10^{-4}$) and with such extreme asymmetry of shape, $\Delta k/k$ is only about 10^{-3}. Usually it would be much smaller.

Secondly, as already mentioned, actual fields deviate slightly from homogeneity. There will therefore be a couple tending to rotate it into the strongest part of the field. This couple was measured for a thin plate of ferric ammonium alum, which crystallizes in the cubic system, when its plane was vertical and at 45° to the field. The length and breadth of the plate in the horizontal plane were 8 mm. and 1 mm. respectively. The couple was "equivalent" to that from a magnetic anisotropy $\Delta k/k = 2 \times 10^{-3}$. Measurements with other crystals also gave values of the same order of magnitude. (These values agree with those obtained with diamagnetic crystals in Part I of this paper, viz., $\Delta k/k = 1{\cdot}5 \times 10^{-3}$.)

Hence for all the crystals studied here, except the manganese salts, for which $\Delta k/k$ ranges from 3 per cent. to 30 per cent., the effect of any ordinary asymmetry of shape will be negligible. For manganese salts, however, this effect had to be eliminated by a special arrangement already mentioned, viz., by surrounding the crystal by a liquid bath of the same volume susceptibility.

5. *Measurements on Magnetic Anisotropy.*

This section deals with measurements on crystals whose anisotropies are so large that they do not require the use of a paramagnetic bath for eliminating the effect of the shape of the crystals. (Feebly anisotropic substances, which require such a bath, are dealt with in the next section.) The anisotropies were measured by the method of oscillations, described in Part I.

Most of the monoclinic crystals described here had their (001) faces very well developed. In the measurement of ψ, therefore, the inclination of this face to the plane normal to the field was directly measured. This gives the inclination of the χ_2-axis to the "a" axis. Denoting this by θ, and taking it as positive towards the obtuse angle β of the monoclinic crystal, we have the equation

$$\frac{\pi}{2} + \theta + \psi = \beta \quad \ldots\ldots\ldots\ldots\ldots \quad (6)$$

Usually in addition to the determination of ψ, *three* oscillation measurements were made for the monoclinic crystal, though two of them are sufficient to give $\chi_1 - \chi_2$ and $\chi_3 - \chi_2$ uniquely. The third offers a check on the accuracy of the measurements. The modes of suspension for the three oscillations were usually

(1) "b" axis vertical;

$$|\Delta\chi| = \chi_1 - \chi_2 \quad \ldots\ldots\ldots\ldots\ldots \quad (7)$$

(2) "a" axis vertical;

$$|\Delta\chi| = \pm (\chi_1 \cos^2\theta + \chi_3 \sin^2\theta - \chi_2) \quad \ldots\ldots\ldots\ldots\ldots \quad (8)$$

the plus or the minus sign being taken according as the "b" axis lies normal to the field or along it;

(3) (001) plane horizontal;

$$|\Delta\chi| = \pm (\chi_1 \sin^2\theta + \chi_2 \cos^2\theta - \chi_3) \quad \ldots\ldots\ldots \quad (9)$$

In some crystals, as, for example, in ferrous ammonium sulphate, the (20$\bar{1}$) plane was developed much better than the (001) plane. In these crystals the inclination of the χ_2-axis to this plane was measured and thence ψ was calculated. The oscillation measurements were made with (1) "b" axis vertical, (2) (20$\bar{1}$) plane vertical, and "b" axis horizontal, and (3) (20$\bar{1}$) plane horizontal.

The results obtained are given in Table II. Since one more measurement is made than is necessary to give $\chi_1 - \chi_2$ and $\chi_1 - \chi_3$, ψ is also treated as an unknown and calculated from the oscillation measurements,* and compared with the directly determined value. Also in order to be quite sure that the asymmetry of shape has no appreciable influence, the measurement of ψ was repeated in several experiments with the crystal immersed in a bath of the same volume susceptibility as that of the crystal along the field. The two values of ψ agree within the limits of experimental error.

The different columns in the table have the same significance as in Tables I and IV in Part I. The values refer to a temperature of about 30° C.

6. *Feebly Anisotropic Crystals.*

As already mentioned, the measurement of feeble anisotropies requires special technique. A convenient method of measurement has been developed by us and we give in this section an account of the measurements made by this method for one typical monoclinic crystal, viz., $MnSO_4 . (NH_4)_2 SO_4 . 6 H_2O$.

The crystal is first suspended with its "b" axis vertical at the end of a calibrated quartz fibre. It is kept surrounded by a paramagnetic solution contained in a rectangular glass cell; the solution has been saturated with the salt, and its volume susceptibility has been adjusted to be the same as the mean susceptibility of the crystal by dissolving suitable amounts of manganese chloride (the method of adjustment is described in the next section). The graduated torsion-head is now rotated so as to make the (001) plane exactly normal to the direction of the field, when the field is zero; in order to avoid the effects of the residual magnetization, if any, of the pole-pieces of the magnet, they are kept as far apart as possible in the course of this adjustment. When the pole-pieces (plane parallel) are moved into position and the field is switched on, the crystal rotates slightly, the direction of rotation being such as to make the normal to the field

* The calculation does not give unique values for ψ. Since, however, ψ is already known from direct measurement, and the calculation is merely for checking the accuracy of the measurements, the known value of ψ is used as a guide in choosing the correct solution for ψ.

TABLE II.

Crystal.	Crystal System.	Mode of Suspension.	Orientation in the Field.	$\lvert\Delta\chi\rvert$	Magnetic Anisotropy.	ψ Calculated.	ψ Measured in Air.	ψ Measured in Bath.
$FeSO_4 . 7H_2O$	Monoclinic $\beta = 104°{\cdot}3$	"b" a.v.* "a" a.v.	$\theta = -7°{\cdot}5$ "b" axis normal to field	1289	$\chi_1 - \chi_2 = 1289$	°	°	°
			"b" " "	1254	$\chi_1 - \chi_3 = 1270$	+21	+22	—
		(001) p.h.	Almost zero		—	—	—	—
$FeSO_4 . K_2SO_4 . 6H_2O$	Monoclinic $\beta = 104°{\cdot}5$	"b" a.v. "a" (001) p.h.	$\theta = -43°{\cdot}8$ "b" axis along field	1841	$\chi_1 - \chi_2 = 1841$			
			"b" " "	1227	$\chi_1 - \chi_3 = -314$	+59·3	+58·3	—
			" " "	1241				
$FeSO_4 . (NH_4)_2SO_4 . 6H_2O$	Monoclinic $\beta = 106°{\cdot}8$	"b" a.v. (20$\bar{1}$) p.v. and a.h. (20$\bar{1}$) p.h.	$\theta = -37°$ "b" axis along field	2582	$\chi_1 - \chi_2 = 2582$			
			"b" axis normal to field	2262	$\chi_1 - \chi_3 = 213$	+54·4	+54	+54·5
				106				
$FeCO_3$	Trigonal	Trigonal a.h.	Trigonal axis along field	6090	$\chi_0 - \chi_1 = 6090$	—	—	—
$CoSO_4 . 7H_2O$	Monoclinic $\beta = 104°{\cdot}7$	"b" a.v. "a" a.v. (001) p.h.	$\theta = +69°{\cdot}1$ "b" axis along field	1928	$\chi_1 - \chi_2 = 1928$			
			" "a" " "	593	$\chi_1 - \chi_3 = 1094$	−54·6	−54·4	—
				854				
$CoSO_4 . K_2SO_4 . 6H_2O$	Monoclinic $\beta = 104°{\cdot}9$	"b" a.v. "a" a.v. (001) p.h.	$\theta = +30°{\cdot}5$ "b" axis normal to field	2532	$\chi_1 - \chi_2 = 2532$			
			"a" " "	1180	$\chi_1 - \chi_3 = 1832$	−15·6	−15·5	−15·5
				47				
$CoSO_4 . (NH_4)_2SO_4 . 6H_2O$	Monoclinic $\beta = 106°{\cdot}9$	"b" a.v. (100) p.h. (001) p.h.	$\theta = +60°$ "b" axis normal to field	3023	$\chi_1 - \chi_2 = 3023$			
			"b" " "	114	$\chi_1 - \chi_3 = 1541$	−43·4	−43	−43·2
				803				

* a.v. = axis vertical; a.h. = axis horisontal; p.h. = plane horizontal; p.v. = plane vertical.

TABLE II—(continued).

Crystal.	Crystal System.	Mode of Suspension.	Orientation in the Field.	$\lvert\Delta\chi\rvert$	Magnetic Anisotropy.	ψ Calculated.	ψ Measured in Air.	ψ Measured in Bath.
$NiSO_4 . 6H_2O$	Tetragonal	Tetragonal a.h.	Tetragonal axis normal to field	109	$\chi_1 - \chi^{11} = 109$	° —	° —	° —
			" c " axis along field	120	$\chi_2 - \chi_3 = 169$	—	—	—
			" c " " "	37	$\chi_2 - \chi_3 = 49$	—	—	—
			" a " " "	169	Cal. $\Delta\chi = 169$	—	—	—
$NiSO_4 . 7H_2O$	Ortho-rhombic	" a " a.v. (110) p.h. " c " a.v.	$\theta = +27°$	158	$\chi_1 - \chi_3 = 158$	−13·1	−12	−12·5
			" b " axis normal to field	120	$\chi_1 - \chi_3 = 155$			
			" b " " "	32				
$NiSO_4 . K_2SO_4 . 6H_2O$	Monoclinic $\beta = 105°·0$.	" b " a.v. " a " a.v. (001) p.h.	$\theta = +31°$	110	$\chi_1 - \chi_3 = 110$	−13·8	−14	−14
			" b " axis normal to field	77	$\chi_1 - \chi_3 = 106$			
			" b " " "	25				
$NiSO_4 . (NH_4)_2SO_4 . 6H_2O$	Monoclinic $\beta = 107°·1$	" b " a.v. " a " a.v. (001) p.h.	$\theta = -88°$	367	$\chi_1 - \chi_3 = 367$	−78·5	−77·5	−77·5
			" b " axis along field	292	$\chi_1 - \chi_3 = 74$			
			" a " " "	73				
$CuSO_4 . K_2SO_4 . 6H_2O$	Monoclinic $\beta = 104°·5$	" b " a.v. " a " a.v. (001) p.h.	$\theta = -61°$	300	$\chi_1 - \chi_3 = 300$	+76·7	+77	+77·5
			" b " axis along field	166	$\chi_1 - \chi_3 = 62$			
			" b " " "	11				
$CuSO_4 . (NH_4)_2SO_4 . 6H_2O$	Monoclinic $\beta = 106°·1$	" b " a.v. " a " a.v. (001) p.h.	$\theta = +66°·7$	2661	$\chi_1 - \chi_3 = 2661$	−52·2	−51·2	—
			" b " axis along field	92				
			" a " " "	1804	$\chi_1 - \chi_3 = 2186$			
$CoSO_4 . CuSO_4 . 7H_2O$*	Monoclinic $\beta = 105°·5$	" b " a.v. " a " a.v. (001) p.h.						

* This crystal is not described by GROTH. The crystallographic data were taken from GMELIN-KRENT, "Handbuch der anorganischen Chemie," vol. 1, p. 1381.

lie in the obtuse angle β; it shows that θ is a positive acute angle. The actual value of θ cannot be measured directly with accuracy, since the restoring couple is too small to be detected until the crystal has been rotated through a considerable angle from the setting position. However, θ is measured indirectly as follows.

The torsion-head is rotated so as to bring back the (001) plane to its original position normal to the field. Let α_1 be the angle of rotation of the torsion-head. Then

$$\alpha_1 = K(\chi_1 - \chi_2) \sin 2\theta, \quad \ldots\ldots\ldots\ldots (10)$$

where

$$K = \frac{1}{2c} \cdot \frac{m}{M} \cdot H^2. \quad \ldots\ldots\ldots\ldots (11)$$

Usually the field is adjusted so as to make α_1 about 500 or 600 degrees.

If now the torsion head is further rotated *very slowly*, at a certain position of the torsion-head the crystal suddenly turns round, through considerably more than 90°. This critical angle of rotation of the torsion-head α_2, say, measured from its initial position, can be determined with accuracy. This corresponds evidently to an orientation of the crystal for which the restoring couple due to the magnetic field is a maximum, *i.e.*, when the principal axes χ_1 and χ_2 are inclined at 45° to the direction of the field. Hence we have

$$\alpha_2 - \left(\frac{\pi}{4} - \theta\right) = K(\chi_1 - \chi_2). \quad \ldots\ldots\ldots\ldots (12)$$

Since in equations (10) and (12), K and the two α's are known, and the above experiment shows that θ is a positive angle less than $\pi/4$, we can easily calculate θ and $\chi_1 - \chi_2$.

Two other measurements are made in a similar manner with the "a" axis of the crystal vertical and the (001) plane horizontal respectively. In these measurements it is easy to determine the setting positions in the field. From a consideration of the symmetry of the crystal, the "b" axis of the crystal must lie either along the field or normal to it. By placing the "b" axis at 45° to the field (for then the couple is a maximum and is therefore easily detected) we can decide between the two alternatives. The values of $\Delta\chi$ can be determined in the same manner as before by noting the critical angle of rotation of the torsion-head that is necessary to turn the crystal round.

The results obtained with $MnSO_4 . (NH_4)_2SO_4 . 6H_2O$ are

$$\theta = +31°·5 \quad \ldots\ldots\ldots (13)$$

$$\chi_1 - \chi_2 = 11·4 \quad \ldots\ldots\ldots (14)$$

$$\chi_1 \cos^2\theta + \chi_2 \sin^2\theta - \chi_3 = 3·7 \quad \ldots\ldots\ldots (15)$$

$$\chi_3 - \chi_1 \sin^2\theta - \chi_2 \cos^2\theta = 1·4 \quad \ldots\ldots\ldots (16)$$

Of these only three are independent. From (14), (15), and (16), treating θ also as an unknown, we obtain

$$\left.\begin{aligned}\chi_1 - \chi_2 &= 11{\cdot}4 \quad .\\ \chi_1 - \chi_3 &= \ 6{\cdot}8 \quad .\\ \theta &= +31°{\cdot}7\end{aligned}\right\} \quad \ldots\ldots\ldots\ldots\ldots (17)$$

This value for θ is in agreement with $\theta = +31°{\cdot}5$ which is the directly calculated value. Adopting for θ the mean of these two values, $\theta = +31°{\cdot}6$, we obtain

$$\psi = -14°{\cdot}6.$$

Before concluding this section we may remark that this method of measuring magnetic anisotropy can also be applied to strongly anisotropic crystals. The method will be very convenient, especially when, as with measurements at low temperatures, the crystal is kept immersed in a liquid bath for the purpose of regulating its temperature with ease.

7. *Absolute Susceptibilities.*

The method used here is essentially the same as that adopted by us for diamagnetic crystals. The magnet is fitted with conical pole-pieces so as to give a highly non-homogeneous field. The crystal is suspended by a long fine quartz fibre at the same height as the axis of the pole-pieces, but slightly to one side of the axis, occupying a position equidistant from the two pole-pieces. It is initially surrounded by a saturated solution of the substance in water. The torsion-head is turned suitably so that there is no rotation of the crystal when the field is put on; the crystal will, however, move laterally. The susceptibility of the bath is adjusted by adding suitable amounts of another aqueous solution that is saturated with the above substance and also with manganese chloride (and is therefore very strongly paramagnetic), until the crystal ceases to move in the field. Under these conditions the volume susceptibility of the crystal along the field is the same as that of the solution.

Susceptibility of the balancing solution.—We now have to find the volume susceptibility of the balancing solution. This was done in the usual manner by weighing a cylindrical column of the solution with one of its ends in the centre of a uniform magnetic field, and the other end well outside the field, and comparing it with the weight of a standard liquid under the same conditions. Water is usually chosen as the standard substance. But for our present purpose a standard liquid or solution whose susceptibility is of the same order of magnitude as that of the balancing solutions is to be preferred; aqueous solutions of nickel chloride are suitable. In the first place the susceptibility of this salt in solution has been measured by Cabrera, Moles and Gunzman, Weiss and Bruins, Miss Brant, Foëx and more recently by Cabrera and Duperier.* Their values are in good agreement and correspond to a magnetic moment for the

* See "International Critical Tables," vol. 6, pp. 351–2.

Ni^{++}-ion equal to 16·05 Weiss magnetons. The value is the same for all concentrations of the salt. Further, they find that the variation of the susceptibility with temperature can be represented accurately by the simple Curie law. Thus the susceptibility of any solution of nickel chloride can be calculated from its concentration.

Standard solutions.—In our present measurements a fairly concentrated solution of Kahlbaum's nickel chloride was prepared. The actual strength of the solution was determined by precipitating the nickel as nickel dimethyl glyoxime, $Ni[(CH_3)_2C_2NOH\,.\,NO]_2$, by the addition of an alcoholic solution of dimethyl glyoxime.* It was found to contain 0·3651 gm. of $NiCl_2$ per c.c. of the solution. On calculation from this concentration, allowing for the diamagnetism of the water, viz., $-0{\cdot}719 \times 10^{-6}$ per gm., and that of the chlorine ions, viz., $-0{\cdot}57 \times 10^{-6}$ per gm., the volume susceptibility of our standard solution at 30° C. comes out as $11{\cdot}34 \times 10^{-6}$ per c.c., with a temperature coefficient of $-0{\cdot}037 \times 10^{-6}$ per 1° C. in the neighbourhood of 30° C. For comparison with strongly paramagnetic balancing solutions a subsidiary standard, in the form of a moderately dilute solution of $MnCl_2$ was used. It was standardized by comparison with the $NiCl_2$ solution, and its susceptibility at 30° C. was $22{\cdot}13 \times 10^{-6}$, with a temperature coefficient of $-0{\cdot}080 \times 10^{-6}$.

It is not necessary to describe the details of the method of comparison of the susceptibility of the balancing solution with that of the standard, since they are well known. The balance used for weighing the solutions in the magnetic field was of the torsion type, and had been developed in this laboratory by Mr. L. M. Das in connection with some delicate measurements on surface tension.

Density of the crystal.—Now, knowing the volume susceptibility of the solution, and hence also of the crystal along the field, it only remains to find, by the usual methods, the density of the particular crystal used.

The results of the measurements are given in Table III. From the susceptibility determined as above along any particular direction in the crystal, the mean susceptibility of the crystal, viz., $\frac{1}{3}(\chi_1 + \chi_2 + \chi_3)$, can be calculated with the help of the data for the anisotropy given in Table II. The measurements were all made at the room temperature, which varied from 30° to 32° C. For the sake of uniformity, all the values have been reduced to 30° C.; the simple Curie law of temperature-dependence has been assumed in making this correction, since the correction is very small.

The unit for the susceptibilities is, as usual, 10^{-6} of a c.g.s. e.m.u.

8. *Comparison with Earlier Measurements.*

Our results are collected together in Table IV, together with the values obtained by earlier investigators. Except when stated otherwise, the values of Rabi may be taken to refer to 27° C., those of Jackson to 17° C., those of Finke to room temperature and

* Treadwell, "Analytical Chemistry," 1924, vol. 2, pp. 134–135.

TABLE III.

Crystal.	Direction of measurement of susceptibility.	Temp. ° C.	Density of Crystal.	Vol. susceptibility.	Corresponding gm. mol. susceptibility.	Mean susceptibility at 30° C.
$FeSO_4 . 7H_2O$	Along "a" axis	31·0	1·894	70·6	10360	10820
$FeSO_4 . K_2SO_4 . 6H_2O$ . .	" "b" "	30·4	2·190	62·3	12350	11550
$FeSO_4 . (NH_4)_2SO_4 . 6H_2O$	" "b" "	31·3	1·858	57·5	12140	11480
$CoSO_4 . 7H_2O$	" "b" "	30·6	1·962	63·2	9060	9170
$CoSO_4 . K_2SO_4 . 6H_2O$ . .	" χ_1 — "	30·0	2·228	58·3	11450	9990
$CoSO_4 . (NH_4)_2SO_4 . 6H_2O$	Normal to $(20\bar{1})$ plane	29·9	1·904	53·4	11090	9590
$NiSO_4 . 6H_2O$	Normal to tetragonal axis	30·0	2·082	32·26	4071	4035
$NiSO_4 . 7H_2O$	Along "a" axis	31·3	1·949	28·43	4099	4043
$NiSO_4 . K_2SO_4 . 6H_2O$.	" "a" "	31·8	2·255	20·26	3927	3970
$NiSO_4 . (NH_4)_2SO_4 . 6H_2O$	" χ_1 "	31·0	1·945	19·82	4025	3967
$CuSO_4 . K_2SO_4 . 6H_2O$.	" χ_1 "	32·0	2·259	7·44	1455	1319
$CuSO_4 . (NH_4)_2SO_4 . 6H_2O$	" "b" "	30·0	1·952	6·79	1392	1333
$CoSO_4 . CuSO_4 . 7H_2O$.	" "b" "	30·6	1·970	43·4	9710	10300
$MnSO_4 . (NH_4)_2SO_4 . 6H_2O$	" χ_1 "	30·8	1·834	64·7	13800	13830

TABLE IV.

Crystal.	ψ	$\chi_1 - \chi_2$.	$\chi_1 - \chi_3$.	Mean χ.	Author.
$FeSO_4 . 7H_2O$	21°· 5	1289	1270	10820	—
	30° 10′	810	1190	11670	FINKE.
				11530	JACKSON, 16°·6.
				11650	ISHIWARA, 23°.
$FeSO_4 . K_2SO_4 . 6H_2O$	58°· 8	1841	— 314	11550	—
	55°	1520	— 320	11440	RABI.
$FeSO_4 . (NH_4)_2SO_4 . 6H_2O$	54°· 3	2582	213	11480	—
	—18° 58′	2080	2230	16670	FINKE.
				12770	JACKSON, 17°·3.
				12510	OOSTERHUIS, 17°.
				12150	FOËX, extrapolated to 30°.
$FeCO_3$	$\chi_{II} - \chi_I =$	6090			—
		6350	—	—	FOËX, 30°.
		6870	—	—	DUPOUY, 28°·2.
$CoSO_4 . 7H_2O$	—54°· 5	1928	1094	9170	—
	—39° 40′	993	344	9784	FINKE.
				10400	JACKSON, 19°.
				10410	ONNES and HOF, 17°.
				8970	WEISS and FOËX, 20°.
				9120	FEYTIS.

TABLE IV—(continued).

Crystal.	ψ.	$\chi_1 - \chi_2$.	$\chi_1 - \chi_3$.	Mean χ.	Author.
$CoSO_4 . K_2SO_4 . 6H_2O$	—15°· 5	2532	1832	9990	—
	—21° 20′	3360	—2090	12750	FINKE.
	20° 2	2370	1670	11080	JACKSON.
				10200	JACKSON, powder.
	—44°	2550	1760	9830	RABI.
$CoSO_4 . (NH_4)_2SO_4 . 6H_2O$	—43°·2	3023	1541	9590	—
	—27°. 31′	2570	2170	10050	FINKE.
	—31° 18′	1530	240	9690	JACKSON.
	—13°	3200	1490	10050	RABI.
$NiSO_4 . 6H_2O$	$\chi_1 - \chi_{II} =$	109	...	4035	—
				4100	FEYTIS.
$NiSO_4 . 7H_2O$	—	$\chi_a - \chi_b =$	$\chi_a - \chi_c =$	—	—
		169	49	4043	—
		— 32	— 136	4231	FINKE.
		40	10	4660	JACKSON.
				4450	ONNES and HOF, 17°.
				4385	GORTER, DE HAAS and VAN DEN HANDEL, 15°.
$NiSO_4 . K_2SO_4 . 6H_2O$.	—12°·5	158	155	3970	—
	—17°	160	180	3870	RABI.
$NiSO_4 . (NH_4)_2SO_4 . 6H_2O$	—13°·9	110	106	3967	—
	—16° 17′	784	325	3655	FINKE.
	— 7°	60	40	4090	RABI
				4220	JACKSON, 13°·5.
$CuSO_4 . K_2SO_4 . 6H_2O$.	—77°·8	367	74	1319	—
	81°	374	136	1308	RABI.
$CuSO_4 . (NH_4)_2SO_4 . 6H_2O$	77°·1	300	62	1333	—
	—74°	284	32	1291	RABI.
$CoSO_4 . CuSO_4 . 7H_2O$.	—51°·7	2661	2186	10300	—
	—52° 54′	2352	1290	10890	FINKE, for the hexahydrate.
$MnSO_4 . (NH_4)_2SO_4 . 6H_2O$	—14°·6	11·4	6·8	13830	—
	14°	40	— 60	13330	RABI.

ours to 30° C. Our values for ψ given in the table are the mean of the values calculated from oscillation measurements, and those measured directly with the crystal in air and in the magnetically balancing liquid bath.

Considering first the absolute susceptibilities of the crystals we find, wherever comparison is possible, that our values agree with those of RABI. The values obtained by the other investigators, however, are usually much higher. Where their measurements have been made on powdered crystals, the higher values probably arise from a non-random distribution. But where the measurements have been made on single crystals,

as in FINKE's determinations or in JACKSON's on cobalt potassium sulphate, the discrepancy must have a different explanation; it perhaps arises from the difficulties of measuring field-gradients with accuracy. These uncertainties are not present in the "null" method of RABI, which we have also adopted.

The considerable agreement that one notices for strongly anisotropic crystals between the values of $\Delta\chi$, as obtained by us by a direct method, and those deduced from RABI's absolute values for the χ's, is indeed further evidence in support of the accuracy of RABI's method; especially considering that agreement between *differences* is a stringent test. Feeble anisotropies cannot be calculated with accuracy from the absolute values, and have to be determined directly by some such method as ours.

As regards ψ our values obtained from the setting position both in air and in the paramagnetic bath, agree well with those calculated from our measurements on oscillations; they are therefore likely to be very near the actual values. They do not, however, agree with those of RABI; but there appears to be some confusion in RABI's results for ψ between the values for the potassium double-sulphates and those for the corresponding ammonium double-sulphates. Table V shows that there is almost certainly an interchange of values between $CoSO_4 . K_2SO_4 . 6\,H_2O$ and $CoSO_4 . (NH_4)_2SO_4 . 6\,H_2O$, and between $CuSO_4 . K_2SO_4 . 6\,H_2O$ and $CuSO_4 . (NH_4)_2SO_4 . 6\,H_2O$. We give under A in that Table RABI's values and under B our values.

TABLE V.—Values for ψ.*

Crystal.	A.	B.
	°	°
$CoSO_4.K_2SO_4.6H_2O$	−44	−15·5
$CoSO_4.(NH_4)_2SO_4.6H_2O$	−13	−43·2
$CuSO_4.K_2SO_4.6H_2O$	+81	−77·8
$CuSO_4.(NH_4)_2SO_4.6H_2O$	−74	+77·1

9. JACKSON's *Values for* $CoSO_4 . (NH_4)_2\,SO_4 . 6\,H_2O$.

Cobalt ammonium sulphate, which has been investigated by JACKSON over a considerable range of temperatures, is discussed in this section. His method of measurement has been described in Section 2. As mentioned there, he assumes both $\chi_3 - \chi_c$ and $\chi_3 - \chi_a$ to be positive; whereas when the crystal is suspended in a uniform

* [*Note added March* 28, 1933.—B. W. BARTLETT has recently ('Phys. Rev.,' vol. 41, p. 818 (1932)) given measurements of susceptibilities of some double-sulphates at different temperatures, using RABI's method. He has also pointed out the interchange that occurs in RABI's values of ψ for some potassium salts and the corresponding ammonium salts. It should be mentioned, however, that for the salts $CuSO_4 . K_2SO_4 . 6H_2O$ and $CuSO_4 . (NH_4)_2SO_4 . 6H_2O$ the interchange persists in BARTLETT's paper as well; his value for the potassium salt is $-102°$ ($= +78°$) and for the ammonium salt $-79°$, as compared with our values $-77°.8$ and $+77°.1$ respectively.]

magnetic field with its (100) plane or its (001) plane horizontal, the "b" axis sets itself, in either case, normal to the field (see Table II); this shows that both χ_a and χ_c are greater than χ_3. This necessitates a recalculation of the magnetic constants of this crystal from the experimental data given in JACKSON's paper. Considering the large range of temperatures over which JACKSON's measurements extend—from 14° K. to the room temperature—and the scarcity of data for single crystals at such low temperatures, we give here the final results of such a recalculation. The second and the third columns in Table VI give the two solutions for ψ obtained from JACKSON's data (see Section 2). We have put in the second column that value of ψ which agrees with that obtained by us for this crystal, and which we presume to be the admissible solution. In the calculation of $\chi_1 - \chi_2$ this value of ψ has therefore been adopted. The values in brackets in the table are those given by JACKSON himself.

TABLE VI.

Temp.	ψ		$\chi_1 - \chi_2$.	$\chi_1 - \chi_3$.
	Rejected.	Adopted.		
	°	°		
290·0 K.	58 59	−42 3 (−31 18)	1530	846 (240)
77·2	61 40	−44 44 (−28 17)	12900	7130 (3120)
20·3	62 50	−45 54 (−27 8)	47800	28500 (3800)
16·7	62 17	−45 21 (−27 41)	60900	35600 (8300)
14·5	62 26	−45 30 (−27 40)	69200	40800 (9100)

If now we compare the recalculated values of JACKSON for 290° K. with our values, we find that the ψ's agree well; but JACKSON's values for $\chi_1 - \chi_2$ and for $\chi_1 - \chi_3$, viz., 1530 and 846 respectively, are almost one half of our values, viz., 3023 and 1541. This is surprising, but on p. 30 of his paper JACKSON defines the angle through which the torsion-head is turned as 2α, whereas in his equations (1) and (1A) on the same page this angle appears as α. If the equations as they appear in the paper had been used in his calculations, the final values for the $\Delta\chi$'s would naturally be *nearly** half the actual values. Sufficient data are not available in the paper to enable us to test this point.

* There is a small correction term in equation (1 A) which would be independent of this factor 2, and hence the values for $\Delta\chi$ would not be *exactly* half. We may also add that the values for ψ would not be affected appreciably by this factor 2.

10. *Discussion of Results.*

Among all the crystals studied by us, manganese ammonium sulphate has the smallest magnetic anisotropy. The difference between the maximum and the minimum principal susceptibilities is only 11·4, in a mean susceptibility of 13830, i.e., 0·08 of one per cent. of the mean value. (The value of $\Delta\chi/\chi$ calculated from RABI's absolute measurements is about 1 per cent.) It is almost of the order of diamagnetic anisotropy. This is clearly what we should expect from the fact that the ground state of the Mn^{++} ion is an S-state.* For the same reason, the crystal may be expected to obey the simple CURIE law. Our mean value for the susceptibility would then correspond to a magnetic moment for the Mn^{++} ion of 29·0 WEISS magnetons, as against the value 29·4 calculated from the spin moments of the five electrons in the outermost shell.

The nickel salts are also feebly anisotropic, the values of $\Delta\chi/\chi$ varying from 2 to 4 per cent. in the different compounds. This has been discussed in detail by VAN VLECK (particularly in relation to the strong anisotropy of the cobalt salts), on the basis of BETHE's calculations regarding the splitting of the atomic energy levels in these crystals. In conformity with the results of the theory, we find that the mean susceptibilities of the various nickel salts, after correcting for their diamagnetism, are practically the same, corresponding to a magnetic moment of 15·8 WEISS magnetons for the Ni^{++} ion.

The strong anisotropy of the iron and cobalt salts is accompanied, as we should expect, by a corresponding dependence of the mean susceptibility on the nature of the crystal. For example, the mean susceptibility of ferrous sulphate is considerably less than that of ferrous potassium or ferrous ammonium sulphate; the anisotropy of ferrous sulphate is also much smaller than for the latter two crystals. Similar results are obtained with the corresponding cobalt salts.

Measurements on the susceptibilities of these crystals at low temperatures have been started; detailed discussion of the CURIE and WEISS constants of the crystals in relation to their structure will be attempted when these measurements are completed.

11. *Summary.*

In this paper are described the results of measurements on the principal susceptibilities of some paramagnetic sulphates and double sulphates, using the methods described in Part I. A critical discussion of earlier measurements on paramagnetic crystals is given, and also a convenient method for the measurement of very feeble anisotropies.

* VAN VLECK, "The Theory of Electric and Magnetic Susceptibilities," Chap. 11 (1932).

NEGATIVE POLARISATION IN FLUORESCENCE

BY

K. S. KRISHNAN

AND

S. M. MITRA

Physics Laboratory, University of Dacca

IN an important paper[1] Wawilow has reported measurements on the polarisation of fluorescence of solutions of some dye-stuffs in glycerine, when excited by radiations of different wave-lengths. Using for excitation the radiations from a mercury lamp, isolated by a quartz monochromator, he finds that the degree of polarisation shows a marked dependence on the wave-length of the exciting light. Starting from the visible region of the spectrum, as the wave-length of the exciting light is diminished the degree of polarisation decreases rapidly, passes through a minimum value (corresponding, in general, to excitation by λ 3125–3131), and rises again as we proceed farther towards the ultra-violet. The minimum value is usually *negative*; that is, the intensity of the fluorescent vibrations along the direction of propagation of the incident light is greater than that of vibrations in the perpendicular direction.

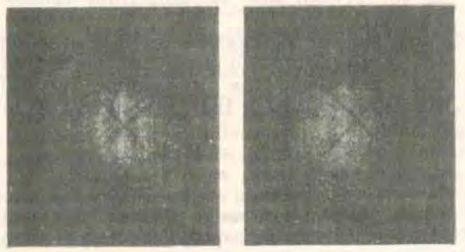

(*a*) (*b*)

FIG. 1.

It is known, however, that the light that issues from a quartz (crystalline) monochromator is, in general, considerably polarised, and that the direction and the extent of polarisation fluctuate as we proceed along the spectrum. We have therefore repeated Wawilow's measurements using linearly polarised light for excitation and observing along the normal to the plane containing the direction of propagation and the direction of vibration of the exciting light. Though our values differ considerably from those calculated from Wawilow's results (the polarisation varies also with the concentration of the dye-stuff), the general nature of the variation of polarisation with the exciting wave-length, and also its negative value for excitation by λ 3125–31, are fully confirmed. The change in sign of the polarisation in the case of fluorescein solution occurring when the exciting wave-length is changed from λ 4358 to λ 3125–31, is seen clearly in Fig. 1 (*a*) and (*b*), which are photographs of the fluorescent radiations excited by λ 4358 and λ 3125–31 respectively, taken through a suitably oriented Savart plate and analyser. The images of a fixed cross-wire which appear in the photographs, serve as reference for the positions of the fringes. It is easily seen that whereas in Fig. 1 (*a*) the centre of the cross-wire falls on a bright fringe, it falls on a dark fringe in Fig. 1 (*b*).

Also observations along different directions show for λ 3125–31 excitation that the intensity of the fluorescent radiations vibrating normal to the direction of the vibrations of the exciting light is always greater than that of fluorescent vibrations along the direction of the exciting vibrations.

[1] *Z. Phys.*, **55**. 690; 1929.

Feeble Anisotropies in Paramagnetic Crystals.

IT is known from the investigations of Rabi[5] and others that at ordinary temperatures single crystals of manganous salts are almost isotropic magnetically; the three principal susceptibilities differ from one another by less than one per cent. This result is what one would expect on the basis of the recent theories of Van Vleck and others[6] since the Mn++ ion is in an S state; and from the point of view of these theories a knowledge of the precise amount of deviation from perfect isotropy in these crystals is of some importance. For the purpose of measuring such feeble anisotropies as are involved here, we have adopted the following method:—

The crystal is suspended at the end of a calibrated quartz fibre so as to lie between the parallel pole-pieces of an electromagnet capable of giving a uniform field. When the field is put on, there will, in general, be two couples tending to rotate the crystal about the axis of suspension: (1) the couple due to the magnetic anisotropy of the crystal in the horizontal plane, and (2) the couple due to small deviations from homogeneity of the field, acting through the asymmetry of shape of the crystal. The latter couple is eliminated by surrounding the crystal with a paramagnetic solution (saturated with the substance) whose volume susceptibility has been adjusted to equal the mean volume susceptibility of the crystal.

The following two measurements suffice to determine the directions of the magnetic axes in the horizontal plane, as well as the difference between the susceptibilities along these axes. The crystal will rotate from the initial position when the field is put on; the first measurement is that of the angle of torsion of the fibre that is necessary to rotate the crystal back to its original orientation.

[5] I. I. Rabi, *Phys. Rev.*, **29**, 174, 1927.
[6] See J. H. Van Vleck, *The Theory of Electric and Magnetic Susceptibilities*, Chap. XI (1932).

If now the torsion head is rotated farther very slowly, at a certain stage the crystal suddenly turns round. This critical orientation of the crystal evidently corresponds to the maximum value of the restoring couple in the field, and therefore to an inclination of the two magnetic axes in the horizontal plane at 45° to the direction of the field. The angle of torsion for this orientation of the crystal is the second quantity measured.

By making similar measurements for other suitable axes of suspension of the crystal, the directions of the principal magnetic axes in the crystal and its anisotropy become known.

By way of illustration we may mention the results obtained by this method in the case of the monoclinic crystal $MnSO_4 . (NH_4)_2SO_4 . 6\,H_2O$. We find that at 30° C.

$$\chi_1 - \chi_2 = 11{\cdot}4$$
$$\chi_1 - \chi_3 = 6{\cdot}8$$
$$\tfrac{1}{3}(\chi_1 + \chi_2 + \chi_3) = 13830$$

where χ_1 and χ_2 denote the two principal gram molecular susceptibilities in the (010) plane, expressed in the usual unit, *viz.*, 10^{-6} of a c.g.s. e.m.u. χ_3 denotes the susceptibility along the '*b*' axis. Also the χ_1 axis is found to lie in the acute angle β at 14·6° to the '*c*' axis. It is seen that the largest difference between the χ's is less than one-tenth of one per cent.

The significance of this small anisotropy will be discussed in detail elsewhere. It may, however, be stated here that when allowance is made for the anisotropy of the diamagnetic part of the susceptibility, the residual anisotropy is of the same order of magnitude as may be expected from the simple magnetostatic influences of the doublets induced in the Mn++ ions.

K. S. KRISHNAN.
S. BANERJEE.

Physics Laboratory,
Dacca University,
February 1, 1933.

Orientations of Molecules in the *p*-Benzoquinone Crystal

THE crystal structure of *p*-benzoquinone has recently been studied by W. A. Caspari[1] by X-ray methods. The crystal belongs to the monoclinic system and is assigned by Caspari to the space-group C^5_{2h}; there are two molecules in the unit cell, the molecules possessing a centre of symmetry. His X-ray measurements are not sufficient to determine uniquely the orientations of the molecules in the unit cell. However, by combining his X-ray data with certain considerations concerning the crystal habit and the dimensions of the molecules, he concludes that the molecular planes are parallel to (201) and that the lines joining the two oxygen atoms of the molecule lie in the (010) plane. This orientation of the molecules secures a large concentration of the oxygen atoms in the (20$\bar{1}$) plane, which concentration, according to Caspari, will account for the exceptional development in the crystal of so peculiar a face as (20$\bar{1}$).

It seems to us that the molecular planes in the crystal are orientated differently. A study of its magne-crystallic properties shows that the (20$\bar{1}$) plane is indeed the mean plane of the molecules. Denoting by χ_1 and χ_2 the principal gram molecular susceptibilities of the crystal in the (010) plane, and by χ_3 the susceptibility along the *b* axis, we find that

$$\left.\begin{aligned}\chi_1 &= -27{\cdot}1\\ \chi_2 &= -64{\cdot}5\\ \chi_3 &= -25{\cdot}4\end{aligned}\right\} \times 10^{-6}\ \text{c.g.s. e.m.u.}$$

The χ_3 axis, which is plainly an axis of approximate magnetic symmetry, is inclined at 20·2° to (001) and at 87·0° to (20$\bar{1}$).

We may compare the above principal susceptibilities of the benzoquinone *crystal* with those for the *molecule* of the substance—deduced from the known constants for the benzene molecule. We then find that χ_1 and χ_3 are about the same as the susceptibility of the molecule for directions in its plane, while χ_2 is nearly equal to the susceptibility of the molecule along the normal to its plane. We may therefore conclude that the molecular planes in the crystal are perpendicular to the χ_2 axis, and are thus almost coincident with the (20$\bar{1}$) plane.

The orientation proposed by us is also supported by the optical properties of the crystal. Since the optical polarisability of the benzene ring for vibrations perpendicular to its plane is known to be considerably smaller than for vibrations in the plane, the refractive index of the crystal for vibrations perpendicular to (20$\bar{1}$) should be a minimum and be much less than the other two principal refractive indices. This is indeed so, since the crystal exhibits a strong negative birefringence, and the acute bisectrix is almost perpendicular to (20$\bar{1}$).[2]

K. S. KRISHNAN.
S. BANERJEE.

Physics Laboratory,
University, Dacca.
March 5.

[1] *Proc. Roy. Soc.*, A, **136**, 82; 1932.
[2] See P. Groth, "Chemische Kristallographie", vol. 4, p. 140.

The Pleochroism and the Birefringence of the NO_3^- Ion in Crystals.

By

K. S. Krishnan and A. C. Dasgupta.

Plate III.

(*Received for publication, June 8, 1933.*)

Abstract.

An account is given in the paper of measurements on the pleochroism and the principal refractive indices of potassium nitrate crystal in the visible and the near ultra-violet regions of the spectrum. The well-known absorption band at about 3000 A. U. due to the NO_3^- ion is found to be strongly polarised, light vibrations in the plane of the ion being absorbed considerably more than vibrations along the normal to the ionic plane. This absorption band is found to have no influence on the principal refractive indices of the ion.

1. *Introduction.*

Halban, Ghosh, Scheibe, Morton and others[1] have studi the absorption spectrum of a large number of nitrates in solution. Their results show that the NO_3^- ion has one absorption band at about 3000 A. U. and another, which is very much stronger, at about 2000 A. U. From a study of the absorption by single crystals of sodium and potassium nitrates, in which all the NO_3^- ions are oriented parallel to one another, it was found by the present writers[2] that both of these absorption bands are strongly polarised, the absorption being considerably more when the electric vector of the incident light wave is in the plane of the ions than when it is along the normal to the plane. In the present paper, we give an account of quantitative measurements of the principal absorption coefficients and refractive indices of potassium nitrate crystal in the visible and the near ultra-violet regions of the spectrum (up to 2500 A. U.).

[1] See H. Ley, 'Handbuch der Physik,' vol. 21, p. 60; also 'International Critical Tables,' vol. 5, pp. 329-31.

[2] 'Nature,' vol. 126, p. 12 (1930).

2. *The Structure of Potassium Nitrate Crystal.*

The crystal of potassium nitrate used in our measurements was of the usual orthorhombic type. X-ray investigations on this crystal show that the NO_3^- ions have a plane structure, the three oxygen atoms lying at the corners of an equilateral triangle with the nitrogen atom at the centre; also the planes of all the ions in the crystal are oriented parallel to one another, *viz.*, in the (001) plane, the '*c*' axis being an axis of pseudo-hexagonal symmetry. The (010) faces of the crystal were well developed and hence a natural plate of the crystal with its faces parallel to this plane could be used conveniently for studying the absorption and refractivity for light-vibrations along the '*c*' and the '*a*' axes, *i.e.*, along the normal to the ionic planes, and along a direction lying in the ionic planes respectively.

3. *Measurement of Pleochroism.*

The experimental arrangement adopted for measuring the pleochroism of the crystal was as follows. A horizontal slit S_1 (see fig. 1) of about 2 or 3 mm. width, was illuminated by the light from a copper arc A condensed by a quartz lens L_1. The slit was covered by a thin plate P of the crystal, its (010) faces being kept perpendicular to the path of the light and its '*c*' axis horizontal. The transmitted light passed through a quartz double-image prism D of the Wollaston type; the

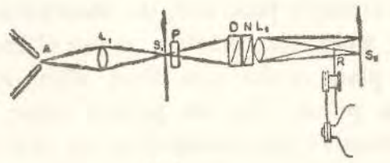

FIG. 4.

prism was so oriented as to separate *vertically* the horizontal and the vertical vibrations. The light then passed through a nicol[3] N and a quartz lens L_2 which focussed the two images on the slit of a spectrograph, the images falling one above the other. Thus the vertical and the horizontal vibrations passing through the crystal could be spectrographed side by side and their intensities could be compared in the following manner.

An Abney sector R rotating just in front of the slit and in the path of the light forming the stronger image, served to diminish its intensity by any desired amount, so as to render it equal to that of the other image. The principal plane of the nicol was in general inclined at 45° to the vertical, and by small rotations of the nicol about this orientation, the final adjustments for equality of intensity of the two images could be made. In practice, with the nicol at 45°, the angle of the rotating sector was first adjusted so as to make the two images appearing in the spectrograms to be of nearly equal intensity for any chosen region of the spectrum. Now keeping the sector angle constant, a series of pictures was taken on a photographic plate, with the principal plane of the nicol at different angles varying from 40° to 50° from the vertical. The exact positions in the spectrum for which the two images are equally intense could be readily located in the various pictures; knowing the angle of the rotating sector and the orientation of the principal plane of the nicol, the ratio of the

[3] The nicol was of the square ended Glan type with an *air film* between the component prisms so as to render the nicol transparent to the ultra-violet.

intensities of the horizontal and the vertical vibrations as transmitted by the crystal, and hence the difference between the two principal absorption coefficients of the crystal, are known for different wave-lengths.

Suppose that k and k_c are the *gram molecular* absorption coefficients of the crystal for vibrations along the 'a' and the 'c' axes respectively. The k's are defined by the usual relation

$$I = I_0\, e^{-\frac{k\rho}{M}\cdot d}, \qquad \ldots\ldots \quad (1)$$

where I is the intensity of light after traversing a thickness of d cms. of the crystal, when the initial intensity is I_0. ρ is the density of the crystal and M is its molecular weight. Let α be the angle (expressed in degrees of arc) of the sector, so that it reduces the intensity of the horizontal vibration (*i.e.*, of the one parallel to the 'c' axis—this was actually the stronger component) in the ratio $\alpha/180$. Also let θ be the angle which the principal plane of the nicol makes with the vertical when the two images are equally intense. Then plainly

$$k_a - k_c = -\frac{M}{\rho}\cdot\frac{1}{d}\log_e\left(\frac{\alpha}{180}\tan^2\theta\right) \qquad \ldots\ldots \quad (2)$$

and can therefore be calculated. (The thickness d of the crystal was measured optically by a method which will be described in a later section.)

The chief advantage in the above experimental arrangement is that the polarisation induced by the quartz (crystalline) parts of the spectrograph and by reflection at the faces of the prism, are automatically eliminated,[4] since the light forming either of the two images on the spectrograph slit has passed through the nicol and so would be affected in the same manner, in their passage through the spectrograph. Before

[4] See K. S. Krishnan and A. Sircar, Ind. Jour. Phys., vol. 6, p. 193 (1931).

any set of measurements was made a blank exposure was always taken with the crystal and the rotating sector removed, and with the nicol at 45°, so as to check the equality of intensity of the two images throughout the range of the spectrum; any small deviations from equality were rectified by suitable adjustment of the lens L_1 and by proper allignment of the other parts of the apparatus.

TABLE I.

$d=0{\cdot}172$ cms.		$d=0{\cdot}109$ cms.		$d=0{\cdot}0872$ cms.	
λ in A.U.	$(k_e-k_o)\times10^{-2}$	λ in A.U.	$(k_e-k_o)\times10^{-2}$	λ in A.U.	$(k_e-k_o)\times10^{-2}$
5890	1·0	4240	2·2	4396	2·0
4390	2·0	4160	2·4	4164	2·4
4000	3·1	3552	4·3	3908	3·1
3523	4·1	3392	6·2		
3508	4·9	3344	7·9		
3404	5·9	3316	9·7		
3396	5·7	3300	11·0		
3304	10·0	3268	14·0		
3244	15·6	3236	17·4		
2758	15·6	3220	20·3		
2748	13·7	3212	23·7		
2726	11·1	2752	14·0		
2716	10·0				
2700	9·0				
2672	7·5				
2636	9·0				
2622	11·1				
2612	13·7				
2604	15·6				

4. *Results.*

Altogether seven crystals of different thicknesses were used for the measurement, and the results are given in Table I. The correction for unequal reflection of the two vibrations at the surfaces of the crystal plate was in general very small.

TABLE I—(*Contd.*).

$d=0{\cdot}0567$ cms.		$d=0{\cdot}0374$ cms.	
λ in A.U.	$(k_e-k_o)\times10^{-2}$	λ in A.U.	$(k_e-k_o)\times10^{-2}$
3204	27·4	3203	27·6
3198	30·5	3175	42·6
3192	33·8	3149	49·0
3188	37·3	3124	56·7
3172	41·5	2952	56·7
2908	46·7	2908	49·0
2888	41·5	2884	42·6
2852	37·3	2860	37·1
2848	33·8	2840	32·0
2836	30·5	2818	27·6
2816	27·4	2800	23·0
2798	21·5	2780	18·3
2772	18·4	2740	13·8
2760	14·8	2616	13·8
2724	11·6		
2620	11·6		
2608	14·8		
2596	18.4		
2588	21·5		
2584	27·4		

TABLE I—(*Contd.*).

$d = 0{\cdot}0197$ cms.		$d = 0{\cdot}0122$ cms.	
λ in A.U.	$(k_a - k_c) \times 10^{-2}$	λ in A.U.	$(k_a - k_c) \times 10^{-2}$
3148	52·1	2924	53·4
3144	55·6	2866	41·3
3141	56·5	2816	28·0
3121	57·4	2589	28·0
3041	62·4	2578	41·3
2949	57·4	2561	53·4
2945	56·5	2553	65·1
2940	55·6		
2924	52·1		
2893	43·5		
2862	35·1		
2821	26·3		
2580	26·3		
2573	35·1		
2567	43·5		
2564	52·1		
2548	60·9		

The values of k_a-k_c are plotted in curve(A) Fig. 2. The strong polarisation of the 3000 A.U. absorption band and of the one in the extreme ultra-violet is plain. This is also strikingly shown in Fig 3, Plate III$_2$ which represents the two images when the rotating sector was removed and the principal plane of the nicol was at 45° to the vertical. The upper image corresponds to vibrations along the 'c' axis and the lower image to vibrations along the 'a' axis. (In the

actual photographs used for measurements, the images were much closer, being just separated from one another so as to facilitate comparison of intensities). As will be seen from the picture, the vibrations parallel to the 'a' axis are more strongly absorbed than those along the 'c' axis, *i.e.*, the NO_3^- ions absorb vibrations along directions lying in their plane more strongly than vibrations along the normal to their plane.

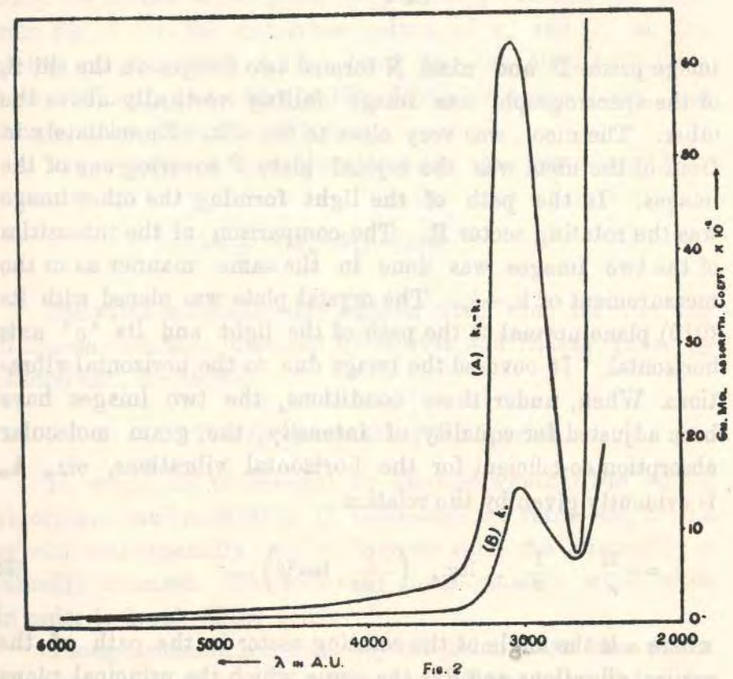

FIG. 2

5. *Absolute Absorption Coefficients.*

Having obtained the difference between k_a and k_c, we now proceed to determine their absolute values. The experimental arrangement adopted for this measurement was somewhat

similar to the previous arrangement. The light from the slit S_1 (see Fig. 4) after passing through the lens L_2 and double

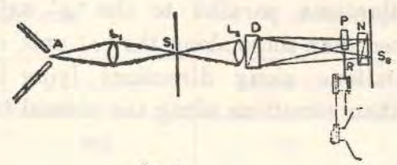

FIG. 4

image prism D and nicol N formed two images on the slit S_2 of the spectrograph, one image falling vertically above the other. The nicol was very close to the slit. Immediately in front of the nicol was the crystal plate P covering *one* of the images. In the path of the light forming the other image was the rotating sector R. The comparison of the intensities of the two images was done in the same manner as in the measurement of $k_a - k_c$. The crystal plate was placed with its (010) plane normal to the path of the light and its 'c' axis horizontal. It covered the image due to the horizontal vibrations. When, under these conditions, the two images have been adjusted for equality of intensity, the gram molecular absorption co-efficient for the horizontal vibrations, *viz.*, k_c, is evidently given by the relation

$$k_c = -\frac{M}{\rho} \cdot \frac{1}{d} \cdot \log_e \left(\frac{\bar{\alpha}}{180} \tan^2\theta \right), \qquad \ldots (3)$$

where α is the angle of the rotating sector in the path of the *vertical* vibrations and θ is the angle which the principal plane of the nicol makes with the *horizontal*. The results are plotted in curve (B), Fig. 2. In this case the correction due to reflection at the faces of the crystal plate is not negligible and has been applied.

It should be mentioned here that these measurements were made with only one crystal, and hence the results are not

likely to be so accurate as those for $k_a - k_c$. Knowing k_c and $k_a - k_c$, k_a is also known.

6. *Absorption by the NO_3-Ion.*

Since the absorption, at any rate for the spectral region we are considering, is presumably due to the NO_3 ion, k_a and k_c may be taken to represent the values of the gram ionic absorption coefficients for NO_3 for vibrations in its plane and along the normal to its plane respectively. It can be seen from Fig. 2 that the maximum values of k_c and k_a at the centre of the 3000 A. U. band (*viz.*, at 3040 A. U.) are $14{\cdot}4 \times 10^2$ and $(14{\cdot}4 + 62{\cdot}4) \times 10^2 = 76{\cdot}8 \times 10^2$ respectively, and thus k_c is less than one-fifth of k_a.

The mean gram ionic absorption for this wave-length is given by

$$k = \frac{1}{3} \quad (2k_a + k_c) = 5{,}600.$$

The value is considerably smaller than that for the ion in *aqueous solutions*, obtained by Morton and Riding (and by others) *viz.*, $k = 16{,}600$.

7. *The Birefringence of the Crystal.*

It would be of interest to enquire whether the strong absorption band at 3000 A. U. influences the refraction of the crystal, and especially its birefringence since the absorption is strongly polarised. The following measurements were made in order to decide these points.

Though potassium nitrate crystal belongs to the orthorhombic system, two of its refractive indices, *viz.*, those for vibrations along its 'a' and 'b' axes are so nearly equal that it can be treated as a uniaxial crystal with its optic axis along 'c'. Using a natural plate of the crystal, with its faces parallel to (010) plane, its birefringence, *viz.*, $\mu_a - \mu_c$ was measured for different wave-lengths in the usual manner by placing the

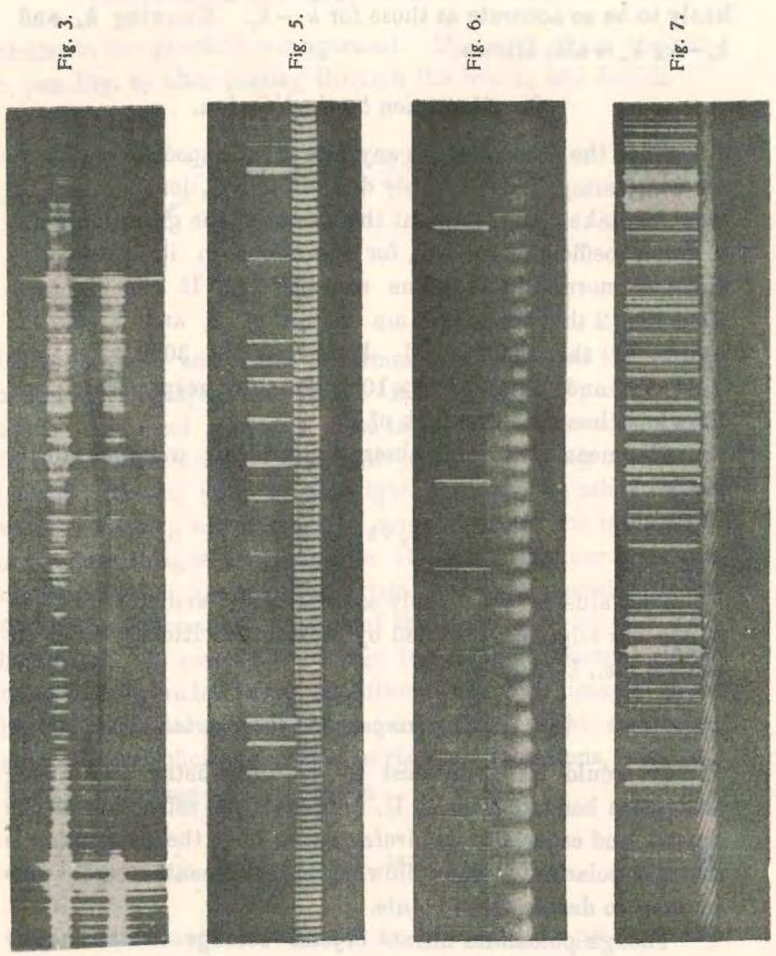

plate between crossed nicols and allowing a parallel beam of white light to pass through the system and analysing spectroscopically the transmitted light. Fig. 5, Plate III, gives a spectrogram of the fringes so obtained, along with a comparison spectrum of copper arc. The wave-lengths of the *dark* bands evidently satisfy the relation

$$(\mu_e - \mu_o)\, d = n\lambda, \quad \ldots \quad \ldots \quad (4)$$

where d is the thickness of the plate and n is an integral number. Thus if we know the thickness of the plate and the value of $\mu_e - \mu_o$ for any one wave-length, the values of n for all the various dark fringes are known, and hence the birefringence for the corresponding wave-lengths. Since, however, the thickness of the crystal used was in general too small to be measured accurately by direct methods, it would be preferable to know the value of $\mu_e - \mu_o$ for two different wave-lengths and thus eliminate d. The principal refractive indices of potassium nitrate have been measured by Schrauf[8] for different wave-lengths in the visible region of the spectrum and his values were used for this calculation.

We should mention here that the calculation gives also the thickness d of the crystal plate. A knowledge of d is useful in connection with absorption measurements on the crystal.

For measurements inside the absorption band, an extremely thin plate of crystal was used. With such thin crystals, besides the exposures being considerably shorter, the visibility of the fringes is much improved. The fringes obtained with one of these crystals is reproduced in Fig. 6, Plate III. The results of the birefringence measurements are given in the last column of Table II.

It may be remarked in this place that equation (4) which defines the positions of the minima of intensity (*i.e.*, of the

[8] See P. Groth, 'Chemische Kristallographie,' vol. 2, p. 75.

dark fringes) holds also inside the absorption band where the two principal vibrations are *unequally* absorbed. The proof of this statement is easy. Only in this case, due to the inequality of absorption, the actual minima of intensity are not equal to zero. However, by a suitable rotation of either the polariser or the analyser from the position for crossing, it is possible to make the minima equal to zero. For example, if the principal plane of the polariser is at 45° to the 'a' and the 'c' axes of the crystal, and that of the analyser at an angle ϕ to the 'a' axis and at $\pi/4+\phi$ to the principal plane of the polariser, it is easily shown that the conditions that the intensity at the minimum may be equal to zero, are

$$\left.\begin{aligned} &(a) \quad (\mu_a-\mu_c)d=n\chi \\ &\qquad\qquad -(k_a-k_c)\cdot\frac{\rho}{M}\cdot d \\ &(b) \quad \tan^2\phi = \varepsilon \end{aligned}\right\} \quad \ldots \quad (5)$$

Relation 5 (b) is of interest. It shows that a knowledge of ϕ, *i.e.*, of the orientation of the analyser for which the "visibility' of the fringes is a maximum, enables us to calculate k_a-k_c. This gives a convenient method of measuring pleochroism in crystals.

8. *Principal Refractive Indices.*

We next proceed to the measurement of μ_a and μ_c separately. For this purpose a Rayleigh interference arrangement was adopted, with the slits horizontal. A lens just in front of the double slit served to focuss the horizontal Rayleigh fringes on the vertical slit of a spectrograph. One of the double slits was closed by a plate of the crystal whose 'c' axis was horizontal and 'a' axis vertical. A nicol with its principal plane horizontal served to isolate the vibrations parallel to the 'c' axis. The fringe system so obtained on the spectrographic camera plate is reproduced in Fig. 7, Plate III. The wavelengths corresponding to points of intersection of the *bright*

fringes with a horizontal line drawn through the centre, evidently satisfy the relations

$$(\mu_c-1)\,d = n\,\lambda. \quad \ldots \quad \ldots \quad (6)$$

Knowing μ_c for two different wave-lengths from Schrauf's data, n and therefore μ_c can be calculated for different wavelengths. * Similarly μ_a was measured by keeping the principal plane of the nicol in the above experimental arrangement vertical, *i.e.*, parallel to the 'a' axis of the crystal.

TABLE II.

λ in A. U.	μ_c	μ_a	$\mu_a-\mu_c$	$\mu_a-\mu_c$ directly measured.
6868	1·4988	1·3328	·1660	·1664
5893	1·5056	1·3346	·1710	·1712
5270	1·5125	1·3367	·1758	·1759
4358	1·5279	1·3410	·1869	·1871
3969	1·5384	1·3435	·1949	·1951
3663	1·5502	1·3460	·2042	·2038
3500	1·5582	1 3479	·2103	·2102
3300	1·5703	1·3499	·2204	·2204
3200	1·5782	1·3514	·2268	·2263
3100	1·5861	1·3526	·2335	·2336
3000	1·5950	1·3543	·2407	·2417
2900	(1·608)	1·356	...	·252
2800	(1·624)	1·358	...	·266
2700	(1·644)	1·361	...	·283
2600	(1·671)	1·364	...	·307
2530	(1·698)	1·367	...	·331

* The thickness of the crystal d can also be calculated from these data. Since some of the crystals used for this measurement had also been used for the birefringence measurements, d calculated there could be compared with the present values. Their close agreement in the actual experiment offers a check on the accuracy of the measurements.

The values of μ_a and μ_c thus obtained are given in columns 2 and 3, Table II. The fourth column gives the values for the birefringence obtained by subtracting μ_c from μ_a. The last column gives the birefringence directly measured. The values of the principal refractive indices are plotted in Fig 8.

It should be remarked here that the accuracy of our present values of the refractive indices are conditioned by that

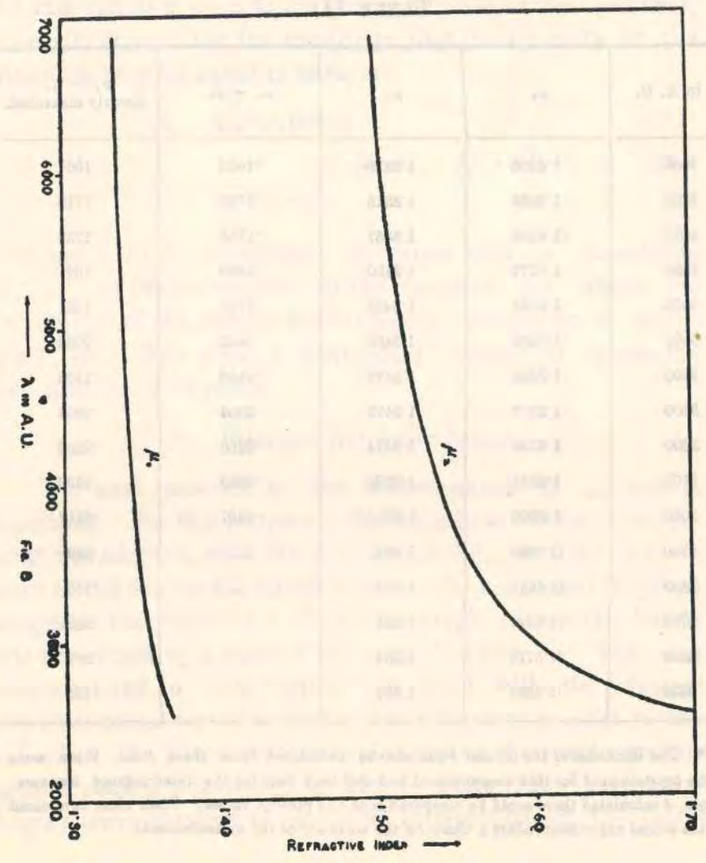

Fig 8

of Schrauf's values for the visible region, which we have used for calibrating the order of the interference fringes appearing in our spectrograms.

9. *Discussion of Results.*

The strong birefringence of the NO_3^- ion has been explained by W. L. Bragg [6] as arising from the mutual influence of the optical doublets induced in the three constituent O^{--} ions which lie in a plane. (The refractivity of the nitrogen atom which has parted with all of its five outer electrons to the oxygen atoms, is naturally very small). Let A be the moment of the optical doublet induced in an O^{--} ion per unit field of the light-wave, when the other two O^{--} ions are moved to a great distance. Suppose now that the latter two O^{--} ions are brought back to their proper positions beside the one we are considering. Let the electric vector of the incident light wave lie along the normal to the plane of the three O^{--} ions. Then the optical moment A_c induced in each of the O^{--} ions per unit field will be given by

$$A_c = \frac{A}{1 + \frac{2A}{r^3}} \quad \ldots (7)$$

where r is the distance between any two of the oxygens. If, on the other hand, the electric vector lies in the plane of the oxygens, the corresponding moment per unit field is given by

$$A_\omega = \frac{A}{1 - \frac{A}{r^3}} . \quad \ldots (8)$$

If the NO_3^- ion is not isolated as contemplated above, but forms part of a uniaxial crystal like sodium nitrate, then the

[6] 'Roy. Soc. Proc.', A, vol. 105, p. 370 and vol. 106, p. 346 (1924).

influence of the doublets in the surrounding NO_3^- ions has also to be taken into account. In this case

$$A_\epsilon \doteq \frac{A}{1 + 2\theta A} \quad \ldots (9)$$

and

$$A_\omega = \frac{A}{1 - \theta A}, \quad \ldots (10)$$

where θ is now equal to $\frac{1}{r^3} - \Delta$, Δ being a small constant which depends on the distribution of the surrounding NO_3^- ions.

The difference between the two principal gram molecular refractivities of the crystal is given by

$$R_\omega - R_\epsilon = \frac{4\pi}{3} N. \; 3 (A_\omega - A_\epsilon), \quad \ldots (11)$$

(where N is the Avogadro number) and is therefore readily calculated when A and r are known. The rapid increase of A_ω as we go towards the ultra-violet, as contrasted with the much slower increase of A_ϵ, follows naturally from equations (9) and (10), since A itself increases with decrease of wavelength. The result is rendered more evident in the following manner. The oxygen ion when it is free from the influence of its neighbours may be taken to have a certain natural frequency ν_0. The effect of its neighbours can be shown to be equivalent to a *decrease* of the natural frequency from ν_0 to ν_ω for vibrations in the plane of the oxygens, and to an *increase* from ν_0 to ν_ϵ for vibrations along the normal to the plane of the oxygens. On this view, since the natural frequency of the oxygens for the ordinary ray is nearer to the spectral region in which we are working, the ordinary refractive index increases very rapidly as we go towards the ultra-violet, while for the extraordinary ray, for which the natural

frequency is farther off, the increase of refractive index is naturally slower.

In consideration of the usefulness of this point of view, especially in connection with the differences in absorption of the NO_3^- ion for the ordinary and the extraordinary rays, we shall deal with it here in some detail.

10. *Natural Frequencies of the NO_3^- Ion.*

Let us consider the case of an *isolated* oxygen ion placed in the path of light. The moment a of the optical doublet induced in the ion by the electric force E of the light wave is given by the well-known relation

$$m\ddot{a} + 4\pi^2\nu_0^2 m\bar{a} = ne^2E, \quad \ldots (12)$$

where m is the mass of an electron, and e is its charge, n is the number of dispersion electrons in the ion, all of which are supposed to have the same natural frequency of oscillation, *viz.*, ν_0.

If now the other two oxygen ions of the nitrate group are brought to their proper positions beside the one we are considering, the electric force acting on the ion will no more be E, but will include in addition the force due to the doublets induced in the other two ions. The latter force will naturally vary with the direction of the incident electric vector. Let us consider the particular case where the electric vector lies along the normal to the plane of the ions. The expression for the oscillating doublet induced in the oxygen ion will then be

$$m\ddot{\bar{a}} + 4\pi^2\nu_0^2 m\bar{a} = ne^2\left(E - \frac{2a}{r^3}\right) \quad \ldots (13)$$

This equation can be rewritten in the form

$$m\ddot{\bar{a}} + 4\pi^2\nu_\epsilon^2 m\bar{a} = ne^2E, \quad \ldots (14)$$

where $$\nu_\epsilon = \left(\nu_0^2 + \frac{ne^2}{2\pi^2 mr^3}\right)^{\frac{1}{2}}, \qquad \ldots \quad (15)$$

from which it is clear that the natural frequency of the oxygen ions is no more equal to ν_0 but is increased owing to their mutual influcnce to ν_ϵ given by equation (15).

On the other hand when the electric vector lies in the plane of the atoms, the total force acting on any of the ions will be $E+\frac{\alpha}{r^3}$ and their natural frequency will be diminished to

$$\nu_\omega = \left(\nu_0^2 - \frac{ne^2}{4\pi^2 mr^3}\right)^{\frac{1}{2}} \qquad \ldots \quad (16)$$

Thus since the natural absorption frequency of the NO_3^- ion for the ordinary rays is nearer to the spectral region in which we have experimented, than the absorption frequency for the extraordinary rays, the former will be more absorbed than the latter; and thus we get an explanation of the observed pleochroism.

PLEOCHROISM AND BIREFRINGENCE IN CRYSTALS

BY
K. S. KRISHNAN
AND
B. MUKHOPADHYAY
210 Bowbazar Street, Calcutta

PROF. W. L. BRAGG[1] explains the strong birefringence of some carbonates and nitrates as being due to the interaction of the optical dipoles induced in the component atoms. For example, X-ray analysis shows that the carbonate ions in calcite have a plane structure, their planes being perpendicular to the optic axis of the crystal. With this arrangement, the interaction of the dipoles results in a much smaller refractivity for vibrations along the optic axis than for perpendicular vibrations.

The effect of the interaction can also be regarded from a slightly different point of view. So far as observations in the visible and in the near ultra-violet regions are concerned, the effect would be equivalent to a change in the natural frequencies of the ions; for the nitrate, carbonate and similar ions, the natural ultra-violet frequencies will be increased for vibrations along their axes, while for perpendicular vibrations the natural frequencies will be diminished. The smaller refractivity for the former vibrations than for the latter, follows then as a natural consequence.

On this view we should expect, as we proceed from the visible region towards the ultra-violet, the absorption of these ions to begin earlier for vibrations perpendicular to the axis than for vibrations along the axis. That this is actually so for the nitrate ion was shown in a previous communication[2]. We have now studied the absorption of several other crystals, namely, calcite, dolomite and ankerite, which are uniaxial, and aragonite and potassium chlorate, which are approximately so. They all show pleochroism in the ultra-violet, which grows stronger with decreasing wave-length, the vibrations along their optic axes being less absorbed than the perpendicular vibrations.

In strong contrast with these crystals are anhydrite, celestite, barite and selenite, which show practically no pleochroism; as is well known, the birefringence of these crystals is very feeble.

[1] *Proc. Roy. Soc.*, A., 105, 370; 1924.
[2] NATURE, 126, 12, July 5, 1930.

Printed in Great Britain by FISHER, KNIGHT & CO., LTD., St. Albans

MOLECULAR ORIENTATIONS IN *p*-DIPHENYLBENZENE CRYSTAL

BY

K. S. KRISHNAN

AND

S. BANERJEE

210 Bowbazar Street, Calcutta

IN recent papers[1] we have shown how a correlation of the principal diamagnetic susceptibilities of an organic crystal with those for the *molecules* of the substance, offers a convenient method for determining the orientations of the molecules in the crystal lattice. The crystal of *p*-diphenylbenzene, the

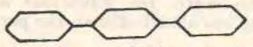

structure of which has recently been analysed by X-ray methods by Miss Pickett[2], is a very suitable substance for determination of molecular orientations by this method. The crystal belongs to the monoclinic system and is found by Miss Pickett to contain two molecules in the unit cell. The molecule has a centre of symmetry; the three benzene rings lie in a plane, and their centres are in a line.

The principal magnetic directions of the molecule are evidently (1) along the line joining the centres of the three benzene rings, (2) along the perpendicular direction in the plane of the rings, and (3) along the normal to the plane of the rings. The susceptibilities along these directions can be calculated from the known values for the benzene molecule (or from those for benzene and for diphenyl molecules) and are found to be

$$K_1 = K_2 = -91$$
$$K_3 = -254$$

respectively, in 10^{-6} c.g.s. e.m.u. per gm. mol.

The principal susceptibilities of the crystal are, in the same units:

$$\chi_1 = -94$$
$$\chi_2 = -203$$
$$\chi_3 = -139.$$

χ_2 is the susceptibility along the b axis; the χ_1-axis, in the (010) plane, is found to lie in the acute angle β, making an angle of 14·3° with the c axis.

From these data the orientations of the two molecules in the unit cell can be deduced in the same manner as was described for diphenyl in a previous communication[3]. It is thus found that the lengths of the molecules lie in the (010) plane, in the acute angle β, making an angle of 14·3° with the c axis, while the planes of the two molecules are inclined at + 56·6° and − 56·6° respectively to the (010) plane. These values are in good agreement with the values 15·3° and ± 56° obtained for these angles by Miss Pickett from her X-ray data.

[1] NATURE, 130, 313, Aug. 27, 1932; and 131, 653, May 6, 1933. *Phil. Trans.*, A, 231, 235; 1933.
[2] *Proc. Roy. Soc.*, A, 142, 333; 1933.
[3] *Phil. Trans.*, A, 231, 256; 1933.

The Principal Optical Polarisabilities of the Naphthalene Molecule

BY

K. S. KRISHNAN.

(*Received for publication, December 20, 1933.*)

1. *Introduction.*

In a previous communication[1] the principal diamagnetic susceptibilities of the naphthalene molecule were calculated from those for the naphthalene crystal and the known orientations of the molecules in the crystal lattice. It was thus found that the two principal susceptibilities of the molecule in the plane of its benzene rings are nearly equal, and are about a fourth of the susceptibility along the normal to the plane of the benzene rings. A knowledge of the principal *optical* polarisabilities of the molecule will also be of great interest. But their evaluation from the known refractivities of the crystal is not so simple as the evaluation of the magnetic constants of the molecule. In the latter case, owing to the extreme feebleness of the diamagnetic moments induced in the molecules, their mutual influence when they are grouped together as in the crystal, is negligible, whereas in the optical case the influence is quite large. This makes the correlation of the optical polarisabilities of the molecule with those of the crystal complicated.

It is, however, possible to calculate the optical polarisabilities of the molecule indirectly from other considerations.

[1] 'Nature', Vol. 130, p. 698 (1932).

It is the purpose of the present paper to give an account of these calculations.

2. *The Principal Optical Polarisabilities.*

The structure of the naphthalene molecule has been studied by x-ray methods by Bragg,[2] Robertson[3] and Banerjee.[4] Considerations of the symmetry of the molecule suggest the following directions for its three principal axes :

(1) along the line joining the centres of the two benzene rings ;

(2) along a direction in the plane of the benzene rings, perpendicular to the first axis ;

(3) along the normal to the plane of the rings.

We shall denote the optical di-pole moments induced in the molecule per unit field of the electric vector of the light-wave, acting respectively along these three directions, by b_1, b_2 and b_3. We shall denote the principal magnetic susceptibilities of the molecule along these directions by a_1, a_2 and a_3 respectively. As has already been mentioned, the a's for the naphthalene molecule are known.

There are three important optical quantities which involve the optical polarisabilities of the molecule :

(1) the well-known Lorentz constant of refraction, which involves $b_1+b_2+b_3$;

(2) the depolarisation factor of the light scattered by the molecules in the fluid state, which involves

$$(b_1-b_2)^2+(b_2-b_3)^2+(b_3-b_1)^2;$$

(3) thirdly, the well-known Cotton-Mouton constant, which involves

$$(a_1-a_2)(b_1-b_2)+(a_2-a_3)(b_2-b_3)+(a_3-a_1)(b_3-b_1).$$

2 ' Proc. Phys. Soc.,' Vol. 34, p. 33 (1921).
3 ' Roy. Soc. Proc.' A, Vol. 125, p. 546 (1929).
4 ' Ind. Jour. Phys.,' Vol. 4, p. 557 (1930).

From a knowledge of the above three physical quantities, it is possible to calculate the three b's.

3. *The Lorentz Constant.*

The Lorentz relation is

$$\frac{n^2-1}{n^2+2}\cdot\frac{M}{\rho}=\frac{4}{3}\pi N.\ \frac{b_1+b_2+b_3}{3}, \qquad \text{.....(1)}$$

where n is the refractive index of the fluid, ρ is its density, M is the gram molecular weight, and N is the Avogadro number per gram molecule. It is well-known that this relation holds, to a first approximation, over such large ranges of densities as correspond to the liquid and the gaseous states.

For naphthalene, taking the gram molecular refractivity $\left(\frac{n^2-1}{n^2+2}\cdot\frac{M}{\rho}\right)$ for the D-lines as 44·37, we obtain

$$b_1+b_2+b_3=52{\cdot}42\times10^{-24}. \qquad \text{.....(2)}$$

4. *The Depolarisation of Light-scattering.*

The depolarisation factor r for the light transversely scattered by a gas, when the incident light is unpolarised, is given by the well-known relation

$$\frac{(b_1-b_2)^2+(b_2-b_3)^2+(b_3-b_1)^2}{(b_1+b_2+b_3)^2}=\frac{10r}{6-7r}. \qquad \text{.....(3)}$$

The value of r is not appreciably affected by small changes in the wave-length of the incident light. For naphthalene vapour r has been measured by Ramanathan,[5] Cabannes[6] and Ramakrishna Rao.[7] Rao's value, which agrees almost exactly with that of Ramanathan, is $r=0{\cdot}079$. Cabannes's value is

5 ' Proc. Ind. Assn. Sc.,' Vol. 9, p. 206 (1926).
6 ' Compt. Rendus,' Vol. 182, p. 885 (1926).
7 ' Ind. Jour. Phys.,' Vol. 2, p. 84 (1927).

higher, *viz.*, 0·10. Adopting the former value, and using the value of $b_1+b_2+b_3$ given in (2) above, we obtain

$$(b_1-b_2)^2+(b_2-b_3)^2+(b_3-b_1)^2=398\cdot4\times10^{-48}. \quad \text{.....(4)}$$

5. *The Cotton-Mouton Constant.*

The Cotton-Mouton constant of a liquid is given by the relation

$$C_m=\frac{n_\parallel-n_\perp}{\lambda H^2} = \frac{3M(n^2-1)^2}{80\pi n\lambda kTN\rho} \cdot \frac{(a_1-a_2)(b_1-b_2)+(a_2-a_3)(b_2-b_3)+(a_3-a_1)(b_3-b_1)}{(b_1+b_2+b_3)^2}, \quad (5)$$

where λ is the wave-lengh of the incident light, H is the magnetic field, $n_\parallel$ and $n_\perp$ are the two principal refractive indices of the liquid in the field, k is the Boltzmann constant per molecule and T is the absolute temperature. Salceanu[8] has recently made extensive measurements on the Cotton-Mouton constant of molten naphthalene at different temperatures. His values refer to $\lambda=0\cdot578\mu$ and the values given in Table I have been calculated for $\lambda=0\cdot589\mu$ (D-lines) from his data with the help of Havelock's relation. The gram molecular refractivity of naththalene for these wave-lengths were taken to be 44·46 and 44·37 respectively. The last column in the table gives the values of

$$a=\frac{(a_1-a_2)(b_1-b_2)+(a_2-a_3)(b_2-b_3)+(a_3-a_1)(b_3-b_1)}{(b_1+b_2+b_3)^2}, \quad \text{... (6)}$$

calculated from these data with the help of relation (5).

TABLE I.

T(°K.)	$C_m\times10^{13}$	a
361·5	18·80	1·46
373	17·26	1·40
377·2	17·03	1·41
387	16·75	1·43
410·5	15·62	1·45
442	14·86	1·55

8 'Compt. Rendus,' Vol. 191, p. 486 (1930).

If we reject the first value which refers to a temperature close to the melting point of the substance (*viz.*, 353° K.), the values of a are found to increase with rise of temperature. This is indeed what we should expect, since it is well known that the effective optical anisotropy of a molecule in the liquid state is appreciably smaller than that for the molecule in the state of vapour, and that in the former state, as the temperature is gradually increased, the value of the effective anisotropy also increases and tends to approach the vapour value at sufficiently high temperatures.[9] We may, therefore, adopt for the value of a of the naphthalene molecule,

$$a=1\cdot60. \quad \text{... ... ... (7)}$$

Hence we obtain, using the value of $b_1+b_2+b_3$ given in (2),

$$(a_1-a_2)(b_1-b_2)+(a_2-a_3)(b_2-b_3)+(a_3-a_1)(b_3-b_1)=4\cdot40\times10^{-51}. \quad (8)$$

The Cotton-Mouton constant of solutions of naphthalene in carbon tetrachloride (which is magneto-optically inactive), has also been measured recently by Chinchalkar in this laboratory, and he obtains a value $C_m=1\cdot56\times10^{-12}$ per gram of naphthalene in 1 c.c. of dilute solution. Using the following relation for C_m for such solutions in an inactive solvent, *viz.*,

$$C_m=\frac{\pi N(n^2+2)^2}{135n\lambda kTM}\cdot\Big[(a_1-a_2)(b_1-b_2)+(a_2-a_3)(b_2-b_3)+(a_3-a_1)(b_3-b_1)\Big], \quad (9)$$

where n is the refractive index of the solution, and M is the molecular weight of the solute, we obtain

$$(a_1-a_2)(b_1-b_2)+(a_2-a_3)(b_2-b_3)+(a_3-a_1)(b_3-b_1)=2\cdot91\times10^{-51}. \quad (10)$$

This value is naturally much less than the value obtained above for higher temperatures.

9 K. S. Krishnan and S. R. Rao, "Ind. Jour. Phys.," Vol. 4, p. 39 (1929).

6. *The Optical Constants of the Naphthalene Molecule.*

Since the a's for the naphthalene molecule are known, the three equations (2), (4) and (8) enable us to calculate the b's. The values of the a's are [10].

$$\left.\begin{aligned} a_1 &= -\ 6{\cdot}50 \\ a_2 &= -\ 7{\cdot}09 \\ a_3 &= -\ 30{\cdot}88 \end{aligned}\right\} \times 10^{-29} \text{ c.g.s. e.m.u.} \quad \ldots \quad (11)$$

Also from considerations of the structure of the molecule, b_1 should be greater than b_2. Hence we obtain from (2), (4) and (8)

$$\left.\begin{aligned} b_1 &= 26{\cdot}8 \\ b_2 &= 14{\cdot}1 \\ b_3 &= 11{\cdot}5 \end{aligned}\right\} \times 10^{-24} \text{ c.g.s. e.s.u.} \quad \ldots \quad \ldots \quad (12)$$

Thus the polarisability of the molecule along its long axis, *viz.*, b_1, is more than double the polarisability b_3 along the normal to the plane of the molecule.

[10] See 'Phil. Trans.' A, Vol. 231, p. 253 (1933). The values of the a's given here were calculated from the principal susceptibilities of naphthalene crystal, on the basis of the orientations given by Banerjee for the two molecules in the unit cell of the crystal, *viz.* that the a_1 axes of the molecules lie in the (010) plane, and their a_3 axes are inclined at plus and minus 25° to the (010) plane. Since the present paper was written, Robertson has published the results of a further x-ray study of the crystal (Roy. Soc. Proc.' A, Vol. 142, p. 678 (1933)), and suggests slightly different orientations for the molecules. The corresponding values of the a's will differ only *slightly* from those given here.

Magnetic Anisotropy of Graphite

GRAPHITE is known from the investigations of Owen, Honda and others to exhibit an exceptionally large magnetic anisotropy. The susceptibilities of the natural crystal along its hexagonal axis and along perpendicular directions are, according to Honda[1]:

$$\chi_1 = -\ 14{\cdot}2 \times 10^{-6}\ ;\ \chi_2 = -\ 2{\cdot}2 \times 10^{-6}$$

respectively, per gm., χ_1 being thus more than six times χ_2. Recently Goetz and his collaborators have found a much higher value for the ratio χ_1/χ_2. Chemically treated pure graphite powder is dispersed by them in a solution of gum Dammar in benzene; the solution is placed in a strong magnetic field and the benzene is allowed to evaporate. All the graphite particles in the solidified medium will then naturally be oriented in the same manner, namely, with their hexagonal axes normal to the direction of the imposed field. From susceptibility measurements on this medium they found[2] for χ_1/χ_2 a value of 13·2. Later[3], using graphite particles dispersed in this manner in a solidified solution of agar, they obtained a still higher value, namely, 18. Their more recent estimate[4], obtained from a similar suspension of graphite particles in gelatine, is so high as 28. It would thus seem desirable to determine the anisotropy of graphite by an independent method.

The following measurements made with some good specimens of Ceylon graphite, by Messrs. B. C. Guha and B. P. Roy in this laboratory, may therefore be of interest. The method adopted in these measurements was the same as was described in previous papers[5]. By suspending the crystal, with its hexagonal axis horizontal, at the end of a calibrated quartz fibre, in a uniform magnetic field, and measuring the couple due to the magnetic anisotropy of the crystal, the *difference* between the two principal susceptibilities, namely, $\chi_1 - \chi_2$, was determined. With the same suspension, the absolute value of χ_2 was measured by magnetically balancing the crystal in a field of large non-homogeneity, against an aqueous solution of potassium iodide, the susceptibility of which could be adjusted by suitable dilution.

Altogether ten different crystals were measured for $\chi_1 - \chi_2$, and the values obtained ranged from $-\ 21{\cdot}8 \times 10^{-6}$ to $-\ 23{\cdot}0 \times 10^{-6}$ per gm. The values for χ_2 varied about a mean value of $-\ 0{\cdot}4 \times 10^{-6}$. Hence the principal susceptibilities of these crystals per gm. are:

$$\chi_2 = -\ 22{\cdot}8 \times 10^{-6},\ \chi_1 = -\ 0{\cdot}4 \times 10^{-6}.$$

210 Bowbazar Street, Calcutta.
Nov. 23.

K. S. KRISHNAN.

[1] "Int. Crit. Tables", 6, 364.
[2] *Phys. Rev.*, 39, 168; 1932.
[3] *Ibid.*, 39, 553; 1932.
[4] *Ibid.*, 40, 1053; 1932.
[5] *Phil. Trans.*, A, 231, 235. 232, 99; 1933.

Large Artificial Crystals of Graphite

Professor Goetz and his collaborators[1, 2] have recently described a new method of producing "large artificial crystals of graphite." Chemically purified graphite particles, of more or less uniform size, are dispersed in a liquid gelatine solution, and the medium is placed in a strong magnetic field; there will naturally result a reorientation of the particles. If the medium is allowed to solidify in the presence of the magnetic field, the solidified mass will contain, embedded in it, a large number of graphite particles having the same orientations as were imposed on them by the field when the medium was still liquid. Professor Goetz assumes that the particles will then be crystallographically parallel to one another, and the medium will be similar to a large single crystal.

It appears to me that under the conditions of the above experiment, the graphite particles will not be parallel to one another. As is well known, a graphite crystal exhibits a large magnetic anisotropy, its diamagnetic susceptibility along its hexagonal axis, *vis.*, $\chi_{\parallel}$, being several times greater than the susceptibility, $\chi_{\perp}$, for directions in its basal plane. Because of this anisotropy, the magnetic field will exert a strong orienting couple on the particles (the couple due to the asymmetric *shape* of the particles will be much smaller in comparison, even in fields of strong inhomogeneity). The crystal flakes will therefore orient themselves in such manner as to bring their basal planes parallel to the direction of the field, i.e., parallel to a line, and therefore *not necessarily parallel to one another*. Indeed, if their orientations are determined solely by the magnetic field (the settling down of the particles under gravity being supposed to have no influence), the hexagonal axes of the different crystals will be oriented at random in the equatorial plane, i.e., in the plane normal to the direction of the field

If this view is correct, the value $\chi_{\parallel}/\chi_{\perp}=28$, obtained by Goetz and Faessler[2] from measurements on such orientated graphite particles, on the assumption that the particles are crystallographically parallel, must be taken to correspond to

$$\tfrac{1}{3}(\chi_{\parallel}+\chi_{\perp})/\chi_{\perp}=28,$$

i.e.,

$$\chi_{\parallel}/\chi_{\perp}=55.$$

In connection with this high value for $\chi_{\parallel}/\chi_{\perp}$, the results of magnetic measurements[3] by Guha and Roy in this laboratory, on some well-developed natural crystals of graphite, may be of interest. Their results are

$$\chi_{\parallel}=-22.8\times10^{-6} \text{ per g,}$$

$$\chi_{\perp}=-0.4\times10^{-6} \text{ per g,}$$

and hence

$$\chi_{\parallel}/\chi_{\perp}=57.$$

Because of the extreme smallness of $\chi_{\perp}$, its value will be sensitive to any traces of impurities that might be present in the crystal, and the above value of $\chi_{\parallel}/\chi_{\perp}$ will be uncertain to that extent. Its closeness, however, to the value deduced from the results of Goetz and Faessler, deserves mention.

K. S. KRISHNAN

210 Bowbazar Street,
Calcutta, India,
November 27, 1933.

[1] Goetz, Focke and Faessler, Phys. Rev. **39**, 169, 553 (1932).
[2] Goetz and Faessler, Phys. Rev. **40**, 1053A (1932).
[3] Reported in a recent communication to Nature.

CRYSTAL STRUCTURE OF 1, 3, 5-TRIPHENYLBENZENE

BY

PROF. K. S. KRISHNAN

AND

S. BANERJEE

210, Bowbazar Street, Calcutta

In a recent communication on the crystal structure of 1, 3, 5-triphenylbenzene, Dr. Kathleen Lonsdale[1] discusses the results of recent X-ray measurements on the crystal and concludes that the planes of the benzene rings of the molecules cannot coincide with the (001) plane of the crystal, as has been suggested by earlier investigators, but must be inclined to this plane.

This conclusion is fully supported by the results of our magnetic measurements on this crystal, and the magnetic data further enable us to calculate approximately the inclinations of the benzene rings to the (001) plane. The crystal is orthorhombic and its principal gram molecular susceptibilities along a, b and c axes are :

$$\chi_a=-141\,;\ \chi_b=-155;\ \chi_c=-309$$

respectively, in 10^{-6} C.G.S. E.M.U.

The c axis is thus an axis of approximate magnetic symmetry, the susceptibility along this axis being numerically greater than that along perpendicular directions by 161×10^{-6} per gram molecule. Had the planes of all the benzene rings in the unit cell been coincident with the (001) plane, the difference between the susceptibilities along the c axis and along perpendicular directions would have been much higher, namely, 216×10^{-6} per gram molecule. This shows that the benzene rings are inclined to the (001) plane, the angle of inclination θ being given by the relation $\cos^2\theta-\frac{1}{2}\sin^2\theta=\frac{161}{216}$; that is, $\theta=24°$.

The optical constants of the crystal also support the above orientation of the benzene rings. The gram molecular refractivities (defined as usual by $R=\frac{n^2-1}{n^2+2}\cdot\frac{M}{\rho}$) of the crystal for vibrations along the a, b and c axes are[2] :

$$R_a=115{\cdot}5\,;\ R_b=115{\cdot}0\,;\ R_c=77{\cdot}6$$

respectively, for the D lines. R_a and R_b are thus nearly equal and much greater than R_c, as we should expect. If we assume all the benzene rings to lie in the (001) plane, and *neglect the mutual influence of the optical dipoles induced in the different benzene rings*, we obtain for the birefringence of the crystal

$$R_a-R_c=R_b-R_c=65.$$

The much smaller birefringence actually observed for the crystal, namely, $R_a-R_c=R_b-R_c=38$, points to an inclination of the benzene rings to the (001) plane, at an angle θ determined, as in the magnetic case, by the equation

$$\cos^2\theta-\tfrac{1}{2}\sin^2\theta=\tfrac{38}{65},\ \text{or}\ \theta=32°.$$

Since the mutual influence of the dipoles is by no means negligible as we have assumed in the calculation, this value of θ must be taken to represent only the *order of magnitude*, and is therefore not inconsistent with $\theta=24°$ obtained from the magnetic data.

[1] NATURE, **133**, 67, Jan. 13, 1934.
[2] Groth, *Chem. Krist.*, 5, 342.

Photo-Dissociation of the NO_3^- Ion and its Dependence on the Polarisation of the Exciting Light-Quantum.

AQUEOUS solutions of several nitrates have been studied for their absorption spectra in the ultra-violet. They all show two absorption bands, one feeble extending from 350 $m\mu$ to 270 $m\mu$ with a maximum at 300 $m\mu$, and a second absorption which is very much stronger, beginning at about 230 $m\mu$ and having its maximum at 206 $m\mu$[1]. Following the explanation given by Henri and his collaborators[2] for the absorption spectra of NO_2, SO_2, CS_2 and other molecules, and of Dutta[3] for SO_3 and N_2O_5, we may attribute the origin of the two absorption bands of the NO_3^- ion to the following photo-chemical reactions. The absorption which begins at 350 $m\mu$ may be taken to correspond to the photo-dissociation of the NO_3^- ion into NO_2^- ion and oxygen atom in the ground state ($^3P_2$) according to the relation

$$NO_3^- \rightarrow NO_2^- + O(^3P_2) - 81 \text{ K cals. } (350\, m\mu). \quad (1)$$

From thermochemical data[4] we have

$$NO_3^- \rightarrow NO_2^- + \tfrac{1}{2}O_2 - 24 \text{ K cals.} \quad .. \quad (2)$$

From (1) and (2) we obtain

$$\tfrac{1}{2}O_2 \rightarrow O(^3P_2) - 57 \text{ K cals.}, \quad .. \quad .. \quad (3)$$

which gives for the energy of dissociation of the O_2 molecule into two unexcited O atoms, the value 114 K cals. This agrees with the value 114·6 K cals. recently obtained by Henri[2] from the predissociation limit of NO_2.

The second absorption band, which begins at about 230 $m\mu$, may be taken to correspond to the dissociation of NO_3^- into NO_2^- and an *excited* O atom according to the relation

$$NO_3^- \rightarrow NO_2^- + O(^1D_2) - 124 \text{ K cals. } (230 m\mu). \quad (4)$$

From (4) and (1) we obtain

$$O(^1D_2) - O(^3P_2) = 43 \text{ K cals.} \quad .. \quad (5)$$

This again agrees with the value 45·1 K cals. obtained from spectroscopic measurements by Frerichs, Hopfield and Paschen.[5]

The photodissociation due to the 206 $m\mu$ absorption band is confirmed by the direct experiments on KNO_3 solutions by Warburg[6] and others; a feeble effect has also been claimed with sun-light having wavelengths greater than 290 $m\mu$, which may be attributed to the 300 $m\mu$ band absorption.

The absorption spectra of nitrates in the crystal state and in the fused state have also been studied, and the absorption curves are very similar to those obtained with aqueous solutions. Thus in these states also, the absorption bands have presumably the same origin and are due to the two types of photo-dissociation of NO_3^- described above.

It is remarkable that when the absorption measurements are made with *single crystals* of KNO_3 and $NaNO_3$, in which the NO_3^- ions are all orientated parallel to one another, the above two absorption bands are very intense when the incident light-vibrations lie in the plane of the NO_3^- ions, while for the vibrations along the normal to the NO_3^- planes the absorptions are much feebler.[7] This experimental result, when considered in relation to the origin of these absorption bands given above, as due to the photo-dissociation of NO_3^- ion to NO_2^- ion and O atom in the ground state and in the excited state respectively, suggests that *the efficiency of the photo-dissociation of the NO_3^- ion is much greater when the exciting light-vibrations are in the plane of the NO_3^- ion than when they are along the normal to its plane.* Experiments are in progress to test this conclusion by direct measurements.

A detailed report of the work will appear in the *Symposium on Molecular Spectra* to be published by the *Indian Academy of Sciences*.

K. S. KRISHNAN.
A. C. GUHA.

210, Bowbazar Street,
Calcutta,
May 28, 1934.

[1] For a typical absorption curve for the nitrate solutions see Fig. 1. Maslakowez, *Zeits. Phys.*, **51**, p. 703, 1928; Fig. 2. The values given in the present letter for the wave-lengths corresponding to the beginnings of the two absorption bands and their maxima, are taken from this curve of Maslakowez.

[2] See article on "Pre-dissociation" by V. Henri, *Leipziger Vortrage*, 1931, English translation, Blackie, pp. 121-143.

[3] *Roy. Soc. Proc.*, **A., 137**, p. 366 and **139**, p. 397, 1932.

[4] *Int. Crit. Tables*, **5**, p. 178.

[5] See Bacher and Goudsmit, *Atomic Energy States*, p. 333. The term values for the $^3P_2$ and $^1D_2$ levels are 109,837 and 93,969 cm^{-1}, so that their difference is equal to 15,868 cm^{-1} or 45·1 K. cal.

[6] *Sitz. Ber. Berliner Akad.*, 1918, p. 1242.

[7] See Krishnan and Das Gupta, *Nature*, **126**, p. 12 (1930) and *Indian Journ. Phys.*, **8**, p. 49 (1933).

Absorption Spectra of Single Crystals of Polynuclear Hydrocarbons.

THE absorption spectra of single crystals of a number of polynuclear hydrocarbons have been studied by us using incident linearly polarised light. Among the crystals studied are anthracene, phenanthrene, 1, 2-benzophenanthrene, 1, 2, 5, 6-dibenzanthracene, fluorene, fluoranthene and pyrene, for which the orientations of the molecular benzene planes in the crystal lattice are known either from X-ray analysis or from the magnetic measurements on the crystals. In all cases, it is found that *the absorption of the crystal is much more intense when the incident light vibrations are parallel to the plane of the benzene rings in the molecules than when the vibrations are along the normal to the benzene planes.*

Fig. 1.

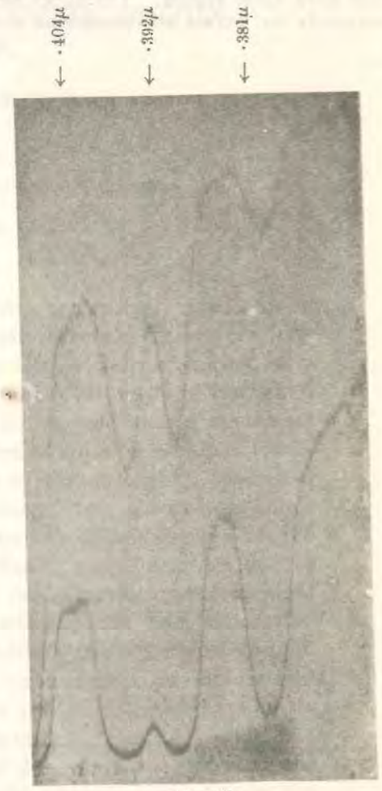

Fig. 2.

As an example, we may take the case of 1, 2, 5, 6-dibenzanthracene. It crystallises in the monoclinic system in the form of thin flakes parallel to the *c* (001) plane. Recent X ray measurements on this crystal by Iball and Robertson, and magnetic measurements by Banerjee in this laboratory, show that the benzene rings in the molecules of the unit cell are nearly parallel to the *b* (010) plane, and that the long axes of the molecules are nearly perpendicular to the *a* axis. Therefore, one of the extinction-directions in the plane of the crystal flake, namely the *a* axis, would correspond predominantly to vibrations in the plane of the benzene rings along the width of the molecules, while the other extinction-direction, namely, that along the *b* axis, would correspond predominantly to vibrations perpendicular to the plane of the benzene rings.

Using one such crystal flake of 1, 2. 5, 6-dibenzanthracene and allowing linearly polarised white light to be incident normally on the flake, its absorption spectra for the above two principal vibrations have been studied by us. Fig. 1 gives a microphotometric record of the absorption spectra in the visible region, the upper curve corresponding to vibrations along the *a* axis, and the lower to vibrations along the *b* axis. It is remarkable that whereas the

absorption bands appear prominently when the vibrations are along the *a* axis, they are quite feeble for vibrations along the *b* axis. Thus, these absorptions are practically confined to vibrations in the plane of the benzene rings, the vibrations along the normal to the plane of the benzene rings being almost freely transmitted.

In Fig. 2 are reproduced the microphotometric records (on a different scale from that of Fig. 1) of these two principal absorptions for the *ultra-violet* region. The upper curve corresponds as before to vibrations along the *a* axis, and the lower curve to vibrations along the *b* axis. Here again, the polarisation of the absorption bands is evident.

The absorption by napthalene, 1, 4-napthoquinone and *p*-benzoquinone also show a similar striking dependence on the direction of the light vibration with reference to the molecular planes.

K. S. KRISHNAN.
P. K. SESHAN.

210, Bowbazaar Street,
Calcutta,
July 12, 1934.

THE ABSORPTION SPECTRA OF NITRATES AND NITRITES IN RELATION TO THEIR PHOTO-DISSOCIATION.

BY PROF. K. S. KRISHNAN, D.Sc.,
AND
A. C. GUHA, M.Sc.,
Indian Association for the Cultivation of Science, Calcutta.

Received September 30, 1934.

1. *Introduction.*

THE absorption spectra of nitrates have been extensively studied by Halban, Scheibe, Morton, Maslakowez and others.[1] There are two absorption bands; one of them is in the near ultra-violet, extending from about 350 $m\mu$ to 260 $m\mu$ with its maximum at about 300 $m\mu$, and the other, which is much more intense, begins at about 230 $m\mu$ and has its maximum at about 200 $m\mu$. Separating the two is a region of more or less free transmission. The spectrum is thus very similar to the absorption spectra of some of the oxides, which have also in general two absorption bands separated by a region of transmission. The absorption spectra in the latter compounds have been explained by Henri[2] and Dutta[3] as due to the photo-dissociation of the molecule under the influence of the incident light. It would be of interest to enquire whether the two absorption bands of the nitrates may not have a similar photo-chemical origin. Further, it is known from measurements on single crystals of sodium and potassium nitrates, in which the NO_3'-ions are all oriented parallel to one another, that the absorption bands are strongly dichroic; when the incident light is linearly polarised, it is found[4] that both the 300 and the 200 $m\mu$ absorptions are much stronger when the electric vector lies in the plane of the NO_3'-ions than when it is along the normal to their plane. The question naturally arises whether this strong dichroism is associated with a corresponding difference in the quantum efficiency of the photo-dissociations

[1] See H. Ley, *Handbuch der Physik.*, 21, 329-31.

[2] See article on "Predissociation" by V. Henri in *Molekulstruktur*, Leipziger Vortrage, 1931.

[3] *Roy. Soc. Proc.*, 1932, A 137, 366; and 139, 397.

[4] See K. S. Krishnan and A. C. Dasgupta, *Nature*, 1930, **126**, 12, and *Ind. Jour. Phys.*, 1933, 8, 49.

for the two directions of vibration of the incident light. In the present paper an attempt is made to answer these and allied questions.

2. *Absorption Spectrum of the NO_3' Ion.*

Among the inorganic nitrates, those of lithium, sodium, potassium, ammonium, calcium, strontium, barium and magnesium, and nitric acid have been studied for their absorption spectra in aqueous solutions of various concentrations. Though for strong solutions, the positions of the absorption bands and also their intensities vary with the nature of the salt and its concentration, in very dilute solutions where the salts are presumably completely ionised, the absorption spectrum is the same for all the salts, being evidently characteristic of the NO_3'-ion.

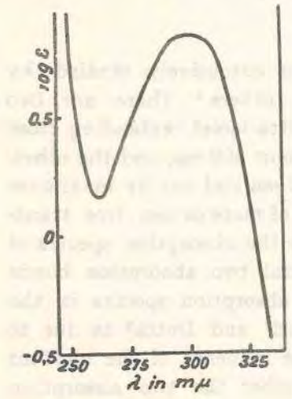

FIG. 1.

Fig. 1, taken from a recent publication by Bonhoeffer and Harteck,[5] gives the typical absorption curve for dilute solutions, in the neighbourhood of 300 $m\mu$. In the figure ϵ is the molar absorption coefficient defined by the usual relation

$$\epsilon = \frac{1}{cd} \log_{10} \frac{I_o}{I}$$

where c is the concentration of the solution in mol. per litre of solution, and I is the intensity of the light after traversing a thickness d cms. of the solution, the initial intensity being I_o.

For our present purpose, the long wave-length limit of the absorption is of special interest, since on the assumption that the absorption is due to photo-chemical dissociation, it gives the minimum energy of the photon effective in inducing the dissociation. In Fig. 1, this wave-length would correspond to the limiting wave-length which the curve would reach asymptotically as it is extrapolated downwards. Though it is difficult to obtain the precise value, it will be clear from the figure that the limiting wave-length cannot differ much from 350 $m\mu$, and we may, therefore, adopt this value as representing the beginning of this absorption band.

The absorption curve in the neighbourhood of the second band is given in Fig. 2, which is taken from Maslakowez's paper.[6] In this figure

[5] *Grundlagen der Photochemie*, Th. Steinkopff, 1933, p. 165, Fig. 63.
[6] *Zeits. f. Phys.*, 1928, 51, 703, Fig. 11.

the actual absorption coefficients k for KNO_3 and KNO_2 solutions of concentration 0·0017%, are plotted against λ. k in the figure corresponds to the definition

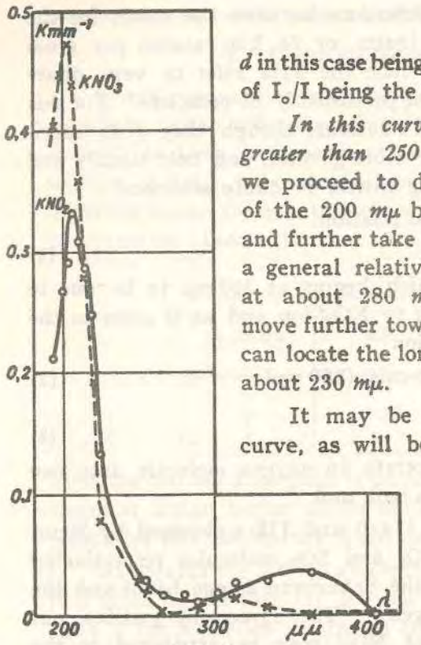

FIG. 2.

$$k = \frac{1}{d} \log_e \frac{I_o}{I}$$

d in this case being expressed in mm. and the logarithm of I_o/I being the base e.

In this curve, the ordinates for all wave-lengths greater than 250 $m\mu$ are magnified 50 times. When we proceed to determine the long wave-length limit of the 200 $m\mu$ band, we have to remember this fact, and further take into consideration the existence of a general relatively feeble absorption, which begins at about 280 $m\mu$ and gradually increases as we move further towards the ultra-violet. Doing so, we can locate the long wave-length limit of this band at about 230 $m\mu$.

It may be mentioned here that Maslakowez's curve, as will be seen from Fig. 2, confirms the value 350 $m\mu$ which we adopted for the beginning of the first band.

3. *The 300 $m\mu$ Band and the Heat of Dissociation of Oxygen.*

The simplest photo-chemical action that may be assumed to be responsible for the absorption will naturally be the dissociation of the nitrate into the nitrite and oxygen. The following table gives the heats of formation, in very dilute solutions, of some nitrates and nitrites.[7]

TABLE I.

Heats of formation in kilojoules per gm. mol.

	Na^+	K^+	NH_4^+	Ba^{++}	Free ion
NO_3'	449·2	460·8	340·9	956·0	208·4
NO_2'	348	359	240·6	753·0	107
Difference	101	102	100·3	2×101·5	101

[7] These thermo-chemical data are taken from the *Inter. Criti. Tables*, 5.

For all the four pairs of salts, as will be seen from the Table, the differences between the heats of formation of the nitrate and the nitrite are the same and are equal to the difference between the values for the NO_3'- and NO_2'-ions, *viz.*, 101 kilo joules, or 24 kilo calories per gram molecule. This is as it should be, since the data refer to very dilute solutions, in which the ionisation must presumably be complete. For this reason, the following thermo-chemical relations, though they refer specifically to the NO_3'- and NO_2'-ions, are more general, and hold equally well for any nitrate and the corresponding nitrite in dilute solutions.

We thus have the thermo-chemical relation,

$$NO_3' \rightarrow NO_2' + \tfrac{1}{2}O_2 - 24 \text{ kilo cals.} \quad .. \quad .. \quad .. \quad .. \quad (1)$$

If now we take the absorption which begins at 350 $m\mu$ to be due to the photo-dissociation of the NO_3'-ion to NO_2'-ion and an O atom in the ground state (^3P), we obtain the relation

$$NO_3' \rightarrow NO_2' + O\ (^3P) - 81 \text{ kilo cals. } (350\ m\mu) \quad .. \quad .. \quad (2)$$

From (1) and (2), we obtain

$$O_2 \rightarrow 2\ O\ (^3P) - 114 \text{ kilo cals.} \quad .. \quad .. \quad .. \quad .. \quad (3)$$

i.e., the energy D required to dissociate an oxygen molecule into two normal oxygen atoms is 114 kilo cals./gm. mol.

This value agrees with the values 114·6 and 115·4 obtained by Henri from the pre-dissociation limits of NO_2 and SO_2 molecules respectively,[8] and 117·3 and 117·0 obtained from the Schumann-Runge bands and the Herzberg bands respectively of oxygen.[9] The agreement justifies our assumption that the 300 $m\mu$ band of NO_3' may be attributed to the photo-dissociation of NO_3'-ion into NO_2'-ion and a normal atom of oxygen.

4. The 200 mμ Band and the Energy of Excitation of the Oxygen Atom.

The beginning of the second absorption band, *viz.*, 230 $m\mu$ is separated from that of the first, *viz.*, 350 $m\mu$ by about 15,000 cm.$^{-1}$, which is nearly the same as the term difference between the ground level (^3P) of oxygen and its $^1D_2$ level. This fact, taken along with the explanation already offered for the 300 $m\mu$ band, suggests the following photo-dissociation as the cause of the second band:

$$NO_3' \rightarrow NO_2' + O\ (^1D_2) - 124 \text{ kilo cals. } (230\ m\mu) \quad .. \quad .. \quad (4)$$

From (2) and (4) we obtain for the energy of excitation of the oxygen atom

$$O\ (^1D_2) - O\ (^3P) = 43 \text{ kilo cals.} \quad .. \quad .. \quad .. \quad .. \quad (5)$$

[8] Debye, *Structure of Molecules*, 1932, Blackie, pp. 134 and 136.
[9] Bonhoeffer and Harteck, *loc. cit.*, pp. 106-112.

The term value of the $^1D_2$ level from spectroscopic data[10] is 109,837 cm.$^{-1}$, while that of the ground level, *viz.*, $^3P_2$ is 93,969 cm.$^{-1}$ The difference, namely, 15,868 cm.$^{-1}$, corresponds to an energy of 45·1 kilo cals., which is nearly the same as the value obtained here.

5. Direct Evidence for Photo-Dissociation.

Direct confirmation of the photo-chemical decomposition of potassium nitrate to nitrite under the influence of light in the neighbourhood of 200 $m\mu$ is available from the experiments of Warburg.[11] With a slightly alkaline solution of KNO_3, of concentration $^1/_3$ N (+ NaOH $^1/_{3000}$ N), he obtains the following values for quantum efficiency γ (number of molecules decomposed per quantum absorbed):

TABLE II.

λ in $m\mu$	207	253	282
γ	0·25	0·17	0·024

Thus the 200 $m\mu$ absorption is photo-chemically active, though the photo-chemical action begins earlier than is contemplated by the theory. The reason for this discrepancy is not clear.

As regards the 300 $m\mu$ absorption band, as has already been mentioned, it is much feebler than the 200 $m\mu$ band; according to Maslakowez,[12] the ratio of the *maximum* absorption coefficients of the two bands is 1 : 1500, so that the photo-chemical action of the 300 $m\mu$ absorption will be correspondingly feebler. Some preliminary observations by Dhar seem to point to the existence of such a feeble photo-chemical action. Under the influence of sunlight, in which wave-lengths shorter than 290 $m\mu$ were absent, Dhar reports a feeble photo-decomposition,[13] and this must evidently be due to the 300 $m\mu$ absorption.

6. Absorption by Nitrates in Other Physical States.

The two absorption bands discussed in the previous sections refer to inorganic nitrates in dilute aqueous solutions, and are characteristic of the NO_3'- ion. For nitrates in other physical states, as also in concentrated

[10] See Bacher and Goudsmit, *Atomic Energy States*, 1933, McGraw-Hill, p. 333.
[11] *Sits. Ber. Berliner Akad.*, 1928, p. 1228.
[12] *Loc. cit.*, 704.
[13] *Jour. Phys. Chem.*, 1925, 29, 926.

solutions, the precise positions and intensities of the absorptions will naturally be different. It is experimentally found, however, that for inorganic nitrates, the deviations are not very large. For example, Schaeffer[14] has studied the absorption by molten potassium nitrate, and finds the maximum of the first absorption band in nearly the same position as for dilute solutions. In solid KNO_3 also he records an absorption in the same region.[15] Using a very thin layer of KNO_3 deposited on a quartz plate by allowing a dilute solution of the substance to evaporate on it, Maslakowez has been able to obtain the second absorption band as well, for the solid state. He gets both the first and the second bands in practically the same positions as for the dilute solutions.[16]

Absorption measurements have also been made with single crystals of sodium and potassium nitrates.[17] Here though the actual absorption coefficients show a striking dependence on the direction of vibration of the incident light, the spectral positions of the bands are independent of the direction of vibration, and are practically the same as for the solutions.

Smakula[18] has recently made some interesting studies on the absorption spectrum of small quantities of KNO_3 and $AgNO_3$ (of the order of 0·1%) dispersed in KCl, and the absorption spectrum is again the same.

The strong similarity of the absorption spectrum of the inorganic nitrates in the fused and solid states to that for dilute solutions, shows that in the former states also, the origin of the absorption must be attributed to the photo-dissociation of the nitrate into the nitrite and oxygen in the normal or excited state, as the case may be. No experiments seem to have been made to test whether such photo-dissociations actually take place in the molten and solid states: the foregoing discussion, however, leaves little doubt as to the results of such experiments.

7. *The Dichroic Nature of the Two Absorption Bands.*

The strongly dichroic nature of both the absorption bands has already been mentioned in the introduction; measurements with incident linearly polarised light show that both the absorption bands appear much more intensely when the electric vector of the incident light lies in the plane of the NO_3'-ions, than when the vector is along the normal to the NO_3' plane. This must naturally be taken to correspond to a much larger quantum efficiency

[14] *Zeits. anorg. Chem.*, 1916, **97**, 285.
[15] *Zeits. f. wiss. Photogr.*, 1910, **8**, 260.
[16] *Loc. cit.*, 702, Fig. 10.
[17] Krishnan and Dasgupta, *loc. cit.*
[18] *Zeits. f. Physik.*, 1927, **45**, 1.

of dissociation for the former direction of polarisation of the incident light than for the latter. This result is of great interest; it shows that while the *energy* required to eject an oxygen atom from the NO_3 group is just the same whether the electric vector is in the plane of the NO_3 group or perpendicular to it, the probability of ejection is very different for the two directions of the electric vector. It is well known that in photo-electric effect with polarised X-rays, the ejection of the electron along the direction of the electric vector is much more probable than along perpendicular directions, though, of course, the energies are the same for both. By analogy, we may expect a similar spatial distribution, favouring the direction of the electric vector, of the oxygen atoms ejected from the NO_3 groups. This is of course a different effect from what is obtained here; taking all the oxygen atoms ejected in various directions into account, what we find here is that the number of such ejected atoms per quantum absorbed, is much larger when the electric vector is in the NO_3 plane than when it is normal to the plane. The fact that for the former direction of the electric vector the dipole-moments induced in the component parts of the NO_3 group tend to increase one another, while for the latter direction they tend to diminish one another, may probably be responsible for the greater probability of photo-dissociation for the former direction.

8. *Absorption Spectra of Nitrites.*

The absorption spectra of sodium and potassium nitrites have been investigated, and are similar to those of the nitrates, excepting that both the absorption bands are shifted towards the longer wave-length side, as will be clear from Fig. 2. The first band begins at 400 $m\mu$ (=71 kilo cal./gm. mol.) and has its maximum at about 360 $m\mu$, while the second one begins at about 240 $m\mu$ (=118 kilo cal./gm. mol.). The difference between the beginnings of the two bands will then be 118−71 or 47 kilo cals., which is roughly the excitation energy of oxygen (which, as we have seen, is equal to 45 kilo cals.). This suggests that the two bands, say of KNO_2, may be attributed to the following photo-chemical reactions:

$$KNO_2 \rightarrow KNO + O\ (^3P) - 71 \text{ kilo cals. } (400\ m\mu).$$
$$KNO_2 \rightarrow KNO + O\ (^1D_2) - 118 \text{ kilo cals. } (240\ m\mu).$$

Excepting that the two relations are inter-consistent as is evidenced by the correct value for $O\ (^1D_2) - O\ (^3P)$ obtained from them, we are not in a position to check the validity of either of the relations separately, since we have no thermo-chemical data for the heat of formation of KNO. However, assuming that our relations are correct, we may proceed conversely and calculate the heat of formation of KNO from the elements under standard

conditions. We thus obtain the value 72 kilo cals. Combining this with the known heat of formation of $K_2N_2O_2$, we get the relation

$$\tfrac{1}{2}\ K_2N_2O_2 \rightarrow KNO - 27{\cdot}3 \text{ kilo cals.}$$

which *a priori* is not improbable.

Summary.

The two well-known absorption bands of inorganic nitrates whose long wave-length limits are at 350 $m\mu$ and 230 $m\mu$ respectively, are attributed to photo-dissociation of the nitrate into the nitrite and an atom of oxygen in the normal state (^3P) and in the excited state ($^1D_2$) respectively. From the above wave-length limits the heat of dissociation of the oxygen molecule into two normal atoms comes out as 114 kilo cals./gm. mol., and the energy of excitation of the oxygen atom from its normal level (^3P) to its ($^1D_2$) level comes out as 43 kilo cals./gm. mol. These are in agreement with the values deduced from spectroscopic data.

The observed strong dichroism of both these absorption bands, which are much more intense when the electric vector of the incident light wave lies in the plane of the NO_3 group than when it is along the normal to the NO_3 plane, is interpreted as due to a corresponding difference in the quantum efficiency of the photo-dissociations for the two directions of polarisation of the exciting light.

The two absorption bands of the nitrites receive a similar explanation as due to the dissociation from the nitrite of one oxygen atom, in the normal state and in the excited state respectively.

Orientations of Impurity Molecules Included in Crystals.

By

K. S. Krishnan and **P. K. Seshan**. Indian Association for the Cultivation of Science, Calcutta.

(With one figure.)

In a recent publication[1]) Winterstein and Schön have shown that the well-known absorption bands at about 478, 448 and 420 $m\mu$ observed with ordinarily pure specimens of chrysene and anthracene, and their intense fluorescence in the visible region, are due to traces of impurities of naphthacene,  . According to these authors, quantities of the order of 10^{-4}% or even less, are quite sufficient to explain the observed intensities of absorption and fluorescence. If the inclusion of this impurity in the crystal is due to "syncrystallisation" in the manner suggested by Gaubert[2]), the molecules of naphthacene may be expected to have some regular orientation with reference to the crystal lattice of the main substance. Now it is known[3]) that the absorption bands of a polynuclear molecule show an exceptionally strong polarisation, appearing much stronger when the light vibrations (electric vector) are in the plane of the benzene rings in the molecule than when they are along the normal to their plane. Hence, from a study of the polarisation of the above naphthacene bands appearing in the absorption spectra of single crystals of ordinary chrysene or anthracene, it would be possible to locate the orientations of the naphthacene molecules included in these crystals.

Let us first consider chrysene,  (1,2-benzophenanthrene). It crystallises in the monoclinic system in the form of thin plates parallel to {001}. One such plate was crystallised from a specimen that was known, from its absorption spectrum, to contain traces of naphthacene. Using incident plane polarised light, the absorption spectra of the crystal plate for light vibrations (i. e., the electric vector of the light wave) along its a-axis and for vibrations along its b-axis, were studied separately. In Fig. 1 are reproduced microphoto-

1) Naturwiss. **22** (1934) 237.

2) Bull. Soc. franç. Minéral. **28** (1905) 286; see also Buckley, H. E., Z. Kristallogr. **85** (1933) 58 and 88 (1934) 248.

3) Krishnan, K. S. and Seshan, P. K., Current Science **3** (1934) 26.

metric records of the absorption spectra for these two directions of vibration; the lower curve corresponsd to vibrations along the a-axis and the upper to those along b. It will be seen that all the three bands are strongly polarised, the b-vibrations being absorbed much more than the a-vibrations. This shows that the naphthacene molecules are so orientated as to have their planes nearly perpendicular to the {001} plane of chrysene and to its a-axis.

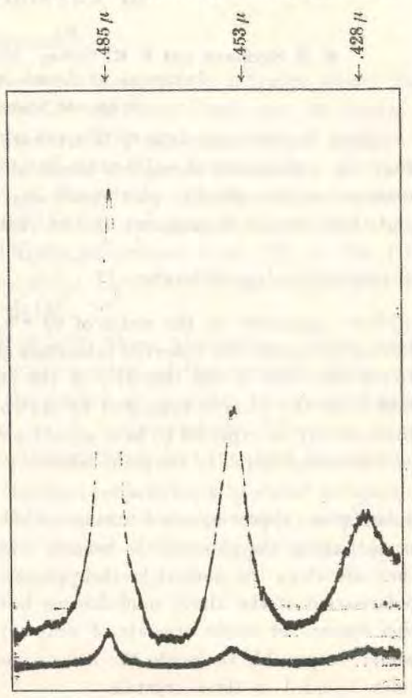

Fig. 1.

Analyses of the structure of chrysene by X-ray methods by Iball[1]) and by the magnetic method by Banerjee and one of us, show that the chrysene molecules in the crystal are so orientated as to have their lengths in the {010} plane, making about 103° with the a-axis and 13° with c; their molecular planes are inclined at plus or minus 28° to the b-axis. We may, therefore, conclude that the naphthacene molecules included as impurity in chrysene crystal, take up orientations nearly parallel to those of the chrysene molecules.

Similar observations with single crystals of anthracene containing traces of naphthacene, point to the same parallelism in orientation of the molecules of the two substances.

Fluorene, 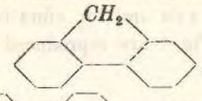 , is usually present as impurity in diphenyl,  . Here again it is found by the same method that the diphenyl molecules induce the fluorene molecules to take up orientations parallel to themselves.

1) Proc. Roy. Soc. London (A) **146** (1934) 140.

Observations on fluorescence also lead to the same conclusion regarding the orientation of impurity molecules. Naphthacene has four fluorescence bands in the visible region, with their centres at 559, 521, 488 and 458 mμ respectively, all of which could be detected with the traces of the substance included in chrysene crystal as impurity. The 436 mμ group of lines from the mercury arc, polarised by passage through a nicol, was allowed to be incident normally on the {001} plane of the crystal, and the fluorescent radiations in the forward direction were studied. It is found that all the fluorescence bands are more intense when the electric vector of the exciting light wave lies along the b-axis, than when it is along the a-axis. This result points clearly to a regularity in the orientations of the naphthacene molecules. It further shows that the intensity of fluorescence in the forward direction is greater when the exciting light vector lies in the plane of the naphthacene molecule, than when it is along the normal to the plane; or in other words the vibration that is absorbed more by the molecule, is found to excite fluorescence more strongly. The result is understandable, if the absorbed light energy is utilised in exciting the molecule, and then reappears as the energy of the fluorescent radiations. In this connection the experimental fact that the long wave-length limits of two of the absorption bands coincide respectively with the short wave-length limits of two fluorescence bands, is significant.

In any quantitative study of fluorescence phenomena in crystals which absorb light strongly, we have naturally to use very thin flakes to minimise absorption, and even with the thinnest flakes that can be used in practice the absorption is not always negligible and has to be allowed for. But using inclusions of orientated molecules in suitable crystalline media we can make their concentration as small as may be desired, and thus we have here a very convenient and elegant method for a quantitative study of fluorescence phenomena, and in particular of the dependence of the intensity and polarisation of fluorescence on the direction of the electric vector of the exciting light with reference to the principal axes of the molecule[1]).

1) A detailed report of the fluorescence phenomena observed with orientated molecules of naphthacene studied by this method, will be published in the Indian Journal of Physics.

210, Bowbazar Street, Calcutta, India, September 6th, 1934.

Received, September 23rd, 1934.

IX—Investigations on Magne-Crystallic Action
III—Further Studies on Organic Crystals

By Professor K. S. KRISHNAN *and* S. BANERJEE

(Communicated by Sir VENKATA RAMAN, F.R.S.—Received October 3, 1934)

CONTENTS

I—INTRODUCTION

In Part I* of this paper a convenient method of measuring the principal magnetic susceptibilities of single crystals was described, and several organic crystals, among others, were studied by this method. The results were discussed particularly in relation to the structure of the molecules and their orientations in the crystal lattice, and it was shown how a correlation of the principal magnetic susceptibilities of the crystal with those for the individual molecules (obtained from measurements on magnetic double-refraction in the liquid state, or from considerations of molecular structure) gives us useful information regarding the orientations of the molecules in the crystal lattice. Indeed, in favourable cases the molecular orientations may thus be determined much more easily, and some of the parameters defining the orientations also more accurately, than by X-ray methods of analysis. Conversely, where the molecular orientations in the crystal lattice are already known from X-ray studies, a knowledge of the principal magnetic susceptibilities of the crystal enables us to

* 'Phil. Trans.,' A, vol. 231, p. 235 (1933).

obtain the magnetic constants of the individual molecules, which are of interest. For example, it is thus found that as one proceeds from benzene to naphthalene and from naphthalene to anthracene, the numerical increase in susceptibility that occurs, is directed predominantly along the normal to the plane of the benzene rings.

In this paper is described another simple method of measuring magnetic anisotropies of crystals, which is as convenient as the oscillational method described in Part I, and which can, moreover, be adopted for measurements with even such small crystals as weigh a fraction of a milligram. Using this method it has been possible to extend the magnetic measurements to a number of organic crystals, specially chosen for their structural or other interest. Many of the crystals extensively studied by X-ray methods by Dr. ROBERTSON, Mrs. LONSDALE, Miss PICKETT, and others, have naturally been included in our list. These magnetic studies are described in Section II of the present Part. In Sections III to VII the results of the magnetic measurements are discussed, especially with a view to co-ordinating them with the X-ray data on the structure of the crystals and with their optical and other properties. The principal magnetic susceptibilities of individual molecules are calculated for a number of substances, and are discussed in relation to chemical and other evidence regarding molecular structure. Of these five Sections, Section III deals with benzene derivatives, Section IV with diphenyl and triphenyl compounds, Section V with naphthalene derivatives and Section VI with polynuclear compounds. Section VII contains some remarks on the optical properties of these crystals.

II—EXPERIMENTAL

Susceptibility measurements on crystals involve, in general,

(1) the determination of the directions of the principal magnetic axes ;
(2) the measurement of the differences between the principal susceptibilities, viz., $\chi_1 - \chi_2$ and $\chi_1 - \chi_3$;
(3) the measurement of the absolute susceptibility along any one convenient direction in the crystal.

1—*The Magnetic Axes*

The determination of the axial directions usually presents no difficulty. In the trigonal, tetragonal, orthorhombic, and hexagonal systems the magnetic axes are naturally defined by considerations of crystal symmetry. For the monoclinic crystal the "*b*" axis must be one of the magnetic axes, and the other two must lie in the (010) plane. By suspending the crystal with its "*b*" axis vertical, in a uniform magnetic field, and determining the orientation of any vertical natural face (*h*0*l*) of the crystal, in the field, the directions of the two magnetic axes in the (010) plane are known. One method of determining the orientation of the face in the field has been described in Part I ; a second method was also adopted in the present measurements and will be described in sub-section 4.

With triclinic crystals the determination of the axial directions is naturally more complicated. Hexamethyl benzene was the only triclinic crystal studied here, and the method of measurement adopted for this crystal will be clear from the data given in Table I below.

2—*Measurement of Magnetic Anisotropy*

Knowing the directions of the three principal magnetic axes, if we measure the magnetic anisotropy $\Delta\chi$ for any two planes in the crystal, then $\chi_1 - \chi_2$ and $\chi_1 - \chi_3$ are known. One method of measuring $\Delta\chi$ that is adopted in the present paper, is the same as was described in Part I. The crystal is suspended at the end of a calibrated quartz fibre, in a uniform magnetic field. The upper end of the fibre is fixed to the centre of a torsion-head which can be rotated about the axis of suspension of the fibre by any known angle. When the field is put on, the crystal will naturally tend to turn round so as to bring the direction of maximum susceptibility in the horizontal plane, along the field. The torsion-head is suitably rotated so that the torsion is nothing in the equilibrium orientation of the crystal. The crystal is now made to execute torsional oscillations of small amplitude about this orientation. Let T be the period of these oscillations and let T′ be the period of similar oscillations outside the field. Then the difference between the maximum and the minimum gram molecular susceptibilities of the crystal in the plane of oscillation is given by the relation

$$\Delta\chi = A\frac{T'^2 - T^2}{T^2}, \quad \ldots\ldots\ldots\ldots \quad (1)$$

where

$$A = \frac{Mc}{mH^2}; \quad \ldots\ldots\ldots\ldots \quad (2)$$

c is the torsional constant of the fibre, H is the field, m is the mass of the crystal, and M is the gram molecular weight. Thus $\Delta\chi$ is readily determined.

3—*Second Method for Measuring Magnetic Anisotropy*

In the present paper a second method has also been used for the measurement of $\Delta\chi$, which is as convenient as the oscillational method, and for crystals of small mass, say a fraction of a milligram,* also more accurate. In the above experimental arrangement, the crystal is allowed to set as before in the equilibrium orientation in the magnetic field under zero torsion of the fibre. If the torsion-head is slowly rotated from this position by an angle α, the crystal will also rotate in the same direction by a smaller angle ϕ. We shall suppose that the torsion of the fibre is chosen to be so small that ϕ will be much smaller than α. The relation between α and ϕ is evidently

$$c(\alpha - \phi) = \tfrac{1}{2}\frac{m}{M} H^2 \Delta\chi \sin 2\phi. \quad \ldots\ldots\ldots\ldots \quad (3)$$

* For a number of substances, *e.g.*, phenanthrene, quaterphenyl, crystals of only this mass could be obtained.

If the rotation of the torsion-head is continued very slowly, there will come a stage when ϕ just reaches the value $\pi/4$. Let α_c be the corresponding value of α. For this position, plainly

$$c\left(\alpha_c - \frac{\pi}{4}\right) = \tfrac{1}{2}\frac{m}{M} H^2 \Delta\chi, \quad \ldots\ldots\ldots\ldots \quad (4)$$

i.e.,

$$\Delta\chi = A\left(2\alpha_c - \frac{\pi}{2}\right), \quad \ldots\ldots\ldots\ldots \quad (5)$$

where A is the same constant as before (see (2)). Hence a knowledge of α_c enables us to calculate $\Delta\chi$.

The determination of α_c is simple and is based on the following property. If from the above position the torsion-head is rotated further by a small angle so as to make α just exceed α_c, ϕ would exceed $\pi/4$, and the restoring couple due to the field, which is proportional to sin 2ϕ, would tend to diminish, and the torsional couple of the fibre would be more than sufficient to compensate the restoring couple due to the field. Hence, the crystal would turn round over a large angle, indeed over $3\pi/4$ if the torsion of the fibre is sufficiently small. Thus, in practice, α_c would be the critical angle of rotation of the torsion-head, from its original position, which is just sufficient to start the crystal to turn round, and can, therefore, be measured accurately.

If after the above rotation the crystal is allowed to come to rest and the torsion-head is further rotated in the same direction as before, when α reaches a value $\alpha_c + \pi$, the crystal rotation ϕ would reach a value $5\pi/4$, which would again correspond to a maximum value of the couple due to the field, and the slightest further rotation of the torsion-head would turn round the crystal in the same manner as before. Again, when α just exceeds $\alpha_c + 2\pi$, there will be still another turning round and so on. From any one of these critical values of α, the value of α_c can be readily calculated, and hence $\Delta\chi$.

4—*Determination of the Orientation of the Crystal in the Field*

With the above experimental arrangement, the *orientation* of the crystal in the magnetic field is also easily determined. Let us consider again the monoclinic crystal suspended with its "b" axis vertical, and suppose that one of the $(h0l)$ faces is well developed. It is required to determine the inclination θ of this face to the equatorial plane of the field. The axis of the observation tele-microscope is adjusted to be horizontal and normal to the direction of the field. Starting now with the equilibrium position of the crystal in the field under zero torsion of the fibre, the torsion-head is gradually rotated in the proper direction so as to bring the $(h0l)$ face to the equatorial plane (as tested by observation through the tele-microscope). Let α_1 be the necessary angle of rotation of the torsion-head. Also let α_c be the critical angle of its rotation, as defined in the previous section. Then θ is given

by the simple relation

$$\sin 2\theta = \frac{\alpha_1 - \theta}{\alpha_c - \frac{\pi}{4}}, \quad \ldots\ldots\ldots\ldots\ldots\ldots \quad (6)$$

and hence θ is known.

5—*Absolute Susceptibilities*

Finally, the absolute susceptibility was measured for a suitable direction in the crystal by the modified form of RABI's null-method described in Parts I and II of this paper. Where, as is usual, the volume susceptibility is numerically less than that of water, a standard solution of $NiCl_2$, suitably diluted, was used for magnetically balancing the crystal.* Where the volume susceptibility was numerically higher than that of water, solutions of KCl or KI were used.

6—*Results*

We explain here briefly the notation adopted in the paper. When the crystal has an axis of symmetry, the gram molecular susceptibility along the axis and that along perpendicular directions are denoted by $\chi_{\parallel}$ and $\chi_{\perp}$ respectively. For the orthorhombic crystal, χ_a, χ_b and χ_c denote the gram molecular susceptibilities along the "*a*," "*b*" and "*c*" axes respectively. For the monoclinic crystal, the gram molecular susceptibility along the "*b*" axis is denoted by χ_3, while the greater of the two principal susceptibilities in the (010) plane is denoted by χ_1 and the smaller by χ_2. The χ_1 axis is inclined at an angle ψ to the "*c*" axis and at $\beta - \psi$ to the "*a*" axis, β being the *obtuse* angle between the "*c*" and "*a*" axes. For many of the monoclinic crystals the (001) faces were well developed, and their inclination to the χ_2 axis was directly measured. This angle is denoted by θ, its relation to ψ being expressed by the equation $\theta + \psi + \frac{1}{2}\pi = \beta$ (obtuse).

The results of the measurements on magnetic anisotropy are given in Table I. In the third column of the table are given the crystallographic data that have been adopted as basis for the description of the various crystal faces. Where X-ray data are available for the dimensions of the unit cell, these data have naturally been adopted in preference to the goniometric data. For those crystals, however, for which such X-ray measurements are not available, the axes and axial ratios adopted for the crystal are those described in GROTH's 'Chemische Kristallographie.' The other columns of the table need no explanation. As has already been mentioned, the determination of $\Delta\chi$ for any *two* planes in the crystal is, in general, sufficient to give $\chi_1 - \chi_2$ and $\chi_1 - \chi_3$. However, as a check on the accuracy of the measurements, an extra measurement was usually made, using a third plane. The calculated value for this plane is included in the table for comparison with the directly measured value.

In Table II are given the results of the measurements on the absolute susceptibilities.

* We wish to correct here an error which appears on p. 245 of Part I. The susceptibility of $MnCl_4$ at 28°·5 C should be $114{\cdot}9 \times 10^{-6}$ per gram, and not $117{\cdot}9 \times 10^{-6}$ as is given there. The other values remain unaffected.

TABLE I

Serial number	Crystal	Crystallographic data	Mode of suspension	Orientation in the field	$\lvert\Delta\chi\rvert$	Magnetic anisotropy
1	*p*-Benzoquinone 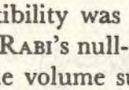	Monoclinic C_{2h}^6 . . . Z = 2 $a = 7{\cdot}08$ A. $b = 6{\cdot}79$ $c = 5{\cdot}80$ $\beta = 101°\,0'$	"*b*" axis vertical	$\theta = -20°{\cdot}2$	40·0	$\chi_1 - \chi_2 = 40{\cdot}0$
			"	"*b*" axis along field .	6·0	$\chi_1 - \chi_3 = -\ 1{\cdot}2$
						$\psi = +31°{\cdot}2$
			(001) plane horizontal	"*b*" " "	37·1	Cal. $\Delta\chi = 36{\cdot}4$
2	Catechol 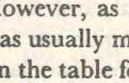	Monoclinic C_{2h}^5 . . . Z = 8 $a = 17{\cdot}46$ A. $b = 10{\cdot}74$ $c = 5{\cdot}48$ $\beta = 94°\,15'$	"*b*" axis vertical	$\psi = +2°{\cdot}2$	30·5	$\chi_1 - \chi_2 = 30{\cdot}5$
			"*c*" " "	"*b*" axis along field .	2·7	$\chi_1 - \chi_3 = 27{\cdot}8$
						$\psi = +2°{\cdot}2$
			(100) plane horizontal	"*c*" " "	27·8	Cal. $\Delta\chi = 27{\cdot}8$
3	Hydroquinol	Trigonal C_{3i}^1 . . . . Z = 18 $a = 22{\cdot}06$ A. $c = 5{\cdot}62$	Trigonal axis horizontal	Trigonal axis along field	1·4	$\chi_{\parallel} - \chi_{\perp} = 1{\cdot}4$

TABLE I—(continued)

Serial number	Crystal	Crystallographic data	Mode of suspension	Orientation in the field	$\lvert\Delta\chi\rvert$	Magnetic anisotropy
4	Hexamethyl benzene . 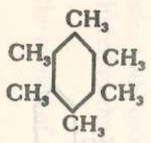	Triclinic C_i^1 . . . . Z = 1 .	(001) plane horizontal	"a" axis at 26½° to field and "b" axis at 93° to field	1·6	$\chi_1 - \chi_3 =$ 1·6 $\chi_1 - \chi_2 =$ 62·7
		a = 9·010 A. b = 8·926 c = 5·344 α = 44° 27′ β = 116° 43′ γ = 119° 34′	"a" axis vertical . .	(001) plane along field	61·4	χ_1 and χ_2 axes lie in the (001) plane, χ_1 making 26½° with "a" axis and 93° with "b" axis
			"b" „ „ .	(001) „ „	62·3	Cal. $\Delta\chi$ = 62·7
			(100) plane horizontal	"b" axis practically along field	59·6	„ „ = 59·5
5	Durene (1, 2, 4, 5-Tetramethyl benzene) 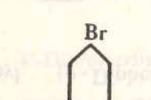	Monoclinic C_{2h}^5 . . . Z = 2	"b" axis vertical . .	$\theta = +3°{\cdot}1$	39·7	$\chi_1 - \chi_3 = 39{\cdot}7$
			(001) plane horizontal	"a" axis normal to field	7·6	$\chi_1 - \chi_2 = 32{\cdot}0$ $\psi = +20°{\cdot}2$
		a = 11·57 A. b = 5·77 c = 7·03 β = 113°·3	"a" axis vertical . .	"b" „ „	31·7	Cal. $\Delta\chi$ = 31·9
6	Hexachlorobenzene . 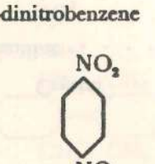	Monoclinic C_{2h}^5 . . . Z = 2	"b" axis vertical . .	$\theta = -25°{\cdot}7$	6·8	$\chi_1 - \chi_3 =$ 6·8
			(100) plane horizontal	"b" axis normal to field	37·4	$\chi_1 - \chi_2 = 41{\cdot}7$ $\psi = +52°{\cdot}6$
		a = 8·07 A. b = 3·84 c = 16·61 β = 116° 52′	"c" axis vertical . .	"b" „ „	39·4	Cal. $\Delta\chi$ = 39·2

TABLE I—(continued)

Serial number	Crystal	Crystallographic data	Mode of suspension	Orientation in the field	$\lvert\Delta\chi\rvert$	Magnetic anisotropy
7	1, 2, 4, 5-Tetrachlorobenzene 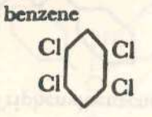	Monoclinic prism . . $a : b : c = 0{\cdot}9041 : 1 : 0{\cdot}3650$ β = 99° 22½′	"b" axis vertical . .	$\psi = -68°{\cdot}9$ . . .	41·7	$\chi_1 - \chi_3 =$ 41·7
			"c" „ „ . .	"b" axis along field .	5·6	$\chi_1 - \chi_2 =$ − 0·2 $\psi = -68°{\cdot}9$
			(100) plane horizontal	"b" „ „ .	36·1	Cal. $\Delta\chi$ = 36·5
8	p-Dichlorobenzene . . 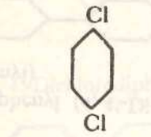	Monoclinic C_{2h}^5 . . . Z = 2	"b" axis vertical . .	$\psi = +86°{\cdot}9$ . . .	36·2	$\chi_1 - \chi_3 =$ 36·2
			"c" „ „ . .	"b" axis normal to field	9·8	$\chi_1 - \chi_2 =$ 9·9 $\psi = +86°{\cdot}9$
		a = 14·83 A. b = 5·88 c = 4·10 β = 112° 30′	(100) plane horizontal	"c" „ „	26·3	Cal. $\Delta\chi$ = 26·2
9	p-Dibromobenzene . .	Monoclinic C_{2h}^5 . . . Z = 2	"b" axis vertical . .	ψ + 87°·0	32·2	$\chi_1 - \chi_3 =$ 32·2
			"c" „ „ . .	"b" axis normal to field	9·0	$\chi_1 - \chi_2 =$ 9·1 $\psi = +87°{\cdot}0$
		a = 15·46 A. b = 5·80 c = 4·11 β = 112° 38′	(100) plane horizontal	"c" „ „	23·3	Cal. $\Delta\chi$ = 23·0
10	p-dinitrobenzene . .	Monoclinic prism . . $a : b : c = 2{\cdot}038 : 1 : 1{\cdot}043$ β = 92°·3	"b" axis vertical . .	$\psi = -36°{\cdot}6$ . . .	53·6	$\chi_1 - \chi_3 =$ 53·6
			"c" „ „ . .	"b" axis normal to field	6·5	$\chi_1 - \chi_2 =$ 41·0 $\psi = -36°{\cdot}6$
			(100) plane horizontal	"b" „ „	21·5	Cal. $\Delta\chi$ = 21·9

TABLE I—(continued)

Serial number	Crystal	Crystallographic data	Mode of suspension	Orientation in the field	$\lvert\Delta\chi\rvert$	Magnetic anisotropy
11	*m*-Nitroaniline 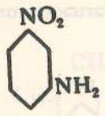	Rhombic C_{2v}^5 . . . . Z = 4	"*c*" axis vertical . .	"*a*" axis along field . 2·0		$\chi_a - \chi_b =$ 2·0
			"*a*" " " . .	"*b*" " " . 10·5		$\chi_a - \chi_c =$ 12·5
		a = 19·23 A.				
		b = 6·48	"*b*" " " . .	"*a*" " " . 12·3		Cal. $\Delta\chi =$ 12·5
		c = 5·06				
12	Terphenyl (*p*-Diphenylbenzene) 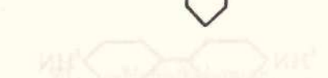	Monoclinic C_{2h}^5 . . . Z = 2	"*b*" axis vertical . .	$\theta = +16°{\cdot}2$ 117		$\chi_1 - \chi_3 =$ 117
			"*a*" " " . .	"*b*" axis normal to field 39·5		$\chi_1 - \chi_2 =$ 48·6
		a = 8·08 A.				$\psi = -$ 14°·3
		b = 5·60				
		c = 13·59	(001) plane horizontal	"*a*" " " 59·8		Cal. $\Delta\chi =$ 59·3
		β = 91° 55′				
13	Quaterphenyl (4, 4′-Diphenyldiphenyl)	Monoclinic C_{2h}^5 . . . Z = 2	"*b*" axis vertical . .	$\lvert\theta\rvert = 17°{\cdot}1$ 168		$\chi_1 - \chi_3 =$ 168
			"*a*" " " . .	"*b*" axis normal to field 55		$\chi_1 - \chi_2 =$ 70
		a = 8·14 A.				$\lvert\theta\rvert =$ 17°·1
		b = 5·64				
		c = 18·4	(001) plane horizontal	"*a*" " " 82		Cal. $\Delta\chi =$ 83
		β = 97°				
14	1, 3, 5-Triphenylbenzene . . . 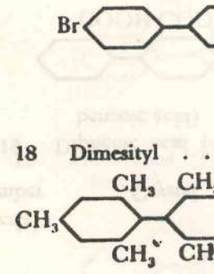	Rhombic C_{2v}^9 . . . . Z = 4	"*a*" axis vertical . .	"*c*" axis along field . 14·9		$\chi_a - \chi_b =$ 14·9
			"*c*" " " . .	"*b*" " " . 158		$\chi_a - \chi_c =$ 173
		a = 7·55 A.				
		b = 19·76	"*b*" " " .	"*c*" " " . 174		Cal. $\Delta\chi =$ 173
		c = 11·22				

TABLE I—(continued)

Serial number	Crystal	Crystallographic data	Mode of suspension	Orientation in the field	$\lvert\Delta\chi\rvert$	Magnetic anisotropy
15	Triphenyl carbinol . . 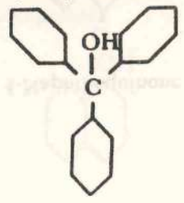	Trigonal . . . . . Z = 3	Trigonal axis horizontal	Trigonal axis along field	5·3	$\chi_{\parallel} - \chi_{\perp} =$ 5·3
		a = 11·25 A.				
		α = 107°				
16	4, 4′-Dichlorodiphenyl . 	Monoclinic prism . . $a:b:c$ = 1·1569 : 1 : 0·7078	"*b*" axis vertical . .	$\psi = -28°{\cdot}5$ . . . 35·1		$\chi_1 - \chi_3 =$ 35·1
			(100) plane horizontal	"*b*" axis along field . 33·4		$\chi_1 - \chi_2 =$ − 25·4
		β = 96° 48′	"*c*" axis vertical . .	"*b*" " " . 52·4		$\psi = -28°{\cdot}5$
						Cal. $\Delta\chi =$ 52·5
17	4, 4′-Dibromodiphenyl 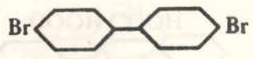	Monoclinic prism . . $a:b:c$ = 1·1181 : 1 : 0·6963	"*b*" axis vertical . .	$\psi = -27°{\cdot}6$ . . . 35·9		$\chi_1 - \chi_3 =$ 35·9
			(100) plane horizontal	"*b*" axis along field . 29·7		$\chi_1 - \chi_2 =$ − 22·0
		β = 94° 30′	"*c*" axis vertical . .	"*b*" " " . 49·7		$\psi = -27°{\cdot}6$
						Cal. $\Delta\chi =$ 50·2
18	Dimesityl	Monoclinic C_{2h}^5 . . . Z = 4	"*b*" axis vertical . .	$\theta = +61°{\cdot}6$ . . . . 27·5		$\chi_1 - \chi_3 =$ 27·5
			(001) plane horizontal	"*b*" axis along field . 2·4		$\chi_1 - \chi_2 =$ 3·8
		a = 8·19 A.				$\psi = -55°{\cdot}8$
		b = 8·54				
		c = 22·1				
		β = 95° 46′	(100) " "	"*b*" " " . 14·9		Cal. $\Delta\chi =$ 15·0

TABLE I—(continued)

Serial number	Crystal	Crystallographic data	Mode of suspension	Orientation in the field	$\lvert\Delta\chi\rvert$	Magnetic anisotropy
19	Diphenic acid (*o*,*o*′-Bibenzoic acid) 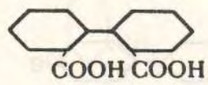	Monoclinic C_{2h}^5 . . . Z = 8 a = 13·70 A. b = 11·95 c = 14·08 β = 91° 40′	"b" axis vertical . . "c" " " . . (100) plane horizontal	$\psi = -3°{\cdot}4$ . . . . "b" axis normal to field "b" " "	17·8 0·3 17·9	$\chi_1 - \chi_2 =$ 17·8 $\chi_1 - \chi_3 =$ 18·0 $\psi = -$ 3°·4 Cal. $\Delta\chi =$ 17·9
20	*o*-Tolidine (4, 4′-Diamido- 3, 3′-dimethyl diphenyl) 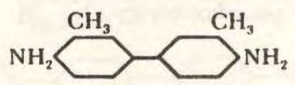	Orth. bisphen. Q^4 (?) . Z = 4 a = 6·47 A. b = 7·48 c = 23·60	"a" axis vertical . . "b" " " . . "c" " " . .	"c" axis along field . "a" " " . "a" " " .	79·6 3·3 82·8	$\chi_a - \chi_b =$ 82·9 $\chi_a - \chi_c =$ 3·3 Cal. $\Delta\chi =$ 82·9
21	1, 4-Naphthoquinone . 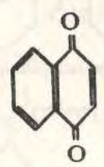	Monoclinic C_{2h}^5 . . Z = 4 a = 13·50 A. b = 7·74 c = 8·25 β = 121° 10′	"b" axis vertical . . "c" " " . . (100) plane horizontal	$\psi = -62°{\cdot}5$ . . . "b" axis along field . "b" " "	87·9 1·8 51·5	$\chi_1 - \chi_2 =$ 87·9 $\chi_1 - \chi_3 =$ 16·9 $\psi = -62°{\cdot}5$ Cal. $\Delta\chi =$ 52·3

TABLE I—(continued)

Serial number	Crystal	Crystallographic data	Mode of suspension	Orientation in the field	$\lvert\Delta\chi\rvert$	Magnetic anisotropy
22	α-Naphthol . . . . . 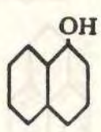	Monoclinic prism . Z = 4 a = 13·1 A. b = 4·9 c = 13·4 β = 117° 10′	"b" axis vertical . . (001) plane horizontal "a" axis vertical . .	$\theta = -1°{\cdot}5$ . . . . "b" axis normal to field "b" " "	51·9 10·0 61·7	$\chi_1 - \chi_2 =$ 51·9 $\chi_1 - \chi_3 =$ 61·9 $\psi = +28°{\cdot}7$ Cal. $\Delta\chi =$ 61·9
23	α-Naphthylamine . . 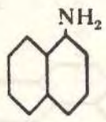	Rhombic bipyr. . . $a : b : c = 1{\cdot}6340 : 1 : 0{\cdot}8156$	"c" axis vertical . . "a" " " . . "b" " " . .	"b" axis along field . "b" " " . "a" " " .	3·4 20·1 16·6	$\chi_a - \chi_b =$ 16·7 $\chi_b - \chi_c =$ 20·1 Cal. $\Delta\chi =$ 16·7
24	Fluorene . . . . . 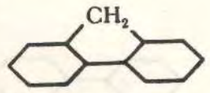	Monoclinic C_{2h}^5 . . . Z = 4 a = 8·48 A. b = 5·73 c = 19·24 β = 101° 30′	"b" axis vertical . . "a" " " . . (001) plane horizontal	$\theta = +0°{\cdot}6$ . . . . "b" axis normal to field "a" " "	84·0 37·0 47·3	$\chi_1 - \chi_2 =$ 84·0 $\chi_1 - \chi_3 =$ 37·0 $\psi = +10°{\cdot}9$ Cal. $\Delta\chi =$ 47·0
25	Fluorenone (Fluorene-ketone) 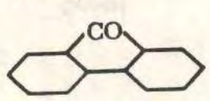	Rhombic bipyr. . . $a : b : c = 0{\cdot}5808 : 1 : 0{\cdot}7788$	"a" axis vertical . . "b" " " . . "c" " " . .	"c" axis along field . "a" " " . "a" " " .	31·7 25·2 56·5	$\chi_a - \chi_b =$ 56·9 $\chi_a - \chi_c =$ 25·2 Cal. $\Delta\chi =$ 56·9

TABLE I—(continued)

Serial number	Crystal	Crystallographic data	Mode of suspension	Orientation in the field	|Δχ|	Magnetic anisotropy
26	Phenanthrene	Monoclinic C_{2h}^5 . . .	" b " axis vertical . .	$\theta = +11°\cdot4$ . . .	126	$\chi_1 - \chi_3 =$ 126
	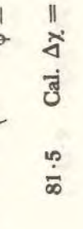	$Z = 4$	" a " " . .	" b " axis normal to field	35·0	$\chi_1 - \chi_3 =$ 39·9
		$a = 8{\cdot}60$ A.				$\psi = -\ 3°\cdot1$
		$b = 6{\cdot}11$	(001) plane horizontal	" a " " "	81·5	Cal. $\Delta\chi =$ 81·2
		$c = 19{\cdot}24$				
		$\beta = 98°\ 15'$				
27	Chrysene (1, 2-Benzo-phenanthrene)	Monoclinic C_{2h}^5 . . .	" b " axis vertical . .	$\theta = +13°\cdot1$	170	$\chi_1 - \chi_3 =$ 170
	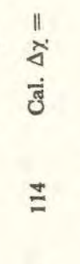	$Z = 4$	" a " " . .	" b " axis normal to field	39·4	$\chi_1 - \chi_3 =$ 48·1
		$a = 8{\cdot}34$ A.				$\psi = +12°\cdot7$
		$b = 6{\cdot}18$	(001) plane horizontal	" a " " "	114	Cal. $\Delta\chi =$ 113
		$c = 25{\cdot}0$				
		$\beta = 115°\cdot8$				
28	Pyrene	Monoclinic prism . .	" b " axis vertical . .	$\theta = -14°\cdot1$	97·5	$\chi_1 - \chi_3 =$ 97·5
	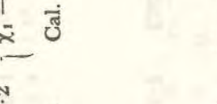	$a : b : c = 1{\cdot}468 :$	(001) plane horizontal	" b " axis normal to field	33·2	$\chi_1 - \chi_3 =$ 125
		$1 : 1{\cdot}781$				$\psi = +25°\cdot0$
		$\beta = 100°\ 53'$	" a " axis vertical . .	" b " " "	118	Cal. $\Delta\chi =$ 119
29	Fluoranthene	Monoclinic prism . .	" b " axis vertical . .	$\theta = -2°\cdot4$	109	$\chi_1 - \chi_3 =$ 109
	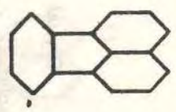	$a : b : c = 1{\cdot}495 :$	" a " " . .	" b " axis normal to field	39·8	$\chi_1 - \chi_3 =$ 40·0
		$1 : 1{\cdot}025$				$\psi = +\ 9°\cdot6$
		$\beta = 97°\ 10'$	(001) plane horizontal	" a " " "	69·9	Cal. $\Delta\chi =$ 69

TABLE II—ABSOLUTE SUSCEPTIBILITIES

Serial number	Crystal	Direction along which susceptibility was measured	Vol suscep-tibility	Density of the crystal	Corres-ponding gm mol suscep	Principal gm mol susceps	Mean suscep-tibility
1	*p*-Benzoquinone	Along χ_1 – axis .	− 0·330	1·324	−27·0	$\chi_1 = -\ 27{\cdot}1$	− 40·0
			− 0·327	1·298	−27·2	$\chi_2 = -\ 67{\cdot}1$	
						$\chi_3 = -\ 25{\cdot}9$	
						$\psi = +\ 31°\cdot2$	
2	Catechol . . .	Along χ_1 – axis .	− 0·604	1·370	− 48·5	$\chi_1 = -\ 48{\cdot}5$	− 67·9
						$\chi_2 = -\ 79{\cdot}0$	
						$\chi_3 = -\ 76{\cdot}3$	
						$\psi = +\ 2°\cdot2$	
3	Hydroquinol .	Along the normal to trigonal axis	− 0·77	1·32	− 64	$\chi_{\parallel} = -\ 63$	− 64·
						$\chi_{\perp} = -\ 64$	
4	Hexamethyl benzene	Along the normal to " b " axis in (001) plane	− 0·636	1·020	−101·1	$\chi_1 = -\ 101{\cdot}1$	−122·5
						$\chi_2 = -\ 102{\cdot}7$	
						$\chi_3 = -\ 163{\cdot}8$	
						For the directions of the axes see Table I	
5	Durene . . .	Along χ_1 – axis .	− 0·596	1·034	− 77·3	$\chi_1 = -\ 77{\cdot}3$	−101·2
						$\chi_2 = -\ 117{\cdot}0$	
						$\chi_3 = -\ 109{\cdot}3$	
						$\psi = +\ 20°\cdot2$	
6	Hexachloro-benzene	Along χ_1 – axis .	− 0·970	2·134	−129·4	$\chi_1 = -\ 129{\cdot}4$	−145·6
						$\chi_2 = -\ 136{\cdot}2$	
						$\chi_3 = -\ 171{\cdot}1$	
						$\psi = +\ 52°\cdot6$	
7	1, 2, 4, 6-Tetra-chlorobenzene	Along χ_1 – axis .	− 0·855	1·829	−100·9	$\chi_1 = -\ 100{\cdot}9$	−114·7
						$\chi_2 = -\ 142{\cdot}6$	
						$\chi_3 = -\ 100{\cdot}7$	
						$\psi = -\ 68°\cdot9$	
8	*p*-Dichloro-benzene	Along the normal to " c " axis in (010) plane	− 0·720	1·510	− 70·1	$\chi_1 = -\ 70{\cdot}0$	− 85·4
						$\chi_2 = -\ 106{\cdot}2$	
						$\chi_3 = -\ 79{\cdot}9$	
						$\psi = +\ 86°\cdot9$	
9	*p*-Dibromo-benzene	Along χ_1 – axis .	− 0·848	2·318	− 86·3	$\chi_1 = -\ 86{\cdot}3$	−100·1
						$\chi_2 = -\ 118{\cdot}5$	
						$\chi_3 = -\ 95{\cdot}4$	
						$\psi = +\ 87°\cdot0$	

TABLE II—(continued)

Serial number	Crystal	Direction along which susceptibility was measured	Vol susceptibility	Density of the crystal	Corresponding gm mol suscep	Principal gm mol susceps	Mean susceptibility
10	*p*-Dinitrobenzene	Along χ_1 — axis .	— 0·366	1·625	— 37·8	$\chi_1 = -37{\cdot}8$ $\chi_2 = -91{\cdot}4$ $\chi_3 = -78{\cdot}8$ $\psi = -36°{\cdot}6$	— 69·3
11	*m*-Nitroaniline	Along " *a* " axis .	— 0·662	1·415	—64·6	$\chi_a = -64{\cdot}6$ $\chi_b = -66{\cdot}6$ $\chi_c = -77{\cdot}1$	— 69·4
12	Terphenyl . .	Along χ_1 — axis .	— 0·516	1·226	— 96·8	$\chi_1 = -96{\cdot}8$ $\chi_2 = -214$ $\chi_3 = -145{\cdot}4$ $\psi = -14°{\cdot}3$	—152
13	1, 3, 5-Triphenyl benzene	Along " *b* " axis .	— 0·607 — 0·609	1·200 1·201	—154·9 —155·2	$\chi_a = -313$ $\chi_b = -155{\cdot}0$ $\chi_c = -140{\cdot}1$	—203
14	Triphenyl carbinol	Along trigonal axis	— 0·777 — 0·773	1·191 1·189	—169·7 —169·1	$\chi_{\parallel} = -169{\cdot}4$ $\chi_{\perp} = -174{\cdot}7$	—172·9
15.	4, 4′-Dichorodiphenyl	Along " *b* " axis .	— 0·663 — 0·667	1·417 1·420	—104·3 —104·7	$\chi_1 = -129{\cdot}9$ $\chi_2 = -165{\cdot}0$ $\chi_3 = -104{\cdot}5$ $\psi = -28°{\cdot}5$	—133·1
16	4, 4′-Dibromodiphenyl	Along " *b* " axis .	— 0·754 — 0·761	1·880 1·911	—125·1 —124·3	$\chi_1 = -146{\cdot}7$ $\chi_2 = -182{\cdot}6$ $\chi_3 = -124{\cdot}7$ $\psi = -27°{\cdot}6$	—151·3
17	Dimesityl . .	Along χ_1 — axis .	— 0·692	1·023	—161·2	$\chi_1 = -161{\cdot}2$ $\chi_2 = -188{\cdot}7$ $\chi_3 = -165{\cdot}0$ $\psi = -55°{\cdot}8$	—171·6
18	Diphenic acid .	Along χ_1 — axis .	— 0·698	1·406	—120·2	$\chi_1 = -120{\cdot}2$ $\chi_2 = -138{\cdot}0$ $\chi_3 = -138{\cdot}2$ $\psi = -3°{\cdot}4$	—132·1
19	*o*-Tolidine . .	Along " *a* " axis .	— 0·680	1·230	—117·3	$\chi_a = -117{\cdot}3$ $\chi_b = -200{\cdot}2$ $\chi_c = -120{\cdot}6$	—146·0
20	α-Naphthoquinone	Along " *b* " axis .	— 0·494 — 0·497	1·402 1·406	— 55·7 — 55·9	$\chi_1 = -38{\cdot}9$ $\chi_2 = -126{\cdot}8$ $\chi_3 = -55{\cdot}8$ $\psi = -62°{\cdot}5$	— 73·8

TABLE II—(continued)

Serial number	Crystal	Direction along which susceptibility was measured	Vol susceptibility	Density of the crystal	Corresponding gm mol suscep	Principal gm mol susceps	Mean susceptibility
21	α-Naphthol	Along χ_1 — axis .	— 0·538	1·282	— 60·5	$\chi_1 = -60{\cdot}5$ $\chi_2 = -112{\cdot}4$ $\chi_3 = -122{\cdot}4$ $\psi = +28°{\cdot}7$	— 98·4
22	α-Naphthylamine	Along " *b* " axis .	— 0·741	1·185	— 89·5	$\chi_a = -92{\cdot}9$ $\chi_b = -89{\cdot}5$ $\chi_c = -109{\cdot}6$	— 97·3
23	Fluorene . . .	Along χ_1 — axis .	— 0·516	1·181	— 72·6	$\chi_1 = -72{\cdot}6$ $\chi_2 = -156{\cdot}6$ $\chi_3 = -109{\cdot}6$ $\psi = +10°{\cdot}9$	—112·9
24	Fluorenone .	Along " *a* " axis .	— 0·502	1·254	— 72·1	$\chi_a = -72{\cdot}1$ $\chi_b = -129{\cdot}0$ $\chi_c = -97{\cdot}3$	— 99·5
25	Phenanthrene .	Along χ_1 — axis .	— 0·49	1·172	— 74	$\chi_1 = -74$ $\chi_2 = -200$ $\chi_3 = -114$ $\psi = -3°{\cdot}1$	—129
26	Chrysene . .	Along χ_1 — axis .	— 0·490	1·270	— 88·0	$\chi_1 = -88{\cdot}0$ $\chi_2 = -258$ $\chi_3 = -136{\cdot}1$ $\psi = +12°{\cdot}7$	—160·7
27	Pyrene . . .	Along χ_1 — axis .	— 0·509 — 0·503	1·274 1·264	— 80·7 — 80·4	$\chi_1 = -80{\cdot}6$ $\chi_2 = -178{\cdot}1$ $\chi_3 = -206$ $\psi = +25°{\cdot}0$	—154·9
28	Fluoranthene .	Along χ_1 — axis .	— 0·542	1·236	— 88·6	$\chi_1 = -88{\cdot}6$ $\chi_2 = -198$ $\chi_3 = -128{\cdot}6$ $\psi = +9°{\cdot}6$	— 138·4

III—MAGNETIC ANISOTROPY IN RELATION TO CRYSTAL STRUCTURE: BENZENE DERIVATIVES

We proceed to discuss the results obtained in the previous Section, in relation to X-ray and other data concerning molecular and crystalline structure. We shall first consider the benzene derivatives.

1—*p*-Benzoquinone

This crystal has been analysed by X-ray methods,* and it is assigned to the space group C_{2h}^5 ($P2_1/a$) in the monoclinic prismatic class, with 2 molecules in the unit cell, the molecules possessing a centre of symmetry. The X-ray measurements are not sufficient to locate the orientations of the two molecules in the unit cell. They can, however, be determined easily from the magnetic data.† As will be seen from Table I, the χ_1 axis makes an angle of 31°·2 with the "*c*" axis and one of 69°·8 with the "*a*" axis, while, from the cell dimensions given by CASPARI, the $(20\bar{1})$ plane is found to be inclined at an angle of 34°·1 to the "*c*" axis and 66°·9 to the "*a*" axis. Thus the χ_1 axis lies practically in the $(20\bar{1})$ plane, which contains of course the χ_2 axis as well, the third magnetic axis, viz., χ_3, being along the normal to $(20\bar{1})$. Moreover, since χ_1 and χ_2 are nearly equal, the normal to the $(20\bar{1})$ plane is an axis of approximate magnetic symmetry. Further, the ratio of the susceptibility of the crystal along this axis to that along perpendicular directions, is equal to $2\chi_2/(\chi_1 + \chi_2) = 2{\cdot}5$, which is nearly the same as the value for the benzene molecule. We may, therefore, conclude that the molecular planes in benzoquinone crystal practically concide with the $(20\bar{1})$ plane.

The optical properties of the crystal also support the molecular orientations suggested here. Since the optical polarizability of the benzene ring for light vibrations along the normal to its plane is much less than for directions in the plane, we should expect α to be much smaller than either β or γ, and further the vibration direction of α to be normal to $(20\bar{1})$. This is actually so, since the crystal exhibits a strong negative birefringence, and the acute bisectrix is nearly perpendicular to $(20\bar{1})$.‡

* W. A. CASPARI, 'Proc. Roy. Soc.,' A, vol. 136, p. 82 (1932).

† A preliminary report on the analysis of molecular orientations in this crystal by the magnetic method was published in 'Nature,' vol. 131, p. 653 (1933).

‡ Since the present paper was written, ROBERTSON ('Nature,' vol. 134, p. 138, July 28 (1934)) has published the results of a complete X-ray analysis of this crystal. He finds that the molecular planes are inclined to the $(20\bar{1})$ plane at an angle between 3° and 7° towards the "*c*" axis, in agreement with the 3° obtained by us from the magnetic data. Besides giving the inclinations of the molecular planes, his X-ray analysis gives complete information regarding the orientations of the molecules. Let us call for convenience the line joining the two O atoms of the molecule as its K_1 axis, the line perpendicular to the K_1 axis in the plane of the molecule as its K_2 axis, and the line normal to its plane as its K_3 axis. ROBERTSON finds that the K_1 axis of the molecule makes 79° with the "*a*" axis of the crystal, 37°·5 with the "*b*" axis, and 54°·5 with the normal to the (001) plane, while the K_2 axis makes 70°, 127° and 44° respectively with these crystal directions. These correspond, in the notation adopted in the later portions of this paper, to $\lambda = 8°{\cdot}6$, $\mu = +29°{\cdot}2$, and $\nu = 52°{\cdot}5$. (The magnetic value of $\mu = +31°{\cdot}2$.) From these orientations the principal susceptibilities of the benzoquinone *molecule* along its K_1, K_2 and K_3 axes can be readily calculated ; they are

$$K_1 = -24{\cdot}2$$
$$K_2 = -27{\cdot}9$$
$$K_3 = -68{\cdot}0.$$

It is clear that the presence of the two oxygen atoms in the para positions produces a small anisotropy in the plane of the molecule, the susceptibility along the line joining the oxygen atoms being numerically the smaller.

2—*Catechol and Hydroquinol*

Catechol (*o*-dioxy-benzene) has also been studied by CASPARI.* It crystallizes in the monoclinic prismatic class in the space group C_{2h}^3 with 8 asymmetric molecules in the unit cell. Regarding the molecular planes, it has been tentatively suggested that they are parallel to (010) plane. The magnetic data, however, point to a different orientation. As will be seen from Table I, two of the principal magnetic susceptibilities of this crystal, viz., χ_2 and χ_3 are nearly equal, so that the χ_1 axis, which almost coincides with the "*c*" axis (actually inclined to it at 2°·2), is an axis of approximate magnetic symmetry. Further, the susceptibility along this axis is numerically smaller than along perpendicular directions by about 29, which is nearly one half of the anisotropy of the benzene molecule, viz., 54/2. This shows that the molecular planes in the unit cell are all parallel to the above symmetry axis, but are orientated relatively to one another in such a manner as to make the two principal susceptibilities perpendicular to the above axis nearly equal. Because, if $K_1 = K_2$ are the two principal susceptibilities of the $C_6H_4(OH)_2$ molecule in its plane, and K_3 that along the normal to its plane, the molecular orientations proposed above will give the following susceptibilities for the crystal :

$$\chi_1 = K_1$$
$$\chi_2 = \chi_3 = \frac{K_1 + K_3}{2};$$
$$\text{therefore } \chi_1 - \chi_2 = \chi_1 - \chi_3 = \frac{K_1 - K_3}{2}.$$

Now, since the anisotropy, $K_1 - K_3$, of the $C_6H_4(OH)_2$ molecule must be the same as for C_6H_6 molecule, and since for the latter it is equal to 53·9, it follows with the molecular orientations proposed here that for catechol crystal both $\chi_1 - \chi_2$ and $\chi_1 - \chi_3$ should be equal to 27, which is about the value required by observation.

These molecular orientations are also supported by the optical properties of the crystal. On the basis of these orientations we should expect first the two refractive indices α and β to be nearly equal and to be much smaller than γ, and secondly, the vibration direction of γ to be nearly along the χ_1 axis. Both these conclusions are experimentally verified ; the principal refractive indices of the crystal for the D lines are :

$$\alpha = 1{\cdot}60, \quad \beta = 1{\cdot}61, \quad \gamma = 1{\cdot}73 ;$$

and further the γ vibration direction makes 6° to 7° with the "*c*" axis, as compared with 2°·2 made by the χ_1 axis.

Hydroquinol (*p*-dioxy-benzene), in one of its hexagonal modifications (α, in CASPARI's notation) was also studied. It is found to be almost isotropic, $\chi_{\parallel} - \chi_{\perp}$ being only 1·4. Also optically ω and ϵ are very close to each other, their values for the D lines being 1·632 and 1·626 respectively.

* 'J. Chem. Soc.,' vol. 129, p. 573 (1926).

3—*Hexamethyl Benzene*

This crystal is of exceptional interest. A complete X-ray analysis has been made by Mrs. LONSDALE,* and the unit cell contains only one molecule. The benzene ring has a plane regular hexagonal structure, and the aliphatic carbon atoms also lie in the same plane. These molecular planes are all parallel to (001) plane of the crystal. Preliminary magnetic measurements on this crystal have been made by BHAGAVANTAM† in this laboratory.

As will be seen from Table I, two of the principal susceptibilities, viz., χ_1 and χ_2 are nearly equal, so that the χ_3 axis, which is normal to the (001) plane, is an axis of magnetic symmetry, as we should expect from the parallelism of the benzene planes to (001). The difference between the susceptibilities along and perpendicular to the symmetry axis is about 61·9, which is slightly higher than the corresponding difference for the benzene molecule, viz., 53·9. This shows that the numerical increase in susceptibility that occurs when a hydrogen atom in benzene is replaced by a methyl group, is not quite isotropic, but has a small preponderance along the normal to the molecular plane. This can be expressed more precisely in the following manner. Consequent on replacing an H by CH_3, let s_1 be the increase in susceptibility along the line of attachment of the CH_3 group to the C atom in benzene, s_2 the increase in a perpendicular direction in the benzene plane, and s_3 the increase along the normal to the benzene plane. The greater anisotropy of $C_6(CH_3)_6$ as compared with that of C_6H_6 shows that s_3 is greater than $\frac{1}{3}(s_1 + s_2 + s_3)$, being actually found, on calculation, to be equal to $0{\cdot}36\ (s_1 + s_2 + s_3)$. The magnetic data for $C_6(CH_3)_6$ do not, however, give us any information regarding the relative values of s_1 and s_2 owing to the hexagonal symmetry of orientation of the s_1 and s_2 axes of the different CH_3 groups.

Before closing this article we should draw attention to the small but definite anisotropy in the (001) plane. Its origin is not clear.

4—*Durene* (1, 2, 4, 5-*Tetramethylbenzene*)

A complete X-ray analysis of this crystal has recently been made by ROBERTSON.‡ It belongs to the space group C_{2h}^5 ($P2_1/a$) in the monoclinic prismatic class, and the unit cell contains two molecules, which are centro-symmetric. ROBERTSON finds its structure to be a plane hexagonal benzene ring with the four methyl groups also in the plane of the ring.

For convenience in description, let us call the line joining the two carbon atoms at positions 3 and 6 (not attached to methyl groups) as the K_1 axis of the molecule, and the perpendicular direction in the plane of the benzene ring as the K_2 axis, and the normal to the molecular plane as the K_3 axis. In order to obtain from the magnetic data the orientations of these molecular axes in the unit cell, let us first place both the molecules with their K_1 axes along the "*c*" axis of the crystal, and

* 'Proc. Roy. Soc.,' A, vol. 123, p. 494 (1929) ; 'Trans. Faraday Soc.,' vol. 25, p. 352 (1929).
† 'Proc. Roy. Soc.,' A, vol. 126, p. 143 (1929).
‡ 'Proc. Roy. Soc.,' A, vol. 142, p. 659 (1933).

their K_3 axes along "*b*." Let us now suppose that, in order to bring them to their final orientations, we have to perform the following rotations :

(1) about the "*c*" axis : one of the molecules by an angle λ and the other by an angle $-\lambda$;
(2) about the "*b*" axis : both the molecules through an angle μ, in the direction from "*c*" axis to "*a*" axis through the obtuse angle β ;
(3) about an axis in the (010) plane perpendicular to the direction of the K_1 axis of the molecule obtaining after rotation (2) has been performed : one of the molecules through an angle ν and the other through $-\nu$.

Evidently $\mu = \psi = +20°{\cdot}2$.

As for λ and ν, we have the following relations*

$$\left.\begin{aligned} \chi_1 &= K_1 \cos^2\nu + (K_2\cos^2\lambda + K_3\sin^2\lambda)\sin^2\nu \\ \chi_2 &= K_2\sin^2\lambda + K_3\cos^2\lambda \\ \chi_3 &= K_1\sin^2\nu + (K_2\cos^2\lambda + K_3\sin^2\lambda)\cos^2\nu \end{aligned}\right\}, \quad \ldots\ldots\ldots (7)$$

from which, if the K's are known, λ and ν can be calculated.

K_3 is readily obtained from the following considerations. We have the relation $K_1 + K_2 + K_3 = \chi_1 + \chi_2 + \chi_3 = -303{\cdot}6$, and further we can obtain the value of $\frac{1}{2}(K_1 + K_2) - K_3$ by interpolating between the anisotropies of C_6H_6 and $C_6(CH_3)_6$ molecules,

$$\tfrac{1}{2}(K_1 + K_2) - K_3 = 53{\cdot}9 + \tfrac{4}{6}(61{\cdot}9 - 53{\cdot}9) = 59{\cdot}2\ ;$$

whence

$$K_3 = -140{\cdot}7.$$

As regards K_1 and K_2, if we take them to be equal, as we might to a first approximation, we obtain for K_1 the value 81. Since it is nearly the value of χ_1, we obtain directly $\cos^2\nu = 1$, *i.e.*, $\nu = 0$, and from the latter two equations in (7) $\lambda = 41°$.

On closer examination, however, we find that the small difference between χ_1 and K_1, which to a first approximation we neglected in the previous paragraph, is in such a direction as to give for $\cos^2\nu$ a value slightly in *excess* of unity. This is evidently due to the uncertainty in the assumption made above, that $K_1 = K_2$. Conversely, taking $\cos^2\nu$ to be actually unity, we can calculate the values of K_1 and K_2 more exactly. We thus obtain†

$$K_1 = -77{\cdot}3$$
$$K_2 = -85{\cdot}6,$$

* See Part I of this paper, p. 256.

† In an earlier section we found that when a CH_3 group replaces an H atom in benzene, of the total increase in susceptibility, equal to $s_1 + s_2 + s_3$ taken in all directions together, about 36% was directed along the s_2 direction, and the remaining 64% along s_1 and s_3. The difference obtained in this section between K_1 and K_2 of durene shows that of the latter 64%, about 38% is along the s_1 direction, and 26% along s_3.

which, when substituted in (7), give $\lambda = 41°{\cdot}0$. We thus have finally

$$\lambda = \quad 41°{\cdot}0$$
$$\mu = +20°{\cdot}2$$
$$\nu = \quad 0\,;$$

i.e., the K_1 axes of both the molecules lie in the (010) plane in the obtuse angle β making an angle of $20°{\cdot}2$ with the "*c*" axis and $93°{\cdot}1$ with the "*a*" axis. Their K_2 axes are inclined at $+41°{\cdot}0$ and $-41°{\cdot}0$ respectively, to the "*b*" axis.

With these may be compared the values obtained by ROBERTSON by X-ray analysis, which correspond to

$$\lambda = \quad 41°{\cdot}4$$
$$\mu = +16°{\cdot}5$$
$$\nu = \quad 1°{\cdot}2.$$

The values of λ and ν agree well with the magnetic values, whereas μ is definitely smaller.*

We may mention here that for naphthalene and anthracene crystals also, the values of μ obtained by X-ray analysis differ slightly from the magnetic values. The X-ray values† are $6°{\cdot}7$ and $5°{\cdot}1$ respectively, whereas the magnetic values‡ are $12°{\cdot}0$ and $8°{\cdot}0$.

4—Hexachlorobenzene

The structure of this crystal has been analysed by Mrs. LONSDALE.§ This crystal also belongs to the space group C_{2h}^5 ($P2_1/c$) in the monoclinic prismatic class, with two centro-symmetric molecules in the unit cell. From observations on the structure-factors in the [010] zone, she finds that this zone has a pseudo-hexagonal structure. This is reflected in the magnetic properties of the crystal, since the two principal susceptibilities in the (010) plane, viz., χ_1 and χ_2 are nearly equal, and differ considerably from the susceptibility along the "*b*" axis.

As regards the positions of the carbon atoms in the unit cell, we can approximately locate them with the help of the magnetic data. Let us assume that the benzene ring in C_6Cl_6 has the same structure as in C_6H_6, and that the chlorine atoms are magnetically isotropic ; the anisotropy of the C_6Cl_6 molecule will then be the same as that of the C_6H_6 molecule. This assumption may not be wholly justified, especially in view of the fact that Mrs. LONSDALE's X-ray results for this crystal

* We should remark here that μ in the magnetic case is the angle ψ which the χ_1 axis makes with the "*c*" axis. Its measurement is simple and involves merely the suspending of the crystal in the magnetic field with its "*b*" axis vertical, and finding the orientation of the (001) face, which is usually well developed ; the measurement is, therefore, capable of yielding accurate values for μ.

† ROBERTSON, 'Proc. Roy. Soc.,' A, vol. 142, p. 675, and vol. 140, p. 79 (1933)

‡ See Part I of this paper, p. 249.

§ 'Proc. Roy. Soc.,' A, vol. 133, p. 536 (1931)

throw some doubt on the regular hexagonal structure of the C_6Cl_6 molecule ; the assumption, however, would not be far from the truth. We should then get for the two principal susceptibilities of C_6Cl_6 in the plane of its benzene ring

$$K_1 = K_2 = -128,$$

and for the susceptibility along the normal to the plane of the ring

$$K_3 = -182.$$

Introducing the same angular parameters λ, μ, and ν as before to define the orientations of the two benzene rings in the unit cell, we obtain by a correlation of the above K's with the χ's for the crystal, with the help of equations (7),

$$\lambda = \quad 66°$$
$$\mu = +52°{\cdot}6$$
$$\nu = \quad 10°.$$

Thus the molecular benzene rings make angles of about 26° with the (010) plane. This is not very different from the angle obtained by Mrs. LONSDALE.

Optically, from the above orientations we should expect the "*b*" axis, which is nearly perpendicular to the molecular planes, to be the vibration direction of the fast ray, and the vibration direction of the slow ray to be close to the χ_1 axis. Experimentally, the axial plane is found to be perpendicular to (010), the obtuse bisectrix making an angle of 74° with the "*c*" axis in the obtuse angle β.

5—1, 2, 4, 5-Tetrachlorobenzene

This crystal does not seem to have been studied by X-ray methods. The orientations of the molecular planes in the crystal lattice can, however, be easily determined from the magnetic data. As will be seen from Tables I and II, two of the principal susceptibilities of the crystal, viz., χ_1 and χ_3 are almost identical, and thus the χ_2 axis, which makes $78°{\cdot}3$ with the "*a*" axis and $21°{\cdot}1$ with "*c*", is an axis of approximate magnetic symmetry. Further, the susceptibility along this axis is numerically greater than along perpendicular directions by $41{\cdot}8$, which is not much short of the anisotropy of the benzene ring, viz., $53{\cdot}9$. This shows that the molecular planes in the crystal must be orientated about the plane* containing the χ_1 and χ_3 axes, making with it small angles θ, given by the relation

$$\cos^2\theta - \tfrac{1}{2}\sin^2\theta = \frac{41{\cdot}8}{53{\cdot}9},$$

i.e., $\theta = 23°$.

Optically, we should expect from the above orientations the two principal refractive indices β and γ to be much greater than α, and the vibration direction of α

* This is not a lattice plane.

to be close to the χ_3 magnetic axis. Sufficient optical observations on the crystal are not available to test these conclusions.

7—*p-Dichloro and p-Dibromo Benzenes*

These two crystals have recently been analysed by HENDRICKS.* They belong to the space group C_{2h}^5 ($P2_1/a$) in the monoclinic prismatic class. Their unit cells, which contain two molecules each, have nearly the same dimensions, and the two crystals are isomorphous. The molecular orientations can be determined from the magnetic data in the same manner as in the other crystals. We shall merely mention here that the orientations of the benzene rings thus obtained are practically the same for the two crystals, and they differ from those suggested in HENDRICK's paper. The complete analysis of the orientations in these two crystals will be published elsewhere.

We shall not consider here the nitro-derivatives of benzene since they do not offer any points of special interest.

IV—MAGNETIC ANISOTROPY IN RELATION TO CRYSTAL STRUCTURE : DIPHENYL AND TRIPHENYL DERIVATIVES

1—*Diphenyl,† Terphenyl, and Quaterphenyl*

These three compounds form an interesting series. The first compound has been analysed by Dhar,‡ and all the three by Miss PICKETT,§ and by HERTEL and RÖMER.‖ They all crystallize in the monoclinic prismatic class in the space group C_{2h}^5 ($P2_1/a$), the unit cell containing two centro-symmetric molecules. The benzene rings are found to have a plane hexagonal structure. All the benzene rings in a molecule lie in a plane, and their centres lie on a line. Let us denote by K_1 the susceptibility of the molecule along the line joining the centres of the constituent benzene rings, and by K_2 the susceptibility along a direction in the plane of the benzene rings perpendicular to the K_1 axis, and by K_3 the susceptibility along the normal to the plane of the benzene rings. The K's can be calculated from the known anistropy of the benzene molecule, and are as given in Table III.

TABLE III

	Benzene	Diphenyl	Terphenyl	Quaterphenyl
		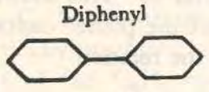	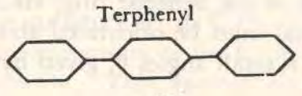	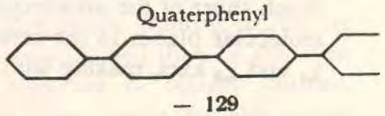
K_1	− 37·3	− 67	− 98	− 129
K_2	− 91·2	− 175	− 260	− 345

* 'Z. Kristallog,' vol. 84, p. 85 (1933).

† Diphenyl has already been considered in detail in Part I of this paper. For the sake of completeness, the results obtained with this crystal are included in this Section.

‡ 'Ind. J. Phys.,' vol. 7, p. 43 (1932).

§ 'Nature,' vol. 131, p. 513 (1933) ; 'Proc. Roy. Soc.,' A, vol. 142, p. 333 (1933).

‖ 'Z. phys. Chem.,' B, vol. 22, p. 292, and vol. 23, p. 226 (1933).

Defining the orientations of the K_1, K_2, and K_3 axes of the last three molecules in their unit cells by the usual parameters λ, μ, and ν, the values of these angles can be readily calculated from the magnetic data. The calculated values are given in Table IV, along with the X-ray values for comparison.

TABLE IV

	Diphenyl		Terphenyl		Quaterphenyl*	
	Magnetic	X-ray	Magnetic	X-ray	Magnetic	X-ray†
λ	31°	32°	32½°	34°	31½°	—
μ	+ 20°·1	+ 20°	− 14°·3	− 15°·3	$\lvert\theta\rvert$ = 17°·1	—
ν	0	0	0	0	0	—

The agreement with the X-ray values is very satisfactory, and emphasizes the powerfulness of the magnetic method for the determination of the orientations of the benzene rings in the crystal lattice.

For all the three molecules, we should expect the K_3 axis, which is normal to the plane of the benzene rings, to be the vibration direction of the fast ray, and the K_1 axis to be that of the slow ray. Since in the crystal, the K_1 molecular axes coincide with the χ_1 axes and since the inclinations of the K_3 axes to the (010) plane are small (about 30°), we should expect the vibration directions of γ and α to lie in the (010) plane, and to be close to the χ_1 and χ_2 magnetic axes respectively. This is actually so, as has been pointed out by Miss PICKETT ; the (010) plane is the axial plane for all the three crystals, and further the directions of the bisectrices are nearly as predicted.

* We are indebted to Dr. P. C. GUHA and Mr. B. H. IYER, of the Indian Institute of Science, Bangalore, for the supply of this compound, and to Miss PICKETT for dimesityl, and we take this opportunity to express our thanks to them.

† [*Note added in proof, February* 19, 1935.—Through the kindness of Miss PICKETT we are able to give here the results of some unpublished X-ray studies by her on the structure of quaterphenyl. She finds that the long axes of the molecules lie in the (010) plane in the acute angle β, making 11°·5 with the "*c*" axis, and that the molecular planes are inclined at 34° to the "*b*" axis. She finds further that β is about 95°. These X-ray results would correspond, in our notation, to

$$\lambda = 34° \quad \mu = -11°{\cdot}5, \textit{ i.e.}, \theta = +16\tfrac{1}{2}° \quad \nu = 0,$$

which are in close agreement with the values deduced from our magnetic data (see Table IV),

$$\lambda = 31\tfrac{1}{2}° \quad |\theta| = 17°{\cdot}1 \quad \nu = 0.$$

The ambiguity in the sign of magnetic θ is due to the circumstance that in the crystals studied by us, none of the prismatic faces was developed, and it was therefore not possible to decide whether the χ_3 — axis, which is inclined at 17°·1 to the (001) plane, lies in the acute angle β or in the obtuse angle β.]

2—1, 3, 5-*Triphenyl Benzene and Triphenyl Carbinol*

s-Triphenyl benzene has recently been analysed by ORELKIN and Mrs. LONSDALE* and is assigned to the space group C_{2v}^9 (*Pna*) in the orthorhombic hemihedral class. The crystal axes and axial ratios adopted in the following descriptions are those given by ORELKIN and Mrs. LONSDALE, and are slightly different from those given by GROTH for this crystal.

The crystal is found to have a pseudo-hexagonal structure, with "*a*" as the pseudo-principal axis. This is reflected in the magnetic data for the crystal, since "*a*" is an axis of approximate magnetic symmetry, χ_b and χ_c being nearly equal. The actual susceptibilities are

$$\chi_a = -313$$

$$\chi_b = -155$$

$$\chi_c = -140.$$

The above large anisotropy of the crystal suggests that the benzene planes must be either parallel to the (100) plane of the crystal or make small angles with it. Their actual orientations can be calculated in the following manner.† We have seen (see Table III) that the susceptibility of the benzene molecule for directions in the plane of the molecule is $-37{\cdot}3$, while along the normal to its plane it is $-91{\cdot}2$. The difference is thus equal to -54. If in the crystal all the four benzene rings of the molecules were orientated parallel to the (100) plane, we should have

$$\chi_a - \chi_b = \chi_a - \chi_c = -216,$$

whereas actually $\chi_a - \chi_b$ and $\chi_a - \chi_c$ are equal to only -166. This shows, in agreement with the conclusions of Mrs. LONSDALE, that the benzene rings cannot be all parallel to the (100) plane, but must make small angles with it.

Assuming that all the rings are inclined at the same angle θ to (100), the value of θ can be calculated from the relation

$$\cos^2\theta - \tfrac{1}{2}\sin^2\theta = \frac{166}{216},$$

$$i.e.,\ \theta = 23°.$$

The optical properties of the crystal also support these orientations. The principal refractive indices of the crystal for vibrations along the "*a*," "*b*" and "*c*" axes are 1·524, 1·867, and 1·872 respectively for the D lines. The corresponding gram molecular refractivities, defined as usual by the LORENTZ Constant $\frac{n^2-1}{n^2+2}\cdot\frac{M}{\rho}$, are

$$R_a = 77{\cdot}6,\ R_b = 115{\cdot}0 \text{ and } R_c = 115{\cdot}5.$$

* 'Proc. Roy. Soc.,' A, vol. 144, p. 630 (1934).

† A preliminary report on the analysis of molecular orientations in this crystal by the magnetic method was published in 'Nature,' vol. 133, p. 497 (1934).

The latter two refractivities, which correspond predominantly to vibrations in the plane of the benzene rings, are nearly equal, and are, as we should expect, much greater than R_a, which corresponds predominantly to vibrations along the normal to the benzene planes. Indeed, just as in the magnetic case, we may find the actual inclinations of the benzene rings to the (100) plane by correlating the observed birefringence, $R_b - R_a$ or $R_c - R_a$ of the crystal with the known birefringence of the benzene rings. The gram molecular refractivities of the benzene molecule for vibrations along the normal to its plane, and along directions in its plane, are 16·4 and 32·6 respectively,* so that the birefringence of the benzene molecule = 16·2. If all the four benzene rings of the molecules were orientated parallel to (100), and if *further it is assumed that the optical moments induced in the different benzene rings exert no influence on one another*, we should have

$$R_b - R_a = R_c - R_a = 65.$$

The actual values, on the other hand, are

$$R_b - R_a = R_c - R_a = 38.$$

From these data, we can calculate θ as in the magnetic case, and we obtain

$$\cos^2\theta - \frac{1}{2}\sin^2\theta = \frac{38}{65},$$

or

$$\theta = 32°.$$

The assumption that the optical dipole moments induced in the different benzene rings do not influence one another is not quite justifiable. The value of θ obtained from the optical constants is, therefore, not inconsistent with the value obtained from the magnetic data, viz., $\theta = 23°$.

In strong contrast with this crystal, in which the benzene rings are orientated more or less parallel to one another, is *triphenyl carbinol*, whose low anisotropy, namely, $\Delta\chi = 5{\cdot}4$, shows that the benzene rings in its unit cell must be so orientated as to form a more or less isotropic group.

3—4, 4′-*Dichlorodiphenyl and* 4, 4′-*Dibromodiphenyl*

These two di-halogen derivatives of diphenyl crystallize in the monoclinic prismatic class, and are isomorphous. They do not seem to have been studied by X-ray methods. The magnetic data for these crystals are very similar, as will be seen from Table V, and they show that the orientations of the benzene rings in the unit cells of these two crystals must also be very similar.

* KRISHNAN, 'Proc. Roy. Soc.,' A, vol. 126, p. 155 (1929).

TABLE V

Crystal	$\chi_1 - \chi_3$	$\chi_3 - \chi_2$	ψ
4, 4′—Dichlorodiphenyl . .	35·1	60·5	− 28°·5
4, 4′—Dibromodiphenyl . .	35·9	57·9	− 27°·6

The actual orientations can be determined from the magnetic data in the same manner as for the other crystals described before. It is found that in both the crystals the different benzene planes in the unit cell are inclined at small angles to the "*b*" axis.

4—*o-Tolidine*

We shall consider here only one more diphenyl derivative *o-tolidine* (4, 4′-diamido : 3, 3′-dimethyl diphenyl). Its structure has been analysed by CLARK and PICKETT* and it probably belongs to the space group Q^1 in the orthorhombic bisphenoidal class. They tentatively place the molecular planes nearly parallel to (010). The magnetic data definitely confirm this orientation. As will be seen from Table I, the "*b*" axis is an axis of approximate magnetic symmetry, the susceptibility along this axis being numerically greater than along perpendicular directions by about 81. Had all the benzene planes in the unit cell been orientated parallel to (010), the above anisotropy would have been about 110. We may, therefore, conclude that the benzene planes are inclined to (010) at small angles

$$\theta = \arcsin \sqrt{\frac{2}{3}\left(1 - \frac{81}{110}\right)} = 25°.$$

Whether the pair of benzene rings constituting a molecule are orientated the same way or not, it is not possible to say from the magnetic data.

The above orientation would correspond optically to the α vibration direction lying along the "*b*" axis, and further α being considerably smaller than either β or γ. Optical observations do not appear to have been made on the crystal.

V—MAGNETIC ANISOTROPY IN RELATION TO CRYSTAL STRUCTURE : NAPHTHALENE DERIVATIVES

1—1, 4-*Naphthoquinone*

An X-ray analysis of this crystal has been made by CASPARI,† and he assigns it to the space group C_{2h}^5 in the monoclinic class, with 4 molecules in the unit cell. From considerations of the dimensions of the molecules and of the unit cell, he places the molecules with their widths (perpendicular to the line joining the two benzene nuclei) along the "*a*" axis, and their lengths nearly along "*b*," the molecular

* 'J. Amer. Chem. Soc.,' vol. 53, pp. 167 and 3826 (1931).

† 'Proc. Roy. Soc.,' A, vol. 136, p. 86 (1932).

planes being thus near about (001). The magnetic data are in accord with these orientations. In the first place two of the principal susceptibilities of the crystal, viz., χ_1 and χ_2, are numerically much smaller than the third, so that the plane containing them must be nearly about the molecular planes. Further, this plane practically coincides with (001) (being inclined to it at 3°·7). Thus the molecular planes must be inclined at small angles to (001).

On calculation from the magnetic data we find that the molecular planes are tilted from (001) by about 31°.

Optically, we should expect α to be much smaller than either β or γ, and the vibration direction of α to be nearly along the normal to (001). Observations are not available which may enable us to check this conclusion.

2—α-*Naphthol*

In Part I β-naphthol was discussed in detail. The molecular orientations in the α-compound can be determined in the same manner. We shall give here the final results only. Denoting by K_1 the long axis of the molecule, by K_2 the short axis in its plane, and by K_3 that along the normal to its plane, the angular parameters λ, μ, and ν that define in the usual manner the orientations of these axes, are as given in Table VI.

TABLE VI

Crystal	λ	μ	ν
α—Naphthol	49½°	+ 28°·7	22°
β—Naphthol	34°	+ 9°·4	34°

VI—MAGNETIC ANISOTROPY IN RELATION TO CRYSTAL STRUCTURE : POLYNUCLEAR COMPOUNDS

1—*Fluorene and Phenanthrene*

Diphenyl, fluorene, and phenanthrene form an interesting series. From the striking similarity in the dimensions of their unit cells (see Table VII) it has been suggested by HENGSTENBERG and MARK* that the molecular orientations in these crystals must be very similar, the lengths of the molecules being nearly along the "*c*" axis, and their breadths at small angles to "*b*." For diphenyl, the precise orientations have since been determined, as we mentioned in an earlier section, and the long axes of the molecules are found to lie in the (010) plane making 20° with "*c*" axis, their planes being inclined at 32° to the "*b*" axis. We shall proceed to inquire what information the magnetic measurements can give us regarding the molecular orientations in the other two crystals.

Let us first consider fluorene. Its χ_1 axis is inclined at + 10°·9 to "*c*," and the susceptibility along it, namely − 72·6, is only slightly higher than that of the

* 'Z. Kristallog.' vol. 80, p. 283 (1929).

diphenyl molecule along its length, namely — 67 (see Table III). Since the fluorene molecule contains one carbon atom more than diphenyl, the above value of — 72·6 might very well be the susceptibility K_1 of the fluorene molecule along its length, and the χ_1 — axis the direction of the long axes of the molecules in the unit cell.

TABLE VII

	Dimensions of the unit cell in A.				Molecular susceptibilities		μ	λ
	a	*b*	*c*	β	$K_1 = K_2$	K_3		
Diphenyl . . .	8·22	5·69	9·50	94°·8	— 67	— 175	+ 20°·1	31°
Fluorene . . .	8·48	5·73	9·62 × 2	101° 30′	— 72·6	— 193·6	+ 10°·9	33½°
Phenanthrene .	8·60	6·11	9·62 × 2	98° 15′	— 74	— 240	— 3°·1	29½°

If now we know the susceptibility of the molecule along its width, K_2, and that along the normal to its plane, K_3, then we can locate their orientations also, from the known values of χ_2 and χ_3. The value of K_2 can be obtained from the following considerations. We have seen that for diphenyl, terphenyl, naphthalene and anthracene molecules, the two principal susceptibilities in the molecular plane are nearly the same, so that for fluorene also we may, to a first approximation, take K_2 to be equal to K_1. We thus obtain for this molecule

$$K_2 = K_1 = - 72·6$$

$$K_3 = - 193·6,$$

from which the inclination of the K_2 axes to "*b*" comes out as

$$\lambda = \tfrac{1}{2} \text{ arc cos } \frac{\chi_2 - \chi_3}{K_3 - K_2} = 33\tfrac{1}{2}°.$$

That is, the lengths of the fluorene molecules in the unit cell lie in the (010) plane making 10°·9 with the "*c*" axis in the obtuse angle β, and the molecular planes are inclined at plus and minus 56½° to (010).

Coming to phenanthrene, adopting a similar course of reasoning, we obtain $K_1 = K_2 = - 74$ and $K_3 = - 240$, which correspond to the following molecular orientations. The K_1 axes (lengths) lie in the (010) plane in the acute angle β at 3°·1 to the "*c*" axis, and the molecular planes are inclined at plus and minus 60½° to (010).

It is remarkable that in many of the monoclinic crystals containing benzene rings, the inclinations of the benzene planes to (010) should be nearly the same, namely, about 60°; naphthalene, anthracene, diphenyl, terphenyl, quaterphenyl, dibenzyl, fluorene, phenanthrene, and chrysene may be cited as examples.

Before closing this article we may mention that in both fluorene and phenanthrene we should expect the (010) plane to contain the vibration directions of both γ and α, the latter being close to the χ_2 axis.

2—Chrysene (1, 2-*Benzophenanthrene*)

A structural analysis of this crystal by X-ray methods has recently been made by IBALL and ROBERTSON.* The crystal belongs to the space group C_{2h}^6 in the monoclinic prismatic class. The dimensions of the unit cell are $a = 8·34$, $b = 6·18$, $c = 25·0$ A., β = 115°·8, and it contains 4 molecules. Let OA be the long axis, and OB the cross axis, of the molecule, which is assumed to have a plane structure as shown in fig. 1. IBALL and ROBERTSON find that in the crystal the OA molecular axis "is tilted about 10° away from the normal to (001) towards the "*c*" axis, but remains practically in the plane of the (010), and the cross axis OB makes an angle of about 16° with the "*b*" axis of the crystal."

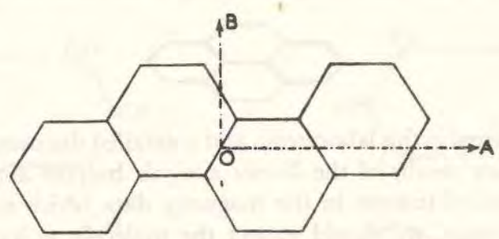

FIG. 1

Now OA and OB will be practically the two principal magnetic axes of the molecule in its plane and let us denote them by K_1 and K_2 respectively, and the third magnetic axis, which would be along the normal to the plane of the molecule, by K_3. Adopting our usual angular parameters λ, μ, and ν, the above molecular orientations would correspond to

$$\lambda = \quad 16°$$

$$\mu = + 15°·8$$

$$\nu = \quad 0.$$

Coming to the magnetic evidence, we find that $\mu = \psi = + 12°·7$. The other two angles are obtained by adopting the same kind of reasoning as for fluorene and phenanthrene. In the first place we may reasonably take K_1 to be the same as K_2 (both of which would of course be numerically much less than K_3). Evidently its value can not be numerically greater than the lowest of the crystal susceptibilities, viz., $\chi_1 = - 88·0$. It cannot also be appreciably less than this value, since even for phenanthrene which contains one benzene ring less, $K_1 = - 74$. We thus obtain $\nu = 0$.

For the molecular susceptibilities we have then

$$K_1 = K_2 = - 88$$

$$K_3 = - 306,$$

* 'Nature,' vol. 132, p. 750 (1933).

from which we obtain $\lambda = 28°$. Collecting the angle values from magnetic data

$$\lambda = \cdot 28°$$
$$\mu = + 12°\cdot 7$$
$$\nu = 0.$$

We find both μ and ν agree with the X-ray values, but λ differs considerably.*

3—*Pyrene*

An X-ray study of this interesting four-ringed compound

has recently been started in this laboratory, and a detailed discussion will be attempted when the preliminary results of the X-ray analysis become available. There are, however, some points of interest in the magnetic data which should be mentioned here. In the first place, we should expect the molecule to have an exceptionally large magnetic anisotropy, the susceptibility along the normal to the plane, say K_3, being several times greater than either K_1 or K_2 along the two axes in the plane. Further, as with the other polynuclear compounds, K_1 and K_2 may be expected to be nearly the same. If we examine the magnetic data for the crystal, we find that the smallest numerical value of its susceptibility, viz., along its χ_1 axis, is equal to $80\cdot 6$, and this fixes the upper limit to $|K_1| = |K_2|$. When, however, we remember that for phenanthrene which has only three rings, $|K_1| = 74$, we can reasonably conclude that for pyrene K_1 cannot differ much from the limiting value $- 80\cdot 6$, and is most probably equal to it. We thus obtain

$$K_1 = K_2 = - 80\cdot 6$$
$$K_3 = - 303.$$

From these data we can deduce the molecular orientations. To quote only the final results, the molecular planes are inclined at plus and minus 42° to (010),

* Since this was written, IBALL, ' Proc. Roy. Soc.,' A, vol. 146, p. 140 (1934) has published the results of a complete X-ray analysis of this crystal. He finds that the OA molecular axis makes $102°\cdot 0$ with the " *a* " axis of the crystal, and $90°\cdot 5$ with the " *b* " axis, and $12°\cdot 0$ with the normal to (001), while the cross axis OB of the molecule makes $118°\cdot 4$, $29°\cdot 0$ and $95°\cdot 4$ respectively with the same crystal directions. These correspond to

$$\lambda = 29°\cdot 0$$
$$\mu = + 13°\cdot 8$$
$$\nu = 0°\cdot 5,$$

which are in close agreement with our magnetic values.

intersecting the latter along a line making $75°\cdot 9$ with the " *a* " axis and $25°\cdot 0$ with " *c*."

Optically, we should expect from these orientations, the vibration direction of γ to be close to the above line in (010). Actually one of the bisectrices lies in (010), making about 37° with " *c* " in the obtuse angle β.

4—*Fluoranthene*

The crystal data given in GROTH's ' Kristallographie '* for the compound of this name, to which he assigns formula (i) ($C_{15}H_{10}$), most probably refer to the compound $C_{16}H_{10}$ having formula (ii), namely, 7, 8-benzo-acenaphthylene† (see fig. 2).

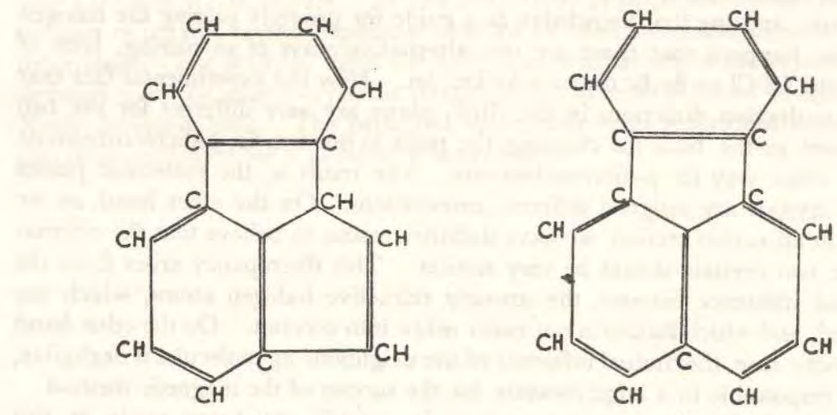

(i) (ii)

FIG. 2

The magnetic data for the crystal suggest that the χ_1 axis, which makes $87°\cdot 6$ with the " *a* " axis and $9°\cdot 6$ with " *c*," cannot deviate much from parallelism to the benzene planes of the molecules, and that the latter are inclined at about 55° to (101).

The magnetic data further suggest that the two optic axes of the crystal should lie in the (010) plane, one of the bisectrices being nearly along the χ_2 axis, *i.e.*, close to " *a* " axis. This is verified by observation.

VII—MOLECULAR ORIENTATIONS IN CRYSTALS AND THEIR OPTICAL PROPERTIES

In the foregoing discussions we have tried wherever possible to correlate the molecular orientations with the optical properties of the crystals also. With the optical properties, however, we are working under serious limitations. We cannot assume, as we do with the magnetic properties, that the crystal polarizability in any

* Vol. 5, p. 430.

† See J. v. BRAUN, ' Ber. deuts. chem. Ges.,' B, vol. 62, p. 145 (1929).

direction is the same as that obtained by the simple superposition of those of the individual molecules constituting it, because of their strong mutual influence. Hence, even under favourable conditions, the optical data can give only qualitative indications. As an example of the uncertainty attendant on the use of the optical data for this purpose, we shall mention *p*-dichloro- and *p*-dibromobenzenes, recently analysed by HENDRICKS (*loc. cit.*). The unit cells of these crystals have practically the same dimensions, and the available X-ray data give the positions of only the halogen atoms in the lattice, which are found to be nearly identical in the two crystals. They do not, however, enable us to choose uniquely the pair of halogen atoms which belong to the same molecule. But we can estimate, from considerations of interatomic distances, the distance between the halogen atoms belonging to the same molecule, and use that knowledge as a guide for properly pairing the halogen atoms. It so happens that there are two alternative ways of so pairing, both of which give the Cl-Cl or Br-Br distance looked for. Now the experimental fact that the optical extinction directions in the (010) plane are very different for the two crystals is used as the basis for choosing the pairs in one way for *p*-dichlorobenzene and in the other way for *p*-dibromobenzene. The result is, the molecular planes in the two crystals are assigned different orientations. On the other hand, as we mentioned in an earlier section, we have definite reasons to believe that the orientations in the two crystals should be very similar. This discrepancy arises from the large mutual influence between the strongly refractive halogen atoms, which has been ignored, and which further is not easily taken into account. On the other hand in the magnetic case, the mutual influence of the neighbouring molecules is negligible, and this is responsible in a large measure for the success of the magnetic method.

Extensive optical measurements on organic crystals are being made in this laboratory, and a detailed discussion of the optical results in relation to crystal structure, in a manner analogous to the treatment presented here of the magnetic problem, will be published shortly.

An optical observation made recently in this laboratory, which is of significance to the present problem,* is that *in compounds containing benzene nuclei, the absorption bands characteristic of the compounds appear much more intensely when the light vibrations (electric vector) are in the plane of the benzene ring than when they are along the normal to the plane.* Observations on the polarizations of the absorption bands in crystals thus supply another useful guide for locating the orientations of the benzene planes.

VIII—CONCLUSION

From the numerous examples worked out in the foregoing pages it will be clear that a knowledge of the magnetic properties of a crystal offers an effective check on the results of the X-ray analysis. In many organic crystals containing benzene rings the orientations of the benzene rings can be predicted successfully from the magnetic data, and the results are found to agree well with those obtained by ROBERTSON and

* KRISHNAN and SESHAN, 'Current Science,' vol. 3, p. 26 (1934).

others by their latest methods of X-ray analysis. The values of the angular parameters defining the orientations of the benzene rings, deduced from the magnetic data, besides being more readily obtained, are sometimes even more accurate than the X-ray values, as for example that of the parameter μ in monoclinic crystals, which is obtained in the magnetic method by the direct measurement of an angle. Thus the magnetic method forms a powerful supplement to the X-ray methods of structural analysis.

IX—SUMMARY

In the present part a new method is described of measuring the magnetic anisotropies of crystals, which can be adopted for even such small crystals as weigh only a fraction of a milligram. By this method the principal susceptibilities of a large number of organic crystals, specially selected for their structural interest, have been determined. For many of them the molecular orientations in the crystal lattice are deduced from the magne-crystallic data, and are in general found to agree with the X-ray determinations. The principal susceptibilities of individual molecules have also been computed for a number of compounds.

Stark Splitting of the ^6S Level of the Manganous Ion in Crystalline Fields

In recent papers, Kramers, Bethe and Van Vleck[1] have discussed theoretically the possibility of a weak Stark splitting of the ^6S levels of Mn++ and Fe+++ ions in crystalline fields. As Van Vleck has shown, such a splitting would lead to two important consequences in the magnetic behaviour of these ions in crystals: (1) it would produce a feeble magnetic anisotropy in the crystal; (2) the temperature dependence of the three principal susceptibilities of the crystal would not exactly conform to the simple Curie law. The first effect, namely, the magnetic anisotropy, can be measured accurately, and can indeed be used, as Van Vleck has pointed out, as a means of calculating indirectly the magnitude of the Stark separation.

Using the special experimental arrangement designed by us for measuring feeble anisotropies[2], we have recently measured the anisotropies of a number of manganous salts of the Tutton series, $MnSO_4.A_2SO_4.6H_2O$, where A = NH_4, Rb, Cs, Tl; $MnSeO_4.A_2SeO_4.6H_2O$, where A = NH_4, Rb, Tl. The differences $\Delta\chi$ between the maximum and the minimum gram molecular susceptibilities of these crystals at about 25° C. range from $11{\cdot}4 \times 10^{-6}$ (c.g.s. e.m.u.) in manganous ammonium sulphate to $7{\cdot}0 \times 10^{-6}$ in manganous cæsium sulphate. For all the crystals the mean of the three principal susceptibilities is about $14{,}000 \times 10^{-6}$.

Part of this anisotropy must be attributed to that of the *diamagnetism* of the crystal. This may be taken, to a first approximation, to be the same as the anisotropy of the corresponding diamagnetic Tutton salt obtained by replacing Mn by Mg. (The anisotropies of the latter salts are found to range from $2{\cdot}5$ to $0{\cdot}9 \times 10^{-6}$.) A further correction is also necessary for the anisotropy arising from the mutual influence of the magnetic moments of neighbouring Mn++ ions, which are not arranged in a cubic lattice.

After making these corrections, we find that the residual anisotropies of the manganous salts correspond to a Stark separation of the ^6S levels of only a small fraction of a cm.$^{-1}$.

K. S. Krishnan.
S. Banerjee.

210 Bowbazar Street,
Calcutta.
Feb. 18.

[1] *Phil. Mag.*, 17, 961; 1934.
[2] *Phil. Trans.*, A, 232, 99; 1933.

Letters to the Editor.

The Photo-dissociation of Single Crystals of Potassium and Sodium Nitrates under Polarised Light.

In a previous communication[1] by Mr. Guha and one of us it was suggested that the well-known absorption bands of inorganic nitrates in the ultra-violet, having their long wave-length limits at about 350 $m\mu$ and 230 $m\mu$ respectively, may be attributed to the following photo-dissociations:—

$NO'_3 \rightarrow NO'_2 + O\ (^3P) - 81$ kilocals. (350 $m\mu$)

$NO'_3 \rightarrow NO'_2 + O(^1D_2) - 124$ kilocals. (230 $m\mu$)

The observation with single crystals of KNO_3, NH_4NO_3, $NaNO_3$, etc., in which the NO'_3 ions are all oriented parallel to one another, that both the absorption bands are strongly polarised, the ordinary rays being absorbed much more strongly than the extraordinary rays, was interpreted as indicating a corresponding difference between the photo-dissociative activities of the two rays.

We have recently made some experiments on the photo-dissociation of solid inorganic nitrates, particularly with a view to testing the above conclusions. The following are the main results obtained:—

(1) All the nitrates studied, namely those of K, Na, NH_4, Sr, Ba, Al, Cd and Pb, showed definite dissociation under the action of light (from a quartz mercury lamp) of wave-lengths shorter than about 250 $m\mu$ (region of the stronger absorption band), as tested by the formation of nitrite. The actual long-wave-length limit of the photo-active region of the spectrum was not determined.

(2) The dissociation appears to be confined to a thin surface layer of the crystal, about 20μ thick. The absence of permanent dissociation in the interior is attributable to the recombination of the products of dissociation.

(3) Experimenting under linearly polarised light (obtained by passing the light from the arc through a quartz double-image prism), with single crystals of KNO_3, NH_4NO_3 and $NaNO_3$, it was found that the dissociation is much greater when the electric vector of the exciting light is in the plane of the NO'_3 ions (ordinary ray) than when it is along the normal to their planes.

(4) $KClO_3$ crystals also show a similar anisotropic photo-dissociation.

K. S. Krishnan.
L. K. Narayanaswamy.

210, Bowbazar Street,
Calcutta,
February 25, 1935.

[1] *Curr. Sci.*, 1943, **2**, 476; *Proc. Ind. Acad. Sc.*, 1934, **1**, 242.

Absorption Spectra of Sulphur-Chlorides and -Oxychlorides in the Vapour State.

In continuation of previous work already reported,[1] it was found necessary to study the absorption spectra of the series of compounds— SCl_2, S_2Cl_2, $SOCl_2$ and SO_2Cl_2. This work is now complete and we present a summary of the results obtained.

[1] *Curr. Sci.*, 1934, **2**, 433.

Substance	A		B			C			D		
	a	*b*	*a*	*b*	*c*	*a*	*b*	*c*	*a*	*b*	*c*
SCl_2	5825	5165 ?	4550	3860	3700	2770	2610	2450	2350	2280	2260
S_2Cl_2						2770	2580	2390			
$SOCl_2$						2900	2450	2400			
SO_2Cl_2									2600—continuous		

a gives the beginning, *b*, the maximum and *c*, the end of absorption in wavelengths (A. U. in air).

An Orthorhombic Crystalline Modification of 1.2; 5.6-Dibenzanthracene.

By

Prof. K. S. Krishnan and S. Banerjee,

Indian Association for the Cultivation of Sciene, Calcutta.

Introduction.

The well-known carcinogenic hydrocarbon, 1.2; 5.6-dibenzanthracene,

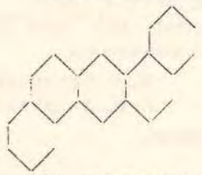

crystallizes in the monoclinic system in the form of thin ill-bounded flakes parallel to (001). The structure of this crystal has been analyzed by X-ray methods by Iball and Robertson[1]). Its space group is either C_{2h}^2 or C_2^2. There are two molecules in the unit cell, whose dimensions are $a = 6.59$, $b = 7.84$, $c = 14.17$ Å; $\beta = 103°.5$.

While trying to crystallize a specimen of 1.2; 5.6-dibenzanthracene (from Kodak) out of solutions in acetic acid and acetic ether, some small well-developed crystals, quite different from the usual variety, also appeared in the crops. On examination they were found to be an orthorhombic modification of the substance. We give in this paper a short account of some crystallographic and other measurements on these crystals.

Crystallographic Data.

The crystals were found to belong to the orthorhombic bipyramidal class, with the axial ratios

$$a : b : c = 0.755 : 1 : 0.546.$$

The prismatic faces {120} and the pyramidal ones {111} were well developed, the side pinacoids {010} also being observable. The angles between these different faces, measured with a single circle goniometer, are given below, together with the corresponding angles calculated from the above axial ratios.

1) Nature 132 (1933) 750.

	Measured	Calculated
(010) : (120)	33° 30′	33° 31
(120) : ($1\bar{2}0$)	67 0	67 2
(120) : (111)	50 32	50 42
(111) : ($\bar{1}11$)	64 54	64 49
(111) : ($1\bar{1}1$)	47 42	47 43
(111) : ($\bar{1}\bar{1}1$)	84 24	84 22

The Chemical Identity of the Crystals.

We shall now give the evidence for identifying the orthorhombic crystals as 1.2; 5.6-dibenzanthracene. On allowing a solution of the orthorhombic crystals in acetic ether to crystallize, and examining the crop of crystals, it was found to contain, in addition to some orthorhombic crystals, a large number of flaky ones of the monoclinic variety. Similarly a solution of the monoclinic flakes alone in acetic ether yielded a crop containing both the monoclinic and the orthorhombic modifications. The appearance of both the monoclinic and the orthorhombic varieties from solutions of either of them, points to the chemical identity of the two types of crystals.

As corroborative evidence we may mention the following. Preliminary X-ray measurements have been made on these orthorhombic crystals by Mr. A. C. Guha in this laboratory, and the mass of the unit cell is found to be nearly four times the molecular weight of dibenzanthracene. Further a micro-analysis of the crystals gave the following results:

Weight of substance taken	= 3.530 mgm.
« « CO_2 obtained by combustion	= 12.343 «
« « H_2O « « «	= 1.659 «

These data correspond to $C = 95.3\%$ and $H = 5.2\%$, which are in agreement with the theoretical values for dibenzanthracene $C_{22}H_{14}$, viz., $C = 94.9\%$, $H = 5.1\%$.

The crystals have a density of 1.282 (as determined by the flotation method), which is practically the same as that of the monoclinic variety. They melt sharply at 260° C., as compared with 262° obtained by Clar[1]) for the compound, and 258—260° given by Kodak. The crystals retained their shape up to the melting point.

A dilute solution of the orthorhombic crystals in benzene was studied for its absorption spectrum. It showed a number of well-defined bands in the same positions as a solution of the monoclinic variety in benzene.

1) Ber. Dtsch. chem. Ges. 62 (1929), 352.

Positions of absorption maxima, in $m\mu$.

Solution of orthorhombic crystal in benzene	395	385	374	365	352	337
Solution of monoclinic crystal in benzene	395	384	374	365	351	336

This further confirms the chemical identity of the two crystals.

We desire to express our thanks to Mr. Madhab Chandra Nath for the micro-analysis, and to Dr. P. B. Sircar for the loan of the goniometer with which the measurements were made.

210, Bowbazar Street, Calcutta (India). 25th April, 1935.

Received 12th May 1935.

The Magnetic Anisotropy and Crystal-Structure of 1.2; 5.6-Dibenzanthracene.

By

K. S. Krishnan and S. Banerjee,

Indian Association for the Cultivation of Science, Calcutta.

(With one figure.)

1. Indroduction.

The structure of 1.2; 5.6-Dibenzanthracene, 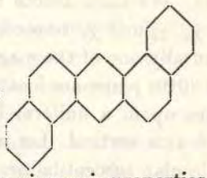

has attracted much interest because of the strong carcinogenic properties of the compound. It crystallizes generally in the monoclinic system in the form of extremely thin flakes, and the structure of these crystals has been analysed by X-ray methods by Iball and Robertson[1]). Recently an orthorhombic crystalline modification of this compound has also been obtained, and studied crystallographically[2]).

In some previous publications[3]) we have shown how a study of the magnetic properties of aromatic organic crystals gives us useful information regarding the orientations of the molecules in the crystal lattice. Dibenzanthracene is a suitable crystal for the study of molecular orientations by this method, owing to the large magnetic anisotropy of its molecules. The present paper concerns itself with such a study.

Crystals of the orthorhombic variety could be obtained in sufficiently large size to enable the magnetic measurements to be made by the usual methods. Those of the monoclinic variety, however, were very small, weighing $^1/_{10}$ mgm. or less. Though this size was sufficient for measurements on the magnetic anisotropy, i. e., the differences between the principal susceptibilities, of the crystals, the absolute value of any of these susceptibilities could not be measured by the usual methods. A simple method applicable to such small crystals is also described in the paper

1) Nature **132** (1933) 750.
2) Z. Kristallogr. **91** (1935) 173.
3) Phil. Trans. Roy. Soc. London (A) **231** (1933) 235.

2. Measurement of Magnetic Anisotropy.

The magnetic measurements on the crystals consist of

1) the location of the principal magnetic axes;
2) the determination of the magnetic anisotropy of the crystals, i. e., the differences between the three principal susceptibilities; and
3) the measurement of the absolute susceptibility along any one convenient direction in the crystal.

For (1) and (2) the methods adopted in the present paper are the same as those described in our recent publications[1]). For the orthorhombic variety, the magnetic axes are of course the crystallographic axes. We shall denote the gram molecular susceptibilities along them by χ_a, χ_b and χ_c respectively. For the monoclinic variety, the b axis is naturally one of the magnetic axes, and the positions of the two axes in the (010) plane are located by finding the orientation which the crystal takes up in a uniform horizontal magnetic field when suspended with its b axis vertical. Let us denote the maximum and the minimum gram molecular susceptibilities in the (010) plane by χ_1 and χ_2 respectively, and the susceptibility along the b axis by χ_3. Suppose further that the χ_1-axis is inclined at an angle ψ to the c axis and $\beta - \psi$ to the a axis.

The differences between the principal susceptibilities are measured as follows. The crystal is suitably suspended in a uniform horizontal magnetic field at the end of a calibrated, long, thin quartz fibre, the upper end of which is fixed to the axis of a graduated torsion-head. The crystal is allowed to take up its equilibrium orientation in the field, under zero torsion of the fibre. If the torsion-head is now slowly rotated through an angle α, the crystal will rotate in the same direction, but through a smaller angle φ. The couple acting on the crystal tending to restore it to its original orientation would be equal to $\frac{1}{2} m/M \, \Delta\chi H^2 \sin 2\varphi$, where m is the mass of the crystal, H is the field, $\Delta\chi$ is the difference between the maximum and the minimum gram molecular susceptibilities of the crystal in the horizontal plane, and M is the molecular weight. This couple is balanced by that due to the torsion of the fibre, viz., $c(\alpha - \varphi)$, where c is the torsional constant of the fibre. As the torsion-head is rotated further, there will come a stage when φ just reaches the value $\pi/4$ (the corresponding value of α being α_c, say), and the couple due to the magnetic field reaches its maximum value. Equating the opposing couples acting on the crystal in this position, we obtain

$$c(\alpha_c - \pi/4) = \tfrac{1}{2} m/M \, \Delta\chi H^2 . \qquad (1)$$

1) Phil. Trans. Roy. Soc. London (A) 231 (1933) 235.

With the slightest further rotation of the torsion-head, the crystal will naturally yield and turn round. On this property is based an accurate measurement of α_c, which, by relation (1), enables us to determine $\Delta\chi$, since the other quantities appearing in (1) are known. In practice $2\alpha_c$ is measured directly by finding the two critical positions of the torsion-head, obtained by clockwise and anti-clockwise rotations of the torsion-head from its initial position.

The measurement of $\Delta\chi$ for any two different suspensions of the crystal gives us $\chi_a - \chi_b$ and $\chi_a - \chi_c$, or $\chi_1 - \chi_2$ and $\chi_1 - \chi_3$.

3. Magnetic Anisotropy of Crystals of 1.2; 5.6-Dibenzanthracene.

The results of the measurements on the magnetic anisotropy of crystals of 1.2; 5.6-dibenzanthracene, of both the monoclinic and the orthorhombic varieties, are given in the following table. The results on the monoclinic crystals, which are not well developed, and which, being flaky, are liable to easy distortion, are not so accurate as those for the orthorhombic crystals.

Table I. The unit for the χ's $= 10^{-6}$ c. g. s. e. m. u.

Crystallographic data	Mode of suspension	Orientation in the field	$\lvert\Delta\chi\rvert$	Magnetic anisotropy
1. Orthorhombic bipyramidal	a ax. vert.	b ax. along field	189	$\chi_a - \chi_c = 130$
$a:b:c$	b " "	a " " "	130	$-\chi_b - \chi_c = 189$
$= .755 : 1 : .546$	c " "	b " " "	59	Calculated $\Delta\chi = 59$
2. Monoclinic	b ax. vert.	(001) plane normal to field	40	$\chi_1 - \chi_2 = 40$
$a = 6.59$ Å				$\chi_1 - \chi_3 = 200$
$b = 7.84$				$\psi = +13°.5$
$c = 14.17$	a ax. vert.	b ax. normal to field	200	
$\beta = 103°.5$	(001) pl. horiz.	b " " " "	160	Calculated $\Delta\chi = 160$

4. Absolute Susceptibilities.

Knowing the anisotropy of the crystal, if now we measure the absolute susceptibility along any one convenient direction in the crystal, its three principal susceptibilities are known. The method adopted for this measurement in our previous papers is as follows. The crystal is suspended suitably at the end of a long, thin quartz fibre, in an inhomogeneous magnetic field, such as obtains between the conical pole-pieces of an electro-magnet. The crystal is kept surrounded by an aqueous solution of some suitable substance, whose susceptibility can be adjusted by

changing the concentration. When the field is put on, the crystal turns round so as to bring the direction of maximum susceptibility in the horizontal plane, along the field; the crystal has, in general, a lateral motion also, along the direction of the gradient of the field. The susceptibility of the bath is now adjusted, by suitably changing its concentration, until there is no such lateral motion. When this condition is secured, the volume susceptibility of the crystal along the direction of the field (i. e., the maximum volume susceptibility of the crystal in the horizontal plane) should evidently be the same as the volume susceptibility of the bath. The latter is readily measured by the usual Gouy or other methods.

In the above experiment, when the crystal is very small, say less than one mgm., it is in the first place difficult to keep the fibre taut; secondly the mass of the shellac used as cement for attaching the crystal to the fibre, which, with large-sized crystals, is quite negligible, is no more so, and the lateral motion in the magnetic field is affected thereby. This difficulty is not so serious in the measurement of anisotropy since the shellac is more or less isotropic magnetically.

If in this arrangement the solution has the same density as the crystal, the quartz suspension is evidently unnecessary, and we can use very small crystals. Two aqueous solutions are prepared, of the same density as the crystal, one diamagnetic, of potassium bromide, and the other paramagnetic, of a mixture of potassium bromide and a small quantity of nickel chloride. A suitable mixture of these two solutions is kept in a thin-walled tube of about 2 mm. bore, and a few well-developed crystals are dispersed in the solution. The tube is placed between the conical pole-pieces of the magnet and adjusted so as to bring one of the crystals to a position slightly below the central axis of the magnet equidistant from the two pole-pieces. The crystal is kept under observation through a tele-microscope. When the field is put on, the crystal brings its principal axis of maximum susceptibility along the field, and moves laterally also, either up or down depending on whether the above principal susceptibility of the crystal per unit volume is greater or less than that of the mixture. The relative proportions of the two solutions which constitute the mixture are now adjusted until there is no such lateral movement in the field. The maximum volume susceptibility of the crystal will then evidently be the same as that of the solution.

With flakes of the monoclinic dibenzanthracene weighing about $^1/_{50}$ mgm. it was possible by this method to determine the susceptibility along the normal to the flake (axis of maximum susceptibility of the crystal).

The results of the absolute measurements are given in Table II.

Table II.

Crystal variety	Direction along which suscep. was measured	Vol. suscep.	Density	Corresponding gm. mol. suscep.
1. Orthorhombic	Along b axis	-0.507	1.277	$\chi_b = -110$
2. Monoclinic	Along χ_1 — axis	-0.50	1.27	$\chi_1 = -109$

Combining these results with those obtained for the anisotropy in the previous section, we obtain the following values for the principal gm. mol. susceptibilities of the two crystals.

1. Orthorhombic variety.

$\chi_a = -169 \quad \chi_b = -110 \quad \chi_c = -299 \quad$ Mean $\chi = -193.$

2. Monoclinic variety.

$\chi_1 = -109 \quad \chi_2 = -150 \quad \chi_3 = -310 \quad \psi = +13°.5 \quad$ Mean $\chi = -190.$

The mean susceptibility is practically the same for the two crystals, as we should expect. (The small apparent difference is within the limits of experimental error in the measurement of the anisotropy of the monoclinic crystals, which were poorly developed.)

5. Molecular Orientation in the Crystals.

As was mentioned in the introduction, the structure of the monoclinic crystal has been analyzed by Iball and Robertson. The crystal belongs to the space-group C_{2h}^2 or C_2^2, with two molecules in the unit cell. The

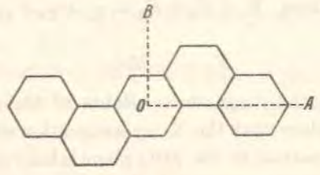

Fig. 1.

benzene rings have most probably a plane regular hexagonal structure as shown in the figure. Let us call for convenience the line OA, joining the centres of the 1st, 3rd and 5th benzene rings, as the length of the molecule, and the line OB, perpendicular to OA in the plane of the molecule, as its

width. Iball and Robertson find that the lengths of the molecules in the unit cell are nearly perpendicular to the (001) plane, and that the planes of the molecules are near to (010).

We shall now consider the evidence from the magnetic data regarding the orientations of the molecules. The three magnetic axes of the molecule may be taken to be along OA, OB, and the normal to the molecular plane, respectively. Let the susceptibilities of the molecule along these directions be K_1, K_2, and K_3 respectively per gram. molecule.

More or less complete X-ray structural analyses by the Fourier method have recently been made by Robertson[1]) of anthracene and naphthalene crystals, and by Iball[2]) of chrysene. Magnetic measurements also have been made on these crystals. From these magnetic data we can obtain by a direct calculation, on the basis of the molecular orientations in the crystals given by the X-ray analyses, the principal susceptibilities of these molecules. We thus find that for all the three molecules the two principal susceptibilities in the molecular plane are nearly equal (and numerically much smaller than the third). As we have shown in a recent paper[3]), this result is very probably true of other molecules also containing condensed benzene rings. We may therefore take for the dibenzanthracene molecule the two susceptibilities in its plane to be equal, and put $K_1 = K_2$.

Regarding the actual value of K_1, we may immediately mention that it can not be numerically greater than the lowest susceptibility for the crystal, namely -110. It can not also be numerically much less than -110, since for the chrysene molecule, which has one benzene ring less, $K_1 = -88$. We can therefore take for the dibenzanthracene molecule

$$K_1 = K_2 = -110,$$

and from the relation $K_1+K_2+K_3 = \chi_a+\chi_b+\chi_c$ (or $\chi_1+\chi_2+\chi_3$), obtain

$$K_3 = -358.$$

Coming now to the magnetic constants of the monoclinic crystal, we find in the first place that the X-ray assignation of the lengths of the molecules along the normal to the (001) plane is fully confirmed, since this direction is one of the magnetic axes of the crystal, namely the χ_1-axis, and the susceptibility along this direction is equal to K_1. Secondly, the susceptibility of the crystal along the b axis, namely χ_3, is numerically

1) Proc. Roy. Soc. London (A) 140 (1933) 79, and 142 (1933) 674.
2) Proc. Roy. Soc. London (A) 146 (1934) 140.
3) In course of publication in Phil. Trans. Roy. Soc. London (A) [No. 739].

much greater than either χ_1 or χ_2, confirming the other conclusion of Iball and Robertson, namely that the molecular planes should lie near to the (010) plane.

The magnetic data enable us further to find the actual inclinations of the molecular planes to (010). Let these inclinations for the two molecules in the unit cell be plus and minus λ respectively. Then we have the evident relations

$$\left.\begin{aligned}\chi_3 &= K_3\cos^2\lambda + K_2\sin^2\lambda\\ \chi_2 &= K_3\sin^2\lambda + K_2\cos^2\lambda\end{aligned}\right\} \quad (2)$$

$$\therefore \lambda = \tfrac{1}{2}\arccos(\chi_2-\chi_3)/(K_2-K_3), \quad (3)$$

from which, by substituting the proper values for the K's and the χ's, we obtain $\lambda = 25°$.

For the monoclinic crystal we thus find from the magnetic data that the lengths of both the molecules in the unit cell lie in the (010) plane at 90° to the a axis, and that the molecular planes are inclined at $+25°$ and $-25°$ respectively, to the (010) plane.

6. Molecular Orientations in the Orthorhombic Crystal.

For the orthorhombic crystal also the molecular orientations can be determined from the magnetic data in the same manner. The observation that χ_b has nearly the same value as K_1 or K_2 suggests immediately that either the lengths OA of the molecules in the unit cell, or their widhts OB, should lie along the b axis. The further observation that the b axis is the direction of vibration of the slow ray shows that it must be the lengths of the molecules that lie along b. Considering next the molecular planes, it is easy to show, by adopting the same argument as before, that they must be inclined to the (001) plane of the crystal at plus and minus $\frac{1}{2}\arccos(\chi_a-\chi_c)/(K_2-K_3) = 29°$.

Thus in the orthorhombic crystal, the lengths of the molecules in the unit cell lie along the b axis, and the molecular planes are inclined at $\pm 29°$ to the (001) plane.

7. Optical Evidence for these Molecular Orientations.

For the monoclinic crystal Bernal[1]) has shown that the optic axial plane is nearly or exactly perpendicular to the a axis, and that the α-vibration is along b, as should be expected from the above molecular orientations.

1) Nature 132 (1933) 751.

The observation by Mr. P. K. Seshan and one of us that the absorption bands of the monoclinic crystal are strongly polarized, light-vibrations along the b axis being much less absorbed than vibrations along the perpendicular directions[1]), is also consistent with the nearness of the molecular planes to the (010) plane.

In the orthorhombic crystal the α-vibration direction is along the c axis, and γ along b. The absorption bands are strongly polarized, being much weaker when the light-vibrations are along the c axis than when they are along directions in the (001) plane. These observations are in agreement with what we should expect from the molecular orientations arrived at from the magnetic data.

Summary.

An account is given of some magnetic measurements on crystals of 1.2; 5.6-dibenzanthracene, of both the monoclinic and the orthorhombic varieties. A simple and convenient method of measuring the susceptibilities of very small crystals is described.

The magnetic data are discussed in relation to the structure of the crystals, and the probable orientations of the molecules in the unit cell are deduced from the magnetic data. It is thus found that in the monoclinic crystal the lengths of the molecules are perpendicular to the (001) plane, and the molecular planes are inclined at $+25°$ and $-25°$ respectively to (010). In the orthorhombic crystal, the lengths of the molecules are along the b axis, and the molecular planes are inclined at $\pm 29°$ to the (001) plane.

The optical data for the crystals, and the observed polarization of the absorption bands, are in conformity with the molecular orientations suggested.

1) Current Science, **3** (1934) 26.

Received 17th May 1935.

THE ENTROPY OF MANGANOUS AMMONIUM SULPHATE AT TEMPERATURES CLOSE TO ABSOLUTE ZERO, IN RELATION TO THE MAGNETIC ANISOTROPY OF THE SALT AT ROOM TEMPERATURES.

By K. S. Krishnan
and
S. Banerjee,
Indian Association for the Cultivation of Science, Calcutta.

Received June 18, 1935.

In a recent paper on the production of very low temperatures by the adiabatic demagnetization method of Debye and Giauque, Kürti and Simon[1] obtain the following important result. If T_i be the initial temperature and H_i the magnetizing field, and if T_f be the final temperature obtained by adiabatically demagnetizing the salt to zero field, then

$$\frac{T_f}{T_i} = \frac{E_m}{E_i} = \frac{k\theta_m}{H_i g\beta}, \qquad \ldots \quad (1)$$

where E_i is the difference in energy between the adjacent m-levels split by the magnetic field H_i; $E_i = H_i g\beta$, g being the Landé factor and β the Bohr magneton. E_m is a certain small energy, characteristic of the crystal in zero magnetic field, which will be of the order of magnitude of the Stark-splitting of the energy levels of the paramagnetic ion under the crystalline fields. The corresponding *characteristic temperature* θ_m is defined by the relation

$$k\theta_m = E_m, \qquad \ldots \quad (2)$$

in which k is the Boltzmann constant. If we assume that the crystalline Stark-splitting is into $(2J+1)$ equally spaced energy levels, then $k\theta_m$ would be the energy difference between adjacent levels.

θ_m is thus an important constant, which determines the deviation of the magnetic entropy of the crystal from its ideal value of $R \log_e (2J+1)$, and therefore defines the entropy-temperature curve at these temperatures. Any method that would enable us to calculate θ_m would therefore be of great interest. Its calculation from the actual Stark-splitting is not easy, since we do not have, at present, sufficient knowledge of either the magnitude

1 *Proc. Roy. Soc.* (A), 1935, 149, 152.

or the dissymmetry of the crystalline fields. Kürti and Simon[2] have suggested an indirect method of calculating θ_m, namely, from the anomaly of the specific heat of the crystal, which begins to appear at temperatures considerably higher than θ_m. For example from measurements on the specific heat of gadolinium sulphate in the range 2°–5° K, they were able to calculate the value of its θ_m, which has since been verified by direct demagnetization experiments on the substance.

The purpose of the present note is to draw attention to another and more convenient method of calculating θ_m, namely from measurements on the magnetic anisotropy of the crystal at *room temperatures*. Let us take as an example the well-known monoclinic Tutton salt $MnSO_4.(NH_4)_2SO_4.6H_2O$. Though, to a first approximation, the crystal is magnetically isotropic and its susceptibility obeys the Curie law, as we should expect from the circumstance that the ground state of the Mn^{++} ion is an S-state ($^6S_{5/2}$), careful measurements reveal a feeble anisotropy.[3] A small part of this anisotropy is that of its diamagnetism, which will be practically the same as that of the isomorphous diamagnetic Tutton crystal obtained by replacing the Mn by Mg or Zn ; it can therefore be corrected for. Another small correction also is necessary, namely, for the anisotropy of the Lorentz-Poisson magnetic polarisation field acting on the Mn^{++} ions in the crystal, the anisotropy being due to the non-cubic distribution of these ions. The residual anisotropy of the manganous salt, after making these two corrections, should evidently be attributed to the feeble Stark-splitting of the S-levels of Mn^{++} in the crystal, *i.e.*, to the same mechanism which is responsible for the diminution of the entropy of the crystal near absolute zero.

This residual anisotropy (due to the Stark-splitting) implies, according to Van Vleck and Penney,[4] a small deviation of the principal susceptibilities of the crystal from the Curie law, the susceptibilities being given by the expressions, of the Weiss type,

$$\chi_1 = \frac{C}{T-\Delta_1}, \chi_2 = \frac{C}{T-\Delta_2}, \chi_3 = \frac{C}{T-\Delta_3}; \quad .. \quad (3)$$

$$\Delta_1 + \Delta_2 + \Delta_3 = 0. \quad .. \quad .. \quad .. \quad .. \quad (4)$$

For manganous ammonium sulphate, taking χ_1 and χ_2 to denote the susceptibilities in the (010) plane, χ_3 that along the 'b' axis, and χ the mean susceptibility, we find experimentally that, at 30° C.,

[2] *Naturwiss.*, 1933, 21, 178.

[3] *Phil. Trans.* (A), 1933, 232, 99.

[4] *Phil. Mag.*, 1934, 17, 961.

$$\left.\begin{aligned}\frac{\Delta_1-\Delta_2}{T} &= \frac{\chi_1-\chi_2}{\chi} = \frac{8}{14{,}000}\\ \frac{\Delta_1-\Delta_3}{T} &= \frac{\chi_1-\chi_3}{\chi} = \frac{6}{14{,}000}\end{aligned}\right\}, \quad .. \quad .. \quad .. \quad (5)$$

from which we obtain

$$\Delta_1 = 0{\cdot}10°,\ \Delta_2 = -0{\cdot}07°,\ \Delta_3 = -0{\cdot}03°\ \text{K}. \quad .. \quad (6)$$

Thus the effect of the Stark-splitting on the magnetic behaviour of the crystal is equivalent to that of feeble magnetic fields of the Weiss type.

For temperatures below Δ_1, the corresponding Weiss field may be taken, as usual, to be equal to

$$H_f = \frac{3k\,\Delta_1}{\mu}, \quad .. \quad .. \quad .. \quad .. \quad .. \quad (7)$$

where $\mu = g\beta\sqrt{s(s+1)}$ is the magnetic moment of the ion.

We shall now assume that, just as the influence of the crystalline fields on the magnetic behaviour of the crystal at room temperatures can be treated as being equal to the effect of a certain Weiss magnetic field, the effect of the crystalline fields in orienting the magnetic moments, and thus diminishing the entropy of the crystal at the low temperatures we are considering, would also be equivalent to the effect of the appropriate Weiss field, H_f.

In the adiabatic demagnetization experiment then, just as the entropy under the initial conditions is that of practically free Mn^{++} ions at temperature T_i placed in a magnetic field[5] H_i, the entropy of the crystal at the final temperature T_f under zero external magnetic field would be that of *free* Mn^{++} ions at temperature T_f placed in a magnetic field H_f. Since in the experiment the two entropies should be equal, we obtain

$$\frac{T_f}{T_i} = \frac{H_f}{H_i} = \frac{3k\,\Delta_1}{H_i\,g\beta\sqrt{s\,(s+1)}}, \quad .. \quad .. \quad .. \quad (8)$$

which is very similar to Kürti and Simon's expression [see (1)]

$$\frac{T_f}{T_i} = \frac{k\,\theta_m}{H_i g\beta} \quad .. \quad .. \quad .. \quad .. \quad .. \quad (9)$$

By comparing the two expressions, we obtain for the characteristic temperature of manganous ammonium sulphate[6]

$$\theta_m = \frac{3\Delta_1}{\sqrt{35/2}\times 7/2} = 0{\cdot}10°\ \text{K}\ (0{\cdot}07\ \text{cm.}^{-1}), \quad .. \quad .. \quad (10)$$

which agrees well with Kürti and Simon's value 0·11° K.

[5] At the initial temperature the influence of the crystalline field on the magnetic entropy would be very small in comparison with that of the applied magnetic field.

[6] The Weiss field H_f for the crystal, at these low temperatures, is found to be about 760 gauss.

The Entropy of Manganous Ammonium Sulphate

Conversely, this agreement may be taken to justify our assumption that the effect of the crystalline field at these low temperatures in orienting the magnetic moments and thus producing a diminution of entropy, is equivalent to the effect of the appropriate Weiss field H_f supposed to act on these moments, which are taken to be otherwise free.

Thus solely from measurements on the magnetic anisotropy of the crystal at room temperatures which can be easily made, it is possible to predict the entropy-temperature curve close to the absolute zero, which (curve) plays an important part in discussions on the production of these low temperatures by adiabatic demagnetization of paramagnetic crystals, and also on their specific heats in this and the neighbouring regions.

GRAPHITE crystal (which is hexagonal and has a perfect basal cleavage) exhibits remarkable magnetic and electrical properties. Its diamagne ic susceptibility[1] along the vertical axis is abnormally large, about -22×10^{-6} pergm., while for directions in the basal plane it is practically the same as that of diamond, *viz.*, $-0{\cdot}5\times10^{-6}$. Electrically, the crystal is a good conductor for directions in the basal plane. These abnormal properties may be traced to the peculiar structure of the crystal. While the three equivalent linkages of the carbon atom in the basal plane of the crystal are homopolar, the fourth weak linkage, which binds the widely separated successive layers of carbon atoms, is generally regarded as "metallic". If the large displacements of these "metallic" electrons under the influence of electric and magnetic fields are confined predominantly to the basal plane, the electrical conductivity along the plane, and the abnormal susceptibility for magnetic fields incident along the normal to the plane, receive a natural explanation.

The "swelling" of graphite to "blue graphite" (as also its further oxidation to graphitic oxide) is generally regarded as corresponding to the adsorption of oxygen atoms between the carbon layers, the metallic linkages being broken thereby.[2] We should therefore expect both the conductivity and the abnormal diamagnetism to disappear on "swelling". It is known that the oxidation of graphite destroys its conductivity. Its effect on the abnormal diamagnetism does not seem to have been studied.

A small single crystal of graphite was treated with a mixture of concentrated nitric and sulphuric acids for about 12 hours. The resulting "blue graphite" was washed in running water for over 12 hours and dried in a desiccator. The specimen had the same hexagonal shape as the original graphite piece, and was also found to be roughly a single crystal, as tested by its X-ray diffraction. On measuring its principal diamagnetic susceptibilities it was found that

(1) for directions in the basal plane, its specific susceptibility is practically the same as that of untreated graphite;

(2) on the other hand the magnetic anisotropy, *i.e.*, the difference $\Delta\chi$ between the two principal susceptibilities, which is as high as 22×10^{-6} per gm. in untreated graphite, is now diminished to about $1{\cdot}3\times10^{-6}$ per gm. of carbon; *i.e.*, the abnormal diamagnetism of graphite along its 'c' axis is almost completely destroyed by the "swelling".

It is significant that the above value for the magnetic anisotropy of oxidised graphite is of the same magnitude as in compounds containing condensed benzene nuclei, *e.g.*, pyrene, for which $\Delta\chi=1{\cdot}2\times10^{-6}$ per gm. content of carbon.

Further it is known that as the size of the graphite particle is continually diminished (to that corresponding to "amorphous" carbon), the distance between the successive layers of carbon increases correspondingly. This has been taken by Randall and Rooksby[3] to indicate a weakening of the metallic valency bonds of the carbons. In that case the diminution in the diamagnetism of graphite powder with the particle size, observed by Honda, Paramasivan and others, would be a natural consequence. In this connection the following observation is of interest. Some preliminary measurements made by us on the principal susceptibilities of crystallites of graphite show that, while the susceptibility along directions in the basal plane is practically independent of particle size, and has a constant value near about $-0{\cdot}5\times10^{-6}$, it is the susceptibility along the 'c' axis, which is abnormal in large crystals, which diminishes with decreasing particle size.

K. S. KRISHNAN.
N. GANGULI.

210, Bowbazar Street,
Calcutta,
March 27, 1935.

[1] Guha and Roy, *Ind. Jour. Phys.*, 1934, **8**, 349.
[2] Hoffmann, *Koll. Zeits.*, 1932, **61**, 297. See also Desch, *Chemistry of Solids*, 1934, p. 180.
[3] See Randall, *Diffraction of X-rays*, London, 1934, p. 192.

A Simple Method for Studying the Magnetic Susceptibilities of Very Small Crystals.

In connection with some magnetic measurements on organic crystals we had occasionally to work with crystals weighing a tenth of a milligram or less. The magnetic anisotropy of these crystals is not difficult to measure.[1] For the measurement of any of the principal susceptibilities of these crystals, however, the usual methods are not applicable. The following simple arrangement, which we have been using for susceptibility measurements with such small crystals, may therefore be of interest.

Two aqueous solutions are prepared, one diamagnetic and the other paramagnetic with respect to the crystal, both having the same density as the crystal. A suitable mixture of the two solutions is kept in a thin-walled tube of about 2 mm. bore, and a few well-developed crystals are dispersed in the liquid. The tube is placed in the strongly inhomogeneous magnetic field obtaining between the usual conical pole-pieces of an electromagnet, and is adjusted so as to bring one of the crystals to a position slightly below the central axis of the field, equidistant from the two pole-pieces. Watching the crystal through a low-power microscope, and putting on the field, we find that the crystal turns round so as to place its axis of maximum susceptibility along the field, and in general moves laterally also, along the direction of the field-gradient. The relative proportions of the two solutions which make up the mixture are now adjusted such that there is no such *lateral* movement of the crystal in the field. The *maximum* susceptibility of the crystal *per unit volume* should then be the same as that of the mixture. The susceptibility of the latter is easily measured.

By changing the inhomogeneous field to a uniform one, and studying the orientations which the crystal takes up, for different initial (*i.e.*, in zero field) orientations, the directions of the principal magnetic axes of the crystal can, of course, be easily located, and the differences between the susceptibilities along these axes studied *qualitatively*.

K. S. Krishnan.
S. Banerjee.

210, Bowbazar Street,
Calcutta,
May, 2, 1935.

[1] Krishnan and Banerjee, *Phil. Trans.* A., 1935.

X—Investigations on Magne-Crystallic Action

IV—Magnetic Behaviour of Paramagnetic Ions in the S-State in Crystals

By K. S. Krishnan and S. Banerjee

(Communicated by Sir Venkata Raman, F.R.S.—Received September 10, 1935.)

Contents

I—Introduction

In Part II* of this paper we gave an account of measurements on the principal susceptibilities of some paramagnetic sulphates and double-sulphates of the iron group of metals. In view of the interest which the subject of crystal magnetism has acquired by the recent theoretical publications of Bethe, Kramers, Van Vleck,

* 'Phil. Trans.,' A, vol. 232, p. 99 (1933). We wish to correct here some errors that appear in in the earlier Parts. In Part I the principal susceptibilities of naphthalene and anthracene should be as follows:

	$-\chi_1$	$-\chi_2$	$-\chi_3$	ψ
Naphthalene	56·0	146·4	76·6	12°·0
Anthracene	75·5	211·8	102·9	8°·0

In Part III, Table I, the value of θ for phenanthrene should read $-11°{\cdot}4$ instead of $+11°{\cdot}4$, and ψ should be equal to $+19°{\cdot}7$.

Penney, and others, further extensive studies on paramagnetic crystals were undertaken. The present part of the paper deals with crystals in which the paramagnetic ions are all in the S-state, which are of special interest. Magnetic studies on the other crystals will be described in a later paper.

II—Van Vleck's Theory

Bethe and Kramers have discussed theoretically the problem of the Stark splitting of the energy-levels of an atom or ion under the influence of crystalline fields. On the basis of their results, Van Vleck, Penney, and Schlapp* have developed a general theory of the magnetic properties of paramagnetic crystals, which explains satisfactorily (1) the relative contributions of the orbital and spin moments to the susceptibility, (2) the magnetic anisotropy of the crystals, and (3) the temperature variation of their principal susceptibilities.

The theory is somewhat as follows. Consider an assemblage of *free* paramagnetic ions having an angular momentum J. In zero magnetic field, the $(2J + 1)$ *m*-states of the ion will naturally all have the same energy. On the application of a magnetic field the degeneracy will be completely removed, *i.e.*, the different *m*-states will split up, the distribution of the ions among these states will become unequal, and the ions will, in consequence, have a resultant magnetic moment along the field. This accounts for their paramagnetism. If, however, the ions had not been free, but had been under the influence of strong asymmetric crystalline electric fields, the degeneracy in respect of the *orbital* moments of the ions would already have been removed by these fields. If, further, the corresponding energy separations of the levels were large compared with kT, the distribution of the ions among these levels will remain practically unaffected by the application of the magnetic field, and there will thus be no contribution from the orbital moments to the effective magnetic moments of the ions.

The *spin* moments, on the other hand, are not affected directly by the crystalline fields, though indirectly they would be, through their coupling with the orbital moments. The latter having been frozen, the coupling of the spins with them would be equivalent to subjecting the spins to local fields, which, because of the asymmetry of the crystalline fields responsible for the freezing of the orbital moments, would also be asymmetric. The result would be: (1) the crystal would exhibit a magnetic anisotropy, (2) the temperature variation of its principal susceptibilities would deviate from the Curie law.

III—Theory Applied to Ions in the S-State

If thus the anisotropy of the crystal and the deviations from the Curie law arise from the coupling of the spins with orbital moments which have been frozen by asymmetric crystalline fields, then both these effects should disappear when the orbital

* *See* Van Vleck, "Theory of Electric and Magnetic Susceptibilities" (Oxford, 1932), chap. xi.

moments are zero, *i.e.*, when the paramagnetic ions are in the S-state. That is, (1) crystals whose paramagnetic ions are in the S-state should be more or less isotropic magnetically, even when the crystals do not belong to the cubic system. This result has been verified by Rabi* and by Jackson† with single crystals of manganous and ferric salts (the ground state for both Mn^{++} and Fe^{+++} ions is $^6S_{5/2}$), for which they find that the three principal susceptibilities do not differ from one another by more than one per cent. (2) The susceptibility should follow the simple Curie law. This result also has been verified for manganous and ferric ions, in the crystal state by Jackson (*loc. cit.*), and in state of solution by A. Bose.‡

IV—Magnetic Anisotropy of S-State Ions

More accurate measurements, however, show that manganous salts do have a definite, though very small, magnetic anisotropy,§ and its explanation offers many points of interest. As we shall show in this paper, a small part of the anisotropy is that of the diamagnetism of the salt, and another part, which should be even smaller, may arise from the mutual influence of the magnetic moments of the Mn^{++} ions. The rest of the anisotropy should be attributed to the following cause: though, as we mentioned in the previous section, the S-levels, to a first approximation, are not affected by the crystalline electric fields, Kramers has shown that when higher order approximations are considered, even the S-levels have a feebly separated Stark multiplet structure; this will naturally lead to an anisotropy, as in other paramagnetic crystals, but of course very much feebler.

If then from the observed anisotropy we can separate the small contributions from the first two causes, and obtain that due to the Stark splitting alone, we can use it to calculate the magnitude of the splitting. This will be of great interest in view of the important part played by this splitting at temperatures close to absolute zero, especially since we do not, at present, possess enough knowledge of either the magnitude or the asymmetry of crystalline fields to be able to calculate the Stark splitting directly.

The present paper concerns itself with a detailed study of the magnetic anisotropy of single crystals of manganous and ferric salts. The different causes which contribute to the anisotropy are discussed, and methods are devised for separating their effects. The anisotropy due to crystalline Stark splitting alone is thus obtained, and the magnitude of the splitting is calculated therefrom. The result is discussed in relation to the entropy and the specific heat of the salt at very low temperatures, and in relation to other physical phenomena that are influenced by the splitting.

* 'Phys. Rev.,' vol. 29, p. 174 (1927).

† 'Proc. Roy. Soc.,' A, vol. 140, p. 695 (1933).

‡ 'Nature,' vol. 133, p. 213 (1934); 'Proc. Ind. Acad. Sci.,' A, vol. 1, pp. 605, 753 (1935).

§ *See* Part II of this paper, 'Phil. Trans.,' A, vol. 232, pp. 105–109 (1933). The values for the magnetic anisotropy of manganous ammonium sulphate crystal given in Part II are too high. *See* Table I of the present paper.

V—Measurements on Manganous and Ferric Salts

We shall first explain the notation adopted in this paper. All the crystals studied were monoclinic. The two principal gram molecular susceptibilities of the crystal in the (010) plane are denoted by χ_1 and χ_2 respectively, χ_1 being greater than χ_2. The third susceptibility, viz., that along the "*b*" axis, is denoted by χ_3. The χ_1- axis is inclined at an angle ψ to the "*c*" axis and at $\beta - \psi$ to the "*a*" axis, β being the obtuse angle between "*c*" and "*a*". Since the (001) faces of the crystals were well-developed, the inclination θ of the χ_2- axis to this face was sometimes directly measured, the positive direction of θ being defined by the relation $\pi/2 + \theta + \psi = \beta$ (obtuse).

The experimental method adopted in the following measurements is the same as that described in Part II of this paper for manganous ammonium sulphate. The measurements consist of two parts.

(1) *The Measurement of the Absolute Susceptibility Along any Convenient Direction in the Crystal*—The crystal is suspended, with its "*b*" axis vertical, at the end of a long, thin quartz fibre, so as to lie between the conical pole-pieces of a magnet, at the same height as the central axis of the magnet, but slightly to one side. The crystal is kept surrounded by a saturated aqueous solution of the substance, which holds in solution suitable amounts of manganous chloride as well. When the field is put on, the crystal turns round so as to bring its χ_1-axis along the field, and further moves laterally along the direction of the field-gradient, either towards the centre of the field or away from it depending on whether the *volume* susceptibility of the crystal along the χ_1-axis is greater or less than that of the liquid bath. Firstly, the torsion-head from which the crystal is suspended is suitably rotated so as to make the torsion on the fibre zero when the χ_1-axis is along the field. Secondly, the concentration of $MnCl_2$ in the bath is adjusted until there is no lateral motion of the crystal. Under these conditions the volume susceptibility of the crystal along the χ_1-axis is the same as that of the solution. The latter is measured by the well-known Gouy method by comparing the weight of the solution in a magnetic field, with that of a standard solution of $NiCl_2$ of known susceptibility in the same field.

(2) *Measurement of Anisotropy*—The conical pole-pieces are now replaced by the usual flat ones in order to obtain a large *uniform* field. The crystal is suspended as before with the "*b*" axis vertical, from the end of the fibre—which has now been calibrated—in the centre of the field ; further, it is kept surrounded by the liquid bath described in the previous paragraph, having the same volume susceptibility as the crystal. Before the field is put on, the torsion-head is suitably rotated in order that the (001) plane of the crystal (which is usually well developed*) may be exactly normal to the direction of the field. The field is now put on, and the direction in

* When any other vertical face (*h*0*l*) was better developed than (001), it was, of course, chosen as the reference plane in preference to (001).

which the crystal tends to rotate is noted—whether the "*c*" axis, which was originally at an angle of $\beta - \pi/2$ to the field, tends to move towards the field direction or away from it. The torsion-head is rotated in the opposite direction, through an angle α_1, say, so as to bring the (001) plane back to normality with the field. If the rotation of the torsion-head is continued in the same direction, there will come a stage when the χ_1 and χ_2 axes just make 45° with the field, and the couple due to the field is a maximum. With the smallest further rotation of the torsion-head, the crystal suddenly turns round. Let α_2 be the angle of rotation of the torsion-head from its initial position, necessary to bring it to the above critical position. Then from the relations

$$\sin 2\theta = \frac{\alpha_1}{\alpha_2 - \pi/4 + \theta}, \quad \ldots\ldots\ldots\ldots \quad (1)$$

and

$$\chi_1 - \chi_2 = \frac{2Mc}{mH^2}(\alpha_2 - \pi/4 + \theta), \quad \ldots\ldots\ldots \quad (2)$$

where c is the torsional constant of the fibre, H is the field, m is the mass of the crystal, and M is its gram molecular weight, both θ and $\chi_1 - \chi_2$ are known.

Measurement of $\Delta\chi$ for one other direction of suspension of the crystal enables us now to determine $\chi_1 - \chi_3$. Usually measurements were made for a third suspension also, so as to have a check on the values obtained.

VI—Results

The results of the measurements on anisotropy are given in Table I. In addition to the paramagnetic crystals, the isomorphous diamagnetic crystals obtained by replacing the Mn in them by Mg or Zn, and the Fe by Al, were also studied by us for their anisotropy. The magnetic data for the latter crystals also are included in Table I, and they are needed for correcting for the anisotropy of the diamagnetic part of the susceptibility of the former. Measurements on some mixed crystals are reported in Tables V and VI. All the measurements were made at room temperature, but, for the sake of uniformity, the results have all been reduced to 30° C. The susceptibilities are expressed in the usual unit, 10^{-6} c.g.s. e.m.u.

The measurements on the absolute susceptibilities of the paramagnetic crystals are given in Table II. In the last column of the table is given the magnetic moment of the Mn^{++} or Fe^{+++} ion in the crystal ; the mean susceptibility of the crystal, given in the penultimate column, was corrected for its diamagnetism, and from the corrected value the moment of the paramagnetic ion was calculated on the assumption that its susceptibility obeys the Curie law, which, as we have seen, is justified since both Mn^{++} and Fe^{+++} ions are in the S-state, viz., $^6S_{5/2}$. The theoretical value of the moment is 29·4 Weiss magnetons. Though the experimental values agree closely with this value, the small deviations that occur are consistently on one side, the experimental values being slightly lower. It is difficult to decide whether this

TABLE I

Serial number	Crystal	Crystallographic data	Mode of suspension	Orientation in the field	$\lvert\Delta\chi\rvert$	Magnetic anisotropy
1	2	3	4	5	6	7
1	$Mn(NH_4)_2(SO_4)_2 . 6H_2O$	Monoclinic prism $a:b:c$ $= 0{\cdot}740 : 1 : 0{\cdot}493$ $\beta = 106° 51'$	"b" axis vertical (001) plane horizontal	$\theta = +33°$ "a" axis normal to field	8·7 0·1	$\chi_1 - \chi_2 =$ 8·7 $\chi_1 - \chi_3 =$ 6·0 $\psi = -16°$
			"a" axis vertical	"b" „ „	3·5	Cal. $\Delta\chi =$ 3·4
2	$MnRb_2(SO_4)_2 . 6H_2O$	Monoclinic prism $a:b:c$ $= 0{\cdot}738 : 1 : 0{\cdot}495$ $\beta = 105° 57'$	"b" axis vertical (001) plane horizontal	$\theta = +28°$ "a" axis normal to field	8·9 0·7	$\chi_1 - \chi_2 =$ 8·9 $\chi_1 - \chi_3 =$ 6·2 $\psi = -12°$
			"a" axis vertical	"b" „ „	4·3	Cal. $\Delta\chi =$ 4·2
3	$MnCs_2(SO_4)_2 . 6H_2O$	Monoclinic prism $a:b:c$ $= 0{\cdot}727 : 1 : 0{\cdot}491$ $\beta = 107° 7'$	"b" axis vertical (001) plane horizontal	$\psi = -12\frac{1}{2}°$ "a" axis normal to field	7·0 0·3	$\chi_1 - \chi_2 =$ 7·0 $\chi_1 - \chi_3 =$ 5·0 $\psi = -12\frac{1}{2}°$
			"a" axis vertical	"b" „ „	3·1	Cal. $\Delta\chi =$ 3·3
4	$MnTl_2(SO_4)_2 . 6H_2O$	Monoclinic prism $a:b:c$ $= 0{\cdot}745 : 1 : 0{\cdot}496$ $\beta = 106° 22'$	"b" axis vertical (001) plane horizontal	$\theta = +33°$ "b" axis normal to field	8·9 0·9	$\chi_1 - \chi_2 =$ 8·9 $\chi_1 - \chi_3 =$ 7·2 $\psi = -16\frac{1}{2}°$
			"a" axis vertical	"b" „ „	4·7	Cal. $\Delta\chi =$ 4·6
5	$MnK_2(SO_4)_2 . 4H_2O$	Monoclinic prism $a:b:c$ $= 1{\cdot}032 : 1 : 1{\cdot}249$ $\beta = 95° 0'$ (does not belong to the Tutton series)	"b" axis vertical. (001) plane horizontal	$\theta = +66°$ "a" axis along field	4·3 0·8	$\chi_1 - \chi_2 =$ 4·3 $\chi_1 - \chi_3 =$ 1·5 $\psi = -61°$
			"a" axis vertical	"b" „ „	2·0	Cal, $\Delta\chi =$ 2·1
6	$Mn(NH_4)_2(SeO_4)_2 . 6H_2O$	Moniclinic prism $a:b:c$ $= 0{\cdot}743 : 1 : 0{\cdot}499$ $\beta = 106° 16'$	"b" axis vertical "a" „ (001) plane horizontal	$\psi = -20°$ "b" axis normal to field "b" „ „	8·9 3·2 0·6	$\chi_1 - \chi_2 =$ 8·9 $\chi_1 - \chi_3 =$ 6·3 $\psi = -20°$ Cal. $\Delta\chi =$ 0·5

TABLE I—(continued)

Serial number	Crystal	Crystallographic data	Mode of suspension	Orientation in the field	$\lvert\Delta\chi\rvert$	Magnetic anisotropy
1	2	3	4	5	6	7
7	$MnRb_2(SeO_4)_2 . 6H_2O$	Monoclinic prism $a:b:c$ $= 0{\cdot}742 : 1 : 0{\cdot}501$ $\beta = 105° 9'$	"b" axis vertical (001) plane horizontal	$\theta = +29°$ "b" axis normal to field	9·0 0·4	$\chi_1 - \chi_2 =$ 9·0 $\chi_1 - \chi_3 =$ 7·3 $\psi = -14°$
			"a" axis vertical	"b" „ „	5·2	Cal. $\Delta\chi =$ 5·2
8	$MnTl_2(SeO_4)_2 . 6H_2O$	Monoclinic prism $a:b:c$ $= 0{\cdot}746 : 1 : 0{\cdot}499$ $\beta = 105° 29'$	"b" axis vertical "a" „ (001) plane horizontal	$\theta = +29\frac{1}{2}°$ "b" axis normal to field "b" „ „	10·2 6·0 0·8	$\chi_1 - \chi_2 =$ 10·2 $\chi_1 - \chi_3 =$ 8·5 $\psi = -14°$ Cal. $\Delta\chi =$ 0·8
9	$K_3Fe(C_2O_4)_3 . 3H_2O$	Monoclinic prism $a:b:c$ $= 0{\cdot}992 : 1 : 0{\cdot}390$ $\beta = 94° 15'$	"b" axis vertical (10$\bar{1}$) plane horizontal both (10$\bar{1}$) and (010) planes vertical	(001) plane nearly along field and (10$\bar{1}$) at 73½° to it "b" axis normal to field "b" „ „	28 51 74	$\chi_1 - \chi_2 =$ 28 $\chi_1 - \chi_3 =$ 77 $\psi = -1°$ Cal. $\Delta\chi =$ 75
10	$Na_3Fe(C_2O_4)_3 . 5H_2O$	Monoclinic prism $a:b:c$ $= 1{\cdot}369 : 1 : 1{\cdot}201$ $\beta = 100° 15'$	"b" axis vertical (001) plane horizontal "a" axis vertical	$\theta = +12°$ "a" axis normal to field "b" „ „	31 6 22	$\chi_1 - \chi_2 =$ 31 $\chi_1 - \chi_3 =$ 24 $\psi = -2°$ Cal. $\Delta\chi =$ 23
	Diamagnetic crystals					
11	$Mg(NH_4)_2(SO_4)_2 . 6H_2O$	Monoclinic prism $a:b:c$ $= 0{\cdot}740 : 1 : 0{\cdot}492$ $\beta = 107° 6'$	"b" axis vertical (001) plane horizontal "a" axis vertical	$\theta = +22°$ "a" axis normal to field "b" „ „	1·1 0·3 0·6	$\chi_1 - \chi_2 =$ 1·1 $\chi_1 - \chi_3 =$ 0·6 $\psi = -5°$ Cal. $\Delta\chi =$ 0·4
12	$Zn(NH_4)_2(SO_4)_2 . 6H_2O$	Monoclinic prism $a:b:c$ $= 0{\cdot}737 : 1 : 0{\cdot}500$ $\beta = 106° 52'$	"b" axis vertical (001) plane horizontal "a" axis vertical	$\theta = +11°$ "a" axis normal to field "b" „ „	1·2 0·4 0·7	$\chi_1 - \chi_2 =$ 1·2 $\chi_1 - \chi_3 =$ 0·8 $\psi = +6°$ Cal. $\Delta\chi =$ 0·8

TABLE I—(continued)

Serial number	Crystal	Crystallographic data	Mode of suspension	Orientation in the field	$\lvert\Delta\chi\rvert$	Magnetic anisotropy
1	2	3	4	5	6	7
13	$MgRb_2(SO_4)_2 . 6H_2O$	Monoclinic prism	"b" axis vertical	$\theta = +3°$	0·9	$\chi_1 - \chi_2 =$ 0·9
		$a : b : c$	(001) plane horizontal	"a" axis normal to field	0·2	$\chi_1 - \chi_3 =$ 0·7
		$= 0·740 : 1 : 0·498$				$\psi = +13°$
		$\beta = 105° 59'$	"a" axis vertical	"b" " "	0·7	Cal. $\Delta\chi =$ 0·7
14	$ZnRb_2(SO_4)_2 . 6H_2O$	Monoclinic prism	"b" axis vertical	$\theta = -7\frac{1}{2}°$	0·9	$\chi_1 - \chi_2 =$ 0·9
		$a : b : c$	(001) plane horizontal	"a" axis normal to field	0·3	$\chi_1 - \chi_3 =$ 0·6
		$= 0·737 : 1 : 0·501$				$\psi = +23\frac{1}{2}°$
		$\beta = 105° 53'$	"a" axis vertical	"b" " "	0·6	Cal. $\Delta\chi =$ 0·6
15	$MgCs_2(SO_4)_2 . 6H_2O$	Monoclinic prism	"b" axis vertical	$\theta = -34°$	1·3	$\chi_1 - \chi_2 =$ 1·3
		$a : b : c$	(001) plane horizontal	"b" axis normal to field	0·1	$\chi_1 - \chi_3 =$ 1·0
		$= 0·728 : 1 : 0·495$				$\psi = +51°$
		$\beta = 107° 6'$	"a" axis vertical	"b" " "	0·5	Cal. $\Delta\chi =$ 0·6
16	$MgTl_2(SO_4)_2 . 6H_2O$	Monoclinic prism	"b" axis vertical	$\theta = +10\frac{1}{2}°$	0·8	$\chi_1 - \chi_2 =$ 0·8
		$a : b : c$	(001) plane horizontal	"b" axis normal to field	0·5	$\chi_1 - \chi_3 =$ 1·3
		$= 0·744 : 1 : 0·500$				$\psi = +6°$
		$\beta = 106° 30'$	"a" axis vertical	"b" " "	1·2	Cal. $\Delta\chi =$ 1·3
			"c" "	"b" " "	0·5	Cal. $\Delta\chi =$ 0·5
17	$MgK_2(SO_4)_2 . 6H_2O$	Monoclinic prism	"b" axis vertical	$\psi = -2°$	1·2	$\chi_1 - \chi_2 =$ 1·2
		$a : b : c$	(001) plane horizontal	"b" axis along field	0·4	$\chi_1 = \chi_3 =$ 0·7
		$= 0·741 : 1 : 0·499$				$\psi = -2°$
		$\beta = 104° 48'$	(100) "	"c" " "	0·7	Cal. $\Delta\chi =$ 0·7
18	$MgNa_2(SO_4)_2 . 4H_2O$ (Bloedite)	Monoclinic prism	"b" axis vertical	$\theta = -55°$	0·5	$\chi_1 - \chi_2 =$ 0·5
		$a : b : c$	"a" "	"b" axis normal to field	0·4	$\chi_1 - \chi_3 =$ 0·7
		$= 1·349 : 1 : 0·672$				$\psi = +66°$
		$\beta = 100° 48'$	(001) plane horizontal	"b" " "	0·6	Cal. $\Delta\chi =$ 0·5
		(does not belong to the Tutton series: isomorphous with $MnK_2(SO_4)_2 . 4H_2O$)				

TABLE I—(continued)

Serial number	Crystal	Crystallographic data	Mode of suspension	Orientation in the field	$\lvert\Delta\chi\rvert$	Magnetic anisotropy
1	2	3	4	5	6	7
19	$Mg(NH_4)_2(SeO_4)_2 . 6H_2O$	Monoclinic prism	"b" vertical	$\theta = +19\frac{1}{2}°$	1·5	$\chi_1 - \chi_2 =$ 1·5
		$a : b : c$	(001) plane horizontal	"a" axis normal to field	0·3	$\chi_1 - \chi_3 =$ 1·0
		$= 0·742 : 1 : 0·497$				$\psi = -3°$
		$\beta = 106° 27'$	"a" axis vertical	"b" " "	0·8	Cal. $\Delta\chi =$ 0·8
20	$MgRb_2(SeO_4)_2 . 6H_2O$	Monoclinic prism	"b" axis vertical	$\theta = +11°$	1·3	$\chi_1 - \chi_2 =$ 1·3
		$a : b : c$	(001) plane horizontal	"a" axis normal to field	0·2	$\chi_1 - \chi_3 =$ 1·1
		$= 0·742 : 1 : 0·501$				$\psi = +4°$
		$\beta = 105° 14'$	"a" axis vertical	"b" " "	1·0	Cal. $\Delta\chi =$ 1·1
21	$MgTl_2(SeO_4)_2 . 6H_2O$	Monoclinic prism	"b" axis vertical	$\theta = +16°$	2·0	$\chi_1 - \chi_2 =$ 2·0
		$a : b : c$	"a" "	"b" axis normal to field	2·4	$\chi_1 - \chi_3 =$ 2·6
		$= 0·749 : 1 : 0·499$				$\psi =$ 0
		$\beta = 105° 36'$	(001) plane horizontal	"b" " "	0·8	Cal. $\Delta\chi =$ 0·8
22	$K_3Al(C_2O_4)_3 . 3H_2O$	Monoclinic prism	"b" axis vertical	$\psi = +19°$	6·9	$\chi_1 - \chi_2 =$ 6·9
		$a : b : c$	(100) plane horizontal	"b" axis normal to field	12·4	$\chi_1 - \chi_3 =$ 13·1
		$= 0·999 : 1 : 0·395$				$\psi = +19°$
		$\beta = 92° 51'$	"c" axis vertical	"b" " "	6·9	Cal. $\Delta\chi =$ 6·9
23	$Na_3Al(C_2O_4)_3 . 5H_2O$	Monoclinic prism	"b" axis vertical	$\theta = +\frac{1}{2}°$	4·9	$\chi_1 - \chi_2 =$ 4·9
		$a : b : c$	"a" "	"b" axis normal to field	8·5	$\chi_1 - \chi_3 =$ 8 5
		$= 1·399 : 1 : 1·198$				$\psi = +9°$
		$\beta = 99° 28'$	(001) plane horizontal	"b" " "	3·6	Cal. $\Delta\chi =$ 3·6

TABLE II

Serial number	Crystal	Direction along which susceptibility was measured	Temp °C	Density of crystal	Vol. susceptibility	Corresponding gm mol susceptibility	Mean gm mol susceptibility at 30° C	Magnetic moment of Mn^{++} or Fe^{+++} in Weiss Magnetons
1	2	3	4	5	6	7	8	9
1	$Mn(NH_4)_2(SO_4)_2 . 6H_2O$	Along χ_1-axis	30·8	1·834	64·7	13,800	13,830	29·0
2	$MnRb_2(SO_4)_2 . 6H_2O$	" χ_1-axis	30·6	2·456	65·8	14,090	14,030	29·2
		" χ_1-axis	28·4	2·473	66·0	14,040		
3	$MnCs_2(SO_4)_2 . 6H_2O$	" χ_1-axis	24·0	2·762	62·5	14,050	13,820	29·0
		" χ_1-axis	21·6	2·734	62·8	14,270		
4	$MnTl_2(SO_4)_2 . 6H_2O$	" "a"-axis	32·3	3·42	61·8	13,800	13,910	29·1
5	$MnK_2(SO_4)_2 . 4H_2O$	" "b"-axis	29·6	2·330	81·1	13,820	13,830	29·0
6	$Mn(NH_4)_2(SeO_4)_2 . 6H_2O$	" χ_1-axis	30·9	2·123	60·4	13,800	13,840	29·0
7	$MnRb_2(SeO_4)_2 . 6H_2O$	" χ_1-axis	25·8	2·748	62·7	14,160	13,980	29·2
		" χ_1-axis	27·1	2·748	62·6	14,150		
8	$MnTl_2(SeO_4)_2 . 6H_2O$	" χ_1-axis	29·5	3·526	58·7	14,290	14,290	29·5
		" "b"-axis	26·0	3·522	59·6	14,520		
9	$Na_2Fe(C_2O_4)_2 . 5H_2O$	" "b"-axis	25·8	1·928	57·7	14,330	14,180	29·3
			26·1	1·919	57·6	14,370		
10	$K_2Fe(C_2O_4)_2 . 3H_2O$	" χ_1-axis	23·8	2·134	62·3	14,330	13,960	29·1
			25·2	2·167	62·5	14,170		

is due to merely experimental errors arising from the imperfections in the crystals, or to a small negative Weiss constant Θ in the expression $\chi = C/(T - \Theta)$ arising from a feeble exchange interaction between the spin moments. The first cause seems to be more probable, especially since the magnitudes of the deviations from 29·4 are quite arbitrary.

VII—Anisotropy of the Diamagnetism of the Crystals

As is well-known, diamagnetic crystals also exhibit a feeble anisotropy, so that a part of the observed anisotropy of the manganous and ferric salts should be that of their diamagnetism. Let us denote it by $(\Delta\chi)_d$. Theoretically, it can be eliminated since it should be independent of temperature, whereas the paramagnetic part of the anisotropy should vary approximately as its inverse square. But practically, this method of separating $(\Delta\chi)_d$ is neither convenient nor accurate, and it is desirable to obtain it *indirectly* in the following manner.

Let us consider manganous Tutton salts, of the type $MnSO_4 . A_2SO_4 . 6H_2O$, or $MnSeO_4 . A_2SeO_4 . 6H_2O$, where A represents a monovalent atom. It is well known that by replacing the Mn in them by either Mg or Zn we obtain a series of diamagnetic crystals which are isomorphous with the corresponding manganous salts. We have studied the magnetic anisotropies of these diamagnetic salts as well, and the results obtained are given in Table I. They reveal the following characteristics. (1) The anisotropies of the diamagnetic Tutton salts are much smaller than those of the manganous salts, suggesting that for the latter salts $(\Delta\chi)_d$ is only a small part of the observed $\Delta\chi$. (2) The diamagnetic anisotropies show only small variations from crystal to crystal. (3) Even these small variations occur only when the monovalent atom A is changed, or when the SO_4 group is replaced by SeO_4; when, on the other hand, the divalent atom Mg is replaced by Zn, there is practically no variation in anisotropy; and it may therefore be presumed that when either of them is replaced by Mn the anisotropy of the diamagnetism of the crystal will still be the same.

Since our present purpose in estimating the diamagnetic part of the anisotropy is merely to separate it from the main anisotropy due to splitting, in which we are specially interested, we can reasonably assume that for any given manganous salt the diamagnetic anisotropy $(\Delta\chi)_d$ is the same as that of the isomorphous diamagnetic salt obtained by replacing the Mn by either Mg or Zn, the other atoms in the molecule being kept the same.

VIII—Anisotropy Due to the Mutual Influence of the Magnetic Moments

Had the paramagnetic ions in the crystal been arranged in a regular cubic lattice, the Poisson-Lorentz magnetic polarization field acting on any of the ions would be isotropic, and equal to $\frac{4}{3}\pi\kappa H$, where κ is the *volume* susceptibility of the crystal and

H is the field in the medium. When, however, as in a manganous ammonium sulphate crystal, the distribution of the Mn^{++} ions surrounding any given one deviates from cubic symmetry, the polarization fields will be asymmetric, and the crystal will be magnetically anisotropic in consequence. The principal susceptibilities will be given by the expressions—

$$\chi_q = \chi_0 (1 + \Phi_q \kappa), \qquad q = 1, 2, 3, \quad . \quad . \quad . \quad . \quad . \quad . \quad . \quad . \quad (3)$$

where

$$\Phi_1 + \Phi_2 + \Phi_3 = 4\pi. \quad . \quad . \quad . \quad . \quad . \quad . \quad . \quad . \quad . \quad . \quad . \quad (4)$$

Φ_1, Φ_2, and Φ_3 are constants characteristic of the distribution of the Mn^{++} ions in the crystal, and χ_0 is the susceptibility of the *free* ions.

The corresponding anisotropy $(\Delta\chi)_m$ due to the mutual influence of the magnetic moments would be equal to $\Delta\Phi\kappa\chi_0$.

The structure of the Tutton salts has been studied in detail by HOFMANN* by X-ray methods. The dimensions of the unit cell are roughly $a = 9{\cdot}2$, $b = 12{\cdot}5$, $c = 6{\cdot}2$ A, $\beta = 107°$, and the two divalent ions in the unit cell occupy the positions (000) and $(\frac{1}{2}\frac{1}{2}0)$. With these positions for the Mn^{++} ions it is possible to calculate the Φ's. The calculation is laborious ; but a rough estimate can be made, and it is found that they cannot differ much from $4\pi/3$, and that the $\Delta\Phi$'s should be much less than unity. Since at room temperature the *volume* susceptibilities κ of the manganous Tutton salts are about 60×10^{-6}, the corresponding anisotropy is given by

$$(\Delta\chi)_m/\chi = \Delta\Phi \,.\, \kappa < 6 \times 10^{-5}\,; \quad . \quad . \quad . \quad . \quad . \quad . \quad . \quad . \quad . \quad . \quad (5)$$

i.e., the anisotropy due to the mutual magnetic influence of the Mn^{++} ions in these crystals can not be greater than a tenth part of the observed anisotropy, and is probably much less. It may therefore be neglected to a first approximation.

IX—THE STARK ANISOTROPY

Thus the correction for the diamagnetic anisotropy is the only appreciable correction to be made, and applying it we obtain directly the anisotropy due to the crystalline Stark splitting of the S-levels.† In making this correction it should be remembered that the principal axes of diamagnetism are not the same as the observed principal magnetic axes, because, as will be seen from Table I, the ψ's for the manganous and the corresponding Mg (or Zn) salts are not identical.

Let OF in fig. 1 be the direction of the χ_1 axis as actually observed, OD that of the diamagnetic χ_1 axis, and OS that of the paramagnetic χ_1 axis. Let their relative inclinations be as marked in the figure. If $(\chi_1 - \chi_2)_f$ be the *observed* anisotropy in

* 'Z. Kristallog.', vol. 78, p. 279 (1931)

† The exchange interactions between the spin moments may also have an influence on the splitting. But for such large magnetic dilutions as obtain in the Tutton salts it should be small. At any rate, we shall neglect it for the present and refer to it again in a later portion of this paper.

the (010) plane, $(\chi_1 - \chi_2)_d$ the diamagnetic part, and $(\chi_1 - \chi_2)_s$ the paramagnetic part (the Stark anisotropy), then*

$$\tan 2\sigma = P/Q, \quad . \quad . \quad . \quad . \quad . \quad . \quad . \quad . \quad . \quad . \quad . \quad . \quad (6)$$

where

$$P = (\chi_1 - \chi_2)_d \sin 2\delta \quad . \quad . \quad . \quad . \quad . \quad . \quad . \quad . \quad . \quad . \quad . \quad . \quad (7)$$

$$Q = (\chi_1 - \chi_2)_f - (\chi_1 - \chi_2)_d \cos 2\delta. \quad . \quad . \quad . \quad . \quad . \quad . \quad . \quad (8)$$

Thus σ, and therefore the directions of the paramagnetic axes, are known.

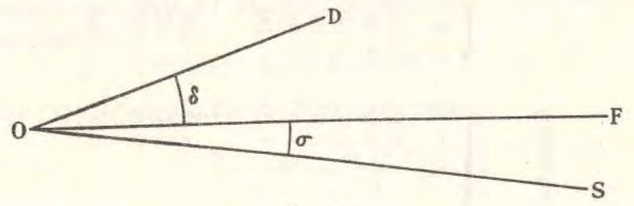

FIG. 1.

The anisotropy of the paramagnetism is given by the expressions

$$(\chi_1 - \chi_2)_s = (P^2 + Q^2)^{\frac{1}{2}}, \quad . \quad . \quad . \quad . \quad . \quad . \quad . \quad . \quad . \quad . \quad . \quad (9)$$

and

$$(\chi_1 - \chi_3)_s = \tfrac{1}{2}\,[(\chi_1 - \chi_2)_s - (\chi_1 - \chi_2)_f + (\chi_1 - \chi_2)_d] + [(\chi_1 - \chi_3)_f - (\chi_1 - \chi_3)_d]. \quad . \quad . \quad . \quad (10)$$

The data given in the last three columns of Table III were calculated in this manner.

X—MAGNITUDE OF THE STARK SPLITTING

We can now use the Stark anisotropies given in the last two columns of Table III to calculate the magnitude of the splitting of the S levels of Mn^{++} under the crystalline fields. The theoretical relations between the splitting and the anisotropy have been worked out in detail by VAN VLECK and PENNEY.† We shall merely quote here their final results. For a crystal whose paramagnetic ions are all in the ^6S state, the three principal susceptibilities are given by the expressions—

$$\chi_1 = C\left(\frac{1}{T} + \frac{2r}{T^2} + \ldots\right) \quad . \quad . \quad . \quad . \quad . \quad . \quad . \quad . \quad . \quad . \quad (11A)$$

$$\chi_2 = C\left(\frac{1}{T} - \frac{r+s}{T^2} + \ldots\right) \quad . \quad . \quad . \quad . \quad . \quad . \quad . \quad . \quad (11B)$$

$$\chi_3 = C\left(\frac{1}{T} - \frac{r-s}{T^2} + \ldots\right) \quad . \quad . \quad . \quad . \quad . \quad . \quad . \quad . \quad (11C)$$

$$C = \frac{N\mu^2}{3k}, \quad . \quad . \quad . \quad . \quad . \quad . \quad . \quad . \quad . \quad . \quad . \quad . \quad . \quad . \quad . \quad (12)$$

* The derivation of these expressions for σ and for the paramagnetic anistropy is simple.

† 'Phil. Mag.,' vol. 17, p. 961 (1934).

TABLE III

Crystal	Observed anisotropy $(\Delta\chi)_f$			Anisotropy of the corresponding Mg salt $(\Delta\chi)_d$			Stark anisotropy $(\Delta\chi)_s$		
	ψ	$\chi_1-\chi_2$	$\chi_1-\chi_3$	ψ	$\chi_1-\chi_2$	$\chi_1-\chi_3$	ψ	$\chi_1-\chi_2$	$\chi_1-\chi_3$
$MnSO_4 . R_2SO_4 . 6H_2O$									
R = NH_4	−16°	8·7	6·0	− 5°	1·1	0·6	−17⅓°	7·7	5·5
Zn salt : + 6°									
Rb	−12°	8·9	6·2	+13°	0·9	0·7	−14⅓°	8·3	5·7
Zn salt : +23½°									
Cs	−12½°	7·0	5·0	+51°	1·3	0·6	−15°	8·6	5·9
Tl	−16½°	8·9	7·2	+ 6°	0·8	1·3	−16°	7·9	5·1
							−18½°	8·3	6·0
$MnSeO_4 . R_2SeO_4 . 6H_2O$									
R = NH_4	−20°	8·9	6·3	− 3°	1·5	1·0	−23°	7·7	5·5
Rb	−14°	9·0	7·3	+ 4°	1·3	1·1	−17°	7·9	6·3
Tl	−14°	10·2	8·5	0	2·0	2·6	−17°	8·5	6·1
$MnSO_4 . K_2SO_4 . 4H_2O$ (does not belong to the Tutton series)	−61°	4·3	1·5	+66°	0·5	0·7	−58°	4·4	1·1

where μ is the magnetic moment of the ion, equal to $g\beta\sqrt{5/2 \times 7/2}$; N is the Avogadro number, k, is the Boltzmann constant, g is the Landé factor (equal to 2), β is the Bohr magneton, $eh/(4\pi mc)$ and T is the absolute temperature ;

$$r = \frac{12a + 8b}{35k}, \qquad s = \frac{4\sqrt{10}\,.\,c + 12\sqrt{2}\,.\,e}{35k}, \quad \ldots\ldots \quad (13)$$

where a, b, c, and e are the constants of the crystalline splitting, which are, of course, very small in comparison with kT at room temperature. The mean susceptibility of the crystal is equal to

$$\chi = (\chi_1 + \chi_2 + \chi_3)/3 = C/T \quad \ldots\ldots\ldots \quad (14)$$

From relations (11) we obtain for the Stark anisotropies

$$\frac{\chi_1 - \chi_2}{\chi} = \frac{3r + s}{T}, \quad \ldots\ldots\ldots\ldots \quad (15A)$$

and

$$\frac{\chi_1 - \chi_3}{\chi} = \frac{3r - s}{T}. \quad \ldots\ldots\ldots\ldots \quad (15B)$$

With the help of these relations we can calculate, from the experimental anisotropies given in Table III, the values of r and s characteristic of the crystalline Stark splitting. Thus, for manganous ammonium sulphate at T = 303° K,

$$\frac{\chi_1 - \chi_2}{\chi} = \frac{7{\cdot}8}{13{,}830} \quad \ldots\ldots\ldots\ldots \quad (16A)$$

$$\frac{\chi_1 - \chi_3}{\chi} = \frac{5{\cdot}5}{13{,}830}, \quad \ldots\ldots\ldots\ldots \quad (16B)$$

whence,

$$r = 0{\cdot}049°, \; s = 0{\cdot}025°. \quad \ldots\ldots\ldots\ldots \quad (17)$$

Substituting these values in (13), we obtain

$$\frac{a + 2b/3}{k} = 0{\cdot}142° \quad \ldots\ldots\ldots\ldots \quad (18A)$$

$$\frac{c + 3e/\sqrt{5}}{k} = 0{\cdot}070°. \quad \ldots\ldots\ldots\ldots \quad (18B)$$

It is not possible from the magnetic data alone to obtain a and b separately, or c and e. We can see, however, that the energy separations of the Stark components should be of the order of $k \times 0{\cdot}1°$.

XI—Some Simplifying Assumptions

To obtain a closer estimate of the crystalline separations of the S-levels, we have to make some simplifying assumptions. Kramers has shown that when the number of electrons in the incomplete shell of the ion is odd, as with Mn^{++}, the (2J + 1)-fold

degeneracy is not completely removed by the crystalline field, however little symmetry there may be in the field ; a two-fold degeneracy is left over. There would thus be only three split levels for the Mn^{++} ion. Let us, however, assume for simplicity, following KÜRTI and SIMON* in their recent discussions on entropies of paramagnetic crystals at very low temperatures, that the degeneracy has been completely removed, and further, that the six Stark levels so produced are equally spaced, at energy intervals of $k\theta_s$, where θ_s is a temperature characteristic of the crystalline splitting.

The effect of the crystalline *electric* fields in splitting the ^6S levels would then be equivalent to that of a *magnetic* field H_s given by the relation

$$g\beta H_s = k\theta_s. \quad \ldots\ldots\ldots\ldots \quad (19)$$

If we can determine this equivalent magnetic field H_s, we obtain directly the characteristic temperature θ_s.

XII—Stark Splitting and the Weiss Field

Returning to our expressions (11) for the principal susceptibilities, since r and s ($\sim 0{\cdot}05°$) are very small in comparison with the room temperature T (303°), we can rewrite the expressions in the form

$$\chi_1 = \frac{C}{T-\Theta_1}, \qquad \chi_2 = \frac{C}{T-\Theta_2}, \qquad \chi_3 = \frac{C}{T-\Theta_3}, \quad \ldots \quad (20)$$

where

$$\Theta_1 = 2r, \qquad \Theta_2 = -(r+s), \qquad \Theta_3 = -(r-s), \quad \ldots\ldots \quad (21)$$

$$\Theta_1 + \Theta_2 + \Theta_3 = 0. \quad \ldots\ldots\ldots\ldots \quad (22)$$

The new expressions (20) are of the Weiss type, and in the usual treatment the Curie temperatures Θ_1, Θ_2, and Θ_3, occurring in them, which in the present crystals really arise from the crystalline fields, would be considered as due to certain internal *magnetic* fields. Let us now enquire what relation our H_s bears to this internal field of the Weiss theory, since both of them are magnetic fields intended to replace effectively the crystalline fields.

The Weiss field, as is well known, is an internal field, which is superposed on the externally applied magnetic field, and is of magnitude αI, where I is the intensity of magnetization per unit volume and α is a constant connexion with the Curie temperature Θ by the relation†

$$\alpha = \frac{3k\Theta}{\mu I_0}, \quad \ldots\ldots\ldots\ldots\ldots \quad (23)$$

in which I_0 is the saturation intensity of magnetization, and μ is the moment of the magnetic ion. It would, therefore, vary with I, and would not be constant as our H_s should be.

* 'Proc. Roy. Soc.,' A, vol. 149, p. 152 (1935).

† *See* Stoner, "Magnetism and Matter" (London, 1934), chap. iv.

This difference between the Weiss field and H_s is due to the following circumstance, which, incidentally, gives also the relation between the two. The Weiss field is the magnetic equivalent of the crystalline field so far as its influence on the magnetization is concerned, where as H_s is the appropriate magnetic equivalent of the crystalline field as regards its effect on the splitting of the ^6S levels. The two fields would be identical only if the crystalline splitting of ^6S were *actually* into six equally spaced levels, which, as we have already mentioned, is not so ; the actual splitting is into three doubly degenerate levels.

Owing to this two-fold degeneracy, which does not differentiate change in the signs of the spin moments, the crystalline splitting does not produce any magnetization by itself. If, however, by the application of an external magnetic field the degeneracy is removed, the crystalline splitting will exert an influence on the magnetization, which will increase continually with the increase in the latter ; when saturation is reached and the spin moments are all aligned along the same direction, the crystalline splitting will contribute its full share to the magnetization. This can be visualized in the following manner. Whereas the crystalline field alone would prefer orientations corresponding to $m = \pm 5/2$, *i.e.*, the maximum numerical value of m, the magnetization field would progressively increase the population corresponding to the positive value of m in strong preference to the negative, and when saturation is reached, and all the ions are in the $m = +5/2$ state, the contribution to the magnetization field as arising from the crystalline splitting would have reached its maximum value, which should naturally be our H_s. We thus obtain

$$H_s = \alpha I_0, \quad \ldots\ldots\ldots\ldots\ldots \quad (24)$$

which, in view of (23), gives

$$H_s = 3k\Theta/\mu. \quad \ldots\ldots\ldots\ldots\ldots \quad (25)$$

In applying this formula to *crystals*, there are three Curie temperatures to be considered. For example, for manganous ammonium sulphate the temperatures are

$$\Theta_1 = 0{\cdot}10°, \qquad \Theta_2 = -0{\cdot}07°, \qquad \Theta_3 = -0{\cdot}03° \text{ K}. \quad \ldots \quad (26)$$

But when we are dealing with phenomena that occur at temperatures not much lower than 0·1° K, as we should be in the next section, the field corresponding to Θ_1 would be the predominant field, and we may put

$$H_s = 3k\Theta_1/\mu. \quad \ldots\ldots\ldots\ldots\ldots \quad (27)$$

Since for Mn^{++}

$$\mu = g\beta\sqrt{5/2 \times 7/2}, \quad \ldots\ldots\ldots\ldots \quad (28)$$

we obtain, using (19), or, in view of relations (19) and (24),

$$\theta_s = 3g\beta\Theta_1/\mu = 3\Theta_1/\sqrt{5/2 \times 7/2}, \quad \ldots\ldots\ldots \quad (29)$$

which, on substituting for Θ_1, yields

$$\theta_s = 0{\cdot}10^\circ\ \mathrm{K}. \quad \ldots\ldots\ldots\ldots \quad (30)$$

This would correspond to a separation of the Stark components of

$$\Delta\nu = 0{\cdot}07\ \mathrm{cm}^{-1}. \quad \ldots\ldots\ldots\ldots \quad (31)$$

This value of θ_s for manganous ammonium sulphate agrees well with the value $0{\cdot}11^\circ$ K obtained by KÜRTI and SIMON from adiabatic demagnetization measurements on this salt at very low temperatures (*see* § XIII).

From (19), the value of the inner field H_s in manganous ammonium sulphate comes out as 750 gauss.

The characteristic temperatures for the other salts can be calculated in the same manner, and are given in Table IV.

TABLE IV

Crystal	Curie temperatures Θ_1	Θ_2	Θ_3	Characteristic temperature θ_s
$MnSO_4 . R_2SO_4 . 6H_2O$				
R = NH_4	$0{\cdot}10^\circ$ K	$-0{\cdot}07^\circ$ K	$-0{\cdot}03^\circ$ K	$0{\cdot}10^\circ$ K
Rb	0·10	−0·08	−0·02	0·10
Cs	0·09	−0·07	−0·02	0·09
Tl	0·10	−0·08	−0·02	0·10
$MnSeO_4 . R_2SeO_4 . 6H_2O$				
R = NH_4	0·10	−0·07	−0·03	0·10
Rb	0·10	−0·07	−0·03	0·10
Tl	0·10	−0·08	−0·02	0·10
$MnSO_4 . K_2SO_4 . 4H_2O$	0·04	−0·06	0·02	0·04

All the manganous Tutton salts have thus practically the same characteristic temperature, namely, $0{\cdot}10^\circ$ K. Manganous potassium sulphate has a considerably lower temperature.

[*Added in proof, May* 18, 1936—In connexion with the calculation of the characteristic temperatures of crystals from their magnetic anisotropies we should make the following remark. In equations (11) we have neglected all the terms higher than those involving T^{-2}, and this is justifiable for the particular crystals that we have been considering. When, however, we are dealing with crystals which are cubic or nearly cubic, the terms involving T^{-2} become small, and the T^{-3} terms may become comparable with them.]

XIII—STARK SPLITTING IN RELATION TO ENTROPY AT VERY LOW TEMPERATURES

The Stark splitting of paramagnetic S-levels plays an important part in very low temperature phenomena. For example, as KÜRTI and SIMON have shown, at temperatures in the neighbourhood of $0{\cdot}1^\circ$ K the entropy temperature curves for these paramagnetic salts are almost wholly determined by it, and consequently also their specific heats at these temperatures. Even the rough model of the splitting of the levels that has been adopted, viz., into six equally spaced ones, having a constant energy difference of $k\theta_s$, enables us to calculate these quantities to a close approximation. We shall merely quote here some of the results obtained by KÜRTI and SIMON.

(1) *Entropy at Very Low Temperatures*—For temperatures in the neighbourhood of $0{\cdot}1^\circ$ absolute, practically the whole of the entropy of these manganous Tutton salts is due to the orientative effect of the crystalline field on the magnetic moments, that due to the lattice oscillations being quite small in comparison. With the assumed constant energy differences between successive Stark levels, viz., $k\theta_s$, the calculation of the entropy can be done in two ways, which are, of course, analytically equivalent.

(*a*) The entropy S can be treated as that of *free* magnetic moments, placed in a magnetic field H_s. The entropy per gram ion is then given by

$$S = S_0 + \int_0^{H_s} \left(\frac{\partial \chi}{\partial T}\right)_H dH, \quad \ldots\ldots\ldots\ldots \quad (32)$$

where S_0 is the entropy when the crystalline fields are absent;

$$S_0 = R \log_e (2J + 1), \quad \ldots\ldots\ldots\ldots \quad (33)$$

and is therefore known. $(\partial\chi/\partial T)_H$ is also easily calculated, since the susceptibility χ in this expression refers to *free* ions.

(*b*) S can also be calculated, as shown by KÜRTI and SIMON, directly from the Stark pattern assumed ;

$$S = R\left[T \frac{d \log_e Q_{(2J+1),\theta_s}}{dT} + \log_e Q_{(2J+1),\theta_s}\right], \quad \ldots\ldots\ldots \quad (34)$$

where

$$Q_{(2J+1),\theta_s} = 1 + e^{-\theta_s/T} + e^{-2\theta_s/T} + \ldots + e^{-2J\theta_s/T}. \quad \ldots\ldots \quad (35)$$

Thus the entropy-temperature curve at these low temperatures can be readily plotted from the known values of θ_s.

(2) *Specific Heats*—The calculation of the specific heats at these temperatures from the entropy-temperature curve is also easy. Denoting by C the heat capacity of the salt per gram ion of its Mn^{++} content.

$$C = T \frac{dS}{dT}. \quad \ldots\ldots\ldots\ldots\ldots \quad (36)$$

The specific heat curve has a pronounced maximum at a temperature slightly lower than θ_s.

Thus, *purely from measurements at room temperature, from which we obtained the characteristic temperatures* θ, *given in Table IV, we can predict the entropy-temperature curve and the specific-heat-temperature curve of these crystals in the neighbourhood of* $0{\cdot}1°$ *absolute.* This is of interest, since at present, short of actual measurements at these low temperatures, we have no other means of predicting these curves.

We should refer in this place to one other phenomenon in which θ, plays a prominent part. It determines, as has been shown by KÜRTI and SIMON, the low temperature that can be obtained by the adiabatic demagnetization method of DEBYE* and GIAUQUE.†

Let the salt be magnetized isothermally at a temperature T_i by a magnetic field H_i, and then demagnetized *adiabatically* by suddenly removing it from the field and let T_f be the final temperature attained by the salt. At the initial temperature, which usually is of the order of 1° K, the crystalline field has little influence, so that the entropy is that of free magnetic ions placed in a field H_i, while at the final temperature it should be equivalent to that of the same *free* magnetic ions under the inner field H_i. Since the two entropies should be equal,

$$\frac{H_i}{T_i} = \frac{H_i}{T_f}, \quad \ldots\ldots\ldots\ldots\ldots \quad (37)$$

which, on substituting for H_i from (19), gives

$$\frac{T_f}{T_i} = \frac{k\theta_i}{g\beta H_i}. \quad \ldots\ldots\ldots\ldots\ldots \quad (38)$$

This relation, obtained by KÜRTI and SIMON, has been experimentally verified by them and they have determined on the basis of it the characteristic temperatures of some paramagnetic salts, from the demagnetization experiments made on them. Only one manganous salt has been experimented by them, namely, manganous ammonium sulphate, for which, as we have seen, the value of θ, thus obtained agrees well with that deduced by us from the magnetic anisotropy of the crystal at room temperatures.

XIV—STARK SPLITTING IN OTHER PHYSICAL PHENOMENA

Among the other phenomena that depend on the crystalline splitting are Faraday rotation, and absorption. Both of them involve, in addition to the splitting of the ground levels, that of the higher levels also, which makes the interpretation more difficult than that of simple susceptibility phenomena. For the manganous salts, however, since the higher level involved would be a P level, whose splitting under the crystalline fields would not be large, we should expect: (1) the paramagnetic Faraday rotation in manganous salts to be small, and vary nearly as the inverse temperature; (2) the absorption frequencies and the absorption coefficients of single crystals

* 'Ann. Physik,' vol. 81, p. 1154 (1926).
† 'J. Amer. Chem. Soc.,' vol. 49, p. 1864 (1927).

of manganous salts to be independent of (*a*) the direction of vibration of the light, unlike in cobalt salts, for example, which should show strong pleochroism, and (*b*) the state of aggregation, and the nature of the anions, again unlike the cobalt salts.

These results have been verified experimentally.*†

XV—INTERACTION BETWEEN THE SPINS

Till now we had neglected, for simplicity, the influence of the interactions between the spin moments, and assumed that the whole of the paramagnetic anisotropy is due to the splitting of the S-levels under the crystalline fields alone. It should be mentioned here that the general results that we have obtained regarding the magnitude of the splitting do not depend on the validity of this assumption. If the interaction is not negligible, it would merely mean that the actual splitting is under the combined action of the crystalline and the interaction fields, and with the assumption of equal spacing of the split levels, the temperatures θ, that we have calculated (*see* Table IV) would still characterize the splitting of the S-levels in the crystal ; only it is not now due to the crystalline field alone. The calculation of the entropy, specific heat, etc., would therefore remain unaffected.

It would, however, be of interest to know how much of the splitting is due to the crystalline field, and how much to the spin interactions. Rough estimates of their relative contributions can be made in the following manner. We have already mentioned that $MnSO_4 . (NH_4)_2 SO_4 . 6H_2O$ and the corresponding diamagnetic salt $MgSO_4 . (NH_4)_2 SO_4 . 6H_2O$ are isomorphous. They readily form mixed crystals, and crystals of any desired composition can be easily grown from aqueous solutions of a suitable mixture of the two. Since the crystalline electric fields which are responsible for the Stark anisotropy are determined by the atoms immediately surrounding the Mn^{++} ions, and since their distributions are presumably independent of the concentration of Mn^{++} in the mixed crystal, we should expect the Stark anisotropy to be independent of the concentration of Mn. The interaction anisotropy, on the other hand, should rapidly fall down as the concentration of Mn in the crystal diminishes.

Let us, for brevity, denote by A the molecule of $MnSO_4 . (NH_4)_2 SO_4 . 6H_2O$ and by B that of $MgSO_4 . (NH_4)_2 SO_4 . 6H_2O$. Consider now a molecule A + nB of the mixed crystal. Its diamagnetic anisotropy may, to a first approximation, be taken to be equal to $(n + 1)$ times that of B, and may be corrected for, as in § IX. The remaining part of the anisotropy would then represent the sum of the Stark and the interaction anisotropies $(\Delta\chi)_s$ and $(\Delta\chi)_i$, say. We can now use the fact that $(\Delta\chi)_s$ should be independent of magnetic dilution of the kind considered, while $(\Delta\chi)_i$ should rapidly diminish with dilution, in order to separate the two.

* BECQUEREL, DE HAAS, and VAN DEN HANDEL, 'Proc. Acad. Sci. Amst.,' vol. 34, p. 1231 (1931).
† GIELESSEN, 'Ann. Physik,' vol. 22, p. 537 (1935).

Some preliminary measurements have been made by us on the magnetic anisotropies of a number of such mixed crystals, and the results obtained are given in Table V.

The measurements were restricted to finding the directions of the χ_1 and χ_2 axes in the (010) plane, and the anisotropy, χ_1 and χ_2, in this plane. The first column in the table gives the composition of the crystal, assumed to be of the form $A + nB$; the value of n for each crystal was determined by analysing it chemically for its Mn constant. Columns 2 and 3 give the observed anisotropy *for a mass consisting of 1 gram molecule of A and n* gram molecules of B. Assuming the diamagnetic part of the anisotropy to be equal to $(n + 1) \times 1{\cdot}1$—$1{\cdot}1$ being the value of $\chi_1 - \chi_2$ for magnesium ammonium sulphate—, and the diamagnetic ψ to be $-5°$—again that of the magnesium salt—, the values of ψ and $\chi_1 - \chi_2$ for the *paramagnetic* part can be calculated in the same manner as in § IX; the calculated values are given in the last two columns of Table V.

TABLE V—

$A = Mn$, $B = Mg$: $(NH_4)_2(SO_4)_2 \cdot 6H_2O$

Composition of the crystal	Magnetic anisotropy: Observed ψ	Observed $\chi_1 - \chi_2$	After correcting for diamagnetism ψ	After correcting for diamagnetism $\chi_1 - \chi_2$
$A + nB$				
$n = 0$	$-16°$	8·7	$-17\frac{1}{2}°$	7·7
0·36	$-17°$	8·3(?)	$-20°$	6·9(?)
1·36	$-18°$	8·6	$-23°$	6·4
1·75	$-18°$	8·4	$-24\frac{1}{2}°$	5·9
3·25	$-16°$	9·5	$-25°$	5·5
5·12	$-15°$	11·2	$-27\frac{1}{2}°$	5·4
B	$-5°$	1·1		

Similar data for mixed crystals for manganous and zinc ammonium sulphates are given in Table VI.

TABLE VI—

$A = Mn$, $B = Zn$: $(NH_4)_2(SO_4)_2 \cdot 6H_2O$

Composition of the crystal	Magnetic anisotropy: Observed ψ	Observed $\chi_1 - \chi_2$	After correcting for diamagnetism ψ	After correcting for diamagnetism $\chi_1 - \chi_2$
$A + nB$				
$n = 0$	$-16°$	8·7	$-19°$	7·8
0·41	$-16°$	8·3	$-21°$	7·2
1·05	$-16°$	8·2	$-24°$	6·6
3·45	$-13°$	8·3	$-32°$	5·3
4·62	$-12°$	9·0	$-36°$	5·3
B	$+6°$	1·2		

Since the diamagnetic corrections are large—for example, for the largest magnetic dilution, namely, that corresponding to $n = 5$, $(\Delta\chi)_d$ is as high as 60 to 70% of the observed anisotropy—the values given in the last column of the Tables V and VI can be taken to represent only the *order of magnitude* of the paramagnetic anisotropy. They indicate, however, a definite fall in the paramagnetic anisotropy with magnetic dilution, from a value 7·8 for pure manganous ammonium sulphate, to 5·3 when it is diluted with 5 molecules of the diamagnetic salt.

Thus, in manganous ammonium sulphate the interactions between the spin moments of Mn^{++} are quite appreciable, and may account for as much as 30% of the observed anisotropy, the remaining 70% being due to crystalline electric fields. This estimate of the relative influences of the interaction and crystalline fields on the splitting of the S levels of Mn^{++} agrees with the results of low temperature demagnetization experiments with these mixed crystals by KÜRTI and SIMON.*

XVI—FERRIC SALTS

Most of the inorganic ferric crystals are hygroscopic, and their anisotropies were difficult to measure. We therefore chose for measurement two organic compounds of iron, namely, $K_3Fe(C_2O_4)_3 \cdot 3H_2O$, and $Na_3Fe(C_2O_4)_3 \cdot 5H_2O$, and the corresponding double oxalates of aluminium, which are diamagnetic. The magnetic data for these crystals are given in Tables I and II. The magnitude of the Stark splitting in the ferric salts can be calculated in the same manner as for the manganous salts. To quote here only the final results, the characteristic temperatures θ, for the potassium and sodium iron oxalates were found to be about 0·7° and 0·3° K respectively. These values are much higher than those for the manganous salts.

Some preliminary measurements on ferric ammonium oxalate show that its characteristic temperature is nearly the same as for the sodium salt, though in its water of crystallization ($3\,H_2O$), and in its crystal structure, it resembles strongly the potassium salt.

We desire to express our thanks to Professor P. C. MAHALANOBIS of the Presidency College, Calcutta, for the loan of the electro-magnet.

XVII—SUMMARY

The paper gives an account of measurements on the magnetic anisotropies of single crystals of manganous and ferric salts. Both the Mn^{++} and Fe^{+++} ions being in the S-state ($^6S_{5/2}$), the anisotropies are naturally very feeble, of the order of one part in a thousand; a special experimental technique is described suitable for the measurement of such feeble anisotropies.

* 'Proc. Roy. Soc.,' A, vol. 149, p. 172 (1935).

The various causes contributing to the anisotropy are discussed. Part of the anisotropy is shown to be that of the diamagnetism of the crystal, and part, much smaller, is that arising from the mutual influence of the magnetic moments and their non-cubic arrangement in the crystal lattice.

The bulk of the anisotropy that is left over after allowing for the above two, arises from the Stark splitting of the ^6S levels under the influence of the crystalline electric fields. A method is described for calculating the magnitude of the Stark separation from the anisotropy, and for calculating the "characteristic temperatures". The part played by the Stark splitting in various low temperature phenomena is reviewed, and it is shown how from magnetic measurements alone at room temperature it is possible to predict the entropy-temperature and specific heat temperature curves of these crystals in the neighbourhood of $0{\cdot}1°$ absolute.

From measurements on the progressive variation of the anisotropy of mixed crystals of $Mn(NH_4)_2(SO_4)_2 . 6H_2O + Mg(NH_4)_2(SO_4)_2 . 6H_2O$, and of $Mn(NH_4)_2(SO_4)_2 . 6H_2O + Zn(NH_4)_2(SO_4)_2 . 6H_2O$, with the concentration of Mn, the effects of the interactions between the spin moments in the crystal are estimated.

Diamagnetic Anisotropy of Crystals in Relation to Their Molecular Structure

By KATHLEEN LONSDALE and Professor K. S. KRISHNAN

(*Communicated by Sir William Bragg, O.M., P.R.S.—Received* 1 *April*, 1936)

In order to determine the fine structure of molecular crystals by means of a Fourier analysis of X-ray data, it is usually necessary that the configuration and orientation of the molecules should be known with considerable accuracy. Only in a few cases can this information be obtained directly from the X-ray data. Typical examples of crystals for which this has been done are hexamethylbenzene* and cyanuric triazide,† both layer lattice structures, and hexamethylene tetramine‡ in the crystal of which the molecule itself possesses high symmetry. In other cases, *e.g.*, anthracene, naphthalene, etc.,§ the "trial and error" structure has been obtained by an intensive study of the X-ray data, a difficult problem involving much expenditure of time and trouble. Any independent physical methods which indicate the approximate orientation of the molecules in the crystal are therefore greatly to be welcomed. Krishnan and his collaborators, in a series of recent papers,‖ have emphasized the fact that a knowledge of the optical and diamagnetic anisotropy of the crystal may, in favourable cases, give very direct information concerning the shape and orientation of the molecules. They point out also that, given the diamagnetic anisotropy of the crystal and the accurate orientation of the molecules in the crystal, the principal diamagnetic susceptibilities of a single molecule can be directly calculated. It is important, therefore, that the exact mathematical relationship between the crystal and molecular diamagnetic susceptibilities and the molecular orientations relative to the crystal axes should be correctly formulated.

TRICLINIC SYSTEM

The triclinic system is in one sense the most complicated and in another the simplest of all the classes. The directions of the three principal

* Lonsdale, 'Proc. Roy. Soc.,' A, vol. 123, p. 494 (1929).
† Knaggs, 'Proc. Roy. Soc.,' A, vol. 150, p. 576 (1935).
‡ Dickinson and Raymond, 'J. Amer. Chem. Soc.,' vol. 45, p. 22 (1923).
§ Robertson, 'Chem. Rev.,' vol. 16, p. 417 (1935).
‖ Krishnan, 'Nature,' vol. 130, pp. 313, 698 (1932); Krishnan, Guha, and Banerjee, 'Phil. Trans.,' A, vol. 231, p. 235 (1933); Krishnan and Banerjee, *ibid.*, vol. 234, p. 265 (1935).

diamagnetic susceptibilities, χ_1, χ_2, χ_3, do not bear any simple relationship to the crystal axes and must therefore be located by experimental investigation; but, on the other hand, since the unit cell contains but one or perhaps two molecules centrosymmetrically arranged, the connexion between molecular and crystal anisotropy is a very simple one.

Assuming, as we must do, that all the molecules which go to build up the crystal are similar in structure, it follows that the absolute values of their principal diamagnetic susceptibilities $|K_1|$, $|K_2|$, $|K_3|$ will be identical. The coordinates of equivalent points in the triclinic system are $x\,y\,z$; $\bar{x}\,\bar{y}\,\bar{z}$ (the highest possible symmetry is a centre), so that the direction cosines of the principal molecular susceptibilities will be the same for both molecules which go to build up the symmetry of the unit cell. Let these direction cosines be

	a	b	c
K_1	$\cos\theta_1$	$\cos\phi_1$	$\cos\psi_1$
K_2	$\cos\theta_2$	$\cos\phi_2$	$\cos\psi_2$
K_3	$\cos\theta_3$	$\cos\phi_3$	$\cos\psi_3$

(Only three of these are independent, since K_1, K_2, K_3 are mutually orthogonal.) The direction cosines of the resultant principal susceptibilities of the crystal will also be $\cos\theta_{1,2,3}$, $\cos\phi_{1,2,3}$, $\cos\psi_{1,2,3}$; in general,

$$\chi_1 = K_1, \quad \chi_2 = K_2, \quad \chi_3 = K_3.$$

The crystal axes in the triclinic system can be taken parallel to any primitive triplet and therefore $\theta_{1,2,3}$, $\phi_{1,2,3}$, $\psi_{1,2,3}$ may have any values, consistent among themselves, depending on the orientation of the molecule or molecules. If θ, ϕ, ψ can be measured for the crystal susceptibilities relative to the chosen axes, then the orientation of the principal molecular susceptibilities relative to those or any other set of crystal axes is known. As an example, consider hexamethylbenzene, for which both the crystalline axes of diamagnetic susceptibility and the molecular structure are known.*

* Bhagavantam, 'Proc. Roy. Soc.,' A, vol. 126, p. 143 (1929); Krishnan and Banerjee, 'Phil. Trans.,' A, vol. 234, p. 265 (1935); Lonsdale, 'Proc. Roy. Soc.,' A, vol. 123, p. 494 (1929).

The molecules of $C_6(CH_3)_6$ have been shown by X-ray analysis to possess a plane pseudo-hexagonal structure and to lie, as accurately as the measurements could reveal, in layers parallel to a good natural cleavage face. This face was called the (001) plane, and it is significant that one principal axis of diamagnetic susceptibility in the crystal is accurately perpendicular to this (001) plane. It follows, therefore, that one principal axis (along which $|\chi_3| = |K_3| = 163{\cdot}8 \times 10^{-6}$ c.g.s. e.m.u./gm. mol.) is perpendicular to the plane of the benzene ring in the molecule, a result which is typical of the plane aromatic molecules (*cf.* naphthalene, anthracene, chrysene, *p*-diphenylbenzene, etc.). The susceptibility along this axis is numerically much larger (algebraically smaller) than either of the other two principal susceptibilities. χ_1 and χ_2 are, of course, perpendicular to χ_3, and therefore they lie *in* the (001) plane—an unexpected simplification due to the layer lattice structure—and hence K_1 and K_2 both lie in the plane of the molecule. They are not, however, quite equal in absolute value:

$$|\chi_1| = |K_1| = 101{\cdot}1, \qquad |\chi_2| = |K_2| = 102{\cdot}7,$$

and their directions do not bear any simple relationship to the geometrical form of the benzene nucleus.

χ_1 (and therefore K_1) makes an angle of about 10° with the line of centres of one pair of carbon atoms and CH_3 groups in the molecule, $\chi_2 = K_2$ being, of course, at right angles to this direction. This feeble anisotropy in the plane of the benzene ring is not surprising in view of the fact that the benzene molecule itself and benzene derivatives in general do not exhibit any symmetry higher than centrosymmetry in the crystalline state. Only a definite asymmetry of the molecular field of force in $C_6(CH_3)_6$ molecules could account for the fact that these molecules form a lattice of triclinic symmetry on crystallization. It seems likely, therefore, that even benzene itself may not possess magnetic symmetry in the plane of the ring and, as will be shown later, $|K_1|$ is not quite equal to $|K_2|$ for any of the benzene derivatives. For the sake of convenience we are obliged to assume in subsequent calculations that these two principal molecular axes, K_1 and K_2, *e.g.*, in anthracene or chrysene, lie respectively parallel to the "long" and the "short" axes of the molecule,* but this is probably only an approximation. It seems fairly well established, however, that K_3 is perpendicular to the plane of the benzene nucleus.

* *Cf.* Robertson, 'Proc. Roy. Soc.,' A, vol. 140, p. 92 (1933).

K. Lonsdale and K. S. Krishnan

Monoclinic System

The maximum symmetry in the monoclinic system is that of reflexion + inversion. (The diamagnetic properties of the crystal are themselves centro-symmetrical, so that lower forms of symmetry, such as reflexion

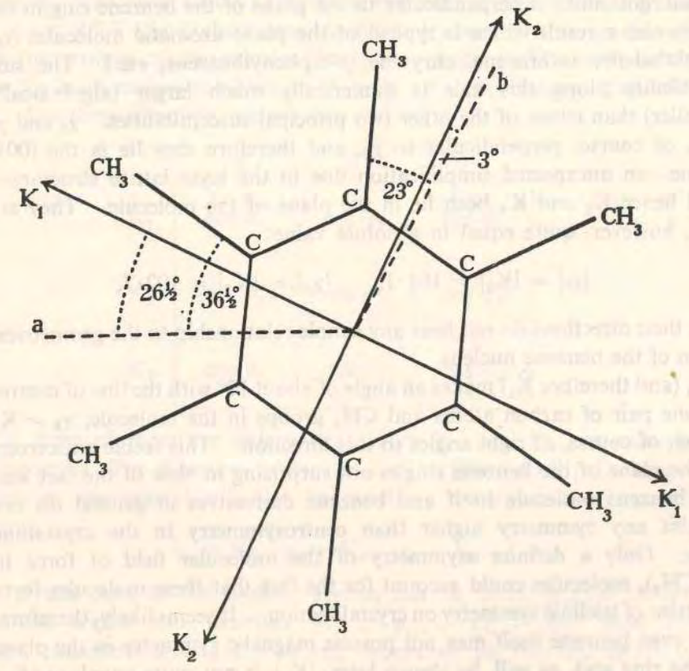

Fig. 1.

or rotation alone, need not be considered.) The coordinates of equivalent points are

$$\pm |x\, y\, z;\ x\, \bar{y}\, z|.$$

In the following calculations it is most convenient to consider only orthogonal systems. The system of coordinates [*a*, *b*, *c*′] consists of the crystal axis *a* (any primitive translation in the (010) reflexion plane), the rotation axis *b*, and the normal to these two directions (*i.e.*, the perpendicular to the (001) plane). Relative to these axes the direction

cosines of the K_1, K_2, K_3 axes of any one molecule and of its inversion will be

	a	*b*	*c*′
K_1	α_1	β_1	γ_1
K_2	α_2	β_2	γ_2
K_3	α_3	β_3	γ_3

only three of these being independent. The direction cosines of the principal axes of the other pair of molecules will be

K_1	α_1	$-\beta_1$	γ_1
K_2	α_2	$-\beta_2$	γ_2
K_3	α_3	$-\beta_3$	γ_3

These two sets of tensors may be combined by considering their components along the *a*, *b*, *c*′ axes. There are nine resultant components which are given (per gram-molecule) by the equations:

$$K_{aa} = K_1\alpha_1^2 + K_2\alpha_2^2 + K_3\alpha_3^2$$
$$K_{bb} = K_1\beta_1^2 + K_2\beta_2^2 + K_3\beta_3^2$$
$$K_{c'c'} = K_1\gamma_1^2 + K_2\gamma_2^2 + K_3\gamma_3^2$$
$$K_{bc'} = K_{c'b} = 0$$
$$K_{c'a} = K_{ac'} = K_1\alpha_1\gamma_1 + K_2\alpha_2\gamma_2 + K_3\alpha_3\gamma_3$$
$$K_{ab} = K_{ba} = 0.$$

Hence we are left with components K_{bb} along the *b* axis and K_{aa}, $K_{c'c'}$, $K_{c'a}$ $K_{ac'}$ in the (010) plane. That is to say, one of the resultant principal axes of the crystal lies along the *b* axis

$$\chi_3 = K_{bb} = K_1\beta_1^2 + K_2\beta_2^2 + K_3\beta_3^2 \qquad (1)$$

and the other two lie in the (010) plane.

Let the resultant susceptibilities in the (010) plane be χ_1, χ_2, where $|\chi_1| < |\chi_2|$ (numerically) and χ_1 makes an angle ϕ with a, ψ with c, where $\phi + \psi = \beta$ (the obtuse monoclinic angle). Then the direction cosines of χ_1, χ_2, χ_3 with respect to $[a, b, c']$ are

	a	b	c'
χ_1	$\cos\phi$	0	$\sin\phi$
χ_2	$-\sin\phi$	0	$\cos\phi$
χ_3	0	1	0

and the equations of transformation of K_{aa}, etc., from the system $[a, b, c']$ to the system $[\chi_1, \chi_2, \chi_3]$ are as follows:

$$K_{\chi_1\chi_1} = K_{aa}\cos^2\phi + K_{c'c'}\sin^2\phi + 2K_{ac'}\cos\phi\sin\phi = \chi_1$$
$$K_{\chi_2\chi_2} = K_{aa}\sin^2\phi + K_{c'c'}\cos^2\phi - 2K_{ac'}\cos\phi\sin\phi = \chi_2$$
$$K_{\chi_3\chi_3} = K_{bb} = \chi_3$$
$$K_{\chi_1\chi_3} = K_{\chi_2\chi_3} = K_{\chi_3\chi_1} = K_{\chi_3\chi_2} = 0$$
$$K_{\chi_1\chi_2} = K_{\chi_2\chi_1} = -K_{aa}\cos\phi\sin\phi + K_{c'c'}\cos\phi\sin\phi + K_{ac'}(-\sin^2\phi + \cos^2\phi).$$

Now the resultant tensors in this system of coordinates are, by definition, χ_1, χ_2, χ_3 along the axes, hence

$$K_{\chi_1\chi_2} = K_{\chi_2\chi_1} = 0,$$

i.e.,

$$-K_{aa}\cos\phi\sin\phi + K_{c'c'}\cos\phi\sin\phi + K_{ac'}(-\sin^2\phi + \cos^2\phi) = 0,$$

$$\tan\phi = \frac{K_{c'c'} - K_{aa} \pm \sqrt{(K_{c'c'} - K_{aa})^2 + 4K_{ac'}^2}}{2K_{ac'}}. \qquad (2)$$

Adding $0 = -K_{\chi_1\chi_3}\cdot\tan\phi$ to each side of the equation

$$\chi_1 = K_{aa}\cos^2\phi + K_{c'c'}\sin^2\phi + 2K_{ac'}\cos\phi\sin\phi,$$

we obtain

$$\chi_1 = K_{aa}\cos^2\phi + K_{c'c'}\sin^2\phi + 2K_{ac'}\cos\phi\sin\phi + [K_{aa}\cos\phi\sin\phi - K_{c'c'}\cos\phi\sin\phi - K_{ac'}(\cos^2\phi - \sin^2\phi)]\tan\phi = K_{aa} + K_{ac'}\tan\phi, \qquad (3)$$

similarly,

$$\chi_2 = K_{c'c'} - K_{ac'}\tan\phi. \qquad (4)$$

Hence

$$\tan\phi = \frac{\chi_1 - K_{aa}}{K_{ac'}} = \frac{K_{c'c'} - \chi_2}{K_{ac'}}, \qquad (2A)$$

$$\chi_1 = \tfrac{1}{2}[K_{aa} + K_{c'c'} \pm \sqrt{(K_{aa} - K_{c'c'})^2 + 4K_{ac'}^2}] \qquad (3A)$$

$$\chi_2 = \tfrac{1}{2}[K_{aa} + K_{c'c'} \mp \sqrt{(K_{aa} - K_{c'c'})^2 + 4K_{ac'}^2}], \qquad (4A)$$

the choice of sign being made so that $|\chi_1| < |\chi_2|$.

$$\chi_1 + \chi_2 + \chi_3 = K_{aa} + K_{bb} + K_{c'c'} = K_1 + K_2 + K_3, \qquad (5)$$

since $\alpha_1^2 + \beta_1^2 + \gamma_1^2 = 1$, etc.

Given χ_1, χ_2, χ_3 and α_1, γ_1, α_2 (or any other three independent direction cosines of the molecule) it is possible to calculate K_1, K_2, K_3 and $\tan\phi$ from the four equations (2), (3), (4), (5). On the other hand, ϕ is directly measurable, and the agreement between the measured and calculated values of ϕ therefore constitutes a check on the determined values of the molecular direction cosines and crystal susceptibilities.

For large plane aromatic molecules, we find that $K_3 \gg K_1$ and K_2 (numerically) and that $K_1 \simeq K_2$.

Substituting $K_1 \simeq K_2$ in the formulae (3A), (4A), (1), and (2) (pp. 601-603) we obtain

$$\begin{cases} \chi_1 \simeq K_1 \\ \chi_2 \simeq K_3 - (K_3 - K_1)\beta_3^2 \\ \chi_3 \simeq K_1 + (K_3 - K_1)\beta_3^2 \\ \tan\phi = \tan(\beta - \psi) \simeq -\dfrac{\alpha_3}{\gamma_3}. \end{cases}$$

(K_1, K_2, K_3 being intrinsically negative and mutually orthogonal.)

From these formulae also it is clear that χ_1 *is the line in which the plane of the molecule cuts the* (010) *plane, if* $K_1 = K_2$, while χ_2 is then the projection on (010) of the K_3 axis, which is normal to the molecular plane.

This is a very important result, as it applies to many of the crystals most suitable for examination by X-ray methods, and the orientation of χ_1 and χ_2 are directly measurable quantities.

In the two papers by Krishnan and his collaborators, referred to above, the statement is made that

$$\psi = \mu,$$

where ψ has the significance given above (*i.e.*, ψ is the angle between χ_1 and the c axis, measured positive from c towards a through the obtuse

angle β) and μ is, by definition, the angle between the *c* axis and the normal projection of the long axis (taken as the direction of K_1) of the molecule on the (010) plane. This statement has led to the assumption that magnetic measurements are capable of yielding a more accurate value of the molecular orientation μ than is obtainable from the analysis of X-ray data (*see* footnotes to the papers by Krishnan, Guha, and Banerjee, *loc. cit.*, p. 252, and Krishnan and Banerjee, *loc. cit.*, p. 285). It will be shown later, however, that magnetic measurements do not give the value of μ at all, except in certain special cases. Magnetic measurements only give ψ, which is not, in general, equal to the angle μ, the relationship between the two angles being a very complicated one except for particular orientations of the molecule. Expanding equation (2),

$$\tan\phi = \tan(\beta-\psi) = \frac{(K_1-K_3)(\gamma_1^2-\alpha_1^2)+(K_2-K_3)(\gamma_2^2-\alpha_2^2) + \sqrt{[(K_1-K_3)(\gamma_1^2-\alpha_1^2)+(K_2-K_3)(\gamma_2^2-\alpha_2^2)]^2+4[(K_1-K_3)\alpha_1\gamma_1+(K_2-K_3)\alpha_2\gamma_2]^2}}{2[(K_1-K_3)\alpha_1\gamma_1+(K_2-K_3)\alpha_2\gamma_2]}$$

Now it is easily shown by spherical trigonometry that

$$\tan(\beta-\mu) = \frac{\gamma_1}{\alpha_1}.$$

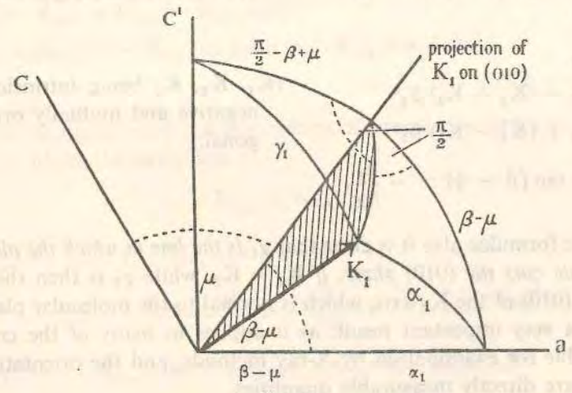

FIG. 2.

If $\psi = \mu$, then those expressions should be exactly equivalent, and this is obviously not true. The expression for $\tan(\beta-\mu)$ is dependent only on the direction of K_1, whereas $\tan\phi = \tan(\beta-\psi)$ is dependent upon the absolute values $|K_1|$, $|K_2|$, $|K_3|$ as well as upon their directions; it depends, in fact, upon *six* variables.

There are special cases in which the expression for $\tan\phi$ simplifies to γ_1/α_1, and in these cases therefore, $\psi = \mu$.

(I). When the molecule is plane and normal to (010):

Then the K_3 axis lies in the (010) plane and must be identical with either χ_1 or χ_2. It follows that $\beta_3 = 0$

$$\chi_3 = K_{bb} = K_1\beta_1^2 + K_2\beta_2^2$$
$$\chi_2 = K_3$$

(since $|K_3| > |K_1|$ and $|K_2|$, and therefore K_3 must be identical with the numerically larger of the two principal susceptibilities in the (010) plane).

Therefore

$$\chi_1 = K_1 + (K_2 - K_1)\beta_1^2$$

since

$$\beta_1^2 + \beta_2^2 = 1.$$

Similarly $\chi_3 = K_2 + (K_1 - K_2)\beta_1^2$

$$\tan\phi = \frac{\chi_1 - K_{aa}}{K_{ac'}} = \frac{K_1 + (K_2-K_1)\beta_1^2 - K_1\alpha_1^2 - K_2\alpha_2^2 - K_3\alpha_3^2}{K_1\alpha_1\gamma_1 + K_2\alpha_2\gamma_2 + K_3\alpha_3\gamma_3} = \gamma_1/\alpha_1,$$

since K_1, K_2, K_3 are orthogonal and $\beta_3 = 0$, $\alpha_1\gamma_2 = \alpha_2\gamma_1$.

(II) When K_1 actually lies in the (010) plane. Then clearly one principal susceptibility will lie along the direction of K_1. Let this be χ_1; then $\beta_1 = 0$

$$\chi_1 = K_1$$
$$\chi_3 = K_{bb} = K_2\beta_2^2 + K_3\beta_3^2 = K_3 + (K_2 - K_3)\beta_2^2$$
$$\chi_2 = K_2 + (K_3 - K_2)\beta_2^2$$

[$\chi_1 < \chi_2$ if $K_1 < K_2 + (K_3 - K_2)\beta_2^2$; otherwise χ_1 and χ_2, β_1 and β_2 can be interchanged. This does not affect the calculation.]

$$\tan\phi = \frac{\chi_1 - K_{aa}}{K_{ac'}} = \frac{K_1 - K_1\alpha_1^2 - K_2\alpha_2^2 - K_3\alpha_3^2}{K_1\alpha_1\gamma_1 + K_2\alpha_2\gamma_2 + K_3\alpha_3\gamma_3} = \gamma_1/\alpha_1,$$

since

$$\beta_1 = 0,$$
$$\alpha_1\alpha_2 + \gamma_1\gamma_2 = 0$$

and

$$\alpha_1\alpha_3 + \gamma_1\gamma_3 = 0.$$

These are the two special cases of structures for which $\psi = \mu$.

In Krishnan's notation* ν is the angle between the actual direction of K_1 and its normal projection on (010), so that $\beta_1 = \sin \nu$. λ is the angle between the axis K_2 and its normal projection on a plane through K_1 perpendicular to (010), *i.e.*, on a plane containing K_1 and the projection of K_1 on (010). Then

$$\beta_2 = \cos \lambda \cos \nu, \qquad \beta_3 = \sin \lambda \cos \nu.$$

The orientation of the molecule is completely defined by μ, ν, λ. Krishnan and Banerjee (*loc. cit.*, p. 284) give three equations:

$$\begin{cases} \chi_1 = K_1 \cos^2 \nu + (K_2 \cos^2 \lambda + K_3 \sin^2 \lambda) \sin^2 \nu \\ \chi_2 = K_2 \sin^2 \lambda + K_3 \cos^2 \lambda \\ \chi_3 = K_1 \sin^2 \nu + (K_2 \cos^2 \lambda + K_3 \sin^2 \lambda) \cos^2 \nu. \end{cases}$$

The last of these is perfectly general; on substitution it becomes identical with equation (1) (p. 601).

The first two of Krishnan's equations are not general. They hold only for the special cases considered above. In case (I) we found $\beta_3 = 0$, so that $\lambda = 0$, and therefore

$$\begin{cases} \chi_1 = K_1 \cos^2 \nu + K_2 \sin^2 \nu = K_1 + (K_2 - K_1)\, \beta_1^2 \\ \chi_2 = K_3. \end{cases}$$

In case (II) we found $\beta_1 = 0$, so that $\nu = 0$, and therefore

$$\begin{cases} \chi_1 = K_1 \\ \chi_2 = K_2 \sin^2 \lambda + K_3 \cos^2 \lambda = K_2 + (K_3 - K_2)\, \beta_2^2. \end{cases}$$

What these two equations do give, are, in general, not χ_1 and χ_2 but the components of the molecular susceptibilities lying in the (010) plane along, and perpendicular to, the projection of K_1. These components, however, do not represent the resultants in the (010) plane except in the special cases referred to above. It is clear, therefore, that, except in such special circumstances, it is inaccurate to use these equations in order to predict the values of ν and λ from magnetic measurements alone, even if K_1, K_2, and K_3 can be correctly estimated. The fact that a considerable measure of success attended the first attempts at such a prediction, *e.g.*, diphenyl, terphenyl, quaterphenyl, durene, chrysene, and benzoquinone,† was due to the fact that the structures chosen happened to approximate to one or

* Krishnan and Banerjee, *loc. cit.*, p. 284.

† Krishnan, Guha, and Banerjee, *loc. cit.*, p. 256; Krishnan and Banerjee, *loc. cit.*, pp. 281–294.

the other of the special cases: in benzoquinone $\lambda \simeq 0$, while in the other crystals $\nu \simeq 0$. In the case of dibenzyl, however, although the values of K_1, K_2, K_3 as estimated by Krishnan and Banerjee were substantially correct, the application of the incorrect formulae led to the orientations $\mu = +83{\cdot}9°$, $\nu = 0°$, $\lambda = 30°$, whereas the correct orientations derived from a Fourier analysis are

$$\mu = +70{\cdot}7°, \quad \nu = 12{\cdot}7°, \quad \lambda = 32{\cdot}1°.*$$

It is true, however, that for most of these large aromatic molecules a perfectly general consideration of the crystalline diamagnetic anisotropy will give a clear indication as to the approximate orientation of the molecule, and will often indicate which substances are likely to yield most easily to X-ray analysis.

Expanding formulae (3A) and (4A) (p. 603),

$$\chi_1 = \tfrac{1}{2}\{K_1(\alpha_1^2 + \gamma_1^2) + K_2(\alpha_2^2 + \gamma_2^2) + K_3(\alpha_3^2 + \gamma_3^2) + \sqrt{[K_1(\alpha_1^2 - \gamma_1^2) + K_2(\alpha_2^2 - \gamma_2^2) + K_3(\alpha_3^2 - \gamma_3^2)]^2 + 4(K_1\alpha_1\gamma_1 + K_2\alpha_2\gamma_2 + K_3\alpha_3\gamma_3)^2}\}$$

$$= \tfrac{1}{2}\{aK_1 + bK_2 + cK_3 + \sqrt{(dK_1 + eK_2 + fK_3)^2 + (lK_1 + mK_2 + nK_3)^2}\}$$

$$\chi_2 = \tfrac{1}{2}\{aK_1 + bK_2 + cK_3 - \sqrt{(dK_1 + eK_2 + fK_3)^2 + (lK_1 + mK_2 + nK_3)^2}\},$$

where

$$a = \alpha_1^2 + \gamma_1^2 \qquad d = \alpha_1^2 - \gamma_1^2 \qquad l = 2\alpha_1\gamma_1$$

$$b = \alpha_2^2 + \gamma_2^2 \qquad e = \alpha_2^2 - \gamma_2^2 \qquad m = 2\alpha_2\gamma_2$$

$$c = \alpha_3^2 + \gamma_3^2 \qquad f = \alpha_3^2 - \gamma_3^2 \qquad n = 2\alpha_3\gamma_3$$

Also

$$\chi_1 + \chi_2 + \chi_3 = K_1 + K_2 + K_3.$$

The solution of these equations, giving K_1, K_2, K_3 in terms of χ_1, χ_2, χ_3, a, b, c, d, e, f, l, m, n is straightforward, though tedious, and will not be given here *in extenso*. In Table I, results of such calculations for various crystals are given and a comparison is made between ψ obs. (measured directly by Krishnan and his collaborators) and ψ calc., as derived from the formula

$$\tan \phi = \tan(\beta - \psi) = \frac{\chi_1 - K_1\alpha_1^2 - K_2\alpha_2^2 - K_3\alpha_3^2}{K_1\alpha_1\gamma_1 + K_2\alpha_2\gamma_2 + K_3\alpha_3\gamma_3}$$

[*i.e.*, using only molecular orientations and absolute values of susceptibilities].

* Robertson, ' Proc. Roy. Soc.,' A, vol. 150, p. 348 (1935).

K. Lonsdale and K. S. Krishnan

Two additional columns give the values of μ (as previously defined) and μ' (the angle between the c axis and the normal projection of K_2 on (010)). It will be seen that the agreement between ψ obs. and ψ calc. is very good, except for durene and dibenzyl. Even here the difference is not great. There is, of course, no agreement between μ or μ' and ψ, except for *p*-benzoquinone, in which the molecular plane is nearly normal to (010), $\left[\tan(\beta-\mu)=\frac{\gamma_1}{\alpha_1},\ \tan(\beta-\mu')=\frac{\gamma_2^2}{\alpha_2};\ \frac{\gamma_1}{\alpha_1}\approx\frac{\gamma_2}{\alpha_2}\text{therefore }\mu\approx\mu'\right]$, and also for chrysene, *p*-diphenylbenzene, and *p*-diphenylbiphenyl, for all of which the long axis K_1 lies near or in the (010) plane [and hence $\mu-\mu'=90°$].

The experimental values of the principal susceptibilities of naphthalene and anthracene, given in Table I, differ from those previously published (Krishnan, Guha, and Banerjee, *loc. cit.*), which were found to be incorrect. It will be observed that the anomalous values of K_1 and K_2 for these two substances have now disappeared, the anisotropies of naphthalene and anthracene falling into line with those of other condensed aromatic compounds such as phenanthrene, chrysene, dibenzanthracene, and pyrene. One of the main facts which emerges from this table is that for all these simple aromatic compounds $|K_2|\approx|K_1|\approx|\chi_1|$, a postulate which has proved exceedingly useful in the estimation of molecular susceptibilities for simple compounds whose structure is not accurately known, but which may prove misleading if applied to more complex substances.

It may be pointed out at this stage that if the unit cell of a crystal contains more molecules than are necessary to provide the symmetry of the class, then the orientations of all the molecules must be taken into account. Assuming as before that magnetically the molecules are identically anisotropic, the formulae connecting principal susceptibilities of crystal and molecule will be

$$\chi_1=\tfrac{1}{2}\left[K_{aa}+K_{c'c'}+\sqrt{(K_{aa}-K_{c'c'})^2+4K_{ac'}{}^2}\right]$$

$$\chi_2=\tfrac{1}{2}\left[K_{aa}+K_{c'c'}-\sqrt{(K_{aa}-K_{c'c'})^2+4K_{ac'}{}^2}\right]$$

$$\chi_3=K_{bb},$$

where

$$K_{aa}=K_1\Sigma\alpha_1{}^2+K_2\Sigma\alpha_2{}^2+K_3\Sigma\alpha_3{}^2$$

$$K_{bb}=K_1\Sigma\beta_1{}^2+K_2\Sigma\beta_2{}^2+K_3\Sigma\beta_3{}^2$$

$$K_{c'c'}=K_1\Sigma\gamma_1{}^2+K_2\Sigma\gamma_2{}^2+K_3\Sigma\gamma_3{}^2$$

$$K_{ac'}=K_1\Sigma\alpha_1\gamma_1+K_2\Sigma\alpha_2\gamma_2+K_3\Sigma\alpha_3\gamma_3,$$

TABLE I

Compound and formula	X-ray data: Long axis α_1	γ_1	μ	X-ray data: Short axis α_2	γ_2	μ'	Observed magnetic data for *crystal* ($\times 10^6$): $-\chi_1$	$-\chi_2$	$-\chi_3$	ψ obs.	Deduced magnetic data for *molecule* ($\times 10^6$): ψ calc.	$-\kappa_1$	$-\kappa_2$	$-\kappa_3$
Naphthalene*,† .... $\rightarrow K_1$	$\overline{0\cdot4278}$	0·8770	6°·7	0·3231	0·3745	73°·5	56·0	146·4	76·6	12°·0	13°·2	56·1	53·9	169·0
Anthracene*,‡..... $\rightarrow K_1$	$\overline{0\cdot4978}$	0·8588	4·9	0·3472	0·3255	81·8	75·5	211·8	102·9	8·0	8·9	75·8	62·6	251·8
Durene§,‖..... $\rightarrow K_1$	0·6551	0·0967	−75·1	$\overline{0\cdot1184}$	0·9926	16·5	77·3	117·0	109·3	20·2	17·6	82·4	77·3	143·9
Dibenzyl¶,** ..... $\rightarrow K_1$	0·6860	0·6936	70·7	$\overline{0\cdot5093}$	0·2418	−38·6	90·5	173·6	118·9	83·9	79·0	90·7	86·7	205·5
p-benzoquinone§,†† .. $\rightarrow K_1$	0·1943	0·5681	29·9	0·2719	0·7521	30·9	27·1	67·1	25·9	31·2	30·5	24·3	28·7	67·1
Chrysene§,‡‡ ..... $\rightarrow K_1$	$\overline{0\cdot2079}$	0·9781	13·8	0·4756	$\overline{0\cdot0811}$	−73·9	88·0	258	136·1	12·7	13·1	88·0	83·3	310·8
	λ	ν	μ			μ′								
p-diphenylbenzene§,§§ $\rightarrow K_1$	34°	0	−15·3			74·7	96·8	214	145·4	−14·3	−15·3	96·8	88·1	271·3
p-diphenylbiphenyl§ $\rightarrow K_1$	34°	0	−11·3			78·7	122	290	192	−12·1	−11·3	122	110	372

* χ_1, χ_2, χ_3 redetermined, as former experimental values were found to be incorrect.
† Robertson, ' Proc. Roy. Soc.,' A, vol. 142, p. 674 (1933).
‡ Robertson, ' Proc. Roy. Soc.,' A, vol. 140, p. 79 (1933).
§ Krishnan and Banerjee, ' Phil. Trans.,' A, vol. 234, p. 265 (1935).
‖ Robertson, ' Proc. Roy. Soc.,' A, vol. 142, p. 659 (1933).
¶ Krishnan, Guha, and Banerjee, ' Phil. Trans.,' A, vol. 231, p. 235 (1933).
** Robertson, ' Proc. Roy. Soc.,' A, vol. 150, p. 348 (1935).
†† *Ibid.*, p. 106.
‡‡ Iball, ' Proc. Roy. Soc.,' A, vol. 146, p. 140 (1934).
§§ Pickett, ' Proc. Roy. Soc.,' A, vol. 142, p. 333 (1933).

the summation being taken over all the independently orientated molecules (not connected by symmetry operations inherent in the space-group) in the unit cell.

If, however, in such circumstances an attempt is made to deduce the molecular orientation from magnetic measurements alone, by using an estimated value of the molecular anisotropy, the results may be quite misleading. This has been pointed out for stilbene* in which the monoclinic unit cell contains two pairs of differently orientated centro-symmetrical molecules. From magnetic measurements alone the molecule was thought to be not centro-symmetrical but folded and twisted in a most peculiar way.† This "molecule" is, in fact, composed of two halves of independently orientated molecules, a fact which could not possibly have been foreseen from a study of the magnetic properties of the crystal.

Orthorhombic System

The coordinates of equivalent points in the most symmetrical orthorhombic class are

$$\pm |x\,y\,z;\ \bar{x}\,y\,z;\ x\,\bar{y}\,z;\ x\,y\,\bar{z}|.$$

Relative to the orthorhombic crystal axes, the direction cosines of the K_1, K_2, K_3 axes of the 8 molecules in the unit cell (centro-symmetrical molecules having identical direction cosines) may be expressed as follows:

	a	*b*	*c*	*a*	*b*	*c*
K_1	α_1	β_1	γ_1	$-\alpha_1$	β_1	γ_1
K_2	α_2	β_2	γ_2	$-\alpha_2$	β_2	γ_2
K_3	α_3	β_3	γ_3	$-\alpha_3$	β_3	γ_3

	a	*b*	*c*	*a*	*b*	*c*
K_1	α_1	$-\beta_1$	γ_1	α_1	β_1	$-\gamma_1$
K_2	α_2	$-\beta_2$	γ_2	α_2	β_2	$-\gamma_2$
K_3	α_3	$-\beta_3$	γ_3	α_3	β_3	$-\gamma_3$

* Robertson, Prasad, and Woodward, 'Proc. Roy. Soc.,' A, vol. 154, p. 187 (1936).
† Krishnan, Guha, and Banerjee, *loc. cit.*, p. 259.

only three of these cosines being independent. The 9 components along the axial directions are obtained as before:

$$K_{aa} = K_1\alpha_1^2 + K_2\alpha_2^2 + K_3\alpha_3^2$$
$$K_{bb} = K_1\beta_1^2 + K_2\beta_2^2 + K_3\beta_3^2$$
$$K_{cc} = K_1\gamma_1^2 + K_2\gamma_2^2 + K_3\gamma_3^2$$
$$K_{bc} = K_{cb} = \tfrac{1}{4}[K_1\beta_1\gamma_1 + K_2\beta_2\gamma_2 + K_3\beta_3\gamma_3 + K_1\beta_1\gamma_1 + K_2\beta_2\gamma_2 + K_3\beta_3\gamma_3 - K_1\beta_1\gamma_1 - K_2\beta_2\gamma_2 - K_3\beta_3\gamma_3 - K_1\beta_1\gamma_1 - K_2\beta_2\gamma_2 - K_3\beta_3\gamma_3] = 0.$$

Similarly,

$$K_{ca} = K_{ac} = K_{ab} = K_{ba} = 0.$$

Hence it follows that the resultant susceptibilities in this system lie along the crystal axes, being given by

$$\left.\begin{aligned}\chi_a &= K_1\,\Sigma\,\alpha_1^2 + K_2\,\Sigma\,\alpha_2^2 + K_3\,\Sigma\,\alpha_3^2\\ \chi_b &= K_1\,\Sigma\,\beta_1^2 + K_2\,\Sigma\,\beta_2^2 + K_3\,\Sigma\,\beta_3^2\\ \chi_c &= K_1\,\Sigma\,\gamma_1^2 + K_2\,\Sigma\,\gamma_2^2 + K_3\,\Sigma\,\gamma_3^2\end{aligned}\right\},$$

where the summation is taken over all the independently orientated molecules (not connected by symmetry operations inherent in the space-group) in the unit cell.

If α_1, α_2, γ_1 are known (and hence the remainder of the direction cosines using the relations

$$\Sigma\,\alpha^2 = \Sigma\,\beta^2 = \Sigma\,\gamma^2 = 1$$
$$\Sigma\,\alpha\beta = \Sigma\,\beta\gamma = \Sigma\,\gamma\alpha = 0),$$

then, knowing also χ_a, χ_b, χ_c, the molecular susceptibilities K_1, K_2, and K_3 may be very directly calculated. It is clear, therefore, that either triclinic or orthorhombic crystals are better than monoclinic for the calculation of the principal molecular susceptibilities.

The reverse process, that is, the deduction of the molecular orientation from the magnetic measurements alone, is not practicable, even though χ_a, χ_b, χ_c are known and K_1, K_2, and K_3 can be accurately estimated. The estimation of K_1, K_2, K_3 involves the use of the equation

$$\chi_a + \chi_b + \chi_c = K_1 + K_2 + K_3,$$

which, in effect, reduces the number of equations in α_1, α_2, γ_1 to two. If it can be assumed, however, that $K_1 = K_2$ (which is nearly true for many aromatic substances), then the equations reduce to

$$\chi_a = K_1 + (K_3 - K_1)\,\alpha_3^2$$
$$\chi_b = K_1 + (K_3 - K_1)\,\beta_3^2,$$

whence α_3, β_3, γ_3 can be calculated. In other words, a correct estimate of $K_1 = K_2$, and of K_3 will locate the orientation of the molecular plane, but not of the atoms or axes in that plane.*

Systems of Higher Symmetry

In systems of higher symmetry the information obtainable from magnetic measurements is less. For tetragonal, trigonal, and hexagonal crystals:

$$\chi_c = K_1\gamma_1^2 + K_2\gamma_2^2 + K_3\gamma_3^2$$

$$\chi_a = \chi_b = K_1\frac{\alpha_1^2+\beta_1^2}{2} + K_2\frac{\alpha_2^2+\beta_2^2}{2} + K_3\frac{\alpha_3^2+\beta_3^2}{2}$$

$$= \tfrac{1}{2}(K_1 - K_2 - K_3 - \chi_c).$$

For cubic crystals

$$\chi_a = \chi_b = \chi_c = \frac{K_1+K_2+K_3}{3}$$

To sum up:

(1) In the triclinic system, measurement of χ_1, χ_2, and χ_3, the principal magnetic susceptibilities of the crystal, gives directly the orientations and numerical values of K_1, K_2, and K_3, the principal molecular susceptibilities.

(2) In the monoclinic system, given χ_1, χ_2, χ_3 and the molecular orientations deduced from a Fourier analysis or in some other reliable way, the numerical values of the susceptibilities along three orthogonal directions in the molecule, $|K_1|$, $|K_2|$, $|K_3|$ may be calculated.

Alternatively, for simple aromatic compounds having a plane configuration, for which $|K_1| \simeq |K_2|$ and $|K_3|$ can be estimated, a knowledge of χ_1, χ_2, and χ_3 will give the line in which the plane of the molecule cuts the (010) symmetry plane, and the inclination of K_3 to the *b* axis.

(3) In the orthorhombic system, $|K_1|$, $|K_2|$, and $|K_3|$ can be calculated directly, given χ_a, χ_b, χ_c and the exact orientations of the molecules. Alternatively, if χ_a, χ_b, and χ_c are measured and if $|K_1| \simeq |K_2|$ and $|K_3|$ can be estimated, the orientation of K_3 can be calculated.

(4) In the tetragonal, trigonal, and hexagonal systems, a knowledge of χ_a ($=\chi_b$) and of χ_c, together with the exact molecular orientations, will not determine $|K_1|$, $|K_2|$, and $|K_3|$ unless the molecule has two of its

* Lonsdale, 'Nature,' vol. 137, p. 826 (1936).

principal susceptibilities equal. If that is the case, so that, for instance, $|K_1| \simeq |K_2|$, then measurement of χ_a and χ_c, together with an estimate of $|K_1|$ and $|K_3|$, will give the inclination of K_3 to the *c* axis, but will not locate it precisely.

(5) In the cubic system, measurement of the principal susceptibility $\chi_a = \chi_b = \chi_c$, will only give the mean molecular susceptibility. No information concerning the molecular orientations can be obtained from magnetic measurements.

One of us (K. L.) is indebted to the Managers of the Royal Institution and to the Trustees of the Leverhulme Research Fellowship Fund for grants defraying the expenses of the research.

Summary

The paper summarizes the mathematical relationships between crystal and molecular diamagnetic susceptibilities and molecular orientations, for the different crystal systems. Special reference is made to the large plane aromatic molecules, whose arrangement in the crystalline state has proved most amenable to accurate determination by X-ray methods. Attention is drawn to an error in the deductions from magnetic measurements, made in previous publications, which has led to a fictitious discrepancy in the results of magnetic and X-ray determinations of molecular orientations. The two methods actually give closely consistent results.

The Magnetic Anisotropy of Copper Sulphate Pentahydrate, $CuSO_4 \cdot 5H_2O$, in Relation to Its Crystal Structure. Part I

K. S. KRISHNAN AND ASUTOSH MOOKHERJI, *Indian Association for the Cultivation of Science, Calcutta*

(Received July 6, 1936)

The magnetic anisotropy of the triclinic crystal $CuSO_4 \cdot 5H_2O$ has been measured. The crystal is found to be nearly uniaxial magnetically, i.e., has an axis of approximate magnetic symmetry, the susceptibility along the axis being less than that along perpendicular directions by about 300×10^{-6} c.g.s. e.m.u. per gram molecule at 26°C. The above axis is inclined at 156°, 65°, and 52°, respectively, to the '*a*', '*b*' and '*c*' axes of the crystal. These results are discussed in relation to the known arrangement of the water molecules and oxygens round the Cu^{++} ions and the resulting crystalline electric fields acting on the latter.

1. INTRODUCTION

IN some recent papers Van Vleck and his collaborators[1] have discussed theoretically the magnetic behavior of some of the Tutton salts of the iron group of metals, particularly in relation to the influence of the strong internal electric fields which are acting on the paramagnetic ions in the crystals. The two copper salts $CuSO_4 \cdot K_2SO_4 \cdot 6H_2O$ and $CuSO_4 \cdot (NH_4)_2SO_4 \cdot 6H_2O$ have been studied in detail by Jordahl[2] and by Janes,[3] and they conclude from the magnetic data that the crystalline electric field acting on the Cu^{++} ion in these crystals has monoclinic symmetry. The field can be split up into two parts, one with cubic symmetry, which is found to be very predominant, and the other with rhombic symmetry, which is much feebler; the over-all Stark separations of the energy levels of Cu^{++} produced by these two fields are about 18,000 cm^{-1} and 350 cm^{-1}, respectively. This predominantly cubic symmetry of the field is a natural consequence of the octohedral arrangement[4] of the six water molecules in the crystal round each Cu^{++} ion, the disposition of the SO_4^{--} and the K^+ or NH_4^+ ions, which are at a greater distance from Cu^{++}, probably producing the feeble rhombic field.

The magnetic susceptibility of the triclinic crystal $CuSO_4 \cdot 5H_2O$ has been measured in the *powder state* over an extensive range of temperatures by de Haas and Gorter,[5] and from these susceptibility data, both Jordahl and Janes concluded that in this crystal also, the crystalline fields acting on Cu^{++} should be predominantly cubic. This result too has recently been shown to be in conformity with the structure of the crystal, by Beevers and Lipson;[6] they find that each Cu^{++} ion in the crystal is at the center of an approximate octohedron formed by four water molecules and two oxygens.

Whether this crystalline field is wholly cubic, or whether there is also a feeble rhombic component, as in the Tutton salts, it is not possible to decide, since the mean susceptibility of the crystal, for which alone experimental data are at present available, is not sensitive to such feeble superposed fields. Measurements on the magnetic anisotropy of the crystal will however give us much information on this point. We have therefore made measurements on the anisotropy of this crystal at different temperatures. In Part I of this paper we give an account of the measurements at room temperature, and discuss the results in relation to the structure of the crystal. Measurements at low temperatures will be dealt with in Part II.

[1] See Van Vleck, *Theory of Electric and Magnetic Susceptibilities*, Oxford (1932), Chapter XI.
[2] Jordahl, Phys. Rev. **45**, 87 (1934).
[3] Janes, Phys. Rev. **48**, 78 (1935).
[4] Regarding the structure of the Tutton salts see Hofmann, Zeits. f. Krist. **78**, 319 (1931).
[5] de Haas and Gorter, Leiden Comm. 210 d (1930).

2. EXPERIMENTAL

Copper sulphate pentahydrate crystallizes in the triclinic system, in the space group C_i^1. An x-ray analysis of the crystal has recently been made by Beevers and Lipson.[7] The unit cell has the dimensions

$a = 6.12A$, $\alpha = 82° 16'$,
$b = 10.7$, $\beta = 107° 26'$,
$c = 5.97$, $\gamma = 102° 40'$,

and it contains 2 molecules of $CuSO_4 \cdot 5H_2O$.

As the crystal is triclinic, the direction of none of its magnetic axes is known directly from considerations of symmetry, as in the other crystal systems. We have therefore to determine experimentally these directions as well.

The experimental procedure adopted is as follows. The crystal is suspended at the end of a calibrated quartz fiber, in a uniform horizontal magnetic field, with some natural face of the crystal horizontal, or some edge in it vertical. The upper end of the fiber is attached axially to a graduated torsion-head. The movements of the crystal are watched through a telemicroscope, whose axis has been adjusted to be horizontal and normal to the direction of the field.

In the first place the torsion-head is rotated suitably so as to make the torsion on the fiber nothing when the crystal takes up its equilibrium orientation in the magnetic field. We shall call this position of the torsion-head as its zero position. We require now to determine (1) the directions of the maximum and minimum susceptibilities of the crystal in the horizontal plane, i.e., the directions which set themselves along and perpendicular to the magnetic field; (2) the difference between the maximum and minimum susceptibilities in the horizontal plane, i.e., the anisotropy in the horizontal plane. The latter is determined by finding the angle α_0 through which the torsion-head has to be rotated from its zero position in order to make the crystal *just* to turn round in the field.[8] The anisotropy $\Delta\chi$ per gram molecule is then given by the relation

$$\Delta\chi = (2Mc/mH^2)(\alpha_0 - \pi/4). \qquad (1)$$

where c is the torsional constant of the fiber, H is the magnetic field, m is the mass of the crystal and M is the gram molecular weight.

To determine the directions of the magnetic axes in the horizontal plane we proceed as follows. When the crystal has taken up its equilibrium orientation in the field under zero torsion of the fiber, let some horizontal edge, or some vertical face of the crystal make a small angle $\varphi (< \pi/4)$ with the direction of observation, i.e., with the direction of the normal to the field. Let α be the angle through which the torsion-head has to be rotated from its zero position in order to bring the above edge or face exactly along the direction of observation. Evidently

$$\sin 2\varphi = (\alpha - \varphi)/(\alpha_0 - \pi/4), \qquad (2)$$

from which φ is known. By finding the inclination φ of two such edges or faces, to the normal to the field, the two magnetic axes in the horizontal plane are fixed uniquely.

The crystal is resuspended so as to make other convenient crystal directions successively vertical, and for each suspension the directions of the

[6] Beevers and Lipson, Proc. Roy. Soc. **A146**, 570 (1934).
[7] See reference 6. See also Tutton, *Crystallography and Practical Crystal Measurement*, Vol. 1 (Macmillan, 1927), p. 297.
[8] See Phil. Trans. **A234**, 265 (1935).

TABLE I. *Magnetic anisotropy of $CuSO_4 \cdot 5H_2O$ at 26°C.*

Serial number	Mode of suspension	Orientation in the field	$\Delta\chi$ ($\times 10^6$)	θ	$\Delta\chi/\sin^2\theta$ ($\times 10^6$)
1	'c' ax. vert.	$(\bar{1}00)$ at 25° to the field and $(\bar{1}\bar{1}0)$ at 51° to it.	183	52°	295
2	'a' ax. vert.	(011) at 2½° to field and $(0\bar{2}1)$ at 17½° to it.	55	24½°	320
3	$(\bar{1}00)$ and $(\bar{1}11)$ vert.	$(\bar{1}00)$ at 45½° to field and $(\bar{1}11)$ at 14° to it.	261	86°	262
4	$(\bar{1}\bar{1}0)$ and $(\bar{1}11)$ vert.	$(\bar{1}\bar{1}0)$ at 60° to field and $(\bar{1}11)$ at 12° to it.	263	79°	273
5	(100) horiz.	'c' ax. at 59½° to field and intersection of $(\bar{1}00)$ and $(\bar{1}11)$ at 7½° to it.	163	45°	326
6	(110) horiz.	'c' ax. at 44° to field, and intersection of $(\bar{1}\bar{1}0)$ and $(\bar{1}11)$ at 12° to it.	220	61°	288
7	$(\bar{1}10)$ horiz.	'c' ax. at 90° to field and intersection of $(\bar{1}10)$ and $(\bar{1}11)$ at 2½° to it.	113	38°	298
8	$(\bar{1}11)$ horiz.	Intersection of $(\bar{1}11)$ and $(\bar{1}00)$ at 22° to field, and intersection of $(\bar{1}11)$ and $(\bar{1}\bar{1}0)$ at 47° to it.	26	16°	342

magnetic axes in the horizontal plane, and the corresponding anisotropy $\Delta\chi$, are determined in the above manner.

3. Results

The experimental results obtained at room temperature are collected together in Table I. The second column gives the manner of suspension of the crystal, and the third the observed orientation of the crystal in the magnetic field; the fourth column gives the value of the anisotropy. The room temperature fluctuated about a mean value of 26°C by a few degrees, and all the values of $\Delta\chi$ have been reduced for uniformity to this temperature by assuming that $\Delta\chi$ varies inversely as the square of the temperature. This temperature correction is small. The last two columns in the table will be explained in the next section.

4. The Magnetic Axes and the Anisotropy of the Crystal

It is convenient to study the experimental data obtained in the previous section with the help of the stereographic projection. For any given suspension of the crystal, there is one plane which is horizontal (which need not necessarily be a natural or a possible crystallographic plane). In Table I we have numbered the different crystal suspensions for which we have made magnetic observations, serially from (1) to (8). In the stereographic projection (see Fig. 1) the poles of the corresponding horizontal planes are denoted by the same numbers. Thus point 1 in the figure is the pole of the plane which would be horizontal when the crystal suspension is 1; and so on.

From each of these poles a great circle is drawn to represent the direction of maximum susceptibility in the particular plane, i.e., the direction which sets itself along the field in the corresponding suspension of Table I. (To be more precise, this great circle is the locus of the poles of all the tautozonal planes which have the above direction of maximum susceptibility as the zone axis.) Only relevant portions of these great circles are shown in the figure.

As will be seen from the figure, all these great circles pass very close to a certain point M which we have marked by a small circle with a central dot. This indicates (1) that the crystal has an axis of approximate magnetic symmetry, namely along the normal to the plane which has M as its pole; this axis is found to make with the a, b and c axes of the crystal the angles 156°, 65° and 52°, respectively: (2) that the susceptibility of the crystal along the above axis is less than that along perpendicular directions; denoting the two susceptibilities by χ_{II} and $\chi_{\perp}$, respectively, χ_{II} should be less than $\chi_{\perp}$.

If the above conclusion regarding the approximate uniaxial symmetry of magnetism of the

crystal is correct, then the anisotropy $\Delta\chi$ for a given plane should be given by the relation

$$\Delta\chi = (\chi_{\perp} - \chi_{II}) \sin^2\theta, \qquad (3)$$

where θ is the angle between the normal to the plane and the axis of symmetry; in other words, $\Delta\chi/\sin^2\theta$ should be nearly constant.

The value of θ corresponding to any given suspension can be directly read from the stereographic projection. The values entered in Table I were obtained in this manner. It will be seen from the last column of the table that except for suspension (8), for which θ is very small (16°), the values of $\Delta\chi/\sin^2\theta$ are near about 300×10^{-6}.

The variations of the individual values of $\Delta\chi/\sin^2\theta$ from the mean offer a rough estimate of the deviation from perfect axial magnetic symmetry. On close examination we find that the values of $\Delta\chi/\sin^2\theta$ are largest for the suspensions (2) and (5), and smallest for (3) and (4), which suggests that the direction of the greater of the two almost equal susceptibilities in the plane M is nearly perpendicular to the planes (3) and (4).

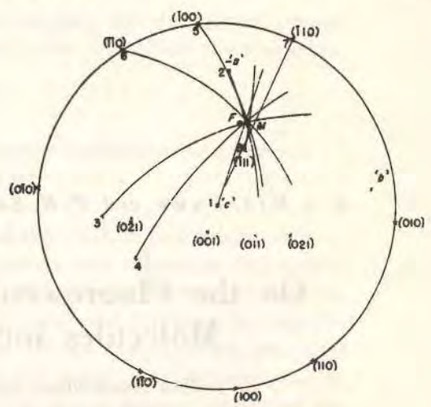

FIG. 1. Stereographic projection.

5. The Crystalline Field and its Axes

The above value for the magnetic anisotropy of $CuSO_4 \cdot 5H_2O$, namely $\chi_{\perp} - \chi_{II} = 300\times10^{-6}$ c.g.s. e.m.u. per gram molecule, points definitely to the existence of a rhombic component in the crystalline field, of nearly the same magnitude as in the Tutton salts of copper.

This small rhombic field is indeed to be expected from the disposition of the water molecules and the oxygens round the Cu^{++} ions in the crystal. From the x-ray analysis by Beevers and Lipson it is found that though each copper ion is at the center of an octohedron formed by four water molecules and two oxygens, the octohedron is only an approximate one; the four water molecules being much closer to Cu^{++} than the two oxygens. The crystalline field acting on Cu^{++} along directions in the plane of the water molecules, should therefore differ slightly from that along the normal to the plane of the water molecules.

There are two Cu^{++} ions in the unit cell, which we shall differentiate by the subscripts I and II. On calculating the orientations of the square of water molecules surrounding Cu_I and that surrounding Cu_{II}, from the parameters given by Beevers and Lipson, we find that the two squares are nearly perpendicular to each other (actually at 82°), and that they are both parallel to a direction F which makes with the a, b and c axes of the crystal the angles 155°, 68° and 50°, respectively. This direction F, as will be seen from the stereographic projection, is very close to the magnetic symmetry axis M, which is inclined at 156°, 65° and 52°, respectively, to the same crystallographic axes.

This coincidence of the magnetic and the crystalline field axes is significant; it points to the asymmetry of the crystalline field acting on the paramagnetic ion as the ultimate cause of the magnetic anisotropy of the crystal, as contemplated in Van Vleck's theory.

K. S. Krishnan and P. K. Seshan (Calcutta).

On the Fluorescence Spectra of Impurity Molecules included in Crystals.

Indian Association for the Cultivation of Science, 210 Bowbazar street, Calcutta, India.

(Received May 12, 1936).

1. *Introduction.*

In a previous paper [1]) we gave an account of some absorption experiments, with polarized light, on single crystals of anthracene and chrysene containing traces of naphthacene as impurity. It was found that the absorption bands due to naphthacene were highly polarized, indicating a strong preferential orientation of the naphthacene molecules in the crystals. Such a medium containing regularly orientated parasitic molecules is very suitable for studying the fluorescence properties of the latter, in particular to investigate the effect of varying the direction of the electric vector of the exciting light-wave with reference to the geometrical axes of the molecules, on the intensity and the polarization of the fluorescent radiations emitted by them. The concentration of these parasitic molecules can be made as small as may be desired, which is an advantage especially when the molecules are strongly absorbing. The present paper gives a short report on the directional properties of fluorescence of naphthacene molecules studied in this manner.

Studies on fluorescence in the vapour state or in solution in suitable liquids, in which the fluorescing molecules are oriented at random, do not

[1]) Zs. Krist. (A) *89*, 338. 1934.

naturally give us the same information regarding the directional properties of fluorescence of the molecules, and in the crystalline state naphthacene does not seem to fluoresce.

2. *Crystals of Chrysene and Anthracene containing Naphthacene as Impurity.*

Chrysene crystallizes out of an alcoholic solution in the form of well-developed plates. When pure, the crystals are colourless and exhibit a feeble bluish fluorescence in day-light. If however a trace of naphthacene has been added to the crystallizing solution, the crystals that separate out exhibit a beautiful green fluorescence. We shall, for brevity, call these green-fluorescing crystals of chrysene, which contain naphthacene as impurity, as „green" chrysene. Similar crystals of anthracene, containing traces of naphthacene as impurity, (which we shall call „green" anthracene can be grown in the same manner.

The question naturally arises as to the actual form in which naphthacene is present in these „green" crystals. That the naphthacene is not present as a crystalline overgrowth on chrysene or anthracene crystals, but is dispersed uniformly in the latter forming some kind of solid solution will be clear from the following considerations. These „green" crystals are quite homogeneous and fluoresce uniformly, whereas crystalline naphthacene does not fluoresce. Further, on comparing the positions of the naphthacene absorption bands appearing in the spectra of crystals of (A) „green" chrysene, (B) „green" anthracene, and (C) pure naphthacene, we find that the positions are not identical; they shift slightly towards the red as we proceed from (A) to (B), or from (B) to (C). Similarly the fluorescence bands of naphthacene appear in slightly different positions in „green" chrysene and „green" anthracene. It will thus be clear that the naphthacene molecules should be intimately mixed with those of the main substance. The „green" crystals are not, however, „mixed crystals" of naphthacene and chrysene, or of naphthacene and anthracene, in the usual crystallographic sense, since the three pure substances are not isomorphous. We have therefore to conclude that the naphthacene molecules go into some kind of solid solution in the crystal. The strong fluorescence of these naphthacene molecules, as contrasted with the absence of fluorescence in crystalline naphthacene, may be intimately connected with this fact. It would be of interest to know the positions which these parasitic molecules take up in the crystal lattice of the parent substance, viz., chrysene or anthracene.

3. *Orientations of the Naphthacene Molecules in the „Green" Crystals.*

We have studied the absorption spectra of single crystals of several aromatic hydrocarbons, with incident polarized light [2]). Though the positions of the absorption bands are practically independent of the direction of vibration of the incident light, the intensites of the bands show a remarkable dependence on the direction of vibration. Connecting this variation of intensity with the known orientations of the benzene rings in the

Fig. 1.

Fig. 2.

Fig. 3.

Fig. 4.

Absorption Spectra of Single Crystals of:

1. Naphthacene.
2. „Green" Anthracene.
3. „Green" Chrysene.
4. 1.2:5.6-Dibenzanthracene.

[2]) Current Science. *4*, 26, 1934; „Symposium on Molecular Spectra". Indian Academy of Sciences, 1934.

crystals, obtained from X-ray and other data, we find that in general the absorption by the molecules is very much stronger when the direction of vibration is in the plane of the benzene rings than when it is along the normal to the plane of the rings.

This result should presumably hold for naphthacene also, and is indeed verified directly by measurements on naphthacene crystal. From preliminary studies on this crystal made by J. Dhar in this laboratory, it is found that one of the extinction directions in the plane of the crystal plate corresponds predominantly to light-vibrations in the plane of the benzene rings while the other extinction direction corresponds predominantly to vibrations along the normal to the plane of the rings. That the former vibrations are much more strongly absorbed by the crystal than the latter will be clear from Fig. 1, in which the absorption spectra for the two directions of vibration are exhibited side by side.

In Figs. 2 and 3 are reproduced similar absorption spectra obtained with „green" anthracene and „green" chrysene. The crystals are monoclinic, and occur in the form of plates parallel to the *c* (001) plane. The two absorption spectra appearing in each picture correspond to the two principal directions of vibration in the plane of the crystal plate, the upper spectrum corresponding to light-vibrations along the *a* axis and the lower to vibrations along *b*. The strong difference in absorption between the *a* and the *b* vibrations points to a strong preferential orientation of the naphthacene molecules in the crystal, and indeed shows that the molecular planes are inclined at small angles to the *b* axis, and are nearly normal to *a*.

4. *Measurements on Fluorescence.*

The experimental arrangement used for studying the fluorescence of these crystals was as follows. The light from a mercury lamp *Q* (see Fig. 5) was rendered slightly convergent with the help of a long focal length lens L_1, and after passing through a nicol *N* and blue glass filter *F*, illuminated strongly the crystal plate *C*, mounted in front of a small square aperture made in a sheet of thick black paper. The crystal plate was mounted with its plane, viz., (001), normal to the path of the light, and its extinction directions vertical and horizontal respectively. The sides of the aperture were also vertical and horizontal.

The fluorescent light issuing from the crystal in the forward („longitudinal") direction passed through a double image prism *D* of the Wollaston type, and a lens L_2, and formed two images of the aperture on

the slit S of a spectrograph, the images lying one just above the other, and corresponding to vertical and horizontal light-vibrations respectively.

By suitably orienting the polarizing nicol, the incident light which excites fluorescence in the crystal may be made to vibrate either along

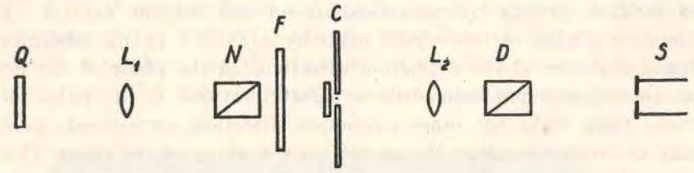

Fig. 5.

the a axis or along the b axis of the crystal. In each case two fluorescent spectra will appear in juxtaposition, in the spectrogram, one representing the component of the fluorescent light that is vibrating along the a axis, and the other the component that is vibrating along b.

The blue glass filter placed in the path of the incident light transmits the 3650, 4047 and the 4358 groups of lines of mercury. Of these the 3650 and 4358 groups excite the fluorescence of the „green" crystals only very feebly, and the 4047 group may therefore be taken to be the effective exciting radiations in our experiments.

5. *Fluorescence of „Green" Anthracene.*

In Figs. 6 and 7 are reproduced the fluorescence spectra of „green" anthracene obtained in this manner. In Fig. 6 the incident light was vibrating along the a axis of the crystal and in Fig. 7 along b. In each figure the upper half corresponds to fluorescent light vibrating along the a axis, and the lower half to fluorescent light vibrating along b.

In the figures these various fluorescent spectra are designated shortly as *aa, ab, ba, bb,* in which the first letter denotes the direction of the electric vector in the exciting light, and the second letter the direction of the electric vector in the particular polarized component of fluorescent radiation that is photographed. Thus *aa* denotes the component of the fluorescent radiation that is photographed. Thus *aa* denotes the component of the fluorescent radiation that is vibrating along the a axis, when the exciting light-vibrations are along the same direction; *ab* denotes the b vibrations of the fluorescent light when the exciting vibrations are along a; and so on.

All the four fluorescence bands that appear in the spectra in the blue-green region, at 574, 533, 495 and 468 $m\mu$ respectively, are due to naphthacene, pure anthracene having no fluorescence bands in this region.

aa
ab

Fig. 6.

ba
bb

Fig. 7.

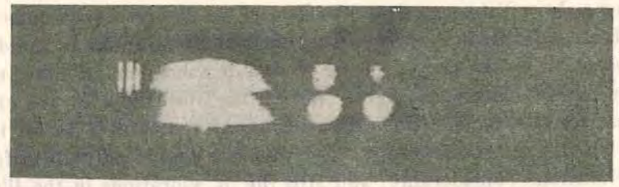

xa
xb

Fig. 8.

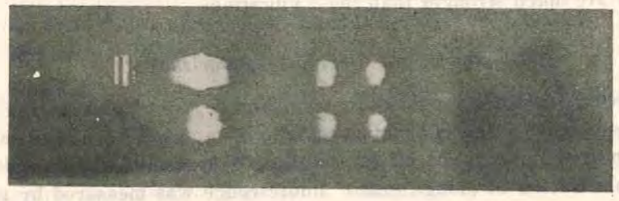

ax
bx

Fig. 9.

Fluorescence Spectra of „Green" Anthracene.

We shall now describe the main results obtained with „green" anthracene.

(1) The fluorescence bands are all partially polarized, and strongly, the degree of polarization being nearly the same for all the bands, as will be clear from the spectrograms.

(2) Whether the exciting light-vibrations are along the *b* axis or along *a*, the direction of polarization of the fluorescent light remains the same, the component of the fluorescent light vibrating along the *b* axis being much more intense than the component vibrating along *a*. In other words the *b* vibration is predominant in the fluorescent light not only when the exciting light-vector is along the same direction — a result normally to be expected — but also when the exciting light-vector is along *a*, which is perpendicular to *b* -- a very striking result. That is, when the exciting light-vibrations are along the *a* axis, the fluorescent vibrations are predominantly along a perpendicular direction, and we have here a conspicuous instance of strong *negative* polarization in „longitudinal" fluorescence.

(3) Closely associated with the above results is the strong polarization exhibited by the „longitudinal" fluorescence even when the exciting light is *unpolarized*. In Fig. 8 are reproduced the double spectra photographed after removing the polarizing nicol *N* from the path of the incident light; the upper component of the fluorescence spectrum corresponds to the *a* vibrations and the lower to *b*. They are designated in the figure as *xa* and *xb* respectively, the letter *x* indicating that the exciting light is unpolarized. As will be seen from the figure, the fluorescence bands in *xb* are much stronger than those in *xa*. This is in no way due to the differential absorption by the crystal of the *a* and *b* vibrations in either the exciting light or the fluorescent light. Indeed the absorption by the crystal is greater for the *b* vibrations than for *a*, and strikingly so for the 4047 region which excites the fluorescence, and this should actually enfeeble the *b* vibrations considerably; and still the *b* vibrations in the fluorescent light are much stronger than the *a* vibrations.

6. *Estimates of the Degree of Polarization*

We have made some rough estimates of the degree of polarization of the fluorescent light. Using a complementary green glass filter in the path of the transmitted light to cut off all the directly transmitted light-radiations, the polarization of „longitudinal" fluorescence was measured by the well-known Cornu method. We shall merely quote here the final results obtained. Denoting the intensities of the different fluorescent spectra appearing in Figs. 6, 7, and 8 by *I* with suitable subscripts, we find

$$\frac{I_{aa}}{I_{ab}} \simeq \frac{1}{4}\,; \quad \frac{I_{ba}}{I_{bb}} \simeq \frac{1}{4}\,.$$

I_{xa}/I_{xb} also is of the same magnitude.

These values would correspond to about 60% $\left(=\frac{4-1}{4+1}\times 100\right)$ polarization of the fluorescent light, for all the three excitations.

The comparison of I_{aa} with I_{ba}, or of I_{ab} with I_{bb}, is naturally more difficult, owing to the strong preferential absorption by the crystal of the *b* vibrations in the exciting light. In the optical arrangement shown in Fig. 5, the double image prism *D* was removed, and two spectrograms were taken, side by side, the polarizing nicol transmitting in one case the *a* vibrations, and in the other the *b* vibrations. The total fluorescence excited respectively by the two vibrations will therefore be recorded in the two spectra. In Fig. 9 these spectra are denoted by *ax* and *bx* respectively. The fluorescence bands appear in the two spectra with nearly the same intensity, I_{bx} being probably slightly greater than I_{ax}. Since the exciting *b* vibrations are strongly absorbed, the above result should be interpreted as indicating that in reality I_{bx} is considerably greater than I_{ax}; which means that the *b* vibrations are much more efficient in exciting fluorescence than the *a* vibrations. We have not, however, made any *quantitative* estimate of I_{bx}/I_{ax}.

7. *Fluorescence of „Green" Chrysene.*

Very similar results are obtained with „green" chrysene. (The various spectra obtained with this crystal are reproduced in Figs. 10 to 13; the double letters used to designate the individual spectra have the same significance as for „green" anthracene). Just as in „green" anthracene, the *b* vibration predominates in the fluorescent light, independent of whether the incident light is unpolarized, or is polarized with its vibration along the *b* axis or along *a*. The fluorescence is however less strongly polarized than in „green" anthracene; $\frac{I_{aa}}{I_{ab}}$ and $\frac{I_{ba}}{I_{bb}}$ are both about ½, corresponding to 30 to 35% polarization of the fluorescent light. As in „green" anthracene, in this crystal also the *b* vibrations in the incident light are more efficient in exciting fluorescence than the *a* vibrations.

8. *Fluorescence of 1.2; 5.6 - Dibenzanthracene.*

We have made similar measurements on the fluorescence of single crystals of some pure aromatic compounds, and we get results very similar to those described in the previous section. For illustration we shall take here 1.2; 5.6-dibenzanthracene, which can be obtained in the form of ex-

tremely thin flakes suitable for fluorescence measurements. This crystal also is monoclinic, and the plane of the flake is (001). X-ray [3]) and the magnetic [4]) measurements on this crystal show that the molecular planes

aa
ab
Fig. 10.

ba
bb
Fig. 11.

xa
xb
Fig. 12.

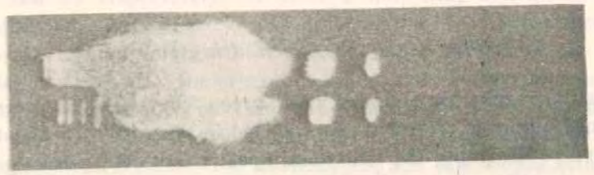

ax
bx
Fig. 13.

Fluorescence Spectra of „Green" Chrysene.

make small angles with the (010) plane, in contrast with the orientations of the naphthacene molecules in „green" anthracene or chrysene, which are nearly perpendicular to the *a* axis.

Experimentally we find that in dibenzanthracene the *a* vibrations are more strongly absorbed than the *b* vibrations (see Fig. 4). The fluorescent radiations are polarized, vibrating predominantly along *a*, inde-

[3]) Iball and Robertson, Nature. *132*. 750. 1933.
[4]) K. S. Krishnan and S. Banerjee. Zs. Krist. (A). *91*. 173, 1935.

pendent of whether the exciting light is unpolarized, or is polarized with its vibrations along *a* or along *b* (see Figs. 14, 15 and 16):

$$\frac{I_{aa}}{I_{ab}} \sim \frac{I_{ba}}{I_{bb}} \sim 2.$$

aa
ab
Fig. 14.

ba
bb
Fig. 15.

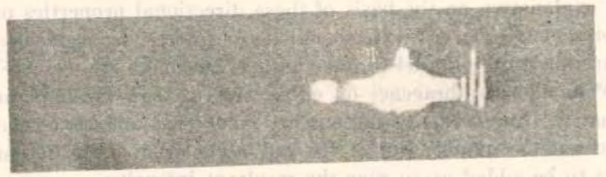

xa
xb
Fig. 16.

ax
bx
Fig. 17.

Fluorescence Spectra of 1.2; 5.6 - Dibenzanthracene.

In this crystal it is the *a* vibrations that are more efficient in exciting fluorescence, and not *b*. (See Fig. 17).

Thus the results for dibenzanthracene are the same as those obtained with the „green" crystals, except for the interchange of the *a* and the *b* axes. This interchange is a natural consequence of the fact that in diben-

zanthracene crystal the molecular planes are nearly perpendicular to the *b* axis, whereas in „green" anthracene or „green" chrysene, the naphthacene molecules are nearly normal to *a*.

9. *Conclusion.*

Considering the above results in relation to the orientations of the molecules in the crystal lattice, we find in the first place that light vibrating in the plane of the molecule excites fluorescence in it much more strongly than light vibrating along the normal to the plane of the molecule; that is, the vibration which is absorbed more strongly by the molecule is also the vibration which excites its fluorescence more strongly. Secondly we find that the fluorescent radiations excited by the former vibrations are also vibrating, either wholly or predominantly, along the same direction.

The strong polarization of fluorescence observed in the crystals with incident unpolarized light is a natural consequence of the above directional properties of fluorescence of the molecules. The negative polarization of fluorescence observed in the „green" crystals with incident *a* vibrations, and in dibenzanthracene with incident *b* vibrations, also receives a natural explanation on the basis of these directional properties of molecular fluorescence when we remember that the fluorescing molecules in the crystals are not quite parallel to one another, but make appreciable angles (about 25° in dibenzanthracene) on either side of their mean planes, and further that the fluorescent radiations are *incoherent* and hence the intensities (and not the amplitudes) of the radiations from the different molecules have to be added up to give the resultant intensity.

We are working out the general theory of fluorescence of crystals consisting of anisotropic molecules, particularly with a view to calculate the degree of polarisation of the fluorescence excited by light vibrating along different directions in the crystal, in terms of the anisotropy of fluorescence of the molecules and their orientations in the crystal lattice.

Temperature Variation of the Abnormal Unidirectional Diamagnetism of Graphite Crystals

As is well-known, graphite crystal exhibits some remarkable magnetic properties. The susceptibility along the hexagonal axis of the crystal, $\chi_{\parallel}$, is about -22×10^{-6} per gm., at room temperature, while that along directions in the basal plane, $\chi_{\perp}$, is $-0{\cdot}5 \times 10^{-6}$ only[1]—the latter value being nearly the same as that of diamond. The abnormal diamagnetism of graphite is thus more or less confined to one direction. Further, this abnormal diamagnetism is very sensitive to any chemical treatment of the crystal. For example, on treating the crystal with a mixture of strong nitric and sulphuric acids, when it swells up to 'blue graphite', $\chi_{\parallel}$ diminishes numerically from -22×10^{-6} to less than -2×10^{-6}, whereas $\chi_{\perp}$ remains practically unchanged. Also an indefinite diminution in the size of the crystal appears to have the same effect.

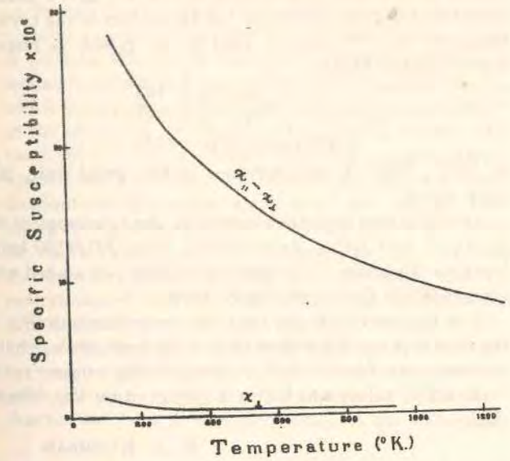

Fig. 1.

We have recently studied the temperature variation of the principal susceptibilities of graphite, and the results may be of some interest in connexion with recent discussions on the contribution of 'free' electrons to diamagnetic susceptibility and its dependence on temperature[2]. The results are represented graphically in Fig. 1. As will be seen from the curves, the magnetic anisotropy of the crystal, namely, $\chi_{\parallel} - \chi_{\perp}$, which was measured directly, diminishes numerically from about -28×10^{-6} at 140° K., to about $-7{\cdot}8 \times 10^{-6}$ at 1,270° K., whereas the corresponding variation of $\chi_{\perp}$ is from about $-1{\cdot}4 \times 10^{-6}$ at 100° K., to $-0{\cdot}5 \times 10^{-6}$ at room temperature, and to $-0{\cdot}4 \times 10^{-6}$ at 940° K.

K. S. KRISHNAN.
N. GANGULI.

210 Bowbazar Street,
Calcutta.
Dec. 3.

[1] NATURE, 133, 174 (1934); *Ind. J. Phys.*, 8, 345 (1934); *Current Science*, 3, 472 (1935); *Phil. Mag.*, 21, 355 (1936).
[2] See Shoenberg and Zaki Uddin, *Proc. Roy. Soc.*, A, 156, 687 (1936); and Stoner, *Proc. Roy. Soc.*, A, 152, 672 (1935).

The Magnetic Anisotropy of $Cs_2[CoCl_4]$

Several salts of cobalt and nickel, chiefly hydrated sulphates, selenates, etc., have recently been studied for their magnetic anisotropy. It is found that while the cobalt salts are strongly anisotropic, $\Delta\chi/\chi$ being of the order of 20 percent to 40 percent, the nickel salts are only feebly so, their $\Delta\chi/\chi$ ranging from 2 percent to 4 percent. This somewhat unexpected difference in the behavior of the two ions, which are both in the F state (d^7 ^4F and d^8 ^3F, respectively) and are adjacent in the periodic table, has been explained elegantly by Van Vleck[1] in the following manner. For a given crystalline electric field which is predominantly cubic in symmetry and has also a feeble rhombic component, the Stark patterns of Co^{++} and Ni^{++} are very similar, except that they are mutually inverted. Since one extreme level in the pattern is a singlet, and the other is a triplet, the inversion naturally makes a great difference to the magnetic anisotropy, which depends on the multiplicity of the lowest level. With the type of cubic crystalline field that obtains in the hydrated sulphates, selenates, etc , the singlet level is lowest for Ni^{++}, which will accordingly be almost isotropic, while for Co^{++} the triplet level is lowest, and will lead to a large anisotropy.

The type of cubic field referred to above as obtaining in the hydrated sulphates corresponds to an octohedral arrangement of 6 negative charges (of the water molecules) around the paramagnetic ion. This arrangement is the usual one. If on the other hand the Co^{++} (or Ni^{++}) ion in a crystal is surrounded by 4 negative charges at the corners of a tetrahedron, or 8 at the corners of a cube, then the terms in the expression for the potential of the field which refer to its cubic part change sign, as has been pointed out by Gorter,[2] and the dispositions of the Stark patterns will be the reverse of those obtaining with the octohedral distribution. The result will be that for Co^{++} the singlet level, and not the triplet level, will now be the lowest, and the crystal will have very little anisotropy.

The tetrahedral type of distribution may be expected to occur in salts in which the Co^{++} ion has a coordination number 4, instead of the usual 6. The blue double chlorides of cobalt with the alkali metals are good examples, and indeed the x-ray analyses of some of these crystals by Powell and Wells[3] show that the Co^{++} ion is closely associated with a group of 4 chlorines, which form a tetrahedron about the Co^{++} at the center.

We have studied the magnetic anisotropy of one such compound, *viz.*, $Cs_2[CoCl_4]$. It forms deep blue crystals, which are orthorhombic. Rough goniometric measurements gave for the axial ratios $a:b:c=0.38:1:0.65$. The results of the magnetic measurements are given below. Denoting the gram molecular susceptibilities of the crystal along the "a," "b" and "c" axes by χ_a, χ_b and χ_c, respectively, we find that

$$\chi_a-\chi_b=\ 143,$$
$$\chi_a-\chi_c=\ 397,$$
$$\chi=\tfrac{1}{3}(\chi_a+\chi_b+\chi_c)=8150$$

at 24°C. The χ's are expressed in the usual unit, 10^{-6} c.g.s. e.m.u.

As will be seen from the above data, the anisotropy of the crystal is very feeble, its maximum value 397/8150 being less than 5 percent. This result is strikingly in accord with the prediction from Van Vleck's theory.

It is further significant that the mean susceptibility of the crystal is much less than that of the hydrated sulphates and selenates of cobalt, and is correspondingly nearer to the "spin-only" value; which also is predicted by Van Vleck's theory.

K. S. Krishnan
Asutosh Mookherji

Indian Association for the Cultivation of Science,
210, Bowbazar Street,
Calcutta, India.
February 8, 1937.

[1] Van Vleck, Phys. Rev. **41**, 208 (1932).
[2] Gorter, Phys. Rev. **42**, 437 (1932).
[3] Powell and Wells, J. Chem. Soc. **359**, (1935).

The Magnetic Anisotropy of Four-Coordinated Co^{++} Ions in Crystals

In a recent communication[1] we described some magnetic measurements on single crystals of the blue cobalt salt $Cs_2[CoCl_4]$. In marked contrast with the ordinary (pink) cobalt salts like the hydrated sulphates and selenates, which are strongly anisotropic, the crystal of $Cs_2[CoCl_4]$ is only feebly so; $\Delta x/x$ is of the order of 20 percent to 40 percent for the former salts, whereas for $Cs_2[CoCl_4]$ it is only 5 percent. This striking difference in the magnetic behavior of the hydrated sulphates and selenates of cobalt on the one hand, and $Cs_2[CoCl_4]$ on the other, is indeed to be expected in view of the different dispositions of negative charges around the Co^{++} ions in the two types of crystals. Whereas in the former salts the cobalt ion is six-coordinated and is surrounded by six negative charges, which occupy the corners of an octahedron with the Co^{++} at the center, in the crystal of $Cs_2[CoCl_4]$, on the other hand, the Co^{++} ion is surrounded by four negative charges, which form a tetrahedron. Though for both the above distributions of charges about Co^{++} the electric fields acting on it will be predominantly cubic in symmetry, and the Stark patterns of Co^{++} produced by the two fields will be very similar, it is found theoretically[2] that the pattern should be inverted as we pass from the octohedral type of distribution to the tetrahedral. Since one extreme level of the Stark pattern is single while the other is triply degenerate, this inversion of the pattern will make a great difference to the magnetic anisotropy, as the latter depends on the degree of degeneracy of the *lowest* level. When the distribution is octohedral the threefold level is lowest, and will therefore lead to a large anisotropy, while with the tetrahedral distribution, such as obtains in $Cs_2[CoCl_4]$, the single level is lowest and the crystal will be almost isotropic.

We have now measured the magnetic susceptibilities of single crystals of another compound of cobalt in which the Co^{++} ion is four-coordinated, namely, $Cs_3[CoCl_4]Cl$. The crystals are tetragonal, and their structure has recently been analyzed by x-ray methods by Powell and Wells.[3] They find that each Co^{++} ion is closely associated with four (negatively charged) chlorine atoms, which form a tetrahedron about it, the fifth chlorine atom standing apart at a much greater distance from it. We should therefore expect the anisotropy of this crystal also to be very feeble. This is actually so, as will be seen from the following results of our magnetic measurements. Denoting the gram molecular susceptibilities of the crystal along its tetragonal axis and along perpendicular directions by $\chi_{\parallel}$ and $\chi_{\perp}$, respectively, we find that, at 30°C, $\chi_{\parallel}-\chi_{\perp}=650\times10^{-6}$, and the mean susceptibility $\chi=(\chi_{\parallel}+2\chi_{\perp})/3=9930\times10^{-6}$, both in c.g.s. e.m.u. The anisotropy is thus quite small, $\Delta x/x$ (=650/9930) being only 6½ percent.

K. S. Krishnan
Asutosh Mookherji

Indian Association for the Cultivation of Science,
210 Bowbazar Street,
Calcutta, India,
March, 1937.

[1] Phys. Rev. **51**, 528 (1937).
[2] See Van Vleck, Phys. Rev. **41**, 208 (1932), and Gorter, Phys. Rev. **42**, 437 (1932).
[3] Powell and Wells, J. Chem. Soc. London 359 (1935).

Magnetic and Optical Properties of Crystals

UNDER this title, Prof. K. S. Krishnan of the Indian Association for the Cultivation of Science (Calcutta) delivered three lectures in the Cavendish Laboratory, Cambridge, on April 26, 29 and 30. In the first lecture he dealt with recent studies of the diamagnetic properties of single crystals, particularly aromatic compounds. The method of deriving the principal susceptibilities of aromatic molecules by combining magnetic measurements with crystal structure determination was described and also the way in which molecular orientation may be predicted on the basis of magnetic measurements alone. A summary of Pauling's method of calculating the principal susceptibilities of any aromatic molecule was given. The experimental method for measuring anisotropy in magnetic susceptibility was demonstrated and also the remarkable property of graphite crystals both as they occur naturally and after exposure to potassium vapour or to oxidizing agents.

The second lecture was devoted to the recent work on paramagnetic crystals. Prof. Krishnan's study of the magnetic properties of $CuSO_4.5H_2O$ has confirmed the predictions concerning the ionic environment made on the basis of theoretical studies and has afforded a remarkable correlation of the magnetic properties with the details of the crystal structure. The influence of the co-ordination on the magnetic anisotropy of the cobalt ion is shown by the comparison of the susceptibilities of $CoSO_4.K_2SO_4.6H_2O$ with those of $Cs_2[CoCl_4]Cl$. The former salt, in which the paramagnetic ion is six co-ordinated, is of great magnetic anisotropy, while the second salt, in which the cobalt is four co-ordinated, has a very small magnetic anisotropy. This result also confirms predictions made on the basis of other physical data. The study of very small magnetic anisotropy of certain manganese salts has made possible the prediction of the entropy of these substances at temperatures near to absolute zero—an important quantity in view of the use to which these salts are put in obtaining very low temperatures by adiabatic magnetization.

The third lecture dealt with the absorption and fluorescent spectra of certain aromatic compounds. Anthracene, naphthacene and chrysene have well-marked pleochroic characters. The absorption spectrum in the ultra-violet region has strong bands for rays vibrating in that principal plane which is most nearly parallel to the plane of the molecules, and weak bands for rays vibrating in that principal plane which is most nearly perpendicular to the planes of the molecules. Naphthacene is a common impurity in anthracene and chrysene, and even when only a few parts per million of the impurity are present a strong fluorescent spectrum is observed. This has the remarkable property of being strongly excited in one plane only, no matter what the relative orientation of the plane of vibration of the incident light. This plane, corresponding to the vibration of the strongly excited spectrum, is coincident with that principal plane which is most nearly parallel to the molecular planes. Some experiments on the photo-dissociation of potassium nitrate in ultra-violet light were also described.

Magnetic Anisotropy of Rare Earth Sulphates and the Asymmetry of their Crystalline Fields

IN an important paper in the *Physical Review* for 1932 Penney and Schlapp[1] have discussed theoretically the Stark-splitting of the energy levels of the rare earth ions in crystals under the influence of the crystalline electric fields, and its influence on the magnetic behaviour of the ions. Experimentally, Spedding and his co-workers[2] have studied the absorption spectra of rare earth salts of the type $M_2(SO_4)_3.8H_2O$, where M = Pr, Nd, Er at different temperatures, and thence deduced the low-lying energy levels of the M^{+++} ions in the crystals. They find that (1) the number of low-lying energy levels and their relative separations are the same as predicted by the theory for a field of cubic symmetry acting on the M^{+++} ions; (2) the intensity of the cubic field required to produce the observed separations is the same in all the three crystals, as should be expected from their isomorphism; (3) the observed separation of the levels is not inconsistent with the available magnetic data for the mean susceptibilities of the crystals. From these and other results, it has been concluded that the fields acting on the M^{+++} ions in these crystals should be almost rigorously cubic in symmetry.

One direct result of such a cubic symmetry in the field would be a magnetic isotropy for the crystal, and any observed deviation from isotropy will give us some idea of the deviation of the field from cubic symmetry. We have recently measured the principal magnetic susceptibilities of single crystals of several rare earth salts, and we give below the values for the anisotropy of the sulphates; $\Delta\chi$ denotes the difference between the maximum and the minimum principal susceptibilities of the crystal, and χ the mean of the three principal susceptibilities.

Crystal	$\Delta\chi/\chi$
$M_2(SO_4)_3.8H_2O$	
M = Pr	0·20
Nd	0·11
Sm	0·21
Er	0·12

$\Delta\chi/\chi$ is not small, and when we remember that the group of atoms associated with each M^{+++} ion in the crystal should have at least this anisotropy, and has very probably more (as the different groups present in the unit cell of the crystal—probably eight in number—will not, in general, be oriented parallel to one another) and that it is the anisotropy of the above group (and not that of the crystal) which corresponds to the asymmetry of the field under consideration, it is easy to realize that the deviation from cubic symmetry should be quite marked. From an inspection of the table it becomes clear, as pointed out by Penney and Kynch[3], that the non-cubic part of the field has produced separations in levels, degenerate in the cubic field, comparable in size with those of the cubic field pattern itself.

A rediscussion of the valuable results on the absorption spectra of these crystals obtained by Spedding and his co-workers, taking into account the non-cubic nature of the crystalline fields as evidenced by the magnetic anisotropy of the crystals, is very desirable.

K. S. KRISHNAN.
A. MOOKHERJI.

210 Bowbazar Street,
Calcutta.
Aug. 19.

[1] *Phys. Rev.*, **41**, 194 (1932).
[2] *J. Chem. Phys.*, **5**, 191, 316, 416 (1937).
[3] NATURE, **140**, 109 (1937).

Crystal Structure and the Magnetic Anisotropy of $CuSO_4.5H_2O$

From a discussion of the magnetic susceptibilities of $CuSO_4.5H_2O$ powder at different temperatures, Jordahl[1] concluded that the crystalline electric field acting on the Cu++ ion in the crystal should be predominantly cubic in symmetry, and further, from the sign of the potential due to this field which fits the magnetic data, that the field should correspond to an octahedral distribution of six equal negative charges around the Cu++ ion. This result is not obvious from general structural considerations, since the crystal is triclinic, and there are five molecules of water and one SO_4 group associated with each Cu++ ion. The result, however, has been beautifully verified by the X-ray studies of Beevers and Lipson[2] on the structure of the crystal. The Cu++ ion is found to be at the centre of an octahedron of six negatively charged oxygen atoms. Four of them belong to four water molecules, and they form a square with the Cu++ ion in the centre. The other two, which are contributed by two sulphate groups, are located centrally above and below this square.

Now this octahedron is only approximately regular, the oxygens of the water molecules being closer to the Cu++ ion than the other two. The crystal field acting on the Cu++ ion should therefore deviate considerably from cubic symmetry, and its intensity along the normal to the plane of the water molecules should be less than for directions in the plane. Now there are two such Cu++ ions in the unit cell of the crystal, and the two corresponding squares of water molecules make with each other an angle of 82°, which is nearly a right angle. One would therefore expect: (1) that the crystal should be magnetically anisotropic, which is a trivial result since the crystal is triclinic; (2) that two of the principal susceptibilities of the crystal should be nearly equal, and greater than the third (that is, the magnetic ellipsoid should be approximately an oblate spheroid); (3) that the axis of this spheroid should lie along the line of intersection of the planes of the two squares of water molecules in the unit cell. All these conclusions have been verified experimentally[3].

The directions of the two nearly equal axes of the ellipsoid can also be predicted from the fine structure of the crystal: the shorter of them should lie in the plane bisecting internally the two squares of water molecules. Since the angle between the two squares differs by only 8° from a right angle, this last conclusion cannot be accepted with the same confidence as the others. From a study of the magnetic anisotropy for a number of planes in the crystal, we have recently determined the directions of these two magnetic axes, and they too lie nearly as predicted from the structure.

Thus the magnetic data confirm in a striking manner the structure proposed by Beevers and Lipson for the crystal.

K. S. Krishnan.
A. Mookherji.

210 Bowbazar Street,
Calcutta.
Sept. 27.

[1] *Phys. Rev.*, **45**, 87 (1934).
[2] *Proc. Roy. Soc.*, A, **146**, 570 (1934).
[3] Krishnan and Mookherji, *Phys. Rev.*, **50**, 860 (1936).

Coupling between the Orbital and the Spin Angular Momenta of Paramagnetic Ions from Magnetic Measurements

In a salt of the iron group, though the spin angular momentum of the paramagnetic ion is not directly affected by the crystalline electric fields acting on the ion, yet indirectly it is, owing to its coupling with the orbital angular momentum of the ion, which is easily affected by these fields. The magnetic anisotropy of the crystal, and the deviations of the temperature dependence of its principal susceptibilities from the Curie law, are the results of such an indirect influence of the crystal fields on the spin angular momentum exerted through the spin-orbit coupling[1], and should be the greater the stronger the coupling. Conversely, from the observed anisotropy or the deviations from the Curie law, it should be possible to calculate the strength of the spin-orbit coupling in the ion.

Such a calculation is simple for a nickel salt, and the necessary theoretical expressions have been worked out by Penney and Schlapp[2]. The magnetic anisotropy $\Delta\chi$ for any given plane in the crystal, that is, the difference between the maximum and the minimum susceptibilities in the plane, per gram molecule, is given by the relation

$$\Delta\chi = \frac{8N\beta^2}{3kT}\left(\cdot 8\lambda - \frac{2\lambda^2}{kT} - 3kT\right) . \Delta\alpha,$$

where λ is the constant of spin-orbit coupling, β is the Bohr magneton, and N, k and T have their usual significance. The factor $\Delta\alpha$ depends on the crystal fields acting on the Ni++ ions, and on the orientation of the selected plane in the crystal. Because of the small coefficient of thermal expansion of the crystal, $\Delta\alpha$ will be almost independent of temperature. From measurements on $\Delta\chi$ at two different temperatures it should therefore be possible to eliminate $\Delta\alpha$ and determine λ.

Using the method described by us in some recent papers[3], we have measured the magnetic anisotropies of the tetragonal crystals $NiSO_4.6H_2O$ and $NiSeO_4.6H_2O$, at the temperature of liquid oxygen and at room temperature. For both the crystals the anisotropy at $-183°$ C. is found to be about 4·8$_6$ times that at 23° C. From this ratio we obtain for the constant of spin-orbit coupling in Ni++ the value $\lambda = -331$ cm.$^{-1}$, which agrees well with the value -335 cm.$^{-1}$ obtained from spectroscopic data[4].

K. S. Krishnan.
A. Bose.

210 Bowbazar Street,
Calcutta.
Jan. 12.

[1] Van Vleck, J. H., *Phys. Rev.*, **41**, 208 (1932).
[2] *Phys. Rev.*, **42**, 666 (1932).
[3] Krishnan, K. S., and Banerjee, S., *Phil. Trans. Roy. Soc.*, A (1933-36).
[4] Laporte, O., *Z. Phys.*, **47**, 761 (1928).

INVESTIGATIONS ON MAGNE-CRYSTALLIC ACTION
V. PARAMAGNETIC SALTS OF THE RARE EARTH. AND THE IRON GROUPS

By Professor K. S. Krishnan and A. Mookherji
Indian Association for the Cultivation of Science, Calcutta

(*Communicated by Sir Venkata Raman, F.R.S.—Received 9 September* 1937)

CONTENTS

I. Introduction

In Part II of this series (Krishnan, Chakravorty and Banerjee 1933) we gave an account of magnetic measurements on single crystals of several sulphates and double sulphates of the iron group, and in Part IV (Krishnan and Banerjee 1936) on crystals whose paramagnetic ions are all in the S-state, which are of special interest. The present Part describes further measurements, on a large number of paramagnetic crystals, among which are many rare earth salts, several double sulphates, double selenates, selenates, sulphato-selenates and fluoberyllates of the iron group, and a few feebly paramagnetic crystals like the chromates, dichromates and ferricyanides. The magnetic data are discussed on the basis of the theory developed by Van Vleck, Penney and Schlapp (1932).

II. Experimental

The experimental method used in these measurements was the same as was described in our previous papers. The magnetic anisotropy of the crystal was measured by both the oscillational and the rotational methods described in Part III (Krishnan and Banerjee 1935) in connexion with the measurements on organic crystals. The values obtained by the two methods were practically the same, the latter method being slightly more convenient. The absolute susceptibility along some convenient direction in the crystal was measured by the modified Rabi method described in Part II.

The double sulphates, double selenates, and sulphato-selenates were prepared by mixing aqueous solutions of the two components in suitable molecular proportions. The fluoberyllates were prepared by the method described by Ray in a recent paper (1932). The fluoberyllate of cobalt ($CoBeF_4$), for example, was prepared in the following manner. First, cobalt nitrite was obtained by the double decomposition of barium nitrite and cobalt sulphate. It was mixed in solution with the required amount of ammonium fluoride. The solution was evaporated, and further heated to decomposition. Cobalt fluoride was left over, which when treated with beryllium fluoride yielded $CoBeF_4$. The double fluoberyllates were obtained by mixing aqueous solutions of the two component fluoberyllates in equimolecular proportions.

The ethyl sulphates of the rare earths were prepared by treating the corresponding hydroxides (obtained by adding ammonia to a solution of any of its salts) with ethyl sulphuric acid. Cerous ethyl sulphate, however, was prepared by the double decomposition of cerous sulphate and barium ethyl sulphate, since the hydroxide is readily oxidized in air.

Praseodymium sulphate was prepared from a specimen of the chloride, of known purity, kindly supplied by Dr P. B. Sircar, to whom we take this opportunity to express our thanks. The salts of samarium, cerium and neodymium were also fairly pure. Those of erbium were not so pure. But judged by the magnetic susceptibility, which was measured for one of these salts in solution, the amount of other rare earths present as impurity should be small.

III. Results

The results of the measurements are collected together in Tables I and II. The different columns in the tables have the same significance as in Part II. The notation adopted is also the same. For the trigonal, tetragonal and hexagonal crystals, which have an axis of magnetic symmetry, the gram-molecular susceptibility along the axis is denoted by $\chi_{\parallel}$, and that along perpendicular directions by $\chi_{\perp}$. For the orthorhombic crystals the principal susceptibilities along the "a", "b" and "c" axes are denoted by χ_a, χ_b and χ_c respectively. For the monoclinic crystals, the two principal

susceptibilities in the (010) plane are denoted by χ_1 and χ_2, χ_1 being the greater of the two. The χ_1 axis is inclined at an angle ψ to the "c" axis, and at $\beta - \psi$ to "a", β being the obtuse angle between "c" and "a". The inclination of the χ_2 axis to "a", which in many of our experiments was directly measured, is denoted by θ, where $\theta = \beta - \pi/2 - \psi$.

The measurements were all made at room temperature. During the measurements on the salts of the iron group the room temperature was about 26° C., and for the sake of uniformity the magnetic data for these crystals have been corrected so as to make them all correspond to 26° C. During the measurements on the rare earth salts and the complex salts the room temperature was about 30° C., and the values for these crystals have accordingly been reduced to 30° C.

IV. Magnetic behaviour of paramagnetic crystals: the theory of Van Vleck, Penney and Schlapp

The three outstanding features in the magnetic behaviour of paramagnetic crystals, which till recently had not been explained satisfactorily, are (1) the magnetic anisotropy of the crystals; (2) the contributions from the orbital and the spin moments of the paramagnetic ions to the susceptibility; (3) the temperature variation of the susceptibility, which, in general, deviates considerably from the Curie law. All of them receive a natural explanation on the basis of the theory developed recently by Van Vleck, Penney and Schlapp (1932).

Let us first consider a gaseous assemblage of paramagnetic atoms (or ions), and assume for simplicity that the coupling between the orbital and the spin moments of the atom is so strong that the multiplet separation is large compared with kT. The magnetic moment of the atom will then be that corresponding to the ground state, and will be given by the simple Hund rule; and the susceptibility of the gas will follow the Curie law. If, however, the multiplet separations are not large in comparison with kT, the "effective" magnetic moment of the particle will not be determined by the ground state alone, but by the immediately higher states as well, which also will be populated to some extent. The effective moment will thus vary with temperature, and the temperature variation of susceptibility will deviate from the Curie law, but in a manner that may be readily predicted.

When we come to the crystal state the problem becomes naturally more complicated, owing to the strong electric fields which are brought to play on the paramagnetic ion in the crystal, as a result of the close proximity of the neighbouring atoms or ions. This will introduce a large constraint on the freedom of rotation of the orbital moment of the paramagnetic ion, and indirectly, through the coupling of the orbital moment with the spin moment, a constraint on the spin moment as well. The effect of the first will be to quench, either partially or wholly, the orbital contribution to the effective magnetic moment of the ion, and of the second to impose on the spin moment what in

Table I

Serial no.	Crystal	Crystallographic data	Mode of suspension	Orientation in the field	$\lvert\Delta\chi\rvert\cdot$	Magnetic anisotropy	ψ Measured	ψ Calculated
			Rare earth salts (the data refer to 30° C.)					
	Sulphates							
1	$Pr_2(SO_4)_3.8H_2O$	Monoclinic prism $a:b:c = 2{\cdot}986:1:1{\cdot}999$ $\beta = 118°$	"b" axis vertical	$\theta = +2°{\cdot}1$	783	$\chi_1-\chi_2 =$ 783	+26°	+26°·5
			"a" "	"b" axis along field	975	$\chi_1-\chi_3 =-$ 975		
			(001) plane horizontal	"b" " "	1757			
2	$Nd_2(SO_4)_3.8H_2O$	Monoclinic prism $a:b:c = 2{\cdot}983:1:1{\cdot}997$ $\beta = 118°\ 8'$	"b" axis vertical	$\theta = +14°{\cdot}5$	806	$\chi_1-\chi_2 =$ 806	+13°·6	+14°·0
			"a" "	"b" axis along field	235	$\chi_1-\chi_3 =-$ 187		
			(001) plane horizontal	"b" " "	945			
3	$Sm_2(SO_4)_3.8H_2O$	Monoclinic prism $a:b:c = 3{\cdot}003:1:2{\cdot}002$ $\beta = 118°\ 16'$	"b" axis vertical	$\theta = -24°{\cdot}4$	433	$\chi_1-\chi_2 =$ 433	+52°·7	+52°·6
			"a" "	"b" axis along field	22	$\chi_1-\chi_3 =$ 52		
			(001) plane horizontal	"b" " "	308			
4	$Er_2(SO_4)_3.8H_2O$	Monoclinic prism $a:b:c = 3{\cdot}012:1:2{\cdot}004$ $\beta = 118°\ 27'$	"b" axis vertical	$\lvert\psi\rvert = 77°{\cdot}2$	8870	$\chi_1-\chi_2 =$ 8870	±77°·2	±77°·3
			"c" "	"b" axis normal to field	7250	$\chi_1-\chi_3 =$ 7680		
			(100) plane horizontal	"c" " "	764			
5	$CeNH_4(SO_4)_2.4H_2O$	Monoclinic prism $a:b:c = 0{\cdot}360:1:0{\cdot}934$ $\beta = 97°\ 15'$	"b" axis vertical	$\psi = +77°{\cdot}3$	136	$\chi_1-\chi_2 =$ 136	+77°·3	+78°·4
			"c" "	"b" axis normal to field	77	$\chi_1-\chi_3 =$ 83		
			(100) plane horizontal	"c" " "	48			
	Nitrates							
6	$Ce_2Mg_3(NO_3)_{12}.24H_2O$	Trigonal	Trigonal axis horizontal	Trigonal axis normal to field	637	$\chi_\parallel-\chi_\perp =-$ 637		
7	$Ce_2Zn_3(NO_3)_{12}.24H_2O$	"	" "	" "	650	− 650		
8	$Pr_2Mg_3(NO_3)_{12}.24H_2O$	"	" "	" "	632	− 632		
9	$Pr_2Zn_3(NO_3)_{12}.24H_2O$	"	" "	" "	653	− 653		
10	$Nd_2Mg_3(NO_3)_{12}.24H_2O$	"	" "	" "	639	− 639		
11	$Nd_2Zn_3(NO_3)_{12}.24H_2O$	"	" "	" "	611	− 611		
12	$Sm_2Mg_3(NO_3)_{12}.24H_2O$	"	" "	" "	176	− 176		

	Ethyl sulphates								
13	$Ce_2(C_2H_5SO_4)_6.18H_2O$	Hexagonal	Hexagonal axis horizontal	Hexagonal axis along field	294	$\chi_{\parallel}-\chi_{\perp}=$	294		
14	$Pr_2(C_2H_5SO_4)_6.18H_2O$	,,	,, ,,	,, ,,	241		241		
15	$Nd_2(C_2H_5SO_4)_6.18H_2O$	,,	,, ,,	,, ,,	600		600		
16	$Sm_2(C_2H_5SO_4)_6.18H_2O$	,,	,, ,,	,, ,,	172		172		
17	$Er_2(C_2H_5SO_4)_6.18H_2O$	,,	,, ,,	Hexagonal axis normal to field	6590		−6590		
	Tutton salts of the iron group of metals (the data refer to 26° C.)								
18	$FeRb_2(SO_4)_2.6H_2O$	Monoclinic prism $a:b:c$ = 0·738 : 1 : 0·500 β = 105° 44′	"b" axis vertical "a" ,, (001) plane horizontal	θ = +43°·0 "b" axis along field "b" ,, ,,	2270 917 1062	$\chi_1-\chi_2=$ 2270 $\chi_1-\chi_3=$ 150		−27°·3	−27°·5
19	$FeCs_2(SO_4)_2.6H_2O$	Monoclinic prism $a:b:c$ = 0·726 : 1 : 0·495 β = 106° 52′	"b" axis vertical "a" ,, (001) plane horizontal	θ = +40°·8 "b" axis along field "b" ,, ,,	2540 502 901	$\chi_1-\chi_2=$ 2540 $\chi_1-\chi_3=$ 570		−23°·9	−23°·6
20	$FeTl_2(SO_4)_2.6H_2O$	Monoclinic prism $a:b:c$ = 0·743 : 1 : 0·500 β = 106° 16′	"b" axis vertical "a" ,, (001) plane horizontal	θ = +42°·5 "b" axis along field "b" ,, ,,	2220 1010 1150	$\chi_1-\chi_2=$ 2220 $\chi_1-\chi_3=$ 30		−26°·2	−26°·9
21	$FeTl_2(SeO_4)_2.6H_2O$	Monoclinic prism $a:b:c$ = 0·745 : 1 : 0·501 β = 105° 27′	"b" axis vertical "a" ,, (001) plane horizontal	θ = +44°·0 "b" axis along field "b" ,, ,,	2230 722 792	$\chi_1-\chi_2=$ 2230 $\chi_1-\chi_3=$ 360		−28°·5	−28°·6
22	$CoSeO_4.6H_2O$	Monoclinic prism $a:b:c$ = 1·571 : 1 : 1·682 β = 98° 14′	"b" axis vertical "a" ,, (001) plane horizontal	θ = −52°·3 "b" axis along field "a" ,, ,,	4030 108 967	$\chi_1-\chi_2=$ 4030 $\chi_1-\chi_3=$ 2440		+60°·5	+60°·9
23	$CoRb_2(SO_4)_2.6H_2O$	Monoclinic prism $a:b:c$ = 0·739 : 1 : 0·501 β = 106° 1′	"b" axis vertical "a" ,, (001) plane horizontal	θ = +40°·5 "b" axis normal to field "a" ,, ,,	2440 163 164	$\chi_1-\chi_2=$ 2440 $\chi_1-\chi_3=$ 1220		−24°·5	−25°·1
24	$CoCs_2(SO_4)_2.6H_2O$	Monoclinic prism $a:b:c$ = 0·727 : 1 : 0·497 β = 107° 8′	"b" axis vertical "a" ,, (001) plane horizontal	θ = +62°·0 "b" axis along field "b" ,, ,,	2600 1515 80	$\chi_1-\chi_2=$ 2600 $\chi_1-\chi_3=$ 500		−44°·9	−44°·6

TABLE I (*continued*)

Serial no.	Crystal	Crystallographic data	Mode of suspension	Orientation in the field	$\lvert\Delta\chi\rvert$	Magnetic anisotropy	ψ Measured	ψ Calculated
25	$CoTl_2(SO_4)_2.6H_2O$	Monoclinic prism $a:b:c$ = 0·741 : 1 : 0·500 β = 106° 25′	"b" axis vertical "a" ,, (001) plane horizontal	θ = +54°·2 "b" axis along field "a" ,, ,,	2010 337 243	$\chi_1-\chi_2=$ 2010 $\chi_1-\chi_3=$ 960	−37°·8	−37°·0
26	$Co(NH_4)_2(SeO_4)_2.6H_2O$	Monoclinic prism $a:b:c$ = 0·745 : 1 : 0·503 β = 106° 23′	"b" axis vertical "a" ,, (001) plane horizontal	θ = +60°·8 "b" axis along field "a" ,, ,,	3120 362 1195	$\chi_1-\chi_2=$ 3120 $\chi_1-\chi_3=$ 1980	−44°·4	−43°·6
27	$CoK_2(SeO_4)_2.6H_2O$	Monoclinic prism $a:b:c$ = 0·752 : 1 : 0·506 β = 104° 17′	"b" axis vertical "a" ,, (001) plane horizontal	θ = +27°·9 "b" axis normal to field "b" ,, ,,	3130 2410 633	$\chi_1-\chi_2=$ 3130 $\chi_1-\chi_3=$ 3090	−13°·6	−13°·4
28	$CoRb_2(SeO_4)_2.6H_2O$	Monoclinic prism $a:b:c$ = 0·743 : 1 : 0·502 β = 105° 14′	"b" axis vertical "a" ,, (001) plane horizontal	θ = +35°·2 "b" axis normal to field "b" ,, ,,	2900 1275 320	$\chi_1-\chi_2=$ 2900 $\chi_1-\chi_3=$ 2250	−20°·0	−20°·2
29	$CoTl_2(SeO_4)_2.6H_2O$	Monoclinic prism $a:b:c$ = 0·746 : 1 : 0·502 β = 105° 40′	"b" axis vertical "a" ,, (001) plane horizontal	θ = +47°·2 "b" axis normal to field "b" ,, ,,	2450 657 794	$\chi_1-\chi_2=$ 2450 $\chi_1-\chi_3=$ 1950	−31°·5	−30°·9
30	$CoK_2SO_4SeO_4.6H_2O$	Monoclinic prism β = 105°	"b" axis vertical "a" ,, (001) plane horizontal	θ = +29°·0 "b" axis normal to field "b" ,, ,,	2960 1904 254	$\chi_1-\chi_2=$ 2960 $\chi_1-\chi_3=$ 2560	−14°	−13°
31	$Co(NH_4)_2(BeF_4)_2.6H_2O$	Monoclinic prism $a:b:c$ = 0·740 : 1 : 0·485 β = 106° 46′	"b" axis vertical "a" ,, (001) plane horizontal	θ = +54°·9 "b" axis along field "a" ,, ,,	2930 375 539	$\chi_1-\chi_2=$ 2930 $\chi_1-\chi_3=$ 1550	−38°·1	−37°·3
32	$NiSeO_4.6H_2O$	Tetragonal $a:c$ = 1·836	Tetragonal axis horizontal	Tetragonal axis normal to field	90	$\chi_{\perp}-\chi_{\parallel}=$ 90		
33	$NiRb_2(SO_4)_2.6H_2O$	Monoclinic prism $a:b:c$ = 0·735 : 1 : 0·502 β = 106° 3′	"b" axis vertical "a" ,, (001) plane horizontal	θ = +27°·0 "b" axis normal to field "b" ,, ,,	144 106 24	$\chi_1-\chi_2=$ 144 $\chi_1-\chi_3=$ 137	−11°·0	−11°·6
34	$NiCs_2(SO_4)_2.6H_2O$	Monoclinic prism $a:b:c$ = 0·727 : 1 : 0·498 β = 107° 2′	"b" axis vertical "a" ,, (001) plane horizontal	θ = +27°·7 "b" axis normal to field "b" ,, ,,	134 97 23	$\chi_1-\chi_2=$ 134 $\chi_1-\chi_3=$ 127	−10°·7	−11°·2

35	$NiTl_2(SO_4)_2.6H_2O$	Monoclinic prism $a:b:c$ $=0{\cdot}740:1:0{\cdot}500$ $\beta=106°\ 23'$	"b" axis vertical "a" „ (001) plane horizontal	$\theta=+27°{\cdot}3$ "b" axis normal to field "b" „ „	114 84 18	$\chi_1-\chi_2=$ 114 $\chi_1-\chi_3=$ 108	−10°·9	−10°·9
36	$Ni(NH_4)_2(SeO_4)_2.6H_2O$	Monoclinic prism $a:b:c$ $=0{\cdot}740:1:0{\cdot}505$ $\beta=106°\ 17'$	"b" axis vertical "a" „ (001) plane horizonal	$\theta=+44°{\cdot}2$ "b" axis normal to field "b" „ „	116 43 33	$\chi_1-\chi_2=$ 116 $\chi_1-\chi_3=$ 96	−27°·9	−26°·2
37	$NiK_2(SeO_4)_2.6H_2O$	Monoclinic prism $a:b:c$ $=0{\cdot}747:1:0{\cdot}506$ $\beta=104°\ 27'$	"b" axis vertical "a" „ (001) plane horizontal	$\theta=+27°{\cdot}5$ "b" axis normal to field "b" „ „	146 113 33	$\chi_1-\chi_2=$ 146 $\chi_1-\chi_3=$ 146	−13°·0	−13°·9
38	$NiRb_2(SeO_4)_2.6H_2O$	Monoclinic prism $a:b:c$ $=0{\cdot}740:1:0{\cdot}503$ $\beta=105°\ 20'$	"b" axis vertical "a" „ (001) plane horizontal	$\theta=+28°{\cdot}2$ "b" axis normal to field "b" „ „	157 110 26	$\chi_1-\chi_2=$ 157 $\chi_1-\chi_3=$ 147	−12°·9	−13°·5
39	$NiCs_2(SeO_4)_2.6H_2O$	Monoclinic prism $a:b:c$ $=0{\cdot}729:1:0{\cdot}499$ $\beta=106°\ 11'$	"b" axis vertical "a" „ (001) plane horizontal	$\theta=+33°{\cdot}8$ "b" axis normal to field "b" „ „	164 85 21	$\chi_1-\chi_2=$ 164 $\chi_1-\chi_3=$ 135	−17°·6	−17°·3
40	$NiTl_2(SeO_4)_2.6H_2O$	Monoclinic prism $a:b:c$ $=0{\cdot}746:1:0{\cdot}502$ $\beta=105°\ 36'$	"b" axis vertical "a" „ (001) plane horizontal	$\theta=+32°{\cdot}7$ "b" axis normal to field "b" „ „	123 80 24	$\chi_1-\chi_2=$ 123 $\chi_1-\chi_3=$ 113	−17°·1	−15°·9
41	$Ni(NH_4)_2SO_4SeO_4.6H_2O$	Monoclinic prism Belongs to the Tutton series $\beta=106°$	"b" axis vertical "a" „ (001) plane horizontal	$\theta=+39°{\cdot}4$ "b" axis normal to field "b" „ „	131 63 31	$\chi_1-\chi_2=$ 131 $\chi_1-\chi_3=$ 113	−23°	−22°
42	$Ni(NH_4)_2(BeF_4)_2.6H_2O$	Monoclinic prism $a:b:c$ $=0{\cdot}737:1:0{\cdot}491$ $\beta=106°\ 40'$	"b" axis vertical "a" „ (001) plane horizontal	$\theta=+31°{\cdot}0$ "b" axis normal to field "b" „ „	107 75 29	$\chi_1-\chi_2=$ 107 $\chi_1-\chi_3=$ 106	−14°·3	−15°·6
43	$CuRb_2(SO_4)_2.6H_2O$	Monoclinic prism $a:b:c$ $=0{\cdot}749:1:0{\cdot}503$ $\beta=105°\ 18'$	"b" axis vertical "a" „ (001) plane horizontal	$\theta=+86°{\cdot}0$ "b" axis along field "a" „ „	350 248 98	$\chi_1-\chi_2=$ 350 $\chi_1-\chi_3=$ 100	−70°·7	−70°·4
44	$CuCs_2(SO_4)_2.6H_2O$	Monoclinic prism $a:b:c$ $=0{\cdot}743:1:0{\cdot}495$ $\beta=106°\ 10'$	"b" axis vertical "a" „ (001) plane horizontal	$\theta=+88°{\cdot}1$ "b" axis along field "a" „ „	339 225 113	$\chi_1-\chi_2=$ 339 $\chi_1-\chi_3=$ 114	−71°·9	−71°·6
45	$CuTl_2(SO_4)_2.6H_2O$	Monoclinic prism $a:b:c$ $=0{\cdot}750:1:0{\cdot}503$ $\beta=105°\ 33'$	"b" axis vertical "a" „ (001) plane horizontal	$\theta=+88°{\cdot}2$ "b" axis along field "a" „ „	283 212 70	$\chi_1-\chi_2=$ 283 $\chi_1-\chi_3=$ 71	−72°·6	−72°·0

TABLE I (*continued*)

Serial no.	Crystal	Crystallographic data	Mode of suspension	Orientation in the field	$\lvert\Delta\chi\rvert$	Magnetic anisotropy	ψ Measured	ψ Calculated
46	$Cu(NH_4)_2(SeO_4)_2.6H_2O$	Monoclinic prism $a:b:c$ $=0{\cdot}748:1:0{\cdot}515$ $\beta=105°\ 30'$	"b" axis vertical "a" „ (001) plane horizontal	$\theta=-51°{\cdot}2$ "b" axis along field "b" „ „	353 96 21	$\chi_1-\chi_2=$ 353 $\chi_1-\chi_3=$ 118	+66°·7	+66°·6
47	$CuK_2(SeO_4)_2.6H_2O$	Monoclinic prism $a:b:c$ $=0{\cdot}751:1:0{\cdot}514$ $\beta=103°\ 25'$	"b" axis vertical "a" „ (001) plane horizontal	$\theta=+66°{\cdot}9$ "b" axis along field "a" „ „	367 220 43	$\chi_1-\chi_2=$ 367 $\chi_1-\chi_3=$ 95	−53°·5	−54°·5
48	$CuRb_2(SeO_4)_2.6H_2O$	Monoclinic prism $a:b:c$ $=0{\cdot}750:1:0{\cdot}507$ $\beta=104°\ 44'$	"b" axis vertical "a" „ (001) plane horizontal	$\theta=+88°{\cdot}0$ "b" axis along field "a" „ „	354 276 78	$\chi_1-\chi_2=$ 354 $\chi_1-\chi_3=$ 78	−73°·3	−75°
49	$CuTl_2(SeO_4)_2.6H_2O$	Monoclinic prism $a:b:c$ $=0{\cdot}753:1:0{\cdot}505$ $\beta=104°\ 59'$	"b" axis vertical "a" „ (001) plane horizontal	$\theta=+87°{\cdot}3$ "b" axis along field "a" „ „	328 255 71	$\chi_1-\chi_2=$ 328 $\chi_1-\chi_3=$ 72	−72°·3	−72°
		Complex salts (the data refer to 30° C.)						
50	$K_3Fe(CN)_6$	Monoclinic prism $a:b:c$ $=1{\cdot}288:1:0{\cdot}801$ $\beta=90°\ 6'$	"b" axis vertical "c" „ (100) plane horizontal	$\lvert\psi\rvert=88°{\cdot}9$ "b" axis normal to field "c" „ „	451 123 328	$\chi_1-\chi_2=$ 451 $\chi_1-\chi_3=$ 123	±88°·9	90°
51	$(NH_4)_2Cr_2O_7$	Monoclinic $a:b:c$ $=1{\cdot}027:1:1{\cdot}766$ $\beta=93°\ 42'$	"b" axis vertical "a" „ (001) plane horizontal	$\theta=+60°{\cdot}9$ "b" axis along field "a" „ „	19·6 7·3 3·6	$\chi_1-\chi_2=$ 19·6 $\chi_1-\chi_3=$ 8·0	−57°·2	−58°
52	K_2CrO_4	Orthorhombic $a:b:c$ $=0{\cdot}569:1:0{\cdot}730$	"b" axis vertical "a" „ "c" „	"a" axis along field "c" „ „ "a" „ „	0·6 0·9 1·5	$\chi_a-\chi_b=$ 1·5 $\chi_a-\chi_c=$ 0·6		
53	$(NH_4)_2CrO_4$	Monoclinic prism $a:b:c$ $=1{\cdot}960:1:1{\cdot}226$ $\beta=115°\ 13'$	"b" axis vertical "a" „ (001) plane horizontal	$\theta=+65°{\cdot}0$ "b" axis along field "b" axis along field	2·6 2·5 0·9	$\chi_1-\chi_2=$ 2·6 $\chi_1-\chi_3=$ −0·4	−40°	−39°

TABLE II

Serial no. 1	Crystal 2	Direction along which susceptibility was measured 3	Temp. ° C. 4	Density of crystal 5	Volume susceptibility 6	Corresponding g.-mol. susceptibility 7	Mean susceptibility at 30° C. 8
1	$Pr_2(SO_4)_3.8H_2O$	Along χ_1 axis	31·1	2·834	35·2	8,870	8,970
			32·5	2·884	35·5	8,790	8,930
2	$Nd_2(SO_4)_3.8H_2O$	"	32·9	2·851	37·0	9,350	9,240
			30·5	2·831	37·1	9,440	9,250
3	$Sm_2(SO_4)_3.8H_2O$	"	31·3	2·978	9·02	2,220	2,070
			31·0	2·990	9·06	2,220	2,070
4	$Ce(NH_4)(SO_4)_2.4H_2O$	"	31·5	2·589	12·13	1,980	1,920
			31·0	2·525	12·03	2,010	1,940
5	$Ce_2Mg_3(NO_3)_{12}.24H_2O$	Normal to trigonal axis	32·0	1·914	4·83	3,860	3,670
			31·0	2·010	5·11	3,890	3,690
6	$Ce_2Zn_3(NO_3)_{12}.24H_2O$	" "	32·1	2·222	5·50	4,090	3,900
			32·0	2·222	5·52	4,110	3,920
7	$Nd_2Mg_3(NO_3)_{12}.24H_2O$	" "	32·8	2·090	10·88	8,010	7,870
			33·2	2·076	10·78	7,990	7,860
8	$Nd_2Zn_3(NO_3)_{12}.24H_2O$	" "	32·0	2·279	10·99	8,010	7,860
			33·0	2·214	10·60	7,950	7,830
9	$Sm_2Mg_3(NO_3)_{12}.24H_2O$	" "	30·1	2·164	3·16	2,260	2,200
			31·9	2·163	3·10	2,220	2,180
10	$Ce_2(C_2H_5SO_4)_6.18H_2O$	Along hexagonal axis	30·2	1·839	5·44	4,010	3,820
			30·3	1·841	5·47	4,030	3,840
11	$Nd_2(C_2H_5SO_4)_6.18H_2O$	" "	31·0	1·924	13·47	9,540	9,170
			31·8	1·910	13·38	9,550	9,210
12	$Sm_2(C_2H_5SO_4)_6.18H_2O$	" "	32·0	1·895	2·83	2,050	1,950
			32·1	1·895	2·82	2,050	1,950
13	$Er_2(C_2H_5SO_4)_6.18H_2O$	Measured in state of solution in water					73,400
							Mean susceptibility at 26° C.
14	$FeRb_2(SO_4)_2.6H_2O$	Along χ_1 axis	25·0	2·511	61·9	12,990	12,140
			24·9	2·506	61·9	13,020	12,160
15	$FeCs_2(SO_4)_2.6H_2O$	"	34·4	2·700	54·8	12,620	11,930
			32·8	2·670	55·6	12,950	12,200

TABLE II. (*continued*)

Serial no. 1	Crystal 2	Direction along which susceptibility was measured 3	Temp. ° C. 4	Density of crystal 5	Volume susceptibility 6	Corresponding g.-mol. susceptibility 7	Mean susceptibility at 26° C. 8
16	$FeTl_2(SO_4)_2.6H_2O$	Along χ_1 axis	24·2	3·653	63·0	13,190	12,360
			24·7	3·630	62·4	13,150	12,340
17	$FeTl_2(SeO_4)_2.6H_2O$	"	30·8	3·626	52·2	12,370	11,700
			31·0	3·623	52·4	12,430	11,780
18	$CoSeO_4.6H_2O$	"	25·5	2·236	81·5	11,310	9,130
			25·0	2·247	83·4	11,520	9,320
19	$CoRb_2(SO_4)_2.6H_2O$	"	24·6	2·515	52·4	11,080	9,770
			24·8	2·507	52·3	11,060	9,760
20	$CoCs_2(SO_4)_2.6H_2O$	"	21·7	2·851	51·0	11,180	9,980
			22·2	2·829	50·5	11,150	9,980
21	$CoTl_2(SO_4)_2.6H_2O$	"	25·7	3·674	50·3	10,520	9,520
			25·3	3·566	48·9	10,530	9,520
22	$Co(NH_4)_2(SeO_4)_2.6H_2O$	"	23·6	2·217	55·2	12,180	10,380
			23·5	2·190	53·8	12,020	10,220
23	$CoK_2(SeO_4)_2.6H_2O$	"	25·0	2·521	58·2	12,280	10,170
			24·3	2·525	58·4	12,290	10,150
24	$CoRb_2(SeO_4)_2.6H_2O$	"	22·5	2·880	54·3	11,770	9,910
			22·4	2·880	54·4	11,800	9,940
25	$CoTl_2(SeO_4)_2.6H_2O$	"	22·7	3·710	53·2	12,360	10,750
			23·7	3·762	53·3	12,220	10,660
26	$CoK_2SO_4SeO_4.6H_2O$	"	23·7	2·336	59·2	12,270	10,330
			21·0	2·315	59·2	12,390	10,340
27	$Co(NH_4)_2(BeF_4)_2.6H_2O$	"	32·0	1·822	52·5	10,750	9,470
			31·9	1·831	52·7	10,740	9,460
28	$NiSeO_4.6H_2O$	Normal to tetragonal axis	25·5	2·328	32·2	4,290	4,250
			26·5	2·329	32·2	4,290	4,270
29	$NiRb_2(SO_4)_2.6H_2O$	Along χ_1 axis	26·8	2·601	20·4	4,160	4,080
			27·0	2·588	20·3	4,160	4,080
30	$NiCs_2(SO_4)_2.6H_2O$	"	22·0	2·858	19·30	4,220	4,080
			21·4	2·846	19·27	4,230	4,080
31	$NiTl_2(SO_4)_2.6H_2O$	"	25·7	3·706	19·92	4,130	4,050
			24·1	3·765	20·21	4,120	4,020
32	$Ni(NH_4)_2(SeO_4)_2.6H_2O$	"	25·5	2·262	19·41	4,200	4,120
			24·0	2·256	19·46	4,220	4,120

33	$NiK_2(SeO_4)_2.6H_2O$	25·7	2·496	19·98	4,250	4,150					
	,,	24·5	2·559	20·64	4,290	4,170					
34	$NiRb_2(SeO_4)_2.6H_2O$	22·0	2·843	19·63	4,310	4,150					
	,,	22·8	2·826	19·55	4,320	4,170					
35	$NiCs_2(SeO_4)_2.6H_2O$	30·5	3·129	18·21	4,180	4,140					
	,,	31·3	3·047	17·90	4,220	4,190					
36	$NiTl_2(SeO_4)_2.6H_2O$	24·2	3.912	19·06	4,200	4,100					
	,,	24·8	3·937	19·25	4,210	4,120					
37	$Ni(NH_4)_2SO_4SeO_4.6H_2O$	32·0	2·064	19·53	4,180	4,180					
	,,	33·0	2·086	19·49	4,130	4,150					
38	$Ni(NH_4)_2(BeF_4)_2.6H_2O$	31·1	1·833	19·97	4,060	4,060					
	,,	31·8	1·839	19·97	4,050	4,060					
39	$CuRb_2(SO_4)_2.6H_2O$	27·4	2·500	6·77	1,450	1,310					
	,,	25·8	2·502	6·77	1,450	1,300					
40	$CuCs_2(SO_4)_2.6H_2O$	21·2	2·86	6·91	1,520	1,340					
	,,	22·1	2·84	6·83	1,510	1,340					
41	$CuTl_2(SO_4)_2.6H_2O$	29·0	3·579	6·69	1,440	1,340					
	,,	28·8	3·634	6·80	1,440	1,340					
42	$Cu(NH_4)_2(SO_4)_2.6H_2O$	26·0	2·202	6·75	1,520	1,360					
	,,	26·2	2·190	6·73	1,520	1,360					
43	$CuK_2(SeO_4)_2.6H_2O$	24·8	2·286	6·93	1,630	1,470					
	,,	24·0	2·408	7·20	1,600	1,440					
44	$CuRb_2(SeO_4)_2.6H_2O$	26·2	2·80I	6·50	1,460	1,320					
	,,	24·7	2·810	6·66	1,470	1,320					
45	$CuTl_2(SeO_4)_2.6H_2O$	25·6	3·761	6·92	1,600	1,470					
	,,	24·5	3·713	6·94	1,620	1,480					
46	$K_3Fe(CN)_6$	31·8	2·117	13·61	2,120	1,940					
	,,	32·1	2·366	15·25	2,120	1,940					
47	$(NH_4)_2Cr_2O_7$	31·8	2·062	0·509	62	53					
	,,										
48	K_2CrO_4	31·0	2·726	0·112	8·0	7·3					
	Along "a" axis										
49	$(NH_4)_2CrO_4$	31·2	1·884	0·098	7·9	7·2					
	Along χ_1 axis										

effect will be equivalent to a local orienting field; this local field will naturally share with the crystalline electric field which it is intended to replace, a certain amount of asymmetry. The results will be (1) a magnetic anisotropy for the crystal, (2) a value for the effective magnetic moment of the ion which will bear no simple relation to its spin and orbital moments, and (3) a complicated deviation from the Curie law.

V. Experimental support for the theory

The theory has received experimental support from various directions. When all the paramagnetic ions in the crystal are in the S-state, and have no orbital moments to be quenched by the crystalline fields, the results are particularly simple. Such crystals should be nearly isotropic magnetically, and should obey the Curie law. Both of these results have been verified experimentally. Indeed even the second order effects, due to a very feeble splitting of the spin levels by the crystal fields, predicted by the theory, have been confirmed. For a detailed discussion of this special class of crystals the reader may be referred to Part IV of this paper (1936).

Van Vleck (1932), Schlapp and Penney (1932), Jordahl (1934), and Janes (1935) have discussed the observed anisotropy and temperature variation of susceptibility of some of the salts of the iron group. They find that the intensity and the degree of asymmetry of the crystal fields required to explain these magnetic properties are of reasonable magnitude.

In particular we may mention that from a theoretical study of the mean susceptibility of the crystal $CuSO_4.5H_2O$ at different temperatures Jordahl predicted that the crystal field acting on the Cu^{++} ion in the crystal should be predominantly cubic in symmetry, and further, from the positive sign of the potential due to this cubic field, that the field should correspond to an octohedral distribution of six equal negative charges around the Cu^{++} ion. This result is not at all obvious from general structural considerations, as the crystal is triclinic, and there are five molecules of water and one SO_4 group associated with each Cu^{++} ion. The result, however, has recently been confirmed by the X-ray studies on the fine structure of the crystal by Beevers and Lipson (1934). It is actually found that each Cu^{++} ion is surrounded by six negatively charged oxygen atoms, which form a nearly regular octohedron. Four of them belong to four water molecules, and they form a square with the Cu^{++} ion at the centre. The other two, which are contributed by the two sulphate groups, are located centrally above and below this square.

As we mentioned just now, this octohedron is only approximately regular, as the oxygens of the water molecules are much closer to the central Cu^{++} ion than the other two. The crystal field acting on the Cu^{++} ion will therefore deviate from cubic symmetry, its magnitude for directions in the plane of the square being greater than along the normal to the square. Now there are two such Cu^{++} ions in the unit cell of the crystal, and the two corresponding squares of water molecules are inclined to each

other at an angle of about 82°. One should therefore expect (1) that the crystal should be magnetically anisotropic, which is of course a trivial result, as the crystal is triclinic; (2) that it should be nearly uniaxial; and (3) that the axis of magnetic symmetry should lie along the line of intersection of the planes of the two squares. All these conclusions are verified by experiment (KRISHNAN and MOOKHERJI 1936).

Finally, we may mention some recent measurements by Mr JOGLEKAR on the magnetic anisotropies of mixed Tutton salts, in which the concentration of the paramagnetic ions in the crystal is varied, over a wide range, by growing mixed crystals with varying amounts of a suitable diamagnetic Tutton salt. The results of these experiments, which are in course of publication, lend strong support to the view underlying VAN VLECK's theory that the magnetic anisotropy of the crystal arises from the asymmetric crystalline electric fields acting on the paramagnetic ions.

VI. CLASSIFICATION OF PARAMAGNETIC CRYSTALS

Following VAN VLECK (1935) we may divide paramagnetic crystals into the following three groups, according to the strengths of the crystalline electric fields acting on the paramagnetic ions: (1) Crystals in which the electric fields are so feeble that the coupling between the orbital and the spin moments remains practically unaffected, e.g. the rare earth salts. The magnetic moments of these ions should approximate to the Hund value. (2) Crystals in which the fields are sufficiently strong to break the spin-orbital coupling, but not strong enough to affect the Russel-Saunders coupling between the moments of the different electrons in the ion; e.g. the sulphates and selenates of the iron group of metals. The magnetic moment of the ion in these crystals should be nearly that due to the spins only. (3) Crystals in which the fields are large enough to break even the Russel-Saunders coupling; e.g. ferricyanide, chromate, etc. The magnetic susceptibilities of these crystals should be very low.

The above conclusions regarding the effective magnetic moments of the ions in the three groups of crystals are verified by experiment.

The magnetic anisotropies of these three groups of crystals, however, may not show such clearly marked differences; because the anisotropy, besides depending on the term-level of the ion, is also sensitive to the asymmetry of the crystalline field, which varies from crystal to crystal more widely than the absolute magnitude of the field (on which the effective magnetic moment depends). But roughly we may expect the crystals of the third group to exhibit the largest anisotropy, and those of the first group the smallest. This is more or less true. Taking $\Delta\chi/\chi$ as a measure of the anisotropy, we find that, among the crystals studied by us, ammonium chromate and dichromate have the highest anisotropies, namely 0·42 and 0·37 respectively, and they belong to the third group. The two other crystals in our list that belong to this group, namely potassium chromate and potassium ferricyanide, have also a large anisotropy. Among the other crystals, the salts of the iron group (except those of nickel) have in general a higher anisotropy than the rare earth salts.

VII. MUTUAL INVERSION OF THE STARK-LEVELS OF SIX-COORDINATED AND FOUR-COORDINATED Co^{++} IONS IN CRYSTALS: THEIR MAGNETIC ANISOTROPIES CONTRASTED

The feeble anisotropy of the nickel salts has just been referred to: $\Delta\chi/\chi$ ranges from 0·02 to 0·04, which is only one-tenth of the anisotropy of the corresponding cobalt salts, for which $\Delta\chi/\chi$ varies from about 0·2 to 0·4. This striking contrast between the anisotropies of the cobalt and the nickel ions, which are both in the F state and are adjacent in the periodic table, requires explanation. An elegant one has been supplied by VAN VLECK (1932), which is as follows. For a given crystalline electric field which is predominantly cubic in symmetry and has also a feeble rhombic component, the Stark patterns of Co^{++} and Ni^{++}, whose ground states are $d^7\,{}^4F$ and $d^7\,{}^3F$ respectively, are very similar, except for this important difference, namely that the pattern for ^4F is inverted with respect to that for ^3F. Since one extreme level in the pattern is a singlet, while the other is a triplet, the inversion of the pattern will naturally make a great difference to the magnetic anisotropy, which depends on the multiplicity of the lowest level. For the type of cubic crystalline field that obtains in the hydrated sulphates, selenates, etc., the singlet level is lowest for Ni^{++}, which will accordingly be almost isotropic, whereas for Co^{++} the triplet level is lowest, and will lead to a large anisotropy; in agreement with observation.

The type of cubic field referred to above as obtaining in the hydrated sulphates corresponds to an octohedral arrangement of six water molecules around the paramagnetic ion. Since the water molecules have a large dipole moment, and will all present their negative ends towards the Co^{++} or Ni^{++} ion, as the case may be, the above arrangement will in effect be equivalent to an octohedral arrangement of six equal negative charges round each paramagnetic ion.

Following VAN VLECK, let us express the potential of the crystalline field in the neighbourhood of the paramagnetic ion in the form

$$\Phi = D(x^4+y^4+z^4)+Ax^2+By^2-(A+B)\,Z^2, \qquad (1)$$

where the fourth power terms refer to the cubic part of the field, and the quadratic terms to the rhombic part; the principal axes of the cubic and the rhombic fields have been assumed, for simplicity, to be coincident.

The cubic field obtaining in the above octohedral arrangement of negative charges will correspond, as GORTER (1932) has pointed out, to a positive value of D, and it is for this type of cubic field that the lowest level is a singlet for Ni^{++} and a triplet for Co^{++}. If, on the other hand, the cubic part of the field corresponds to a *negative* value of D, as it will if the paramagnetic ion were surrounded by eight equal negative charges at the corners of a cube, or four at the corners of a tetrahedron, then the disposition of the Stark pattern will be the reverse of that obtaining with the octohedral distribution;

in such a crystal the lowest level in the Stark pattern of Co^{++} will be the singlet, and not the triplet, and the crystal will in consequence be almost isotropic.

The tetrahedral type of distribution may be expected to occur in salts in which the Co^{++} ion has a coordination number four, instead of the usual six, as for example in the blue double chlorides of cobalt with the alkali metals. Indeed one such crystal, namely Cs_3CoCl_5, has recently been studied for its structure by X-ray methods by POWELL and WELLS (1935). The crystal is tetragonal, with the axial lengths $a = 9{\cdot}18$, $c = 14{\cdot}47$ A. It is found that each cobaltous ion in the crystal is closely associated with a group of four (negatively charged) chlorine atoms, which form an approximately regular tetrahedron with the cobalt at the centre, the fifth chlorine atom standing apart at a much greater distance; the structure thus corresponding to the coordination formula $Cs_3^{1+}[CoCl_4]^{2-}\,Cl^{1-}$. We should accordingly expect the magnetic anisotropy of this crystal to be quite small, in marked contrast with the hydrated sulphates and selenates of cobalt. This is actually so, as will be seen from the following results of our magnetic measurements on this crystal.

We find that at 30° C. $\chi_{\parallel} - \chi_{\perp} = 650$

and $\chi = (\chi_{\parallel} + 2\chi_{\perp})/3 = 9930.$

$\Delta\chi/\chi$ is thus quite small, being only 6·5 %.

We have also measured the principal susceptibilities of another double chloride of cobalt with caesium, namely $Cs_2[CoCl_4]$, in which also the $[CoCl_4]$ group has presumably a tetrahedral structure. Some well-developed deep blue crystals of this substance were grown out of an aqueous solution containing suitable amounts of the two chlorides. (An analysis of the crystals for their chlorine content gave Cl = 30·4 %, as compared with 30·39 % given by the above formula.) The crystals are orthorhombic, and from rough goniometric measurements the axial ratios were found to be

$$a : b : c = 0{\cdot}38 : 1 : 0{\cdot}65.$$

The following are the results of the magnetic measurements made on the crystal at 24° C.:

"a" axis vertical	"b" axis sets along the field	$\chi_b - \chi_c = 254$
"b" axis vertical	"a" axis sets along the field	$\chi_a - \chi_c = 397$
"c" axis vertical	"a" axis sets along the field	$\chi_a - \chi_b = 146,$

as against 143 calculated from the results for the first two directions.

The absolute gram-molecular susceptibility of the crystal (density 3·46) along its "b" axis was found to be 8190.

Collecting the results, we have

$$\chi_a - \chi_b = 143$$
$$\chi_a - \chi_c = 397$$
$$\text{Mean } \chi = 8150$$

The maximum anisotropy of the crystal, equal to 397/8150, is thus less than 5 %.

It is further significant that for both these crystals the mean susceptibilities are smaller than for the other cobalt salts listed in our table (in which the cobalt ions are six-coordinated), and are correspondingly nearer to the "spin-only" value. This result also follows from VAN VLECK's theory.*

We have not been able to obtain any four-coordinated nickel salt which is not diamagnetic.

VIII. CONSTANTS OF THE CRYSTAL FIELD IN NICKEL SALTS

We shall now discuss in some detail the anisotropy of nickel salts with positive D, in relation to their crystal fields. These salts lend themselves readily to a quantitative discussion. The necessary theoretical expressions have been developed by SCHLAPP and PENNEY. Assuming for simplicity, that the principal axes of the cubic and the rhombic parts of the crystal field are coincident, and that they are the same for all the paramagnetic ions in the unit cell, and that the potential of the field in the neighbourhood of the paramagnetic ion can be expressed by the relation (1) given in the previous section, namely, $\Phi = D(x^4+y^4+z^4) + Ax^2 + By^2 - (A+B)\,z^2$, they have calculated the three principal susceptibilities, χ_1, χ_2 and χ_3 of the crystal along the z, y and x axes respectively of the crystal field. We shall merely quote here their final results. For χ_1 they obtain the expression

$$\chi_1 = \frac{8N\beta^2}{3kT}\left[1 + 8\lambda\alpha_1 + \frac{\theta_1}{kT} + \ldots\right] - 8N\beta^2\alpha_1, \qquad (2)$$

and for χ_2 and χ_3 two similar expressions, in which λ is the constant of the spin-orbit coupling ($= -335$ cm.$^{-1}$), β is the BOHR magneton ($= eh/4\pi mc$), and N is the Avogadro number:

$$\theta_1 = \tfrac{2}{3}\lambda^2(\alpha_2 + \alpha_3 - 2\alpha_1); \qquad (3)$$

α_1, α_2 and α_3 are constants which depend on the crystal field in the manner to be described below.

* It should be mentioned here that the feeble anisotropies of these two crystals may be imagined to arise alternatively in the following manner: (*a*) the $[CoCl_4]$ groups may have a perfectly regular tetrahedral structure, and the rhombic component of the field may be totally absent; this is highly improbable; (*b*) the different $[CoCl_4]$ groups that are present in the unit cell may be oriented relatively to one another in such a manner as to form a more or less isotropic combination; the low mean susceptibilities of these crystals as compared with those of the six-coordinated compounds, do not support this possibility.

Instead of the constants D, A and B appearing in (1), SCHLAPP and PENNEY introduce the new constants* Dq_0, aA and aB, where $q_0/12$ and a are the ratios of the matrix elements of the actual system with 8 electrons to those for a one-electron system, for the cubic and the rhombic fields respectively.

Denoting $a(A+B)/2$ by σ, and $a(A-B)/2$ by δ, the α's are given by the expressions

$$\left.\begin{aligned}\alpha_1 &= \frac{p^2}{r_2-r_{-2}}+\frac{q^2}{r_2-r_0},\\ \alpha_2 &= \frac{r^2}{r_2-r_{-1}}+\frac{s^2}{r_2-r_{-3}},\\ \alpha_3 &= \frac{t^2}{r_2-r_1}+\frac{u^2}{r_2-r_3},\end{aligned}\right\} \tag{4}$$

in which

$$\left.\begin{aligned}(r,s) &= (\cos\theta_1, \sin\theta_1), \text{ where } \tan 2\theta_1 = \frac{-2\times 15^{\frac{1}{2}}(3\sigma+\delta)}{6(\sigma-\delta)+8Dq_0},\\ (t,u) &= (\cos\theta_2, \sin\theta_2), \text{ where } \tan 2\theta_2 = \frac{-2\times 15^{\frac{1}{2}}(3\sigma-\delta)}{8Dq_0+6(\sigma+\delta)},\\ (p,q) &= (\cos\theta_3, \sin\theta_3), \text{ where } \tan 2\theta_3 = \frac{4\times 15^{\frac{1}{2}}.\delta}{8Dq_0-12\sigma},\end{aligned}\right\} \tag{5}$$

$$\left.\begin{aligned}r_2 &= -18Dq_0,\\ r_{-3} &= r^2\times 6(\sigma-\delta)+s^2\times -8Dq_0+2rs\times -15^{\frac{1}{2}}(3\sigma+\delta),\\ r_{-1} &= r^2\times -8Dq_0+s^2\times 6(\sigma-\delta)-2rs\times -15^{\frac{1}{2}}(3\sigma+\delta),\\ r_1 &= t^2\times -8Dq_0+u^2\times 6(\sigma+\delta)+2tu\times 15^{\frac{1}{2}}(3\sigma-\delta),\\ r_3 &= t^2\times 6(\sigma+\delta)+u^2\times -8Dq_0-2tu\times 15^{\frac{1}{2}}(3\sigma-\delta),\\ r_{-2} &= p^2\times -8Dq_0+q^2\times -12\sigma+2pq\times -2\times 15^{\frac{1}{2}}.\delta,\\ r_0 &= p^2\times -12\sigma+q^2\times -8Dq_0-2pq\times -2\times 15^{\frac{1}{2}}.\delta.\end{aligned}\right\} \tag{6}$$

Thus from the known values of χ_1, χ_2 and χ_3 at any given temperature, it is possible to calculate the three α's, and thence the constants Dq_0, σ and δ of the crystal field. We have made the calculation for all the nickel salts whose susceptibilities we have measured.

The first part of the calculation, namely the evaluation of the α's from the χ's, is easily done with the help of the following relations. The expression for the mean susceptibility,

$$\chi = \tfrac{1}{3}(\chi_1+\chi_2+\chi_3) = \frac{8N\beta^2}{3kT}\left[1+(\alpha_1+\alpha_2+\alpha_3)\left(\frac{8\lambda}{3}-kT\right)\right] \tag{7}$$

may be put equal to

$$\frac{p_B^2 N\beta^2}{3kT}, \tag{8}$$

* We use the letter q_0 in place of SCHLAPP and PENNEY's q, so as to avoid confusion with another q which also appears in the expression, and has a different significance.

where p_B is the "effective BOHR magneton value" of the magnetic moment of Ni^{++} in the crystal, and we thus obtain

$$\alpha_1+\alpha_2+\alpha_3 = \frac{3(p_B^2-8)}{8(8\lambda-3kT)}. \tag{9}$$

Further, from (2) and (3)

$$\frac{\alpha_1-\alpha_2}{\chi_1-\chi_2} = \frac{\alpha_1-\alpha_3}{\chi_1-\chi_3} = \frac{3kT}{8N\beta^2(8\lambda-2\lambda^2/kT-3kT)}. \tag{10}$$

With the help of (8), (9) and (10) the three α's are readily calculated from the χ's.

The second part of the calculation, namely the evaluation of Dq_0, σ and δ from the three α's, is more laborious; it requires the solving of equations which involve these quantities in a very complicated manner, and the solving has therefore to be done by the trial and error method. We give below the results of the calculations.

As already mentioned, the axes x, y and z of the crystal field have been chosen to be respectively along the χ_3, χ_2 and χ_1 magnetic axes of the crystal. In order to make this definition of the choice of the crystal field axes applicable to the orthorhombic and tetragonal crystals also (in which the χ's along the different magnetic axes have been differentiated, in our notation, by the subscripts a, b, c, or $\parallel$ and $\perp$, instead of by 1, 2 and 3), we have adopted the following convention: χ_1, χ_2 and χ_3 are taken to correspond in orthorhombic crystals with χ_a, χ_b and χ_c respectively, and in tetragonal crystals with $\chi_\parallel$, $\chi_\perp$ and $\chi_\perp$ respectively.

It is clear from Table III that the value of Dq_0 is of nearly the same magnitude in all the crystals. In other words, the cubic part of the field acting on the Ni^{++} ion, which is also the predominant part, is more or less the same in all the crystals. This suggests that the octohedron of water molecules surrounding the Ni^{++} ion has nearly the same size in all the crystals.

The values of aA and aB, on the other hand, do depend on the structure of the crystal. This may indicate a real dependence of the rhombic part of the field on the structure of the crystal, or it may be merely a consequence of the simplifying assumption that we made, namely, that the axes of the crystalline fields acting on all the Ni^{++} ions in the crystal are coincident. Speaking in relation to the group of atoms associated with each Ni^{++} ion, this is equivalent to assuming that all such groups present in the unit cell of the crystal are oriented parallel to one another, and that consequently the observed magnetic anisotropy of the crystal represents that of each such group contained in it. But actually these groups will not in general be oriented parallel, and the anisotropy of the group will therefore be greater than the observed anisotropy of the crystal by an amount which will be determined by the orientations of these groups relative to one another, and therefore indirectly by the symmetry of the crystal. Thus the rhombic part of the field calculated from the crystal anisotropy on the assumption of parallelism of the constituent groups will naturally differ from the real field to an extent which will depend on the crystal symmetry. The dependence of the values of

aA and *aB* in Table III on the nature of the crystal may, at least partly, arise from this cause, and to that extent the dependence is only apparent.

TABLE III. CONSTANTS OF THE CRYSTAL FIELD IN NICKEL SALTS

Crystal	Dq_0	$aA=\sigma+\delta$	$aB=\sigma-\delta$
$NiSO_4.6H_2O$	1328	492	492
$NiSeO_4.6H_2O$	1096	333	333
$NiSO_4.7H_2O$	1333	675	−1137
Double sulphates			
$NiSO_4.A_2SO_4.6H_2O$:			
A = K	1356	909	−995
NH_4	1314	744	−812
Rb	1231	748	−830
Cs	1183	687	−755
Tl	1218	666	−732
Double Selenates			
$NiSeO_4.A_2SeO_4.6H_2O$:			
A = K	1129	680	−732
NH_4	1152	590	−690
Rb	1118	674	−750
Cs	1079	620	−738
Tl	1110	597	−667
$Ni(NH_4)_2SO_4SeO_4.6H_2O$	1112	599	−689
$Ni(NH_4)_2(BeF_4)_2.6H_2O$	1250	687	−739

IX. AN INTERESTING FEATURE OF THE MAGNETIC ANISOTROPY OF THE SALTS OF THE IRON GROUP

Before leaving the salts of the iron group, we may notice one interesting feature of the magnetic anisotropy of these crystals. As will be seen from Table I, and also from the data given in an earlier paper in this series (Part II, 1933), there seems to be a general tendency, except in the cobalt salts, for the magnetic ellipsoid to approximate to a spheroid; the spheroid being oblate (susceptibility along the axis being minimum) for the ferrous and the cupric Tutton salts, and for the hydrated sulphates and selenates of nickel and copper; and prolate (susceptibility along the axis being a maximum) for the nickel Tutton salts and for ferrous sulphate heptahydrate.

X. SPLITTING OF THE ENERGY LEVELS OF THE RARE EARTH IONS IN CRYSTALS IN RELATION TO THEIR MAGNETIC PROPERTIES AND ABSORPTION SPECTRA

The general theory of the magnetic properties of the rare earth salts in relation to the Stark-splitting of the energy levels of the rare earth ions in the crystals has been worked out by PENNEY and SCHLAPP (1932). Let us consider first the salts of neodymium. The ground state of the Nd^{+++} ion is $^4K_{9/2}$, and since its J has a half integral value, a twofold (KRAMERS) degeneracy will be left over, however asymmetric the crystal field

may be; and thus there will be two coincident groups, each containing five energy levels. *When the field has cubic symmetry*, the five levels are constituted as follows: a single level, which is lowermost, and two doubly degenerate levels separated from the former by $-11{\cdot}84A$ and $-40{\cdot}54A$ respectively, where A is a certain negative quantity, having the dimensions of energy, whose value depends on the magnitude of the field (and on the quantum state $^4K_{9/2}$ of the free Nd^{+++} ion).

As a result of this separation of the levels the susceptibility of the ion in the crystal will differ from that of the free ion, i.e. from the Hund value, by an amount which will be determined by this quantity A, and in a simple manner. Granting that the field is cubic, it should therefore be possible theoretically to calculate the value of A from the observed deviation of the susceptibility of the crystal from the Hund value, and thus to predict the Stark-separation of the ground levels of the rare earth ion in the crystal. But actually we are not able to do this at present, as the deviation from the Hund value is small, and the measurements on the mean susceptibility of the crystal are not sufficiently accurate. For example in the crystal of $Nd_2(SO_4)_3.8H_2O$, as PENNEY and SCHLAPP have pointed out, the magnetic values of GORTER and DE HAAS (1931) over a wide range of temperature correspond to $A=-20{\cdot}6$ cm.$^{-1}$, whereas CABRERA's measurements (1925) give practically the Hund value, corresponding to $A=0$, while ZERNICKE and JAMES (1926) and ST MEYER (1925) obtain intermediate values.

SPEDDING and his co-workers (1937), on the other hand, have looked for a verification of the theory regarding the Stark-separation of the energy levels of the rare earth ions in crystals, in their absorption spectra. In a series of papers published recently in the *Journal of Chemical Physics* they have studied the absorption spectra of several rare earth salts in the crystal state at different temperatures, and deduced therefrom the low-lying energy levels of the rare earth ions in the crystals. In the crystal of $Nd_2(SO_4)_3.8H_2O$, for example, they obtain three levels, at 0, 77 and 260 cm.$^{-1}$ respectively, whose relative spacings are the same as those predicted by the theory for a cubic field, since $77:260\approx-11{\cdot}84A:-40{\cdot}54A$. The actual separation evidently corresponds to $A=-\frac{260}{40{\cdot}54}$ cm.$^{-1}=-6{\cdot}4$ cm.$^{-1}$, which is not an improbable value as it fits well with the magnetic susceptibility measurements of ZERNICKE and JAMES, which extend over a wide range of temperatures, and of ST MEYER at room temperature.

In the crystal of $NdCl_3.6H_2O$ they obtain similarly three levels, at 0, 62 and 250 cm.$^{-1}$ respectively, and these separations correspond to $A=-6{\cdot}2$ cm.$^{-1}$.

For the Pr^{+++} ion, the theoretical Stark-pattern in a cubic field consists of four levels, at 0, $-336A$, $-576A$, and $-1296A$ respectively. Experimentally from the absorption spectrum of the crystal of $Pr_2(SO_4)_3.8H_2O$ SPEDDING, HOWE and KELLER (1937) deduce the same number of levels, with their relative positions as predicted by theory. Similarly for Er^{+++} theory predicts for a cubic field a Stark-pattern consisting of five levels (SPEDDING 1937), and experimentally four levels have been

observed (two of the theoretical levels being too close together to be resolved properly), which have the predicted relative spacings.

Further the actual separations of the levels of Pr^{+++}, Nd^{+++} and Er^{+++} in the respective octohydrated sulphates, as deduced from their absorption spectra, correspond to practically the same intensity of field in all the three crystals; a result which is to be expected in view of the isomorphism of the crystals,* and which is particularly satisfactory since some earlier discussions of the magnetic data of Pr and Nd sulphates seemed to give widely different fields in the two crystals.

The above results and the further observation that all the levels are single, including those which theoretically are degenerate and should be expected to split up if the field had a lower symmetry than the cubic, are taken by Spedding to indicate a practically rigorous cubic symmetry for the field. Indeed the evidence for this from the absorption spectra is apparently so strong that it has been suggested that the separation of the energy levels as deduced from the absorption data may be used for checking the observed susceptibility values for the crystal. On this criterion it is surmised, for example, that for $Nd_2(SO_4)_3.8H_2O$ the values of Gorter and de Haas should be too low, and of Cabrera too high, and those of Zernicke and James and of St Meyer should be nearly correct. Further since the splitting constant A is proportional to $(Z-\sigma)^4$, where Z is the atomic number and σ is the screening constant, it has been further suggested that by comparing the values of A (deduced from the absorption spectra) for any two of the rare earth ions under identical crystal fields (a condition which will practically obtain if the two ions are present in the same mixed crystal, or in two different crystals which are isomorphous), we may estimate the screening constants for the two ions.

XI. The magnetic anisotropy of the rare earth sulphates, and the asymmetry of their crystal fields

In view of these developments based on the presumed cubic symmetry of the fields acting on the rare earth ions in the crystals, and of the indirect nature of the evidence from the absorption spectra for such a cubic symmetry, it would be desirable to obtain some independent evidence regarding the symmetry.

One direct result of a cubic field would be a magnetic isotropy for the crystal, and any observed deviation from magnetic isotropy will give us some idea of the deviation of the field from cubic symmetry. Let us consider again the hydrated sulphates, and

* That the crystal fields acting on the Pr^{+++} ion in the crystal of $Pr_2(SO_4)_3.8H_2O$ and on the Nd^{+++} ion in the crystal of $Nd_2(SO_4)_3.8H_2O$, should have practically the same intensity, is also suggested by the observation of Spedding (1937) that the absorption lines of neodymium sulphate present as a small impurity in the crystal of $Pr_2(SO_4)_3.8H_2O$ are in practically the same positions as in the crystal of $Nd_2(SO_4)_3.8H_2O$.

denote the difference between the maximum and the minimum principal susceptibilities of the crystal by $\Delta\chi_m$. The values of the anisotropy $\Delta\chi_m/\chi$ for these crystals are as given below:

Table IV

Crystal	$\Delta\chi_m/\chi$
$M_2(SO_4)_3.8H_2O$	
M = Pr	0·20
Nd	0·11
Sm	0·21
Er	0·12

$\Delta\chi_m/\chi$ is not small, and when we remember that the group of atoms associated with each M^{+++} ion in the crystal should have at least this anisotropy, and has very probably more (as the different such groups—eight in number—present in the unit cell of the crystal, will not in general be oriented parallel to one another), and that it is the anisotropy of the above group (and not that of the crystal) that corresponds to the asymmetry of the crystalline field under consideration, it is easy to realize that the deviation from cubic symmetry should be quite marked.

Considering now those energy levels whose degeneracy has not been removed by the cubic field, but will be by a field of lower symmetry, one may safely conclude from the figures given in Table IV that the separation of these levels by the non-cubic part of the field will not be small in comparison with the separation between them and their neighbours produced by the cubic part of the field. The interpretation of the absorption spectra will naturally be more complicated, and the determination of the energy levels therefrom correspondingly difficult. A rediscussion of the valuable results on the absorption spectra of these crystals obtained by Spedding and his co-workers, taking into account the non-cubic nature of the crystalline fields as evidenced by the magnetic anisotropy of the crystals, is very desirable.

[*Note added on correction of proof, 9 December* 1937.] Mr D. C. Chakrabarty and one of us have recently studied the absorption spectra of single crystals of some of these rare earth salts, using *polarized* light. Many of the absorption lines are found to be strongly polarized, some of them being confined almost wholly to one or another of the principal directions of vibration in the crystal. We are making a preliminary classification of the absorption lines on the basis of their polarization, in the hope that such a classification may be helpful in any attempt at complete analysis of the absorption spectra of these crystals, which are rather complicated.]

We may mention here that the other rare earth salts that we have studied have also a fair degree of anisotropy; except the ethyl sulphate of praseodymium, which is almost isotropic, with $\Delta\chi_m/\chi$ only 3 %, and is in strong contrast with its octohydrated sulphate, for which $\Delta\chi_m/\chi$ is about 20 %.

XII. Further remarks on the rare earth salts

When the present measurements were started, no data were available for the magnetic anisotropy of any of the rare earth salts. Recently, however, Fereday and Wiersma (1935) have measured the anisotropy of some of the ethyl sulphates over a large range of temperature. Our results for these crystals at room temperature agree with theirs, as will be seen from the following table; except for erbium ethyl sulphate, for which our value, besides being nearly two and a half times theirs, has also the opposite sign. As we mentioned in the introduction, the specimen of erbium salt with which the present measurements were made was not quite pure; but it does not seem probable that the large discrepancy in the results can be due to this cause. We are trying to obtain a pure specimen with which to repeat the measurements.

Table V

Crystal $M_2(C_2H_5SO_4)_6.18H_2O$ $M=$	$\chi_\parallel-\chi_\perp$ at 30° C. Fereday and Wiersma extrapolated	Present measurements
Ce	300	294
Pr	300?	241
Nd	600	600
Er	2590	−6590

Powder measurements have been made on the hydrated sulphates by several investigators, and the results obtained by some of them are given in the following table, for comparison with the mean of the three principal susceptibilities for single crystals obtained in the present measurements. Instead of giving the susceptibilities we have entered in the table the effective Bohr magneton values, p_B, calculated with the help of the relation

$$p_B = \sqrt{\frac{3k\chi_A T}{N\beta^2}}, \qquad (11)$$

Table VI. Values of p_B for the rare earth ions

$M_2(SO_4)_3.8H_2O$ $M=$		Pr	Nd	Sm
Theoretical, for the free ion:				
Hund		3·58	3·62	0·84
Van Vleck and Frank		3·62	3·68	1·55 1·65
Observed, for the ion in the crystal:				
Zernicke and James (1926)	20° C.	3·48	3·54	1·56
Freed (1930)	17°·6	—	—	1·58
Gorter and de Haas (1931)	15–16°	3·43	3·38	—
Selwood (1933)	20°	—	3·56	—
Rodden (1934)	23–26°	3·63	3·72	1·69
Present measurements	30°	3·35	3·41	1·69

where χ_A is the mean susceptibility of the crystal per gram ion of the rare earth, obtained after correcting for the diamagnetism of the crystal. In making this correction we have taken the diamagnetism of the group $(SO_4^{--})_3.8H_2O$ to be −204 and that of the rare earths ions to be −28.

Summary

An account is given of measurements on the magnetic anisotropy and the mean susceptibility of a large number of paramagnetic crystals, among which are several salts of the rare earths, many of the iron group, and some feebly paramagnetic salts. The results are discussed, on the basis of the theory of Van Vleck, Penney and Schlapp, in relation to the Stark-splitting of the energy levels of the paramagnetic ions under the influence of the strong crystalline electric fields acting on the ions. A detailed calculation is given of the constants of the crystal field in the nickel salts.

The striking contrast in the magnetic behaviour of the six-coordinated and the four-coordinated cobalt compounds, predicted by the theory, is verified experimentally. The former salts are strongly anisotropic magnetically, while the latter are only feebly so. The mean susceptibilities of the former deviate more from the "spin-only" value than those of the latter.

All the salts of the iron group, except those of cobalt, have two of their principal susceptibilities nearly equal; i.e. the magnetic ellipsoids of these crystals approximate to a spheroid.

The conclusion drawn from studies on the absorption spectra of some of the rare earth salts that the fields acting on the rare earth ions in these crystals should be almost cubic in symmetry is not supported by observations on the magnetic anisotropy of these crystals.

References

Beevers, C. A. and Lipson, H. 1934 *Proc. Roy. Soc.* A, **146**, 570–82.
Cabrera, B. 1925 *C. R. Acad. Sci., Paris*, **180**, 668–71.
Fereday, R. A. and Wiersma, E. C. 1935 *Physica, 's Grav.*, **2**, 575–81.
Freed, S. 1930 *J. Amer. Chem. Soc.* **52**, 2702–12.
Gorter, C. J. 1932 *Phys. Rev.* **42**, 437–8.
Gorter, C. J. and de Haas, W. J. 1931 *Comm. Phys. Lab. Leiden*, **218** *b*.
Janes, R. B. 1935 *Phys. Rev.* **48**, 78–83.
Jordahl, O. M. 1934 *Phys. Rev.* **45**, 87–97.
Krishnan, K. S., Chakravorty, N. C. and Banerjee, S. 1933 *Philos. Trans.* A, **232**, 99–115.
Krishnan, K. S. and Banerjee, S. 1935 *Philos. Trans.* A, **234**, 265–98.
—— —— 1936 *Philos. Trans.* A, **235**, 343–66.
Krishnan, K. S. and Mookherji, A. 1936 *Phys. Rev.* **50**, 860–3.
Meyer, St 1925 *Phys. Z.* **26**, 51–4, 478–9.
Penney, W. G. and Schlapp, R. 1932 *Phys. Rev.* **41**, 194–207.
Powell, H. M. and Wells, A. F. 1935 *J. Chem. Soc.* pp. 359–62.

INVESTIGATIONS ON MAGNE-CRYSTALLIC ACTION

Ray, N. N. 1932 *Z. anorg. Chem.* **205**, 257–67.
Rodden, C. J. 1934 *J. Amer. Chem. Soc.* **56**, 648–9.
Schlapp, R. and Penney, W. G. 1932 *Phys. Rev.* **42**, 666–86.
Selwood, P. W. 1933 *J. Amer. Chem. Soc.* **55**, 3161–77.
Spedding, F. H. 1937 *J. Chem. Phys.* **5**, 316–20.
Spedding, F. H., Howe, J. P. and Keller, W. H. 1937 *J. Chem. Phys.* **5**, 416–29.
Spedding, F. H., Hamlin, H. F. and Nutting, G. C. 1937 *J. Chem. Phys.* **5**, 191–8.
Van Vleck, J. H. 1932 "The Theory of Electric and Magnetic Susceptibilities", Chap. XI. Oxford: Clarendon Press.
—— 1932 *Phys. Rev.* **41**, 208–15.
—— 1935 *J. Chem. Phys.* **3**, 807–13.
Zernicke, J. and James, C. 1926 *J. Amer. Chem. Soc.* **48**, 2827–31.

The Polarization of the Absorption Lines of Single Crystals of Rare Earth Salts

The absorption spectra of rare earth salts of the type $M_2(SO_4)_3 \cdot 8H_2O$ have been studied in great detail, at different temperatures, by Spedding and his collaborators.[1] From a preliminary analysis of these spectra they have concluded that the electric fields acting on the rare earth ions in these crystals, which are responsible for the splitting of the energy levels of the ions, should be nearly cubic in symmetry. Since the absorption spectra of these crystals are complicated and their analysis difficult, it would be desirable to verify this conclusion by an independent method. One direct result of such a cubic symmetry for the electric fields is that the crystals should be magnetically isotropic. But actually many of these crystals are strongly anisotropic,[2] showing that the fields should deviate considerably from cubic symmetry.

The purpose of the present note is to show that some of the features of the absorption spectra themselves point to such a deviation from cubic symmetry in the internal electric fields. From a study of the absorption spectra of single crystals of these salts in polarized light, it is found that many of the absorption lines are strongly polarized, some of them being confined almost wholly to vibrations along one or another of the principal axes of the optical ellipsoid of the crystal, and that these variations in the direction of polarization occur even among the lines of the same group; in other words, among the Stark components

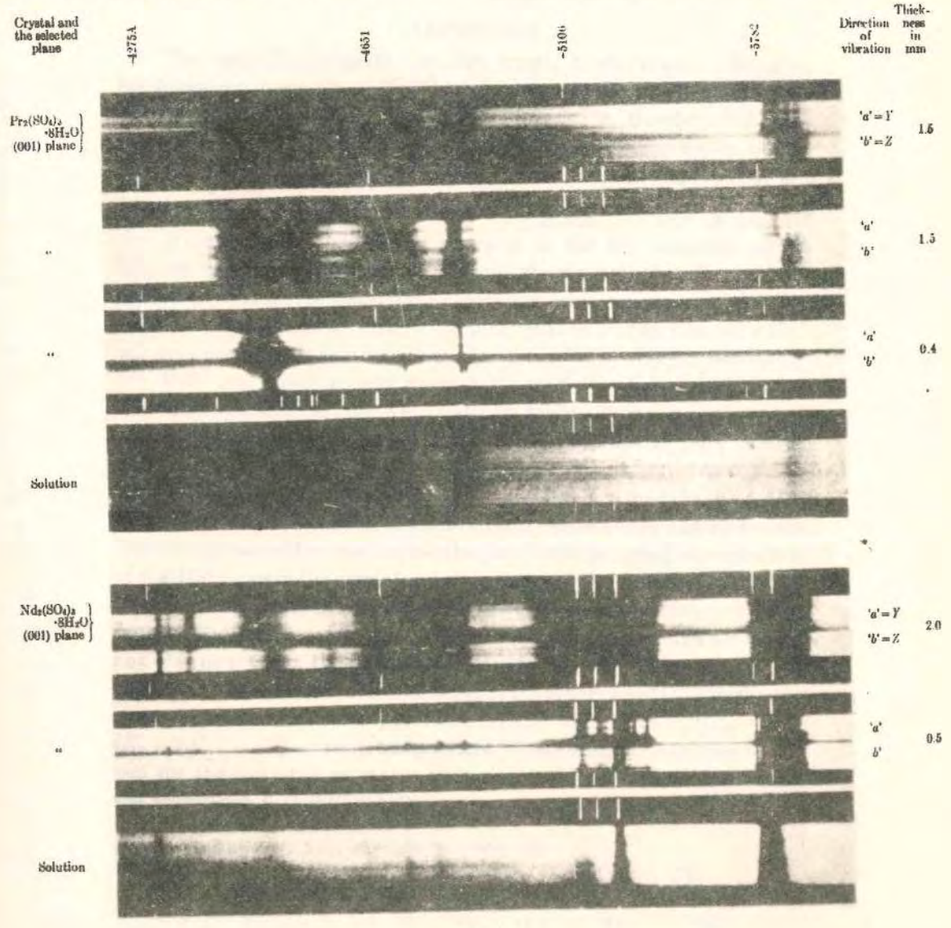

FIG. 1.

which originate from the same absorption line of the free ion, some are polarized strongly in one direction and some strongly in another.

We reproduce in Fig. 1 some typical absorption photographs which show the polarization. The crystals are monoclinic, and the upper and the lower halves in each photograph correspond to light vibrating respectively along the two extinction lines in the particular crystal plane selected for study.

The strong polarization, and the variation in its direction, observed among the members of a Stark group, show that the electric fields which produce the Stark splitting should be strongly asymmetric. Since there are 8 rare earth ions in the unit cell of the crystal, and the principal axes of the electric fields acting on these 8 ions may not be all parallel, the noncubic parts of the fields may be even much larger than the observed polarizations would suggest.

We are studying the polarization of the lines in some detail in the hope that the results may be helpful in the analysis of these complicated spectra.

K. S. Krishnan
D. C. Chakrabarty

Indian Association for the Cultivation of Science,
210 Bowbazar Street,
Calcutta, India,
January, 24, 1938.

[1] Several papers in this journal, 1937.
[2] K. S. Krishnan and A. Mookherji, Nature **140**, 549 (1937), and paper in course of publication in Phil. Trans. Roy. Soc. A.

Magnetic Studies on Rhodochrosite, $MnCO_3$.

By Prof. K. S. Krishnan and S. Banerjee,
Indian Association for the Cultivation of Science, Calcutta.

1. Introduction.

The magnetic properties of the crystal rhodochrosite (dialogite, manganspar: composition $MnCO_3$) have been studied in detail by Dupouy[1]) at different temperatures. The crystal is rhombohedral, and belongs to the calcite group. The two principal susceptibilities of the crystal, along the trigonal axis and perpendicular to it respectively, are found to fit well with the formulae $K_{\parallel} = \frac{C}{T-70}$ and $K_{\perp} = \frac{C}{T-53}$, of the Weiss type; C has the same value in the two formulae, about 387×10^{-6} per gm. of the crystal. Though the magnetic behaviour of the crystal is thus of the usual type, there are some serious difficulties in explaining these results. Firstly, the observed value of C, viz., 387×10^{-6} per gm., corresponds to a magnetic moment of 3.0 Weiss magnetons for the Mn^{2+} ion, which is very much lower than the theoretical value of 29.4 corresponding to the $^6S_{5/2}$ state of Mn^{2+}. Further, some recent measurements by Sucksmith[2]) on artificially prepared pure $MnCO_3$ do give a high susceptibility for the substance, viz., 96×10^{-6} per gm. at room temperature, as compared with 1.7×10^{-6} obtained from the above data for rhodochrosite. Secondly, though the large values of 53 and 70 for the Curie temperature θ are not improbable, in view of the great concentration of the Mn^{2+} ions in the crystal and the consequent large exchange interactions that may obtain between their electronic spin moments, yet they differ, both in magnitude and in sign, from the value estimated by Van Vleck and Penney[3]) from the temperature variation of the Verdet constant of the crystal[4]); the latter value of θ being of the order of $-11°$. Thirdly, the observed magnetic anisotropy of the crystal, viz. $\Delta K/K = 3(K_{\parallel}-K_{\perp})/(K_{\parallel}+2K_{\perp}) = 7\%$ at room temperature, is much higher than that observed for the hydrated sulphates and selenates of manganese, for which the anisotropy is 0.06% only[5]).

1) G. Dupouy, Ann. Physique **15** (1931) 495.
2) W. Sucksmith, Proc. Roy. Soc. London (A) **133** (1931) 179.
3) J. H. Van Vleck and W. G. Penney, Philos. Mag. (7) **17** (1934) 961.
4) J. Becquerel, W. J. de Haas and J. van den Handel, Leiden Comm. **218** (1931).
5) K. S. Krishnan and S. Banerjee, Philos. Trans. Roy. Soc. London (A) **235** (1936) 343.

The magnetic properties of manganous salts, and in particular their anisotropies, are of interest theoretically. Since the Mn^{2+} ions are in the S state, the mechanism which is responsible for their anisotropy in the crystals, namely the feeble Stark-splitting of their S levels under the action of the strong and asymmetric crystalline electric fields, is also the mechanism which determines the thermal behaviour of these crystals in the neighbourhood of the absolute zero of temperature[1]). Unlike the other manganous salts studied by us earlier for their anisotropy, rhodochrosite has a simple structure, and the distribution of the negative charges surrounding the Mn^{2+} ions in the crystal, which determines the electric fields acting on these ions, is also known.

Recently we were able to obtain some well-developed, large, transparent crystals of rhodochrosite. In view of the discrepancies in the available magnetic data for the crystal, and the importance of the magnetic data, we have remeasured the magnetic anisotropy and the mean susceptibility with these crystals. We give below a short account of these magnetic studies.

2. The Chemical Purity of the Crystals.

Four different crystals were measured, and all of them, on analysis, were found to contain about 96% $MnCO_3$ and 4% diamagnetic carbonates. The amount of $FeCO_3$ present was separately estimated, and was found to be 0.036, 0.066, 0.144 and 0.241 per cent respectively in the four crystals. No ferric iron was detectable.

3. Measurements on Magnetic Susceptibility.

Since the volume susceptibility of the crystal is very large, about 370×10^{-6} per c. c., it was not possible to use the magnetic balancing method adopted by us in our measurements on other crystals; no balancing solution could be prepared having such a large susceptibility. The mean susceptibility of the crystal was therefore measured in the powder form by the well-known Föex-Forrer method[2]). As will be seen in the next section, the magnetic anisotropy of the crystal is quite feeble, about 0.1%, so that any tendency of the crystalline particles constituting the powder to orient in the magnetic field, will not appreciably affect the measurements.

We will give here only the final results of our measurements. The susceptibility of the powder was found to be 100×10^{-6} per gm. at 28°.4 C., and was practically the same for all the four specimens.

1) See Note 5 on previous page 499.

2) G. Föex and R. Forrer, J. Physique Radium 7 (1926) 180.

After correcting for the 4% of diamagnetic carbonates present in the mineral, we obtain for pure rhodochrosite the value

$$K = 104\times10^{-6} \text{ per gm. at } 28°.4 \text{ C.},$$

as compared with 96×10^{-6} obtained by Sucksmith for the artificially prepared carbonate of manganese.

4. Temperature Variation of the Susceptibility.

The above value of K corresponds to a gram molecular susceptibility of about $12{,}000\times10^{-6}$ at 28°.4 C. Though this high value is very satisfactory, it is still appreciably lower than that obtained for the hydrated double sulphates and double selenates of manganese, namely about $14{,}000\times10^{-6}$ at room temperature. The lower value obtained for rhodochrosite may be due to two causes:

(1) A finite negative value of θ in the Weiss formula $K=C/(T-\theta)$, i. e. an appreciable demagnetizing exchange interaction between the spin moments of the Mn^{2+} ions. In view of the large concentration of the Mn^{2+} ions in rhodochrosite a large exchange interaction is not improbable, and since the interaction it is a demagnetizing one in most non-ferromagnetic crystals, it may very well be so in rhodochrosite also. As we mentioned in the Introduction the observed temperature variation of the Verdet Constant of the crystal also requires a finite negative value of θ, of the order of $-11°$.

(2) An effective magnetic moment for the Mn^{2+} ion in the crystal which is actually short of the value corresponding to a spin angular momentum of 5/2.

In order to decide between these two causes, we have made some measurements on the temperature variation of the susceptibility of the crystal. The results of these measurements are given in Table I.

Table I.

T	K observed	K corrected for diamagnetism $=\left(\frac{K}{0.960}+0.4\right)$	Susceptibility per gm. ion of Mn^{2+} in the crystal
301.5° K	100.1×10^{-6}	104.6×10^{-6}	12010×10^{-6}
378.5	80.0	83.7	9620
417.8	72.8	76.2	8760
459.3	67.2	70.4	8090
495.5	61.6	64.5	7410
531.8	58.5	61.3	7050

The second column in the table gives the observed susceptibility K of the crystal, per gm. This value is now corrected for (1) the 4% of diamagnetic carbonates present in the crystal, and (2) the diamagnetism of $MnCO_3$ itself, which may be taken to be roughly -0.4×10^{-6} per gm.; and the corrected value is entered in column 3. The last column gives the gram ionic susceptibility of Mn^{2+} in the crystal, χ, obtained by multiplying the value entered in the previous column by the gram molecular weight of $MnCO_3$.

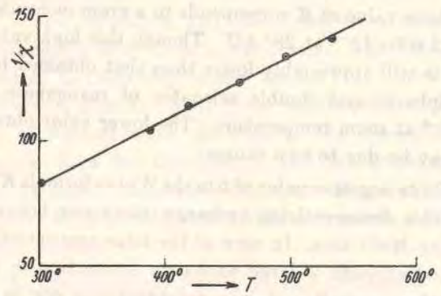

Fig. 1.

On plotting $1/\chi$ against T (see Fig. 1) we find that the values lie nearly on a straight line, namely that defined by

$$\chi = \frac{3.81}{T + 13}.$$

The Curie constant of 3.81 per gm. ion of Mn^{2+} corresponds to a magnetic moment of 27.5 Weiss magnetons, as against the theoretical value of 29.4 for the free Mn^{2+} ion.

Since the temperature range in our measurements is not large, the values obtained here for θ and for the magnetic moment of Mn^{2+} should be regarded as only approximate. We may, however, note with satisfaction that our value for θ, namely $-13°$, is practically the same as that deduced by Van Vleck and Penney from the temperature variation of the Verdet constant of the crystal, to which we referred in an earlier section.

5. Measurements on Magnetic Anisotropy.

The magnetic anisotropy of the crystal was measured by the same method that was adopted by us in our earlier measurements on manganous salts. The crystal is suspended in a uniform magnetic field, at the end of a calibrated quartz fibre. The upper end of the fibre is attached to a

graduated torsion-head. The torsion-head is first rotated suitably such that when the crystal takes up its equilibrium orientation in the magnetic field the torsion on the fibre is zero. As the torsion-head is rotated from this position by an angle α, the crystal also will rotate in the same direction, but by a smaller angle φ. In our experiments φ is very much smaller than α. Let α_c be the value of α when φ is equal to $\pi/4$. Now the couple acting on the crystal is a maximum. With a small further rotation of the torsion-head the crystal becomes unstable and suddenly spins round in the magnetic field. Experimentally, this property is made use of to determine α_c, from which the anisotropy ΔK of the crystal in the horizontal plane, per gm., is caculated with the help of the relation

$$\lambda = \tfrac{1}{2}\frac{mH^2}{c}\cdot\Delta K = \alpha_c - \pi/4,$$

where m is the mass of the crystal, H is the magnetic field, and c is the torsional constant of the fibre.

In deducing this expression it has been assumed that α is much greater than φ, i. e. α_c is much greater than $\pi/4$, which is the case in our experiments, since α_c is always much more than one rotation. Since the expression is sometimes quoted unconditionally, we may give here the exact relation between α_c and ΔK. If α_c is the observed critical angle of rotation of the torsion-head necessary to bring the crystal just to the unstable position, then the simple, but approximate, relation $\lambda = \alpha_c - \pi/4$ should be replaced by the exact relation

$$\lambda = \frac{\alpha_c - \pi/4 - \sigma}{\cos 2\sigma},$$

where λ stands for $\frac{1}{2}\frac{mH^2}{c}\cdot\Delta K$, as before, and

$$\sin 2\sigma = \frac{1}{2\lambda}.$$

Experimentally σ is the extra angle, in excess of $\varphi = \pi/4$, over which the crystal rotates before becoming unstable.

When $\alpha_c = 360°$ the error involved in using the approximate formula for calculating λ, and thence ΔK, is less than $\frac{1}{2}\%$, and for larger values of α_c it is quite negligible. For small values of α_c the error is large, and we have naturally to use the exact relation.

6. The Magnetic Anisotropy of Rhodochrosite.

In our previous measurements on the anisotropy of manganous salts we used the crystal in its natural form. Owing to its asymmetry in shape and the consequent asymmetry in the Lorentz-Poisson distribution

of induced magnetism on the surface of the crystal, there would be in general a disturbing couple acting on the crystal in any actual field, which rarely is perfectly homogeneous. This was eliminated by surrounding the crystal by an aqueous solution of manganous chloride or nitrate, adjusted to have the same volume susceptibility as the crystal; under these conditions the couple acting on the crystal is that due to its magnetic anisotropy alone. For rhodochrosite, however, it was not possible to do this, because of its very large volume susceptibility. We therefore cut a cylinder out of the crystal, with its axis perpendicular to one of the faces of the natural rhombohedon (for convenience in cutting), and the cylinder was suspended with its axis vertical. As an extra precaution to avoid the surface effects, the crystal cylinder was kept surrounded by a saturated aqueous solution of manganous nitrate.

In the magnetic field the crystal cylinder takes up an orientation such that the projection of the trigonal axis on the horizontal plane lies along the field; which shows that $K_{\parallel} > K_{\perp}$. The anisotropy ΔK of the crystal in the horizontal plane (i. e. in the plane perpendicular to the axis of the cylinder), which is directly measured, will evidently be equal to $(K_{\parallel}-K_{\perp}) \sin^2 \varrho$, where ϱ is the angle which the axis of the cylinder makes with the trigonal axis. For our cylinder $\varrho = 43°.4$.

In the measurement of the mean susceptibility of the crystal the presence of $FeCO_3$ as a small impurity does not affect the results, since the susceptibilities of $FeCO_3$ and $MnCO_3$ are of comparable magnitude. In the measurement of the anisotropy, however, it has a serious disturbing effect; since $FeCO_3$ has an anisotropy about 2500 times greater than that of $MnCO_3$. We have therefore studied in detail the dependence of the anisotropy of rhodochrosite on its iron content. The results are given in the following table.

Table II.

% $FeCO_3$	.036	.066	.144	.241
$(K_{\parallel}-K_{\perp})\times 10^6$	.0288	.0506	.0689	.1126

We should mention here that in Dupouy's measurements also $K_{\parallel} - K_{\perp}$ was measured directly, and it is gratifying that his values of $K_{\parallel} - K_{\perp}$ are of the same magnitude as ours. For example his value $K_{\parallel} - K_{\perp} = 0.107 \times 10^{-6}$ at room temperature (17°.3 C.) would correspond, according to our table, to about 0.22% $FeCO_3$, which is very reasonable. (No data are given in his paper for the iron content of his crystal.)

In addition to measuring $K_{\parallel} - K_{\perp}$, he measures $K_{\parallel}/K_{\perp}$ by comparing the forces acting on the crystal, shaped suitably, when it is placed in the same part of an inhomogeneous magnetic field, with its trigonal axis first along the field and then perpendicular to it. (Actual experimental data for $K_{\parallel}/K_{\perp}$ are not given in the paper.) From the values of $K_{\parallel}-K_{\perp}$ and $K_{\parallel}/K_{\perp}$, those of $K_{\parallel}$ and $K_{\perp}$ separately are calculated.

As we have seen, his values for $K_{\parallel} - K_{\perp}$ are of the proper magnitude. Hence the very low values which he obtains for $K_{\parallel}$ and $K_{\perp}$ separately must be due to the uncertainties in the measurement of $K_{\parallel}/K_{\perp}$, which are difficult to avoid since $K_{\parallel}/K_{\perp}$ differs very little from unity.

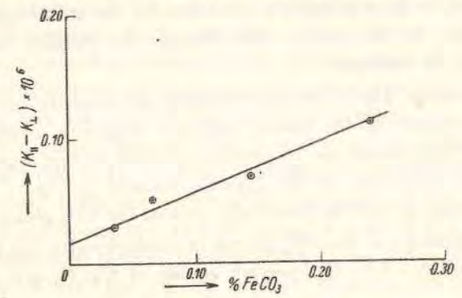

Fig. 2.

On plotting the values entered in Table II and extrapolating (see Fig. 2), we find (1) that when the iron content of the crystal is nothing, its anisotropy should be about 0.016×10^{-6} per gram; and (2) from the slope of the curve that the anisotropy of $FeCO_3$ present as impurity should roughly correspond to $K_{\parallel} - K_{\perp} = 41 \times 10^{-6}$ per gram of $FeCO_3$.

Taking the latter result first, we may mention that it is of the same order of magnitude as the anisotropy of siderite $FeCO_3$, namely 51×10^{-6} per gm[1]). When we remember (1) that the highest concentration of $FeCO_3$ in our crystals is only a quarter per cent, and is thus too small to give us any accurate value for the anisotropy of $FeCO_3$, and (2) that the anisotropy of $FeCO_3$ present as impurity in $MnCO_3$ may not actually be the same as that of pure $FeCO_3$, since the crystal fields acting on the Fe^{2+} ions in the two crystals may not be identical[2]), the value 41×10^{-6} obtained above may be considered to be quite satisfactory.

1) K. S. Krishnan, N. C. Chakravorty and S. Banerjee, Philos. Trans. Roy. Soc. London (A) 232 (1933) 99.

2) We are now studying the magnetic anisotropies of specimens of siderite containing large percentages of carbonates of the alkaline earths or of manganese, with a view to follow the progressive changes in the crystalline fields acting on the Fe^{2+} ions which might accompany the changes in the concentration of these ions.

In any case the precise value which we adopt for the anisotropy of $FeCO_3$ will not appreciably affect the extrapolated value

$$K_{\parallel} - K_{\perp} = 0.016 \times 10^{-6}$$

which we obtained above for rhodochrosite of zero iron content, and of composition 96% $MnCO_3$ and 4% diamagnetic carbonates.

7. The Paramagnetic Anisotropy of the Crystal.

In order to obtain from the above result the paramagnetic anisotropy of the crystal, we have to apply a correction for the anisotropy of the CO_3 group present in the crystal; the diamagnetic metallic ions may be presumed to be isotropic.

In a previous paper[1]) we have studied the magnetic anisotropies of several carbonates of the calcite and the aragonite series. In these crystals the CO_3 groups are all oriented parallel to one another so that the observed anisotropy of the crystals, namely $\chi_{\parallel} - \chi_{\perp} = -5.0 \times 10^{-6}$ per gram molecule, will be practically that of the CO_3 group.

The anisotropy of the CO_3 groups in rhodochrosite will therefore be roughly equal to -5.0×10^{-6} per gm. molec. of $MnCO_3$ or -0.044×10^{-6} per gm.

Applying the correction for this, and remembering that only 96% of our rhodochrosite is $MnCO_3$, we obtain for the paramagnetic anisotropy of pure rhodochrosite $K_{\parallel} - K_{\perp} = \frac{0.016 + 0.044}{0.96} \times 10^{-6}$, or 0.063×10^{-6}, per gm. This would correspond to

$$\chi_{\parallel} - \chi_{\perp} = 7.2 \times 10^{-6} \text{ per gm. ion of } Mn^{2+}.$$

This value is practically the same as that obtained by us for the various manganous Tutton salts, namely 7.7 to 8.3×10^{-6}.

8. The Magnetic Anisotropy of the Mn^{2+}-Ion in the Crystal.

As we mentioned in a previous section the paramagnetic anisotropy of a crystal arises from that of the paramagnetic ions in the crystal, and the anisotropy of the latter is due to the asymmetry of the crystalline electric fields acting on them. Now since the field acting on any given ion is determined by the distribution of the charged atoms immediately surrounding it, what we have called for brevity the anisotropy of the ion in the crystal is really that of the small group consisting of the paramagnetic ion and

1) K. S. Krishnan, B. C. Guha and S. Banerjee, Philos. Trans. Roy. Soc. London (A) **231** (1932) 235.

the charged atoms immediately surrounding it. Now the unit cell of the crystal contains usually more than one such ion, and their surroundings will not in general be identical; i. e. the atomic groups, associated each with one paramagnetic ion, may not be similar, and even when they are, they may not be oriented parallel to one another. Thus the observed anisotropy of the crystal will not represent that of the individual paramagnetic ions, but will be less than the latter by an amount depending on the mutual inclinations of the groups associated severally with these ions.

In our previous work on the manganous Tutton salts, for want of information regarding the mutual orientations of the two paramagnetic groups present in the unit cell, we made the convenient assumption that the observed anisotropy of the crystal is really that of the ions; in other words that both the paramagnetic groups present in the unit cell are identical and are oriented parallel to one another.

In rhodochrosite, however, the crystal structure is known. There are two Mn^{2+} ions in the unit cell, and from the known distribution of the atoms about them, the crystal fields acting on them may be expected to have trigonal symmetry, and the principal axes of the fields acting on the two ions to be parallel to one another. Hence the paramagnetic anisotropy of 7.2×10^{-6} per gm. ion of Mn^{2+} observed for the crystal, is also the actual anisotropy of the Mn^{2+} ion in the crystal.

9. The Magnetic Anisotropy and the Stark-Separation of the Energy Levels of Mn^{2+} in the Crystal.

Judging from the value of $-13°$ for θ, the exchange interaction between the spin moments of the different Mn^{2+} ions in the crystal is not small. This would not, however, produce any appreciable anisotropy, and the observed anisotropy should therefore be attributed almost wholly to the Stark-separation of the energy levels of Mn^{2+} by the asymmetric crystalline electric fields.

In the paper on manganous salts we have given a detailed discussion of the relation between the magnetic anisotropy of the Mn^{2+} ion, and the magnitude of the Stark-separation of its energy levels. The observed anisotropies of about 8×10^{-6} per gm. ion of Mn^{2+}, in the manganous Tutton salts, were shown to correspond to a separation between the adjacent levels in the Stark-pattern of Mn^{2+} of the order of $K \times 0.1°$ (where K is the Boltzmann constant) or 0.07 cm.$^{-1}$. In rhodochrosite also, since $\Delta\chi$ has practically the same value, namely 7.2×10^{-6} per gm. ion of Mn^{2+}, the separation of the Stark-components should be of the same magnitude.

10. Summary.

The paper gives a report of measurements on the magnetic anisotropy, and on the mean susceptibility at different temperatures, of rhodochrosite ($MnCO_3$). The mean susceptibility of the crystal is of the order of $12{,}000\times10^{-6}$, per gm. molec. of $MnCO_3$, at room temperature, and its temperature variation conforms to the formula $\chi=\frac{3.84}{T+13}$, from which the magnetic moment of the Mn^{2+} ion comes out as 27.5 Weiss magnetons. The anisotropy of the crystal is very feeble, as should be expected, being about 7.2×10^{-6} per gm. molec. at room temperature, which is only 0.06% of the mean susceptibility. This corresponds to a separation between adjacent levels in the Stark-pattern of Mn^{2+}, produced by the crystalline electric fields acting on it, of the order of 0.07 cm^{-1}.

Received 23 May 1938.

OCTOBER 1, 1938 PHYSICAL REVIEW VOLUME 54

The Magnetic Anisotropy of Copper Sulphate Pentahydrate, $CuSO_4\cdot5H_2O$, in Relation to its Crystal Structure. Part II

K. S. Krishnan and A. Mookherji
Indian Association for the Cultivation of Science, Calcutta, India

(Received July 5, 1938)

In Part I of this paper were reported some magnetic measurements on the crystal of $CuSO_4\cdot5H_2O$. The crystal, though triclinic, has nearly uniaxial magnetic symmetry, and the symmetry axis is the direction of minimum susceptibility for the crystal. This observed uniaxial symmetry and the negative sign of the anisotropy were shown to follow naturally from the known fine structure of the crystal, and the direction of the symmetry axis also is nearly that predicted from the structure. In the present paper are described further magnetic studies on the crystal, and a more detailed correlation with its structure. The magnetic data are also discussed in relation to the magnitude and the asymmetry of the internal electric fields acting on the Cu^{++} ions in the crystal. A general method is described for determining, for any triclinic crystal, the principal magnetic axes and susceptibilities, i.e., the constants of the magnetic ellipsoid.

1. Explanation of the Magnetic Anisotropy of Paramagnetic Crystals

In some recent papers[1,2] we have discussed the magnetic anisotropy of several organic crystals in relation to the anisotropy of the constituent molecules and their relative orientations in the crystal lattice. When the molecular anisotropy is known, either from measurements on the magnetic double refraction of the substance in the liquid state or in state of solution in suitable solvents, or theoretically from considerations of the structure of the molecules, we can utilize the observed data for the anisotropy of the crystal to obtain much useful information regarding the orientations of the molecules in the unit cell of the crystal. On the other hand, if the molecular orientations in the crystal are already known from x-ray analysis, the magnetic measurements on the crystal may be used for calculating the molecular anisotropy, which is an important molecular constant.

[1] Krishnan and Mookherji, Phys. Rev. **50**, 860 (1936), which is Part I of this paper.
[2] Krishnan, Guha and Banerjee, Phil. Trans. Roy. Soc. **A231**, 235 (1932); Krishnan and Banerji, Phil. Trans. Roy. Soc. **232**, 99 (1935); Zeits. f. Krist. **A91**, 173 (1935).

In a paramagnetic crystal also the anisotropy of the crystal may be regarded as arising from that of certain paramagnetic units; the magnitude of the crystal anisotropy will depend on the anisotropy of these units and their orientations relative to one another. These anisotropic units, however, are not the molecules as in the organic crystals, but are constituted as follows: Each paramagnetic ion (or atom) in the crystal is under the influence of the strong, and generally asymmetric, electric fields of the neighboring electrically charged atoms. Under the influence of these fields the paramagnetic ion may exhibit, as was shown by Van Vleck,[3] Penney and Schlapp,[4] a magnetic anisotropy. The magnitude and the asymmetry of these fields will be determined practically by the positions of the atoms *immediately* surrounding the paramagnetic ion, those that are further away contributing relatively very little to the fields. Thus the paramagnetic ion and the charged atoms immediately surrounding it constitute a group which may be magnetically anisotropic; and such a group forms the anisotropic paramagnetic unit which we referred to previously. There will be in general more than one such group in the unit cell of the crystal, and the magnetic anisotropy of the crystal as a whole will therefore be determined by the anisotropy of these groups and their orientations relative to one another; in the same manner in which the anisotropy of an organic crystal is determined by the anisotropy, and the relative orientations, of the constituent molecules. The relative *positions* (or the density of packing) of the paramagnetic groups in the crystal lattice, as distinguished from the *orientations* of the groups relative to one another, will not appreciably affect the anisotropy, again as in the organic crystals, since the mutual influence of their magnetic moments will be very small.[5]

If we know the structure of the above paramagnetic groups, i.e., if we know the distributions of the charged atoms around the paramagnetic ions, it should be possible, at any rate theoretically, to calculate the magnitude and the asymmetry of the electric fields acting on the paramagnetic ions, and thence to calculate the principal magnetic susceptibilities of the groups. Further if we know the relative orientations of the different groups present in the unit cell of the crystal, it should be possible to predict the principal magnetic susceptibilities of the crystal. Conversely, from the observed principal susceptibilities of the crystal, and the known orientations of the different paramagnetic groups present in the unit cell, we can readily calculate the principal susceptibilities of these groups, i.e., the principal susceptibilities which the crystal would have if all the paramagnetic groups in it were identical and their orientations parallel.[6] We can then try to correlate these magnetic data deduced for the group with its structure. Thus a study of the magnetic properties of paramagnetic crystals can throw light on some aspects of their fine structure.

The crystal of copper sulphate pentahydrate is very suitable for illustrating some of these points.

2. Temperature Variation of the Susceptibility of $CuSO_4 \cdot 5H_2O$ Powder and the Structure of the Crystal

The crystal of $CuSO_4 \cdot 5H_2O$ is triclinic, in the space group C_i^1. Its unit cell has the dimensions[7]

$$a = 6.12\text{A} \qquad \alpha = 82°16'$$
$$b = 10.7 \qquad \beta = 107°26'$$
$$c = 5.97; \qquad \gamma = 102°40';$$

and it contains two molecules of $CuSO_4 \cdot 5H_2O$.

Jordahl[8] has discussed theoretically the magnetic susceptibility of $CuSO_4 \cdot 5H_2O$ powder at different temperatures, in relation to the splitting of the energy levels of the Cu^{++} ion under the action of the crystalline electric fields. In particular, he found that the observed deviation of the effective magnetic moment of the Cu^{++} ion in the crystal from the theoretical value for the free ion corresponds to a field of predominantly

[3] Van Vleck, *Theory of Electric and Magnetic Susceptibilities* (Oxford University Press, 1932), Chap. XI; Phys. Rev. **41**, 208 (1932).

[4] Penney and Schlapp, Phys. Rev. **41**, 194 (1932) and **42**, 666 (1932).

[5] We are considering here the simple magnetic interaction between the moments induced in neighboring groups, which will be of the order of the volume susceptibility of the crystal and negligible. The exchange interactions, in paramagnetic crystals, between neighboring spin-moments, even when appreciable, will not produce an anisotropy.

[6] Studies on the susceptibility of the crystal powder at different temperatures can also give us a rough estimate of the anisotropy of these paramagnetic groups.

[7] Beevers and Lipson, Proc. Roy. Soc. **A146**, 570 (1934).

[8] Jordahl, Phys. Rev. **45**, 87 (1934).

TABLE I. *Tetragonal angles of* Cu^{++} *ions in unit cells of crystal.*

	'a'	'b'	'c'
z_I	78°	130°	52°
z_{II}	70°	41°	69°
Normal to the $z_I - z_{II}$ plane	155°	68°	50°

cubic symmetry. We can state this result in a slightly different way thus. Taking the Cu^{++} ion under consideration as the origin of a suitably oriented system of rectangular coordinates, and denoting the potential of an electron placed at the point $x\ y\ z$, because of the electric field, by an expression of the type[9]

$$\Phi = D(x^4+y^4+z^4) + Ax^2 + By^2 - (A+B)z^2, \quad (1)$$

he found that the terms involving the fourth power, which are due to the cubic part of the field, are much greater than the square terms, which are due to the rhombic part. He further found that the direction of the deviation from the free ion value corresponds to a positive value of D; which shows that the cubic field should be due to an octahedral distribution of six equal negative charges round the Cu^{++} ion; since four negative charges at the corners of a tetrahedron, or eight at the corners of a cube, will give a negative value for D.[9]

This prediction has been verified experimentally by the recent x-ray analysis of the structure of this crystal by Beevers and Lipson.[7] It is actually found that each Cu^{++} ion in the crystal is surrounded by six negatively charged oxygen atoms which form an approximately regular octahedron. Four of them, which belong to four water molecules, form a square, of side equal to about 2.8A, with the Cu^{++} ion at the center; the other two oxygens, which are contributed by two SO_4 groups, lie nearly centrally above and below this square. The distance between either of these two oxygens and any of the water oxygens at the corners of the square is about 3.1A.

3. The Tetragonal Symmetry of the Internal Electric Fields Acting on the Cu^{++} Ions and the Magnetic Anisotropy of the Crystal

As we mentioned just now, the octahedron of oxygen atoms is only approximately regular; those belonging to the water molecules are closer to the central Cu^{++} ion than the other two. The octahedron will thus be drawn out along one of its diagonals, namely along the line joining the two sulphate oxygens. As a consequence, the field acting on the Cu^{++} ion should have approximately tetragonal symmetry, with the above long diagonal of the octahedron as the tetragonal axis. In other words the expression for the potential of the field should approximate to the form

$$\Phi = D(x^4+y^4+z^4) + A(x^2+y^2-2z^2), \quad (2)$$

and the susceptibility of the ion along the z axis (the tetragonal axis) should be greater than that along the other two axes.

Now there are two such Cu^{++} ions in the unit cell of the crystal, and their respective tetragonal axes z_I and z_{II} are found, from the parameters given by Beevers and Lipson, to make the angles with the 'a,' 'b,' 'c' crystallographic axes given in Table I. The angle between z_I and z_{II} is about 98°, *which is nearly a right angle*. We should therefore expect: (1) the normal to the plane containing the z_I and z_{II} axes to be one of the principal magnetic axes of the crystal; (2) the susceptibility of the crystal along this axis to be less than the other two principal susceptibilities, which should be nearly equal. In other words the crystal should be nearly uniaxial magnetically, and the symmetry axis should be the direction of minimum susceptibility for the crystal, and should lie along the normal to the plane containing the z_I and z_{II} axes, i.e., along the direction which makes angles of 155°, 68° and 50°, respectively, with the 'a,' 'b,' 'c' axes.

All these results deduced from the structure of the crystal are verified by the magnetic measurements described in Part I of this paper. Two of the principal susceptibilities of the crystal are nearly equal, and greater than the third (by about 300×10^{-6} per gram molecule of $CuSO_4 5H_2O$, at room temperature), and the axis of minimum susceptibility makes with the 'a,' 'b,' 'c' axes angles of 156°, 65° and 52°, respectively, which are nearly the angles predicted from the structure.

The directions of the other two principal magnetic axes of the crystal, of nearly equal susceptibility, can also be predicted from the structure. They should lie along the two bisectors

[9] Gorter, Phys. Rev. **42**, 437 (1932).

of the angle between z_1 and z_2, the interior bisector (i.e., of the acute angle) corresponding to the larger susceptibility. We shall show presently that these two directions also, predicted from the structure, agree with observation.

4. Determination of the Magnetic Constants of a Triclinic Crystal

Before describing the magnetic studies on $CuSO_4 \cdot 5H_2O$, we may offer some preliminary remarks on the determination of the magnetic constants of a triclinic crystal, i.e., the directions of the three principal magnetic axes and the susceptibilities α, β, γ along them; $\alpha \leq \beta \leq \gamma$. Instead of measuring α, β and γ directly, it is more convenient experimentally to determine the anisotropies $\gamma-\beta$ and $\beta-\alpha$, and the susceptibility along any one convenient direction in the crystal, or the susceptibility of the powder, $(\alpha+\beta+\gamma)/3$.

Taking up first the determination of the magnetic axes, we may mention that if one of them is located, the other two may be obtained easily, by suspending the crystal at the end of a thin fiber in a uniform horizontal magnetic field, with the known principal magnetic axis vertical, and finding the directions in the horizontal plane which tend to lie along the field and perpendicular to it, respectively. It should be possible to locate the γ axis (the axis of maximum susceptibility for the crystal) by mounting it in a suitably designed light "universal" rotating stage in which the crystal can turn round freely in any direction, and by placing it in a uniform magnetic field; the γ axis will naturally place itself along the field. The rotating parts of the mount have to be of a material whose susceptibility is almost nothing, so that the rotating couple due to the field acting on them will be negligible.

The method however offers at present serious experimental difficulties.

5. The M Axes

Analogous to the two optic axes of a crystal, there are two magnetic directions, which we may call the M axes,[10] which are the normals to the two central circular sections of the magnetic ellipsoid. The two M axes will naturally lie in the $\alpha\gamma$ plane, i.e., the plane containing the directions of the minimum and the maximum susceptibilities of the crystal, and make with the γ axis angles of V and $-V$, respectively, where[11]

$$\tan^2 V = (\beta-\alpha)/(\gamma-\beta). \qquad (1)$$

Instead of determining the three principal magnetic axes, and the anisotropies $\gamma-\beta$ and $\beta-\alpha$, we may therefore alternatively determine the two M axes, and the anisotropy $\Delta\chi$ for any one selected plane in the crystal.

If the crystal is suspended with either of the M axes vertical in a uniform horizontal magnetic field, it will behave like an isotropic crystal, and it should be possible to utilize this property to determine directly the M axes. Here again the experimental difficulties are great, and are similar to the difficulties of determining the γ axis. We have therefore to depend on indirect methods for the determination of these directions.

6. Magnetic Data for $CuSO_4 \cdot 5H_2O$

Coming back to copper sulphate, we determined in Part I, by suspending the crystal in a uniform horizontal magnetic field with different known planes successively horizontal, the directions of maximum and minimum susceptibilities in each of these planes, and the anisotropy $\Delta\chi$ (i.e., the difference between the maximum and the minimum susceptibilities) in each plane. Since the number of crystal planes for which such measurements were made was large, (actually eight) the data obtained should be much more than sufficient to give the magnetic axes and the anisotropies. However, since two of the principal susceptibilities of $CuSO_4 \cdot 5H_2O$ are nearly equal, i.e., since $\gamma-\beta$ is very small in comparison with $\beta-\alpha$, in order to locate the γ and the β axes with certainty, it would be desirable to use more accurate data than those given in Part I. We have therefore repeated the magnetic measurements described there using the following more precise technique.

The crystal was kept immersed in a liquid medium having the same volume susceptibility as the mean volume susceptibility of the crystal. The medium was an aqueous solution of manganous sulphate of suitable concentration, which had been saturated with copper sulphate so as to prevent the crystal from going into solution. With this arrangement the small rotating couple which may act on the crystal in the magnetic field, because of the asymmetry of shape of the crystal and the imperfect homogeneity of the field, is eliminated. The rotating couple acting on the crystal under these conditions should be due to its anisotropy alone.

In calculating the anisotropy $\Delta\chi$ for any given plane in the crystal from the observed critical angle of rotation of the torsion-head, namely α_0, we used in Part I the simple formula (see Eq. (1), p. 861 of reference 1)

$$\lambda = \alpha_0 - \pi/4, \qquad (2)$$

where λ denotes $\Delta\chi \cdot mH^2/(2Mc)$. It should be emphasized here that this formula is only approximate, though a sufficiently good one under the usual conditions of measurement of anistropy; it is correct to less than 0.5 percent when $\alpha_0 = 2\pi$ (i.e., one rotation), and in our measurements α_0 is always much greater than this angle. When, however, the observed critical angle α_0 is small, we have to use the more rigorous formula

$$\lambda = (\alpha_0 - \pi/4 - \sigma)/\cos 2\sigma, \qquad (3)$$

where

$$\sin 2\sigma = 1/2\lambda. \qquad (4)$$

σ is the extra angle in excess of $\pi/4$ (measured from the equilibrium position of the crystal in the field) over which the crystal turns before reaching the unstable position.

The experimental results are given in Table II. The $\Delta\chi$'s are expressed in the usual unit, 10^{-6} c.g.s. e.m.u., and refer to one gram molecule of $CuSO_4 \cdot 5H_2O$. The last three columns in the table will be explained later.

7. Location of the M Axes

From the data given in Table II the two M axes may be located in either of the following ways.

(1) We may utilize the observational data for the directions of maximum and minimum susceptibilities for the different crystal planes. For brevity we may call these two directions in a given plane the "setting-directions;" when the crystal is suspended in the magnetic field with the plane horizontal, it sets with the above directions along and perpendicular to the field, respectively. The setting-directions in a plane are thus analogous to the extinction-lines in crystal optics, and our present problem of determining the two M axes from observations on the setting-directions for the requisite number of planes, n (equal to 4 for a triclinic crystal, as we shall see presently), in the crystal is equivalent to the problem in crystal optics of determining the two optic axes of a biaxial crystal when the

Table II. *The magnetic data refer to 26°C.*

Serial Number	Mode of Suspension	Orientation in the Field	$\Delta\chi$	θ	θ'	$\Delta\chi/(\sin\theta \cdot \sin\theta')$
1	'c' ax. vert.	(I00) at 27°.2 to the field and (II0) at 53°.3 to it.	183	49°	55°	296
2	'a' ax. vert.	(011) at 2°.7 to the field and (021) at 17°.6 to it.	60	24	31	286
3	(I00) and (I11) vert.	(I00) at 45°.5 to the field and (I11) at 14°.0 to it.	263	86	105	273
4	(II0) and (I11) vert.	(II0) at 62°.6 to the field and (I11) at 9°.5 to it.	264	92	108	278
5	(100) horiz.	'c' ax. at 58°.9 to the field and the intersection of (I00) and (I11) at 8°.0 to it.	146	43	51	276
6	(110) horiz.	'c' ax. at 43°.9 to the field and intersection of (II0) and (I11) at 12°.6 to it.	213	55	71	275
7	(I10) horiz.	'c' ax. at 90°.0 to the field and the intersection of (I10) and (I11) at 2°.5 to it.	117	44	36	286
8	(I11) horiz.	The intersection of (I11) and (I00) at 20°.2 to the field and the intersection of (I11) and (II0) at 45°.4 to it.	26	17	18	288
						Mean = 282

[10] The name "magnetic axes" would have been preferable, but it has come into general use to denote the principal axes of the magnetic ellipsoid.

[11] Analogous to the expression $\tan^2 V = (\gamma^2/\alpha^2)(\beta^2-\alpha^2)/(\gamma^2-\beta^2)$ defining the angle between the two optic axes.

TABLE III. *Location of the M axes and of the principal magnetic axes.*

	'a'	'b'	'c'
M_1	156°	74°	49°
M_2	149°	53°	55°
α	154°	64°	51°
β	66°	85°	42°
γ	80°	27°	103°

TABLE IV. *Directions of principal magnetic axes as deduced from structure.*

		'a'	'b'	'c'
Normal to z_I and z_{II}: (α)		155°	68°	50°
Bisectors of the angle between z_I and z_{II}	exterior: (β)	66°	86°	42°
	interior: (γ)	85°	22°	100°

extinction-lines on n different faces have been observed. The optical problem has been discussed in detail by Weber,[12] Johnsen,[13] and Hilton.[14] It has been shown that a unique solution is possible when $n=1$, 2 or 4 according as the crystal is orthorhombic, monoclinic or triclinic. (It is, of course, assumed that all the n faces have general positions.) A further observation on one such face to find out which of the two extinction lines on the face corresponds to the larger refractive index will determine whether the γ axis is the acute bisectrix or the obtuse bisectrix of the angle between the two optic axes. Practical methods have been developed, both graphical and analytical, to determine the optic axes from the observed extinction-lines on the required number of faces.

Thus in the crystal of $CuSO_4 \cdot 5H_2O$, which is triclinic, observations on the setting directions for four faces are sufficient to determine uniquely the two M axes. Actually we have such data for eight faces, and from these data we have tried to locate the two M axes, both by the geometrical method of Hilton and by the trial and error method described by Johnsen. We find, however, that, because of the small angle between the two M axes, though its acute bisectrix is determined accurately in this manner, there is some uncertainty in the location of the M axes themselves. We have therefore adopted the following alternative method which utilizes the experimental data for the anisotropy for different crystal planes.

(2) For a given plane in the crystal whose normal makes angles θ and θ' with the two M axes, the magnetic anisotropy $\Delta\chi$ is given by the simple relation

$$\Delta\chi=(\gamma-\alpha)\sin\theta\cdot\sin\theta'. \qquad (5)$$

The location of the M axes reduces therefore to finding two directions such that $\Delta\chi/(\sin\theta\cdot\sin\theta')$ may have the same value for all the planes; θ and θ' are the angles which the two directions make with the normal to the plane for which the anisotropy is $\Delta\chi$.

This is conveniently done by the trial and error method, by using stereographic projection for the measurement of angles. The angular parameters for the two M axes given in Table III were obtained in this manner. The corresponding values of θ, θ' and $\Delta\chi/(\sin\theta\cdot\sin\theta')$ for the different crystal planes are given in the last three columns of Table II; as will be seen from the table, $\Delta\chi/(\sin\theta\cdot\sin\theta')$ has practically the same value for all the planes, namely about 280.

8. The Principal Magnetic Axes and the Anisotropy of the Crystal

Knowing the M axes, we can deduce readily the α, β and γ axes of the magnetic ellipsoid, since the α and the γ axes are the two bisectors (the interior and the exterior bisectors, respectively, in this crystal), of the angle between the two M axes. Their directions also are given in Table III.

Further, from the directions of the M axes given in Table III the magnetic axial angle $2V$ comes out as 159°. From this value, and the equation $\Delta\chi/(\sin\theta\cdot\sin\theta')=280$, we obtain

$$\gamma-\alpha=280, \quad \gamma-\beta=10.$$

9. The Magnetic Constants of the Crystal Deduced from its Structure

The directions of the principal magnetic axes of the crystal, deduced from its structure, are given in Table IV. On comparing these values with the corresponding values given in Table III, we find that they agree well. This is very gratifying, and may be taken to be a striking confirmation on the one hand of the structure proposed by Beevers and Lipson for the crystal from x-ray studies, and on the other of the theory

[12] Weber, Zeits. f. Krist. **56**, 1 and 96 (1921).
[13] Johnsen, Centralblatt Min. 1919, p. 321.
[14] Hilton, Mineral. Mag. **19**, 233 (1921).

of Van Vleck, Penney and Schlapp, which attributes the magnetic anisotropy of paramagnetic crystals to the asymmetry of the internal electric fields acting on the paramagnetic ions in the crystals.

10. The Asymmetry of the Internal Electric Fields Acting on the Cu^{++} Ions

Let us consider again the paramagnetic unit groups, each consisting of a Cu^{++} ion in the center, and six negatively charged oxygen atoms forming an octahedron about it, with one of its diagonals, the z axis, drawn out. Let us denote the gram molecular susceptibility of the group along the z axis, i.e., the axis of tetragonal symmetry, by K_{II}, and that along directions perpendicular to the tetragonal axis by $K_\perp$. Let us further denote the obtuse angle between the z axes of the two paramagnetic groups in the unit cell, i.e., between z_I and z_{II}, by 2φ. (As we mentioned in an earlier section, the x-ray data of Beevers and Lipson give $2\varphi=98°$.) Then evidently

$$\left.\begin{aligned}\alpha&=K_\perp\\ \beta&=K_\perp\sin^2\varphi+K_{II}\cos^2\varphi\\ \gamma&=K_\perp\cos^2\varphi+K_{II}\sin^2\varphi\end{aligned}\right\}, \qquad (6)$$

$$\therefore\quad \left.\begin{aligned}\gamma-\alpha&=(K_{II}-K_\perp)\sin^2\varphi\\ \beta-\alpha&=(K_{II}-K_\perp)\cos^2\varphi\end{aligned}\right\}. \qquad (7)$$

From these relations we obtain

$$\tan^2\varphi=(\gamma-\alpha)/(\beta-\alpha), \qquad (8)$$

which, in view of relation (1) for the tangent of the half-angle between the two M axes, *viz.*, $\tan^2 V=(\beta-\alpha)/(\gamma-\beta)$, gives

$$\tan\varphi=\operatorname{cosec} V. \qquad (9)$$

Substituting for V the value $\frac{1}{2}\times159°$, obtained from our magnetic measurements, we get

$$2\varphi=91°,$$

as compared with 98° obtained from the x-ray data. The difference is small, and is not unexpected, since the tetragonal symmetry which we have assumed for the paramagnetic groups is only approximate; the line joining the two sulphate oxygens, which we have taken to be an axis of tetragonal symmetry, is not exactly perpendicular to the square of water oxygens, but deviates from that direction by a small angle.

Coming back to Eqs. (7), we further obtain

$$K_{II}-K_\perp=(\gamma-\alpha)+(\beta-\alpha), \qquad (10)$$

i.e., $$K_{II}-K_\perp=550.$$

In other words, if all the octahedra in the crystal were identical and were oriented in the same way (i.e., with their tetragonal axes along the same direction), two of the principal susceptibilities of the crystal would be equal and *less* than the third by about 550×10^{-6} per gram molecule of $CuSO_4 \cdot 5H_2O$, at 26°C; the third susceptibility is along the common direction of the tetragonal axes of all the paramagnetic groups. This anisotropy characteristic of the paramagnetic unit group, as distinguished from the observed anisotropy for the crystal as a whole, is the proper measure of the asymmetry of the electric fields acting on the Cu^{++} ions in the crystal.

We should mention here that the mean susceptibility of the crystal, equal to $(\alpha+\beta+\gamma)/3$, or $(K_{II}+2K_\perp)/3$, is about 1420×10^{-6} per gram molecule, at 26°C. The magnetic anisotropy of the paramagnetic group, *viz.*, $K_{II}-K_\perp=550\times10^{-6}$, is thus about 40 percent of the mean susceptibility, and is very large.

NOVEMBER 15, 1938 PHYSICAL REVIEW VOLUME 54

The Magnetic Anisotropy of Copper Sulphate Pentahydrate, $CuSO_4 \cdot 5H_2O$, in Relation to its Crystal Structure. Part III.

K. S. KRISHNAN AND A. MOOKHERJI
Indian Association for the Cultivation of Science, Calcutta, India

(Received September 21, 1938)

Measurements have been made of the magnetic anisotropy of $CuSO_4 \cdot 5H_2O$ at different temperatures from 26°C to −190°C. The crystal is nearly uniaxial magnetically, and its two principal susceptibilities conform roughly to the Curie law, with different Curie constants. The observed anisotropy of the crystal may be attributed to the anisotropy induced in the Cu^{++} ion under the influence of the asymmetric electric field of the neighboring negatively charged atoms. From the known positions of these atoms the field should be expected to have tetragonal symmetry. The two principal susceptibilities of the Cu^{++} ion, along the tetragonal axis of the field, and perpendicular to the axis, respectively, are calculated. The corresponding effective magneton numbers are calculated therefrom, and it is found (1) that these magneton numbers vary little with temperature, and (2) that the magneton numbers corresponding to the two principal susceptibilities of the ion are widely different.

1. INTRODUCTION

IN Parts I and II[1] of this paper we gave an account of some magnetic studies on $CuSO_4 \cdot 5H_2O$ at room temperature, and a discussion of the results in relation to the structure of the crystal. The results verify in a striking manner the views advanced by Van Vleck,[2] and Penney and Schlapp[3] regarding the origin of magnetic anisotropy in a paramagnetic crystal, namely that it is due to the asymmetry of the internal electric fields acting on the paramagnetic ions in the crystal. The crystal of $CuSO_4 \cdot 5H_2O$ is triclinic and its unit cell contains two Cu^{++} ions. Each of these ions is in the center of an octahedron formed by six negatively charged oxygen atoms.[4] The octahedron is not regular, but may be regarded as derived from a regular one by drawing out symmetrically one of its diagonals. This diagonal will thus be an axis of tetragonal symmetry for the octahedron, and therefore also for the electric field acting on the Cu^{++} ion located at the center of the octahedron. Now the tetragonal axes of the two octahedra in the unit cell make with each other an angle of 82°. We should therefore expect the internal and the external bisectors of this angle, and the normal to the two bisectors, to be the three principal magnetic axes of the crystal. The susceptibility along the first direction should be the maximum for the crystal, and that along the third the minimum; and further, since the angle between the two tetragonal axes is nearly a right angle, the intermediate susceptibility should be nearly the same as that along the first direction, i.e., should be close to the maximum. All these results deduced from the structure of the crystal are verified experimentally.

Denoting the susceptibility of the Cu^{++} ion along the tetragonal axis of the field acting on it by $K_{\parallel}$, and that perpendicular to the tetragonal axis by $K_{\perp}$, we find that at 26°C, $K_{\parallel} - K_{\perp} = 550 \times 10^{-6}$ per gram ion, and that the mean susceptibility $K = (K_{\parallel} + 2K_{\perp})/3$ at this temperature is about 1520×10^{-6} (equal to the mean susceptibility of the crystal, corrected for its diamagnetism). The anisotropy of the Cu^{++} ion in the crystal is thus about 36 percent of its mean susceptibility, and it points to a strong asymmetry in the crystalline field acting on Cu^{++}.

The present paper deals with the temperature variation of the anisotropy and the principal susceptibilities of the crystal, and of the principal susceptibilities, $K_{\parallel}$ and $K_{\perp}$ of the Cu^{++} ion in it, from the temperature of the room to that of liquid air. The earlier theories are shown to be inadequate to explain the temperature variation of the anisotropy, and the results are considered on the basis of Van Vleck's theory.

2. THE CURIE-WEISS LAW

The magnetic behavior of paramagnetic ions in crystals naturally differs from that of the free ions. The most striking departures are the magnetic anisotropy exhibited by the crystal, and the deviations of the temperature variations of the principal susceptibilities from the Curie law.[5] These were explained on the older theories as arising from certain internal magnetic fields, which were presumed to be of the same nature as the inner fields in ferromagnetics, and were taken to be proportional to the intensity of magnetization. On this basis the temperature variations of the three principal susceptibilities are given by the simple formulae

$$\chi_i = C/(T - \Theta_i); \qquad i = 1, 2, 3; \qquad (1)$$

the Curie constant C, which is determined by the magnetic moment of the paramagnetic ion, which is assumed to be capable of turning around freely in the crystal, will naturally be the same for all the three directions, while the Θ's which are determined by the internal magnetic fields developed in the presence of the applied field, may depend on the direction of the latter in the crystal. When the Θ's are small, the mean susceptibility of the crystal, i.e., the powder susceptibility, will also conform to a formula of the same type,

$$\chi = (\chi_1 + \chi_2 + \chi_3)/3 = C/(T - \Theta), \qquad (2)$$

where

$$\Theta = (\Theta_1 + \Theta_2 + \Theta_3)/3. \qquad (3)$$

Coming back to the crystal of $CuSO_4 \cdot 5H_2O$, its susceptibility in the powder state has been measured by de Haas and Gorter[6] over a wide range of temperatures, from 14° to 290°K, and it conforms closely to the formula

$$\chi = 0.456_9/(T + 0.70), \qquad (4)$$

where χ refers to one gram ion.

The temperature variation thus approximates practically to the Curie law, and the value of 0.456_9 for the Curie constant gives for the magnetic moment of Cu^{++} 1.92 Bohr magnetons, as compared with the theoretical value of 1.73 for the single spin moment. These results would suggest, on the basis of these older theories, (1) that the inner magnetic fields are very feeble; and (2) that as in many other salts of the iron group, the contribution from the orbital angular momentum of the paramagnetic ion to the observed magnetic moment is small. We should then expect the anisotropy of the crystal to be small, and the temperature variations of the three principal susceptibilities to conform to formula (1), in which the Θ's should be small, and the Curie constant C should have the same value, namely about 0.457, for all the three principal directions.

We have already seen that the anisotropy of the crystal is by no means small. We shall show presently that the principal susceptibilities also do not conform to Eq. (1).

3. EXPERIMENTAL

The general method adopted in the present measurements is the same as that described by us and Mr. Bose in a recent paper.[7] The main part of the apparatus is the cryostat for maintaining the temperature of the crystal constant at any desired value. The crystal is suspended freely inside a thin-walled copper tube, closed at the bottom, and immersed deeply in a liquid

[1] Krishnan and Mookherji, Phys. Rev. **50**, 860 (1936) and **54**, 533 (1938).
[2] Van Vleck, *The Theory of Electric and Magnetic Susceptibilities* (Oxford, 1932).
[3] Penney and Schlapp, Phys. Rev. **41**, 194 (1932).
[4] Beevers and Lipson, Proc. Roy. Soc. **A146**, 570 (1934).
[5] If the higher multiplet levels of the paramagnetic ion, being low, are also occupied, and the magnetic moments corresponding to these levels differ from that of the ground state, e.g. Eu^{+++}, Sm^{+++}, the temperature variation of the susceptibilities of even the free ions may deviate from the Curie law, but in a manner that may be readily predicted.
[6] de Haas and Gorter, Leiden Comm. 210 d (1930).
[7] In course of publication in Phil. Trans. Roy. Soc. London.

bath of petroleum ether of boiling point 30°–50°C. The temperature of the bath was controlled automatically by a constant volume air-thermometer, of thin-walled copper, immersed in the bath. When the temperature of the bath rises above the desired value, the air in the thermometer expands and closes the electric circuit of an air-pump which slowly sucks liquid air into a small copper vessel immersed in the bath and thus cools it. When the temperature of the bath falls below the desired value, the air in the thermometer contracts, the electric current through the air-pump circuit is cut off automatically, and that through a small heating coil, also immersed in the cryostatic bath, is made, and the temperature of the bath rises. In practice the two circuits, through the air-pump and the heating coil respectively, alternate in quick succession, and the temperature remains steady to within 0.1°C.

Below about −140°C the petroleum ether becomes very viscous, and temperatures lower than this cannot be maintained with the above arrangement. The only temperatures lower than this at which measurements are made are those of liquid oxygen or air, used as bath liquid instead of the petroleum ether, and allowed to evaporate at atmospheric pressure. The electrical connections for temperature control are cut off in this arrangement.

All the temperature measurements are made with a calibrated copper-constantan thermocouple.

The magnetic measurements are made in the same manner as in Part II. The suspension for the crystal, however, now consists of two parts. The upper part is a calibrated quartz fiber, which remains at room temperature always, and its torsional constant is therefore independent of the temperature of the cryostat; and the lower part is a much stouter fiber which may be regarded as practically rigid.

4. Results

Measurements of magnetic anisotropy are made for five different suspensions of the crystal, which are numbered in the same manner as in Parts I and II; suspensions (2), (7) and (8) which correspond to low anisotropies, are omitted in the present measurements. The results are given in Tables I to V.

Suppose the torsion-head has been adjusted such that the torsion on the quartz fiber may be zero when the crystal has taken up its natural orientation in the magnetic field, namely with the direction of the maximum susceptibility for the crystal in the horizontal plane along the field. Let us call this position of the torsion-head its zero-position. Let α_0 be the angle through which the torsion-head has to be rotated from the above zero position so as to bring the crystal just to its unstable orientation in the field. Let us denote by λ the quantity $\Delta\chi \cdot mH^2/(2Mc)$, where m is the mass of the crystal, M is its molecular weight, H is the magnetic field, c is the constant of torsion of the suspension fiber, and $\Delta\chi$ is the difference between the maximum

Table I. *Suspension (1): 'c' axis vertical. $(\bar{1}00)$ sets at $27°+\epsilon$, and $(\bar{1}\bar{1}0)$ at $53°+\epsilon$, to the field; ϵ increases from 0 at room temperature to 1.5° at 82°K. $\Delta\chi = 183\times10^{-6}$ at 299°K.*

Temp. °K	304.9	270.8	251.8	231.5	210.7	191.5	170.2	148.2	137.8	90.1	81.5
ρ	0.98	1.10	1.16	1.26	1.38	1.51	1.68	1.95	2.02	3.01	3.26

Table II. *Suspension (3): $(\bar{1}00)$ and $(\bar{1}11)$ vertical. $(\bar{1}00)$ sets at 45½°, and $(\bar{1}11)$ at 14°, to the field; except at the two lowest temperatures, where the setting angle differs from the above by about 1°. $\Delta\chi = 263\times10^{-6}$ at 299°K.*

Temp. °K	295.8	270.6	248.7	231.0	211.6	194.5	189.4	174.3	148.1	90.1	82.0
ρ	1.01	1.08	1.14	1.22	1.33	1.46	1.48	1.59	1.86	2.87	3.00

Table III. *Suspension (4): $(\bar{1}\bar{1}0)$ and $(\bar{1}11)$ vertical. $(\bar{1}\bar{1}0)$ sets at 62½°, and $(\bar{1}11)$ at 9½°, to the field, at all the temperatures. $\Delta\chi = 264\times10^{-6}$ at 299°K.*

Temp. °K	271.1	251.9	231.8	211.0	194.5	171.1	143.1	90.1	83.0
ρ	1.08	1.14	1.23	1.33	1.45	1.63	1.95	2.90	3.08

Table IV. *Suspension (5): (100) horizontal: 'c' axis sets at $59°+\epsilon$, and the intersection of $(\bar{1}00)$ and $(\bar{1}11)$ at $8°-\epsilon$, to the field; ϵ increases from 0 at room temperature to ½° at 90°. $\Delta\chi = 146\times10^{-6}$ at 299°K.*

Temp. °K	304.9	271.4	251.0	230.2	210.1	194.5	176.0	158.9	148.4	90.1
ρ	0.99	1.08	1.13	1.23	1.33	1.42	1.52	1.67	1.77	2.70

Table V. *Suspension (6): (110) horizontal. 'c' axis sets at $44°+\epsilon$, and the intersection of $(\bar{1}\bar{1}0)$ and $(\bar{1}11)$ at $12½°-\epsilon$, to the field; ϵ increases from 0 at room temperature to 2° at 90°K. $\Delta\chi = 213\times10^{-6}$ at 299°K.*

Temp. °K	271.4	250.2	231.1	211.0	194.5	190.5	170.1	149.8	90.1
ρ	1.09	1.14	1.21	1.33	1.41	1.44	1.60	1.77	2.71

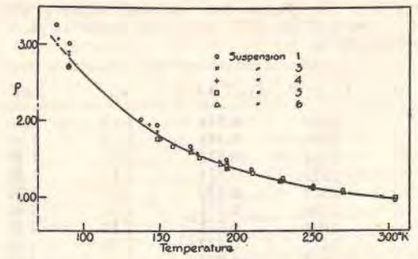

Fig. 1.

and the minimum susceptibilities of the crystal in the horizontal plane, per gram molecule. The quantity λ is connected with the observed critical angle α_0 by the relation (see Part II)

$$\lambda = (\alpha_0 - \pi/4 - \sigma)/\cos 2\sigma \qquad (5)$$

where

$$\sin 2\sigma = 1/(2\lambda). \qquad (6)$$

From observations on α_0 at different temperatures with the suspension and the field the same, we can calculate with the help of relations (5) and (6) the corresponding values of λ.

The quantity ρ in the tables denotes the ratio of the value of λ at any given temperature to that at 26°C. Obviously, this will also be the ratio of the anisotropies $\Delta\chi$ at the two temperatures.

The values of ρ for the different suspensions are plotted against temperature in Fig. 1.

5. Some General Features of the Temperature Variation of the Anisotropy of the Crystal

An examination of the data entered in the above tables, shows firstly that the setting directions are practically independent of temperature; the largest variation as we pass from room temperature to that of liquid air is only 2°; and secondly that the value of ρ at any given temperature is more or less the same for all the five suspensions. This is exhibited clearly in Fig. 1, where the experimental points for all the suspensions are seen to lie close to the mean curve; the values for suspension (1) lie slightly above the curve, and those for the suspensions (5) and (6) slightly below it.

We may conclude from these results that the principal magnetic axes of the crystal are practically the same at all the temperatures. We have seen that at room temperature the crystal is nearly uniaxial magnetically, and the axis makes with the a, b and c axes of the crystal angles of 154°, 64° and 51°, respectively. Denoting the susceptibilities along the axis and perpendicular to it by $\chi_{\parallel}$ and $\chi_{\perp}$, respectively, we found in Part II that at room temperature, namely 299°K, $\chi_{\perp} - \chi_{\parallel} = 275\times10^{-6}$. The present measurements show that at the other temperatures also, the crystal will remain approximately uniaxial, and the direction of the axis will remain the same; and the anisotropy $\chi_{\perp} - \chi_{\parallel}$ may be taken to be roughly equal to $\rho\times275\times10^{-6}$, where ρ is the value obtained from the mean curve plotted in Fig. 1. The values of $\chi_{\perp} - \chi_{\parallel}$ given in Table VI were obtained in this manner.

Combining these data with the values for the mean susceptibility, $\chi = (\chi_{\parallel} + 2\chi_{\perp})/3$, obtained by de Haas and Gorter, we can calculate the principal susceptibilities of the crystal, $\chi_{\parallel}$ and $\chi_{\perp}$, separately, at different temperatures. These

Table VI. *Principal susceptibilities of copper sulphate pentahydrate crystal.*

Temp. °K	ρ	$(\chi_{\perp}-\chi_{\parallel})\times10^6 = 275\rho$	$\chi = (\chi_{\parallel}+2\chi_{\perp})/3 \times10^6$	$\chi_{\parallel}\times10^6$	$\chi_{\perp}\times10^6$	$\chi_{\parallel}(T-2.0)$	$\chi/(T+1.8)$
299	(1.00)	275	1525	1342	1617	0.399	0.486
280	1.06	291	1628	1434	1725	0.399	0.486
260	1.12	308	1753	1548	1856	0.399	0.486
240	1.19	327	1899	1681	2008	0.400	0.485
220	1.28	352	2070	1835	2187	0.400	0.485
200	1.40	385	2277	2020	2405	0.400	0.485
180	1.54	424	2529	2246	2670	0.400	0.485
160	1.72	473	2844	2529	3002	0.400	0.486
140	1.95	536	3248	2891	3427	0.399	0.486
90.1	2.84	781	5032	4511	5292	0.398	0.486
						mean = 0.399	

calculated values are also entered in Table VI. All the χ's have been corrected for the diamagnetism of the crystal. The anisotropy of the diamagnetism of the crystal, as judged from the observed anisotropy of diamagnetic sulphates,[8] should be negligible.

As will be seen from the figures given in the last two columns of the table, the two principal susceptibilities of the crystal conform closely to the formulae

$$\chi_{\parallel}=0.399/(T-2.0) \qquad (7)$$

and

$$\chi_{\perp}=0.486/(T+1.8). \qquad (8)$$

Though both of them are of the Weiss type, the Curie constants for the two directions are widely different, a result which, as we mentioned before, is not expected on the Weiss theory.

Since the Θ's are small, the mean susceptibility also naturally obeys a formula of the same type. It is easily verified that Eqs. (7) and (8) lead to expression (4) for the mean susceptibility, as they should.

6. The Principal Susceptibilities of the Cupric Ion in the Crystal

Viewing these results on the basis of Van Vleck's theory, we can calculate the anisotropy, $K_{\parallel}-K_{\perp}$, of the Cu^{++} ion in the crystal, due to the asymmetry of the crystalline electric field acting on it. Since the field has tetragonal symmetry, and the tetragonal axes of the fields acting on the two Cu^{++} ions in the unit cell are nearly perpendicular to each other, we have the simple relation (see Part II)

$$K_{\parallel}-K_{\perp}=2(\chi_{\perp}-\chi_{\parallel}), \qquad (9)$$

from which $K_{\parallel}-K_{\perp}$ is known at different temperatures. Since further $K_{\parallel}+2K_{\perp}=\chi_{\parallel}+2\chi_{\perp}$ (the χ's, as we mentioned before, denote the principal susceptibilities of the crystal, which have been corrected for its diamagnetism), we can calculate from the data given in Table VI, the values of $K_{\parallel}$ and $K_{\perp}$ separately, at different temperatures. The results are given in Table VII.

[8] Krishnan and Banerjee, Phil. Trans. Roy. Soc. **A235**, 343 (1936).

TABLE VII. *The effective Bohr magneton values of the magnetic moment of the* Cu^{++} *ion in the copper sulphate pentahydrate crystal.*

Temp. °K	$K_{\parallel}\times10^6$	$K_{\parallel}(T+4\cdot5)$	$n_{\parallel}$	$n_{\perp}$
299	1892	0.574	2.13	1.80
280	2016	0.574	2.13	1.80
260	2164	0.572	2.13	1.80
240	2335	0.571	2.12	1.80
220	2539	0.570	2.12	1.80
200	2790	0.571	2.12	1.80
180	3094	0.571	2.12	1.81
160	3475	0.572	2.12	1.81
140	3963	0.573	2.11	1.81
90.1	6073	0.574	2.10	1.81
		mean = 0.572		

Since evidently $K_{\perp}=\chi_{\parallel}$, and the values for $\chi_{\parallel}$ have already been given, the values for $K_{\perp}$ have not been entered in the table.

Let us denote the effective Bohr magneton values of the magnetic moment of the Cu^{++} ion when the applied magnetic field is along the tetragonal axis of its crystalline field, and when it is perpendicular to it, by $n_{\parallel}$ and $n_{\perp}$, respectively;

$$n_{\parallel}^2/K_{\parallel}=n_{\perp}^2/K_{\perp}=3kT/(N\beta^2), \qquad (10)$$

where $\beta=eh/4\pi mc$ is the Bohr magneton, N is the Avogadro number and k is the Boltzmann constant. The values of $n_{\parallel}$ and $n_{\perp}$, calculated from $K_{\parallel}$ and $K_{\perp}$ in relation (10), are also given in Table VII.

The most striking feature of the anisotropy of the Cu^{++} ion under the crystal fields is that whereas the effective magneton numbers for both the principal directions of the field vary little with temperature, showing that both the principal susceptibilities of the Cu^{++} ion obey practically the Curie law of inverse dependence on T, the magneton numbers for the two principal directions are widely different. To be more precise, the two principal susceptibilities of the ion conform to the formulae

$$K_{\parallel}=0.572/(T+4.5) \qquad (11)$$

and

$$K_{\perp}=0.399/(T-2.0), \qquad (12)$$

with small Curie temperatures, and widely different Curie constants.

Magnetic Anisotropies and the Valencies of Paramagnetic Atoms in Crystals

Studies on the magnetic anisotropies of paramagnetic crystals are of interest because of the variety of information one can obtain from them under favourable conditions, on such widely different topics as (1) the magnitude and the asymmetry of the internal electric field acting on the paramagnetic ion in the crystal; (2) the geometry of distribution of the negatively charged atoms immediately surrounding the paramagnetic ion, and hence the co-ordination number of the ion; (3) the magnitude of the Stark-separation of the energy levels of the ion in the above field (in the special case when the paramagnetic ion in the crystal is in the S-state, the Stark-separation of its levels is naturally feeble, and it plays an important part in determining the thermal behaviour of the crystal at very low temperatures, in the neighbourhood of 0·1° K.); (4) the strength of coupling between the orbital and the spin angular momenta of the electrons in the incomplete shell of the ion, etc. In some recent papers[1] we have dealt with these various aspects of paramagnetic studies on single crystals. In the present note we wish to direct attention to another useful application, namely, to questions concerning the valency of the paramagnetic atom in the crystal.

We shall take, for example, the well-known crystal manganite, the chemical composition of which corresponds to that of hydrated hemitrioxide of manganese. On the basis of the available chemical evidence, the manganese in the compound is sometimes regarded as trivalent, corresponding to the formula, 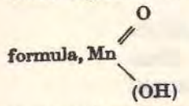 and sometimes as half divalent and half tetravalent, corresponding to the formula, 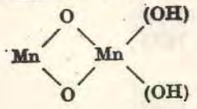

A measurement of the magnetic anisotropy of the crystal should enable us to decide readily between these two alternatives. The Mn^{++} ion is in the S-state (^6S), and should therefore be almost isotropic. The Mn^{++++} ion, which is in the ^4F-state, and resembles Cr^{+++}, should also have very little anisotropy. On the other hand, the Mn^{+++} ion, the ground state of which is ^5D, should have a relatively large anisotropy in the asymmetric crystalline field. A measurement of the anisotropy of the crystal, that is, the difference between its maximum and minimum susceptibilities, to find whether it is of the same order of magnitude as in manganous and chromic salts, namely, 10^{-5} per gram atom of manganese at room temperature, or is very much greater, will therefore decide whether the manganese atoms in the crystal are half of them divalent and the other half tetravalent, or all of them trivalent.

The crystal is monoclinic, and at 31° C. its maximum anisotropy, namely, $\chi_c-\chi_a$, is found to be $4\cdot0\times10^{-4}$ per gram atom of manganese; which shows that the manganese atoms in the crystal cannot be trivalent.

The mean susceptibility of the crystal does not give us similar information. The susceptibility of Mn^{+++} lies almost midway between those of Mn^{++} and Mn^{++++}; and further, the exchange interaction between the spin moments of Mn, which should be large in this crystal owing to the large concentration of manganese, affects the mean susceptibility considerably, and to an uncertain extent, whereas its influence on the anisotropy is almost nothing.

K. S. Krishnan.
S. Banerjee.

Indian Association for the Cultivation of Science, Calcutta.
Aug. 30.

[1] *Phil. Trans. Roy. Soc.*, 1933–38.

DIRECTIONAL VARIATIONS IN THE ABSORPTION AND THE FLUORESCENCE OF THE CHRYSENE MOLECULE.

By K. S. Krishnan and P. K. Seshan.

1. *Single Crystals as Suitable Media for Studying the Directional Variations in Some of the Properties of Aromatic Molecules.*

Complete X-ray analyses of the structures of several organic compounds, particularly of the aromatic class, have been made recently by Robertson (1933–38) and others. Since the molecules of these compounds retain their individuality in the crystal state, and their orientations in the crystals are known from the X-ray studies, the crystals are very suitable for the study of the directional variations of some of the properties of the molecules.

The directional variations in the magnetic and the optical polarisabilities of many of the aromatic molecules have been studied in this manner. Conversely, when the principal polarisabilities of the molecules are already known, the magnetic or the optical studies on the crystals can be utilized to obtain information regarding the orientations of the molecules in the crystals (Krishnan, 1929; Bhagavantam, 1929; Krishnan and Banerjee, 1933, 1935; Bernal and Crowfoot, 1935; Banerjee, 1938).

The absorption spectra of some of these crystals have been studied under polarised light (Krishnan and Seshan, 1934; Obreimov and Prikhotjko, 1936), and it is found that for plane aromatic molecules much of the absorption is confined to light vibrating along directions in the plane of the benzene rings, vibrations along the normal to the plane being much less absorbed. Hence a study of the "pleochroism" of aromatic crystals can also be utilized for determining the molecular orientations in the crystals. Studying in this manner the polarisation of the absorption by single crystals of anthracene and chrysene, containing traces of naphthacene (2, 3-benzanthracene) as impurity, crystals of diphenyl containing fluorene as impurity, etc., one finds that the impurity molecules are oriented with their planes nearly parallel to those of the host molecules which accommodate them (Krishnan and Seshan, 1934).

The concentrations of the impurities can be controlled, and these crystals form therefore very convenient media for studying the fluorescence of the impurity molecules, and in particular the directional variations in their fluorescence, since the orientations of the impurity molecules in the crystals

are known approximately and we can excite the fluorescence by light vibrating along known directions with reference to the molecule, and can analyse the fluorescent radiations emitted along different directions for their polarisation. Some preliminary experiments on the fluorescence of naphthacene molecules, included as impurity in anthracene and chrysene crystals, showed that the excitation of fluorescence is due mostly to light-vibrations in the plane of the naphthacene molecule, vibrations along the normal to the plane exciting very little fluorescence. Similar results were also obtained from studies on the fluorescence of single crystals of 1, 2, 5, 6-dibenzanthracene, which could be obtained in very thin flakes.

In the present paper we report quantitative studies on the fluorescence and light-absorption of single crystals of pure chrysene. This substance was chosen because its crystal structure is known in detail from X-ray studies, and pure synthetic chrysene free from naphthacene and other fluorescent impurities could be easily obtained.

2. *The Orientations of the Molecules in Chrysene Crystal.*

A quantitative X-ray analysis of the structure of this crystal has been made by Iball (1934). The crystal is monoclinic in the space group C_{2h}^6 (I 2/c) or C_s^4 (I c). Its unit cell has the dimensions

$$a = 8{\cdot}34,\ b = 6{\cdot}18,\ c = 25{\cdot}0 \text{ A.U.};\ \beta = 115°{\cdot}8$$

and it contains 4 molecules of $C_{18}H_{12}$.

The molecule has a plane structure and it consists of four regular hexagons arranged as shown in Fig. 1. Let OA and OB be two directions in the plane of the molecule located as marked in the diagram.

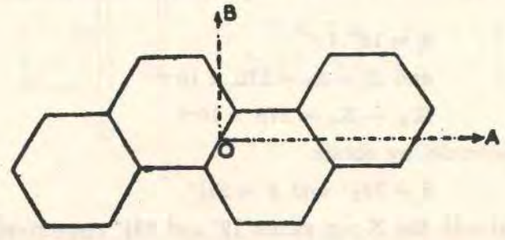

Fig. 1.

Two of the molecules in the unit cell of the crystal are oriented in the same way, and their OA directions make with the a and the b crystallographic axes angles of 102°·0 and 90°·5 respectively, while their OB directions make

with the [illegible] axes angles of 118°·4 and 29°·0 respectively. The orientations of the other two molecules in the unit cell are obtained from the above orientations by reflection from the (010) plane.

The crystal as usually prepared is in the form of a flake parallel to the c(001) plane. From the above angles defining the molecular orientations it is easily seen (1) that the molecular planes are nearly perpendicular to the plane of the flake, actually making with it an angle of 79°; (2) that their intersections with the plane of the flake make angles of $\pm 29\frac{1}{2}°$ with the b-axis; and (3) that these intersections are very close to the OB axes of the molecules.

The orientations of the molecules in the crystal can also be deduced from measurements on its magnetic anisotropy, and are found to be practically the same as those obtained above from the X-ray analysis. Let δ be the angle which the molecular planes make with (001), and $+\phi$ and $-\phi$ the angles which the intersections of the molecular planes with (001) make with 'b'. Let χ_1 and χ_2 be the maximum and the minimum susceptibilities of the crystal in the (010) plane, and θ the angle which χ_2 axis makes with a. Also let K_1 be the susceptibility of the *molecule* along the normal to its plane and $K_\perp$ that for directions in the plane. (The susceptibility will be practically the same along different directions in the molecular plane.) Then we can easily show that

$$\cos\delta = \sin\theta \,.\, \sqrt{\frac{\chi_1 - \chi_2}{K_\perp - K_{||}}};$$

$$\cos\phi = \cot\theta \,.\, \cot\delta.$$

Using these expressions, and the experimental values (Krishnan and Banerjee, 1935)

$$\theta = 13°.1$$

$$\text{and } \chi_1 - \chi_2 = 170 \times 10^{-6}$$

$$K_\perp - K_{||} = 218 \times 10^{-6}$$

per gram molecule, we obtain

$$\delta = 78\tfrac{1}{2}° \text{ and } \phi = 28\tfrac{1}{2}°,$$

as compared with the X-ray values 79° and $29\frac{1}{2}°$ respectively.

Since the molecular planes are nearly perpendicular to the plane of the crystal flake, and the OB axis of the molecule lies nearly in the plane, the directional variations in the absorption and the fluorescence of the molecule as we pass from the normal to the molecular plane to the OB axis in the plane can be easily followed.

3. Measurements on Fluorescence.

We shall first take up the study of the fluorescence. Chrysene has three diffuse fluorescence bands in the visible region, with their maxima at 4490, 4380 and 4200 A.U. respectively. Using a quartz mercury lamp as the source of light, and suitable light-filters for isolating some of the mercury lines, we found that the above fluorescence bands are excited strongly by the 3650 group of lines, and hardly, if at all, by the 4047 and the 4358 groups.

A thin flake of the crystal of about 1/20 mm. thickness was used in our measurements. As we mentioned before, the plane of the flake is the (001) plane, and the two extinction lines in the plane will naturally be the a and the b axes. The general plan of the experiments was to excite the fluorescence by the radiations of the 3650 group incident normally on the crystal flake, either unpolarised, or polarised with the electric vector along the a or the b axis, and to study the fluorescence in the forward direction for its polarization and intensity. A sketch of the experimental arrangement used is given in Fig. 2. The light from a mercury lamp M is focussed, with the help of a lens L_1 on a square aperture A having its sides vertical and horizontal respectively. Between L_1 and A are inserted a nicol N_1 to polarise the light suitably, and a Corning glass-filter F to isolate the 3650 group of radiations. C is the crystal flake mounted just behind the aperture and covering it completely, with its plane perpendicular to the path of the light, and its a or b axis vertical. The fluorescence in the forward direction, after passing

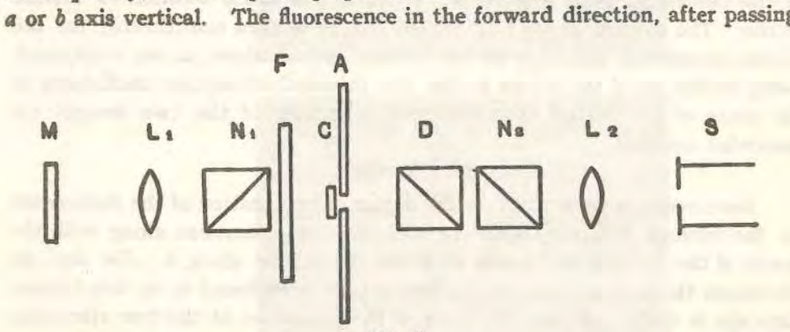

FIG. 2.

through a double-image prism D, so oriented as to separate the images vertically, a nicol N_2, and a lens L_2, forms two images of the aperture A on the slit S of the spectrograph, one of them just above the other. The polarization of the fluorescence is determined by suitably rotating the nicol N_2 so as to make the intensities of the two images of the fluorescence bands appearing in the spectrograms equal.

We shall mention here one simple result which enables us to dispense with the spectrograph; this is an advantage in view of the feeble intensity of the fluorescence. For any given excitation, *all the three fluorescence bands are found to be polarised to nearly the same extent.* Indeed as far as can be judged from the spectrograms every small region inside the bands also appears to have nearly the same polarization (except in the extreme violet, beyond about 4100 A.U., where the two principal absorption coefficients in the plane of the crystal flake, which are unequal, begin to increase rapidly). This will be clear from Fig. 3, Plate XVI, which was taken with the principal plane of the analyser N_2 at 35° to the direction of the *a* axis of the crystal.

It would therefore be sufficient to compare the total intensities of the two polarised images of the fluorescent light formed at S, without analysing them spectroscopically; the photographic plate may be placed at S, and the images photographed directly. For this purpose, however, it would be necessary to cut off any of the incident radiations that may be transmitted by both the Corning glass-filter and the crystal. The filter transmits, in addition to the 3650 group of lines, some of the long wave-length lines also. Though the 1/20 mm. thick crystal used in the experiment completely cuts off the 3650 group and the lines in its neighbourhood, some of the long wave-length lines transmitted by the filter are transmitted feebly by the crystal also. These were eliminated in our measurements by placing in the path of the fluorescent light a glass cell containing a dilute solution of sodium nitrite. The sodium nitrite filter served also to weaken considerably the tail of the fluorescence spectrum in the extreme violet, where, as we mentioned, owing to the rapid variations in the two principal absorption coefficients in the plane of the crystal, the apparent intensities of the two images are somewhat unequal.

4. *Results.*

Measurements were made on the degree of polarization of the fluoresence in the forward direction, with the incident light-vibrations along with the *a*-axis of the crystal, and again with the vibrations along *b*. *For both the excitations* the *a* vibrations in the fluorescence were found to be less intense than the *b* vibrations, and the ratio of the intensities of the two vibrations was also the same for both, namely 0·49.

Now since the polarization of the forward fluoresence is the same whether the incident light-vibrations are along *a* or along *b*, we should naturally expect the same polarization with incident unpolarized light also. Removing the nicol N_1 in the experimental arrangement we measured again the polarization of fluoresence in the forward direction. The ratio of the intensities of the *a* and the *b* vibrations was the same as before, namely 0.49.

FIG. 3

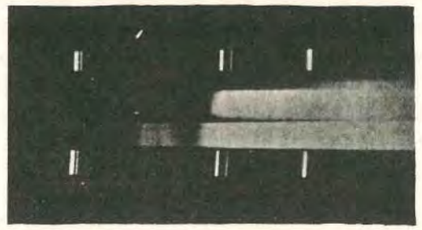

FIG. 4

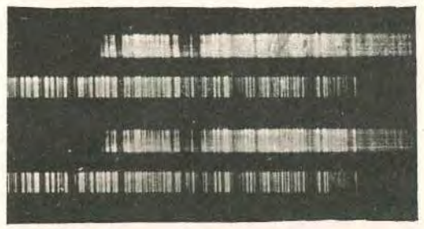

FIG. 5

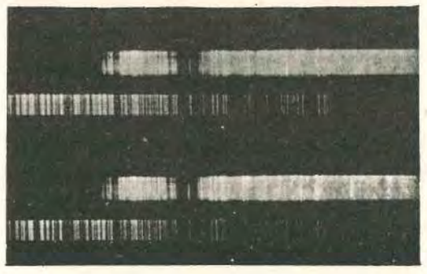

FIG. 6

The value of 0·49 obtained in all the three measurements above for the ratio ρ of the intensities of the *a* to the *b* vibrations in the forward fluorescence requires correction on two accounts. (1) The *b* vibrations in the fluorescence are absorbed more strongly by the crystal than the *a* vibrations. From a measurement of the absorption coefficients in the fluorescence region it was estimated that the *b* vibrations are weakened in relation to the *a* vibrations on this account in the ratio 0.85 : 1. Since the ratio changes slightly with wave-length, this estimate of its effective value should be regarded as only approximate. (2) The *b* vibrations of the fluorescent light lose by reflection at the back surface of the crystal about 4% more than the *a* vibrations. Making these two corrections we obtain for the true ratio of the intensities of the *a* to the *b* vibrations in the fluorescence the value $\rho = 0 \cdot 40$.

5. *The Significance of the Results.*

The result that the ratio ρ is independent of whether the incident light-vibrations are along the *a* axis or along *b* is very significant. It shows that in the (001) plane, *to which we shall confine our attention at present*, there are two unique directions, one on either side of the *b* axis, and making equal angles with it, such that it is only the resolved components of the incident electric vector along one or the other of these two directions, as the case may be, which can excite fluorescence in any given molecule. The electric vector of the fluorescent radiations from the molecule will also naturally be along the same direction. The ratio of the intensities of the *a* to the *b* vibrations in the fluorescence of the crystal as a whole, namely ρ, will then be determined only by the inclinations of the above directions to the *a* and the *b* axes. If $+\Phi$ and $-\Phi$ are the angles which these directions make with *b*, evidently

$$\rho = \tan^2 \Phi,$$

and one can readily understand why the ratio ρ should be independent of the direction of the incident electric vector in the (001) plane, and also why, over the whole region of fluorescence, ρ should have the same value. The absolute intensities of the *a* or the *b* vibrations, unlike their ratio ρ, will of course depend on the direction of the incident electric vector, and we shall postpone the consideration of their separate intensities to a later section, confining ourselves here to their ratio ρ.

The experimental value of ρ namely 0·40, corresponds to

$$\Phi = \tan^{-1} \sqrt{0 \cdot 40} = 32°;$$

i.e., the two unique directions mentioned above should lie on either side of the *b*-axis, making with it angles of 32°,

Now these two directions nearly coincide with the intersections of the molecular planes with the plane of the crystal flake (001), since the intersections make angles of 29½° with b on either side. In other words, Φ is nearly the same as ϕ. We can conclude therefrom that among the various directions lying on the (001) plane, along which the electric vector may be incident, the excitation of fluorescence in any given molecule is a maximum when the electric vector is in the plane of the molecule, and it is practically nothing when it is along the projection of the normal to the molecular plane on (001). Considering the latter direction, along which the excitation of fluorescence is practically nothing, since there is no direction in the molecular plane which is closer to it than 79°, and since the normal to the molecular plane makes with it an angle of 11° only, we are forced to conclude that when the incident electric vector is along the normal to the plane of the molecule, there is hardly any fluorescence excited.

Our present experiments, beyond demonstrating that when the electric vector is incident along the OB direction in the plane of the molecule there is a strong excitation of fluorescence, do not enable us to draw any conclusions as to how the efficiency of excitation will vary with the change of direction of the electric vector in the plane of the molecule.

6. *The Polarization of Fluorescence in State of Solution cannot give Information regarding the Anisotropy of Fluorescence of the Molecule.*

We should mention here that measurements on flourescence in the liquid state or in state of solution in suitable solvents, even when the medium is made so highly viscous that molecular rotations are completely stopped, cannot give us any information regarding the anisotropy of flourescence of the molecules. Suppose a parallel beam of plane polarised light with its electric vector along the z-axis traverses the solution in the x-direction, and that observations are made on the polarization of the fluorescence either in the forward direction (x), or in the transverse direction (y). Let us denote by r the ratio of the intensity of the weak component to that of the strong in the partially polarised fluorescent light. Let us suppose there is a unique direction in the molecule such that when the electric vector is incident along this direction there is maximum excitation of fluorescence, and that the fluorescent radiations so excited also vibrate along the same direction; and further that when the incident electric vector is along any direction perpendicular to the above unique direction in the molecule, there is no excitation of fluorescence at all. In other words, we assume that the fluorescence of the molecule would be that of a single linear oscillator fixed to the molecule. Assuming that the molecules in the medium have fixed random orientations,

the ratio r, as Perrin (1931) has shown, would be theoretically equal to 1/3, corresponding to a 50 per cent. polarization of the flourescent light.

If instead of the fluorescence being due to a single linear oscillator, it is regarded as due to more than one oscillator, along different directions fixed to the molecule, then because of the incoherence between the incident and the fluorescent radiations and the consequent incoherence in phase between the different oscillators in the same molecule, they will behave as though they were all independent of one another, and the resulting polarizations of fluorescence of the medium along the forward or the transverse direction would still only be 50 per cent., *i.e.*, r would still be only 1/3.

If the medium is not sufficiently viscous and the molecules are free to rotate, then owing to the finite duration of the molecule in the excited state, the observed value of r would naturally be greater than 1/3; we are not concerned with this aspect of the problem, which has been discussed in great detail by Perrin. What we wish to emphasise here is the result, which is not generally realised, that the polarization of the fluorescence of the solution, in which the molecules are oriented at random, is independent of the anisotropy of fluorescence of the molecule and cannot therefore give any information about the latter; and only measurements on a medium in which the molecules are regularly oriented, as in a crystal, can give such information. In this respect there is an essential difference between the phenomena of scattering and fluorescence.

In this connection it is very significant that in all highly viscous solutions, whatever the fluorescing molecule may be, the ratio r does experimentally tend to approach a value close to 1/3, *i.e.*, the limiting value of the polarization for infinite viscosity is close to 50 per cent. (Perrin, 1931; Mitra, 1933, 1934).

7. *The Intensities of Fluorescence Excited Separately by the* a *and the* b *Vibrations Compared.*

Coming back to the observations on the chrysene crystal, if the explanation given in a previous section for the observed value of ρ, namely $\rho = \tan^2\Phi = \tan^2\phi$, is correct, then we should expect that for a *very thin crystal*, so thin that the absorption of the 3650 radiations which excite the fluorescence is negligible, the total intensity of forward fluorescence excited parallel to the a axis should be less than that excited by vibrations of the same intensity incident along the b axis, in the ratio $\tan^2\Phi : 1$.

It was not practicable, however, to verify this result directly, since even the thinnest crystal absorbs both the a and the b vibrations of 3650 very strongly, and to very different extents. In any actual crystal, owing to the

much stronger absorption of the *b* vibrations of the exciting light than of the *a* vibrations, the observed ratio R of the intensities of fluorescence excited separately by the two vibrations will naturally be greater than the theoretical value of $\tan^2\Phi$ predicted for an ideally thin film. Actually with our 1/20 mm. thick crystal, which absorbed both the *a* and the *b* vibrations of the incident 3650 radiations *completely*, the fluorescence excited by the *a* vibrations was found to be just stronger than that excited by the *b* vibrations; *i.e.*, for such a thick crystal, R is practically unity.

We can deduce from this observation one important result. Since both the *a* and the *b* vibrations of the exciting light are completely absorbed, and the *b* vibrations much more strongly than *a*, the penetration, or the effective thickness of the crystal producing the observed fluorescence, should be much greater when the incident vibrations are along *a* than when they are along *b*. To be more precise, the effective thickness for the two vibrations should be in the inverse ratio of the corresponding absorption coefficients. Since the observed ratio R is unity, instead of being equal to $\tan^2\Phi$, as it would have been had the effective thicknesses been the same for both the vibrations, we should infer that the effective thickness for the *a* vibration is greater than that for *b* in the ratio $1 : \tan^2\Phi$, and since the effective thicknesses are inversely proportional to the absorption coefficients, that the absorption coefficient of the crystal for the 3650 region for the *a* vibrations should bear to the coefficient for the *b* vibrations the ratio $\tan^2\Phi : 1$.

Now since Φ is nearly equal to ϕ, the angle which the intersections of the molecular planes with (001) make with *b*, the obvious interpretation of the above result is this. We found that light-vibrations incident along the normal to the plane of the molecule do not excite its fluorescence and it is only vibrations in the plane that do. We are now forced to the conclusion that the molecular absorption also is practically nothing when the incident light-vibrations are along the normal to the plane of the molecule, and it is only vibrations in the plane that are absorbed by the molecule.

The close correspondence between the absorption spectra of the crystal for the *a* and the *b* vibrations is then easily understandable, since on the view presented here the effect of changing over from the *a* to the *b* vibrations, on the absorption, will be roughly equivalent to increasing the thickness of the crystal from $\tan^2\phi$ to 1.

8. *Direct Comparison of the Absorption Coefficients for the* a *and* b *Vibrations.*

Because of the very strong absorption of the 3650 group for both the vibrations, it was not possible to measure the absorption coefficients directly

and verify whether they bear the ratio $\tan^2\Phi : 1$. We have, however, made such measurements in the region of the first absorption band, which has a maximum, not very strong, at about 3970 A.U. (see Fig. 4, Plate XVI).

The light from an iron arc was rendered nearly parallel, and after passing through a large-sized nicol, was incident axially on the slit of a spectrograph. In front of the slit and close to it was mounted a screen with two small square apertures, one just below the other. One of them was covered completely by the crystal plate, with its *a* or *b* axis vertical. A rotating sector mounted just in front of the open aperture served to reduce the intensity of the light falling on it by a constant known amount, in the ratio 2·5 : 100 in our experiments. A further reduction in intensity which was necessary in order to equalize it in the 3970 region with the light transmitted through the crystal, was secured by shutting out the light through the open aperture after a certain fixed interval of time, while the exposure through the crystal was continued for a longer time, which was increased progressively in the different exposures. A few typical photographs near about the point of matching for the 3969 line of iron, which is the region of maximum of the first absorption band, is reproduced in Figs. 5 and 6 (Plate XVI). In Fig. 5 the incident light vibrations were along the *a* axis, and in Fig. 6 along *b*.

The thickness of the crystal was measured by an optical method. The crystal flake was placed between two crossed nicols with its *a* and *b* axes at nearly 45° to the principal planes of the nicols; white light was allowed to traverse the system, and after transmission was analysed by a spectrograph. The refractive indices of the crystal for the *a* and the *b* vibrations, according to some unpublished measurements by Mr. Sundararajan in this laboratory, are 1·615 and 1·787 respectively for the 5461 line, and 1·648 and 1·849 respectively for the 4358 line. The birefringence of the crystal plate is thus known for the two wave-lengths, and by counting the number of fringes which appear between these two lines in the above spectrogram—the number was actually 8·1—the thickness of the plate was calculated and was found to be 0·0055 cm.

Coming back to the absorption measurements, we shall give here only the final results. For the 3969 line, which, as we mentioned, is the region of maximum absorption in the first band, the ratio of the intensity of the transmitted light to that of the incident light (after correcting for the loss by reflections at the two surfaces) was 0.18 for the *a* vibrations, and 0.0037 for the *b* vibrations. Equating these ratios to $e^{-k_a t}$ and $e^{-k_b t}$ respectively, where *t* is the thickness of the crystal (0·0055 cm.), and k_a and k_b are the absorption coefficients for the 3969 line for the *a* and the *b* vibrations respectively, we obtain

$$k_a = 310$$
$$k_b = 1020$$

approximately. The ratio $k_a/k_b = 310/1020 = \tan^2 29°$. The last angle is practically the X-ray angle ϕ which gives the inclination to the b-axis of the intersections of the molecular planes with (001). The value of Φ deduced in an earlier section from the fluorescence measurements was 32°.

Thus the conclusion that the absorption coefficients of the crystal for the a and the b vibrations should bear approximately the ratio $\tan^2 \Phi : 1$ is verified experimentally, and hence also the obvious inference therefrom that light-vibrations incident along the normal to the molecular plane are not absorbed at all by the molecule.

Since the vibrations which excite fluorescence strongly are also the vibrations which are absorbed strongly, and those which do not excite fluorescence are not absorbed at all, one is tempted to enquire whether after all the absorption by the molecule may not represent the energy expended in exciting fluorescence. Such a simple connection between fluorescence and absorption however, offers difficulties, since some of the absorption bands are in regions whose wave-lengths are too long to excite fluorescence, and they are polarised just as strongly as the other absorptions. We are continuing the studies on fluorescence with a view to elucidate the connection between the absorption and the fluorescence of these molecules.

Summary.

Chrysene crystal is monoclinic, and as usually prepared is in the form of a flake parallel to (001). The molecular planes are inclined at 79° to (001), and their intersections with (001) make angles of $+\phi$ and $-\phi$ with the b-axis, where $\phi = 29\frac{1}{2}°$.

The fluorescence of the crystal was excited by the 3650 group of lines of the mercury arc, incident normally on the flake, and was analysed in the forward direction for its polarizations and intensity. The following results may be mentioned here :

(1) Whether the incident vibrations are along a or along b, the a vibrations in forward fluorescence are much weaker than the b vibrations, the ratio of their intensities being 0·40, which is nearly equal to $\tan^2 \phi$. From this it is concluded that when the incident light-vibrations are along the normal to the plane of a molecule there is hardly any fluorescence excited in it, and that it is only vibrations in the plane that excite fluorescence.

(2) With a crystal thick enough to absorb *completely* the exciting radiations, the intensities of forward fluorescence excited by the a and the b

vibrations separately, are practically equal. From this observation it follows that the absorption coefficients for the a and the b vibrations should bear the ratio $\tan^2 \Phi : 1$. This conclusion is verified by direct measurements on the absorption coefficients.

The obvious interpretation of this result is that when the incident light-vibrations are along the normal to the molecular plane there is hardly any absorption ; and it is only vibrations in the plane that are absorbed.

(3) The relation between fluorescence and absorption is discussed.

REFERENCES.

Banerjee, S. .. Paper in course of publication in *Zeits. Kristall.*
Bhagavantam, S. .. *Proc. Roy. Soc.*, (A), 1929, **124**, 545 ; **126**, 143.
Bernal, J. D., and Crowfoot, D. *Journ. Chem. Soc., London*, 1935, 94.
Iball, J. .. *Proc. Roy. Soc.*, (A), 1934, **146**, 140.
Krishnan, K. S. .. *Proc. Ind. Sci. Congress*, 1929.
———, and Banerjee, S. .. *Phil. Trans.*, (A), 1932, **231**, 235.
——— *Ibid.*, (A), 1935, **234**, 265.
Krishnan, K. S., and Seshan, P. K. *Curr. Sci.*, 1934, **3**, 26.
——— .. *Zeits. Kristall.*, (A), 1934, **89**, 538.
——— .. *Acta Phys. Polonica*, 1936, **5**, 289.
Mitra, S. M. .. *Ind. Jour. Phys.*, 1934, **8**, 171 and 445.
Obreimov, I. W., and Prikhotjko *Phys. Zeits. Sowjet.*, 1936, **9**, 34.
Perrin, F. .. *Fluorescence*, Hermann, Paris, 1931.
Robertson, J. M. .. Various papers in *Proc. Roy. Soc.*, (A), 1933–1938.

INVESTIGATIONS ON MAGNE-CRYSTALLIC ACTION
VI. FURTHER STUDIES ON PARAMAGNETIC CRYSTALS

By Professor K. S. Krishnan, A. Mookherji and A. Bose
Indian Association for the Cultivation of Science, Calcutta

(*Communicated by Sir Venkata Raman, F.R.S.—Received 5 September* 1938)

CONTENTS

1. Introduction

In some of the earlier papers in this series (Part II, 1933; Part IV, 1936; Part V, 1938) we gave an account of magnetic studies on single crystals of several paramagnetic salts of the rare earth and the iron groups, and a discussion of the results on the basis of the recent theoretical work of Van Vleck (1932 *a*, *b*), and Penney and Schlapp (1932), on the influence of the strong local electric fields acting on the paramagnetic ions in the crystals on their magnetic behaviour. Paramagnetic studies on single crystals are of interest because of the variety of information one can obtain from them under favourable conditions—on such widely different topics as the magnitude and the asymmetry of the electric field acting on the paramagnetic ion in the crystal; the geometry of distribution of the negatively charged atoms immediately surrounding the paramagnetic ion, and

hence the co-ordination number of the ion; the strength of coupling between the orbital and the spin angular momenta of the electrons in the incomplete shell of the ion; and in those crystals in which the paramagnetic ions are all in the S-state, the magnitude of the Stark separation of the S-levels, which plays an important part in determining the thermal properties of the crystal at very low temperatures ($\doteqdot 0{\cdot}1°$ K); etc. Several examples were given, in the papers referred to, to illustrate these various aspects of the magnetic studies on paramagnetic crystals.

Encouraged by these results we have now made measurements at low temperatures, down to about 90° K, on the anisotropies of some typical salts of the iron and the rare earth groups. The low temperature measurements naturally supply much useful material for an extended application of the theory. We have also made measurements at room temperature on a number of crystals specially selected for their structural or other interest. The present paper gives an account of these magnetic studies.

2. A cryostat for measurements on the magnetic anisotropy of crystals at low temperatures

The cryostat. We shall take up first the low temperature measurements. In fig. 1 is given a sketch of the apparatus used, of which the main part is the cryostat for maintaining the temperature of the crystal constant at any desired value. The liquid used as the cryostatic bath is petroleum ether, of boiling-point 30–50° C, which remains sufficiently fluid to about −140° C. It is contained in a long cylindrical silvered Dewar vessel D_1, of about 3 in. external diameter, which is mounted between the large flat pole-pieces *PP* of the electromagnet, on a wooden block *W* shaped suitably to receive the bottom of the vessel. The vessel is covered by an ebonite disk *E*, which is kept in position by a rubber ring R_1. The bath liquid is kept well stirred by a stirrer *F* driven by a small motor. The shaft of the stirrer is enclosed in a metal sheath passing through *E*, and is connected to the driving motor by the cross-pinions p_1 and a flexible steel cord *C* enclosed in a flexible metal sheath *s*. The stirrer when connected to the motor in this manner runs more smoothly than with the usual pulley and cord connexion.

Temperature control. The control of the temperature of the bath is effected automatically by a constant volume air thermometer. The bulb of the thermometer C_1 is a thin-walled cylinder of copper, which takes up the temperature of the bath with very little time-lag. The bulb has a capacity of 30 c.c., and the volume of dead space of the thermometer is made as small as possible. The bulb is connected to the capillary tube T_1 of pyrex glass through the metal-glass soldered joint J_1, and thence to the pressure rubber tubing *t*, which is filled with clean mercury. The other mechanical parts in this arm of the apparatus will be clear from the figure, and they serve to adjust the pressure of the air inside the thermometer suitably, and to maintain it constant, and also to adjust the level of the mercury at e_1 at any desired height.

e_1 and e_2 are two tungsten electrodes fused through the glass tube. e_2 is always under the mercury in the tube, while e_1 is just at the mercury level. There are two electric circuits, one or the other of which is closed according as the mercury level is in contact, or loses contact, with e_1.

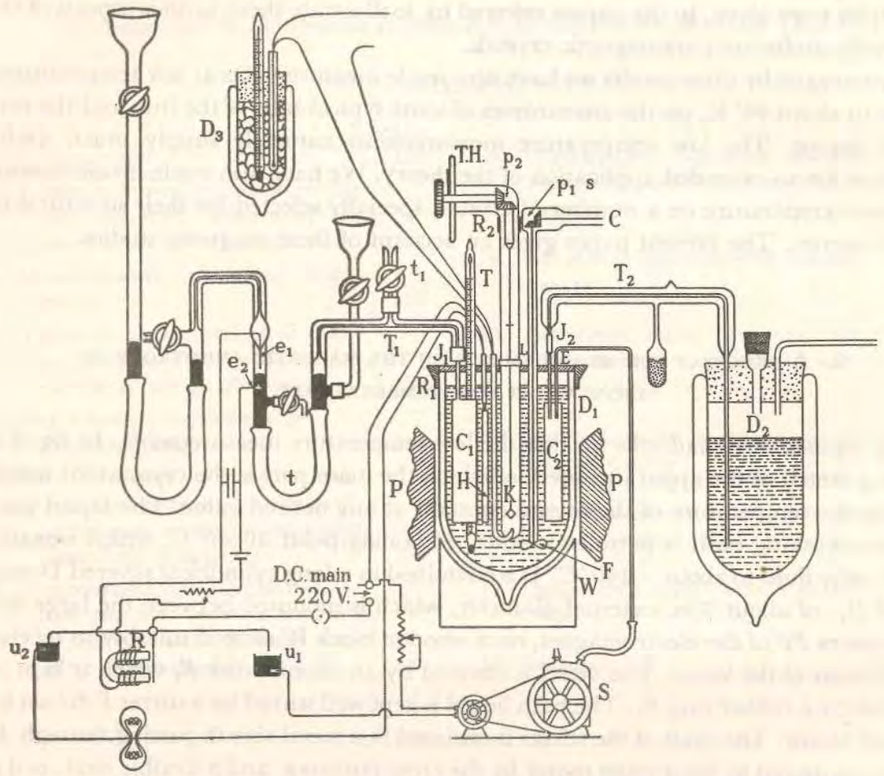

FIG. 1

The first circuit is that through the motor of the air-pump S which slowly sucks liquid air from the Dewar flask D_2 through the thin-walled copper chamber C_2 immersed in the cryostatic bath. The liquid air evaporates in the chamber, and thus cools it and the surrounding bath. The tube T_2 through which the liquid air is delivered to the chamber is double-walled, and the space between the two walls has been well evacuated. It is connected to C_2 through the glass-metal joint J_2.

The second circuit is that through the heating coil H immersed in the bath. The coil is of fine enamelled copper wire wound on a mica sheet, and takes a current of about $\frac{1}{2}$ amp. The leads to the coil have naturally to be well insulated, since any sparking near the bath of petroleum ether is dangerous.

The electrical connexions to the two circuits will be clear from the figure. The current through the relay magnet R is made or broken according as there is contact between e_1 and the mercury or not. The yoke which is connected to the relay arm, and is of the double-contact type, dips accordingly into one or the other of the mercury cups u_1, u_2, and thus closes the first or the second of the two circuits mentioned above.

In order to avoid sparking at the mercury contact at e_1, the mercury surface is covered by a drop of glycerine, and a condenser, of 6 μF capacity, is connected across the terminals e_1 and e_2.

The cryostat in actual working. In order to lower the temperature of the bath, the tap t_1 is opened to the atmosphere, and the mercury level is adjusted so that it just makes contact with e_1. The air pump is now in action, and the bath cools slowly, and the air thermometer takes up the temperature of the bath without appreciable time-lag. Since the air of the thermometer is in communication with the atmosphere, the mercury levels are not altered.

When the bath has cooled down to the required temperature, the tap t_1 is closed. If there is any further cooling, the air in the thermometer will contract, and break the contact at e_1, and close the circuit of the heating coil. The air then expands and pushes the mercury to contact with e_1, thus closing the cooling circuit. In practice the two processes alternate in rapid succession all the time, and the temperature of the bath remains steady to within 0·1° C.

In order to raise the temperature of the bath, t_1 is opened and the mercury level lowered so as to cut off contact with e_1. When the temperature has risen to the desired value, the mercury level is adjusted so as to be just in contact with e_1, and t_1 is closed again.

The thermostat is very economical in its working; about 2 l. of liquid air are sufficient for a complete series of measurements from room temperature to −140° C and back, extending over about 8 hrs.

Measurement of temperature. The temperature measurements in the crystal chamber are made with a copper-constantan thermocouple enclosed in a Pyrex tube, and inserted into the crystal chamber of copper through a suitable airtight copper-glass seal at the bottom of the chamber. The other junction of the thermocouple is kept immersed in a mixture of pure ice and distilled water kept in the Dewar flask D_3. The thermocouple, before insertion in the apparatus, is calibrated at the following temperatures: (1) the temperature of liquid oxygen boiling at atmospheric pressure, namely

$$-183°{\cdot}0\,\mathrm{C}+(p-760)\times 0{\cdot}0126°\,\mathrm{C},$$

where p is the atmospheric pressure in mm. of mercury (the liquid usually contains a little dissolved nitrogen, which slightly lowers the boiling-point; but as the liquid evaporates the nitrogen is progressively removed, and the temperature reaches a steady value, which is the temperature of boiling pure oxygen); (2) the temperature of a mixture of solid carbon dioxide and ethyl ether, namely, −78°·64 C; (3) the tempera-

ture of the room, measured with a calibrated mercury thermometer; and (4) that of steam at about 100° C: the other end of the thermocouple is kept in melting ice all the time. A four-constant formula of the type $E = at+bt^2+ct^3+dt^4$, in which E is the observed potential difference between the two ends of the thermocouple and t is the temperature in ° C of the measuring end, is used for calculating the temperatures.

In the actual experiments a pentane thermometer, previously calibrated with the thermocouple, and immersed deeply in the cryostatic bath, serves to indicate directly the *approximate* temperatures.

Modification of the cryostat for the temperature of boiling oxygen. Below about −140° C the petroleum ether becomes very viscous, and therefore unsuitable for the bath. The only temperature lower than this at which measurements were made was that of oxygen boiling at atmospheric pressure. The cryostatic arrangement for this temperature is naturally simple. The petroleum ether is removed and liquid oxygen in sufficient quantity is directly introduced into the Dewar vessel D_1 and allowed to evaporate at atmospheric pressure. The arrangement for thermostatic control is cut off.

In some of the measurements, we used in the above arrangement, in place of liquid oxygen, a mixture of solid carbon dioxide and ethyl ether, which gives a constant temperature of −78°·6 C.

3. Measurements on magnetic anisotropy

Crystal suspension. The crystal K is suspended in a separate chamber formed by a long thin-walled cylindrical copper tube, of large diameter, closed at the lower end, and immersed in the cryostatic bath as deeply as possible. The copper tube is attached at the upper end to a long glass tube T, which rests on a cup-shaped collar L attached to the copper tube; the junction is sealed airtight with soft wax. The glass tube carries at its upper end a graduated torsion-head, $T.H.$, which is attached to the tube by a piece of large diameter rubber tubing R_2. The axis of the torsion-head is horizontal, and its scale vertical, so that the scale can be read conveniently. The axis of the torsion-head is coupled to the vertical torsion-pin, from which the crystal is suspended, by means of a cross-pinion p_2 having no backlash, so cut that the angle of rotation of the torsion-pin about the vertical axis is accurately the same as that of the pointer on the torsion-head about the horizontal axis.

The crystal is suspended, with any desired direction vertical, from the end of the torsion-pin. The suspension fibre consists of two parts. The upper part is a very thin quartz fibre whose torsional constant has been determined previously. The lower part is a glass fibre which is sufficiently stout, relatively to the quartz fibre, to be regarded as rigid. To the lower end of this glass fibre is attached the crystal, and it lies in the centre of the homogeneous, horizontal magnetic field obtaining between the large flat pole-pieces of the electromagnet. The whole length of the quartz fibre is sufficiently above the cryostat to remain always at room temperature, and its torsional constant

thus remains independent of the temperature of the cryostat.* A small horizontal glass fibre, attached centrally to the glass suspension near its upper end, serves as a pointer for observing the rotatory movements of the crystal.

Measurements on magnetic anisotropy. The experimental method adopted by us for measuring the magnetic anisotropy is essentially the same as that used in our previous measurements at room temperature. For any given suspension of the crystal, the anisotropy $\Delta\chi$ in the horizontal plane is determined by finding the critical angle by which the torsion-head has to be rotated from its normal position (corresponding to zero torsion of the fibre when the crystal has taken up its equilibrium orientation in the magnetic field), in order to bring the crystal just to its unstable orientation in the field. For the details of the method the reader may be referred to Part III of this paper, pp. 268–9. In calculating $\Delta\chi$ from the observed critical angle α_c, we used in Part III the simple, but approximate, formula

$$\lambda = \alpha_c - \pi/4, \tag{1}$$

where λ stands for $\Delta\chi mH^2/(2Mc)$. Under the usual conditions of measurement of anisotropy, in which α_c is large, usually several rotations, this formula is a sufficiently good approximation.†

In the present measurements, which concern the variation of $\Delta\chi$ with temperature, $\Delta\chi$ is found to increase in some crystals more than 10 times as we pass from room temperature to that of liquid oxygen; and λ naturally increases in the same ratio. Hence, in order to avoid inconveniently large values of α_c at low temperatures, its value at room temperature has to be kept moderate. In this case the simple relation $\lambda = \alpha_c - \pi/4$ is not sufficiently accurate, and we have to use in its place the more rigorous relation

$$\lambda = (\alpha_c - \pi/4 - \sigma)/\cos 2\sigma, \tag{2}$$

where

$$\sin 2\sigma = 1/(2\lambda) \tag{3}$$

and λ stands for $\Delta\chi mH^2/(2Mc)$, as before.

When the crystal just reaches its unstable orientation in the field, the direction of the largest susceptibility in the horizontal plane will make an angle of $\pi/4+\sigma$ with the direction of the field, and as will be seen from (2) and (3), if α_c is not large, σ may be considerable.

4. The magnetic anisotropy of paramagnetic ions in the S-state in crystals: inverse T^2 law

We shall first consider the special class of crystals whose paramagnetic ions are all in the S-state; their magnetic moments are due wholly to the spin moments of their electrons. Since the spin moments are affected little by the crystalline electric fields—

* Some recent measurements by Mr W. J. John on the torsional constants of quartz fibres at different temperatures show that the temperature coefficient of torsion is very small.

† When $\alpha_c = 2$ rotations ($=4\pi$) the error involved in using the approximate formula (1) instead of (2) is 0·1%, and even when α_c is only one rotation, the error is less than ½%.

in other words since the splitting, in the Stark manner, of the S-levels of the paramagnetic ions under these fields is very narrow—the theory predicts a simple magnetic behaviour for these crystals; particularly when, as in the substances that we are studying, the concentration of the paramagnetic ions is not large. At any given temperature T, the principal susceptibilities of the crystal conform to the simple formulae (Van Vleck and Penney 1934)

$$\chi_i = \frac{C}{T}\left(1+\frac{\Theta_i}{T}\right), \quad i = 1, 2, 3, \tag{4}$$

where the Θ's are small temperatures, of the order of 0·1° K, which are determined by the magnitude and the asymmetry of the crystalline fields acting on the paramagnetic ions, and satisfy the relation

$$\Theta_1+\Theta_2+\Theta_3 = 0. \tag{5}*$$

For this class of crystals we should therefore expect the following simple results:

(1) From equations (4) and (5)

$$\chi = (\chi_1+\chi_2+\chi_3)/3 = C/T. \tag{6}$$

i.e. the mean susceptibility of the crystal should conform closely to the Curie law. This result has been verified experimentally by Jackson, de Haas and others, for manganous, ferric and gadolinium salts.

(2) The anisotropy of the crystal is given by

$$\Delta\chi/\chi = \Delta\Theta/T, \tag{7}$$

and should therefore be very feeble. This result also is verified experimentally for both manganous and ferric salts. (Salts of gadolinium will be considered in the next section.) To be more precise, from measurements on the mean susceptibility χ and the anisotropies $\chi_1-\chi_2$ and $\chi_1-\chi_3$ at any one temperature, say at room temperature, we can easily calculate, with the help of relations (4) and (6), the Θ's. For manganous salts, as we showed in Part IV, the Θ's so obtained have nearly the same magnitude as that deduced from the observations of Kürti and Simon on the lowering of the temperature of the crystals when they are demagnetized adiabatically at very low temperatures.

(3) There is another feature of the anisotropy of these salts, which we shall consider here in some detail. It is clear from equation (7) that for given asymmetric fields acting on the paramagnetic ions, the crystal anisotropies $\Delta\chi$ should be proportional to χ/T, i.e. to the inverse square of the temperature. Now the coefficients of thermal expansion of the crystals being small, the distributions of the negatively charged atoms immediately surrounding the paramagnetic ions in the crystals will remain practically unaffected by temperature, and hence also the electric fields acting on the ions. The temperature variation of $\Delta\chi$ for these crystals should therefore conform to the inverse T^2 law.

* The Θ's being small compared to T at all ordinary temperatures, it is readily seen that equation (4) reduce to the familiar equations $\chi_i = C/(T-\Theta_i)$ of the classical Weiss theory.

With the experimental arrangement described in the previous section we have measured the magnetic anisotropy of the monoclinic crystal $MnSO_4 . (NH_4)_2SO_4 . 6H_2O$ at different temperatures. In our previous measurements on this crystal, which were made at room temperature, we used the crystal in its natural form. The distribution of induced magnetism (of the Poisson type) on the surface of the crystal will be asymmetric, and since the magnetic fields used are not ideally homogeneous, there may be a small disturbing couple tending to rotate the crystal. In order to eliminate it the crystal was kept surrounded by a liquid of the same volume susceptibility as the crystal. Since it is not convenient to use this technique at low temperatures, the crystals are used in the present measurements in the form of cylinders cut with their axes along different known directions in the crystal, and suspended in the horizontal magnetic field with the cylinder axes vertical.

The results of the magnetic measurements on the crystal are given in Table I. The crystal is monoclinic, having the axial elements $a:b:c = 0{\cdot}740:1:0{\cdot}493$; $\beta = 106° 51'$. χ_1 and χ_2 are the two principal susceptibilities in the (010) plane, and χ_3 is that along the "b" axis. They refer to one gram molecule, and are expressed in the usual unit, 10^{-6} c.g.s. e.m.u. ψ denotes the angle which the χ_1-axis makes with the "c" axis of the crystal, the positive direction of ψ being defined by the condition that the χ_1-axis makes with "a" the angle $\beta-\psi$, where β is the obtuse angle between the "c" and the "a" axes.

TABLE I

		$\Delta\chi$		
Mode of suspension	Orientation in the magnetic field	303° K	194°·5 K	90° K
"b" axis vertical	$\psi = -16°$ at all the three temperatures	8·7	21	93
"a" axis vertical	"b" axis normal to the field	3·4	6·7	21

From these data we obtain the following values for the anisotropy.

TABLE II

Temp. ° K	$\chi_1-\chi_2$	$\chi_1-\chi_3$	ψ
303	8·7	6·0	−16°
194·5	21	13	−16°
90	93	49	−16°

That ψ has the same value at all the three temperatures justifies our assumption that the crystal fields remain practically unaffected by changes in temperature.

The values of $\chi_1-\chi_2$ and $\chi_1-\chi_3$ entered in Table II, particularly those at room temperature, require correction for the anisotropy of the diamagnetism of the crystal. To a first approximation the latter anisotropy may be taken to be the same as that of the diamagnetic crystal $MgSO_4 . (NH_4)_2SO_4 . 6H_2O$, or $ZnSO_4 . (NH_4)_2SO_4 . 6H_2O$, which is isomorphous with the manganese salt. The corrections for $\chi_1-\chi_2$ and $\chi_1-\chi_3$ will then be 1·0 and 0·6 respectively (see Part IV), to be subtracted from the values given in Table II.

The corrected values of $\chi_1-\chi_2$ at the three temperatures bear the ratios

$$7{\cdot}7 : 20 : 92 = 1 : 2{\cdot}6 : 11{\cdot}9,$$

and those of $\chi_1-\chi_3$ the ratios

$$5{\cdot}4 : 12{\cdot}4 : 48{\cdot}4 = 1 : 2{\cdot}3 : 9{\cdot}0.$$

With these may be compared the ratios of the inverse squares of the temperatures,

$$1 : 2{\cdot}4 : 11{\cdot}3.$$

In view of the low values of the anisotropies at room temperature and their consequent sensitiveness to the diamagnetic correction, which is not known with certainty, the agreement between the experimental and the inverse T^2 ratios may be regarded as satisfactory.

5. The magnetic anisotropy of $Gd_2(SO_4)_3.8H_2O$

The Gd^{+++} ion is in the S-state (^8S) and has a large magnetic moment. Its salts are therefore very suitable for use as working material in demagnetization experiments at very low temperatures, and were used in the classic experiments of Giauque. The magnetic and the thermal properties of these salts have been studied extensively at these temperatures. It would be of interest to study their magnetic anisotropies also, which naturally should be expected to be very feeble.

Through the kindness of Professor Giauque we were able to obtain some good crystals of the octahydrated sulphate, $Gd_2(SO_4)_3.8H_2O$. The crystal is monoclinic, having the axial elements $a : b : c = 3{\cdot}009 : 1 : 2{\cdot}007$, $\beta = 118°\,2'$. The results of our magnetic measurements on the crystals, used in the form of suitably cut cylinders, are given in Tables III and IV; they refer to a gram molecule having the formula $Gd_2(SO_4)_3.8H_2O$, i.e. to a mass of the crystal containing two gram ions of Gd^{+++}.

Table III

Mode of suspension	Orientation in the magnetic field	$\Delta\chi$ 303° K	$\Delta\chi$ 194°·5 K	$\Delta\chi$ 90° K
"b" axis vertical	$\psi = +15\frac{1}{2}°$ at all the three temperatures	750	1960	8100
(001) plane horizontal	"b" axis along the field	710	1640	5840

Table IV

Temp ° K	$\chi_1-\chi_2$	$\chi_3-\chi_2$	ψ
303	750	745	$+15\frac{1}{2}°$
194·5	1960	1730	$+15\frac{1}{2}°$
90	8100	6220	$+15\frac{1}{2}°$

Considering first the room temperature values, we find that the crystal, though monoclinic, is nearly uniaxial magnetically, the axis of magnetic symmetry being along the χ_2-axis, i.e. along a direction in the (010) plane which makes with the "a" and the "c" axes angles of $12\frac{1}{2}°$ and $105\frac{1}{2}°$ respectively.

Measurements on the mean susceptibility of the crystal at room temperature gave

$$\chi = (\chi_1+\chi_2+\chi_3)/3 = 52{,}300 \text{ at } 30° \text{ C},$$

which corresponds to a magnetic moment of 8·00 Bohr magnetons for the Gd^{+++} ion, as compared with the theoretical value of 7·94 for the ^8S-state. Comparing with this value the data given in Table IV, we find that at room temperature the anisotropy of the crystal, namely $\chi_1-\chi_2$ or $\chi_3-\chi_2$, is only 1·4 % of the mean susceptibility.

According to the data supplied by Professor Giauque the specimen of gadolinium from which the salt was prepared contained as impurity 0·5 % samarium and 1 % terbium. Because of the low susceptibility of the Sm^{+++} ion, its presence will not contribute appreciably to the observed anisotropy. The effect of the terbium impurity cannot be calculated exactly at present, since no measurements have been made on the anisotropy of terbium salts. We can, however, fix an upper limit to its contribution, and conclude that for the octahydrated sulphate of gadolinium at 30° C

$$(\chi_1-\chi_2)/\chi = (\chi_3-\chi_2)/\chi = 0{\cdot}014 \pm 0{\cdot}003.$$

From these values for the anisotropy and the relations (4) and (6), we obtain

$$\Theta_1 = \Theta_3 = -\tfrac{1}{2}\Theta_2 = (1{\cdot}4 \pm 0{\cdot}3)° \text{K}.$$

We shall presently show that these values for the Θ's, though small, are yet considerably higher than what we should expect from the known temperature variation of the entropy of the salt at very low temperatures.

Assuming a cubic symmetry for the crystalline fields acting on the Gd^{+++} ions in the crystal and denoting by δ the *over-all* Stark separation of the ^8S-levels of Gd^{+++} under these fields, Hebb and Purcell (1937) find that the value

$$\delta = 0{\cdot}98 \text{ cm.}^{-1} = 1{\cdot}4° \text{ K}$$

fits well with the experimental entropy-temperature curve over the whole of the available range, namely 0·25° to 1·5° K. But actually, judging from the large observed magnetic anisotropy of the octahydrated sulphates of the other rare earths, which are isomorphous with $Gd_2(SO_4)_3.8H_2O$, the crystalline fields acting on the Gd^{+++} ions should deviate considerably from cubic symmetry. Nevertheless the over-all Stark separation δ, under these asymmetric fields, which would fit the experimental entropy-temperature data, should be of the above order of magnitude.

Now we should expect the Θ's, which define the asymmetry of the crystalline fields, to be considerably smaller than the over-all separation δ. For the following reason the

observed Θ's may be still smaller. Since the unit cell of the crystal contains more than one Gd^{+++} ion (probably eight), and since the principal axes of the crystalline fields acting on these different Gd^{+++} ions may not be parallel to one another, the observed anisotropy of the crystal, and hence the Θ's deduced therefrom, may be smaller than would correspond to the actual asymmetry of the fields acting on the Gd^{+++} ions.

But actually the Θ's for the crystal are of nearly the same magnitude as δ, i.e. the Θ's are much larger than we should expect from the thermal properties of the crystal at low temperatures. This result suggests that much of the observed anisotropy of the crystal must arise from causes other than the splitting of the S-levels by the crystalline electric fields. If the Gd^{+++} ions in the crystal are not sufficiently widely separated, and if their arrangement in the crystal lattice does not conform to cubic symmetry, then the crystal may exhibit an anisotropy in the magnetic field; and at the same time, *in the absence of the applied magnetic field*, the internal *magnetic* fields acting on the Gd^{+++} ions due to the neighbouring Gd^{+++} ions, i.e. the local magnetic fields of the Onsager type, may be so small that the resulting separation of the S-levels, and the contribution to the entropy in the absence of the external magnetic field, may be very little.*

At present we have not enough information regarding the positions of the Gd^{+++} ions in the unit cell which would enable us to estimate the anisotropy that may arise in the above manner, i.e. from the mutual interaction of the magnetic moments. If the large observed anisotropy is really due to this cause, we should expect it to diminish rapidly as the crystal is diluted magnetically, in contrast with the behaviour of the manganous salts which we have studied previously (Part IV), in which the effect of magnetic dilution on the anisotropy is not large. We are trying to grow mixed crystals of gadolinium sulphate with yttrium sulphate, which is diamagnetic, in order to verify this result.

Whether the anisotropy is due to the splitting of the S-levels of Gd^{+++} under the asymmetric electric fields of the neighbouring negative charges, or under the asymmetric magnetic fields of the neighbouring Gd^{+++} ions, in either case it should vary approximately as the inverse square of the temperature. This is actually so, as will be seen from the data given in Table IV. The values of $\chi_1-\chi_2$ at the three temperatures bear the ratios $750 : 1960 : 8100 = 1 : 2{\cdot}6 : 10{\cdot}8$, and those of $\chi_3-\chi_2$ the ratios $745 : 1730 : 6220 = 1 : 2{\cdot}3 : 8{\cdot}4$, as compared with the ratios of the inverse squares of the temperatures, $1 : 2{\cdot}4 : 11{\cdot}3$.

* Professor Giauque has kindly informed us that demagnetization experiments on gadolinium salts at low temperatures also suggest a large magnetic interaction. The exchange interactions between the spins of the neighbouring Gd^{+++} ions, which fall off exponentially with their separation, in contrast with the magnetic interactions which vary as the inverse cube of the separation, will be small in the hydrated crystals. Even if it is not small, it will not produce an anisotropy.

6. The influence of the orbital angular momenta of paramagnetic ions on their magnetic behaviour in crystals

It is well known that in many of the salts of the iron group the "effective" magnetic moment of the paramagnetic ion conforms closely to the spin-only value. The inference sometimes drawn from this observation that the orbital angular momentum of the paramagnetic ion plays an insignificant part in determining its magnetic behaviour is, however, incorrect. It is true that the orbital angular momentum is more or less completely quenched by the crystalline electric fields, and is not therefore capable of orienting in the applied magnetic field and thus contributing directly to the magnetic moment developed in the crystal; and that practically the whole of this moment is contributed by the spin momentum of the paramagnetic ion. But *indirectly* the frozen orbital momentum, by virtue of its coupling with the spin momentum, can exercise a large orienting couple on the latter, and thus influence the magnetization. The older way of regarding these local orienting couples acting on the spins as arising from certain internal magnetic fields, whose origin was not properly understood, but which were presumed to be of the same nature as the local fields in ferromagnetics, is in a large measure responsible for the insignificant part assigned to the orbital momentum in determining the magnetic behaviour of the crystal. It is now well established that the local couples tending to orient the spin momentum are ultimately due to the internal electric fields in the crystal, which are generally strong and asymmetric. The spin momentum is not directly affected by these fields to any appreciable extent, but indirectly it is, as we mentioned just now, owing to its coupling with the orbital momentum, which is easily affected. The magnetic anisotropy of the crystal, and the deviations from the simple Curie law, of the temperature variation of its principal susceptibilities, are the results of this indirect influence exercised by the asymmetric crystalline fields on the spin momentum through the spin-orbit coupling. Both these effects, viz. the anisotropy and the deviations from the Curie law, should therefore be the greater the stronger the spin-orbit coupling; and conversely, from observations on the principal susceptibilities of the crystal or its anisotropy at different temperatures, it should be possible to calculate the strength of the spin-orbit coupling.

7. The coupling between the orbital and the spin angular momenta in Ni^{++} evaluated from magnetic measurements

The theoretical expressions necessary for such a calculation come out simple for nickel salts, and have been worked out by Schlapp and Penney (1932). For any given plane in the crystal the anisotropy $\Delta\chi$, i.e. the difference between the maximum and the minimum susceptibilities in the plane, per gram molecule, is given by the relation

$$\Delta\chi = \frac{8N\beta^2}{3kT}\left(8\lambda - \frac{2\lambda^2}{kT} - 3kT\right)\Delta\alpha, \qquad (8)$$

where λ is the constant of spin-orbit coupling, $\beta = eh/(4\pi mc)$ is the Bohr magneton, N is the Avogadro number, and k is the Boltzmann constant. $\Delta\alpha$ is a constant which depends on the crystalline electric fields acting on the paramagnetic ions in the unit cell of the crystal, and on the inclination of the selected plane to the principal axes of these crystal fields. At present we have not enough knowledge of these fields to be able to calculate $\Delta\alpha$ directly. We may, however, assume as before that these fields, and therefore $\Delta\alpha$ also, will be practically independent of temperature. By comparing the values of $\Delta\chi$ at any two convenient temperatures we can then eliminate $\Delta\alpha$ and calculate the constant of spin-orbit coupling λ.

For this purpose measurements at the temperature of the room and that of liquid oxygen, which are the two extreme temperatures in our experiments, would be very suitable. We have made such measurements with the hexahydrated selenate and sulphate of nickel, $NiSeO_4 . 6H_2O$ and $NiSO_4 . 6H_2O$, which are both tetragonal, and the results are given in Table V. ρ denotes the ratio of the anisotropy at $-183°{\cdot}0$ C to that at $21°{\cdot}0$ C.

TABLE V

Crystal	ρ	λ
$NiSeO_4 . 6H_2O$	4·76	-330 cm.$^{-1}$
$NiSO_4 . 6H_2O$	$4{\cdot}8_1$	-340 cm.$^{-1}$

In obtaining the ratios ρ we made the room temperature measurements both before and after the low temperature measurements. While for the selenate the ratio obtained was independent of the order of the measurement, for the sulphate the value obtained by making the room temperature measurement first, and then the low temperature measurement, was considerably lower than that obtained by making the measurements in the reverse order. This result was found to be due to an appreciable dehydration of the sulphate at the low temperature, and the formation of a thin whitish crust of the dehydrated micro-crystals on the surface. The value $4{\cdot}8_1$ given above is that obtained by making the low temperature measurement first, since this will approximate more closely to the real value than the one obtained from measurements made in the reverse order.

For this reason the value of λ obtained for the sulphate is not entitled to the same weight as that obtained for the selenate, and we may adopt the latter value, namely

$$\lambda = -330\,\text{cm.}^{-1},$$

as the result of our magnetic measurements.

Spectroscopically, the Ni^{++} ion is in the $^3F_4$ state, and the over-all multiplet width, according to Laporte (1928), is 2347 cm.$^{-1}$. From this we obtain, using the relation $\lambda S(2L+1) = 2347$ cm.$^{-1}$, $\lambda = -335$ cm.$^{-1}$. It is gratifying that the value deduced from the magnetic data agrees well with this value.

8. Temperature variation of the magnetic anisotropy of nickel salts

We have also made measurements of the anisotropy of these two nickel salts at several intermediate temperatures, and the results are given in Tables VI and VII. ρ denotes the ratio of the anisotropy at the given temperature T to that at $21°{\cdot}0$ C. The theoretical values of ρ, calculated from equation (8) using for λ the value -330 cm.$^{-1}$, are also given in the tables for comparison with the experimental values.

The measurements on the sulphate were made with increasing temperatures, beginning at about $-130°$ C, and care was taken not to keep the crystal unduly long at temperatures below $-80°$ C, where dehydration is appreciable. For the selenate it was immaterial whether the measurements were made with increasing or with decreasing temperatures.

TABLE VI. $NiSeO_4 . 6H_2O$

Temp. ° K	ρ Obs.	ρ Calc.
294·1	(1·000)	(1·000)
270·9	1·096	1·096
268·4	1·110	1·108
251·2	1·192	1·195
248·6	1·207	1·209
240·0	1·261	1·261
231·0	1·321	1·319
221·6	1·389	1·387
212·0	1·462	1·464
207·8	1·494	1·500
203·4	1·544	1·540
190·3	1·673	1·674
175·3	1·863	1·860
171·0	1·917	1·921
168·5	1·955	1·958
164·0	2·023	2·029
148·8	2·309	2·310
147·2	2·345	2·345
145·0	2·389	2·392

TABLE VII. $NiSO_4 . 6H_2O$

Temp. ° K	ρ Obs.	ρ Calc.
294·1	(1·000)	(1·000)
272·7	1·090	1·087
251·9	1·190	1·191
232·7	1·307	1·308
230·5	1·323	1·323
225·5	1·364	1·358
210·2	1·477	1·479
191·0	1·667	1·666
170·8	1·925	1·924
151·0	2·262	2·265
146·7	2·355	2·355

As will be seen from the tables, the agreement between the experimental and the theoretical values of ρ is very satisfactory, and may be taken as a quantitative verification of Schlapp and Penney's theory.

Regarding the absolute values of the anisotropy, we may mention that at 21° C $\chi_\perp - \chi_\parallel$ is about 92 for the selenate and 112 for the sulphate. These anisotropies should be regarded as very feeble, since they are less than 3 % of the mean susceptibilities of the crystals at this temperature. They give for $\Delta\alpha$ reasonable magnitudes, as we showed in Part V.

We may further mention here that measurements on the temperature variation of

the principal susceptibilities can also serve for the verification of the theory. The principal susceptibilities are given by

$$\chi_1 = \frac{8N\beta^2}{3kT}(1+8\lambda\alpha_1+\theta_1/kT)-8N\beta^2\alpha_1, \tag{9}$$

where

$$\theta_1 = 2\lambda^2(\alpha_2+\alpha_3-2\alpha_1)/3, \tag{10}$$

and two similar expressions. The α's are determined by the crystalline fields and the inclinations to one another of the field axes associated separately with the different Ni^{++} ions in the unit cell of the crystal. Like $\Delta\alpha$, the α's also will be practically independent of temperature.

Experimentally, however, the temperature variations of the principal susceptibilities are more difficult to measure accurately than the temperature variations of the anisotropies. Moreover, in the expressions for the principal susceptibilities, namely equation (9), the predominant term is independent of λ and α, unlike the predominant term in the expression for $\Delta\chi$.

9. The feeble anisotropy of chromic salts

The chromic salts also lend themselves to a simple discussion on the basis of the theory of Schlapp and Penney. The ground state of the Cr^{+++} ion is an F state, as in Ni^{++}, but with a spin moment of 3/2 instead of the moment 1 in Ni^{++}. The over-all multiplet width of Cr^{+++}, according to Laporte, is 912 $cm.^{-1}$, from which we obtain for the constant of spin-orbit coupling $\lambda = +87\ cm.^{-1}$. This is numerically only a fourth of the value for Ni^{++}. In the expression for the anisotropy of a chromic salt, analogous to (8) for a nickel salt, the λ^2 term will therefore be negligible; moreover, the other two terms, which will be of comparable magnitudes, will have opposite signs. The anisotropy should therefore be much smaller than that of nickel salts, and when we remember that even for the latter salts it is only 2–3 % of the mean susceptibility, for the chromic salts it should be very small indeed.

We have measured the anisotropy of one such salt, namely ammonium chromium oxalate, $(NH_4)_3Cr(C_2O_4)_3.3H_2O$, and the results are given below. The crystal is monoclinic prismatic; $a:b:c = 0{\cdot}983:1:0{\cdot}387$; $\beta = 95°\,18'$. At 30° C:

$$\chi_1-\chi_2 = \quad 4{\cdot}3,$$
$$\chi_1-\chi_3 = -10{\cdot}3,$$
$$|\psi| = \quad 29°,$$
$$\chi = (\chi_1+\chi_2+\chi_3)/3 = 5440.$$

The maximum anisotropy, namely $\chi_3-\chi_2 = 14{\cdot}6$, is only $\frac{1}{4}$ % of the mean susceptibility. This is not much higher than the anisotropy which might be expected even from

the direct influence of the crystalline fields on the spins, as distinguished from the influence exerted on them indirectly through the spin-orbit coupling, which we have considered here. The low anisotropy predicted by the theory is thus verified.

In fact the observed anisotropy of the crystal is of the same order of magnitude as its diamagnetic anisotropy, as will be clear from the following data for the anisotropy of the diamagnetic crystal $K_3Al(C_2O_4)_3.3H_2O$, which is isomorphous with the above chromic salt (see Part IV of this paper, p. 351):

$$\chi_1-\chi_2 = \quad 6{\cdot}9,$$
$$\chi_1-\chi_3 = \quad 13{\cdot}1,$$
$$\psi = +19°.$$

The low anisotropy of the salts of trivalent chromium—nearly as low as if the Cr^{+++} ion were in the S-state, instead of in ^4F—is very significant, and explains the suitability of these salts as working material for the production of low temperatures by the Debye-Giauque method.

The close conformity of the mean susceptibility of crystal to the spin-only value is generally taken as a criterion for judging its suitability for this purpose. This is not, however, a reliable test, since it only ensures the efficient quenching of the orbital momenta, and the consequent inability of the latter to contribute directly to the effective magnetic moment of the ion. Indirectly, as we remarked in the previous section, the orbital momenta, by virtue of their coupling with the spins, can appreciably hamper the freedom of rotation of the latter. On the other hand, a very feeble anisotropy for the crystal (except of course when it is due to a cubic or a pseudo-cubic symmetry in the structure of the crystal or in the crystal field) is a more reliable and sensitive test for the freedom of rotation of the spin-moments, and hence of the suitability of the crystal for the production of low temperatures by demagnetization.

Coming back to ammonium chromic oxalate, we have also studied the temperature variation of its anisotropy for two suspensions of the crystal. With the "b" axis vertical, we find firstly that the value of ψ changes by about 78° as the temperature is lowered from 30° to −183° C, and the value of $\chi_1-\chi_2$ increases 1·9 times. The large variation in ψ and the small increase in $\chi_1-\chi_2$ are both to be expected, since the diamagnetic part of the anisotropy, which is a large part, will be independent of temperature, and the values of ψ will not be the same for the diamagnetic and the paramagnetic parts.

With the "c" axis vertical, the anisotropy in the horizontal plane increases about 12 times as we pass from room temperature (30° C) to that of liquid oxygen.

Before closing this section we should mention that the mean susceptibility of 5440 at 30° C observed for the crystal, or 5660 after correcting for its diamagnetism, gives for the magnetic moment of Cr^{+++} 3·72 Bohr magnetons, as compared with the spin-only value of 3·87. Now, theoretically, the effective moment of Cr^{+++} in the crystal should bear to the spin-only moment approximately the ratio $1-2\lambda/(5Dq)$, where Dq

is the constant of the cubic part of the crystalline field, which would be the predominant part. The above experimental value for the magnetic moment of Cr^{+++} corresponds to $Dq \doteqdot 900\,cm.^{-1}$, which is of reasonable magnitude.

10. The Curie-Weiss law and the temperature variation of magnetic anisotropy

As we mentioned in a previous section the crystalline electric fields acting on the paramagnetic ions may be regarded as producing an orienting couple on the magnetic dipoles, and to this extent they will simulate a local magnetic field. But there is this essential difference between the inner magnetic field of the Weiss theory and this field, namely that, in general, the latter field will not be proportional to the intensity of magnetization. The Weiss law of temperature variation, $\chi = C/(T-\Theta)$, has not therefore much significance on the new theory.

Experimentally also, the validity of the Weiss law is very limited. In order to realize this properly one has to remember that the so-called "cryomagnetic anomalies", which occur at low temperatures, are really deviations from the Weiss law, and it is only at low temperatures that the conditions are suitable for a proper test of the law. Even at ordinary temperatures, where the test is not stringent, deviations from the law are not uncommon, and in particular if we follow the temperature variations of the three principal susceptibilities of the crystal separately, instead of the variation of their mean value, the deviations from the Weiss law,

$$\chi_i = C/(T-\Theta_i), \quad i = 1, 2, 3, \tag{11}$$

where the Curie constant C should be the same for all the three principal directions, while the Θ's may be different, become more conspicuous. On the new theory, on the other hand, these deviations are not only to be expected but receive a natural explanation.

But the most striking success of the new theory is in explaining the anisotropy and its variation with temperature. We shall consider here one particular feature of the temperature variation of anisotropy. Whereas according to (11), at all ordinary temperatures, the anisotropy $\Delta\chi$ should increase with fall of temperature, on the new theory the temperature variation of $\Delta\chi$ is not so simple. Since the energy levels of the paramagnetic ions have already separated under the influence of the crystalline fields, and the lower levels may not always correspond to larger magnetic moments, the anisotropy $\Delta\chi$ may, under suitable conditions, even decrease with fall of temperature. If the natural multiplet width of the free ion is not large, then also we may expect similar results.

This is well illustrated by the ethylsulphates of praseodymium and samarium; as the temperature is continually lowered their anisotropies first increase, pass through a maximum and then diminish.

11. Ethylsulphates of praseodymium and samarium

The magnetic anisotropies of some of the rare earth ethylsulphates, having the formula $M_2(C_2H_5SO_4)_6 \cdot 18H_2O$, have been studied by Fereday and Wiersma (1935) over a wide range of temperatures. (The crystals are hexagonal, and we shall denote their susceptibilities along the hexagonal axes, and perpendicular to the hexagonal axes by $\chi_\parallel$ and $\chi_\perp$ respectively, per gram molecule—containing two gram ions of M^{+++}.) Among them, the ethylsulphate of praseodymium is of special interest. At liquid hydrogen temperatures its anisotropy $\chi_\parallel - \chi_\perp$ has a large negative value, about $-36{,}900$ at $14°{\cdot}44$ K, and as the temperature is raised the value increases (algebraically) rapidly, reaching -3610 at $77°{\cdot}8$, -19 at $137°$, 370 at $167°{\cdot}6$ and 318 at $290°$. The anisotropy, besides changing sign, thus passes through a maximum, in contrast with the behaviour of the other ethylsulphates studied by them, for which $\chi_\parallel - \chi_\perp$ is always positive and decreases continually with increase of temperature.

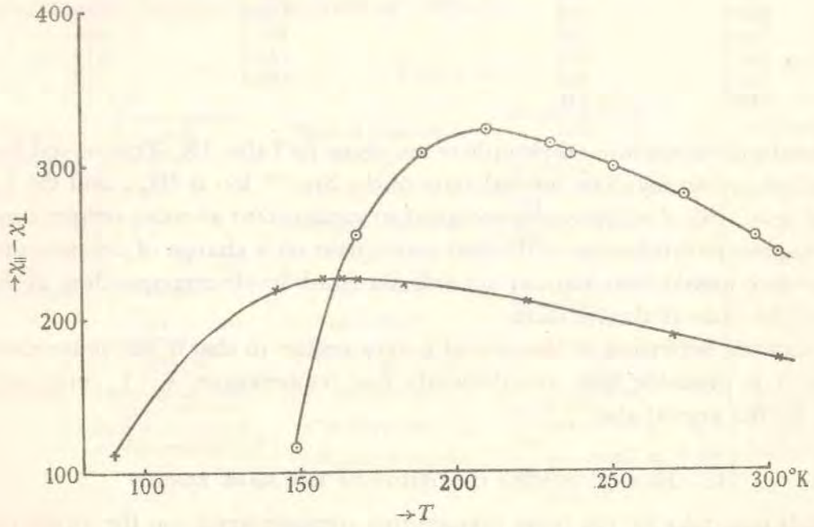

Fig. 2. The circles refer to praseodymium ethylsulphate and the crosses to samarium ethylsulphate.

We had made some low temperature measurements on this crystal. Though our temperature range is much smaller, it includes the region on either side of the maximum of anisotropy, and since only two of the observations of Fereday and Wiersma lie in this region, our detailed measurements in this region may be of some interest. The results are given in Table VIII, and they are plotted in Fig. 2.

Now the normal state of the Pr^{+++} ion is $^3H_4$, and in the Stark pattern produced by the crystalline fields the lowest level is a singlet, which corresponds to a smaller magnetic moment than the higher levels. As the temperature falls, and the population in the

ground level increases, the effective magnetic moment of the Pr^{+++} ion naturally diminishes, and the increase in susceptibility is therefore much less than in the inverse proportion to the temperature. Now the diminution in the effective magnetic moment is much greater when the applied magnetic field is along the hexagonal axis than when it is perpendicular to it. In other words $\chi_\parallel$, which at room temperature is greater than $\chi_\perp$, increases much less slowly than $\chi_\perp$, the result being that $\chi_\parallel - \chi_\perp$ passes through a maximum and then diminishes rapidly, reaching a large negative value, as experimentally observed.

TABLE VIII. $Pr_2(C_2H_5SO_4)_6.18H_2O$

Temp. °K	$\chi_\parallel - \chi_\perp$
303·1	241
296·0	252
273·0	279
250·9	297
237·1	306
230·6	313
210·0	322
189·7	307
168·1	254
148·7	116

TABLE IX. $Sm_2(C_2H_5SO_4)_6.18H_2O$

Temp. °K	$\chi_\parallel - \chi_\perp$
303·1	172
269·4	187
223·0	210
183·3	221
168·4	226
163·4	226
157·2	226
142·2	219
90·1	112

The results for samarium ethylsulphate are given in Table IX. This crystal has not been studied previously. The normal state of the Sm^{+++} ion is $^6H_{5/2}$ and the higher multiplet level with $J = 7/2$ is also occupied to some extent at room temperature; in considering the redistribution of the ions consequent on a change of temperature, we have therefore to take into account not only the Stark levels corresponding to the 5/2 state, but also those of the 7/2 state.

The magnetic behaviour of this crystal is very similar to that of the praseodymium salt, and it is probable that at sufficiently low temperatures $\chi_\parallel - \chi_\perp$ may become negative for this crystal also.

12. HEXAHYDRATED CHLORIDES OF THE RARE EARTHS

We shall now take up the room temperature measurements, on the anisotropy of some of the chlorides of the rare earth and the iron groups.

The absorption spectra of several rare earth salts of the type $M_2(SO_4)_3.8H_2O$ and $MCl_3.6H_2O$ have been studied in detail at different temperatures, and from a preliminary analysis of the spectra it has been inferred that the electric fields acting on the rare earth ions in these crystals should be nearly cubic in symmetry. A direct result of such a cubic symmetry is that the crystals should be magnetically isotropic, even when crystallographically they do not belong to the cubic system. In the sulphates, which have been studied magnetically, this result is not verified; they exhibit a marked anisotropy (Part V) showing that, in these salts at any rate, the crystalline fields deviate considerably from cubic symmetry.

Some of the features of the absorption spectra of these crystals also point to this conclusion. If we take the absorption lines which form a close group, many of which are presumably the Stark components originating from the same line of the *free* rare earth ion, the lines are in general strongly polarized, some of them along one, and some along another, of the principal axes of the optical ellipsoid of the crystal (Krishnan and Chakrabarty 1938).

If then in the sulphates, which are octahydrated, the crystalline fields are not cubic in symmetry, there seems to be a general impression that at least in the chlorides, which are hexahydrated, they should be so (Kynch 1937). Since there are just six water molecules associated with each rare earth ion, the octahedron formed by them is presumed to be regular, with the rare earth ion in the centre, and hence the electric field acting on the latter is presumed to be cubic.

In order to test the above surmise we have measured the magnetic anisotropies of some of these chlorides, using the same methods as were adopted by us in our earlier measurements. The results are given in Table X.

TABLE X

Crystal	Crystallographic data	Mode of suspension	Orientation in the field	$\Delta\chi$	Magnetic anisotropy
$NdCl_3.6H_2O$	Monoclinic	"b" axis vertical	(100) plane at 78°·6 to the field	860	$\chi_1 - \chi_2 = 860$
		"c" axis vertical	"b" axis normal to field	230	$\chi_1 - \chi_3 = 265$
		(100) plane horizontal	"c" axis normal to field	560	$\lvert\psi\rvert = \begin{cases}78°{\cdot}6 \text{ obs.}\\ 78°{\cdot}4 \text{ cal.}\end{cases}$ Temp. = 26° C
$SmCl_3.6H_2O$	Monoclinic $a:b:c = 1{\cdot}471:1:1{\cdot}218$ $\beta = 93°\ 26'$ (Pabst 1931)	"b" axis vertical	(100) plane at 59°·1 to the field	340	$\chi_1 - \chi_2 = 340$
		"c" axis vertical	"b" axis along field	42	$\chi_1 - \chi_3 = 50$ $\lvert\psi\rvert = \begin{cases}59°{\cdot}1 \text{ obs.}\\ 58°{\cdot}9 \text{ cal.}\end{cases}$
		(100) plane horizontal	"b" axis along field	200	Temp. = 30° C
$ErCl_3.6H_2O$	Monoclinic, with nearly the same axial elements as the samarium salt	"b" axis vertical	(100) plane at 64°·1 to the field	8650	$\chi_1 - \chi_2 = 8650$
		"c" axis vertical	"b" axis normal to field	5900	$\chi_1 - \chi_3 = 7600$ $\lvert\psi\rvert = \begin{cases}64°{\cdot}1 \text{ obs.}\\ 63°{\cdot}8 \text{ cal.}\end{cases}$
		(100) plane horizontal	"b" axis normal to field	640	Temp. = 31° C

All the three crystals are monoclinic and isomorphous. In the particular specimens on which our magnetic measurements were made the side faces were not properly developed, and we were not therefore able to fix the sign of the angle ψ, i.e. to decide whether the χ_1-axis lies in the obtuse or the acute angle β between the "a" and the "c" axes.

With the "b" suspension (see Table X) both ψ and $\chi_1 - \chi_2$ are determined, and with one other suspension $\chi_1 - \chi_3$ also. We made, however, measurements with one more suspension of the crystal, so as to have a check on the results. From the measured anisotropies for the three suspensions the value of ψ is calculated, and compared with its value as measured directly with the "b" suspension. The two values agree well, as will be seen from the last column of the table.

In Table XI we give for the hydrated chlorides the values of the maximum anisotropy, i.e. the difference between the maximum and the minimum susceptibilities of the crystal. Similar values for the corresponding hydrated sulphates, taken from Part V, are also given in the table, for comparison with the chloride values.

TABLE XI. VALUES OF THE MAXIMUM ANISOTROPY

	$MCl_3.6H_2O$	$\frac{1}{2}\times M_2(SO_4)_3.8H_2O$
M=Nd	860 (26° C)	500 (30° C)
Sm	340 (30° C)	220 (30° C)
Er	8650 (31° C)	4440 (30° C)

As will be seen from the table the chlorides have much larger anisotropies per rare earth ion than the corresponding sulphates. When we remember that even in the sulphates the anisotropies are by no means small, it is easy to realize that in the chlorides also the crystalline electric fields acting on the rare earth ions should be highly asymmetric.

As we mentioned in an earlier part of this paper, the proper measure of the asymmetry of the electric field acting on the rare earth ion is not the anisotropy of the crystal as a whole, but the anisotropy of the ion in its actual surroundings of negatively charged atoms. The latter anisotropy cannot be less than that of the crystal, but may be much greater, since the unit cell of the crystal contains more than one rare earth ion,* and the principal axes of the electric fields acting on the different ions in the cell will not, in general, be parallel to one another. The asymmetry of the electric fields acting on the rare earth ions may therefore be even larger than is suggested by the observed magnetic anisotropy of the crystal.

For the same reason, namely, that the crystal anisotropy gives only a lower limit to the anisotropy of the rare earth ion, and therefore to the asymmetry of the electric field acting on it, the higher crystal anisotropies observed for the chlorides as compared with the sulphates cannot be taken to imply that the electric fields in the chlorides are necessarily more asymmetric than in the sulphates. From the values given in Table XI we can, however, definitely conclude that in both the salts the asymmetry should be large.

13. DIHYDRATED CUPRIC ALKALI CHLORIDES

We have also measured at room temperature the anisotropies of some of the double chlorides of copper with the alkali atoms, of the type $R_2CuCl_4.2H_2O$, where $R = NH_4$, K or Rb. The crystals are tetragonal, and their structures have been studied by X-ray methods by Hendricks and Dickinson (1927) and by Chrobak (1929). A detailed discussion of the structures is given in a recent paper by Chrobak (1934). Two alternative structures are proposed, between which it seems to be difficult to decide from the

* Actually eight in the sulphates (Zachariasen 1935); no data are available for the chlorides.

available X-ray data. According to the first, which is essentially that proposed by Hendricks and Dickinson, each Cu^{++} ion in the crystal is in the centre of an octahedron, formed by two oxygen atoms at the opposite corners and four chlorines, the diagonal joining the two oxygens being along the "c" axis. According to the second structure, each Cu^{++} ion in the crystal is in the centre of a cube formed by eight chlorine atoms. (The centres of two opposite faces of the cube are occupied by two oxygens, the line joining them being along the "c" axis.) Chrobak finds, after a detailed Fourier analysis, that though in the ammonium salt it is not possible to decide uniquely between the two structures, in the potassium salt the X-ray data favour the first structure.

The magnetic data for these crystals should throw some light on this question. Following Van Vleck, we may represent the potential of the electric field acting on the Cu^{++} ion by the expression

$$\Phi = D(x^4+y^4+z^4)+Ax^2+By^2-(A+B)z^2, \qquad (12)$$

where the fourth power terms refer to the cubic part of the field and the quadratic terms to the rhombic part. The first structure, which corresponds to an octahedral distribution of six negative charges around the Cu^{++} ion, will give a positive value for D, the second a negative value (Gorter 1932); and a change in the sign of D will be equivalent to an inversion of the Stark pattern. Van Vleck has shown that for a given field, i.e. for a given sign of D, the Stark pattern for Cu^{++} is inverted with respect to that of Fe^{++}. Hence the pattern for Cu^{++} with negative D will be similar to that of Fe^{++} with positive D. Now since the spin-orbit coupling in Cu^{++} ($852\,cm.^{-1}$) is much stronger than in Fe^{++} ($100\,cm.^{-1}$), we should expect the anisotropy, $\Delta\chi/\chi$, of Cu^{++} with negative D to be much greater than that of Fe^{++} with positive D; and since experimentally the anisotropies of Cu^{++} and Fe^{++} in hydrated sulphates, selenates, etc., in which D is positive, are of comparable magnitude, we may conclude that the anisotropy of Cu^{++} should be much greater in crystals with negative D than in crystals with positive D; assuming of course, as we might justifiably, that the rhombic parts of the field are of comparable magnitude in the two classes of crystals. Thus an experimental study of the anisotropy of our double chlorides to find whether the anisotropy is of the same order of magnitude as in the hydrated sulphates and selenates, or is much higher, should enable us to decide whether the crystal has the first or the second of the structures proposed.

Feytis has measured the mean susceptibilities of the ammonium and the potassium salts, and finds that for both of them $\chi = 1370$ at 17° C.

TABLE XII. MAGNETIC ANISOTROPY OF $R_2CuCl_4.2H_2O$

Crystal	$\chi_\perp - \chi_\parallel$	Temp. ° C
$R=NH_4$	260	31·0
K	268	31·5
Rb	265	31·5

On comparing these values for the hydrated double chlorides with the corresponding values for the hydrated sulphates and selenates of copper, given in Parts II and V of this paper, we find (1) that their mean susceptibilities are the same as in the latter salts; and (2) that their anisotropies also are of the same order of magnitude as in the latter salts. The magnetic data for our double chlorides are thus decisively in favour of the first structure, namely that of Hendricks and Dickinson, which gives a positive D, as against the second.

The magnetic data further show that the crystals are typical double salts, whose composition can be represented by the formula $2R\mathrm{Cl}.\mathrm{CuCl_2}.2\mathrm{H_2O}$, rather than a complex salt.

We have much pleasure in expressing our thanks to Professor W. F. Giauque for the gift of gadolinium sulphate, and to Dr S. Banerjee and Mr N. Ganguli for helping us in making some of the low temperature measurements.

14. Summary

The magnetic anisotropies of some typical salts of the rare earth and the iron groups have been measured at low temperatures down to about 90° K. A simple cryostat, with automatic temperature control, suitable for measurements of the magnetic anisotropies of crystals at low temperatures, is described. The results are discussed on the basis of the theory of paramagnetism in crystals developed by Van Vleck, Penney and Schlapp.

1. In those crystals in which the paramagnetic ions are all in the S-state, e.g. $\mathrm{Gd_2(SO_4)_3.8H_2O}$, $\mathrm{Mn(NH_4)_2(SO_4)_2.6H_2O}$, the anisotropy $\Delta\chi$ is found to vary inversely as the square of the absolute temperature.

2. In $\mathrm{Gd_2(SO_4)_3.8H_2O}$ the maximum anisotropy, though only 1·4 % of the mean susceptibility at room temperature, is still much larger than should be expected from the Stark separation of the S-levels of Gd^{+++} under the crystalline electric fields. The bulk of the observed anisotropy appears to arise from the magnetic interaction between the neighbouring Gd^{+++} ions.

3. Chromic salts have a very feeble anisotropy, almost as feeble as if the Cr^{+++} ion were in the S-state. The criterion for judging the suitability of a paramagnetic salt as working material in the production of low temperatures by the Debye-Giauque method is discussed.

4. From measurements on the magnetic anisotropy of nickel salts at different temperatures, the strength of the coupling between the orbital and the spin angular momenta of Ni^{++} is calculated, and is found to agree with the spectroscopic value.

5. Praseodymium and samarium ethylsulphates are of special interest. As we go down to low temperatures their anisotropies increase at first, reach a maximum, and then diminish rapidly.

6. The crystal fields in the rare earth chlorides, which are hexahydrated, are as strongly asymmetric as in the sulphates, which are octahydrated.

7. Magnetic measurements on the cupric alkali chlorides enable us to decide between the alternative structures proposed for these crystals from X-ray studies.

References

Chrobak, L. 1929 *Bull. int. Acad. Cracovie*, p. 497.
— 1934 *Z. Kristallogr.* **88**, 35–47.
Fereday, R. A. and Wiersma, E. C. 1935 *Physica, 's Grav.*, **2**, 575–81.
Gorter, C. J. 1932 *Phys. Rev.* **42**, 437–8.
Hendricks, S. B. and Dickinson, R. G. 1927 *J. Amer. Chem. Soc.* **49**, 2149–62.
Hebb, M. H. and Purcell, E. M. 1937 *Phys. Rev.* **5**, 346.
Krishnan, K. S. and Banerjee, S. 1935 *Philos. Trans.* A, **234**, 265–98, III.
— — 1936 *Philos. Trans.* A, **235**, 343–66, IV.
Krishnan, K. S. and Chakrabarty, D. 1938 *J. Chem. Phys.* **6**, 224–5.
Krishnan, K. S., Chakravorty, N. C. and Banerjee, S. 1933 *Philos. Trans.* A, **232**, 99–115, II.
Krishnan, K. S. and Mookherji, A. 1937 *Nature, Lond.*, **140**, 549.
— — 1938 *Philos. Trans.* A, **237**, 135–59, V.
Kynch, G. J. 1937 *Trans. Faraday Soc.* **33**, 1403.
Laporte, O. 1928 *Z. Phys.* **47**, 761–69.
Pabst, A. 1931 *Amer. J. Sci.* **22**, 426–30.
Penney, W. G. 1933 *Phys. Rev.* **43**, 485–90.
Penney, W. G. and Kynch, G. J. 1937 *Nature, Lond.*, **140**, 109–10.
Penney, W. G. and Schlapp, R. 1932 *Phys. Rev.* **41**, 194–207.
Schlapp, R. and Penney, W. G. 1932 *Phys. Rev.* **42**, 666–86.
Van Vleck, J. H. 1932*a* "The Theory of Electric and Magnetic Susceptibilities." Oxford.
— 1932*b* *Phys. Rev.* **41**, 208–15.
Van Vleck, J. H. and Penney, W. G. 1934 *Phil. Mag.* **17**, 961–87.
Zachariasen, W. H. 1935 *J. Chem. Phys.* **3**, 197–8.

THE MAGNETIC ANISOTROPY OF MANGANITE CRYSTAL IN RELATION TO ITS STRUCTURE.

By K. S. Krishnan and S. Banerjee.

Received 30th September, 1938.

1. The Chemical Composition of Manganite and the Valency of its Manganese Atoms.

The chemical composition of the mineral manganite is that of hydrated sesquioxide of manganese, $Mn_2O_3 . H_2O$. Its structure has been the subject of a long-standing controversy.[1] The hydrogen in the mineral is generally regarded as occurring in the form of hydroxyl groups and not as water, and this view receives strong support from the observation of Coblentz that the infra-red absorption spectrum of the mineral shows the characteristic band of hydroxyl, and no water bands. The main contention about the structure of the mineral concerns the valency of its manganese atoms, whether they are trivalent, or half of them divalent and the other half tetravalent. If the former, the structural formula would be 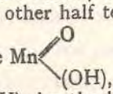 and the compound may be regarded as derived from $Mn(OH)_3$ by the loss of one molecule of water. Some of the available chemical evidence supports this view. On the other hand, on suitable treatment with an acid, half of the manganese in the mineral is converted into the corresponding manganous salt and the other half into hydrated manganese dioxide. This observation supports strongly the second alternative, and suggests the formula

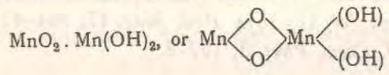

2. Evidence from X-ray Studies.

The structure of manganite has been studied by X-ray methods by Garrido,[2] and more recently, and in great detail, by Buerger.[3] According to the latter author the crystal is monoclinic, and its unit cell has the dimensions

$$a = 8{\cdot}86,\ b = 5{\cdot}24,\ c = 5{\cdot}70 \text{ A.};\ \beta = 90°,$$

and contains 8 molecules of MnO(OH). Its structure is found to be similar to that of arsenopyrite, FeSAs, rather than to that of marcasite, FeS_2, as suggested by the earlier work. This is to be expected in view of the difference between O and (OH).

[1] See Mellor, *Treatise on Inorganic Chemistry*, vol. 12, p. 239.
[2] *Bull. Soc. Franc. Mineral.*, 1935, **58**, 224.
[3] *Z. Krist.*, 1936, **95**, 163.

Each Mn atom in the crystal is found to be at the centre of an irregular octahedron formed by three oxygens and three (OH) groups. All the Mn atoms in the crystal are apparently identical, and this result would correspond to all of them having the same valency, namely three.

3. The Magnetic Anisotropy of the Crystal in Relation to the Valency of its Mn Atoms.

Observations on the magnetic anisotropy of the crystal should throw some light on the question of the valency of the Mn atoms in it. The Mn^{++} ion is the *S*-state, ${}^6S_{5/2}$, and since the spin angular momenta of the electrons are affected very little by the crystalline electric fields, *i.e.*, since the Stark-separation of the *S*-levels should be very narrow, the Mn^{++} ions in crystals should have very little magnetic anisotropy even when the crystalline fields are highly asymmetric. This result has been verified by us for a large number of manganous salts;[4] the anisotropy $\Delta\chi$, *i.e.* the difference between the maximum and the minimum principal susceptibilities of the crystal, is about 8×10^{-6} per gram ion of Mn^{++} at room temperature.

We shall next consider the Mn^{++++} ion. Its ground state is ${}^4F_{3/2}$ and in its Stark-pattern, produced in the crystalline field, the lowermost level is non-degenerate. Owing to this circumstance, and the feebleness of the coupling between the orbital and the spin angular momenta of the electrons in the incomplete shell of Mn^{++++} (the constant of spin-orbit coupling is 121 $cm.^{-1}$ only), this ion also should have very little anisotropy even in highly asymmetric crystalline fields. Experimentally, though salts of tetravalent manganese have not been studied for their magnetic anisotropy, salts containing the Cr^{+++} ion, whose ground state is also ${}^4F_{3/2}$, have been studied, and they are found to be almost as feebly anisotropic as manganous salts.

On the other hand, the Mn^{+++} ion, whose ground state is ${}^5D_0$, should have relatively a large anisotropy in crystals, indeed several times larger than that of the manganous or the chromic ion under the same conditions. For example, manganic acetylacetone at 31° C. has an anisotropy of 75×10^{-6} per gram ion of Mn^{+++}, whereas chromic acetylacetone, which is isomorphous with the manganic compound, has an anisotropy of $3{\cdot}2 \times 10^{-6}$ only per gram ion of Cr^{+++}.

Hence a measurement of the magnetic anisotropy of manganite to find out whether it is of the same order of magnitude as in manganous and chromic salts, *i.e.*, of the order of 8×10^{-6} at room temperature, or very much greater and of the order of 75×10^{-6}, should decide whether the Mn atoms in the crystal are half of them divalent and the other half tetravalent, or all of them trivalent.

We should mention here that the mean susceptibility of the crystal does not enable us to decide between the two alternatives. In the first place the spin-only value of the magnetic moments of Mn^{++}, Mn^{+++} and Mn^{++++} are 5·92, 4·90, and 3·87 Bohr magnetons respectively, so that in magnetically dilute crystals their susceptibilities would bear the ratios $5{\cdot}92^2 : 4{\cdot}90^2 : 3{\cdot}87^2 = 2{\cdot}34 : 1{\cdot}60 : 1{\cdot}00$. The susceptibility of Mn^{+++} would thus be almost midway between those of Mn^{++} and Mn^{++++}. Further, in a crystal like manganite, in which the concentration of the Mn atoms is large, the exchange interactions between their

[4] *Phil. Trans. Roy. Soc., A*, 1936, **235**, 343.

spin moments would be large, and would affect the susceptibility considerably and to an uncertain extent. From the observed mean susceptibility of the crystal it is not therefore easy to conclude whether it corresponds to Mn^{+++} ions, or to Mn^{++} and Mn^{++++} ions in equal numbers.

The exchange interactions would not, however, produce any anisotropy in the crystal.

4. Measurements of Magnetic Anisotropy.

Measurements of magnetic anisotropy were made with a well-developed crystal of manganite, which was practically free from iron—the iron content was less than 0·01 per cent. Though the crystal is monoclinic, the two principal magnetic axes in the (010) plane practically coincide with the "a" and the "c" axes ($\beta = 90°$). Denoting the susceptibilities along the three crystallographic axes, which, as we mentioned, are also the principal magnetic axes, by χ_a, χ_b and χ_c respectively, we obtain at 31° C,

$$\chi_c - \chi_a = 4{\cdot}0 \times 10^{-6}$$
$$\chi_c - \chi_b = 3{\cdot}0 \times 10^{-6}.$$

The data refer to a mass of the crystal that contains one gram atom of Mn.

The anisotropy is thus very feeble, and is of the same order of magnitude as in chromic and manganous salts. Indeed it is not much higher than the anisotropy of the diamagnetism of the crystal.

This result shows that the Mn atoms in the crystal are not trivalent, and are presumably half of them divalent and the other half tetravalent. All the Mn atoms in the crystal will not then be identical, but will be of two kinds, and a rediscussion of the X-ray results taking this into account is desirable.

In the corresponding iron mineral, göthite ($Fe_2O_3 . H_2O$), it should be possible in the same manner to decide about the valency of the iron atoms. The Fe^{+++} ion is in the S-state, ${}^6S_{5/2}$ and should therefore have very little anisotropy, whereas Fe^{++} under the same conditions should exhibit an anisotropy at least a hundred times greater. We are trying to get a good single crystal of göthite for making measurements of the anisotropy.

Summary.

From the observed feeble magnetic anisotropy of manganite crystal it is concluded that the Mn atoms in it cannot be trivalent, and are presumably half of them divalent and the other half tetravalent.

Indian Association for the
Cultivation of Science, Calcutta.

Jahn-Teller Theorem and the Arrangement of Water Molecules around Paramagnetic Ions in Aqueous Solutions

It is well known from X-ray studies that in many of the highly hydrated salts of the iron and the rare earth groups the cation is surrounded by an octahedron of water molecules. This distribution fits well with the observed magnetic properties of these salts; first, it gives an electric field of predominantly cubic symmetry about the central cation, as required by the magnetic data, and secondly, it gives the potential of the electric field the proper sign demanded by the magnetic data. The magnetic data, however, further require (1) that the field, though predominantly cubic in symmetry, should deviate from it considerably, since the cation in these crystals exhibits, in general, a strong magnetic anisotropy, and (2) that for a given cation the magnitude and the asymmetry of the electric field about it should be nearly the same in the different hydrated salts containing the ion, since the magnetic anisotropy of the ion is found to be of the same order of magnitude in all these salts. These requirements will be satisfied in a simple manner if the octahedron, instead of being regular, deviates from it slightly—a small deviation is permitted by the available X-ray data—and the deviation is determined by the nature of the cation in the centre. This arrangement appears very probable in view of the important theoretical result obtained recently by Jahn and Teller[1], namely, that if the electronic state of the central ion is degenerate, the system will be stable only if there is enough asymmetry in the system to remove the degeneracy (except, of course, the special two-fold degeneracy of Kramers). This minimum asymmetry required for stability supplies then the mechanism by which the cation can in a manner determine the geometry of distribution of the water molecules around it.

Such an asymmetric arrangement of the water molecules about the cation seems to persist even in the aqueous solutions of these salts. Freed and his collaborators[2] have found in the observed multiplicity of the absorption lines of the rare earth ions in aqueous solutions evidence for asymmetric electric fields, nearly the same as in the corresponding hydrated crystals. A comparison of the magnetic behaviour of some of the paramagnetic ions, both of the rare earth and the iron groups, in aqueous solutions, with the ideal free-ion behaviour on one side, and with the behaviour of the ions in the hydrated crystals on the other, also leads to the same conclusion.

The large magnetic double-refraction exhibited by aqueous solutions of these salts[3] follows as a natural result. Owing to the asymmetry in the distribution of the water molecules about the paramagnetic ion, and the consequent asymmetry of the electric field about the ion, the group as a whole will be magnetically anisotropic, and will tend to orient in the magnetic field. Since the group will also be optically anisotropic, the solution will exhibit double-refraction. Now these anisotropies, according to the views presented here, should depend indirectly on the incipient degeneracy of the electronic state of the central paramagnetic ion, and in particular on the orbital degeneracy. The observation by Chinchalkar[4] that the double refraction depends on the orbital angular momentum of the paramagnetic ion, and that in particular the double refraction is almost nothing when the ion is in the S-state, (for example, Gd^{+++}) is significant. Indeed, from the known magnetic anisotropy of the group in the crystal state, and its birefringence, a rough estimate can be made of the magnetic double refraction of the solution, and it is found to be of the right order of magnitude.

K. S. Krishnan.

Indian Association for the
Cultivation of Science,
Calcutta.
Feb. 15.

[1] *Proc. Roy. Soc.*, A, **161**, 220 (1937); **164**, 117 (1938).
[2] *J. Chem. Phys.*, **6**, 297 and 654 (1938).
[3] Raman, C. V., and Chinchalkar, S. W., Nature, **128**, 758 (1931); Haenny, C., *C.R.*, **193**, 931 (1931); **195**, 219 (1932).
[4] *Phil. Mag.*, **20**, 856 (1935).

Temperature Variation of the Magnetic Anisotropy of Graphite.

By K. S. Krishnan and N. Ganguli,
Indian Association for the Cultivation of Science, Calcutta.

1. Introduction.

Graphite crystal belongs to the hexagonal system and occurs in the form of a thin flake parallel to the basal plane. The crystal exhibits some remarkable magnetic properties. Whereas its susceptibility along directions in the basal plane, $\chi_\perp$, is normal, and has the value $-0.5 \cdot 10^{-6}$ per gm., which is nearly that of diamond, the susceptibility along the hexagonal axis, χ, has more than 40 times this value, namely about $-22 \cdot 10^{-6}$ per gm., at room temperature[1]). This abnormal diamagnetism of graphite along the hexagonal axis is due to its peculiar structure. The carbon atoms are arranged in layers parallel to the basal plane. The atoms in each layer form a regular hexagonal net-work, and are strongly bound to their neighbours in the plane. On the other hand, the binding between adjacent layers, which are rather widely separated, is very weak. Three of the electrons of each carbon atom take part in binding the atom to its three immediate neighbours in the same layer, while the fourth electron is more or less free, and can wander about in the plane of the hexagonal net-work. The large orbits which these odd electrons can execute in the basal plane under the influence of a magnetic field incident along the normal to the plane, explains the abnormal diamagnetism along the latter direction.

Now these "free" electrons probably take part in loosely binding together the adjacent layers of carbon atoms, and any disturbance which alters the distance between the adjacent layers, will naturally interfere with the freedom of these odd electrons, and will therefore tend to diminish the abnormal diamagnetism along the hexagonal axis. In other words, the abnormal part of the diamagnetism of graphite should be markedly structure-sensitive. This is verified experimentally[2]). On treating the crystal, for example, with a mixture of strong sulphuric and nitric acids, to which has been added a pinch of potassium chlorate—when the crystal swells up to "blue graphite"—$\chi_\perp$ diminishes (numerically)

1) Krishnan, Nature 133 (1934) 174; Guha and Roy, Ind. Jour. Phys. 8 (1934) 345.

2) Krishnan and Ganguli, Current Sc. 3 (1935) 472; Ganguli, Phil. Mag. 21 (1936) 355.

rapidly from $-22 \cdot 10^{-6}$ to less than $-2 \cdot 10^{-6}$, whereas $\chi_\perp$ remains practically unaffected. In this treatment it is the distance between the loosely bound adjacent layers of carbon atoms that changes, while the distances between the atoms in any given layer are not altered; i. e. the swelling is confined to one direction, namely the hexagonal axis of the crystal.

A similar effect is observed on treating the crystal with potassium vapour, when it forms a metallic-looking, copper-coloured alloy. Here also the swelling is along the hexagonal axis, and it is the abnormal diamagnetism along this direction that diminishes rapidly, whereas the diamagnetism in the basal plane, which is normal, remains practically unaffected. An indefinite diminution in the size of the crystal, beyond a certain low value, also appears to have a similar effect.

In view of the structure-sensitiveness of the abnormal part of the diamagnetism of the crystal, temperature changes also may be expected to have a large influence. We have therefore made measurements of the principal susceptibilities of the crystal over a large range of temperatures, from the temperature of liquid oxygen, $-183°$C, to about $800°$C. The present paper gives an account of these measurements[1]).

2. Measurements of Magnetic Anisotropy at Low Temperatures.

Since one of the principal susceptibilities of the crystal, namely χ, is much larger than the other, $\chi_\perp$, and since the difference between the two is easier to measure accurately than either of them separately, we have made measurements of the anisotropy $\chi_\perp - \chi_{||}$, and of the smaller susceptibility $\chi_\perp$, at different temperatures.

We shall take up first the low temperature measurements of the anisotropy. The method of measurement adopted is essentially the same as that described in a recent paper[2]) on the measurement of the magnetic anisotropies of some paramagnetic crystals at low temperatures. The crystal is suspended at the end of a calibrated quartz fibre inside a thin-walled copper cylinder which is kept deeply immersed in the liquid bath of a cryostat. The liquid used for the bath is petroleum ether of low boiling point, kept in a large Dewar cylinder. The bath is kept continually stirred, and its temperature is maintained steady at any desired value by automatic control by a constant-volume air-thermometer of thin-walled copper, immersed completely in the bath. There

1) A preliminary report of the results was published in Nature, 139 (1937) 155.

2) Krishnan, Mookherji and Bose, in course of publication in Phil. Trans. Roy. Soc. A.

are two electrical circuits, one through the motor of an air pump which can suck slowly liquid oxygen into a small copper chamber immersed in the bath, and the other through a small heating coil, also immersed in the bath. One or the other of the two circuits is automatically closed according as the volume of the air in the controlling thermometer is higher or lower than a certain pre-adjusted value, depending on the temperature at which it is desired to maintain the bath.

Below about −140°C the petroleum ether becomes very viscous, and hence unsuitable as a bath liquid. We could therefore work at only one temperature below this, namely the boiling point of oxygen. For this temperature, liquid oxygen is used directly as the bath liquid, in place of petroleum ether, and is allowed to evaporate freely at atmospheric pressure; no temperature control is necessary in this case.

Measurements of the temperature of the crystal are made with a copper-constantan thermocouple, one junction of which is inside the crystal chamber, just below the crystal, and the other is kept at the temperature of melting ice. The thermocouple is calibrated by keeping the former junction at the following temperatures:— (1) the temperature of liquid oxygen boiling at atmospheric pressure, namely −183°.0 C $+(p-760)\cdot 0.0126°$ C, where p is the atmospheric pressure in mm. of mercury; (2) the temperature of a mixture of solid carbon dioxide and ethyl ether, namely −78°.64 C; (3) the temperature of the room, measured with a calibrated mercury thermometer; (4) the boiling point of water at atmospheric pressure. A four-constant formula, of the type $E = at + bt^2 + ct^3 + dt^4$, is used to express the relation between the temperature t of the measuring junction of the thermocouple, in degrees centigrade, and the observed potential difference E between its two junctions.

The magnetic measurements are made by the torsional method described in earlier papers from this laboratory. The crystal is suspended inside the copper-tube immersed in the cryostatic bath, mentioned previously, with its plane vertical. The suspension for the crystal consists of two parts. The upper part is a fine quartz fibre, which has been calibrated previously, and the lower part is a thick glass fibre, sufficiently stout in comparison with the quartz fibre to be regarded as rigid. The whole length of the quartz fibre is above the cryostat, and is practically at room temperature all the time, so that its torsional constant is independent of the temperature of the cryostat. The whole of the cryostatic arrangement is placed between the flat pole-pieces of a large electromagnet, so that the crystal may be in the centre of the field.

The upper end of the quartz fibre is attached centrally to the pin of a graduated torsion-head. The torsion-head is initially adjusted so that when the crystal takes up its natural orientation in the magnetic field, namely with its plane along the field, the torsion on the fibre is zero. If the torsion-head is now slowly rotated from this position there will come a stage when the equilibrium of the crystal in the field becomes unstable and the crystal suddenly turns. If α_c is the total angle by which the torsion-head has been rotated from its original position, then the anisotropy $\chi_\perp - \chi_\parallel$ per gm., will evidently be given by the relation

$$\lambda = \frac{\alpha_c - \pi/4 - \sigma}{\cos 2\sigma}, \qquad (1)$$

where

$$\sin 2\sigma = \frac{1}{2\lambda}, \qquad (2)$$

and λ stands for $\frac{mH^2}{2c}(\chi_\perp - \chi_\parallel)$: m is the mass of the crystal, H is the magnetic field and c is the torsional constant of the fibre.

Since α_c is large in our measurements, corresponding to 3 or 4 rotations of the torsion-head, the expression for λ reduces to the simple form

$$\lambda = \alpha_c - \pi/4.$$

Three different crystals were measured and the results are collected together in Table I.

Table I.

I crystal		II crystal		III crystal	
Temp. °K	$\chi_\perp - \chi_\parallel \cdot 10^6$	Temp. °K	$\chi_\perp - \chi_\parallel \cdot 10^6$	Temp. °K	$\chi_\perp - \chi_\parallel \cdot 10^6$
293.6	21.2	301.2	21.0	295.6	21.0
270.6	22.0	272.8	21.9	272.4	21.9
252.9	22.6	241.8	23.0	209.4	24.7
231.2	23.4	212.2	24.2	189.9	25.5
211.4	24.7	186.4	25.4	169.6	26.4
191.8	25.3	160.6	27.0	146.2	27.4
165.4	26.8	137.1	28.0	130.6	28.3
148.9	27.3	99.1	29.1		
90.1	28.8				

3. Measurements of Anisotropy at High Temperatures.

For the high temperature measurements the crystal is suspended inside a large-sized tube of unglazed porcelain, closely wound on the

outside with "nicrome" wire, over which is rolled tightly a thin sheet of asbestos. By sending a steady electric current through the wire, the temperature inside can be maintained at any desired value, up to about 800° C. With this arrangement the temperature of the crystal chamber is not so steady as in the cryostatic bath; but owing to the much slower variation of $\chi_\perp - \chi$ at the higher temperatures, the effect of the small fluctuations in the temperature of the crystal chamber on the measurement of $\chi_\perp - \chi$ is very small.

The temperature is measured by a copper-constantan thermocouple, one junction of which is inside the crystal chamber, just below the crystal, and the other junction is at the temperature of melting ice. The thermocouple is calibrated by keeping the latter junction at 0° C, and the former successively at the temperature of steam at 100° C, and the temperatures of melting of tin (231°.8), lead (327°.4), zinc (419°.4), antimony (630°.5) and silver (960°.5), and the temperature of sulphur boiling at atmospheric pressure (444°.6). The temperatures given inside the brackets are in degress centigrade. Though the metals chosen were pure, yet in order to guard against any possible uncertainties in their melting points due to impurities, we have utilized for calibration 7 temperatures, 3 more than necessary.

The suspension for the crystal consists of two parts; the upper one is a fine quartz fibre as before, and is at room temperature, but the lower one is now a thin copper wire, to the lower end of which is tied rigidly the crystal, with its plane vertical. The copper wire stands the high temperatures better than the stout glass fibre used in the low temperature measurements, and the use of cements for attaching the crystal is also thus avoided. The wire does not show any anisotropy.

Table II.

I crystal		II crystal		III crystal	
Temp. °K	$\chi_\perp - \chi_\parallel \cdot 10^6$	Temp. °K	$\chi_\perp - \chi \cdot 10^6$	Temp. °K	$\chi_\perp - \chi_\parallel \cdot 10^6$
304.5	21.0	304.5	21.0	304.4	21.1
362.5	19.4	365.8	19.2	435	17.8
451	17.3	446	17.3	911	10.6
621	14.0	617	14.0	1273	7.8
825	11.3	911	10.3		
1080	9.0	1047	8.8		
		1264	7.8		

The results of the high temperature measurements on the anisotropy are given in Table II. The crystals are all different from those used in the low temperature measurements.

4. Measurement of $\chi_\perp$.

In view of the small value of $\chi_\perp$, and its sensitiveness to small traces of iron which are usually present as impurity in graphite crystal, and the large temperature variation of the disturbing effect of the iron impurity, only rough measurements were made on $\chi_\perp$. The crystal was suspended with its plane vertical, at the end of a long quartz fibre, in an inhomogeneous part of the magnetic field, so that the plane of crystal may be along the field and perpendicular to the direction of its gradient. The crystal was inside the copper tube of the cryostat in the low temperature measurements, and inside the heated porcelain tube in the high temperature measurements.

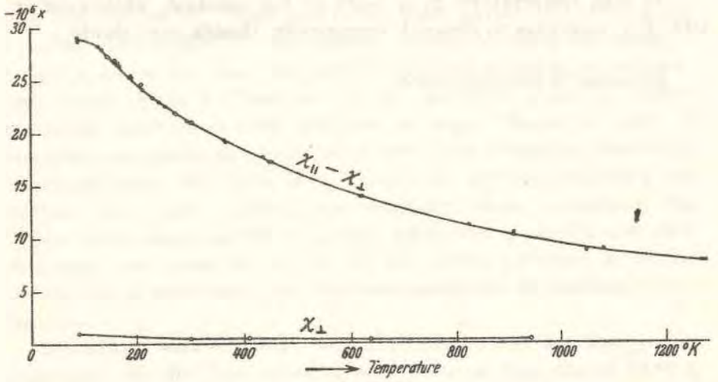

Fig. 1.

The motion of the crystal along the direction of the field gradient when the current through the magnet coils is switched on, is followed by watching through a low power microscope the shift of the suspension fibre at a point as low as possible, i.e. where it emerges from the crystal chamber. The shift is read directly on the eye-piece scale of the microscope.

Owing to the small value of $\chi_\perp$, the movement of the crystal in the field is small, and we may therefore take the susceptibilities at different temperatures to be roughly proportional to the lateral shifts

of the suspended crystal, or to the lateral displacements of the fibre in the field of view of the microscope, produced by switching on the current through the magnet coils. The results are given in Table III.

Table III.

Temp. °K	90	301	409	637	943
$\chi_\perp \cdot -10^6$	1.0	0.5	0.5	0.4	0.4

5. Temperature Variation of the Principal Susceptibilities.

The values of $\chi_\perp - \chi_\parallel$ and of $\chi_\perp$, at different temperatures are plotted in Fig. 1. As will be seen from the graphs, both $\chi_\parallel$ and $\chi_\perp$ increase numerically as the temperature is lowered, $\chi_\perp$, however, remaining always very much smaller than $\chi_\parallel$. At the temperature of liquid oxygen the curve for $\chi_\parallel$ tends to flatten, suggesting that it may not increase much as we go to still lower temperatures.

At high temperatures $\chi_\perp$ is more or less constant, while even at 1000° C $\chi_\parallel$ continues to diminish numerically, though very slowly.

Received 16 December 1938.

Magnetic Studies on Braunite, $3Mn_2O_3 \cdot MnSiO_3$.

By K. S. Krishnan and S. Banerjee,
Indian Association for the Cultivation of Science, Calcutta.

1. Some General Features of the Magnetic Properties of Manganese Salts.

In some recent papers we have described magnetic studies on single crystals of several manganese salts[1]). These salts are of great interest magnetically. Let us first consider ionic salts of divalent manganese. The Mn^{2+} ion is in the S-state, ${}^6S_{5/2}$, and the Stark-splitting of its energy levels in the strong, and generally asymmetric, electric fields obtaining in the crystals is naturally very narrow. These salts have therefore very little magnetic anisotropy, and their susceptibilities follow closely the Curie law, $\chi = C/T$. and the salts are very suitable as working materials for the production of low temperatures by the adiabatic demagnetization method of Debye and Giauque.

Let us next consider ionic salts of tetravalent manganese. The Mn^{4+} ion is in the ${}^4F_{3/2}$ state. and in the Stark-pattern produced in the crystalline electric fields. the lowermost level has no orbital degeneracy—though it has a four-fold spin degeneracy—and at ordinary temperatures almost all the Mn^{4+} ions will occupy this level, since the separation of the other levels from this level is large. Hence the salts of tetravalent manganese also should have very little magnetic anisotropy, and should obey the Curie law. Though no crystals containing the Mn^{4+} ion have been studied experimentally, those containing the Cr^{3+} ion, which also is in the ${}^4F_{3/2}$ state, have been studied[2]), and their anisotropies are found to be very small, almost as small as if the Cr^{3+} ion were in the S-state, and their susceptibilities do conform to the Curie law.

In contrast with the Mn^{2+} and Mn^{4+} ions, which are both feebly anisotropic, the Mn^{3+} ion, whose ground state is ${}^5D_0$, should have a relatively large anisotropy. This result also is verified experimentally. In a recent paper we utilized this contrast in the magnetic behaviour

1) Philos. Trans. Roy. Soc. London 235 (1936) 343, double sulphates and double selenates of manganese, of the Tutton type; Z. Kristallogr. 98 (1938) 499, rhodochrosite, $MnCO_3$; Nature 142 (1938) 717, manganite $MnO(OH)$.

2) Krishnan, Mookherji and Bose, Philos. Trans. Roy. Soc. London, 238 (1939) 125.

of the Mn^{2+} and Mn^{4+} ions on one side, and the Mn^{3+} ions on the other, to decide the question of the valency of the manganese atoms in manganite, $MnO(OH)$; from the observed feeble anisotropy of the crystal it was concluded that the Mn atoms in it can not be trivalent, and are presumably half of them divalent and the other half tetravalent[1]).

2. The Chemical Composition of Braunite and the Valencies of its Mn-Atoms.

The chemical composition of braunite is generally represented by he formula $3\,Mn_2O_3 \cdot MnSiO_3$, according to which one of the Mn atoms in the molecule is divalent and the remaining six are trivalent. It has been observed, however, that chemically the oxide in braunite behaves in many ways differently from the artificially prepared hemitrioxide of manganese, and in particular that it behaves more like a salt than like an oxide. The formula $Mn\,MnO_3$ has therefore been suggested in preference to Mn_2O_3[2]). In other words, braunite is regarded as a manganous salt of metamanganous acid, mixed with the metasilicate $MnSiO_3$. According to this formula the manganese atoms in braunite are four of them divalent, and the remaining three tetravalent; none of them is trivalent. The magnetic anisotropy of the crystal should then be very feeble, whereas the presence of trivalent manganese will give the crystal, which is tetragonal, a relatively large anisotropy. A measurement of the magnetic anisotropy of the crystal should therefore enable us to decide, in the same manner as in manganite, between the two alternative structures.

3. Earlier Magnetic Measurements on Braunite.

Some rough measurements have been made by Rao[3]) on the magnetic properties of this crystal at room temperature. The specimen with which he worked was of density 4.8, and had the following composition:—Mn 54%, Fe 2.5%, and the rest silica and oxygen. He found the susceptibility of the crystal along its tetragonal axis to be less than that for directions perpendicular to the axis by about 2%, and the mean susceptibility to be about 400×10^{-6} per c.c., or 83×10^{-6} per gram, of the crystal. This value for the mean susceptibility is apparently very low, and we have therefore made fresh measurements on the magnetic constants of this important mineral.

1) Nature, loc. cit.; Trans. Faraday Soc. in course of publication.

2) See J. W. Mellor, Treatise on Inorganic Chemistry 12, 236, and L. L. Fermor, Mem. Geol. Survey India 37 (1909) 52.

3) K. Seshagiri Rao, Proc. Indn. Assocn. Cultn. Sc. 6 (1920) 87.

4. Measurement of the Mean Susceptibility.

We shall first take up the measurement of the mean susceptibility. This was done with the powdered crystal, by the well-known Föex-Forrer method, and the results are given in Table I. K denotes the mean susceptibility per gram of the crystal.

Table I.

Temp. ° K	$K \times 10^6$	$K(T-76)$
301.8	145.5	.0329
315.1	137.3	.0328
337.5	124.5	.0326
375.6	107.3	.0322
418.2	94.5	.0323
454.8	86.3	.0327
495.4	77.3	.0324
527.7	72.6	.0328
578.9	65.4	.0329
628.7	59.7	.0330
653.1	57.4	.0331
668.1	55.2	.0327
		mean = .0327

In Fig. 1 the reciprocal of the susceptibility is plotted against the absolute temperature T. (We have not corrected the values of K for the diamagnetism of the crystal, scine the diamagnetism will be of the order of 0.4×10^{-6} per gram, which even at the highest temperature of our measurement is only 0.7% of the observed susceptibility, and is therefore very small.) As will be seen from the figure, the values of $1/K$ plot into the straight line defined by the equation

$$K = \frac{0.0327}{T - 76}.$$

The large value of the Curie temperature, namely 76° K, is

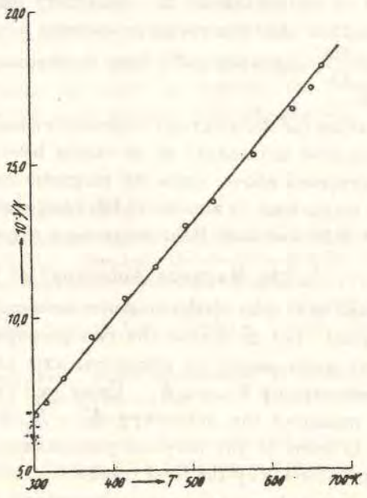

Fig. 1.

understandable in view of the high concentration of the *Mn* atoms in the crystal, and the consequent large interaction between their spin moments.

Now the mineral with which we made the susceptibility measurements, had the following composition: manganese 54%—the formula $3Mn_2O_3 \cdot MnSiO_3$ gives 63.6% manganese—iron (ferrous) 1.2%, and the rest practically oxygen and silica. Since ferrous salts have roughly the same mean susceptibility as manganese salts, the correction for the iron impurity is easily made; its effect will be equivalent to increasing the percentage of *Mn* in the mineral from 54 to 54+1.2 or 55.

The value of 0.0327, per gram of braunite, obtained above for the Curie constant, C, will then correspond to $\frac{0.0327 \cdot 54.9}{0.55}$ or 3.27 per gram atom of *Mn*. If we assume that all the elementary magnets in the crystal are alike, then their effective magnetic moment μ, defined by the usual relation $C = \frac{N\mu^2}{3k}$, comes out as 5.1 Bohr magnetons, which is of reasonable magnitude.

This value for the average magnetic moment of the manganese ion in braunite does not enable us to decide between the two alternative formulae proposed above, since the magnetic moment of Mn^{+3}, namely 4.90 Bohr magnetons, is almost midway between the moments of Mn^{+2} and Mn^{+4}, 5.92 and 3.87 Bohr magnetons respectively.

5. The Magnetic Anisotropy of Braunite.

We shall next take up the measurements on the magnetic anisotropy of the crystal. Let us denote the two principal susceptibilities of the crystal, per gram, along its tetragonal axis and perpendicular to the axis respectively, by $K_\parallel$ and $K_\perp$. Using well developed single crystals, we have measured the anisotropy $K_\parallel - K_\perp$ by the torsional method described in some of the previous publications from this laboratory[1]). We shall give here only the final results.

For a crystal having the same composition as before, the anisotropy at room temperature, namely 27.8° C, was found to be

$$K_\perp - K_\parallel = 0.364 \times 10^{-6} \text{ per gram.}$$

Comparing this value with that of the mean susceptibility at the same temperature, (see Table I), we find that at this temperature the anisotropy is only a quarter per cent of the mean susceptibility.

The anisotropy of the crystal being small, the question naturally arises how much of it is due to the mineral and how much is due to the

1) See for example Z. Kristallogr. 99 (1938) 199.

ferrous iron impurity, since ferrous salts are known to have a very large anisotropy, of the order of 10^{-3} per gram ion of Fe^{++}, and the 1.2% of ferrous iron present in our braunite is therefore capable of producing an anisotropy of the same order of magnitude as the observed anisotropy. In particular we have to find whether the contribution from the ferrous iron impurity to the anisotropy $K_\perp - K_\parallel$ will be positive or negative; if the former the real anisotropy of the mineral should be much less than the observed anisotropy (which already is small), and if the latter the real anisotropy should be larger than the observed anisotropy. In order to decide this question, and also roughly to estimate the magnitude of the contribution from the ferrous iron, we have measured the anisotropy of another crystal of braunite, from a different source, whose iron content was about 2.5%, and was as before wholly ferrous. The value of $K_\perp - K_\parallel$ was found to be 0.54×10^{-6} per gram. This crystal was slightly twinned, and on this account the value of $K_\perp - K_\parallel$ may be somewhat higher than 0.54×10^{-6} per gram.

This value suggests that more than half of the observed value of 0.364×10^{-6} for the first crystal should be attributed to its iron content. Hence the anisotropy of iron—free braunite should be less than 0.17×10^{-6} per gram., which is roughly 1/8% of the mean susceptibility.

This is of the same order of magnitude as for S-state ions, and much less than we should expect for the Mn^{3+} ions. The observed low anisotropy of braunite may therefore be taken to support the formula $3MnMnO_3 \cdot MnSiO_3$ as against the usual formula $3Mn_2O_3 \cdot MnSiO_3$.

Received May 23, 1939.

Eingegangene Bücher.

E. Albers-Schönberg, **Hochfrequenzkeramik** (= Industrielle Keramik, Band 2). XI, 171 Seiten mit 97 Abb. Dresden, Theodor Steinkopff. 1939

D. Balarew, **Der disperse Bau der festen Systeme.** Allgemeine Theorie der Verunreinigung fester Systeme (= Sonderausgabe aus »Kolloid-Beihefte«, Band 50). VI, 240 Seiten mit 45 Abb. Dresden, Theodor Steinkopff. 1939.

C. Ch. Beringer, **Das Werden des erdgeschichtlichen Weltbildes im Spiegel großer Naturforscher und Denker aus zwei Jahrhunderten.** V, 88 Seiten. Stuttgart, F. Enke. 1939.

W. Biltz, **Ausführung qualitativer Analysen.** 5. erweiterte Auflage. IX, 180 Seiten mit 14 Abb. Leipzig, Akademische Verlagsgesellschaft m. b. H. 1939.

M. Volmer, **Kinetik der Phasenbildung** (= Die chemische Reaktion, Band IV). XII. 220 Seiten mit 61 Abb. und 15 Tabellen. Dresden, Th. Steinkopff. 1939.

Large Anisotropy of the Electrical Conductivity of Graphite

GRAPHITE is a hexagonal crystal with a perfect basal cleavage. The carbon atoms in it are arranged in layers parallel to the basal plane, the atoms in each layer forming a regular hexagonal net-work[1]. The distance between adjacent layers is 3·4 A., which is much larger than the distance between adjacent atoms in the same layer, namely, 1·42 A. The crystal exhibits some remarkable magnetic properties. Whereas its susceptibility along directions in the basal plane is about $-0{\cdot}5 \times 10^{-6}$ per gm., which is nearly that of diamond, the susceptibility along the normal to the plane is more than forty times greater, being equal to -22×10^{-6} per gm. at room temperature[2]. The abnormal diamagnetism along the latter direction shows a striking temperature dependence[3], and is structure-sensitive[2].

Associated with the abnormal diamagnetism along the normal to the basal plane, we should naturally expect a much larger electrical conductivity in the basal plane than along the normal to the plane. On examining the available literature, we find that conductivity measurements on single crystals of graphite have been made along directions in the basal plane only[4]. We have therefore made measurements both along these directions and along the normal to the basal plane, using some well-developed single crystals from Ceylon. We find that the conductivity in the basal plane is at least *ten thousand* times larger than that along the normal to the plane. Whereas the specific resistance in the basal plane is of the order of $1C^{-4}$ ohm-cm., the specific resistance along the normal to the plane is 2–3 ohm-cm.

K. S. KRISHNAN.
N. GANGULI.

Indian Association for the
Cultivation of Science,
Calcutta.
Sept. 1.

[1] Bernal, *Proc. Roy. Soc.*, A, **106**, 749 (1924).
[2] Krishnan, NATURE, **133**, 174 (1934); Ganguli, *Phil. Mag.*, **21**, 355 (1936).
[3] Krishnan and Ganguli, NATURE, **139**, 155 (1937); *Z. Krist.*, A, **100**, 530 (1939).
[4] Koenigsberger and Weiss, *Ann. Phys.*, **35**, 1 (1911); Roberts, *Ann. Phys.*, **40**, 455 (1913); Ryschkewitsch, *Z. Elektrochem.*, **29**, 474 (1923).

SECTION OF PHYSICS

President :—K. S. KRISHNAN, D.Sc., F.N.I., F.R.S.

Presidential Address

(Delivered on Jan. 4, 1940)

THE DIAMAGNETISM OF THE MOBILE ELECTRONS IN AROMATIC MOLECULES

Considerable progress has been made during recent years in our understanding of the structures of aromatic molecules, and in particular of benzene. Much of this progress is due, on the theoretical side, to the application of quantum mechanics to study the nature of the linkage between the carbon atoms in the benzene ring and the part played by the valency electrons in the linkage, and on the experimental side, to the detailed investigations on the Raman and the infra-red spectra of benzene and its deutero-isomers, which have established the symmetry properties of benzene and the nature of its vibrations. One important result that emerges from these structural studies on benzene is that one electron in each carbon atom in the ring is mobile and is more or less free to migrate from atom to atom over the whole of the ring, a result of great significance to the sixty-year-old controversy regarding the location of the extra bonds in the benzene ring.

These mobile electrons have interesting magnetic properties, and I propose in this address to discuss some of these properties. In many respects the magnetic behaviour of these electrons is not dissimilar to that of the free electrons in metals, and the theoretical treatment in the two cases follows nearly the same course. I shall therefore deal first with the properties of free electrons, which are simpler.

THE PARAMAGNETISM OF AN ELECTRON GAS

All the characteristic properties of a metal are explained satisfactorily on the assumption that a certain number of electrons get detached from their atoms and are free to migrate from atom to atom throughout the metal. Taking for example the alkali metals, there is considerable evidence from their optical properties, their Hall coefficients, the fine structure of their emission spectra in the soft X-ray region, theoretical studies on metallic cohesion, etc., to show that the number of such free electrons should be just one per atom. The paramagnetic

properties of these electrons, regarded as forming a free-electron gas, are easily investigated. In the magnetic field the spin-moments of the electrons will place themselves either parallel or anti-parallel to the field, the number with parallel orientations preponderating, because of their lower energy in the field. Assuming that the preponderance of the parallel spins over the anti-parallel ones is determined by the classical statistics of Boltzmann, the susceptibility per unit volume of the gas will be given by the Curie law

$$\kappa_p = \frac{n\mu^2}{kT}, \quad .. \quad .. \quad .. \quad (1)$$

where n is the number of electrons per unit volume, μ is the Bohr magneton, and the other letters have their usual significance.

In order, however, that the classical statistics may be applicable, the uncertainty Δq in the location of the position of the electron, which is determined by the Heisenberg relation

$$\Delta q \approx h/\Delta p \approx h/(mkT)^{1/2},$$

should be much less than the average distance between neighbouring electrons in the metal, namely $n^{-1/3}$. This would be the case only at temperatures much higher than

$$T_0 \approx \frac{h^2 n^{2/3}}{mk}.$$

For the alkali metals, with the number of free electrons equal to one per atom, this temperature will be of the order of 10^5 degrees. Hence at all ordinary temperatures the electron gas in these metals will be almost completely degenerate, and the electrons will occupy, in pairs with opposite spins, all the energy levels permitted by Pauli's Exclusion Principle, up to $E \approx kT_0$. A few stray electrons having energies near about kT_0 will occupy their energy levels singly. To put it more precisely, the energy distribution of the electrons will conform to the statistics of Fermi and Dirac.

Now it is only the few stray electrons which occupy their energy levels singly, that can orient in the magnetic field and contribute to the magnetic moment. Their number, n' per unit volume, will obviously be much smaller than n, roughly in the ratio of T to T_0, and the susceptibility will therefore be given by the expression

$$\kappa_p = \frac{n'\mu^2}{kT} \approx \frac{n\mu^2}{kT_0}.$$

This gives the order of magnitude only. Detailed calculation gives for the spin-susceptibility of the degenerate gas

$$\kappa_p = \frac{3}{2}\frac{n\mu^2}{kT_0}, \quad .. \quad .. \quad .. \quad (2)$$

where T_0, the degeneracy temperature, is given by

$$T_0 = \frac{h^2}{8mk}\left(\frac{3n}{\pi}\right)^{2/3} \quad .. \quad .. \quad .. \quad (3)$$

This in outline is the celebrated explanation given by Pauli for the feeble, temperature-independent paramagnetism exhibited by the alkali metals, which initiated the modern theories of the properties of electrons in metals.

The Diamagnetism of a Free-Electron Gas on the Classical Theory

That on the pure classical theory a free-electron gas should have no diamagnetism at all, seems to have been first demonstrated by Bohr. This result is at first sight surprising, since in the magnetic field the electrons will all describe paths whose projections on a plane perpendicular to the direction of the field will be circles, and the direction of motion in all the circles will be the same, and such as to give a negative moment along the direction of the field. On more careful consideration, however, it will be seen that the outer electrons in the medium which are too close to the boundary wall to execute complete circles will be reflected repeatedly from the wall, as shown in the diagram, (in which the boundary is assumed to be cylindrical),

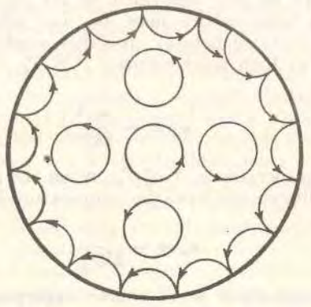

Fig. 1.

and will describe cuspidal paths; obviously this is equivalent to a creeping of these electrons along the boundary wall in a direction opposite to the direction of motion of the inner electrons. Though the creeping will be slow, yet because of the very large orbits in which these electrons creep, their contribution to the magnetic moment will be considerable, and on calculation we

find that it exactly neutralizes the diamagnetic contribution from the inner electrons.

This null result is independent of the nature of the boundary; in fact the boundary may be removed altogether. The result is even more general, and is applicable, as Miss van Leeuwen has demonstrated, not only to an electron gas, but to any dynamical system obeying pure classical statistics. The success of Langevin's apparently classical theory of diamagnetism, which explains so elegantly the diamagnetic properties of atoms and molecules, is due to the initial assumption of well-defined electronic orbits, which is a quantum result.

Landau's Discovery

To Landau we owe the discovery that if the motions of the free electrons in the magnetic field are quantized, as they should be according to our quantum mechanical ideas, the balancing between the diamagnetic moments of the inner electrons which execute uninterrupted paths, and the apparently paramagnetic contributions of the boundary electrons, is disturbed, much in favour of the former, and the result is a large diamagnetic moment. The argument by which the result is deduced is somewhat difficult to appreciate intuitively, and I shall therefore merely quote Landau's result, which has been checked by others, and with other models too. The diamagnetism of the free-electron gas is found to be just one-third of its spin-paramagnetism, whatever the temperature may be, i.e. whether the gas is degenerate or non-degenerate. In other words, the diamagnetic susceptibility at high temperatures, $T \gg T_0$, should conform to the Curie law

$$\kappa_d = -\frac{n\mu^2}{3kT}, \quad .. \quad .. \quad .. \quad (4)$$

and at low temperatures, $T \ll T_0$, when the gas is degenerate, the susceptibility should have the temperature-independent value

$$\kappa_d = -\frac{n\mu^2}{2kT_0}. \quad .. \quad .. \quad .. \quad (5)$$

The diamagnetism is of course superposed on the spin-paramagnetism, which will predominate, and the resultant susceptibility will be given by

$$\kappa = \kappa_p + \kappa_d.$$

Experimental Verification of Landau's Diamagnetism

It would be of great interest to verify experimentally Landau's result, which is essentially a quantum result and has no counterpart in the classical theory. There are, however, two

serious difficulties in verifying this diamagnetism, firstly the predominant paramagnetism with which it is normally associated, and secondly the enormous degeneracy temperatures for the free electrons in most metals, 10^4 to 10^5 degrees, which render only the degenerate state accessible for experimenting. There is, however, one substance in which, owing to certain special conditions, both these difficulties are eliminated. I mean the crystal of graphite.

Graphite is a hexagonal crystal with a perfect basal cleavage. The carbon atoms in it are arranged in layers parallel to the basal plane, the atoms in each layer forming a regular hexagonal network. The binding between neighbouring layers is extremely loose, and is probably of the van der Waals type, as is evidenced by the very large distance of separation between them, viz. 3·4 A.U., as compared with the distance of 1·42 A.U. between adjacent atoms in the same layer. Three of the electrons in each carbon atom will be utilized in binding it to its three neighbours in the basal plane, and the fourth will be practically free to migrate from atom to atom in the basal plane, much in the same manner as the free electrons in a metal. The probability of the electron jumping to the next layer will be very small.

The conditions obtaining in graphite are very favourable for a verification of the Landau diamagnetism. With a magnetic field incident along the hexagonal axis, we are concerned with the motions of the electrons in the basal plane only, and these motions, as we have seen, are free; the diamagnetic properties of the medium will therefore be similar to those of a free-electron gas. The restriction of the freedom of the electrons practically to the basal plane actually proves to be an advantage; the restriction will be equivalent to an enormously increased effective mass for the electron for motion along the normal to the plane, and as a result the spacing of the energy levels along this direction will become much narrower, and hence the degeneracy temperature much smaller, than for electrons that are free to move in all directions. Lastly, the spin-moments of the electrons in graphite are paired in such a manner as to give zero paramagnetism.

Experimentally, graphite crystal does have an abnormal diamagnetism, which is confined to the direction of the hexagonal axis (the susceptibility in the basal plane being practically the same as that of diamond), and which conforms to the Curie law (4) at high temperatures, and to the temperature-independent value (5) at low temperatures, with the *number of free electrons n equal to one per carbon atom and the degeneracy temperature* $T_0 = 520°K$. At all temperatures (in the range investigated) the diamagnetism per carbon atom is found to be the same as the Landau diamagnetism per electron of a free-electron gas having a degeneracy temperature of 520°K. The theoretical values for the specific susceptibility (per gm.) of graphite

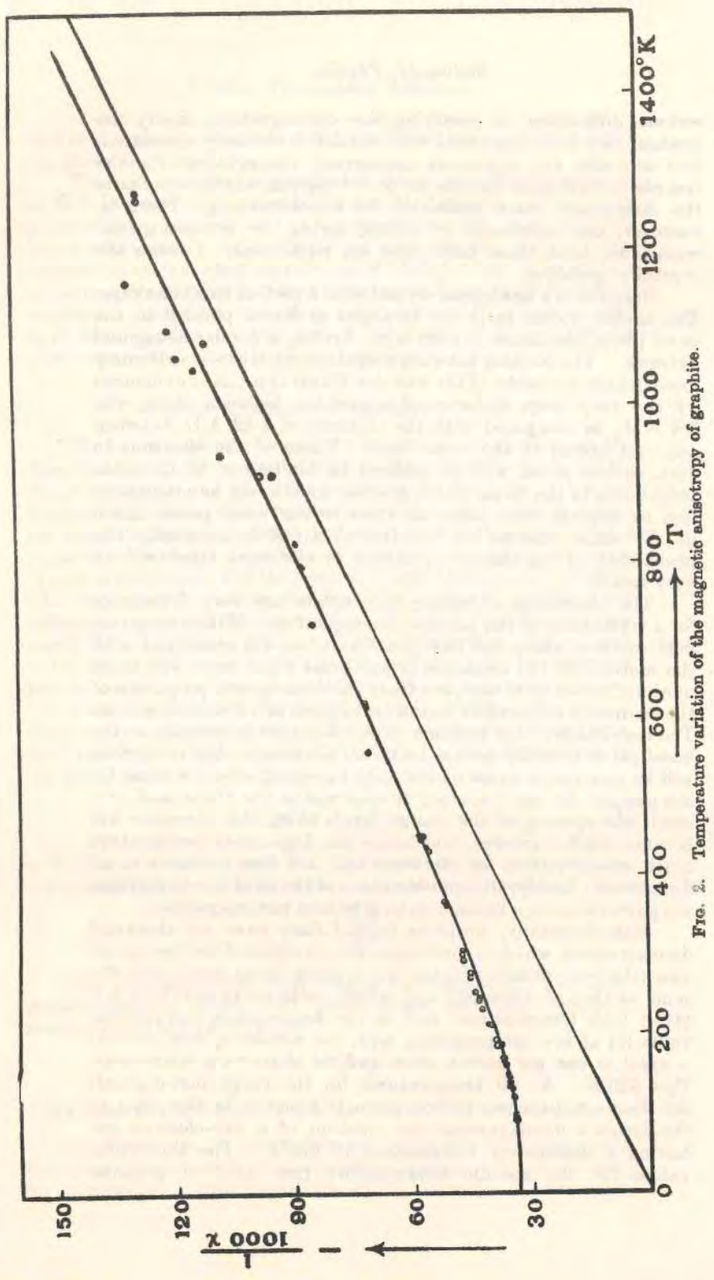

Fig. 2. Temperature variation of the magnetic anisotropy of graphite.

calculated on this basis are represented by the curve drawn in Fig. 2. The straight line which the curve tends to reach asymptotically at high temperatures, namely that corresponding to the Curie law (4), is also drawn in the figure. The circles denote the experimental values obtained by Mr. Ganguli and the present writer, and it will be seen that they all lie close to the theoretical curve.

That one electron per carbon atom should be free to move about in the basal plane agrees, as we have just seen, with the known structure of the crystal. It is further gratifying to find that there is a Brillouin zone which can just accommodate 3 electrons per carbon atom, which is a flat hexagonal prism bounded by $\{000,2\}$ and $\{2\bar{1}\bar{1},0\}$, and the energy-discontinuities across all the faces of the zone are large. There is a bigger zone bounded by $\{000,2\}$ and $\{2\bar{2}0,0\}$ which can just contain all the 4 valency electrons, but the energy-discontinuity across $\{2\bar{2}0,0\}$ is small.

The restriction of the freedom of motion of the metallic electrons in graphite to the basal plane is also evidenced by the enormously greater electrical conductivity of the crystal in the basal plane than along the normal to the plane; the ratio of the two conductivities, according to some recent measurements by Mr. Ganguli and the present writer, is larger than 10^4, probably very much larger.

The agreement between the experimental and the theoretical values plotted in Fig. 2 may be regarded as an experimental demonstration of the Landau diamagnetism of a free-electron gas, and of its temperature variation in accordance with the statistics of Fermi and Dirac.

The Mobile Electrons in Aromatic Molecules

Further, the magnetic data for graphite lend support to the view that one electron per carbon atom in the crystal is practically free to migrate from atom to atom through the whole layer. Following Lennard-Jones we shall call it the mobile electron, so as to distinguish it from the other three valency electrons in each carbon atom, which are localized and take part in binding it to its three neighbours. The occurrence of such mobile electrons is characteristic of all aromatic molecules—each layer in graphite can be regarded as a single molecule consisting of a very large number of condensed benzene rings—and is an essential feature of the quantum mechanical theories of the structures of these molecules. Their mobility is a necessary consequence of the Uncertainty Principle, according to which the larger the region assigned to these electrons, the smaller would be their kinetic energy. Any localization of these mobile electrons, such as is implied, for example, in the conventional

double-bond (in which a pair of such electrons is involved), will naturally correspond to a very large kinetic energy for these electrons; it is equivalent to restricting the wave-lengths of the standing electron waves to small values of the order of the length of the double-bond, whereas if the electrons are mobile, greater wave-lengths, of the order of the dimensions of the whole molecule, will also be permitted, thus conducing to a lowering of the energy, and to a correspondingly increased stability.

This is essentially the solution offered by quantum mechanics to the old controversy regarding the locations of the extra bonds in the benzene ring: they are not located at all! If we prefer it, we may, following Pauling and Wheland, express the same result in this form: the actual structure of the benzene ring is that obtained by the 'resonance' between the following

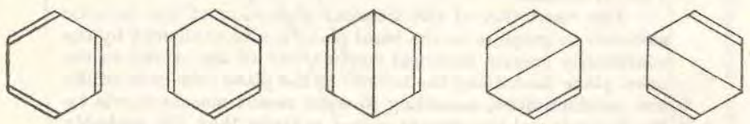

Fig. 3.

five canonical structures, the coefficients to be attached to the wave-functions representing these structures being given by

$$\psi = 0{\cdot}622\,(\psi_{\mathrm{I}} + \psi_{\mathrm{II}}) + 0{\cdot}271\,(\psi_{\mathrm{III}} + \psi_{\mathrm{IV}} + \psi_{\mathrm{V}}).$$

The first and the second of these structures can be recognized as Kekulé's and the remaining three as Dewar's. The structures proposed by Claus, Ladenburg and others, can all be obtained from the above five by suitable combinations.

The number of such canonical structures becomes very large even for the simplest of condensed ring molecules. For example for naphthalene 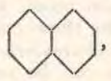 , the number of such structures is 42, and for the three-ringed molecules anthracene  and phenanthrene 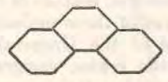 , the number is 429, and so on. If one has a partiality for any particular model, he can with a little diligence find his favourite in this list.

The Diamagnetism of the Mobile Electrons

One direct consequence of the freedom of the mobile electrons in benzene to migrate from atom to atom over the whole ring, would be an abnormal diamagnetism, confined to the direction perpendicular to the plane of the ring, because the diamagnetic moment is proportional to the area of the orbits described by the electrons under the influence of the magnetic field, and the mobile electrons can describe very much larger orbits in the plane of the benzene ring than the localized electrons. These diamagnetic effects should be even more marked in plane condensed ring molecules like naphthalene, anthracene, etc., in which the migrations of the mobile electrons can be more extensive. This explains the remarkable diamagnetic anisotropy exhibited by aromatic molecules. For example in benzene, the diamagnetic susceptibility along the normal to the plane of the molecule is nearly $2\frac{1}{2}$ times that along directions in the plane. Indeed the observed large diamagnetic anisotropies of these molecules offer the most striking evidence for the presence of the mobile electrons.

When such magnetically anisotropic molecules are arranged in a regular manner as in a crystal—in most organic crystals the molecules retain their individuality—the crystal as a whole will naturally exhibit an anisotropy, whose magnitude will depend on the anisotropy of the individual molecules and on their orientations relatively to one another. The closeness of approach of the molecules, which may not be the same along different directions in the crystal, will have practically no effect on the crystal anisotropy, since the diamagnetic moments induced in them will be too feeble to influence one another. In other words, the susceptibility of the crystal along any given direction will be merely the sum of the susceptibilities along this direction of all the constituent molecules.

When the magnetic constants of the molecule are already known, from measurements of the magnetic double-refraction of the substance in the liquid state or in state of solution in suitable solvents, magnetic studies on the crystal should enable us, in favourable cases, to obtain useful information about the orientations of the molecules in the crystal lattice. Such information will be very helpful in any structural analysis of the crystal by X-ray methods, since it may save much labour in the preliminary analysis, and will in any case offer an independent check on some of the results of the X-ray analysis.

I shall not deal further with this aspect of the magnetic studies on single crystals, and I shall now take up the converse aspect, namely that when the molecular orientations are already known from detailed X-ray studies, the crystal data enable us to calculate the principal magnetic constants of the molecules, which interest us here. This is a more direct, and more

accurate method for calculating the molecular magnetic constants, than the one based on measurements of the magnetic double-refraction in the liquid state, and besides is more general in its applicability.

The Magnetic Anisotropies of Some Plane Aromatic Molecules

Extensive measurements have been made by Bhagavantam, Banerjee, Mrs. Lonsdale and the present writer on the magnetic properties of organic crystals, particularly of the aromatic class. For some of these crystals complete X-ray analyses have been made by Robertson and others, by the Fourier method. I give in the following Table the magnetic constants for some plane aromatic molecules, calculated from these data. K_1, K_2 and K_3 represent the three principal diamagnetic susceptibilities of the molecule, per gm. mol., and are expressed in the usual unit 10^{-6} c.g.s. e.m.u.; K_3 refers to the direction normal to the plane of the molecule; the directions of K_1 and K_2 in the plane of the molecule are as marked at the head of the Table. In those crystals in which the X-ray data are not sufficiently precise to enable us to calculate K_1 and K_2 separately, only one value is given in the Table, which will be a good approximation to either of them.

It will be seen from the Table that for all the molecules, the susceptibility along the normal to the molecular plane, namely K_3, is numerically much larger than either K_1 or K_2, in the plane, and that K_1 and K_2 are of comparable magnitudes. The difference, $\Delta K = K_3 - \frac{1}{2}(K_1 + K_2)$, which may be taken to be the contribution from the mobile electrons, wholly directed along the K_3 axis, is given in the last column of the Table; it is roughly proportional to the number of benzene rings in the molecule.

Optical Evidence for the Mobile Electrons in Aromatic Molecules

The restriction of the freedom of migration of the mobile electrons in these molecules to the molecular plane, is also evidenced by the striking directional variations in some of the optical properties of these molecules, observed some time ago by Mr. P. K. Seshan and the present writer. Let us take for example the plane condensed ring compounds naphthacene 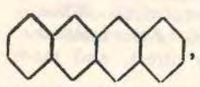 , chrysene 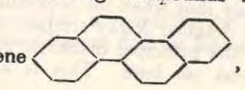 , 1, 2; 5, 6—

Table I

Molecule	K_2 / K_1	$-K_1$	$-K_2$	$-K_3$	$-\Delta K = \frac{1}{2}(K_1+K_2)-K_3$
Benzene		37	37	91	54
Hexamethylbenzene	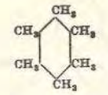	102	102	164	62
Hexaethylbenzene	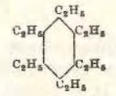	165	165	231	66
Durene	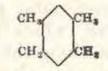	82	77	144	65
Diphenyl		63		182	119
Terphenyl		97	88	271	178
Quaterphenyl	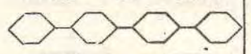	122	110	372	256
Tolane	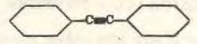	80	67	197	123
Fluorene	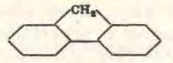	73		194	121
Naphthalene		56	54	169	114
Anthracene		76	63	252	183
Phenanthrene		74		240	166
Naphthacene	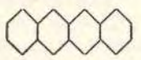	93		295	202
Chrysene		88	83	311	226
Pyrene	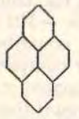	81		303	222
1, 2; 5, 6—Dibenzanthracene	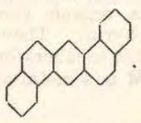	110		358	248

dibenzanthracene 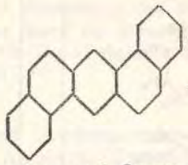 , etc. They all have characteristic absorption and fluorescence bands in the visible region of the spectrum, which are presumably due to the transitions of the mobile electrons. It is found experimentally that it is only the component in the molecular plane of the electric vector of the incident light-wave, which is absorbed by the molecule, whereas the component along the normal to the plane is not absorbed at all. In fluorescence also it is the component of the electric vector parallel to the molecular plane which excites fluorescence, the perpendicular component being quite inactive. An elegant quantum mechanical interpretation of these properties has recently been published by F. London.

Other Conjugated Systems

Besides the benzene ring there are other plane ring structures which, on the conventional view, have alternate single and double bonds. Their diamagnetic properties should be very similar to those of the benzene ring, since they also must have mobile electrons which can migrate all over the ring. I shall mention here two such compounds, studied recently for their magnetic properties by Mrs. Lonsdale. One is cyanuric trichloride 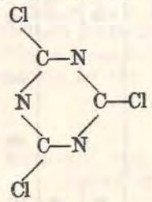 . The two principal susceptibilities of this molecule in the plane of the cyanuric ring are −70·9 and −71·2 respec ively, whereas the third susceptibility, which is along the normal to the ring, is −101·3, which is numerically much larger. The diamagnetic contribution from the mobile electrons is thus about −40, as compared with the value −54 of the mobile electrons in the benzene ring.

The second compound is metal-free phthalocyanine. The phthalocyanines are complex organic compounds, which are related to the natural porphyrins. They have been studied extensively by Linstead and his collaborators, and they have the formula $C_{32}H_{16}N_8M$, where M is a metal atom like Ni, Cu, etc.

The metal atom can be removed altogether, and the metal-free compound has the formula $C_{32}H_{18}N_8$. A complete X-ray analysis of the structure of this compound has been made recently by Robertson, and the molecule is found to have the following structure:—

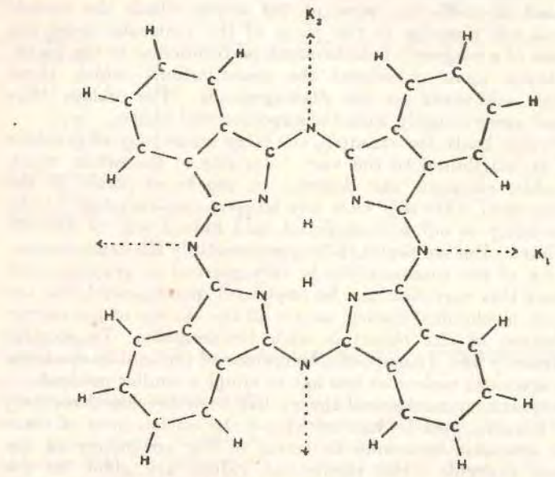

Fig. 4. Metal-free phthalocyanine molecule.

The most interesting part of this molecule, from our present point of view is the central zig-zag ring. It is a 16-membered ring of alternate carbon and nitrogen atoms, with two hydrogen atoms somewhere in the interior. This ring should exhibit resonance phenomena like the benzene and the cyanuric rings, and in view of its very large size, its diamagnetism along the normal to the plane of the ring should be enormous.

This is verified experimentally. The principal susceptibilities of the molecule are $K_1 = -120$, $K_2 = -165$, $K_3 = -982$. The susceptibility along the normal to the molecular plane is thus nearly 7 times that for directions in the plane. Even after allowing for the contributions from the outer rings, the contribution from the central 16-membered ring should be very large indeed, reminding one of the magnitudes involved in graphite.

Some Theoretical Considerations

Attempts have been made to calculate theoretically the magnitude of the diamagnetic anisotropy in some simple aromatic

molecules. Adopting a semi-classical theory—which we have adopted here in our description of the diamagnetic properties of the aromatic molecules—Pauling and Mrs. Lonsdale have evaluated the effective sizes of the orbits which the mobile electrons will describe in the plane of the molecule under the influence of a magnetic field incident perpendicular to the plane, and thence have calculated the contributions which these electrons will make to the diamagnetism. The values thus obtained agree roughly with the experimental values.

On this basis, for example, the large anisotropy of graphite would be attributed to the very large size of the orbits which the mobile electrons can describe in the basal plane, in the magnetic field. On this view any temperature-variation of the susceptibility is not contemplated, and indeed will be difficult to explain. But we found that experimentally the temperature-variation of the susceptibility is very marked in graphite, and also that this variation can be explained quantitatively on the quantum mechanical theory, as due to the change of the energy distribution of the electrons with temperature. To explain satisfactorily the diamagnetic behaviour of the mobile electrons in the aromatic molecules one has to adopt a similar method.

A quantum mechanical theory has been developed recently by F. London, and he has calculated the anisotropies of some simple aromatic molecules in terms of the anisotropy of the benzene molecule. His theoretical values are given in the following Table along with the experimental values for comparison :—

TABLE II

Molecule	$\frac{\Delta K}{\Delta K_{\text{benzene}}}$	
	Theoretical	Experimental
Naphthalene	2·19	2·11
Anthracene	3·45	3·39
Phenanthrene	3·19	3·07
Pyrene	4·46	4·11
Diphenyl	2·21	2·20

Attention may be drawn to one or two features in the experimental values, which are not obvious on Pauling's theory, but which follow from London's calculation: the anisotropy of diphenyl is found to be considerably larger than twice that of benzene; and there is a marked difference between the anisotropies of anthracene and phenanthrene.

It is interesting that experimentally the diamagnetic susceptibilities of the mobile electrons in chrysene, pyrene, and other condensed ring compounds do show an appreciable temperature-variation. This variation, however, is much smaller than in graphite, suggesting that the kinetic energies of the mobile electrons in these molecules should be much larger than in graphite. This is indeed to be expected.

Landau Diamagnetism and the Fermi-Dirac Energy Distribution of the Metallic Electrons in Graphite

It was discovered by Landau[1] that an electron gas should have, besides its spin paramagnetism, an appreciable diamagnetism due to the quantized orbital motions of the electrons in the magnetic field. If the electrons are *free*, the diamagnetic susceptibility per unit volume of the gas, when it is non-degenerate, is given by the Curie law

$$K = -\frac{n\mu^2}{3kT}, \quad . \quad . \quad . \quad (1)$$

and when it is completely degenerate by the temperature-independent value

$$K = -\frac{n\mu^2}{2kT_0}, \quad . \quad (2)$$

where n is the number of electrons per unit volume, μ is the Bohr magneton, T_0 is the degeneracy temperature defined by

$$kT_0 = \frac{h^2}{2m}\left(\frac{3n}{8\pi}\right)^{2/3}, \quad . \quad (3)$$

and the other letters have their usual significance. For such a gas the paramagnetic susceptibility is numerically three times the diamagnetic susceptibility and therefore predominates.

For the electrons in any actual metal, which are under the influence of the lattice field, the expressions for the two susceptibilities are naturally more complicated. In particular, the 3 : 1 ratio between them does not hold, and under special conditions the paramagnetic part of the susceptibility may become negligible in comparison with the diamagnetic part. When further, as in graphite, the metallic electrons can move about freely in a plane, and the freedom of movement is confined practically to the plane, the susceptibility along the normal to the plane will conform to equation (1) at high temperatures, and to (2) at low temperatures, the degeneracy temperature T_0 appearing in (2) being, however, much smaller than that given by (3) for electrons that are free to move in all directions.

These results have been verified in graphite. Its abnormal diamagnetism, which is confined to the direction of its hexagonal axis, conforms to equation (1) at high temperatures, and to (2) at low temperatures, with n corresponding to *one electron per carbon atom*, and $T_0 = 520°$ K.; at all temperatures (in the range investigated) the susceptibility per carbon atom is found to be the same as the diamagnetic susceptibility per electron of a Fermi free-electron gas the degeneracy temperature of which is 520° K. The theoretical values for the specific susceptibility (per gram) of graphite, χ, calculated on this basis, are represented by the accompanying curve, and it will be seen that the experimental values, which are denoted by circles, lie close to the curve[2]. The straight line which the curve tends to reach asymptotically at high temperatures is also drawn in the graph, and corresponds to equation (1).

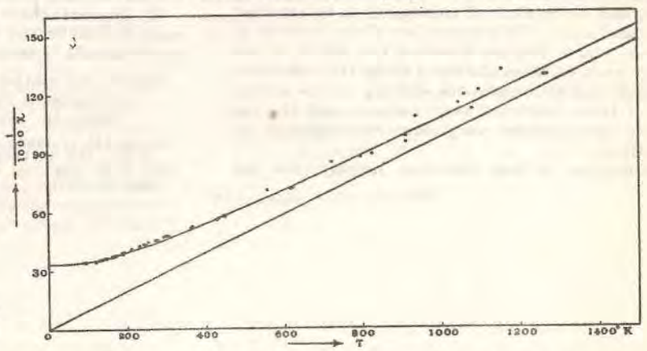

That one electron per carbon atom should be free to move about in the basal plane agrees with the known structure of graphite. There is a Brillouin zone which can just accommodate 3 electrons per atom, which is a flat hexagonal prism bounded by {000,2} and {$2\bar{1}\bar{1}$,0}, and the energy discontinuities across all the faces of the zone are large. There is a bigger zone bounded by {000,2} and {$2\bar{2}$0,0} which can just contain 4 electrons per atom, but the energy discontinuity across {$2\bar{2}$0,0} is small.

The agreement between the experimental data and the theoretical curve plotted in the graph may be regarded as a convincing demonstration of Landau's value for the diamagnetism of a free-electron gas, and of its temperature variation in accordance with the statistics of Fermi and Dirac.

K. S. KRISHNAN.

Indian Association for the
Cultivation of Science,
Calcutta.
Oct. 21.

[1] *Z. Phys.*, **64**, 629 (1930).

[2] The theoretical curve was plotted with the help of the tables for the Fermi-Dirac integrals given by Stoner, *Proc. Leeds Phil. Soc.*, **3**, 403 (1938). The experimental values are from the measurements by Krishnan and Ganguli, *Z. Krist.*, A, 100, 530 (1939), and some unpublished measurements by Ganguli.

Electronic Specific Heat of Graphite

In a previous communication[1] it was shown that the observed large diamagnetism of graphite along its hexagonal axis is that of its 'free' electrons, and is of the Landau type. At high temperatures it conforms to the Curie law $K = -n\mu^2/(3\ kT)$, and at low temperatures it tends to the temperature-independent value $K = -n\mu^2/(2\ kT_0)$, where n, the number of free electrons, is found to be just one per carbon atom, and T_0, the degeneracy temperature, is found to be about 520° K.; μ is the Bohr magneton.

These results fit well with the known electronic structure of graphite. From structural considerations we should expect one electron per carbon atom to be free, and its freedom of movement to be confined to the basal plane. This restriction of the freedom to the basal plane, besides directing the whole of the diamagnetism of these electrons along the normal to the plane, will also make the spacing of the energy levels of these electrons very narrow, and the degeneracy temperature very low, as required by observation.

This number of free electrons, namely, one per atom, together with the very low degeneracy temperature of the electron gas, should make the electronic specific heat of graphite at room temperature, and at low temperatures, much larger than that of most metals. Now the electronic contribution is most easily evaluated at very low temperatures, where the contribution from the lattice becomes relatively small. The available experimental data[2] for graphite extend down to about 29° K. only, and from these data the electronic part of the specific heat at low temperatures may be estimated roughly as 20×10^{-4} T. cal. deg.$^{-1}$ per gm. atom. This is more than ten times the electronic specific heat of copper or silver, and is of nearly the same magnitude as that of the transition metals, nickel, platinum and palladium.

It appears that even at 40° K. the electronic contribution to the specific heat of graphite greatly predominates over the contribution from the lattice.

K. S. Krishnan.

Indian Association for the Cultivation of Science,
Calcutta. Feb. 9.

[1] Nature, **145**, 31 (1940); see also presidential address to the Physics Section, Ind. Sci. Congress, Madras Session, 1940.

[2] Nernst, W., *Ann. Phys.*, **36**, 395 (1911); Magnus, A., *Ann. Phys.*, **303**, 70 (1923).

Dimorphism of Diphenyl Octatetraene Crystals

The crystal structures of the diphenyl polyenes, having the general formula 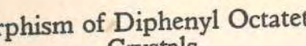 , have been studied by Hengstenberg and Kuhn[1] by X-ray methods. They find that while the lower members of the series, with $n = 1$ to 4, crystallize in the monoclinic system, the higher members studied by them, for which $n = 5$ to 7, crystallize in the orthorhombic system.

Recently, in the course of some electrical and optical measurements on this important series of compounds possessing conjugate double bonds, we had occasion to study the crystal structure of one of them, namely, diphenyl octatetraene, corresponding to $n = 4$. On allowing this substance to crystallize from its solution in acetic ether, we found that in addition to some flaky crystals which were monoclinic and had the axial dimensions described by Hengstenberg and Kuhn, there also appeared in the same crop stout well-developed crystals which were orthorhombic. The chemical identity of the two types of crystals is verified by the observation that both types appear in the crops obtained by the evaporation of the solutions in acetic ether of either of them separately.

n	a	b	c
	in A.		
5	10·25	7·66	21·2
6	10·20	7·60	23·58
7	10·2	7·57	25·95

The orthorhombic crystal belongs to the bipyramidal class, and its unit cell has the dimensions $a = 9{\cdot}95$, $b = 7{\cdot}55$, $c = 19{\cdot}75$ A., and contains 4 molecules of 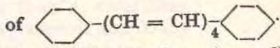 . These dimensions fit well with the dimensions of the unit cells of the higher members of the series—all of which contain 4 molecules—obtained by Hengstenberg and Kuhn, and reproduced in the accompanying table.

K. S. Krishnan.
S. L. Chorghade.
T. S. Ananthapadmanabhan.

Indian Association for the Cultivation of Science,
Calcutta.
June 15.

[1] *Z. Kristallog.*, A, **75**, 301 (1930).

ON AN ORTHORHOMBIC CRYSTALLINE MODIFICATION OF DIPHENYL OCTATETRAENE.

By K. S. KRISHNAN, S. L. CHORGHADE and T. S. ANANTHAPADMANABHAN.

Received 4th September, 1940.

The diphenyl polyenes, having the general formula

$$C_6H_5—(CH=CH)_n—C_6H_5,$$

with alternate single and double bonds in the central chain, are an interesting class of compounds from many different points of view. The crystal structures of several of them have been studied by X-ray methods by Hengstenberg and Kuhn,[1] who find that while the earlier members of the series, namely those for which $n = 1$ to 4, crystallise in the monoclinic system, the higher members investigated by them, namely those for which $n = 5$ to 7, crystallise in the orthorhombic system. Recently while crystallising some diphenyl octatetraene (the compound with $n = 4$) from its solution in ethyl acetate, there appeared in the crop, along with the many flaky crystals, which were monoclinic and had the axial dimensions given by Hengstenberg and Kuhn, also several thick

[1] *Z. Kristallog. A*, 1930, **75**, 301.

plates, which were found to be orthorhombic and to belong to the same series in which the higher polyenes, with n greater than 4, crystallise. In the present paper * is given an account of some goniometric and X-ray studies on this orthorhombic modification of diphenyl octatetraene.

Preparation of Diphenyl Octatetraene and its Identification.

The compound was prepared by the method described by Kuhn and Winterstein,[2] namely by the condensation of cinnamaldehyde with succinic acid in the presence of lead monoxide, and purified by repeated crystallisations. The substance is golden yellow and can be crystallised from solutions in any of the usual organic solvents. The crop of crystals obtained from a solution in ethyl acetate contains, as we mentioned just now, both the monoclinic (usually large and flaky) and the orthorhombic (usually stout and well-developed) varieties. The crystals obtained from a solution in benzene, or in ethyl acetate to which has been added some benzene, are predominantly of the monoclinic variety, whereas those obtained from a solution in chloroform are predominantly of the orthorhombic variety. The chemical identity of the two types of crystals is verified by the observation that starting from either type of crystals one can obtain, by dissolving in suitable solvents and recrystallising, both the types. The monoclinic crystals had a melting-point of 227° C., which agrees well with the value 232° C. given by Kuhn and Winterstein. The orthorhombic crystals too had practically the same melting-point, namely 226° C.

Both the varieties answered to the following chemical tests given by Kuhn and Winterstein. When melted with *s*-trinitrobenzene, they gave a reddish brown solution, and with cold concentrated sulphuric acid they gave a violet colour, which after some time deepened to dark pink. Further a solution in chloroform was found to decolourise a dilute solution of bromine in chloroform, as should be expected from the presence of double bonds in the molecule.

Finally, an X-ray analysis of the flaky crystals, by the rotation method, gave the following dimensions for the unit cell :

$$a = 6{\cdot}24,\ b = 7{\cdot}42,\ c = 16{\cdot}09\ \text{A},\ \beta \sim 90°,$$

which agree well with the dimensions

$$a = 6{\cdot}25,\ b = 7{\cdot}44,\ c = 16{\cdot}03\ \text{A},\ \beta \sim 90°$$

obtained by Hengstenberg and Kuhn. The cell contains 2 molecules of $C_6H_5—(CH=CH)_4—C_6H_5$.

Orthorhombic Modification : Goniometric Measurements.

The stout, well-developed crystals of diphenyl octatetraene, were measured goniometrically, and were found to belong to the orthorhombic bipyramidal class, having the axial elements

$$a : b : c = 1{\cdot}319 : 1 : 2{\cdot}615.$$

The crystals were thick plates parallel to {001}, with the side faces {010}, {012} and {111} also well-developed. The measured angles between the various faces are given in Table I, along with the angles calculated from the above axial ratios for comparison.

TABLE I.

	Measured.	Calculated.
(111) : (001)	73° 3′	—
(111) : (010)	40 20	—
(111) : (1$\bar{1}$1)	80 40	80° 41′
(111) : ($\bar{1}$11)	70 41	70 36
(111) : (11$\bar{1}$)	33 54	33 53
(012) : (001)	52 29	52 36

* A preliminary note appeared in *Nature*, 1940, **146**, 333.

[2] *Helv. Chim. Acta*, 1928, **11**, 87.

KRISHNAN, CHORGHADE, ANANTHAPADMANABHAN

Orthorhombic Modification : X-ray Studies.

Rotation photographs taken about the *a*, *b*, and *c* axes gave the following dimensions for the unit cell :

$$a = 9{\cdot}95,\ b = 7{\cdot}55,\ c = 19{\cdot}75\ \text{A},$$

which bear the ratios

$$a : b : c = 1{\cdot}318 : 1 : 2{\cdot}616,$$

which are almost the same as the goniometric ratios. The density of the crystal, as measured by the flotation method, was 1·140 g./c.c., and it corresponds to 4 (3·95) molecules of C_6H_5—(CH=CH)$_4$—C_6H_5 in the unit cell.

Comparison of the Unit Cell Dimensions with those of the Higher Polyenes.

The above cell dimensions fit well with the dimensions of the unit cells of the higher members in the series, as will be seen from the following table. The number of molecules in the unit cell is 4 in all the crystals. Thus diphenyl octatetraene is dimorphous, and one of the modifications belongs to the monoclinic system, in which the earlier members of the diphenyl polyenes crystallise, and the other to the orthorhombic series to which the higher members belong. We are now studying the crystal structures of the adjacent members in the polyene series, namely those for which $n = 3$ and 5 respectively, to find whether they too exhibit similar dimorphism and appear in both the monoclinic and the orthorhombic modifications.

TABLE II.

n.	*a* (A).	*b* (A).	*c* (A).
4	9·95	7·55	19·75
5	10·25	7·66	21·2
6	10·20	7·60	23·58
7	10·2	7·57	25·95

Summary.

The crystal structures of the diphenyl polyenes having the general formula C_6H_5—(CH=CH)$_n$—C_6H_5 have been studied before, by Hengstenberg and Kuhn, and it is known that while the earlier members in the series with $n = 1$ to 4 crystallise in the monoclinic system, the higher members studied by them crystallise in the orthorhombic system. In the present paper it is shown that diphenyl octatetraene (the compound with $n = 4$) is dimorphous ; it crystallises not only in the monoclinic system, as the earlier members do, but also in the orthorhombic system in the same series as the higher members.

Indian Association for the
Cultivation of Science, Calcutta.

Magnetic and Thermal Properties of Crystalline Copper Sulphate at Low Temperatures

THE principal magnetic susceptibilities of crystalline copper sulphate ($CuSO_4.5H_2O$) have been measured from room temperature down to about 90° K.[1]. From a detailed analysis of these magnetic data, Jordahl[2] finds that they can be explained quantitatively on the assumption that the crystalline electric field in the neighbourhood of the Cu++ ion in the crystal is predominantly cubic in symmetry, with a small tetragonal component superposed on it. The ground state of the Cu++ ion is ^2D, and the crystalline field postulated is such that under the influence of its cubic part the energy levels split up into two sets, the lower set having a two-fold *orbital* degeneracy, and the upper a three-fold one, the separation between the two sets being about 18,300 cm.$^{-1}$; the tetragonal part of the field separates the levels of either set by about 2,550 cm.$^{-1}$. Each of these separated levels will have a two-fold *spin* degeneracy, which, being of the Kramers type, will not be removed by the crystalline field.

The type of crystalline field postulated above for explaining the magnetic data appears, from the known structure of the crystal[3], to be plausible. Each copper atom in the crystal is surrounded by 6 oxygen atoms, 4 of which belong to 4 water molecules forming a square with the copper atom at the centre, and the other two belong respectively to two SO_4 groups, and are located centrally above and below the square. The copper-oxygen distance for the 4 water oxygens is about 2·0 A., and for the other two about 2·4 A.

The splitting of the ^2D levels of Cu++ that would occur in the above field cannot, however, be reconciled with two important observations made recently at the Mond Laboratory in Cambridge. Ashmead[4] has observed that the specific heat of $CuSO_4.5H_2O$ shows a maximum in the region of liquid helium temperatures, and Reekie[5] has found that the effective magnetic moment of Cu++, deduced from susceptibility measurements on the powdered crystal, falls rapidly in the same temperature region. These observations indicate that there are two low-lying energy levels for the paramagnetic ion in the crystal, separated by a few cm.$^{-1}$, the lower of which is non-magnetic. The pattern of splitting of the ^2D levels contemplated above cannot be made to conform to these requirements.

A closer examination of the structure of the crystal, however, suggests a simple explanation. The distance between the copper atom and the 4 water oxygens, namely 2·0 A., is much smaller than would correspond to an ionic binding between Cu++ and these oxygens, and is just the distance that one should expect for a *covalent* type of binding between them. Such a planar quadri-covalent binding is indeed common in the cupric salts[6]. Such a binding, according to Pauling's theory of directed valence, will involve the orbitals dsp^2, and the odd electron in Cu++ displaced from the 3*d* orbital will now occupy the 4*p* orbital. The ground state of the $[Cu(H_2O)_4]$++ complex will thus be a $^2\Pi$ state, and the magnetic properties of the complex will, therefore, be somewhat similar to those of the nitric oxide (NO) molecule, which have been investigated theoretically in detail by Van Vleck[7] and are well known. If the coupling between the spin moment and the component of the orbital moment conserved along the normal to the plane of the complex is very weak, and of the order of a few cm.$^{-1}$ (as against 121 cm.$^{-1}$ in NO), and the antiparallel coupling between them corresponds as usual to the smaller energy, then the results obtained by Reekie and Ashmead will follow naturally.

The experimental finding[4] that the *orbital* contribution to the magnetic moment of the $[Cu(H_2O)_4]$++ complex is directed predominantly along the normal to the plane of the complex is significant.

K. S. KRISHNAN.

Indian Association for the
Cultivation of Science,
Calcutta.
Nov. 18.

[1] Krishnan and Mookherji, *Phys. Rev.*, **54**, 841 (1938).
[2] Abstract published in *Phys. Rev.*, **57**, 349 (1940).
[3] Beevers and Lipson, *Proc. Roy. Soc.*, A, **146**, 570 (1934).
[4] NATURE, **143**, 853 (1939).
[5] *Proc. Roy. Soc.*, A, **173**, 367 (1939).
[6] See Pauling, "Nature of the Chemical Bond" (Cornell Univ. Press, 1939), p. 100.
[7] See Van Vleck, "Theory of Electric and Magnetic Susceptibilities", (Oxford Univ. Press, 1932), p. 269.

The magnetic and other properties of the free electrons in graphite

By N. Ganguli and K. S. Krishnan, F.R.S.

Indian Association for the Cultivation of Science, Calcutta

(*Received* 16 *August* 1940)

1. Graphite crystals have a large free-electron diamagnetism, which is directed almost wholly along the hexagonal axis. Over the whole range of temperature over which measurements have been made, namely, from 90 to 1270° K, this free-electron diamagnetism of graphite per carbon atom is found to be equal to the Landau diamagnetism per electron of a free-electron gas obeying Fermi-Dirac statistics and having a degeneracy temperature of 520° K.

2. From this experimental result it is concluded (*a*) that the number of free or mobile electrons in graphite is just one per carbon atom; (*b*) that the effective mass of these electrons for motion in the basal plane is just their actual mass, showing that the movements in this plane are completely free and uninfluenced by the lattice field; (c) that on the other hand their effective mass for motion along the normal to the basal plane is enormous, about 190^3 times the actual mass, which indicates that the mobile electrons belonging to any given basal layer of carbon atoms are tightly bound to the layer, though, according to (*b*), they can migrate quite freely over the whole of the layer; (*d*) that this tight binding accounts for the observed low degeneracy temperature of the electron gas in the crystal.

3. The electron gas in graphite thus conforms to a simple model which is easily amenable to theoretical treatment, and it has a low degeneracy temperature which is conveniently accessible for experimenting. It therefore forms a suitable medium for studying the properties of an electron gas.

4. The conclusions stated in 2 are in accord with the quantal views of the electronic structure of graphite, and also with its Brillouin zones. There is one zone which can just accommodate three electrons per atom, and the energy discontinuities at all of its boundary surfaces are large. There is a bigger zone which can just accommodate all the four valency electrons, but the energy discontinuities at those of its faces that are perpendicular to the basal plane are very small.

1. Introduction

As is well known, graphite crystals exhibit an abnormal diamagnetism, directed almost wholly along the hexagonal axis of the crystal, and having a large temperature coefficient. This diamagnetism is evidently due to the presence of 'free' electrons in the crystal, and a detailed study of the diamagnetism should enable us to obtain at least some of the general

characteristics of these free electrons. In the present paper is given a discussion of the diamagnetism of graphite from this point of view, and it is found that the magnetic data indeed reveal all the main features of the free electron gas in the crystal. For example, it is found that the number of free electrons is just one per carbon atom, that under the influence of the lattice field the movements of these electrons along the normal to the basal plane are severely restrained, whereas their movements in the basal plane remain almost completely free, and lastly, that as a result of the restraint imposed on the movements along the former direction, and the peculiar structure of the Brillouin zones of the crystal, the degeneracy temperature of the electron gas becomes very low indeed, sufficiently low to be easily accessible for experimenting in the laboratory.

This simple picture of the free electron gas in graphite revealed by the magnetic data naturally makes graphite a very suitable medium for studying in general the properties of an electron gas. An account of some of these studies will be given in Part II.

2. The magnetic properties of a free-electron gas

It was discovered by Landau (1930) that an electron gas should have, besides its spin-paramagnetism, an appreciable diamagnetism also, superposed on it, due to the quantized orbital motions of the electrons in the magnetic field. For a *free*-electron gas both the diamagnetic and the paramagnetic susceptibilities are easily calculated. Neglecting terms that are dependent on the magnetic field, the diamagnetic susceptibility per unit volume of the gas is given by the expression (see Stoner 1935)

$$K_d = -\frac{n\mu^2}{3kT}\frac{F'(\eta)}{F(\eta)}, \tag{1}$$

where n is the number of electrons per unit volume, μ is the Bohr magneton,

$$F(\eta) = \int_0^\infty \frac{x^{\frac{1}{2}}\,dx}{e^{x-\eta}+1}, \tag{2}$$

$$F'(\eta) = \frac{\partial}{\partial\eta}F(\eta), \tag{3}$$

$$= \frac{1}{2}\int_0^\infty \frac{x^{-\frac{1}{2}}\,dx}{e^{x-\eta}+1},$$

$$\eta = \zeta/kT, \tag{4}$$

ζ being the thermodynamic potential per electron. k and T have their usual significance.

The numerical values of $F(\eta)$ and $F'(\eta)$ for different values of η can be obtained from the tables for Fermi-Dirac integrals given by McDougall and Stoner (1938).

To the same approximation, the paramagnetic susceptibility per unit volume is given by

$$K_p = \frac{n\mu^2}{kT}\frac{F'(\eta)}{F(\eta)}, \tag{5}$$

which is just three times the diamagnetic susceptibility.

The resultant susceptibility, namely, $K = K_p + K_d$, will therefore be paramagnetic.

Let us define the degeneracy temperature T_0 of the gas by the usual expression

$$T_0 = \zeta_0/k \tag{6}$$

$$= \frac{h^2}{2mk}\left(\frac{3n}{8\pi}\right)^{\frac{2}{3}}, \tag{7}$$

where ζ_0 is the value of ζ at the absolute zero of temperature, or the maximum kinetic energy of an electron in the gas when it is completely degenerate. At very high temperatures, $T \gg T_0$, F'/F tends to reach asymptotically the value 1, and the two susceptibilities will then conform to the Curie laws

$$K_d = -\frac{n\mu^2}{3kT} \quad \text{and} \quad K_p = \frac{n\mu^2}{kT}, \tag{8}$$

respectively. At very low temperatures, $T \ll T_0$, the expressions for the two susceptibilities will reduce to the temperature-independent values

$$K_d = -\frac{n\mu^2}{2kT_0} \quad \text{and} \quad K_p = \frac{3n\mu^2}{2kT_0}. \tag{9}$$

3. Effect of the lattice field

When the electrons are not quite free, but are under the influence of the lattice field, as the conduction electrons in any actual metal are, the expressions for the two susceptibilities, particularly for the diamagnetic susceptibility, will naturally be complicated. But in the special case, which is of practical interest, when the surfaces of constant energy of these

electrons in k-space* may be represented by the family of similar ellipsoids,

$$E = \frac{h^2}{2m}(\alpha_1 k_x^2 + \alpha_2 k_y^2 + \alpha_3 k_z^2), \tag{10}$$

the two susceptibilities can be evaluated easily (see Mott and Jones 1936, chap. VI, § 6.2). We shall take the number of electrons per unit volume of this gas also to be n, and denote the various quantities relating to this gas by the same letters as for the free-electron gas, but with the subscript g attached to them.

The degeneracy temperature T_{0g} of this gas can be shown to be related to that of a free-electron gas of the same density by the equation

$$T_{0g} = T_0(\alpha_1\alpha_2\alpha_3)^{\frac{1}{3}}. \tag{11}$$

The effect of the lattice field is thus to increase the degeneracy temperature by a factor $(\alpha_1\alpha_2\alpha_3)^{\frac{1}{3}}$. Its effect on the paramagnetism of the electron gas, given by expression (5), will therefore be to increase the argument in the functions F' and F from η to η_g, where

$$\eta_g = \eta(\alpha_1\alpha_2\alpha_3)^{\frac{1}{3}} = \frac{\zeta}{kT}(\alpha_1\alpha_2\alpha_3)^{\frac{1}{3}}. \tag{12}$$

At high temperatures, $T \gg T_{0g}$, the paramagnetic susceptibility will thus be the same as for a free-electron gas of the same density, namely,

$$K_{pg} = \frac{n\mu^2}{kT}. \tag{13}$$

At low temperatures, $T \ll T_{0g}$, when the gas is completely degenerate,

$$K_{pg} = \frac{3n\mu^2}{2kT_{0g}} \tag{14}$$

$$= \frac{3n\mu^2}{2kT}(\alpha_1\alpha_2\alpha_3)^{-\frac{1}{3}}, \tag{15}$$

as compared with the value

$$K_p = \frac{3n\mu^2}{2kT_0}$$

for a free-electron gas of the same density.

Considering next the effect of the lattice field on the diamagnetism of these electrons, we may notice here that the effect is two-fold. The first is due to the increase in the degeneracy temperature, by the factor $(\alpha_1\alpha_2\alpha_3)^{\frac{1}{3}}$, and will

* k is here taken to be equal to $1/\lambda$, where λ is the electronic wave-length.

be similar to the effect of the lattice field on the paramagnetism of the gas. The second is more direct and arises from the fact that the kinetic energies of the electrons conform to equations of the type (10), which shows that the electrons behave as though their 'effective masses' were $m/\alpha_i (i = 1, 2, 3)$, instead of m. This will be so in the equations of motion of the electrons in the magnetic field also. Taking the direction of the magnetic field to be along the z-axis of the energy ellipsoid, the equations of motion of the electrons in the xy-plane will thus differ from the equations for free electrons in having an effective magnetic moment $\mu_g = \mu(\alpha_1\alpha_2)^{\frac{1}{2}}$, in the place of μ for the free electrons. The diamagnetic susceptibility along the z-axis will therefore be given by

$$K_{dg} = -\frac{n\mu_g^2}{3kT}\frac{F'(\eta_g)}{F(\eta_g)}$$

$$= -\frac{n\mu^2}{3kT}\frac{F'(\eta_g)}{F(\eta_g)}\alpha_1\alpha_2, \tag{16}$$

where η_g has the value (12). Hence at high temperatures, $T \gg T_{0g}$,

$$K_{dg} = -\frac{n\mu^2}{3kT}\alpha_1\alpha_2, \tag{17}$$

and at low temperatures, $T \ll T_{0g}$,

$$K_{dg} = -\frac{n\mu^2}{2kT_{0g}}\alpha_1\alpha_2 \tag{18}$$

$$= -\frac{n\mu^2}{2kT_0}\left(\frac{\alpha_1^2\alpha_2^2}{\alpha_3}\right)^{\frac{1}{3}}. \tag{19}$$

On comparing (17) with (13), and similarly (18) with (14), it will be seen that the ratio of the diamagnetic to the paramagnetic susceptibility is no longer equal to $\frac{1}{3}$, but is equal to $\frac{1}{3}\alpha_1\alpha_2$. When $\frac{1}{3}\alpha_1\alpha_2$ is very large, the paramagnetic part of the susceptibility will become relatively insignificant.

4. Graphite a suitable crystal for studying the properties of an electron gas

The conditions obtaining in the crystal of graphite, as we shall see presently, are exceptionally favourable for verifying some of the results given in the previous section. Graphite, as is well known, is a hexagonal crystal, with a perfect basal cleavage. The carbon atoms in it are arranged in layers parallel to the basal plane, the atoms in each layer forming a regular

hexagonal network. The distance of separation between adjacent layers is 3·40 A, which is much larger than the distance between adjacent atoms in the same layer, namely, 1·42 A, which shows that the binding between adjacent layers is extremely loose, and is probably of the van der Waals type.

The diamagnetic properties of this crystal have been studied by us in detail in some recent papers (1934, 1937, 1939). The specific susceptibility per g. of the crystal perpendicular to the hexagonal axis, $\chi_\perp$, is about $-0{\cdot}5 \times 10^{-6}$, which is nearly that of diamond. On the other hand, the susceptibility along the hexagonal axis, $\chi_\parallel$, is numerically very large, and it varies much with temperature. At room temperature $\chi_\parallel$ is about $-21{\cdot}5 \times 10^{-6}$ per g., and is thus more than 40 times $\chi_\perp$.

The abnormal part of the susceptibility of graphite, which we may take as equal to $\chi_\parallel - \chi_\perp$, and which we shall denote by χ_e, appears to be the contribution from the free or the mobile electrons in graphite. We shall assume that it is so, and further that an explanation can be found for the absence of a paramagnetic contribution from these electrons. The experimental finding that χ_e is directed wholly along the normal to the basal plane then indicates that the mobility of these electrons is practically confined to the basal plane. Adopting the language of the Bloch theory this would mean, in view of the layered structure of graphite, that the mobile electrons belonging to any given layer of carbon atoms, parallel to the basal plane, are tightly bound to the layer, the probability of their migrations to the adjacent layers being very small. This is indeed to be expected from the large separation, which we referred to just now, between adjacent layers, and the looseness of the binding between them.

Though the mobile electrons belonging to any given basal layer are tightly bound to the layer, the magnetic data require, as we found just now, that there should be large movements of these electrons in the plane of the layer. The magnetic data further require, as we shall find in § 6, that these movements in the basal plane should be *completely* free, i.e. quite uninfluenced by the lattice field.

We thus have in graphite a particularly simple model of an electron gas, the electrons behaving in their movements in the basal plane as though they were completely free, and in their movements perpendicular to the plane as though they were tightly bound. Moreover, as we shall again find in § 6, the number of mobile electrons is just one per carbon atom, and this finding further enhances the simplicity of the model.

Now the observed large temperature variation of χ_e shows that the electron gas in graphite should have, in spite of its large density, a low degeneracy temperature. This result, as we shall show in § 8, is a consequence

of the tight binding of the electrons along the hexagonal axis, and the peculiar structure of the Brillouin zones of the crystal.

The electron gas in graphite, conforming as it does to a simple model which is amenable to easy theoretical treatment, and having a low degeneracy temperature which is conveniently accessible in the laboratory, offers a very suitable medium for studying the magnetic and other properties of an electron gas.

5. The magnetic data for graphite

Detailed measurements of the temperature variation of the diamagnetic anisotropy of graphite, namely, $\chi_\parallel - \chi_\perp$, denoted by χ_e, from the temperature of liquid oxygen to about 1270° K, were given by us in a previous paper (1939). These data need some supplementing. In the first place there was a gap between 90 and 130° K in the low temperature measurements, since we used a liquid bath of light petroleum ether for maintaining steady temperatures in the cryostat, and the liquid became too viscous for use below about 130° K. The only temperature lower than this, at which measurements were made, was that of liquid oxygen itself. The region included between these two temperatures is rather important, since $\chi_\parallel - \chi_\perp$ is almost independent of temperature at 90°, while at 130° it has a large temperature coefficient. We have now made measurements in this region, with a new type of cryostat* in which the use of a liquid bath for maintaining steady temperatures is eliminated altogether.

Secondly, the high temperature measurements were made previously inside a furnace from which oxygen from air could not be wholly excluded. There was consequently a slight oxidation of the graphite crystal at high temperatures. Immediately after each magnetic measurement, the crystal was quickly cooled and its mass determined; this was taken to be the mass of the crystal when the measurement at the high temperature was made. This would make the numerical values of $\chi_\parallel - \chi_\perp$ reported before for the highest temperatures slightly too high. We have now repeated these measurements in an air-tight furnace in an atmosphere of nitrogen, and under these conditions there was no detectable change in the crystal even at the highest temperatures. These new values of $\chi_\parallel - \chi_\perp$ are found to differ only slightly from the old values, and both the sets of values are included in the present paper.

* We wish to express here our thanks to Mr Akshayananda Bose for designing the cryostat. A detailed description of the apparatus will be published by him elsewhere.

6. Discussion of the magnetic data

Plotting the values of $\chi_\parallel - \chi_\perp = \chi_e$ per gram of graphite against the reciprocal of the temperature, we find (see figure 1) that at high temperatures the susceptibility tends to reach asymptotically the value

$$\chi_e = -0{\cdot}010/T,$$

and at low temperatures it tends to reach the temperature-independent value

$$\chi_e = -30 \times 10^{-6},$$

and the curve in general resembles closely the theoretical susceptibility curve for a free-electron gas whose energy distribution conforms to Fermi-Dirac statistics.

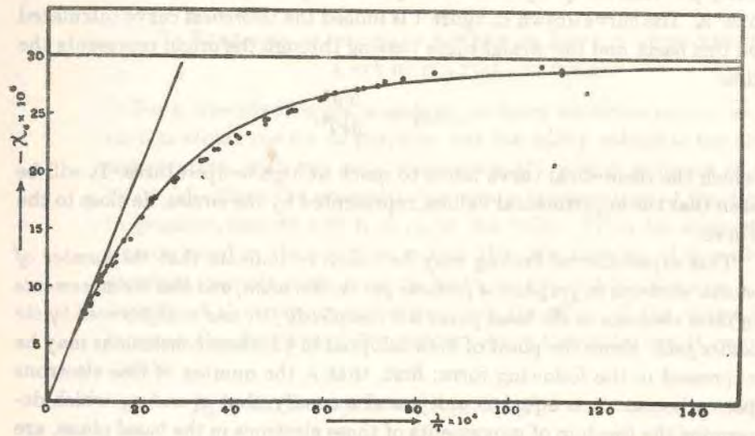

Figure 1

On more detailed examination of the curve we find that the high temperature values, namely, $\chi_e = -0{\cdot}010/T$, conform closely to the formula

$$A\chi_e = -\frac{0{\cdot}12}{T} = -\frac{N\mu^2}{3kT}, \tag{20}$$

where A is the atomic weight of carbon and N is the Avogadro number.*

* We may mention here that the volume susceptibility K and the specific susceptibility χ are connected by the relation

$$K/n = A\chi/N. \tag{20a}$$

Similarly the temperature-independent value of χ_e at low temperatures conforms to the formula

$$A\chi_e = -360 \times 10^{-6} = -\frac{N\mu^2}{2kT_{0g}}, \tag{21}$$

where T_{0g} has the value 520° K. At all temperatures, in the range investigated, the curve is found to fit well with the formula

$$A\chi_e = -\frac{N\mu^2}{3kT}\frac{F'(\eta)}{F(\eta)}, \tag{22}$$

in which the value of η is the same as for a free-electron gas whose degeneracy temperature is 520° K. In other words, *the observed electronic susceptibility of graphite per carbon atom is the same as the Landau susceptibility per electron of a free-electron gas having a degeneracy temperature of* 520° K. The curve drawn in figure 1 is indeed the *theoretical* curve calculated on this basis, and the straight line passing through the origin represents the line

$$A\chi_e = -\frac{N\mu^2}{3kT},$$

which the theoretical curve tends to reach at high temperatures. It will be seen that the experimental values, represented by the circles, lie close to the curve.

This experimental finding may be taken to indicate that *the number of mobile electrons in graphite is just one per carbon atom, and that the movements of these electrons in the basal plane are completely free and uninfluenced by the lattice field*. From the point of view adopted in § 3, these conclusions may be expressed in the following form: first, that ν, the number of free electrons per carbon atom, is equal to unity, and secondly, that α_1 and α_2, which determine the freedom of movements of these electrons in the basal plane, are also equal to unity.

It should be mentioned immediately that these conclusions do not follow *uniquely* from the magnetic data. On comparing the experimental relations (20) and (21) with the theoretical relations (17) and (18) respectively, and in view of (20*a*), one can see that the experimental data merely require that

$$\nu\alpha_1\alpha_2 = 1. \tag{23}$$

The obvious conclusion that we drew from the magnetic data in the previous paragraph, namely, that

$$\nu = 1 \quad \text{and} \quad \alpha_1 = \alpha_2 = 1, \tag{24}$$

is only a particular solution. This solution, however, appears from other considerations to be the most probable one. For example, it fits well with the modern quantal views regarding the electronic structure of aromatic molecules in general, and of graphite in particular—indeed each layer of carbon atoms in graphite may be regarded as a giant aromatic molecule—according to which one electron per carbon atom is free to migrate from atom to atom over the whole condensed network. Incidentally such a migration is also the solution for the sixty-year-old controversy regarding the location of the extra bonds in the benzene ring—the bonds are not localized at all! (Ingold 1938).

7. Surfaces of constant energy in k-space approximately a set of coaxial cylinders

For a free-electron gas containing as many electrons per c.c. as there are carbon atoms per c.c. of graphite, one can easily calculate the degeneracy temperature, with the help of equation (7), and it is found to be about 98,000° K. Now the observed degeneracy temperature of the electron gas in graphite, namely 520° K, is $\frac{1}{190}$ of this value. From the magnetic data it was deduced in the previous section that the number of free electrons in graphite, namely ν per atom, is given by the relation $\nu\alpha_1\alpha_2 = 1$. For this density of electrons, remembering that the effect of the lattice field is to increase the degeneracy temperature by a factor $(\alpha_1\alpha_2\alpha_3)^{\frac{1}{3}}$ (see (11)), we obtain

$$T_{0g} = 520° = 98{,}000° \times \nu^{\frac{1}{3}} \times (\alpha_1\alpha_2\alpha_3)^{\frac{1}{3}}, \quad \text{or} \quad \alpha_1\alpha_2/\alpha_3 = 190^3, \tag{25}$$

which indicates a very high eccentricity for the ellipsoidal surfaces of constant energy in the k-space. Indeed the eccentricity is so large that one may regard these surfaces as a set of coaxial cylinders, with their common axis along the 'c' axis of the crystal.

Now the 'effective mass' of an electron is $1/\alpha_i$ times the actual mass, where α_1 has the value α_1 or α_2 for motion in the basal plane, and the value α_3 for motion perpendicular to the plane. The very large value of $\alpha_1\alpha_2/\alpha_3$ obtained in (25) indicates that the effective mass for motion perpendicular to the plane is enormous, as indeed it should be, because of the tight-binding of the mobile electrons to their respective layers. The effective mass for motion in the basal plane will be much smaller, and if we adopt the conclusion provisionally accepted in the previous section, namely $\alpha_1 = \alpha_2 = 1$, it will be just the actual mass.

8. Brillouin zones of graphite

We shall next consider these results in relation to the Brillouin zones in the crystal. The unit cell of graphite has the dimensions

$$a = 2{\cdot}46, \quad c = 6{\cdot}79\,\text{A},$$

and it contains four atoms of carbon. The structure factors for the various crystallographic planes are given in table 1 (see Mott and Jones 1936, p. 163).

Table 1

Plane	$\{1\bar{1}0, 0\}$	$\{2\bar{2}0, 0\}$	$\{2\bar{1}\bar{1}, 0\}$	$\{000, 1\}$	$\{000, 2\}$
S	1	1	4	0	4

The energy discontinuities across $\{000, 2\}$, and across $\{2\bar{1}\bar{1}, 0\}$ are the strongest. Let us consider the Brillouin zone in k-space (k is taken to be equal to $1/\lambda$, as before) bounded by these sets of planes. It will be a flat hexagonal prism of the second order, with its axis along 'c'. The height of the prism will be $2/c$, and its cross section, by the basal plane, will be a regular hexagon of side $2/(\sqrt{3}a)$ (see figure 2, the inner hexagon). The volume of this Brillouin

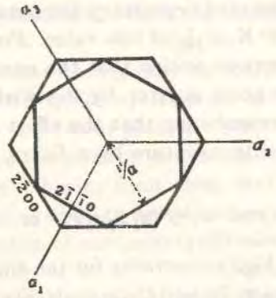

Figure 2

zone in the k-space will be $4\sqrt{3}/(a^2c)$. Since each unit volume in the k-space will correspond to two electrons per unit volume of graphite, and since the atomic volume of carbon in the crystal is $\sqrt{3}a^2c/8$, it can be readily seen that the above Brillouin zone can contain just three electrons per carbon atom.* The energy discontinuities at all the faces of the zone are large, and hence these three electrons in each carbon atom may be regarded as forming a closed group.

* The Brillouin zone described by Mott and Jones on p. 163 of their book is really this three-electron zone.

There is a bigger zone which can just accommodate all the four valency electrons of the carbon atom, namely, the one bounded by $\{000, 2\}$ and $\{2\bar{2}0, 0\}$. This zone also is a flat hexagonal prism, of the same height as before, but of the first order, whose cross-section is a hexagon of side $4/(3a)$ (the outer hexagon in figure 2). But the energy discontinuities across $\{2\bar{2}0, 0\}$, as will be clear from the values given in table 1, are small.

We mentioned just now that the three electrons per carbon atom that can be accommodated in the smaller Brillouin zone, whose bounding faces are all surfaces of large energy discontinuity, may be regarded as forming a closed group. The remaining electrons, namely one per carbon atom, may occupy any of the outer zones. Using reduced wave numbers, it can be easily seen that there is much overlapping of these zones into one another, and on this account the maximum kinetic energy of the electrons will be much smaller than it would be otherwise. Further, in view of the small value of α_3 (which is only $1/190^2$ of $\alpha_1\alpha_2$), the electrons will take up all the permitted values of k_z in the zones under consideration right up to the boundary surface parallel to the basal plane. For the same reason, neither k_x nor k_y will reach high values; in other words, along the x and y directions the zones will be 'nearly empty'. In terms of the Brillouin zones, one thus gets a natural explanation why in spite of the large density of free electrons in graphite, namely one per atom, the degeneracy temperature is so low, and also why for motion in the basal plane (i.e. in the xy-plane) the electrons behave as if they were completely free, whereas for motion along the normal to the plane (i.e. along the z-axis) they behave as if they were tightly bound.

9. An alternative view of the free-electron diamagnetism of graphite

We have seen that a particularly simple solution of the experimental finding that $\nu\alpha_1\alpha_2 = 1$ is to put

$$\nu = 1 \quad \text{and} \quad \alpha_1 = \alpha_2 = 1,$$

and that this solution receives much support from general structural considerations, and also from a consideration of the Brillouin zones. Assuming, for the sake of argument, that this solution is not acceptable, the only other permissible solution seems to be to regard the larger Brillouin zone, which can accommodate all the four valency electrons, as the proper zone, and to attribute the diamagnetism to the few electrons that may overlap into the next zone. ν will then represent the number of such overlap electrons per atom, and will be much less than unity. The surfaces of constant energy in

the k-space in the region immediately outside any pair of parallel surfaces $\{2\bar{2}0, 0\}$ bounding the Brillouin zone may still be represented by ellipsoids of the type (10), the origin of the coordinate system being now taken at the surface. Taking the z-axis as before along the 'c' axis of the crystal, and the x-axis along the normal to the surfaces of energy discontinuity under consideration, it can be shown (see Mott and Jones 1936, p. 84) that both α_2 and α_3 should be of the order of unity, whereas α_1 should be very large; indeed the larger it is, the smaller is the energy discontinuity. The relation $\alpha_1\alpha_2/\alpha_3 = 190^3$ deduced from the observed degeneracy temperature of the electron gas in graphite will then give for α_1 the value

$$\alpha_1 \sim 190^3.$$

Such a large value of α_1 indicates an extremely small energy discontinuity at the surface, of the order of 10^{-4} or 10^{-5} electron volt, and this will be the case at all the $\{2\bar{2}0, 0\}$ faces of the four-electron Brillouin zone. We may then legitimately disregard these discontinuities altogether, regard the one electron per carbon atom that cannot be accommodated in the smaller Brillouin zone to be effectively free, and shift the origin of the coordinate system to the beginning of the one-electron zone. We will then have

$$\nu = 1, \quad \alpha_1 = \alpha_2 = 1, \quad \alpha_3 = 1/190^3.$$

This is precisely the first alternative view, which we had adopted.

In other words, in order to explain, on the second alternative view, the experimental finding that the number of electrons overlapping beyond the four-electron Brillouin zone bears a definite relation to the α's in the basal plane—the relation being $\nu\alpha_1\alpha_2 = 1$—the energy discontinuities across the $\{2\bar{2}0, 0\}$ planes have to be negligibly small. The existence of the discontinuities can then be ignored altogether, in which case the second alternative view reduces itself to the first. This is very gratifying.

10. Absence of spin-paramagnetism

Now we have to explain why the spin-paramagnetism of the free-electrons, which normally should have predominated over their diamagnetism, is practically absent. According to the second alternative view proposed in the preceding section, this is merely a consequence of the large value of $\alpha_1\alpha_2/3$, which, as we noticed in §3, represents the ratio of the diamagnetic to the paramagnetic susceptibility. But we have already preferred, on other grounds, the first alternative. The absence of paramagnetism has then to be explained in the following manner. Each permitted energy level of the

electron gas can accommodate, according to Pauli's exclusion principle, two electrons, with opposing spin moments. Under the conditions usually obtaining in an electron gas all the lower energy levels will be so occupied by electron pairs, but some of the higher energy levels, near about $\zeta_0 = kT_{0g}$, will be occupied by single electrons, and the higher the temperature the larger will be the number of such energy levels occupied by single electrons. In graphite, in order to explain the absence of paramagnetism, we have to assume that *all* the occupied energy levels are occupied each by a pair of electrons, and none of the levels by single electrons. This will be the case if there is some coupling between the opposite spin moments, and the energy of coupling is large in comparison with kT even at the higher temperatures of our measurement, and therefore large in comparison with kT_{0g} also. Such a pairing of the electron spins is indeed contemplated in the quantal theory of the mobile electrons in aromatic molecules.

In spite of such a coupling—which will result in an energy level being either occupied by an electron pair or not occupied at all—if the occupied energy levels are so closely spaced that they may be regarded as almost continuous (this condition is satisfied ordinarily), the energy distribution will be practically the same as when the spin-spin coupling is absent. The coupling will not therefore affect the diamagnetism of the electron gas, and the temperature variation of the diamagnetism will still be in accordance with the statistics of Fermi and Dirac, as is actually observed.

At sufficiently high temperatures, however, we should expect the paramagnetism to become more and more important relatively to the Landau diamagnetism of the electrons, and ultimately to predominate over the latter in the ratio of 3 : 1.

Thus in addition to the observed degeneracy temperature of 520° K, which when multiplied by k represents the maximum kinetic energy which an electron in the gas will have at very low temperatures, there must be another characteristic temperature T_s for the electron gas in graphite, much higher than 520° K, such that kT_s will represent the energy of dissociation of the components of a pair of electrons with opposite spins. The temperature T_s will be somewhat analogous to the Curie temperature of a ferromagnetic body.

11. The Landau diamagnetism and the Fermi-Dirac energy distribution of the electron gas

Treating the abnormal diamagnetism of graphite as the Landau diamagnetism of its electron gas, we found that the various results deduced

from the magnetic data are just what we should expect from other and independent considerations. Arguing conversely, we may regard the observed magnetic data for graphite, especially at very high and very low temperatures, at which the magnetic behaviour is particularly simple, as providing an experimental demonstration of Landau's value for the diamagnetism of an electron gas. The region that we have studied extends from the completely degenerate to the almost completely non-degenerate state; and includes in particular the region of transition from the one to the other. The close agreement between the theoretical curve plotted in figure 1, calculated on the basis that the energy distribution of the electrons is in accordance with Fermi-Dirac statistics, and the experimental values may therefore be regarded as verifying experimentally the Fermi-Dirac distribution over the whole range from temperatures very much lower than the degeneracy temperature to temperatures much higher than the latter. This is very gratifying, since ordinarily it is only the degenerate state that is accessible for experimenting, whereas for verifying the Fermi-Dirac distribution, it is the transition region between the degenerate and the non-degenerate states that is most interesting.

In conclusion we wish to express our thanks to Dr D. N. Wadia, Government Mineralogist at Ceylon, for his kind present of some of the graphite crystals with which the measurements described in this paper were made.

References

Ganguli, N. 1936 *Phil. Mag.* **21**, 355.
Ingold, C. K. 1938 *Proc. Roy. Soc.* A, **169**, 149.
Krishnan, K. S. 1934 *Nature, Lond.*, **133**, 174.
Krishnan, K. S. and Ganguli, N. 1937 *Nature, Lond.*, **139**, 155.
—— —— 1939 *Z. Kristallogr.* A, **100**, 530.
Landau, L. 1930 *Z. Phys.* **64**, 629.
McDougall, J. and Stoner, E. C. 1938 *Phil. Trans.* A, **237**, 67.
Mott, N. F. and Jones, H. 1936 *The theory of the properties of metals and alloys.* Oxford Univ. Press.
Stoner, E. C. 1935 *Proc. Roy. Soc.* A, **152**, 672.

PROCEEDINGS
OF THE
NATIONAL ACADEMY OF SCIENCES
INDIA
SECTION A

Volume 14] 1944 [Part 4

Investigations on the Resistivities of Binary Alloys
Part I. Order-Disorder Alloys of the CuZn Type under Equilibrium Conditions

By Professor K. S. Krishnan, F.R.S., and A. B. Bhatia
Physics Department, Allahabad University
(*Received September* 23, 1944)

1. Introduction

The electrical resistivity of a metal, as is well known, may be attributed to the scattering of the electron waves passing through it and representing the electric current, by the thermally agitated atoms of the metal (Frenkel 1928, 1936). The wave-length of these waves will be that corresponding to the Fermi surface of the free electrons in the metal, since it is only the electrons near the Fermi surface that can make collisions and thus take part in electrical conduction. On this view the calculation of the electrical resistivity of a metal reduces to the calculation of the attenuation coefficient due to scattering of these electron waves passing through the metal. In order to calculate the attenuation coefficient, one may adopt the same method as is usually employed to calculate the attenuation coefficient of light waves passing through a transparent medium due to scattering. If the scattered waves from the different atoms in the medium were of *random* phases, the attenuation coefficient μ would simply be equal to $\nu\sigma$, where ν is the number of atoms per unit volume, and σ is the scattering cross-section of an atom. In actual metals, however, in which the atoms are close-packed, the scattered waves from neighbouring atoms cannot be regarded as being of random phases. Even then the attenuation coefficient can be calculated on a phenomenological basis, by attributing the scattering to local fluctuations in density caused by thermal agitation. The calculation becomes particularly simple when the electronic wave-length λ is large in comparison with the interatomic distance. One can then divide the medium into volume elements whose linear dimensions are small in

comparison with λ, and which at the same time are large enough to contain a great number of atoms. The scattered waves from the different parts of any given volume element may then be taken to be all of the same phase, and the fluctuations in density occurring in different volume elements to be uncorrelated with one another. Under these conditions, and at temperatures T sufficiently above the Debye temperature to make the energy of thermal agitation proportional to T (for most metals this is so at room temperature), the attenuation coefficient will be given by the expression (Frenkel *loc. cit.*)

$$\mu = \nu^2 k T \beta . \sigma, \qquad .. \quad (1)$$

where k is the Boltzmann constant and β is the isothermal compressibility.*

Now the condition that λ must be large in order that μ may be given by (1) is not, however, stringent, as we shall show in the body of the paper ; λ may be just a few times the interatomic distance, and in crystalline media it need only be slightly greater than λ_0, where λ_0 is the longest wave-length for which a Bragg reflection from *any* set of reflecting planes in the crystal can occur in the backward direction. (λ_0 is equal to $2d_{110}$ in body-centred, and to $2d_{111}$ in face-centred, cubic crystals). In other words, in a crystal, the electronic wave-length corresponding to the Fermi surface of the free electrons need not be much longer than that corresponding to the sphere inscribed in the first Brillouin zone, in order that the simple expression for μ given above may hold. This is fortunate, since in good metals like the alkali and the noble metals, the electronic wave-length involved in conduction is of just this magnitude, being actually $1{\cdot}14\ \lambda_0$ in the alkali metals, which are body-centred cubic, and $1{\cdot}11\ \lambda_0$ in the noble metals, which are face-centred cubic.

The observed resistivities of the alkali and the noble metals are in accord with an attenuation coefficient given by (1), and a scattering cross-section σ of the order of πa^2, where a is the radius of the scattering atom ; which is reasonable, since we know from direct measurements on elastic scattering of slow electrons in rare gases that for electronic wave-lengths of the order of $2a$ the scattering cross-section is roughly of this magnitude (Mott and Massey 1933).

In the case of *light*-scattering by a binary mixture, it is wellknown that in addition to the density scattering referred to above, arising from the local fluctuations in the density of the mixture, there is an extra scattering due to the local fluctuations in concentration, which also are the result of thermal agitations, the concentration scattering becoming particularly conspicuous in the neighbourhood of the critical solution temperature of the mixture. Similarly in a binary alloy , since the electrical resistivity arises ultimately from the scattering of the electron waves in their passage through the medium, we should expect, in addition to the contribution to the resistivity from the density scattering, an extra contribution from the concentration scattering. This should be conspicuous when

* In any actual solid metal, even an isotropic one, the expression for μ involves not only the compressibility, but also the other elastic constants, and in a complicated manner. As we shall show in a separate communication, at least in the alkali and the noble metals, expression (1) is a good enough approximation.

the atoms of the two kinds that consititute the alloy are capable of exchanging freely their positions, i.e. in random alloys. In some alloys this tendency for the atoms of the two kinds to exchange their places is hampered by the presence of a finite ordering force, and the result will be the exhibition of the well-known order-disorder phenomena. In these alloys too there will be a concentration scattering which will be large when the degree of order is small, i.e. in the neighbourhood of the Curie temperature and at all higher temperatures.

Viewed on this basis, the well-known abnormal increase in the electrical resistance observed in such alloys as one approaches the Curie temperature from the low temperature side, is a natural consequence of the rapid increase of the concentration scattering in this region. On this basis the calculation of this extra resistance also turns out to be simple. All that one needs for such a calculation is to be able to evaluate the fluctuations in concentration. This can be done readily when once we have formulated the expression for the free energy of the alloy in terms of its concentration, and this formulation has already been done by earlier investigators (see Section 7 below).

The electrical resistivities of binary alloys, both of the order-disorder type and of the random type—the latter is merely a particular case of the former, namely with the Curie temperature very small or zero—are investigated in the present paper from this point of view. The various results obtained are discussed in detail in relation to the available experimental data. These data are extensive, and include among others those for (1) the order-disorder alloys CuZn (Steinwehr and Schulze 1934, Webb 1939), Cu_3Au (Sykes and Jones 1936), and CuAu (Kurnakow and Ageew 1931), over a wide range of temperatures on both sides of the Curie temperature ; (2) the same alloys at different concentrations in the ordered state (Webb 1939, Johansson and Lindo 1936), and CuAu alloys of different concentrations in the disordered quenched state (Johansson and Linde 1936) ; (3) numerous random alloys at various concentrations and temperatures (see International Critical Tables, Vol. VI, 1927). It is found that all the essential features in the electric behaviours of these alloys, and in particular the absolute value of the resistivity, and its dependence on the concentration of the alloy, its temperature, and the degree of order present, receive a natural and quantitative explanation on the basis of the proposed theory.

The usual method of calculating the resistivity of an alloy is based on the calculation of the perturbing potentials produced at the lattice sites under the actual conditions of thermal agitation and of distribution—either random (Nordheim 1931), or partially or completely ordered (Muto 1936), as the case may be—of the component atoms in the lattice of the alloy. The expression for resistivity deduced on this basis involves constants which are not easy to evaluate in terms of observable physical quantities. In the case of ordered alloys, attempts have also been made to connect empirically the extra resistivity due to alloying with the degree of order present in it (Bragg 1934).

In the present investigations, however, the extra resistivity due to alloying is attributed to the scattering due to local thermal fluctuations in the concentration of the alloy. These fluctuations, and also the equilibrium degree of order present, are both directly connec-

ted with the free energy of the alloy at the given temperature and concentration. The expression for electrical resistivity deduced on this basis involves only constants that can be directly evaluated in terms of observable physical quantities, and hence this method of approach gives us a better physical insight into the problem than the method of perturbing potentials. In some of its aspects it bears a close analogy to the well-known theory of light scattering in binary liquid mixtures of Einstein (1910) and of Raman and Ramanathan (1923).

Further in the case of ordered alloys the results obtained on this basis differ in some important respects from those obtained on the current theories. In a random binary alloy, i.e. an alloy for which the Curie temperature is zero, and the disordering is complete at all temperatures, the extra resistance due to alloying, which ultimately is due to the disorder, will naturally be independent of temperature. In an ordered alloy also, according to the current theories, when the temperature exceeds the Curie temperature and the long range order has become zero, the extra resistance, which according to these theories depends on the long range order alone, becomes temperature-independent. In other words, according to the current theories, the extra resistance of an alloy which does not exhibit any long range order, must be temperature independent, irrespective of whether the alloy is of the random type, or is of the order-disorder type and above the Curie temperature*. On the other hand, according to the theory developed here, it is only in the random alloy that the temperature coefficient of the extra resistance comes out to be zero, whereas in an order-disorder alloy above the Curie temperature, the coefficient remains not only finite, but large, and tends to zero at very high temperatures only. Indeed for order-disorder alloys above the Curie temperature, the extra resistance, as we shall see in the body of the paper, is a function of Θ/T, where Θ is the Curie temperature. Hence, given a binary alloy under *equilibrium conditions*, which is known to have no long range order, measurement of the temperature-coefficient of its extra resistance should enable us to estimate its Curie temperature, and in particular, if it is zero, to identify the alloy as a random alloy.

The present point of view is also helpful in understanding the effects of quenching on the electrical properties of alloys. The relaxation time corresponding to the thermal *oscillations* of the atoms about their mean positions is very small, whereas the relaxation time corresponding to the *migrations* of atoms between neighbouring lattice sites, as for example in order-disorder alloys, will be much larger, and under favourable conditions may be of the order of days or even weeks. The quenching effects, where present, will, therefore be confined to the part of the electrical resistance associated with the migrations of atoms between lattice sites as distinguished from the oscillations.

Part I of the present paper deals with the resistance properties of the CuZn type of order-disorder alloys, *under equilibrium conditions*, from the above point of view. The

* Except for a second order dependence due to the small change with temperature, of the perturbing potentials due to atomic oscillations.

resistivities of Cu_3Au, CuAu and other types, and those of random alloys, and also the effects of quenching and allied processes on the resistivites, will be dealt with in the succeeding Parts of the paper.

2. Even with the short electron waves involved in electrical conduction expression (1) for the attenuation coefficient shown to be applicable to crystals

As a preliminary to the discussion of the electrical resistivities of alloys on the basis of electronic scattering in the media, we shall consider those of pure metals. As is well known the specific resistance of a good metal like the alkali and the noble metals is given by

$$\rho = \frac{h}{n e^2 \lambda} \cdot \mu \qquad .. \quad (2)$$

where n is the effective number of free electrons per unit volume (one per atom for the alkali and the noble metals), e is the electronic charge and λ is the wave-length of the electron waves concerned in conduction, i.e. the wave-length corresponding to the Fermi surface, and given by

$$\lambda=(8\pi/3n)^{\frac{1}{3}}. \qquad .. \quad (3)$$

When λ is large in comparison with the interatomic distance, the calculation of μ, as mentioned in the Introduction, becomes simple. We may then divide the medium into volume elements whose linear dimensions are small in comparison with λ, and which at the same time contain a great many atoms each. Under these conditions (a) the scattered radiations from the different parts of any given volume element will all be in sensibly the same phase, and (b) the fluctuations in density occurring in the different volume elements will be uncorrelated with one another. μ will then be given by

$$\mu = \sum_v \overline{\Delta N^2} \cdot \sigma,$$

where $\overline{\Delta N^2}$ is the mean square of the deviation of the number of atoms in a volume element v containing on the average $N = v\nu$ atoms, and the summation extends to all the volume elements in unit volume. Confining ourselves to temperatures much higher than the Debye temperature such that the thermal energy is proportional to T, we have

$$\overline{\Delta N^2} / \bar{N}^2 = kT\beta/v.$$

Using this relation we obtain expression (1) for the attenuation coefficient, namely

$$\mu = \nu^2 kT\beta\cdot\sigma.$$

Now in the alkali and the noble metals the electronic wave-length λ concerned in conduction, and given by $\lambda=(8\pi/3n)^{1/3}$, is not really very large in comparison with the interatomic distance, being just 1.14 λ_0 for the alkali metals (body-centred cubic) and 1.11 λ_0 for the noble metals (face-centred cubic), where λ_0 is the wave-length corresponding to the sphere inscribed in the first Brillouin zone, as mentioned in the introduction ; λ_0 is equal to $2d_{110}$ in the former metals and to $2d_{111}$ in the latter metals. It is the main purpose of this

section to show that even with such short wave-lengths, it is possible to divide the crystal into volume elements satisfying both the requirements (a) and (b) stated above, and hence to calculate the attenuation coefficient due to scattering in terms of the density fluctuations in the simple manner indicated. The volume elements into which the crystal may be so divided are thin slabs parallel to the plane bisecting the direction of propagation of the electron waves and the particular direction of scattering under consideration, each slab being just one layer of atoms.

Detailed theoretical and experimental studies have been made on the effect of thermal agitations on the intensities of regular reflections of *X-rays* at the Bragg angles from crystal planes, in different orders of spectra (Bragg 1939). Considering any one such reflecting layer of atoms, the effect of the thermal agitations will be equivalent to a diffuseness, or spread of the atomic *centres* from their mean plane. One consequence of such a spread will be a diminution of the intensity of Bragg reflection, particularly in the higher orders of spectra, as compared with the corresponding intensity at low temperatures. Such a diminution has been observed. Assuming the thermal spread to be of the Gaussian type (Darwin 1914), the probability of finding an atom centre at a distance x from the mean plane, measured along the normal to the plane, will be given by $p_x=p_o e^{-x^2/\xi^2}$, where ξ is the distance at which, at the given temperature, p_x falls to $1/e$ of its value at $x=0$, and may therefore be taken as a measure of the amplitude of the thermal oscillations of the atom at that temperature. From the observed diminution of the intensities of the Bragg reflections with rise of temperature, it is possible to estimate ξ at any given temperature, and it is found that even at high temperatures ξ is only a small fraction of the interatomic distance.*

Further it has been observed that though there is such a marked effect of thermal agitations on the *intensities* of Bragg reflections, the *sharpness* of these reflections remains practically unaffected. In other words *the resolving power of the crystal, regarded as a reflection grating, remains practically unaffected by these thermal agitations* (Bragg, *loc. cit.* p.218). These experimental results, namely the diminution of intensity of Bragg reflections, without however any appreciable diminution in the resolving power of the grating, can only be understood on the basis that at *the high temperatures that we are considering*, there is no marked correlation between the thermal vibrations of even adjacent layers of atoms†, and hence between the density fluctuations in adjacent atomic layers; thus satisfying requirement (b).

Incidentally it shows that the postulate of practical independence of the thermal vibrations of even neighbouring atoms in a monatomic crystal usually made in discussions

* This is in accordance with the well-known result that in a monatomic solid the amplitude of the thermal oscillations even at the melting point is only 10% to 12% of the distance between neighbouring atoms (Lord Cherwell, Encyclo. Brit. 14th edn., *Theory of the solid state*).

†The Gaussian distribution referred to represents the time-average of the distribution of the atomic centres under the thermal agitations. The acutal distribution, however, will fluctuate from instant to instant from this mean, and it is these fluctuations that are responsible for producing the scattering with which we are concerned in the calculation of the electrical resistance. This scattering is analogous to the "diffuse scattering" of X-rays in crystals due to thermal agitation.

on the electrical resistance of a metal from the atomic or microscopic point of view, as distinguished from the phenomenological point of view adopted here, is justifiable at the high temperatures that we are considering.

Having shown that requirement (b) is satisfied even when the elementary slab consists of only one layer of atoms, we can readily show that with λ of the order of λ_o, requirement (a) also is effectively secured. Consider an atomic layer parallel to the plane bisecting the angle φ between the direction of propagation of the electron waves and the direction of scattering under consideration. Had there been no thermal spreading of the atomic centres from their mean plane, the scattered radiations from all the atomic centres in the plane, in the direction considered, would have been in the same phase (by Huygens's Principle). Owing to the thermal spread, however, they will not be so. Now in order to satisfy requirement (a), all that is necessary is that the effective phase-width produced by the thermal spreading must be a small fraction of 2π. Adopting the Rayleigh limit of $\lambda/4$ for the extreme difference of path between the rays that may be allowed without the intensity's diminishing sensibly from the value corresponding to no difference of path, the condition reduces to

$$4\xi \sin\frac{\varphi}{2} < \frac{\lambda}{4}.$$

As we have seen, ξ, even at the melting point, is only 10% to 12% of the distance between neighbouring atoms, whereas λ is greater than twice this distance. Hence $\xi<\lambda/16$, and the above condition is clearly satisfied even for the backward direction of scattering, $\varphi=\pi$.

Both the requirements (a) and (b) having been secured, we may now readily calculate the attenuation coefficient μ in terms of the density fluctuations in the manner indicated, provided that λ is at least slightly greater than λ_o, where λ_o is the *longest* wave-length that can suffer a Bragg reflection in the backward direction from *any* set of reflecting planes in the crystal. This proviso is equivalent to ensuring that the Fermi surface is well within the sphere inscribed in the first Brillouin Zone in the crystal. This is actually the case in the alkali and the noble metals, λ/λ_o being equal to 1·14 and 1·11 respectively in these metals. Under these conditions no Bragg reflection can occur at any real angle $\varphi\leqslant\pi$, and in view of the sharp falling off of the intensity of reflection as we move away from the Bragg angle, the intensity of the electronic scattering even in the backward direction will be practically that given by the density fluctuations, and hence the total scattering in all directions, namely μ per unit volume, will be that given by expression (1).

As mentioned in the Introduction, the observed resistivities of the alkali and the noble metals are in good agreement with the expressions (1) to (3), at room temperature and at higher temperatures, with $n=1$ per atom and with a temperature-independent value of the atomic scattering cross-section σ, of the order of πa^2, where a is the radius of the scattering atom*.

*The ratio μ/ν may be regarded as the *effective* cross-section of scattering *per* atom under the conditions of scattering in the medium. The cross-section appearing in Frenkel's discussions on electrical conductivity (*Wave Mechanics, Elementary Theory*, Oxford Univ. Press 1936, p. 261) is this effective cross-section, and not σ.

In liquid metals like the molten alkali and noble metals, the interatomic distance, and hence λ_0 corresponding to the first diffraction maximum's occurring in the backward direction, $\varphi=\pi$, will be nearly the same as in the solid metal. Here also the electronic wave length λ involved in conduction will be slightly greater than λ_0, i.e. slightly too large to give a diffraction maximum at any real angle $\varphi\leqslant\pi$. There will be, however, this important difference between the liquid and the solid. The diffraction halo for the liquid will be diffuse, unlike the diffraction rings due to randomly oriented crystals, and hence the electronic scattering by the liquid metal, in the neighbourhood of the backward direction, will be considerably larger than in the solid metal. In these molten metals then, the attenuation coefficient μ will be correspondingly greater than that given by expression (1), and the specific resistance given by (2) correspondingly higher. This is verified experimentally, since the observed increase of resistance of the alkali and the noble metals on melting is found to be much larger than can be accounted for by the known changes in density and compressibility that accompany melting*.

It follows incidentally from the above discussion that at temperatures sufficiently above the Debye temperature, the intensity of *X-ray* scattering by a crystal, not only in the neighbourhood of the forward direction, but in all directions, will be given by the Einstein–Smoluchowski formula, down to wave-lengths nearly, but not quite, as short as λ_0. Even in a liquid if the wave-length is a few times λ_0 (λ_0 will be about twice the interatomic distance), the intensity of scattering will be only slightly greater than that given by the Einstein-Smoluchowski formula.

3. The phenomenological and the microscopic methods of approach to the problem of electical conductivity shown to be equivalent

It would be interesting to compare the expression deduced above, on a phenomenological basis, for the specific resistance of a good metal, namely [see (1), (2) and (3)]

$$\rho=\frac{h}{ne^2\lambda}\cdot\mu=\left(\frac{3}{8\pi}\right)^{1/3}\frac{hn^{-2/3}}{e^2}\cdot\nu^2kT\beta\sigma, \qquad .. \quad (4)$$

with the expression deduced by the usual method (Mott and Jones 1936), namely

$$\rho=\frac{2\pi Cm^2}{Me^2nh}\cdot\frac{T}{k\theta^2}\cdot W^2, \qquad .. \quad (5)$$

where n is the number of electrons per unit of volume as before, M and m are the masses of the atom and the electron respectively, θ is the Einstein characteristic temperature, and W is the kinetic energy of the electron at the boundary of the atomic polyhedron, i.e. at a distance r_0 from the nucleus nearly equal to half the interatomic distance, and C is a

*We shall deal with the change of electrical resistance of good metals on melting from this point of view in a separate communication.

numerical constant of the order of unity. Whereas (4) involves the compressibility β and the scattering cross-section of the atom σ, (5) involves the characteristic vibration frequency of the atoms and the electronic energy at the boundary of the atomic polyhedron. Comparing the two expressions, and confining ourselves as before to the alkali and the noble metals, for which $n=\nu$, we obtain

$$\beta\sigma=2\pi C\left(\frac{8\pi}{3}\right)^{1/3}\frac{m\iota^2}{M\,\nu^{7/3}}\cdot\frac{W}{k^2\theta^2h^2},$$

which can be put in the form

$$\beta\sigma=\left\{\frac{h^2}{k^2}\cdot\frac{1}{A^{2/3}\rho^{1/3}\theta^2\,M_H^{2/3}}\cdot E\right\}\cdot\left\{\frac{2\pi C(8\pi/3)^{1/3}}{E}\cdot\frac{m^2W^2}{h^4\nu^2}\right\} \qquad .. \quad (6)$$

The first factor on the left hand side can be readily identified as the well-known expression for β of Einstein, in which E is simply a numerical constant, taken by Einstein to be equal to $10{\cdot}8\times10^{-2}$. We thus get for σ

$$\sigma=\frac{2\pi C(8\pi/3)^{1/3}}{10{\cdot}8\times10^{-2}}\cdot\frac{m^2W^2}{h^4\nu^2}, \qquad .. \quad (7)$$

which can be readily seen to be of the order of a^2.

4. Concentration scattering in an alloy and its contribution to the electrical resistivity of the alloy

We have regarded till now, for simplicity, the thermal agitations as corresponding to *oscillations* of the various atoms about their mean positions. Actually the thermal agitations may not be wholly of this type; it is likely that under favourable conditions the atoms will migrate from one lattice point to an adjacent lattice point, the fraction of the time spent by the atoms in passing from the neighbourhood of their initial positions to the neighbourhood of their final positions in the lattice being small in comparison with the total time. The possibility of such migrations will not affect our results, which refer to equilibrium conditions, because we have connected the electrical resistance directly with the fluctuations in the density, and the latter with the observed compressibility, and the procedure is thus independent of the precise mechanism of the thermal agitations, and in particular independent of whether they correspond merely to vibrations of the atoms about their mean positions or to migrations of atoms between adjacent lattice points. Where, however, the thermal state of the metal is not the equilibrium state at that temperature, as may happen for example in quenched metals, the effects of the oscillations and the migrations of atoms on the density scattering may have to be differentiated since the relaxation time associated with the migrations may under favourable conditions be large, unlike the relaxation time of the oscillations. We shall confine ourselves here to equilibrium states, and postpone consideration of quenching and allied phenomena to a subsequent Part of the paper.

Considering now *binary* alloys, we know that the atoms of the two types constituting them may exchange places, and that the order-disorder phenomena exhibited by some of the alloys result from this mechanism. Owing to the possibility of such exchanges between atoms, a fluctuation in concentration also becomes possible*, with a corresponding extra electronic scattering and an extra resistance in these alloys.

The magnitude of this extra scattering can be calculated in a manner analogous to that adopted for the calculation of density scattering. Let σ_1 and σ_2 be respectively the scattering cross-sections of the atoms of the two kinds that constitute the *binary* alloy, and let c be the atomic concentration of one of the components, i.e. a fraction c of the total number of atoms present will be of the first kind, and $1-c$ of the second kind. Denoting by $\overline{dc^2}$ the mean square of the fluctuations in concentration in a volume element v containing $vv=N$ atoms in all, the total scattering per unit volume, or the attenuation coefficient μ, will be given by (see Section (5)]

$$\begin{aligned}\mu &= \mu_d + \mu_c \\ &= \Sigma_v \overline{\Delta N^2}\,\sigma + \Sigma_v \bar{N}^2\,\overline{dc^2}\,(\sigma_1-\sigma_2),\end{aligned} \qquad \ldots (8)$$

where the summations extend to all the volume elements in unit volume, and μ_d and μ_c represent the contributions to μ separately from the density scattering and the concentration scattering respectively, and σ is given by expression (10) below.

The corresponding expression for the specific resistance of the alloy will be (see 2)

$$\rho = \rho_d + \rho_c = \frac{h}{ne^2\lambda}\left(\mu_d + \mu_c\right), \qquad \ldots (9)$$

in which the two terms will represent the contributions to resistance from the density and the concentration scatterings respectively.

Now the scattering cross-sections σ_1 and σ_2 for the atoms of two kinds may be obtained either from the known resistances of the pure metals, or from other considerations, as we shall show in Section 9. Knowing σ_1 and σ_2, and the compressibility of the *alloy*, the density scattering and the corresponding attenuation coefficient μ_d and the resistance ρ_d can be readily calculated, since for this purpose one may regard all the atoms in the alloy as having the same cross-section σ, namely

$$\sigma = c\sigma_1 + (1-c)\,\sigma_2. \qquad \ldots (10)$$

We now proceed to the calculation of $\overline{dc^2}$ and thence of μ_c and ρ_c.

5. Expression for $\overline{dc^2}$, the mean square of the fluctuations in concentration

The local fluctuations in concentration in a given volume element can be calculated in the following manner. For an alloy the expression for the thermal fluctuations in the

*The fluctuation in concentration due to the thermal oscillation of the atoms, as distinguished from that due to their migrations between sites, will be relatively very small.

number of atoms N_i of the i^{th} component present in the volume element is given according to Tolman (1938) by

$$\frac{\overline{N_i^2} - \bar{N}_i^2}{\bar{N}_i^2} = \frac{kT}{\bar{N}_i^2}\left(\frac{\overline{\delta N_i}}{\delta \eta_i}\right), \qquad \ldots (11)$$

where η_i is the chemical potential of the i^{th} component, per atom, and is equal to $\left(\frac{\partial A}{\partial N_i}\right)_{T\,;\,a_1,\,a_2,\ldots\,;\,N}$, in which A is the Helmholtz free energy of the volume element of the alloy ; the subscripts to $\left(\frac{\partial A}{\partial N_i}\right)$ indicate that the temperature and the external conditions defined by the parameters $a_1, a_2 \ldots$, are to be kept constant. The inclusion of N among the subscripts signifies that all N's other than N_i in the given volume element are also to be kept constant.

In order to calculate $\overline{dc^2}$ for a *binary* alloy, we may proceed as follows. We may write as usual

$$\overline{\Delta N_1^2} = c^2\,\overline{\Delta N^2} + \bar{N}^2\,\overline{\Delta c^2} + 2\bar{N}c\,\overline{\Delta N\,\Delta c}. \qquad \ldots (12)$$

The first term represents the fluctuations in the total number of atoms present in the volume element, the ratio of the two components remaining the same, and the second term the fluctuations in the concentration c, the total number of atoms in the volume element remaining the same, the two fluctuations being regarded as occurring independently of each other, and the two together representing wholly the fluctuations that actually take place. The last term will evidently be negligible in comparison with the other two. The independence of these two fluctuations justifies our regarding in expression (8) the total attenuation coefficient μ as obtained by the simple addition of the attenuation coefficients μ_d and μ_c due separately to the two types of scattering.

Now with the help of (11), remembering that statistical expressions can be replaced by their thermodynamical analogues, and *vice versa*, we may express $\overline{\Delta N_1^2}$ in the following form also ;

$$\begin{aligned}\overline{\Delta N_1^2} &= kT\,\frac{\delta N_1}{\delta \eta_1} \\ &= kT\,\frac{\delta(\bar{N}c)}{\delta\left(\frac{1}{c}\frac{\partial A}{\partial N} + \frac{1}{\bar{N}}\frac{\partial A}{\partial c}\right)} \\ &= kT\left\{c^2\frac{\delta N}{\delta \eta} + \bar{N}^2\frac{\delta c}{\delta \eta_c} + \bar{N}c\left(\frac{\delta N}{\delta \eta_c} + \frac{\delta c}{\delta \eta}\right)\right\},\end{aligned} \qquad \ldots (13)$$

in which $\eta = \frac{\partial A}{\partial N}$ and $\eta_c = \frac{\partial A}{\partial c}$, and the last term can be neglected. Comparing (12) and

(13), it is evident that the first term represents the density fluctuations, and the second the concentration fluctuations. Hence we obtain

$$\overline{dc^2} = kT\frac{dc}{d\eta_c} = \frac{kT}{\frac{d}{dc}\left(\frac{\partial A}{\partial c}\right)}$$

where A is the Helmholtz free energy expressed in terms of the number of atoms present in the volume element. In obtaining $\frac{\partial A}{\partial c}$, the temperature, order, volume and other parameters are kept constant, whereas in differentiaing $\frac{\partial A}{\partial c}$ with respect to c, in order to obtain $\frac{d}{dc}\left(\frac{\partial A}{\partial c}\right)$, the temperature remains constant, but the other parameters are assumed to vary in such a manner as to maintain equilibrium. We now proceed to get an expression for the free energy A, equal to E—Ts, where s is the entropy (the quantities refer, as we have mentioned, to the volume element v containing N atoms) in a form suitable for differentiation with respect to c.

Evidently the free energy of a *binary alloy* will consist of (i) the vibrational free energy and (ii) the configurational free energy. We shall assume that the effective vibrational partition functions of the individual atoms of the two types are independent of both the degree of long-range order and their relative concentrations. This will be so approximately if the atomic sizes of the two components constituting the alloy do not differ much, and the alloy remains throughout its volume and throughout the range of concentration under consideration, in the same phase. If the effective vibrational partition functions of the two types of atoms be $J_\alpha(T)$ and $J_\beta(T)$ respectivly, then the complete free energy can be expressed in the form

$$A = -NkT\{c \log J_\alpha(T) + (1-c) \log J_\beta(T)\} + F,$$

where N is the total number of atoms in the volume element v, and F is the configurational part of the free energy. Hence

$$\overline{dc^2} = \frac{kT}{\frac{d}{dc}\left(\frac{\partial F}{\partial c}\right)}. \qquad .. \quad (14)$$

6. Application to CuZn type of alloys : long and short range order and the configurational partition function

We shall consider here the application of the above expressions to one typical order-disorder alloy, namely CuZn alloy in the β-phase, whose structure has been studied in detail by X-ray methods, and for which expressions are already available for the configurational free energy in terms of the concentration. The crystal lattice of this alloy is a body-centred cubic lattice, which, as is well-known, may be regarded as formed of two interpenetrating

simple cubic sublattices, which we shall denote by I and II, the lattice points of I, say, forming the corners, and of II the centres, of the body-centred cube. The total number of sites in the two together will evidently be equal to the total number of atoms of the two kinds, A and B, that are to be accommodated. Each site of sublattice I has eight neighbours, all of which belong to the sublattice II, and *vice versa*. When the alloy is completely ordered, and when further the number N_A of A atoms is equal to the number N_B of B atoms, all the sites of I will be occupied exclusively by A atoms and of II exclusively by B atoms. If their numbers are not equal, let $N_A < N_B$; then such of the B atoms as cannot be accommodated in II—their number will evidently be equal to $N_B - \frac{N_A+N_B}{2}$ — will occupy the vacant sites in I, whose number also will be the same.

We referred just now to the tendency of the A and the B atoms to occupy certain preferred sites, say α and β respectively, in the lattice. Following the usual practice, we shall designate the order associated which such a tendency as the *long range order* (as distinguished from another type of order, namely the *short range order* to be described presently) and define it by the expression

$$S = \frac{p-\theta}{q-\theta}, \qquad .. \quad (15)$$

where p is the fraction of α sites that is occupied by A atoms at the given temperature, and q and θ are the values of p at perfectly ordered and random states respectively. S will then be zero at all temperatures higher than the Curie temperature, and will tend to unity at sufficiently low temperatures.

In the ordered state the geometry of the dispositions of the A and the B atoms in the lattice requires a preponderence of B atoms around A and similarly of A around B, which will tend to reach their respective maxima, characteristic of the lattice and of the ratio between the numbers of A and B atoms, as the order becomes perfect. This can be interpreted as due to a general tendency for any given atom to prefer unlike atoms as neighbours. This tendency leads to another kind of order, which, as it relates to the ordering of neighbouring atoms, is generally designated as 'short range order' and is defined by

$$S' = \frac{\gamma-\gamma_{min}}{\gamma_{max}-\gamma_{min}}, \qquad .. \quad (16)$$

where γ is the total number of nearest neighbour pairs of atoms in the alloy that are unlike, and γ_{max} and γ_{min} are the values of γ in the states of perfect order and of randomness respectively.

The short range order will evidently remain finite even above the Curie temperature, i.e. even when the degree of long range order has become zero, and it will tend to zero at only very high temperatures.

Bethe defined this tendency of atoms to have unlike atoms as their neighbours (which as we have seen, is responsible for producing both the short range and the long range orders)

in terms of certain interaction energies between the various types of nearest neighbour pairs of atoms, the interaction energies being χ_{AA}, χ_{BB} and χ_{AB} respectively such that $\chi_{AA}+\chi_{BB}-2\chi_{AB}$, equal to 2χ say, is positive. χ is the well-known Bethe interaction energy. Now a theoretical study of the dependence of S, the long range order as defined in (15), on temperature, consists essentially in constructing the configurational partition function, which may be put in the form $\Gamma(T)=g(S).\, e^{-E(S)/(kT)}$, where $g(S)$ is the number of ways in which the system can be arranged with the given degree of order S, and E(S) is the energy of the configuration corresponding to this value of S. Though for a given S, $g(S)$ can be evaluated rigorously, E(S) can be evaluated only approximately, since the variables determining it, namely the numbers of nearest neighbour pairs of the three types, depend on S or on $g(S)$ in a complicated manner. Hence the partition function $\Gamma(T)$ can be constructed only approximately.

In Bragg-Williams (1934, 1935) approximation the atoms in each sublattice are assumed to be randomly distributed at all temperatures, which is equivalent to neglecting the short range order altogether and retaining the long range order alone. Though neglecting the short range order is not logically consistent with the postulate of a finite χ which leads to the long range order, such a procedure considerably simplifies the problem. It is further found that the general results are not much affected by this neglect; at any rate the uncertainties so introduced are not much greater than those introduced by the usual simplifying assumptions, namely, that the interaction is confined to the nearest neighbours only, and that the interaction energy remains independent of the degree of order. Hence Bragg-Williams approximation has found much favour in the discussion of order-disorder phenomena. For temperatures below the Curie temperature, we too shall adopt this approximation, and merely indicate the general nature of the improvements to be expected on other approximations which attempt to include the effects of the short range order also, e.g. those of Bethe, Kirkwood, and Fowler and Guggenheim*.

It may be pointed out here that Bethe did not evaluate the complete partition function, but got the dependence of S on temperature indirectly. But recently Fowler and Guggenheim (1940) have constructed the complete partition function for the CuZn type of alloys by assuming a quasi-chemical relation between the various pairs, of the type

$$\frac{\left[\begin{matrix}A & B\\ I & II\end{matrix}\right]\left[\begin{matrix}A & B\\ II & I\end{matrix}\right]}{\left[\begin{matrix}A & A\\ I & II\end{matrix}\right]\left[\begin{matrix}B & B\\ I & II\end{matrix}\right]}=e^{\frac{2\chi}{kT}} \qquad \ldots (17)$$

They have also shown that this relation is a direct consequence of the hypothesis of non-interference of pairs, and that it leads to the same results as obtained by Bethe with his approximation†. We shall adopt the approximation of Fowler and Guggenheim in calcu-

*For a good account of these approximations see Fowler and Guggenheim, *Statistical Thermodynamics*, Camb. Univ. Press, 1939. We shall refer to this book briefly as F.G.

†No such equivalence has yet been established for other lattice types, e.g. Cu_3Au and CuAu.

lating the configurational free energy, and thence the resistance of the CuZn alloy, at temperatures above the Curie temperature, since at these temperatures, unlike at lower temperatures at which the long-range order is finite, the expression for the fluctuations in concentration is not complicated.

7. Expression for the configurational free energy of the CuZn type of alloy

The Helmholtz free energy F can be written as $-kT \log \Gamma(T)$. The expressions for F for various lattice types are given in F. G. , and the results concerning the free energy of the CuZn type of alloys quoted in this section are taken from this book. In deducing these expressions it is assumed that the lattice and its modes of vibration, and the interaction energy χ, remain independent of the degree of order, and further that all interactions except those between nearest neighbours are negligible. We shall have, later in this section, some comments to make on the validity and the consequences of these assumptions.

Denoting by N the total number of atoms in the alloy, and by Nc and N (1—c) the numbers of A and B atoms separately, we obtain for the CuZn type of lattice $0 < c \leqslant \frac{1}{2}$;

$$F=kT\frac{N}{2}\Big[c(1+S)\log c(1+S)+\{1-c(1+S)\}\log\{1-c(1+S)\}+c(1-S)\log c(1-S) +\{1-c(1-S)\}\log\{1-c(1-S)\}\Big]+Nz\chi c^2(1-S^2), \quad \ldots (18)$$

where z is the number of nearest neighbours, equal to eight in CuZn. Now the equilibrium states are characterised by the stationary values of F, i. e. by $\frac{\partial F}{\partial S}=0$, the minima of F corresponding to stable equilibrium, and the maxima of F to unstable equilibrium. The condition $\frac{\partial F}{\partial S}=0$ gives

$$\log\frac{c(1+S)\{1-c(1-S)\}}{c(1-S)\{1-c(1+S)\}}=\frac{4z\chi}{kT}cS. \qquad \ldots (19)$$

Detailed study of (18) and (19) shows that there exists a certain critical temperature such that above this temperature S=0 is the only root of (19), and corresponds to stable equilibrium, while below it (19) has two roots one of which is again S=0, but corresponds now to unstable equilibrium, and the other, $0<S<1$, corresponds to stable equilibrium. The critical temperature referred to is evidently the Curie temperature for the alloy of concentration c, and is given by

$$S=0,\ \frac{\partial F}{\partial S}=0,\ \text{and}\ \frac{\partial^2 F}{\partial S^2}=0$$

Or,

$$\Theta_c=\frac{2z\chi}{k}c(1-c). \qquad \ldots (20)$$

Incidentally it will be seen that Θ_c is a maximum at $c=\frac{1}{2}$, as is actually observed.

As will be seen from (19) S falls catastrophically to zero as one approaches Θ from the low temperature side, and remains at this value at all higher temperatures.

We should emphasize in this place that the assumption of χ's remaining independent of S will not be quite justifiable in the neighbourhood of the Curie temperature, since the coefficient of thermal expansion attains large values in this region, and χ is presumably sensitive to changes in the lattice constant of the crystal. This will make χ fall appreciably as we approach Θ from the low temperature side. The effect of this fall in χ in the neighbourhood of Θ will be to make the fall in the order more rapid than it would be otherwise. Indeed an expression of the type $\chi=\chi_0(1+CS^2)$, where C is a constant, has been found empirically by Williams (1935) to fit with observation. In view, however, of the difficulty of taking the effect of the variation of χ with order into account, we shall regard χ as being independent of S, but remember in making detailed comparison of the results obtained on this basis, with the experimental data, that the effect of taking the variation of χ into account will be to make the calculated variation of the order in the neighbourhood of Θ steeper.

8. General features of the concentration scattering and of its contribution to the extra resistance in the CuZn type of alloys

We may now utilize expression (18) for the configurational free energy F for the CuZn type of alloy, in terms of its concentration c, for calculating the variation of F with c, and thence the value of $\overline{dc^2}$ according to expression (14). Assuming that χ, the Bethe interaction energy, is independent of both the degree of order S and the concentration c, and remembering that $\frac{d}{dc}\left(\frac{\partial F}{\partial c}\right)=\frac{\partial^2 F}{\partial c^2}+\frac{\partial^2 F}{\partial c \partial s}\cdot\frac{ds}{dc}$, where $\frac{ds}{dc}$ can be obtained from the equilibrium condition (19), the mean square of the fluctuations in concentration $\overline{dc^2}$ in an element of volume v, containing altogether N atoms, will be given by

$$\frac{1}{N\overline{dc^2}}=\frac{2z\chi}{kT}\,ab+\tfrac{1}{2}\left(\frac{2}{c}+\frac{a^2}{1-ac}+\frac{b^2}{1-bc}\right)$$

$$-\tfrac{1}{2}c\left(\frac{a}{1-ac}+\frac{b}{1-bc}-\frac{4z\chi}{kT}S\right)^2\Big/\left(\frac{2}{ab}+\frac{c}{1-ac}+\frac{c}{1-bc}-\frac{4z\chi}{kT}c\right), \quad .. \quad (21)$$

where $a=1+S$ and $b=1-S$.

The resistance due to concentration scattering will evidently be given by

$$\rho_c=\frac{h}{ne^2\lambda}\sum_v N^2\,\overline{dc^2}\cdot(\sigma_1-\sigma_2), \quad .. \quad (22)$$

where the summation extends as before to all the volume elements in unit volume. Hence

$$\rho_c=\frac{h}{ne^2\lambda}\,\nu\,(\sigma_1-\sigma_2)\,N\,\overline{dc^2}, \quad .. \quad (23)$$

where ν is the total number of atoms of the two kinds together per unit volume, and $N\overline{dc^2}$ is given by (21).

In order to calculate ρ_c we thus require in addition to $N\overline{dc^2}$, the values of $\sigma_1-\sigma_2$ and of n, the effective number of free electrons per unit volume, both of which, as we shall show presently, are easily obtained. Before making detailed calculations, one may draw attention here to some of the general features of the electrical resistivities of this type of alloy predicted by expressions (23) and (21).

We have already seen (page 168) that the drop in the degree of order from unity at low temperatures to zero at $T=\Theta$ is confined to the neighbourhood of Θ. Hence the *development* of the concentration scattering, and of the extra resistance associated with it, will take place in the immediate neighbourhood of the Curie temperature. This accounts for the abnormal increase in resistance as we approach the Curie temperature from the low temperature side. As we shall show presently, ρ_c continues to increase even when T exceeds Θ. The temperature coefficient of ρ_c in the region $T>\Theta$ will, however, be small in comparison with the coefficient on the low temperature side of Θ.

The expression for ρ_c in the general case when both c and S may have any values, is complicated, as can be seen from expression (21) for $N\overline{dc^2}$. There are, however, three particular cases for which the expression becomes simple, and fortunately these are the only cases that are physically important.

Case I : When the concentration is in the neighbourhood of 1/2, and further S is nearly unity, such that $\frac{z\chi}{kT}$ is small in comparison with $1/(1-S^2)$, expression (21) which refers to $c\leqslant 1/2$, and similar expression which may be obtained for concentrations $c\geqslant 1/2$, reduce respectively to

$$c\leqslant\tfrac{1}{2}\;;\; N\,\overline{dc}\sim\tfrac{1}{2}\,(\tfrac{3}{2}-S-c) \quad .. \quad (24a)$$

$$c\geqslant\tfrac{1}{2}\;;\; N\,\overline{dc^2}\sim\tfrac{1}{2}\,(\tfrac{1}{2}-S+c) \quad .. \quad (24b)$$

We shall discuss this case in section 13.

Case II. When $c=1/2$, as in the ideal CuZn 1 : 1 alloy, the expression for ρ_c reduces to

$$\rho_c=\frac{K/4}{\frac{1}{1-S^2}+\frac{z\chi}{2kT}} \quad .. \quad (25)$$

$$=\frac{K/4}{\frac{1}{1-S^2}+\frac{\Theta}{T}} \quad .. \quad (26)$$

where $$K=\frac{h}{ne^2\lambda}\,\nu\,(\sigma_1-\sigma_2). \quad .. \quad (27)$$

We shall now consider the relative importance of the two terms $1/(1-S^2)$ and Θ/T appearing in the denominator of expression (26). At all temperatures lower than Θ, but not close to it,

S will be nearly unity as we have seen, and hence the first term will be the predominant term. ρ_c will then be given by

$$\rho_c = \frac{K}{4}(1-S^2). \qquad .. \quad (28)$$

The proportionality of ρ_c to $(1-S^2)$ is significant, since such a relation between the extra resistance in an ordered alloy and the degree of order S, has been proposed by Webb (1939) on certain *a priori* considerations.

At other temperatures, i.e. at temperatures above Θ, and also below it and in its neighbourhood, at which S is zero or small, the second term, namely Θ/T, will be comparable with the first term $1/(1-S^2)$. Indeed, at the Curie temperature the two terms become equal, since when S=0 expression (26) reduces to

$$\rho_c = \frac{K/4}{1+\Theta/T}. \qquad .. \quad (29)$$

It can be seen from (29) that when T is increased above the Curie temperature ρ_c will continue to increase, even though the degree of order has already become zero and remains at zero. At high temperatures ρ_c tends to reach asymptotically the value K/4 which is actually double the value at $T=\Theta$. We shall have more to say on the temperature-dependance of ρ_c above the Curie temperature in the next section.

Case III : When the degree of order is zero, i.e. at the Curie temperature and higher temperatures, the expression for ρ_c becomes simple for *any* concentration, and not merely for $c=\frac{1}{2}$, since it is then given by

$$\rho_c = \frac{K\,c(1-c)}{1+\frac{2z\chi}{kT}c(1-c)} \qquad .. \quad (30)$$

This expression holds for a face-centred cubic lattice also, as we shall show in a subsequent Part of the paper ; the value of z, which denotes the number of nearest neighbours, will, however, be 12 in the face-centred lattice, whereas it is 8 in the body-centred one.

In real random alloys, for which $\chi=0$, the above expression reduces to

$$\rho_c = K\,c(1-c). \qquad (31)$$

The alloys contemplated in Nordheim's (1931) treatment are presumably of this type, and it is gratifying that the proportionality of the extra resistance due to alloying to $c(1-c)$, deduced theoretically by him, and verified in detail experimentally, is retained in our results. In Nordheim's expression the constant of proportionality is difficult to evaluate, whereas in ours, as we shall show presently, it is easily calculated.

The finite temperature coefficient of ρ_c, indicated by (30), above the Curie temperature, i.e. even after the disordering has become complete, is significant, since such a temperature dependence is not contemplated in the current theories (Nordheim, Muto, Bragg, *loc. cit.*) whereas it will be clear from the expression (30) that it is only in the special case when $\chi=0$ or $\Theta=0$, i.e. in random alloys, that the temperature coefficient of ρ_c is zero. When χ is finite the temperature coefficient remains finite, and tends to zero at very high temperatures only.

Thence we obtain $\sigma_1=\pi(1{\cdot}97\text{Å})^2$, which is a reasonable value, since 1·97Å is of the magnitude of the atomic radius of copper.

In the case of Zn, however, there is some difficulty in estimating n. Pure zinc crystallizes in the hexagonal system and its first Brillouin zone can accommodate only 1·79 electrons per atom, whereas there are 2 electrons per atom to be accommodated. Hence there will be a strong overlapping with the outer zones, and since the energy discontinuities at the bounding planes of the first Brillouin zone are not very large, and are not known accurately, it will be difficult to estimate correctly from the known resistance of the metal the effective number of free electrons, n. We cannot, therefore, calculate the scattering cross-section σ_2 for Zn from the known resistivity of the pure metal, as we did for copper.

Even if σ_2 is known, there is a further difficulty that arises from a similar uncertainty in estimating the effective number of free electrons in the *alloy*. At high temperatures, at which the degree of order present in the alloy is small or zero, the innermost Brillouin zone will be the rhombic dodecahedron bounded by planes of the type (110). The sphere inscribed in this zone can accommodate about 1·48 electrons per atom. Now for the ideal ratio Cu : Zn = 1 : 1, the number of free electrons per atom that has to be accommodated will evidently be 1·5. This ideal ratio, however, does not actually occur in the β-phase, the closest approach to it in this phase being Cu : Zn = 1·08 : 1, which corresponds to 1·48 electrons per atom. This is almost the same as the number of electrons that can be accommodated in the sphere inscribed in the first Brillouin Zone. The coincidence between these two numbers is not accidental, since this is just the condition that determines the limit of the phase (Mott and Jones, *loc. cit.*, p. 170).

Now since the Fermi surface is close to the boundary of the Brillouin Zone, the *effective* number of free electrons will be less than 1·48, but near to it. Hence to the same approximation to which the Cu : Zn ratio is taken to be 1 : 1, the effective number of free electrons at these high temperatures may be taken to be 1·5 per atom.

At low temperatures, however, owing to the setting in of order, and because of the difference in the scattering cross-sections of the two types of atoms, the innermost Brillouin Zone will not be the dodecahedron bounded by (110) planes, but the cube bounded by (100) planes, and the latter zone can accommodate only one electron per atom. The energy discontinuity across the (100) planes will depend on the difference between the scattering cross-sections σ_1 and σ_2, and on the degree of order. Hence the discontinuity will be nothing at high temperatures, where the atoms of the two kinds occupy the lattice sites randomly, and it will increase with the increase of order. At low temperatures, as for example at room temperature, at which the degree of order is nearly unity, n should therefore be much closer to 0·5 per atom than to 1·5.

We shall first consider the region of high temperatures for which, as we have seen, $n\sim1{\cdot}5$ per atom. In order to get over the difficulty of estimating the scattering cross-section of the zinc atom σ_2, we adopt the following indirect procedure. Since the bulk of the resistance ρ at the Curie temperature is that due to the concentration scattering, namely

Taking an alloy for which the degree of order S is known to be zero, observations on ρ_c at different temperatures will thus enable us to decide whether it is a random alloy, (for which ρ_c will be independent of temperature,) or merely an order-disorder alloy above the Curie temperature, (for which the temperature coefficient of ρ_c will be finite). In the latter case the observations will further enable us to calculate the Curie temperature (or the interaction energy χ) of the alloy*.

Expression (30) bears a close analogy to the well-known Curie-Weiss expression for the paramagnetic susceptibility of a ferromagnetic at temperatures above the ferromagnetic Curie temperature, the deviation of the temperature variation of susceptibility from the the simple Curie law enabling one to deduce the ferromagnetic Curie temperature, and hence the interaction energy between the magnetic particles, i.e. between the spins of the free electrons. That in a disordered alloy ρ_c should continue to increase even after the disordering has become complete, need not, therefore, occasion surprise, since the Bethe interaction will persist even above the Curie temperature, in the same manner as the interation between the electron spins in a ferromagnetic persists above the Curie temperature and leads to a deviation of the temperature variation of susceptibility from the simple Curie law.

9. Detailed calculations for Cu : Zn=1 : 1 alloy at different temperatures

We shall now take up the detailed verification of the expressions for ρ_d and ρ_c for the CuZn (1 : 1) alloy ($c=\frac{1}{2}$) deduced in the previous sections, namely

$$\rho_d = \frac{h}{ne^2\lambda}\, \nu^2 kT\beta \frac{\sigma_1+\sigma_2}{2}, \qquad .. \quad (32)$$

$$\rho_c = \frac{\frac{h}{ne^2\lambda}\nu\,(\sigma_1-\sigma_2)}{4/(1-S^2)+4\Theta/T} = \frac{K/4}{1/(1-S^2)+\Theta/T}. \qquad .. \quad (33)$$

We thus require to know n, the effective number of free electrons, and the scattering cross-sections σ_1 and σ_2 of the atomic cores of Cu and Zn respectively, which form the scattering centres in the lattice of the alloy. At first sight it appears that the σ's should be capable of easy evaluation from the known resistivities of the corresponding pure metals. This is true enough of Cu, since the Fermi surface of the free electrons in the metal is well inside the sphere inscribed in the first Brillouin Zone, and the sphere can accommodate 1·36 electrons per atom. Hence the effective number of free electrons n will be 1 per atom, a result confirmed by other evidence (Mott and Jones, *loc. cit.* p. 316). We shall adopt this value for n and the following values (taken from Landolt-Börnstein Tables) for the specific resistance and the compressibility of copper at 100°C, which may be regarded as sufficiently high in comparison with the Debye temperature :—

$$\rho = 2{\cdot}23\ \mu\ \Omega\ \text{cm}; \qquad \beta = 0{\cdot}75\times10^{-12}\ \text{cm}^2\ \text{dyne}^{-1}.$$

* It may be emphasized again that we are concerned here, as elsewhere in this Part, with equilibrium conditions alone, at the temperature of measurement. If the relaxation time corresponding to the migrations of atoms between adjacent lattice sites is large, as it will be at low temperatures, the observed conditions of disordering will be determined by those at the lowest temperature above the temperature of observation at which the relaxation time becomes large. In that case many of the results regarding temperature coefficient of ρ_c will be modified. We shall postpone discussion of these and other effects associated with quenching, to a subsequent Part of this paper.

ρ_c, and it is proportional to $\sigma_1-\sigma_2$, and the small part due to density scattering namely ρ_d, is proportional to $\sigma_1+\sigma_2$, and since we know the scattering cross-section σ_1 for Cu, it is easy, using the observed value of ρ, equal to $\rho_c+\rho_d$, at the Curie temperature, to calculate σ_2, by the method of successive approximations. First ρ_d for the alloy at the Curie temperature is calculated to a first approximation by putting $\sigma_1+\sigma_2=2\sigma_1$. Deducting this value of ρ_d from ρ we obtain the concentration part of the resistance, and thence $\sigma_1-\sigma_2$. Since σ_1 is known, σ_2 and $\sigma_1+\sigma_2$ become known to the next approximation. By such successive approximations σ_2 can be evaluated to the same degree of accuracy as σ_1. Actually three such approximations are found to be sufficient.

Taking the observed value of the specific resistance of the CuZn alloy at the Curié temperature (741°K) as 14·10 $\mu\,\Omega$ cm, the total number of Cu and Zn atoms together per c.c. as $7{\cdot}6\times10^{22}$, and the compressibility the same as at room temperature*, namely $0{\cdot}93\times10^{-12}$ cm²/dyne, we obtain

$$\rho_d = 3{\cdot}33\ \mu\ \Omega\ \text{cm}, \quad \rho_c = 10{\cdot}77\ \mu\ \Omega\ \text{cm}, \quad \text{and} \quad \sigma_1-\sigma_2 = \pi\times0{\cdot}67\,\text{Å}^2$$

whence σ_2, the scattering cross-section of the zinc atom comes out as $\pi(1{\cdot}80\,\text{Å})^2$

This value of σ_2 is reasonable. Using this cross-section and the observed specifi resistance of pure zinc, namely 5·92 $\mu\ \Omega$ cm, one obtains for the effective number of free electrons in this metal 0·33 per atom. This is consistent with the facts that the first Brillouin zone can accommodate only 1·79 electrons per atom, and that the discontinuities at the bounding faces of this zone are not large (Wilson 1939). The relative values of the scattering cross-sections of copper and zinc atoms can also be seen to be of the proper magnitude, since $\sqrt{\sigma_1/\sigma_2}=1{\cdot}10$ agrees well with the ratio of the radii of the two ions, i.e. the inverse ratio of (the atomic number *minus* the screening constant for the two ions) $=(30-21{\cdot}5)/(29-21{\cdot}5)=1{\cdot}13$.

Adopting these values of σ_1 and σ_2, and the value $n=1{\cdot}5$ per atom, we have calculated ρ_d and ρ_c for temperatures above 600°K (this temperature is about 130° below the Curie temperature). The values of ρ_d and ρ_c so calculated, and also of ρ equal to $\rho_d+\rho_c$, are given in Fig. 1, in curves 1, 2 and 3 respectively.

10. Comparison with experimental data

Experimental data for the specific resistance of the CuZn alloy in the β-phase over a wide range of temperatures, from 273°K to about 830°K, (Curie temperature is 742°K) are available from the measurements of Webb (1939) on a large number of single crystals, and from an earlier measurement over the same temperature range by Steinwehr and Schulze (1934) for one single crystal. Though the absolute values of the resistance obtained by the latter authors do not agree with those of Webb, the values of $\rho_T/\rho_{273}{}^\circ{}_K$ obtained in the two

*In a pure metal β increases slowly with the rise of temperature, $1/\beta\times d\beta/dt\sim2\times10^{-4}$. In an order-disorder alloy, superposed on this small increase in β with temperature there will be an increase due to progressive disordering, which also will be of nearly the same magnitude (see F.G. p. 607). Thus the increase in β will be altogether small, and since at high temperatures the density scattering is a small fraction of the total scattering, this increase will not appreciably affect the total resistance.

investigations agree well. Hence in adopting the values of Steinwehr and Schulze we have reduced them so as to make the absolute value of the resistance at 273°K coincide with that of Webb. We have plotted in Fig. 1 the experimental values of Webb, and also those of Steinwehr and Schulze so reduced, both of them for comparison with the values calculated in this paper. It will be seen from the figure that the calculated values plotted therein refer only to the region where the order is zero, or small, for which $n \sim 1{\cdot}5$ per atom. Before discussing the values plotted in this region, we may offer the following remarks regarding the calculation of the resistance of the alloy at lower temperatures.

As the order develops, the energy discontinuities across planes of the type (100) in the Brillouin Zone will become appreciable, and the calculation of the effective number of electrons correspondingly uncertain. All that one can infer safely is that the number should tend to diminish from 1·5 to much lower values with the development of the order; until at sufficiently low temperatures e.g. at room temperature, at which the degree of order is nearly unity, and the energy discontinuities fairly large, it will be only the electrons outside this zone, namely about 0·5 per atom, that will be effectively free. The observed resistance of the alloy at room temperature does correspond to such a low value of n; since the resistance calculated on the basis $n=0{\cdot}5$ per atom comes out as

$$\rho=\rho_d+\rho_c=(2{\cdot}60+0{\cdot}83)\ \mu\ \Omega\ \text{cm}=3{\cdot}43\ \mu\ \Omega\ \text{cm},$$

as compared with the value 4·02 observed, and the value 1·65 $\mu\ \Omega$ cm, calculated on the basis of $n=1.5$ per atom. It will be seen further from the values given above, that at room temperature, the bulk of the observed resistance is due to the density scattering, the contribution from the concentration scattering being much smaller, which is to be expected since the degree of order is nearly unity.

The effective number of free electrons thus changes from about 1·5 per atom at high temperatures at which the order is small, to about 0·5 at low temperatures at which the order is nearly complete, but its actual value at any intermediate temperature will be difficult to estimate.

Coming back to the region of low order for which $n=1{\cdot}5$, to which all the plots in Fig 1 refer, we can see immediately that the theoretical curve fits fairly well with the experimental curve. Since the bulk of the resistance at the Curie temperature is due to the concentration scattering and its variation on the low temperature side particularly is very steep, the agreement between the theoretical and the experimental curves is significant and should be regarded as verifying the essential validity of attributing the extra resistance in the alloy to the concentration scattering. Since σ_2 for Zn has been chosen to fit the experimental curve at the Curie temperature, it may appear at first sight that the agreement between the two curves referred to merely verifies the *variation of resistance with temperature* in this range and not the absolute values of the resistance. Even so it will be significant, but as we have seen, the value of σ_2 so chosen is reasonable, and hence the absolute values also stand verified.

In the next section we shall take up for detailed consideration the temperature variation of ρ on the high temperature side of the Curie temperature. On the low temperature side, we may mention here that even such discrepancy as exists between the calculated and the experimental values of ρ plotted in Fig. 1, is in the direction to be expected in view of (1) the complete neglect of the short range order in calculating the configurational free energy, and (2) the assumption of a constant χ, which is not quite justifiable in the close

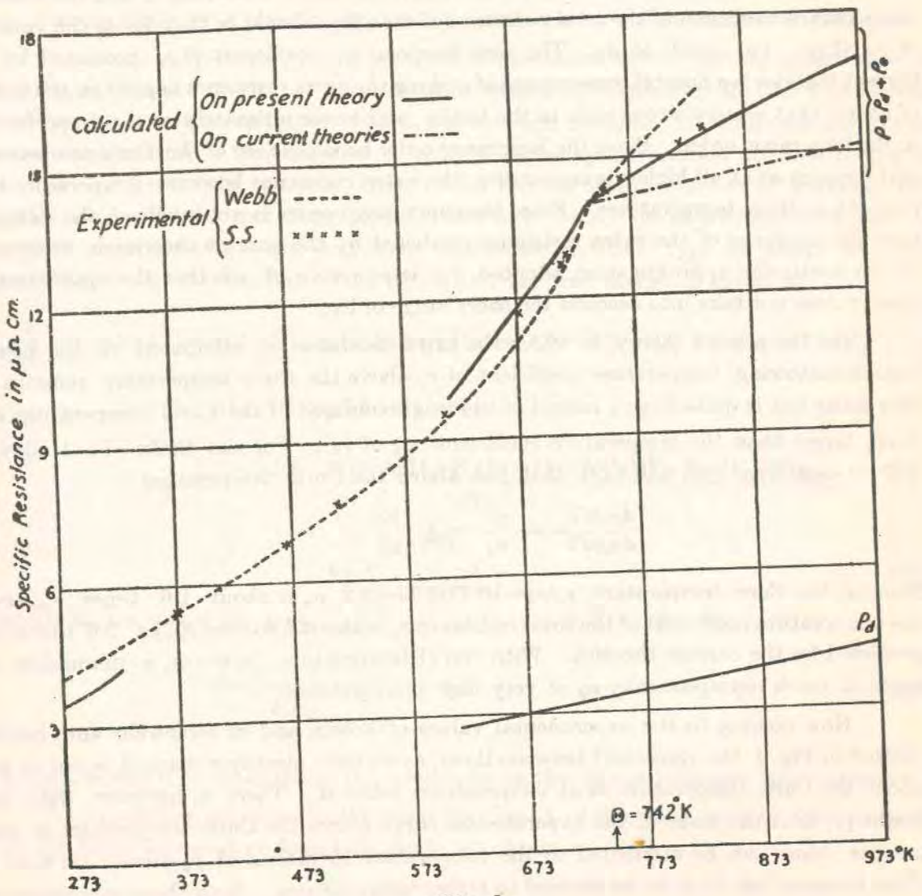

Fig. 1.

neighbourhood of Θ on the low temperature side, where owing to the large thermal expansion of the alloy, evidently connected with the rapid fall in order, χ will diminish appreciably. Both these effects, if taken into account, will make the theoretical ρ vs T curve steeper than that given in the figure, and hence closer to the experimental curve.

11. Temperature coefficient of ρ_c finite even above the Curie temperature

One important feature of the present theory, which distinguishes it from the current theories connecting the extra resistance of an alloy with the disorder is the finite temperature coefficient, say α_c, of the extra resistance ρ_c, even above the Curie temperature, predicted by the present theory. The coefficient tends to zero at very high temperatures only. On the other hand according to the current theories the temperature coefficient of the extra resistance should be zero at all temperatures above the Curie temperature, and the observed temperature coefficient of the total resistance of the alloy should be that due to the variation of ρ_d alone, i.e. equal to α_d. The zero temperature coefficient of ρ_c predicted by the current theories is a natural consequence of making the extra resistance depend on the number of atoms that occupy wrong sites in the lattice, and hence ultimately on the imperfections in the long range order. Since the long range order becomes zero at the Curie temperature, and remains so at all higher temperatures, the extra resistance becomes temperature-independent at these temperatures. Since the short range order is not involved, the temperature-independence of the extra resistance predicted by the current theories is irrespective of the particular approximation adopted, i.e. irrespective of whether the approximation does or does not take into account the short range order.

[1]On the present theory, in which the extra-resistance is attributed to the concentration scattering, temperature coefficient of ρ_c above the Curie temperature remains not only finite but is quite large; indeed in the neighbourhood of the Curie temperature it is much larger than the temperature coefficient α_d of ρ_d. For the CuZn=1 : 1 alloy, it will be seen from (32) and (33), that just above the Curie temperature

$$\frac{d\rho_c/dT}{d\rho_d/dT} = \frac{\alpha_c}{\alpha_d} = \tfrac{1}{2}\frac{\rho_c}{\rho_d}. \qquad .. \quad (34)$$

Since at the Curie temperature, $\rho_c/\rho_d = 10{\cdot}77/3{\cdot}33 = 3{\cdot}2$, α_c is about 1·6 times α_d, and α, the temperature coefficient of the total resistance ρ, is about 2.6 times α_d, i.e. 2·6 times that predicted by the current theories. With rise of temperature, however, α diminishes and tends to reach asymptotically α_d at very high temperatures.

Now coming to the experimental values of Webb, and of Steinwehr and Schulze, plotted in Fig. 1, the agreement between them, as we have already remarked, is not so good above the Curie temperature as at temperatures below it. There is, however, very little doubt (1) that the slope of the experimental curve above the Curie temperature is much steeper than can be attributed to the temperature coefficient of ρ_d alone; (2) that the slope becomes less steep as we proceed to higher temperatures. Both these conclusions are in agreement with the results of the present theory.

A closer comparison between the theoretical and the experimental curves shows that in the neighbourhood of the Curie temperature, though the theory predicts a temperature coefficient nearly 2·6 times that of ρ_d alone, even this slope falls appreciably short of the experimental slope. This is indeed to be expected because of our neglect of the short range

order in calculating the free energy and thence the fluctuations in concentration. We shall now show that the small discrepancy left over between the theoretical slope, and the experimental slope, of the ρ *vs* T curve above the Curie temperature, is considerably reduced, if not wholly eliminated, by pushing to a higher order the approximation adopted in calculating the free energy.

12. Calculation of ρ_c above the Curie temperature to a higher approximation

Though at temperatures below the Curie temperature, where the long range order is finite, the adoption of the higher approximation makes the expression for the fluctuations in concentration very complicated, this is not so when S=0, i.e. at temperatures above the Curie temperature. We, therefore, adopt the higher approximation at these temperatures. We prefer for this purpose, from considerations of convenience of working, the approximation of Fowler and Guggenheim (1940) to Bethe's; but as we mentioned earlier, these two approximations are equivalent in the case of CuZn type of alloy. On this approximation and for concentrations $0<c\leqslant 1/2$, the free energy is given by

$$\frac{F}{2NkT} = c(1+S)\log c(1+S) + c(1-S)\log c(1-S) + \{1-c(1+S)\}\log\{1-c(1+S)\}$$
$$+\{1-c(1-S)\}\log\{1-c(1-S)\}$$
$$+\frac{z}{2}\int \frac{[1+\{2(1-2c)+4c^2(1-S^2)\}y+(1-2c)^2y^2]^{\frac{1}{2}}-1-(1-2c)y}{y(y+1)}dy,$$

where

$$y = e^{2\chi/(kT)} - 1 \qquad .. \quad (35)$$

from which, we obtain for $c=\frac{1}{2}$

$$\Theta = \frac{\chi}{k\log\frac{z}{z-2}}, \qquad .. \quad (36)$$

as against $\Theta = z\chi/(2k)$ obtained by us previously on the Bragg-Williams approximation.

Now confining ourselves to the ratio Cu : Zn=1 : 1, i.e. $c=\frac{1}{2}$, and to temperatures above the Curie temperature for which, S=0, we obtain

$$N\overline{dc^2} = \frac{1}{4+2z\left(e^{\chi/kT}-1\right)},$$

as against the approximate ex ion

$$N\overline{dc^2} = \frac{1}{4+2z\chi/(kT)},$$

which we obtained previously.

The expression for ρ_e will now become

$$\rho_e = \frac{K/4}{1+\frac{z}{2}\left(e^{X/(aT)}-1\right)}, \qquad \ldots (37)$$

which evidently will correspond to a slightly steeper slope of the ρ *vs* T curve than the expression obtained previously (29).

Taking as before the observed value of the specific resistance $\rho=\rho_d+\rho_e$ at the Curie temperature as 14·10 $\mu\Omega$ cm, and $\sigma_1=\pi$ (1·97Å)^2, we have recalculated σ_2 on the basis of (37), and we obtain

$$\sigma_1 - \sigma_2 = \pi \times 0{\cdot}78\text{Å}^2$$

and

$$\sigma_2 = \pi \times (1{\cdot}77\text{Å})^2$$

as against

$$\sigma_1 - \sigma_2 = \pi \times 0{\cdot}67\text{Å}^2$$

$$\sigma_2 = \pi \times (1{\cdot}80\text{Å})^2$$

obtained previously.

The values of ρ above the Curie temperature plotted in Fig. 1, have been calculated on the basis of these values and expression (37). It will be seen that the theoretical curve fits well with the experimental values of Steinwehr and Schulze. The experimental values of Webb, however, are appreciably higher.

Thus on the high temperature side of the Curie temperature also the theory is verified satisfactorily.

13. Variation of ρ_e of the CuZn alloy with concentration when S is nearly unity

Finally we may take up *Case* I referred to in Section 8, namely the variation of ρ_e of the CuZn alloy with concentration, in the neighbourhood of $c=\frac{1}{2}$, i.e. Cu : Zn=1 : 1, and when the order is nearly unity. The expressions for ρ_e on the two sides of $c=\frac{1}{2}$, reduce when S$\sim$1, and c is in the neighbourhood of 1/2, roughly to [See (24)]

$$c \leqslant 1/2\,; \quad \rho_e = \frac{K}{2}\left(\frac{3}{2} - S - c\right) \qquad .. \quad (38a)$$

$$c \geqslant 1/2\,; \quad \rho_e = \frac{K}{2}\left(\frac{1}{2} - S + c\right) \qquad .. \quad (38b)$$

where K has the same significance as before [see (27)].

From these expressions it will be seen that ρ_e is a minimum at $c=\frac{1}{2}$, and rises sharply and symmetrically on both sides of it, the curve being V shaped, suggesting proportionality of the increase in resistance with the change in concentration.

The occurrence of such a minimum, and the increase on either side proportionately to the change in concentration, are verified experimentally. Indeed both these results have

already been predicted by others from direct considerations, by regarding the excess atoms of Cu or Zn as the case may be, over that corresponding to the concentration Cu : Zn=1 : 1, as impurity atoms alloyed with CuZn, the latter being regarded as the pure phase. Actually, however, the value of c at which the resistance is a minimum corresponds to the ratio Cu : Zn=1·08 : 1, and not to 1 : 1 ; the former ratio is the closest approach to 1 : 1 at which the alloy can exist in the β-phase. For larger concentrations of Zn than this, the alloy is hexagonal. On the β-phase side, to which expression (38b) applies, the actual variation of ρ_e with c is not quite so steep as predicted theoretically. One should not, however, expect a closer agreement, since we are here dealing with the alloy at room temperature at which the relaxation time of the alloy for attaining equilibrium conditions may be large. This may also be the explanation of the wide discrepancy between Webb's results and those of Houghton and Griffiths quoted by him in his paper.

14. Summary

Since the electrical resistance of a metal or an alloy may be regarded as arising from the scattering of the electron waves passing through the medium and representing the electric current, by the thermally agitated atoms of the medium, the calculation of the electrical resistance reduces to one of calculating the attenuation coefficient of the waves due to scattering. The attenuation coefficient, and thence the resistance, of a binary alloy are calculated in terms of the local fluctuations in the density and in the concentration of the alloy, both due to thermal agitation. A well known method adopted in calculating the attenuation coefficient of a medium for light waves due to scattering, in terms of the thermal fluctuations in the medium, is to divide the medium into volume elements which are small in comparison with the wave-length such that the scattered radiations from the different parts of the element may be of sensibly the same phase, and which at the same time are large enough to contain a great many atoms, such that the fluctuations in neighbouring volume elements will be uncorrelated. Such a subdivision is shown to be possible in a crystal even for wave-lengths only slightly longer than twice the inter-atomic distance. Hence this method is shown to be applicable to the calculation of the attenuation coefficient of the electron waves that are involved in electric conduction, and whose wave-lengths are roughly of this magnitude.

Detailed calculations of the electrical resistance are given for one typical order-disorder alloy, namely CuZn. The part of the resistance due to "density scattering" is easily calculated in terms of the compressibility and the known cross-sections of the atoms for scattering. The part due to "concentration scattering" is calculated in the following manner. Starting with the expression for the configurational free energy of the alloy in terms of its concentration, one can readily obtain by suitable differentiations, the expression for the fluctuations in concentration, and thence the part of the resistance due to concentration scattering. For temperatures below the Curie temperature Bragg-Williams approximation is adopted for calculating the free energy, since the adoption of higher approximations makes the expression for fluctuations in concentration very complicated. At temperatures higher than the Curie temperature, the calculation of the resistance due to concentration scattering is carried to a higher approximation.

The following special cases, which are the only cases of practical interest, are discussed in detail ;

I : when the concentration is in the neighbourhood of Cu : Zn = 1 : 1, and the degree of order is nearly unity ;

II : when Cu : Zn ratio is just 1 : 1, for all degrees of order from 1 to 0 ;

III : when the temperature is above the Curie temperature, for all concentrations.

The theory is satisfactorily verified in all the three cases, if the effective number of free electrons is taken to be 1·5 per atom, (which is also the actual number) when the degree of order is small, and about 0·5 per atom when the order is nearly complete. These values for the effective number are just what should be expected, since at low order the first Brillouin Zone can accomodate two electrons per atom, whereas with the development of order a smaller zone appears that can accommodate only one electron per atom.

One striking feature of the new results is the finite and large temperature-coefficient of the extra resistance of the alloy due to concentration scattering, even above the Curie temperature. Such a finite temperature-cofficient is not contemplated in the current theories, but is verified experimentally. This finite temperature coefficient of the extra resistance distinguishes order-disorder alloys above Curie temperature from genuine random alloys for which the Curie temperature is zero, and for which the temperature-coefficient of the extra resistance also is zero.

For random alloys the proportionality of the extra resistance to $c(1-c)$, i.e. to the product of the concentrations of the two components, originally derived by Nordheim, is verified in the present theory, and the constant of proportionality, unlike in Nordheim's treatment, can be evaluated in terms of known physical quantities.

References

Bethe, H. A. 1935 Proc. Roy. Soc. A, *150*, 552.
Bragg, W. H. and Bragg, W. L. 1939, *The Crystalline State*, Bell, London pp. 218.
Bragg, W. L. 1934 Proc. Roy. Soc. A, *145*, 699.
Bragg, W. L. and Williams, E. J. 1935 Proc. Roy. Soc. A, *151*, 504.
Darwin, C. G 1914 Phil. Mag. *1*, 315.
Einstein, A. 1910 Ann. d. Physik. *33*, 1294.
Fowler, R. H. and Guggenheim, E. A. 1940 Proc. Roy. Soc. A, *174*, 189.
Frenkel, J. 1928 Zeits. f. Phys. *47*, 819.
Frenkel, J. 1936 *Wave Mechanies, Elementary Theory*, Oxford Univ. Press, §35 pp. 257-03.
Johansson, C. H. and Linde, J. O. 1936 Ann. d. Physik *26*. 1.
Mott, N. F. and Jones, H. 1936 The *Theory of the Properties of Metals and Alloys*, Oxford Univ. Press, p. 264.
Mott, N. F. and Massey, H. S. W. 1933 *The Theory of Atomic Collisions*, Clarendon Press, Oxford, p. 134.
Kurnakov, N. S. and Ageew, N. W. 1931 J. Inst. Metals, *46*, 481.
Muto, T. 1936 Inst. Phys. and Chem. Research, Tokyo, Sci. Papers No. 653, p. 99.
Nordheim, L. 1931 Ann. d. Physik, *9*, 607.
Raman, C. V. and Ramnathan, K. R. 1923 Phil. Mag. *45*, 213.
Steinwehr, H. V. and Schulze, A. 1934 Phys. Zeits. *35*. 385.
Sykes, C. and Jones, F. W. 1936 Proc. Roy. Soc. A, *157*, 213.
Tolmann, R. C. 1938 *The Principles of Statistical Mechanics*, Oxford, Clarendon Press, p. 641,
Webb, W. 1939 Phys. Rev. *55*, 297.
Williams, E. J. 1935 Proc. Roy. Soc. A, *152*, 231.

Electrical Resistance of Liquid Metals

The electrical resistance of a metal arises from the scattering of the electron waves passing through it. The fraction of these electron waves scattered in all directions in a unit volume, which will be called the attenuation coefficient, μ, is equal to the reciprocal of the mean free path of the electrons. From this the specific resistance ρ can be calculated from the formula.

$$\rho = \frac{h}{n\nu e^2\lambda} \cdot \mu, \quad . \quad . \quad . \quad . \quad . \quad . \quad (1)$$

where ν is the number of atoms per unit volume, n is the number of conduction electrons per atom, and λ is the wave-length corresponding to the Fermi surface.

In the alkali metals in the solid state, this wave-length is 14 per cent greater than the wave-length that will give the first Bragg reflexion in the backward direction. In a recent paper[1], we have shown that this magnitude for λ is sufficient to make the scattering coefficient *even in the backward direction* conform to the Einstein-Smoluchowski formula

$$\left.\begin{aligned} E_\varphi &= \varepsilon \,.\, \nu\sigma_\varphi, \\ \varepsilon &= \nu kT\beta \end{aligned}\right\} \quad . \quad . \quad . \quad (2)$$

where E_φ is the scattering coefficient in any direction making an angle φ with the direction of motion of the electrons, defined for unit volume and for unit solid angle ; β is the isothermal compressibility, and σ_φ is the scattering coefficient for a single isolated atom. (σ_φ will be proportional to the square of the atomic structure factor as usually defined.) T is taken to be sufficiently large in comparison with the Debye temperature for the thermal energy to be regarded as proportional to kT.

The attenuation coefficient will then be given by

$$\mu = \int_0^\pi E_\varphi \,.\, 2\pi \sin\varphi d\varphi \quad . \quad . \quad . \quad . \quad (3)$$

$$= \varepsilon \,.\, \nu\sigma, \quad . \quad . \quad . \quad . \quad . \quad . \quad . \quad (4)$$

where $\sigma = \int_0^\pi \sigma_\varphi \,.\, 2\pi \sin\varphi d\varphi$ is the cross-section of the atom for scattering in all directions.

In the alkali metals in the liquid state also, λ is about 13 per cent longer than λ_0, where λ_0 is the wave-length for which the first diffraction maximum is in the backward direction, $\varphi = \pi$. Though the diffraction halo of the liquid is much more diffuse than the Bragg reflexions in the solid, the above magnitude of λ is still sufficient to exclude all the intense parts of the halo. A portion of its long tail, however, extends into the observable range, $\varphi \ll \pi$. This forms an excess scattering in the neighbourhood of the backward direction over that given by (2), and hence μ will be in excess of the value determined by (4) by a corresponding amount. On calculation, this extra scattering in the liquid is found to account for the observed increase in resistance of about 50 per cent of the alkali metals on melting. (The increase due to changes in β and ν on melting is relatively small, about 10 per cent.)

Since the method adopted for this calculation is general, and is applicable to polyvalent liquid metals also, we will briefly describe the method here. Denoting by x_φ and s_φ the quantities in X-ray scattering analogous to E_φ and σ_φ respectively in electron scattering, we have

$$\frac{x_\varphi}{\nu s_\varphi} = \frac{E_\varphi}{\nu\sigma_\varphi}, = R_\varphi \text{ say.} \quad . \quad . \quad . \quad . \quad (5)$$

Now x_φ, s_φ and R_φ involve φ and λ through $\sin\frac{1}{2}\varphi/\lambda$ alone. Hence knowing the intensity distribution in X-ray scattering by the liquid metal, and the X-ray atomic structure factor, for any convenient wave-lengths, we know R_φ. The Fermi electronic wave-length for the metal is also easily calculated ; for this purpose we regard *all* the valency electrons as conduction electrons. If now the atomic structure factor for the scattering of electron waves of this particular wave-length is known, the electronic scattering coefficient E_φ for the metal in different directions can be calculated, and thence, using relations (3) and (1) respectively, the attenuation coefficient μ and the specific resistance ρ can be calculated.

We have calculated the electrical resistances of some typical liquid metals by this method, using the known distribution of intensity in the X-ray diffraction pattern of the liquid[2] and the known X-ray atomic structure factors. Data for atomic structure factors for electron scattering for such low-velocity electrons as are involved in conduction are available for the rare gas atoms only[3], and they have been adopted roughly as the appropriate values for the corresponding alkali atoms in the metal. For other atoms, for want of similar data, the electronic scattering coefficient of the atom σ_φ is assumed to be the same in different directions, and equal to $\sigma/(4\pi)$.

Now plotting R_φ against $\sin\frac{1}{2}\varphi/\lambda = \xi$, say, it is found that in all liquid metals there is one prominent maximum for R_φ, the value of this maximum being about 2 or 3. When ξ is increased further, R_φ falls below unity, and after two or three oscillations about the value $R_\varphi = 1$, with progressively diminishing amplitudes, settles down at this value. As we proceed from the prominent maximum to smaller values of ξ, in most liquids R_φ falls quickly to a very low value, which according to the theory must be the Einstein-Smoluchowski value $R_\varphi = \varepsilon \ll 1$, and must remain so at all smaller values of ξ. In a few liquids, for example, zinc and aluminium, R_φ passes through a subsidiary maximum, before falling to ε.

Now the attenuation coefficient, and hence the resistance, of a given liquid metal will depend on how much of the diffraction pattern, the intensity of which is highly concentrated in the neighbourhood of the prominent halo, is included in the range $0 < \varphi \ll \pi$, or $0 < \xi \ll 1/\lambda$, where λ is the Fermi wave-length of the metal. In monovalent metals this range includes little beyond the Einstein-Smoluchowski region ; whereas in the other extreme case when the valency is sufficiently high ($n = 5$ or 4), it includes the whole of the diffraction pattern where R_φ deviates significantly from unity. For intermediate valencies ($n = 2$ or 3), the region includes the major portion of the prominent halo, but not the whole of it.

We may mention here one striking result to which we are led by these considerations. Whereas in monovalent liquid metals the attenuation coefficient is of the order of the Einstein-Smoluchowski value, namely, $\mu = \varepsilon \times \nu\sigma$, in polyvalent liquid metals it approximates to what may be called the Rayleigh value, namely, $\mu = \nu\sigma$, which is much larger. The experimental values for the electrical resistances of liquid alkali and noble metals verify the former value, and those for liquid bismuth, lead and tin the latter, with reasonable values for σ.

The exceptional electric behaviour of mercury is

due to the following circumstance. Its prominent diffraction halo, which is very sharp, is much closer to the centre than in other liquids; the spherical zone in phase space the boundary of which corresponds to this maximum can accommodate only 0·9 electrons per atom, whereas in the other liquid metals studied this number varies from 1·2 to 1·7 per atom.

K. S. KRISHNAN.
A. B. BHATIA.

University of Allahabad,
Allahabad.
June 20.

[1] *Proc. Nat. Acad. Sci. India*, in the press. We owe to Frenkel the idea of calculating the coefficient of electronic scattering in a metal in terms of the thermal fluctuations in density.
[2] For collected data, see Gingrich, N. S., *Rev. Mod. Phys.*, **15**, 90 (1944).
[3] Ramsauer, C., and Kollath, R., *Ann. Phys.*, **12**, 529 (1932).

Light-scattering in homogeneous media regarded as reflexion from appropriate thermal elastic waves

BY A. B. BHATIA, D.PHIL. AND SIR K. S. KRISHNAN, F.R.S.
University of Allahabad

(*Received* 21 *May* 1947)

Attributing the scattering of light in a homogeneous transparent liquid to the local fluctuations in density, and the latter to the superposition of the thermal elastic waves of different wave-lengths maintained in the enclosure, one may, following Einstein, evaluate the scattering coefficient of the liquid along any given direction. The expression for the scattering coefficient involves a triple infinite series, which Einstein evaluates by suitably replacing it by a triple integral. The series, however, can be directly summed, and the contributions from different progressive waves to scattering studied in detail. This method brings out prominently the appropriateness of regarding scattering as regular Bragg reflexions from suitable elastic waves, and also reveals some interesting features which are missed when the summation is replaced by integration.

The intensities of the Brillouin components are calculated on this basis, both in a fluid medium and in a crystal; and in the latter case the expression for the overall intensity of the Brillouin components is shown to be identical with the well-known expression of Waller in X-ray scattering.

1. EINSTEIN'S TREATMENT OF LIGHT-SCATTERING IN A LIQUID

The intensity of light scattered by a homogeneous liquid is calculated by Einstein (1910) in the following manner. Consider for simplicity a *monatomic* liquid contained in a large cube of edge-length L, $0<x<L$, $0<y<L$, $0<z<L$. The local fluctuations in the density of the liquid, due to thermal agitation, which ultimately produce the scattering, may be expressed in terms of the stationary elastic waves maintained in the cube:

$$D = D_0+\Delta,$$

$$\Delta = \sum_{\rho}\sum_{\sigma}\sum_{\tau} B_{\rho\sigma\tau}\sin\frac{2\pi\rho x}{2L}\sin\frac{2\pi\sigma y}{2L}\sin\frac{2\pi\tau z}{2L}\exp\left[i(2\pi N_{\rho\sigma\tau}t-\theta_{\rho\sigma\tau})\right], \qquad (1)$$

where Δ is the fluctuation in density at any point xyz from the mean value D_0, and $\rho\sigma\tau$ are positive integers which define as usual the stationary elastic waves; a stationary wave defined by given $\rho\sigma\tau$ will consist in general of *eight* progressive waves whose wave-length $\Lambda_{\rho\sigma\tau}$ is equal to $2L/(\rho^2+\sigma^2+\tau^2)^{\frac{1}{2}}$, and the direction-cosines of whose wave-normals (one in each octant of co-ordinate space) are given by the eight combinations of $(\pm\rho, \pm\sigma, \pm\tau)/(\rho^2+\sigma^2+\tau^2)^{\frac{1}{2}}$,

$$N_{\rho\sigma\tau} = V_{\rho\sigma\tau}/\Lambda_{\rho\sigma\tau}, \qquad (2)$$

where $N_{\rho\sigma\tau}$ is the frequency, and $V_{\rho\sigma\tau}$ is the phase velocity, of elastic waves of wave-length $\Lambda_{\rho\sigma\tau}$.

Consider a small cube of edge-length l of the liquid, with its edges parallel to those of the large cube. The fraction of the incident light scattered by this element

of volume l^3, per unit solid angle, along a direction making an angle ϕ with the incident direction, will then be given by

$$S_\phi l^3 = \frac{l^6}{64 D_0^2} n^2 \sigma_\phi \sum_\rho \sum_\sigma \sum_\tau \overline{B^2_{\rho\sigma\tau}} \frac{\sin^2\xi}{\xi^2} \frac{\sin^2\eta}{\eta^2} \frac{\sin^2\zeta}{\zeta^2}, \tag{3}$$

where S_ϕ is the scattering coefficient per unit volume of the liquid per unit solid angle along the direction considered, and σ_ϕ is the corresponding coefficient for an *individual* (not isolated) atom in the liquid, n is the number of atoms per unit volume, $\overline{B^2_{\rho\sigma\tau}}$ is the time average of $B^2_{\rho\sigma\tau}$, and

$$\xi = \frac{\pi}{2}\frac{l}{L}(\rho - \rho_0), \quad \eta = \frac{\pi}{2}\frac{l}{L}(\sigma - \sigma_0), \quad \zeta = \frac{\pi}{2}\frac{l}{L}(\tau - \tau_0), \tag{4}$$

where $\rho_0\sigma_0\tau_0$ are positive numbers, not necessarily integers, which analogously to $\rho\sigma\tau$ define certain wave-normal directions, and a wave-length, and are such that

(1) one of the four pairs of wave-normals defined by them is along the bisector of the exterior angle $\pi - \phi$ between the directions of incidence and of observation;

(2) the wave-length $\Lambda_0 = 2L/(\rho_0^2 + \sigma_0^2 + \tau_0^2)^{\frac{1}{2}}$ defined by them satisfies the Bragg condition for reflecting the incident light-waves along the direction of observation, namely,

$$2\Lambda_0 \sin\tfrac{1}{2}\phi = \lambda, \tag{5}$$

where λ is the wave-length of the incident light.

In other words, if there were elastic waves in the liquid of the above wave-length, and progressing along the above bisector in either direction, the coefficient of reflexion of the incident light-waves from these elastic waves would be a maximum in the direction selected for observation of scattering.

In (3) we have expressed the scattering coefficient S_ϕ of the liquid along any given direction ϕ in terms of the scattering coefficient of the atom, i.e. the atomic cross-section for scattering, along the same direction, namely, σ_ϕ. The σ_ϕ introduced here is analogous to the well-known atom form factor for intensity in X-ray scattering. σ_ϕ will be proportional to M^2, where M is the dipole moment induced in the atom per unit 'field in the medium', and since the actual field acting on the atom which produces the dipole moment M is not merely the field in the medium but includes the polarization field due to surrounding atoms, σ_ϕ will not be an atomic constant, but will depend also on the density of packing of the atoms in the medium.

We may mention here that in Einstein's derivation, S_ϕ is expressed in terms of the local fluctuations in the refractivity of the liquid accompanying the fluctuations in density. We shall discuss the value of σ_ϕ in the liquid in relation to the density of packing of the atoms, and the refractivity of the liquid, in § 6 of this paper.

We should, however, emphasize here a fundamental assumption that underlies the derivation of relation (3). Consider a small element of volume v in the liquid containing on an average N atoms, the linear dimensions and the disposition of the volume element being such that the scattered radiations from the different parts of the element reach the observer in practically the same phase. If $\overline{\Delta N^2}$ is the mean

square of the fluctuation in the number of atoms in the volume element from its average value N, the assumption referred to is that the contribution from this volume element to the scattering by the liquid is given by

$$S_\phi v = \overline{\Delta N^2}\sigma_\phi. \tag{6}$$

We shall discuss the validity and the implications of this assumption when we take up in § 6 below the question of the relation between the atomic scattering coefficient in the liquid, and the density and the refractivity of the liquid.

2. Evaluation of the series appearing in (3) by integration

Coming back to expression (3) for S_ϕ, since the wave-length of light is long in comparison with the interatomic distance, the values of $\rho_0\sigma_0\tau_0$, even for the backward direction of observation, will be much smaller than the maximum values of $\rho\sigma\tau$ for the elastic waves, and since the significant values of $\sin^2\xi/\xi^2$, $\sin^2\eta/\eta^2$ and $\sin^2\zeta/\zeta^2$ are confined to small values of ξ, η and ζ respectively, the summations in (3) may be taken to extend over all permitted (discrete) values of ξ or η or ζ as the case may be, from $-\infty$ to $+\infty$.

Now $\rho\sigma\tau$ vary in steps of unity, and for given directions of incidence and observation, i.e. for given $\rho_0\sigma_0\tau_0$, the corresponding steps in the variation of $\xi\eta\zeta$ will be $\frac{1}{2}\pi l/L$, and can be made infinitesimally small by making l sufficiently small in comparison with L. Doing so, and regarding $\overline{B^2_{\rho\sigma\tau}}$ as independent of $\rho\sigma\tau$—which will be practically the case at room temperature, which is high enough for the thermal energies of the long elastic waves that are involved here to be nearly proportional to the absolute temperature—we obtain

$$\Sigma\Sigma\Sigma\, \overline{B^2_{\rho\sigma\tau}} \frac{\sin^2\xi}{\xi^2}\frac{\sin^2\eta}{\eta^2}\frac{\sin^2\zeta}{\zeta^2} = \overline{B^2}\left(\frac{2}{\pi}\frac{L}{l}\right)^3 \int_{-\infty}^{+\infty}\!\!\int\!\!\int \frac{\sin^2\xi}{\xi^2}\frac{\sin^2\eta}{\eta^2}\frac{\sin^2\zeta}{\zeta^2} d\xi\, d\eta\, d\zeta$$

$$= \overline{B^2}\left(\frac{2L}{l}\right)^3, \tag{7}$$

from which we obtain

$$S_\phi = n^2\sigma_\phi \frac{\overline{B^2}L^3}{8D_0^2}. \tag{8}$$

At the high temperatures that we are considering

$$\frac{\overline{B^2}L^3}{8D_0^2} = kT\beta, \tag{9}$$

where β is the isothermal compressibility of the liquid, and k is the Boltzmann constant, and we obtain for the scattering coefficient per unit volume, per unit solid angle, along the direction considered

$$S_\phi = n^2\sigma_\phi kT\beta. \tag{10}$$

For a gas obeying Boyle's law, $nkT\beta = 1$, and S_ϕ becomes equal to $n\sigma_\phi$, as should be expected since the scattered radiations even from neighbouring atoms will then be of *random* phases. In the other extreme case where all the atoms scatter in the *same* phase, S_ϕ will evidently be equal to $n^2\sigma_\phi$.

3. Direct summation of the series

We wish to point out here that the series appearing on the left-hand side of (7) may be summed up directly, and to draw attention to certain interesting features in scattering that are revealed by the summation, and are missed when it is replaced by integration in the manner described above. What is required is the sum of the values of $\sin^2\xi/\xi^2$, etc., at equal intervals $\alpha = \frac{1}{2}\pi l/L$, and it can be shown that

$$\sum_{n=-\infty}^{+\infty} \frac{\sin^2(n\alpha+\theta)}{(n\alpha+\theta)^2} = \frac{\pi}{\alpha}, \tag{11}$$

where n is an integer, $0<\alpha\leqslant\pi$, and θ is a constant. (θ in our problem is equal to $\frac{1}{2}\pi l/L$ times the fractional part of ρ_0 or σ_0 or τ_0, as the case may be.) The proof is as follows:

Consider the well-known series*

$$\sum_{n=1}^{\infty}\left[\frac{\sin\{(n+\beta)y\}}{n+\beta}+\frac{\sin\{(-n+\beta)y\}}{-n+\beta}\right] = -\frac{\sin\beta y}{\beta}+\pi \quad (0<y<2\pi), \tag{12}$$

in which β is a constant and n an integer. In the interval $0\leqslant y<2\pi$, the series in (12) can be integrated term by term (i.e. the sum of the series of integrals thus obtained will be equal to the integral of the sum), since it is uniformly convergent except in the neighbourhood of zero, and is boundedly convergent over the whole interval including zero. Replacing each sine term in (12) by the product of a sine and cosine term, and integrating, we have

$$2\sum_{n=1}^{\infty}\left[\frac{\sin^2\{(n+\beta)y/2\}}{(n+\beta)^2}+\frac{\sin^2\{(-n+\beta)y/2\}}{(-n+\beta)^2}\right] = -\frac{2}{\beta^2}\sin^2\frac{\beta y}{2}+\pi y. \tag{13}$$

Putting $\frac{1}{2}y=\alpha$, $\alpha\beta=\theta$, transposing $\frac{2}{\beta^2}\sin^2\frac{\beta y}{2}$ to the left-hand side, and dividing both sides by α^2, $\alpha\neq 0$, we obtain for $0<\alpha<\pi$

$$\sum_{n=-\infty}^{+\infty} \frac{\sin^2(n\alpha+\theta)}{(n\alpha+\theta)^2} = \frac{\pi}{\alpha}.$$

This can be readily seen to be true for $\alpha=\pi$ also, and hence (11) holds over the interval $0<\alpha\leqslant\pi$.†

We notice in particular that the sum in (11) is independent of θ.

Coming back to the series appearing on the left-hand side of (7), we obtain using (11)

$$\sum_{\xi}\sum_{\eta}\sum_{\zeta}\bar{B}^2_{\rho\sigma\tau}\frac{\sin^2\xi}{\xi^2}\frac{\sin^2\eta}{\eta^2}\frac{\sin^2\zeta}{\zeta^2} = \bar{B}^2\left(\frac{\pi}{\alpha}\right)^3 = \bar{B}^2\left(\frac{2L}{l}\right)^3, \tag{14}$$

the same result as obtained in (7) by integration.

* See, for example, J. Bromwich, *An Introduction to the Theory of Infinite Series* (Macmillan, 1931, p. 371).

† We are thankful to Professor Norbert Wiener for the following elegant alternative proof of (11).

Let
$$g(v) = \frac{1}{\sqrt{(2\pi)}}\int_{-\infty}^{+\infty} f(u)\, e^{iuv}\,du$$

Since the series can be summed up, it is not necessary to make l small. One may choose l as large as one likes, *even make it equal* L, in which case α becomes equal to $\frac{1}{2}\pi$, and still satisfies the condition $0<\alpha\leqslant\pi$.

Making $l=L$, one obtains from (3)

$$S_\phi = n^2\sigma_\phi\frac{L^3}{(64l)_0^2}\bar{B}^2\sum_{\rho}\sum_{\sigma}\sum_{\tau}, \tag{15}$$

where
$$\sum_{\rho} = \sum_{n=-\infty}^{+\infty}\frac{\sin^2(\frac{1}{2}n\pi+\theta_\rho)}{(\frac{1}{2}n\pi+\theta_\rho)^2}, \quad \text{etc.,} \tag{16}$$

and $\theta_\rho = \frac{1}{2}\pi$ times the fractional part of ρ_0, etc.

Each of the three sums appearing in (15) is obviously equal to 2, giving for S_ϕ the same value (8) as before.

4. Light-scattering regarded as reflexion from appropriate elastic waves

Expressions (15) and (16) for S_ϕ give us the following information:

(1) For any given stationary wave (specified by given $\rho\sigma\tau$) (15) and (16) give the variation of its contribution to S_ϕ with the change in the direction of incidence, or of observation, i.e. with the change in $\rho_0\sigma_0\tau_0$. The variation is as

$$\sin^2\xi/\xi^2\,.\,\sin^2\eta/\eta^2\,.\,\sin^2\zeta/\zeta^2;$$

$$\xi=0, \quad \text{when} \quad \rho_0=\rho, \quad \text{etc.,}$$

and
$$d\xi/d\rho_0 = d\eta/d\sigma_0 = d\zeta/d\tau_0 = \tfrac{1}{2}\pi.$$

(2) For any given directions of incidence and of observation, i.e. for any given $\rho_0\sigma_0\tau_0$, (15) and (16) give the contributions to S_ϕ from different stationary waves,

---

be the Fourier transform of the function

$$f(u) = \frac{\sin^2(u+\theta)}{(u+\theta)^2} = \frac{\sin^2 w}{w^2}, \quad \text{say.}$$

Then
$$g(v) = \frac{e^{-iv\theta}}{\sqrt{(2\pi)}}\int_{-\infty}^{+\infty}\frac{\sin^2 w}{w^2}e^{iwv}\,dw$$
$$= \frac{e^{-iv\theta}}{\sqrt{(2\pi)}}\pi\left[1-\frac{|v|}{2}\right], \quad \neq 0 \quad \text{when } -2<v<2.$$

Now according to Poisson's formula,

$$\sum_{n=-\infty}^{+\infty} f(n\alpha) = \frac{\sqrt{(2\pi)}}{\alpha}\sum_{n=-\infty}^{+\infty} g\left(\frac{2\pi n}{\alpha}\right),$$

where n is an integer, and $\alpha>0$. If further, as in our problem, α is not greater than π, there is only one value of n for which $g\left(\frac{2\pi n}{\alpha}\right)$ differs from 0, namely $n=0$; and $g(0)=\sqrt{(\frac{1}{2}\pi)}$, and is independent of θ. Hence

$$\sum_{n=-\infty}^{+\infty} f(n\alpha) = \frac{\sqrt{(2\pi)}}{\alpha}\sqrt{\frac{\pi}{2}} = \frac{\pi}{\alpha}.$$

i.e. stationary waves of differing $\rho\sigma\tau$; these contributions also are proportional to $\sin^2\xi/\xi^2 . \sin^2\eta/\eta^2 . \sin^2\zeta/\zeta^2$, ξ being zero when $\rho = \rho_0$, etc., and a change of ρ or σ or τ by unity, as will occur when we pass from one stationary wave to the adjacent one, corresponding to a change of $\frac{1}{2}\pi$ in ξ, or η, or ζ, respectively.

It can be readily seen that the resolving power of the stationary waves regarded as forming a reflexion grating is just half that necessary to resolve, in the Rayleigh sense, the reflexions from adjacent stationary waves, by which we mean stationary waves whose ρ or σ or τ values differ by unity. Hence the significant part of the contribution to S_ϕ comes from waves whose $\rho\sigma\tau$ lie close to $\rho_0\sigma_0\tau_0$, and practically lie in the range $\rho_0 \pm 2$, $\sigma_0 \pm 2$, $\tau_0 \pm 2$. Hence it is not now necessary to assume the independence of $\overline{B^2_{\rho\sigma\tau}}$ on $\rho\sigma\tau$. We choose for $\overline{B^2}$ the value appropriate to the neighbourhood of $\rho_0\sigma_0\tau_0$.

On the other hand, when the scattering volume is restricted to a small element l^3, $l \ll L$, the resolving power of the elastic waves inside the element regarded as forming a reflexion grating naturally becomes smaller by a factor l/L, and hence not only the few elastic waves whose $\rho\sigma\tau$ values lie in the close neighbourhood of $\rho_0\sigma_0\tau_0$, but waves corresponding to a much wider range, $(\rho_0 - 2L/l) < \rho < (\rho_0 + 2L/l)$, etc., will apparently contribute to the scattering along any given direction.

Now when $l = L$ each of the sums $\sum_{\xi=-\infty}^{+\infty} \sin^2\xi/\xi^2$, etc., appearing in (15) is equal to 2, which is just twice the value of $\sin^2\xi/\xi^2$ at $\xi = 0$, etc. Their product will therefore be 8 times the value at $\xi = \eta = \zeta = 0$. Now in reflexion from a stratified medium, it will be seen by applying Huyghens's principle, that the variations in density along the normal to the reflecting plane alone will affect the intensity of reflexion in the Bragg direction. Hence the above result indicates that S_ϕ is *eight times* the coefficient of reflexion along the Bragg direction of reflexion from a pair of progressive elastic waves, extending over the whole volume L^3 of the liquid, the two progressive waves travelling in opposite directions along the bisector of the exterior angle between the directions of incidence and of observation, the wave-length of these waves,

$$\Lambda_0 = 2L/(\rho_0^2 + \sigma_0^2 + \tau_0^2)^{\frac{1}{2}} = \lambda/(2\sin\tfrac{1}{2}\phi),$$

being that appropriate for giving a Bragg reflexion of the incident light-waves of wave-length λ along the direction of observation, and the energy of each of the two progressive waves being *one-eighth* of the energy associated with a normal mode of vibration,* or *one-eighth* of the energy of a Planck oscillator of frequency N_0 corresponding to the wave-length Λ_0. It follows that S_ϕ may also be taken to be just the coefficient of reflexion along the Bragg direction of reflexion, from these two progressive waves, provided we assign to each of these waves the full energy of a Planck oscillator of the appropriate frequency N_0.

* Since *eight* such progressive waves constitute one normal mode of vibration.

5. Intensity of scattering in terms of the energy and velocity of propagation of the reflecting elastic waves

In the last section we noticed that practically the whole of the contribution to the observed scattering along any given direction comes from the few elastic waves in the close neighbourhood of those in a position to reflect, in the Bragg sense, the incident light-waves along the direction of observation, i.e. from those elastic waves whose $\rho\sigma\tau$ values lie in the close neighbourhood of $\rho_0\sigma_0\tau_0$, and hence expression (8) for S_ϕ, namely,

$$S_\phi = n^2\sigma_\phi \frac{\overline{B^2} L^3}{8D_0^2},$$

will be valid even under conditions when $\overline{B^2_{\rho\sigma\tau}}$ may not be independent of $\rho\sigma\tau$, e.g. at low temperatures, provided we use for $\overline{B^2}$ the value appropriate for $\rho_0\sigma_0\tau_0$. In that case it will be convenient to express $\overline{B^2_{\rho_0\sigma_0\tau_0}}$ in terms of the energy and the velocity of propagation of the elastic waves defined by $\rho_0\sigma_0\tau_0$, instead of in terms of $kT\beta$ as we did at the high temperatures. The expression for S_ϕ will now be of the form

$$S_\phi = n^2\sigma_\phi \frac{E(N_0)}{V_0^2 D_0}, \tag{17}$$

where $E(N_0)$ is the energy of a Planck oscillator of frequency N_0 and is equal to $hN_0/(e^{hN_0/kT} - 1) + \frac{1}{2}hN_0$, and V_0 is the velocity of propagation of elastic waves of this frequency in the liquid,

$$V_0/N_0 = \Lambda_0 = 2L/(\rho_0^2 + \sigma_0^2 + \tau_0^2)^{\frac{1}{2}}.$$

For the long elastic waves $\Lambda_0 \gg n^{-1}$ involved in light-scattering, V_0 will be practically independent of the wave-length Λ_0, and will be equal to $(\beta D_0)^{-\frac{1}{2}}$, leading to the same expression for S_ϕ as before.

We have confined ourselves till now to a fluid medium, in which the elastic waves concerned in reflecting the incident light-waves, and thus producing the observed scattering, are longitudinal waves, the direction of displacement of the atoms under these waves being along the wave-normal, i.e. along the normal to the reflecting plane. This will be the case in an elastically isotropic solid also. If, however, the medium is an elastically anisotropic solid, the wave-length Λ_0 and the direction of the wave-normal, say $\mathbf{n}_0$, of the elastic waves which by reflexion of the incident light-waves produce the scattering, will still be determined in the same manner as before, namely by $\rho_0\sigma_0\tau_0$, but the frequency N_0, and the velocity of propagation V_0, of these elastic waves will now be dependent on the direction of the wave-normal $\mathbf{n}_0$ in the crystal, and will have three different values, corresponding to the three directions of displacement in the crystal associated with elastic waves of a given wave-length, and given wave-normal direction. Further, the directions of displacement will not in general be parallel and perpendicular respectively to the direction of the wave-normal $\mathbf{n}_0$, as in an elastically isotropic medium, but will be inclined to this direction.

Let $\omega_1, \omega_2, \omega_3$ be the angles which the three directions of displacement make with the direction of the wave-normal of the elastic waves. According to Huyghens's principle it is only the components of the displacements along the normal to the reflecting plane that will determine the intensity of reflexion. Hence the scattering coefficient S_ϕ will now be given by

$$S_\phi = \frac{n^2\sigma_\phi}{D_0}\sum_{i=1}^{3}\frac{E(N_i)\cos^2\omega_i}{V_i^3}, \tag{18}$$

where $N_i = V_i/\Lambda_0$, and V_i, $i = 1, 2, 3$, are the frequencies and the velocities of propagation of the three polarized elastic waves associated with the wave-length Λ_0, and the wave-normal $\mathbf{n}_0$, both defined by $\rho_0\sigma_0\tau_0$.

Expression (18) can be readily recognized as Waller's (1925) expression for the intensity of scattering of X-rays of wave-length λ for the case when

$$\Lambda_0 = \lambda/(2\sin\tfrac{1}{2}\phi) \gg n^{-\frac{1}{3}}.$$

V_i can be expressed as usual in terms of the elastic constants of the crystal, which for such long wave-lengths Λ_0 as are involved here, will be practically the same as the static elastic constants of the crystal.

6. The atomic cross-section for scattering

Coming back to the liquid medium, we proceed to evaluate the cross-section of the atom in the liquid for scattering, namely σ_ϕ. If the incident light is linearly polarized, and the direction of observation makes an angle θ with the electric vector of the incident light (and ϕ with the direction of propagation of the incident light, as before) σ_ϕ, as we have defined it, will evidently be given by

$$\sigma_\phi = (2\pi/\lambda)^4 M^2 \sin^2\theta, \tag{19}$$

where M is the dipole moment induced in the atom per unit 'field in the medium', as usually defined, of the electric vector of the incident light-wave, and is given by

$$M = \chi/n = \frac{\epsilon-1}{4\pi n}, \tag{20}$$

where χ is the optical susceptibility and ϵ is the square of the refractive index, of the liquid.

Hence
$$\sigma_\phi = \frac{\pi^2(\epsilon-1)^2}{n^2\lambda^4}\sin^2\theta. \tag{21}$$

We should emphasize here that the field actually acting on the atom, and producing the dipole moment M, is not merely the field in the medium, say E, but also includes the polarization field P due to the dipole moments similarly induced in all the surrounding atoms. Hence χ in expression (20) will not be just proportional to n (except in a gas where $\epsilon \sim 1$), but will be greater. If the polarization field P has the Lorentz value, namely $P = 4\pi\chi E/3$, the total field which acts on an atom and

induces the dipole moment M, will be $1+4\pi\chi/3$ or $(\epsilon+2)/3$ times E, where ϵ is the mean dielectric constant of the medium. Hence neither M, nor σ_ϕ as we have defined it, which is proportional to M^2, will be atomic constants, but will depend also on the density of packing of the atoms in the medium. If the dielectric constant conforms to the Lorentz formula, σ_ϕ will be proportional to $\left(\frac{\epsilon+2}{3}\right)^2$, and will be correspondingly much higher in the liquid than in the gaseous state.

Expressions (19) and (20) are intended to refer to the case when the incident light is linearly polarized, and the direction of observation makes an angle θ with the direction of the electric vector of the incident light-wave. If the incident light is unpolarized, $\sin^2\theta$ in the above expressions will have to be replaced by $(1+\cos^2\phi)/2$, and for other polarizations of the incident light by a suitable factor $f(P)$ which can be readily calculated.

Substituting the value of σ_ϕ deduced here in expression (10) for S_ϕ, we obtain

$$S_\phi = \frac{\pi^2 kT\beta}{\lambda^4}(\epsilon-1)^2 f(P). \tag{22}$$

7. Comparison with Einstein's value

We expressed S_ϕ in the first place in terms of the atomic scattering coefficient σ_ϕ, and thence deduced expression (22) for S_ϕ, whereas in Einstein's derivation, as we mentioned in an earlier section, S_ϕ is connected directly with the local fluctuations in the refractivity of the liquid accompanying the fluctuations in density. The two are related in the following manner.

$n^2\sigma_\phi$ in our notation gives the scattering per unit volume from an element of volume when all the atoms in the element scatter in the same phase. This would correspond in Einstein's derivation to $\pi^2/\lambda^4(D\partial\epsilon/\partial D)^2 f(P)$. In evaluating $\partial\epsilon/\partial D$ Einstein adopts the Lorentz relation

$$\frac{\epsilon-1}{\epsilon+2}\frac{1}{D} = \text{constant}, \tag{23}$$

which gives on differentiating with reference to D

$$D\frac{\partial D}{\partial\epsilon} = (\epsilon-1)\frac{\epsilon+2}{3}, \tag{24}$$

which leads to Einstein's expression for S_ϕ, namely

$$S_\phi = \frac{\pi^2 kT\beta}{\lambda^4}(\epsilon-1)^2\left(\frac{\epsilon+2}{3}\right)^2 f(P). \tag{25}$$

This differs from (22) in that it includes the factor $\left(\frac{\epsilon+2}{3}\right)^2$ which is not present in (22).

This discrepancy is due to the following circumstance. $\partial\epsilon/\partial D$ occurring in Einstein's expression for S_ϕ denotes the fluctuation in ϵ in any small element of volume of the

liquid accompanying the fluctuation in its density D, per unit value of the latter. Adopting a suitable formula connecting ϵ and D for the liquid, for example the Lorentz formula (23), as we have done, we would not be justified in obtaining the required value of $\partial\epsilon/\partial D$ by differentiating ϵ in the expression with reference to D. Such a differentiation would give the change in ϵ consequent on a change of D, per unit value of the latter, when the density D of the liquid is varied uniformly throughout the liquid, whereas the variations of density we are concerned with here are local fluctuations, the fluctuations in different regions being uncorrelated with one another. In order to obtain the value of $\partial\epsilon/\partial D$ appropriate for such local variations in density, we need to know how the polarization field at any point, which is equal to $4\pi\chi/3 = (\epsilon-1)/3$ times the field in the medium, and which together with the latter gives a total field $(\epsilon+2)/3$ times the field in the medium, varies with the fluctuations of density at the point. Now the polarization field at any point will be determined not only by the density of distribution of the atomic dipoles in its *close* neighbourhood but in the whole of the surrounding regions. Hence though ϵ appearing in the numerator of (23) will vary in accordance with the fluctuations in density at the point, ϵ occurring in the denominator of (23), which comes through the factor $(\epsilon+2)/3$ which gives the ratio of the actual field to the field in the medium, both at the point, will not vary in the same manner. From some arguments put forward by Ramanathan (1927) it appears that to a first approximation the polarization field at any point in the medium should be independent of the fluctuation in density at the point. In other words the value of $\partial\epsilon/\partial D$ appropriate to our problem would approximate more closely to the expression

$$D\frac{\partial\epsilon}{\partial D} = \epsilon - 1, \tag{26}$$

rather than to $$D\frac{\partial\epsilon}{\partial D} = (\epsilon-1)\frac{\epsilon+2}{3}$$

obtained by direct differentiation of Lorentz's expression, and given in (24).

The fundamental assumption underlying our derivation of expression (3) for S_ϕ, namely that the contribution to S_ϕ from a small element of volume v in the liquid containing on an average N atoms, and so small that the scattered radiations from different parts of the volume may be regarded as being in practically the same phase, is given by (6), $S_\phi v = \overline{\Delta N^2}\sigma_\phi$, is indeed equivalent to assuming that the Lorentz polarization field at any point in the liquid is practically independent of the local fluctuation of density at the point. Hence the absence of the factor $\left(\frac{\epsilon+2}{3}\right)^2$ in our expression for S_ϕ, as compared with Einstein's.

The available experimental data for light-scattering in a large number of liquids, as was shown by one of us several years ago (Krishnan 1926), point definitely to the need for deleting the factor $\left(\frac{\epsilon+2}{3}\right)^2$ from Einstein's expression (20) for the scattering coefficient in a liquid.

8. Brillouin splitting in light-scattering

We have neglected till now the small changes in frequency accompanying scattering, i.e. the enhancement and degradation in frequency accompanying the reflexions respectively from the two sets of progressive waves travelling in opposite directions, to which attention was first drawn by Brillouin (1914, 1922). Consider an elastic wave defined by $\rho\sigma\tau$ and having a frequency $N_{\rho\sigma\tau}$, and extending over the whole volume L^3 of the liquid. The contribution from this wave to the scattering coefficient S_ϕ along the direction ϕ selected for observation of scattering, which we shall denote by $[S_\phi]_{\rho\sigma\tau}$, will now consist of two terms, as Brillouin (1933) has shown, namely

$$[S_\phi]_{\rho\sigma\tau} = [S_\phi]^+_{\rho\sigma\tau} + [S_\phi]^-_{\rho\sigma\tau}, \tag{27}$$

where the two terms with superscripts + and − correspond respectively to scattering of enhanced and degraded frequencies, namely $\nu' = \nu \pm N_{\rho\sigma\tau}$. Let us denote by k_x, k_y and k_z the components of the wave-vector $\mathbf{k}$ of the incident light-wave, and by k'_x, k'_y and k'_z the components of the wave-vector $\mathbf{k}'$ of the scattered radiation; $k = 1/\lambda = \nu/v$, and $k' = 1/\lambda' = \nu'/v'$, where v and v' are the velocities in the liquid of the incident and the scattered radiations respectively; v' besides being slightly different from v, will also be slightly different for the two values of k'. Either of the two terms in (27) will now be given by

$$[S_\phi]^\pm_{\rho\sigma\tau} = n^2\sigma_\phi \frac{L^3}{128D_0^2}\overline{B^2_{\rho\sigma\tau}}\frac{\sin^2\xi}{\xi^2}\frac{\sin^2\eta}{\eta^2}\frac{\sin^2\zeta}{\zeta^2}, \tag{28}$$

in which $\xi\eta\zeta$ are now given by

$$\left.\begin{aligned}\xi &= \tfrac{1}{2}\pi\rho - \pi L\,|\,k_x - k'_x\,|\\ \eta &= \tfrac{1}{2}\pi\sigma - \pi L\,|\,k_y - k'_y\,|\\ \zeta &= \tfrac{1}{2}\pi\tau - \pi L\,|\,k_z - k'_z\,|\end{aligned}\right\}, \tag{29}$$

$[S_\phi]^+_{\rho\sigma\tau}$ and $[S_\phi]^-_{\rho\sigma\tau}$ corresponding respectively to the two values of k'.

It will be seen from (29) that the condition $\xi = \eta = \zeta = 0$, which defines the directions of maximum intensity of reflexion for the two frequencies, is not now the same as the Bragg condition, namely $\rho = \rho_0$, $\sigma = \sigma_0$ and $\tau = \tau_0$, but corresponds to slightly different values of $\rho\sigma\tau$, which we shall denote by $\rho'_0\sigma'_0\tau'_0$ respectively. $\rho'_0\sigma'_0\tau'_0$ will also be slightly different for the two Brillouin components.

In the special case when k' is put equal to k, i.e., when we neglect the change in frequency accompanying reflexion, $\rho'_0\sigma'_0\tau'_0$ reduce to $\rho_0\sigma_0\tau_0$ as they should, and $[S_\phi]^+_{\rho\sigma\tau}$ will then be equal to $[S_\phi]^-_{\rho\sigma\tau}$, and $[S_\phi]_{\rho\sigma\tau}$ will be twice the value given by the right-hand side of (28).

Considering the general case, and confining ourselves to a given direction of incidence, and a given direction of observation, it will be readily seen from (29) that as we pass from one elastic wave to another, the corresponding change in ξ (and similarly in η or ζ) will be given by

$$\Delta\xi/\Delta\rho = \tfrac{1}{2}\pi + \pi L\Delta k'_x/\Delta\rho, \tag{30}$$

which in view of the relation $K_x = \rho/(2L)$, where K_x is the x-component of the elastic wave-vector $\mathbf{K}$, and $K = (\rho^2+\sigma^2+\tau^2)^{\frac{1}{2}}/(2L)$, becomes

$$\frac{\Delta\xi}{\Delta\rho} = \frac{\pi}{2}\left[1+\frac{\Delta k'_x}{\Delta K_x}\right] = \frac{\pi}{2}\left[1+\frac{k'_x}{k'}\frac{K_x}{K}\frac{\Delta k'}{\Delta K}\right]. \tag{31}$$

Now
$$\frac{\Delta(\nu'k')}{\Delta\rho} = \pm\frac{\Delta N}{\Delta\rho} = \pm\frac{\Delta(VK)}{\Delta\rho}. \tag{32}$$

Hence
$$\frac{\Delta k'}{\Delta K} = \pm\frac{\Delta N/\Delta K}{\Delta\nu'/\Delta k'} = \pm\frac{G}{g'}, \tag{33}$$

where g' and G are the group velocities of the scattered light-waves, and of the elastic waves in the neighbourhood of the wave-number K, respectively. Therefore

$$\frac{\Delta\xi}{\Delta\rho} = \frac{\pi}{2}\left[1\pm\frac{k'_x}{k'}\frac{K_x}{K}\frac{G}{g'}\right]. \tag{34}$$

In the second term inside the square brackets, k'_x/k' and K_x/K are direction-cosines, and hence will not exceed unity, and G/g' will *in general* be of the same order of magnitude as V/v', the ratio of the velocity of sound to that of light, and hence the second term will be negligible in comparison with the first term, and $\Delta\xi/\Delta\rho$, and similarly $\Delta\eta/\Delta\sigma$ and $\Delta\zeta/\Delta\tau$, will be almost exactly equal to $\frac{1}{2}\pi$. In other words as we pass from one stationary elastic wave to the adjacent one, and the ρ or σ or τ values change by steps of unity, the corresponding changes in $\xi\eta\zeta$ will be in steps of practically $\frac{1}{2}\pi$ as before.

Since $\Delta\xi/\Delta\rho$, etc., are practically $\frac{1}{2}\pi$, $[S_\phi]^+_{\rho\sigma\tau}$ or $[S_\phi]^-_{\rho\sigma\tau}$ will be significant for only a few values of $\rho\sigma\tau$ in the close neighbourhood of the corresponding $\rho'_0\sigma'_0\tau'_0$, or practically of $\rho_0\sigma_0\tau_0$, since $\rho'_0-\rho_0$, etc., can be readily shown to be less than $4Lk$. V/v, and hence less than 1 when L is of the order of unity. In other words the frequencies $N_{\rho\sigma\tau}$, and the mean square of amplitude $\overline{B^2_{\rho\sigma\tau}}$ for the elastic waves concerned *effectively* in scattering either of the Brillouin components, will be practically those corresponding to $\rho_0\sigma_0\tau_0$. In other words for any given direction of incidence, and of observation at an angle ϕ, the changes in frequency will be practically $\pm N_0$, and the intensity of either component will be given by

$$S^+_\phi = S^-_\phi = n^2\sigma_\phi\frac{L^3\overline{B^2}}{128D_0^2}\sum_\rho\sum_\sigma\sum_\tau\frac{\sin^2\xi}{\xi^2}\frac{\sin^2\eta}{\eta^2}\frac{\sin^2\zeta}{\zeta^2} \tag{35}$$

$$= n^2\sigma_\phi\frac{L^3\overline{B^2}}{16D_0^2}$$

$$= n^2\sigma_\phi\frac{E(N_0)}{2V^2D_0}. \tag{36}$$

Thus the coefficient of scattering of either of the Brillouin components separately, of enhanced or degraded frequency, $\nu' = \nu\pm N_0$ per unit volume, per unit solid angle, will as before be equal to eight times the maximum intensity of reflexion from a

progressive wave of the appropriate frequency N_0 travelling along the appropriate direction, and extending over the whole volume L^3 of the liquid, and having one-eighth the energy of a Planck oscillator of frequency N_0.

This result is the same as that obtained by Brillouin (1933) who assumed the two progressive waves that give rise respectively to the two spectral components in scattering as each having the full energy of a Planck oscillator, and further arbitrarily took the scattering coefficient as equal to the reflexion coefficient *at the maximum* corresponding to $\xi = \eta = \zeta = 0$.

In a crystal too, the wave numbers of the elastic waves which effectively contribute to the scattering along any given direction, will be defined as before by $\rho'_0\sigma'_0\tau'_0$, and practically by $\rho_0\sigma_0\tau_0$, but in general there will be three different values of N_0 associated with the three velocities of propagation of a wave whose wave-length and wave-normal are defined by $\rho_0\sigma_0\tau_0$, and hence there will be three pairs of Brillouin components whose frequencies are

$$\nu'_i = \nu\pm N_i \quad (i = 1, 2, 3).$$

On this basis the intensities of the Brillouin components corresponding to the same frequency shift on either side, will be the same, whereas the intensities of the three components on any one side, corresponding to the three values of N_i, will be widely different, the intensities of the three being given respectively by (see (18))

$$S^\pm_{\phi i} = \frac{n^2\sigma_\phi}{2D_0}\frac{E(N_i)\cos^2\omega_i}{V_i^2} \quad (i = 1, 2, 3); \tag{37}$$

and ω_i and N_i, and hence V_i also, being widely different for the three components.

9. Relative intensities of the Stokes and the anti-Stokes Brillouin components

From the point of view adopted above, which regards the Brillouin components on either side as Doppler shifts accompanying reflexions from the appropriate progressive waves moving in opposite directions, the enhanced and degraded frequencies corresponding to the same frequency shift N_i should be of the same intensity. Though this will be true at all ordinary temperatures $T \gg hN_i/k$, where k is the Boltzmann constant, this will not be the case at low temperatures. The intensities will then have to be calculated on the quantum theory, as in the case of the intensities of the Raman spectra. Indeed the Brillouin components are the Stokes and the anti-Stokes Raman lines respectively, due to *acoustic* frequencies, whereas the usual Raman spectra are due to the vibrational and rotational frequencies characteristic of the medium, i.e. due to the *optical* branches of the elastic waves, which also will be present in general, and which for simplicity, we have neglected till now, in the crystal explicitly, and in the liquid implicitly by assuming the liquid to be monatomic.

There is one striking difference between Raman spectra due to the acoustic and the optical branches of the elastic waves. Whereas for the optical branch of the elastic

waves the frequency N_i is practically independent of the wave-length $\Lambda \sim \lambda/(2 \sin \frac{1}{2}\phi)$, and hence the corresponding Raman shifts $\Delta\nu_i = \pm N_i$ are independent of Λ, and therefore of the direction of scattering, for the acoustic branch N_i is nearly proportional to $1/\Lambda$, and hence the frequency shifts of the Brillouin components are proportional to $1/\Lambda$, and hence vary as $\sin \frac{1}{2}\phi$.

The effect of including the optical branch will be twofold. Besides the appearance of the usual Raman spectra the polarization characteristics of ordinary scattering also will be greatly altered, since σ_ϕ for the scattering atoms will be a function of the direction of the electric vector of the incident light-wave in relation to the dispositions of the different atoms. In other words the optical branch of the elastic spectrum will not only produce Raman spectra corresponding to much larger frequency shifts than are involved in Brillouin splitting, but will affect the polarization of ordinary scattering—in a liquid the effect will be the same as that attributed in the usual treatment to the optical anisotropy of the molecules in the medium.

Summary

The intensity of light scattered by a homogeneous monatomic liquid can be calculated readily, following Einstein, by attributing the scattering to the local fluctuations in density, and regarding the latter as due to the superposition of the standing or progressive elastic waves of different wave-lengths. The expression for the scattering coefficient along any given direction involves a triple infinite series, each of which is of the form $\sum_{n=-\infty}^{+\infty} \alpha \frac{\sin^2(n\alpha+\theta)}{(n\alpha+\theta)^2}$, where n is an integer, and α and θ are positive constants. By splitting the medium into small volume elements, α may be made sufficiently small, and the summation may be replaced by integration, and this is usually done. But this is not necessary, since the series can be summed even when α is not so small, provided $0 < \alpha \leqslant \pi$, which is actually the case, since, even when the volume element chosen is the whole of the medium α is just $\frac{1}{2}\pi$.

Taking the medium as a whole, one finds that the elastic waves regarded as forming a reflexion grating, have a high resolving power, actually half that necessary to resolve in the Rayleigh sense the reflexions from adjacent elastic waves; and hence it becomes convenient to regard scattering in terms of reflexion from the appropriate elastic waves.

On this basis, the coefficient of scattering along any given direction comes out to be eight times the coefficient of reflexion at the maximum from just two progressive waves in the medium which satisfy the Bragg law, each of the two waves having one-eighth the energy of a Planck oscillator of the same frequency as the waves.

These two progressive waves give rise respectively to the two Brillouin components in scattering, and the intensity of either of them deduced in the above manner agrees with that given by Brillouin, who assumed each of the progressive waves to have the full energy of a Planck oscillator, and who further arbitrarily took the scattering coefficient as equal to the reflexion coefficient at its maximum.

The calculation of intensity is extended to a crystalline medium, and the expression for the total intensity of all the Brillouin components together, is shown to be identical with Waller's expression for X-ray scattering.

For more precise calculation of intensity the Brillouin components have to be regarded as the Raman spectra due to acoustic frequencies, as distinguished from the usual Raman spectra, which also will be present when the elastic spectrum consists of optical branches also.

References

Brillouin, L. 1914 *C.R. Acad. Sci., Paris*, **158**, 1331.
Brillouin, L. 1922 *Ann. Phys., Paris*, **17**, 88.
Brillouin, L. 1933 *La diffraction de la lumière par des ultra-sons*. Paris: Hermann.
Einstein, A. 1910 *Ann. Phys., Lpz.*, **33**, 1294.
Krishnan, K. S. 1926 *Proc. Indian Ass. Cult. Sci.* **9**, 251.
Ramanathan, K. R. 1927 *Indian J. Phys.* **1**, 413.
Waller, I. 1925 *Uppsala Univ. Årsk.*

'Diffuse scattering' of the Fermi electrons in monovalent metals in relation to their electrical resistivities

By A. B. Bhatia, D.Phil. and Sir K. S. Krishnan, F.R.S.

(*Received* 27 *November* 1947)

The main step in the calculation of the electrical resistivities of monovalent metals, in which the conduction electrons are almost completely degenerate, is the calculation of the relaxation time τ of the electrons at the Fermi surface, which in these metals is a sphere, and is well inside the first Brillouin zone. Since the wave-length λ, and hence the group velocity v, of the Fermi electrons is known, the calculation of τ means also the calculation of the mean free path $l = v\tau$ of these electrons. Now the finite mean free path of these electrons arises from the scattering—particularly the large-angle scattering—of these electrons in their passage through the crystal, by the thermally agitated atoms. Hence a detailed knowledge of the scattering coefficient of the crystal for the Fermi electrons, incident and scattered along different directions in the crystal, will enable us to calculate τ or l.

Now the scattering coefficient depends on two factors.

1. The atom form factor for scattering, which in monovalent metals may be taken to be isotropic, i.e. independent of the direction of incidence or of scattering separately, but dependent on the angle of scattering ϕ between them, and on λ. (Extensive measurements are available on the scattering of slow electrons by the rare gases, which give us information regarding the atom form factors for the scattering of the Fermi electrons in the corresponding alkali metals, and the variation of these factors with ϕ.)

2. The structure factor of the crystal, which, besides being a function of λ, will vary, even in a cubic crystal, with the direction of incidence and of scattering, but will, however, be independent of the nature of the waves, i.e. independent of whether they are X-rays, or electron or neutron waves. (The 'diffuse scattering' of *X-rays* of *long* wave-lengths in crystals has been studied in great detail, both theoretically and experimentally, from which one can calculate the structure factors of the monovalent metals for their respective Fermi wave-lengths, for different directions of incidence and of scattering in the crystals.)

Using these data for the atom form factor and for the structure factor of the crystal, the mean free path of the Fermi electrons is calculated in detail in the present paper for different directions of incidence, for one typical monovalent metal, namely sodium crystal. The free path l is given by

$$1/l = \Psi\nu^2 kT\beta\sigma,$$

where ν is the number of atoms per unit volume, σ is the cross-section of the atom for total scattering in all directions, β is the compressibility, and Ψ is a numerical factor which varies from a maximum of about 2·2 for incidence along [110] to a minimum of about 0·9 for incidence along [100], its average value being close to the minimum, and nearly unity.

With Ψ actually unity, the right-hand side of the above expression for $1/l$ can be seen to be just the Einstein-Smoluchowski expression for the attenuation coefficient of a liquid medium for *long* waves: which shows that in sodium, and presumably in the other monovalent metals also, the mean free path of the Fermi electrons may be taken roughly as the reciprocal of the attenuation coefficient of the crystal due to scattering, and the scattering may be regarded as due almost wholly to the local thermal fluctuations in density, and the Fermi wave-length as long enough for the Einstein-Smoluchowski formula for density-scattering to be applicable.

1. Introduction

In an electronic conductor, e.g. a metal crystal, it is only the electrons near the Fermi surface that can make effective collisions and thus take part in conduction. Hence a detailed knowledge of the coefficient of scattering along different directions in the crystal, of the Fermi electrons, will be helpful in our understanding its

electrical properties. In general the wave-lengths of these electrons are of the order of the interatomic distance. Now the scattering coefficient of a crystal depends both on the atom form factor, i.e. the cross-section of the atom for scattering, and on the structure factor of the crystal. For waves much shorter than the interatomic distance, or much longer, both these factors are easily evaluated, but for intermediate wave-lengths, such as are involved in electrical conduction, the evaluation is more difficult, but has been done by earlier workers. The atom form factor for scattering of electrons of such wave-lengths has been studied theoretically by Faxén & Holtsmark (1927), and experimentally by Ramsauer & Kollath (1932), and others. The technique for the calculation of the structure factor of the crystal for scattering of these wave-lengths is also available, since the structure factor for 'diffuse scattering' of X-rays has been studied extensively, both theoretically and experimentally, and the structure factor of a crystal for the scattering of electrons—or of any other waves—is the same as for the scattering of X-rays of the same wave-length. (In the usual discussions on diffuse scattering of X-rays, however, attention is directed mainly to the neighbourhood of the Bragg spots, whereas in the scattering of the Fermi waves we shall be concerned mainly with the region between the central spot and the immediately surrounding Bragg spots.)

In *good* metals like the alkali or the noble metals, i.e. metals of the first group in the Periodic Table, in which the Fermi surface is well within the first Brillouin zone, and is a sphere, the calculation of the scattering coefficient for the Fermi electrons becomes much simpler, since all the Fermi electrons have the same wave-length, and this wave-length is too long to give any Bragg reflexion; in the alkali metals, which are body-centred cubic, this wave-length is 14 % longer, and in the noble metals, which are face-centred cubic, 11 % longer, than that necessary to give the first Bragg reflexion in the backward direction.

Detailed calculations are given in the present paper of the structure factor of sodium crystal for scattering of wave-lengths too long to give any Bragg reflexion. Some rough estimates can be made of the atom form factor for scattering of the Fermi electrons by the atoms in the metal. These data are then utilized to calculate the relaxation time of the Fermi electrons in the metal, and thence its electrical resistivity.

In a previous paper (Krishnan & Bhatia 1944) it was shown from certain general considerations, that in the alkali and the noble metals the mean free path of the Fermi electrons may be taken roughly to be equal to the reciprocal of the attenuation coefficient of the metal for the passage of these electrons, the attenuation being due to scattering by the thermally agitated atoms in the metals; and that for the Fermi wave-length the scattering may be taken to be due predominantly to the local thermal fluctuations in density and the attenuation coefficient to be given practically by the Einstein-Smoluchowski formula. The detailed calculations made in the present paper for sodium crystal show that these results are good approximations for this metal, and presumably for other monovalent metals too. It is needless to add that they simplify considerably the calculation of electrical resistivities.

2. Electrical resistivity in relation to the scattering of the Fermi electrons

As is well known the specific resistance ρ of a *good* metal or alloy is given by the expression

$$\rho = \frac{m}{n\nu e^2}\frac{1}{\tau} \tag{1}$$

$$= \frac{h}{n\nu e^2 \lambda}\frac{1}{l}, \tag{2}$$

where τ is the relaxation time of the Fermi electrons, of wave-length $\lambda = (8\pi/3n\nu)^{\frac{1}{3}}$ and of group velocity $v = h/m\lambda$, $l = v\tau$ is their mean free path, ν is the number of atoms per unit volume, and n is the number of conduction electrons per atom, and the other letters have their usual significance (see Mott & Jones 1936; Fröhlich 1936). All the quantities in (1) and (2) are known except τ (or l), and the main problem in calculating the electrical resistivities of good metals or alloys is therefore one of calculating τ (or l) in terms of the scattering of the Fermi electrons by the thermally agitated atoms.

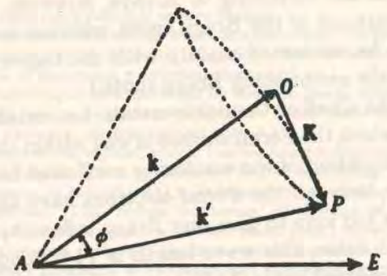

Figure 1

Let AE (see figure 1) be the direction of the applied electric field. Consider electrons at the Fermi surface moving along any given direction AO, and scattered along AP, the angle of scattering being ϕ. The wave-vectors $\mathbf{k}$ and $\mathbf{k}'$ ($k' \approx k$) of the incident and the scattered electron-waves respectively, are as marked in the figure. $\mathbf{K}$ is the wave-vector of the elastic wave that produces the scattering, where $K \approx 2k \sin \frac{1}{2}\phi$. Consider now the quantity $\Delta p_E/p_E = \Delta k_E/k_E$, where $p = \hbar k$ is the momentum of the incident Fermi electron, and $\Delta p = \hbar \Delta k$ is the change in its momentum due to scattering, and the subscripts E denote the components along AE of these quantities. $\Delta\mathbf{k}$ will evidently be equal to $\mathbf{K}$.

Let $S_{kk'}$ be the fraction of the Fermi electrons moving along direction $\mathbf{k}$ which is scattered per unit volume of the crystal, per unit solid angle,* along direction $\mathbf{k}'$. The reciprocal of the mean free path appearing in (2) will then be given by

$$\frac{1}{l} = \frac{1}{v\tau} = \frac{1}{4\pi}\iint S_{kk'}\frac{\Delta k_E}{k_E}\, d\omega_k d\omega_{k'}, \tag{3}$$

* The probability that a Fermi electron travelling along $\mathbf{k}$ is scattered per unit time per unit solid angle along $\mathbf{k}'$ is given by

$$P_{kk'} = S_{kk'} v,$$

where v is the velocity of the electron.

where $d\omega_k$ and $d\omega_{k'}$ are elements of solid angles about the directions $\mathbf{k}$ and $\mathbf{k}'$ respectively, and both the integrations extend over the whole of the 4π solid angle. It will be seen from (3) that $1/l$ may also be regarded as 4π times the average value of $S_{kk'}\Delta k_E/k_E$, the average being taken over all directions of scattering $\mathbf{k}'$, and all directions of incidence $\mathbf{k}$ of the Fermi electrons.*

Even in a cubic crystal, because of its elastic anisotropy, the scattering coefficient $S_{kk'}$ will be a function of $\mathbf{k}$ and $\mathbf{k}'$. Even so, with a detailed knowledge of $S_{kk'}$ as a function of $\mathbf{k}$ and $\mathbf{k}'$, which as we shall show in the present paper is not difficult to obtain, the integration in (3) can be done numerically.

In the usual discussions on the electrical resistivities of these metals, it is assumed for convenience that $S_{kk'}$ is a function of the angle of scattering ϕ between $\mathbf{k}$ and $\mathbf{k}'$, and is independent of $\mathbf{k}$ and $\mathbf{k}'$ separately. This assumption will hold when the crystal is elastically isotropic, and when further the Fermi wave-length is much longer than is necessary to give any Bragg reflexion, i.e. $\lambda \gg 2d \sin \frac{1}{2}\phi$, where d is the lattice spacing corresponding to the first Bragg reflexion. Neither of these conditions, however, is satisfied in the alkali or the noble metals, since many of them are elastically anisotropic, and λ, as we have seen, is only slightly greater than $2d$. Holding for the present to the assumption that $S_{kk'}$ is a function of ϕ alone, which we can denote by S_ϕ, we may evaluate (3) in a simple manner, since we can now keep one of the directions $\mathbf{k}$, $\mathbf{k}'$, say $\mathbf{k}$ fixed, and find the average value of $S_\phi \Delta k_E/k_E$ over all directions of the other, namely $\mathbf{k}'$. We can do this averaging in two steps. First we keep ϕ, and hence S_ϕ, constant, and average $\Delta k_E/k_E$ over all *azimuths* of scattering; the average is just $K \sin \frac{1}{2}\phi/k$, or $(1 - \cos\phi)$, which gives for $1/l$ the value

$$\frac{1}{l} = \frac{1}{v\tau} = \int_0^\pi S_\phi (1 - \cos\phi)\, 2\pi \sin\phi\, d\phi, \tag{4}$$

which is independent of the direction of incidence $\mathbf{k}$ in the crystal.

Though we do not adopt the approximation that $S_{kk'}$ is a function of ϕ alone, and is independent of $\mathbf{k}$ or $\mathbf{k}'$ separately, we shall have occasion to use expression (4), since even in elastically anisotropic crystals like the alkali metals there are regions in reciprocal space in which for certain directions of incidence the scattering coefficient is roughly a function of ϕ alone.

3. Diffuse scattering as due to thermal agitation

The influence of the thermal agitations of the atoms in a crystal on the intensities of the Bragg reflexions and of the 'diffuse scattering' along other directions, has been discussed among the earlier investigators by Darwin (1914) and by Debye (1914). Let R be the structure factor of the crystal, defined as usual by

$$R = \frac{S}{\nu s},$$

* In the derivation of expression (1) it is implicit that $1/\tau$ is the same for all the Fermi electrons, i.e. for all directions of incidence since in the metals that we are considering all the Fermi electrons have the same wave-length. When $1/\tau$ varies with the direction of incidence, one may as an approximation, use the average value of $1/\tau$ taken over all directions of the Fermi electrons, as we have done in expression (3).

where s is the scattering coefficient of an atom in the crystal per unit solid angle, or the atom form factor for intensity, all the three quantities R, S and s referring to the given wave-length and to *the same directions of incidence and of observation*. In the *monatomic* metals that we are considering, s may be regarded as practically isotropic, i.e. a function of only ϕ and λ in the combination $\sin\frac{1}{2}\phi/\lambda$.

The major effect of the thermal spread of the atomic centres about their mean positions will be to make the atom form factor at temperature T, namely s_T, fall off more rapidly with increase of $\sin\frac{1}{2}\phi/\lambda$ than the corresponding form factor s_0 of the non-vibrating atom, according to the well-known expression

$$\left.\begin{aligned} s_T &= s_0 e^{-2M}, \\ M &= 8\pi^2\overline{\xi^2}(\sin\tfrac{1}{2}\phi/\lambda)^2, \end{aligned}\right\} \qquad (5)$$

where $\overline{\xi^2}$ is the mean square of the amplitude of the thermal oscillations taken along the external bisector of the angle between the directions of incidence and of scattering, and is given at room temperature, which in these metals is sufficiently high in comparison with the Debye temperature to make the thermal energy proportional to T, by

$$4\pi^2\nu_e^2 m\overline{\xi^2} \approx kT,$$

where ν_e is the Einstein vibration frequency and m the mass of the atom. The result is a rapid fall of intensity of the Bragg reflexions particularly of higher orders, with rise of temperature. This is observed, and the fall is roughly in accordance with (5).

The question naturally arises as to what happens to the energy represented by the diminution of the intensities of the Bragg reflexions consequent on increase of temperature. Obviously it should appear as diffuse scattering along other directions, and besides, if a sufficient number of higher order Bragg reflexions is included in the range $0 < \phi \leqslant \pi$, we should have for any given direction of incidence

$$\nu\int s_0\,d\omega - \nu\int s_T\,d\omega = \int S\,d\omega, \qquad (6)$$

where the integrations extend over the whole of the 4π solid angle of scattering.

If the only effect of the thermal agitations may be regarded as a static swelling up or inflation of the scattering atoms, as is implied in the above treatment, then, in addition to the integrated value of S over all directions being equal to the difference between the integrated values of νs_0 and of νs_T over these directions, as given by (6), S will be equal to $\nu(s_0 - s_T)$ along *every* direction. Though some extensive measurements by Jauncey and his collaborators (1935) apparently lend support to this conclusion, it is now realized, both from theoretical considerations, and from scattering experiments made with a narrow parallel pencil of incident monochromatic X-rays, which verify the theory, that such a detailed balancing between $\nu(s_0 - s_T)$ and S does not occur.

4. Calculation of diffuse scattering

A detailed calculation of the directional distribution of intensity of the diffuse scattering of X-rays in crystals due to thermal agitation has been made by Faxén (1923) and by Waller (1923, 1925, 1928), and more recently, and from a different

point of view, by Raman (1941). We may mention immediately that in crystals in which *all* the normal modes of vibration are of the acoustic type, e.g. those of the alkali and the noble metals, the Faxén-Waller treatment and the treatment by Raman give identical results. (The criterion adopted by Raman for distinguishing between the 'acoustic', and the 'optical', normal modes of vibration of a crystal, is not, however, the same as the criterion adopted here.)

The Faxén-Waller treatment has been simplified, or made more rigorous, by Zachariasen, Born, Weigel, and Jahn,* among others. We shall use here the results as presented by Jahn (1942*a*) since they are in a form directly applicable to our problem.

Consider the reciprocal lattice of a given cubic crystal and the first Brillouin zones surrounding each of the points of the reciprocal lattice, including (000). These zones will be filled by a quasi-continuous and uniform distribution of cells, each cell defining a wave-vector **K** associated with the elastic standing waves that represent the normal modes of vibration of the crystal. Each K-cell will correspond to *three* normal modes of vibration of the crystal answering respectively to the three directions of vibration or displacement—and the three frequencies—associated with the particular value of **K**.

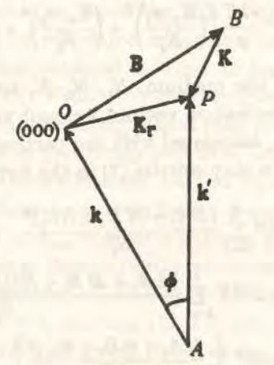

Figure 2

In the alkali metals, which are body-centred cubic, the first Brillouin zone surrounding each point of the reciprocal lattice is the rhombic dodecahedron bounded by faces of the type {110}. The distance from the reciprocal point forming the centre of the dodecahedron to the faces of the dodecahedron will be $1/2d_{110}$, where d_{110} is the grating spacing of the (110) planes in the crystal. In the noble metals, which are face-centred cubic, the first Brillouin zone is the orthotetrakaidekahedron, or the 14-hedron, bounded by {111} and {200} faces, i.e. the octahedron {111} truncated by the cubic faces {200}. In both the alkali and the noble metals *these first zones can accommodate just one K-cell per atom, i.e. all the normal modes of vibration of the crystal*

* For a good account of the subject see symposia of papers on the subject in *Proc. Ind. Acad. Sci.* 14, 1941, and in *Proc. Roy. Soc.* A, 179, 1942, and the reports by Mrs Lonsdale and by Max Born in *Reports on Progress in Physics*, Physical Society, London, 1942–43.

will be of the acoustic type, and further the first zones surrounding the various reciprocal lattice points will be similar and similarly oriented, and these zones will fill up the whole of the reciprocal space without overlapping. (As is well-known, both the rhombic dodecahedron and the orthotetrakaidekahedron described above are 'space-fillers'.)

Consider now a narrow pencil of monochromatic electron waves of wave-number $k = 1/\lambda$ incident along AO (see figure 2), where O is the origin (000) of the reciprocal lattice, and consider the radiations scattered along AP, where $AP = k' \approx k$, and ϕ is the angle between AO and AP or the angle of scattering as before. Let P—which, following Laval, we may call the 'pole of diffusion'—lie in the zone associated with the reciprocal lattice point B. Let $\mathbf{B}$ denote the vector OB, and $\mathbf{K}$ the elastic wave-vector from B to P. The vector $\mathbf{K}_r$ defined by

$$\mathbf{K}_r = \mathbf{B} + \mathbf{K}$$

will bisect externally the angle between the direction of incidence $\mathbf{k}(AO)$ and the direction of observation $\mathbf{k}'(AP)$. The structure factor R of the crystal for the given direction of incidence and of scattering will be given, according to Jahn, by*

$$R = e^{-2M}\frac{vkT}{\rho}\left\{\left(\frac{\mathbf{K}_r, \mathbf{e}_1}{N_1}\right)^2 + \left(\frac{\mathbf{K}_r, \mathbf{e}_2}{N_2}\right)^2 + \left(\frac{\mathbf{K}_r, \mathbf{e}_3}{N_3}\right)^2\right\}, \tag{7}$$

where ρ is the density of the medium, N_1, N_2, N_3 are the three frequencies and $\mathbf{e}_1$, $\mathbf{e}_2$, $\mathbf{e}_3$ the three unit polarization vectors, i.e. unit vectors along the directions of displacement of the atoms, associated with the particular elastic wave-vector $\mathbf{K}$.

Following again Jahn, we may rewrite (7) in the form

$$\begin{aligned} R = e^{-2M}\frac{vkT}{\rho}\Bigg[& B^2 \sum_{i=1}^{3} \frac{(LA_i + MB_i + NC_i)^2}{N_i^2} \\ & + 2BK \sum_{i=1}^{3} \frac{(LA_i + MB_i + NC_i)(lA_i + mB_i + nC_i)}{N_i^2} \\ & + K^2 \sum_{i=1}^{3} \frac{(lA_i + mB_i + nC_i)^2}{N_i^2}\Bigg], \end{aligned} \tag{8}$$

where L, M, N are the direction cosines of $\mathbf{B}$, l, m, n those of $\mathbf{K}$, and A_i, B_i, C_i those of the polarization vectors $\mathbf{e}_i$, $i = 1, 2, 3$.

In the special case when the pole of diffusion P lies in the central Brillouin zone, i.e. in the zone associated with (000), the first two terms in (8) vanish, since for this zone $B = 0$ (and $\mathbf{K}_r \equiv \mathbf{K}$), and we are left with the third term alone. The expression for R then reduces to

$$R = e^{-2M}\frac{vkT}{\rho}\sum_{i=1}^{3}\frac{(lA_i + mB_i + nC_i)^2}{V_i^2}, \tag{9}$$

where $V_i = N_i/K$ is the phase velocity of the elastic wave.

* Except for a constant of proportionality which is left undetermined in Jahn's expression, but is easily evaluated when we regard scattering as reflexion from the appropriate thermal elastic waves in the crystal (Krishnan & Bhatia 1948), and is included in (7).

5. Scattering regarded as reflexion from appropriate thermal elastic waves

In a previous paper, on the scattering of light-waves, i.e. of very long waves, in homogeneous media (Krishnan & Bhatia 1948), we showed that the scattering coefficient S may also be regarded as equal to the maximum value of the coefficient of reflexion from the two sets of progressive elastic waves (the two progressing in opposite directions) whose wave-normals and wave-lengths satisfy the Bragg condition for reflexion, either set consisting of three progressive waves corresponding to the three directions of displacement, the energy of each of the waves, *filling the whole of the medium*, being that of a Planck oscillator of the same frequency, or kT under the present assumptions. The expression for R comes out on this basis as (Krishnan & Bhatia 1948)

$$R = \frac{vkT}{\rho}\sum_{i=1}^{3}\frac{\cos^2\omega_i}{V_i^2}, \tag{10}$$

where ω_i is the angle between $\mathbf{K}$ and $\mathbf{e}_i$.

Expression (10), deduced here for long waves, can be seen to be identical with the Faxén-Waller expression (9), except for the factor e^{-2M}, which for long waves is practically unity.

For shorter wave-lengths also, i.e. when the pole of diffusion P lies outside the central Brillouin zone, R can be calculated in terms of reflexions from the elastic waves, and the expression thus obtained is found to be identical with the corresponding expression (7) of Faxén-Waller. We demonstrate this equivalence below.

Consider any one set of atomic reflecting planes (hkl) in the crystal, which, under suitable conditions, can give rise to a Bragg reflexion, and let the spacing of these layers be d_{hkl}. This regular layered structure may be regarded as the limiting case of a plane condensational acoustic wave with its wave-normal perpendicular to the planes, its wave-length equal to d_{hkl}, and *its velocity of propagation zero*. Actually since the distribution of matter in these layers is not sinusoidal, but is concentrated near the plane of the atomic centres, we shall have to take into account the upper partials also, corresponding to the spacings 1/2, 1/3, etc. times d_{hkl}. These shorter grating spacings may be regarded as giving rise to Bragg reflexions of the second, third and higher orders, corresponding to the reciprocal lattice points $2(hkl)$, $3(hkl)$, etc., and since these reciprocal lattice points are considered separately, we shall confine ourselves here to the fundamental spacing d_{hkl} corresponding to the point (hkl) of the reciprocal lattice.

Consider now one of the elastic waves representing a normal mode of vibration of the crystal, whose wave-vector is $\mathbf{K}$, and consider also a regular stratification of the crystal of spacing d_{hkl}. Because of this stratification the above wave may also be regarded as an elastic wave whose wave vector $\mathbf{K}_r$ is given by

$$\mathbf{K}_r = \left(\overrightarrow{\frac{1}{d_{hkl}}}\right) + \mathbf{K}.$$

We shall refer to such waves obtained by the superposition of elastic waves on the stratified layers of the scattering medium, as *resultant* elastic waves, as distinguished from the *primary* elastic waves. Whereas the wave numbers of the latter, namely $\mathbf{K}$,

are restricted in our crystals to the limits of the first Brillouin zone, the wave numbers $\mathbf{K}_r$ of the resultant elastic waves may have very large values, $K_r \approx n/d_{hkl}$.

The frequency of the resultant elastic wave, the displacement of the atoms under it, and the energy per unit volume associated with it, will all be the same as for the primary elastic wave producing it, but the velocity of the resultant wave will naturally be smaller than that of the primary wave in the ratio

$$V_r/V = K/K_r.$$

When the primary wave is a long one, such that $K \ll K_r$ the velocity of the resultant wave can become quite small.

These resultant waves can reflect the incident X-rays in the same manner as the primary elastic waves, and thus account for scattering along directions corresponding to positions of P outside the central Brillouin zone, i.e. along directions for which there can be no direct reflexion from any of the primary waves.

It will be seen from relation (10) that when the total energy in the medium associated with the elastic wave remains fixed, namely at kT, the intensity of reflexion from the elastic wave, which determines the scattering along the direction concerned, is inversely proportional to the square of its velocity, and hence the intensity of reflexion from the resultant wave, because of its low velocity, will be larger than that of the reflexion from the primary wave by a factor $(K_r/K)^2$, which, as K becomes small, or as P approaches the reciprocal point corresponding to the Bragg reflexion from the particular set of reflecting planes considered, will become very large.

The intensity of scattering along these directions will also be conditioned by the following.

(1) Just as in reflexion by a primary elastic wave, i.e. when P lies in the central Brillouin zone, it is the components of the three displacements along the wave-normal $\mathbf{K}$ of the reflecting elastic wave that determine the intensity of scattering, so also in the case of reflexion by the secondary elastic wave referred to above, i.e. when P lies outside the central Brillouin zone, it is the components of the displacements along $\mathbf{K}_r$ that determine the intensity, but the absolute directions of these displacements in the crystal will be determined by the direction of propagation (lmn) of the primary wave alone, according to relation (12) to be given in the next section.

(2) For the short wave-lengths λ that we are considering now, the temperature factor e^{-2M} will deviate considerably from unity, and will have to be retained.

These considerations obviously lead to an expression for R identical with expression (7) given above, of Faxén & Waller.

For these short waves we should remember that the atom form factor s_0 will vary markedly with ϕ unlike for long waves.

6. Remarks on the calculation of τ for some special directions of electron waves

Consider the locus of the pole of diffusion P in reciprocal space when the direction of incidence is kept fixed and the direction of scattering is varied over the whole of the 4π solid angle. The locus will evidently be a sphere passing through the origin,

of diameter $2k$, the diameter through the origin being along the direction of incidence. Following the usual practice we shall call this the 'sphere of propagation'. Since equal areas on the sphere correspond to equal solid angles of scattering, the calculation of $1/l$ for the given direction of incidence is equivalent to integrating

$$\frac{1}{k^2} S_{kk'} \frac{\Delta k_E}{k_E} dA,$$

where dA is an element of area on the surface of the sphere of propagation, over the whole of the sphere.

We saw in § 2 that when S is a function of ϕ alone, the average value of $S_\phi(\Delta k_E/k_E)$ over all azimuths of scattering corresponding to a given angle of scattering ϕ, is just equal to $S_\phi(1-\cos\phi)$. Even when the crystal is cubic like ours, $S_{kk'}$ is not a function of ϕ alone. If, however, the incidence is along [100], [110] or [111], which are axes of tetragonal, digonal and trigonal symmetry respectively, and we consider all the *crystallographically equivalent* directions ϕ, θ_i corresponding to the same angle of scattering ϕ and to equivalent azimuthal angles θ_i, then $S_{kk'} = S_{\phi\theta_i}$ will be the same for all these directions of scattering, and the average value of $\Delta k_E/k_E$ over these directions will again be $(1-\cos\phi)$. Hence for the above special directions of incidence in a cubic crystal, the expression for $1/l$ may be written in the form

$$\frac{1}{l} = \int_{\phi=0}^{\pi}\int_{\theta=0}^{2\pi} S_{kk'}(1-\cos\phi)\sin\phi\, d\phi\, d\theta. \tag{11}$$

In other words the weightage factor that takes into account the relatively large contribution to $1/l$ from large angle scattering, is equal to $(1-\cos\phi)$, and hence the same as when $S_{kk'}$ is a function of ϕ alone.

7. Sphere of propagation wholly inside the first Brillouin zone

Before proceeding to calculate $1/l$ for the alkali and the noble metals, for their respective Fermi wave-lengths, for which the sphere of propagation extends into the second Brillouin zone also, it will be useful to calculate its value for the special case when λ is large, i.e. when the sphere of propagation is *well* within the first Brillouin zone. This case is simple since then for every point P on the sphere the velocity of propagation, and the directions of the displacements, are independent of the *wave-number* K of the elastic wave, though of course they will vary with the *direction* of $\mathbf{K}$; and V_i, and A_i, B_i, C_i, occurring in (9), can then be expressed in terms of the static elastic constants c_{11}, c_{12} and c_{44} of the cubic crystal, by the relations

$$\left.\begin{aligned}
\{c_{11}l^2 + c_{44}(m^2+n^2) - \rho V_i^2\}A_i + (c_{12}+c_{44})(lmB_i + nlC_i) &= 0,\\
\{c_{11}m^2 + c_{44}(l^2+n^2) - \rho V_i^2\}B_i + (c_{12}+c_{44})(lmA_i + mnC_i) &= 0,\\
\{c_{11}n^2 + c_{44}(l^2+m^2) - \rho V_i^2\}C_i + (c_{12}+c_{44})(lnA_i + mnB_i) &= 0.
\end{aligned}\right\} \tag{12}$$

In view of these relations, expression (9) reduces, as Jahn has shown, to

$$R = e^{-2M}\nu kT \frac{c_{44}^2 + 2c_{44}\epsilon(l^2m^2+m^2n^2+n^2l^2) + 3\epsilon^2 l^2m^2n^2}{c_{11}c_{44}^2 + c_{44}(c_{11}+c_{12})\epsilon(l^2m^2+m^2n^2+n^2l^2) + (c_{11}+2c_{12}+c_{44})\epsilon^2 l^2m^2n^2} \tag{13}$$

$$= e^{-2M}\nu kT.F_{lmn}, \text{ say,} \tag{14}$$

where ϵ is the elastic anisotropy of the crystal, given by

$$\epsilon = c_{11} - c_{12} - 2c_{44}.$$

Moreover in this region e^{-2M} is practically unity, and s_ϕ practically independent of ϕ, and equal to $\sigma/4\pi$, where σ is the cross-section of the atom for *total scattering in all directions*, and is given by

$$\sigma = \int_0^\pi s_\phi \, 2\pi \sin\phi \, d\phi. \tag{15}$$

Consider incidence of long electron waves along one of the principal directions [100], [110] or [111] of the cubic crystal. Expression (11) for $1/l$ reduces under the above conditions to the simple form

$$1/l = \nu^3 kT(\sigma/4\pi)\, J, \tag{16}$$

where

$$J = \int_{\phi=0}^{\pi}\int_{\theta=0}^{2\pi} F_{lmn}(1-\cos\phi)\sin\phi \, d\phi \, d\theta. \tag{17}$$

When the crystal is elastically isotropic, i.e. when $\epsilon = 0$, F becomes independent of lmn, and equal to $1/c_{11}$. In that case expression (17) holds whatever may be the direction of incidence, and the factor $(1-\cos\phi)$ appearing in (17) intended to give the proper weightage for scattering at large angles, over scattering at small angles, becomes quite ineffective ultimately, and the expression for $1/l$ merely reduces to

$$1/l = \mu = \nu^3 kT\sigma/c_{11}, \tag{18}$$

where μ is the total scattering in all directions, per unit volume of the crystal, or the attenuation coefficient of the crystal for the passage of electron waves along the direction considered, the attenuation being due to scattering, and the coefficient μ being defined by

$$I_d = I_0 e^{-\mu d},$$

where I_d is the intensity after traversing a distance d in the crystal.

If further $c_{44} = 0$, c_{11} becomes equal to c_{12} and to $1/\beta$, where β is the compressibility of the crystal, and the expression for the attenuation coefficient due to scattering then reduces to the Einstein-Smoluchowski value for a liquid (Krishnan & Bhatia 1948), namely

$$1/l = \mu = \nu^3 kT\beta.\sigma \tag{19}$$

as it should.

Coming back to the elastically anisotropic cubic crystal, and considering first incidence of long electron waves along [$\bar{1}$00], we may express F_{lmn} defined by (13) and (14), in the form*

$$F_{lmn} = \frac{a + b(l^2m^2 + m^2n^2 + n^2l^2) + cl^2m^2n^2}{a' + b'(l^2m^2 + m^2n^2 + n^2l^2) + c'l^2m^2n^2}$$
$$= \frac{A + B\sin^2 2\theta}{A' + B'\sin^2 2\theta}, \tag{20}$$

where

$$A = a + \tfrac{1}{2}b\sin^2\phi, \quad B = \tfrac{1}{2}\cos^4\tfrac{1}{2}\phi(b + c\sin^2\tfrac{1}{2}\phi),$$

and A' and B' have similar values in terms of a' and b'.

* We should remember here that lmn are the direction cosines of the elastic wave-vector K which bisects externally the angle between k and k', and when k is along [$\bar{1}$00], is related to the angle ϕ, and the azimuth θ, of scattering by the relations

$$l = \sin\tfrac{1}{2}\phi, \quad m = \cos\tfrac{1}{2}\phi\cos\theta, \quad n = -\cos\tfrac{1}{2}\phi\sin\theta.$$

In view of expression (20) for F in which A, B, A', B' are all independent of θ, the integration in (17) with reference to θ can be done readily. Doing so we obtain

$$J = \int_0^\pi Y(1-\cos\phi)\sin\phi \, d\phi, \tag{21}$$

where

$$Y = \int_0^{2\pi} F_{lmn}\, d\theta$$
$$= 2\pi\left\{\frac{B}{B'} + \frac{AB' - A'B}{B'(A'+B')}\sqrt{\frac{A'+B'}{A'}}\right\}. \tag{22}$$

Changing the variable in (21) by putting $f = 1-\cos\phi$ we obtain

$$J = \int_0^2 Yf\,df. \tag{23}$$

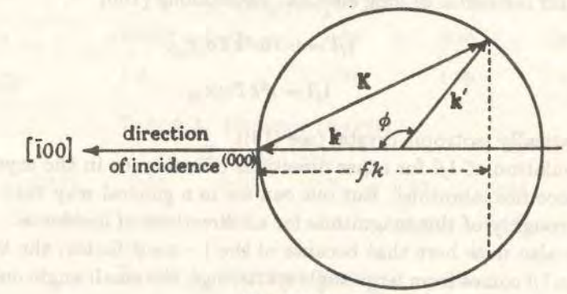

FIGURE 3

Obviously fk represents the perpendicular distance from (000) of the plane perpendicular to the direction of incidence which by its intersection of the sphere of propagation defines ϕ (see figure 3).

The integration in (23) can be done numerically, since we can calculate readily the values of Y corresponding to different values of f in the range $0 \leqslant f \leqslant 2$.

The elastic constants of sodium crystal have been determined by Quimby & Siegel (1938) at different low temperatures, which on extrapolation, give for room temperature (see Lonsdale & Smith 1940)

$$c_{11} = 0{\cdot}52, \quad c_{12} = 0{\cdot}40, \quad c_{44} = 0{\cdot}41,$$

all of them in 10^{11} dynes/cm.^{2}. Or

$$c_{12} = 0{\cdot}77c_{11}, \quad c_{44} = 0{\cdot}79c_{11}, \quad \epsilon = -1{\cdot}35c_{11}. \tag{24}$$

Using these data, we have calculated the values of Y for different values of f in the range $0 \leqslant f \leqslant 2$ at intervals of 0·2. The values are entered in table 1.

TABLE 1

	0 forward direction	0·2	0·4	0·6	0·8	1·0	1·2	1·4	1·6	1·8	2·0 backward direction
$Y.c_{11}/2\pi$	0·84	0·77	0·69	0·60	0·53	0·50	0·59	0·74	0·86	0·95	1·0

It will be seen from the expression for B' that it becomes zero when $\sin^2\frac{1}{2}\phi = -b'/c'$, or when $f = 0{\cdot}62$. Since B' appears as a multiplying factor in the denominator of both the terms in expression (22) for Y, it appears at first sight that Y may become infinite at $f = 0{\cdot}62$. But actually on making B' small, and expanding the two terms and taking them together and then making B' tend to zero, the Y *vs* f curve is found to decrease smoothly at this point.

B' becomes again zero at $\phi = \pi$, i.e. at $f = 2$; but it can be readily seen that both the terms in (22) are separately finite at this point since B' occurs in the combination B/B', and B/B' remains finite at $\phi = \pi$.

Using the values given in table 1, and Simpson's rule for numerical integration, we obtain

$$J = 2\pi \times 1{\cdot}52/c_{11},$$

and hence for incidence of long electron waves along [100]

$$1/l = 0{\cdot}76\nu^3 kT\sigma/c_{11}, \tag{25}$$

as against

$$1/l = \nu^3 kT\sigma/c_{11}$$

for the elastically isotropic crystal (see (18)).

The calculation of $1/l$ for other directions of incidence in the crystal, even [110] or [111], becomes laborious. But one can see in a general way that for long waves $1/l$ will be roughly of this magnitude for all directions of incidence.

We may also note here that because of the $1-\cos\phi$ factor, the bulk of the contribution to $1/l$ comes from large angle scatterings, the small angle ones contributing very little to it.

8. Variation of R with the wave-length λ

In the region of reciprocal space close to (000), corresponding to $\lambda \gg 2d\sin\frac{1}{2}\phi$, the velocities V_i and the directions of displacements $\mathbf{e}_i$ defined by A_i, B_i, C_i, and hence also R, will be independent of the magnitude of the elastic wave-vector $\mathbf{K}$ (but will of course depend on the direction of $\mathbf{K}$). This will not be true, however, when the pole of diffusion P approaches the boundary of the Brillouin zone. One has a rough idea how at least the velocity varies as one approaches the boundary, which may be taken to indicate in a general way the variation of the displacements also. Calculations have been made by Kellerman (1940) of the phase velocities V_i of the elastic waves in rock salt crystal. Though the velocities decrease as one approaches the boundary, the total drop, even for the [111] direction, for which it is a maximum, is only 25 %, and much of this drop is confined to the close neighbourhood of the boundary. Calculations have also been made for crystals of tungsten (Fine 1939), and of KCl (Blackman 1937), of the density of distribution of the normal modes of vibration of the crystal, on the *frequency* scale, i.e. $p(N)$ as a function of the frequency N, where $p(N)\,dN$ gives the number of normal modes of vibration whose frequencies lie between N and $N+dN$. Now the corresponding distribution on the K scale, i.e. $P(K)$ as function of K, where $P(K)\,dK$ gives the number of normal modes of vibration between K and $K+dK$, is known to be uniform over the whole of the

Brillouin zone. A comparison of the distributions on the two scales, using the simple relations*

$$N/K = V \quad \text{and} \quad dN/dK = G, \tag{26}$$

where V is the phase-velocity, and G the group-velocity of the elastic waves, gives a rough estimate of the change in the phase-velocity as we approach the boundary of the zone. These estimates also show that the total drop in the phase-velocity as we approach the boundary is a fraction, of the order of 1/4, most of the change again occurring in the neighbourhood of the boundary. (The group-velocity G will of course diminish much more rapidly than V in this region, and tend to zero at the boundary of the zone.) The result will be an excess of scattering in the close neighbourhood of the boundary of the Brillouin zone, which, however, being highly localized, will contribute little to the total scattering taken over all directions.

Table 2. (Sodium crystal)

K_r along [100]

$K_r d_{110}$	$<0{\cdot}707\dagger = 1/\sqrt{2}$	0·75	0·80	0·877‡
$R\,c_{11}/e^{-2M}\nu kT$	1·0	1·31	1·70	2·73

Table 3. (Sodium crystal)

K_r along [110]

$K_r d_{110}$	$<0{\cdot}5\dagger$	0·55	0·60	0·70	0·80	0·85	0·877‡
$R\,c_{11}/e^{-2M}\nu kT$	0·60	0·89	1·34	3·12	9·55	19·2	30·5

Table 4. (Copper crystal)

K_r along [100]

$K_r d_{111}$	$<0{\cdot}58\dagger = 1/\sqrt{3}$	0·60	0·70	0·80	0·90‡
$R\,c_{11}/e^{-2M}\nu kT$	1·0	1·17	2·36	5·08	12·6

Table 5. (Copper crystal)

K_r along [111]

$K_r d_{111}$	$<0{\cdot}5\dagger$	0·55	0·60	0·70	0·80	0·85	0·90‡
$R\,c_{11}/e^{-2M}\nu kT$	0·71	1·06	1·60	3·72	11·4	22·8	58·8

When we move outside the first Brillouin zone, the value of R, which is now determined by $\mathbf{K}_r$, will naturally vary not only with the direction of $\mathbf{K}_r$ but also with its magnitude, as can be seen from (7). In order to get an idea of the variation of R

* In the special case when the medium is non-crystalline and $P(K) = 3\times 4\pi K^2$, we obtain

$$p(N)\,dN = 3\times 4\pi N^2\,dN/(V^3 G).$$

† These values of K_r correspond to the upper limit of the first Brillouin zone. For values of K_r greater or smaller than this limiting value, *but not close to it*, R can be calculated on the basis of formula (8), and the values entered in the tables are those calculated on the basis. When K_r is close to this limiting value, the value of R given by (8) will be too low, as we mentioned earlier in this section.

‡ These values of K_r correspond to backward scattering ($\phi = \pi$) of electrons having the Fermi wave-length.

in this region, we have calculated for sodium the variation of R with $\sin\frac{1}{2}\phi/\lambda$ for two directions of $\mathbf{K}_r$, namely [100] and [110]. The special advantage of these directions is that for all positions of P on these lines $\mathbf{K}_r$ can be obtained in a unique way, and the directions of $\mathbf{B}$, $\mathbf{K}$ and $\mathbf{K}_r$ are identical (neglecting the sense of the direction) so that R will continue to be a function of $\sin\frac{1}{2}\phi/\lambda$, as in the central region.

The values of R for different positions of P along [100] and [110] for sodium crystal, and along [100] and [111] for copper crystal, are entered in tables 2 to 5. The distances from the origin are expressed in terms of $1/d_{110}$ for sodium, and in terms of $1/d_{111}$ for copper, i.e. in terms of the distance in reciprocal space of the first Bragg spot from (000).

9. The atom form factor s and its variation with ϕ

We have seen that for the Fermi wave-length the sphere of propagation extends much beyond the first Brillouin zone, and that for the regions on the sphere remote from (000) R may vary rapidly. Though this will be the major factor affecting S, two other factors also affect it considerably.

(1) The factor e^{-2M}, which in the region near (000) is practically unity, will now be appreciably less, and will diminish with increase of ϕ. For sodium crystal at room temperature (300° K), and for its Fermi wave-length

$$\lambda = 2{\cdot}28 d_{110} = 6{\cdot}93\,\text{A}\,(3{\cdot}12\,\text{eV}), \quad e^{-2M} = e^{-0{\cdot}27\sin^2\frac{1}{2}\phi}$$

decreases by about 24 % as we pass from the forward to the backward direction.*

Table 6

ϕ (degrees)	s_ϕ (A)	ϕ (degrees)	s_ϕ (A)
15	0·220	105·5	0·148
28	0·214	121	0·131
43	0·218	137	0·120
59	0·220	152	0·117
74·5	0·207	167	0·112
90	0·173		

(2) The atom form factor s, which in the region near (000) is practically independent of ϕ will not be so now. Knowing, however, the Fermi wave-length λ, and the electronic distribution in the atoms of these metals, it is possible theoretically to calculate the variation of s with ϕ. The calculation is rather laborious. But we can get the data concerning the variation of s with ϕ required for our present purpose from the extensive measurements made by Ramsauer & Kollath (1932) on the scattering coefficients S_ϕ of rare gases for different angles of scattering ϕ and for different wave-lengths λ. The scattering medium in their experiments being gaseous, these data give directly the atom form factors s_ϕ, since $s_\phi = S_\phi/\nu$. The data for neon gas for 3·12 eV, i.e. for electrons having the same wave-length as the Fermi electrons in sodium metal, are given in table 6.

* The value $2M = 0{\cdot}27\sin^2\frac{1}{2}\phi/\lambda^2$ given here is on the basis of the Debye temperature of sodium being 150° K.

It will be seen from table 6 that s_ϕ is practically independent of ϕ up to about $\phi = 75°$, after which it drops down, reaching about half the value at about $\phi = 125°$, and remains afterwards practically constant at this value. The general variation of s_ϕ with ϕ observed here holds not only for 3·12 eV, but also for electrons having energies in the neighbourhood of this value, and for other rare gases too. We may, therefore, take this result to be applicable to the scattering atoms in the alkali metals also, and as a rough approximation take s_ϕ to be constant and equal to s_1 over the whole of the range $0 \leqslant \phi \leqslant \phi_0$, and again constant and equal to $s_2 = \frac{1}{2}s_1$ over the remaining angles of scattering $\phi_0 < \phi \leqslant \pi$, where ϕ_0 is about 100°.

10. Calculation of τ for the Fermi electrons in sodium crystal

We now proceed to calculate $1/l$ for one typical crystal, namely sodium, and for its Fermi wave-length of 6·93 A, when the direction of incidence is along $[\bar{1}\bar{1}0]$, i.e. to evaluate the integral

$$\frac{1}{l} = \int_{\phi=0}^{\pi}\int_{\theta=0}^{2\pi} S_{kk'}(1-\cos\phi)\sin\phi\, d\phi\, d\theta$$

over the whole of the corresponding sphere of propagation. *The value of $1/l$ will be a maximum for this direction of incidence in the alkali metals.* For the purpose of the integration we split the surface of the sphere into two parts, namely that included in the central zone, and that outside respectively. The critical angle of scattering ϕ_0 defining the transition from the former to the latter region is about 98°, corresponding to (see § 7) $f_0 = 1-\cos 98° = 1{\cdot}14$, and in view of the remarks made at the end of the previous section we may to a first approximation take s_ϕ to be constant and equal to s_1 over the whole of the former part, $0 \leqslant \phi \leqslant 98°$, and again constant and equal to $s_2 = s_1/2$ over the latter part $98° < \phi \leqslant \pi$, the average value of s over the whole of the sphere being given by

$$\bar{s} = \sigma/(4\pi) = \tfrac{1}{2}(1{\cdot}14 s_1 + 0{\cdot}86 s_2) = 0{\cdot}79 s_1. \tag{27}$$

Let us denote by $(1/l)_1$ the contribution to $1/l$ from the part of the sphere included in the first Brillouin zone, corresponding to $0 \leqslant \phi \leqslant 98°$, and by $(1/l)_2$ the contribution from the part of the sphere that lies outside the first zone and corresponding to $98° < \phi \leqslant \pi$.

The calculation of $(1/l)_1$ is done immediately. Since $(1/l)_1$ is the contribution to $1/l$ from forward angles of scattering and is a small part of $1/l$, we may in view of (23) take it to be just $(f_0/2k)^2$ times the value of $1/l$ for the complete sphere of propagation, *the whole of the sphere being taken for this purpose to be well within the first Brillouin zone*, or

$$(1/l)_1 = \nu^2 kT \,.\, 4\pi s_1 (0{\cdot}76/c_{11})\,(1{\cdot}14k/2k)^2$$
$$= 0{\cdot}3\nu^2 kT\sigma/c_{11}. \tag{28}$$

The contribution to $1/l$ from the part of the sphere outside the central zone, which we have denoted by $(1/l)_2$, and which is the major contribution to $1/l$, is calculated in the following manner, remembering that in this region also s_ϕ may be taken to be independent of ϕ, but equal to s_2. The major factor that determines variation of S

in this region will be the variation of R, which will be particularly marked in the regions of the sphere facing the reciprocal point (110). Jahn (1942*b*) has discussed in the case of X-rays the variation of R for scattering by sodium crystal, for different positions of P in the neighbourhood of the reciprocal point (110), and has investigated in particular the shape of the 'isodiffusion' surfaces, i.e. the loci of P corresponding to different constant values of the coefficient R_ϕ. The portions of these isodiffusion surfaces in the neighbourhood of the line [110] and the reciprocal point (110), are found to be portions of highly oblate ellipsoids, with their short axis along [110], and hence the intersections of these surfaces with the sphere of propagation will be practically planes perpendicular to the above line and perpendicular to the plane of the paper in figure 4.

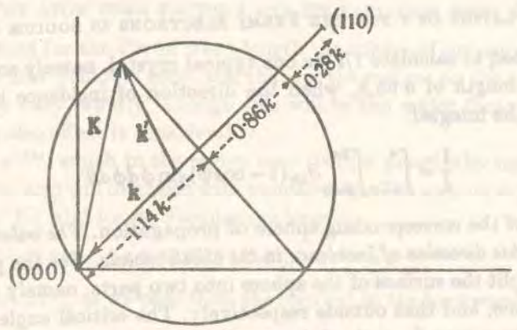

FIGURE 4

In order to give an idea how flat these surfaces are, we give in table 7 for a few of the isodiffusion ellipsoids surrounding (110), the magnitudes of the semi-axes along the three principal directions of the ellipsoid, which are also the directions of displacement e_i, I along [110]; II along [$\bar{1}$10]; and III along [001]. The semi-axes are all expressed in terms of the Fermi wave-number $k = 1/(2{\cdot}28d_{110})$ as unit. (The shortest distance from (110) to the surface of the sphere of propagation is $0{\cdot}28k$.) The calculation of the axes is based on the data for the elastic constants of sodium crystal given in § 7.

TABLE 7. SEMI-AXES OF SOME OF THE ISODIFFUSION ELLIPSOIDS AROUND (110) AND CLOSE TO THEIR [110] AXES

I	II	III	$R\frac{c_{11}}{e^{-2M}\nu kT}$
0·28	1·23	0·48*k*	30·5
0·4	1·90	0·73	13·2
0·5	2·55	1·00	7·6
0·75	4·90	2·10	2·48
0·9	7·06	4·04	1·40
1·0	10·89	—	0·98

It will be seen that the II and III semi-axes are much longer than I, especially as we move out some distance from (110) and as the area of intersection of these

isodiffusion surfaces with the sphere of propagation expands; and hence we may take these intersections practically as planes perpendicular to [110].

This feature of the isodiffusion surfaces makes the computation of the structure factor R_ϕ, and of the scattering coefficient S_ϕ, for the portions of the sphere of propagation outside the central Brillouin zone, and facing (110), and the numerical integration of $S_\phi(1-\cos\phi)$ over this region of the surface of the sphere, easy; since for the purpose of this integration we may divide the surface of the sphere in the neighbourhood of B into zones of equal area, by equally spaced planes perpendicular to [110]. In other words S in this region is determined wholly by the distance fk from (000) measured along [110], where $f = 1-\cos\phi$, $98° < \phi \leqslant \pi$.

On this basis expression (7) for R, for the part of the sphere outside the central zone at a distance fk from (000) measured along [110] will be given by

$$R = e^{-2M}\frac{\nu kT}{\rho V_l^2}\left(\frac{K_r}{K}\right)^2 = e^{-2M}\frac{\nu kT}{\rho V_l^2}\left(\frac{f}{2{\cdot}28-f}\right)^2, \tag{29}$$

where V_l is the velocity of the longitudinal elastic wave of wave-number K travelling along [110], and is given by (see (12))

$$\rho V_l^2 = \tfrac{1}{2}(c_{11}+c_{12}+2c_{44}), \tag{30}$$

which for sodium crystal becomes $c_{11}/0{\cdot}60$. Hence we obtain

$$R = e^{-2M}\nu kT(0{\cdot}60/c_{11})f^2/(2{\cdot}28-f)^2 \tag{31}$$

and

$$\left(\frac{1}{l}\right)_2 = \int_{\phi_0}^{\pi} Rvs_2(1-\cos\phi)\,2\pi\sin\phi\,d\phi = \frac{\nu^2kT\sigma}{c_{11}} \times 0{\cdot}190\int_{1{\cdot}14}^{2} e^{-2M}\frac{f^3\,df}{(2{\cdot}28-f)^2}. \tag{32}$$

The integral can be evaluated numerically, and is found to be equal to about 12·0, whence we obtain

$$(1/l)_2 = 2{\cdot}3\nu^2kT\sigma/c_{11}. \tag{33}$$

From (28) and (33) we obtain

$$1/l = (1/l)_1 + (1/l)_2 = 2{\cdot}6\nu^2kT\sigma/c_{11}. \tag{34}$$

Though the above method of calculating $(1/l)_2$ by taking the intersections of the sphere of propagation by the isodiffusion surfaces to be *planes* is a good approximation, it can be readily seen that it is on the side of an over-estimate, since R will fall off slightly more rapidly as we move away from (110) than is implied in the above approximation. Hence we may express $1/l$ for the Fermi electrons in sodium crystal in the form

$$1/l = \Phi\,\nu^2kT\sigma/c_{11}, \tag{35}$$

where for incidence along [110], Φ is slightly less than 2·6, which as we mentioned *is the highest value of Φ for any direction of incidence of the Fermi electrons.*

11. Incidence of Fermi electrons along [100]

The calculation of Φ for other directions of incidence of the Fermi electrons is more laborious, but we can see in a general way that in a body-centred cubic crystal, just as Φ is a maximum for incidence along [110], it is a minimum for incidence along [100]. For the latter direction of incidence the portion of the sphere of propagation that is included in the first Brillouin zone varies with the azimuthal plane of scattering, and for (001) and similar azimuthal planes corresponds to $0 \leqslant f \leqslant 0{\cdot}66$. Now the structure factor R does not reach a high value in *any* part of the sphere of propagation, as it does when the incidence is along [110], the highest values of $Rc_{11}/(e^{-2M}\nu kT)$ now reached being only 2·7 (see table 2), for the backward direction of scattering, i.e. for $f = 2$, and falling down to unity as we move back to the boundary of the Brillouin zone. The above value of R would correspond to

$$S_{\max.} = e^{-0{\cdot}27} \times 2{\cdot}7\nu^2 kT s_3/c_{11}$$
$$= 1{\cdot}3\frac{\nu^2 kT}{c_{11}}\frac{\sigma}{4\pi}.$$

Hence for this direction of incidence Φ should lie between 1·3 and 0·76, and a rough estimate shows it is about 1·1.

12. The average value of $1/l$ taken over all directions of incidence

Having fixed the approximate upper and lower limits for Φ, namely 2·6 and 1·1, for incidence of the Fermi electrons along [110] and [100] respectively, it now remains to determine the average value of Φ taken over all directions of incidence of these electrons. The high value of $\Phi = 2{\cdot}6$ for incidence along [110] is due to the close proximity of the extreme outer regions of the sphere of propagation to the reciprocal lattice point (110); indeed of the total value of 2·6 for Φ for this direction of incidence, about 1·7 is contributed by the small region $1{\cdot}75 < f \leqslant 2$, the rest of the sphere, namely $0 \leqslant f \leqslant 1{\cdot}75$, contributing about 0·9 only. Hence as the direction of incidence is varied even slightly away from [110], Φ will drop down considerably, and hence one can reasonably take the average value of Φ to be very close to its minimum value of 1·1, and take the mean value of $1/l$ or $1/v\tau$ required in calculating the specific resistance of sodium to be given by $\overline{1/l} = \overline{\Phi}\,\nu^2 kT\sigma/c_{11}$,

where $\overline{\Phi}$ is about 1·2 or 1·3.

Till now we have expressed $1/l$ for sodium in terms of its elastic constant c_{11}. We may also, for convenience, express it in terms of its compressibility β, which in a cubic crystal is given by $\beta = 3/(c_{11} + 2c_{12})$,

and which in sodium is equal to $3/(2{\cdot}54c_{11}) = 1{\cdot}18/c_{11}$. The mean free path $1/l$ can then be expressed in the form

$$\overline{1/l} = \Psi\,\nu^2 kT\beta\sigma, \qquad (36)$$

where Ψ is a numerical factor, which in sodium crystal will be seen to be close to unity. With $\Psi = 1$, one can easily recognize the right-hand side of equation (36) to be just the Einstein-Smoluchowski expression for the attenuation coefficient of a liquid medium for *long* waves (see Einstein (1910)).

Now in a liquid, the local inhomogeneities produced by thermal agitation, which ultimately account for the scattering, is represented almost wholly by the local fluctuations in density. In a crystalline medium, however, the local inhomogeneities which produce scattering will naturally be more complicated, and will involve, besides the compressibility β, the other elastic constants too. As a result of this, in sodium crystal, and for small values of $\sin\frac{1}{2}\phi/\lambda$, the structure factor R is considerably less than the Einstein value, almost half of it when K is along [110]. On the other hand, when the pole of diffusion P moves out of the first Brillouin zone, R as we have seen rises above the Einstein value, and for certain directions of incidence, and in the neighbourhood of the backward direction, becomes several times the Einstein value. But since these high values are highly localized their contribution to $1/l$ is not so large. Indeed the average value of $1/l$ for the Fermi electrons, taken over all directions of incidence and of scattering, as we have seen, is roughly just the Einstein value, *as though we might regard the mean free path l of the Fermi electrons in sodium to be just the reciprocal of the attenuation coefficient due to scattering, and the scattering to be determined almost wholly by the local thermal fluctuations in density*. This simple approximation is a result of the rough balancing of the different varying factors that determine the mean free path, R_ϕ and $1 - \cos\phi$ increasing, e^{-2M} and s_ϕ decreasing, as we pass from the forward to the backward directions of scattering.

Had λ been considerably shorter, i.e. had the Fermi surface been much closer to the boundary of the Brillouin zone, owing to the rapid increase of R as one approaches the boundary, and the consequent increase of the scattering coefficient S, the free path and the relaxation time would be much shorter. The result would be a correspondingly enhanced specific resistance.

In the usual treatment of the electrical resistivities of metals (see Mott & Jones 1936) for convenience in calculation, the medium is regarded as elastically isotropic, and the longitudinal thermal elastic waves alone as contributing to the scattering, which is equivalent to regarding the scattering as produced by the fluctuations in density due to thermal agitation. The detailed calculations made in the present paper show that in sodium metal, this is a good approximation, and it is presumably so in other monovalent metals too.

Now the Fermi wave-length λ, as we have seen, is not much longer than necessary to give the first Bragg reflexion in the backward direction, i.e. not much longer than $2d$. Even so, it was shown in an earlier paper (Krishnan & Bhatia 1944) from certain general considerations, that it should be regarded as long enough for the Einstein formula—which is derived explicitly on the basis of λ's being very long in comparison with the interatomic distance—to be applicable. The present calculations show that the intensity of scattering, particularly along the backward direction will deviate considerably from the Einstein value, but the total scattering in all directions, i.e. the attenuation coefficient, remains roughly at this value.

13. Fermi surface close to the boundary of the Brillouin zone

We have already emphasized that if the electronic wave-length were to be reduced considerably below the Fermi value, the total scattering, and hence the specific

resistance, would increase very rapidly. This would be attributed in the usual theory of electrical conduction in metals to the approach of the Fermi surface to the boundary of the Brillouin zone, and the consequent enhanced influence of the ionic lattice on the freedom of movement of the electrons. The effect would be regarded as equivalent to either an increase in the effective mass of the electron near the boundary of the zone, or a decrease in the effective number of conduction electrons, whereas from the point of view adopted in the present paper the effect is an enhanced scattering and a corresponding reduction in the mean free path of the Fermi electrons. All the three alternatives are of course equivalent, and correspond to an enhanced specific resistance. But the viewpoint adopted here, which regards the enhancement of the resistance when the Fermi surface approaches any of the reciprocal points as due to enhanced scattering of the Fermi electrons, has certain advantages, especially in dealing with the electrical resistivities of liquid metals (Krishnan & Bhatia 1945). We postpone detailed consideration of this aspect to a separate paper.

References

Blackman, M. 1937 *Proc. Roy. Soc.* A, **159**, 416.
Darwin, C. G. 1914 *Phil. Mag.* **1**, 315.
Debye, P. 1914 *Ann. Phys., Lpz.*, **43**, 49.
Einstein, A. 1910 *Ann. Phys., Lpz.*, **33**, 1294.
Faxén, H. 1923 *Z. Phys.* **17**, 266.
Faxén, H. & Holtsmark, J. 1927 *Z. Phys.* **45**, 307.
Fine, P. C. 1939 *Phys. Rev.* **54**, 355.
Fröhlich, H. 1936 *Theorie der Metalle.* Berlin: Springer.
Jahn, H. A. 1942*a* *Proc. Roy. Soc.* A, **179**, 320.
Jahn, H. A. 1942*b* *Proc. Roy. Soc.* A, **180**, 476.
Jauncey, G. E. M. See Compton, A. H. & Allison, S. H. 1935 *X-rays in theory and experiment.* London: Macmillan & Co.
Kellerman, E. W. 1940 *Phil. Trans.* A, **238**, 513.
Krishnan, K. S. & Bhatia, A. B. 1944 *Proc. Nat. Acad. Sci. India*, **14**, 153.
Krishnan, K. S. & Bhatia, A. B. 1945 *Nature*, **156**, 503.
Krishnan, K. S. & Bhatia, A. B. 1948 *Proc. Roy. Soc.* A, **192**, 181.
Lonsdale, K. & Smith, H. 1940 *Nature*, **149**, 21.
Mott, N. F. & Jones, H. 1936 *Theory of properties of metals and alloys.* Oxford Univ. Press.
Quimby, S. L. & Siegel, S. 1938 *Phys. Rev.* **54**, 293.
Raman, Sir C. V. 1941 *Proc. Ind. Acad. Sci*, **13**, 1.
Ramsauer, C. & Kollath, R. 1932 *Ann. Phys., Lpz.*, **12**, 529.
Waller, I. 1923 *Z. Phys.* **17**, 398.
Waller, I. 1925 *Diss.* (*Uppsala*).
Waller, I. 1928 *Z. Phys.* **51**, 213.

A Simple Result in Quadrature

In calculating the intensity of light scattered by a transparent homogeneous medium, one comes across the infinite series[1]

$$\sum_{n=-\infty}^{+\infty}{}^{\alpha} \frac{\sin^2(n\alpha+\theta)}{(n\alpha+\theta)^2}, \qquad (1)$$

in which θ is a constant and n an integer. α is a positive number, which under the conditions under which light-scattering is generally studied is very small, and hence the sum of the above series is usually replaced by the corresponding integral

$$\int_{-\infty}^{+\infty} \frac{\sin^2 x}{x^2}\,dx, \qquad (2)$$

which evidently is equal to π.

It can be shown[1], however, that the equality of (1) and (2) holds not only in the limit when $\alpha \to 0$, but for any value of α in the range $0 < \alpha \leqslant \pi$. An obvious interpretation of this result is that the area subtended between the curve $y = \sin^2 x/x^2$ and the x-axis can be obtained by taking the sum of the ordinates at equal intervals α, $0 < \alpha \leqslant \pi$, and multiplying by α, that is, by simple rectangulation, just as well as by integration. In erecting these ordinates at equal intervals, we may start from any value θ of x.

The main purpose of this note is to direct attention to this property, namely,

$$\sum_{n=-\infty}^{+\infty}{}^{\alpha} f(n\alpha+\theta) = \sum_{n=-\infty}^{+\infty}{}^{\alpha} f(n\alpha) = \int_{-\infty}^{+\infty} f(x)\,dx, \qquad (3)$$

where $0 < \alpha \leqslant$ a certain constant α_0, which characterizes $f(x) = \sin^2 x/x^2$, and to show that numerous other functions can be constructed that have this property. A method of evaluating (1) given by Prof. Wiener, and quoted in the paper referred to[1], suggests the criterion by which to construct such functions.

Consider an even function $F(x)$ $[= F(-x)]$ the Fourier transform of which,

$$g(v) = \frac{1}{\sqrt{(2\pi)}} \int_{-\infty}^{+\infty} F(x)\,\exp\,(ivx)dx, \qquad (4)$$

has non-zero values when $|v|$ is less than a certain constant v_0, and is zero otherwise. Then by Poisson's summation formula[2]

$$\sum_{n=-\infty}^{+\infty}{}^{\alpha} F(n\alpha+\theta) = \sqrt{(2\pi)} \sum_{N=-\infty}^{+\infty} \cdot \exp\,[-i2\pi N\theta/\alpha]. \; g(2\pi N/\alpha), \qquad (5)$$

where n and N are integers and $\alpha > 0$. If now α is chosen to be $\leqslant 2\pi/v_0$, then all the terms on the right-hand side of (5) except the one corresponding to $N = 0$ vanish, and we obtain

$F(x)$	$\sqrt{(2\pi)} \cdot g(v)$	v_0
$\dfrac{\sin\,[a(x^2+\lambda^2)^{1/2}]}{(x^2+\lambda^2)^{1/2}}$	$\pi J_0\,[\lambda(a^2-v^2)^{1/2}]$	a
$\cos\,[a(x^2+\lambda^2)^{1/2}] - \cos ax$	$-\dfrac{\pi a\lambda J_1\,[\lambda(a^2-v^2)^{1/2}]}{(a^2-v^2)^{1/2}}$	a
$\dfrac{1}{\Gamma(\alpha+x)\,\Gamma(\beta-x)}$	$\dfrac{(2\cos 1/2v)^{\alpha+\beta-2}\{-\frac{1}{2}\exp iv(\alpha-\beta)\}}{\Gamma(\alpha+\beta-1)}$	π [4]

$$\sum_{n=-\infty}^{+\infty}{}^{\alpha} F(n\alpha+\theta) = \sqrt{(2\pi)}\,g\,(0),$$

which can be seen from (4) to be equal to $\int_{-\infty}^{+\infty} F(x)\,dx$;

and hence the function F satisfies (3).

Since the Fourier integrals of a large number of functions have been tabulated by Campbell and Foster[3] and by others, it is easy to select, or construct, examples of functions F the Fourier transforms of which satisfy the above criterion, and which satisfy (3). $F(x) = \sin^m x/x^n$, where m and n are positive integers, $m \geqslant n$, both of them odd or both of them even, is one such function with $v_0 = m$; when $m = 1$, the range of v over which $g(v) \neq 0$ includes $v = 1$. A few other examples are given below.

A more detailed account will be published shortly in the *Journal of the Indian Mathematical Society*.

K. S. Krishnan
National Physical Laboratory of India,
Delhi. June 6.

[1] Bhatia, A. B., and Krishnan, K. S., *Proc. Roy. Soc.*, A, **192**, 181 (1947).
[2] See Titchmarsh, "Introduction to the Theory of Fourier Integrals", 60 (Oxford, 1937).
[3] Bell Tel. Sys. Tech. Pub. Monograph B584 (1931).
[4] From Ramanujan, "Collected Papers", 216.

ON THE EQUIVALENCE OF CERTAIN INFINITE SERIES AND THE CORRESPONDING INTEGRALS

BY

K. S. KRISHNAN, *National Physical Laboratory of India, Delhi.*

[Received 15 March, 1948.]

1. In calculating the intensity of light scattered in a homogeneous medium, one comes across the infinite series

$$\alpha \sum_{n=-\infty}^{+\infty} \frac{\sin^2(n\alpha+\theta)}{(n\alpha+\theta)^2},$$

where θ is a constant, and n an integer. α is a positive number which under the conditions under which light-scattering is generally studied, can be made arbitrarily small, and hence the sum is usually replaced by the corresponding integral*

$$\alpha \sum_{n=-\infty}^{+\infty} \frac{\sin^2(n\alpha+\theta)}{(n\alpha+\theta)^2} = \int_{-\infty}^{\infty} \frac{\sin^2 x}{x^2}\,dx = \pi. \qquad (1)$$

It is easy to show†, however, that (1) holds not only in the limit when α tends to zero, but for any value of α in the range $0 < \alpha \leqslant \pi$. The proof is as follows.

Consider the series‡

$$\sum_{n=-\infty}^{\infty} \frac{\sin(n+\beta)z}{n+\beta} = \pi, \qquad (2)$$

where β is a constant, n an integer, and $0 < z < 2\pi$. The series can be integrated term by term with respect to z in any closed interval (γ, δ), where $0 < \gamma < \delta < 2\pi$, since it is uniformly convergent in this interval. We thus obtain

* Einstein. *Ann. der Physik*, 33 (1910), 1294.

† Bhatia and Krishnan, *Proc. Royal Soc.* A., 192 (1947), 184.

‡ Bromwich, *An introduction to the theory of infinite series*, (1931), 371, Ex. 5.

$$\sum_{n=-\infty}^{\infty} \frac{\cos(n+\beta)\gamma}{(n+\beta)^2} - \sum_{n=-\infty}^{\infty} \frac{\cos(n+\beta)\delta}{(n+\beta)^2} = \pi(\delta-\gamma). \qquad (3)$$

Keeping δ constant and making $\gamma \to 0$, (3) reduces to

$$\sum_{n=-\infty}^{\infty} \frac{1-\cos(n+\beta)\delta}{(n+\beta)^2} = \pi\delta,$$

since the first series on the left side of (3) is uniformly convergent and therefore represents a continuous function of γ. Putting now $\delta = 2\alpha$, $\alpha\beta = \theta$, and dividing both sides by 2α $(\neq 0)$, we obtain for $0 < \alpha < \pi$,

$$\alpha \sum_{n=-\infty}^{\infty} \frac{\sin^2(n\alpha+\theta)}{(n\alpha+\theta)^2} = \pi. \qquad (4)$$

This can be seen to be true for $\alpha = \pi$ also, and hence (4) holds over the interval $0 < \alpha \leqslant \pi$.

The above result implies that the area subtended between the curve $y = \sin^2 x/x^2$ and the x-axis may be obtained just as well by adding up the ordinates at equal intervals α, and multiplying by α (i.e. by simple rectangulation), as by integration, provided $0 < \alpha \leqslant \pi$. It may be noted here that the sum in (4) is independent of θ, which shows that we may start the division of the x-axis into equal steps α from any value of x. In particular, $x = 0$ need not be one of the points of division.

2. As we shall show presently, the same property, viz.

$$\alpha \sum_{n=-\infty}^{\infty} f(n\alpha+\theta) = \alpha \sum_{n=-\infty}^{\infty} f(n\alpha) = \int_{-\infty}^{\infty} f(x)\,dx \qquad (5)$$

for a suitable range of values of α, $0 < \alpha \leqslant l$, say, holds for several other functions too. Before considering such functions, we shall refer here to an alternative proof of (4), given by Prof. Norbert Wiener.* The proof is very

* See Bhatia and Krishnan, *loc. cit.*, foot-notes on pp. 184 and 185.

suggestive, and enables us to determine the conditions for the validity of the equations (5).*

Consider an even function $f(x) = f(-x)$, and its Fourier transform defined by

$$g(v) = \frac{1}{(2\pi)^{\frac{1}{2}}} \int_{-\infty}^{\infty} f(x) e^{ivx} dx. \qquad (6)$$

Let $f(x)$ be such that $g(v)$ has non-zero values in the range $-a < v < a$, where a is a positive number. Obviously $f(x) = \sin^2 x/x^2$ satisfies this condition, since $g(v) = (\pi/2)^{\frac{1}{2}}(2 - |v|)$, if $0 \leqslant |v| \leqslant 2$, and $= 0$ if $|v| \geqslant 2$.

According to Poisson's summation formula,†

$$\sum_{n=-\infty}^{\infty} f(n\alpha) = \frac{(2\pi)^{\frac{1}{2}}}{\alpha} \sum_{N=-\infty}^{\infty} g\left(\frac{2\pi N}{\alpha}\right), \qquad (7)$$

where N is an integer. If now $0 < \alpha \leqslant 2\pi/a$, there is only one value of N, viz. $N = 0$, for which $g(2\pi N/\alpha)$ differs from 0.

Hence

$$\sum_{n=-\infty}^{\infty} f(n\alpha) = \frac{(2\pi)^{\frac{1}{2}}}{\alpha} g(0), \qquad (8)$$

whence substituting for $g(0)$ from (6) we obtain

$$\alpha \sum_{n=-\infty}^{\infty} f(n\alpha) = \int_{-\infty}^{\infty} f(x)\,dx. \qquad (9)$$

Further, for a fixed θ, it can be seen that

$$\int_{-\infty}^{\infty} f(x+\theta) e^{ivx} dx = e^{-iv\theta} \int_{-\infty}^{\infty} f(x) e^{ivx} dx, \qquad (10)$$

which shows that for $v = 0$, the Fourier transform of $f(x+\theta)$ is the same as that of $f(x)$. Hence it follows that

* $f(x) =$ constant is a trivial example that satisfies (5).

† See Titchmarsh, *Introduction to the Theory of Fourier Integrals*, p. 60, where Poisson's summation formula is proved with reference to the Fourier cosine transform,

$$g_c(v) = \left(\frac{2}{\pi}\right)^{\frac{1}{2}} \int_0^{\infty} f(x) \cos vx\, dx;$$

but, for the *even* functions that we are considering, the exponential and the cosine transforms become identical.

if $f(x)$ be such that its Fourier transform $g(v)$ has non zero values when $|v| < a$, and zero value otherwise, then

$$\alpha \sum_{n=-\infty}^{\infty} f(n\alpha+\theta) = \alpha \sum_{n=-\infty}^{\infty} f(n\alpha) = \int_{-\infty}^{\infty} f(x)dx, \qquad (11)$$

provided that $0 < \alpha \leqslant 2\pi/a$.

We have seen that $\sin^2 x/x^2$ is such a function, the range of α over which (11) holds being $0 < \alpha \leqslant \pi$. *More generally*, the functions $f_{m,n}(x) = \sin^m x/x^n$, where m and n are positive integers, both odd or both even, and $n \leqslant m$, are examples of such functions; their Fourier transforms $g_{m,n}(v)$ can be seen to have zero value if $|v| \geqslant n$ ($|v| > n$ when $n = 1$), and non-zero values otherwise, and hence for these functions, relations (11) will be valid if

$$0 < \alpha \leqslant 2\pi/n \quad (0 < \alpha < 2\pi/n \text{ when } n = 1).$$

The Fourier transforms of $(\sin x/x)^m$, $m = 1, 2, 3$, are plotted in Fig. 1, *a*, *b*, *c*.

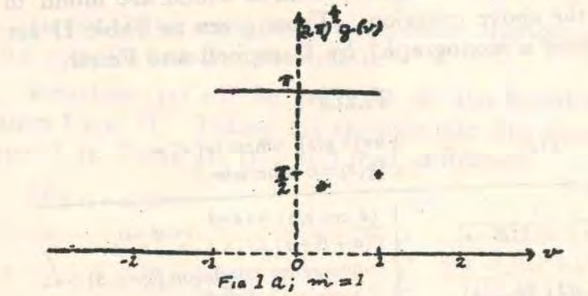

Fig 1 a; $m = 1$

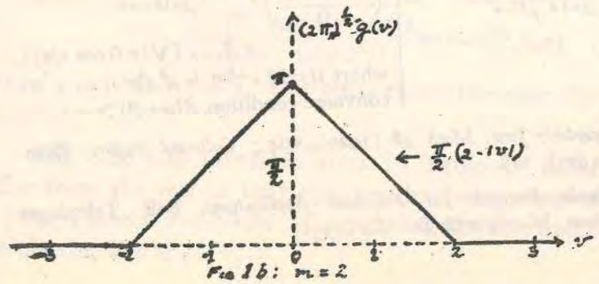

Fig 1 b: $m = 2$

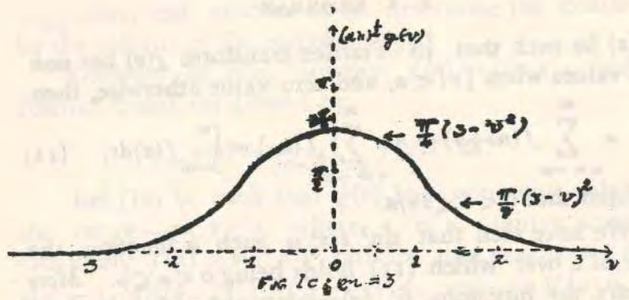

FIG. 1 (c = 3)

3. Since the Fourier transforms are known for a large number of functions, and many of them have been conveniently tabulated, it is easy to select other examples of functions that satisfy the criterion stated above, and for which therefore relations (10) are valid. We give in the following tables a few. Those given in Table I are taken from a paper by Ramanujan,* entitled *A class of definite integrals*, in which among others are given the values of several Fourier integrals, some of which are found to satisfy the above criterion. Those given in Table II are taken from a monograph† by Campbell and Foster.

TABLE I.

$f(x)$	$(2\pi)^{\frac{1}{2}} g(v)$, when $\lvert v\rvert < \pi$ [$g(v)=0$ otherwise.]
$\frac{1}{\Gamma(\alpha+x)\,\Gamma(\beta-x)}$	$\frac{(2\cos v/2)^{\alpha+\beta-2}}{\Gamma(\alpha+\beta-1)} e^{\frac{1}{2}iv(\beta-\alpha)}$, convergence condition $R(\alpha+\beta)>1$
$\frac{J_{\alpha+x}(\lambda)\,J_{\beta-x}(\mu)}{\lambda^{\alpha+x}\,\mu^{\beta-x}}$	$\left(\frac{2\cos v/2}{\Omega}\right)^{\frac{1}{2}(\alpha+\beta)} e^{\frac{1}{2}v(\beta-\alpha)i} + J_{\alpha+\beta}[\sqrt{(2\Omega\cos v/2)}]$, where $\Omega=\lambda^2 e^{-\frac{1}{2}vi}+\mu^2 e^{\frac{1}{2}vi}$, converge condition $R(\alpha+\beta)>-1$.

* *Quarterly Jour. Math.* 48 (1920), 294; *Collected Papers*, Cambridge (1927), 216.

† *Fourier Integrals for Practical Applications*, Bell Telephone Publications, Monograph B—584 (1931).

TABLE II.

$f(x)$	$(2\pi)^{\frac{1}{2}} g(v)$, when $\lvert v\rvert \leqslant a$ [$g(v)=0$ otherwise.]
$\frac{\sin a(x^2+\lambda^2)^{\frac{1}{2}}}{(x^2+\lambda^2)^{\frac{1}{2}}}$	$\pi J_0[\lambda(a^2-v^2)^{\frac{1}{2}}]$
$\frac{\sin a(x^2-\lambda^2)^{\frac{1}{2}}}{(x^2-\lambda^2)^{\frac{1}{2}}}$	$\pi I_0[\lambda(a^2-v^2)^{\frac{1}{2}}]$
$\cos a(x^2+\lambda^2)^{\frac{1}{2}}-\cos ax$	$-\frac{\pi a\lambda J_1[\lambda(a^2-v^2)^{\frac{1}{2}}]}{(a^2-v_2)^{\frac{1}{2}}}$
$\frac{\sin a(1-x)}{1-x}+\frac{\sin a(1+x)}{1+x}$	$2\pi\cos v$
$\frac{\sin^2 a(1-x)/2}{1-x}+\frac{\sin^2 a(1+x)/2}{1+x}$	$\pi\sin v$
$\frac{\sin ax}{x^2}-\frac{a\cos ax}{x}$	$i\pi v$.

In the above, a is a positive real finite number, and λ is a complex number, not infinite.

Relations (11) will be valid for all the functions in Tables I and II. Taking for example the first function entered in Table II, (11) will read as follows:

If $0<\alpha\leqslant 2\pi/a$,

$$\alpha\sum_{n=-\infty}^{\infty}\frac{\sin a\{(n\alpha+\theta)^2+\lambda^2\}^{\frac{1}{2}}}{\{(n\alpha+\theta)^2+\lambda^2\}^{\frac{1}{2}}}=\alpha\sum_{n=-\infty}^{\infty}\frac{\sin a(n^2\alpha^2+\lambda^2)^{\frac{1}{2}}}{(n^2\alpha^2+\lambda^2)^{\frac{1}{2}}}=\int_{-\infty}^{\infty}\frac{\sin a(x^2+\lambda^2)^{\frac{1}{2}}}{(x^2+\lambda^2)^{\frac{1}{2}}}dx=\pi J_0(\lambda a). \quad (12)$$

When $\lambda=0$ and $a=1$, this reduces to the case $f(x)=\sin x/x$.

The last two functions given in Table II however differ from the rest in that $g(v)$, besides being zero when $\lvert v\rvert > a$, is zero at $v=0$ also. Considering the last function, we obtain, if $0<\alpha<\pi$,

$$\alpha \sum_{n=-\infty}^{\infty} \left[\frac{\sin(n\alpha+\theta)}{(n\alpha+\theta)^2} - \frac{\cos(n\alpha+\theta)}{n\alpha+\theta} \right]$$

$$= \alpha \sum_{n=-\infty}^{\infty} \left[\frac{\sin(n\alpha)}{n^2\alpha^2} - \frac{\cos(n\alpha)}{n\alpha} \right]$$

$$= \int_{-\infty}^{\infty} \left(\frac{\sin x}{x^2} - \frac{\cos x}{x} \right) dx \qquad (13)$$

$$= g(0) = 0.$$

That the value of the integral in (13) is zero is otherwise obvious. We thus obtain when $0 < \alpha < \pi$ and $n\alpha+\theta$ is not equal to θ for any value of n,

$$\sum_{n=-\infty}^{\infty} \frac{\sin(n\alpha+\theta)}{(n\alpha+\theta)^2} = \sum_{n=-\infty}^{\infty} \frac{\cos(n\alpha+\theta)}{n\alpha+\theta} \qquad (14)$$

The corresponding integrals $\int_{-\infty}^{\infty} \frac{\sin x}{x^2}\, dx$ and $\int_{-\infty}^{\infty} \frac{\cos x}{x}\, dx$ are however infinite.

The last but one function entered in Table II, for which too $g(a) = 0$ at $v = 0$, as also when $|v| > a$, yields similarly, if $0 < \alpha < \pi/a$,

$$\sum_{n=-\infty}^{\infty} \frac{\sin^2 a(n\alpha+\theta)}{n\alpha+\theta} = \sum_{n=-\infty}^{\infty} \frac{\sin^2 a(n\alpha+\theta+2)}{n\alpha+\theta+2}, \qquad (15)$$

though

$$\int_{-\infty}^{\infty} \frac{\sin^2 ax}{x}\, dx = 0.$$

4. The class of functions that we have been considering here, which is characterized by the Fourier transforms being zero when $|v|$ is greater then a certain positive number a, has other interesting properties. Analogous to Poisson's summation formula, which we have used, and which we may write in the more familiar form

$$\sqrt{\alpha}\left\{ \tfrac{1}{2} f(0) + f(\alpha) + f(2\alpha) + \dots \right\}$$

$$= \sqrt{\beta}\left\{ \tfrac{1}{2} g_c(0) + g_c(\beta) + g_c(2\beta) + \dots \right\}, \qquad (16)$$

where $\alpha\beta = 2\pi$, there are others of the same type due to Ramanujan*. Two of the typical formulae are given below.

$$\sqrt{\alpha}\left\{ f(\alpha) - f(3\alpha) - f(5\alpha) + f(7\alpha) + f(9\alpha) - \dots \right\}$$

$$= \sqrt{\beta}\left\{ g_c(\beta) - g_c(3\beta) - g_c(5\beta) + g_c 7(\beta) + g_c(9\beta) - \dots \right\}, \qquad (17)$$

where $\alpha\beta = \pi/4$;

$$\sqrt{\alpha}\left\{ f(\alpha) - f(5\alpha) - f(7\alpha) + f(11\alpha) + f(13\alpha) - \dots \right\}$$

$$\sqrt{\beta}\left\{ g_c(\beta) - g_c(5\beta) - g_c(7\beta) + g_c(11\beta) + g_c(13\beta) - \dots \right\}, \qquad (18)$$

where $\alpha\beta = \pi/6$, and 1, 5, 7, 11, 13, ..., are the numbers prime to 6.

Unlike in Poisson's formula (16), in which the first term on the right side is $\frac{1}{2} g_c(0)$, the first term in (17), (18) and similar formulae, is $g_c(\beta)$. If now $\beta > a$, i.e. if α is chosen small enough to make $\beta > a$, then all the terms on the right side of (17) and (18) vanish, and we get the following interesting results. From (17), for example, we obtain, if $0 < \alpha < \pi/4a$,

$$f(\alpha) + f(7\alpha) + f(9\alpha) + f(15\alpha) + f(17\alpha) + \dots$$

$$= f(3\alpha) + f(5\alpha) + f(11\alpha) + f(13\alpha) + \dots \qquad (19)$$

Similarly, from (18), if $0 < \alpha < \pi/6a$,

$$f(\alpha) + f(11\alpha) + f(13\alpha) + f(23\alpha) + f(25\alpha) + \dots$$

$$= f(5\alpha) + f(7\alpha) + f(17\alpha) + f(19\alpha) + \dots \qquad (20)$$

Taking $\sin x/x$ as an example of such a function, we obtain from (19), if $|\alpha| < \pi/4$,

$$\frac{\sin \alpha}{\alpha} + \frac{\sin 7\alpha}{7\alpha} + \frac{\sin 9\alpha}{9\alpha} + \dots$$

$$= \frac{\sin 3\alpha}{3\alpha} + \frac{\sin 5\alpha}{5\alpha} + \frac{\sin 11\alpha}{11\alpha} + \dots$$

$$= \frac{1}{8\alpha} \int_{-\infty}^{\infty} \frac{\sin x}{x}\, dx = \frac{\pi}{8\alpha}. \qquad (21)$$

More generally,

Collected papers, p. 63; *Messenger of Maths.*, 44 (1915), 75.

$$\frac{\sin^m\alpha}{\alpha^n}+\frac{\sin^m 7\alpha}{(4\alpha)^n}+\frac{\sin^m 9\alpha}{(9\alpha)^n}+\cdots$$
$$=\frac{\sin^m 3\alpha}{(3\alpha)^n}+\frac{\sin^m 5\alpha}{(5\alpha)^n}+\frac{\sin^m 11\alpha}{(11\alpha)^n}+\cdots$$
$$=\frac{1}{8\alpha}\int_{-\infty}^{\infty}\frac{\sin^m x}{x^n}\,dx, \qquad (22$$

where $|\alpha|\leqslant\frac{\pi}{4n}$, m and n are positive integers both odd or both even, and $0<n\leqslant m$.

Now the Fourier transform of $f(x+\theta)$ differs from that of $f(x)$ by a multiplying factor $e^{-iv\theta}$, or $\cos v\theta$ in the case of cosine transforms, and hence the g's on the right side of (17) and (18) will remain zero even when $f(x)$ is changed to $f(x+\theta)$. Hence, we obtain from (22), even more generally,

$$\frac{\sin^m(\alpha+\theta)}{(\alpha+\theta)^n}+\frac{\sin^m(\alpha-\theta)}{(\alpha-\theta)^n}+\frac{\sin^m(7\alpha+\theta)}{(7\alpha+\theta)^n}+\frac{\sin^m(7\alpha-\theta)}{(7\alpha-\theta)^n}$$
$$+\frac{\sin^m(9\alpha+\theta)}{(9\alpha+\theta)^n}+\frac{\sin^m(9\alpha-\theta)}{(9\alpha-\theta)^n}+\cdots$$
$$=\frac{\sin^m(3\alpha+\theta)}{(3\alpha+\theta)^n}+\frac{\sin^m(3\alpha-\theta)}{(3\alpha-\theta)^n}+\frac{\sin^m(5\alpha+\theta)}{(5\alpha+\theta)^n}+\frac{\sin^m(5\alpha-\theta)}{(5\alpha-\theta)^n}+\cdots \qquad (23)$$

under the same conditions as before.

Similar series can be constructed from (20) and the other formulae analogous to Poisson's, and for all the functions in Tables I and II.

Indeed, equations (19), (21), 22) and (23) can be seen to be special cases of

$$\sum_{n=-\infty}^{\infty} f(nA+\Omega)=\frac{1}{A}\int_{-\infty}^{\infty}f(x)\,dx, \qquad (24)$$

and therefore independent of Ω, when $0<A<2\pi/a$, and $g(v)=0$ when $|v|>a$. By putting $A=8\alpha$, it can be seen that the left sides of (19), (21) and (22) correspond to $\Omega=\alpha$, and the right sides to $\Omega=3\alpha$; the left side of (23)

corresponds to $\Omega=\alpha\pm\theta$ while the right side corresponds to $\Omega=3\alpha\pm\theta$, if we remember that f is an even function, so that $f(-nA+\Omega)=f(nA-\Omega)$.

Equation (24) moreover enables us to evaluate the series in all these equations.

Similarly, (20) corresponds to $A=12\alpha$ and $\Omega=\alpha$ and 5α respectively.

5. Till now, we have confined ourselves to the Fourier cosine or exponential transforms. There are formulae analogous to Poisson's, applicable to Fourier sine transforms, again due to Ramanujan*, of which we shall quote here just one.

If $g_s(v)=\left(\frac{2}{\pi}\right)^{\frac{1}{2}}\int_0^\infty f(x)\sin vx\,dx$, then

$$\alpha\{f(\alpha)-f(3\alpha)+f(5\alpha)-\cdots\}=g_s(\beta)-g_s(3\beta)+g_s(5\beta)-\cdots \qquad (25)$$

where $\alpha\beta=\pi/2$.

If $f(x)$ be such that its Fourier sine transform $g_s(v)$ is zero for $|v|>a$, and if $\beta>a$, i.e. if $0<\alpha<\pi/2a$, all the terms on the right side of (25) vanish, and we obtain

$$\sum_{n=0}^{\infty}f\left[(4n+1)\alpha\right]=\sum_{n=0}^{\infty}f\left[(4n+3)\alpha\right]. \qquad (26)$$

As examples of such functions, we may mention†

$$(1)\begin{cases}f(x)=2^{\nu-\frac{1}{2}}\,\Gamma(\nu-\frac{1}{2})\;x^{1-\nu}\,J_\nu(x)\\ g_s(v)=v(1-v^2)^{\nu-\frac{3}{2}}\text{ if }0<v<1\\ \quad=0\qquad\qquad\text{if }v>1\quad;\end{cases} \qquad (27)$$

$$(2)\begin{cases}f(x)=2^{\nu-\frac{1}{2}}\,\Gamma(\nu+\frac{1}{2})\;x^{-\nu}\,H_\nu(x)\\ g_s(v)=(1-v^2)^{\nu-\frac{1}{2}}\quad\text{if }0<v<1\\ \quad=0\qquad\qquad\text{if }v>1\quad,\end{cases} \qquad (28)$$

where $H_\nu(x)$ is Struve's function of order ν.

* *Collected Papers*, p. 64.

† Titchmarsh: *loc. cit.* pp. 179 and 180.

Anharmonicity of the Lattice Oscillations in the Alkali Halide Crystals

In my note under the above title, published in *Nature* of July 15, there are two errors to which I wish to direct attention.

(1) The oscillation discussed there, namely, of the two interpenetrating lattices of Na^+ and Cl^- ions respectively, relatively to each other, is unique among the normal modes of oscillation of the crystal in that it polarizes the medium[1]. The effect of this is to reduce the coefficient of r^2 in equation (2) from a to $a-\frac{4\pi}{3}-\frac{e^2}{8d^3}$. Equating this coefficient to $\pi^2\mu\nu_0^2$, we get the frequency ν_0, the value of which remains the same as given in the note.

(2) The coefficient f appearing in equations (4) and (5) refers to a *pair* of ions, and will be double that defined by (3). This will make the magnitude of the anharmonicity and the rate of fall of C_v with temperature twice those given in the note.

K. S. Krishnan

National Physical Laboratory of India,
New Delhi.
Aug. 18.

[1] See Kellermann, *Phil. Trans. Roy. Soc.*, A, 238, 513 (1940).

Anharmonicity of the Lattice Oscillations in the Alkali Halide Crystals

The oscillations of the two interpenetrating lattices of the alkali and the halide ions respectively, in alkali halide crystals, with respect to each other, have been studied in detail, particularly in relation to the infra-red and the Raman spectra of the crystals, and the contribution of the electric dipole moments associated with these oscillations to the dielectric constants of the crystals. These oscillations are presumed to be anharmonic—the anharmonicity being attributed sometimes to the size of the amplitude of the oscillations—and the anharmonicity is invoked to explain the occurrence of certain combination frequencies in Raman spectra, and the temperature variation of the specific heat at constant volume at high temperatures. No attempt, however, seems to have been made to estimate the magnitude of the anharmonicity, though it can be done readily on the basis of any simple model of the crystal, as, for example, Born's, which regards the lattices of the positive and the negative ions respectively as held together by electrostatic forces between the ions, and by Van der Waals forces of repulsion between them, which die down much more rapidly with distance than the electrostatic forces. (The inclusion of forces due to the polarizabilities of the ions does not appreciably affect the results.)

Let us consider a halide of the NaCl type. Neglecting Van der Waals repulsions except between nearest neighbours, and taking the repulsion potential between two neighbouring ions to be $A\exp(-R/\rho)$, where R is the distance between them, we obtain, for the potential energy of the crystal per ion,

$$U = \tfrac{1}{2}\{-\alpha e^2/R + 6A\exp(-R/\rho)\}, \qquad (1)$$

in which $\alpha = 1{\cdot}748$ is the Madelung constant. Now using the equilibrium condition $(\partial U/\partial R)_{R=d} = 0$, where d is the distance between the sodium and chloride ions, we may eliminate A in the usual manner, and with the help of the relation $(\partial^2 U/\partial R^2)_{R=d} = 9d/\beta$, where β is the isothermal compressibility, determine ρ. We thus find that, in sodium chloride, d/ρ, which we shall denote by δ, is about 9.

Now taking the cubic axes of the crystal as the xyz axes of a co-ordinate system, and separating the Na^+ and the Cl^- lattices from each other by a small distance r in the direction lmn, we obtain for the potential energy of the deformed crystal per ion the expression

$$U = U_0 + ar^2 + br^4 + cr^4(l^4 + m^4 + n^4), \qquad (2)$$

in which

$$U_0 = -\frac{e^2\alpha}{2d}\left(1-\frac{1}{\delta}\right) = -6{\cdot}4\times10^{-12}$$

$$a = \frac{e^2}{d^3}\alpha\frac{(\delta-2)}{12} = 1{\cdot}05\times10^{4} \qquad (3)$$

$$b = \frac{e^2}{d^5}\left\{\frac{21}{8} - \frac{7}{27\sqrt{3}} - \alpha\frac{(2\delta^2+3\delta+3)}{48}\right\} = -0{\cdot}59\times10^{20}$$

$$c = \frac{e^2}{d^5}\left\{-\frac{35}{8} + \frac{35}{81\sqrt{3}} + \alpha\frac{(\delta^2+6\delta^2+15\delta+15)}{144}\right\} = 1{\cdot}62\times10^{20}.$$

In the expressions for a, b and c, the terms involving α arise from Van der Waals repulsion, and the other terms in them from electrostatic interaction. In the numerical values, which refer to sodium chloride, the energies are expressed in ergs, and r in cm.

It will be seen that the r^2 term, which determines the frequency ν_0 of the oscillations of the two lattices with respect to each other, arises wholly from Van der Waals repulsion, the electrostatic forces contributing nothing to it, and that it is independent of the direction of the oscillations. Equating its coefficient to $2\pi^2\mu\nu_0^2$, where $1/\mu = 1/m_1 + 1/m_2$ and m_1 and m_2 are the masses of sodium and chloride ions respectively, one obtains $\nu_0 = 4{\cdot}8\times10^{12}$, which is of the right magnitude.

The coefficient of r^4, which we shall denote by f, determines the anharmonicity of the oscillation. It will be seen that both the electrostatic and the Van der Waals interactions contribute to f, and further, that f varies with the direction of the oscillation, and is a maximum, equal to $b + c$—positive and large—when the oscillation is along any of the cubic axes, and is a minimum, equal to $b + c/3$—negative and numerically small—when the oscillation is along any of the octahedral directions [111].

The energy of the oscillator is given by[1]

$$W = (n+\tfrac{1}{2})h\nu_0 + \frac{3}{64\pi^4}(2n^2+2n+1)\frac{h^2f}{\mu^2\nu_0^2}. \qquad (4)$$

When the oscillation is along [100], the anharmonicity will correspond to the frequency of the octave being 1·1 per cent greater than twice that of the fundamental.

The anharmonicities of other modes of oscillation of this crystal, and of the oscillations of the other alkali halides, may be calculated in the same manner.

The specific heat of the crystal at constant volume at high temperatures due to any such *linear* oscillation will be given by[2]

$$c_v = k\left(1 - \frac{3fkT}{8\pi^4\mu^2\nu_0^4}\right) \qquad (5)$$

For Na versus Cl oscillation along [100], expression (5) corresponds to a fall in the value of c_v of about 1 per cent per 50° C., and for oscillation along [111] to practically no temperature variation. Some rough estimates of c_v of sodium chloride crystal made by Eucken and Dannohl[3] on the basis of extrapolated values for the compressibility at high temperatures do point to a fall in c_v, and of this order of magnitude, which suggests that any observed fall in c_v at high temperatures may be attributed to the anharmonicity of the thermal oscillations.

K. S. Krishnan
National Physical Laboratory of India,
New Delhi.
April 26.

[1] See, for example, Pauling and Wilson, "Introduction to Quantum Mechanics", 161 (McGraw-Hill, 1935).
[2] See Born and Mayer, "Handbuch der Physik", 24/2, 676 (Julius Springer, 1933).
[3] *Z. Elektrochem.*, 40, 814 (1934).

The frequencies and the anharmonicities of the normal modes of oscillation of alkali halide crystals

I. Lattice oscillations

By Sir K. S. Krishnan, F.R.S. and Sanat Kumar Roy, Ph.D.
National Physical Laboratory of India, New Delhi

(*Received* 12 *January* 1951)

The frequencies and the anharmonicities of the lattice oscillations of alkali halide crystals, i.e. the oscillations of the interpenetrating lattices of the alkali and the halide ions respectively, with respect to each other, are calculated on the basis of the Born model. If r be the small relative displacement of the two lattices, and lmn the direction cosines of r with reference to the cubic axes of the crystal, it is found that the potential energy can be expressed in the form

$$U = U_0 + ar^2 + br^4 + cr^4(l^4 + m^4 + n^4) + \ldots,$$

in which the constants U_0, a, b and c are readily evaluated. The coefficient of r^2 determines the frequency, and of r^4 the anharmonicity, of the lattice oscillation.

This oscillation is characterized by the development of a homogeneous electric polarization in the medium. It is found that the polarization field acting on an ion tending to *displace* the ion has just the Lorentz value, whereas the field tending to *polarize* the ion is almost nothing.

The anharmonicity of the lattice oscillation, unlike its frequency, is found to vary with the direction of the oscillation, from a large positive value along [111]: to a small negative value along [100]. Its effect on the frequency of the octave, and on the specific heat at constant volume, are discussed.

1. Introduction

The frequencies of the various normal modes of oscillation of the sodium chloride crystal have been calculated by Kellermann (1940) on the basis of the Born model, and the frequencies of the other alkali halide crystals, of both the NaCl and the CsCl types, can be calculated in the same manner. The frequencies of some of the simple modes have also been calculated by Raman (1947) and by Ramanathan (1947) in terms of certain force constants that define the restoring forces acting on the ions when they are given certain specific small displacements from their equilibrium positions. These oscillations in general are presumed to be anharmonic, and their anharmonicities have been invoked frequently to explain the occurrence of some of the octaves and combination frequencies in the infra-red and the Raman spectra of these crystals, and also to explain the possibility of a temperature variation of the specific heats of these crystals *at constant volume* at high temperatures (Born & Brody 1921). No attempt, however, seems to have been made to estimate the magnitudes of the anharmonicities of these oscillations, though they can be calculated on the basis of the Born model just as readily as the frequencies (Krishnan 1950).

It is the main purpose of this paper to calculate the anharmonicities of the various normal modes of oscillation of the alkali halide crystals. Part I concerns itself with the oscillations of the two interpenetrating lattices of the alkali and the halide ions respectively with respect to each other. These oscillations, unlike those in other

normal modes, are characterized by the development of a homogeneous electric polarization in the crystals. Hence the calculation of the frequencies of these oscillations on the Born model is also of interest, as it throws light incidentally on the magnitude of the polarization fields in these crystals, and in particular brings out the essential difference in behaviour between the polarization due to the relative displacements of the positive and the negative ions and that due to the dipoles induced in these ions, and the almost complete lack of interaction between the two polarizations. These and other aspects of the polarization fields are also discussed in this part.

2. The Born model

In crystals of the alkali halides, as is well known, the alkali and the halide ions form interpenetrating lattices, both the lattices being face-centred cubic in the NaCl type of crystals, and body-centred cubic in the CsCl type. The ions in the crystal may be regarded, according to Born†, as held in their respective positions by the electrostatic forces between the charges carried by them, and by short-range forces of repulsion between them. Indeed, the fall of the repulsive forces with increase of distance is so rapid that all repulsion interactions except between the nearest neighbours may be neglected. Other types of interaction, as, for example, the interaction between the dipoles that may be induced in the ions, will be much smaller, and may be neglected to a first approximation. Further, in view of the spherical symmetry of the ions, we may regard both the electrostatic and the repulsion interactions to be central. These assumptions, which are good approximations, render the model simple.

Taking the energy of repulsion interaction between any two neighbouring ions separated by a distance R to be given by $\phi(R)$, the potential energy U of the crystal per pair of ions will be given by

$$U = -\alpha e^2/R + n_0\phi(R), \tag{1}$$

in which n_0 is the number of nearest neighbours, equal to 6 in the NaCl type and 8 in the CsCl type, and α is the Madelung constant, equal to 1·748 in the NaCl type and to 1·763 in the CsCl type (Sherman 1932).

The condition for equilibrium of the crystal, namely,

$$(\partial U/\partial R)_{R=d} = 0, \tag{2}$$

where d is the value of R when the crystal is in equilibrium, gives

$$\phi'(d) = -\alpha e^2/(n_0 d^2). \tag{3}$$

Using the further relation $$(\partial^2 U/\partial R^2)_{R=d} = 9/(N\beta d^2), \tag{4}$$

where β is the isothermal compressibility of the crystal, and N is the number of ion pairs per unit volume, we obtain

$$\phi''(d) = 2\alpha e^2/(n_0 d^3) + 9/(n_0 N\beta d^2), \tag{5}$$

where N is equal to $1/(2d^3)$ in the NaCl type and to $3\sqrt{(3)}/(8d^3)$ in the CsCl type.

† For a good account see Born & Göppert-Mayer (1933) or Sherman (1932, p. 116).

Both d and β appearing in these expressions refer to the absolute zero of temperature. Though d may be obtained by extrapolation accurately enough, a reliable estimate of β at absolute zero (and at zero pressure) is difficult to make.

The higher derivatives of ϕ, namely, $\phi'''(d)$, $\phi^{IV}(d)$, etc., may similarly be obtained from the known variation of the compressibility of the crystal with pressure at different pressures. Since the experimental data on pressure variation of compressibility are not sufficiently precise for this purpose, we may obtain the values of the higher derivatives of $\phi(R)$ more satisfactorily by assuming for it, as usual, a suitable simple form like

$$\phi(R) = A\,e^{-R/\rho}, \tag{6}$$

in which the two constants A and ρ can be evaluated with the help of relations (2) and (4). For such functions, involving only two constants, not only $\phi'(d)$ and $\phi''(d)$, but all the higher derivatives also become known from (2) and (4).

The exponential law of variation of repulsion interaction with distance postulated in (6), besides being convenient, is justifiable, as is well known, on other considerations. Adopting (6), and denoting d/ρ by δ, we obtain from (3) and (5),

$$\delta - 2 = 9d/(N\alpha e^2\beta). \tag{7}$$

Other simple functions, like $\phi(R) = BR^{-m}$, have also been proposed for the repulsion interaction between neighbours, in which the constant B can be eliminated as before with the help of (3), and the number m evaluated with the help of (5). It will be readily seen that

$$m - 1 = 9d/(N\alpha e^2\beta), \tag{8}$$

and hence m is equal to $\delta - 1$.

3. Potential energy corresponding to small relative displacement of the two interpenetrating lattices

We shall now consider the oscillation of the interpenetrating lattices formed by the alkali and the halide ions respectively, with respect to each other. Starting with the crystal in equilibrium, and taking the co-ordinate axes along the cubic axes of the crystal, and the origin at the lattice point occupied by an alkali ion, let the lattice formed by the alkali ions be displaced with reference to the lattice of the halide ions by a small distance r ($r \ll d$) in the direction lmn. The alkali ion which was originally at the origin will now be at xyz, where $x = rl$, $y = rm$, $z = rn$. Let us now calculate the potential energy of the pair of ions formed by the alkali ion at xyz and each of the surrounding ions taken in succession. The sum of these potential energies will obviously be the potential energy of the deformed crystal per pair of ions. Denoting it by U, one may express it as a power series in r, in which, owing to the centre of symmetry of the lattice points in these crystals, terms involving odd powers of r will obviously be absent. U may therefore be expressed in the form

$$U = U_0 + ar^2 + fr^4 + \ldots. \tag{9}$$

The term U_0, which is independent of r, will evidently be the same as for the undeformed crystal, and will be given by

$$U_0 = -\alpha e^2/d + n_0\phi(d). \tag{10}$$

The coefficient of r^2 will determine the frequency of the oscillation that we are considering, i.e. the reststrahlen frequency of the crystal, and the coefficient of r^4 the anharmonicity of this oscillation.

We now proceed to calculate these coefficients. Since the positions of the other *alkali* ions relative to the one at xyz remain the same as before, the potential due to them will obviously be independent of xyz. Hence, in calculating the r^2 and r^4 terms in the expression for the potential energy of the alkali ion at xyz due to the surrounding ions, it is sufficient to consider the effect of the halide ions alone.

4. Expression for potential energy

Let us confine attention to one of these halide ions located at say $\xi\eta\zeta$, and the alkali ion at xyz, and denote the interaction energy between them by $\psi(R)$, where

$$\psi(R) = -e^2/R + \phi(R), \tag{11}$$

R is their distance of separation, given by

$$R^2 = (\xi - x)^2 + (\eta - y)^2 + (\zeta - z)^2 \tag{12}$$

$$= R_0^2 + r^2 - 2QR_0r, \tag{13}$$

R_0 is the distance of the halide ion from the origin, and

$$Q = (l\xi + m\eta + n\zeta)/R_0 \tag{14}$$

denotes the cosine of the angle θ between the radius vectors r and R (see figure 1).

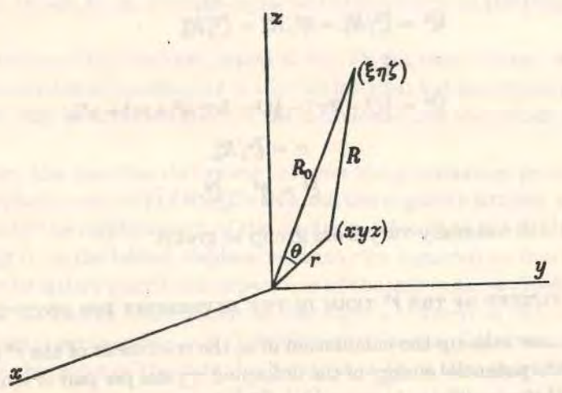

Figure 1

Keeping lmn constant, and varying the magnitude of r, we may express $\psi(R)$ in the form

$$\psi(R) = \psi(R_0) + r(\partial\psi/\partial r)_{r=0} + (r^2/2!)\,(\partial^2\psi/\partial r^2)_{r=0} + \ldots, \tag{15}$$

in which $R \to R_0$ as $r \to 0$.

With the help of (13) we may replace the differential coefficients in (15) with respect to r, at $r = 0$, by the corresponding coefficients with respect to R, at $R = R_0$. The r^3 and r^4 terms in (15) will then reduce to

$$Ar^3 = (r^3/2!)\,[(1-Q^2)\,\psi'/R_0 + Q^2\psi''] \tag{16}$$

and

$$Fr^4 = (r^4/4!)\,[3(1-Q^2)\,(5Q^2-1)\,(\psi'/R_0^3 - \psi''/R_0^2) + 6Q^2(1-Q^2)\,\psi'''/R_0 + Q^4\psi^{iv}], \tag{17}$$

respectively. The differential coefficients of ψ appearing in (16) and (17), and in the equations to follow, are with respect to R, at $R = R_0$.

Owing to the symmetry of the crystal, corresponding to every lattice point $(\xi\eta\zeta)$ occupied by a halide ion, there are others at points obtained by the various combinations of $(\pm\xi, \pm\eta, \pm\zeta)$, in which the co-ordinates are interchangeable. Their number n, i.e. the number of negative ions at a distance $R_0 = (\xi^2+\eta^2+\zeta^2)^{\frac{1}{2}}$ from the origin will be 48 when ξ, η, ζ are all different and different from zero, but will ordinarily be less. Knowing the values of n and of R_0 for these groups of halide ions, the coefficients a and f of the r^2 and r^4 terms respectively, appearing in (9), can be calculated, since

$$a = \Sigma(n\bar{A}), \tag{18}$$

$$f = \Sigma(n\bar{F}), \tag{19}$$

where the bar indicates the average value taken over the n ions forming one such group, and the summation extends over all such groups.

In calculating $\bar{A}$ and $\bar{F}$, we need to know the corresponding mean values of Q^2 and Q^4 appearing in equations (16) and (17). Obviously

$$\bar{Q}^2 = \bar{\xi}^2/R_0^2 = \bar{\eta}^2/R_0^2 = \bar{\zeta}^2/R_0^2 \tag{20}$$

$$= \tfrac{1}{3}; \tag{21}$$

$$\bar{Q}^4 = \tfrac{1}{2}(1-3\sigma) - \tfrac{1}{2}(1-5\sigma)\,(l^4+m^4+n^4), \tag{22}$$

in which

$$\sigma = \bar{\xi}^4/R_0^4, \tag{23}$$

and

$$\bar{\xi}^4 = \bar{\eta}^4 = \bar{\zeta}^4. \tag{24}$$

n, R_0 and σ will naturally vary from group to group.

5. Coefficient of the r^2 term in the expression for potential energy

We shall now take up the calculation of a, the coefficient of the r^2 term in expression (9) for the potential energy of the deformed crystal per pair of ions. Substituting for Q^2 in (16) its average value, namely, $\bar{Q}^2 = \frac{1}{3}$ (see (21)), we obtain

$$a = \Sigma\{n(2\psi'/R_0 + \psi'')/6\}, \tag{25}$$

in which R_0 and n vary, as we have seen, from group to group, and the summation extends over all the groups of negative ions surrounding the positive ion at xyz.

Considering first the electrostatic interaction, i.e. putting $\psi(R) = -e^2/R$ in (25), one can readily see that (25) reduces to zero. In other words, the electrostatic

interactions between the various ions contribute nothing to the r^2 term in expression (9) for the potential energy of the crystal.†

Considering next the repulsion interactions, i.e. putting $\psi(R) = \phi(R)$, and confining ourselves to the interactions between the nearest neighbours, one can readily see from (25), in view of relations (3) and (5), that their contribution to the coefficient a in expression (9) is given by

$$a_1 = 3/(2N\beta d^2). \tag{26}$$

Taking the law of repulsion interaction to be exponential, a_1 can also be expressed, in view of (7), in the form

$$a_1 = \alpha e^2(\delta-2)/(6d^3). \tag{27}$$

The magnitude of a_1, as calculated here, will obviously be independent of the explicit formulation of $\phi(R)$ as a function of R.

6. The effect of the polarization of the medium

Among the various normal modes of vibration of the crystal, the particular one that we are considering, namely, the oscillation of the lattice of alkali ions with respect to that of the halide ions, is unique in that it corresponds to the development of a homogeneous electric polarization in the crystal. As a result of this polarization, which will be proportional to the displacement r, and, as mentioned just now, will be the same throughout the crystal, the force acting on any given ion in the crystal, tending to restore it to its equilibrium position, instead of being $2a_1 r$, where a_1 has the value (26), will be less by an amount equal to the force due to the polarization field.‡

Now the polarization of the medium, equal to say Pr per unit volume, will arise primarily from the relative *displacement* r of the two lattices; but accompanying this displacement there *may* be a polarization of the individual ions also, since the ions are polarizable.

There is, however, this essential difference between the polarization produced by a small relative displacement $r \ll d$ of the positive and the negative lattices, and that induced in the ions by the displacement of the electrons relative to the nucleus. The polarization arising from the lattice displacement may be regarded as due to small dipoles, located at the lattice points, the separation of charges in these dipoles being much smaller than d. On the other hand, in the dipoles induced in the ions, the separation of charges is comparable to d. This difference in size of the two types of dipoles renders the character of the field due to them in their *close* neighbourhood quite different (Heckmann 1925; see also Mott & Gurney 1940). We shall denote by $P_1 r$ and $P_2 r$ ($P_1 + P_2 = P$) the contributions to the polarization of the crystal per unit volume, from the lattice displacement and from the dipoles induced in the ions respectively, and consider the polarization fields, due to P_1 and P_2 acting on an ion,

† There is, however, an indirect contribution to the r^2 term arising from the electric polarization developed in the crystal as a result of the relative displacement of the positive and the negative ions; this will be considered in the next section.

‡ The direction of the latter force is such as to *increase* the separation r of the two lattices.

that are effective (i) in displacing the ion, and (ii) in polarizing the ion. Let us designate the polarization fields effective in (i) by

$$p_1 P_1 er \quad \text{and} \quad p_2 P_2 er, \quad \text{respectively,} \tag{28}$$

and those effective in (ii) by

$$p_3 P_1 er \quad \text{and} \quad p_4 P_2 er, \quad \text{respectively.} \tag{29}$$

The elementary dipoles arising from the displacements of the ions being practically point dipoles, we should expect p_1 to be equal to $\frac{4}{3}\pi$, i.e. the polarization field concerned to have the proper Lorentz value. The other p's, however, will be much smaller than $\frac{4}{3}\pi (p_4 < p_3 \simeq p_2 \ll \frac{4}{3}\pi)$ their actual magnitudes depending on the degree of overlap of the electric charges of neighbouring ions. Anticipating the results to be obtained in the next section, we may mention here that the experimental data point to p_1 being $\frac{4}{3}\pi$, and all the other p's being practically zero. In other words, the experimental data show that P_2 is practically zero, and the only polarization in the medium is that due to the displacement of the ions alone. The polarization per unit volume is then given by $Pr = P_1 r = Ner$, and the force acting on an ion tending to increase the displacement has the full Lorentz value $(\frac{4}{3}\pi) Ne^2 r$.

Remembering that the displacement r of the positive ions is relative to the negative ions which may be regarded as kept fixed, the corresponding potential energy of the crystal *per pair of ions* will be given by

$$a_2 r^2 = -2\pi N e^2 r^2/3, \tag{30}$$

which will be the contribution to the coefficient a in (9) from the polarization of the crystal.

Adding this to (27), we obtain for the coefficient of r^2 in expression (9),

$$a = a_1 + a_2 = \alpha e^2 (\delta - 2)/(6d^3) - 2\pi N e^2/3. \tag{31}$$

Knowing a, the reststrahlen frequency ν of the alkali halide crystal is readily calculated from the relation† $$2\pi^2 \mu \nu^2 = a, \tag{32}$$

where $$1/\mu = 1/m_1 + 1/m_2, \tag{33}$$

and m_1 and m_2 are the masses of the two ions. Equations (32) and (31) determining the frequency ν of the lattice oscillation are the same as those obtained by Kellermann.

† [*Note added in proof* 3 *May* 1951.] A relative displacement r of the positive and the negative lattices may also be regarded as produced by a field E *in the medium*, where

$$Ee = 2ar = 4\pi^2 \mu \nu^2 r.$$

The internal field E_i is given by $E_i = E + 4\pi Ner/3$,

and the corresponding force acting on an ion of charge e will be given by

$$E_i e = 2a_1 r.$$

The polarization of the crystal per unit volume, per unit field in the medium, will be given by the usual expression

$$\chi = (K - n_\infty^2)/(4\pi) = Ne^2/(4\pi^2 \mu \nu^2),$$

where K is the dielectric constant of the crystal for a steady field, and $K - n_\infty^2$ is the contribution to K from the relative displacements of the positive and the negative ions. The same expression may also be obtained by equating the energy per unit volume of the crystal, namely $Na r^2$, to $(K - n_\infty^2) E^2/(8\pi)$.

7. The reststrahlen frequencies of the alkali halides

The constants needed in the calculation of the frequencies are obviously d, δ and μ. For all the alkali halides, both of the NaCl and CsCl types, the values of m, equal to $\delta - 1$ (see (8)), have already been calculated from the compressibility data extrapolated to the absolute zero of temperature, by Slater (1924), and from certain independent general considerations by Pauling (1928). We have adopted Pauling's values of m to give us δ. The values of a_1 calculated therefrom, and of a_2, are given in columns 5 and 6 table 1.

Table 1

crystal	d (Å)	$\delta = m+1$ (Pauling)	$1/\mu \times 10^{-23}$	$a_1 \times 10^{-4}$	$a_2 \times 10^{-4}$	$\nu \times 10^{-12}$ calculated	$\nu \times 10^{-12}$ observed (Barnes 1932)
			NaCl type				
LiF	2·01	7·0	1·186	4·13	−2·97	8·4	9·1
NaF	2·31	8·0	0·579	3·27	−1·96	6·2	7·4
KF	2·67	9·0	0·472	2·47	−1·27	5·4	—
RbF	2·82	9·5	0·389	2·25	−1·08	4·8	—
CsF	3·00	10·5	0·363	2·11	−0·89	4·7	—
LiCl	2·57	8·0	1·039	2·37	−1·42	7·1	—
NaCl	2·81	9·0	0·432	2·11	−1·09	4·7	4·9
KCl	3·14	10·0	0·324	1·74	−0·78	4·0	4·2
RbCl	3·27	10·5	0·241	1·63	−0·69	3·4	3·5
LiBr	2·75	8·5	0·944	2·10	−1·16	6·7	—
NaBr	2·98	9·5	0·338	1·90	−0·91	4·1	4·2
KBr	3·29	10·5	0·230	1·60	−0·68	3·3	3·4
RbBr	3·43	11·0	0·146	1·50	−0·60	2·6	2·6
LiI	3·00	9·5	0·916	1·86	−0·89	6·7	—
NaI	3·23	10·5	0·310	1·69	−0·72	3·9	3·5
KI	3·53	11·5	0·202	1·45	−0·55	3·0	2·9
RbI	3·66	12·0	0·118	1·37	−0·49	2·3	2·3
			CsCl type				
CsCl	3·56	11·5	0·215	1·43	−0·69	2·8	2·9
CsBr	3·71	12·0	0·121	1·33	−0·61	2·1	2·2
CsI	3·95	13·0	0·093	1·21	−0·51	1·8	—

It will be seen from the table that except in some of the fluorides the calculated values of ν agree well with the observed values.

It will also be seen that $|a_2|$ is a large fraction of a_1. If in (28) and (29) the factors p_3 and p_4 determining the magnitude of the polarization fields that are effective in inducing dipole moments in the ions, and the factor p_2 determining the polarization field due to these induced dipoles, tending to displace the ions, had all of them the Lorentz value of $\frac{4}{3}\pi$, like p_1, the contribution to a from the polarization of the medium, instead of being equal to $-2\pi Ne^2/3$, would be given by

$$a_2 = -(2\pi N e^2/3)(n_\infty^2 + 2)/3, \tag{34}$$

where n_∞ is the refractive index of the crystal extrapolated for long wave-lengths. In NaCl, for example, $\frac{1}{3}(n_\infty^2 + 2) = 1{\cdot}4$, and in some of the other crystals much higher,

and if introduced in the expression for a_2 would considerably *decrease* the calculated value of ν. Even if p_2 and p_3, which should be of comparable magnitudes, were equal to $\frac{4}{3}\pi$, and p_4, which might be much smaller, were equal to zero, the effect would be considerable. Hence the observed agreement between the experimental values of ν and those calculated from (32) and (31), may be regarded as demonstrating empirically

(1) that the polarization of the medium is due *wholly* to the displacements of the ions, and that these displacements do not induce any polarization in the ions;

(2) that the effective polarization field acting on an ion and tending to displace it has just the Lorentz value, namely $\frac{4}{3}\pi$ times the polarization per unit volume of the crystal.

Similar conclusions have been drawn by Mott & Littleton (1938) for the NaCl type of crystals from the observed difference between the dielectric constant for static fields and the square of the refractive index extrapolated for long wave-lengths. This difference obviously represents the contribution from the relative displacement of the positive and the negative ion lattices.

8. The Lorentz polarization field

These results are indeed gratifying. The experimental finding that the observed variation of the refractivity of these crystals with density does not conform to the Lorentz formula has sometimes been regarded as throwing doubt on the validity of the Lorentz derivation of the polarization factor $\frac{4}{3}\pi$ even in cubic crystals. The fundamental assumption implicit in this derivation is that the elementary dipoles present in the crystal to which the polarization of the medium is due, are point dipoles, i.e. that the distance of separation of the charges in the dipoles is small in comparison with d. The dipoles induced in the ions in these crystals, as for example in refraction, do not generally satisfy this condition, since the separation of charges in the ions is of the magnitude of the diameter of the ions, and hence in the larger ions comparable with the interionic distance. The polarization factor under these conditions, instead of being equal to $\frac{4}{3}\pi$ as deduced by Lorentz, will be much smaller, and, judging from the experimental data, almost nothing in the alkali halides. In other words, the Lorentz factor $\frac{4}{3}\pi$ fails just in the case to which it was intended to apply, namely, in determining the polarization field in refracting media.

This should not, however, be interpreted as casting doubt on the validity of the Lorentz derivation of the factor $\frac{4}{3}\pi$. Where the polarization of the crystal arises from a small relative displacement of the positive and the negative ion lattices, it may be regarded, as we have seen, as due to *point* dipoles located at the lattice points. In this case, the experimental data for the reststrahlen frequency do point to the factor p_1 determining the polarization field, having just the Lorentz value $\frac{4}{3}\pi$.

Before concluding this section we wish to make two observations. We have here regarded the effect of the overlap of the electric charge on an ion with the charges on its immediate neighbours as affecting the magnitude of the polarization field due to the latter acting on the former. *Alternatively*, we may also regard the effect of the overlap as equivalent to a reduction of the effective charge on the ions from e to $e^* < e$ (Fröhlich 1949).

The second observation concerns the method referred to in the Introduction, for calculating the frequencies of some of the simple modes of oscillation of these crystals on the basis of certain specified force-constants between the atoms. Since these constants are not known functions of the distance of separation between the interacting atoms, the method is not capable of giving information regarding the anharmonicity of the oscillations, in which we are specially interested in this paper. Even in the calculation of the frequencies by this method, since no attempt is made to distinguish between the contributions to the force constants from electrostatic interaction and from other types of interaction, and the electric charges on the ions are not therefore invoked explicitly in calculating the forces between them, any co-operative effect of the electric charges, like the polarization of the medium that may accompany the oscillation, is completely overlooked in this method. When such a polarization occurs, as in the lattice oscillation of the alkali halides considered in this paper, the effect of the polarization field on the restoring forces acting on the ions, and thence on the frequency of the oscillation, as we have seen, can be quite large.

We shall have more to say on the force constants between the atoms in alkali halide crystals when we calculate the frequencies of some of the other modes of oscillation of these crystals in part II.

9. The r^4 term in expression (9) for potential energy

The contribution to the potential energy from the polarization of the medium is confined, as we have seen, to the r^2 term. But both the repulsion and the Coulomb interactions will contribute to the r^4 term. It will be seen from (17), (21) and (22) that this term is of the form

$$fr^4 = br^4 + cr^4(l^4 + m^4 + n^4), \tag{35}$$

and is thus a function of the direction of the relative displacement r of the two lattices.

As in the calculation of the r^2 term, in the present case also, it will be convenient to consider separately the contributions from the repulsion and the electrostatic interactions, and denote them by the subscripts 1 and 2 respectively, so that

$$b = b_1 + b_2 \tag{36}$$

and

$$c = c_1 + c_2. \tag{37}$$

Considering the repulsion interactions first, and adopting for them the exponential law (6), and ignoring interactions except between nearest neighbours, we obtain from (17)

$$b_1 = \frac{\alpha e^2}{d^5}\left(\frac{\delta^3 + 2\delta^2 + 9\delta + 9}{48} - \frac{\delta^3 + 6\delta^2 + 15\delta + 15}{16}\sigma\right), \tag{38}$$

$$c_1 = -\frac{\alpha e^2}{d^5}\frac{\delta^3 + 6\delta^2 + 15\delta + 15}{48}(1 - 5\sigma), \tag{39}$$

respectively.

In the NaCl type, in which the immediate neighbours are six, at $(\pm d, 0, 0)$, etc.,

$$\sigma = \tfrac{1}{3}, \tag{40}$$

whence (38) and (39) reduce to

$$b_1 = -\frac{\alpha e^2}{d^5}\frac{2\delta^2+3\delta+3}{24}, \tag{41}$$

$$c_1 = \frac{\alpha e^2}{d^5}\frac{\delta^3+6\delta^2+15\delta+15}{72}, \tag{42}$$

respectively.

Similarly in the CsCl type, in which the nearest neighbours are eight, at $(\pm d/\sqrt{3}, \pm d/\sqrt{3}, \pm d/\sqrt{3})$,

$$\sigma = \tfrac{1}{9}, \tag{43}$$

and the values of b_1 and c_1 are given by

$$b_1 = \frac{\alpha e^2}{d^5}\frac{\delta^3+6\delta+6}{72}, \tag{44}$$

$$c_1 = -\frac{\alpha e^2}{d^5}\frac{\delta^3+6\delta^2+15\delta+15}{108}. \tag{45}$$

In calculating the corresponding contributions b_2 and c_2 from the Coulomb interactions, which are long-range ones, we have naturally to include many more of the negative ions surrounding the positive ion at xyz. Substituting $-e^2/R$ for $\psi(R)$ in (17), and putting

$$R_0/d = \Delta, \tag{46}$$

we obtain

$$b_2 = -\frac{21}{16}\frac{e^2}{d^5}\Sigma\left(n\frac{1-5\sigma}{\Delta^5}\right), \tag{47}$$

$$c_2 = \frac{35}{16}\frac{e^2}{d^5}\Sigma\left(n\frac{1-5\sigma}{\Delta^5}\right). \tag{48}$$

The values of n, Δ and σ will naturally vary from one group to another, and their values for the different groups of negative ions surrounding any given positive ion in the crystal are given in table 2.

TABLE 2

n	Δ^2	typical co-ordinates	σ	$n(1-5\sigma)/\Delta^5$
		NaCl type		
6	1	$d, 0, 0$	$\frac{1}{9}$	−4·000
8	3	d, d, d	$\frac{1}{9}$	0·228
24	5	$2d, d, 0$	$\frac{17}{75}$	−0·057
24	9	$2d, 2d, d$	$\frac{11}{81}$	0·032
6	9	$3d, 0, 0$	$\frac{1}{9}$	−0·016
24	11	$3d, d, d$	$\frac{83}{363}$	−0·009
24	13	$3d, 2d, 0$	$\frac{97}{507}$	0·002
			total	−3·82
		CsCl type		
		$D = d/\sqrt{3}$		
8	1	D, D, D	$\frac{1}{9}$	3·556
24	$\frac{11}{3}$	$3D, D, D$	$\frac{83}{363}$	−0·133
24	$\frac{19}{3}$	$3D, 3D, D$	$\frac{163}{1085}$	0·059
8	$\frac{27}{3}$	$3D, 3D, 3D$	$\frac{1}{9}$	0·015
24	$\frac{37}{3}$	$5D, D, D$	$\frac{209}{729}$	−0·043
48	$\frac{51}{3}$	$5D, 3D, D$	$\frac{101}{525}$	0·004
			total	3·46

It will be seen from the last column of table 2 that $n(1-5\sigma)/\Delta^5$ decreases rapidly with increase of Δ, and the value of $\Sigma(n(1-5\sigma)/\Delta^5)$, appearing in (47) and (48), in which the summation extends over all the surrounding groups, is therefore calculated easily. Its value is −3·82 for crystals of the NaCl type, and 3·46 for those of the CsCl type. Using these values, those of b and c can be calculated with the help of (47) and (48) respectively. The values of $b = b_1+b_2$ and of $c = c_1+c_2$ thus calculated are entered in columns (2) and (3) of table 3.

TABLE 3

crystals	$b\times10^{-20}$	$c\times10^{-20}$	$f_{100}\theta\times100$	$f_{111}\theta\times100$	$\bar{f}\theta\times100$	$\Theta/100$
			NaCl type			
LiF	−2·72	7·03	6·5	−0·6	2·3	44
NaF	−2·20	5·84	3·3	−0·2	1·2	64
KF	−1·52	4·21	2·4	−0·1	0·9	72
RbF	−1·35	3·80	2·1	−0·1	0·8	70
CsF	−1·28	3·79	2·0	0	0·8	70
LiCl	−1·29	3·43	4·1	−0·3	1·5	58
NaCl	−1·18	3·26	2·4	−0·1	0·9	64
KCl	−0·90	2·60	1·8	0	0·7	70
RbCl	−0·84	2·47	1·5	0	0·6	68
LiBr	−1·12	3·01	3·7	−0·2	1·4	62
NaBr	−1·02	2·89	2·0	−0·1	0·7	66
KBr	−0·81	2·39	1·5	0	0·6	68
RbBr	−0·74	2·23	0·2	0	0·5	68
LiI	−0·98	2·78	3·2	−0·1	1·2	60
NaI	−0·89	2·62	1·8	0	0·7	66
KI	−0·71	2·20	1·5	0	0·6	62
RbI	−0·66	2·08	1·0	0	0·6	64
			CsCl type			
CsCl	1·39	−1·34	0·1	1·3	0·4	42
CsBr	1·30	−1·24	0·1	0·9	0·8	44
CsI	1·23	−1·16	0·1	0·8	0·5	44

Now the extreme values of Σl^4 are

$$\Sigma l^4 = 1$$

when the direction of oscillation is along any of the cubic axes, i.e. along (100), etc., and

$$\Sigma l^4 = \tfrac{1}{3}$$

when it is along any of the long diagonals of the cube, i.e. along (111), etc., and its average value, taken over all directions, is given by

$$\overline{\Sigma l^4} = \tfrac{3}{5}.$$

The corresponding extreme values of f (see (35)) are

$$f_{100} = b+c \tag{49}$$

$$f_{111} = b+\tfrac{1}{3}c \tag{50}$$

and its average value is

$$\bar{f} = b+\tfrac{3}{5}c. \tag{51}$$

10. Energy levels of the anharmonic oscillator

The energy levels of an anharmonic oscillator of the above type are given by†

$$W_n = (n+\tfrac{1}{2})h\nu_0 + 3h^2 f(2n^2+2n+1)/(64\pi^4\mu^2\nu_0^2), \tag{52}$$

which may be written in the form

$$W_n = h\nu_0[n+\tfrac{1}{2}+(n^2+n+\tfrac{1}{2})f\theta], \tag{53}$$

where

$$\theta = 3h/(32\pi^4\mu^2\nu_0^3), \tag{54}$$

and $f\theta$ is a measure of the anharmonicity of the oscillator, which varies, as we have seen, with the direction of the oscillation. In these expressions we may use for ν_0 the value of ν given in table 1.

The 'first differences' between the energy levels will be given by

$$W_{n+1} - W_n = h\nu_0 + 2(n+1)f\theta h\nu_0, \tag{55}$$

and the 'second differences' by $2f\theta h\nu_0$, which is a constant. We obtain for example from (53)

$$\nu_2 = (W_2 - W_0)/h = 2\nu_0 + 6\nu_0 f\theta, \tag{56}$$

$$\nu_1 = (W_1 - W_0)/h = \nu_0 + 2\nu_0 f\theta, \tag{57}$$

so that the ratio of the frequency ν_2 of the first overtone (second harmonic) to twice the frequency of the fundamental is given by

$$s = \nu_2/(2\nu_1) = 1 + f\theta. \tag{58}$$

The frequency of the octave will obviously vary with the direction of the oscillation, unlike the frequency of the fundamental.

The two extreme values of the anharmonicity factor $f\theta$ are given in columns (4) and (5) of table 3, which give us a measure of the spread of the spectrum of the octave on either side of twice the frequency of the fundamental.

The anharmonicities of the oscillations of several *diatomic* molecules have been studied in detail both theoretically and experimentally. There are two features that distinguish them from the anharmonicities of the lattice oscillations of the alkali halides. In the first place the main term determining the anharmonicity in diatomic molecules is the r^3 term, whereas in the alkali halides it is the r^4 term, the r^3 term being absent. The sign of the anharmonic factor in diatomic molecules is negative, i.e. the energy levels come closer together as n increases, and the Condon Parabola tends to widen out as one moves to high energy levels. In the lattice oscillations, on the other hand, the anharmonicity factor varies with the direction of oscillation, from large positive to small negative values.

From the values of the anharmonicity factor $f\theta$ entered in table 3 it will be seen that its magnitude decreases as we proceed from the fluorides to the iodides, and again from the lithium salts to the corresponding salts of caesium.

† See for example, Ta-You-Wu (1946) and Pauling & Wilson (1935).

11. Influence of the anharmonicity on the specific heat

For *linear* oscillators having an anharmonicity of the above type, the specific heat at constant volume at sufficiently high temperatures, will be given by (Born & Brody 1921)

$$c_v = k(1 - T/\Theta), \tag{59}$$

where

$$\Theta = 8\pi^4\mu^2\nu_0^4/(3fk). \tag{60}$$

The significance of Θ is that the specific heat at constant volume of an assemblage of such linear anharmonic oscillators will fall from its theoretical value k per oscillator characteristic of harmonic oscillators, by 1 % per $\Theta/100$ degrees rise in temperature. Using for f its average value, namely, $\bar{f} = b + \frac{3}{5}c$, the values of Θ have been calculated and are entered in the last column of table 3.

We naturally need to know similarly the anharmonicities of all the other normal modes of oscillation of these crystals, before we can correlate them with the observed temperature variation of c_v of these crystals. On the observational side also, only rough estimates of c_v are available, and those too for one crystal, namely sodium chloride. Direct measurements naturally give the specific heat at atmospheric pressure, and in order to calculate from these data the specific heat at constant volume, one needs to know the compressibilities of the crystal at these very high temperatures, whereas the available compressibility measurements are at ordinary temperatures only, and only very rough estimates can be made by extrapolation. Using such extrapolated values for the compressibility of sodium chloride, Eucken & Dannöhl (1934) find that c_v attains nearly the theoretical value characteristic of an assemblage of harmonic oscillators at about 300° C, and then *falls* off almost linearly by about one sixth in 500° C. This would correspond roughly to an effective value of 3000° C for Θ, which is of the same sign, and of the same *order of magnitude*, as that calculated for the lattice oscillations.

We shall resume this discussion after the anharmonicities of all the other modes of oscillation have also been calculated.

We wish to thank Mr K. S. Sarma and Mr K. D. Baveja for helpful discussions.

References

Barnes, R. B. 1932 *Z. Phys.* **75**, 723.

Born, M. & Brody, E. 1921 *Z. Phys.* **6**, 132.

Born, M. & Göppert-Mayer, M. 1933 *Handbuch der Physik*, **24/2**, p. 676. Berlin: Springer.

Eucken, A. & Dannöhl, W. 1934 *Z. Elektrochem.* **39**, 792.

Fröhlich, A. 1949 *Theory of dielectrics*, p. 158. Oxford.

Heckmann, G. 1925 *Z. Phys.* **33**, 646.

Krishnan, K. S. 1950 *Nature*, **166**, 114, 571.

Kellermann, E. W. 1940 *Phil. Trans*, A, **238**, 513.

Mott, N. F. & Gurney, W. 1940 *Electronic processes in ionic crystals*. Oxford.

Mott, N. F. & Littleton, M. J. 1938 *Trans. Faraday Soc.* **34**, 485.

Pauling, L. 1928 *Z. Krystallogr.* **67**, 377.

Pauling, L. & Wilson, E. B. 1935 *Introduction to quantum mechanics*, p. 161. New York: McGraw-Hill.

Raman, C. V. 1947 *Proc. Indian Acad. Sci.* A, **26**, 370.

Ramanathan, K. G. 1947 *Proc. Indian Acad. Sci.* A, **26**, 493.

Sherman, J. 1932 *Chem. Rev.* **11**, 116, 107.

Slater, J. C. 1924 *Phys. Rev.* **23**, 488.

Ta-You-Wu 1946 *Vibrational spectra and structure of polyatomic molecules*, p. 48. J. W. Edwards.

Elastic Constants of Alkali Halide Crystals

ADOPTING the simple Born model for an alkali halide crystal, in which the ions are regarded as held in their respective positions by the electrostatic and the repulsion interactions between the ions, one may readily calculate the velocities of propagation v of long acoustic waves of wave-length λ along the principal directions [100], [110] and [111], and hence along any direction, in the crystal:

$$v^2 = \sum_n (A_{1n}\Delta^2_{1n})/(m_1 + m_2), \qquad (1)$$

where m_1 and m_2 are the masses of the two ions, $2\pi\Delta_{1n}/\lambda$ denotes the difference in phase of the acoustic wave at any two ions 1 and n, and $\sum_n$ denotes summation over all the ions, except 1, in the crystal. (If D is the distance up to which the electrostatic interactions remain significant, λ is regarded as sufficiently large in comparison with D that $\cos(2\pi D/\lambda)$ can be put equal to $1 - \frac{1}{2}(2\pi D/\lambda)^2$.)

$$A_{1n} = (\psi'/R_{1n}^0)(1 - Q^2) + \psi'' Q^2, \qquad (2)$$

where $\psi(R_{1n})$ is the interaction energy between the two ions 1 and n, separated by a distance R_{1n}, and ψ' and ψ'' are its differential coefficients with respect to R_{1n} at its equilibrium value R_{1n}^0. Q is the cosine of the angle between R_{1n}^0 and the direction of displacement of the ions under the acoustic wave. Since the values of v^2 for different directions of propagation and corresponding directions of displacement are also known in terms of the elastic constants c_{11}, c_{12} and c_{44}, we obtain, by comparing them with the values obtained from (1), expressions for the elastic constants in terms of the interactions between the ions. We shall denote by ε_{11}, ε_{12}, ε_{44} the contributions to c_{11}, c_{12}, c_{44} respectively from the electrostatic interactions, which are of long range, and by ρ_{11}, ρ_{12}, ρ_{44} the contributions from repulsion interactions, which are assumed to fall exponentially with the increase in the distance of separation of the interacting ions. In view of the short range of these repulsion interactions, we regard them as confined to the immediate neighbours only.

Let us first consider a crystal of the sodium chloride type, and take the co-ordinate axes along the cubic axes of the crystal, and the origin at the equilibrium position of ion 1. It is found that the ε's and the ρ's can be expressed in terms of the following two series, in which ξ, η, ζ are integers, which, multiplied by d, the sodium–chlorine distance, define the co-ordinates of all the lattice points:

$$\Sigma(-1)^{\xi_n+\eta_n+\zeta_n}/(\xi_n^2 + \eta_n^2 + \zeta_n^2)^{1/2} = -\alpha, \text{ say}, \qquad (3)$$

which can be recognized as the Madelung series, and

$$\Sigma(-1)^{\xi_n+\eta_n+\zeta_n}(\xi_n^4 + \eta_n^4 + \zeta_n^4)/(\xi_n^2 + \eta_n^2 + \zeta_n^2)^{5/2} = -\chi, \text{ say}, \qquad (4)$$

which also is a known series[1]. It is further known that $\alpha = 1{\cdot}748$ and $\chi = 3{\cdot}139$. The values of the elastic constants thus calculated, which refer to very low temperatures, are given in the following table in terms of $e^2/(12d^4)$, in which e is the electronic charge. δ in the table is a number such that d/δ gives the distance over which the repulsion interaction drops to 1/e of its value ($\delta = 9$ in the case of sodium chloride).

	11	12	44
ε	$2\alpha - 6\chi$	$-5\alpha + 3\chi$	$-\alpha + 3\chi$
ρ	$2\alpha\delta$	2α	-2α
c	$2\alpha(\delta + 1) - 6\chi$	$-3\alpha + 3\chi$	$-3\alpha + 3\chi$

Since the interaction forces have been assumed to be central, c_{12} naturally comes out equal to c_{44}, though ε_{12} and ρ_{12} are not separately equal to ε_{44} and ρ_{44} respectively. The final values for the c's are the same as those obtained by Kellermann[2] and also agree with the experimental values. Our values of ε_{12}, ε_{44} and of ρ_{12}, ρ_{44}, however, differ from his.

Similar expressions are obtained from the cæsium chloride type of crystals, in terms of two series α' and χ' that are similar to (3) and (4).

It is remarkable that for the sodium chloride type, c_{12} and c_{44}, as also the corresponding ε's and ρ's, depend on the lattice constant alone. This result, however, does not hold for the cæsium chloride type.

K. S. KRISHNAN
S. K. ROY

National Physical Laboratory of India,
New Delhi. May 26.

[1] Löwdin, Per-Olov, "A Theoretical Investigation into some Properties of Ionic Crystals", 47 (Dissertation, Uppsala, 1948).
[2] Kellermann, E. W., *Phil. Trans. Roy. Soc.*, A, 238, 513 (1940).

The frequencies and the anharmonicities of the normal modes of oscillation of alkali halide crystals
II. Low-frequency acoustic modes

BY SIR K. S. KRISHNAN, F.R.S., AND SANAT KUMAR ROY, PH.D.
National Physical Laboratory of India, New Delhi

(*Received* 17 *September* 1951)

In the present part are deduced, on the basis of Born's model, expressions for the frequency and the ratio of the amplitudes of the alkali and the halide ions in an alkali halide crystal, for any general normal mode of oscillation of the crystal. The results are applied in detail to the special case of low-frequency acoustic modes. Since the amplitudes of the two ions are not in general the same, there is a resultant electric polarization of the medium accompanying the oscillations, and consequently a polarization field. The force acting on an ion due to this field is found to be comparable with the force of interaction with the other ions, not only in the optical branch, in which the displacements of adjacent positive and negative ions are in opposite directions and in which, therefore, the polarization is large, but also in general in the acoustic branch, in which their displacements are in the same direction. A detailed calculation, however, shows that for low frequency acoustic modes, though the ratio of the amplitudes of the two ions is affected by the polarization field, *the frequency remains completely unaffected by it.*

The expressions deduced for the frequencies of the acoustic modes give us also the velocities of propagation of the corresponding acoustic waves, and since the latter are already known in terms of the elastic constants of the crystal, we obtain, incidentally, simple expressions for these constants. The elastic constants so calculated are found to agree with observation.

Unlike the principal oscillation of the crystal dealt with in part I, these low-frequency acoustic modes have negligible anharmonicity.

1. INTRODUCTION

In part I of this paper (Krishnan & Roy 1951*a*; see also Krishnan 1950) the oscillation of the lattice of positive ions in alkali halide crystals with respect to the lattice of negative ions was discussed in detail, on the basis of the simple Born model. Among

other results it was found that the electric polarization of the crystal that accompanies the oscillation plays an important part in determining its frequency. The force acting on any given ion, due to this polarization field, is comparable in magnitude with the force due to its interactions with the other ions. For example, in sodium chloride crystal the force due to the polarization is nearly half that due to the interactions with the other ions, and, being in opposite direction to the latter, is almost of the same magnitude as the resultant force.

The model enables us also to calculate the anharmonicity of this oscillation, since the expression for the potential energy of the crystal contains, in addition to the prominent term proportional to the square of the relative displacement of the two lattices, which term determines the frequency, also a term proportional to its fourth power. The latter term, unlike the square term, varies with the direction of the displacement, and hence the anharmonicity, unlike the frequency, varies with the direction of the oscillation.

In the present part are deduced, on the basis of the same model, general expressions for the frequency and the ratio of the amplitudes of the positive and the negative ions for any general normal mode of oscillation of the alkali halide crystal. The results are applied in detail to the special case of low-frequency acoustic modes.

These and other modes of oscillation of the alkali halide crystal have been discussed previously by several authors, and particularly by Kellermann (1940). But the present treatment is in some ways much simpler, and yields some new results of interest.

2. The potential energy of an ion displaced by an elastic wave in the crystal

Consider an alkali halide crystal of the NaCl type, and propagation in it of a plane elastic wave of wave-length λ, and consider one of the three principal directions of displacement of the ions in the crystal associated with this wave, the displacements being small in comparison with the distance d between neighbouring ions. Choosing as the co-ordinate axes the cubic axes of the crystal, and as the origin the equilibrium position of an alkali ion, we denote by lmn the direction-cosines of the wave-normal, and by LMN the direction-cosines of the displacements, and by r_m the displacement at any given instant t of an ion m whose equilibrium position corresponds to the co-ordinates $(\xi_m, \eta_m, \zeta_m)\,d$, where $\xi_m \eta_m \zeta_m$ are integers. Let $\psi(R)$ be the energy of interaction between any two ions separated by a distance R. For simplicity $\psi(R)$ may be assumed, as in part I, to be of the form

$$\psi(R) = \pm e^2/R + A\,e^{-R/\rho}, \tag{1}$$

where the second term on the right-hand side represents the repulsion interaction between the ions, and the first term the electrostatic interaction between them, the + or the − sign being chosen according as the second ion, say n, is of the same type as the first, or is different. It will be the former when

$$(\xi_n + \eta_n + \zeta_n) - (\xi_m + \eta_m + \zeta_m)$$

is even, and the latter when it is odd. e in the first term denotes the electronic charge.

The repulsion interactions, which are of short range, are regarded in this paper as confined to the nearest neighbours only, and hence we use in (1) *single* constants A and ρ which refer to the interactions between near ions of the opposite types only. Other interactions, like those of the van der Waals type between the dipoles induced in the ions, are neglected.

Considering now the interactions between the various ions in the crystal, all of which have been displaced appropriately to correspond to the same instant t, we obtain for the potential energy of the crystal

$$U = \tfrac{1}{2} \sum_{m} \sum_{m+n} \psi_{mn}, \tag{2}$$

where ψ_{mn} is used for brevity in place of $\psi(R_{mn})$.

Let us denote by U_m the potential energy involved in displacing *one* of the ions, say ion m, from its equilibrium position to the position appropriate to time t, the other ions being displaced ***synchronously*** from their respective equilibrium positions to the positions corresponding to t. U_m can be readily obtained, except for a constant term independent of the displacements, in which we are not at present interested, by putting

$$U_m = \int_0^{r_m} (\partial U/\partial r_m)\, dr_m, \tag{3}$$

in which while differentiating U with respect to r_m all the other displacements are kept constant, whereas in the integration all the displacements are increased from 0 to their final value characteristic of time t, synchronously with r_m, i.e. before integrating, all the other displacements r_n occurring in the expression for $\partial U/\partial r_m$ are to be expressed in terms of r_m and the appropriate differences in phase between them, so that for the purpose of this integration $\partial U/\partial r_m$ may be regarded as a function of r_m only.

In obtaining the differential coefficient $\partial U/\partial r_m$ occurring in (3) we may, therefore, omit straightway all those terms in expression (2) for U that obviously do not involve r_m, and rewrite (3) in the simpler form

$$U_m = \int_0^{r_m} \frac{\partial}{\partial r_m} \Big[\sum_{n+m} \psi_{mn} \Big]\, dr_m. \tag{4}$$

3. Expansion as a power series

Now the interaction energy ψ between the alkali ion near the origin and any other ion at a distance R from it may be expressed in the form of a Taylor expansion

$$\psi(R) = \psi(R_0) + r(\partial\psi/\partial r)_{r=0} + (r^2/2!)\,(\partial^2\psi/\partial r^2)_{r=0} + \ldots, \tag{5}$$

where r is the displacement of the former ion with respect to the latter. In view of the relation

$$R^2 = R_0^2 + r^2 - 2QR_0 r, \tag{6}$$

in which Q is the cosine of the angle between the directions of r and R_0, and in which therefore $R \to R_0$ as $r \to 0$, we may express the differential coefficients of ψ with

respect to r at $r = 0$ in terms of the differential coefficients of ψ with respect to R, at $R = R_0$. We shall, for simplicity, designate the latter coefficients by $\psi', \psi'', \psi''', \ldots$. Obviously

$$\left.\begin{aligned}
(\partial\psi/\partial r)_{r=0} &= -Q\psi', \\
(\partial^2\psi/\partial r^2)_{r=0} &= (1-Q^2)\,\psi'/R_0 + Q^2\psi'' \\
&= F, \text{ say}, \\
(\partial^3\psi/\partial r^3)_{r=0} &= 3Q(1-Q^2)\,(\psi'/R_0^2 - \psi''/R_0) - Q^3\psi''' \\
&= G, \text{ say}, \\
(\partial^4\psi/\partial r^4)_{r=0} &= 3(1-Q^2)\,(5Q^2-1)\,(\psi'/R_0^3 - \psi''/R_0^2) \\
&\quad + 6Q^2(1-Q^2)\,\psi'''/R_0 + Q^4\psi'''' \\
&= H, \text{ say},
\end{aligned}\right\} \tag{7}$$

where

$$Q = (L\xi + M\eta + N\zeta)/(\xi^2+\eta^2+\zeta^2)^{\frac{1}{2}}. \tag{8}$$

Since ψ_{mn} can thus be expressed as a power series in r_m, U_m also, as we shall show presently, can be expressed as a power series in r_m, and in particular U_0, the potential energy of the alkali ion near the origin as a power series in r_0.

4. Interaction of an ion with a pair centro-symmetric to it

As a first step towards expressing U_0 as a power series in r_0, we shall confine attention to the interaction between the alkali ion near the origin and the pair of ions at $\pm(\xi_n, \eta_n, \zeta_n)\,d$ respectively, and designated n and n' respectively, n' being the inverse of n with respect to the origin. Now choosing the positive direction of the displacement to be the same for all the ions, and the positive direction of R_{0n} to be from the origin to the lattice point n under consideration, one can readily see that Q_{0n} and $Q_{0n'}$ are of the same magnitude, but have opposite signs. Hence putting $Q_{0n} = -Q_{0n'} = Q$, and denoting by ψ_0 the value of ψ_{0n} when both the ions 0 and n are in their equilibrium positions, we obtain

$$\begin{aligned}
\psi_{0n} + \psi_{0n'} = 2\psi_0 &- Q\psi'[(r_0 - r_n) - (r_0 - r_{n'})] \\
&+ (F/2!)\,[(r_0 - r_n)^2 + (r_0 - r_{n'})^2] \\
&+ (G/3!)\,[(r_0 - r_n)^3 - (r_0 - r_{n'})^3] \\
&+ (H/4!)\,[(r_0 - r_n)^4 + (r_0 - r_{n'})^4] + \ldots.
\end{aligned} \tag{9}$$

Now the amplitudes of the alkali and the halide ions will in general be different. Denoting by q the ratio of the latter amplitude to the former, and by ϕ_{0n} the difference in phase of the elastic wave at the ions 0 and n, we obtain

$$\left.\begin{aligned}
r_n/r_0 &= q\,e^{-i\phi_{0n}} \\
r_{n'}/r_0 &= q\,e^{i\phi_{0n}}
\end{aligned}\right\}, \tag{10}$$

in which q will be unity if n and n' are alkali ions, but otherwise will, in general, be different from unity, and will be positive in the acoustic branch in which the displacements of *adjacent* positive and negative ions are in the same direction, and will be negative in the optical branch in which the displacements of the two ions are

in opposite directions. ϕ_{0n} will evidently be equal to $2\pi k\Delta_{0n}$, where $k = 1/\lambda$, and Δ_{0n} is the *path* difference between 0 and n, and is given by

$$\Delta_{0n} = (l\xi_n + m\eta_n + n\zeta_n)\,d. \tag{11}$$

In other words, Δ_{0n} is the projection of R_0 on the wave-normal.

Now equation (4) for U_0 may be written in the form

$$U_0 = \Sigma \int_0^{r_n} \frac{\partial}{\partial r_0}(\psi_{0n} + \psi_{0n'})\,dr_0, \tag{12}$$

in which the summation extends over all pairs nn'. The differential coefficient appearing in it may be obtained by differentiating (9) with respect to r_0, remembering that in this operation r_n and $r_{n'}$ are to be treated as constants independent of r_0 (see remarks at the end of § 2). The coefficient thus obtained will naturally involve r_n and $r_{n'}$ in addition to r_0. Now by substituting for r_n and $r_{n'}$ from (10), we can express the integrand as a function of r_0 alone, and thus obtain U_0 as a function of r_0, or, to be more precise, as a power series in r_0.

5. The r_0^2 term in the expression for U_0 and the effect of the polarization field

In expression (12) for U_0 we shall consider separately the terms that involve the different powers of r_0, and take first the r_0^2 term, which is the first non-vanishing term. Now

$$\begin{aligned}
\frac{\partial}{\partial r_0}(\psi_{0n} + \psi_{0n'}) &= F[2r_0 - (r_n + r_{n'})] \\
&= 2Fr_0[1 - q\cos\phi_{0n}],
\end{aligned} \tag{13}$$

and hence

$$\int_0^{r_n} \frac{\partial}{\partial r_0}(\psi_{0n} + \psi_{0n'})\,dr_0 = Fr_0^2(1 - q\cos\phi_{0n}). \tag{14}$$

In equations (13) and (14), as in (10), q is to be put equal to unity whenever nn' are alkali ions, i.e. are of the same type as the ion at the origin. Hence the r_0^2 term in expression (12) for U_0 will be given by

$$a_1 r_0^2 = \tfrac{1}{2}r_0^2[\Sigma_1 F(1 - q\cos\phi_{0n}) + \Sigma_2 F(1 - \cos\phi_{0n})], \tag{15}*$$

in which Σ_1 denotes summation over all the ions for which $s = \xi + \eta + \zeta$ is odd, and similarly Σ_2 denotes summation over all the ions for which s is even.

If m_1 be the mass of the alkali ion, $-2a_1/m_1$ will obviously be the acceleration of the ion per unit displacement under the interaction forces under consideration. If these were *all* the forces acting on the ion, $2a_1/m_1$ should be equal to the square of the frequency of oscillation of the ion, and therefore of the elastic waves.

* Equation (14) refers to the interaction between the alkali ion near the origin and the pair of ions n and n'. Hence in obtaining the potential energy U_0 of the ion 0, due to interactions with all the other ions, we have to sum up the effects of all such *pairs* nn'. In (15), however, for convenience in doing the summations, we have regarded the ion n and its inverse n' *separately*, and to rectify the double counting thus introduced, we have inserted the multiplying factor $\frac{1}{2}$ on the right-hand side of (15).

In part I we showed that the interactions ψ between the ions, on the basis of which we have calculated a_1, do not include the effects of any *co-operative* phenomenon like the electric polarization of the crystal that may accompany the oscillations. Such a polarization obviously accompanies what are usually described as polar oscillations of the crystal, in which the displacements of adjacent positive and negative ions are in opposite directions. The oscillation of the lattice of positive ions with respect to the lattice of negative ions is a special case of such polar oscillations, and is characterized by $k = 0$, and hence by a *homogeneous* polarization, i.e. polarization that is the same throughout the medium. In part I, in which this case was discussed in detail, it was found that the force acting on any ion due to the polarization field is comparable in magnitude with the force due to interaction with the surrounding ions. In NaCl for example, it is roughly half of the latter, and being opposed to it, is of nearly the same magnitude as the resultant restoring force. It was also found that any polarization *induced* in the ions by the displacement of the electrons with reference to the corresponding nuclei does not contribute to the force acting on an ion and tending to *displace* the ion as a whole.

The polarization field plays an important part in many of the other modes of oscillation too of the alkali halide crystal, and will be discussed in detail elsewhere. We shall merely note here the following results which are relevant to our present purpose.

(1) Even when the polarization of the medium is not quite homogeneous, the polarization field acting on an ion may be nearly as large as when it is homogeneous, but will now depend markedly on whether the displacements of the ions that produce the polarization are longitudinal or transverse to the direction of the gradient of the polarization, i.e. to the wave-normal.

(2) Considering elastic waves having their wave-normals along [111] such a polarization occurs not only for the *optical* branch, in which the displacements of adjacent positive and negative ions are in opposite directions, but also for the *acoustic* branch in which the displacements are in the same direction, because the magnitudes of the displacements of the two ions are different as a result of the difference in their masses. For a given amplitude of one of the ions, the polarization thus produced will of course be much smaller than in the corresponding optical branch, but the frequencies involved now are also correspondingly smaller, and hence the polarization fields acting on the ions will still remain comparable with the forces of interaction between the ions displaced from their respective equilibrium positions by the acoustic wave.

When k is small in comparison with $1/d$, and the polarization is nearly homogeneous over regions covering a large number of ions, the polarization per unit volume in the neighbourhood of the origin will be given by $Ne(1-q)r_0$, where N is the number of ion pairs per unit volume; the direction of the polarization will naturally be that of the direction of displacement of the ions under the elastic wave. (Consistently with the finding in part I, we neglect here the polarization due to the electronic displacements, as distinguished from the polarization due to the relative displacements of the positive and the negative ions, since the former polarization does not affect the displacements of the ions, in which alone we are interested

here.) Hence the extra force due to the polarization field acting on the alkali ion near the origin, and tending to increase its displacement will be equal to $pNe^2(1-q)r_0$, and the corresponding contribution to the potential energy U_0 of this ion will be given by $-\frac{1}{2}pNe^2(1-q)r_0^2$, in which p is the polarization factor, which will depend on whether the direction of the polarization is along or transverse to the direction of the gradient of the polarization, i.e. whether the displacements under the elastic wave, that cause the polarization, are longitudinal or transverse. In the latter case p will evidently have the Lorentz value $4\pi/3$, for the same reason for which the usual Lorentz treatment of dielectric polarization is applicable not only for an incident static electric field, but also for the field of an electromagnetic wave whose wave-length is much longer than the interatomic distance, as is the case with the elastic waves that we are considering now.

Even when k is not small, the extra potential energy of the ion near the origin due to the polarization produced in the medium by the elastic wave may still be put equal to $-\frac{1}{2}pNe^2(1-q)r_0^2$, in which p will not now be merely the polarization factor; its value will depend not only on whether the displacements are longitudinal or transverse, but also on the magnitude of k in relation to $1/d$, but it can be calculated.

Adding this to the right-hand side of (15) we obtain for the r_0^2 term in the expression for U_0, which determines the frequency of the mode, the value

$$\tfrac{1}{2}r_0^2[\Sigma F - \Sigma_2(F\cos\phi_{0n}) - pNe^2(1-q) - q\Sigma_1(F\cos\phi_{0n})]. \tag{16}$$

Equating this to $\frac{1}{2}m_1\omega^2 r_0^2$, and putting

$$\Sigma_1(F\cos\phi_{0n}) = c_1 \tag{17}$$

and

$$\Sigma F - \Sigma_2(F\cos\phi_{0n}) - pNe^2 = g, \tag{18}$$

we obtain

$$q = \frac{g - m_1\omega^2}{c_1 - pNe^2}. \tag{19}$$

By shifting the origin of the co-ordinate system from the equilibrium position of an alkali ion, where we have located it at present, to that of a halide ion, we obtain similarly

$$\frac{1}{q} = \frac{g - m_2\omega^2}{c_1 - pNe^2}, \tag{20}$$

in which m_2 is the mass of the halide ion, and Σ_1 and Σ_2 occurring in the expressions for c_1 and g denote as before summations over all odd and even values respectively of s.

6. Expressions for the frequency and the ratio of the amplitudes of the two ions

For any given value of k, which determines the phase differences ϕ of the elastic wave between the ions, one may eliminate either q or ω^2 from (19) and (20), and obtain

$$m_1m_2\omega^4 - (m_1+m_2)g\omega^2 + g^2 - (c_1 - pNe^2)^2 = 0, \tag{21}$$

whence

$$\omega^2 = \frac{(m_1+m_2)g \mp \sqrt{\{(m_1-m_2)^2g^2 + 4m_1m_2(c_1-pNe^2)^2\}}}{2m_1m_2}, \tag{22}$$

and similarly $$m_2(c_1-pNe^2)q^2+(m_1-m_2)gq-m_1(c_1-pNe^2)=0, \tag{23}$$

whence $$q=-\frac{(m_1-m_2)g\mp\sqrt{\{(m_1-m_2)^2g^2+4m_1m_2(c_1-pNe^2)^2\}}}{2m_2(c_1-pNe^2)}. \tag{24}$$

In both (22) and (24) the upper sign corresponds to the acoustic branch of the elastic modes, and the lower sign to the optical branch.

7. Particular case when k is small

Let u be the distance up to which the electrostatic interactions between ions, which are of long range, remain significant, and let k be sufficiently small that $\cos\phi = 2\pi k\Delta$ can be put equal to $1-\phi^2/2$ even when Δ is as large as u. Expression (24) for q then reduces to

$$q=1-\frac{1}{2}\frac{m_1-m_2}{m_1+m_2}\frac{\Sigma(F\phi_{0n}^2)}{\Sigma_1F-pNe^2} \tag{25}$$

in the acoustic branch, and to

$$q=-\frac{m_1}{m_2}\left(1+\frac{1}{2}\frac{m_1-m_2}{m_1+m_2}\frac{\Sigma(F\phi_{0n}^2)}{\Sigma_1F-pNe^2}\right) \tag{26}$$

in the optical branch. Similarly, expression (22) for ω^2 reduces to

$$\omega^2=\frac{\Sigma(F\phi_{0n}^2)}{m_1+m_2} \tag{27}$$

in the acoustic branch and to

$$\omega^2=\frac{\Sigma_1F-pNe^2}{\mu}+\frac{\Sigma_2(F\phi_{0n}^2)}{2\mu}-\frac{\Sigma(F\phi_{0n}^2)}{m_1+m_2} \tag{28}$$

in the optical branch, where $$\frac{1}{\mu}=\frac{1}{m_1}+\frac{1}{m_2}. \tag{29}$$

In the special case when $k\to 0$,

$$q\to 1 \quad \text{or} \quad -\frac{m_1}{m_2}. \tag{30}$$

The first value corresponds obviously to an acoustic wave of infinite wave-length, for which the amplitudes of the two ions will naturally be the same, and the second value to the oscillations of the lattice of the alkali ions with respect to the lattice of the halide ions, in which their displacements will be in opposite directions, and the amplitudes inversely proportional to their respective masses. Similarly, when $k\to 0$,

$$\omega^2\to 0 \quad \text{or} \quad (\Sigma_1F-pNe^2)/\mu, \tag{31}$$

the first value in (31) referring to the acoustic, and the second to the optical branch. In the latter case, in which the polarization is homogeneous, $p=4\pi/3$, and is independent of the direction of the displacement of the lattice of positive ions with respect to the lattice of the negative ions. This expression for the optical frequency is identical with that obtained in part I, where too it was found to be independent of the direction of displacement.

8. Long acoustic waves: velocities and amplitudes

From now on we shall confine our attention to low-frequency acoustic modes, and postpone to later parts of this paper the consideration of the other modes.

It will be readily seen from the expressions derived in the previous section that the ratio of the amplitudes is considerably influenced by the polarization field, in both the acoustic and the optical branches, and the frequency too in the optical branch. *But the frequency of long acoustic waves, as is evident from* (27), *remains completely unaffected by the polarization field.* This result is significant, since otherwise the validity of the well-known Christoffel relations between the elastic constants and the velocities of propagation of long acoustic waves for different directions of the wave-normal, and the corresponding displacements, which we need to use in the next section, will be disturbed. One can understand in a general way how in the case of long acoustic waves this happens, in spite of the restoring force acting on an ion due to the polarization field, being still quite large and comparable with the force due to the interactions. The frequencies of the oscillations of adjacent positive and negative ions, which are determined jointly by the interactions with all the surrounding ions and the polarization field, have naturally to be identical, and this is secured by a suitable automatic adjustment in the crystal of the relative amplitudes of the two ions. The relative amplitudes and, in general, the frequencies also will, therefore, depend very much on whether the polarization field is present or not. In the case of low-frequency acoustic modes, however, it happens that the condition that the frequencies of the neighbouring ions remain equal in spite of the extra polarization forces, incidentally ensures that these frequencies remain quite unaffected by these extra forces, the whole effect of these extra forces being now confined to changing the relative amplitudes of the two ions.

Now expression (27) for ω^2 for low-frequency acoustic modes of vibration of the crystal leads to the following expression for the velocities of propagation v of the corresponding long acoustic waves in the crystal, namely,

$$Dv^2=N\Sigma(F\Delta_{0n}^2), \tag{32}$$

in which D is density of the crystal, and is given by

$$D=N(m_1+m_2). \tag{33}$$

The calculation of the velocities of long acoustic waves thus reduces, on Born's model, to evaluating $\Sigma(F\Delta_{0n}^2)$. It becomes particularly simple when, as in the case of propagation along [100], [110] and [111], the acoustic waves can be regarded as longitudinal and transverse respectively. The restriction of the calculation to these special cases does not involve any loss of generality, since for any given general direction of the wave-normal the directions of the displacements and the corresponding velocities of propagation can be obtained from the data for these particular directions.

Since p is known, the ratio of the amplitudes of the two ions can also be calculated for the above directions of the wave-normal.

9. Evaluation of $\Sigma(F\Delta^2)$

We now proceed to calculate $\Sigma(F\Delta^2)$ for these special directions. (For convenience we are dropping the subscripts from Δ.) The summation can be done conveniently in two stages, as similar summations were done in part I. In a cubic crystal of the alkali halide type, corresponding to every lattice point (ξ, η, ζ) there are others whose co-ordinates are obtained by the various permutations of $\pm\xi$, $\pm\eta$, $\pm\zeta$. Their number τ when all the three co-ordinates are different and different from zero will be 48, and otherwise will be smaller. For any such group of ions round the origin, $|R_0|$ will remain the same, and hence the average value of $F\Delta^2$ taken over all the ions in the group, which we shall denote by $\overline{F\Delta^2}$, can be calculated easily, and hence also the contribution of $\Sigma(F\Delta^2)$ from all the ions in this group, namely, $\tau\overline{(F\Delta^2)}$. The summation can then be extended over all such groups.

Moreover, in expression (7) for F we may separate the contributions from the electrostatic and the repulsion interactions by substituting for ψ given by (1) either the first or the second term only, and thus get *separately* the contributions to $\Sigma(F\Delta^2)$ from the electrostatic and the repulsion interactions. The repulsion interactions being of short range may be restricted to the six immediate neighbours only, whereas in the electrostatic case we have to include interactions over a much wider range.

In order to calculate the average value of $F\Delta^2$ taken over all the ions in any particular group, i.e. over the ions whose co-ordinates may be obtained by the permutations of $(\pm\xi, \pm\eta, \pm\zeta)d$, we merely require the average values of the following functions of these co-ordinates, all of which are readily obtained. Putting

$$\xi^2+\eta^2+\zeta^2 = S, \tag{34}$$

we obtain

$$\left.\begin{aligned} &\overline{\xi^2} = S/3; \quad \overline{\xi\eta} = 0; \quad \overline{(\xi+\eta+\zeta)^2} = 3\overline{\xi^2} = S; \\ &\overline{(\xi+\eta)^2} = \overline{(\xi-\eta)^2} = 2S/3; \quad \overline{\xi^2\eta^2} = S^2/6 - \overline{\xi^4}/2; \\ &\overline{(\xi^2-\eta^2)^2} = -S^2/3 + 3\overline{\xi^4}; \quad \overline{(\xi+\eta)^4} = S^2 - \overline{\xi^4}; \\ &\overline{(\xi+\eta+\zeta)^4} = 3S^2 - 6\overline{\xi^4}. \end{aligned}\right\} \tag{35}$$

The results of the calculation are entered in table 1. The first column in the table gives the direction of the wave-normal, and the second the direction of the displacement. The third column gives the contribution to $\Sigma(F\Delta^2)$ from repulsion interaction, which, being restricted to the six immediate neighbours, is readily calculated, and needs no comment. Following the notation used in part I the repulsion interaction is expressed in terms of $\delta = d/\rho$.

The calculation of the electrostatic contribution, however, presents certain features of interest. Considering the interaction between the alkali ion at 0 with any particular ion n whose co-ordinates are $(\xi, \eta, \zeta)d$, we find that the value of $F\Delta^2$ can be expressed in the form

$$(F\Delta^2)_{\text{elec.}} = (-1)^s (AS^{-\frac{1}{2}} + BS^{-\frac{1}{2}})(e^2/d), \tag{36}$$

where A and B are functions of the co-ordinates, and also vary with the direction of the wave-normal and of the displacement. The values of A and B for different

directions are entered in columns 4 and 5 of table 1. Now it is found that the average value of $(F\Delta^2)_{\text{elec.}}$ taken over the group of ions whose co-ordinates are obtained by the permutations of $(\pm\xi, \pm\eta, \pm\zeta)d$ can be expressed in the form

$$\overline{(F\Delta^2)}_{\text{elec.}} = -(-1)^s [aS^{-\frac{1}{2}} + b(\xi^4+\eta^4+\zeta^4)S^{-\frac{1}{2}}](e^2/d), \tag{37}$$

where a and b are found to be *independent of the co-ordinates* and therefore have the same value for all the groups. (They, however, depend on the direction of the wave-normal and of the displacement.) We are thus led to the important result *that the*

Table 1. NaCl type

direction of wave-normal	direction of displacement	repulsion interaction $\Sigma(F\Delta^2)/(e^2/d)$	electrostatic interaction $F\Delta^2=(-1)^s(e^2/d)\ (AS^{-\frac{1}{2}}+BS^{-\frac{1}{2}})$ $\Sigma(F\Delta^2)=(-1)^s\ (e^2/d)(a\alpha+b\chi)$ A	B	a	b	$Dv^2=N\Sigma(F\Delta^2)$ in terms of the elastic constants
[100]	[100]	$\alpha\delta/3$	$-\xi^2$	$3\xi^4$	$\frac{1}{3}$	-1	c_{11}
	[010], [001]	$-\alpha/3$		$3\xi^2\eta^2$, $3\xi^2\zeta^2$	$-\frac{1}{6}$	$\frac{1}{2}$	c_{44}
[110]	[110]	$\alpha(\delta-1)/6$	$-(\xi+\eta)^2/2$	$3(\xi+\eta)^4/4$	$-\frac{5}{12}$	$\frac{1}{4}$	$(c_{11}+c_{12}+2c_{44})/2$
	[1$\bar{1}$0]			$3(\xi^2-\eta^2)^2/4$	$\frac{7}{12}$	$-\frac{3}{4}$	$(c_{11}-c_{12})/2$
	[001]	$-\alpha/3$		$3(\xi^2+\eta^2)\,\zeta^2/2$	$-\frac{1}{6}$	$\frac{1}{2}$	c_{44}
[111]	[111] $\perp$ to [111]	$\alpha(\delta-2)/9$	$-(\xi+\eta+\zeta)^2/3$	$(\xi+\eta+\zeta)^4/3$	$-\frac{2}{9}$	$\frac{2}{3}$	$(c_{11}+2c_{12}+4c_{44})/3$
				$(\xi+\eta+\zeta)^2Q^2$	$\frac{1}{3}$	$-\frac{1}{3}$	$(c_{11}-c_{12}+c_{44})/3$

net electrostatic contribution from all the ions to $\Sigma(F\Delta^2)$ is as though each ion contributed just two terms, both unique, one to the series $(e^2/d)\,a\alpha$ and the other to the series $(e^2/d)\,b\chi$, where

$$\alpha = -\Sigma(-1)^s(\xi^2+\eta^2+\zeta^2)^{-\frac{1}{2}}, \tag{38}$$

$$\chi = -\Sigma(-1)^s(\xi^4+\eta^4+\zeta^4)(\xi^2+\eta^2+\zeta^2)^{-\frac{1}{2}}, \tag{39}$$

in which $\xi\eta\zeta$ take all integral values except $\xi = \eta = \zeta = 0$. In other words, the electrostatic part of $\Sigma(F\Delta^2)$ can be expressed in the form

$$\Sigma(F\Delta^2)_{\text{elec.}} = (a\alpha + b\chi)\,e^2/d, \tag{40}$$

in which a and b are known functions of the direction of propagation and of displacement. The values of a and b for the principal directions are entered in columns 6 and 7 of table 1.

α can be readily identified as the well-known Madelung series, and χ also is a known series (see, for example, Löwdin 1947, 1948). Their values are $\alpha = 1{\cdot}75$ and $\chi = 3{\cdot}14$.*

10. Expressions for the elastic constants

As is well known, for any given direction of the wave-normal of an acoustic wave in a cubic crystal, the three directions of displacement, and the corresponding velocities, can be readily calculated in terms of the known elastic constants c_{11}, c_{12}, c_{44} with the help of Christoffel relations. (See, for example, Love 1927.) The values of

* Both α and χ have been computed numerically to seven places of decimals; $\alpha = 1{\cdot}7475578$; $\chi = 3{\cdot}1385558$ (Löwdin 1947).

Dv^2 thus obtained in terms of the elastic constants are entered in the last column of table 1. At the same time, we have in equation (32), namely,

$$Dv^2 = N\Sigma(F\Delta^2) = \Sigma(F\Delta^2)/(2d^3),$$

an expression for Dv^2 for crystals of the NaCl type, in terms of α, χ and δ, all of which are known. From a comparison of these two values of Dv^2 we obtain expressions for the elastic constants of the crystal in terms of α, χ, δ, and also the contributions to these constants from the electrostatic and the repulsion interactions separately.

The data entered in table 1 offer nine relations between the elastic constants, and α, χ and δ. Three of these relations are repetitions, and any three of the remaining six will enable us to calculate the three elastic constants, or rather to calculate c_{11} and c_{12} and to verify the Cauchy relation, namely, $c_{12} = c_{44}$, which we should expect the crystal to satisfy on the basis of the model adopted by us, in which both the repulsion and the Coulomb forces are 'central'. The three extra relations offer an effective check on our calculation.

We shall denote the contributions to c_{11} from the repulsion and the electrostatic interactions by ρ_{11} and ϵ_{11} respectively, and similarly the contributions to c_{12} by ρ_{12} and ϵ_{12}, and to c_{44} by ρ_{44} and ϵ_{44} respectively. Their values are entered in table 2, and are expressed in terms of $e^2/(12d^4)$.

TABLE 2. NaCl TYPE

	11	12	44
ϵ	$2\alpha - 6\chi$	$-5\alpha + 3\chi$	$-\alpha + 3\chi$
ρ	$2\alpha\delta$	2α	-2α
$c = \epsilon + \rho$	$2\alpha(\delta+1) - 6\chi$	$-3\alpha + 3\chi$	$-3\alpha + 3\chi$

It will be seen immediately (1) that the Cauchy relation is verified, c_{12} being equal to c_{44}, *though the components* ϵ_{12} *and* ρ_{12} *are not separately equal to* ϵ_{44} *and* ρ_{44} *respectively*; and (2) that the compressibility

$$\beta = 3/(c_{11} + 2c_{12}) = 18d^4/\{e^2\alpha(\delta - 2)\} \qquad (41)$$

is the same as the value $9d/\{Ne^2\alpha(\delta-2)\}$ obtained in part I (equation 7), from direct considerations (in view of the relation $N = 1/(2d^3)$ for the NaCl type of crystals that we are now considering).

The values of the elastic constants obtained here agree with those calculated by Kellermann on the basis of the same model. His expressions, however, involve more complicated series than χ. It should also be mentioned here that the values of ϵ_{12} and ρ_{12}, and of ϵ_{44} and ρ_{44} obtained by Kellermann differ from the corresponding values obtained by us.

The numerical values of the elastic constants calculated from the expressions given above, which obviously refer to very low temperatures, are entered in table 3, along with the observed values wherever available. The values of δ used in the calculation are those given by Pauling (1928) and used by us in part I, and are entered in column 2 of the table. The agreement between the calculated and the observed values of the elastic constants is satisfactory.

Frequencies and anharmonicities of normal modes of oscillation

It will also be seen from table 3 that in the NaCl type of crystal the elastic constant $c_{12} = c_{44}$, as calculated on Born's simple model, depends on the lattice constant d only, and is inversely proportional to its fourth power. This result is verified by observation. This result, however, does not apply to the CsCl type, as we shall see presently.*

TABLE 3.

The elastic constants are expressed in 10^{11} dynes/cm^2.

crystals	d (in Å)	δ (Pauling)	c_{11} calc.	c_{11} obs.	$c_{12} = c_{44}$ calc.	c_{12} obs.	c_{44} obs.
			NaCl type				
LiF	2·01	7·0	10·7	9·8	4·9	5·2	—
NaF	2·31	8·0	8·5	—	2·8	—	—
KF	2·67	9·0	6·1	—	1·6	—	—
RbF	2·82	9·5	5·4	—	1·3	—	—
CsF	3·00	10·5	5·1	—	1·0	—	—
LiCl	2·57	8·0	5·5	—	1·8	—	—
NaCl	2·81	9·0	5·0	4·8	1·3	—	—
KCl	3·14	10·0	3·9	3·9	0·8	0·8	0·7
RbCl	3·27	10·5	3·6	—	0·7	—	—
LiBr	2·75	8·5	4·8	—	1·4	—	—
NaBr	2·98	9·5	4·3	(3·3)	1·0	1·3	—
KBr	3·29	10·5	3·5	3·4	0·7	0·6	0·6
RbBr	3·43	11·0	3·2	—	0·6	—	—
LiI	3·00	9·5	4·2	—	1·0	—	—
NaI	3·23	10·5	3·8	—	0·7	—	—
KI	3·53	11·5	3·1	2·7	0·5	0·4	—
RbI	3·66	12·0	2·8	—	0·4	—	—
			CsCl type				
CsCl	3·56	11·5	4·0	—	0·6	—	—
CsBr	3·71	12·0	3·5	—	0·6	—	—
CsI	3·95	13·0	2·8	—	0·6	—	—

The experimental values of the elastic constants have been taken from Bridgman (1929), Voigt (1928), Huntingdon (1947), Galt (1948) and Ramachandran (1949).

11. THE ELASTIC CONSTANTS FROM STEADY DISPLACEMENTS

Our main interest in the present part is the calculation of the frequencies and the amplitudes of the acoustic modes of oscillation in the crystal and their harmonicities, on the simple Born model, and the expressions obtained for the frequencies are used *incidentally*, by making k small, to give us the elastic constants. If our main purpose had been to calculate the elastic constants of the alkali halides, we could have calculated directly the potential energy associated with certain specific homogeneous strains produced in the crystal, and thence evaluated the elastic constants; for example, $c_{11} - c_{12}$ by increasing slightly the distances between the ions along the x-axis and decreasing simultaneously by the same amount the distances along the y-axis, those along the z-axis remaining unaltered, and c_{44} by a shearing strain in

* A preliminary report of the results on the elastic constants has been communicated to *Nature*.

a plane parallel to two of the cubic axes. In general, for a cubic crystal, adopting the usual Voigt notation (Voigt 1928), and denoting by x_1, x_2, x_3 the three tension components of the strain tensor, and by x_4, x_5, x_6 the shear components, and expressing the energy E per unit volume of the crystal in terms of the strains

$$E = \tfrac{1}{2}\sum_{ij} c_{ij} x_i x_j, \tag{42}$$

we obtain

$$c_{ij} = c_{ji} = \frac{\partial^2 E}{\partial x_i \partial x_j}. \tag{43}$$

The calculation of E involves, as mentioned just now, the same technique as used in the earlier sections of this part, and leads naturally to the same expressions for the elastic constants as obtained here from the velocities of acoustic waves of long wave-lengths.

12. Alkali halides of the CsCl type

Though the discussion till now has been made to refer explicitly to the NaCl type of alkali halides, most of it will apply equally well to the CsCl type also. Choosing again as the origin the equilibrium position of an alkali ion, the co-ordinates of all the other ions will now be given by $(\xi, \eta, \zeta)\, d/\sqrt{3}$, where, as before, d is the distance between neighbouring ions, and $\xi\eta\zeta$ are integers, but are now all of them odd, in which case they refer to a halide ion, or all of them even, in which case they refer to an alkali ion. The number of ion pairs N per unit volume will now be given by $3\sqrt{3}/(8d^3)$, instead of by the value $1/(2d^3)$ characteristic of the NaCl type. The contribution to $\Sigma(F\Delta^2)$ from the repulsion interactions will also be different, since the number of nearest neighbours is now 8 instead of 6, and so will be the contribution from the electrostatic interactions. The latter, however, can still be expressed in the form $(a'\alpha' + b'\chi')\, e^2/d$, where $a' = a\sqrt{3}$ and $b' = b\sqrt{3}$, in which a and b have the same values as for NaCl (see table 1), and

$$\alpha' = -\Sigma(-1)^s (\xi^2+\eta^2+\zeta^2)^{-\frac{1}{2}}, \tag{44}$$

$$\chi' = -\Sigma(-1)^s (\xi^4+\eta^4+\zeta^4)(\xi^2+\eta^2+\zeta^2)^{-\frac{1}{2}}. \tag{45}$$

Though α' and χ' have the same form as α and χ, they are really different from them, since $\xi\eta\zeta$ do not now take all integral values as before, but are restricted to where they are all odd, or are all even. ($\xi = \eta = \zeta = 0$ is excluded in both the cases). α' is obviously the Madelung constant for the CsCl type of crystal, and has been calculated by several investigators (see, in particular, Sherman 1932) and is equal to 1·018.

It should be remembered here that the Madelung constant used in part I for the CsCl type of crystal, namely, $\alpha = 1{\cdot}763$, is defined by

$$-\alpha/d = \Sigma(-1)^s/R,$$

where R is the distance of the ion from the origin and is equal to $S^{\frac{1}{2}} \times d/\sqrt{3}$. Hence our $\alpha' = 1{\cdot}763/\sqrt{3}$.

The series χ', however, does not seem to have been studied, but can be evaluated in the following manner. The CsCl type of crystal is body-centred cubic, with two

ions in the unit cell. If we divide the crystal into such unit cells and calculate in the usual manner the contributions from such cells to χ', the terms are found to converge very slowly, and one needs to take contributions from several thousand cells before even the second decimal place can be decided with certainty. This method of cubic summation, which is usually adopted for the computation of such series, is not, therefore, helpful in the present case. There is, however, an alternative choice of the elementary cells, which we find on trial to give terms that are much more rapidly convergent. Choosing as before the equilibrium position of an alkali ion as the origin, consider the cube of eight halide ions immediately surrounding it. The corners of the cube will correspond in our notation to $\xi\eta\zeta = \pm 1, \pm 1, \pm 1$. Join the origin to any three adjacent corners of this cube, say, 111, 1−11, 11−1. The parallelopiped formed with these three lines as the adjoining edges will form a suitable unit cell with one ion at each of its corners, half of them positive, and the other half negative. By considering these eight ions forming the corners of such a cell as forming a group, and regarding every alternate cell as unoccupied, one can calculate readily the contributions from these cells to χ', and they are found, after the first few terms, to converge fairly rapidly. Detailed calculations have been made by this method by Mr K. D. Baveja and Mr Gyan Mohan in this laboratory, and will be published elsewhere. We shall merely quote here the final result of their computation, namely,

$$\chi' = -1{\cdot}08.$$

Coming back to the calculation of $\Sigma(F\Delta^2)$ and thence of the elastic constants of alkali halides of the CsCl type, on the Born model, the results obtained are given in table 4, and are expressed in terms of $e^2/(16d^4)$.

Table 4. CsCl type

	11	12	44
ϵ	$6\alpha' - 18\chi'$	$-15\alpha' + 9\chi'$	$-3\alpha' + 9\chi'$
ρ	$2\alpha'(\delta-2)$	$2\alpha'(\delta+4)$	$2\alpha'(\delta-2)$
$c = \epsilon + \rho$	$2\alpha'(\delta+1) - 18\chi'$	$\alpha'(2\delta-7) + 9\chi'$	$\alpha'(2\delta-7) + 9\chi'$

Here again though $c_{12} = c_{44}$ as should be expected, the contributions to c_{12} from the repulsion and the electrostatic interactions, namely ρ_{12} and ϵ_{12}, are not separately equal to ρ_{44} and ϵ_{44} respectively.

Further

$$\beta = 3/(c_{11} + 2c_{12}) = 8d^4/\{e^2\alpha'(\delta-2)\}, \tag{46}$$

which is the same as the value obtained in equation (7) of part I from direct considerations.

13. The anharmonicities of the low frequency acoustic modes

Coming back to expression (12) for U_0 (see also (9)) we shall now consider the terms in it that involve higher powers of r_0 than r_0^2. These terms will evidently determine the anharmonicity of the oscillation, in the same manner in which the r_0^2 term determines the frequency. The r_0^4 term, which we shall consider first, will be given by

$$hr_0^4 = \Sigma \int_0^{r_0} \frac{\partial}{\partial r_0}\left[\frac{H}{4!}\{(r_0 - r_n)^4 + (r_0 - r_{n'})^4\}\right] dr_0, \tag{47}$$

where H has the value defined by (8) and where, while differentiating with respect to r_0, r_n and $r_{n'}$ are to be treated as constants, whereas before integrating, both r_n and $r_{n'}$ are to be expressed in terms of r_0. Doing so, we obtain for the coefficient of r_0^4

$$h = \Sigma\left[\frac{H}{4!}(1 - 3q\cos\phi + 3q^2\cos 2\phi - q^3\cos 3\phi)\right], \tag{48}$$

where the summation extends over all the ions.

For the low-frequency modes, for which $\cos\phi$ can be put equal to $1-\phi^2/2$, q is given by (25), which we may rewrite for convenience in the form

$$q = 1 - Wk^2, \tag{49}$$

where the second term is of the same order of magnitude as ϕ^2. After some simple reductions, we find that the terms in (48) that are independent of ϕ cancel each other out, and that the first non-vanishing term corresponds to

$$h = -\Sigma_1\left(\frac{H}{8}Wk^2\phi^2\right), \tag{50}$$

and is of the same order of magnitude as $\Sigma(H\phi^4)$.

There is thus an essential difference between the optical modes and the low-frequency acoustic modes. In the optical branch, the coefficients of the r_0^2 and r_0^4 terms in the expression for potential energy are of the order of ΣF and ΣH respectively, and the ratio of the latter to the former is of the order of $10^{-16}\,\mathrm{cm}^2$. In other words, the r_0^4 term will become comparable with the r_0^2 term only when the amplitude becomes as large as an ångström, which may be taken as a rough measure of the anharmonicity.

On the other hand, for the low-frequency acoustic modes that we are now considering, the r_0^2 and the r_0^4 terms are of the order of $\Sigma(F\phi^2)$ and $\Sigma(H\phi^4)$ respectively. The ratio of the latter to the former will now be of a lower order of magnitude than for the optical modes, lower by a factor ϕ^2.

The calculation of the r_0^3 term is slightly more complicated, but here again, the coefficient is of the order of ϕ^3.

Hence for the low-frequency acoustic modes, the anharmonicities are of a lower order of magnitude than for the optical branch, and will be the smaller the lower the frequency, and quite insignificant.

We wish to thank Mr K. D. Baveja and Mr Gyan Mohan for undertaking the numerical computation of the series χ', and for making available to us their results.

References

Bridgman, P. W. 1929 *Proc. Amer. Acad. Arts Sci.* **64**, 19.
Galt, J. K. 1948 *Phys. Rev.* **73**, 1460.
Huntingdon, H. B. 1947 *Phys. Rev.* **72**, 321.
Kellermann, E. W. 1940 *Phil. Trans.* A, **238**, 513.
Krishnan, K. S. 1950 *Nature, Lond.*, **166**, 114, 571.
Krishnan, K. S. & Roy, S. K. 1951*a* *Proc. Roy. Soc.* A, **207**, 447.
Krishnan, K. S. & Roy, S. K. 1951*b* *Nature, Lond.* **168**, 869.

Love, A. E. H. 1927 *A treatise on the mathematical theory of elasticity*. Cambridge University Press.
Löwdin, P. O. 1947 *Ark. Mat. Astr. Fys.* **35**, no. 9.
Löwdin, P. O. 1948 A theoretical investigation into some properties of ionic crystals. Dissertation, Uppsala.
Pauling, L. 1928 *Z. Kristallogr.* **67**, 377.
Ramachandran, G. N. 1949 Thesis, Cambridge University.
Sherman, J. 1932 *Chem. Rev.* **11**, 107, 116.
Voigt, W. 1928 *Lehrbuch der Kristallphysik*. Leipzig: Teubner.

Thermionic Constants of Graphite

Some years ago, one of us (K. S. K.) suggested a new method of determining the thermionic constants of solids. The method is based on the determination of the saturation vapour pressure of the electron gas in equilibrium with the substance at different known temperatures. In practice, this is done by finding the rate of effusion into vacuum of electrons out of a small hole in a thin wall of a chamber scooped out of the substance. Using a well-known thermodynamic relation, analogous to the Clapeyron–Clausius equation connecting the temperature variation of the saturation vapour pressure of a given substance with its latent heat of evaporation, one obtains readily the thermionic constants. The work function of graphite was determined by this method by Dr. A. S. Bhatnagar[1], and of a few other substances by Dr. S. B. L. Mathur[2]; but the A coefficients in Richardson's equation were not determined by these authors, owing to uncertainties in some of the absolute measurements.

We have now improved the experimental technique, particularly to keep the temperature of the chamber uniform throughout, and the apparatus is now enclosed in a sealed glass vessel; this enables us to work in a better vacuum, and to ensure a mean free path of the electrons much larger than the dimensions of the apparatus. In order to eliminate the electrons emitted by the graphite surface adjoining the effusion hole, the surface is suitably covered by a thin mica sheet; a hole punctured in the sheet serves as the effective effusion hole. The area of the effusion hole is determined indirectly from the observed rate of loss of a suitably selected substance like naphthalene, or *p*-dichlorobenzene, kept inside the chamber, in vacuum, the loss being due to the sublimation of the substance and its subsequent effusion through the hole.

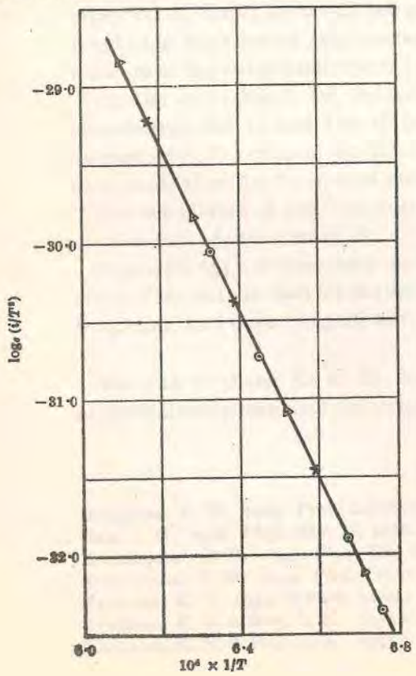

We reproduce in the graph the results obtained in three typical sets of measurements with graphite, in which $\log_e(i/T^2)$ is plotted against $1/T$, where i is the saturation current in amperes corresponding to effusion, per unit area of the effusion hole, in all directions, and T is the absolute temperature. The slope of the curve determines $-\varphi/k$, where k is the Boltzmann constant and φ is the work function, and it is found to correspond to:

$$\varphi = 4{\cdot}62 \pm 0{\cdot}02 \text{ eV}.$$

The intercept of the curve on the y-axis at $1/T = 0$ gives $\log_e A$, from which we find

$$A = 60 \pm 2 \text{ amp. cm.}^{-2} \text{ deg.}^{-2}.$$

This is almost exactly the value that one obtains for good metals.

This method of determining the thermionic constants has certain merits over the usual methods, in that it does not involve a knowledge of the effective area of the emitting surface, which is difficult to determine, or of the reflexion coefficient of the electrons at the surface of emission. Any localized stray impurities in the chamber, as, for example, small bits of copper or zinc deliberately introduced, are found to have no influence on the observation; this is understandable, since the contact potential between the material of the walls of the chamber and the inserted metal will be almost exactly the difference between their work functions.

K. S. Krishnan
S. C. Jain

National Physical Laboratory of India,
New Delhi.
Nov. 14.

[1] *Proc. Nat. Acad. Sci., Ind.*, A, 14, 5 (1944).
[2] Doctorate thesis, University of Allahabad; see also *Proc. Ind. Sci. Cong. Assoc.* 1950, p. 23.

Polarization Field and the Acoustic Modes of Oscillation of Alkali Halide Crystals

In a recent paper[1], the frequency of the principal lattice oscillation of an alkali halide crystal, in which the lattice of the alkali ions oscillates with respect to the lattice of the halide ions, was calculated on the basis of the simple Born model. It was found that the electric polarization of the crystal that accompanies this oscillation leads to a polarization field of the Lorentz type which tends to increase the relative displacement of the two lattices and has thus a marked influence on the principal frequency. Microscopically, this polarization may be regarded as due to small dipoles located at the lattice points. Because of the small amplitude of the oscillation, these dipoles will be practically point-dipoles, and since they are also cubically arranged, the polarization field will have just the Lorentz value, namely, $4\pi/3$ times the polarization per unit volume. (Indeed, this appears to be the only case where the conditions postulated by Lorentz for obtaining the factor $4\pi/3$ are rigorously satisfied.)

The important part which the polarization field plays in determining the resonance frequency of the crystal is indeed to be expected from other considerations. Let us consider, for example, the dielectric constant of the crystal, and confine attention to the contribution from the relative displacements of the positive and the negative ions, as distinguished from the electronic polarizations of the ions themselves. Then the effect of the polarization field on the dielectric constant may be taken into account in two alternative ways. We may regard the effective field that produces the polarization as consisting of not only the 'field in the medium', but also the polarization field, in which case we obtain a formula of the Lorentz type:

$$\frac{K_\omega - 1}{K_\omega + 2} = \frac{C/3}{\Omega_i^2 - \omega^2}, \qquad (1)$$

in which Ω_i is *not* the resonance frequency of the crystal but a certain hypothetical frequency which the crystal would have, had there been no polarization field to affect it. Resonance will occur when the right-hand side of (1) tends to unity, that is, when

$$\omega^2 \to \omega_i^2 = \Omega_i^2 - C/3. \qquad (2)$$

Alternatively, we may regard the effect of the polarization field as confined wholly to changing the hypothetical frequency Ω_i to the actual resonance frequency ω_i of the crystal, in which case we obtain the Drude formula:

$$K_\omega - 1 = \frac{C}{\omega_i^2 - \omega^2}, \qquad (3)$$

in which C has the same value as in (1).

The relation between the two frequencies ω_i and Ω_i may also be expressed in the form:

$$\Omega_i^2 = \omega_i^2 \left(\frac{K_0 + 2}{3}\right), \qquad (4)$$

or more generally,

$$\Omega_i^2 - \omega^2 = (\omega_i^2 - \omega^2) \left(\frac{K_\omega + 2}{3}\right). \qquad (5)$$

The acoustic modes of oscillation also lead to a finite polarization of the crystal, since the amplitudes of the two ions are in general different, as a result of the difference in their masses. Though the polarization now is much smaller than in the optical oscillations, the resulting polarization field is still comparable with the field due to the electrostatic and the repulsion interactions between the ions displaced by the acoustic wave.

We have studied the effect of this polarization field on the low-frequency acoustic oscillations in detail, and we find that the polarization field affects considerably the relative amplitudes of the two ions, but their frequencies remain completely unaffected by it (unlike the optical frequencies). This is very satisfactory, since otherwise the well-known Christoffel relations connecting the velocities of propagation of acoustic waves in the crystal with its elastic constants will be disturbed.

Note added in proof, June 30. Detailed investigations on the effect of the polarization field on the acoustic modes of oscillation have since been published (Krishnan and Roy, *Proc. Roy. Soc.*, A, 210, 481 (1951)).

K. S. Krishnan
S. K. Roy

National Physical Laboratory of India,
New Delhi.
Jan. 5.

[1] *Proc. Roy. Soc.*, A, 207, 447 (1951).

The thermionic constants of metals and semi-conductors
I. Graphite

By S. C. Jain and Sir K. S. Krishnan, F.R.S.
National Physical Laboratory of India, New Delhi

(*Received* 1 *February* 1952)

The thermionic constants of graphite are determined by finding by Knudsen's effusion method the saturation vapour pressure of the electron gas in a graphite chamber, at different known temperatures, and applying the well-known Clapeyron-Clausius thermodynamic relation. The work function ϕ of graphite determined in this manner is $4{\cdot}62 \pm 0{\cdot}02$ eV, and the effusion constant A, analogous to the emission constant in Richardson's equation, is 60 ± 2 A cm^{-2} deg.$^{-2}$.

The introduction of metals like platinum or tungsten into the graphite chamber does not affect the rate of effusion detectably, i.e. does not affect either ϕ or A determined therefrom, and these constants are also quite insensitive to any contamination of the graphite surface by normal adsorption, even in conditions in which the emission of electrons from the surface is greatly suppressed. These observations emphasize the advantages of this method of determining the thermionic constants of graphite over the usual methods. They further suggest that (1) the contact potential between graphite and the metal introduced into the chamber almost exactly compensates for the difference between their work functions; (2) the effusion coefficients A of these metals are practically the same as for graphite, namely, 60 A cm^{-2} deg.$^{-2}$; (3) surface contamination of the walls of the chamber behaves in the same way as the metals introduced in it; (4) any observed differences in the emission coefficients of these metals should be attributed to differences in the reflexion coefficients of their surfaces for electrons; and (5) contamination of the surface affects its reflexion coefficient very markedly.

Measurements are also reported incidentally for the spectral emissivity of graphite for electromagnetic radiations in the neighbourhood of 6550 Å at different temperatures.

1. Introduction

Some years ago a new method was suggested by one of us for the determination of the thermionic constants of a metal. The method is based on the measurement of the saturation vapour pressure of the electron gas in equilibrium with the metal at different known temperatures, and the application of a well-known thermodynamic equation analogous to the Clapeyron-Clausius relation connecting the saturation vapour pressure of a substance with its latent heat of evaporation. In practice, the saturation vapour pressure of the electrons is measured by finding the rate at which electrons effuse into vacuum out of a small hole in a thin wall of a chamber scooped out of the substance. In order to eliminate the electrons emitted by the surface adjoining the effusion hole, which also is at the same temperature as the chamber, the surface is suitably covered with a mica sheet; a small hole punctured in the mica sheet, which comes just in front of a considerably larger hole in the wall, serves actually as the effusion hole.

The method thus involves the measurement of (1) the temperature of the chamber, which is readily done with an optical pyrometer; (2) the area of the effusion hole, which is done indirectly by finding the rate of loss of a suitably chosen substance like naphthalene, whose vapour pressure is known, which is kept in the chamber,

in vacuo, the loss being due to the sublimation of the substance and its subsequent effusion through the hole; (3) the saturation current corresponding to the effusion of electrons through the hole. As we shall see in the present paper, the thermionic constants determined from effusion, are found to be quite insensitive to the contamination of the surfaces of the chamber by adsorption; whereas the corresponding constants determining thermionic emission from the surface, are sensitive to surface adsorption, the work function, slightly, and the emission constant in Richardson's equation, extremely. The method avoids uncertain factors like the reflexion coefficient of the metal surface for electrons incident on it, which are involved in the determination of the thermionic constants by the usual methods, from emission by the heated surface.

A preliminary study of the work function of graphite by this method was made by Bhatnagar (1944), and of a few other substances by Mathur (1950, 1951). The experimental technique has now been improved considerably, which enables the effusion constant A, analogous to the emission constant in Richardson's equation, also to be determined accurately. The present part deals with the determination of the thermionic constants of graphite by this method. By suitably coating the surfaces of the graphite chamber with various metals, of sufficient thickness, the thermionic constants of these metals also are determined by the same method. An account of these latter measurements will be given in part II.

Incidentally, the present studies clarify the relation between the constants that determine the saturation vapour pressure of the electrons in equilibrium with the metal surface, and those that determine the emission of electrons by the surface, and also throw light on the influence of adsorption of gases by the surface on the latter constants.

2. Some relevant expressions for the thermionic constants

As is well known (Dushman 1923; for a general account see, for example, Jones 1936; Herring & Nichols 1949) the saturation vapour pressure p of the electron gas in equilibrium with a metal at temperature T is given by

$$p = \Delta T^{\frac{1}{2}} e^{-\phi/kT}, \tag{1}$$

where Δ is the vapour-pressure constant, which in the case of a monovalent metal will be the same as the Sackur-Tetrode value for a monatomic gas, except for an extra multiplying factor 2 which is now introduced to take into account the spin of the electrons (Fowler 1929). For a monovalent metal, Δ is thus given by

$$\Delta = 2(2\pi m)^{\frac{3}{2}} k^{\frac{5}{2}}/h^3. \tag{2}$$

ϕ is the work function of the metal, and the other letters in (1) and (2) have their usual significance.

Consider a chamber scooped out of the substance, and the electrons that effuse out of a *small* hole of area s in a thin wall of the chamber, into vacuum. The number that effuse out per second in all directions, i.e. over the whole of the semi-solid angle 2π, will be given by

$$n = sp/\sqrt{(2\pi mkT)}. \tag{3}$$

The saturation current, as usually defined, and extrapolated to zero applied field, corresponding to this effusion, per unit area of the effusion hole, will be given by

$$i = ne/s = AT^2 e^{-\phi/(kT)}, \tag{4}$$

where

$$A = 4\pi emk^2/h^3, \tag{5}$$

for a monovalent metal, but may have other values for other metals.

Now equation (4) is very similar to Richardson's equation for the emission of electrons from a hot surface, and we shall denote the corresponding constants that appear in the latter equation by A' and ϕ' respectively, to distinguish them from the unprimed constants that appear in equation (4) for effusion. For an ideally pure surface ϕ' will obviously be the same as ϕ, whereas A' will be equal to $A(1-\rho)$, where ρ is the reflexion coefficient of the emitting surface for electrons incident on the surface and having sufficient energy to cross the barrier. For a pure surface ρ is generally quite small.

Thus the effusion from an aperture in a thin wall of the chamber is identical with the emission from an equal area of the pure surface of the metal kept at the same temperature, except for the transmission coefficient $1-\rho$ that appears in the latter. This correspondence between the effusion of electrons from a cavity, and the emission from a hot surface, is *analogous* to the correspondence between the electromagnetic radiations from a cavity and from the surface of a hot body; the factor $1-\rho$ in electronic emission from the surface taking the place of the emissivity ϵ in the electromagnetic case.

The appearance of the multiplying factor $1-\rho$ in the expression for the emission of electrons from the surface, but not in the expression for the saturation vapour pressure of the electron gas in equilibrium with the surface, or in the expression for its effusion, is important, and we shall have occasion to invoke it in a later section of this part. It is to be expected from general considerations also. Emission from the surface involves the passage of electrons in one direction only, namely, from the metal to vacuum, and $1-\rho$ is the transmission coefficient of the surface for electrons having sufficient energy to cross the barrier. On the other hand, under equilibrium conditions there is an exchange of electrons between the metal and the gas, and the effects of the reflexions from the surface on passage in the two directions being equal, compensate each other.

Equation (4) gives the saturation current i corresponding to effusion over the whole of the semi-solid angle 2π, but the emission *per unit solid angle* is not the same in all directions in the hemisphere, and can be readily seen to vary, as in the case of electronic emission from the surface, or of electromagnetic radiations from it, with the cosine of the angle θ between the direction concerned, and the normal to the aperture. Denoting by A_θ the value of A per unit solid angle along any direction θ,

$$A_\theta = A_0 \cos\theta, \tag{6}$$

where A_0 is the value for effusion along the normal to the plane of the aperture, and is twice the *average* value of A taken over the whole of the 2π solid angle;

$$\bar{A}_\theta = A/(2\pi) = \tfrac{1}{2}A_0. \tag{7}$$

In the actual experiment the number of electrons that effuse out within a well-defined small cone with its axis along the normal to the hole, is measured, at different temperatures T, whence the saturation currents i corresponding to effusion per unit area of the hole over the whole of the semi-solid angle 2π at these temperatures are known. $\ln(i/T^2)$ is then plotted against $1/T$, and the plot is found experimentally to be a straight line, showing that both A and ϕ are nearly independent of the temperature. The slope of the curve obviously gives $-\phi/k$, and the value of $\ln(i/T^2)$ extrapolated to $1/T \to 0$ gives similarly A.

3. The experimental arrangement

The use of a thin-walled graphite tube as a furnace that can be heated to high temperatures in a reducing atmosphere, or *in vacuo*, by passing a heavy electric current through it, is well known (Northrup 1913; Saha & Tandon 1936). The method of determining the vapour pressure of a gas in a chamber from the rate of its effusion into vacuum through a small hole in the wall of the chamber is also well known, and has been used by Knudsen (1900, 1909) for determining the vapour pressures of mercury and lead, and more recently the method has been used by Srivastava (1938, 1940*a*, *b*) and by Bhatnagar (1943, 1947*a*, *b*) for studying the thermal ionization of some metallic vapours. We have adopted a similar arrangement. Whereas in these earlier studies the graphite chamber is used as a container for heating the substances in, the chamber in the present measurements just contains the electron gas which is in equilibrium with graphite and whose vapour pressure is to be determined.

A diagrammatic sketch of the essential parts of the apparatus, drawn roughly to scale, is given in figure 1*a* and *b*. T is the graphite tube which has been turned on the lathe from a thick rod of Acheson graphite to the shape indicated in the diagram, and is of one piece. It consists of a central portion T_1, which forms the graphite chamber, the front wall of which, namely, W_1, has an aperture in the centre, of about $1\frac{1}{2}$ mm diameter. T_2 is an extension of the tube having the same internal diameter as T_1 but with its outer diameter slightly tapering so as to make the thickness progressively smaller. T_3 is a further extension, also thin, but of much wider diameter, and the thick copper strip C (see figure 1*b*, which gives a section) from the electrode E_1 of the generator is clamped on to this end with the help of the two graphite blocks G_1 and G_2 which are bolted on to the end of T_3. The surfaces of G_1 and G_2 bearing on T_3 are shaped precisely, so as to give a perfect fit, and avoid sparking. M is the metal diaphragm, ground on to the end of T_3 which serves to restrict the solid angle of the effusion electrons that can reach the Faraday cylinder F. Both M and T_3 are effectively earthed.

The extension of the graphite tube at the other end, namely, T_4, is also of slightly tapering thickness, and at the end is shaped suitably to take the graphite blocks similar to G_1, G_2, which can be bolted on to it, and which carry the copper strip leading to the other electrode E_2 of the generator. The electrodes E_1 and E_2 consist of double-walled tubes of thick chromium-plated brass, which are fitted to the bed glass plate, and which are water-cooled. A long hollow plug of graphite, P, shaped conically at the farther end, is ground on to T_4, and the inner end of P is a flat disk

W_2 which just touches edgewise the wall of the graphite tube, but is insulated from it with a ring R of mica. W_2 forms the back wall of the graphite chamber.

S_1 is a thin mica disk, which fits on the outer surface of W_1 and which carries the effusion hole H, and S_2 is a cylinder of mica which extends from W_1 to near M. S_1 and S_2 screen effectively the Faraday cylinder from the electrons emitted by the graphite surfaces.

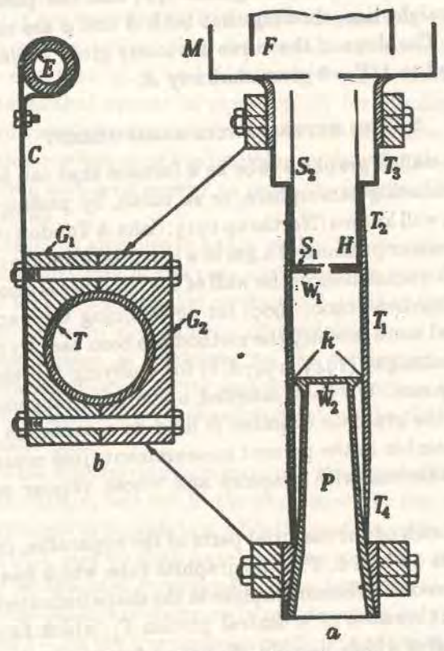

FIGURE 1. Sketch of the apparatus.

The whole apparatus is enclosed in an inverted Dewar vessel which can be evacuated. By sending a suitably large electric current through the graphite tube, *in vacuo*, it can be raised to any desired high temperature up to about 2500° K. At the higher temperature, however, the rate of sublimation of graphite becomes large, and its deposition on the walls of the Dewar vessel, with the consequent uncertain absorption of the radiation from the graphite tube reaching the pyrometer, renders the temperature measurements correspondingly uncertain.

The electrical lead to the Faraday cylinder is enclosed in a double-walled insulation tube between the walls of which is circulated oil from an insulated reservoir, so as to keep it at constant temperature.

The main improvements in technique adopted in the present measurements are the following:

(i) As already mentioned, the apparatus is now enclosed in an all-glass chamber, which enables us to work in a much higher vacuum and to ensure practically

uninterrupted free path for the electrons. The chamber consists of a bed plate of glass $\frac{3}{4}$ in. thick, and an inverted cylindrical unsilvered Dewar vessel of Pyrex glass which is ground on to the plate. Water is circulated in the space between the two walls of the Dewar vessel, so as to keep it at nearly room temperature. The vessel is evacuated with a two-stage oil-diffusion pump, working with Apiezon B oil, and the pump is connected directly to the bed plate to ensure the maximum speed of exhausting which the pump is capable of. In our measurements the pressure in the vessel could be maintained over long periods at less than 10^{-6} cm of mercury, as measured on a cold-cathode ionization gauge connected to the chamber. Now, the mean free path of the molecules in *nitrogen gas* at 20° C and at this pressure is about 7 m, and the free path of electrons in the same gas will be much longer, and in any case several times the dimensions of the vessel. On the other hand, in the earlier measurements, the vacuum chamber was a metallic one of large size, in which naturally the pressure of the residual gas was much higher, and further, the chamber had to be degassed frequently.

(ii) In order to ensure uniformity of temperature over the whole of the graphite chamber, including its end-walls, which is essential in any measurement of saturation vapour pressure, the graphite tube is made to extend considerably beyond the ends of the chamber. Now, in spite of these extensions, if the thickness of the graphite tube was quite uniform over its whole length, there would be a small temperature gradient in the chamber along its axis, the temperature falling off slightly as one moved axially from the centre of the chamber towards its ends. To correct for this the thickness of the extensions of the graphite tube beyond the walls of the chamber is made slightly smaller than that of the main chamber.

(iii) The heating current is taken from a low-voltage generator with a separately excited field, and the current can be maintained steady over long periods. The measurement of temperature also is made more precise so as to enable us to determine the effusion constant A also, which is very sensitive to uncertainties in temperatures, particularly if they are systematic.

(iv) The metal screen with the aperture restricting the solid angle of the effusion electrons that can reach the Faraday cylinder is ground on to the extension end of the graphite tube, which enables the effective solid angle of effusion to be determined accurately.

(v) The electrons emitted by the graphite surface adjoining the effusion holes and also by the near regions of the inner surface of the extension of the graphite tube, which are at the same temperature as the chamber, can also reach the Faraday cylinder, and even when the surfaces are undegassed, because of their large area in comparison with that of the effusion hole, the corresponding contribution to the current through the Faraday cylinder is considerable. In the present measurements, as mentioned in an earlier section, the Faraday cylinder is shielded from these electrons by covering these surfaces suitably with mica.

(vi) The effective area of the effusion hole, which is of irregular shape, is determined more accurately by the method described in the introduction than directly under the microscope, as was done in the earlier measurements.

4. Measurement of temperature

As mentioned in §2, the temperature that we need to measure is that of the inside of the graphite chamber, and the method that normally suggests itself is to use a suitable thermocouple, e.g. platinum/platinum-rhodium couple. Since, however, the introduction of a foreign material inside the chamber *may* disturb the vapour pressure of the electrons in the chamber, the temperature determinations were made with an optical pyrometer. The pyrometer used, which was of the 'disappearing filament' type, was first calibrated with the help of the cavity radiations from a muffled glow furnace, whose temperature was measured with a platinum/platinum-rhodium thermocouple, which in its turn was calibrated with the known melting-points of the following substances in the pure state: sodium chloride (1073° K), copper in a reducing atmosphere (1356° K), lithium metasilicate (1475° K) and nickel (1725° K).

Now the pyrometer measurements relate to the radiation from the outer surface of the graphite tube, which has passed through the double wall of the Dewar vessel with water circulating between the walls, and therefore these measurements require correction on three accounts: (1) for the loss of intensity of the radiation in its passage through the walls of the Dewar vessel; (2) for the deviation of the spectral emissivity of the graphite surface from unity; and (3) for the small difference in temperature that will obtain between the inside of the graphite chamber and its outer surface whose temperature is measured by the pyrometer.

We shall consider (1) first. A closely wound coil of tungsten wire kept in the same position as the graphite chamber, and covered with a small bell-jar which could be kept evacuated, was raised to different constant high temperatures by passing through it a suitable current. Its apparent temperature was determined with the optical pyrometer, (*a*) with the outer Dewar vessel in position, the coil being viewed by the pyrometer through the same part of the walls of the Dewar vessel as in the measurement of the temperature of the graphite tube, and (*b*) with the Dewar vessel removed. Since the optical filter fitted to the pyrometer transmits only a narrow region of the spectrum, namely, in the neighbourhood of 6550 Å, a comparison of the pyrometer temperatures T_a and T_b obtained with the Dewar vessel in position and without it respectively, gives the fraction f of the radiation in this region that is transmitted by the walls of the vessel. Using Wien's formula, which is a good-enough approximation for this purpose, it can be shown that

$$f = \exp\left[-\frac{hc}{k\lambda}\left(\frac{1}{T_a}-\frac{1}{T_b}\right)\right]. \qquad (8)$$

Table 1 gives the corresponding temperatures T_a and T_b obtained in our measurements, and they are expressed in degrees Kelvin. As will be seen from the table, $1/T_a - 1/T_b$ is practically constant, as should be expected. Its mean value, namely, $5{\cdot}3 \times 10^{-6}$, is found to correspond to $f = 0{\cdot}89$, or a loss of 11 %; this loss is due mostly to reflexions at normal incidence at the two air-glass surfaces, and at the two glass-water surfaces. We may mention in passing that this method of measuring f is in essence a photometric method, and the value obtained is therefore of nearly the same accuracy as will be obtained by direct measurement.

Table 1

T_a	1222	1281	1352	1368	1425	1441	1481	1549	1573	1619
T_b	1230	1290	1362	1378	1436	1452	1493	1562	1586	1633
$(1/T - 1/T_b) \times 10^6$	5·3	5·4	5·4	5·3	5·4	5·3	5·4	5·4	5·2	5·3 mean = 5·3

For any apparent temperature T_a as measured by viewing through the glass walls of the Dewar vessel, the corresponding temperature T_b that would be obtained had there been no loss of intensity at these walls, is determined readily from the known value of $1/T_a - 1/T_b$.

The second correction is for the deviation of the actual emissivity of graphite from unity. The spectral emissivity of Acheson graphite in the neighbourhood of 6550 Å, which is the region generally utilized in optical pyrometry, has been measured by Prescott & Hincke (1928) over a wide range of temperatures, and their values of the emissivity could have been used for our purpose, as our graphite tube also was prepared from an Acheson graphite rod. Their values, however, show a very wide spread, and since further the emissivity is sensitive to the nature of the surface, and the values quoted in the literature for the emissivity of high-grade gas carbon (*International critical tables* 1929*a*) are widely different from the values of Prescott & Hincke for Acheson graphite, it was considered desirable to determine directly the temperature of the cavity, without having to invoke a knowledge of the emissivity.

For this purpose a hole of about 1 mm diameter is bored through the wall of the graphite tube after the completion of the thermionic measurements, and the tube is heated as before to different high temperatures, by passing suitably controlled electric current through it.

The ratio of the diameter of the hole (1 mm) to the internal diameter of the graphite tube (11·6 mm) is sufficiently small, according to the criterion of Buckley (1934), to make the radiation from this hole approximate closely to that of a black body.

Let T_a and T_a be the corresponding temperatures of the cavity as viewed through the hole in the wall of the graphite tube, and of the surface of the tube respectively, both as measured with the pyrometer, and with the Dewar vessel in position. Correcting T_a for the loss of intensity at the walls of the vessel, as described in an earlier part of this section, one obtains directly the temperature T of the cavity, corresponding to any observed pyrometer temperature T_a of the surface of the tube as viewed through the Dewar vessel. The value of T so obtained is quite independent of the small gradient in temperature that will obtain between the inner and the outer surfaces of the graphite chamber. In practice a chart was used in which could be read directly the actual temperature T of the cavity corresponding to any observed pyrometer temperature T_a of the outer surface of the graphite chamber.

5. The emissivity of graphite

Incidentally, the data also enable us to determine the emissivity ϵ of the surface of the graphite tube at different temperatures. Under the conditions of heating of the tube, it can be shown that when the conditions have become steady, the

difference in temperature between the inner and the outer surfaces of the tube will be given by

$$\Delta T = \frac{\sigma T^4}{\kappa_T}\left(\frac{r_1}{2} - \frac{r_1 r_2^2}{r_1^2 - r_2^2}\ln\frac{r_1}{r_2}\right), \tag{9}$$

which in view of the thickness of the tube $t = r_1 - r_2$ being much smaller than the radius of the tube, reduces to

$$\Delta T = \frac{\sigma T^4}{\kappa_T}\frac{t}{2}, \tag{10}$$

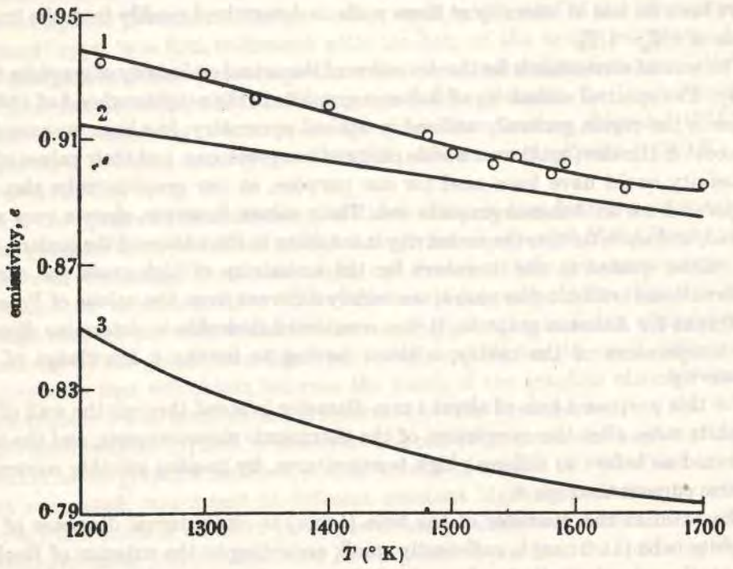

FIGURE 2. The spectral emissivity of graphite in the neighbourhood of 6550 Å.

where r_1 and r_2 are the external and the internal radii of the graphite tube, 6·4 and 5·8 mm respectively, σ is Stefan's radiation constant, equal to $5{\cdot}7 \times 10^{-12}$ J cm^{-2} s^{-1} deg.$^{-4}$, and κ_T is the thermal conductivity of graphite at temperature T, for which we use the value (*International critical tables* 1929*b*)

$$\kappa_T = (1{\cdot}635 - 4{\cdot}95 \times 10^{-4}T)\,\mathrm{J\,s^{-1}\,cm^{-1}\,deg.^{-1}}. \tag{11}$$

In deriving (9) the total emissivity of graphite has been taken to be unity.

To give some idea of the magnitude of the gradient of temperature between the inner and the outer walls of the graphite tube, we may mention that according to expression (10) ΔT is about 0·4° C at 1215° K, and 1·8° C at 1700° K.

Now knowing the corresponding pyrometer temperatures T_c and T_a of the cavity and of the surface of the graphite tube respectively, and their real temperatures T and $T - \Delta T$ respectively, the emissivity ϵ can be obtained from the expression

$$\epsilon = \exp\left[-\frac{hc}{k\lambda}\left(\frac{1}{T_a} - \frac{1}{T_c - \Delta T}\right)\right], \tag{12}$$

which refers to a temperature $T - \Delta T$ of the emitting surface.

The values of the emissivity of graphite at different temperatures obtained in this manner are plotted in figure 2, curve 1. Curve 2 in the figure corresponds to the empirical formula

$$\epsilon = 0{\cdot}984 - 5{\cdot}8 \times 10^{-5}T \tag{13}$$

deduced by Prescott & Hincke (1928) from their experimental data, which, as we mentioned, have a very wide spread, the individual values of ϵ obtained by them varying sometimes by as much as 0·15 from the straight line defined by (13). Curve 3 in the figure is a plot of the values for high grade gas carbon quoted in *International critical tables* (1929*a*).

6. The size of the effusion hole

An obvious method of determining the area of the effusion hole is to measure it directly under the microscope. Since the effusion hole in mica is of odd shape the determination of the effective aperture by this method presents some difficulty. In the present measurements this is done *indirectly* as mentioned already, by finding the rate at which a substance like naphthalene or *p*-dichlorobenzene (the latter could, however, be used only in winter) whose vapour pressure at room temperature is known, loses weight when it is kept in the chamber, *in vacuo*, the loss being due to the sublimation of the substance, and its subsequent effusion through the hole. This determination was done in the same high-vacuum chamber in which the effusion of electrons from the graphite chamber was determined. It takes about 10 min before the vacuum reaches its final high value, and hence the sublimation is allowed to proceed over a long interval, so as to minimize the uncertainty of this duration. The following are the results of a typical experiment. With naphthalene in the chamber, the loss at about 32° C, over an interval of 5 h, was found to be 5·19 g. Taking the vapour pressure of naphthalene at this temperature to be $1{\cdot}66 \times 10^{-3}$ cm of mercury (*International critical tables* 1928), the area of the aperture comes out as $4{\cdot}60 \times 10^{-3}$ cm^2. Any slow adsorption of naphthalene vapour by the walls of the graphite chamber will naturally not affect the result.

This method of determining the area of the effusion hole was checked with a light test-tube in which was kept naphthalene, and whose mouth was closed with a thin platinum foil in which was punctured with a clean pin a small circular hole. The area of the hole determined from the rate of effusion *in vacuo* agreed well with the area as measured under the microscope, which could now be done accurately since the hole is in a thin foil and is circular.

7. Results

As we mentioned in an earlier section, the electrons that reach the Faraday cylinder are those that effuse out of the hole in the graphite chamber in all directions insider the cone subtended by the metal diaphragm at the effusion hole, the diaphragm and the graphite chamber being kept at the same potential. By applying gradually increasing positive potentials to the Faraday cylinder, the corresponding currents are measured in the usual manner. The results obtained in a typical measurement are plotted in figure 3.

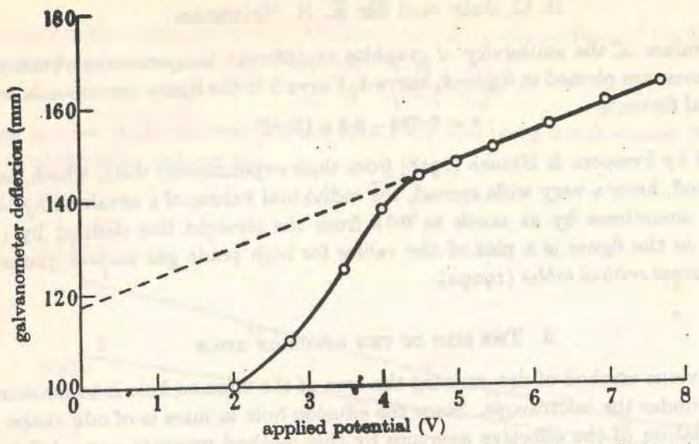

FIGURE 3. Variation of the electronic current through the Faraday cylinder with the applied voltage.

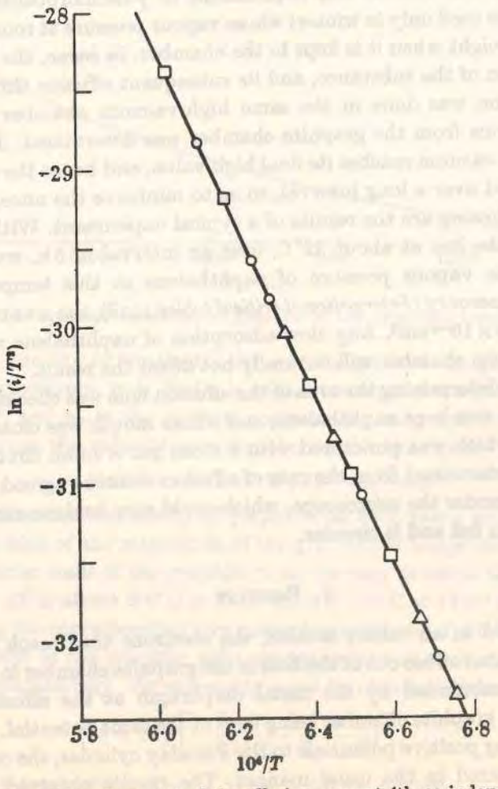

FIGURE 4. The Richardson plot of the effusion current (three independent sets).

It will be seen from the figure that above a certain low voltage the current increases practically *linearly with the increase of the applied voltage V*. By extrapolating backwards the linear portion of the curve, one obtains in the usual manner the saturation current I corrected for the effects of space charge, and the effect of the penetration of the applied electric field into the region between the metal diaphragm and the effusion hole.

Now if r is the radius of the aperture in the metallic screen that limits the solid angle of effusion of the electrons that reach the Faraday cylinder, and d is the distance of the plane of the screen from the effusion hole, then

$$\frac{I}{s} = \frac{i}{\pi}\int_0^{\arctan(r/d)} \cos\theta\, 2\sin\theta\, d\theta$$
$$= \frac{r^2}{r^2+d^2} i, \qquad (14)$$

whence the saturation current i corresponding to effusion, per unit area of the hole, over the whole of the 2π solid angle is known..

It should be mentioned here that a preliminary test made *without* the effusion hole in the mica sheet, i.e. with the sheet in position but before puncturing the hole in it, gave no detectable current. In figure 4 are plotted $\ln(i/T^2)$ against $1/T$. It will be seen from the figure that the plot is a straight line, which shows that, in the temperature range studied, the work function of graphite is practically independent of temperature. The slope of the curve, which gives $-\phi/k$, is found to correspond to

$$\phi = 4{\cdot}62 \pm 0{\cdot}02\,\text{eV},$$

and the intercept of the curve on the y-axis at $1/T \to 0$ gives

$$A = 60 \pm 2\,\text{A cm}^{-2}\,\text{deg.}^{-2}.$$

8. The effect of introducing foreign metals in the graphite chamber

We should mention here some observations made by Mathur (1951) and by ourselves on the effect of introducing foreign metals into the graphite chamber, which may be of significance. A roll of thin platinum foil with a total surface area of about 6 cm² was introduced into the graphite chamber by attaching it to the centre of the plug at the farther end of the chamber without its touching the walls of the graphite tube, since otherwise the distribution of the heating current through the graphite tube may be affected, and as a result of it the uniformity of temperature in the chamber too. It was found that with the platinum foil in, the effusion current was practically the same as without the foil. In other words, both ϕ and A as determined by the present method remain completely unaffected by the insertion of platinum into the chamber.

A bunch of twenty-eight tungsten wires, each about a centimetre long and about 0·4 mm in diameter, introduced into the chamber, in place of the platinum foil, gave the same negative result; and so did small quantities of copper and zinc introduced in the chamber.

That ϕ remains unaffected by the introduction of these metals is immediately understandable, since the finite difference between the work function of graphite and that of the metal introduced will be almost exactly compensated for by the contact potential between the two. That the A coefficient also remains unaffected is a significant result. But before we consider its implications it is desirable to examine in some detail the relation between the values of the thermionic constants ϕ and A obtained from the effusion measurements, and which determine the saturation vapour pressure of the electron gas in equilibrium with the surface, and the corresponding constants ϕ' and A' that determine the emission of electrons from the surface itself. Theoretically, we found in §2 that if the surface is ideally pure, $\phi' = \phi$, and the emission constant A' is $(1-\rho)$ times the effusion constant A, where ρ is the reflexion coefficient of the surface for these electrons.

9. Effusion from the hole and emission from the graphite surface compared

The measurements described in the previous section were repeated with an identical tube in which the thin partition wall bounding the chamber has no aperture, and has no mica sheet to screen it, so that the electrons that now reach the Faraday cylinder are due wholly to the emission from the graphite surface which is practically at the same temperature as the graphite chamber. In order to ensure that this surface was at the same temperature as the chamber a direct comparison was made of the temperatures of this surface and of the graphite tube with the pyrometer. There was no detectable difference. Denoting by i' the saturation current corresponding to emission from unit area of the surface over the 2π solid angle, and plotting as before $\ln(i'/T^2)$ against $1/T$, ϕ' was found to be about 4·4 eV, while *A' was less than a hundredth part of A*.

This result is very suggestive. It is well known that both ϕ' and A' corresponding to electronic emission from a surface are sensitive to any adsorbed gases on the surface, ϕ' slightly, and A' extremely. The surface has to be degassed by repeated heating in vacuum at very high temperatures before ϕ' and A'—particularly the latter—tend to approach the values characteristic of the pure surface. Our present observations suggest (1) that the graphite surface studied for emission, and hence presumably the graphite surfaces inside the chamber too, which had been treated in exactly the same way, are far from being degassed; and (2) that the adsorbed gases do not affect the saturation vapour pressure inside the chamber, though they are effective enough to suppress the value of A' to less than a hundredth of its real value.

It thus appears that the adsorbed layers at the inner surface of the graphite chamber, like the platinum foil or the tungsten wires introduced into it, do not affect either the work function ϕ or the A coefficient determining the saturation vapour pressure of the electrons in the chamber, whereas they do affect the corresponding quantities ϕ' and A' determining the direct emission from such a surface.

This emphasizes incidentally the advantage of the present method of determining the thermionic constant of a metal from the saturation vapour pressure of the

electron gas in equilibrium with it, which is not affected by adsorption, over the usual method from the emission of electrons from the heated surface of the metal, which is very sensitive to it.

We are now studying more extensively the effect of introducing other metals into the graphite chamber, on the saturation vapour pressure of the electron gas in it, and it may be premature to draw any definite conclusions. We may, however, mention this in passing. If the negative result observed with platinum and tungsten introduced into the chamber turns out to be more general, it will imply that (1) the effusion constant A has nearly the same value for all the metals; (2) any observed differences in the A' values of different metals, even after complete degassing, should be attributed to the differences in the reflexion coefficients ρ of the surfaces of these metals for electrons, as $A' = A(1-\rho)$; and (3) the observed abnormal influence of adsorbed gases in suppressing the value of A' is due ultimately to its large effect on the reflexion coefficient ρ, making ρ tend to unity as the adsorption progresses.

Table 2

author and year	method	ϕ' (eV)	A' (A cm^{-2} deg.$^{-2}$)
Langmuir (1913)	emission from carbon filament	2·5	5×10^{-4}
Langmuir (1916) (quoted by Reimann)		3·9	5·9
Lester (1916)	calorimetric measurement using filaments of much-used carbon lamps	4·5	—
Dushman (1929) (quoted in *Int. crit. tables*)	—	4·0	60·2
Reimann (1938)	emission from carbon filament	4·34	30
Braun & Busch (1947)	emission from a graphite rod	4·39	15
Glockler & Sausville (1949)	emission from an extruded filament	4·35 ± 0·6	48 ± 25
Ivey (1949)	emission from carbon filament max. temp. used for degassing:		
	1610° K	4·44	22
	2125° K	4·61	45
	2335° K	4·59	48
present method	—	4·62	60

In the previous section we found that the contribution from the free surface of graphite to the saturation current through the Faraday cylinder was low in comparison with the contribution from the effusion hole; in spite of the much larger area of the former, its contribution was of the order of a fifth of the current due to the latter. This current remained practically unaffected by the normal heating involved in making these measurements, showing that in the temperature range used there was hardly any degassing. Hence in some of our earlier measurements the hole in the graphite wall was made small enough to serve directly as the effusion hole. No attempt was made to screen the Faraday cylinder from the electrons emitted by the graphite surfaces adjoining the hole, but using the data for emission from the unpunctured graphite surface at different temperatures a correction was made for the latter contribution.

It may be mentioned here that the corrected values of i per unit area of the effusion hole thus obtained agree well with the values obtained with the mica effusion hole. Since, however, these corrected values are not quite as precise as the values obtained with the mica aperture, they are not reported in detail here.

10. Comparison with earlier values

In table 2 are collected together the values for the thermionic constants of graphite obtained by earlier workers for comparison with the present values.

We wish to thank Dr Swami Jnanananda, for helpful discussions.

References

Bhatnagar, A. S. 1943 *Proc. Nat. Acad. Sci. India*, **13**, 243.
Bhatnagar, A. S. 1944 *Proc. Nat. Acad. Sci. India*, **14**, 5.
Bhatnagar, A. S. 1947*a* *Proc. Nat. Acad. Sci. India*, **16**, 45.
Bhatnagar, A. S. 1947*b* *Proc. Nat. Acad. Sci. India*, **16**, 53.
Braun, A. & Busch, G. 1947 *Helv. phys. acta*, **20**, 33.
Buckley, H. 1934 *Phil. Mag.* **17**, 576.
Dushman, S. 1923 *Phys. Rev.* **21**, 263.
Dushman, S. 1929 *International critical tables*, **6**, 53.
Fowler, R. H. 1929 *Proc. Roy. Soc.* A, **122**, 36.
Glockler, G. & Sausville, J. W. 1949 *J. Electroch. Soc.* **95**, 292.
Herring, C. & Nichols, M. H. 1949 *Rev. Mod. Phys.* **21**, 185.
International critical tables 1928 **3**, 208.
International critical tables 1929*a* **5**, 245.
International critical tables 1929*b* **5**, 217.
Ivey, H. F. 1949 *Phys. Rev.* **76**, 567.
Jones, T. J. 1936 *Thermionic emission*. London: Methuen and Co.
Knudsen, M. 1900 *Ann. Phys., Lpz.*, **29**, 179.
Knudsen, M. 1909 *Ann. Phys., Lpz.*, **28**, 999.
Langmuir, I. 1913 *Phys. Rev.* **2**, 450.
Lester, H. 1916 *Phil. Mag.* **31**, 197.
Mathur, S. B. L. 1950 *Proc. Indian Sci. Congr. Ass.* p. 23.
Mathur, S. B. L. 1951 D.Sc. Thesis, University of Lucknow (unpublished).
Northrup, E. F. 1913 *Princeton Met. Chem. Engng*, **12**, 31.
Prescott, C. H. & Hincke, W. B. 1928 *Phys. Rev.* **31**, 130.
Reimann, A. L. 1938 *Proc. Phys. Soc.* **50**, 496.
Saha, M. N. & Tandon, A. N. 1936 *Proc. Nat. Acad. Sci. India*, **6**, 212.
Srivastava, B. N. 1938 *Proc. Nat. Inst. Sci. India*, A, **4**, 365.
Srivastava, B. N. 1940*a* *Proc. Roy. Soc.* A, **175**, 26.
Srivastava, B. N. 1940*b* *Proc. Roy. Soc.* A, **176**, 343.

Evjen's Method of Evaluating the Madelung Constant

K. S. Krishnan and S. K. Roy
National Physical Laboratory of India, New Delhi, India

(Received April 8, 1952)

A convenient method of evaluating the Madelung series is first to group the terms into unit cells and then sum the contributions from the different cells. It is emphasized that even such a grouping, which involves neighboring terms only, may affect the sum. This happens, for example, with the CsCl type of lattice, if the unit cell chosen is the usual body-centered cube, whereas by choosing an oblique elementary cell containing one ion, the sum remains unaltered. A criterion is given for the choice of a suitable elementary cell.

THE Madelung series has been evaluated by several methods.[1] Among them we shall consider here in particular the method adopted by Evjen,[2] in which the contributions from the ions in a unit cell are summed first, and then the contributions from the different unit cells in the crystal. Let us consider for example a crystal of CsCl, whose unit cell is a cube of side $2a$ which contains 2 ions, one at the center and the other, of opposite sign, at each of the corners of the cube. Each of the latter ions will contribute $\frac{1}{8}$ to the cell. Expressing all the charges in terms of $|e|$ where e is the electronic charge, and the distances in terms of a, and taking the coordinate axes along the cubic axes of the crystal, and the origin at a lattice point occupied by a positive ion, the potential at the origin, due to all the surrounding ions, will be given by the Madelung sum

$$S=\sum_{(\xi,\eta,\zeta)}(-1)^{\xi+\eta+\zeta}(\xi^2+\eta^2+\zeta^2)^{-\frac{1}{2}}, \qquad (1)$$

in which ξ, η, ζ are integers which define the coordinates of the ions, all three of them being odd if the ion is negative, and even if the ion is positive; $\xi=\eta=\zeta=0$ is naturally excluded. Series (1) can be shown to be convergent, but not absolutely convergent. By dividing the medium into such unit cells, the original triple series (1) can be converted into a new triple series in which each term is the contribution from a unit cell. Consider one of these cells whose center is at a distance ρ from the origin. The contribution from this cell to the potential at the origin can be expressed as a power series in $1/\rho$, in which, as Evjen has shown, the first nonvanishing term is that involving $1/\rho^5$. Hence the new triple series will be absolutely convergent, and can therefore be summed in any manner that is convenient.

Since the preliminary grouping of the ions into unit cells is among neighboring ions only, and is the same at all distances from the origin, it may appear at first sight that the rearrangement of terms involved in such a grouping will not alter the sum, and that the sum of the resulting absolutely convergent series, which can be obtained without ambiguity, should be the same as that of the original series, namely, S. It is the main purpose of this note to emphasize that this would not in general be the case, and in order that the sum might remain unaltered by the grouping, the group, i.e., the elementary cell selected, should be such that its faces do not carry a net electric charge. In CsCl the unit cell that we have chosen, namely, a cube of side $2a$, does not satisfy this condition, and actually, depending on whether the cell chosen contains a negative ion at the center and positive ions at the corners, or a positive ion at the center and negative ions at the corners, the resulting absolutely convergent series has different sums, namely, $S_I=S-\pi/4$ and $S_{II}=S+\pi/4$, respectively, as we shall show presently.

It is however possible to construct an elementary cell of this crystal that does satisfy the condition stated above. Consider for example the parallelopiped whose three adjacent edges are the lines joining the center of the unit cube to any three adjacent corners of the cube. This new elementary cell has one ion at each of its corners, and these ions are alternately positive and negative. By dividing the medium into such oblique cells, series (1) can again be converted into an absolutely convergent triple series, but now with its sum unaltered.[3]

Coming back to the division into cubic unit cells, consider the infinite plane defined by $\xi=n$, the distances being expressed as before in terms of a. This plane will contain exclusively positive or negative ions depending on whether n is even or odd. Denoting the contribution to the potential at the origin from the ions in this plane by $(-1)^n\tau_n$, where τ_n is positive, one can readily see that τ_n will be infinite. On the other hand $\tau_n-\tau_{n+1}$ tends to a finite value independent of n, when n becomes large in comparison with unity, namely, $\pi/2$. This follows from $\tau_n-\tau_{n+1}$ being the potential at the origin due to a uniform double layer of moment $\frac{1}{4}$ per unit area, and subtending at the origin a solid angle 2π.

Considering now the absolutely convergent series obtained by dividing the crystal into cubic unit cells, the sum of this series should be independent of the mode of grouping these cells (keeping of course the cells intact). In particular we may group these cells in

[1] See J. Sherman, Chem. Revs. **11**, 93 (1932).
[2] H. M. Evjen, Phys. Rev. **39**, 675 (1932).

[3] An analogous lattice sum has been evaluated by us by dividing the crystal into cells of this type. See K. S. Krishnan and S. K. Roy, Proc. Roy. Soc. (London) **A210**, 481 (1951).

infinite layers or perpendicular to ξ-axis, each shell being one cell thick. The contribution to the potential at the origin from one such shell when n is large, will be given by

$$s_n = (-1)^n(\tfrac{1}{2}\tau_n - \tau_{n+1} + \tfrac{1}{2}\tau_{n+2}), \qquad (2)$$

in which n will be consistently even for all the shells, or consistently odd, depending on how the unit cell has been chosen, whether with a negative ion at the center or with a positive ion there. n will take both positive and negative values, s_n obviously tends to zero as n becomes large, and the sum of the series $\sum s_n$, n increasing in steps of 2, is finite, as it is the sum of an absolutely convergent series. In other words, depending on the particular choice of the cubic unit cell, the resulting absolutely convergent series $\sum s_n$ will have different sums S_{I} and S_{II} the difference between them being $\tau_{n+1} - \tau_n = -\pi/2$. The same result can also be obtained by grouping the unit cells into cubic shells about the origin as center, each shell being again one cell thick. Thus the rearrangement of the terms of the series (1) involved in grouping them into cubic cells alters the sum.

As we mentioned earlier the positive and the negative ions in CsCl separate out in layers parallel to faces of the type {100}. Any unit cell whose faces are parallel to these faces will not therefore be suitable for our present purpose. The condition stated above requiring the electrical neutrality of the faces of the unit cell is to preclude such a choice.

On the other hand when the parallelopiped described above is chosen as the unit cell, there can be no such separation of charges. The resulting absolutely convergent series, besides giving the same sum S as the original series, is also found to be rapidly convergent, and can therefore be used conveniently for the numerical computation of S.

Thermionic Constants of the Iron Group of Metals

In a recent communication[1], we gave an account of a new method of determining the thermionic constants of graphite, which is based on the determination of the saturation vapour pressure of the electron gas in equilibrium with the substance at different known temperatures, and application of the well-known thermodynamic relation of Clausius and Clapeyron. In the actual experiments, the saturation vapour pressure of the electron gas in a graphite chamber is determined by finding the rate of effusion of the gas into vacuum through a small hole in a thin wall of the chamber. The chamber is in the form of a thin-walled tube, and can be heated to any desired high temperature by sending a suitable heavy electric current through it. In order to eliminate the electrons emitted by the graphite surface adjoining the effusion hole, the surface is covered by a thin sheet of mica, with a small hole punctured in it; this comes just in front of a bigger one in the graphite wall and serves as the effective effusion hole.

This method of determining the thermionic constants, and in particular the coefficient A in Richardson's equation, has advantages over the other methods, since it is insensitive to the usual type of contamination of the emitting surface; and further, it does not require a knowledge of the effective area of the emitting surface or of the reflexion coefficient of the electrons at the surface.

The inner walls of the graphite chamber, as also the regions close to the effusion hole, can be coated suitably with other metals, and the method can thus be used for the determination of the thermionic constants of these metals also. We have determined in this manner the thermionic constants of chromium, iron, cobalt and nickel, depositing the metals both electrolytically and by evaporation from a tungsten wire coated previously with the metal, or carrying small rings of the metal. The results were found to be independent of the method used for the deposition of the metal and were reproducible.

The observations fit well with Richardson's equation:

$$i = AT^2 \exp(-\varphi/kT), \qquad (1)$$

in which A and φ are independent of temperature, and have the values given in the accompanying table.

Metal	φ (eV.)	A (amp. cm.$^{-2}$ deg.$^{-2}$)
Chromium	4·58	60
γ-Iron	4·31 ±0·02	60 ±2
Cobalt	4·41	60
Nickel	4·50	120 ±5
Note added in proof, October 8.		
Titanium	3·95	44
Vanadium	4·12	50
Manganese	3·83	34

As is well known, the observed fit of the experimental data with formula (1) with temperature-independent constants A and φ cannot be regarded as excluding a small linear variation of the actual work function with temperature, since such a variation will be equivalent to a temperature-independent change in A. Apart from the normal thermal expansion of the metal, which will lead to a small temperature variation of the work function, there is a further source of such variation in these metals. The d- and the s-energy bands of these metals overlap, the former being nearly full, and having a much larger density of energy-states than the latter. As a result, (1) the electronic specific heat in the condensed phase will be considerable, and (2) on change of temperature there will be a transference of electrons from one band to the other, and a consequent change in the work function[2]. Hence experimental data for the thermionic constants of the transition elements are of special interest.

K. S. Krishnan
S. C. Jain
National Physical Laboratory of India,
New Delhi. April 15.

[1] *Nature*, **169**, 702 (1952). See also Bhatnagar, A. S., *Proc. Nat. Acad. Sci. India*, A, **145** (1944). Mathur, S. B. L., doctorate thesis, University of Lucknow (1951). Krishnan, K. S., and Jain, S. C., *Proc. Roy. Soc.*, A. (In the press).

[2] Wohlfarth, E. P., *Proc. Phys. Soc.*, **61**, 360 (1948).

The Dispersion Formulae and the Polarization Fields

By Sir K. S. Krishnan, F.R.S., and S. K. Roy
The National Physical Laboratory of India, New Delhi*

[Received June 18, 1952]

In the usual derivation of the Drude formula for the dielectric constant of a dense medium as a function of the frequency of the incident waves, since one does not invoke the presence of a polarization field, and since further it is known that the Lorentz dispersion formula reduces to the Drude formula in the special case when the polarization field is made to vanish, any verification of the Drude dispersion formula is sometimes taken to imply the absence of a polarization field. This conclusion is not justified, and it is the main purpose of this note to emphasize that the Drude formula for the dielectric constant as a function of the frequency of the incident waves (as distinguished from the formula for the dielectric constant as a function of the density) is perfectly consistent with the occurrence of a polarization field having the Lorentz value, or any other value. This will be the case even when the polarization field factors

* Communicated by the Authors.

p_{ij} defining the polarization field acting on any oscillator of type i due to all the oscillators of type j in the medium differ from the Lorentz value $4\pi/3$, and differ from one another. In other words, irrespective of the actual polarization field that occurs in the medium, i.e. irrespective of the actual values of p_{ij} that define this field, the observational data for the dispersion of the dielectric constant can always be represented by the Drude formula

$$\epsilon_\omega - 1 = \Sigma_i \frac{A_i}{\omega_i^2 - \omega^2}, \quad \ldots\ldots\ldots \quad (1)$$

the characteristic frequencies ω_i that appear in the formula being the resonance frequencies of the medium.

The same observational data can also be fitted alternatively into a formula of the type

$$\epsilon_\omega - 1 = 4\pi\chi = 4\pi\Sigma_i \chi_i, \quad \ldots\ldots\ldots \quad (2)$$

where

$$\chi_i = \frac{B_i}{\Omega_i^2 - \omega^2}(1 + \Sigma_j p_{ij}\chi_j), \quad \ldots\ldots\ldots \quad (3)$$

in which j can take all values $i, j, k, \ldots$. When all the p_{ij}'s have the same value, equal to p say, $\Sigma_j p_{ij}\chi_j = p\chi$, and eqn. (2) reduces to the form

$$\frac{\epsilon_\omega - 1}{\epsilon_\omega + \alpha} = \Sigma_i \frac{C_i}{\Omega_i^2 - \omega^2}, \quad \ldots\ldots\ldots \quad (4)$$

where

$$\alpha = \frac{4\pi}{p} - 1, \quad \ldots\ldots\ldots \quad (5)$$

and

$$C_i = pB_i. \quad \ldots\ldots\ldots \quad (6)$$

When p has the Lorentz value $4\pi/3$, it will be seen that α reduces to 2 and eqn. (4) to the simple Lorentz formula. For convenience we shall describe the type of dispersion formula defined by (2) and (3) as a generalized Lorentz formula, as distinguished from the simple Lorentz formula corresponding to $\alpha = 2$ in eqn. (4).

Thus any observational data on the dispersion of the dielectric constant of a dense medium can be fitted into a Drude formula, or alternatively into a generalized Lorentz formula involving any given set of polarization factors p_{ij}. This fitting into the alternative formulae can be done irrespective of what the *actual* polarization field in the medium may be, and even if there is no polarization field at all.

The equivalence of the Drude and the simple Lorentz formulae for the dispersion of the dielectric constant of a dense medium was first demonstrated by Livens (1912) for the case when the medium has a single resonance frequency, and by Herzfeld and Wolf (1925) for the case when the medium may have more than one resonance frequency. The equivalence extends, as we have just seen, also to the generalized Lorentz

formula corresponding to any specified set of polarization factors p_{ij} defining the interactions between the dipole moments of the different oscillators.

This equivalence arises from the following circumstance. The effect of any polarization field that may be present in a dense medium on its dielectric constant may be taken into account in two alternative ways, which are equivalent. The effective field that polarizes the medium may be taken to include, in addition to what is usually defined as 'the field in the medium', the polarization field also, in which case the dispersion formula will be of the Lorentz type and the characteristic frequencies that appear in the formula will be the frequencies Ω_i of the individual oscillators, regarded as unaffected by the presence of the polarization field, i.e. unaffected by their mutual interactions. Alternatively one may also regard the polarization field as effective in changing the frequencies Ω_i to the corresponding resonance frequencies ω_i of the medium, and its effect on the dielectric constant as exercised indirectly through these frequencies. The result is the Drude dispersion formula. (The important part played by the polarization field in determining the infra-red resonance frequency of the alkali halide crystal, in which the polarization field involved is readily calculated, is discussed by us in a recent paper (Krishnan and Roy 1951).)

Conversely, starting with the Drude formula, and the known resonance frequencies ω_i that appear in the formula, and taking them to correspond to zero polarization field, one may postulate any desired polarization field and reduce the Drude formula to one of the Lorentz type. The frequencies Ω_i that appear in the latter formula will be different from the corresponding resonance frequencies ω_i by amounts that will be determined by the polarization field postulated.

Hence dispersion data as such can not give us any information regarding the nature of the polarization field that exists in the medium, though they enable us to obtain the resonance frequencies, directly if the data are expressed in the Drude form, since the characteristic frequencies ω_i that appear in this formula are just these frequencies, or after a simple calculation from the corresponding Ω_i if the data are expressed in the Lorentz form.

The position, however, is very different with expressions for the dielectric constant as a function of the density, where the equivalence of the Drude and the Lorentz types does not hold.

References

Herzfeld, K. F., and Wolf, K. L., 1925, *Ann. d. Physik*, **78**, 35.
Krishnan, K. S., and Roy, S. K., 1951, *Proc. Roy. Soc.* A, **207**, 447
Livens, G. H., 1912, *Phil. Mag.*, **24**, 268.

Thermionic constants of metals and semiconductors
II. Metals of the first transition group

By S. C. Jain and Sir K. S. Krishnan, F.R.S.
National Physical Laboratory of India, New Delhi

(*Received* 8 *August* 1952)

The method described in part I for the determination of the thermionic constants of graphite, which is based on finding the saturation vapour pressure of the electron gas in a graphite chamber at different known temperatures, and applying the well-known thermodynamic relation of Clausius and Clapeyron, can be used for determining the constants of most metals by simply coating the inner walls of the graphite chamber with a thick layer of the metal to be studied. The present part reports measurements made by this method of the thermionic constants of the metals of the iron group from Ti to Ni.

1. Introduction

In part I of this paper (Jain & Krishnan 1952) was described a new method for determining the thermionic constants of a substance, which is based on finding the saturation vapour pressure of the electron gas in equilibrium with the substance at different known temperatures. The saturation vapour pressure actually measured is that of the electron gas in a chamber scooped out of the substance, and the measurement of pressure is done indirectly by finding the rate of effusion of the electrons from the chamber into a vacuum through a small effusion hole in a thin wall of the chamber. In part I the thermionic constants of graphite were determined by this method. Graphite is particularly suited for this purpose since the chamber, which in the experiment is formed from a thin-walled cylindrical tube of graphite, can be conveniently heated and maintained at any desired high temperature in a vacuum chamber by sending a suitable heavy electric current through it.

As is well known, the thermionic constants determined by the usual diode method, which is based on finding the rate of emission of electrons by a known area of the heated surface, are very sensitive to the adsorption of gases at the surface, such as may occur even on a casual exposure of the surface to air. This is particularly the case with the A coefficient in Richardson's equation for thermionic emission. Hence the emitting surface has to be degassed by repeated heating before the emission settles down to the value characteristic of the pure surface. In the present method, however, such surface contaminations are found to have very little influence on the constants, which is understandable, since the major effect of the adsorbed layers will be on the reflexion coefficient of the surface, and this coefficient is involved in the expression for the emission of electrons from the surface, but not in the expression for their effusion from the chamber. The effect of the adsorbed layers on the *work function* will be compensated by the contact potential between the bulk material and its surface layers. Further, the usual uncertainties of determining the *effective* area of the emitting surface do not arise in the present method.

Now the walls of the graphite chamber can be readily coated with various metals or alloys, or with semi-conductors with a suitable base if desired. The coating can be done either by thermal deposition in a vacuum or by electrolytic deposition, and to any desired thickness. Hence the same experimental arrangement as was used in part I for determining the thermionic constants of graphite can be used to determine the constants of these substances also, many of which cannot be prepared in the form of filaments suitable for study by the usual diode method.

The present part describes measurements on the thermionic constants of the first transition group of elements. The transition groups are of special interest theoretically owing to the overlap of the energy bands of the free electrons in these metals and the consequent high density of the energy states at the Fermi surface, and the possibility of transference of electrons from one band to another when the temperature is varied. The specific heat of the electrons in the condensed phase, namely the metal, which in general is negligible, is quite large in the transition elements. These factors make the case of the transition elements particularly interesting.

2. Thermal deposition of the metals

As was mentioned in the Introduction, the walls of the graphite chamber were coated with the metals both by thermal and by electrolytic methods. The quantity of metal generally needed for thermal deposition is small and that needed for the present purpose is even smaller, since the coating is confined to the *inner* walls of the graphite chamber. Hence specimens of very high purity could be used. The specimen of chromium used for thermal deposition was from Johnson Matthey & Co. and was of spectroscopic purity, and the other pure metals were made available through the kindness of the Pure Metals Committee of the Department of Scientific and Industrial Research of the United Kingdom. In the electrolytic deposition, on the other hand, the electrolytes used were not of the same high original purity as the metals, and they had to be further purified for the present purpose. The methods used for this purification will be described in the next section.

The thermal deposition is done in the following manner. As was described in part I, the graphite chamber consists of a long thin-walled graphite tube with a thin partition wall in the middle, the partition wall having a small hole in the centre. This hole is covered ultimately by a sheet of mica which carries the effusion hole. The other end of the tube is closed by a detachable hollow graphite plug. The thermal deposition of the metal is made in a separate vacuum chamber. The surface of the graphite tube is first cleaned electrolytically in an alkali bath, and is washed with dilute acid, and then with water, before use. A twisted pair of tungsten wires (cleaned previously by boiling in an alkali solution) is stretched along the length of the graphite tube, and passes through the hole in the partition wall, and is made to carry in its folds small pieces of the metal to be deposited. In order to make the deposit on the walls of the chamber uniform, the tungsten wire is made to stretch axially over most of its length, and form a loop near the partition wall before it emerges, again axially, through the hole. This loop is nearly parallel with, and lies close to, the partition wall and is so shaped as to enable the adjoining corners of the chamber also to receive the deposit.

The chamber is evacuated and then filled with hydrogen gas, and an electric current is sent through the twisted tungsten pair just enough to melt the metal pieces and make them spread over the whole of the surface of the tungsten wires. Without the hydrogen atmosphere metals like chromium show a tendency to sublime when heated, and hence the pieces of metal held in the folds of the twisted pair of tungsten wires drop down without melting, whereas in the hydrogen atmosphere these pieces melt and spread over the tungsten wires just like other metals. Though the hydrogen atmosphere might not be necessary for melting many of the metals, it was used generally.

After thus spreading the metal over the whole of the tungsten wires the vacuum chamber is evacuated to a very low pressure. On sending a suitable electric current now through the tungsten wires the metals evaporate and become deposited in the usual manner, quite uniformly over the walls of the chamber, including the regions on the other side of the partition wall and in its neighbourhood. The surface of the graphite plug which will form the back wall of the chamber, is coated in the same manner, but separately.

3. The electrolytic deposition of the metal

All the metals studied here, except Ti and V, were also deposited electrolytically. Here again the graphite surface is first cleaned by the same method as previously. The anode used in electrolysis consists of a rod running axially over the whole length of the chamber, with an auxiliary anode of the same material, which can pass through the small hole in the partition wall of the chamber. The graphite tube is kept filled with the electrolyte, which is maintained fresh by a steady flow of the electrolyte into and out of the tube.

The electrolytes used for the deposition of the metals were respectively (1) dilute chromic acid to which is added a small quantity of sulphuric acid, (2) solution of manganous sulphate with some ammonium sulphate, (3) solution of ferrous ammonium sulphate, (4) solution of cobalt sulphate with some boric acid and ammonium chloride, and (5) solution of nickel sulphate with some of the chloride and boric acid.

The anodes used for the deposition of iron and nickel are rods of these metals, prepared by melting the pure metals in a hydrogen atmosphere. The anode used for the deposition of chromium is of antimonized lead, which serves to oxidize the trivalent chromium in the bath to chromic acid. In the case of manganese and cobalt, for which sufficient quantities of the pure metal were not available for use as anode rods, thin rods of pure graphite were used as anodes.

4. Purification of the electrolytes

All the electrolytes used are purified by a preliminary electrolysis with scrap cathodes, using an appropriate low current density, and a suitable temperature. The chromic acid used was of sufficient purity that no further purification was considered necessary. In the case of manganous sulphate any Ni, Co or Cu that may be present is removed by precipitation as sulphides, and by adding a little ferrous

sulphate and precipitating it as ferric hydroxide (at an optimum pH value of 7); all Fe, and along with it any As, Mo, colloidal S or sulphides that may be present, also get removed. In the case of iron, metallic impurities such as Cu, As, etc., are removed in the process of initial electrolysis using scrap cathodes. Some ferric salts are always present in the electrolyte, because of which the surface of the deposited film appears rough, and shows some cracks. To convert all the ferric iron into ferrous iron a small quantity of HCl is added to the bath and pure iron wires are hung in it. If the acid added is too much the cathode efficiency becomes less. Hence in the case of the iron electrolyte its pH value is the critical controlling factor.

The purification of the cobalt and the nickel electrolytes is slightly more elaborate. In the course of the preliminary electrolysis, which is carried out at 140° F and with a current density of 1 to 3 amps per sq.ft., Cu, Zn and Pb are eliminated. To eliminate Fe the pH value of the electrolyte is raised to about 5 by adding nickel carbonate. A small amount of hydrogen peroxide is then added and the bath is vigorously agitated for several hours. The precipitate of ferric hydroxide is filtered off and the pH value is restored to about 3·8 by adding pure sulphuric acid.

All the electrolytes are finally treated with activated carbon so as to remove any organic impurities that may be present.

The thickness of the deposit is conditioned by the requirement that it should be possible to heat the coated graphite tube to the requisite high temperatures by sending an electric current through it. In our experiments the thickness varies from about 50 to 100μ. As we shall see in a later section, this thickness is sufficient to ensure that the thermionic properties of the metal coating are the same as for the metal in bulk.

5. The thermionic measurements

Except that the inner walls of the graphite chamber are now completely covered by the metal, the arrangement remains exactly the same as in part I. The saturation current determined by the rate of effusion of electrons through the hole in the mica sheet now corresponds to effusion from a chamber of the metal, and is proportional to the saturation vapour pressure of the electron gas in equilibrium with the metal. As shown in part I, a straight forward application of Clapeyron's equation connecting the saturation vapour pressure of the substance at any given temperature with its latent heat of evaporation, gives directly the thermionic constants.

Since the outer surface of the graphite tube is not coated, the data given in part I for the optical emissivity of graphite can be utilized for the temperature measurements, and the corrections to be applied to the observed pyrometer temperatures in order to get the actual temperature therefore remain the same as before. The gradient in temperature between the coated metal surface inside, and the outer surface of the graphite tube which is directly accessible to the optical pyrometer, may now be slightly different. But since the total difference between the inside and outside is of the order of 2° C, and the thickness of the metal is much smaller than the thickness of the graphite wall, the changes will be negligible. In any case a fresh measurement of the inside temperature was made by boring a hole on the

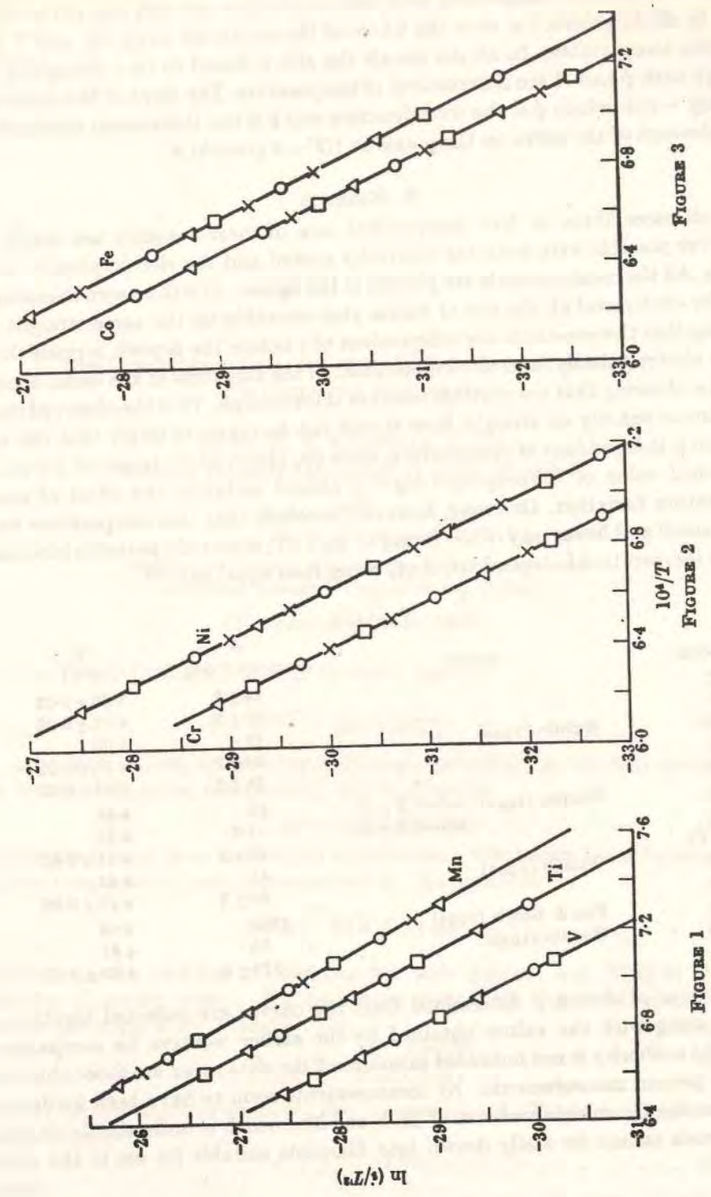

Figure 3

Figure 2

Figure 1

side of the coated tube and compared with the surface temperature. No difference could be detected between the simple graphite tube and the coated graphite tube.

In figures 1 to 3 are plotted the values of $\ln(i/T^2)$ against $1/T$, where i is the saturation current corresponding to effusion of electrons per unit area of the effusion hole, in all directions, i.e. over the whole of the semi-solid angle 2π, and T is the absolute temperature. In all the metals the plot is found to be a straight line, as though both ϕ and A are independent of temperature. The slope of the curve gives directly $-\phi/k$, where ϕ is the work function and k is the Boltzmann constant, and the intercept of the curve on the y-axis at $1/T \to 0$ gives $\ln A$.

6. Results

In all cases three or four independent sets of measurements are made, and wherever possible with both the thermally coated and the electrolytically coated metals. All the measurements are plotted in the figures. It will be seen immediately that for each metal all the sets of values plot smoothly on the same straight line, showing that the constants are independent of whether the deposit is made thermally or electrolytically, and also independent of the thickness of the metal coatings used; i.e. showing that the coatings used are thick enough. That the observed results plot almost exactly on straight lines should not be taken to imply that the work function is independent of temperature, since the observed deviation of A from the theoretical value of 120 amp cm^{-2} deg^{-2} is almost certainly the effect of such a temperature variation. One may, however, conclude that this temperature variation is small and linear, say of the form $\phi = \phi_0 + \alpha T$, since only in such a case can A remain temperature independent, A/A_0 being then equal to $e^{-\alpha/k}$.

Table 1

metal	author	A (amp cm^{-2} deg^{-2})	ϕ (eV)
Ti		44 ± 2	3·95 ± 0·02
V		50 ± 2	4·12 ± 0·02
Cr	Wahlin (1948)	48	4·60
Cr		60 ± 2	4·58 ± 0·02
Mn		34 ± 2	3·83 ± 0·02
Fe	Wahlin (1942): below β-γ pt.	26	4·48
	above β-γ pt.	1·5	4·21
γ-Fe		60 ± 2	4·31 ± 0·02
Co	Wahlin (1942)	41	4·41
Co		60 ± 2	4·41 ± 0·02
Ni	Fox & Bowie (1933)	1380	5·03
Ni	Wahlin (1942)	30	4·61
Ni		120 ± 5	4·50 ± 0·02

The values of A and ϕ determined from the curves are collected together in table 1, along with the values obtained by the earlier workers for comparison. Where the authority is not indicated in column 2 the data given are those obtained from the present measurements. No measurements seem to have been made previously on the thermionic emission of Ti, V and Mn, which is understandable since these metals cannot be easily drawn into filaments suitable for use in the diode method.

References

Fox, G. W. & Bowie, R. M. 1933 *Phys. Rev.* **44**, 345.
Jain, S. C. & Krishnan, Sir K. S. 1952 *Proc. Roy. Soc.* A, **213**, 143.
Wahlin, H. B. 1942 *Phys. Rev.* **61**, 509.
Wahlin, H. B. 1948 *Phys. Rev.* **73**, 1458.

The Temperature Variation of the Thermodynamic Potential of a Degenerate Electron Gas

By Sir K. S. Krishnan, F.R.S.
National Physical Laboratory of India, New Delhi
and
P. G. Klemens
Division of Physics, Commonwealth Scientific and Industrial Research Organization, Sydney*

[Received August 25, 1952]

In the Fermi–Dirac distribution function, namely

$$f(E) = \frac{1}{e^{(E-\zeta)/kT}+1}, \quad \ldots\ldots\ldots \quad (1)$$

ζ, as is well known, is the thermodynamic potential, or the free energy at constant pressure, per electron, and is given by

$$\zeta = u - Ts + pv, \quad \ldots\ldots\ldots \quad (2)$$

where the letters have their usual significance. Obviously ζ is a function of the temperature, and is determined by the equation

$$n = 2\int_0^\infty N(E) f(E)\, dE, \quad \ldots\ldots\ldots \quad (3)$$

where n is the number of electrons per unit volume, and $N(E)$ is the density of energy states. For an almost completely degenerate gas, i.e. at temperatures $T \ll T_0$, where

$$T_0 = \zeta_0/k = \frac{h^2}{2mk}\left(\frac{3n}{8\pi}\right)^{2/3} \quad \ldots\ldots\ldots \quad (4)$$

is the degeneracy-temperature, the integration of (3) yields to a first approximation

$$\zeta = \zeta_0(1 - \gamma T^2/6), \quad \ldots\ldots\ldots \quad (5)$$

where

$$\gamma = \pi^2 k^2/2\zeta^2. \quad \ldots\ldots\ldots \quad (6)$$

* Communicated by the Authors.

Since the second term in (5) is merely a correction term, ζ appearing in the denominator of (6) may be replaced by ζ_0, or by ζ_0^*, which we shall define presently, which are both of nearly the same magnitude as ζ.

In expression (5) ζ_0 is frequently referred to as the value of ζ at $T=0$, and for that reason is sometimes regarded as independent of T, and hence the temperature variation of ζ is taken to be determined completely by the second term, which involves T explicitly. It is the main purpose of this note to emphasize that this will be the case only if the density of electrons n is kept constant, whereas at constant pressure the density n, and hence also ζ_0 as will be seen from (4), will vary with the temperature. In other words ζ_0 will not represent the free energy at the same pressure at $T=0$. The latter energy will be given by

$$\zeta_0^*=\zeta_0(1+\gamma T^2/3), \quad . \quad . \quad . \quad . \quad . \quad . \quad . \quad (7)$$

and the expression for the temperature variation of ζ at constant pressure will therefore be given by

$$\zeta=\zeta_0^*(1-\gamma T^2/2). \quad . \quad . \quad . \quad . \quad . \quad . \quad . \quad (8)$$

Physically $\zeta_0^*-\zeta$ has the following significance. Let ϕ_T be the thermionic work function, as usually defined, of a metal at temperature T. If the electrons in the metal, i.e. in the condensed phase, can be regarded as an almost completely degenerate assemblage, having a finite latent heat of evaporation, then the temperature variation of ϕ *due to the temperature variation of* ζ will be given by

$$\phi_T-\phi_0=\zeta_0^*-\zeta. \quad . \quad . \quad . \quad . \quad . \quad . \quad . \quad (9)$$

Incidentally it may be mentioned that thermodynamically

$$\zeta_0^*-\zeta=T\int_0^T\frac{c_p}{T}dT-\int_0^T c_p\,dT, \quad . \quad . \quad . \quad . \quad . \quad (10)$$

where c_p is the specific heat of the electrons in the condensed phase at constant pressure. In view of (8) and (10) one obtains

$$c_p=\gamma T, \quad . \quad . \quad . \quad . \quad . \quad . \quad . \quad . \quad (11)$$

which is the same expression as for c_v.

It should be mentioned here that if the electronic structure of the metal, instead of corresponding to a nearly empty parabolic band, as we have taken it to be till now, corresponds to a nearly full parabolic band, the expressions for c_p and c_v will remain the same as before, but will now refer to the holes, and hence $\zeta_0^*-\zeta$ in eqns. (8), (9) and (10) should be replaced by $\zeta-\zeta_0^*$. In other words ζ will now increase with the increase of the temperature, though the specific heats remain positive as they should.

That in a highly degenerate electron gas, the specific heat at constant pressure should be the same as that at constant volume can also be demonstrated otherwise. At higher temperatures naturally c_p will increase more rapidly than c_v, and they will tend to the values $\frac{5}{2}k$ and $\frac{3}{2}k$ respectively per electron.

The Polarization Fields and the Resonance Frequencies of the Alkali Halide Crystals

By Sir K. S. Krishnan, F.R.S., and S. K. Roy
National Physical Laboratory of India, New Delhi*

[Received August 7, 1952]

Abstract

The effect of the polarization field on the dielectric constant of a medium can be taken into account in two alternative ways, which are equivalent. It may be regarded as enhancing the actual field that produces the polarization, or as determining the resonance frequencies of the medium, which will be different from the frequencies of the individual oscillators that constitute the medium. The dispersions of the alkali halides are discussed from the latter point of view. Though the polarization factors defining the interactions between the infra-red oscillators have the Lorentz value $4\pi/3$, those defining the interactions of the *electronic* oscillators are found to be zero. The electronic overlap between the neighbouring ions in their equilibrium positions seems to be just the one that corresponds to negligible interactions between the electronic oscillators.

§1. Introduction

The part played by the polarization field in dielectric phenomena has been discussed in detail by Lorentz (1908), and following him by several authors. (For a good account of the subject see Debye 1928, Fröhlich 1949, or Rosenfeld 1951.) An obvious method of considering the influence of the polarization field on the dielectric constant is to regard the effective field that produces the polarization as including the polarization field in addition to 'the field in the medium', to which the polarization field will naturally be proportional. The result will be an enhanced susceptibility and a correspondingly enhanced dielectric constant. This method of calculating the effect of the polarization field is the one usually adopted.

The polarization field is also known (Krishnan and Roy 1951) to play an important part in determining the observed resonance frequencies of the medium. Hence its effect on the dielectric constant may also be regarded as exercised indirectly through its influence on the resonance frequencies. The dispersion of the dielectric constant of the alkali halide crystals is discussed in the present paper from the latter point of view. The alkali halides are particularly suitable for this purpose.

* Communicated by the Authors.

The point of view adopted here throws also some light on the relation between the different types of dispersion formulae, and in particular on the relation between the characteristic frequencies that appear in these formulae.

§ 2. The Effect of the Polarization Field on the Principal Lattice Oscillation of an Alkali Halide Crystal

In a recent paper (Krishnan and Roy 1951) the frequency of the principal mode of oscillation of an alkali halide crystal, in which the lattice of the alkali ions oscillates with respect to the lattice of the halide ions, was calculated on the basis of the simple Born model. It was found that the electric polarization of the crystal due to the separation of the charges accompanying the oscillation, plays an important part in determining the frequency. Separating the two lattices by a small distance r one can obviously express the potential energy of the crystal thus deformed as a power series in r, in which owing to the centre of symmetry of the lattice points of the undeformed crystal, terms involving odd powers of r will naturally be absent. We shall confine attention at present to the r^2 term, which is the first non-vanishing, and also the predominant, term involving r, and which determines the frequency. We shall denote this term in the potential energy per *pair* of ions by

$$W=ar^2=\tfrac{1}{2}\mu\omega_i^2 r^2, \quad \ldots\ldots\ldots \quad (1)$$

where μ is the reduced mass of the pair given by $1/\mu=1/m_1+1/m_2$ and m_1 and m_2 are the masses of the two ions, and ω_i is the angular frequency of the principal mode of oscillation.

The essential part of the problem is to evaluate the contributions to a from the different types of interactions. This has been done in the paper referred to, and we shall merely quote here the relevant results. It will be seen immediately, in view of the centre of symmetry of all the lattice points, that the electrostatic interactions contribute nothing to a. As regards the repulsion interactions, they may be taken to be of the form $Ae^{-R/\rho}$, where R is the distance between the interacting ions, and they are of short range, since ρ is found to be much shorter than the equilibrium distance d between the neighbouring ions. Hence these interactions may be regarded as confined to the immediate neighbours only. Their contribution to a is found to be equal to

$$\frac{3}{2N\beta d^2}=\frac{\alpha e^2(\delta-2)}{6d^3}=a_1 \text{ say}, \quad \ldots\ldots \quad (2)$$

where N is the number of ion-pairs per unit volume, β is the compressibility of the crystal, α is the Madelung constant, d is the equilibrium distance between neighbouring ions, $\delta=d/\rho$ and e is the electronic charge. The interactions of the van der Waals type involving the dipole moments induced in the ions contribute relatively little to a, and they are neglected throughout.

Had a_1 been the *whole* of the contribution to a, the frequency of the principal lattice oscillation of the crystal would be given by

$$a_1=\tfrac{1}{2}\mu\Omega_i^2. \quad \ldots\ldots\ldots \quad (3)$$

But actually the contribution to a from the polarization field is considerable. For a given relative displacement r between the two lattices the polarization per unit volume is given by

$$P=Ner. \quad \ldots\ldots\ldots \quad (4)$$

In the paper referred to it was shown (1) that owing to the electronic overlap between the neighbouring ions, this polarization does not induce any *electronic* polarization in the ions, and (2) that the polarization field acting on an ion and tending to displace it as a whole, has just the Lorentz value, namely $(4\pi/3)P$, and hence (3) that the corresponding contribution to a is given by

$$a_2=-\tfrac{2}{3}\pi Ne^2. \quad \ldots\ldots\ldots \quad (5)$$

This term is negative since the polarization field is in a direction that tends to *increase* the relative displacement r between the two lattices.

In NaCl, for example, a_2 is found to be numerically nearly half of a_1 and since they are of opposite signs, a_2 is of almost the same magnitude as a, the net coefficient of the r^2 term, namely

$$a=a_1+a_2. \quad \ldots\ldots\ldots \quad (6)$$

For most of the alkali halide crystals the frequency ω_i calculated in this manner by taking the polarization field into account, agrees well with the observed reststrahlen frequency (Krishnan and Roy 1951).

§3. The Magnitude of the Polarization Field

As is well known the internal field F in a dielectric may differ considerably from the field E in the medium, the difference between them being the polarization field

$$F=E+p\chi E, \quad \ldots\ldots\ldots \quad (7)$$

in which χ is the susceptibility of the medium, i.e., the polarization per unit volume per unit field in the medium, and p is the polarization factor, which is rather difficult to evaluate except under certain simple conditions. When the elementary dipoles in the medium, which together make up the polarization of the medium, are *point*-dipoles, and when they are arranged in a cubic lattice, or are distributed at random, p, as Lorentz has shown, will be equal to $4\pi/3$ (see also Van Vleck 1937).

But actually, as was shown in the paper referred to, the dipoles concerned in refraction phenomena, for which Lorentz's theory was originally intended to apply, are by no means point-dipoles; they are due primarily to the displacement of the electrons in an atom with respect to its positively charged nucleus, and the separation of charges will be of atomic dimensions, and comparable with the distances between neighbouring dipoles. Thus the Lorentz polarization factor $p=4\pi/3$ may fail

just where it was originally intended to apply, namely to electronic polarization as is involved in refraction phenomena in the visible and in the ultra-violet regions of the spectrum. But the polarization produced in ionic crystals like the alkali halides by a small relative displacement of the two lattices, with which we are concerned here, is in a different category altogether, since we can now regard the polarization as due to dipoles of small dimensions of the order of r located at the lattice points. This can be readily seen from the following considerations. Electrostatically the effect of deforming the original lattice, which we shall designate by A, into B will be equivalent to superposing on A the following two lattices: the lattice A' obtained from A by changing the signs of all the ions in it, and the lattice B. The superposition of A' and B will be equivalent to locating a small dipole of moment er at each of the positive, *or* each of the negative lattice points, which again will be equivalent to locating a dipole $er/2$ at every lattice point, whether positive or negative. Since r can be made as small as we desire, these dipoles will be practically point-dipoles, and the corresponding polarization factor p will therefore be expected to approximate closely to the Lorentz value $4\pi/3$, and this is just the value which we have used in the calculation of ω_i and which, as we mentioned, is confirmed experimentally.

§4. The Resonance Frequency of an Assemblage of Harmonic Oscillators

Coming back to the calculation of the energy ar^2 per pair of ions from which the resonance frequency ω_i of the crystal is evaluated using relation (1), it may appear at first sight that when the electrostatic interactions between all the ions of the positive and the negative lattices displaced relatively to each other by r are taken into account, the effect of the polarization field also, which is a direct result of this displacement, gets included in it automatically, and it should not therefore be necessary to invoke separately the effect of the polarization field. But actually the necessity arises from the following circumstance. It was shown just now that separating the two lattices by a small distance r is equivalent to developing small dipoles at the lattice points. The oscillating crystal will be equivalent to harmonic oscillators, all of the same moment, located one at each of the lattice points of the crystal. The frequency Ω_i which we would have obtained from a_1 with the help of relation (3), i.e. the frequency which we would have obtained by ignoring the polarization field, would be the frequency of these *individual* oscillators, whereas the frequency ω_i that we are trying to calculate is the resonance frequency of the assemblage of these oscillators, which will be different from Ω_i, and the difference is determined by the polarization field. (That Ω_i is itself dependent on the density of the medium does not affect the argument.)

Anticipating the results concerning the energies associated with the polarization of the medium to be given in § 6, we may mention immediately that

$$Nar^2=\tfrac{1}{2}N\mu\omega_i^2r^2=\tfrac{1}{2}PE,$$

where E is the field in the medium, whereas the energy that is obtained from the Coulomb and the repulsion interactions is equal to $PF/2$, where F is the internal field, which includes in addition to E the polarization field pP. Hence one has to subtract from Na_1r^2 the work done by the polarization field, namely $pP^2/2$ $(=2\pi P^2/3$ in the case of the alkali halides), before it can be equated to $\frac{1}{2}N\mu\omega_i^2r^2$.

§5. The Dielectric Constant of the Crystal and the Drude and the Lorentz Formulae

Let us for the present ignore the electronic polarization, i.e. the polarization due to the displacements of the electrons in the ions with reference to their respective nuclei, and regard the medium as consisting of ions that can only be bodily displaced. For any given relative displacement r of the positive and the negative lattices the polarization per unit volume will be given by (4), namely $P=Ner$. This polarization may also be regarded as produced by a field E in the medium, such that

$$Ee=2ar=\mu\omega_i^2r. \qquad (8)$$

The corresponding internal field F will be given by

$$Fe=Ee+\frac{4\pi}{3}Ne^2r=2a_1r=\mu\Omega_i^2r, \qquad (9)$$

where, as we have seen, Ω_i is the frequency which we would have obtained for the principal oscillation of the crystal if we had neglected the effect of the polarization field, as distinguished from the actual resonance frequency ω_i.

It will be seen from (8) that the susceptibility χ_0 of the medium for static electric fields will be given by

$$\epsilon_0-1=4\pi\chi_0=\frac{C_i}{\omega_i^2}, \qquad (10)$$

where

$$C_i=\frac{4\pi Ne^2}{\mu} \qquad (11)$$

and ϵ_0 is the corresponding dielectric constant. Equation (10) can be readily identified with the well-known expression of Born's (see *Handbuch der Physik*). The two frequencies Ω_i and ω_i are connected by the relation

$$\Omega_i^2=\omega_i^2+\frac{C_i}{3}, \qquad (12)$$

or

$$\Omega_i^2=\omega_i^2\frac{\epsilon_0+2}{3}. \qquad (13)$$

Similarly

$$\left.\begin{aligned} a_1&=a\frac{\epsilon_0+2}{3},\\ a_2&=-a\frac{\epsilon_0-1}{3}. \end{aligned}\right\} \qquad (14)$$

Hence eqn. (10) can also be written in the form

$$\frac{\epsilon_0-1}{\epsilon_0+2}=\frac{C_i/3}{\Omega_i^2}. \quad . \quad . \quad . \quad . \quad . \quad . \quad . \quad . \quad . \quad (15)$$

Similarly the dielectric constant at any frequency ω can be expressed either in the form

$$\epsilon_\omega-1=\frac{C_i}{\omega_i^2-\omega^2} \quad . \quad . \quad . \quad . \quad . \quad . \quad . \quad . \quad . \quad (16)$$

or, in view of (12), in the form

$$\frac{\epsilon_\omega-1}{\epsilon_\omega+2}=\frac{C_i/3}{\Omega_i^2-\omega^2}, \quad . \quad . \quad . \quad . \quad . \quad . \quad . \quad . \quad (17)$$

which are indeed identical relations (Livens 1912).

Just as the equivalence of (10) and (15) is based on relation (13), the equivalence of (16) and (17) corresponds to a relation which is analogous to (13), and which is a corollary to it, when we are concerned, as we are now, with only one frequency that influences the polarization, the relation being

$$\Omega_i^2-\omega^2=(\omega_i^2-\omega^2)\frac{\epsilon_\omega+2}{3}. \quad . \quad . \quad . \quad . \quad . \quad . \quad . \quad (18)$$

It can be readily seen that (16) and (17) reduce to (10) and (15) respectively when $\omega\to 0$.

In (16) resonance occurs obviously when $\omega=\omega_i$ and in (17) when the right hand side tends to unity, i.e. when $\Omega_i^2-\omega^2=C_i/3$ which in view of (12) corresponds again to $\omega=\omega_i$ as it should.

One may thus take into account the effect of the polarization field on the dielectric constant explicitly by taking the field that is effective in producing the polarization as $(1-4\pi\chi_\omega/3)$ times E or $(\epsilon_\omega+2)E/3$ where E is the field in the medium, in which case the formula obtained is of the Lorentz type, and the characteristic frequency appearing in the expression is the frequency Ω_i; or *alternatively*, one may regard the effect of the polarization field as confined to changing Ω_i to the actual resonance frequency of the crystal ω_i such that the relation (18) is satisfied, in which case the formula is of the Drude type.

§6. The Electric Fields Associated with the Separation of the Lattices

Now the potential energy Nar^2 per unit volume, due to separating the two lattices by a small distance r can also be regarded as due to the incidence of a 'field E in the medium' such that eqn. (8) is satisfied, or such that

$$Nar^2=\frac{E^2}{8\pi}(\epsilon_0-1)$$

$$=\tfrac{1}{2}EP. \quad . \quad . \quad . \quad . \quad . \quad . \quad . \quad . \quad (19)$$

Similarly

$$Na_1r^2=\tfrac{1}{2}FP, \quad . \quad . \quad . \quad . \quad . \quad . \quad . \quad . \quad (20)$$

and the energy per unit volume associated with the occurrence of the polarization field will be given by

$$Na_2r^2=-\tfrac{1}{2}pP^2, \quad . \quad . \quad . \quad . \quad . \quad . \quad . \quad . \quad (21)$$

where pP is the polarization field. In the alkali halides, as we have seen, $p=4\pi/3$.

As is well known, the field in the medium E at any given lattice point O includes not only the field due to all the surrounding dipoles, but also a certain averaged field at O due to the dipole at O also, i.e., the averaged self-field of the dipole at O also, whereas the inner field F does not include the latter (Fröhlich 1949). Though we refer to the latter field for convenience as the self-field, it depends very much on the polarization of the surroundings, which will be realized immediately when we remember that the self-field will be just compensated by the field that would obtain at the point O in the cavity produced by removing from the medium the doublet located at O.

Now the effect at O of all the dipoles including the one at O will be equivalent to the field at O due to the charges developed on the surface of the medium due to polarizing it. Hence the averaged self-field of the doublet at O will be just the difference between the field at O due to the charges developed on the surface of the medium as a result of polarizing it, and the field at the same point due to all the surrounding dipoles in the medium. Since the difference between F and E is the polarization field, the latter field can be regarded as equal to the averaged self-field, but of opposite sign to it.

Now the self-field of a dipole should depend only on the fine structure of the medium, and in particular should be independent of the external shape. One may, therefore, use any convenient shape like a sphere or an infinite parallel plate, and show that the self-field is equal to

$$-\left(\frac{4\pi}{3}+f\right)P=-pP, \quad . \quad . \quad . \quad . \quad . \quad . \quad . \quad (22)$$

where fP is the field at O due to all the surrounding doublets in an infinite medium. In the case of the alkali halides f will obviously be zero.

§7. The Dispersion Formulae for a Dense Medium

We have specifically discussed till now the case when the only frequency affecting the dielectric constant is that of the principal lattice oscillation of the crystal. One good reason for confining ourselves to this case is that the polarization factor involved here is very definite, and is known to be equal to $4\pi/3$. But the main results obtained are applicable equally well to the case when the medium has more than one resonance frequency, and when some or all of these are electronic frequencies, instead of lattice frequencies. Let us denote these frequencies and the physical constants associated with them by the subscripts $i, j, k, \ldots n$. The polarization factor p_{ij} defining the polarization field acting on any oscillator i due

to the dipole moments of all the oscillators j in the medium will not in general be equal to $4\pi/3$ but will depend on both i and j. The dielectric constant of the medium will then be given by

$$\epsilon-1=4\pi\chi=4\pi\Sigma_i\chi_i, \quad \ldots\ldots\ldots \quad (23)$$

where χ_i is the contribution to the susceptibility, i.e. to the polarization per unit volume per unit field in the medium, from the oscillators of type i.

$$4\pi\chi_i=\frac{C_i}{\Omega_i^2-\omega^2}(1+\Sigma_j p_{ij}\chi_{ij}), \quad \ldots\ldots\ldots \quad (24)$$

in which the summation extends over all values of j namely $i, j, \ldots n$.

$$C_i=\frac{4\pi n_i f_i e^2}{\mu_i}, \quad \ldots\ldots\ldots \quad (25)$$

where n_i is the number of oscillators of type i present per unit volume of the medium, f_i is the oscillator strength, and μ_i is the effective mass of the oscillator. Ω_i is the frequency of the oscillator in the free state, to be more precise, the frequency which it will have if the influence of the interactions of the surrounding dipoles is eliminated.

In the special case when all the p_{ij}'s have the same value, say p, eqns. (23) and (24) reduce to

$$\frac{\epsilon-1}{\epsilon+\alpha}=\Sigma_i\frac{B_i}{\Omega_i^2-\omega^2}, \quad \ldots\ldots\ldots \quad (26)$$

where

$$B_i=\frac{pC_i}{4\pi};\ \alpha=\frac{4\pi}{p}-1. \quad \ldots\ldots\ldots \quad (27)$$

When further all the polarization factors have just the Lorentz value, namely $p=4\pi/3$, it will be seen from (27) that α reduces to 2, and eqn. (26) to the well-known Lorentz formula.

Herzfeld and Wolf (1925) have shown that the simple Lorentz formula

$$\frac{\epsilon-1}{\epsilon+2}=\Sigma_i\frac{B_i}{\Omega_i^2-\omega^2}, \quad \ldots\ldots\ldots \quad (28)$$

is mathematically convertible into the Drude formula

$$\epsilon-1=\Sigma_i\frac{C_i}{\omega_i^2-\omega^2} \quad \ldots\ldots\ldots \quad (29)$$

and *vice versa*. Using the same method it can be readily shown that the more general formula corresponding to (23) and (24) in which the polarization factors p_{ij} may all be different, can also be reduced to the Drude formula (28) or to the simple Lorentz formula, and conversely the Drude or the simple Lorentz formula can also be transformed to a formula of the type (24), *with any specified values of* p_{ij}.

It will be seen immediately, whatever may be the actual polarization fields that may obtain in the medium, and even if there is no polarization field at all, that the dispersion data can be fitted, as may be desired, into

a Drude formula, or a simple Lorentz formula, or a generalized Lorentz formula of the type (23) and (24) with any postulated set of polarization factors p_{ij}. The characteristic frequencies that appear in these alternative formulae with which the same set of observational data can be fitted, will naturally be different; those that appear in the Drude formula will be the actual resonance frequencies ω_i of the medium, and in the other formulae the frequencies will differ from ω_i by amounts which are determined by the polarization fields postulated on which the formulae are based. Hence dispersion data by themselves can yield information regarding only the resonance frequencies of the medium and their oscillator strengths, and none at all regarding the polarization field.

It may not be out of place here to emphasise these results. Though the mathematical equivalence of the Drude and the simple Lorentz formulae, which was demonstrated long ago by Herzfeld and Wolf, is generally conceded, the agreement between the characteristic frequencies appearing in these formulae, and the observed absorption frequencies is sometimes invoked in order to decide between the alternative formulae as regards their experimental validity. On considerations of convenience, the Drude dispersion formula, in which the characteristic frequencies that appear are also the observed absorption frequencies, is naturally preferable to any alternative formulae, but the latter formulae too should be regarded as having the same experimental validity as Drude's.

It should be mentioned immediately that the equivalence between the different alternative formulae relates to the formulation of the dielectric constant as a function of the frequency of the incident electromagnetic waves, with which we are concerned here, and *does not extend to the expressions for the dielectric constant as a function of the density of the medium*. Since the polarization field will depend on the density the latter formula will be conditioned by the actual polarization field. Even here, the frequencies Ω_i of the individual oscillators, and the polarization field factors p_{ij} may also be dependent on the degree of close-packing. We shall postpone consideration of these aspects to a later section of the paper.

§8. The Case of the Alkali Halides.

The case of the alkali halides is exceptional, as we have mentioned already. The only infra-red resonance frequency that is involved in the dispersion formula is that of the principal lattice oscillation of the crystal. Making the subscript i refer to this frequency, p_{ii} as we have seen, has just the Lorentz value $4\pi/3$. The other frequencies, denoted by the subscripts $j, k, \ldots$, will all be electronic and the separation of the charges in the corresponding dipoles will be comparable with the distance between the neighbouring ions. Hence the distribution of the field in the neighbourhood of any of the latter dipoles will differ considerably from that of a point-dipole. Indeed, even the order of magnitude of the field may become different when the approach to the dipole is close.

In other words, when there is considerable overlap of the electronic clouds of neighbouring ions, as is the case with the neighbouring ions in the alkali halide crystals, the polarization factors of the type p_{ij}, p_{ik}, . . . will be much less than $p_{ii}=4\pi/3$, and the factors p_{jj}, p_{kk}, . . . may be still smaller.

In the paper referred to, it was shown that in the alkali halides all the p's except p_{ii} have practically zero values. This circumstance, namely, that only one of the p's has a finite value, and the rest have zero value renders the case of the alkali halides exceptional.

The expression for the dielectric constant of these halides will, therefore, be of the form

$$\epsilon_\omega-1=\frac{C_i}{\omega_i^2-\omega^2}+\sum_j\frac{C_j}{\omega_j^2-\omega^2}, \quad . \quad . \quad . \quad . \quad . \quad . \quad (30)$$

where the electronic resonance frequencies ω_j, ω_k, . . . will be practically the same as for the individual (not isolated) atoms, namely, Ω_j, Ω_k, . . . respectively, whereas the lattice frequency ω_i will naturally be very different from Ω_i.

In particular, in the region of very long wavelengths in which the contribution to the dispersion from the electronic frequencies, namely

$$n_\omega^2-1=\sum_j\frac{C_j}{\omega_j^2-\omega^2}, \quad . \quad . \quad . \quad . \quad . \quad . \quad . \quad . \quad (31)$$

is practically independent of ω, and is nearly the same as for $\omega=0$, we obtain

$$\epsilon_\omega-n_0^2=\frac{C_i}{\omega_i^2-\omega^2}, \quad . \quad . \quad . \quad . \quad . \quad . \quad . \quad . \quad (32)$$

or alternatively,

$$\frac{\epsilon_\omega-n_0^2}{\epsilon_\omega-n_0^2+3}=\frac{C_i/3}{\Omega_i^2-\omega^2}, \quad . \quad . \quad . \quad . \quad . \quad . \quad . \quad (33)$$

the relation between Ω_i and ω_i being given as before (see (12) and (13)) by

$$\Omega_i^2=\omega_i^2+\frac{C_i}{3}=\omega_i^2\left(\frac{\epsilon_0-n_0^2+3}{3}\right). \quad . \quad . \quad . \quad . \quad (34)$$

In particular one obtains from (31) for the dielectric constant in a static field, the well-known expression of Born

$$\epsilon_0=n_0^2+\frac{C_i}{\omega_i^2}. \quad . \quad . \quad . \quad . \quad . \quad . \quad . \quad . \quad (35)$$

§ 9. Discussion of the Available Experimental Data

The available experimental data for the refractive indices of the alkali halides, which extend over a wide spectral range, have been discussed by Herzfeld and Wolf (1925), by Fuchs and Wolf (1928), and more recently by Ramachandran (1947) and by Radhakrishnan (1948). Attention may be drawn in particular to the following results.

(1) When the data are fitted into a dispersion formula of the Drude type, the characteristic frequencies that appear in the formulae are found to agree well with the observed resonance frequencies. Since the fitting is done empirically, it will be more correct to say that the available experimental data can be fitted satisfactorily into a Drude dispersion formula, using the *observed* resonance frequencies of the crystal as the characteristic ones that should appear in the formula. For details regarding the fitting with the experimental data reference may be made to the original papers. The formula in general, involves three frequencies in the far ultra-violet, and the principal lattice frequency in the infra-red.

(2) Since the only infra-red frequency involved in the formula is that of the principal lattice oscillation of the crystal the corresponding oscillator strength C_i will be that defined by (16), and given by (11). Hence it will be possible to compare the values of C_i calculated from (11) with the numerical values appearing in the empirical formulae given by Ramachandran and Radhakrishnan. They are collected together in table 1 which includes all the crystals for which experimental dispersion formulae are available.

Table 1

Crystal	LiF	NaF	NaCl	KCl	KBr
$C_i\times10^{-26}$ from (11)	210	68	28	15	10
$C_i\times10^{-26}$ from dispersion	230	74	33	18	11

(3) Now the measurements on dispersion usually extend at the infra-red end to about 22 μ for some of the crystals, and to about 9 μ only for most others. Since even at the former limit the contribution to n^2-1 from the infra-red term in the dispersion formula is very small, the experimental value of C_i appearing in the infra-red terms is slightly uncertain, except where the value of the dielectric constant for either steady fields or for the usual radio frequencies has also been utilized in determining the constants of the dispersion formula. Actually this has been done only for a few crystals, by Radhakrishnan. Hence it will be of interest to compare the calculated and observed values of $k_0-n_0^2$ in which k_0 is the dielectric constant for static fields, and n_0^2 is the square of the refractive index extrapolated to $\omega\rightarrow0$. The experimental value of n_0^2 is readily obtained from the dispersion formula by taking the contributions at $\omega=0$ from all the terms except the infra-red one. The experimental values of $k_0-n_0^2$ thus calculated are given in table 2 along with the values calculated from (34), in which we have used for the frequency of the principal lattice oscillation of the crystal the values calculated by us in an earlier paper, on the basis of Born's model, from

the known Coulomb and repulsion interactions between the ions (Krishnan and Roy 1951). The value as was shown in the paper agrees well with the observed reststrahlen frequency.

Table 2

Crystals	k_0	n_0^2	$k_0-n_0^2=Ne^2/\pi\mu\nu^2$	
			Observed	Calculated
LiF	9·3	1·9	7·4	7·6
NaF	6·0	1·7	4·3	4·5
NaCl	5·6	2·3	3·3	3·2
KCl	4·7	2·2	2·5	2·4
KBr	4·8	2·4	2·4	2·2

§10. Dependence on Density

Extensive data are also available for the temperature variation of the refractive index of the alkali halides, and for some of them for the variation of the refractive index with the density also. One may therefore compare the observed values of $(\partial n/\partial t)$ and $-\rho(\partial n/\partial\rho)\alpha$ where α is the coefficient of thermal expansion, in order to find whether the change of refractive index with temperature is due wholly to the change of density accompanying the temperature change, or whether there is in addition a pure temperature effect due to the thermal agitations of the ions. From the values of $\partial n/\partial t$ and of $-\alpha\rho(\partial n/\partial\rho)$ given in table 3 it will be seen that the pure temperature effect, if any, is practically negligible.

Table 3

Crystals	$10^5\alpha$	$\rho(\partial n/\partial\rho)$	$10^5(dn/dt)$	
			Observed	Calculated
NaCl	12·0	0·24	−3·8	−2·9
KCl	11·4	0·23	−3·6	−2·6
KBr	12·0	0·35	−3·6	−4·2
KI	13·5	0·43	−5·0	−5·8

Now the available data for the temperature variation of the refractive index which extend from the extreme quartz ultra-violet to the infra-red

in most crystals, have been analysed by Ramachandran and by Radhakrishnan. They find that the temperature variation can be expressed empirically in the form*

$$2n\frac{dn}{dt}=-\alpha(n^2-1)+\Sigma\frac{2C_j\psi_j}{(\omega_j^2-\omega^2)^2}+\frac{2C_i\psi_i}{(\omega_i^2-\omega^2)^2}+\frac{D}{\omega_i^2-\omega^2}, \quad . \quad (36)$$

where

$$\psi_j=-\omega_j\frac{\partial\omega_j}{\partial t}. \quad . \quad . \quad . \quad . \quad . \quad . \quad . \quad . \quad . \quad (37)$$

The first term on the right hand side of (36) is due directly to the change in density, since the expression for n^2-1 will contain a factor proportional to ρ, and this term accounts for the bulk of the temperature variation. Attention may be drawn here to the extra term involving the infra-red frequency and proportional to $1/(\omega_i^2-\omega^2)$.

We have referred to the experimental finding that in the alkali halides all the polarization factors are zero except p_{ii}, which is equal to $4\pi/3$. Any change of density is not likely to affect p_{ii}. If the other factors also remain unchanged, i.e. continue to be zero, it will be difficult to explain either the change in the ω_i's suggested by the analysis of the experimental data, or the extra infra-red term proportional to $1/(\omega_i^2-\omega^2)$ which corresponds to a change of the oscillator strength with temperature. The obvious inference is that though all the p's except p_{ii} are quite small, their variations with density, and therefore also with temperature, are considerable. Further the form of the empirical formula suggests that coefficients of the type $(\partial p_{jj}/\partial t)$, $(\partial p_{kk}/\partial t)$ . . . relating to the interactions of the electronic oscillators of the same frequency, and terms like $\partial p_{ii}/\partial t$ which define the interaction of the infra-red frequency with the other frequencies, are the predominant ones. These differential coefficients can be calculated from the experimental data. We shall merely mention that $\partial p/\partial t$ is of the order of 10^{-4}.

§11. Further Remarks on the Electronic Overlap of the Neighbouring Ions

In the previous sections the effect of the electronic overlap between the neighbouring ions has been regarded as affecting the polarization field, and rendering it almost nothing when the ions are at their equilibrium positions. Alternatively, the effect of the overlap can also be regarded as reducing the effective charge on an ion from e to fe where f is a factor which is determined by the degree of overlap, and is less than unity, while the polarization field is allowed to have the Lorentz value (Fröhlich 1949). The former point of view, in which the overlap is regarded as reducing the polarization field to nothing, has certain advantages over the alternative point of view, and has therefore been adopted here.

* Actually these authors use wave-lengths instead of frequencies, but the latter are used here for convenience.

That in all the alkali halides the electronic polarization field is found to be practically zero when the ions are at their equilibrium positions may be theoretically significant. According to the simple Born model on which the foregoing discussions are based, the ions in the lattice are held in their equilibrium positions by the Coulomb electrostatic interactions between the charges carried by the ions, and the repulsion interactions between the neighbouring ions. When the ions have taken their equilibrium positions under the corresponding attractive and repulsive forces respectively, there will be a certain optimum overlap between the neighbouring ions, and this overlap is apparently also the one that corresponds to zero polarization field. This view receives strong support from the observation referred to in the previous section, namely this: though the polarization field is zero for the equilibrium positions of the ions, it varies rapidly about this value with change of density.

References

Born, M., and Mayer, G. M., 1933, *Handbuch der Physik*, **24/2**, 623.
Debye, P., 1928, *Polar Molecules* (New York: Dover Publication).
Fröhlich, H., 1949, *Theory of Dielectrics* (Oxford: Clarendon Press), pp. 21–36.
Herzfeld, F. F., and Wolf, K. L., 1925, *Ann. d. Physik*, **78**, 35.
Krishnan, K. S., and Roy, S. K., 1951, *Proc. Roy. Soc.* A, **207**, 447.
Livens, G. H., 1912, *Phil. Mag.*, **24**, 268.
Lorentz, H. A., 1908, *Theory of Electrons* (Leipzig: Teubner), Section 117 and note 54.
Radhakrishnan, T., 1948, *Proc. Ind. Acad. Sci.* A, **27**, 165.
Ramachandran, G. N., 1947, *Proc. Ind. Acad. Sci.* A, **25**, 481.
Rosenfeld, L., 1951, *Theory of Electrons* (Amsterdam: North Holland Publishing Co.).
Van Vleck, J. H., 1937, *J. Chem. Phys.*, **5**, 556.

Thermionic constants of metals and semiconductors
III. Monovalent metals

By S. C. Jain and Sir K. S. Krishnan, F.R.S.
National Physical Laboratory of India, New Delhi

(*Received 22 December* 1952)

In this part are described measurements on the thermionic constants of the monovalent metals copper, silver and gold, made by the effusion method. Owing to the low melting-points of these metals, and the consequent low vapour pressure of the electron gas in thermal equilibrium with them, the effusion holes used had to be much larger than in the measurements with the other metals. The maximum size of the effusion hole that can be used with an electron gas chamber of given dimensions without disturbing appreciably the equilibrium condition in the chamber, and the effect of the large size of the effusion hole on the saturation current, are discussed in some detail.

For all the three metals, the A coefficient in Richardson's equation for thermionic emission is found to be only slightly short of the theoretical value of 120 amp cm^{-2} deg^{-2}. This experimental finding is of significance, since the lowering of the thermodynamic potential of the degenerate electron assemblage in these metals, consequent on the thermal expansion of the metal, is considerable.

1. Introduction

In the earlier parts of this work (Jain & Krishnan 1952*a*, *b*) was described a new method for determining the thermionic constants of metals, which is based on measuring the rate of effusion of electrons through a small hole, from a chamber of electron gas in thermal equilibrium with the metal. The chamber is made from a thin-walled tube of graphite, and its inner walls (and the region adjoining the effusion hole) are coated completely with the metal to be studied. The chamber can be heated to any desired high temperature *in vacuo* by sending a suitable heavy electric current through the tube. In this part are described measurements on the monovalent metals copper, silver and gold, made by the same method. Since the conduction electrons in these metals are highly degenerate at all working temperatures, and they approximate closely to the model of a free-electron gas, the thermionic constants of these metals, and in particular the A coefficients in the Richardson equation for thermionic emission, are of special theoretical interest.

All the metals whose thermionic constants were determined earlier by this method were studied at high temperatures, up to about 1600° K, and this was possible because of their high melting-points. The metals studied in this part, however, have much lower melting-points, and since their thermionic constants are of the same order of magnitude as in the former metals, they have much lower electronic vapour pressures in the range of temperatures over which they can be studied. This necessitates certain modifications in the experimental technique, and these modifications raise questions regarding the maximum size of the effusion hole that can be used with a chamber of given dimensions without disturbing appreciably the equilibrium in the chamber, and also regarding the effect of a large effusion hole on

the magnitude of the saturation current. These questions also are discussed in this part.

It may be mentioned here that the usual diode method is particularly unsuitable for determining the thermionic constants of metals having low melting-points. Their surfaces have to be degassed by repeated heating before the thermionic emissions from them settle down to their proper values, and the heat treatment for degassing becomes efficient only at very high temperatures. On the other hand, the present method, as we have shown in parts I and II, is quite insensitive to surface adsorption.

It may be mentioned here that the actual vapour pressure of the electrons in the chamber is very small; and the effusion is into vacuum where the pressure of the residual gas also is very small. The mean free paths in both are much larger than the over-all dimensions of the apparatus. Hence the equilibrium in the electron gas chamber is maintained through collisions with the inner walls of the chamber, in much the same manner in which the density of electromagnetic radiations inside a hot chamber is maintained.

2. Modifications required in the experimental technique

In the measurements reported in parts I and II, the chamber containing the electron gas was a cylinder of internal diameter 11·6 mm and of length about 30 mm. The effusion hole was circular and had a diameter of about 2·4 mm. A metal plate having a circular aperture of about 20 mm diameter, and placed at a distance of about 20 mm from the effusion hole, and coaxial with it, served to restrict the solid angle of effusion electrons reaching the Faraday cylinder to about $\frac{1}{2}\pi$ about the axis of the effusion hole. The metal plate bearing the diaphragm was kept in electrical contact with the graphite tube, so as to keep the region between the effusion hole and the metal diaphragm field-free. The dimensions given above varied slightly in the different measurements, but they serve to give an idea of the order of magnitude of these quantities in the previous experimental arrangement.

By applying a difference of potential between the Faraday cylinder and the diaphragm, the effusion electrons are collected in the cylinder. As was mentioned in part I, the current through the Faraday cylinder increases at first rapidly, and then slowly and linearly, with the increase of the applied voltage. It is therefore possible to extrapolate backwards from the linear portion, and obtain with accuracy the saturation current corresponding to effusion under zero applied potential.

For the monovalent metals studied here, whose work functions are in the range of 4·3 to 4·5 eV, and whose A coefficients have nearly the theoretical value of 120 amp $cm^{-2} deg^{-2}$, the lowest temperature at which the saturation current corresponding to effusion can be measured with some precision with the dimensions given above for the effusion hole and for the solid angle of collection, is about 1350° K. Now, the melting-points of the monovalent metals studied in the present part are of this magnitude, and in order to be able to measure the saturation currents with accuracy it therefore becomes necessary to enlarge considerably either the solid angle of collection, or the size of the effusion hole. Enlarging the solid angle does not help much, but on the other hand introduces uncertainties regarding the

penetration of the applied field into the region behind the metal diaphragm, and consequently also uncertainties in the effective solid angle of effusion of the electrons collected by the Faraday cylinder. One has therefore to depend on enlarging the effusion hole, and this necessitates a corresponding enlargement of the size of the chamber containing the saturated electron gas from which effusion takes place.

We may mention immediately the dimensions of the apparatus finally adopted in the present measurements, with which the currents through the Faraday cylinder could be measured accurately in the range of temperatures studied. The cylindrical chamber had an internal diameter of 46 mm and a length of 100 mm, and the effusion hole was a circle of diameter 16 mm. These dimensions correspond to a total area W of the inner walls of the chamber about 87 times the area s of the effusion hole. Though the temperature range over which the present measurements extend is lower than in the measurements on the other metals, owing to the enlarged dimensions of the chamber, the electric current needed for heating was much heavier, namely 400 to 450 amp, as compared with about 250 amp in the previous measurements.

3. Effect of the large size of the effusion hole on the saturation current

The use of a large effusion hole raises immediately two important points for consideration. First, how large can the effusion hole be in relation to the dimensions of the chamber without the saturation pressure of the electron gas in the chamber being disturbed by too rapid an effusion? This will be considered in detail in the next section. The other point is a geometrical one, and arises in the following manner. As we have seen, the effusion electrons collected by the chamber are restricted by an aperture of radius r_0 in a metal plate kept at a distance d from the plane of the effusion hole. As long as the effusion hole is small, the saturation current corresponding to the electrons passing through the restricting diaphragm and reaching the Faraday cylinder, will naturally be proportional to the area s of the effusion hole. This will not, however, be the case when this area is not small, as we shall see presently.

Now the rate of effusion of electrons from any given small element of area, per unit solid angle, at an angle θ to the normal to the plane of the effusion hole, is known to be proportional to $\cos\theta$. Let i be the saturation electric current corresponding to effusion per second, per unit area of the effusion hole, *over all directions*, i.e. over the whole of the 2π solid angle, corresponding to the range $\theta = 0$ to $\frac{1}{2}\pi$. This will be the current occurring in the Richardson equation

$$i = AT^2 e^{-\phi/kT}. \qquad (1)$$

As a result of the cosine law, the corresponding value for effusion per unit area *per unit solid angle* along a direction θ will obviously be $(i/\pi)\cos\theta$.

Let I be the saturation current actually observed, which will correspond to effusion from the whole area of the effusion hole, the effusion being confined to directions restricted by the diaphragm used. *If the area s of the effusion hole is small* and the hole is on the axis of the circular diaphragm, as was the case in the measure-

ments described in parts I and II, one can immediately see (see equation (14) of part I) that

$$I = \frac{is}{\pi}\int \cos\theta\,\mathrm{d}\omega = \frac{is r_0^2}{r_0^2+d^2}. \tag{2}$$

In equation (2) $\mathrm{d}\omega$ denotes the element of solid angle. Using this relation, i can be readily obtained from the observed value of I.

On the other hand, if s is not small, which is the case in the present measurements, it is easily shown that the relation between I and i is given by the more general expression

$$I = \frac{i}{\pi}\iint \cos\theta\,\mathrm{d}s\,\mathrm{d}\omega$$

$$= \frac{i}{\pi d^2}\iint \cos^4\theta\,\mathrm{d}s\,\mathrm{d}S, \tag{3}$$

where $\mathrm{d}s$ and $\mathrm{d}S$ are elements of area in the effusion hole and in the limiting aperture respectively, and θ is the angle which the line joining the two surface elements makes with the normal to the two planes.

Equation (3) may, for convenience in practical application, be expressed in the form

$$I = is\frac{r_0^2}{r_0^2+d^2}f, \tag{4}$$

where f may be regarded as a correction factor which is determined by the dimensions of the effusion hole, and of the diaphragm, and their separation. We now proceed to evaluate the integral appearing in (3), and thence the correction factor f.

4. Evaluation of the integral

The integral may be evaluated in the following manner. Let the elements of area be defined by $\mathrm{d}s = \rho\,\mathrm{d}\rho\,\mathrm{d}\alpha$ and $\mathrm{d}S = r\,\mathrm{d}r\,\mathrm{d}\beta$ respectively. Then the integral may be expressed in the form

$$X = \iint \cos^4\theta\,\mathrm{d}s\,\mathrm{d}S = d^4\int_{\rho=0}^{\rho_0}\int_{r=0}^{r_0}\int_{\alpha=0}^{2\pi}\int_{\beta=0}^{2\pi}\frac{\rho r\,\mathrm{d}\rho\,\mathrm{d}r\,\mathrm{d}\alpha\,\mathrm{d}\beta}{(B-C\cos\gamma)^2}, \tag{5}$$

where

$$\left.\begin{aligned} B &= \rho^2+r^2+d^2,\\ C &= 2\rho r,\\ \gamma &= \beta-\alpha. \end{aligned}\right\} \tag{6}$$

One can immediately see that when ρ is small, X becomes proportional to the area $s = \pi\rho_0^2$ of the effusion hole.

Taking up first the integration over β, this may be replaced where ρ, r and α are kept constant, by integration over γ between the limits 0 and 2π. Substituting

$$\tan\frac{\gamma}{2} = t, \tag{7}$$

and remembering that the integration between the limits 0 and π gives the same value as integration between π and 2π, one obtains

$$Y = \int_0^{2\pi}\frac{\mathrm{d}\gamma}{(B-C\cos\gamma)^2}$$

$$= 2\int_0^{\infty}\frac{2(1+t^2)\,\mathrm{d}t}{[B(1+t^2)-C(1-t^2)]^2}$$

$$= \frac{4}{(B+C)^2}\int_0^{\infty}\frac{\mathrm{d}t}{t^2+\frac{B-C}{B+C}} + \frac{8C}{(B+C)^3}\int_0^{\infty}\frac{\mathrm{d}t}{\left(t^2+\frac{B-C}{B+C}\right)^2}. \tag{8}$$

The first integral in (8) is directly evaluated, and the second by applying the reduction formula

$$2k(n-1)\int\frac{\mathrm{d}x}{(x^2+k)^n} = \frac{x}{(x^2+k)^{n-1}} + (2n-3)\int\frac{\mathrm{d}x}{(x^2+k)^{n-1}}. \tag{9}$$

One thus obtains

$$Y = \frac{2\pi B}{(B^2-C^2)^{\frac{1}{2}}}. \tag{10}$$

Coming back to (5), the next step after integrating over β will be to integrate over α, which now is just equivalent to multiplying by 2π. Hence

$$X = 4\pi^2 d^4\int_0^{\rho_0} Z\rho\,\mathrm{d}\rho, \tag{11}$$

where

$$Z = \int_{r=0}^{r_0}\frac{B r\,\mathrm{d}r}{(B^2-C^2)^{\frac{1}{2}}}. \tag{12}$$

Now B^2-C^2, which for convenience may be denoted by Q, may be written in the form

$$Q = B^2-C^2 = r^4+2r^2(d^2-\rho^2)+(d^2+\rho^2)^2, \tag{13}$$

and B in the form

$$B = (r^2+d^2-\rho^2)+2\rho^2. \tag{14}$$

Doing so, one obtains

$$Z = \int_{r=0}^{r_0}\frac{\mathrm{d}Q}{4Q^{\frac{1}{2}}} + \int_{r=0}^{r_0}\frac{2\rho^2 r\,\mathrm{d}r}{Q^{\frac{1}{2}}}. \tag{15}$$

By substituting

$$r^2+d^2-\rho^2 = 2\rho d\tan\delta, \tag{16}$$

and remembering that

$$(r^2+d^2-\rho^2)^2+(2\rho d)^2 = Q,$$

the second integral in (15) also can be seen to reduce to a simple form, namely, to

$$\frac{1}{4d^2}\int_{r=0}^{r_0}\cos\delta\,\mathrm{d}\delta.$$

The expression (11) for X thus reduces to

$$X = \pi^2 d^2\int_0^{\rho_0}\rho d\rho - \pi^2 d^2\int_0^{\rho_0}\frac{\rho^3+\rho(d^2-r^2)}{Q_0^{\frac{1}{2}}}\mathrm{d}\rho, \tag{17}$$

where Q_0 is the value of Q for $r = r_0$, and as a function of ρ can be written in the convenient form

$$Q_0 = \rho^4+2\rho^2(d^2-r_0^2)+(d^2+r_0^2)^2, \tag{18}$$

from which it will be seen that the second term in (17) reduces to the simple form

$$-\frac{\pi^2 d^2}{4}\int_{\rho=0}^{\rho_0}\frac{dQ_0}{Q_0^{\frac{1}{2}}}.$$

One thus obtains finally

$$X = \tfrac{1}{2}\pi^2 d^2(\rho_0^2 + r_0^2 + d^2 - \sqrt{\{(\rho_0^2 + r_0^2 + d^2)^2 - 4\rho_0^2 r_0^2\}}). \tag{19}$$

It is significant that ρ_0 and r_0 in the expression for X may be interchanged, which shows that the effusion hole and the collecting aperture may be interchanged without affecting the saturation current.

For any given values of ρ_0, r_0 and d, X is readily evaluated from (19), and hence the correction factor f also, which as defined by equations (3) and (4) has the value

$$f = \frac{r_0^2 + d^2}{sSd^2}X, \tag{20}$$

where $s = \pi\rho_0^2$ and $S = \pi r_0^2$ are the areas of the effusion hole and the aperture respectively.

Again it will be seen from (19) that when ρ_0 is small in comparison with either r_0 or d, X reduces to $sSd^2/(r_0^2 + d^2)$, and hence f reduces to unity, as should be expected.

5. The maximum size of the effusion hole that can be used with a chamber of given dimensions

As was pointed out in part I the relation between the effusion of electrons from a chamber of the saturated electron gas, through a small hole, and emission directly from an equal area of the surface of the metal, bears a close analogy to the relation between the black body radiation from a cavity through an aperture, and the direct radiation from the heated surface. Corresponding to the emissivity of the surface ϵ in the radiation problem, ϵ' may be taken to represent in the electronic case the ratio of direct emission from the surface to effusion from the chamber of saturated vapour through an equal area of the effusion hole. When the surface is an ideal one, i.e. when it has been completely degassed, ϵ' will obviously be equal to $1-r$, where r is the reflexion coefficient of the surface of the metal for electrons incident on it, and $1-r$ is its transmission coefficient. But for any normal surface, i.e. a surface which has not been specially treated for degassing, which is the case in our present measurements, ϵ' may be considerably smaller. We have made some quantitative measurements with a normal surface of nickel, and ϵ' is found to be about 1/5, and it may be presumed that for the other metals also it will be of this order of magnitude. Graphite, however, is an extreme case, in which the emission coefficient ϵ' for the untreated surface is much smaller, about 1/15 at 1300° K, about 1/70 at 1600° K, and still smaller at higher temperatures.

The main purpose of invoking here the analogy of the relation between the electromagnetic radiation from the surface and from the cavity, with the corresponding relation between electronic emission from the surface and effusion from the chamber, is this. It is possible to utilize some of the results already available for the case of radiation from a cavity to our present problem, namely to determine the

maximum size of the effusion hole that can be used with a chamber of given dimensions without disturbing appreciably the equilibrium pressure of the electron gas in the chamber.

The type of source that has been studied in detail in the radiation problem is a cylindrical furnace closed at one end and open at the other. We should refer here in particular to the investigations of Buckley (1927, 1928*a*, *b*, 1934) and Yamauti (1933). Obviously the greater the ratio of the length l of the cylinder to its radius R, and the higher the emissivity of surface, the closer will be the approximation of the radiation from the cavity to that of an ideal black body. For example, for a permitted defect of 1 % of the actual cavity radiation from that of a black body, the values of the ratio l/R corresponding to different values of ϵ, as obtained by Buckley, are given in table 1. The significance of the entries in the bottom row of the table will be made clear presently.

Table 1

ϵ	0·75	0·5	0·3	0·25
l/R	3·8	5·8	8·0	9·0
$W\epsilon/s$	6	6	5	5

One can also deduce from certain general considerations a rough criterion that the radiation from such a cylinder may approximate to that of a black body. The criterion is that the total radiation from the walls of the chamber, namely $W\epsilon$, where W is the area of the walls of the chamber, should be much larger than the emission from the aperture, which will be practically s. In other words $W\epsilon/s$, $= p$ say, should be much larger than unity.

One has now to estimate for a given value of ϵ how large p should be in order that the radiation may approach that of a black body to any desired degree of approximation. As was mentioned above, the larger will p have to be the closer the approximation required. One can also see in a general way that p should depend on ϵ, which becomes obvious when one remembers that for an ideally black surface p can be as small as unity.

In the last row of the table are entered the values of $W\epsilon/s$, calculated from Buckley's data for an accuracy of 1 %. In view of what was stated just now regarding the dependence of p on ϵ, the apparent constancy of the values of $W\epsilon/s$ entered in the last row of the table shows first that the variation of $W\epsilon/s$ with ϵ is small in the range considered, and that if ϵ is not much smaller than 0·25, a value of p of the order of 5 is ample to make the approximation to the black body as close as 1 %.

It may not be permissible to extrapolate from these data to the case when the open end of the cylinder is restricted to a small aperture in the centre, or when ϵ' is small. But since one is concerned here with orders of magnitude only, $W\epsilon'/s > 5$ may safely be taken as a good enough general criterion for the electronic case also. Adopting this criterion, one can readily see that with the dimensions of the chamber and of the effusion hole used in the present measurements, i.e. with $W/s = 87$, the value of ϵ' can be as low as 1/17, and this requirement is clearly satisfied not only for the metals at all working temperatures, but also for the exceptional case of graphite up to about 1300° K. For graphite at higher temperatures the deviation from the ideal value *may* exceed 1 %.

6. Experimental verification of the effect of a wide effusion hole

In the last section it was found that even in the extreme case of graphite, except probably at very high temperatures, the large size of the effusion hole that is used in the present measurements is small enough not to disturb the equilibrium in the chamber. In order to check this result experimentally, and incidentally also to check the geometrical correction factor calculated in an earlier section, we have made some systematic measurements on the saturation current for graphite, which as we have seen is an extreme case, using effusion holes varying in area from 4·5 to 314 mm², and at different temperatures. The effusion holes were circular holes punched in sheets of mica, and backed by a bigger hole in the end wall of the graphite chamber, as in the measurements made in part I. Three different sets of measurements were made, in which the size of the effusion hole was varied over the range given just now; the values of r_0 and d in the three sets were (22, 18), (16, 20) and (10, 18) respectively, in mm.

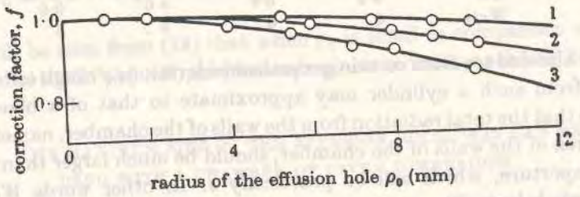

Figure 1

The full curves 1, 2 and 3 in figure 1 give the values of f corresponding to these three cases, calculated on the basis of equations (20) and (19). The circles in the figure denote the experimental values of f. Each such circle, corresponding to one of the sizes used for the effusion hole, represents the results obtained at different temperatures, and since they agree closely no attempt is made to indicate them separately in the figure. It will be seen that the experimental points lie practically on the theoretical curves, even for the largest value of the aperture used. This finding, besides verifying the relations (20) and (19) for the evaluation of f from the dimensions of the apparatus, also shows that even the largest effusion hole used is too small to disturb appreciably the equilibrium in the chamber.

Incidentally it is also found that for the small effusion holes used in the measurements described in parts I and II, the correction factor f differs negligibly from unity.

These measurements also throw light on an important point that arises in connexion with the use of effusion holes made in a mica sheet. The main purpose of using the mica sheet is to shield the Faraday cylinder from the electrons that would be emitted by the front surface of graphite if the effective effusion hole had been a hole in the graphite wall itself, since the wall also is at the same temperature as the chamber. The point that naturally arises in this connexion is the possibility of an accumulation of charge on the mica sheet, and the effect of this charge on the effusion of electrons. If the surface charge has any effect it will evidently be most pronounced with narrow effusion holes, and will be practically nothing with large

holes. The agreement of the experimental values plotted in figure 1 with the values calculated from the dimensions, suggests that the effect if any, of the surface charge on effusion even through holes of about 4·5 mm² area, which was the smallest hole used in any of our measurements, is negligible.

7. Measurements with copper, silver and gold

The thermionic constants of these metals were determined in the same manner as those of the transition metals in part II. The inner walls of the graphite chamber, and the regions adjoining the effusion hole, were coated with the metal to be studied, by thermal deposition, and in the case of copper and silver electrolytically also. The specimen of silver used was of spectroscopic purity and was supplied by Johnson, Matthey and Co. The specimen of gold used was of 99·99 % purity and was kindly

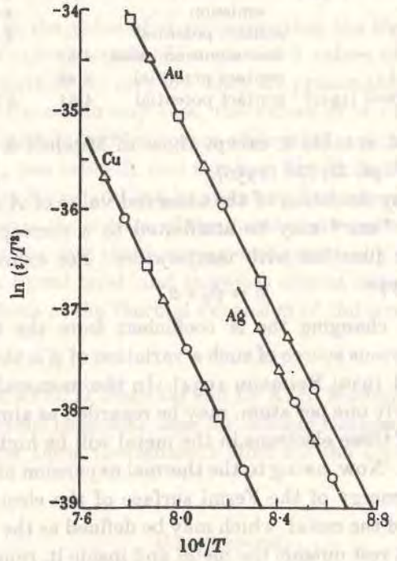

Figure 2

supplied by The Chief Assayer of the India Government Mint. The specimen of copper also was of high purity and was further purified by electrolysis. The Richardson plots of $\ln (i/T^2)$ against $1/T$ for the three metals are given in figure 2, in which the values of i used in the plotting have been corrected for the large size of the effusion holes used. The values of the thermionic constants of these metals deduced from these plots are entered in Table 2.

In table 3 are collected together the results obtained by other workers; those obtained earlier than 1938 are not included in this list. The available data for the A coefficients are very meagre, and they vary widely. They are all very low, the values reported earlier being 65 for copper (Goetz 1927), 0·76 for silver (Ameiser 1931) and 40 for gold (Goetz 1927), in the usual unit amp cm^{-2} deg^{-2}. These low

values, as mentioned in the Introduction, may be due to the difficulty of effectively degassing the surfaces at temperatures below their melting-points, as these temperatures are not high enough for this purpose.

TABLE 2

metal	ϕ (eV)	A (amp cm^{-2}deg^{-2})
copper	$4{\cdot}50 \pm 0{\cdot}02$	110 ± 5
silver	$4{\cdot}31 \pm 0{\cdot}03$	107 ± 6
gold	$4{\cdot}25 \pm 0{\cdot}02$	100 ± 4

TABLE 3. EARLIER VALUES FOR THE WORK FUNCTIONS IN eV

author	method	copper	silver	gold
Klein & Lange (1938)	contact potential	4·46	4·44	4·46
Farnsworth & Winch (1940)	photo-electric emission	—	4·75 (111) 4·81 (100)	—
Anderson (1941)	contact potential	—	4·79 (100)	—
Dyke (1946)	thermionic emission	4·55	—	—
Anderson (1949)	contact potential	4·46	—	—
Mitchell & Mitchell (1952)	contact potential	4·61	4·35	—

All the data entered in table 3, except those of Mitchell & Mitchell (1952), are taken from *J. Appl. Phys.* **21**, 536 (1950).

As is well known any deviation of the observed value of A from the theoretical value of 120 amp deg^{-2} cm^{-2} may be attributed to a corresponding small linear variation of the work function with temperature. For example, a temperature variation of ϕ of the type

$$\phi = \phi_0 + \alpha T \tag{21}$$

will be equivalent to changing the A coefficient from the theoretical value of A_0 to $A_0 e^{-\alpha/k}$. One obvious source of such a variation of ϕ is the thermal expansion of the metal (Herzfeld 1930; Reimann 1934). In the monovalent metals the conduction electrons, nearly one per atom, may be regarded as almost completely free, and the assemblage of these electrons in the metal will be highly degenerate at all working temperatures. Now, owing to the thermal expansion of the metal there will be a lowering of the energy of the Fermi surface of the electrons. If the energy barrier at the surface of the metal, which may be defined as the difference in energy between an electron at rest outside the metal and inside it, remains independent of the change of temperature, the lowering of the Fermi surface will lead to an equal increase in ϕ.

Now the energy ζ of the Fermi surface, measured from the bottom of the electronic energy band, will be proportional to $n^{\frac{2}{3}}$, where n is the number of electrons per unit volume, and therefore also practically the number of atoms per unit volume. Hence

$$\frac{1}{\zeta}\frac{d\zeta}{dT} = -\tfrac{2}{3}\Delta, \tag{22}$$

where $\Delta = -\dfrac{1}{n}\dfrac{dn}{dT}$ is the coefficient of thermal expansion of the metal. The corresponding thermal coefficient of ϕ will then be given by

$$\alpha = \frac{d\phi}{dT} = -\frac{d\zeta}{dT} = \tfrac{2}{3}\zeta\Delta, \tag{23}$$

where the Fermi energy ζ is given by the well-known expression

$$\zeta = \frac{h^2}{2m}\left(\frac{3n}{8\pi}\right)^{\frac{2}{3}}. \tag{24}$$

The values of Δ, and of ζ and α calculated from (24) and (23) respectively, are given in table 3. On this basis the A coefficients should be a fraction $e^{-\alpha/k}$ of A_0, and the values of this fraction are entered in the last column of the table.

TABLE 4

metal	$10^6\,\Delta$(deg^{-1})	ζ (eV)	$10^4\,\alpha$(eV deg^{-1})	$e^{-\alpha/k}$
copper	5·01	7·0	2·3	0·07
silver	5·76	5·5	2·1	0·09
gold	4·17	5·5	1·5	0·18

Such a lowering in the value of A accompanying the thermal expansion of the metal *is not verified experimentally*. Though the A values of these metals obtained by the usual diode method are very low, they are presumably due to the insufficient degassing of the surfaces. In any case, the values of A obtained by the present method, which are not affected by surface adsorption, are only slightly short of the theoretical value A_0 (see table 2), and this is so for all the three metals.

This finding is significant and can be shown to be a consequence of the lowering of the energy barrier at the surface of the metal that must accompany the thermal expansion of the lattice, and this lowering is of practically the same magnitude as the lowering of the Fermi level, and therefore almost exactly compensates for it. These and other effects of the thermal expansion of the lattice will be discussed in part IV.

We wish to thank Mr G. D. Joglekar and Dr K. N. Mathur for help in the installation of the high current generator used for heating the graphite chamber, and the Chief Assayer of the India Government Mint for the supply of gold of 99·99 % purity.

REFERENCES

Ameiser, I. 1931 *Z. Phys.* **69**, 111.
Buckley, H. 1927 *Phil. Mag.* **4**, 753.
Buckley, H. 1928*a* *Phil. Mag.* **6**, 447.
Buckley, H. 1928*b* *Rec. Trav. Com. Int. Eclair*, 7e Sess., p. 888.
Buckley, H. 1934 *Phil. Mag.* **17**, 576.
Goetz, A. 1927 *Z. Phys.* **43**, 531.
Herzfeld, K. F. 1930 *Phys. Rev.* **35**, 248.
Jain, S. C. & Krishnan, Sir K. S. 1952*a* *Proc. Roy. Soc.* A, **213**, 143 (part I).
Jain, S. C. & Krishnan, Sir K. S. 1952*b* *Proc. Roy. Soc.* A, **215**, 431 (part II).
Mitchell, E. W. J. & Mitchell, J. W. 1952 *Proc. Roy. Soc.* A, **210**, 270.
Reimann, A. L. 1934 *Nature, Lond.*, **133**, 833.
Yamauti 1933 *Com. gén. Poids Mes.* **16**, 243.

Temperature Distribution along a Wire Electrically Heated *in vacuo*

THE distribution of temperature along a thin rod or wire electrically heated *in vacuo* has been studied both theoretically and experimentally by several authors. A knowledge of this distribution is of practical importance in connexion with the design of sealed-in heating elements for thermionic or illumination purposes, and also otherwise.

The distribution is determined uniquely by three parameters, which for convenience may be taken to be (1) the temperature T_l at the centre of the rod, (2) the temperature T_m to which T_l tends as the length of the rod is increased indefinitely, the heating current being kept constant, and (3) a simple constant $a = \frac{2}{5}\frac{p\varepsilon\sigma}{\varkappa\omega}$, where $\varkappa$ is the thermal conductivity, σ is the Stefan constant of radiation, ε is the total (as distinguished from spectral) emissivity from the surface, and p and ω are the perimeter and the area respectively of the cross-section of the rod. The effect of the radiations from the surrounding walls is wholly accounted for by their effect on T_m.

The temperature distribution is given by an integral which can be readily formulated. It is found, however, that the integration cannot be done directly, and it has therefore been done numerically by previous workers. The purpose of this communication is to report that the integrand can be expanded as a power series, and the integration can be done term by term. The resulting series is found to be rapidly convergent, and may therefore be used conveniently for computation, the first few terms being quite adequate for this purpose. It is found that the rod divides itself naturally into two regions, region A in the middle corresponding to $0 \leqslant t \leqslant t_c$, and region B corresponding to $t > t_c$, where t is the drop in temperature as compared with that at the centre of the rod, and $t_c = (T_m^4 - T_l^4)/(2T_l^3)$. The power series into which the distribution integral may be expanded is different in the two regions, but the transition from one to the other is continuous, and hence either series can be used close to the boundary separating A and B.

The temperature variation in region A is found to be parabolic, and it is practically independent of the temperature coefficients of $\varkappa$, ρ and ε, where ρ is the specific resistance of the rod. When the rod is too short to have any B-region at all, the expressions become particularly simple, including the expression for T_l as a function of the length of the rod.

The distribution of temperature in an infinitely long rod is obtained readily. The distribution in the B-region of a *finite* rod is found to be practically the same as in the corresponding end region of an infinitely long rod, the discrepancy between the two increasing progressively as one approaches the upper limit of B in the finite rod, but remaining quite small at this limit, even for a short rod. The effect of the finite temperature coefficients of $\varkappa$, ρ and ε on the temperature distribution in the B-region can also be taken into account in a simple manner.

The well-known logarithmic formula for the temperature variation near the centre, usually derived on the basis $t \ll T_m$, is found to have a much wider applicability, extending far into the B-region even in short rods. The criterion for its validity is found to be $t/(2 \log t) \ll T_m$, which is a much less stringent condition than $t \ll T_m$. The additive constant in the logarithmic formula, which in the usual derivation has to be left undetermined, is also evaluated now.

Experimental results are available for the temperature distribution in tungsten filaments and in thin rods of Acheson graphite, but the lengths used are so great that T_l approximates closely to T_m in these measurements. Hence these measurements have been extended by us to shorter lengths, and also to wires of platinum and a few other metals. The observations verify in detail the results deduced theoretically.

An account of some of these investigations is in course of publication in the *Proceedings of the Royal Society*.

K. S. KRISHNAN
S. C. JAIN

National Physical Laboratory of India,
New Delhi.
Nov. 12.

The distribution of temperature along a thin rod electrically heated *in vacuo*

I. Theoretical

BY S. C. JAIN AND SIR K. S. KRISHNAN, F.R.S.
National Physical Laboratory of India, New Delhi

(*Received* 10 *July* 1953)

The paper describes a detailed investigation of the distribution of temperature along a thin rod or wire electrically heated *in vacuo*. The distribution is determined uniquely by three parameters, namely, (1) the temperature at the centre of the rod, (2) that at the centre of a similar infinitely long rod heated by the same current, and (3) a simple constant that involves directly the cross-section of the rod, its thermal conductivity and the emissivity of its surface. Though the integral that determines the temperature distribution cannot be evaluated directly, it is shown that it can be expanded as a convergent power series. The rod may be divided for this purpose into two well-defined regions, region A comprising a certain length in the middle of the rod, and region B consisting of the portions outside A, the appropriate series for the evaluation of the integral being different in the two regions. The temperature coefficients of the physical constants involved can also be taken into account in the evaluation.

The temperature distribution in the A-region is found to be parabolic. Hence when the rod is too short to have any B-region at all, the theoretical relations become particularly simple, and are also practically independent of the finite temperature coefficients of the physical constants involved.

The distribution in the B-region is found to be practically the same as in the corresponding end-portions of an infinitely long rod, except near the upper limit of the B-region when this region is very short.

An analytical expression is also obtained for the temperature at the centre of the rod as a function of its length.

The criterion for the validity of the well-known logarithmic formula for temperature distribution is shown to be much less stringent than is generally taken to be; the range of its applicability is thus extended far into the B-region even when the rod is not long. The additive constant in the formula, which previously had to be left undetermined, also gets evaluated now.

1. INTRODUCTION

The distribution of temperature along a thin rod or a thin-walled tube heated *in vacuo* by sending a heavy electric current through it is of interest experimentally. When the rod or the tube is sufficiently long, there is a considerable portion in the middle in which the temperature is sensibly constant. In this region practically the whole of the heat generated by the passage of the electric current is dissipated by radiation from the outer surface; the loss of heat by conduction from the centre outwards, and, in the case of the tube, also by radiative transfer occurring in the cavity, will then be negligible.

The occurrence of such a region of sensibly uniform temperature is utilized for various purposes experimentally, and it is therefore of some importance to know how long any actual thin rod or tube has to be in order that a specified length about the centre may be of sensibly uniform temperature, i.e. in order that the maximum deviation in temperature in this range may not exceed a specified small tolerance. More generally, it is desirable to know in detail the distribution over its whole length irrespective of whether it is long or short, and also to know the rate at which

heat is conducted away at the ends. Such detailed information, apart from its intrinsic interest, will also be helpful in connexion with the design of sealed-in heating elements such as are used for thermionic or illumination purposes.

In this part (I) of the paper is given a theoretical investigation of the distribution of temperature along a thin rod. Extensive experimental data are available for tungsten, and some for Acheson graphite, which have been supplemented by some fresh measurements made by the present authors. Part II of the paper will be concerned with a discussion of these data in relation to the results deduced theoretically in part I.

The case of a *tube*, even when it is thin-walled, is slightly more complicated because of the radiative transfer of heat from the centre towards the ends that will occur in the cavity of the tube, which is more difficult to take into account.

2. Formulation of the problem and earlier work

Let κ be the thermal conductivity of the material, ρ its specific resistance and ϵ the total emissivity of the surface, i.e. the emissivity over the whole of the significant range of its emission spectrum. Neglecting to a first approximation the temperature coefficients of these quantities, and neglecting also, since the rod is taken to be thin, the radial gradient of temperature in the rod, the equation of conduction in the steady state may be written in the form (Carslaw & Jaeger 1947)

$$\frac{\mathrm{d}^2T}{\mathrm{d}x^2}-\frac{p\epsilon\sigma}{\kappa\omega}(T^4-T_0^4)+\frac{I^2\rho}{\kappa\omega^2}=0, \tag{1}$$

in which x is the distance of the point under consideration from the near end of the rod, ω is the cross-sectional area of the rod, p is the perimeter of the cross-section, T_0 is the temperature of the walls of the chamber and also of the ends of the rod, σ is Stefan's constant of radiation, and I is the heating electric current. The current is taken to be an alternating one, in which case the two halves of the rod will be symmetrical about its centre. The loss of energy due to thermionic emission is in general negligible and hence is not included here.

Following Carslaw & Jaeger and using the boundary conditions

$$\left.\begin{aligned} &T=T_0 \quad \text{when} \quad x=0,\\ \text{and}\quad &\frac{\mathrm{d}T}{\mathrm{d}x}=0 \quad \text{when} \quad x=l,\end{aligned}\right\} \tag{2}$$

where $2l$ is the length of the rod, one obtains

$$x=\int_{T_1}^{T}\frac{\mathrm{d}T}{[a(T^5-T_1^5)-b(T-T_1)]^{\frac{1}{2}}}, \tag{3}$$

in which T_1 is the temperature at the centre of the rod, i.e. at $x=l$,

$$a=\frac{2}{5}\frac{p\epsilon\sigma}{\kappa\omega}, \tag{4}$$

$$b=\frac{2I^2\rho}{\kappa\omega^2}+\frac{2p\epsilon\sigma T_0^4}{\kappa\omega}. \tag{5}$$

Evidently

$$l=\int_{T_1}^{T_1}\frac{\mathrm{d}T}{[a(T^5-T_1^5)-b(T-T_1)]^{\frac{1}{2}}}. \tag{6}$$

Now for a rod of given material and cross-section, and for a known heating current, (6) may be regarded as defining the temperature T_1 at the centre of the rod when its length is $2l$. Knowing T_1, (3) enables one to obtain the temperature T at every other point x on the rod.

It does not seem to be possible to do the integration in (6) directly. Bush & Gould (1927) have done the integration with the help of a differential analyzer, and the temperature distribution in a heated tungsten wire obtained in this manner has been used by them for determining the distribution of thermionic emission along the wire. In using the differential analyzer for calculating the temperature distribution they found it possible also to include the known temperature variations of κ, ρ and ϵ. The integration of (3) has also been done numerically by Baerwald (1936). Using the known values of κ, ρ and ϵ for molybdenum at different temperatures, the temperature gradient $\mathrm{d}T/\mathrm{d}x$ is first evaluated at different points of the rod, and thence the distribution integral is evaluated by him numerically. Some of the steps in the integration have also been done graphically by Worthing (see Worthing & Halliday 1948). The distribution function has also been discussed by Langmuir & Taylor (1936) and by Cox (1943).

When the rod is very long there will be naturally a considerable region in the middle where the temperature will be sensibly constant. The loss of heat from the centre by conduction will in this case be negligible in comparison with the loss due to radiation. Confining attention to such a rod, and to a region where t, defined by

$$t=T_m-T, \tag{7}$$

is small in comparison with T_m, the equation of conduction (1) may be shown to reduce to the simple form

$$\mathrm{d}^2t/\mathrm{d}x^2-At=0, \tag{8}$$

which can be directly solved. The solution is

$$x\sqrt{A}=D-\ln t, \tag{9}$$

in which A is known, but not the integration constant D, since it cannot be determined directly from the boundary values.

The logarithmic formula—to be more precise the formula in its exponential form $t=\exp(D-x\sqrt{A})$—has been discussed by Worthing (1914, 1922), Stead (1920), Prescott & Hincke (1928), Bearwald (1936) and others. We may emphasize here an important result that emerges from the observations of Prescott & Hincke. Their plots of the experimental data for Acheson graphite show that the logarithmic formula (9) is verified even for regions where the fundamental basis for its derivation, namely, that t should be small in comparison with T_1, cannot be justified at all. Further, Baerwald has compared the values obtained by the numerical evaluation of the integral with the corresponding values given by the logarithmic formula. His curves show that the two sets of values practically coincide up to

$$t/T_1=300°/1300°,$$

which is by no means a small fraction.

In view of these it is desirable to be able to discuss the temperature distribution analytically in order to follow more closely the implications of these and other

findings. It is the main purpose of this paper to show that even in the general case of a rod of *any* length it is possible to expand the integrand in (3) as a convergent power series, and do the integration term by term. The convergence is found to be rapid, and one can therefore evaluate the integral to any desired degree of approximation in this manner. One also gets thus a proper estimate of the degree of approximation involved in any particular step that may be taken.

3. Expansion of the integrand in (3) as a series

At any point x the energy generated, and the energy radiated, per second per unit length of the rod are given by $I^2\rho/\omega$ and $p\epsilon\sigma(T^4-T_0^4)$ respectively. Neglecting as before the temperature variations of κ, ρ and ϵ—they will be taken into account in a later section—it is convenient to define a temperature T_m such that

$$p\epsilon\sigma(T_m^4-T_0^4)=I^2\rho/\omega. \tag{10}$$

Obviously (10) corresponds to the condition that the heat generated is dissipated away wholly by radiation, i.e. it corresponds to a region where the transfer of heat by conduction is negligible, and hence where the temperature is sensibly constant. This will evidently be the case near the centre of a very long rod. In other words T_m will be the value to which the temperature T_l at the centre tends when $l\to\infty$. For shorter lengths of the rod, however, T_l will be smaller than T_m, and hence

$$I^2\rho/\omega-p\epsilon\sigma(T_l^4-T_0^4) \tag{11}$$

will be finite, and quite large for short rods.

Now, in view of (4), (5) and (10),

$$b/a=5T_m^4. \tag{12}$$

Hence (3) may be written in the form

$$x\sqrt{a}=\int_{T_0}^{T}[5T_m^4(T_l-T)-(T_l^5-T^5)]^{-\frac{1}{2}}\,\mathrm{d}T. \tag{13}$$

Putting as before $T_l-T=t$, one obtains from (13)

$$x\sqrt{a}=\int_{t}^{t_0=T_l-T_0}[5(T_m^4-T_l^4)\,t+10T_l^3t^2-10T_l^2t^3+5T_lt^4-t^5]^{-\frac{1}{2}}\,\mathrm{d}t. \tag{14}$$

The temperature distribution is thus determined uniquely by the three parameters T_l, T_m and a. Now the dependence on a (which includes the dependence on the dimensions p and ω of the cross-section of the rod) is particularly simple, and by expressing the lengths along the rod in terms of $1/\sqrt{a}$ (as has been done in plotting the curves in figure 1), the temperature distribution may be made to depend on the two parameters T_l and T_m only.

Before proceeding to consider the integration of (14) it is desirable to make a small generalization of the problem. Till now the ends of the rod had been taken to be at the same temperature T_0 as the walls of the chamber. This need not necessarily be the case. The effect of the temperature T_0 of the walls is wholly confined to determining the temperature T_m as defined in (10), and hence changing the temperature of the walls is merely equivalent to changing suitably the value of T_m appearing in equation (14).

In the discussion that follows, the temperature of the walls is taken to be T_0, and that of the two ends of the rod as zero. The results obtained therefrom can be readily adapted to the case where the ends are kept at any other temperature Θ, since it is equivalent merely to ignoring the portions in the theoretical rod whose temperatures are below Θ. It can also be adapted to the case when the two ends of the rod are at different temperatures.

4. Separation of the rod into two regions

For a given length $2l$ of the rod and given heating current, both T_l and T_m appearing in (14) may be regarded as constants independent of x. It is convenient to define a certain critical value of t, namely, t_c, such that

$$t_c=(T_m^4-T_l^4)/(2T_l^3). \tag{15}$$

Depending on whether $t<t_c$ or $>t_c$, the first term inside the square brackets in (14), will be greater than, or less than, the second. The manner in which the integrand in (14) is to be expanded as a power series will therefore depend on whether $t<t_c$ or $>t_c$; there is, however, a continuity between the two regions which makes the two series overlap in a small range in the close neighbourhood of t_c.

One may accordingly divide the rod into two regions, one in the middle of the rod in which $0<t<t_c$, which may be designated as region A, and the other outside this range, corresponding to $t>t_c$, which may be designated as region B. When l is not sufficiently great, t_c may exceed the total fall in temperature, namely, T_l over the whole length of the rod, in which case obviously the whole of the rod will be included in region A, and there will be no B-region at all.

5. Region A considered in detail

Taking up first the A-region, (14) may be expressed in the form

$$q[5a(T_m^4-T_l^4)]^{\frac{1}{2}}=\int_0^t t^{-\frac{1}{2}}(1+y)^{-\frac{1}{2}}\,\mathrm{d}t, \tag{16}$$

in which $q=l-x$ is the distance as measured from the centre of the rod, of the point under consideration whose temperature is t, and

$$y=\frac{t}{t_c}\left(1-\frac{t}{T_l}+\frac{t^2}{2T_l^2}-\frac{t^3}{10T_l^3}\right). \tag{17}$$

The upper limit of the integral in (16), namely, the temperature t at the point under consideration, may extend, when the rod is long enough to have a B-region to $t=t_c$, and when the rod is too short to accommodate the whole of A, to $t=T_l<t_c$. It can be readily seen that for any position of the point in this range, y remains less

than unity, so that the integrand in (16) may be expanded as a power series and the integration may be done term by term. Doing so, one obtains

$$q^2 = \frac{4t(1-S)^2}{5a(T_m^4 - T_l^4)}, \tag{18}$$

where
$$S = \frac{1}{2\sqrt{t}}\left[\int_0^t \tfrac{1}{2}t^{-\frac{1}{2}}y\,dt - \int_0^t \tfrac{3}{8}t^{-\frac{1}{2}}y^2\,dt + \int_0^t \tfrac{5}{16}t^{-\frac{1}{2}}y^3\,dt - \ldots\right]. \tag{19}$$

S is a number which can be seen to be small in comparison with unity, and may be readily evaluated from (19), since even when y is close to unity, which will be the case when the rod is very long and the point under consideration is close to the upper limit of the A-region, i.e. when $t = t_c \ll T_l$, the convergence of the series (19) is rapid enough for convenient numerical computation. This value of S, which naturally is an extreme one, is found to be about 0·13. But, in general, S will be much smaller than this, and when there is no B-region at all, actually less than 0·08. Hence, in general, whether the rod is short or long, S may be neglected in comparison with unity, and thus one obtains

$$q^2 = \frac{4t}{5a(T_m^4 - T_l^4)}. \tag{20}$$

In other words, as one moves out from the centre the observed temperature variation will be parabolic, and will continue to be practically so over the whole of the A-region.

In order to have some idea of the magnitude of the factor $T_m^4 - T_l^4$ appearing in (20), it may be mentioned that when the rod is just long enough to accommodate the whole of the A-region, $t_c = T_l$, and hence in view of (15)

$$T_l/T_m = (\tfrac{1}{2})^{\frac{1}{4}} = 0{\cdot}76. \tag{21}$$

As the length is increased, T_l will obviously approach closer to T_m. (The case of shorter rods will be considered in detail in the next section.)

Now the linear extent q_c of the A-region will be given by

$$q_c = \left(\frac{2}{5aT_l^3}\right)^{\frac{1}{2}}, \tag{22}$$

and it varies from $2^{\frac{1}{2}}/(5aT_m^3)^{\frac{1}{2}}$ for an infinitely long rod, to $3^{\frac{1}{2}}.2^{\frac{1}{2}}/(5aT_m^3)^{\frac{1}{2}}$ for a rod just long enough to include only the A-region; thus the length of the A-region remains of the same *order* of magnitude in spite of the enormous range of l.

The total drop in temperature over the whole of the A-region, namely lt_c, will naturally be the smaller the longer the rod.

6. Short rods, $l < q_c$

When the length of the rod falls short of q_c, equation (20), which gives the temperature distribution, will be an even closer approximation than before. Now the total drop in temperature over the whole length becomes T_l. Substituting this value for t in (20), one obtains

$$l^2 = \frac{4T_l}{5a(T_m^4 - T_l^4)}. \tag{23}$$

For such short rods, (23) determines the dependence of T_l on l, and on the heating current, which naturally determines T_m.

As the length of the rod is reduced, T_l^4 will at some stage become small enough to be negligible in comparison with T_m^4. At any given distance q from the centre, the temperature drop t, which will be seen from (20) to be proportional $T_m^4 - T_l^4$, will then become practically independent of T_l and therefore of l. In other words, the temperature distribution curves t against q for such short rods will be nearly parallel to one another, their relative separations being along the t axis and independent of q.

7. The series applicable to the B-region

Considering the B-region defined by $t > t_c$, the second term inside the square brackets in (14) now becomes larger than the first term, unlike in the A-region. Equation (14) may now be written in the form

$$x(10aT_l^3)^{\frac{1}{2}} = \int_t^{T_l} t^{-1}\left[1 + \frac{t_c}{t} - \frac{t}{T_l} + \frac{1}{2}\frac{t^2}{T_l^2} - \frac{t^3}{10T_l^3}\right]^{-\frac{1}{4}} dt. \tag{24}$$

All the terms inside the square brackets in (24) that involve t are separately and together less than unity, and hence the integrand can be expanded again as a power series

$$x(10aT_l^3)^{\frac{1}{2}} = \int_t^{T_l}\left[\frac{1}{gt} + \frac{1}{2T_l g^3} - \frac{t}{4T_l^2}\left(\frac{1}{g^3} - \frac{3}{2g^5}\right) + \ldots\right] dt, \tag{25}$$

where
$$g^2 = 1 + t_c/t. \tag{26}$$

The integration in (25) can be done term by term. Doing so one obtains x as the sum of three convergent power series, namely

$$x(10aT_l^3)^{\frac{1}{2}} = [U + V + W]_t^{T_l}, \tag{27}$$

where
$$U = \ln t + \frac{t}{2T_l}\left(1 + \frac{t}{8T_l} - \ldots\right), \tag{28}$$

$$V = 2\ln(g+1) + \frac{t_c}{T_l}\left(\frac{1}{g} - \frac{3}{4}\ln\frac{g+1}{g-1}\right) - \frac{t_c^2}{2T_l^2}\left(\frac{7}{2g} + \frac{1}{2g^3} + \frac{19}{16}\frac{g}{g^2-1} - \frac{75}{32}\ln\frac{g+1}{g-1}\right) + \ldots, \tag{29}$$

$$W = \frac{(g-1)t}{2T_l}\left(1 + \frac{t}{8T_l} - \ldots\right). \tag{30}$$

Thus in both the regions A and B, the integral on the right-hand side of (14) can be evaluated to any desired approximation, though the series involved in the evaluation are naturally different for the two regions.

8. Infinitely long rod

Before considering (27), applicable to the B-region of a rod of any length $2l$, it is desirable to consider the special case when the rod is infinitely long, for which $T_l = T_m$ and hence $t_c = 0$ and $g = 1$. It will be seen from (29) and (30) that in this case both $[V]_t^{T_m}$ and W vanish, and (27) reduces to

$$x(10aT_m^3)^{\frac{1}{2}} = [U]_t^{T_m} = D - \left(\ln t + \frac{t}{2T_m}\left(1 + \frac{t}{8T_m} - \frac{t^2}{120T_m^2} + \ldots\right)\right), \tag{31}$$

in which D is a constant given by

$$D = \ln T_m + \chi, \tag{32}$$

where

$$\chi = \tfrac{1}{2} + \tfrac{1}{12} - \tfrac{1}{240} + \ldots. \tag{33}$$

Equation (31) gives the distribution over the whole length of an infinitely long rod.

This expression could also have been obtained directly from (3) by putting $T_l = T_m$. The integrand could then have been expanded in the form of a series and integrated term by term.

Consider now a region of the rod in which $t/(2\ln t) \ll T_m$. The temperature distribution in this region will be given by

$$x(10aT_m^3)^{\frac{1}{2}} = D - \ln t. \tag{34}$$

Thus one obtains the same logarithmic formula as was obtained in (9) from certain direct considerations. The constant A appearing in (8) and (9) can be readily shown, in view of (10) and (4), to be equal to $10aT_m^3$, which is identical with the corresponding value appearing in (34).

Further, the integration constant D appearing in the logarithmic formula, which previously had to be left undetermined, now gets determined uniquely, and is given by expression (32). This expression, like all the other expressions in this paper, refers to the case when the end-temperatures are zero. If the ends are kept at any other temperature Θ the additive constant D appearing in (34) may be shown to be

$$D = \ln \tau + \frac{\tau}{2T_m} + \frac{\tau^2}{16T_m^2} - \frac{\tau^3}{240T_m^3} + \ldots, \tag{35}$$

where $\tau = T_m - \Theta$. It may be seen that (35) reduces to (32) when $\Theta = 0$.

Further the criterion for the validity of the logarithmic formula now comes out to be $t/(2\ln t) \ll T_m$, which is not quite so stringent as $t \ll T_m$, on the basis of which (9) was deduced. Taking, for example, $T_m = 1500°\,\mathrm{K}$ and a fraction $\frac{1}{150}$ of it as negligible in comparison with it, the present criterion will make the logarithmic formula valid over the range $0 < t < 100°$, whereas the corresponding range contemplated in the derivation of (9) is only a tenth of it.

At first sight it may seem a little surprising that the range of t over which the logarithmic formula (34) holds is much wider than that over which its *equivalent* differential equation (8) holds. That this should be so may be seen from the following argument. Retaining one more term on the right-hand side of (34), one obtains

$$x\sqrt{A} = D - \ln t - \frac{t}{2T_m}, \tag{36}$$

in which $t \ll T_m$. It can be readily seen by differentiating it twice that

$$\frac{\mathrm{d}^2 t}{\mathrm{d}x^2} = At\left(1 - \frac{3t}{2T_m}\right). \tag{37}$$

Whereas in (36) the correction will become negligible when $t \ll 2T_m \ln t$, the corresponding correction term in (37) will be negligible only when $t \ll \frac{2}{3}T_m$.

The increased range of validity of the logarithmic formula in a long rod is in agreement with the results of the numerical calculations of Baerwald referred to in § 2, and also with the observations of Prescott & Hincke.

This extension of the range of applicability of the logarithmic formula has an important consequence, as we shall see in the next section, namely, that even in rods that will be normally regarded as not long enough, there is a considerable range in which the formula holds.

9. The B-region further considered

It will be seen from (27) which gives the temperature distribution over the B-region, and from (30), that W is practically negligible over the whole of this region. It is also found after a little calculation that *the temperature at any given distance x from the end of the rod is practically the same as in a similar infinitely long rod.* Indeed, the difference between the two becomes detectable only near the upper limit of the B-region of the finite rod, and even there only when the B-region is small. This is an important result, which may be readily verified from the expressions (27) and (31). It can also be seen to be the case from the following argument. From (13) one obtains for the gradient of the temperature along the rod

$$\phi = \mathrm{d}T/\mathrm{d}x = a^{\frac{1}{2}}T_m^{\frac{1}{2}}\left[\frac{5T_l}{T_m} - \frac{T_l^5}{T_m^5} - \left(\frac{5T}{T_m} - \frac{T^5}{T_m^5}\right)\right]^{\frac{1}{2}}. \tag{38}$$

As will be seen from (38) the difference in slope between a rod of finite length and one of infinite length, both at the same T, is determined by the defect of T_l from T_m. Denoting the gradients for the infinitely long rod and the finite rod, both at temperature T, by ϕ_∞ and ϕ_l respectively, it can be seen that $(\phi_\infty - \phi_l)/\phi_\infty$, i.e. the relative difference between the two slopes, will be a minimum at the end of the rod, and will be the largest near the upper limit of the B-region.

We shall now consider the two extreme cases (1) when the B-region is just present, and (2) when the B-region is extensive, in both cases at the upper limit of the B-region. Taking up (1) first, this corresponds to T being very small and $T_l^4/T_m^4 = \frac{1}{3}$. It can be readily seen that in this case

$$\left.\begin{aligned} \phi_\infty &= 2a^{\frac{1}{2}}T_m^{\frac{1}{2}}, \\ \phi_l &= (14^{\frac{1}{2}}/3^{\frac{1}{2}})\,a^{\frac{1}{2}}T_m^{\frac{1}{2}}, \end{aligned}\right\} \tag{39}$$

the difference between the two being about 6 % of either.

When the B-region is very extensive, we may regard $T_m - T_l$, equal to Δ, say, as small in comparison with T_m. At $T = T_l - t_c$ it can be seen from (38) that

$$\left.\begin{aligned} \phi_\infty &= 90^{\frac{1}{2}}a^{\frac{1}{2}}T_m^{\frac{1}{2}}\Delta, \\ \phi_l &= 80^{\frac{1}{2}}a^{\frac{1}{2}}T_m^{\frac{1}{2}}\Delta, \end{aligned}\right\} \tag{40}$$

the difference between the two being now about 5 %.

In other words, the slope at the upper limit of the B-region of a finite rod differs from that of an infinitely long rod at the same temperature by about 5 to 6 %,

irrespectively of whether the finite rod has just a B-region present, or has an extensive B-region. The difference between the two slopes drops down rapidly as one moves inside the B-region.

Since the gradient of temperature ϕ_l at every temperature T inside the B-region is thus practically the same as ϕ_∞ at the same temperature in an infinitely long rod, the actual temperature T at any given distance x from the end will also be the same for the two rods. Since again $(\phi_\infty - \phi_l)/\phi_\infty$ has its largest value, namely, 5%, at the upper limit of B, and as one moves into the B-region it drops down rapidly, the difference in temperature between the two rods at any given distance x from the end will be much less than 5% even at the top of the B-region.

That the temperature distribution over practically the whole of the B-region of a finite rod is the same as in an infinitely long rod, apart from its intrinsic interest has also an important consequence. If the B-region is long enough, there will be a considerable range in it in which t is sufficiently small in comparison with $2T_m \ln t$ to make the distribution correspond to the logarithmic formula (34) characteristic of the infinitely long rod; t appearing in the formula will continue to denote $T_m - T$ in the case of the finite rod also.

Since the distribution of temperature in the B-region is nearly that of an infinitely long rod, the length of the B-region, equal to x_c, say, may be obtained from (31) by putting $t = t_c + T_m - T_l$. To a first approximation, which will be a fairly close one, one thus finds

$$x(10\alpha T_m^3)^{\frac{1}{2}} = \ln \frac{2T_l^3 T_m}{T_m^4 + 2T_l^3 T_m - 3T_l^4} + \frac{3T_l^4 - T_m^4}{4T_l^3 T_m}. \tag{41}$$

Obviously
$$x_c + q_c = l, \tag{42}$$

which is an important relation defining T_l as a function of l. This relation has many useful applications.*

10. The temperature coefficients of κ, ρ and ϵ included

Till now the quantities κ, ρ and ϵ were regarded, for convenience, as temperature-independent. It is not, however, difficult to take into account their temperature variations too. The differential equation corresponding to equation (1) will then be

$$\frac{\mathrm{d}}{\mathrm{d}x}\left(\kappa_T \frac{\mathrm{d}T}{\mathrm{d}x}\right) + \frac{I^2 \rho_T}{\omega^2} - \frac{p \epsilon_T \sigma}{\omega}(T^4 - T_0^4) = 0. \tag{43}$$

* [*Note added in proof*, 28 *December* 1953.] Equation (1) may also be written in the form

$$\frac{\mathrm{d}^2 T}{\mathrm{d}x^2} + \tfrac{5}{2}\alpha(T_m^4 - T_l^4) + \tfrac{5}{2}\alpha(T_l^4 - T^4) = 0.$$

In the close neighbourhood of the centre of a *finite* rod the third term on the left-hand side becomes negligible in comparison with the second. One then obtains the parabolic law (20).

On the other hand at *any* point of an infinite rod, or at a point sufficiently removed from the centre of a finite rod, the second term may become negligible in comparison with the third, in which case one obtains (13). The transition from the A- to the B-region in a finite rod corresponds to the third term growing to a magnitude comparable with the second.

Let κ_l, ρ_l and ϵ_l be the values of κ, ρ and ϵ at $T = T_l$. Further, let their temperature variations be linear,* and let the temperature coefficients be α, β and δ respectively. Equation (43) then reduces to

$$(1-\alpha t)\frac{\mathrm{d}^2 t}{\mathrm{d}x^2} - \alpha\left(\frac{\mathrm{d}t}{\mathrm{d}x}\right)^2 = \tfrac{5}{2}\alpha[T_m^4(1-\beta t) - (1-\delta t)(T_l - t)^4 + (\beta - \delta) t T_0^4], \tag{44}$$

where the physical constants involved in defining a are to be assigned values appropriate to $T = T_l$. Multiplying both sides by $2(1-\alpha t)$ and doing the first integration with respect to x one obtains

$$(1-\alpha t)^2\left(\frac{\mathrm{d}t}{\mathrm{d}x}\right)^2 = 5\alpha t\left[T_m^4 - T_l^4 + T_l^4\left(\frac{2a_1 t}{T_l} - \frac{2a_2 t^2}{T_l^2} + \frac{a_3 t^3}{T_l^3} - \frac{a_4 t^4}{5T_l^4} + \frac{a_5 t^5}{6T_l^5} - \frac{a_6 t^6}{7T_l^6}\right)\right]$$
$$= Q, \quad \text{say}, \tag{45}$$

where
$$\left.\begin{aligned} a_1 &= \tfrac{1}{4}\{4 + (\alpha+\delta)T_l - (\alpha+\beta)T_m^4/T_l^3 + (\beta-\delta)T_0^4/T_l^3\},\\ a_2 &= \tfrac{1}{8}\{6 + 4(\alpha+\delta)T_l + \alpha\delta T_l^2 - \alpha\beta T_m^4/T_l^2 + \alpha(\beta-\delta)T_0^4/T_l^2\},\\ a_3 &= \tfrac{1}{4}\{4 + 6(\alpha+\delta)T_l + 4\alpha\delta T_l^2\},\\ a_4 &= 1 + 4(\alpha+\delta)T_l + 6\alpha\delta T_l^2,\\ a_5 &= (\alpha+\delta)T_l + 4\alpha\delta T_l^2,\\ a_6 &= \alpha\delta T_l^2. \end{aligned}\right\} \tag{46}$$

From (45) one obtains
$$x = \int_t^{T_l} \frac{1-\alpha t}{Q^{\frac{1}{2}}}\,\mathrm{d}t. \tag{47}$$

It will be seen that in the special case when $\alpha = \beta = \delta = 0$ each of the coefficients $a_{1,\ldots,6}$ defined by (46) reduces to unity, and (47) reduces to (14) as it should. Even otherwise a_1 will remain practically at unity.

Now let us consider first the case of an infinitely long rod, for which $T_l = T_m$. Equation (47) can in this case be shown to reduce to

$$x(10aa_1 T_m^3)^{\frac{1}{2}} = \int_t^{T_m} \frac{(1-\alpha t)\,\mathrm{d}t}{t\left(1 + \frac{b_1 t}{T_m} + \frac{b_2 t^2}{T_m^2} + \frac{b_3 t^3}{T_m^3} + \frac{b_4 t^4}{T_m^4} + \frac{b_5 t^5}{T_m^5}\right)^{\frac{1}{2}}}, \tag{48}$$

where
$$b_1 = -a_2/a_1, \quad b_2 = a_3/(2a_1), \quad b_3 = -a_4/(10a_1),$$
$$b_4 = a_5/(12a_1), \quad b_5 = -a_6/(14a_1),$$

and the values of $a_{1,2,\ldots,6}$ are now those corresponding to $T_l = T_m$.

Expanding the integrand in (48) as a power series in t/T_m and integrating term by term, one obtains

$$x(10aa_1 T_m^3)^{\frac{1}{2}} = \ln T_m + \chi' - \left[\ln t + \frac{A_1 t}{T_m} + \frac{A_2 t^2}{T_m^2} + \frac{A_3 t^3}{T_m^3} + \ldots\right], \tag{49}$$

where
$$\left.\begin{aligned} A_1 &= -(b_1/2 + \alpha T_m), \quad A_2 = \tfrac{1}{2}(3b_1^2/4 + \alpha b_1 T_m - b_2),\\ A_3 &= \tfrac{1}{48}(12b_1 b_2 - 6b_1^3 \alpha T_m + 8b_2 \alpha T_m - 8b_3 - 5b_1^3),\\ \chi' &= A_1 + A_2 + A_3 + \ldots. \end{aligned}\right\} \tag{50}$$

* This assumption considerably simplifies the expressions and hence is adopted here. But it is possible to take into account the actual temperature variations of these quantities even if they are not linear. In general, α is negative and β and δ positive.

Again it will be seen that when α, β and δ vanish, A_1, A_2 and A_3 tend to $\frac{1}{2}$, $\frac{1}{12}$ and $-\frac{1}{240}$ respectively, $\chi' \to \chi$, and (49) reduces to (31) as it should.

Now the effect of the finite temperature coefficients of κ, ρ and ϵ on the temperature distribution is twofold:

(1) the effect on the additive constant, which is now χ' instead of χ; this effect is naturally independent of t and is also independent of the length of the rod;

(2) the effect on the terms involving t, which will be the greater the larger the value of t.

The investigation in the A-region of a finite rod, which will be given presently, shows that even when the rod contains just the A-region, and t is of the order of t_c or T_l, the second effect is negligible. Hence the total effect of the finite temperature coefficients on the distribution in these regions, $t \lesssim t_c$, of an infinitely long rod, is to elongate x by

$$\Delta x = (\chi - \chi')/(10\alpha T_m^3)^{\frac{1}{3}}. \tag{51}$$

The constant D appearing in the logarithmic formula will also be similarly increased by $\chi - \chi'$.

One can also investigate in the same manner the effect of the temperature coefficients of κ, ρ and ϵ in the case of a finite rod. It will suffice to quote here the final results. Taking up the A-region first, it is found that instead of (18), which holds when the temperature coefficients are zero, one now obtains

$$q^2 = \frac{4t(1-f)^2}{5a(T_m^4 - T_l^4)}, \tag{52}$$

where

$$f = \tfrac{1}{6}(a_1 + 2\alpha t_c)\frac{t}{t_c} - \frac{1}{5}\left(\frac{3a_1^2}{8} + \frac{a_2 t_c}{2T_l} + \frac{a_1 \alpha t_c}{2}\right)\frac{t^2}{t_c^2} + \ldots. \tag{53}$$

In the case of temperature-independent κ, ρ and ϵ it was found in § 5 that $f \leqslant 0{\cdot}13$, and it was regarded as negligible in comparison with unity. The effect of the finite temperature coefficients is equivalent to multiplying f by a factor of the order of $1 + \alpha t_c$, which under normal working conditions will still be close to unity. Hence (20) will continue to represent the temperature distribution in the A-region and to the same degree of approximation, as with zero temperature coefficients. This will be the case even for very short rods.

Considering next the B-region of a finite rod, the temperature distribution in it will be given by an expression similar to (27) in which the right-hand side will now be

$$[U' + V' + W']_{T_l}^{T_1}, \tag{54}$$

and the temperature at a given distance x from the end will be the same as for an infinitely long rod, and differ appreciably from it only when the B-region is short and in addition t is close to t_c. Hence the temperature distribution in the B-region will be the same as for an infinitely long rod just as in the temperature-independent case. In particular, in regions close to t_c the effect of the finite temperature coefficients of κ, ρ and ϵ will be merely to elongate x by Δx defined by (51).

Since the temperature distribution in the A-region remains unaffected, this will be equivalent to extending by the same amount the total half-length l of the rod corresponding to a given T_l and T_m.

Comparing now two rods having the same T_l and T_m, one in which κ, ρ and ϵ have finite temperature coefficients and the other in which κ, ρ and ϵ are temperature-independent and have the same values as the former at $T = T_l$, the two curves diverge slightly near the origin, but soon settle to a constant displacement along the x axis, of the former curve with respect to the latter, by an amount given by (51). This will be the case also when the two rods are infinitely long.

11. Some relevant graphs

As was mentioned in an earlier section, when the physical constants involved are temperature-independent, the three parameters T_l, T_m and a determine uniquely the temperature distribution along the rod. Taking for example $T_m = 1500°\,\mathrm{K}$, and expressing the lengths in terms of $1/\sqrt{a}$, the temperature distribution curves have been plotted in figure 1 for different selected values of T_l. The values plotted were

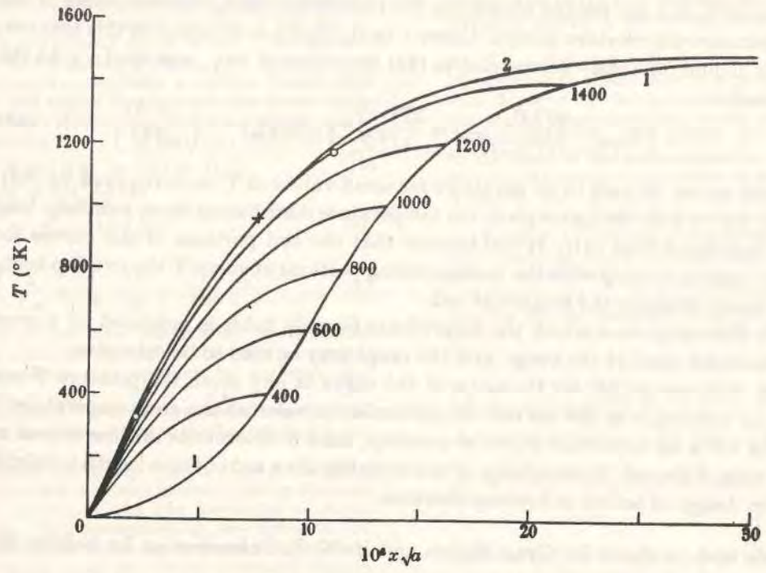

Figure 1. Temperature distribution curves for $T_m = 1500°\,\mathrm{K}$. and various values of T_l marked in the figure.

calculated on the basis of the relations (18) and (27) respectively in the A- and the B-regions, i.e. treating κ, ρ and ϵ as independent of temperature. *The same curves may also be utilized to give the temperature distribution in the case when the temperature coefficients of κ, ρ and ϵ are finite*, in the following manner. The abscissa should now be taken to represent not $x\sqrt{a}$, but

$$x\sqrt{a} - \left\{(\chi' - \chi) - (A_1 - \tfrac{1}{2})\frac{t}{T_m} - \ldots\right\}(10T_m^3)^{-\frac{1}{3}}. \tag{55}$$

We shall draw attention here to some of the important features of the curves plotted in figure 1, and the corresponding results deduced in the previous sections which they help to illustrate.

(1) The limit of the A-region is indicated by a small circle on the curve. The horizontal distance from the circle to the end of the curve, corresponding to $T = T_l$ gives the linear extension q_c of the A-region. The variation of q_c with T_l or l obtained in (22) may be readily verified.

(2) The value of T_l corresponding to $l = q_c$ is given by $T_l = T_m/3^{\frac{1}{4}} = 1140°$. Hence curves for which $T_l < 1140°$ correspond to short rods, $l < q_c$, which have no B-region at all. These curves are all parabolic. From the curves of T against x plotted here the corresponding curves of t against q can be easily obtained by suitably displacing the former curves horizontally. These t against q curves for short rods may be seen to be parallel to one another (see § 6).

(3) Having plotted the temperature-distribution curves for different selected values of T_l, one can readily obtain the $T_l - l$ curve by joining the end points of the temperature distribution curves. Curve 1 in the figure is obtained in this manner, and it should obviously correspond to (23) for values of $l < q_c$, and for $l > q_c$ to the expression

$$l = \left(\ln \frac{2T_l^3 T_m}{T_m^4 - 3T_l^4 + 2T_l^3 T_m} + \frac{3T_l^4 - T_m^4}{4T_l^3 T_m}\right)(10aT_m^3)^{-\frac{1}{2}} + \left(\frac{2}{5aT_l^3}\right)^{\frac{1}{2}}. \qquad (56)$$

The curve can be seen to be parabolic for small values of T_l, as is required by (23).

(4) Curve 2 in the figure gives the temperature distribution in an infinitely long rod calculated from (31). It will be seen that the end portions of the curves for finite lengths overlap with the corresponding portions of curve 2, the overlap being the more extensive the longer the rod.

(5) The range over which the logarithmic formula holds is indicated by a cross at the lower limit of the range, and the range may be seen to be extensive.

(6) Expression (38) for the slope of the curve at any given temperature T can also be verified from the curves. In particular its value at the end-temperature Θ of the rod is an important physical quantity, since it determines the loss of heat at the ends of the rod. A knowledge of this quantity for a rod of finite length is helpful in the design of sealed-in heating elements.

We wish to thank Mr Gyan Mohan and Mr N. R. Subramanian for helpful discussions.

REFERENCES

Baerwald, H. G. 1936 *Phil. Mag.* **21**, 641.
Bush, V. & Gould, K. E. 1927 *Phys. Rev.* **29**, 337.
Cox, M. 1943 *Phys. Rev.* **64**, 241.
Carslaw, H. S. & Jaeger, J. C. 1947 *Conduction of heat in solids*, p. 135. Oxford: Clarendon Press.
Langmuir, I. & Taylor, J. B. 1936 *Phys. Rev.* **50**, 68.
Prescott, C. H. & Hincke, W. B. 1928 *Phys. Rev.* **31**, 130.
Stead, G. 1920 *J. Instn Elect. Engrs*, **58**, 107.
Worthing, A. G. 1914 *Phys. Rev.* **4**, 523.
Worthing, A. G. 1922 *J. Franklin Inst.* **194**, 597.
Worthing, A. G. & Halliday, D. 1948 *Heat*, p. 171. New York: John Wiley and Sons.

Temperature Distribution in an Electrically Heated Filament

THE distribution of temperature in a filament electrically heated *in vacuo* has been studied by several previous authors. The differential equation defining the steady state is:

$$\frac{d^2T}{dx^2} + \frac{5}{2}\,a\,(T_m^4 - T^4) = 0, \qquad (1)$$

in which T is the temperature at a distance x from one of the ends, T_m is the value to which the temperature T_l at the centre tends as the length $2l$ of the filament is increased indefinitely, keeping the heating current the same, and a is a constant determined by the cross-section of the filament, its thermal conductivity and the emissivity of its surface. Using the boundary conditions $T = \Theta$ when $x = 0$, and $dT/dx = 0$ when $x = l$, one obtains[1]

$$x = \int_\Theta^T [5aT_m^4\,(T_l - T) - a\,(T_l^5 - T^5)]^{-\frac{1}{2}}\,dT, \qquad (2)$$

the value of T_l occurring in (1) being determined by the condition that, when the upper limit of the integral is made equal to T_l, x should become l.

In a recent paper[2] it was shown that though the integral cannot be evaluated directly, it can be expanded as a convergent power series. The filament can be divided for this purpose into two distinct regions, region A comprising a certain length near the middle, and region B outside it, the power series referred to being different in the two regions.

Now, denoting $T_m - T$ by Δ, it can be shown that:

$$\Delta \exp f(\Delta) = \exp \pm x\sqrt{A} \qquad (3)$$

are solutions of (1), where

$$A = 10\,a\,T_m^3 \qquad (4)$$

and

$$f(\Delta) = \frac{1}{2}\frac{\Delta}{T_m} + \frac{1}{16}\frac{\Delta^2}{T_m^2} - \frac{1}{240}\frac{\Delta^3}{T_m^3} - \cdots \qquad (5)$$

The effect of the finite temperature coefficient of the thermal conductivity, and of the other constants, can also be taken into account by replacing the factors $\frac{1}{2}$, $\frac{1}{16}$, $-\frac{1}{240}$, ... by A_1, A_2, A_3, ... which can be calculated. For a tungsten filament with $T_m = 2{,}400°$ K., $A_1 = 0{\cdot}75$, and the other A's are much smaller.

In the region where $\exp f(\Delta)$ is close to unity, a general solution for the finite filament can be obtained by suitably combining the two particular solutions given by (3). The corresponding two terms in the general solution are obviously such that one of them increases rapidly and the other decreases rapidly as we move away from the centre of the filament. If $T_m - T_l$ is sufficiently small, the latter term may become negligible in comparison with the former, while Δ still remains small enough to permit our combining the two particular solutions. When this has happened, the need to keep $\exp f(\Delta)$ close to unity disappears. We thus obtain a *practical* general solution that is applicable over the whole length of the filament, namely:

$$\begin{aligned}\Delta \exp f(\Delta) &= \Delta_0 \exp f(\Delta_0)\,[\exp - x\sqrt{A} + \exp\{-(2l - x)\sqrt{A}\}] \\ &= \Delta_0 \exp f(\Delta_0) \exp - l\sqrt{A}\,(\exp q\sqrt{A} + \exp - q\sqrt{A}),\end{aligned} \qquad (6)$$

where $\Delta_0 = T_m - \Theta$, and $q = l - x$ is the distance measured from the centre.

Now for a filament for which $T_m - T_l$ is small in comparison with T_m, which we shall refer to for convenience as a 'long' filament, the limit of the A-region is given by $\Delta_c \sim 3(T_m - T_l)$. At this point it is found that the ratio of the second term inside the brackets in (6) to the first term has decreased to about $\exp(-3{\cdot}6)$, that is, below 3 per cent. Taking for convenience this fraction, namely 0·03, as small in comparison with unity, we can readily investigate how small $T_m - T_l$ should be in comparison with T_m in order that (6) may hold over the whole length of the filament to at least this degree of accuracy.

It may appear at first sight that the criterion for our being able to combine the two particular solutions, namely, that $\exp f(\Delta)$ should be close to unity, will become increasingly difficult to satisfy as Δ increases. But actually, owing to the disparity in the magnitudes of the two terms to be combined, which increases rapidly as one moves away from the centre, the working criterion becomes $f(T_m - T_l) < 0{\cdot}03$, or $(T_m - T_l) < 0{\cdot}04T_m$. When this is secured, (6) will fit with observation to a much closer accuracy than 3 per cent, the accuracy increasing rapidly as one moves away from the centre of the filament.

The results obtained earlier for such a filament, on the basis of the series-expansion of the integral—namely, the parabolic variation of temperature in the A-region, the closeness of the distribution outside the A-region to that of a similar infinitely long filament heated by the same current and the logarithmic distribution at the top of this range—all come out as special cases of (6).

By putting $x = l$ in (6), one obtains a useful relation for the temperature T_l at the centre of a long filament, as a function of its length, namely:

$$T_l = T_m - 2\Delta_0 \exp f(\Delta_0) \times \exp - l\sqrt{A}, \qquad (7)$$

in view of which (6) may also be written in the convenient form,

$$\Delta \exp f(\Delta) = \tfrac{1}{2}\,(T_m - T_l)\,(\exp q\sqrt{A} + \exp - q\sqrt{A}), \qquad (8)$$

which is applicable over the whole length of a long filament.

K. S. KRISHNAN
S. C. JAIN
National Physical Laboratory of India,
Hillside Road,
New Delhi 12.
Feb. 12.

[1] See Carslaw, H. S., and Jaeger, J. C., "Conduction of Heat in Solids", 135 (Oxford: Clarendon Press, 1947).
[2] Krishnan, Sir K. S., and Jain, S. C., *Nature*, 173, 166 (1954); *Proc. Roy. Soc.*, A (in course of publication).

The distribution of temperature along a thin rod electrically heated *in vacuo* II. Theoretical (continued)

By S. C. Jain and Sir K. S. Krishnan, F.R.S.
National Physical Laboratory of India, New Delhi
(*Received* 22 *January* 1954)

For a thin rod electrically heated *in vacuo* the differential equation defining the distribution of temperature in the steady state has been formulated previously. If the rod is not too short, a solution can be obtained by suitably combining the two particular solutions for a similar infinitely long rod heated by the same current, which is applicable over the whole length of the rod. The solution is discussed in relation to some formulae that had been proposed by Stead. The solution also leads to a very useful expression for the temperature at the centre of a finite long rod as a function of its length.

1. Introduction

In part I (Jain & Krishnan 1954) of this paper was reported a theoretical investigation of the distribution of temperature along a thin rod electrically heated *in vacuo*. The integral defining the distribution cannot be evaluated directly, but it can be expanded as a convergent power series, the convergence being rapid in most parts of the rod. The rod is divisible for this purpose into two well-defined regions, region A comprising a certain length in the middle of the rod, and region B outside it, the appropriate series for the evaluation of the integral being different for the two regions. The main features of the distribution of temperature in the two regions are also different, and they have been investigated in detail in part I.

In the context of these investigations, an additive formula proposed originally by Stead (1920) connecting the temperature distribution in a finite rod, with that obtaining in a similar infinitely long rod heated by the same current, becomes significant. This formula of Stead's was derived by him as an approximation to a certain multiplicative formula. Though the latter formula, as we shall see in the present paper, is not justifiable, the additive formula is known to fit with observation. It suggests that it may be possible to formulate a solution of the differential equation defining the temperature distribution in a finite rod in terms of the appropriate particular solutions for an infinitely long rod. This method of approach to the problem has proved helpful, and the present part is an extension of the theoretical investigations given in part I, from this point of view.

2. Stead's formulae

On the basis of some detailed measurements on the distribution of temperature along a very long tungsten filament electrically heated *in vacuo*, Worthing (1914) found that the temperature at any distance x from the cold end can be expressed in the form

$$T_x = T_m[1-e^{-\mu(x+x_0)}]^n, \tag{1}$$

in which T_m is the temperature to which T_x tends as $x\to\infty$. In formulating (1) Worthing was guided partly by theory and partly by the requirements of the experimental data. For temperatures T_x close to T_m the terms inside the brackets could be justified theoretically, though even here the constant x_0 was not determinable theoretically. The index n was introduced in order to make a single formula applicable over a wider range of T_x.

But the most significant part of this expression, which has been utilized by Stead, is the proportionality of T_x to T_m. Had there been no conduction towards the cold end of the rod, the temperature at every point would have been equal to T_m, the value of T_m being determined by the balancing between the heat generated in the rod by the electric current and the radiation of energy from the surface of the rod. But owing to the loss of energy by conduction the actual temperature T_x is smaller. The proportionality of T_x to T_m observed by Worthing implies that in an infinitely long rod the effect of the cold end is to reduce the temperature at any distance x from the end by a factor F, where F is a function of the distance. Denoting by primed letters the temperatures along an infinitely long rod, in order to distinguish them from those relating to finite rods,

$$F(x) = T'_x/T_m. \tag{2}$$

Generalizing from this, Stead formulated that in a *finite* rod, since there are two cold ends through which heat is conducted away, the temperature at any given distance x from one of the ends should be given by

$$T_x/T_m = F(x)\,F(2l-x), \tag{3}$$

where $2l$ is the length of the rod.

Though in deriving (3) in this manner no restriction is imposed on the length of the rod, Stead finds that the formula is applicable to long rods only. Considering such a rod, for which T_m-T_l is small in comparison with T_m, where T_l is the temperature at the centre, and confining attention to a region where T_m-T_x also is small, it may be seen that $F(l)$, $F(x)$ and $F(2l-x)$ will all be close to unity, and that (3) then reduces to the additive formula

$$T_m-T_x = (T_m-T'_x)+(T_m-T'_{2l-x}). \tag{4}$$

It is in this form that the formula has been applied by Stead, and verified experimentally.

Any formula defining the temperature distribution has naturally to be a solution of the differential equation determining the steady state. As we shall see presently, an expression of the type (3) cannot be a solution, and hence the derivation of (4) in the manner indicated before may not be justifiable. On the other hand, Stead's additive relation (4) is known to fit with the experimental data for long rods. We proceed to investigate whether it would be possible directly to obtain a solution of the type (4) for the differential equation for such rods, irrespective of the validity of (3) on which Stead's derivation is based.

3. General solution of the differential equation of the steady state

The differential equation determining the steady state may be written in the form (see (1) and (10) of part I)

$$d^2T/dx^2+\tfrac{4}{3}a(T_m^4-T^4) = 0, \tag{5}$$

where the subscript x of T_x has been omitted for convenience. The equation applies naturally to the infinitely long rod also. The letter a appearing in (5) and the other

letters which we shall use later in this part, have the same significance as in part I. Neglecting for the present the temperature coefficients of κ, ρ and ϵ, which have been taken into account in part I, but which are not quite relevant to the present discussion, and denoting $T_m - T$ by Δ, (5) may be written in the form

$$d^2\Delta/dx^2 = \tfrac{1}{2}a(4T_m^3\Delta - 6T_m^2\Delta^2 + 4T_m\Delta^3 - \Delta^4). \tag{6}$$

Multiplying both sides by $2d\Delta/dx$ and integrating with respect to x, and putting $10aT_m^3 = A$, one obtains

$$\left(\frac{d\Delta}{dx}\right)^2 = A\Delta^2\left(1 - \frac{\Delta}{T_m} + \frac{\Delta^2}{2T_m^2} - \frac{\Delta^3}{10T_m^3}\right), \tag{7}$$

whence

$$\pm x\sqrt{A} = \int \frac{d\Delta}{\Delta\left(1 - \frac{\Delta}{T_m} + \frac{\Delta^2}{2T_m^2} - \frac{\Delta^3}{10T_m^3}\right)^{\frac{1}{2}}} \tag{8}$$

or

$$\Delta e^{f(\Delta)} = e^{\pm x\sqrt{A}}, \tag{9}$$

where

$$f(\Delta) = \frac{\Delta}{2T_m} + \frac{\Delta^2}{16T_m^2} - \frac{\Delta^3}{240T_m^3} - \ldots. \tag{10}$$

The *physical* solution applicable to the infinitely long rod is

$$\Delta e^{f(\Delta)} = c e^{-x\sqrt{A}}, \tag{11}$$

in which c may be eliminated from the boundary condition that when $x = 0$, $\Delta = \Delta_0 = T_m - \Theta$, where Θ is the temperature of the cold ends, which may have any value down to zero. One thus obtains

$$\Delta e^{f(\Delta)} = \Delta_0 e^{f(\Delta_0)} e^{-x\sqrt{A}}, \tag{12}$$

which can be seen to be identical with (31) of part I, remembering that the temperature coefficients of κ, ρ and ϵ are being neglected here. If desired, the temperature coefficients may be included by suitably modifying the expression for $f(\Delta)$ in the manner indicated in part I.

It can be readily seen from (12) that a multiplicative formula of the type (3) cannot possibly be fitted with (12). On the other hand, as will be shown in the next section, the additive formula (4) can be obtained by a suitable combination of the two particular solutions obtained in (9). We now proceed to demonstrate this, and to determine the conditions under which this can be done.

4. Solution for the finite rod as combination of particular solutions for the infinitely long rod

Now $\Delta \leqslant \Delta_0 \leqslant T_m$. Even when $\Delta = T_m$, which will be the case at the cold end of a rod when the end is kept at zero temperature,

$$f(T_m) = \tfrac{1}{2} + \tfrac{1}{16} - \tfrac{1}{240} - \ldots = 0{\cdot}56. \tag{13}$$

For other values of Δ, $f(\Delta)$ will be smaller, and when Δ is small in comparison with T_m, $e^{f(\Delta)}$ will be practically unity.

In any case, in a finite rod and in a region where Δ is small, a general solution of the differential equation may be obtained by suitably combining the two particular solutions in (9), which is now permissible since $e^{f(\Delta)}$ is now practically unity. The condition that Δ be small implies first that the rod is long enough to make $T_m - T_l$ small, and secondly that the point concerned is not too far away from the centre of the rod. The general solution is

$$\Delta = c_1 e^{-x\sqrt{A}} + c_2 e^{x\sqrt{A}}, \tag{14}$$

which could also have been obtained directly as solutions of

$$d^2\Delta/dx^2 = A\Delta, \tag{15}$$

to which (6) reduces when Δ is small.

The two constants c_1 and c_2 appearing in (14) may be evaluated from the following conditions:

$$\left.\begin{aligned} d\Delta/dx = 0 \quad &\text{when} \quad x = l, \\ \Delta = \Delta_1, \text{ say}, \quad &\text{when} \quad x = x_1, \end{aligned}\right\} \tag{16}$$

where x_1 represents a distance which is considerably smaller than l, but is still within the range where Δ remains small in comparison with T_m. Using these conditions one obtains

$$c_1 = \frac{\Delta_1 e^{l\sqrt{A}}}{e^{(l-x_1)\sqrt{A}} + e^{-(l-x_1)\sqrt{A}}}, \tag{17}$$

$$c_2 = \frac{\Delta_1 e^{-l\sqrt{A}}}{e^{(l-x_1)\sqrt{A}} + e^{-(l-x_1)\sqrt{A}}}. \tag{18}$$

Now if it is possible to find a value of x_1 such that Δ at this point, namely, Δ_1, remains small in comparison with T_m, i.e. *$e^{f(\Delta_1)}$ remains close to unity, and at the same time $e^{-2(l-x_1)}$ has become negligibly small in comparison with unity,* then (14) will reduce to

$$\Delta = \Delta_1 e^{x_1\sqrt{A}}[e^{-x\sqrt{A}} + e^{-(2l-x)\sqrt{A}}]. \tag{19}$$

If, further, Δ_1, which represents the temperature of the *finite* rod at a distance x_1, can also be shown to be the temperature of the infinite rod at the same distance x_1, then obviously

$$\Delta_1 e^{x_1\sqrt{A}} = \Delta_0 e^{f(\Delta_0)}. \tag{20}$$

The general solution (19) for regions $T_m - T_l < \Delta < \Delta_1$ will then reduce to

$$\Delta = \Delta_0 e^{f(\Delta_0)}[e^{-x\sqrt{A}} + e^{-(2l-x)\sqrt{A}}]. \tag{21}$$

The two terms in (21) can then be seen to be separately the solutions for an infinitely long rod.

Equation (21) can be seen to be the same as Stead's additive relation (4), except that (21) gives also the actual values of the two particular solutions, which (4) does not.

It now remains to investigate whether the conditions imposed in the derivation of (21) can be actually secured, and the range over which this can be done. Before doing so we shall briefly indicate an alternative method of deriving (19), which is helpful in understanding the significance of the conditions imposed above. It also enables us incidentally to follow in detail the temperature variation in the A-region, which also is needed for our present purpose.

5. An alternative solution

Taking the case of a finite rod of *any* length, and confining attention to a region close to the centre, where $t = T_1 - T$ is small in comparison with T_1, the differential equation defining the steady state can be written in the form

$$d^2t/dq^2 - Pt - Q = 0, \tag{22}$$

where

$$P = 10aT_1^3, \tag{23}$$

$$Q = \tfrac{5}{2}a(T_m^4 - T_1^4), \tag{24}$$

and $q = l - x$ is the distance measured from the centre. Solving (22) with the boundary conditions $t = 0$, and $dt/dq = 0$, when $q = 0$, one obtains

$$t = \frac{Q}{P}[\cosh(q\sqrt{P}) - 1]. \tag{25}$$

Expression (25) is applicable to *any* rod, short or long, provided that t is small, the linear extent of this region depending on how long the rod is, since the variation of t is the slower the longer the rod. When $q\sqrt{P}$ is sufficiently small that q^2P is negligible in comparison with unity, (25) reduces to

$$t = \tfrac{1}{2}Qq^2, \tag{26}$$

which is identical with the parabolic relation obtained in part I. As q increases, the temperature variation naturally deviates increasingly from the parabolic law. This deviation, which was investigated for the general case in part I with the help of a complicated series, comes out more elegantly, for small values of t, as just the deviation of $\cosh(q\sqrt{P})$ from $1 + \frac{1}{2}Pq^2$. For a given small t the deviation will be the smaller the smaller the value of P, i.e. the shorter the rod, which is in agreement with the result obtained in part I.

For a long rod for which $T_m - T_1$ is small, the deviation from the parabolic law is a maximum. In this case, and at the upper limit of the A region, where $t_c = 2Q/P$, the deviation of the actual value of q from that calculated from the parabolic law comes out as 10 %. This again is the same as the value calculated in part I.

For such a rod, $t_c = 2Q/P = 2(T_m - T_1)$. Thus even at the limit of the A-region, Δ is only thrice $T_m - T_1$, and therefore remains small in comparison with T_m.

Returning to (25) one can see that when $T_m - T_1$ is small in comparison with T_m, $Q/P = T_m - T_1$ and $P = A$. Remembering that $t = \Delta - (T_m - T_1)$, (25) can be readily seen to reduce to (19).

6. A More general expression applicable over the whole rod

Coming back to the general solution (19), it will be seen that the ratio of the two terms is equal to $e^{-2q\sqrt{A}}$, and that it decreases rapidly with the increase of q. Even at the limit of the A-region, where Δ still remains small in comparison with T_m, and hence (19) remains valid, $2q\sqrt{A}$ has increased to 3·6. Hence this ratio has become as small as $e^{-3\cdot6}$, which is less than 3 %. Hence as one moves into the B-region, only

one of the two particular solutions in (19) will be significant, the other having become relatively negligible.

It will be remembered that the condition that Δ also be small was invoked in order to enable us to combine the two particular solutions. Now that one of them has vanished, the necessity for this condition also vanishes. In other words the distribution of temperature over the rest of the rod will be practically the same as for a similar infinitely long rod heated by the same current, the agreement between the two becoming the closer the nearer one approaches the cold end. Incidentally it also shows that for such rods for which $T_m - T_1$ is small in comparison with T_m, the expression for Δ will reduce to the simple exponential form at the top of the B-region, which is in conformity with the result obtained in part I.

When we move further inside the B-region, since we have now to deal with only one solution, and it is characteristic of an infinitely long rod, one may use the more precise form (12).

Consider now the general expression

$$\Delta\, e^{f(\Delta)} = \Delta_0\, e^{f(\Delta_0)}[e^{-x\sqrt{A}} + e^{-(2l-x)\sqrt{A}}]. \tag{27}$$

Though as such it may not satisfy the differential equation, it will be a solution in the following two special cases, as we have shown:

(a) if $e^{f(\Delta)} \approx 1$;

(b) even when $e^{f(\Delta)}$ differs much from unity, if one of the terms inside the brackets in (27) vanishes.

For a rod for which $T_m - T_1$ is small in comparison with T_m, we have shown that these two conditions are so related that one or the other of them is satisfied at *every* point of the rod. Indeed, there is a considerable range where (a) and (b) are *both* sensibly satisfied.* Hence (27) may be regarded *practically* as a solution of the differential equation over the whole length of the rod.

Now equation (27) may be seen to be the same as Stead's additive formula (4), and that it gives much more detailed information regarding the temperature distribution than (4). The necessary condition for its validity is that $T_m - T_1$ be small in comparison with T_m, and when this condition is satisfied, the formula will be valid over the whole length of the rod, not only in regions where $T_m - T$ is small in comparison with T_m, for which region (4) was supposed to be a good approximation to the correct formula, but also over regions where $T_m - T$ may have become as large as T_m itself. On the other hand, the multiplicative formula, of which (4) was regarded as an approximation, has no validity except in so far as it may approximate to (4).

* [*Note added in proof*, 16 *June* 1954.] It should be emphasized here that the condition for our being able to combine the two solutions, namely, that $e^{f(\Delta)}$ be close to unity, is indeed the most stringent near the centre, where the two terms to be combined are of the same magnitude. This is so in spite of the fact that Δ itself has the *minimum* value here. As we move away from the centre, because of the progressively growing disparity in the magnitudes of the two terms to be combined, the permitted tolerance, i.e. the permitted deviation of $e^{f(\Delta)}$ from unity increases progressively with the distance from the centre (Krishnan & Jain, *Nature, Lond.*, 1 *May* 1954). Putting $f(T_m - T_1) = \theta \ll 1$, equation (27) will represent the temperature distribution near the centre to an accuracy of θ in 1, and the accuracy will increase progressively as we move away from the centre.

From (27), which is applicable to a long rod over its whole length, one can readily obtain by putting $x = l$, an expression for T_l as a function of l. The expression is

$$T_l = T_m - B\,e^{-l\sqrt{A}}, \tag{28}$$

where

$$B = 2\Delta_0 e^{l(\Delta_0)}. \tag{29}$$

Experimentally (28) is a very useful relation.

For the temperature distribution in short rods one has to fall back on the detailed solutions (25) and (11) respectively in the regions A and B, or the corresponding ones given in part I.

REFERENCES

Jain, S. C. & Krishnan, Sir K. S. 1954 *Proc. Roy. Soc.* A, **222**, 167 (part I).
Stead, G. 1920 *J. Instn Elect. Engrs*, **58**, 107.
Worthing, A. G. 1914 *Phys. Rev.* **4**, 523.

The distribution of temperature along a thin rod electrically heated *in vacuo*

III. Experimental

BY S. C. JAIN AND SIR K. S. KRISHNAN, F.R.S.

National Physical Laboratory of India, New Delhi

(*Received* 5 *February* 1954)

The present part is concerned with a detailed experimental verification of the main results obtained theoretically in the earlier parts. Thin rods of Acheson graphite were used for this purpose, and were found very suitable. In addition to the experimental data for the temperature distribution along rods of different lengths, and heated by alternating currents of different densities, one also needs for such a verification, data for the thermal and the electrical conductivities, and the spectral and the total emissivities of the surface, at different temperatures. These measurements also have been made.

The observed temperature variation along the rod is itself used to determine the thermal conductivity and its temperature variation. The thermal conductivity is found to decrease and tend to a constant value at high temperatures, as it should. The other physical constants are determined directly. At low temperatures the spectral emissivity is found to be much larger than the total emissivity, and they tend to approach each other at high temperatures. Further, the spectral emissivity is found to decrease rapidly with increase of wave-length, as in the case of metals.

Coming back to the temperature distribution, the main results that are verified here relate to the range of validity of the logarithmic formula in the B-region of a long rod, the constants involved in the formula, the deviation from the formula as one moves further into the B-region, the effect of the temperature coefficients, the parabolic law of variation near the centre, and the nature of the deviation from the parabolic law in long and short rods as one moves further away from the centre.

1. INTRODUCTION

In parts I and II (Jain & Krishnan 1954*a*, *b*) were reported some theoretical investigations on the distribution of temperature along a thin rod or filament electrically heated *in vacuo*. The present part is concerned with the experimental verification of the main results obtained there.

Extensive experimental data are available for the temperature distribution in electrically heated filaments of tungsten (Worthing 1914), and some for thin-walled tube of Acheson graphite (Prescott & Hincke 1928). The lengths used in these measurements, however, are such as to make the temperature over the whole of the A-region sensibly constant. The data for rods of medium and short lengths afford naturally a more stringent test of the theory. Such short rods do not seem to have been studied previously.

The experimental verification requires also a knowledge of some of the physical constants of the material, which are not available. Hence we have made detailed studies of the temperature distribution in thin rods of Acheson graphite, using a wide range of lengths and heating currents, and we have also made measurements on the physical constants required for the experimental verification of the results obtained in parts I and II. As we shall see later in this part, Acheson graphite is a very suitable material for this purpose.

2. THE PARAMETERS INVOLVED

The distribution function is determined uniquely, as was found in part I, by three parameters, which can be taken to be conveniently the following: (1) the temperature T_l at the centre of the rod, or its semi-length l; (2) the temperature T_m to which T_l tends as l is increased indefinitely, keeping the heating current I constant; T_m is determined by the condition

$$p\epsilon\sigma(T_m^4 - fT_w^4) = I^2\rho/\omega; \tag{1}$$

(3) a constant defined by

$$a = \tfrac{2}{3}p\epsilon\sigma/(\kappa\omega); \tag{2}$$

where ω is the cross-sectional area of the rod, p is the perimeter of the cross-section, ρ is the specific resistance and κ is the thermal conductivity, σ is Stefan's constant of radiation, and T_w is the temperature of the glass walls of the large vacuum chamber in which the measurements were made. The chamber was double-walled and between the two walls was circulated water at room temperature, and hence T_w could be taken to be practically the room temperature. Just as ϵ is the total emissivity at temperature T_m, $f\epsilon$ is the absorptivity of the same surface at the same temperature T_m for radiations from a black body at temperature T_w. As will be seen in the next section, the spectral emissivity ϵ_λ of graphite is a function of the wave-length, and it decreases as the wave-length is increased. Since the effective wave-length of the radiations from the walls at T_w is much longer than that of the radiations at T_m, f will be less than, but of the order of, unity. In order to avoid the uncertainty in our knowledge of f, most of our measurements were made at temperatures T greater than 1100° K, for which $T_w^4 \sim 300^4$ becomes small in comparison with T^4. There is a further advantage in using these high temperatures; the basis for the derivation of relation (1) is that the loss of energy from the central region of the rod towards the ends by conduction is negligible in comparison with the loss due to radiation. Though this will be true in any case for long rods, the length can be the shorter the higher the temperature T_m near the centre.

In investigating the temperature distribution, the known temperature dependence of κ, ρ and ϵ can also be taken into account. It was shown in part I that the temperature distribution in the *A*-region, expressed as a function of the distance from the centre, and relatively to the temperature at the centre, remains unaltered by the finite temperature coefficients of these quantities, while in the *B*-region the effect may be regarded as a small correction Δx to the distance x from the end of the rod, of any point having a temperature T, and Δx may be readily obtained from the known temperature coefficients. Thus the physical constants involved in the theoretical expressions are κ, ρ and ϵ at different temperatures in the range concerned. Now the measurement of the temperature at any point on the surface of the heated rod is most conveniently done with the help of an optical pyrometer, and for this purpose a knowledge of the *spectral* emissivity ϵ_λ of the surface, as distinguished from the *total* emissivity ϵ, is also needed.

We now proceed to describe briefly the experimental determination of these physical constants for Acheson graphite at high temperatures.

3. The spectral and the total emissivities

A thin-walled tube of Acheson graphite was heated *in vacuo* by sending a suitable *alternating* current through it. The tube used in the experiment was long enough to make the temperature in the middle of the tube sensibly constant over a considerable length of the tube. Under these conditions, the loss of heat from this region is due almost wholly to radiation from its surface, and very little of it is due either to the thermal conduction from the centre of the tube towards the ends, or to the radiative transfer occurring in the cavity of the tube. By puncturing a small hole in the wall of the tube near the centre, the temperature inside the cavity as viewed through this hole can be measured directly with the help of the optical pyrometer, since the temperature concerned is that of a *black body*.

By making the walls of the tube sufficiently thin, the temperature of the outer surface can be made to approximate to the temperature inside. The small difference in temperature between the inner and the outer surfaces, due to the finite thermal conductivity of the material of the wall, is readily obtained when κ is known. Even a very rough value of κ will serve this purpose. Knowing thus the real temperature T_m and the apparent temperature T_a of the surface as determined directly by the pyrometer,* the spectral emissivity ϵ_λ at this temperature, for the narrow spectral region transmitted by the glass filter of the optical pyrometer, namely, about $0{\cdot}655\,\mu$, is obtained with the help of the relation

$$\epsilon_\lambda = \exp\left[-\frac{hc}{k\lambda}\left(\frac{1}{T_a}-\frac{1}{T_m}\right)\right]. \qquad (3)$$

Measurements on the spectral emissivity of Acheson graphite made in this manner were reported in a recent paper (Jain & Krishnan 1952) in the temperature range 1200 to 1700° K. The measurements have now been extended to 2100° K,

* A small correction is made for the loss of intensity of the radiation in its passage through the glass walls of the chamber (Jain & Krishnan 1952).

and the results are plotted in the upper curve in figure 1. Conversely, for any temperature T_a of the graphite surface obtained directly with the optical pyrometer, the corresponding true temperature T is obtained with the help of this curve and (3). Our measurements of the surface temperature of the graphite rod at different points along the rod were made in this manner.

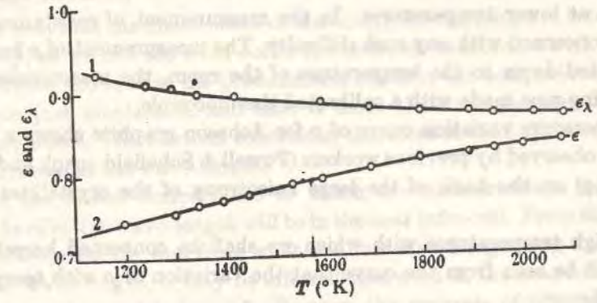

Figure 1. The spectral and the total emissivities of Acheson graphite.

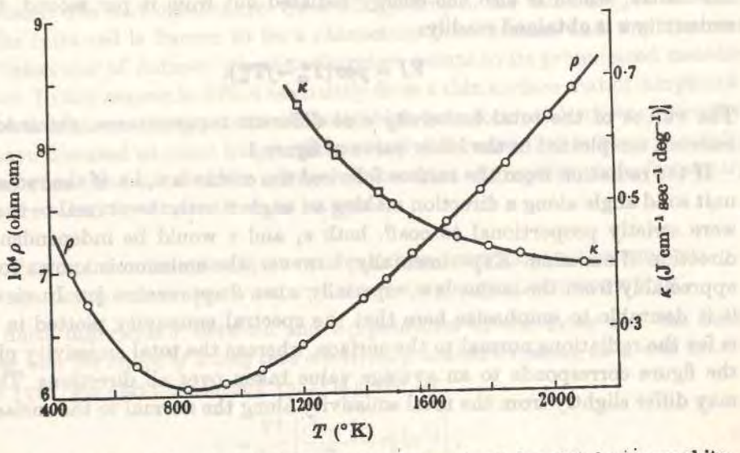

Figure 2. The electrical resistivity and the thermal conductivity of Acheson graphite.

It should be mentioned immediately that the emissivity of the surface naturally depends on the nature of the polish of the surface. For example, any rubbing of the graphite surface with the fingers reduces the emissivity appreciably. However, after maintaining the tube at a temperature of 2000° K for about an hour, the emissivity reaches a steady value that is reproducible. The data plotted in figure 1 refer to such a conditioned surface, which is also the surface of the thin rod along which the temperature distribution is to be studied.

Now the potential gradient V in the central region, where the temperature is sensibly constant, is obtained with the help of two electrical probes. Now, knowing

the heating current I, the specific resistance ρ of Acheson graphite at temperature T_m is readily obtained. By suitably varying I, the value of ρ at any other desired high temperature can be obtained. The results are plotted in figure 2.

The restriction of the low-temperature limit in our other measurements to 1100° K, referred to in an earlier section, was to avoid the uncertainty in the theoretical expressions due to the radiation from the walls of the chamber, which will be appreciable at lower temperatures. In the measurement of resistance, however, one is not concerned with any such difficulty. The measurement of ρ has therefore been extended down to the temperature of the room, the measurement of temperature being now made with a calibrated thermocouple.

The temperature variation curve of ρ for Acheson graphite shows a minimum, as had been observed by previous workers (Powell & Schofield 1939), and explained (Bowen 1949) on the basis of the large anisotropy of the crystallites and their finite size.

At the high temperatures with which we shall be concerned hereafter in the paper, it will be seen from the curve that the variation of ρ with temperature is practically linear.

Knowing the energy generated per second per unit length of the long tube near the centre, which is also the energy radiated out from it per second, the total emissivity ϵ is obtained readily:

$$VI = p\epsilon\sigma(T_m^4 - fT_w^4). \tag{4}$$

The values of the total emissivity ϵ at different temperatures, obtained in this manner, are plotted in the lower curve of figure 1.

If the radiation from the surface followed the cosine law, i.e. if the radiation per unit solid angle along a direction making an angle θ with the normal to the surface were strictly proportional to $\cos\theta$, both ϵ_λ and ϵ would be independent of the direction of emission. Experimentally, however, the emission is known to deviate appreciably from the cosine law, especially when θ approaches $\frac{1}{2}\pi$. In view of this it is desirable to emphasize here that the spectral emissivity plotted in figure 1 is for the radiations normal to the surface, whereas the total emissivity plotted in the figure corresponds to an average value taken over all directions. The latter may differ slightly from the total emissivity along the normal to the surface.

4. The data for the two emissivities compared

It will be seen immediately from figure 1 that at the lower temperatures, ϵ is considerably smaller than ϵ_λ, and the two curves tend to approach each other at high temperatures. An obvious conclusion to be drawn from this is the following. There are two effects associated with the change in temperature. One is the direct effect of the temperature as such on the spectral emissivity in every spectral region. For the red region, as will be seen from the upper curve, the spectral emissivity falls off with the increase of temperature, and it may be presumed that this will be the case for the other spectral regions also. Hence the direct effect of increasing the temperature will be to reduce the total emissivity.

The second effect is indirect. As a consequence of increasing the temperature, the effective wave-length of the radiation, to which the total emissivity refers, will decrease. If ϵ_λ is a function of the wave-length also, as we should expect it to be, there will be an indirect effect of the change of temperature on the total emissivity due to the change in the effective wave-length accompanying the change of temperature.

We have seen that the direct effect of increasing the temperature is to decrease ϵ. But actually, as we can see from curve 2, ϵ is found to increase with rise of temperature, which shows that the predominant effect of the temperature on ϵ is the indirect one just mentioned, and that it more than compensates for the pure temperature effect. The obvious conclusion therefore is that ϵ_λ decreases rapidly with the increase in the wave-length.

Now, at the lowest temperature to which our measurements refer, namely, 1100° K, the effective wave-length will be in the near infra-red. From the magnitude of ϵ at this temperature, and from what was just stated regarding the dependence of ϵ_λ on the wave-length, it may be inferred that even in the near infra-red region ϵ_λ should have dropped below 0·7. Further, the progress of the curve indicates that it should be much lower in the farther infra-red.

This conclusion is of significance. Such a large drop in the value of ϵ_λ as we move to the far infra-red is known to be a characteristic of metals, and the observed similar behaviour of Acheson graphite therefore points to its pronounced metallic character. In this respect it differs essentially from a thin surface coat of lampblack, for which it is known that ϵ_λ continues to be high even for very long wave-lengths.

We have discused at some length the marked difference that is experimentally found between the total and the spectral emissivities of graphite, since frequently the two are taken for convenience to be equal.

5. The finite difference in temperature between the outer and the inner surfaces in relation to the thermal conductivity

The finite difference τ between the temperatures of the inner and the outer surfaces, *near the centre of a long tube* electrically heated *in vacuo*, as is well known (Angell 1911; see also Glazebrook 1922) is given by

$$\tau = \frac{V^2}{2\kappa\rho}\left[\frac{r_1^2 - r_2^2}{2} - r_2^2 \ln\frac{r_1}{r_2}\right], \tag{5}$$

where r_1 and r_2 are the outer and the inner radii respectively. It is assumed that the radial variations of the thermal and the electrical conductivities due to the finite radial gradient of the temperature are negligible. The error involved in this neglect is equivalent to neglecting $\alpha\tau$ in comparison with unity, where α is of the order of the temperature coefficient of either of the conductivities; $\alpha\tau$ will be of the order of 10^{-3}.

Relation (5) may be made the basis for a determination of κ from the observed temperature difference τ between the inner and the outer surfaces of the tube; τ may be made sufficiently large for this purpose by making the thickness of the walls large (Angell 1911). In practice, however, though it is easy to measure the inner tem-

perature accurately, that of the outer surface cannot be measured so readily. It will therefore be more appropriate to make the tube thin-walled, and thus make τ small, and utilize any rough value of κ determined by other methods in order to calculate τ. In this case (6) reduces to the simple form

$$\tau = V^2(r_1-r_2)^2/(2\kappa\rho) = VI(r_1-r_2)/(4\pi\kappa). \tag{6}$$

As Prescott & Hincke (1928) first pointed out, the temperature variation *along* the tube itself in the logarithmic region provides the value of κ required for this purpose. (Actually the observed temperature variation in this region has been utilized by them to eliminate κ from (6) and thence to calculate τ.) Knowing τ the precise temperature T_m of the outer surface is obtained from the known temperature of the inner surface. It is this value of T_m that has been used by us in obtaining the spectral emissivity, and later the total emissivity, of graphite.

Indeed, as will be shown in the next section, the temperature variation along the rod, which can be measured accurately, may be made the basis for an accurate determination of not only κ, but also of its temperature coefficient.

It will be clear from the discussion given above that a thin-walled tube is the most convenient form for the determination of the temperature of the outer surface near the centre, and thence to determine ϵ_λ at this temperature. Graphite can be turned into a tube conveniently on the lathe. Without making the tube walls unduly thin, one can secure enough electrical resistance for heating it to high temperatures.

6. The *B*-region

We now proceed to describe the experimental studies on the distribution of temperature in a thin rod electrically heated *in vacuo*, and to utilize the experimental data thus obtained to verify the main results deduced theoretically in parts I and II.

We shall take up first the case of a rod long enough to include a considerable length of the *B*-region. For such a rod $T_m - T_l$ will be small in comparison with T_m. In part II was deduced a general expression for the temperature distribution in such a rod, which is applicable over its whole length. The expression is

$$\Delta\, e^{f(\Delta)} = \Delta_0\, e^{f(\Delta_0)}[e^{-x\sqrt{A}} + e^{-(2l-x)\sqrt{A}}], \tag{7}$$

in which

$$\Delta = T_m - T, \tag{8}$$

$$\Delta_0 = T_m - \Theta, \tag{9}$$

Θ is the temperature of the ends, and

$$f(\Delta) = \frac{\Delta}{2T_m} + \frac{\Delta^2}{16T_m^2} - \frac{\Delta^3}{240T_m^3} - \cdots. \tag{10}$$

When the temperature coefficients of κ, ρ and ϵ are also taken into account, $f(\Delta)$ may be expressed in the form

$$f_1(\Delta) = \frac{A_1\Delta}{T_m} + \frac{A_2\Delta^2}{T_m^2} + \frac{A_3\Delta^3}{T_m^3} + \ldots, \tag{11}$$

where A_1, A_2 and A_3 have the same significance as in part I. They are now functions of the temperature coefficients, and they naturally reduce to $\frac{1}{2}$, $\frac{1}{16}$ and $-\frac{1}{192}$

respectively when these coefficients become negligible. In order to give an idea of the magnitudes of these quantities it may be mentioned that for Acheson graphite and for $T_m \sim 2000°$ K, A_1 is of the order of unity, A_2 is about 0·2 and $|A_3|$ is still smaller. Since the highest value of Δ/T_m involved in our measurements is less than $\frac{1}{3}$, the second term in (11) is about 10 % of the first or less. Now, $f_1(\Delta)$ itself occurs as an additive term to $\ln\Delta_0 \sim 7$ (see (14) below). Even when $\Delta = \Delta_0$ the A_2 term in $f_1(\Delta_0)$ can be seen to be less than 1 % of $\ln\Delta_0$. Hence it would be ample if the A_1 term alone is retained in the expression for $f_1(\Delta)$.

Now

$$A_1 = \tfrac{1}{2} - \alpha T_m + c. \tag{12}$$

The second term on the right-hand side of (12) involves the temperature coefficient of κ alone, namely α, whereas c involves the coefficients of κ, ρ and ϵ (see equation (50) of part I).

Returning now to (7) it was shown in part II that even at the upper limit of the *B*-region the ratio of the second term inside the square brackets to the first is $e^{-3\cdot6}$, or less than 3 %. As we move inside the *B*-region the ratio will become still smaller. In other words, the distribution becomes independent of l, and is the same as for an infinitely long rod.

Equation (7) then reduces to

$$x\sqrt{A} = D - \ln\Delta - f_1(\Delta), \tag{13}$$

where D denotes the part that is independent of Δ, and is given by

$$D = \ln\Delta_0 + f_1(\Delta_0). \tag{14}$$

As was mentioned in part I, a simple logarithmic formula of the type

$$x\sqrt{A} = D - \ln\Delta \tag{15}$$

had been derived previously on the basis that Δ is small in comparison with T_m, and had been verified experimentally. The additive constant D, however, could not be determined from those simple considerations.

On the other hand, (13) and (14) not only enable us to determine the additive constant D, but also give the actual law of deviation from (15) when Δ is not sufficiently small. One therefore obtains further a criterion for the range of validity of (15), namely, that $\Delta/\ln\Delta$ should be small in comparison with T_m, which is a much less stringent criterion than that Δ should be small in comparison with T_m, on the basis of which (14) had been previously derived.

All these conclusions are verified experimentally. The temperature distribution was studied in thin long rods of different lengths and with different heating currents. In figure 3 are plotted the values of $\ln\Delta$ against x for a typical case, namely, for $T_m = 2100°$ K. The data for other rods are not plotted in the figure since they overlap much on one another. These data are, however, summarized in table 1.

It will be seen from figure 3 that there is a considerable portion in the lower ranges of Δ, where the plot is a straight line, from the slope of which $\sqrt{A}$, and hence the thermal conductivity κ, can be readily obtained. The values of κ obtained in this manner are entered in table 1, and they are also plotted in figure 2.

We should emphasize again that this method of determining the thermal conductivity and its temperature variation at these high temperatures,* is more reliable than the method based on measuring the difference in temperature between the inner and the outer surfaces in the middle of a long tube electrically heated *in vacuo*.

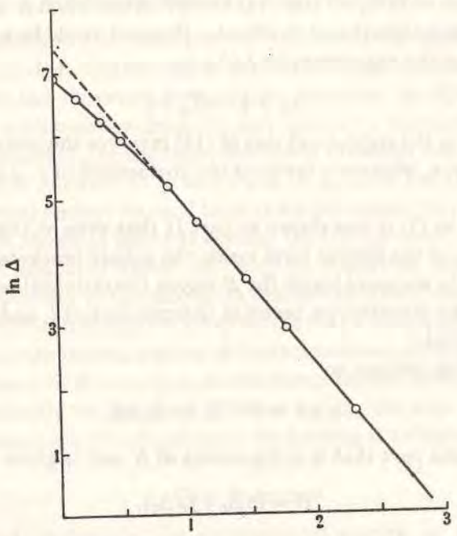

FIGURE 3. The temperature distribution in the B-region when $T_m = 2100°$ K.

Had the logarithmic formula been valid over the whole length of the rod, the additive constant D, which is given by the intercept of the straight line on the $\ln\Delta$ axis at $x = 0$, would also have been the value of $\ln\Delta$ at this point, i.e. D would have been equal to $\ln(T_m - \Theta)$. But actually D is considerably larger, since the curve can be seen to curve downwards, the deviation from the straight line increasing progressively with the increase of Δ. The difference according to (13) should be equal to $f_1(\Delta) \sim A_1\Delta/T_m$. This is verified quantitatively.

In table 1 are given the experimental values for all the long rods studied by us, and the corresponding theoretical values for comparison. The values of α at different temperatures T_m needed for the calculation of A_1 were taken from the κ-T curve given in figure 2. Considering that the quantities compared in the last two rows in

* A graphical method of determining the thermal conductivity from the observed temperature distribution in a filament has been described by Worthing & Halliday (1948). The method is based on finding by graphical integration the total energy generated, and that radiated out, in the whole of the region on the hotter side of the cross-section under consideration, up to the centre of the filament. The difference between the two gives the heat conducted across this section. Knowing the gradient in temperature at this section the conductivity can be calculated.

the table refer to the small deviations from the logarithmic formula, these deviations also may be taken to be verified satisfactorily.

Incidentally it may be mentioned that at $T_m = 2100°$ K, $A_1 = 0{\cdot}95$, which is very much in excess of 0·50, which it would be if the temperature coefficients were neglected. This shows that the deviation from the straight line is due nearly as much to the finite temperature coefficients as to the other factors, their relative contributions to A_1 being 0·45 and 0·50 respectively.

TABLE 1. THE LOGARITHMIC LAW AND THE DEVIATION FROM IT

T_m (° K)		1300	1500	1700	1800	1900	2100
$\sqrt{A}$	from the curve	0·92	1·27	1·66	1·84	2·03	2·45
κ (J cm^{-1} sec^{-1} deg^{-1})		0·60	0·50	0·44	0·43	0·42	0·40
$D - \ln\Delta_0$		0·23	0·28	0·33	0·36	0·39	0·46
$A_1\Delta_0/T_m$		0·23	0·30	0·32	0·36	0·38	0·44

Thus all the important results deduced theoretically for the temperature distribution in this region are verified quantitatively, namely, (1) the slope of the straight-line part of the curve, (2) the additive constant D, (3) the precise deviation from the straight line when Δ is not sufficiently small, and in particular the contribution to the deviation from the finite temperature coefficients, and finally (4) the wider range of validity of the simple logarithmic formula than is implied by the criterion that Δ should be small in comparison with T_m, on which basis (15) had been derived previously. Since the deviation from the straight line is verified in detail, it amounts to a verification of the temperature distribution over the whole of the B-region of the rod.

7. THE A-REGION

Moving now into the A-region, and still confining attention to the long rod, it will be seen that $e^{f(\Delta)}$ will now be practically unity, and the temperature variation will be given by

$$\Delta = \Delta_0 e^{f(\Delta_0)} e^{-q\sqrt{A}} (e^{q\sqrt{A}} + e^{-q\sqrt{A}}). \tag{16}$$

This expression will hold not only in the A-region but over a considerable portion of B too, as long as $\Delta/\ln\Delta$ remains small in comparison with T_m, i.e. over the whole of the range in B where the simple logarithmic formula holds. When $q = 0$, Δ should be equal to $T_m - T_l$. Hence (16) may also be written in the form

$$t = \tfrac{1}{2}(T_m - T_l)(e^{q\sqrt{A}} + e^{-q\sqrt{A}} - 2), \tag{17}$$

which reduces, when q is small, to the parabolic law

$$t = \tfrac{1}{2}(T_m - T_l) A q^2. \tag{18}$$

Curve 1, figure 4, in which t is plotted against q^2, relates to such a long rod, for which $T_m = 1500°$ K and $T_l = 1450°$ K. The thick line represents the theoretical curve (17), and the circles denote the experimental points. As should be expected for long rods (see next section), the straight-line portion of the curve corresponding to the parabolic variation of temperature near the centre is relatively short.

The slope of the straight-line portion, extended in the figure by the dotted line, will obviously be $\frac{1}{2}(T_m - T_i)A$, and it can be utilized as before to give us A, and thence κ. The value of κ at 1450° K plotted in figure 2 was obtained in this manner.

It should be mentioned here that the value of A needed in plotting the theoretical curve was taken from the straight-line portion of the experimental curve. It will be seen that all the experimental points lie almost exactly on the theoretical curve, which includes some part of the B-region too.

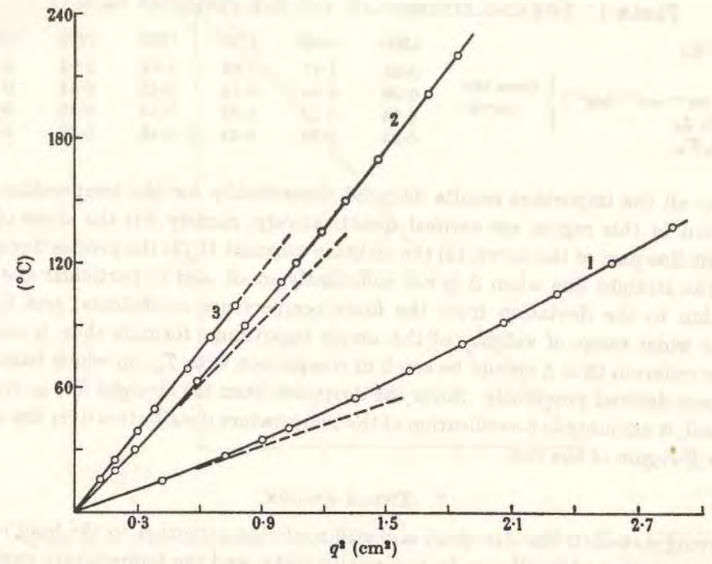

FIGURE 4. Temperature distribution in the A-region.

8. SHORT RODS

For short rods also the temperature variation near the centre is given by a parabolic law, namely,

$$t = \tfrac{1}{2}Qq^2, \tag{19}$$

where

$$Q = \tfrac{1}{2}a(T_m^4 - T_i^4), \tag{20}$$

and at larger distances from the centre by the more precise relation

$$t = \tfrac{1}{2}Qq^2/(1-S)^2, \tag{21}$$

where S is a small fraction which can be expressed as a power series in t/t_c (see (19) of part I), and can be easily calculated.

Curves 2 and 3 in figure 4 refer to such short rods for which $T_m = 1500°$ K, and $T_i = 1320$ and 1200° K respectively.

The slope of the straight-line portion can again be utilized to give Q and thence κ. The values of κ plotted in figure 2 for 1320 and 1200° K were obtained in this manner.

Now for a given q, which is not small, the deviation of t from the straight line will be given according to (21) by $2tS$. The full lines in curves 2 and 3 of figure 4 are the theoretical curves plotted on the basis of (21). The values of Q required for the theoretical plot were taken from the straight portions of the experimental curves, and the calculated values of $2tS$ gave the deviations from the straight line.

Here again the experimental values may be seen to lie almost exactly on the theoretical curves.

The result deduced in part II, namely, that for a given t the deviation from the parabolic law should be the larger the longer the rod, is obviously verified from the curves 1, 2 and 3 of figure 4.

Coming back to the curve for the temperature variation of κ, plotted in figure 2, it will be seen that all the experimental values plot smoothly on a *single* curve. When we remember that the values plotted here have been obtained from widely different considerations, some from the logarithmic variation in long rods, some from the parabolic variation in short rods, and one of them from the variation in the central region of a long rod, their smooth plot into a single curve becomes significant. It is yet another experimental verification of the theoretical results obtained in parts I and II.

We wish to thank Mr S. S. S. Agarwala for help in making some of the calculations.

REFERENCES

Angell, M. F. 1911 *Phys. Rev.* **33**, 421.
Bowen, D. 1949 *Phys. Rev.* **76**, 1878.
Glazebrook, Sir Richard 1922 *Dictionary of applied physics*, **1**, 447. London: Macmillan and Co.
Jain, S. C. & Krishnan, Sir K. S. 1952 *Proc. Roy. Soc.* A, **213**, 143.
Jain, S. C. & Krishnan, Sir K. S. 1954*a* *Proc. Roy. Soc.* A, **222**, 167 (part I).
Jain, S. C. & Krishnan, Sir K. S. 1954*b* *Proc. Roy. Soc.* A, **225**, 1 (part II).
Powell, R. W. & Schofield, F. H. 1939 *Proc. Phys. Soc.* **51**, 153.
Prescott, C. H. & Hincke, W. B. 1928 *Phys. Rev.* **31**, 130.
Worthing, A. G. 1914 *Phys. Rev.* **4**, 523.
Worthing, A. G. & Halliday, D. 1948 *Heat*, p. 171. New York: John Wiley and Sons.

The distribution of temperature along a thin rod electrically heated *in vacuo*

IV. Many useful empirical formulae verified

By S. C. Jain and Sir K. S. Krishnan, F.R.S.

National Physical Laboratory of India, New Delhi

(*Received* 11 *March* 1954)

On the basis of extensive measurements made on the distribution of temperature, and on the distribution of other physical characteristics which are known functions of the temperature, along tungsten filaments heated *in vacuo*, several empirical formulae have been proposed by Worthing, and they have found wide practical application. Many of these formulae are shown in the present part to follow naturally from the theoretical expressions deduced in parts I and II, as special cases. The conditions for their validity also get determined.

The other formulae of Worthing are shown to be good approximations, and the degrees of their closeness to the corresponding theoretical formulae are estimated.

1. Introduction

Extensive experimental work has been done on the distribution of temperature, and of several temperature-dependent physical characteristics like thermionic emission, brightness, total radiation, electrical resistivity, etc., along tungsten filaments electrically heated *in vacuo* (Worthing 1914*a*,*b*, 1922; Langmuir 1916*a*,*b*,*c*, 1922, 1930; Stead 1920; Forsythe & Worthing 1925; Worthing & Halliday 1948). The experimental data have been analyzed in detail, and many useful empirical formulae have been deduced therefrom. These formulae have been used extensively in designing, and in studying the performance of, sealed-in heating elements, such as are used in thermionic tubes, filament lamps, optical pyrometers and the cathodes of X-ray tubes; and, in particular, in calculating the effect of the 'end-losses'.

In parts I and II (Jain & Krishnan 1954*a*,*b*) of this paper it was shown that a practical general solution of the differential equation defining the steady state of the temperature distribution can be obtained when the filament is long, and for shorter lengths the solution can be expanded as a power series which is found to be rapidly convergent in most parts of the filament. In part III (Jain & Krishnan 1954*c*) were described detailed measurements on thin rods of Acheson graphite, which verify the various theoretical results obtained in parts I and II. Knowing the distribution of temperature along the filament, the distribution of any other physical characteristic like thermionic emission, which is a known function of the temperature, can also be readily formulated.

In the light of these investigations many of the empirical formulae referred to acquire a new significance. The present part is devoted to an appraisal of the theoretical significance of some of the formulae that are widely used. One such

formula of practical importance, namely, that due to Stead (1920), has been discussed in part II in connexion with obtaining the general solution of the differential equation of the steady state.

2. Temperature distribution in reduced co-ordinates

Consider a filament in which $T_m - T_l$ is small in comparison with T_m, where T_l is the temperature at the centre of the filament, and T_m is the value to which T_l tends as the length of the filament is increased indefinitely keeping the heating current constant. For convenience we shall refer to such a filament as a *long* one, though the actual length of the filament will depend on how low is the temperature T_0 of the cold ends, i.e. of the junction of the leads and the filament, as compared with T_l.

(1) Denoting $T_m - T$ by Δ, where T is the temperature at a distance x measured from one of the ends, it is well known that in regions where Δ is small in comparison with T_m, x varies linearly with $\ln \Delta$. Worthing defines a certain natural unit of length λ which is the distance over which Δ in this region drops to a fraction $1/e$. Using the reduced lengths $X = x/\lambda$, the temperature distribution in this region may be written in the form

$$X = D - \ln \Delta. \tag{1}$$

(2) Using tungsten filaments of different cross-sections, in which, however, the heating currents are so adjusted as to give the same central temperature T_m in all of them, he finds that the corresponding values of λ, determined experimentally from the logarithmic region, vary as $\sqrt{r}$, as was expected, where r is the radius of the cross-section of the filament.

(3) The second set of measurements of Worthing were made on one such filament, using different heating currents, so that r remains constant in these measurements, but T_m varies over a wide range. Plotting the reduced temperature $\tau = T/T_m$ against X, Worthing finds that the temperature distribution in the filament for all the different heating currents can be represented by a single τ-X curve.

(4) Worthing gives also plausible reasons for expecting this result to hold in the logarithmic range.

(5) Incidentally, he finds that the logarithmic region extends considerably beyond the range over which Δ is small in comparison with T_m, which is the basis on which equation (1) is generally derived.

We now proceed to show that these experimental findings of Worthing follow naturally from the theoretical expressions deduced in parts I and II, which further enable us to formulate the conditions for the validity of these findings. Some of these findings are found to be particular cases of more general theoretical results.

(1) The natural unit of length λ chosen by Worthing can be readily identified with the length $1/\sqrt{A}$ deduced theoretically in part I, which is equal to $(10 a a_1 T_m^3)^{-\frac{1}{4}}$, where $a = \frac{2}{5} p\epsilon\sigma/(\kappa\omega)$, κ is the thermal conductivity, ϵ is the total emissivity, σ is Stefan's radiation constant, and p is the perimeter and ω the area of cross-section of the filament. a_1 is a function of the temperature coefficients of ρ and ϵ, where ρ is the specific resistance. a_1 was evaluated in part I, and is found to be close to unity, and reduces to it when the temperature coefficients are negligible.

Now, equation (1) can be derived from certain simple theoretical considerations, which also enable us to calculate λ (Prescott & Hincke 1928) in the special case when the temperature coefficients referred to are negligible.

(2) Now, for a circular cross-section of radius r, p/ω is obviously equal to $2/r$, and hence the proportionality of λ to $\sqrt{r}$ is verified.

(3) The simple theoretical considerations referred to, on the basis of which (1) may be derived, do not, however, enable us to determine the integration constant D that appears in (1) (Jain & Krishnan 1954*a*). They do not also tell us in what manner D is dependent on T_m, or on the end temperature T_0, since the validity of (1) may not extend to the end of the filament.

Using now the reduced co-ordinates, (1) can be expressed in the form

$$\ln(1-\tau) = -(X+\xi), \tag{2}$$

where

$$\xi = \ln T_m - D. \tag{3}$$

Not knowing theoretically how D depends on T_m or T_0, it is not possible to infer the dependence of ξ on these quantities, and much less to demonstrate that ξ does not involve T_m (except probably through τ_0), which demonstration is essential for verifying theoretically, in the logarithmic region, Worthing's finding regarding the identity of the τ-X curves for the different heating currents.

We emphasize this point here since the appearance of ξ in (2) as an integration constant has been taken by Worthing to imply that it should be independent of T_m; and his observation that the τ-X curve for a filament is independent of the heating current, i.e. independent of T_m, is taken to follow from it as a natural consequence in this region. On the other hand, the appearance of D or ξ as an integration constant in (1) or (2) merely signifies that it is independent of T and x, but not necessarily independent of T_m.

(4) It has been shown in part I that the integration constant D, and hence also ξ, can be evaluated theoretically, though not from the simple considerations on which (1) and (2) had been derived previously. As we shall see presently, ξ depends on τ_0 only, and does not involve T_m separately.

(5) It has also been shown in part I that the criterion for the validity of the logarithmic formula is that $\Delta/\ln\Delta$ should be small in comparison with T_m, which naturally holds over a much wider range than the condition that Δ be small in comparison with T_m.

(6) As we shall show presently, the temperature distribution in all long filaments over their whole lengths, irrespective of their actual lengths or cross-sections, or the heating currents used, or even the materials of which the filaments are made, can be represented by a single τ-X curve, provided that the point $X = 0$ from which measurements of lengths are made is chosen to have the same reduced temperature τ_0 in all of them.

This result is a precise one when the temperature coefficients of κ, ρ and ϵ are neglected, but is otherwise a close approximation.

Worthing's observation on the identity of the τ-X curves for a long filament heated by different currents follows as a particular case of this general result since τ_0, though not kept constant, remains roughly so in his measurements.

(7) For shorter filaments the A-region becomes experimentally significant, and has to be differentiated from the B-region:

(*a*) In the B-region the temperature distribution can be represented by the same τ-X curve as for a similar long filament heated by the same current.

(*b*) The temperature distribution in the A-region also can be represented by a single reduced curve, but the units of length and temperature to be used for the reduction are different from those applicable to the B-region.

We shall take up the case of long filaments first, to which Worthing's measurements refer; and obtain a general expression for the τ-X curve, applicable to all long filaments.

3. A general expression for the τ-X curve

It was shown in part II that in the logarithmic region, and over the rest of the filament on the colder side, the temperature distribution in a long filament is given by

$$\Delta\, e^{f(\Delta)} = \Delta_0\, e^{f(\Delta_0)} e^{-x/\lambda}, \tag{4}$$

where

$$f(\Delta) = \frac{1}{2}\frac{\Delta}{T_m} + \frac{1}{16}\frac{\Delta^2}{T_m^2} - \frac{1}{240}\frac{\Delta^3}{T_m^3} - \cdots \tag{5}$$

$$= \phi(\tau), \quad \text{say.} \tag{6}$$

In terms of the reduced co-ordinates that have been adopted, (4) can be expressed in the form

$$(1-\tau)\, e^{\phi(\tau)} = (1-\tau_0)\, e^{\phi(\tau_0)-X}, \tag{7}$$

which will hold over the whole of the filament, down to $\tau = 0$ if the ends are cold enough for it. Equation (7) is obviously *independent of the material and the length and the cross-section of the filament, and also independent of* T_m, *provided that* τ_0, *which denotes the temperature of the point from which the lengths are measured, is chosen the same for all the filaments.*

This condition is roughly secured in Worthing's second set of measurements, on which is based his finding that the τ-X curve is independent of T_m. The same long filament is heated to different central temperatures T_m. Since no special arrangement is made to control the end temperatures, these temperatures will be the higher the higher the value of T_m. Though, as we shall see in a later section, this increase in T_0 was not quite in proportion to the increase in T_m, which is needed to secure the constancy of τ_0, it was nearly so.

In the earlier parts the distances were measured for convenience from one of the ends of the filament. Since now the origin of X has to be chosen to correspond to the same temperature τ_0 in all the filaments, one has naturally to distinguish between this temperature and the temperatures $\tau_e = T_e/\lambda$ of the ends. Negative values of X also will now be significant, and will correspond to $\tau_e < \tau < \tau_0$.

The effect of the temperature coefficients of κ, ρ and ϵ can also be taken into account by expressing $f(\Delta)$ in the form (see (49) and (50) of part I)

$$f_1(\Delta) = \frac{A_1\Delta}{T_m} + \frac{A_2\Delta^2}{T_m^2} + \frac{A_3\Delta^3}{T_m^3} + \ldots, \tag{8}$$

where $A_1, A_2, A_3, \ldots$ are functions of the temperature coefficients and of T_m, and are readily calculated. They tend to $\frac{1}{2}, \frac{1}{16}, -\frac{1}{240}, \ldots$, respectively, when the temperature

coefficients vanish. Actually only the first term in (8) is significant, and further A_1 is found to be only slightly higher than $\frac{1}{2}$, even this small deviation from $\frac{1}{2}$ depending more on the material of the filament than on T_m. Hence (7) will hold to a close approximation even when the temperature coefficients of κ, ρ and ϵ are taken into account.

The expression for A_1 given in part I was on the basis that the temperature variations of κ, ρ and ϵ may be taken to be linear, which is justified when the temperature range involved is not large. In Worthing's measurements, however, this range is quite large. Hence in calculating A_1 for tungsten applicable to Worthing's measurements we have to take into account the known variation with temperature, which is not quite linear for ρ and ϵ, though it is for κ. The value of A_1 thus obtained for tungsten is 0·75.

In the region where Δ is small, $e^{\phi(\tau)} \sim 1$, and (7) can be seen to reduce to the logarithmic formula (2), in which, however, the integration constant ξ and hence also D, now stand evaluated:

$$\begin{aligned} -\xi &= \ln(1-\tau_0)+\phi(\tau_0) \\ &= \ln(1-\tau_0)+A_1(1-\tau_0), \end{aligned} \tag{9}$$

which is known when the temperature τ_0 corresponding to $X = 0$ is known. ξ is thus a function of τ_0 alone, and does not involve T_m separately. This will be so even when the temperature coefficients of κ, ρ and ϵ are finite, except that in this case the magnitude of a trivial part of A_1 depends on T_m.

It may appear at first sight odd that (7) ultimately involves only *two* parameters, namely, T_m and λ, and is independent of the length of the filament. This is because we are dealing here with *long* filaments, and with regions not too close to the centre —actually outside the A-region as defined in part I. The complete expression for a finite long filament is (part II, equation (27))

$$\Delta\, e^{f(\Delta)} = \Delta_0\, e^{f(\Delta_0)}[e^{-X}+e^{-(2L-X)}], \tag{10}$$

where $2L = 2l/\lambda$ is the reduced length of the filament. Outside the A-region the second term inside the brackets becomes negligible.

Inside the A-region also, whether the filament is short or long, the temperature distribution can be represented, as we shall show in a later section, by a single curve, involving again just two parameters, which are, however, different from those applicable to the B-region of long filaments.

For long filaments of the type used by Worthing, the temperature variation in the A-region is negligible, and hence the exclusion of the A-region from the range of applicability of (7) is not significant in his experiments.

4. Corresponding distances in a filament heated to different central temperatures

It would be relevant to refer here to some curves plotted by Worthing to demonstrate the identity of the τ-X curves for a given filament heated to different T_m's. These curves also serve to emphasize the necessary condition for this identity, namely, that the origin of X should be so chosen that the corresponding temperatures τ_0 are the same for all of them.

As mentioned previously, a long filament is heated by different currents, so that the corresponding temperatures T_m at the centre can be made to have different values. He chooses the case when $T_m = 2400°$ K as reference. Let x be the distance from the cold end to the point whose reduced temperature is τ. Let x' be the corresponding distance from the cold end to the point τ when T_m has a different value. Worthing finds that x' plotted against x is a straight line, and its slope is given by λ'/λ, where λ' and λ are the units of length determined by the two values of T_m concerned.

In these measurements of Worthing no special precaution is taken to keep the reduced end temperature τ_0 the same when the heating currents are varied. Naturally Worthing could not have been aware of this requirement for securing the identity of the curves.

Now from (7) and (9) it will be seen that

$$(1-\tau)\, e^{\phi(\tau)} = e^{-(x/\lambda+\xi)}. \tag{11}$$

Since τ is the same for both x and x'

$$x' = (\lambda'/\lambda)\, x+\lambda'(\xi-\xi'). \tag{12}$$

One may draw from (12) the following conclusions:

(1) The plots of x' against x are straight lines, whose slopes are λ'/λ, which is also Worthing's experimental finding.

(2) They will not pass through the origin, since the necessary condition for it, namely, $\xi'-\xi = 0$, which is equivalent to $\tau_0' = \tau_0$, is not secured in Worthing's experiments.

(3) From the natural variation of τ_0 with T_m mentioned earlier, namely, that τ_0 should be expected to decrease slightly with the increase of T_m, it will be seen that the intercepts of these straight lines on the x'-axis at $x = 0$ should be negative for the curves corresponding to $T_m < 2400°$ K, and positive for the curves for which $T_m > 2400°$ K. This conclusion is verified in Worthing's curves.

(4) Indeed by adjusting the origin of x in the different experiments to correspond to the same τ_0, all the three straight lines can be made to pass through the origin. If, further, the distances plotted are the reduced ones, namely, $X' = x'/\lambda'$ and $X = x/\lambda$, then all the straight lines will obviously become identical. In other words, a single straight line, passing through the origin, and inclined at 45° to the axes, will represent the corresponding distances for all the different heating currents.

5.[4] Distances corresponding to any given drop in temperature with reference to that at the centre

Worthing (Forsythe & Worthing 1925) has also determined experimentally, again for long filaments, the distance x_d at which τ has just approached unity to within 10^{-3}. Taking $\tau_0 = \frac{1}{4}$ he finds that x_d can be represented by the empirical formula

$$x_d/\lambda = 7{\cdot}0, \tag{13}$$

which is a very useful relation.

Actually Worthing's determination of the numerical constant appearing in (13) is equivalent to determining experimentally the integration constant ξ of the logarithmic formula (2), since the point corresponding to x_d lies in the logarithmic region. Obviously

$$X_d = x_d/\lambda = -(\xi + \ln 10^{-3}). \tag{14}$$

Since the integration constant ξ has already been evaluated theoretically (see (9)), one obtains therefrom, for the case $\tau_0 = \frac{1}{4}$, which was the end temperature in Worthing's measurements,

$$-\xi = \ln \tfrac{3}{4} + 0{\cdot}75 \times \tfrac{3}{4}, \tag{15}$$

from which one obtains

$$X_d = 7{\cdot}18, \tag{16}$$

which is in close agreement with Worthing's experimental determination,* namely, $X_d = 7{\cdot}0$.

When once the constant appearing in the logarithmic formula has been determined, one can evaluate X_d readily for other values of τ too. Worthing gives the values $X_d = 7{\cdot}0 \pm \frac{7}{8}$ for $1-\tau = 10^{-4}$ and 10^{-2} respectively. Now 7·0 is the value of X_d for $1-\tau = 10^{-3}$, as we have seen, and $\frac{7}{8}$ is close to ln 10. His filaments are long enough for all the three points to lie in the logarithmic region.

Obviously similar calculations can also be made for end temperatures other than $\tau_0 = \frac{1}{4}$.

6. L as a function of T_l

Worthing has extrapolated these results to include the case of shorter filaments too, in which $T_m - T_l$ may be considerable, though still small in comparison with T_m. Specifying, for example, that $(T_m - T_l)/T_m$ should be less than 10^{-3}, his formula for the corresponding semi-length of the filament is as follows. The value of X_d in a long filament corresponding to $1-\tau = 10^{-3}$ is 7·0, as we saw in the last section. In order that $(T_m - T_l)/T_m$ in the shorter filament might be less than 10^{-3}, Worthing's criterion is that its reduced semi-length should be at least 13 % larger than 7·0.

We have shown in part II that the drop in temperature $T_m - T_l$ at the centre of a long filament of semi-length l will be double the value of Δ at the same distance l in a similar infinitely long filament heated by the same current. Hence $L = l/\lambda$ should be theoretically equal to $X_d + \ln 2$. Now $\ln 2 = 0{\cdot}7$, and it can be seen to be just 10 % of the value of $X_d = 7{\cdot}0$ appropriate to the particular tolerance specified, namely, 10^{-3}. This is not very different from the value of 13 % estimated by Worthing.

7. Temperature variation outside the logarithmic region

As was mentioned in a previous section, the criterion for the validity of the logarithmic formula is that $\Delta/\ln\Delta$ should remain small in comparison with T_m. Outside this region the deviation from the logarithmic formula increases progressively with the increase of Δ. In order to cover this deviation an empirical formula has been proposed by Worthing (1914*a*), which is found to extend the region

* In reducing his observed x_d to X_d Worthing uses an experimentally determined value of λ which is slightly greater than the theoretical value. When the latter value of λ is used, as it should be, in reducing his x_d to X_d, the small discrepancy between his 7·0 and our 7·18 disappears.

of fit with observation considerably beyond the logarithmic range, but not, however, over the whole length of the filament, even though the end temperature τ_0 in these measurements was kept as high as 0·62. The formula is

$$\frac{T}{T_m} = [1 - e^{-(X+c)}]^n, \tag{17}$$

which can be expanded in the form

$$\frac{\Delta}{T_m} = n e^{-(X+c)} - \tfrac{1}{2}n(n-1)e^{-2(X+c)} + \tfrac{1}{6}n(n-1)(n-2)e^{-3(X+c)} - \ldots. \tag{18}$$

Substituting values for the constants n and e^{-c} appropriate to tungsten and to the boundary conditions in Worthing's measurements—these values will be determined presently—the series is found to be fairly rapidly convergent even at $X = 0$. The convergence is naturally the more rapid the larger the distance X from the end.

If now all the terms on the right-hand side of (18) after the first can be neglected, as they can be when X is large enough, the formula obviously reduces to the simple logarithmic formula (2), $\ln n - c$ being then equal to $-\xi$ of (2).

The corresponding theoretical expression is (see (4))

$$\Delta e^{f(\Delta)} = \Delta_0 e^{f(\Delta_0)} e^{-X}, \tag{19}$$

which may be put in the form

$$\Delta e^{f(\Delta)} = T_m e^{-(X+\xi)}. \tag{20}$$

Where Δ is small, $e^{f(\Delta)} \sim 1$, and (20) reduces, as we have seen, to the simple logarithmic formula. The deviation of $e^{f(\Delta)}$ from unity, which increases progressively with the increase of Δ, accounts for the observed progressive deviation from the logarithmic formula. It may be mentioned immediately that (20) fits with Worthing's observational data over the whole range including the region near the leads, and also with other data of his which extend to $\tau = \frac{1}{4}$.

We now proceed to compare Worthing's empirical relation (17), of which (18) is an expansion, with (20). Obviously (17) cannot be identified with (20), but one can investigate the degree of approximation to which (17) may be made to conform to (20). We obtain from (20), for this purpose, an expression for Δ/T_m as a power series in $e^{-(X+\xi)}$ as before, which can be compared term by term with the series (18). Putting

$$e^{f(\Delta)} \approx e^{A_1\Delta/T_m} \approx 1 + A_1\Delta/T_m \tag{21}$$

to a first approximation, equation (20) reduces to the quadratic form

$$\frac{A_1\Delta^2}{T_m^2} + \frac{\Delta}{T_m} - e^{-(X+\xi)} = 0, \tag{22}$$

the solution of which is

$$\frac{\Delta}{T_m} = \frac{1}{2A_1}[\sqrt{\{1 + 4A_1 \exp -(X+\xi)\}} - 1]. \tag{23}$$

Now the quantity inside the square root in (23), and hence the expression for Δ/T_m also, can be expanded as a convergent power series in $e^{-(X+\xi)}$ if $4A_1 e^{-(X+\xi)}$,

which is known to be positive, is less than unity. In view of (9) this corresponds to the criterion

$$4A_1(1-\tau_0)\,e^{A_2(1-\tau_0)-X} < 1, \tag{24}$$

which can be secured at $X = 0$, and hence for all positive values of X, when $\tau_0 > 0{\cdot}61$. This condition is just satisfied in Worthing's measurements to which he applies his formula (17); the lowest temperature of measurement corresponds to $\tau = 0{\cdot}62$. Hence (23) may now be expanded in the form

$$\frac{\Delta}{T_m} = e^{-(X+\xi)} - A_1 e^{-2(X+\xi)} + 2A_1^2 e^{-3(X+\xi)} - \ldots. \tag{25}$$

Like (18) this series also is fairly rapidly convergent even at $X = 0$. This being so, one can adjust the first two terms in (18) to be the same as the corresponding terms in (25) for all values of X, by putting

$$n\,e^{-c} = e^{-\xi}, \tag{26}$$

$$\tfrac{1}{2}n(n-1)\,e^{-2c} = A_1 e^{-2\xi}, \tag{27}$$

from which the two constants n and e^{-c} can be determined in terms of the known quantities A_1 and ξ:

$$\left.\begin{aligned} n &= -\frac{1}{2A_1-1}, \\ e^{-c} &= -(2A_1-1)\,e^{-\xi}. \end{aligned}\right\} \tag{28}$$

Using (28) the first three terms in Worthing's expansion (which is convergent even when $X = 0$) may be written in the form

$$\frac{\Delta}{T_m} = e^{-(X+\xi)} - \left(\frac{1}{2}-\frac{1}{2n}\right)e^{-2(X+\xi)} + \frac{(n-1)(n-2)}{6n^2}e^{-3(X+\xi)} - \ldots, \tag{29}$$

in which the coefficient of the second term, namely, $\frac{1}{2}-\frac{1}{2n}$, takes the place of A_1 in (25). Having adjusted the first two terms in (18) to be the same as the corresponding terms in (25), naturally it will not be possible to secure equality of the succeeding terms in the two series. However, comparing the third term in (29), namely, $\frac{1}{6}(n-1)(n-2)/n^2$, with that in (25), namely, $2A^2$, it will be seen that they are of the same sign, though not of the same magnitude. Hence Worthing's formula (17) can be made to fit with the theoretical formula (25) to a slightly closer approximation than would correspond to the neglect of the third and the succeeding terms. Obviously the approximation depends on X too, and hence for any specified approximation one can estimate the lower limit of X for which the third and the succeeding terms may become negligible. At all distances greater than this the agreement of (17) with observation will naturally be closer than the tolerance prescribed.

Now the coefficients of the second terms, as we have seen, are $\frac{1}{2}-\frac{1}{2n}$ and A_1 respectively. In the special case when the temperature coefficients of κ, ρ and ϵ are negligible, $A_1 = \frac{1}{2}$. Hence $-1/(2n)$, which gives the difference between A_1 and $\frac{1}{2}$,

is determined almost wholly by the finite temperature coefficients, and is therefore small. As we have seen, the deviation of A_1 from $\frac{1}{2}$ is determined more by the material of the filament than by T_m. Hence n should also be practically independent of T_m and the dimensions of the filament, which is also Worthing's observation.

For the same reason again, almost any value of n which does not change the sign or the order of magnitude of $\frac{1}{2}-\frac{1}{2n}$, for example, any positive value greater than unity, or any small negative value, will extend the fit with observation beyond the logarithmic region. It is significant in this connexion that Worthing uses the value $n = 1{\cdot}87$, whereas the theoretical value is negative and about $-2{\cdot}0$.

Even with the latter value for n, the validity of formula (17) does not extend much beyond $\tau = 0{\cdot}7$. The discrepancy becomes quite large when applied to other measurements of Worthing which extend to $\tau = \frac{1}{4}$. This is not surprising, since for such low values of τ (20) cannot even be expanded in a form that would permit comparison with (18).

Hence one has to fall back on (20) for this region. Taking $\tau_0 = 0{\cdot}25$, $e^{-\xi}$ comes out as 1·17. Using this value, and $A_1 = 0{\cdot}75$ and the known thermal conductivity of tungsten at $T_m = 2400°$ K, namely, 0·96 W cm^{-1} deg^{-1}, the temperature distribution calculated on the basis of (20) is found to agree very closely with the distribution observed by Worthing over the whole length of the filament.

8. The distribution of other physical characteristics along the filament

Knowing the distribution of temperature along the filament, the distribution of any other physical characteristic which is a known function of the temperature can also be investigated theoretically. Some of these characteristics are listed in table 1. In the case of tungsten, the temperature dependence of all of them can be expressed, according to Langmuir (1930), in the form

$$F_i(T) = A_i e^{\gamma_i} e^{-\Theta_i/T}, \tag{30}$$

where $F_i(T)$ denotes the particular physical characteristic studied, and γ_i and Θ_i are constants whose values are known and are entered in table 1. For some of the characteristics like thermionic emission and the rate of evaporation, (30) can be deduced theoretically, and for others it is an empirical relation.

Table 1

property	electrical resistance	total radiation	brightness	thermionic emission	rate of evaporation
γ_i	1·2	5·1	0	2	0
Θ_i	0	0	25200	52600	94100

Worthing (1922) has made extensive measurements on the distribution of these various characteristics along heated tungsten filaments, except the rate of evaporation, and he has plotted $F_i(T)/F_i(T_m) = \psi_i$, say, against the distance from the end. Since all his measurements refer to the same filament, it is not material whether

the plot is against the reduced distance or the actual distance. He finds that in the logarithmic region ψ_i can be represented by the formula

$$\psi_i = 1 - e^{-(X+\xi_i)}, \tag{31}$$

in which ξ_i is a constant independent of X and T. In other words, he finds that in this region the curves for the different characteristics are laterally displaced along the x-axis relatively to one another by constant amounts, that is by amounts that are independent of X. He observes further in a general way that this constancy of shift extends over a wider range than the logarithmic region. In an earlier paper (1914*b*) he has also found in the case of one of these properties, namely, the total radiation, that its observed distribution along the filament can be fitted over most parts of the filament by a formula very similar to his formula (17) for the distribution of temperature. This formula is

$$\psi_i = [1 - e^{-(X+c_i)}]^{n_i}. \tag{32}$$

This can be seen to reduce in the logarithmic range to (31) if $n_i e^{-c_i} = e^{-\xi_i}$.

We now proceed to demonstrate that these observations of Worthing can be verified theoretically, and that the constants appearing in them can also be evaluated, in the same manner in which the constants in (17) were evaluated earlier. Adopting Langmuir's expression (30) for $F_i(T)$ as an explicit function of T, it can be shown that

$$\psi_i = 1 - (\gamma_i + \Theta_i/T_m)\,\Delta/T_m + [\tfrac{1}{2}\Theta_i^2/T_m^2 + (\gamma_i - 1)(\tfrac{1}{2}\gamma_i + \Theta_i/T_m)]\,\Delta^2/T_m^2 - \ldots. \tag{33}$$

Since we are here concerned with regions not much beyond the logarithmic region, one may substitute for Δ/T_m from (25), and obtain

$$\psi_i = 1 - e^{-(X+\xi_i)} + B_{i1}\, e^{-2(X+\xi_i)} - \ldots, \tag{34}$$

where

$$\xi_i = \xi - \ln(\gamma_i + \Theta_i/T_m), \tag{35}$$

$$B_{i1} = [A_1(\gamma_i + \Theta_i/T_m) + \tfrac{1}{2}\Theta_i^2/T_m^2 + (\gamma_i - 1)(\tfrac{1}{2}\gamma_i + \Theta_i/T_m)]/(\gamma_i + \Theta_i/T_m)^2. \tag{36}$$

By securing

$$\left.\begin{aligned} n_i e^{-c_i} &= e^{-\xi_i}, \\ \frac{1}{2} - \frac{1}{2n_i} &= B_{i1}, \end{aligned}\right\} \tag{37}$$

the first three terms in series (34) can be made to be identical with the first three terms in the expansion of (32), which shows that an expression of the type (32) can be made to cover an appreciably wider range than the exponential formula (31), in the same manner in which (17) extends (2). Like (17), formula (32) also has serious limitations in the range of its applicability.

The differences in the value of ξ_i for the different curves represent naturally their relative shifts along the x-axis, and it can be seen from the expressions that these shifts are independent of X over the range over which formula (31) holds.

Worthing has given some numerical values for the shift along the x-axis, in the logarithmic region, of the distribution curves for the different characteristics with reference to the curve for the temperature distribution. These values are entered in table 2 along with the corresponding values calculated from (35). The agreement between the calculated and the observed values is quite satisfactory.

On the basis of the observation that the temperature distribution in a long filament heated by different currents can be represented by a single τ-X curve, and the further observation that in the logarithmic region the other distribution curves for the filament, namely ψ_i plotted against X, are displaced with reference to the τ-X curve along the x-axis by amounts independent of X, Worthing draws the following conclusion. Just as the distribution of temperature along a given long filament heated by different currents, can be represented by a single τ-X curve, the distribution of any of these other characteristics along the filament should also be representable by a single ψ_i-X curve. This conclusion, however, is not justified. What is implied by the observed relative shifts is that in the logarithmic region ξ_i is independent of X and T, whereas Worthing's inference would require that ξ_i be independent of T_m also. As will be seen from equation (35), this will be the case for only such characteristics for which $\Theta_i = 0$, like electrical resistance and total radiation, but not for example for thermionic emission, or for brightness. For any of the latter characteristics, for which $\Theta \neq 0$, the distribution curves for filaments heated by different currents, will obviously be shifted parallel to one another along the x-axis by amounts determined by their respective T_m's.

TABLE 2

property		electrical resistance	total radiation	brightness	thermionic emission	rate of evaporation
$\lambda(\xi - \xi_i)$ (cm)	obs.	0·04	0·39	0·60	0·82	—
	calc.	0·045	0·39	0·59	0·79	0·90

Having obtained an analytical expression for the distribution of these characteristics along the heated filament, namely (33), it is easy to integrate it over the whole length, or any part, of the filament, and in particular to calculate the correction due to the end-losses, for the purpose for which the filament is intended to be used.

The corrections due to the end-losses for many of these characteristics have been calculated by Worthing by graphical integration of the observed distribution curves for these characteristics. For such of the properties for which Θ_i is zero, and for which the distribution curve with reduced co-ordinates is independent of T_m, the values given by Worthing are naturally *generally* applicable. On the other hand for properties like thermionic emission for which $\Theta \neq 0$, the values given by Worthing hold only for filaments for which the temperature T_m at the centre has the particular value for which his calculations have been made, namely 2400° K. Naturally, not being aware of the significant difference between these two classes of physical characteristics, in being reproducible uniquely or not by a single curve in reduced co-ordinates, Worthing has not differentiated the data for these two classes.

Worthing has verified in detail in one case the correction calculated by him for the end losses, namely for the radiation output, with the help of the data obtained for different filaments and heated by different currents. He concludes therefrom that the end corrections given by him for the other characteristics also should be similarly valid. It so happens that the radiation output is one of those characteristics for which $\Theta_i = 0$, and this is true also of two others in his table, namely, heat

content and energy input. On the other hand, the other two characteristics for which also he gives end losses, namely, thermionic emission and brightness, do not belong to this category.

Since the end-loss corrections are important practically, and an adequate treatment of it will be beyond the scope of the present part, we postpone the treatment of end losses to a later part.

9. Short filaments

Till now we have confined attention to long filaments in which $T_m - T_l$ is small in comparison with T_m, in which case the A-region is practically unimportant, since the temperature variation inside it is negligible. We shall now consider shorter filaments, in which the A-region becomes important. It was shown in part I that the A-region is defined by $0 < t < t_c$, where $t = T_l - T$, and

$$t_c = (T_m^4 - T_l^4)/(2T_l^3), \tag{38}$$

and the temperature distribution is given by (see (25) of part II)

$$t = \tfrac{1}{2}t_c[\cosh(q/\lambda_A) - 1], \tag{39}$$

where q is the distance measured from the centre, and $\lambda_A = (10aT_l^3)^{-\frac{1}{2}}$ is now the appropriate unit of length. Expressing t in terms of t_c and q in terms of λ_A, (39) takes the simple form

$$\tau_A = \tfrac{1}{2}(\cosh q_A - 1), \tag{40}$$

where τ_A and q_A are the reduced temperature and length respectively. The expression involves only these two quantities, and is even more general than (7) applicable to the B-region, since the latter requires at least τ_0 to be adjusted the same in all the filaments.

Outside the A-region (7) would be applicable, for a short filament also, with the appropriate value of T_m, which now will not be the temperature at the centre.

10. Summary

Many interesting empirical formulae relating to the distribution of temperature, and of some of the temperature-dependent physical characteristics, along heated filaments, which were originally proposed by Worthing, and have since found wide practical application, are discussed in the present part in relation to the theoretical expressions obtained in parts I and II. The following are some of the main results.

(1) Expressing temperatures in terms of the temperature at the centre, and lengths in terms of a certain natural unit, Worthing finds that the observed temperature distribution curves for a long tungsten filament heated by different currents become identical. This is shown to follow as a special case of the following general result. The temperature distribution in long filaments of different materials, of different lengths and cross-sections, and heated to different central temperatures, can all be represented by a single distribution curve in reduced co-ordinates, involving ultimately only two parameters, provided that the origin from which distances are measured is chosen to have the same reduced temperature in all the cases considered.

This general result is a precise one when the small temperature coefficients of the physical constants involved are neglected, but is otherwise a close approximation.

(2) It is further shown that the same reduced curve may be made to represent the distribution in the B-region of a short filament, provided that in reducing the temperature the unit used is not the actual temperature at the centre, but the temperature that would obtain at the centre of a similar long filament heated by the same current.

(3) The temperature distribution in the A-region of a filament, long or short, can also be similarly represented by a single curve, which however, is different from that applicable to the B-region. This curve also involves only two parameters.

(4) These two parameters, though different from those involved in the B-region, are not independent of them, the total number required for describing uniquely both the regions being three (in which number are not included temperature coefficients of the physical quantities involved).

(5) The distribution of the temperature-dependent physical characteristics cannot, in general, be so represented by single curves; this can be done only in the special case when the property is proportional to a constant power of the temperature. This is so for example for radiation output, but not for thermionic emission.

(6) Worthing's expressions for the distance from the end to the point where the temperature has just approximated to that at the centre to any given degree of approximation are verified.

(7) Similar expressions formulated by Worthing for the total length of a filament such that the temperature at its centre might approach to a given degree of closeness that at the centre of a similar long filament heated by the same current also verified.

(8) A simple generalization of the logarithmic formula was proposed by Worthing which extends its applicability considerably beyond the logarithmic region. The range of validity of this extended formula, and its limitations are discussed.

(9) Similar formulae for the distribution of certain physical characteristics which are known functions of the temperature, along the filament, are also considered in detail.

References

Forsythe, W. E. & Worthing, A. G. 1925 *Astrophys. J.* **61**, 146.
Jain, S. C. & Krishnan, Sir K. S. 1954*a* *Proc. Roy. Soc.* A, **222**, 167 (part I).
Jain, S. C. & Krishnan, Sir K. S. 1954*b* *Proc. Roy. Soc.* A, **225**, 1 (part II).
Jain, S. C. & Krishnan, Sir K. S. 1954*c* *Proc. Roy. Soc.* A, **225**, 7 (part III).
Langmuir, I. 1916*a* *Phys. Rev.* **7**, 154.
Langmuir, I. 1916*b* *Phys. Rev.* **7**, 302.
Langmuir, I. 1916*c* *Gen. Elect. Rev.* **19**, 208.
Langmuir, I. 1922 *Trans. Faraday Soc.* **17**, 634.
Langmuir, I. 1930 *Phys. Rev.* **35**, 478.
Prescott, C. H. & Hincke, W. B. 1928 *Phys. Rev.* **50**, 68.
Stead, G. 1920 *J. Instn Elect. Engrs*, **58**, 107.
Worthing, A. G. 1914*a* *Phys. Rev.* **4**, 524.
Worthing, A. G. 1914*b* *Phys. Rev.* **4**, 535.
Worthing, A. G. 1922 *J. Franklin Inst.* **194**, 597.
Worthing, A. G. & Halliday, D. 1948 *Heat.* New York: John Wiley and Sons.

Thermionic constants of metals and semiconductors
IV. Monovalent metals (continued)

By S. C. Jain and Sir K. S. Krishnan, F.R.S.
National Physical Laboratory of India, New Delhi

(*Received* 7 *April* 1954)

In a monovalent metal, in which the valency electrons may be regarded as forming a free-electron assemblage, the assumption of a temperature-independent energy barrier at the surface of the metal is shown to be equivalent to taking the free electrons in the condensed phase, namely, the metal, and the electrons in the gaseous phase in thermal equilibrium with it, as forming a homogeneous single component system. The temperature variation of the work function is then determined by the temperature variation of the thermodynamic potential of the electrons in the condensed phase, when the external pressure is kept constant at the value of the saturation vapour pressure of the electrons, which is equivalent to keeping the pressure of the electron assemblage in the condensed phase also constant, since the energy barrier at the surface is independent of temperature. It is further shown that for a degenerate, or nearly degenerate, electron assemblage the specific heat at constant pressure is the same as that at constant volume, and it is easily calculated. The temperature coefficient of the work function calculated therefrom corresponds to an apparent lowering of about 8 to 10% in the value of the A coefficient in thermionic emission. This agrees with observation.

On the other hand, the thermal expansion of the lattice is found to be about 25 to 50 times that to be expected thermodynamically for the electron assemblage in the condensed phase. This result, when viewed against the nearly normal observed value of the A coefficient, shows that the energy barrier at the surface of the metal should decrease with increase of temperature by the same amount by which the thermodynamic potential of the electrons in the condensed phase decreases as a result of the thermal expansion of the lattice.

A detailed calculation is made of the effect of both the thermal expansion of the lattice, and the increased thermal oscillations of the atoms in the lattice, associated with the rise in temperature, on the energy of the barrier at the surface. The net effect is found to be a lowering of this energy of the required magnitude.

1. Introduction

In the early measurements on the thermionic constants of the monovalent metals the A coefficients in Richardson's equation for thermionic emission were found to be in general much less than the theoretical value of 120 amp deg.$^{-2}$ cm^{-2}. Two obvious explanations suggest themselves. One is the insufficient degassing of the metal surface. The adsorption of gases at the surface is known to depress the intensity of thermionic emission from the surface, and the low melting-points of these metals do not permit their being raised to temperatures high enough for efficient degassing. The other explanation is the thermal expansion of the metal (Herzfeld 1930; Reimann 1934). The conduction electrons in a monovalent metal form a degenerate assemblage whose thermodynamic potential is naturally a function of the density of the electrons—actually proportional to $n^{\frac{2}{3}}$, where n is the number of free electrons per unit volume. Hence the thermal expansion of the metal will lead to a lowering of the thermodynamic potential. *If the energy barrier at the surface of the metal may be regarded as remaining independent of the temperature*, the negative temperature coefficient of the thermodynamic potential will mean an equivalent positive temperature coefficient for the work function. Any such small linear increase of the work function with temperature will not be distinguishable in practice from a temperature-independent reduction in the value of the A coefficient.

In part III (Jain & Krishnan 1953) were described measurements on the thermionic constants of the monovalent metals copper, silver and gold, made by the effusion method, which is quite insensitive to the contamination of the surface of the metal by adsorbed gases. The measurements yield for all the three metals A values only slightly short of the theoretical value of 120 amp deg.$^{-2}$ cm^{-2}. The observed values of A were 110, 107 and 100 respectively for the three metals. Had the energy barrier been independent of temperature, the thermal expansion alone, as was shown in part III, would have reduced these values to an eleventh of the theoretical value in copper, to a fourteenth in silver, and to less than a fifth in gold.

In the light of these results it becomes desirable to re-examine the question of the temperature variation of the work function of a monovalent metal, which because of the simplicity of its electronic structure is somewhat amenable to theoretical treatment. The various factors that might contribute to the variation of the work function of a metal with temperature have been discussed by Herzfeld (1930), Reimann (1934), Wigner (1936), Seely (1941), Seitz (1940) and others. The present part is concerned with the detailed evaluation of the effects of these factors on the energy barrier at the surface of the metal, and on the thermodynamic potential of the electrons, and hence on the work function, which represents the difference between these two energies.

2. Statement of the problem

Any method of evaluating theoretically the rate of emission of electrons from the surface of a heated metal reduces *ultimately* to one of determining the saturation vapour pressure of the electron gas in thermal equilibrium with the metal. Since the saturation pressure of the vapour at all working temperatures is very small, the

vapour can be regarded as a perfect gas obeying the classical laws. The number of electrons in this gas that cross a unit area from one side to the other per second, equal to N say, is therefore readily known. The number of electrons that enter the metal from the vapour phase per unit area per second will be the above number multiplied by a factor $1-r$, where r is the reflexion coefficient, and $1-r$ the transmission coefficient, of the surface for electrons incident on it. Since r should be the same whether the electrons are incident on the surface from the vapour phase or from the condensed phase, the condition for equilibrium between the electrons in the metal phase and in the vapour phase requires that the number of electrons emitted per second per unit area of the metal surface should be the same as the number $N/(1-r)$ crossing the surface in the opposite direction.

Consider the electron gas in thermal equilibrium with the metal in a chamber scooped out of it, and consider the electrons that *effuse* out of the chamber through a small aperture in a thin wall of the chamber. The number of electrons that effuse out per second per unit area of the aperture will be just N, the uncertain factor $1-r$ that appears in the expression for direct emission from the surface being now eliminated. We shall confine ourselves to this case, as it is also of interest experimentally (Jain & Krishnan 1952*a*, *b*, 1953), and the results obtained may be made applicable to direct emission also, by including the factor $1-r$.

Indeed, the difference between effusion from the saturated vapour and emission directly from the surface is analogous, as was shown in the earlier parts, to the difference between the electromagnetic radiations from a cavity and from the surface directly of a hot body.

The simplest way in which the saturation vapour pressure of the electrons in thermal equilibrium with the metal can be evaluated, as is well known, is to regard the system of electrons in the two phases as forming *a single component system* having a finite latent heat of evaporation, which represents the work done per electron in transferring it from the condensed phase to the gaseous phase at the saturation pressure of the latter. On this basis, and without any further approximations, the saturation vapour pressure may be evaluated readily by applying the well-known thermodynamic relation of Clapeyron and Clausius connecting the saturation vapour pressure at any given temperature with the latent heat of evaporation at this temperature and under this pressure.

We should mention immediately that the basic assumption that the *electrons in the metal and in the vapour phase form a single component system* implies the following. Though initially the number of free electrons per unit volume in the condensed phase, and the thermodynamic properties of this electron assemblage, are determined wholly by the density of the atoms in the lattice, any change in the volume or the pressure of the electron assemblage due to a change in the temperature is taken to be completely determined by the initial conditions of the electrons in the condensed phase, and not by the actual thermal expansion of the lattice, which, as we shall see in a later section, is 25 to 50 times larger.

On this model the work function of the metal at the absolute zero of temperature will be the same as the latent heat of evaporation of the electrons at this temperature, and it can be shown (see § 5) that the temperature variation of the work

function with its sign changed, will then be just that of the thermodynamic potential of the electrons in the condensed phase *at constant pressure*, namely, the saturation pressure of the electron gas in equilibrium with it.

Now the occurrence of a large latent heat of evaporation implies also a large energy barrier between the electrons inside the metal and outside it, and hence one can also determine thermionic emission by finding the number of electrons in the metal that strike unit area of the surface per second whose components of momenta along the normal to the surface are large enough to enable them to cross the barrier. In a single-component system this energy barrier, which may be defined as the difference in energy between an electron at rest in the vapour phase, and an electron at rest in the condensed phase, i.e. at the bottom of the energy band of the free electrons in the metal, *can be shown to be independent of the temperature* (see § 4). Conversely, the usual model in which the energy barrier as defined just now is taken to be independent of temperature can be shown to be equivalent to the model that regards the electrons in the two phases as constituting a single-component system. Hence on the postulate of a temperature-independent energy barrier also the temperature variation of the work function, except for its sign, will be that of the thermodynamic potential of the electrons in the condensed phase at *constant pressure*, and not at constant volume as it is generally taken to be. This distinction, as we shall see in a later section, is material.

Considering an actual monovalent metal, the thermal expansion of the ionic lattice is much larger than the expansion at constant pressure that we should expect for the electrons in the condensed phase from the initial conditions—for example, about 50 times in silver. That in spite of this large thermal expansion, the temperature variation of the work function remains small, as evidenced by the small deviation of the observed A coefficient from the theoretical value, shows that the energy barrier is by no means temperature-independent. Before discussing the effect of the thermal expansion of the lattice, and of the thermal agitations of the atoms in the lattice, on the energy barrier and on the thermodynamic potential of the electrons, it is desirable to investigate the full implications of treating the electrons in the two phases as forming a single-component system.

3. The saturation vapour pressure of the electron gas in equilibrium with a metal

Consider the electrons in the condensed and in the vapour phases as forming a *homogeneous single-component system*, and consider the thermodynamic potential, or the Gibbs free energy of the system, per electron, defined by

$$\zeta = u - Ts + pv, \tag{1}$$

where u, s and v are the internal energy, the entropy and the volume, per electron. Using the subscripts C and G to indicate that the quantity concerned refers to the condensed and the gaseous phases respectively, one can see that the thermodynamic potential *of the gaeous phase* is given by (see, for example, Planck 1926)

$$\zeta_{T,\mathrm{G}} = kT\ln p - c_{p,\mathrm{G}}T\ln T - kT\ln\Delta + \chi, \tag{2}$$

in which p is the saturation vapour pressure of the electron gas, and $c_{p,G}$ is the specific heat per electron in the gaseous phase. Δ is the well-known Sucker-Tetrode constant for a monatomic gas, with an extra multiplying factor 2 to take into account the spin of the electrons (Fowler 1929), and is given by

$$\Delta = 2(2\pi m)^{\frac{3}{2}} k^{\frac{5}{2}}/h^3. \tag{3}$$

χ is the temperature-independent additive constant that appears in the expression for the heat function for the gas

$$h_{T,G} = u + pv = c_{p,G} T + \chi. \tag{4}$$

In other words, χ is the value of the heat function of the gas at $T = 0$.

Now the thermodynamic potential *in the condensed phase* will be given by

$$\zeta_{T,C} = h_{T,C} - Ts_C = h_{T,C} - T\int \frac{c_{p,C}}{T} dT. \tag{5}$$

Equating the expressions (2) and (5) for the thermodynamic potentials in the gaseous and in the condensed phases respectively, and treating the vapour as a perfect gas, for which $c_{p,G} = \frac{5}{2}k$, one obtains

$$p = \Delta T^{\frac{5}{2}} e^{-\phi_T/(kT)}, \tag{6}$$

in which

$$\phi_T = \chi - h_{T,C} + T\int_0^T \frac{c_{p,C}}{T} dT. \tag{7}$$

Now the latent heat of evaporation L_0 at $T = 0$ will be given by

$$L_0 = \chi - h_{0,C}. \tag{8}$$

Further,

$$h_{T,C} - h_{0,C} = \int_0^T c_{p,C} dT, \tag{9}$$

from which one obtains

$$\phi_T = L_0 + \epsilon_T = \phi_0 + \epsilon_T, \tag{10}$$

where

$$\epsilon_T = T\int_0^T \frac{c_{p,C}}{T} dT - \int_0^T c_{p,C} dT. \tag{11}$$

It will be seen from (5) and (7) that

$$\zeta_T = \chi - \phi_T. \tag{12}$$

Hence the temperature variation of the thermodynamic potential of either phase will be given by an expression similar to (10), namely,

$$\zeta_T = \zeta_0 - \epsilon_T. \tag{13}$$

Thus *for a single-component system* the temperature variation of both ϕ and ζ can be readily obtained in terms of the specific heat of the electrons in the condensed phase at constant pressure, namely, the saturation vapour pressure of the electron gas in thermal equilibrium with the condensed phase.

4. The energy barrier in a single-component system independent of temperature

It is desirable here to interpret the constants appearing in these thermodynamic equations in terms of the energy levels. We shall take, as before, the energy of an electron at rest inside the metal, i.e. the bottom of the energy band of the free electrons, as the zero level. From the expressions given in the previous section it will then be seen (1) that the constant χ appearing in the expression for the heat function $h_{T,G}$ in the vapour phase will represent the energy of an electron at rest outside the metal; i.e. χ will be the energy barrier at the surface as we have defined it in the previous sections; (2) that $\zeta_0 = h_{0,C}$ will be the energy of the Fermi level at $T = 0$, i.e. the Fermi level of the completely degenerate electron assemblage in the condensed phase; and (3) that at all ordinary temperatures $T \ll \zeta_0/k$, the difference between χ and the thermodynamic potential ζ_T, which obviously is a function of the temperature, represents the work function ϕ_T.

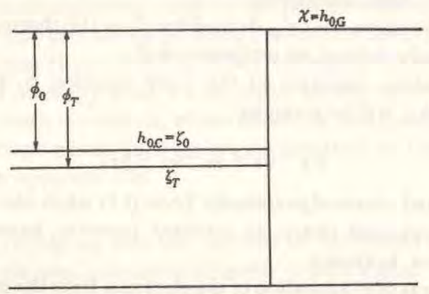

FIGURE 1. Energy levels of a single-component system.

Incidentally it may be mentioned that in equation (2) the first term tends to a finite value, namely, ϕ_0 as T tends to 0, and ζ then tends to $\chi - \phi_0$.

Obviously the identification of the energy barrier with the temperature-independent constant χ that appears in expression (4) for the heat function of the gas, leads to the following significant result, which needs emphasis here, namely, that in a single-component system, the energy barrier at the surface is independent of the temperature, and conversely that the usual model on which thermionic emission is calculated, in which the energy barrier at the surface is taken to be independent of temperature, is ultimately equivalent to taking the electrons in the metal phase and in the vapour phase as forming a homogeneous single-component system.

5. The thermionic constants of the metal

Consider a chamber scooped out of the metal, and consider the effusion of electrons from the saturated electron gas in the chamber through a small hole in a thin wall of the chamber. The number of electrons that effuse out per second per unit area of the hole in all directions, i.e. over the whole of the semi-solid angle 2π, is given by

$$N = p/\sqrt{(2\pi mkT)}. \tag{14}$$

When these electrons are collected in a positively charged Faraday cylinder in the usual manner (see Jain & Krishnan 1952*a*) the corresponding saturation current, extrapolated to zero space charge, is given by

$$i = Ne = AT^2 e^{-\phi_T/(kT)}, \tag{15}$$

where

$$A = 4\pi emk^2/h^3. \tag{16}$$

In other words, the expression for the rate of effusion of electrons from a chamber through a small hole has the same form as the expression for emission from a corresponding area of the surface of the heated metal, but with this difference; whereas the expression for emission from the surface involves the transmission coefficient $1-r$ as a multiplying factor, the expression for effusion from the chamber does not include it.

One can immediately draw the following conclusions for the single-component system that we have been considering:

(i) Equation (15) shows that ϕ_T defined by (7) is the thermionic work function of the metal as usually defined, at temperature T.

(ii) The temperature variation of the work function ϕ, and of the thermodynamical potential ζ, will be given by

$$\phi_T - \phi_0 = \zeta_0 - \zeta_T = \epsilon_T, \tag{17}$$

and can be calculated thermodynamically from (11) when the specific heat of the electrons in the condensed phase, at constant pressure, namely, the pressure of the saturated vapour, is known.

(iii) The latent heat of evaporation of the electrons from the metal at the absolute zero of temperature, namely, L_0, is the same as the work function ϕ_0 at this temperature, but at any other temperature T, $L_T \neq \phi_T$. Since by definition L_T is the heat per electron required to change to the vapour under the constant pressure of its saturated vapour,

$$L_T = L_0 + c_{p,G}T - \int_0^T c_{p,C}\mathrm{d}T, \tag{18}$$

whereas

$$\phi_T = L_0 + T\int_0^T \frac{c_{p,C}}{T}\mathrm{d}T - \int_0^T c_{p,C}\mathrm{d}T. \tag{19}$$

6. Thermionic emission on the basis of a temperature-independent energy barrier at the surface

Before proceeding to discuss the temperature variation of ϕ, which except for its sign is the same as that of ζ, in terms of the specific heat $c_{p,C}$ of the electrons in the condensed phase, it is desirable to refer to an apparent discrepancy regarding the order of approximation, between the Richardson expression for thermionic emission obtained here and that obtained in the usual manner on the basis of a temperature-independent energy barrier at the surface of the metal, which, as we have seen, is equivalent to the present model. The number of electrons in the metal striking unit area of the surface per second whose components of momenta along

the normal to the surface exceed $\sqrt{(2m\chi)}$ can be shown to be equal to (Sommerfeld & Bethe 1933; Fowler & Guggenheim 1939)

$$N = \frac{2}{h^3}\int_{-\infty}^{+\infty}\int_{-\infty}^{+\infty}\int_{E_0}^{\infty} \frac{\mathrm{d}p_y\mathrm{d}p_z\mathrm{d}E}{e^{(E-\zeta)/(kT)}+1}, \tag{20}$$

where

$$E = (p_x^2+p_y^2+p_z^2)/(2m), \tag{21}$$

$$E_0 = \chi + (p_y^2+p_z^2)/(2m). \tag{22}$$

Neglecting unity in comparison with $\exp\{(E-\zeta)/(kT)\}$, which will be justified at all ordinary temperatures $T \ll \zeta/k < \chi/k$, one obtains immediately from (20)

$$i = Ne = AT^2 e^{-(\chi-\zeta)/(kT)},$$

which is the same expression as (15).

It may appear at first sight surprising that expression (15), which was obtained as a *precise* result thermodynamically, should now turn out as a first approximation only. The answer is that neglecting unity in comparison with $\exp\{(E-\zeta)/(kT)\}$ for the electrons whose energies are large enough to enable them to cross the barrier is equivalent to treating these electrons as conforming to the classical statistics of Boltzmann, which is precisely what we are doing already with the electron gas in thermal equilibrium with the metals, whose density is comparable with the density in the metal of electrons whose energies are greater than χ. Thus the discrepancy referred to is only an apparent one.

7. The internal and the external pressures of the assemblage of electrons in the metal

We now proceed to calculate the specific heat of the electrons in the condensed phase, which is required for the evaluation of the various expressions occurring in §§ 3 and 5, and in particular the expression for the temperature variation of ϕ. It should be emphasized here that the constant pressure to which the specific heat $c_{p,C}$ refers is the saturation pressure of the electron gas in thermal equilibrium with the condensed phase.

Since the assemblage of electrons in the condensed phase may also be treated as an electron gas, but highly degenerate, it will have its own pressure, which for convenience we designate as the *internal pressure*, in order to distinguish it from the pressure of the vapour with which we have been concerned till now, and which we shall refer to hereafter as the *external pressure*.

Now for a monovalent metal a simple calculation shows that the internal pressure should be of the order of a million atmospheres, whereas the pressure of the saturated vapour is a very small fraction of an atmosphere, of the order of 10^{-12} even at the highest working temperatures. This large difference in pressure is really maintained by the presence of the energy barrier. Now the difference between the internal and the external pressures is a function of χ, and for a single component system since χ remains independent of the temperature, the specific heat $c_{p,C}$ of the electrons in the condensed phase at constant external pressure, which we need to know in order to calculate the temperature variation of ϕ, will be the same as the specific heat of

the electron assemblage in the condensed phase when its own pressure, i.e. the internal pressure, is kept constant.

It will be seen from equations (5) and (11) that the first integral in expression (7) for ϵ_T originates from the expression for the entropy, and the second from the expression for the heat function, of the electrons in the condensed phase, and that in both these integrals $c_{p,C}$ may therefore be replaced by the specific heat c_p of these electrons at constant internal pressure. It is the latter quantity that is calculated in the next section.

8. The specific heat of a degenerate electron gas at constant pressure shown to be the same as that at constant volume

For simplicity we shall confine attention to the case when the assemblage of electrons in the condensed phase is nearly degenerate. If n is the number of electrons per unit volume at temperature T, the internal energy u per electron is given by the well-known expression (Sommerfeld & Bethe 1933)

$$u = \tfrac{3}{5}\zeta_0 + \tfrac{1}{2}\gamma T^2 + \ldots, \tag{23}$$

where

$$\zeta_0 = \frac{h^2}{2m}\left(\frac{3n}{8\pi}\right)^{\frac{2}{3}}. \tag{24}$$

ζ_0 is a function of n, and therefore also of the temperature.

$$\gamma = \frac{\pi^2 k^2}{2\zeta_0}. \tag{25}$$

The specific heat at constant volume will obviously be given by

$$c_v = \left(\frac{\partial u}{\partial T}\right)_v = \gamma T. \tag{26}$$

Denoting the heat function of the assemblage per electron by

$$h_C = u + pv, \tag{27}$$

where $v = 1/n$ is the volume per electron, and remembering that

$$pv = \tfrac{2}{3}u, \tag{28}$$

one obtains for the specific heat of the assemblage at constant pressure the expression

$$c_p = (\partial h_C/\partial T)_p = \tfrac{5}{3}(\partial u/\partial T)_p = (\partial \zeta_0/\partial T)_p + \tfrac{5}{3}\gamma T. \tag{29}$$

Since ζ_0 is proportional to $n^{\frac{2}{3}}$, one obtains

$$(\partial \zeta_0/\partial T)_p = -\frac{2}{3}\frac{\zeta_0}{v}(\partial v/\partial T)_p. \tag{30}$$

Now

$$(\partial v/\partial T)_p = -(\partial p/\partial T)_v/(\partial p/\partial v)_T, \tag{31}$$

which in view of relation (28) is readily evaluated, since

$$(\partial p/\partial T)_v = \tfrac{2}{3}c_v/v, \tag{32}$$

and

$$(\partial p/\partial v)_T = -\tfrac{2}{3}\zeta_0/v^2. \tag{33}$$

Thus one obtains

$$(\partial \zeta_0/\partial T)_p = -\tfrac{2}{3}c_v, \tag{34}$$

and hence from (32) the significant relation*

$$c_p = c_v = \gamma T. \tag{35}$$

That for a degenerate, or nearly degenerate, electron assemblage the specific heat at constant pressure comes out to be the same as that at constant volume need not occasion any surprise, since any increase in volume consequent on an increase in temperature at constant pressure brings down the degeneracy temperature and hence the zero point energy of the gas, and to the approximation aimed here, namely $kT \ll \zeta_0$, the energy gained thereby is just sufficient to do the work involved in the expansion of the gas against the constant pressure under which the gas is expanding.

At higher temperatures, when the assemblage of electrons in the condensed phase becomes less and less degenerate, c_p will naturally become greater than c_v, and they will tend to approach the classical values $\frac{5}{2}k$ and $\frac{3}{2}k$ respectively.

Incidentally we obtain from (31), (32) and (33) an expression for the coefficient of thermal expansion of the electron assemblage in the condensed phase at constant pressure, namely,

$$\beta = \frac{1}{v}(\partial v/\partial T)_p = c_v/\zeta_0. \tag{36}$$

9. The temperature variation of ζ in a single-component system

Considering again the single-component system, and the case when the electron assemblage in the condensed phase is highly degenerate, and using the result that $c_{p,C}$ is equal to c_p derived in an earlier section, one obtains from (11) and (35)

$$\epsilon_T = T\int_0^T \gamma\,\mathrm{d}T - \int_0^T \gamma T\,\mathrm{d}T = \tfrac{1}{2}\gamma T^2, \tag{37}$$

where γ has the value given by (25). In view of (17), equation (37) gives the temperature variation of both ϕ and ζ for a single-component system

$$\mathrm{d}\phi/\mathrm{d}T = -\mathrm{d}\zeta/\mathrm{d}T = \gamma T. \tag{38}$$

The temperature variation of ζ can also be calculated alternatively from the following consideration. Consider the Fermi distribution function of the electrons in the metal,

$$f(E) = \frac{1}{e^{(E-\zeta)/(kT)}+1}, \tag{39}$$

in which ζ is the thermodynamic potential defined by (1). Obviously the number of electrons in the condensed phase per unit volume is given by

$$n = 2\int_0^\infty f(E)\,N(E)\,\mathrm{d}E, \tag{40}$$

* For a preliminary report of the results embodied in equations (34) and (35) see Krishnan & Klemens (1952).

in which $N(E)\,dE$ gives the number of energy states between E and $E+dE$. In other words $N(E)$ is the density of the energy states at E. Taking as usual the energy distribution to be parabolic, i.e. taking the density of the energy states to be given by

$$N(E) = KE^{\frac{1}{2}}, \tag{41}$$

where K is a constant, and taking the electron assemblage to be highly degenerate, the thermodynamic potential will be given by (Sommerfeld & Bethe 1933)

$$\zeta = \zeta_0 - \tfrac{1}{6}\gamma T^2. \tag{42}$$

In (42) ζ_0 is not the actual value of ζ at $T = 0$, but the value which it would have at $T = 0$ *had the density remained constant.*

In the usual discussions on the temperature variation of ϕ on the model in which the energy barrier is taken to be independent of temperature, the whole of the variation is attributed to the variation of ζ, and the latter variation is taken to be given by (42), in which n and hence ζ_0 are regarded as remaining constant. One then obtains

$$d\phi/dT = -d\zeta/dT = \tfrac{1}{3}\gamma T, \tag{43}$$

which is only a *third* of the value obtained in (38) for the single-component system, which as we have seen, is equivalent to the model based on a temperature-independent energy barrier.

But actually, as we have shown, $d\phi/dT$ should be equal to $-d\zeta/dT$ at constant *pressure*, so that the variation of ζ_0 in (42) with temperature has also to be taken into account. Doing so one obtains

$$d\phi/dT = -(d\zeta/dT)_p = \tfrac{1}{3}\gamma T - (d\zeta_0/dT)_p. \tag{44}$$

The second term $-(d\zeta_0/dT)_p$ on the right-hand side of (44) can be seen, in view of (34) and (35), to reduce to $\frac{2}{3}\gamma T$, and hence the expression for the total variation of ζ with temperature will become identical with (38), as it should.

The first term on the right-hand side of (44) gives the variation of ζ with temperature as such, and the second the variation due to the change in the density of the electron assemblage accompanying the temperature change. The former accounts for one-third of the total change of ζ with temperature and the latter for the remaining two-thirds.

10. The monovalent metals treated as a single-component system

Having calculated the temperature variation of ζ, which, except for the sign, is also that of ϕ for a single-component system, we shall now extend the calculation to actual metals. We shall confine attention again to the monovalent metals copper, silver and gold. The number of electrons per unit volume in the condensed phase, which determines ζ, is practically the number of *atoms* per unit volume in these metals, and hence is known, as also the coefficient of thermal expansion β of this electron assemblage at constant pressure, namely the saturation vapour pressure. In table 1 are entered the values of the expected coefficient of thermal expansion β for the electron assemblage treated as a single-component system, as also the values of the actual coefficient of expansion δ of the lattice. It will be seen that δ is

enormously greater than β. The obvious conclusion to be drawn from this is that the system cannot be regarded as a single-component one.

Treating it, however, *provisionally* as a single-component one, one can see from (17) and (37) that for these metals

$$\phi_T \doteq \phi_0 + \tfrac{1}{2}\gamma T^2. \tag{45}$$

The temperature variation of ϕ is thus not linear, and hence the saturation current i cannot be represented by an equation of the Richardson type (see (15)) in which both A and ϕ are temperature-independent constants. However, since the second term on the right-hand side of (45) is much smaller than the first, and the actual thermionic measurements extend over a small temperature range only, we may still regard A as roughly constant over this range. One thus obtains

$$A/A_0 = e^{-\gamma T/k} \sim 1 - \gamma T/k. \tag{46}$$

The values of $\gamma T/k$ at 1300° K, which is roughly the middle of the temperature region in which the thermionic constants of these metals were measured, are given in table 1. As will be seen from the entries in the last column of the table, one should expect the observed A coefficients of these metals to be short of the theoretical value by about 10 %.

Table 1

metal	$10^{-4}\zeta_0/k$	$10^5\gamma/k$	$10^5\beta$	$10^5\delta$	$-\Delta A/A_0 = -\gamma T/k$ at 1300° K
Cu	8·1	6	0·10	5·0	0·08
Ag	6·4	8	0·16	5·8	0·10
Au	6·4	8	0·16	4·2	0·10

The actual values of A, as were reported in part III of this paper, are practically of this magnitude. One may therefore conclude that the temperature variation of the work function of a monovalent metal, to which is due the deviation of A from its theoretical value, *is as though it were a single-component system.* This result is particularly significant since we know from the observed large coefficient of thermal expansion of the lattice $\delta \gg \beta$, that there should be a marked deviation from the single-component behaviour; which means that the different thermal effects on the work function roughly balance one another.

11. Thermal effects on the work function

The various factors associated with a change in the temperature that might influence the work function of an *actual* metal, as distinguished from a single-component system, have been discussed by several authors, and in particular by Herzfeld, Wigner, Bardeen, Seitz and Seely, and the present position of the subject is reviewed critically by Herring & Nichols (1949). The two major factors are (1) the thermal expansion of the lattice, and (2) the thermal agitation of the atoms in the lattice. Since we have chosen the energy of an electron at rest in the metal as the zero energy level, the investigation of the temperature variation of ϕ would reduce to one of finding the effects of these two factors, namely, thermal expansion and

thermal agitation, on ζ and on χ. Taking up first ζ, the effect of the thermal expansion is readily calculated on the basis of the free electron gas model, to which the electron assemblage in a monovalent metal closely approximates. On this basis, the extra coefficient of ζ is given by

$$\mathrm{d}\zeta/\mathrm{d}T = -\tfrac{2}{3}\zeta(\delta-\beta) \sim -\tfrac{2}{3}\zeta\delta. \tag{47}$$

The effect of the thermal agitation on ζ will be much smaller and will be to reduce only slightly the depression given by (47).

The observed value of A for the monovalent metal, which is known to be only slightly short of the theoretical value of 120 amp deg.$^{-2}$ cm^{-2}, would therefore imply that the energy barrier χ also is lowered by nearly the same amount as ζ, so that the difference between χ and ζ, which determines ϕ, remains practically unaltered.

12. The influence of the temperature on the energy barrier

We shall now proceed to show that the depression of the energy barrier χ accompanying a rise of temperature is of the required magnitude, i.e. just sufficient to compensate for the lowering in ζ.

The decrease of χ with temperature can be estimated roughly in the following manner. To a first approximation we may take χ to be inversely proportional to the interatomic distance (Seely 1941), i.e. proportional to $n^{\frac{1}{3}}$, in which case the effect of the thermal *expansion* of the lattice on χ will be given by

$$(\mathrm{d}\chi/\mathrm{d}T)_{\mathrm{expn}} = -\tfrac{1}{3}\chi\delta. \tag{48}$$

The effect of the thermal oscillations of the atoms, as distinguished from the simple expansion of the lattice with the atoms in their mean positions to which (48) refers, can be expressed roughly in the form

$$\left(\frac{\mathrm{d}\chi}{\mathrm{d}T}\right)_{\mathrm{oscn}} = -\frac{\mathrm{d}}{\mathrm{d}T}\left(\frac{2}{3}\frac{\pi}{V}e^2\overline{\xi^2}\right), \tag{49}$$

where V is the atomic volume, e is the electronic charge, and $\overline{\xi^2}$ is the mean square of the displacement of the atom, given by

$$\overline{\xi^2} = \frac{h^2T}{4\pi^2Mk\Theta^2}, \tag{50}$$

where M is the mass of the atom, and Θ is the Einstein characteristic temperature, which at the high temperatures that are being considered here, may be taken to be roughly three quarters of the Debye characteristic temperature (Mott & Gurney 1940), for which data are available from the standard tables. We thus obtain

$$\frac{\mathrm{d}\chi}{\mathrm{d}T} = -\tfrac{1}{3}\chi\delta - \frac{1}{6}\frac{e^2h^2}{\pi VMk\Theta^2}. \tag{51}$$

Table 2

metal	$-\frac{1}{k}\left(\frac{\mathrm{d}\chi}{\mathrm{d}T}\right)_{\mathrm{expn}}$	$-\frac{1}{k}\left(\frac{\mathrm{d}\chi}{\mathrm{d}T}\right)_{\mathrm{oscn}}$	$-\frac{1}{k}\frac{\mathrm{d}\chi}{\mathrm{d}T}$	$-\frac{1}{k}\frac{\mathrm{d}\zeta}{\mathrm{d}T}$
Cu	2·2	0·3	2·5	2·8
Ag	2·2	0·3	2·5	2·5
Au	1·6	0·3	1·9	1·8

In columns (2) and (3) of table 2 are entered the temperature coefficients of χ due to the thermal expansion and to the oscillations respectively, calculated from (48) and (49), and in the penultimate column the resultant temperature coefficient of χ. In the last column are entered the temperature coefficients of ζ calculated from (47). It will be seen from the values entered in the last two columns of the table that $\mathrm{d}\chi/\mathrm{d}T$ and $\mathrm{d}\zeta/\mathrm{d}T$ are of practically the same magnitude and their effects on the work function $\phi = \chi - \zeta$ practically cancel each other, and the whole of the observed temperature variation may be regarded as due to the electronic specific heat alone.

This result may have a wider significance. In the monovalent metals the thermal oscillations of the atoms in the lattice, and the accompanying thermal expansion (which as we have seen is much larger than that to be expected for the electron assemblage in the metal) are apparently so conditioned that maintaining the external pressure constant while varying the temperature becomes equivalent to maintaining the internal pressure of the electron assemblage also constant. Hence the observed temperature variation of ϕ is *as though* the electrons in the metal and in the vapour formed the two phases of a single-component thermodynamic system.

References

Fowler, R. H. 1929 *Proc. Roy. Soc.* A, **122**, 36.

Fowler, R. H. & Guggenheim, E. A. 1939 *Statistical thermodynamics.* Cambridge University Press.

Herring, C. & Nichols, M. H. 1949 *Rev. Mod. Phys.* **21**, 185.

Herzfeld, K. F. 1930 *Phys. Rev.* **35**, 248.

Jain, S. C. & Krishnan, Sir K. S. 1952*a* *Proc. Roy. Soc.* A, **213**, 143 (part I).

Jain, S. C. & Krishnan, Sir K. S. 1952*b* *Proc. Roy. Soc.* A, **215**, 431 (part II).

Jain, S. C. & Krishnan, Sir K. S. 1953 *Proc. Roy. Soc.* A, **217**, 451 (part III).

Krishnan, Sir K. S. & Klemens, P. G. 1952 *Phil. Mag.* **43**, 1224.

Mott, N. F. & Gurney, W. 1940 *Electronic processes in ionic crystals.* Oxford: Clarendon Press.

Planck, M. 1926 *Treatise on thermodynamics.* New York: Dover publications.

Reimann, A. L. 1934 *Nature, Lond.*, **133**, 833.

Seely, S. 1941 *Phys. Rev.* **59**, 75.

Seitz, F. 1940 *The modern theory of solids.* New York: McGraw Hill Book Company Inc.

Sommerfeld, A. & Bethe, H. A. 1933 Electronentheorie der Metalle, in *Handbuch der Physik*, XXIV/2. Berlin: Julius Springer.

Wigner, E. P. 1936 *Phys. Rev.* **49**, 696.

ORIGINAL CONTRIBUTIONS

Determination of thermal conductivities at high temperatures

By Sir K. S. Krishnan, F.Inst.P., F.R.S., and S. C. Jain, M.Sc., National Physical Laboratory of India, New Delhi

[*Paper first received* 21 *April, and in final form* 12 *July*, 1954]

The usual electrical methods of determining thermal conductivities either cannot be used at high temperatures or their use is restricted to substances like carbon or graphite which satisfy certain special requirements. It is shown that the observed temperature distribution along a metal filament electrically heated in a vacuum can be used for the determination of the thermal conductivity at high temperatures. The temperature distribution near the centre of a short filament, which is known to be parabolic, or the distribution in regions slightly removed from the centre of a long filament, which is known to be logarithmic, are particularly suitable for this purpose. Measurements are reported on the thermal conductivity of platinum in the temperature region 1300 to 1800° K made in this manner.

THE DIFFERENTIAL EQUATION DEFINING THE STEADY STATE

Consider a filament electrically heated in a vacuum, so that the transfer of heat by convection in the surrounding atmosphere is avoided. The heat generated per unit length of the filament per second is $I^2\rho/\omega$, where I is the heating current, ρ is the specific resistance, and ω is the area of cross-section of the filament. The rate of loss of energy per unit length by radiation is $p\epsilon\sigma(T^4 - T_0^4)$, where p is the periphery of the cross-section, ϵ is the total emissivity from the surface, as distinguished from the spectral emissivity ϵ_λ, and σ is Stefan's constant of radiation. Owing to the conduction of heat towards the ends, the energy abstracted per second per unit length is $-\kappa\omega d^2T/dx^2$, where κ is the thermal conductivity. Hence the steady state is determined by the well-known differential equation[1]

$$\kappa\omega d^2T/dx^2 - p\epsilon\sigma(T^4 - T_0^4) + I^2\rho/\omega = 0 \qquad (1)$$

Now the existence of a temperature gradient along the filament is a consequence of the finite thermal conductivity of the filament. Hence if we had an analytical solution of equation (1), we might utilize the observed distribution of temperature along the filament to determine experimentally the thermal conductivity. But an analytical solution of the differential equation in the general case was not available till recently. Hence some of the earlier experimental methods for the determination of κ, as for example those of Kohlrausch,[2] and of Callendar,[2] were so designed as to reduce equation (1) to a readily integrable form, namely to

$$d^2T/dx^2 = f \qquad (2)$$

where f is an explicit function of κ. Obviously the solution is

$$T = \tfrac{1}{2}fx^2 + Bx + C \qquad (3)$$

in which the constants B and C may be determined from the boundary conditions. The actual techniques used in these methods for securing equation (3), however, restrict the applicability of these methods to temperatures in the neighbourhood of the room temperature.

On the other hand Worthing and Halliday[3] have adopted a graphical method for the determination of the thermal conductivity from the observed distribution of temperature in heated filaments, which in essence is equivalent to solving the differential equation (1) graphically. Knowing all the physical constants involved in equation (1) except κ, κ then becomes known. Actually they integrate graphically the total heat generated in a selected finite length of the filament, and similarly also the total heat radiated out from this length. The difference between the two gives $\kappa\omega(G_1 - G_2)$, where G_1 and G_2 are the temperature gradients at the colder and the hotter ends respectively of the length selected. By making one end of the selected length coincide with the centre of the filament, G_2 can be made zero.

This method of determining κ is obviously applicable to high temperatures also.

In some recent papers[4,5,6] we have investigated in detail the analytical solution of equation (1). In the case of a long filament it is possible to obtain a general solution of equation (1), and in the case of shorter filaments too a solution can be obtained in terms of a power series which is rapidly convergent over most parts of the filament. It is the main purpose of this paper to show that the observed temperature distribution along such filaments, which can be readily measured with an optical pyrometer, can be made the basis of a convenient and direct method for determining thermal conductivities at high temperatures. This is of interest experimentally. The only other method that is available now, namely, that of Angell,[7] is based on the measurement of the difference in temperature between the inner and the outer surfaces in the middle portion of a long tube electrically heated in a vacuum. This method has been used by Powell and Schofield[8] to determine the thermal conductivity of carbon and of Acheson graphite; in which the walls of the tube can be made thick enough to secure a considerable difference in temperature between the inner and the outer surfaces, and at the same time the electrical resistance of the tube remains sufficiently large to permit our heating it to high temperatures without using inconveniently large currents. This cannot, however, be done with good metals.

It is significant that the only high temperature data for thermal conductivities available at present are those for tungsten, tantalum and carbon obtained by Worthing's graphical method, and those for carbon and graphite obtained by Angell's method.

THE METHODS OF KOHLRAUSCH AND CALLENDAR AS DEVICES FOR SIMPLIFYING THE TEMPERATURE DISTRIBUTION

In Kohlrausch's method, which has been developed experimentally by Jaeger and Diesselhorst,[2] the loss by radiation is practically eliminated by surrounding the conductor with a suitable wadding of insulating material. The differential equation (1) now reduces to

$$d^2T/dx^2 + I^2\rho/(\kappa\omega^2) = 0 \qquad (4)$$

which is readily solved.

In Kohlrausch's method the distances x are not measured directly, but in terms of the corresponding potential drops

$$v = (I\rho/\omega)x \qquad (5)$$

Since there is no loss by radiation, and therefore no gradient of temperature *across* the length, one may use, as these authors do, a rod or a bar of large cross-section, instead of a filament.

On the other hand, in Callendar's method a low heating current is used so as to make $T - T_0$ sufficiently small over the whole length of the filament that the radiation loss may be regarded as proportional to $T - T_0$ instead of to $T^4 - T_0^4$, that is, the radiation cooling follows Newton's law. The temperature range being now small, the variation of the specific resistance with temperature may be taken to be linear. Hence the resistance at every point may be split into a constant term characteristic of the temperature T_0, and an extra term proportional to $T - T_0$. Consider now the heating due to the latter part of the resistance, which will be proportional to I^2 and to $T - T_0$. By suitably adjusting the heating current I, this part of the heat generated can be made to balance the loss due to radiation, at every point of the filament, since both are proportional to $T - T_0$. When this condition is secured, the energy that is abstracted per unit length in the process of conduction becomes constant, i.e. the same at all points along the filament. This is essentially the condition for the temperature distribution to be parabolic. In the actual measurements the increase in resistance due to the heating, which can be readily calculated in terms of the parabolic distribution, is measured, rather than the distribution of temperature as such.

Both these methods, by the limitations imposed by the special techniques involved in securing the parabolic distribution, are applicable only to temperatures in the neighbourhood of the room temperature.

We now proceed to show that independently of any such special devices the temperature distribution near the centre of any finite filament is naturally parabolic, and can be utilized in the same manner as in Kohlrausch's and Callendar's special arrangements, to determine κ. Unlike these special arrangements, this method is applicable to high temperatures too.

ACTUAL DISTRIBUTION NEAR THE CENTRE SHOWN TO BE PARABOLIC AND UTILIZED TO DETERMINE κ

Let T_l be the temperature at the centre of the filament, and T_m the value to which T_l tends as $2l$, the length of the filament, is increased indefinitely, keeping the heating current constant. Obviously

$$p\sigma\epsilon(T_m^4 - T_0^4) = I^2\rho/\omega \qquad (6)$$

Returning to equation (1), and eliminating T_0 with the help of equation (6), one obtains

$$\frac{d^2T}{dx^2} + \frac{p\epsilon\sigma}{\kappa\omega}(T_m^4 - T^4) = 0 \qquad (7)$$

which in the case of a finite rod for which $T_l \neq T_m$ can be written in the form

$$\frac{d^2T}{dx^2} + \frac{p\epsilon\sigma}{\kappa\omega}(T_m^4 - T_l^4) + \frac{p\epsilon\sigma}{\kappa\omega}(T_l^4 - T^4) = 0 \qquad (8)$$

If $T_m - T_l$ is considerable, as will be the case when the filament is not long, one may confine attention to a region close to the centre, where the temperature-dependent term in equation (8), namely, the third term on the left-hand side, becomes negligible in comparison with the second term. Equation (8) then reduces to

$$d^2T/dq^2 - f_1(\kappa) = 0 \qquad (9)$$

where

$$f_1(\kappa) = \frac{p\epsilon\sigma}{\kappa\omega}(T_m^4 - T_l^4) \qquad (10)$$

and $q = l - x$ is now the distance measured from the centre. Using the boundary conditions that when $q = 0$, $T = T_l$ and $dT/dq = 0$, one obtains

$$t = T_l - T = \tfrac{1}{2}f_1q^2 \qquad (11)$$

Thus from the observed temperature distribution in this region it is possible to determine f_1 and then κ in the same manner as before. Since the largest deviation of the temperature in the parabolic region from T_l, that is, the highest value of t involved in this region, is small, the quantity $p\epsilon/(\kappa\omega)$ appearing in equation (10) for f_1 may be assigned the value appropriate to the temperature T_l.

κ FROM THE LOGARITHMIC REGION

Consider a long filament in which $T_l \simeq T_m$. In this case, if one is not too close to the centre, that is, if T is not too close to T_l, the second term on the left-hand side of equation (8) may be neglected in comparison with the third. Consider a region sufficiently removed from the centre, but where $T_m - T = \Delta$ is still small in comparison with T_m. Equation (8) then takes the simple form

$$d^2\Delta/dx^2 = A\Delta \qquad (12)$$

where

$$A = \frac{4p\epsilon\sigma T_m^3}{\kappa\omega} \qquad (13)$$

Neglecting for the present the temperature variation of the physical quantities involved, one then obtains the well-known solution

$$x\sqrt{A} = D - \ln\Delta \qquad (14)$$

in which $1/\sqrt{A}$ is obviously the distance over which Δ changes by a factor e. Hence A can be determined experimentally, and κ can be evaluated therefrom.

We should mention here that the temperature distribution along a thin-walled tube electrically heated in a vacuum is somewhat similar to that along a filament. When the tube is long, the temperature distribution in regions slightly removed from the centre is given by equation (14), in which A has the same significance as in a filament, except that the cross-sectional area ω occurring in the expression for A is now the area of the annular ring. A part of A, namely $\epsilon\sigma/\kappa$, occurs also in the expression for the difference in temperature between the inner and the outer surfaces of the tube. In determining this difference in temperature Prescott and Hincke[9] have used the observed temperature distribution in the logarithmic region, in order to eliminate $\epsilon\sigma/\kappa$ from the expression for this difference. Obviously the experimental data for the temperature distribution in the logarithmic region could have been used to determine κ also.

Coming back to the filament, we should mention also the following results which were derived in our earlier papers, and which are relevant to our present purpose.

(1) Though the condition under which equation (14) has been derived, namely that Δ be small in comparison with T_m, is a sufficient one, it is not necessary, the necessary condition being that $\Delta \ln \Delta$ be small in comparison with T_m, which

obviously holds over a much wider range than the former condition.

(2) The region near the centre that is excluded corresponds to a total range of temperature equal to a few times $T_m - T_l$, and hence experimentally trivial.

(3) Now in formulating equation (12) we have neglected for convenience the temperature variations of the different physical quantities involved, namely $\kappa\omega$, ρ/ω and $p\epsilon$. The effect of the temperature coefficients of these quantities on equation (12) is essentially different from that in the parabolic region. As we shall see presently, even when attention is confined to a *narrow* region in the logarithmic range, the effect of the temperature coefficients will be appreciable, unlike in the parabolic range. This is due to the following circumstance. In the differential equation (9), which defines the temperature distribution in the parabolic range, the effect of the temperature coefficients is in the form of a contribution to the term proportional to f, which in any case may be neglected since t is chosen small. In other words equation (9) will hold even when the temperature coefficients are considerable, provided that the value of $p\epsilon/(\kappa\omega)$ occurring in the expression for f_1 is made to refer to the temperature T_l.

On the other hand in the logarithmic region the effect of the temperature variation of ρ/ω and $p\epsilon$ is to introduce an extra small term which varies linearly with temperature, which now cannot be neglected. Taking the values of $\kappa\omega$, ρ/ω and $p\epsilon$ to refer to the temperature T_m, the effect of the finite temperature coefficients of these quantities—the temperature coefficient of $\kappa\omega$ has very little effect in this region—is to introduce in equation (12) a small extra term proportional to Δ. In other words the expression for A in equations (12) and (13) will include a multiplying factor a_1 of the order of unity, whose deviation from unity is determined by the temperature coefficients of ρ/ω and $p\epsilon$, and by T_m.

The calculation of a_1 was given in a recent paper,[4] in which, however, the coefficient of thermal expansion, which normally is much smaller than the coefficients of κ, ρ and ϵ, was neglected. The expression for a_1 obtained in the paper can, however, be made to include thermal expansion also by replacing the temperature coefficients of κ, ρ and ϵ given in that paper by the coefficients of $\kappa\omega$, ρ/ω and $p\epsilon$ respectively.

We shall merely mention here the final result, namely, that for platinum, with which we shall be concerned in the present paper, a_1 varies from 0·97 for $T_m = 1800°$ K to 1·00 for $T_m = 1300°$ K.

TEMPERATURE DISTRIBUTION IN OTHER REGIONS ALSO UTILIZED TO GIVE κ

In the case of a long filament one can also obtain a general solution of equation (1) applicable over the whole length of the filament. Neglecting provisionally the temperature coefficients, the solution is

$$\Delta \exp [f(\Delta)] = \Delta_0 \exp [f(\Delta_0)]\{\exp(-x\sqrt{A}) + \exp[-(2l - x)\sqrt{A}]\} \quad (15)$$

where

$$\Delta_0 = T_m - T_0 \quad (16)$$

T_0 being the temperature of the point from which x is measured, and

$$f(\Delta) = \tfrac{1}{2}\Delta/T_m + \tfrac{1}{6}\Delta^2/T_m^2 - \ldots \quad (17)$$

Now in a long filament the region near the centre where $\exp[-(2l - x)\sqrt{A}]$ is significant, is not of experimental interest since the total variation of temperature in this region is a few times $T_m - T_l$, which is negligible. Outside this region, where $\exp[-(2l - x)\sqrt{A}]$ is negligible in comparison with $\exp(-x\sqrt{A})$, equation (15) reduces to the simple form

$$\Delta \exp [f(\Delta)] = \Delta_0 \exp [f(\Delta_0)] \exp(-x/A) \quad (18)$$

Now expressing all distances in terms of $1/\sqrt{A}$ and all temperatures in terms of T_m, that is, using the reduced co-ordinates $X = x\sqrt{A}$ and $\tau = T/T_m$, equation (18) may be seen to reduce to

$$(1 - \tau) \exp [\phi(\tau)] = (1 - \tau_0) \exp [\phi(\tau_0)] \exp(-X) \quad (19)$$

where $\phi(\tau) = f(\Delta)$. Obviously equation (19) is a very general expression, which implies that a *single* $\tau - X$ curve will represent the temperature distribution in all *long* filaments, independently of the nature of the filament, its length, its cross-section, or even the heating current used, provided that the reduced temperature τ_0 of the point from which the distances are measured is chosen the same in all the plots.

Hence, knowing T_m in any actual experiment, one can easily plot τ against x. This curve may be compared with the theoretical plot of τ against X, taking τ_0 from which x is measured, as the origin of distance in the $\tau - X$ curve too. The only difference between the two curves should be in the scales representing the abscissae. In other words it should be possible to transform the experimental $\tau - x$ curve into the theoretical $\tau - X$ curve by increasing the abscissae of the former by a *constant* factor F, that is, by a factor which is independent of x, and which can be experimentally determined. This factor should obviously be equal to $\sqrt{A}$, from which κ can be determined.

Here again we have neglected the temperature coefficients of the different quantities. Taking them into account would introduce a factor q_1 in the expression for A, as in the logarithmic region, and a factor a_2 in the expression for $\phi(\tau)$. For platinum a_2 varies from 1·4 for $T_m = 1800°$ K, to 1·8 for $T_m = 1300°$ K.

Confining now attention to the top of the region that we are considering, in which Δ is small enough to keep $\exp\phi(\tau)$ close to unity, equation (19) will obviously reduce to the logarithmic formula, as it should.

In reduced co-ordinates the temperature distribution in the logarithmic region is given by

$$\ln(1 - \tau) = \ln(1 - \tau_0) + \phi(\tau_0) - X \quad (20)$$

Hence, if the reduced temperature τ_0 from which distance measurements are made is taken to be the same in all the measurements, the plot of $\ln(1 - \tau)$ against the distance will be a series of straight lines, all of them passing through the point τ_0, and having different slopes. The slopes give directly $\sqrt{A}$, and hence κ, taking into account the temperature coefficients of ρ/ω and $p\epsilon$.

When one moves out of the logarithmic region $\phi(\tau)$ grows fairly rapidly and the effect of the temperature coefficients on $\phi(\tau)$ also becomes significant. Now $\phi(\tau)$ involves in addition to the temperature coefficients of ρ/ω and $p\epsilon$ which are known, the temperature coefficient of $\kappa\omega$ too. Hence in the same manner in which temperature distribution in a long filament in the logarithmic range can be used to give κ, the distribution outside the logarithmic range can be made to yield both κ and its temperature coefficient α.

In practice, however, it is found more convenient to determine κ at different temperatures from the logarithmic range, by suitably varying the heating currents and varying the temperatures T_m to which κ refers. This has been done in the measurements described below.

EXPERIMENTAL

It has been shown that the thermal conductivity can be determined from the temperature distribution either in the parabolic region near the centre of any finite filament, preferably a short one, or in the logarithmic or any other region of a long filament. We have made measurements with a platinum wire, of spectroscopic purity (obtained from Johnson and Matthey and Co. Ltd.). The main part of the experiment is the determination of the temperature at different points along the heated wire. This was done with an optical pyrometer and for this purpose one needs to know the spectral emissivity ϵ_λ for the spectral region utilized in the pyrometer, namely the neighbourhood of 0·655 μ, at different temperatures.

This was determined in the following manner. In a recent paper we described some measurements on the spectral emissivity of Acheson graphite.[10] Using a thin-walled, long tube of graphite, electrically heated in a vacuum, the temperature of the inner surface of the tube near its centre is readily obtained by boring a small hole in the wall, and by measuring directly with the pyrometer the temperature of the cavity as viewed through the hole. The small difference in temperature between the inner and the outer surfaces is estimated easily from any rough value of the thermal conductivity. Thus the temperature of the outer surface near the centre is known. Knowing also the brightness temperature of the surface as measured with the optical pyrometer, the spectral emissivity ϵ_λ is obtained directly. By suitably adjusting the heating current, the spectral emissivity can be obtained at different known temperatures. Conversely, knowing ϵ_λ, the actual temperature of the surface corresponding to any observed brightness temperature can also be readily obtained.

For our present purpose, namely, the determination of the spectral emissivity of platinum at different temperatures, we used one of these thin-walled long graphite tubes, and wound round it in a thin groove cut round the middle of the tube, a single ring of platinum wire. The presence of either the groove or the platinum wire in the middle does not affect the temperature distribution. Knowing the actual temperature of the wire, which is that of the graphite surface adjoining it, and the brightness temperature of the wire as obtained with the optical pyrometer, its spectral emissivity is known. By suitably varying the heating current, values of ϵ_λ can be obtained at different temperatures. They are plotted in Fig.

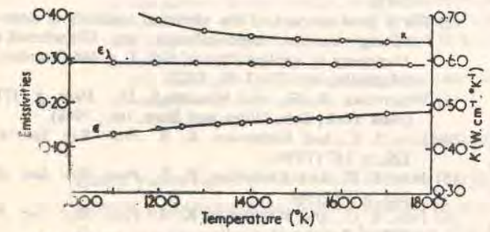

Fig. 1. The temperature variation of the thermal conductivity of platinum and of the spectral and the total emissivities

The first series of measurements that we made on the spectral emissivity of platinum was with a foil rolled into a cylinder, which just surrounded the graphite tube without touching it. It was fixed to the supporting block at one end. The external diameter of the graphite tube was 8 mm, and the clearance space between the graphite tube and the tube of platinum foil was about $\frac{1}{2}$ mm. The tube of platinum foil extended over nearly the whole length of the graphite tube, but not completely. This was to avoid passage of electric current through the platinum foil. Hence the temperature of the foil, particularly near the centre, where it is sensibly constant, will be just that of the graphite tube underneath, and that of the annular space between the two tubes. A small hole of about 1 mm diameter punctured in the platinum foil, and also in the wall of the graphite tube just underneath it, enabled the temperature in the cavity near the middle of the graphite tube to be measured directly. Knowing this temperature, and the small difference between the inner and the outer surfaces of the graphite tube, the temperature of the platinum surface adjoining the hole is known. From this temperature and the brightness temperature of the platinum surface as measured with the pyrometer, the spectral emissivity of platinum is readily determined.

The spectral emissivity data for platinum obtained in this manner were found to agree closely with the measurements reported, which were made with a ring of platinum wire wound round the central portion of the graphite tube.

The available data for the spectral emissivity of platinum obtained by different authors vary widely, and the differences have sometimes been attributed to the probable differences of the surfaces of the specimens used. The close agreement between our measurements with the surface of the platinum foil and of the wire does not, however, support this view. Even so, since the specimen with which the thermal conductivity measurements were made, was in the form of a wire, we considered the measurements on ϵ_λ made with the same specimen to be more appropriate for our present purpose than the measurements made with the foil. The results of the latter measurements, which are not incorporated in the graph, are given in the following table.

$T°$ K	1120	1250	1400	1525	1600	1690	1750
ϵ_λ	0·28	0·30	0·29	0·28	0·29	0·29	0·30

The single coil of the platinum wire wound in a small groove round the middle of the graphite tube involves negligible change in the heat capacity, and is therefore not likely to disturb the temperature distribution sensibly. The agreement between the values of ϵ_λ obtained by the two methods, supports this conclusion. Observations made with the optical pyrometer also confirmed that the temperature of the graphite surface in the close neighbourhood of the ring of platinum wire did not show any detectable variation.

The experimental error in the measurement of ϵ_λ is estimated to be less than $\pm 0{\cdot}02$.

Referring again to the temperature measurements, two sets of temperature measurements were made on platinum wires of 0·5 mm diameter (s.w.g. 25) heated in a vacuum by an alternating current. In the first set the wire was a medium long one, and the temperature measurements were made in the parabolic region near the centre. In Fig. 2 are plotted the values of t against q^2. In one series of measurements T_m and T_l were 1600 and 1400° K respectively, while in the other series 1500 and 1200° K respectively. The plot can be seen to be a straight line for small values of q^2, and its slope according to equation (11) gives $\frac{1}{2} f_1$, from which κ can be calculated. It can also be seen that t increases slightly more rapidly than in proportion to q^2, since the last one or two points are slightly above the straight line. This is to be

expected theoretically. But the straight line portion is long enough to enable the slope to be determined accurately. The values of κ for 1200 and 1400° K plotted in Fig. 1 were obtained in this manner.

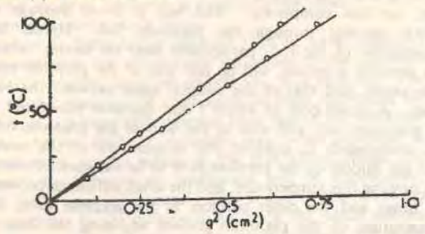

Fig. 2. The parabolic variation of temperature near the centre of the filament

In the second set measurements were made with a *long* platinum wire in the logarithmic region, using different heating currents. In Fig. 3 are plotted the values of $\ln(\Delta/T_m)$ against the distance. The plot is a straight line over the whole of the temperature region included in the curves. The slope gives $\sqrt{A}$, from which again κ can be calculated.

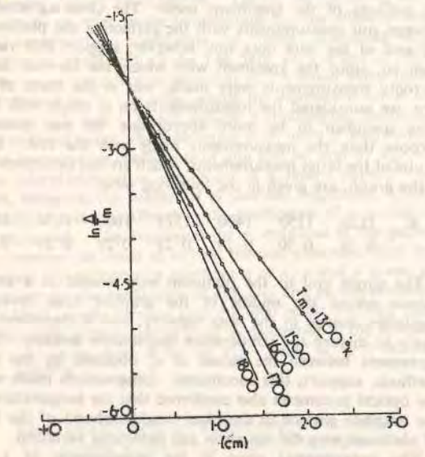

Fig. 3. Temperature variation in the logarithmic region

In order to obtain κ from f_1 or from A one needs to know also the total emissivity ϵ, as distinguished from the spectral emissivity. All that one needs for this purpose is the potential gradient g in the centre of a long wire heated by different currents, since

$$p\epsilon\sigma(T_m^4 - T_0^4) = Ig \qquad (21)$$

ϵ in equation (21) is the value of the total emissivity at temperature T_m.

The potential gradient g is easily measured with the help of two probes. The values of ϵ thus obtained are also plotted in Fig. 1. It is very significant that, whereas the spectral emissivity is almost independent of temperature, the total emissivity drops with the decrease of temperature.

DATA FOR THERMAL CONDUCTIVITY

The values of κ obtained from the parabolic and the logarithmic regions are also plotted in Fig. 1. The values for 1200 and 1400° K were obtained from the former region, and the remaining values from the latter. It will be seen that both the sets plot smoothly on a single curve.

It will also be seen that κ tends to a constant value at high temperatures, as should be expected at temperatures much above the Debye temperature.

THE LORENZ RATIO FOR PLATINUM

In the course of the determination of the total emissivity described in a previous section, one obtains incidentally from the potential gradient and the current, the electrical resistivity at different temperatures. Since we now have data for the thermal conductivities also, we can obtain directly the values of the Lorenz ratio $\kappa\rho/T$ at different temperatures. Since it is an important physical quality, for which at present data are not available for platinum at high temperatures, we have plotted in Fig. 4 this ratio.

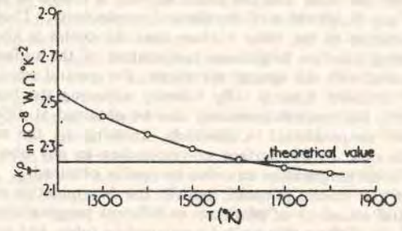

Fig. 4. Lorenz ratio for platinum

It will be seen from Fig. 4 that the Lorenz ratio for platinum decreases slightly with the increase of temperature, and remains close to the theoretical value of $2{\cdot}23 \times 10^{-8}\,\mathrm{W}\,\Omega\,^{\circ}\mathrm{K}^{-2}$.

REFERENCES

(1) Carslaw, H. S., and Jaeger, J. C. *Conduction of heat in solids*, p. 135 (London: Oxford University Press, 1947).

(2) For a good account of the electrical methods of determining thermal conductivities see Glazebrook's *Dictionary of Applied Physics*, Vol. I, p. 446 (London: Macmillan and Co. Ltd., 1922).

(3) Worthing, A. G., and Halliday, D. *Heat*, p. 171 (New York: John Wiley and Sons, Inc., 1948).

(4) Jain, S. C., and Krishnan, K. S. *Proc. Roy. Soc. A*, **222**, p. 167 (1954).

(5) Jain, S. C., and Krishnan, K. S. *Proc. Roy. Soc. A*, **225**, p. 1 (1954).

(6) Jain, S. C., and Krishnan, K. S. *Proc. Roy. Soc. A*, **225**, p. 7 (1954).

(7) Angell, M. F. *Phys. Rev.*, **33**, p. 421 (1911).

(8) Powell, R. W., and Schofield, F. H. *Proc. Phys. Soc.*, **51**, p. 153 (1939).

(9) Prescott, C. H., and Hincke, W. B. *Phys. Rev.*, **31**, p. 130 (1928).

(10) Jain, S. C., and Krishnan, K. S. *Proc. Roy. Soc. A*, **213**, p. 143 (1952).

The distribution of temperature along a thin rod electrically heated *in vacuo*. V. Time lag

By S. C. Jain and Sir K. S. Krishnan, F.R.S.
National Physical Laboratory of India, New Delhi

(*Received* 2 *July* 1954)

On the basis of the expressions obtained in parts I and II of this series for the distribution of temperature in the *steady* state along a filament electrically heated *in vacuo*, the growth of temperature accompanying a small increase in the heating current is investigated in the present part. Over a considerable region about the centre of the filament, which is the region of practical interest, it is found that to a close approximation the growth of temperature can be completely represented by a simple exponential law involving a *single* relaxation time, whose magnitude is readily calculated.

This method of investigating the time lag, which is general and applicable to any filament, is compared with the well-known method of Fourier expansion developed by Straneo for the special case where the temperature everywhere in the filament is only slightly higher than the room temperature, and hence the loss by radiation conforms to Newton's law of cooling. Each of the Fourier terms is assigned in his method a separate relaxation time that will make the term separately satisfy the differential equation and the boundary conditions. In principle the Fourier method also should be applicable to any filament. But the actual temperature distribution is in general too complicated for an analytical Fourier expansion.

In the special case treated by Straneo the temperature distribution over practically the whole length of the filament is parabolic. The actual distribution near the centre of any filament is also known to be parabolic. Hence a comparison of the results obtained by the two methods in the above special case suggests a convenient adaptation of the Fourier method also to the calculation of the time lag near the centre of any filament. The adaptation lies essentially in the use of a certain effective length to determine the period of the Fourier expansion, instead of the actual length generally used. The magnitude of this length is obtained from the results of the present investigation. The distinction between the two lengths is not significant in the special case treated by Straneo, but it is in other cases.

Though the occurrence of a single effective relaxation time is not directly obvious from the Fourier expansion, it is shown to follow from it as a close approximation. This result is convenient for practical application.

For a given central temperature the relaxation time is found to vary inversely as the ratio of the surface to the volume, and is therefore smaller for a ribbon filament than for one of circular cross-section, as observed by Prescott & Morrison. For a given central temperature and length, the ribbon filament is found to approximate closer than one of circular section, to an infinitely long one.

The variation of the relaxation time near the centre with the length of the filament is investigated in some detail.

1. Introduction

Many years ago Prescott & Morrison (1939) made the following important observation on a filament electrically heated *in vacuo*. When the heating current is changed, there is naturally a time lag between the change of current and the attainment of the corresponding steady state. Their observation was that this time lag is considerably shorter in a ribbon filament than in a filament of circular cross-section. Denoting by ω the area, and by p the periphery, of the cross-section of the filament, they found that the time lag is the shorter the larger the value of p/ω. Obviously p/ω will be a minimum when the cross-section is circular.

There has been some difference of opinion between these authors on one side and Wensel on the other regarding the mechanism by which an increase in p/ω effects

a reduction in the time lag. The two views are stated in detail in the discussion accompanying a paper by Prescott (1941). Whereas according to Prescott & Morrison the effect of the large ratio of the surface of the filament to the volume, which obtains in a ribbon filament, on the time lag, is through its 'minimizing the heat capacity', according to Wensel it is through its 'minimizing the heat conduction loss (from the central part) to the leads'. The general impression left on the reader after a perusal of this discussion is that, independently of the controversy, there is need for a detailed theoretical investigation of the growth of temperature in a filament with time when a current is switched on it, or when the heating current is varied. The investigation will also be useful otherwise. In the optical pyrometer, for example, which is used extensively for the measurement of high temperatures, the heating current through the filament is adjusted so as to make the brightness of the filament match that of the background whose temperature is being measured. The efficiency of this matching depends naturally on how small is the time lag referred to above. Indeed, the original use of the ribbon filament by Prescott & Morrison was in an optical pyrometer, and was intended specifically to reduce the time lag.

Some special cases, where either the loss of heat due to conduction through the ends of the filament, or the loss due to radiation from the surface, is wholly eliminated, have been investigated by Fischer (1938*a*, *b*, *c*), and in connexion with the study of the bearing loads of fuse wires by Wintergerst (1950). But the most important earlier work is that of Straneo (1898) on a filament whose temperature at every point is only slightly above the room temperature, such that the rate of cooling due to radiation may be taken to conform to Newton's law. Though the temperatures that we shall be concerned with in the optical pyrometer are naturally of a different order of magnitude, and the loss due to radiation is by no means Newtonian, the method developed by him is a general one. The method is this. Since the temperature distribution is known for his filament both in the final and in the initial steady states, the difference between them is known as a function of the distance. When the temperature is growing the expression for the difference between the final temperature at any point and the actual temperature there can be expressed as a Fourier sine series, *each term in the series having its own characteristic relaxation time*, the relaxation time chosen being such that each term separately satisfies the differential equation and the boundary conditions. Hence the growth of the current may be followed at every point of the filament in detail.

In Straneo's problem the temperature distribution along the filament is practically parabolic, and can be expressed conveniently as a Fourier sine series. But the filaments that are of practical interest are the long ones, worked at high temperatures, in which the temperature distribution is much more complicated, and hence the Fourier method in its usual form becomes a laborious one.

In parts I and II (Jain & Krishnan 1954*a*, *b*) was given a theoretical investigation of the distribution of temperature in an electrically heated filament in the steady state. On the basis of the results obtained therein the time lag in electrical heating in the central portion (which is the region of practical interest) of any filament, long or short, is investigated in the present part, taking into account the loss of heat due both to the conduction at the ends, and to the radiation from the surface, which is

not Newtonian. The direct method, besides being applicable generally to a filament of any length, has also some advantages over the Fourier method. Even where, as in Straneo's problem, the temperature distribution along the filament is parabolic, and the Fourier expansion convenient, there are some features which may be missed altogether by the Fourier method. For example, it is found by the present method that the whole course of the growth of temperature near the centre of the filament, in which we are particularly interested, corresponds practically to a single relaxation time. Though this result should be implicit in the Fourier expansion, it is by no means obvious from the expansion.

2. Formulation of the differential equation

Now in a heated filament the heat generated per second per unit length of the filament is $I^2\rho/\omega$, and the rate of loss of heat per unit length is $p\epsilon\sigma(T^4 - T_0^4)$, where T is the temperature of the element, and T_0 that of the walls of the chamber, I is the heating current, ρ is the specific resistance, ϵ is the total (as distinguished from the spectral) emissivity of the surface, and σ is Stefan's constant of radiation. The heat conducted away from this element, per unit length per second, is $-\kappa\omega \mathrm{d}^2T/\mathrm{d}x^2$, where x is the distance along the filament, and κ is the thermal conductivity.

When the conditions are *steady*, the temperature distribution along the filament will be given by the well-known differential equation (see Carslaw & Jaeger 1947)

$$-\kappa\omega \mathrm{d}^2T/\mathrm{d}x^2 = I^2\rho/\omega - p\epsilon\sigma(T^4 - T_0^4). \tag{1}$$

Had there been no loss due to conduction, the temperature of the filament at every point would have been equal to T_m, where

$$p\epsilon\sigma(T_m^4 - T_0^4) = I^2\rho/\omega. \tag{2}$$

Obviously T_m will be the value to which the temperature T_l at the centre of the filament tends as the length $2l$ tends to infinity, the heating current being kept constant.

In view of (2) the equation for the steady state may be written in the convenient form

$$-\kappa\omega \mathrm{d}^2T/\mathrm{d}x^2 = p\epsilon\sigma(T_m^4 - T^4). \tag{3}$$

It will be seen from (3) that the temperature T_0 of the walls of the chamber does not appear explicitly in the expression, and the whole effect of this temperature is exercised through its influence on T_m.

Now if a heating current is switched on or off, or the current is changed, the temperature distribution at any later instant t can be obtained from the following considerations. Since the temperature T in the element is changing, a quantity equal to $c\delta\omega \mathrm{d}T/\mathrm{d}t$, where δ is the density and c is the specific heat of the material of the filament, will be taken up in this process per second per unit length of the element, and this quantity has to be included on the left-hand side of (3). Hence the differential equation defining the growth of temperature at any point of the filament is

$$-\kappa\omega\, \partial^2T/\partial x^2 + c\delta\omega\, \partial T/\partial t = p\epsilon\sigma(T_m^4 - T^4), \tag{4}$$

which may be written in the form

$$\partial T/\partial t = \alpha \partial^2 T/\partial x^2 + \beta(T_m^4 - T^4), \tag{5}$$

where
$$\alpha = \kappa/(c\delta) \tag{6}$$

and
$$\beta = p\epsilon\sigma/(c\delta\omega). \tag{7}$$

To T_m appearing in (4) is to be assigned the value appropriate to the final steady state. α is the thermal *diffusivity* as usually defined.

It follows directly from (4) that the time lag should be the greater the smaller the value of p/ω, as observed by Prescott & Morrison. Further, the first term on the left-hand side of (4) is the one associated directly with the loss due to the conduction towards the ends. What part this conduction plays in determining the time lag depends on the magnitude of its contribution to $\partial T/\partial t$ as compared with that from the term on the right-hand side.

Let T_1 and T_2 be the initial and the final steady temperatures at the point x, i.e. when $t = 0$ and $t \to \infty$ respectively. Following the usual procedure adopted in solving problems of this type, we may put $T = T_2 - \tau$, where τ is a function of the time (and also of the distance x). Substituting this value of T in (5) one obtains from it *two* differential equations, one defining the temperature distribution in the final steady state, i.e. defining T_2 as a function of x, and the other defining the variation of τ with time. These equations are

$$\alpha \mathrm{d}^2 T_2/\mathrm{d}x^2 + \beta(T_m^4 - T_2^4) = 0 \tag{8}$$

and
$$-\partial\tau/\partial t = \beta[T_2^4 - (T_2 - \tau)^4] - \alpha\partial^2\tau/\partial x^2, \tag{9}$$

respectively.

3. The relaxation time at the centre of a long filament

Our main objective is to solve (9), and equation (8) for the steady state is invoked for the purpose of evaluating $\partial^2\tau/\partial x^2$, which is required for the solution of (9). In the special case when $\partial^2\tau/\partial x^2$ is zero, the solution of (9) may be obtained directly without the aid of (8), though even here one has to invoke (8) in order to determine the conditions under which $\partial^2\tau/\partial x^2$ vanishes. It will be seen from (8) that *in the steady state*, the value of $\mathrm{d}^2T/\mathrm{d}x^2$ at any point x is proportional to $T_m^4 - T^4$, where T is the temperature at the point. At the centre of a long filament, where $T = T_l$, and T_l is practically the same as T_m, $\mathrm{d}^2T/\mathrm{d}x^2$ should be negligible. This is due essentially to the central portions of such a long filament being too far removed from the ends, through which the heat is conducted away, to be affected by the conduction. Hence when the heating current is growing, the value of $\partial^2\tau/\partial x^2$ in this region should remain negligible. The differential equation (9) defining the growth of temperature now reduces to

$$-\partial\tau/\partial t = \partial T/\partial t = \beta(T_m^4 - T^4). \tag{10}$$

This equation is identical with the equation for the rate of cooling of a mass of water kept at a high temperature, the temperature being maintained the same throughout the mass, which has been discussed by Jaeger (1951). This is also the expression obtained by Wintergerst for a filament in which the loss in heat is due wholly to

radiation. Since the solution is well-known, we shall merely give the final result here namely,

$$\frac{T_m - T}{T_m + T} \mathrm{e}^{-2 \arctan (T/T_m)} = C\,\mathrm{e}^{-t/t_0}, \tag{11}$$

where
$$t_0 = 1/(4\beta T_m^3) = c\delta\omega/(4p\epsilon\sigma T_m^3) \tag{12}$$

is a constant having the dimension of time, which may be called the relaxation time, and C is the constant of integration which can be determined from the boundary conditions $T = T_0$ when $t = 0$ and $T \to T_m$ when $t \to \infty$. One thus obtains

$$C = \frac{T_m - T_0}{T_m + T_0} \mathrm{e}^{-2 \arctan (T_0/T_m)}. \tag{13}$$

It may be mentioned immediately that the relaxation time t_0 obtained here is not directly that of τ, but of a certain function of τ.

In deriving expression (11) for the growth of the temperature near the centre of a long filament, the whole current is taken to be switched on directly, i.e. T is made to grow from the room temperature T_0 to a high temperature T_m. But in actual practice one is not generally concerned with such a large change in the heating current, but with a small adjustment of the current so as to vary T in the neighbourhood of the final temperature. In other words, the initial value of the temperature at the centre, which ultimately grows to T_m, is not T_0, but a certain temperature T_1 close to T_m. In this case the growth of temperature is given by the simpler expression

$$\partial T/\partial t = 4\beta T_m^3 (T_m - T) \tag{14}$$

with the boundary conditions

$$T = T_1 \quad \text{when} \quad t = 0$$
$$T \to T_m \quad \text{when} \quad t \to \infty.$$

The solution is

$$T_m - T = \tau = (T_m - T_1)\,\mathrm{e}^{-\nu_0 t}, \tag{15}$$

where the relaxation time $t_0 = 1/\nu_0$ has the same value as in (12). For convenience we shall refer to the reciprocal of the relaxation time as the attenuation coefficient.* The relaxation time is obviously a measure of the time lag. We shall note in passing that for a given material for the filament, and a given central temperature T_m, t_0 is *inversely proportional to p/ω, as observed by Prescott & Morrison. It is also inversely proportional to the cube of the temperature at the centre.*

4. The magnitude of the time lag in a long filament

Wensel gives some numerical data regarding the performance of an optical pyrometer, in which the filament can be regarded as a long one. Using a tungsten three-mil filament (of diameter 0·0075 cm) he makes the heating current drop from the value corresponding to $T_m = 1200°$ K to the value corresponding to $T_m = 1000°$ K. He finds that the time taken for the temperature to approach to within 1° of the final temperature is 10 to 20 s.

* The same expressions (11) and (15) will obviously hold when the heating current is switched off or reduced.

Using the following data for tungsten at about 1100° K, taken from Worthing & Halliday (1948), namely, $c = 0{\cdot}14\,\mathrm{J\,g^{-1}\,deg.^{-1}}$, $\delta = 19\,\mathrm{g\,cm^{-3}}$ and $\epsilon = 0{\cdot}12$, we obtain the value $t_0 = 1{\cdot}8$s, from which the above-mentioned time comes out as 10s. This compares well with the estimate of 10 to 20s made by Wensel. Since the accuracy of measurement of temperature with an optical pyrometer is of the order of a degree, Wensel's estimate, which refers to the time needed for approach to the final temperature to within a degree, must be regarded as very rough.

5. Criterion for regarding the filament as long

The relaxation time calculated in the previous section for the growth of temperature at the centre of a long filament naturally raises the question how long the filament should be in order that the temperature T_l at the centre might approximate to T_m to any given degree of approximation. In parts I and II we have discussed in detail the distribution of temperature along a filament electrically heated *in vacuo*. For a long filament in which $T_m - T_l$ is small in comparison with T_m, the temperature at the centre is given by

$$T_l = T_m - 2\Delta_0\, e^{f(\Delta_0)}\, e^{-l\sqrt{A}}, \tag{16}$$

where l is the semi-length of the filament,

$$A = 4p\epsilon\sigma T_m^3/(\kappa\omega), \tag{17}$$

$$\Delta_0 = T_m - \Theta, \tag{18}$$

and Θ is the temperature of the ends. Till now we had taken the temperature of the ends of the filament to be that of the room. For generality we shall henceforth take the temperature of the ends, which is kept constant, to be Θ, as distinguished from the temperature T_0 of the room which occurs in the expression for the radiation. $f(\Delta_0)$ in equation (16) is defined by

$$f(\Delta_0) = \tfrac{1}{2}\Delta_0/T_m + \tfrac{1}{16}\Delta_0^2/T_m^2 - \tfrac{1}{240}\Delta_0^3/T_m^3 + \ldots. \tag{19}$$

It is significant that it is not directly the length $2l$, but $2l\sqrt{A}$, which may be called the reduced length, whose magnitude determines how close T_l is to T_m. For a given length the approximation will be the closer the larger the value of A, i.e. the larger the value of p/ω or of T_m^3. Here again the ribbon filament has the advantage over a filament of circular cross-section.

Indeed, the two effects, namely, the reduction of the relaxation time, and the reduction of the actual length of filament needed for securing a given approximation to the infinitely long filament, both accompanying an increase in p/ω or in T_m^3, are closely related. It can be seen from the expressions for t_0 and A that

$$t_0 = c\delta/(A\kappa), \tag{20}$$

and hence any factor like p/ω or T_m^3 that tends to increase A will automatically reduce the relaxation time.

6. The criterion for a definite relaxation time for τ

Coming back to the differential equation (9) defining the growth of temperature, when once we decide to confine attention to small values of τ only, it reduces to the simple form

$$-\partial\tau/\partial t = 4\beta T_2^3\tau - \alpha\partial^2\tau/\partial x^2. \tag{21}$$

Now if τ is to have a definite relaxation time, $-\partial\tau/\partial t$ should be proportional to τ. In other words, the two terms on the right-hand side of (21) should be separately proportional to τ. The first term can be directly seen to be so. We now proceed to investigate whether the proportionality of the second term also, namely, $\partial^2\tau/\partial x^2$, to τ can be secured at least in the central region, which is of practical interest.

7. The relaxation time near the centre of any filament

We have shown in parts I and II that the steady temperature distribution near the centre of any filament, long or short, is given by*

$$T_2 = T_{l2} - \tfrac{1}{2}Q_2 q^2, \tag{22}$$

where $q = l - x$ denotes the distance measured from the centre,

$$Q = (\beta/\alpha)(T_m^4 - T_l^4) = (p\epsilon\sigma/\kappa\omega)(T_m^4 - T_l^4), \tag{23}$$

and Q_2 and T_{l2} are the values of Q and T_l respectively appropriate to the final steady state. From (22) and a similar expression for the distribution of the initial temperature T_1, one obtains

$$T_2 - T_1 = (T_{l2} - T_{l1}) - \tfrac{1}{2}(Q_2 - Q_1)\,q^2, \tag{24}$$

which may be written in the convenient form

$$T_2 - T_1 = \Delta T_l\left(1 - \frac{1}{2}\frac{\Delta Q}{\Delta T_l}q^2\right). \tag{25}$$

It can be seen directly from the form of (25) that $\dfrac{\partial^2}{\partial q^2}(T_2 - T_1)$ cannot be rigorously proportional to $T_2 - T_1$, e.g., $\partial^2\tau/\partial q^2$ cannot be *rigorously* proportional to τ, even for small values of q. But at the same time one can also see that for small values of q, $1 - \frac{1}{2}(\Delta Q/\Delta T_l)\,q^2$ can be put equal to $\cos(\Delta Q/\Delta T_l)^{\frac{1}{2}}q$, and hence *to this approximation* $\partial^2\tau/\partial q^2$ may be taken to be proportional to τ. Therefore one may write

$$\tau = (T_2 - T_1)\,e^{-\nu t} = \Delta T_l[1 - \tfrac{1}{2}(\Delta Q/\Delta T_l)\,q^2]\,e^{-\nu t}, \tag{26}$$

in which, however, ν will not now be quite independent of t, and for any given q may be expressed in the form

$$\nu = \nu_1 + (\partial\nu/\partial t)\,t. \tag{27}$$

Hence from (21), (26) and (27) one obtains

$$(1/\tau)\,\partial^2\tau/\partial q^2 = -(\Delta Q/\Delta T_l)\,[1 + 2q(\partial\nu/\partial q)\,t]/[1 - \tfrac{1}{2}(\Delta Q/\Delta T_l)\,q^2] + (\partial\nu/\partial q)^2 t^2 + (\partial^2\nu/\partial q^2)\,t, \tag{28}$$

from which it will be seen that ν_1 which will be the value of ν for small values of t, is given by

$$\begin{aligned}\nu_1 &= 4\beta T_2^3 - \alpha(1/\tau)\,\partial^2\tau/\partial q^2 \\ &= 4\beta T_2^3 + \alpha(\Delta Q/\Delta T_l)/[1 - \tfrac{1}{2}(\Delta Q/\Delta T_l)q^2] \\ &= \nu_a + \nu_{b1}, \quad \text{say.}\end{aligned} \tag{29}$$

* (22) could also have been obtained directly as a solution of (8) in the special case when T is close to T_1.

The expression will obviously hold over the whole range of q over which the parabolic law (22) or (24) holds. As t increases (29) continues to hold, as we shall show in a later section, but its validity is restricted to a progressively decreasing range of q, and though it is not now a precise result, it is a close approximation. At the centre of the filament, in particular, which is of practical interest, (29) holds as a close approximation for all values of t, the approximation being the closer the smaller the value of t.

When the filament is a long one, such that T_l is practically the same as T_m, both Q_2 and Q_1 vanish, and hence ν_b also vanishes. This confirms our earlier finding based on certain very plausible direct considerations that $\partial^2 T/\partial x^2$ should be equal to zero at the centre of a long filament, not only for the steady temperature distribution but also for a growing one.

8. The case when the temperature distribution is parabolic throughout

We referred in the previous section to the temperature distribution near the centre being always parabolic, irrespective of the length of the filament or the heating current. Under suitable conditions the whole length of the filament can be included in this region. In other words (22) and (24) will then be applicable over the whole of the range $0 \leqslant q \leqslant l$. Before considering the time lag in such a filament it will be useful to know the criterion for the distribution to be parabolic over the whole length of the filament.

In part II it was shown that the temperature distribution over a wider region than the parabolic region is given by

$$T_{l2} - T_2 = (Q_2/P_2)\,[\cosh q\,\sqrt{P_2} - 1], \tag{30}$$

where

$$P = 4p\epsilon T_l^3/(\kappa\omega). \tag{31}$$

It can be seen immediately that when $q\,\sqrt{P_2}$ is sufficiently small that the higher powers of $q\,\sqrt{P_2}$ than the second are negligible in comparison with unity, (30) reduces to the parabolic expression (22) obtained previously. The range of validity of the parabolic law is therefore determined by this criterion.

Just as in a long filament it is not the absolute length $2l$, but $2l\,\sqrt{A}$ that determines how close T_l is to T_m, so also in the shorter filaments it is not directly l but $l\,\sqrt{P}$ that determines the parabolic range. P differs from A in having the factor T_l^3 in place of the T_m^3 that appears in the expression for A. If the central temperature T_l is small, the actual length l can be quite large, and yet the whole of it can be well within the parabolic range. This is the case, for example, when the temperature over the whole filament is close to the room temperature, as in Straneo's problem.

The hyperbolic expression (30) is invoked here, not merely for determining the extent of the parabolic region, which can be done otherwise, but also because we need this expression in a later section.

Considering now such a filament, in which the parabolic relation (22) holds over the whole length of the filament $0 \leqslant q \leqslant l$, T_2 should now become equal to the end-temperature Θ when in (22) q is put equal to l. We thus obtain

$$Q_2/(T_{l2} - \Theta) = 2/l^2. \tag{32}$$

Obviously this should also be the value of $Q_1/(T_{l1} - \Theta)$ corresponding to the initial steady state, from which it follows that

$$(Q_2 - Q_1)/(T_{l2} - T_{l1}) = \Delta Q/\Delta T_l = 2/l^2. \tag{33}$$

Hence for the parabolic filament, the expression for ν_{b1} (see (29)) reduces to the simple form

$$\nu_{b1} = 2\alpha/(l^2 - q^2), \tag{34}$$

and the expression for τ reduces to

$$\tau = \tfrac{1}{2}\Delta Q l^2 (1 - q^2/l^2) \exp - [4\beta T_{\frac{1}{2}}^3 + 2\alpha/(l^2 - q^2)]\,t, \tag{35}$$

as compared with the corresponding general expression for any filament

$$\tau = \Delta T_l [1 - \tfrac{1}{2}(\Delta Q/\Delta T_l)\,q^2] \exp - \left[4\beta T_{\frac{1}{2}}^3 + \alpha \left(\frac{\Delta Q}{\Delta T_l}\right) \Big/ \left(1 - \frac{1}{2}\frac{\Delta Q}{\Delta T_l} q^2\right)\right] t. \tag{36}$$

Before taking up the general case we shall consider expression (35) obtained here for the wholly parabolic distribution, in relation to the corresponding expression obtained by Straneo's method.

9. Time lag in parabolic distribution by Straneo's method

As was mentioned in the Introduction the growth of temperature in a filament in which the temperature at any point is only slightly higher than the room temperature such that the loss by radiation may be taken to conform to Newton's law has been discussed by Straneo. A good account of Straneo's method is given in Carslaw & Jaeger (1947). The expression given by Carslaw & Jaeger for the temperature distribution, after making it conform to the present notation and to a finite end-temperature Θ, is

$$T_2 - \Theta = \frac{Q_2}{P_2} \cosh l\,\sqrt{P_2} \left[1 - \frac{\sinh (l+q)\,\sqrt{P_2} + \sinh (l-q)\,\sqrt{P_2}}{\sinh 2l\,\sqrt{P_2}}\right], \tag{37}$$

which will be seen to reduce to

$$T_2 - \Theta = \frac{Q_2}{P_2} \cosh l\,\sqrt{P_2} \left[1 - \frac{\cosh q\,\sqrt{P_2}}{\cosh l\,\sqrt{P_2}}\right], \tag{38}$$

which in its turn can be seen to follow from (30), since T_l is now sufficiently small to make the whole of the filament conform to (30).

The expressions for the initial and the final temperatures as functions of the distance may be expanded into the appropriate sine series, and they yield*

$$\tau = \frac{16l^2}{\pi} \sum_{n=1}^{\infty} \frac{(-1)^{n-1}}{2n-1} (A_{n2} - A_{n1}) \cos \frac{(2n-1)\,\pi q}{2l} \exp - \left[4\beta T_{\frac{1}{2}}^3 + \frac{\alpha (2n-1)^2 \pi^2}{4l^2}\right] t, \tag{39}$$

where

$$A_n = \frac{Q}{(2n-1)^2 \pi^2 + l^2 P}. \tag{40}$$

* In Straneo's filament the loss by radiation, which conforms to Newton's law, is proportional to $T_2 - T_\theta$, and the constant of proportionality is $4\beta T_{\frac{1}{2}}^3$. Though it is not quite independent of q, it is practically so, since the maximum variation of temperature over his filament is small.

By making l^2P much smaller than π^2, equation (37), on the basis of which (39) has been expanded, reduces to the parabolic law over the whole length of the filament.* Hence by making the corresponding approximation in (32), by which A_n becomes equal to $Q/[(2n-1)^2\pi^2]$, equation (39) may be made to represent the growth of temperature in a filament whose length is wholly in the parabolic region.

Incidentally it may also be mentioned that in the experimental arrangement intended to be covered by (37), where the temperature everywhere is close to the room temperature, T_l is actually small enough to make the whole of the filament conform to the parabolic law. The parabolic distribution obtains also in the special case when the radiation from the surface is completely eliminated. This is secured for example in the well-known method of Kohlrausch for the determination of thermal conductivities. The problem has been investigated theoretically by Wintergerst using the method of Laplace transforms. He obtains the same infinite series as (39) without l^2P, and naturally without ν_a too.

Comparing now equation (35) obtained by the present method with the corresponding expression (39) one obtains the following results. For small values of t, for which $\exp\{-\alpha(2n-1)^2\pi^2t/4l^2\}$ can be put equal to $1-\alpha\{(2n-1)^2\pi^2/4l^2\}t$, it can be shown that (39) is identical with (35) for all values of q. Making this substitution we obtain

$$\tau = \frac{16l^2}{\pi^3}\Delta Q \exp(-4\beta T_2^3 t)\sum_{n=1}^{\infty}\frac{(-1)^{n-1}}{(2n-1)^3}\cos\frac{(2n-1)\pi q}{2l} - \frac{4}{\pi}\Delta Q\alpha t\exp(-4\beta T_2^3 t)\sum_{n=1}^{\infty}\frac{(-1)^{n-1}}{2n-1}\cos\frac{(2n-1)\pi q}{2l}. \quad (41)$$

Using the well-known relations (see Sommerfeld 1949)

$$\sum_{n=1}^{\infty}\frac{(-1)^{n-1}}{(2n-1)^3}\cos\frac{(2n-1)\pi q}{2l} = \sin\frac{\pi x}{2l}+\frac{1}{3^3}\sin\frac{3\pi x}{2l}+\frac{1}{5^3}\sin\frac{5\pi x}{2l}+\ldots = \frac{\pi}{8}\left[\frac{\pi^2 x}{2l}-\left(\frac{\pi x}{2l}\right)^2\right] = \frac{\pi^3}{32}(1-q^2/l^2) \quad (42)$$

and† $$\sum_{n=1}^{\infty}\frac{(-1)^{n-1}}{2n-1}\cos\frac{(2n-1)\pi q}{2l} = \sin\frac{\pi x}{2l}+\tfrac{1}{3}\sin\frac{3\pi x}{2l}+\tfrac{1}{5}\sin\frac{5\pi x}{2l}+\ldots = \frac{\pi}{4}, \quad (43)$$

(41) can be seen to reduce to

$$\tau = \tfrac{1}{2}\Delta Q l^2(1-q^2/l^2)\exp(-4\beta T_2^3 t)\left(1-\frac{2\alpha t}{l^2-q^2}\right) = \tfrac{1}{2}\Delta Q l^2(1-q^2/l^2)\exp-\left[4\beta T_2^3+\frac{2\alpha}{l^2-q^2}\right]t, \quad (44)$$

which is identical with (35).

This is indeed very gratifying especially since we are now dealing with a single term having a single relaxation time, instead of an infinite series each term of which has its own characteristic relaxation time. Equation (44) also enables us to follow in detail the variation of the relaxation time with q for small values of t.

* This can be seen to be consistent with the criterion obtained earlier for the whole of the filament to be in the parabolic range, namely that higher powers of $l\sqrt{P}$ than the second are negligible in comparison with unity.

† Equation (43) may be shown to follow from (42) by differentiating both sides of (42) twice with respect to q.

As t increases it can be seen from (39) that the terms involving high values of n get progressively weakened out, because of the exponential factor involving n and t, and the expression for τ ultimately settles down to

$$\tau = \frac{16l^2}{\pi^3}\Delta Q l^2\cos\frac{\pi q}{2l}e^{-\nu_2 t}, \quad (45)$$

where $$\nu_2 = 4\beta T_2^3+\alpha\pi^2/(4l^2). \quad (46)$$

From the following considerations it will be seen that in the *central regions where q is small*, (45) is not very different from (44). (1) The limiting value ν_2 to which ν tends as $t\to\infty$ is not very different from the value

$$\nu_1 = 4\beta T_2^3+2\alpha/l^2, \quad (47)$$

which holds for small values of t. The difference between them is in the second term only, and corresponds to dropping a factor $\frac{1}{8}\pi^2$ from it, which differs only slightly from unity. (2) As $t\to\infty$ the coefficient of the exponential term in the Fourier expansion tends to $(16/\pi^3)\Delta Q l^2\cos\pi q/(2l)$. The corresponding coefficient from the present calculation, which remains independent of t, is $\frac{1}{2}\Delta Q l^2(1-q^2/l^2)$. Remembering that $32/\pi^3\approx 1$, the two coefficients again can be seen to agree to the same approximation to which ν_{b1} and ν_{b2} agree, provided that q is small enough to make

$$1-q^2/l^2\approx\cos(q\sqrt{2}/l).$$

Confining attention to regions close to the centre, it is thus seen that expression (35) for the growth of temperature will hold for all values of t; for small values of it as a precise result, and for larger values as a close approximation, the approximation remaining as close as $\frac{1}{8}\pi^2$ to 1, or $\frac{1}{32}\pi^3$ to 1, even when $t\to\infty$.

We have discussed at some length the special case where the temperature distribution over the whole filament is parabolic, for two reasons. It is the only case where the Fourier method can be conveniently applied, and where the results obtained in the present paper can be compared with those obtained by the Fourier method. But the more important reason is that the actual distribution in any filament near the centre is parabolic, and the comparison made just now between the two methods as applied to the special case, enables us to adapt the Fourier method for the investigation of the time lag near the centre of any filament, though the temperature distribution taken over the rest of the filament would be too complicated for a direct Fourier expansion, besides involving a relaxation time that varies markedly with q.

10. General case of any filament

Returning to the general case for which the growth of temperature is given by (36), it can be readily seen that in the region where the temperature distribution is parabolic, it has precisely the same validity as the corresponding expression (35) for a shorter filament which was discussed in the previous section. Considering first the expression for T_2-T_1, namely, ,

$$T_2-T_1 = \Delta T_l[1-\tfrac{1}{2}(\Delta Q/\Delta T_l)q^2],$$

one may, without invoking any special mechanism, identify it with the infinite series

$$T_2 - T_1 = \frac{32}{\pi^3}\Delta T_l \sum_{n=1}^{\infty} \frac{(-1)^{n-1}}{(2n-1)^3} \cos\frac{(2n-1)\pi q}{2\lambda}, \tag{48}$$

where λ is now a certain *effective length* defined by

$$\lambda = \left(\frac{2}{\Delta Q/\Delta T_l}\right)^{\frac{1}{4}}. \tag{49}$$

Assigning to each of the terms in (48) the appropriate time factor that will satisfy the differential equation,* we obtain

$$\tau = \frac{32}{\pi^3}\Delta T_l \sum_{n=1}^{\infty} \frac{(-1)^{n-1}}{(2n-1)^3} \cos\frac{(2n-1)\pi q}{2\lambda} \exp\left[-\{4\beta T_2^3 + \alpha(2n-1)^2\pi^2/(4\lambda^2)\}t\right]. \tag{50}$$

Equation (50) is a complete and precise description of the growth of the temperature at every point in the parabolic range of any filament, just as (39) is for the special case when the whole filament is within the parabolic range. Indeed, (50) can be seen to reduce to (39) when $\Delta Q/\Delta T_l$ is put equal to $2/l^2$, which is its appropriate value for the latter filament. In the general case considered just now, the usual Fourier representation, in which the actual length of the filament determines the period, would have involved coefficients A_n which would have been difficult to evaluate. On the other hand by using the effective length λ the representation over the whole of the parabolic range takes the elegant form (50). In the choice of the appropriate λ we are guided by the results of the present investigation.

Comparing now (36) with (50) one can see that the relation between them is exactly the same as the relation between (35) and (39). For small values of t, (36) and (50) are identical over the whole range of q over which the temperature distribution in the steady state is parabolic. Further (36) can be seen to be a close approximation to (50) at any value of t, if q is made sufficiently small. The degree of approximation is exactly the same as that of (35) to (39).

This is a very satisfactory result, since it implies that the growth of temperature near the centre of any filament, long or short, can always be represented to a close approximation by a single relaxation time $t_r = 1/\nu$, where

$$\nu = 4\beta T^3 + \alpha\Delta Q/\Delta T_l.$$

The first term on the right-hand side is a constant contribution which is independent of time. The correct value of the second term, however, should vary slightly with time, and since we are trying to represent it also by a constant term the approximation, which is perfect for small values of t, slightly deteriorates with time, the approximation, however, remaining as close as $\frac{1}{2}\pi^2$ is to 1 even when t tends to infinity.

The possibility of representing the growth of temperature near the centre of any filament by a simple exponential law involving a single relaxation time effects naturally a considerable simplification of the problem, and further makes the practical application convenient.

* The value of ν_a, equal to $4\beta T^3$, appearing in (50) is not quite independent of q. It will be, however, practically so, since over the range where $4\beta T_2^3$ is significant it can be shown to be close to $4\beta T_1^3$.

The simplification is due ultimately to the following circumstances:

(1) The distribution of temperature both in the initial and in the final states, near the centre of any filament, is parabolic.

(2) The parabola can be represented by a Fourier series which is very simple when the length involved is suitably chosen.

(3) With the proper choice of the *effective* length the first term in the Fourier expansion is by itself a close approximation to the parabola.

(4) Hence the growth of temperature near the centre can be represented by a simple exponential law involving a single effective relaxation time.

11. Variation of the time lag at the centre of a filament with its length

The general expression for ν at the centre of the filament may also be written in the following convenient form. Using relation (23) for Q, namely, $\alpha Q = \beta(T_m^4 - T_l^4)$, one obtains

$$\alpha\Delta Q/\Delta T_l = 4\beta[T_m^3\Delta T_m/\Delta T_l - T_l^3], \tag{51}$$

whence

$$\nu = \nu_0\Delta T_m/\Delta T_l, \tag{52}$$

where $\nu_0 = 4\beta T_m^3$, as we have seen, is the attenuation coefficient at the centre of an infinitely long filament having the same T_m. Equation (52) is a convenient relation since it combines both ν_a and ν_b into a single term.

It can be further shown that for a filament in which the temperature distribution is wholly parabolic

$$(\beta/\alpha)(T_m^4 - T_l^4) = (2/l^2)(T_l - \Theta),$$

and if Θ is small* in comparison with T_l,

$$\Delta T_m/\Delta T_l = \frac{T_m^4 + 3T_l^4}{4T_m^3 T_l} = \frac{1+3\theta^4}{4\theta}, \tag{53}$$

where $\theta = T_l/T_m$ depends on the length of the filament.

For long filaments, as $T_l \to T_m$, $\Delta T_m/\Delta T_l \to 1$, and this is also the value to which (53) tends. Presumably the variation of $\Delta T_m/\Delta T_l$ in the intermediate range of lengths also is given by the same expression, namely (53).

The filaments used in practice are long ones in which θ is close to unity. In such filaments obviously even a major change in length will not much affect the relaxation time. Thus the major factors that affect it then are p/ω and T_m^3.

12. Dependence of the time lag on p/ω and on T_m^3

The expression for the relaxation time for any filament, namely,

$$t_r = \frac{c\delta\omega}{p\epsilon\sigma T_m^3}\frac{\Delta T_l}{\Delta T_m}, \tag{54}$$

shows that for a given value of T_m, the relaxation time is inversely proportional to p/ω. If, however, the heating current through the filament is kept constant when p/ω is varied, an increase in p/ω will reduce T_m, since $(T_m^4 - T_0^4)\,p/\omega$ has now to

* Equation (52) will obviously hold for any value of Θ.

remain constant. If T_0^4 can be neglected in comparison with T_m^4, then t_0 will be proportional to $(p/\omega)^{-\frac{1}{4}}$, and the effect of an increase in p/ω is then not quite so striking. But in practice it is no inconvenience to maintain the same T_m by suitably increasing the heating current in the ribbon, and thus ensure a great reduction on the time lag. We should also emphasize here the inverse proportionality of t_0 to T_m^3, and the consequent advantage of using high central temperatures in reducing the time lag.

It will be seen from (54) that the expression for the relaxation time involves in addition to p/ω and T_m^3 two other factors, namely, $c\delta$ and $\Delta T_l/\Delta T_m$. An increase in p/ω will in effect be equivalent to a decrease in the heat capacity $c\delta$, and hence the effect of an increase of p/ω on the time lag may be taken to be through minimizing the heat capacity. This effect will be independent of whether the filament is long or short. On the other hand the magnitude of the factor $\Delta T_l/\Delta T_m$ depends on the conduction losses through the ends, and it tends to unity at the centre of a long filament. Hence in a short filament where ΔT_l will be much larger than ΔT_m, the effect of an increase in p/ω is equivalent to making ΔT_l approach ΔT_m, and so would be equivalent to minimizing also the heat loss due to conduction. When the filament is long and we are considering a region near the centre, the question of conduction loss does not arise. But at other points, particularly near the ends it would.

In any case, the advantage of a ribbon filament over one of circular cross-section for use particularly in an optical pyrometer is very definite. Apart from the reduction of the time lag secured by the use of a ribbon filament, the actual length of the filament needed for ensuring a given approximation to the ideally long one is also smaller, as we have shown, in a ribbon filament than in a filament of circular cross-section. The larger area which the ribbon can present is also a help in matching it against the background whose temperature is to be measured, if the background is a broad one.

References

Carslaw, H. S. & Jaeger, J. C. 1947 *Conduction of heat in solids*, p. 135. Oxford: Clarendon Press.

Fischer, J. 1938*a* *Z. tech. Phys.* **19**, 25.

Fischer, J. 1938*b* *Z. tech. Phys.* **19**, 57.

Fischer, J. 1938*c* *Z. tech. Phys.* **19**, 105.

Jaeger, J. C. 1951 *An introduction to applied mathematics*, p. 50. Oxford: Clarendon Press.

Jain, S. C. & Krishnan, Sir K. S. 1954*a* *Proc. Roy. Soc.* A, **222**, 167 (part I).

Jain, S. C. & Krishnan, Sir K. S. 1954*b* *Proc. Roy. Soc.* A, **225**, 1 (part II).

Prescott, C. H., Jr. 1941 *Temperature, its measurement and control in science and industry*, p. 1199. New York: Reinhold Publishing Corporation.

Prescott, C. H., Jr. & Morrison, J. 1939 *Rev. Sci. Instrum.* **10**, 36.

Sommerfeld, A. 1949 *Partial differential equations in physics*, pp. 12, 13. New York: Academic Press, Inc.

Straneo, P. 1898 *R.C. Accad. Lincei*, **7**, 197.

Wintergerst, E. 1950 *Z. angew. Phys.* **2**, 167.

Worthing, A. G. & Halliday, D. 1948 *Heat*, pp. 492, 496. New York: John Wiley and Sons.

The distribution of temperature along a thin rod electrically heated *in vacuo*

VI. End-losses

By S. C. Jain and Sir K. S. Krishnan, F.R.S.

National Physical Laboratory of India, New Delhi

(*Received* 16 *September* 1954—*Revised* 21 *February* 1955)

On the basis of the known distribution of temperature along a filament electrically heated *in vacuo*, the distributions of some of the other physical characteristics that are known functions of the temperature were investigated in part IV. By means of the expression thus obtained for the distribution of any given characteristic, the over-all performance of the filament for this particular purpose can be obtained by integration, and can be expressed in terms of a certain equivalent length of an ideal filament in which the loss by conduction at the ends is completely eliminated. The difference between the actual and the equivalent lengths, which is generally referred to as the correction for the end-losses, is calculated in the present part for some typical physical properties that are of practical interest. Among them are

(1) properties like the heat capacity, the heat generated, and the total output of radiation, which are proportional to known powers of the temperature T;

(2) properties like brightness and the rate of evaporation, which are proportional to known powers of exp $(1/T)$;

(3) properties like thermionic emission, which are proportional to known powers of T and of exp $(1/T)$.

The corrections for the end-losses thus calculated for a long filament of tungsten for the different properties are found to agree closely with those computed graphically by Worthing from the observed distributions of these properties along the filament.

It is further shown that the correction for a filament of *medium* length, such as is used in high-frequency power-tubes, is practically the same as for a similar *long* filament heated by the same current.

1. Introduction

In parts I and II of this paper (Jain & Krishnan 1954*a*, *b*) the distribution of temperature along a thin filament electrically heated *in vacuo* was investigated in detail, and simple expressions were obtained for the temperature as a function of the distance. Parts III and IV (Jain & Krishnan 1954*c*, *d*) were concerned with the experimental verification of the various results obtained in I and II. On the basis of the known distribution of temperature along the filament, the distributions of other physical characteristics which depend on the temperature, and which can be expressed as explicit functions of the temperature, were also investigated in IV.

The most convenient way of appraising the over-all performance of a heated filament used for any specific purpose is to compare the performance with that of an ideal filament in which the loss of heat by conduction through the ends is eliminated, and in which, therefore, the temperature remains constant at T_m throughout its length. Obviously T_m would be the temperature at the centre of a filament similar to the filament actually used, but very long, and heated by the same current.

Let F_t be the particular physical property under consideration, which is a known function of the temperature T. Now denoting by ψ_t the ratio $F_t/F_{t,m}$, where $F_{t,m}$ is the value of F_t at $T = T_m$, the effective length is given by

$$L_e = \int_0^L \psi_t \, dX, \tag{1}$$

where $X = x\sqrt{A}$ is the reduced distance as defined in part IV, and $L = l\sqrt{A}$ is the reduced semi-length of the filament. Now $L - L_e$, which we shall denote by η, is generally called the correction for the end-loss at each end. It is a useful physical quantity which enables us to appraise the efficiency of performance of the filament for the particular purpose for which it is to be used. The present part is concerned with the calculation of the corrections for the end-losses for some of the typical temperature-dependent properties that are of practical interest.

2. General expression for the correction in a long filament

We shall first consider the case of a long filament in which the temperature T_l at the centre is sensibly the same as T_m. As was shown in II and IV, the temperature distribution along such a filament is given by

$$v \exp f(v) = v_0 \exp\{f(v_0) - X\}, \tag{2}$$

where
$$v = (T_m - T)/T_m \tag{3}$$

and
$$f(v) = A_1 v + A_2 v^2 + A_3 v^3 + \ldots, \tag{4}$$

and v_0 denotes the value of v at the ends. The coefficients A_n in (4) have the same significance as in I, and are readily evaluated. Thus one obtains

$$dX/dv = -v^{-1}(1 + A_1 v + 2A_2 v^2 + 3A_3 v^3 + \ldots). \tag{5}$$

Under the usual conditions of working, v is considerably smaller than unity, even at the ends of the filament, and since the coefficients A_n also decrease with increasing n, the terms in (5) involving $A_3, A_4, \ldots$ are found to be negligible.

In view of (1) and (5), one obtains the following expression for the correction for the end-loss,

$$\eta = \int_0^{v_0} (1 - \psi_t) v^{-1}(1 + A_1 v + 2A_2 v^2) \, dv. \tag{6}$$

Several physical properties have been studied in detail for their temperature-dependence, and many of them, as Langmuir (1930) has shown, may be expressed, at any rate empirically, by the relation

$$F_t = A_t T^{\gamma_t} \exp(-\Theta_t/T), \tag{7}$$

where A_t, γ_t and Θ_t are constants characteristic of the particular property F_t under consideration. Some of these properties were tabulated in IV. For such properties the value of $1 - \psi_t$ appearing in expression (6) can be expressed as a power series in v, namely,

$$1 - \psi_t = a_1 v + a_2 v^2 + a_3 v^3 + \ldots, \tag{8}$$

and the integration in (6) can be done term by term. One thus obtains

$$\eta = a_1 v_0 + \tfrac{1}{2}(a_2 + a_1 A_1) v_0^2 + \tfrac{1}{3}(a_3 + a_2 A_1 + 2a_1 A_2) v_0^3 + \tfrac{1}{4}(a_4 + a_3 A_1 + 2a_2 A_2) v_0^4 + \ldots. \tag{9}$$

Hence one needs to know only the magnitudes of $a_1, a_2, a_3, \ldots$ for the different properties, in order to be able to calculate the corresponding corrections for the end-losses.

3. Properties for which $\Theta_t = 0$

We shall first consider the end-losses for the special case of those properties for which $\Theta_t = 0$, as, for example, the electrical resistance, or the energy generated (which is proportional to the resistance), or the total output of radiation, all of which have been studied in detail for tungsten. These quantities are also of practical importance. For example, since the energy input is proportional to the electrical resistance, the end-loss correction for the resistance will enable us to determine the voltage to be maintained between the terminals of a filament in order that the temperature T_m at the centre may have any specified value. Similarly, the end-loss correction for total radiation will enable us to estimate the efficiency of performance of a sealed-in filament lamp to be used for radiation heating.

Equation (1) now reduces to the simple form

$$F_t = A_t T^{\gamma_t}, \tag{10}$$

so that
$$\psi_t = (1 - v)^{\gamma_t}. \tag{11}$$

(From now on we shall drop the subscripts t for convenience.) For these properties the expression for $1 - \psi$ will obviously conform to (8), and that for η to (9), in which

$$a_1 = \gamma, \quad a_2 = -\tfrac{1}{2}\gamma(\gamma - 1), \quad a_3 = \tfrac{1}{3}\gamma(\gamma - 1)(\gamma - 2). \tag{12}$$

Worthing (1922) has studied experimentally the distribution of several physical properties along a long filament of tungsten electrically heated *in vacuo*. By plotting the experimental values of F/F_m against X, and by finding graphically the area subtended between the curve and the X-axis, he has computed the effective lengths L_e for these properties, and thence the end-loss corrections. In all his measurements the temperature T_m at the middle point of the filament was 2400° K, and the temperature of the point from which the distances X were measured was $0{\cdot}25T_m$, so that $v_0 = 0{\cdot}75$. The values of η obtained graphically by Worthing for all the properties of tungsten studied by him for which $\Theta = 0$ are entered in table 1.

The values of η calculated from (9) and (12) are also entered in the table for comparison. Now the values of A_1 and A_2 appearing in (9) are readily calculated, as was shown in I, from the known values of T_m and of the temperature coefficients of the physical quantities involved. Among the latter the coefficient of the thermal conductivity κ exercises the predominant influence. The temperature coefficient of κ, which we shall denote by α, has been determined by Worthing himself for the specimen of tungsten used by him, and he obtains a small *positive* value. Later measurements by Osborne (1941), on the other hand, yield a small *negative* value for α, which appears more probable from general theoretical considerations. Osborne

attributes the positive α obtained by Worthing to the inadequate ageing of the specimen used by him.

Whatever may be the reason for the discrepancy, since we are calculating the end-losses for Worthing's specimen (for comparison with the values computed by him graphically for the same specimen) we use here his α in preference to Osborne's, remarking, however, that the choice of the one or the other value of α makes very little difference to η. The agreement between the values obtained by Worthing graphically and those calculated is satisfactory.

TABLE 1. VALUES OF η FOR A LONG FILAMENT OF TUNGSTEN

property		heat content	energy input	total radiation
	$\Theta = 0;\ \gamma =$	1	1·2	5·1
η	calculated	0·9	1·1	2·4
η	obtained graphically by Worthing	0·9	1·0	2·3

4. PROPERTIES FOR WHICH $\gamma = 0$

We shall consider next the other special case in which $\gamma = 0$ but Θ remains finite. The brightness and the rate of evaporation, for example, belong to this category. In this case

$$\psi = \exp\{-\Theta(1/T - 1/T_m)\} = \exp\{-\theta v/(1-v)\}, \tag{13}$$

where

$$\theta = \Theta/T_m. \tag{14}$$

Expression (13) can then be seen to conform to (8), and the corresponding expression for η to (9), where

$$a_1 = \theta, \quad a_2 = \theta - \tfrac{1}{2}\theta^2, \quad a_3 = \theta - \tfrac{1}{2}\theta^2 + \tfrac{1}{6}\theta^3. \tag{15}$$

Since we shall have occasion to use separately the values of a_n given by (12) and by (15), we shall denote them by b_n and c_n respectively.

5. THE CONVERGENCE OF THE SERIES FOR η

There is an essential difference between the two special cases $\Theta = 0$ and $\gamma = 0$ considered in the last two sections, which has an important bearing on the convergence of the power series representing η. In Worthing's measurements $v_0 = 0{\cdot}75$. Hence in the power series of v_0 the decrease of v_0^n with the increase of n is not by itself rapid enough for convenient numerical computation. In the case when $\Theta = 0$, however, this is not a serious inconvenience, since the coefficients of v_0^n, namely, b_n, decrease rapidly with the increase of n. Even for the highest value of γ that we have to deal with, namely, 5·1, which occurs in the expression for the total radiation, it is found that the fourth term in the expression for η has dropped much below 2 % of the first term, and the fifth term is practically negligible.

On the other hand, when $\gamma = 0$ and Θ is finite, the corresponding coefficients c_n that occur in the expression for η actually increase in the early stages of the increase of n before decreasing. This is due to θ being greater than unity. Indeed, it is much

greater, being about 10·5 for brightness, and about 39 for the rate of evaporation. Hence the coefficients c_n continue to grow till we reach very high values of n.

For the same reason, namely, that $\theta \gg 1$, for which the coefficients c_n of the terms in the expansion of η as a power series in v_0 remain large till we reach high values of n, the value of F, which is proportional to $\exp(-\Theta/T)$ will drop down rapidly with the decrease of T, i.e. with the increase of v. Hence the contribution to L_ϵ may become negligible long before v has approached v_0. In other words, the significant portion of the contribution to L_ϵ may be confined to the region $0 \leqslant v \leqslant v_s$, where $v_s \ll v_0$. Or from the point of view of η the contribution to it from the range $0 \leqslant X \leqslant X_s$, where X_s is the distance of the point v_s, will be just the length X_s of the range, and the contribution from the rest of the filament can be expressed as a power series in v_s, which will be rapidly convergent.

Aiming at an accuracy of say 1 % in the evaluation of η, one obtains

$$\exp\{-\theta v_s/(1-v_s)\} \approx 0{\cdot}01, \tag{16}$$

which for optical brightness, for which $\theta = 10{\cdot}5$, yields $v_s = 0{\cdot}3$. With these values it is found that the number of terms to be retained in the evaluation of η gets reduced to seven, as against a number of the order of 100 to be retained if the expansion had been in powers of v_0. When θ is larger, as is the case with the rate of evaporation, the saving in the number of terms is correspondingly larger.

The values of η for brightness and for the rate of evaporation calculated in this manner are entered in table 2. The value obtained by Worthing by graphical computation for the former case can be seen to be close to the calculated value. No experimental data are available for evaporation.

TABLE 2. END-LOSS CORRECTIONS FOR TUNGSTEN

property		brightness	rate of evaporation
	$\gamma = 0;\ \Theta =$	25 200	94 100
η	calculated	3·2	4·6
η	obtained graphically by Worthing	3·0	—

6. PROPERTIES FOR WHICH Θ AND γ ARE BOTH FINITE

We shall next consider the more general case where both Θ and γ are finite. Thermionic emission is a typical example of such a property. In this case

$$\begin{aligned}\psi &= (1-v)^\gamma \exp\{-\theta v/(1-v)\} \\ &= (1 - b_1 v - b_2 v^2 - b_3 v^3 - \ldots)(1 - c_1 v - c_2 v^2 - c_3 v^3 - \ldots),\end{aligned} \tag{17}$$

which can be seen to reduce to the same form as (8), where now

$$a_1 = b_1 + c_1, \quad a_2 = b_2 + c_2 - b_1 c_1, \quad a_3 = b_3 + c_3 - b_1 c_2 - b_2 c_1. \tag{18}$$

Here again the filament can be divided conveniently into two regions $0 \leqslant v \leqslant v_s$ and $v_s \leqslant v \leqslant v_0$ respectively, the contribution to η from the latter region being practically the same as the length X_s of the region, and the contribution from the former region being expressible as a rapidly convergent power series in v_s. Taking

$\Theta = 52\,600$ and $\gamma = 2$, the correction for thermionic emission from an electrically heated long tungsten filament calculated in this manner, comes out as 4·0, as compared with the value 3·9 computed by Worthing graphically.

7. Same expressions applicable to filaments of medium length

Even when the filament is not long, but long enough to include the logarithmic region, it was shown in IV that the temperature distribution over the whole length of the filament will conform to an additive formula of the type proposed by Stead. Now the temperature-dependent characteristics that we are considering vary more rapidly than in proportion to the temperature, and hence they too should conform to a similar additive formula, namely

$$1-\psi_L(X) = [1-\psi_\infty(X)]+[1-\psi_\infty(2L-X)], \tag{19}$$

where $\psi_L(X)$ denotes the value of ψ at distance X in a filament of reduced semi-length L.

Multiplying both sides of (19) by $\mathrm{d}X$ and integrating between the limits $X = 0$ and $X = L$, one obtains for the end-loss correction in the finite filament

$$\eta_L = \int_0^L [1-\psi_L(X)]\,\mathrm{d}X = \int_0^L [1-\psi_\infty(X)]\,\mathrm{d}X + \int_0^L [1-\psi_\infty(2L-X)]\,\mathrm{d}X. \tag{20}$$

The second integral on the right-hand side of (20) can be shown to reduce to $\int_L^{2L} [1-\psi_\infty(X)]\,\mathrm{d}X$, and the whole of the right-hand side to $\int_0^{2L} [1-\psi_\infty(X)]\,\mathrm{d}X$.

Consistently with the basic assumption that the additive law holds, the value of $\psi_\infty(X)$ will remain at unity for all values of X beyond $2L$. Hence the upper limit of the integral may be extended from $2L$ to ∞, and η_L will have practically the same value as η_∞.

The filaments used for example in high-frequency power-tubes belong to this category.

8. Short filaments

In the case of filaments which are too short to include the logarithmic region, the distribution of temperature is given by

$$t = T_l - T = \frac{Q}{P}[\cosh(q\sqrt{P})-1], \tag{21}$$

in which the constants Q and P are known (see II), and $q = l-x$ is the actual distance measured from the centre. The correction due to the end-loss can be calculated in the same manner as for the longer filaments, but it will now be a large fraction of the total length. Since, however, such short filaments are not of practical interest, we do not give here the detailed calculations.

We wish to thank Mr S. Vedantham for help in some of the numerical calculations.

References

Jain, S. C. & Krishnan, Sir K. S. 1954*a* *Proc. Roy. Soc.* A, **222**, 167 (part I).
Jain, S. C. & Krishnan, Sir K. S. 1954*b* *Proc. Roy. Soc.* A, **225**, 1 (part II).
Jain, S. C. & Krishnan, Sir K. S. 1954*c* *Proc. Roy. Soc.* A, **225**, 7 (part III).
Jain, S. C. & Krishnan, Sir K. S. 1954*d* *Proc. Roy. Soc.* A, **225**, 19 (part IV).
Jain, S. C. & Krishnan, Sir K. S. 1955 *Proc. Roy. Soc.* A, **227**, 141 (part V).
Langmuir, I. 1930 *Phys. Rev.* **35**, 478.
Osborne, R. H. 1941 *J. Opt. Soc. Amer.* **31**, 428.
Worthing, A. G. 1922 *J. Franklin Inst.* **194**, 597.

THE POLARIZATION FIELD IN AN IONIC CRYSTAL AND ITS INFLUENCE ON THE RESTSTRAHLEN FREQUENCY

By

Sir K. S. KRISHNAN, F.R.S., & S. K. ROY

National Physical Laboratory of India, New Delhi

ABSTRACT

By displacing the lattice of positive ions in an ionic crystal like the alkali halide with reference to the lattice of negative ions, one naturally produces a polarization in the medium. When the displacement is small the polarization may be regarded as due to point-dipoles located at the lattice points of the crystal Associated with the polarization there will naturally be a polarization field acting on the ions tending to increase this displacement. Knowing the potential energy corresponding to a small displacement, one obviously obtains the reststrahlen frequency of the crystal. In calculating this potential energy, however, one has to include in addition to the work done against the forces due to the Coulomb and the repulsion interactions between the ions, also the work done by the polarization field in effecting this displacement. If the latter work were not included, the frequency that one would get would be that of the individual dipoles isolated from one another, whereas the reststrahlen frequency is that of the assemblage of such dipoles. Owing to their mutual interactions in the assemblage the latter frequency may be markedly different from that of the isolated dipoles. It is precisely these interactions that are taken into account when the effect of the polarization field is included in the calculation of the potential energy.

The characteristic frequencies that appear in the well-known Drude formula for dispersion are the resonance frequencies of the medium, in which the effect of the polarization field has been included automatically, and hence the formula will be of general validity irrespective of the magnitude of the polarization field acting on the oscillators. On the other hand in the Lorentz formula, in which the polarization field is taken into account explicity, the characteristic frequencies that occur are those which the oscillators constituting the medium would have if they had been isolated from one another, *i.e.*, if there had been no polarization field to influence them.

The paper includes also a discussion on the nature of the polarization field in ionic crystals.

1. INTRODUCTION

Some years ago we calculated the frequency and the anharmonicity of the polar oscillations of the alkali halide crystals (Krishnan and Roy 1950 ab, 1951) on the basis of the following simple model. The positive and the negative ions in the crystal lattice are regarded as held in their respective positions of equilibrium by the electrostatic and the repulsion interactions between the ions. Whereas the electrostatic interactions are long range ones, the repulsion interactions are practically confined to the adjacent ions only. Now displacing the lattice of positive ions in the crystal with respect to that of the negative ions by a small distance r, the potential energy due to such a relative displacement may be readily calculated on the basis of this model, and expressed as a power series in r, in which, owing to the centre of symmetry of the lattice points of the crystal, the terms involving the odd powers of r will be absent. The coefficient of the r^2 term in this expression will obviously determine the frequency, and that of the r^4 term the anharmonicity, of the polar oscillations of the crystal. For most of the alkali halides, the frequency thus obtained was found to agree closely with the known reststrahlen frequency of the crystal. It was further found that the sign and the magnitude of the anharmonicity calculated in this manner for KCl crystal fitted well with the known decrease of the specific heat

of the crystal at constant volume with increase of temperature at high temperatures. Among the alkali halides this happens to be the only crystal for which such specific heat data are available.

Now the relative displacement r of the positive and the negative lattices naturally leads to a homogeneous polarization of the crystal, and in calculating the r^2 term in the expression for the potential energy we had to take into account, in the paper referred to, besides the electrostatic and the repulsion interactions between the ions, separately the work done by the polarization field also in effecting this displacement.

A question has been raised in the course of some discussions on the subject whether in considering the electrostatic interactions with all the surrounding ions in the crystal, all of them occupying their respective displaced positions, the effect of the polarization field also has not been indirectly taken into account. The answer to this question is an unambiguous one, namely, that in calculating the reststrahlen frequency one should take into account explicitly the effect of the polarization field, in addition to taking into account the effect of the electrostatic and the repulsion interactions. Even so, the very posing of the question points to the need for a further elucidation of the issues involved. Such an elucidation incidentally helps also to clarify some of the basic concepts regarding the nature of the polarization field itself.

2. CALCULATION OF THE RESTSTRAHLEN FREQUENCY

Since our main purpose is the elucidation of the basic issues, and it can be done with any typical crystal, we shall confine attention for the present to a crystal of the NaCl type. Again, since we are concerned here with the calculation of the frequency only, and not its anharmonicity, we shall retain the r^2 term alone in the expression for the potential energy. Knowing the potential energy W per pair of ions, the frequency of the polar oscillations of the crystal may be readily obtained from the relation

$$W = \tfrac{1}{2}\mu\omega_0^2 r^2, \tag{1}$$

where ω_0 is 2π times the frequency, and μ is the reduced mass of the ion-pair.

Considering now the calculation of W, it is found that the contribution to W from the electrostatic interactions between the ions is nothing, owing to the centre of symmetry of the lattice points, and that from the repulsion interactions is given by $a_1 r^2$, where

$$a_1 = 3/(2\,N\,\beta\,d^5) = \alpha\,e^2\,(\delta-2)/(6d^5)\,; \tag{2}$$

d is the distance between the neighbouring ions, α is the Madelung constant, N is the number of ion-pairs per unit volume of the crystal, β is the compressibility, and δ is a number which defines the repulsion interaction between two adjacent ions as a function of the distance of separation R between them :

$$\phi = A \exp(-\delta R/d). \tag{3}$$

Now the relative displacement of the two lattices will produce a homogeneous polarization in the medium, both directly as a result of this separation, and indirectly by polarizing the ions themselves, *i.e.*, by displacing the electronic cloud in each ion relatively to its nucleus. As a result of this polarization there will be a polariz-

ation field acting on the ions, which will be in a direction that will help the further relative separation of the ions. Hence $a_1 r^2$ will be correspondingly too high an estimate of the potential energy W required for the calculation of the reststrahlen frequency ω_0 with the help of equation (1).

Let Br be the total polarization per unit volume. Then pBr will be the polarization field acting on an ion, where p is the polarization field factor. The corresponding contribution to the potential energy will then be

$$a_2 r^2 = -\tfrac{1}{2} e\, pB\, r^2, \tag{4}$$

where e is the magnitude of the electronic charge. Hence the net value of the potential energy per pair of ions, due to the relative displacement r of the two lattices, will be given by

$$W = (a_1 + a_2)\, r^2 = a\, r^2, \text{ say.} \tag{5}$$

We shall quote here some of the major results obtained in the papers referred to, relating to the quantities involved in (5) and relevent to our purpose.

1. Since the relative displacement r of the two lattices is small in comparison with the inter-ionic distance d, the detailed structure of the polarization due to this displacement corresponds to locating at each point of the lattice of positive ions a point-dipole, of moment er, with its direction along that or r.

2. The polarization field associated with the ionic displacements r was found to have just the Lorentz value, namely $4\pi/3$ times the polarization per unit volume, which is to be expected since the medium consists now of point-dipoles occupying the points of a simple cubic lattice, and Lorentz's original calculation which led to the factor $4\pi/3$ was concerned specifically with this case.

3. It was further found that the relative displacement of the two lattices does not induce any electronic polarization in the ions, and hence the total polarization per unit volume is just Ner.

The experimental evidence for this finding is this. The observed reststrahlen frequency is just what should be expected if the total polarization of the medium had been Ner per unit volume. Any appreciable electronic polarization induced by the ionic displacements r, would have lowered correspondingly the reststrahlen frequency below its observed value.

In other words the mutual interactions between the displacement dipoles $e\,r$ correspond to a polarization field factor $p=4\pi/3$, whereas the interactions between these dipoles and the electronic cloud of the ions correspond to $p\simeq 0$. This is due to the following circumstance. The polarization due to the displacement of the electronic cloud with respect to its nucleus cannot be replaced by a point-dipole, except for its effect at large distances. The extent of overlap of the electronic clouds of neighbouring ions is obviously such as to make $p=0$ for interactions involving electronic polarizations.

In view of these findings, one obtains

$$a_2 r^2 = -\tfrac{2}{3}\pi N e^2 r^2 \tag{6}$$

The reststrahlen frequencies of all the alkali halide crystals were calculated in this manner using (1) and (5), and including in (5) explicitly the contribution $a_2 r^2$ from the polarization field to the potential energy. The calculated frequencies were found to agree well with the observed ones.

3. THE FREQUENCIES INVOLVED IN THE DISPERSION FORMULAE OF DRUDE AND LORENTZ

Just as one obtains from the potential energy $W=ar^2$ a certain frequency ω_0 which can be identified with the resonance frequency of the crystal, one can also calculate another characteristic frequency Ω_0 from the expression $W_1 = a_1 r^2$ using a relation analogous to (1). The difference between ω_0 and Ω_0 is that in calculating the former the contribution to the protential energy from the polarization field has been included, whereas in calculating Ω_0 this contribution has not been included. As was shown by us in some later papers (Krishnan and Roy 1952, 1953) Ω_0 also has a physical significance. It is the frequency which the individual dipoles located at the lattice points would have, had they been isolated from one another, as distinguished from the reststrahlen frequency ω_0 which is that of the assemblage of these oscillators. That the resonance frequency ω_0 of the assemblage is different from the frequency Ω_0 of the isolated dipoles is indeed to the expected, and is due to the mutual interactions of the dipoles in the assemblage. It was further shown in the papers referred to that the effect of their mutual interactions on their frequency is equivalent to the effect of the polarization field in the assemblage on the frequency.

This manner of distinguishing between ω_0 and Ω_0 throws new light on the well-known dispersion formulae of Drude and Lorentz. Again, since we are concerned here with illustrating the basic results, it will be convenient to take the simple case when the medium has just one frequency, namely, the reststrahlen frequency ω_0, the corresponding frequency of the isolated oscillators calculated from $W_1=a_1r^2$ being Ω_0. Now the dielectric constant of such a crystal for any applied frequency ω is given by the relation,

$$K_\omega = 1 + 4\pi x, \tag{7}$$

where x is the polarization that would be induced in unit volume, per unit field in the medium' as usually defined. If γ is the moment induced in an isolated oscillator per unit field incident on it, then obviously

$$\gamma = \frac{e^2}{\mu\,(\Omega_0^2 - \omega^2)}. \tag{8}$$

There are N such oscillators in the medium but x will not be merely N times γ, but may differ from it considerably, owing to the mutual interactions of these oscillators.

The effect of these interactions on x, and hence also on $K\omega$, can be taken into account in two alternative, but equivalent, ways.

1. The actual field producing the polarization in each of the oscillators in the medium, still regarded as retaining its natural frequency Ω_0, is not the field in the medium, say E, but will be greater by $\frac{4}{3}\pi x E$, so that

$$x = N\gamma\,(1 + \tfrac{4}{3}\pi x) = N\gamma\,(K_\omega + 2)/3. \tag{9}$$

The expression for K_ω then takes the well-known Lorentz form

$$\frac{K_\omega - 1}{K_\omega + 2} = \tfrac{4}{3}\pi\, N \frac{e^2}{\mu(\Omega_0^2 - \omega^2)}.$$

2. The alternative way in which the mutual interactions between the dipoles can be regarded as influencing the dielectric constant, is through their effect on the frequency of the oscillators, their frequency ω_0 in the assemblage being different from that in the isolated state, namely Ω_0. The field that produces the polarization in the oscillator is now just the field in the medium E.

In this cae
$$\varkappa = \frac{Ne^2}{\mu(\omega_0^2-\omega^2)} \tag{11}$$

and hence
$$K_\omega - 1 = 4\pi N \frac{e^2}{\mu(\omega_0^2-\omega^2)}. \tag{12}$$

The two expressions (10) and (12) will become idential when

$$\Omega_0^2-\omega^2 = \frac{K_\omega+2}{3}(\omega_0^2-\omega^2), \tag{13}$$

From (12) one can readily obtain

$$\frac{K_0-1}{K_\omega-1} = \frac{\omega_0^2-\omega^2}{\omega^2} \tag{14}$$

Eliminating ω between (13) and (14) one can see that the criterion for securing the identity of (10) and (12), namely (13), reduces to

$$\Omega_0^2 = \frac{K_0+2}{3}\omega_0^2. \tag{15}$$

It can be readily seen that the values of Ω_0^2 and ω_0^2 obtained from a_1 and a respectively would lead to precisely this relation, since

$$a_1 = \tfrac{1}{2}\mu\,\Omega_0^2 = a + \tfrac{2}{3}\pi Ne^2 = \tfrac{1}{2}\mu\omega_0^2\,(1+\frac{K_0-1}{3}). \tag{16}$$

Thus one can readily see that by including in the expression for the potential energy W the contribution from the polarization field, one obtains the reststrahlen frequency ω_0 of the medium, *i.e.* of the assemblage of oscillators, whereas without it one gets the frequency Ω_0 which the same oscillators would have, had they been isolated from one another.

4. THE NATURE OF THE POLARIZATION FIELD

We now return to the question posed in an earlier section. If the polarization of the medium arises from the relative separation of the lattices of positive and negative ions, and if in obtaining the potential energy from which the reststrahlen frequency is to be calculated the contribution to it from all the positive and the negative ions, in their displaced positions, has been taken into account, is not the effect of the polarization field also included in it automatically? The answer is supplied indirectly by the results obtained in the previous section, and it is quite definite, namely, that the polarization field has to be taken into account separately, since the frequency that we are trying to calculate is the resonance frequency ω_0 of the crystal, and not Ω_0 of the corresponding isolated oscillators.

One can also approach the question from certain direct considerations regarding the mechanism of the polarization field. Consider a medium of induced point-dipoles arranged in a simple cubic lattice. Consider one of these lattice points, say O. Now the field in the medium E as usually defined, is that at O when it is made the centre of a very thin long cylindrical cavity scooped out of the medium with its axis along the direction of the polarization. Hence E will consist of the applied field, if any, and the field due to the charges developed on the surface of the medium as a consequence of the polarization of the medium. The surface charges, and hence the field at O due to them, will obviously be determined by *all* the dipoles in the medium, *including that at O also*. On the other hand, the inner field E_i, again as usually defined, will be the field at O when the dipole at O is removed without disturbing the surrounding dipoles. Obviously the difference between E and E_i is this: whereas the former includes a certain averaged self-field at O due to the dipole at O, the latter does not include it. Since this self-field is negative, E will be smaller than E_i. The excess of E over E is by definition the polarization field. For a cubic distribution of point-dipoles, as Lorentz has shown,

$$E_i = E + \tfrac{4}{3}\pi \varkappa E, \tag{17}$$

where $\varkappa E$ is the total polarization per unit volume.

Now one can readily appreciate the equivalence of the two alternative ways described earlier in this paper, of taking into account the effect of the mutual interaction of the dipoles. Consider one of the dipoles say the one at O. It may be regarded as having the frequency Ω_0 and placed in the cavity, created by removing the dipole at O, and thus subject to a field E_i, or alternatively as being an intergral part of the medium with its frequency the same as that of the medium, namely ω_0, the field that determines its polarization being now the field in the medium E. The difference between E_i and E, as we have seen, is $\frac{4}{3}\pi$ times the polarization per unit volume, *i. e.* $\frac{4}{3}\pi Ner$.

One thus obtains the relations

$$\left.\begin{aligned} 2a_1 r &= \mu\,\Omega_0^2 r = E_i e \\ 2ar &= \mu\omega_0^2 r = Ee \end{aligned}\right\} \tag{18}$$

from which one further obtains

$$a - a_1 = a_2 = \tfrac{1}{2}(E-E_i)\,e/r = -\tfrac{2}{3}\pi Ne^2, \tag{19}$$

which is just equation (6).

The relations will again be consistent with the expression for the potential energy per unit volume of the crystal due to the relative separation of the lattices of positive and negative ions, namely,

$$NW = Na r^2 = \tfrac{1}{2} N\mu\omega_0^2 r^2 = (K_0-1)\,E^2/(8\pi), \tag{20}$$

from which one obtains

$$K_0 - 1 = \frac{4\pi Ne^2}{\mu\omega_0^2}, \tag{21}$$

which is just relation (12) in the relevant special case when $\omega = 0$.

5. SOME GENERAL CONSIDERATIONS

Returning to the calculation of the potential energy W, one may re-examine here the contributions from the electrostatic and the repulsion interactions. The repulsion interactions are confined practically to the nearest neighbours, and there is no ambiguity in culculating them. On the other hand, the electrostatic interactions are long-range ones, and in calculating for example the interactions between any two distant ions we have taken the force between them to be given by $\pm e^2/R^2$, as though they were *in vacuo*, and we have ignored the presence of the intervening ions. For very distant ions one may take the intervening medium as having the appropriate dielectric constant K so that the force between them is now $\pm e^2/(KR^2)$. But for the nearer ions the effective value of the dielectric constant to be used in this expression will be difficult to estimate. In any case the usual calculation of the interactions in which the presence of the intervening ions is ignored, which is equivalent to putting $K=1$, is obviously not justifiable. It may appear at first sight that by taking the influence of the intervening ions into account in calculating the electrostatic interactions it may not be necessary to take account explicitly the effect of the polarization field.

This conclusion also would not be justified. It is sufficient to mention in this connection that the actual contribution from the electrostatic interactions to the r^3 term in the expression for W is nothing, and even if the appropriate dielectric constants were to be taken into account in calculating the electrostatic forces their contribution to the r^3 term would still be zero because of the cubic symmetry of the lattice, though the contribution to the r^4 term will be affected.

Thus we are forced to the same conclusion as previously, namely, that in calculating the potential energy W, and thence the reststrahlen frequency ω_0, the contribution to W from the polarization field has to be explicitly taken into account. Otherwise the frequency that one obtains would be that of the isolated oscillators, namely Ω_0, whereas the reststrahlen frequency is the resonance frequency ω_0 of the assemblage of these oscillators, which owing to the mutual interaction of these oscillators, may be markedly different from the frequency Ω_0 of the isolated oscillators.

6. THE OVERLAP OF THE ELECTRONIC CLOUDS OF ADJACENT IONS

In the foregoing discussions we have taken the charges on the ions to be $\pm e$, where e is the electronic charge. This will be the case rigorously if the neighbouring ions did not influence each other, *i.e.*, if the electronic clouds of adjacent ions did not overlap appreciably. But actually the overlap will be considerable. The major effect of the overlap from the point of view adopted by us comes to this. As a result of the separation of the positive and the negative lattices there is polarization of the crystal. This polarization might induce the electronic polarization of the ions, *i.e.* produce a shift of the electronic cloud of an ion relatively to the nucleus of the ion. The effect of the overlap is to make the electronic polarization induced by the relative displacement of the two lattices negligible; while the charges on the ions retain the magnitude of the electronic charge. This method of taking the overlap into account is simple, and fits well, as we have seen, with observation.

On the other hand one may, alternatively, assume the polarization fields, associated not only with the ionic displacement, but also with the shift of the electrons with respect to their nuclei, to have the Lorentz value, and the effective

charges to be correspondingly smaller than $|e|$ in magnitude. There are some major difficulties in accepting this view. Apart from the difficulty of determining theoretically the magnitude of the overlap, and thence the effective charges on the ions, the polarization field associated with the electronic polarization is known from other phenomena to deviate considerably from the Lorentz field. For exmple, considering the temperature variation of refractivity, which is practically the variation due the change in density accompanying the change in temperature— it is found that the terms involving the electronic frequencies behave very differently from the term involving the reststrahlen frequency.

From a detailed analysis of the experimental data for the dispersion, and for its temperature variation, in the alkali halides, Ramachandran (1947) found that in the expression for $dK\omega/dt$ the term involving the reststrahlen frequency ω_0 is proportional to $1/(\omega_0^2-\omega^2)$, whereas the terms involving the ultraviolet frequencies ω_i are proportional to $1/(\omega_i^2-\omega^2)^2$, which points to a marked difference in the behaviour of the two sets of frequencies. The difference can be attributed to the reststrahlen oscillators being practically point-dipoles, whereas the electronic oscillators are not. The result will be that the polarization field corresponding to the mutual interactions of the reststrahlen oscillators will have just the Lorentz value, as we have seen, whereas the interactions between the reststrahlen oscillators and the electronic oscillators, or between the electronic oscillators themselve, would be much smaller. Actually the experimental finding quoted above, obtained from the temperature variation of the dispersion, points to the interactions involving the electronic oscillators being negligible. This was precisely also the conclusion to which we were led from the magnitude of the contribution to W from the polarization field, *i.e.*, the magnitude of a_4 required to explain the observed reststrahlen frequency.

Indeed all the observational data receive a natural and quantitative explanation on the basis of the approximation that the effective charges on the ions are just $\pm e$ and that the whole affect of the overlap of the electronic clouds of the neighbouring ions is to suppress completely the interactions between the reststrahlen oscillators and the electronic ones, and also those among the electronic oscillators themselves. On the other hand, the mutual interactions between the reststrahlen oscillators among themselves are considerable, and correspond to a polarization field having just the Lorentz value.

REFERENCES

Krishnan, Sir K. S. and Roy, S. K. 1950 *a*, *Nature* **166**, p. 114.

_____ 1950, *b* ,, **166**, p. 574.

_____ 1951, *Proc. Roy. Soc.* A. **207**, 447.

_____ 1952, *Phil. Mag.* **43**, 1000.

_____ 1953, ,, ,, **44**, 10.

Ramachandran, G. N. 1947 *Proc. Ind. Acad. Sc.* **25**, 481.

Thermionic Constants of Semi-Conductors

In some recent papers[1], we have described a convenient method of determining the thermionic constants of metals. The method consists essentially in determining, at different known temperatures, the rate of effusion of electrons through a small hole in a thin wall of a chamber made of the metal, instead of determining the direct emission from the surface. The advantage of the effusion method over the emission method is this. The expression for emission involves the transmission coefficient of the surface for electrons having the requisite momentum to cross the surface. This coefficient is very sensitive to adsorption of gases at the surface, and may differ considerably from unity. This coefficient, however, is eliminated in the expression for effusion, in the same manner in which the emissivity of the surface for electromagnetic radiations is eliminated when we take the electromagnetic radiations from a cavity through a small hole, instead of directly from the radiating surface. When the transmission coefficient is eliminated, any observed deviation of the A-coefficient in Richardson's equation from its theoretical value may be attributed to a small linear variation of the work function with temperature. Thus one is enabled by this method to determine not only the work function correctly, but also its temperature coefficient.

The thermionic constants of several metals have been determined by this method, using for this purpose a graphite chamber the walls of which were coated completely with the metal under study, by thermal or electrolytic deposition.

The main purpose of this communication is to direct attention to a new application of this method, namely, for the determination of the thermionic constants of semi-conductors, and to report some preliminary results obtained with nickel ribbons coated with the triple carbonates of barium, strontium and calcium in the molar percentages 47·5, 46·0 and 6·5 respectively. The ribbons were kindly supplied by Dr. D. A. Wright, of the Research Laboratories of the General Electric Co., Ltd., at Wembley. The ribbons were cut into pieces about 2 cm. in length, and a sheaf of them, held together at one end by a platinum foil, was fixed to the back of the graphite chamber, so that the ribbons did not come directly into contact with the graphite surface. The total surface area of these ribbons was more than twenty-five times the area of the effusion hole in our earlier measurements, and about fifty times in our later ones. The coated filaments were activated in the usual manner, and the effusion currents, corresponding to the saturation electronic vapour pressure of the oxide coat, in the temperature range 950°–1,160° K., were measured in the same manner as in our measurements on metals. (The electronic vapour pressure due to graphite, or platinum, is negligible at these temperatures.)

The currents corresponding to zero field were found to fit well with Richardson's equation, with $\varphi = 1{\cdot}55$ eV., and $A = 48$ amp. cm.$^{-2}$ deg.$^{-2}$. The latter value corresponds to a temperature coefficient of the work function $d\varphi/dT = 8 \times 10^{-5}$ eV. per deg., which is of the same order as in many metals. At 1,000° K. the current corresponding to effusion over the whole of the 2π-solid angle would be about 0·75 amp. per sq. cm. The corresponding current obtained by Elizabeth Grey[2] for maximum space-charge-limited pulsed emission directly from the surface of the oxide coat is 8 amp. per sq. cm., which is about eleven times as great. This ratio is of the order to be expected.

We thank Dr. Wright for supplying the coated ribbons, and for helpful discussions.

K. S. Krishnan
S. C. Jain
National Physical Laboratory of India,
New Delhi.
Nov. 27.

[1] Jain, S. C., and Krishnan, Sir K. S., *Proc. Roy. Soc.*, A, **213**, 143, and **215**, 431 (1952).
[2] Grey, Elizabeth, *Nature*, **167**, 522 (1951).

XCIV. *The Drude Dispersion Formula shown to be Applicable to any Medium irrespective of the Polarization Field*

By Sir K. S. Krishnan, F.R.S., and S. K. Roy
National Physical Laboratory of India, New Delhi†

[Received April 10, 1956]

Abstract

It is shown that the well known dispersion formula of Drude is applicable to a dense medium even when the polarization fields associated with the different types of oscillators may all be different. The parameters involved in the formula are naturally the frequencies and the oscillator strengths of the oscillators in the medium, both of them as influenced by the mutual interactions between the oscillators, i.e. as influenced by the polarization fields. The observed data on dispersion will enable us to determine these parameters. In the Lorentz type of dispersion formula, on the other hand, the frequencies and the oscillator strengths involved are those of the *isolated* oscillators, which naturally are independent of the polarization field, and hence the effect of the polarization field on dispersion has to be taken into account explicitly. Because of this, the Lorentz type of formula needs for its formulation explicit information regarding the polarization field, which cannot be supplied by the observed dispersion data alone. The reduction of the Drude formula to one of the Lorentz type, and the appropriate information regarding the polarization field that is needed for this purpose, are also discussed in the paper.

§ 1. The Dispersion Formulae of Drude and of Lorentz

The well known dispersion formula of Lorentz for a dense medium is

$$\frac{K_\infty - 1}{K_\infty + 2} = \frac{4\pi}{3}\sum_{i=1}^{n}\frac{N_i F_i e_i^2}{\mu_i(\Omega_i^2 - \omega^2)} = \frac{4\pi}{3}\sum_{i=1}^{n}\frac{A_i}{(\Omega_i^2 - \omega^2)}, \text{ say} \quad . \quad . \quad (1)$$

where K_∞ is the dielectric constant of the medium for frequency ω, N_i is the number per unit volume, F_i the oscillator strength, and μ_i the reduced mass, of oscillators of frequency Ω_i. This formula is derived on the basis that the actual field acting on an oscillator in the medium is not merely the field in the medium but includes in addition the polarization field, which is further taken to be $4\pi/3$ times the polarization per unit

† Communicated by the Authors.

volume. This introduces in the expression for $K_\omega - 1$ a multiplying factor $[1+(4\pi/3)\chi_\omega]=(K_\omega+2)/3$, where χ_ω is the polarization of the medium per unit volume per unit field in the medium.

On the other hand the Drude formula, namely

$$K_\omega - 1 = 4\pi \sum_{i=1}^{n} \frac{N_i f_i e_i^2}{\mu_i(\omega_i^2 - \omega^2)} = 4\pi \sum_{i=1}^{n} \frac{a_i}{\omega_i^2 - \omega^2}, \text{ say, } \quad . \quad . \quad . \quad (2)$$

which had been derived much earlier, did not naturally contemplate the presence of a polarization field. Hence the Drude formula is generally regarded as a special case of the Lorentz formula, applicable to media in which the polarization field is known to be zero.

For convenience in discussion we shall refer to the quantities A_i and a_i briefly as the oscillator strengths of the oscillators concerned in the two formulae, though actually they refer to N_i oscillators.

Many years ago Herzfeld and Wolf (1925) showed, however, that formula (1) *can always be reduced algebraically to* (2), the ω_i's and a_i's appearing in (2) being calculable functions of Ω_i's and A_i's. They derived (2) from (1) in the simple case when the number of frequencies involved in the formula is just two, but as they themselves pointed out, the reduction of (1) to (2) can be done also in the general case when the frequencies are more than two.

Further since the number of parameters involved in the two formulae is the same, it should be possible conversely to reduce (2) to (1), though the actual reduction, as we shall see later in the present paper, is not quite so simple as the reduction of (1) to (2).

From these considerations it follows that if the experimental data for the dispersion of any substance can be fitted with one of these formulae, they can be fitted equally well with the other formula too. The characteristic frequencies appearing in the two formulae will naturally be very different. From this circumstance it has been concluded by some of the later workers that by comparing the frequencies occurring in the two formulae with the observed frequencies of the medium it should be possible to decide between the two formulae: in other words to decide whether there is a polarization field of magnitude $4\pi/3$ times the polarization per unit volume, as contemplated in the derivation of the Lorentz formula, or it is zero as is taken to be implied by the Drude formula.

§ 2. The Dispersion Data can give no Information regarding the Polarization Field

In some earlier papers (Krishnan and Roy 1952, 1953) we have shown that such an appeal to observation, namely to find which set of frequencies deduced from the observed dispersion agrees with the observed resonance frequencies, whether it is the Ω_i's or the ω_i's, will not enable us to decide

on the existence or otherwise of a polarization field in the medium, and much less to determine its magnitude. Irrespective of whether a polarization field occurs or not, and irrespective of its magnitude when it occurs, the Drude formula (2) will always express correctly the observed dispersion, and the frequencies appearing in this formula will be the actual resonance frequencies of the medium. Since (2) can always be reduced algebraically to (1), again irrespective of the presence or not of an actual polarization field, the observed validity of (1) has by itself no physical significance, *unless the magnitude of the polarization field can be verified independently, or the frequencies Ω_i, whose significance will be stated presently, are known from other considerations.*

This arises from the following circumstance. The effect of the polarization field, whatever may be its magnitude, on the dielectric constant, can be taken into account in two alternative ways, which are mathematically equivalent, and which lead to the Lorentz and the Drude formulae respectively:

(1) The frequencies and the oscillator strengths may be taken to be those of the oscillators when isolated from one another, namely Ω_i and A_i respectively, and the effect of the polarization field on the dielectric constant is then taken into account explicitly.

(2) Alternatively, one may use the frequencies and the oscillator strengths, of the oscillators as influenced by the mutual interactions of the oscillators, i.e. as influenced by the polarization field, namely ω_i and a_i, in which case the whole effect of the polarization field on the dielectric constant is taken into account automatically.

The difference between the two approaches lies in this: whereas ω_i and a_i can be obtained directly from the dispersion data, Ω_i and A_i cannot be.

§ 3. Scope of the Present Paper

It was also emphasized in these papers that the polarization fields associated with the different types of oscillators present in the medium, as for example the electronic and the reststrahlen oscillators in the alkali halide crystals, may be widely different. It was further mentioned, without a statement of the proof, that the Drude formula (2) will hold even in the most general case when the polarization field acting on an oscillator of type i due to all the oscillators of type j in the medium is p_{ij} times χ_j, where χ_j is the contribution from oscillators of type j to the polarization per unit volume per unit field in the medium, and the p_{ij}'s *may all be different*. Since this result is of some importance, and the proof is not obvious, the proof is given in the present paper.

The conditions under which the Drude formula, which is generally applicable to any medium, can be reduced to one of the Lorentz type are also discussed in this paper.

§ 4. The Basic Expression for Refractivity and its Reduction to the Drude Formula

When the different p_{ij}'s, which we may refer to as the polarization field factors, may be different, the basic expression for the dielectric constant of the medium takes the form

$$K_\omega - 1 = 4\pi\chi = 4\pi \sum_{i=1}^{n} \chi_i, \quad \ldots \ldots \quad (3)$$

where

$$\chi_i = \frac{N_i F_i e_i^2}{\mu_i(\Omega_i^2 - \omega^2)} \left(1 + \sum_{j=1}^{n} p_{ij}\chi_j\right) \quad \ldots \ldots \quad (4)$$

Obviously the χ's, like K, would be functions of the incident frequency ω, but for convenience in writing, we have dropped the subscripts ω except in the case of K.

We now proceed to demonstrate that the basic eqns. (3) and (4) can be reduced to formula (2) of Drude.

Using the n equations similar to (4), and using also (3), one can eliminate all the χ_i's and obtain therefrom

$$\begin{vmatrix} -\chi & 1 & 1 & \ldots & \ldots & 1 \\ 1 & p_{11} - \frac{1}{b_1} & p_{12} & \ldots & \ldots & p_{1n} \\ 1 & p_{21} & p_{22} - \frac{1}{b_2} & \ldots & \ldots & p_{2n} \\ \ldots & \ldots & \ldots & \ldots & \ldots & \ldots \\ \ldots & \ldots & \ldots & \ldots & \ldots & \ldots \\ 1 & p_{n1} & p_{n2} & \ldots & \ldots & p_{nn} - \frac{1}{b_n} \end{vmatrix} = 0, \quad \ldots \quad (5)$$

where

$$b_i = \frac{N_i F_i e_i^2}{\mu_i(\Omega_i^2 - \omega^2)} = \frac{A_i}{\Omega_i^2 - \omega^2} \quad \ldots \ldots \quad (6)$$

Let

$$\Delta = \begin{vmatrix} p_{11} - \frac{1}{b_1} & p_{12} & \ldots & \ldots & p_{1n} \\ p_{21} & p_{22} - \frac{1}{b_2} & \ldots & \ldots & p_{2n} \\ \ldots & \ldots & \ldots & \ldots & \ldots \\ \ldots & \ldots & \ldots & \ldots & \ldots \\ p_{n1} & p_{n2} & \ldots & \ldots & p_{nn} - \frac{1}{b_n} \end{vmatrix} \quad \ldots \quad (7)$$

which is a polynomial of degree n in ω^2, which cannot be zero for all values of ω^2.

Now let P_{ij} be the co-factor of the ijth element in the determinant Δ. One then obtains from (5)

$$\chi = -\sum_{i,j=1}^{n} P_{ij}/\Delta. \quad \ldots \ldots \quad (8)$$

In (8) the P_{ij}'s are polynomials of degree $n-1$ in ω^2, whereas Δ is of degree n in ω^2. Hence the right-hand side of (8) can be expanded into partial fractions, thus leading to the expression

$$K_\omega - 1 = 4\pi\chi = 4\pi \sum_{i=1}^{n} \frac{a_i}{\omega_i^2 - \omega^2}, \quad \ldots \ldots \quad (9)$$

where $\omega_1^2, \omega_2^2, \ldots \omega_n^2$ are the n roots of the equation $\Delta(\omega^2)=0$. ω_i and a_i will be functions of the Ω's, the A's and the p's, and will be independent of ω.

Equation (9) can be immediately recognized as the Drude formula.

§ 5. The Dispersion Data in Relation to the Polarization Field

This derivation emphasizes the basic nature of the Drude formula for dispersion. Far from being a special case of the Lorentz formula for zero polarization field, it is physically a more significant formula than Lorentz's, even when there is a polarization field, which may be large and complicated. Just as for the isolated oscilators, their optical behaviour is determined uniquely by their characteristic frequencies Ω_i and their oscillator strengths A_i, so also the optical behaviour of a dense assemblage of such oscillators is determined by the corresponding quantities ω_i and a_i characteristic of the medium. The parameters involving explicitly the polarization fields get eliminated.

For the same reason the dispersion data by themselves cannot give any information regarding the polarization field. If the medium has n characteristic frequencies, the observed dispersion data, which obviously should fit into (9), can supply $2n$ parameters, namely the ω_i's and the a_i's which would be just sufficient to determine the frequencies Ω_i and the oscillator strengths A_i of the n oscillators, *when all the p_{ij}'s are known*.

Now if the p_{ij}'s were all different their number would be n^2, in which case, the p's would be too numerous to be calculated from the $2n$ parameters available from the dispersion data, even if all the Ω_i's and the A_i's were known; except in the trivial case when $n=1$. But actually the p_{ij}'s are not quite so many, since in general p_{ij} should be equal to p_{ji}, in which case the number of different p_{ij}'s reduces to $\frac{1}{2}n(n+1)$. If the Ω_i's and the A_i's are known, then all the p_{ij}'s should be determinable from the dispersion data when $n \leqslant 3$. With $n=3$ or even with $n=2$, it would be possible in practice to describe satisfactorily the dispersion over a fairly wide region of the spectrum.

The result obtained just now may be of even deeper practical interest. Till now we have been concerning ourselves with the dispersion formula alone, i.e. the expression for K as *a function of the frequency* ω, which

enables us directly to determine only the parameters ω_i and a_i, and in which the polarization fields do not appear explicitly. On the other hand the expression for K as *a function of the density of the medium* would involve the polarization field explicitly. In particular, for molecular substances like benzene, naphthalene and other organic compounds, in which the molecules retain their individuality in the condensed state, one can obtain the Ω_i's and the A_i's from the dispersion in the vapour state, in which the polarization fields are negligible, and the corresponding ω_i's and a_i's in the condensed phase from the dispersion data for this phase. A comparison of the two sets, referring respectively to the two phases, should enable us to determine all the p_{ij}'s, provided we choose a spectral region in which 3 frequencies would be adequate to represent correctly the dispersion data.

On the other hand the variation of dispersion with density, in the condensed phase, which may be secured by varying the temperature, would not be so helpful, since the p's also are functions of the density.

§ 6. Reduction of the Basic Formula to One of the Lorentz Type

Having shown that the basic formulae of dispersion, namely (3) and (4), do reduce to Drude's even when the p_{ij}'s are all different, we may proceed to enquire whether in this general case, (3) and (4) can also be reduced to one of the Lorentz type, by which we mean a formula of the type

$$\phi(K)=4\pi\sum_{i=1}^{n}\frac{A_i}{\Omega_i^2-\omega^2}, \quad \ldots\ldots\ldots \quad (10)$$

in which the Ω_i's and the A_i's refer to the *isolated* oscillators, and have the same significance as in (1). The answer is that this can not be done in the general case when the p_{ij}'s are all different.

The problem is really one of finding an expression for K, i.e. for χ, which will not involve the component polarizabilities χ_i separately. One obvious method of doing this is to eliminate the χ_i's between (3) and (4), and this procedure, as we have seen, yields the Drude formula, which involves the characteristic frequencies ω_i of the medium, and not the frequencies Ω_i of the isolated oscillators, which we now wish to retain. On a closer examination of (4) and (3) one can see that the separate χ_i's can be eliminated, without at the same time eliminating the Ω_i's also, only when the p_{ij}'s have all the same value, say p.

When this is the case, the explicit expression for $\phi(K)$ appearing in (10) becomes

$$\frac{\chi}{1+p\chi}=\sum_{i=1}^{n}\frac{A_i}{\Omega_i^2-\omega^2} \quad \ldots\ldots\ldots \quad (11)$$

or

$$\frac{K-1}{K+\alpha}=p\sum_{i=1}^{n}\frac{A_i}{\Omega_i^2-\omega^2} \quad \ldots\ldots\ldots \quad (12)$$

where $\alpha=4\pi/p-1$,

§ 7. Reduction of the Drude Formula to one of the Lorentz Type

We have shown that the basic formulae of dispersion, namely (3) and (4), can be reduced to the Drude formula (9) even when the p_{ij}'s are all different, and that in the special case when they have all the same value p, (3) and (4) reduce to (12) also. Hence it follows when all the p_{ij}'s have the same value, it should be possible directly to reduce (9) to (12), i.e. to obtain the constants Ω_i and A_i in terms of ω_i and a_i when $\alpha=4\pi/p-1$ is known. The reduction is done in the following manner.

Starting with (10), and remembering that $\alpha=4\pi/p-1$, one obtains immediately

$$\frac{K-1}{K+\alpha}=\left(p\sum_{i=1}^{n}\frac{a_i}{\omega_i^2-\omega^2}\right)\Big/\left(1+p\sum_{i=1}^{n}\frac{a_i}{\omega_i^2-\omega^2}\right)$$

$$=\frac{p\sum_{i=1}^{n}a_i\prod_{\substack{j=1\\j\neq i}}^{n}(\omega_j^2-\omega^2)}{\prod_{i=1}^{n}(\omega_i^2-\omega^2)+p\sum_{i=1}^{n}a_i\prod_{\substack{j=1\\j\neq i}}^{n}(\omega_j^2-\omega^2)} \quad \ldots\ldots \quad (13)$$

Now knowing ω_i and a_i and knowing further that every p_{ij} has the same value $p=4\pi/(\alpha+1)$, we may put the denominator on the right-hand side of (13)=0, and treating it as an equation in ω^2, obtain the n roots of the equation, namely $M_1^2, M_2^2, \ldots M_n^2$, and thence obtain

$$\frac{K-1}{K+\alpha}=\frac{p\sum_{i=1}^{n}a_i\prod_{\substack{j=1\\j\neq i}}^{n}(\omega_j^2-\omega^2)}{\prod_{i=1}^{n}(M_i^2-\omega^2)} \quad \ldots\ldots\ldots \quad (14)$$

Since the M_i's are now known, the numerator on the right hand side can be put equal to $p\sum_i C_i\prod_{\substack{j=1\\j\neq i}}^{n}(M_j^2-\omega^2)$ where the C_i's can be readily obtained. We thus obtain

$$\frac{K-1}{K+\alpha}=p\sum_{i=1}^{n}\frac{C_i}{M_i^2-\omega^2}, \quad \ldots\ldots\ldots \quad (15)$$

in which the C_i's are obviously independent of ω.

Comparing (15) with (12) one can immediately see that if the basic assumption that every p_{ij} has the same value, namely p, is correct, then every M_i and C_i appearing in (15) should be identical with every Ω_i and A_i respectively.

But the important point to emphasize is that the values of M_i and C_i thus obtained will represent correctly the frequencies and the oscillator strengths of the isolated oscillators only to the extent to which our knowledge of the polarization field is dependable. Since the dispersion data themselves do not supply any information regarding the polarization

field, one may choose any arbitrary α, and find the corresponding M_i and C_i which will make (15) algebraically identical with (9). Since the Drude formula (9) represents correctly the observed dispersion, (15) too, with the appropriate choice of the M_i's and C_i's corresponding to our choice of α, will represent equally well the observed dispersion, and this will be so irrespective of the actual values of the different p_{ij}'s; but then the M_i's and C_i's that appear in the formula will not be the actual Ω_i's and the A_i's of the isolated oscillators.

References

Herzfeld, F. F., and Wolf, K. L., 1925, *Ann. d. Physik*, **78**, 35.
Krishnan, K. S., and Roy, S. K., 1952, *Phil. Mag.*, **43**, 1000; 1953, *Ibid.*, **44**, 19.

Radiative Transfer of Energy in the Core of a Heated Tube

While investigating the temperature distribution along a thin-walled tube heated by passing an electric current through it *in vacuo* we had naturally to calculate the radiative transfer of energy occurring in the hollow core of the tube[1]. Taking the tube to be a circular cylinder of diameter D, and considering an annular ring of width dx, the net gain in energy by the ring due to radiative transfer can be readily calculated. If the ring is not too near the ends, this is found to be equal to:

$$4\pi\sigma D^3T^3\,(dT/dx)^3\,dx + \frac{4}{3}\,\pi\sigma D^3T^3\,(d^3T/dx^3)dx$$

which may be expressed in the form:

$$\frac{d}{dx}\left(\frac{4}{3}\,\pi\sigma D^3T^3\,dT/dx\right)dx$$

where σ is Stefan's constant of radiation, and the emissivity of the walls is taken to be unity. It is as though the hollow core had a thermal conductivity of magnitude:

$$\varkappa_r = \frac{16}{3}\,\sigma DT^3 \qquad (1)$$

One may compare this with the expression obtained by Bosworth[2] for the radiational conductivity of a very hot gas, in which the photons emitted by the molecules, as distinguished from the molecules themselves, are regarded as diffusing into the gas, his expression being:

$$\varkappa_{rg} = \frac{16}{3}\,\sigma l_0T^3 \qquad (2)$$

where l_0 is the mean free path of the photons, which may be taken to be the reciprocal of the absorption coefficient of the gas for the photons. Indeed, the radiational conductivity of the hollow core may be regarded as the limiting case of the conductivity of a hot gas filling the core, when the pressure of the gas is reduced to zero and the free path of the photons is thus limited by the dimensions of the tube. In this limiting case the source of the photons will recede to the walls. Taking (2) to remain valid in this limiting case also, and comparing (1) with it, one can see that the mean free path of the photons in the hollow core is just D.

There is a close analogy between expression (2) for the radiational conductivity of a gas at high temperatures, and that for the lattice conductivity of a dielectric crystal at low temperatures, in which the transport of energy is by the low-frequency thermal elastic waves or phonons in the medium[3]. The closeness of the analogy arises ultimately from two factors: the upper limit to the wave number set by the Brillouin zone ceases to be of significance for these low-frequency waves, and, secondly, the frequencies are proportional to the wave numbers, as for the photons in a gas. These are also just the factors that lead to the T^3 law for the lattice specific heat.

The expression obtained by Casimir[3] for the lattice conductivity of a dielectric cylinder at temperatures low enough for the free path of the phonons to be limited by its diameter is analogous to that obtained here for the radiational conductivity of the hollow core—again as though the mean free path so limited is just D.

When the emissivity of the walls falls short of unity, one has to know how the fraction $(1 - \varepsilon)$ of the incident radiation that is not absorbed is returned to the enclosure. When it is in the form of specular reflexion, it is found that the thermal conductivity of the core is on this account increased by a factor $(2 - \varepsilon)/\varepsilon$, which is similar to the factor obtained by Berman, Simon and Ziman[4] in their expression for the lattice thermal conductivity of a cylindrical specimen at low temperatures, and also similar to the 'coefficient of slip' of a rarefied gas in its passage through a narrow tube[5].

K. S. Krishnan
R. Sundaram

National Physical Laboratory,
New Delhi. Aug. 23.

[1] *Proc. Roy. Soc.* (In the press).
[2] Bosworth, R. C. L., "Heat Transfer Phenomena", 60 (John Wiley, New York, 1952). The expression given by Bosworth corresponds to $\frac{4}{3}\,\sigma l_0T^3$, which is due to his taking the density of radiational energy per unit volume as $\sigma T^4/c$, whereas actually it should be four times this.
[3] Casimir, H. B. G., *Physica*, **5**, 595 (1938).
[4] Berman, R., Simon, F. E., and Ziman, J. M., *Proc. Roy. Soc.*, A, **220**, 176 (1953).
[5] Maxwell, J. C., *Phil. Trans. Roy. Soc.*, Part 1, 332 (1879); or "The Scientific Papers of James Clerk Maxwell", 708.

The distribution of temperature along electrically heated tubes and coils
I. Theoretical

By Sir K. S. Krishnan, F.R.S. and R. Sundaram
National Physical Laboratory, New Delhi

(*Received* 29 *March* 1960)

The distribution of temperature along a filament electrically heated *in vacuo* has been studied in detail in previous papers, both theoretically and experimentally. The investigations are extended in the present paper to the case of a thin-walled tube. The major new factor that appears here is the radiational transfer of energy in the core of the tube, and if one can evaluate the rate of gain in energy by a given annular ring on this account one can readily formulate the differential equation governing the distribution of temperature along the tube.

Taking ϵ to be the emissivity, and hence also the absorptivity, of the surface, and taking the fraction $(1-\epsilon)$ of the radiation incident on the surface that is not absorbed by it to be specularly reflected, we have calculated the radiational gain by the annular ring per second; the expression consists of two terms, proportional to $(dT/dx)^3$ and to d^3T/dx^3 respectively, and their coefficients point to a temperature-dependent thermal conductivity of the core equal to $\frac{4}{3}\sigma DT^3(2-\epsilon)/\epsilon$. It is as though the conduction is due to the thermal diffusion of the photons, and they had a mean free path equal to the diameter D of the tube, enhanced by a factor $(2-\epsilon)/\epsilon$ as a result of the specular reflexions, in the same manner in which the 'coefficient of slip' of the molecules of a rarefied gas in its passage through a narrow tube is enhanced by the specular reflexions of the molecules from the walls of the tube.

The expression for the conductivity of the core bears a close analogy to the corresponding expression for other transport phenomena in which the mean free path of the diffusing particle is limited by the dimensions of the medium or of the enclosure, e.g. the thermal conductivity of a hot gas in a narrow tube due to the diffusion of the photons emitted by the molecules, or the thermal conductivity of a dielectric cylinder at low temperatures due to the diffusion of thermal phonons.

Though the differential equation determining the temperature distribution along a tube is more complicated than that for a filament, a practically general solution can be obtained; it is found to be similar to that for the filament, except that the natural length is now considerably greater, and the longitudinal variation of the temperature considerably flatter, than in the filament.

The case of a closely wound coil is very similar to that of the tube, except that the conductivity through the material of the walls is now through the wire and hence much smaller than in the tube.

1. Introduction

A thin-walled tube of graphite electrically heated *in vacuo* by the passage of a heavy current serves as a convenient high-temperature furnace for many purposes. While designing one such furnace in which a certain prescribed length of the furnace tube near the centre had to be of sensibly constant temperature, we felt the need for a theoretical investigation of the general problem of distribution of temperature along a thin-walled tube electrically heated *in vacuo*. Such an investigation, besides serving the immediate purpose in view, would at the same time cover the case of the closely wound coil, which also is of practical importance. Since, however, no general solution was available even for the simpler case of an electrically heated *filament*, the investigation of this latter case was taken up first, by Dr S. C. Jain and one of us, and the results have been reported in a series of six papers in these *Proceedings* (Jain & Krishnan 1954 and 1955).

The practically complete solution that could be obtained for the filament, and the wide range of results that could be derived therefrom, encourage one to undertake the more general problem of the tube. The new factor that appears here is the transference of heat along the tube by the radiations in the core of the tube, besides the normal conduction through the material of the walls of the tube. The present paper is concerned with this more general problem of distribution in thin-walled tubes and closely wound coils. In part I are reported the theoretical investigations. and in part II some experimental studies on such tubes and coils.

Apart from the practical importance of the problem, the investigation also throws light incidentally on the part played by specular reflexions in radiative transfer in tubes, and particularly on the performance of cylindrical furnaces as close approximations to black bodies. Since the heat transfer in such tubes occurs under conditions that correspond to a mean free path of the photons that is determined by the dimensions of the tube, some of the results bear a close analogy to corresponding results concerning the passage of a rarefied gas through a narrow tube, and the thermal conductivity of a cylindrical dielectric at very low temperatures. Both these fields have been studied extensively, the former by Maxwell (1879), Knudsen (1909), Smoluchowski (1910) and others, and the latter by Casimir (1938), and by Berman, Simon & Ziman (1953), and others.

2. Formulation of the differential equation determining the distribution of temperature

Consider a thin-walled cylindrical tube of length $2l$ of circular cross-section whose external and internal radii are r_e and r_i respectively; $(r_e-r_i) \ll r_i \ll l$. Taking the axis of the cylinder as the x-axis of a co-ordinate system, and one end of the tube as corresponding to $x = 0$, consider a thin annular ring between x and $x+dx$. Now if I be the heating current, the heat generated in the annular ring by the current $= I^2\rho\,dx/\omega$ per second, where ρ is the specific resistance, and $\omega = \pi(r_e^2-r_i^2)$ is the cross-section of the material of the tube. The gain in energy per second in the element due to conduction $= \kappa\omega(d^2T/dx^2)\,dx$. The loss due to radiation from the outer surface of the element $= 2\pi r_e\epsilon\sigma(T^4-T_0^4)\,dx$, where T is the temperature at x, which is regarded as constant over the whole of the cross-section at x, and T_0 is the temperature of the walls of the enclosing vacuum chamber; σ is Stefan's constant, and ϵ is the emissivity of the surface. Denoting by $W\,dx$ the *net* gain in energy by the element dx per second due to radiational transfer in the core of the tube, we can write the differential equation determining the temperature distribution along the tube in the form

$$I^2\rho/\omega + \kappa\omega\,d^2T/dx^2 + W - 2\pi r_e\epsilon\sigma(T^4-T_0^4) = 0. \qquad (1)$$

Now W is the only quantity appearing in (1) for which we do not have an explicit expression. It can be evaluated indirectly by first evaluating the net flux of radiation F that crosses the core-section at x and differentiating it with respect to x; since $W\,dx = -(dF/dx)\,dx$. There are, however, some advantages, as we shall see presently, in evaluating $W\,dx$ *directly*, and we therefore adopt the latter method.

Obviously

$$W\,dx = \epsilon J\,dx - 2\pi r_i\epsilon\sigma T^4\,dx, \qquad (2)$$

where $J\,dx$ is the radiational energy *received* per second by the inner walls of the annular ring from the rest of the tube, and ϵ times this will be the energy *absorbed* by it. The second term on the right-hand side of (2) represents the radiation emitted by the inner walls of the ring. We have already included in equation (1) explicitly the radiation from the outer walls of the ring.

We now proceed to evaluate J.

3. Some basic expressions concerning radiative transfer in a tube

Consider two annular rings dx_1 and dx_2 respectively at x_1 and x_2. Consider the elements of area ds_1 and ds_2 of the inner walls of these two rings, whose co-ordinates are $x_1, r_i\sin\theta$, $r_i\cos\theta$, and $x_2, r_i\sin\theta_2$, $r_i\cos\theta_2$ respectively. Then the radiation *received* by ds_1 from ds_2 is given by

$$di = \frac{\epsilon\sigma T_2^4}{\pi}\frac{\cos\alpha_1\cos\alpha_2}{R^2}\,ds_1\,ds_2, \tag{3}$$

where α_1 and α_2 are the acute angles which the normals to the two elements ds_1 and ds_2 make with the line joining the two elements, and R is the distance between them. It can be readily shown that

$$di = \frac{\epsilon\sigma T_2^4}{4\pi}dx_1\,dx_2\left[\frac{1-\cos(\theta_1-\theta_2)}{p-\cos(\theta_1-\theta_2)}\right]^2 d\theta_1\,d\theta_2, \tag{4}$$

where
$$p = (2h^2+D^2)/D^2;\quad h = x_2-x_1;\quad D = 2r_i. \tag{5}$$

Now the radiation received by the whole of the ring dx_1 from the ring dx_2, equal to dj say, is given by

$$\begin{aligned} dj &= \frac{1}{4\pi}\epsilon\sigma T_2^4\,dx_1\,dx_2\int_0^{2\pi}d\theta_2\,2\int_{\theta_2}^{\theta_2+\pi}\left[\frac{1-\cos(\theta_1-\theta_2)}{p-\cos(\theta_1-\theta_2)}\right]^2 d\theta_1 \\ &= \epsilon\sigma T_2^4\zeta(h)\,dx_1\,dx_2, \end{aligned} \tag{6}$$

where

$$\zeta(h) = \int_0^\pi\left(\frac{1-\cos\theta}{p-\cos\theta}\right)^2 d\theta \tag{7}$$

$$= \left[\theta+\frac{p-1}{p+1}\frac{\sin\theta}{p-\cos\theta}-\frac{2(p+2)(p-1)^{\frac{1}{2}}}{(p+1)^{\frac{3}{2}}}\tan^{-1}\left\{\left(\frac{p+1}{p-1}\right)^{\frac{1}{2}}\tan\tfrac{1}{2}\theta\right\}\right]_0^\pi$$

$$= \pi\left[1-\frac{|h|(2h^2+3D^2)}{2(h^2+D^2)^{\frac{3}{2}}}\right] \tag{8}$$

is just a geometrical factor depending on the diameter and the distance of separation of the two rings.

4. Radiative contribution predominantly from adjoining regions and the consequent simplification

The total radiation received by the ring dx_1 from the rest of the tube is obtained by integrating $dx_1\epsilon\sigma T_2^4\zeta(h)\,dx_2$ over x_2, i.e. over all values of h from $-x_1$ to $2l-x_1$. This integration is rendered possible by the fact that not only $\zeta(h)$ but

even $\zeta(h)\,h^m$, where m is a small number, decreases rapidly with increase of h, as will be seen from table 1.

Table 1

h/D	0	0·5	0	2	3	4
$\zeta(h)/\pi$	1	0·374	0·116	0·016	0·004	0·001
$\zeta(h)\,h^2/\pi D^2$	0	0·094	0·116	0·064	0·036	0·022

This feature, which implies that the significant part of the radiation received by dx_1 comes from the adjoining regions, namely a few times D, $\ll l$, makes it possible for us to express T_2 as a Taylor expansion in terms of the temperature and its derivatives with respect to x at x_1, and further with the first few terms only in the expansion. We thus obtain

$$T_2^4 = T_1^4 + ah + bh^2, \tag{9}$$

where
$$\left.\begin{aligned} a &= 4T_1^3(dT/dx)_1, \\ b &= 6T_1^2(dT/dx)_1^2 + 2T_1^3(d^2T/dx^2)_1. \end{aligned}\right\} \tag{10}$$

Thus the total *direct* radiation received by dx_1 from either side of the tube separately will be given by

$$J_i\,dx_1 = dx_1\epsilon\sigma\sum_{m=0}^{2}A_m\int_0^L\zeta(h)\,h^m\,dh, \tag{11}$$

where A_m takes the values T_1^4, a and b respectively when $m = 0$, 1 and 2, and L takes the values $2l-x_1$ or x_1 as the case may be. The integrals over the portions of the tube on the two sides of dx_1 will add up when m is even and will be of opposite signs when m is odd.

5. Evaluation of the integral

In order to evaluate the definite integral appearing in (11) it will be convenient to start with expression (7) for $\zeta(h)$ and instead of integrating with respect to θ first* and then with respect to h, to express the integral involved, namely

$$I_m = \int_0^L\zeta(h)\,h^m\,dh = \int_0^L h^m\,dh\int_0^\pi\left(\frac{1-\cos\theta}{p-\cos\theta}\right)^2 d\theta, \tag{12}$$

in the form
$$I_m = \int_0^\pi(1-\cos\theta)^2\,d\theta\int_0^L\frac{h^m\,dh}{(p-\cos\theta)^2}. \tag{13}$$

Putting $h = Du$, $L = D\lambda$ and $\frac{1}{2}\theta = \phi$, one obtains

$$I_m = 2D^{m+1}\int_0^{\pi/2}\sin^4\phi\,d\phi\int_0^\lambda\frac{u^m\,du}{(u^2+\sin^2\phi)^2}. \tag{14}$$

Taking the second integral in (14) first, namely

$$Q_{m\lambda} = \int_0^\lambda\frac{u^m\,du}{(u^2+\sin^2\phi)^2}, \tag{15}$$

we are already aware that the significant contributions to it come from small values of u of the order of unity. Hence we may first evaluate $Q_{m\infty}$ and then formulate the

* In order to demonstrate the rapid decrease of $\zeta(h)$ with h, the integration had to be done over θ in the previous section, for the simple case $m = 0$.

correction to be applied to it in order to obtain $Q_{m\lambda}$, remembering that $\lambda > 1$ and $m < 3$. Now putting $u = z\sin\phi$ one obtains

$$Q_{m\infty} = \frac{1}{\sin^{3-m}\phi}\int_0^\infty \frac{z^m\,\mathrm{d}z}{(1+z^2)^2}$$
$$= \frac{1}{\sin^{3-m}\phi}\tfrac{1}{2}\Gamma\left(\frac{m+1}{2}\right)\Gamma\left(\frac{3-m}{2}\right). \tag{16}$$

The difference between $Q_{m\lambda}$ and $Q_{m\infty}$, which we may regard as a correction term, is given by

$$Q_{m\lambda} - Q_{m\infty} = \int_\infty^\lambda \frac{u^m\,\mathrm{d}u}{(u^2+\sin^2\phi)^2} = \int_\infty^\lambda \frac{1}{u^{4-m}}\left(1+\frac{\sin^2\phi}{u^2}\right)^{-2}\mathrm{d}u$$
$$= \sum_{n=1}^{\infty}(-1)^n \frac{n\sin^{2n-2}\phi}{2n+1-m}\frac{1}{\lambda^{2n+1-m}}. \tag{17}$$

Going back to the integrals I_m (see (14)), which may now be designated more specifically as $I_{m\lambda}$, one obtains

$$I_{m\lambda} = 2D^{m+1}\int_0^{\pi/2} Q_{m\lambda}\sin^4\phi\,\mathrm{d}\phi. \tag{18}$$

Here again replacing $Q_{m\lambda}$ by $Q_{m\infty}$ *plus* $Q_{m\lambda} - Q_{m\infty}$, we obtain the two corresponding integrals, namely

$$I_{m\infty} = D^{m+1}\int_0^{\pi/2}\Gamma\left(\frac{m+1}{2}\right)\Gamma\left(\frac{3-m}{2}\right)\sin^{m+1}\phi\,\mathrm{d}\phi$$
$$= D^{m+1}/(m+1)\,\Gamma\left(\frac{m+2}{2}\right)\Gamma(\tfrac{1}{2})\,\Gamma\left(\frac{3-m}{2}\right), \tag{19}$$

which can be seen to have the values $\pi D/2$, $\pi D^2/4$ and $\pi D^3/3$ when $m = 0$, 1 and 2, respectively; and the correction term,

$$I_{m\lambda} - I_{m\infty} = 2D^{m+1}\sum_{n=1}^{\infty}(-1)^n\frac{n}{2n+1-m}\frac{1}{\lambda^{2n+1-m}}\int_0^{\pi/2}\sin^{2n+2}\phi\,\mathrm{d}\phi$$
$$= \frac{D^{m+1}}{\lambda^{3-m}}\sum_{n=1}^{\infty}(-1)^n\frac{n}{2n+1-m}\frac{\Gamma\tfrac{1}{2}(2n+3)\,\Gamma(\tfrac{1}{2})}{\Gamma(n+2)}\frac{1}{\lambda^{2n-2}}. \tag{20}$$

The values of $I_{m\lambda}$ calculated from the above expressions for $m = 0, 1$, and 2, are entered in table 2.

TABLE 2

m	$I_{m\lambda}/\pi$
0	$\frac{1}{2}D - \frac{1}{8}D/\lambda^3 + \frac{1}{8}D/\lambda^5 - \ldots$
1	$\frac{1}{4}D^2 - \frac{3}{16}D^2/\lambda^2 + \frac{5}{32}D^2/\lambda^4 - \ldots$
2	$\frac{1}{6}D^3 - \frac{3}{8}D^3/\lambda + \frac{5}{24}D^3/\lambda^3 - \ldots$

6. Effect of specular reflexions

Till now we had confined attention to direct radiations only, which are naturally proportional to T_2^4 and to the emissivity ϵ, which will also be the absorptivity of the surface. Now the question arises as to the manner in which the fraction $(1-\epsilon)$ of the radiation that is incident on the surface and is not absorbed, is returned to the

enclosure. In the usual discussions on radiations from a heated cylinder (see, for example, Buckley 1927, 1934), it is assumed that this fraction is diffusely radiated according to the cosine law, by analogy with the fraction ϵ that is absorbed and re-emitted. A perfectly diffuse radiation of this type which does not also involve absorption is difficult to secure in practice. We shall therefore confine ourselves to the alternative case where the whole of the fraction $(1-\epsilon)$ that is not absorbed is specularly reflected. This condition can be secured experimentally by suitably polishing the surface, particularly since the radiations will be predominantly in the infra-red region. In any case we shall regard this condition to hold in the tube that we are considering.

We have seen that the radiation from $\mathrm{d}x_2$ that is directly received by $\mathrm{d}x_1$ is given by

$$\mathrm{d}j_0 = \epsilon\sigma T_2^4\zeta(h)\,\mathrm{d}x_1\,\mathrm{d}x_2, \tag{21}$$

where the subscript 0 attached to j is to indicate that it relates to the unreflected direct radiation. It can be readily seen that the radiation from $\mathrm{d}x_2$ that is received by $\mathrm{d}x_1$ after r reflexions will be given by

$$\mathrm{d}j_r = \sigma T_2^4\epsilon(1-\epsilon)^r\frac{1}{r+1}\zeta\left(\frac{h}{r+1}\right)\mathrm{d}x_1\,\mathrm{d}x_2, \tag{22}$$

where the multiplying factor $1/(r+1)$ on the right-hand side is to take into account the $(r+1)$ times larger linear spread of the reflected beam reaching $\mathrm{d}x_1$ as compared with the width of the source $\mathrm{d}x_2$. Hence the total radiation received from the whole of the tube on one side, either directly or after one or more reflexions will be given by

$$J_i\,\mathrm{d}x_1 = \mathrm{d}x_1\,\epsilon\sigma\sum_{r=0}^{\infty}(1-\epsilon)^r\int_0^L T_2^4\zeta\left(\frac{h}{r+1}\right)\frac{\mathrm{d}h}{r+1}$$
$$= \mathrm{d}x_1\,\epsilon\sigma\sum_{m=0}^{2}\sum_{r=0}^{\infty}A_m(1-\epsilon)^r(r+1)^m\int_0^{h'=L_i(r+1)}\zeta(h')\,h'^m\,\mathrm{d}h'. \tag{23}$$

The integral appearing in (23) is the same integral as before, except that the upper limit now is $L/(r+1)$ instead of L, and hence the values given in table 2 can be used directly in the evaluation of the integral, except that λ will now be replaced by $\lambda/(r+1)$.

The correction terms involving λ will now be of the type $c(r+1)^n/\lambda^n$, so that we shall be left with only the evaluation of the series

$$S_N = \sum_{r=0}^{\infty}(1-\epsilon)^r(r+1)^N, \tag{24}$$

in which $N = m$, or $m+n$, as the case may be.

Now the series can be readily seen to be convergent, since in the limit $r\to\infty$, the ratio of the two consecutive terms u_q and u_{q+1} remains finite and > 1;

$$\lim_{r\to\infty}\frac{u_q}{u_{q+1}} = \lim_{r\to\infty}\left(\frac{r+1}{r+2}\right)^N\frac{1}{1-\epsilon} = \frac{1}{1-\epsilon} > 1. \tag{25}$$

The series S_N can be evaluated in the following manner. It can be seen that

$$S_{N+1} = S_N - (1-\epsilon)\,\mathrm{d}S_N/\mathrm{d}\epsilon, \tag{26}$$

so that the value of S_N for any N can be based on that of S_{N-1}, and ultimately on that of S_0, which obviously is equal to $1/\epsilon$.

The values of S_N thus obtained are entered in table 3.

TABLE 3

N	0	1	2	3	4
S_N	$1/\epsilon$	$1/\epsilon^2$	$(2-\epsilon)/\epsilon^3$	$(6-6\epsilon+\epsilon^2)/\epsilon^4$	$(24-36\epsilon+14\epsilon^2-\epsilon^3)/\epsilon^5$

7. The tube very long on both sides of dx_1

Before we take up the case of the finite tube, it will be convenient to consider the case where the tube is very long on *both* sides of dx_1. In this case the contributions from the two sides will add up for even values of m, and will just cancel each other out when m is odd. We thus obtain for the radiation *absorbed* by dx_1, which is ϵ times the radiation *received* by it, the value

$$\epsilon J\,dx_1 = 2\epsilon^2\sigma[S_0 I_{0\infty} T_1^4 + S_2 I_{2\infty} b]\,dx_1 = [\pi D\epsilon\sigma T_1^4 + \tfrac{2}{3}\pi\sigma D^3 b(2-\epsilon)/\epsilon]\,dx_1, \qquad (27)$$

where b has the value defined by (10).

The first term on the right-hand side of (27) is just balanced by the radiation emitted by dx_1, and we thus obtain finally for the radiational energy accumulating in dx_1 per second, when both sides are long, the expression

$$W\,dx_1 = \tfrac{2}{3}\pi\sigma D^3(2-\epsilon)/\epsilon\left[6T_1^2\left(\frac{dT}{dx}\right)_1^2 + 2T_1^3(d^2T/dx^2)_1\right]dx_1. \qquad (28)$$

8. Radiation from inside a long tube kept at uniform temperature as approximation to that of a black body

Going back to (23), we see that $J_i\,dx_1$ obviously represents the total radiation received by the annular ring dx_1 at the mouth of a tube of length L. When $L\to\infty$, the integral appearing in (23) becomes independent of r. Now comparing the expression for $J_i\,dx_1$ in this case with the corresponding expression for the *direct* radiations only received by dx_1, one can see that in place of the multiplying factor ϵ that appears in the latter expression there now appears the factor ϵS_m as a result of the specular reflexions. In other words, ϵS_m is the factor by which the corresponding expression for the ideal case when $\epsilon = 1$ has to be multiplied in order to take into account the actual defect of ϵ from unity and the consequent occurrence of specular reflexions. One can immediately see that for all values of m, $\epsilon S_m \to 1$ when $\epsilon \to 1$, as should be expected.

We may draw attention here to the special case when the whole of the long tube is kept at a constant temperature. Now m takes only one value, namely 0, and ϵS_m has the value $\epsilon S_0 = \epsilon\sum_{r=0}^{\infty}(1-\epsilon)^r$, which is just unity, and therefore independent of ϵ. It is as though only the *direct* radiations from the tube were concerned and these radiations were effectively those of an ideally black surface. In other words the flux that will issue from the mouth of a tube of any material, provided the tube is sufficiently long, will be that of a black body. We merely refer to this result here, in passing, and since it is of some importance, we shall deal with it in detail elsewhere.

9. The radiational conductivity of the core

Coming back to equation (28), we can write it in the form

$$W\,dx_1 = \frac{d}{dx}\left(\tfrac{1}{3}\pi\sigma D^3 T^3\,\frac{2-\epsilon}{\epsilon}\,\frac{dT}{dx}\right)dx_1. \qquad (29)$$

The radiational transfer of energy corresponds to a net flux of amount

$$\tfrac{4}{3}\pi\sigma D^3 T^3\{(2-\epsilon)/\epsilon\}\,(dT/dx)$$

per second, proportional to the gradient of temperature. It is as though the core had a thermal conductivity

$$\kappa_r = \tfrac{16}{3}\sigma D T^3(2-\epsilon)/\epsilon. \qquad (30)$$

We now proceed to compare (30) with corresponding expressions obtained in analogous phenomena, and it will be convenient for this purpose to consider separately the expression $\kappa_r = \frac{16}{3}\sigma D T^3$ characteristic of a tube with black walls, and the factor $(2-\epsilon)/\epsilon$ which arises from the specular reflexions and tends to unity when $\epsilon \to 1$.

10. Conductivity of core as limiting case of that of a rarefied hot gas

One may first compare the expression obtained here for a black tube with the radiational conductivity of a very hot gas, which plays an important part in radiative transfer in stellar atmospheres. Treating the conductivity as being due to the diffusion into the gas of the photons emitted by the molecules of the gas, and taking the mean free path of the photons as l_0, Bosworth (1952) obtains for the thermal conductivity of the gas the expression*

$$\kappa_{rg} = \tfrac{16}{3}\sigma l_0 T^3. \qquad (31)$$

l_0 will naturally be determined by the absorption coefficient of the gas for the photons, and can be put equal to the reciprocal of the absorption coefficient.

If the gas is enclosed in a cylindrical tube, and at a high pressure such that $l_0 \ll D$, and the pressure of the gas is gradually reduced, the mean free path of the photons will naturally increase, almost inversely in proportion to the pressure, and there will come a stage when the free path is limited by the dimensions of the tube only, and not by the absorption coefficient of the gas, and thereafter the free path will remain constant at this value l_D unaffected by any further reduction in the pressure. The radiational transfer *in vacuo* in the hollow core of the tube that we have been considering would correspond to this limiting case, and the corresponding value of the conductivity will be

$$\kappa_r = \tfrac{16}{3}\sigma l_D T^3, \qquad (32)$$

which may be compared with the value (30) calculated directly. Doing so one obtains for the effective mean free path of the photons in the vacuum core of the tube of diameter D the value

$$l_D = D, \qquad (33)$$

* The actual expression obtained by Bosworth corresponds to $\frac{4}{3}\sigma l_0 T^3$. This arises from his taking the radiational energy per unit volume as $\sigma T^4/c$, whereas actually it should be four times this quantity.

which is to be expected from direct considerations, with the extra factor $(2-\epsilon)/\epsilon$ as a consequence of the specular reflexions when $1-\epsilon$ is finite.

11. Analogy with the thermal conductivity of a cylindrical dielectric at low temperatures

The thermal conductivity of the hollow core due to radiational transfer is closely analogous to the conductivity of a dielectric at very low temperatures by the thermal elastic waves, or the phonons, whose *natural* free path in the dielectric is much longer than the dimensions of the specimen, and whose *actual* free path is therefore determined by the dimensions of the specimen. Taking the specimen in the form of a long cylinder, and taking the reflexions of the phonons from the surface of the cylinder to correspond to *complete* absorption and re-emission according to the cosine law, on the basis of the analogy with the emission of photons from the surface of a *black body*, and further taking the temperature gradient along the cylinder to be constant, Casimir (1938) has calculated the net energy transferred across any given cross-section of the cylinder, and thence the thermal conductivity; he obtains for the conductivity of a cylinder of a crystal dielectric the expression*

$$\kappa_a = \frac{16}{45}\frac{\pi^5 k^4 D T^3}{h^3}\sum_{i=1}^{3}\frac{1}{v_i^2}, \tag{34}$$

where k and h are the Boltzmann and the Planck constants respectively, and the v_i's represent the velocities of the three principal acoustic waves associated with a given wave vector. For the long acoustic waves with which we are concerned here the v_i's may be taken to be independent of the wave number.

The energy density per unit volume in this case is given by

$$\delta = \frac{4}{15}\frac{\pi^5 k^4 T^4}{h^3}\sum_{i=1}^{3}\frac{1}{v_i^3}. \tag{35}$$

Now $v_i\delta/(4\pi)$ may be put equal to $\sigma_a T^4/\pi$, where σ_a is the acoustical analogue of Stefan's constant. Expressing κ_a in terms of σ_a one obtains

$$\kappa_a = \tfrac{16}{3}\sigma_a D T^3, \tag{36}$$

which is analogous to the expression for κ_r obtained previously in (30), in the special case when $\epsilon = 1$.

Comparing the above expression for the thermal conductivity of the crystal due to the transference of energy by the phonons, with the usual kinetic expression for the thermal conductivity of a gas, namely

$$\kappa_g = \tfrac{1}{3}c_v v l_g, \tag{37}$$

and taking l_g to represent now the mean free path of the phonons, which in this case is determined by the dimensions of the crystal specimen, and further remembering that in the acoustic case $c_v = \mathrm{d}\delta/\mathrm{d}T$, one can calculate the mean free path l_g of the

* A factor $2/\pi$ is missing in Casimir's expression for κ_a, but is restored in the later expressions that appear in his paper. This has been noticed by earlier workers too.

Wherever appropriate we use the same symbols used earlier in the case of electromagnetic radiational transfer to denote the analogous quantities in the corresponding acoustic case.

phonons in the tube. Berman *et al.* (1953) have calculated l_g in this manner, and they obtain, as we can readily check from the expressions given here, $l_g = D$. This is gratifying since it is also the value obtained here for the mean free path of the photons in the heated tube, when its walls have the ideal emissivity unity.

It is worth mentioning in passing that the expression for conductivity obtained by Casimir is for the case when the temperature gradient is constant. But equation (28) of this paper shows that expression (30) for the radiational conductivity of the core of our tube, and hence also the analogous expression obtained by Casimir for the conductivity of the cylindrical crystal at low temperatures, will remain valid even when $\mathrm{d}^2T/\mathrm{d}x^2$ is finite and significant, as is actually the case in the heated tube.

12. Effect of specular reflexions on heat transfer equivalent to enhancement of the mean free path of photons

The factor $(2-\epsilon)/\epsilon$ that appears in the expression for the net transference of radiation, as a consequence of the multiple specular reflexions, is the same as that obtained by Berman *et al.* in the expression for the thermal conductivity of a crystal cylinder at low temperatures. The appearance of this factor is equivalent, as they have pointed out in the case of the phonons concerned in thermal conductivity, to a corresponding increase in the free path of the phonons, and of the photons in our case, as a result of the specular reflexions.

A similar factor appears, as pointed out by these authors, also in the expression obtained by Smoluchowski (1910) for the passage of a rarefied gas through a narrow cylindrical tube. The series that leads to the factor $(2-\epsilon)/\epsilon$ in Smoluchowski's problem is

$$\epsilon[1+3(1-\epsilon)+5(1-\epsilon)^2+\ldots]. \tag{38}$$

It is as if, on the average, the molecules that are reflected r times have a weightage $2r+1$. This series can be readily seen to be equivalent to the series $\sum_{r=0}^{\infty}\epsilon^2(1-\epsilon)^r(r+1)^2$ obtained by us here.

This is also the factor, as Maxwell demonstrated nearly eighty years ago (1879), by which 'coefficient of slip' of the molecules striking the walls of the tube is enhanced as a result of specular reflexions.

13. Corresponding expressions for a tube of finite length

Coming back to the finite tube, since we are taking its length $2l \gg D$, at least one of the two lengths, either x_1 or $2l-x_1$, will still be sufficiently long to justify the approximation of large L, and hence it will be sufficient to discuss how closely $\mathrm{d}x_1$ can approach the nearer end before the deviations from the long distance approximation become significant. Obviously it has to be at least a few times D. If it is put equal to λD, $1/\lambda$ would be small enough to justify neglect of $1/\lambda^2$ in comparison with unity.

On this basis one can readily calculate the total radiation received by $\mathrm{d}x_1$ located at a distance λD from the nearer end, from the rest of the tube, using for this purpose the values of the integral $\int_0^L \zeta(h)\,h^m\,\mathrm{d}h$ and of the series S_N, entered in tables 2 and 3

respectively. Doing so, and remembering that the contributions from the two sides add up when m is even, and are of opposite signs when m is odd, one obtains

$$W = \tfrac{2}{3}\pi\sigma D^3 b(2-\epsilon)/\epsilon - \pi\sigma\{(6-6\epsilon+\epsilon^2)/\epsilon^2\}\left[\frac{1}{8}\frac{D}{\lambda^3}T_1^4 - \frac{3}{16}\frac{D^2}{\lambda^2}a + \frac{3}{8}\frac{D^3}{\lambda}b\right]. \quad (39)$$

The three correction terms on the right-hand side of (39), except for the numerical factors $\frac{1}{8}$, $\frac{3}{16}$ and $\frac{3}{8}$ respectively, and their signs, are in the same ratio as the first three terms in the Taylor expansion (9) for T_2^4. Especially near the ends of the tube, with which we are concerned now, the three terms will be of comparable magnitudes. Taking for example the last term, which can be directly compared with the main term, since they both involve b, their ratio can be seen to be equal to

$$\frac{9}{16\lambda}\,\frac{6-6\epsilon+\epsilon^2}{\epsilon(2-\epsilon)}.$$

With $\epsilon = 0{\cdot}75$ and $\lambda = 10$, this ratio is about $\frac{1}{8}$. Hence if dx_1 is not closer to either end of the tube than $10D$, the radiational conductivity at this section can be taken to conform to the value obtained in (30).

14. General solution of the differential equation

Coming back to the differential equation (1) defining the temperature distribution, and substituting in it the value of W obtained in (28), one obtains

$$[\kappa\omega + \tfrac{4}{3}\pi\sigma D^3T^3(2-\epsilon)/\epsilon]\,d^2T/dx^2 + 4\pi\sigma D^3T^2\{(2-\epsilon)/\epsilon\}\,(dT/dx)^2 + I^2\rho/\omega - \pi\epsilon\sigma D_e(T^4 - T_0^4) = 0, \quad (40)$$

where $D_e = 2r_e$ is the external diameter of the tube. It can be seen that when the tube is made very long, keeping the heating current the same, the temperature at the centre will tend to a value T_m given by

$$I^2\rho/\omega - \pi\epsilon\sigma D_e(T_m^4 - T_0^4) = 0. \quad (41)$$

Hence (40) may be written in the form

$$d^2T/dx^2 + \frac{3\xi T^2}{1+\xi T^3}(dT/dx)^2 + \frac{\eta}{1+\xi T^3}(T_m^4 - T^4) = 0, \quad (42)$$

where
$$\left.\begin{aligned}\xi &= \frac{4}{3}\frac{\pi\sigma D^3}{\kappa\omega}\frac{2-\epsilon}{\epsilon},\\ \eta &= \frac{\pi\epsilon\sigma D_e}{\kappa\omega}.\end{aligned}\right\} \quad (43)$$

If we put $T = T_m - \Delta$ and $d\Delta/dx = y$, (42) may be seen to reduce to

$$\frac{d(y^2)}{d\Delta} - 2\,\frac{3\xi(T_m-\Delta)^2}{1+\xi(T_m-\Delta)^3}y^2 = \frac{2\eta(4T_m^3\Delta - 6T_m^2\Delta^2 + 4T_m\Delta^3 - \Delta^4)}{1+\xi(T_m-\Delta)^3} = \frac{\Phi(\Delta)}{1+\xi(T_m-\Delta)^3}, \text{ say,} \quad (44)$$

which has the solution

$$y^2\{1+\xi(T_m-\Delta)^3\}^2 = \int \Phi(\Delta)\{1+\xi(T_m-\Delta)^3\}\,d\Delta; \quad (45)$$

i.e.

$$\begin{aligned}&(d\Delta/dx)^2(1-\alpha t+\alpha t^2-\tfrac{1}{3}\alpha t^3)^2\\ &= \frac{8\eta T_m^3}{1+\xi T_m^3}\int\{1-(\alpha+\tfrac{3}{2})t+(\tfrac{5}{2}\alpha+1)t^2-(\tfrac{17}{6}\alpha+\tfrac{1}{4})t^3+\tfrac{7}{4}\alpha t^4-\tfrac{7}{12}\alpha t^5+\tfrac{1}{12}\alpha t^6\}\,\Delta\,d\Delta\\ &= \mu\Delta^2\Psi(t), \quad \text{say,}\end{aligned} \quad (46)$$

where
$$\left.\begin{aligned}&t = \Delta/T_m; \quad \alpha = 3\xi T_m^3/(1+\xi T_m^3),\\ &\mu = 4\eta T_m^3/(1+\xi T_m^3),\\ &\Psi(t) = 1-\tfrac{1}{3}(2\alpha+3)t+\tfrac{1}{4}(5\alpha+2)t^2-\tfrac{1}{10}(34\alpha+3)t^3+\tfrac{17}{12}\alpha t^4-\tfrac{1}{3}\alpha t^5+\tfrac{1}{48}\alpha t^6.\end{aligned}\right\} \quad (47)$$

Now $[\Psi(t)]^{-\frac{1}{2}}$ can be expanded, and hence taking the square roots of both sides of (46) and integrating again one obtains

$$\begin{aligned}&\int\frac{1-\alpha t+\alpha t^2-\frac{1}{3}\alpha t^3}{\Delta[\Psi(\Delta)]^{\frac{1}{2}}}\,d\Delta\\ &= \int\{1-\tfrac{1}{6}(4\alpha-3)t-\tfrac{1}{72}(4\alpha^2-9\alpha+3)t^2+\ldots\}\,d\Delta/\Delta = \pm\mu^{\frac{1}{2}}x + \text{a constant},\end{aligned} \quad (48)$$

for which one obtains the two particular solutions

$$\Delta\,e^{f(\Delta)} = C\,e^{\pm x\sqrt{\mu}}, \quad (49)$$

where
$$f(\Delta) = \tfrac{1}{6}(3-4\alpha)t+\tfrac{1}{48}(3+9\alpha-4\alpha^2)t^2+\ldots. \quad (50)$$

One may immediately see that the particular solutions obtained here for the tube, namely (49), are similar to those obtained for the case of the filament, though the differential equations determining the temperature distribution in the tube appear more complicated. Further one can verify easily that when the internal diameter D_i of the tube tends to zero, the solutions obtained here reduce to those of a filament, as they should. In this case obviously ξ defined by (43) tends to zero, and hence μ reduces to $4\eta T_m^3$, which is the value characteristic of the filament; similarly $\alpha \to 0$ and hence
$$f(\Delta) \to \tfrac{1}{2}t+\tfrac{1}{16}t^2+\ldots, \quad (51)$$
which also can be recognized as the value obtained previously for the filament.

One can further show that as in the case of the filament, if the tube is not too short, $f(\Delta)$ would be sufficiently small in the middle of the tube, and $e^{f(\Delta)}$ sufficiently close to unity, to justify our combining the two particular solutions given in (49) so as to obtain the *practically* general solution

$$\Delta\,e^{f(\Delta)} = C_1e^{x\sqrt{\mu}} + C_2e^{-x\sqrt{\mu}}. \quad (52)$$

Moreover, as in the case of the filament, the term on the right-hand side of (52) that decreases exponentially with distance as one moves away from the centre, becomes

negligible, in comparison with the other term that increases exponentially, *while yet* $f(\Delta)$ *remains small*. In other words, over the whole of the region over which both the terms on the right-hand side of (52) remain significant, $f(\Delta)$ remains small enough to justify our combining the two particular solutions in the manner indicated in (52), while on the other hand, when we move out of this region, one of the terms ceases to be significant, and hence there is no special requirement for $f(\Delta)$'s remaining small in order to justify the combination. Hence for all practical purposes the solution given in (52) will apply over the whole length of the tube. The constants C_1 and C_2 appearing in (52) can be readily evaluated from the boundary conditions, i.e. from the temperatures at the centre and at the ends of the tube respectively.

Hence, from the known results for the filament, one would expect the temperature variation in the tube also to be parabolic near the centre, to be logarithmic farther out, and the variation near the ends to be the same as for an infinitely long tube. The details of the distribution will be taken up along with their experimental verification in part II of the paper.

We shall, however, draw attention here to a major feature that distinguishes the tube from the filament. As will be seen from (49), $1/\sqrt{\mu}$ represents the length over which the temperature in the logarithmic region drops down by a factor e, and may be regarded as a natural unit of length characteristic of the tube under the conditions of heating. The effect of the radiational conductivity of the core is to make the natural unit of length the larger the higher the temperature, and the central plateau in the temperature-distance curve will as a consequence be flatter and more extensive than in the absence of this radiational conduction.

15. Closely wound coils

A closely wound cylindrical solenoid naturally approximates to a tube, except that:

(1) the effective emissivity or absorptivity ϵ is not quite the emissivity of the surface of the wire, but will be greater owing to exchange of radiations between adjoining coils;

(2) the conductivity through the material of the coil is not now through a cross-section $\pi(r_e^2 - r_i^2)$ as in a tube, but through the cross-section $\pi\rho^2$, where ρ is the radius of the wire, which is much smaller, and the temperature gradient corresponding to the latter conduction is not $\mathrm{d}T/\mathrm{d}x$ but $(\mathrm{d}T/\mathrm{d}x)/2\pi rn$, where n is the number of turns in the coil per unit length. Hence in place of $\kappa\omega\,\mathrm{d}T/\mathrm{d}x$ of the tube we now have $\kappa\rho^2(\mathrm{d}T/\mathrm{d}x)/(2rn)$.

Hence the conduction along the material will be much smaller than the radiational conduction through the core, particularly at high temperatures. These and other features can be discussed more appropriately and significantly in relation to the experimental data, which will be reported in part II of this paper.

In conclusion we wish to express our thanks to Professor Thiruvenkatachar, Dr S. C. Jain and Mr A. K. Mustafy for many helpful discussions.

References

Berman, R., Simon, F. E. & Ziman, J. M. 1953 *Proc. Roy. Soc.* A, **220**, 176.
Bosworth, R. C. L. 1952 *Heat transfer phenomena*, p. 60. New York: John Wiley and Sons.
Buckley, H. 1927 *Phil. Mag.* **4**, 753.
Buckley, H. 1934 *Phil. Mag.* **17**, 596.
Casimir, H. B. G. 1938 *Physica*, **5**, 595.
Jain, S. C. & Krishnan, Sir K. S. 1954–55 *Proc. Roy. Soc.* A, **222–229**.
Knudsen, M. 1909 *Ann. Phys, Lpz.* **28**, 75, 999.
Maxwell, J. C. 1879 *Phil. Trans.* part I, 332 or *The scientific papers of James Clerk Maxwell*, p. 708. New York: Dover Publications Inc.
Smoluchowski, M. v. 1910 *Ann. Phys., Lpz.* **33**, 1559.

PHYSICS

Effect of Specular Reflexions on the Radiation Flux from a Heated Tube

A QUESTION of some importance that arises in problems of radiational transfer of energy in an enclosure is this: If ε is the emissivity, and hence also the absorptivity, of the surface, in what manner is the fraction $(1 - \varepsilon)$ of the incident radiation that is not absorbed returned to the enclosure? In most investigations on the radiation from the inside of a uniformly heated cylinder it is assumed that the whole of this fraction is diffusely radiated according to the cosine law[1]. The alternative case where the whole of this fraction is specularly reflected does not seem to have been investigated. This case also is of interest, since it can be secured in practice by suitably polishing the wall surface, and secondly since it lends itself to a more precise and elegant theoretical treatment than the corresponding case of perfectly diffuse reflexion.

Consider, for example, the flux of radiation that issues from the mouth of a cylinder, open at both ends, the temperature of which is kept uniform over its whole length. In order to evaluate the flux one may adopt a method somewhat similar to that used by Berman, Simon and Ziman[2] for calculating the effect of specular reflexions of thermal phonons of long free path from the walls of a cylindrical crystal on its thermal conductivity at low temperatures—though these authors were concerned, unlike here, with transport of energy under a gradient in temperature. The flux can be readily shown to be equal to:

$$F_L = \sigma T^4 \sum_{r=0}^{\infty} \varepsilon^r (1 - \varepsilon)^r \int_0^L \mu\left(\frac{h}{r+1}\right) dh \qquad (1)$$

where:

$$\mu(h) = \pi\left[h - \frac{2h^2 + D^2}{2(h^2 + D^2)^{1/2}}\right] \qquad (2)$$

σ being Stefan's constant, L the length of the tube and D its internal diameter.

When the tube is long, that is, when $L \to \infty$, the expression for the flux reduces to:

$$F_\infty = \sigma T^4 \varphi(\varepsilon) \int_0^\infty \mu(h')\,dh' \qquad (3)$$

where:

$$\varphi(\varepsilon) = \sum_{r=0}^{\infty} \varepsilon^r (1 - \varepsilon)^r (r + 1) \qquad (4)$$

is the factor by which the corresponding expression for the ideal case when the walls of the tube are black has to be multiplied in order to take into account the defect of actual ε from unity and the consequent occurrence of specular reflexions.

It can be readily seen that:

$$\varphi(\varepsilon) = \varepsilon^2[1 + 2(1 - \varepsilon) + 3(1 - \varepsilon)^2 + \ldots] = 1 \qquad (5)$$

That $\varphi(\varepsilon)$ is independent of ε and is equal to unity, as though the direct radiations only were involved and they corresponded to those of a black body, is significant. It can be further seen that $\int_0^\infty \mu(h)dh = \frac{1}{4}\pi D^2$, which is just the area S of the mouth of the tube, and that $F_\infty = S\sigma T^4$, which is just the radiation that one would expect from a black body of this area.

The equivalence of the flux from the mouth of the cylinder to the radiation from a black surface holds for all directions over the 2π solid angle.

When the other end of the tube is closed, the flux from the mouth includes, in addition to F_L, two more terms, F_L' and F_L'', relating to the radiations that originate from the side walls and are reflected from the end wall, and those that originate from the end wall, respectively:

$$F'_L = \sigma T^4 \sum_{r=0}^{\infty} \varepsilon^2 (1 - \varepsilon)^r \int_L^{2L} \mu\left(\frac{h}{r+1}\right) dh \qquad (6)$$

$$F_L'' = \sigma T^4 \sum_{r=0}^{\infty} \varepsilon^2 (1 - \varepsilon)^r \xi\left(\frac{L}{r+1}\right) \qquad (7)$$

where:

$$\xi(L) = \tfrac{1}{4}\pi[2L^2 + D^2 - 2L(L^2 + D^2)^{1/2}] \qquad (8)$$

With $\varepsilon = 0{\cdot}75$, the flux issuing from the mouth of a tube of length $5D$, closed at the other end, is short of that from a black body by about 1 per cent. In the alternative case of perfectly diffuse reflexion, even though the flux along some directions may approximate even more closely to that from a black surface, the total flux over all directions is considerably short of it, and remains so however much the cylinder may be extended.

K. S. KRISHNAN

National Physical Laboratory,
New Delhi 12.
March 3.

[1] See, for example, Buckley, H., *Phil. Mag.*, **4**, 753 (1927).
[2] Berman, R., Simon, F. E., and Ziman, J. M., *Proc. Roy. Soc.*, A, **220**, 171 (1953).

Quenching of Cation Vacancies in Doped Crystals of Sodium Chloride

As is well known, the thermodynamic defects developed by alkali halide crystals at high temperatures are predominantly of the Schottky type. The number of cation and anion vacancies in equilibrium with the crystal, at temperatures near the melting point, for example, may be as large as 10^{-4} of the total number of atoms. Attempts have, therefore, been made to quench those vacancies by very rapid cooling from these high temperatures, but without success, judging from the very similar values obtained for the electrical conductivities of the quenched and the annealed specimens[1]. (From the melt, however, some of the defects can be quenched.) This, however, is not surprising, since the relaxation times corresponding to the migration of vacancies, leading either to formation of pairs or to their exit from the crystal, remain small, even at temperatures several hundred degrees below the melting point.

Cation vacancies can also be introduced, as is well known, by suitably doping the crystal. For example, by doping sodium chloride with cadmium chloride, it is easy to see that at sufficiently high temperatures the number of cation vacancies produced by the doping will be just the number of Cd^{++} ions held in solution. We find experimentally that such vacancies, unlike the natural Schottky ones, can be quenched effectively. There are many advantages, as we shall see presently, in working with such quenched crystals, since the number of cation holes is then known definitely, and can be made fairly large. It may be mentioned incidentally that though extensive work has been done on annealed specimens of doped crystals, by Maurer *et al.*[1], quenched specimens do not seem to have been studied.

In the present experiments large clear crystals of sodium chloride containing known molar concentrations c of cadmium chloride, ranging from 2×10^{-5} to 7×10^{-4}, were grown from the melt in the usual manner. They were annealed at about 1,050° K., which is 27° below the melting point of the pure crystal, and then suddenly dropped into liquid nitrogen and thus allowed to cool rapidly. Although many of the crystals developed cracks, it was possible to obtain specimens free from cracks that were large enough for electrical conductivity measurements. Fig. 1 gives a plot of the conductivity σ of the quenched crystals at four different temperatures up to about 720° K. These temperatures were low enough to leave the quenching undisturbed. The observed small residual conductivity of the 'pure' crystal at these temperatures was corrected for. It corresponded to a doping concentration of cadmium chloride of about $4{\cdot}6 \times 10^{-6}$. It will be seen that they plot into straight lines, naturally passing through the origin. In Fig. 2 are plotted the values of $\log(\sigma T/c)$ against $1/T$, from which it will be seen that the values for all the concentrations plot on the same straight line. One may draw the following conclusions from this: (1) that even at the highest temperature of measurement, namely, 720° K., the number of cation vacancies produced by quenching remains undisturbed, and is therefore independent of the temperature of measurement; (2) that this number is proportional to the concentration c up to the highest concentration studied, namely, 7×10^{-4}, and must, therefore, be the number obtaining at the high temperature, and hence the same as the number of Cd^{++} ions doped into the lattice; in other words, while all the cation vacancies produced by the dope at 1,050° K. have

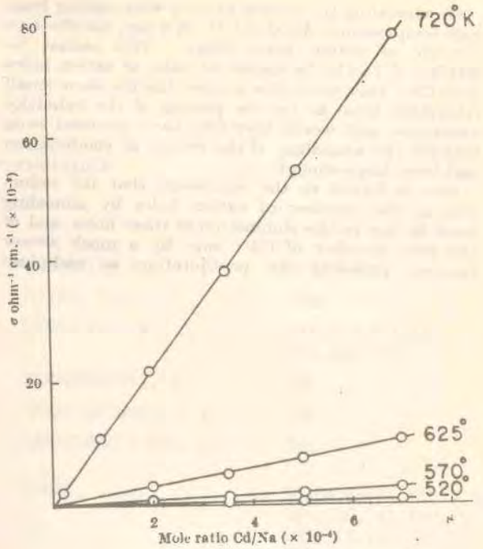

Fig. 1

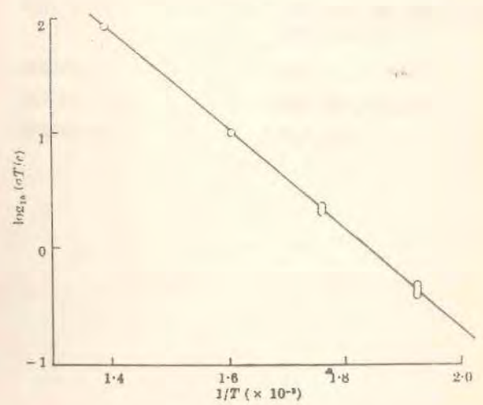

Fig. 2

been frozen intact, almost none of the natural cation vacancies of the Schottky type, the number of which also is considerable at this high temperature, has been frozen; (3) since the relaxation time corresponding to the migration of a cation hole to the neighbourhood of Cd^{++} is small, that the observed proportionality of the quenched number of holes to the concentration of cadmium points to a low value for the energy of pairing of a cation vacancy with a Cd^{++} ion.

Using the well-known expression for the conductivity, namely, $\sigma = ne\mu$, where $\mu = (ea^2/kT)\exp(-U/kT)$ is the mobility of the cation vacancy, and $U = U_0 - \alpha T$ is the activation energy corresponding to the mobility, one obtains from the slope of the straight line in Fig. 2, $U_0 = 0{\cdot}85$ eV., and from the intercept on the y-axis the value $\exp(\alpha/k) = 460$, which is large, but of the right order of magnitude. This value of α would correspond to a temperature coefficient of U given by $-(1/U)(dU/dT) = 5 \times 10^{-4}$.

On annealing the crystal by very slow cooling from high temperatures, by about 15° in a day, the effective number of cation holes drops. This cannot be attributed to the formation of pairs of cation holes with Cd^{++} ions, since this process has the same small relaxation time as for the pairing of the Schottky vacancies, and would therefore have occurred even without the annealing, if the energy of combination had been large enough.

One is forced to the conclusion that the reduction in the number of cation holes by annealing must be due to the elimination of these holes, and of the same number of Cd^{++} ions, by a much slower process, probably by precipitation as cadmium chloride. This accounts for the possibility of quenching these cation vacancies, but not the Schottky vacancies. Such precipitation may be merely a consequence of the decrease in the solubility of cadmium chloride with decrease of temperature. The development of turbidity by these crystals on annealing lends support to such a precipitation.

K. S. KRISHNAN
S. C. JAIN

National Physical Laboratory,
New Delhi.

[1] For a detailed review of the work, see Lidiard, A. B., *Handbuch der Physik*, 20, 246 (Berlin, 1957).

Co-AUTHOR INDEX